

Proceedings of

1st International Conference on Sustainable Chemical & Environmental Engineering



31st Aug - 4th Sep 2022

Rethymno, Crete, Greece

hybrid event

www.susteng.eu

ISBN: 978-618-86417-0-9



www.susteng.eu





Proceedings of the 1st International Conference on Sustainable Chemical and Environmental Engineering

SUSTENG 2022, 31 Aug – 04 Sep 2022, Rethymno, Crete, Greece

ISBN: 978-618-86417-0-9

Publisher:

Design of Environmental Processes Laboratory

School of Chemical and Environmental Engineering, Technical University of Crete, Greece.

Editor-in-Chief:

Prof. Petros Gikas

Conference Chair, Head of the Design of Environmental Processes Laboratory, School of Chemical and Environmental Engineering, Technical University of Crete, Greece.

Editors:

Ms. Anthoula Manali

Chemist M.Sc., Design of Environmental Processes Laboratory, School of Chemical and Environmental Engineering, Technical University of Crete, Greece.

Ms. Xanthi Evangelia Manaroli

Architect Engineer M.Sc., School of Chemical and Environmental Engineering, Technical University of Crete, Greece.

Mr. George Makaroglou

Environmental Engineer, Design of Environmental Processes Laboratory, School of Chemical and Environmental Engineering, Technical University of Crete, Greece.

Mr. Konstantinos Tsamoutsoglou

Environmental Engineer, Design of Environmental Processes Laboratory, School of Chemical and Environmental Engineering, Technical University of Crete, Greece.

Editorial Office:

Ms. Anthoula Manali

SUSTENG 2022 Conference Secretariat

Email: secretariat@susteng.eu

Telephone: +30 2821037839

Website: www.susteng.eu

SUSTENG 2022 Conference - Review

On behalf of the Organizing Committee, I am pleased to announce that the 1st International Conference on Sustainable Chemical and Environmental Engineering (SUSTENG2022), which was held both physically and virtually, in the town of Rethymno, on the island of Crete, Greece, between 31st August to 4th September 2022, has been successfully completed.

The conference included 27 sessions and was held in 3 parallel presentation rooms. During the conference, 211 abstracts were presented, out of which 162 were oral presentations, while the remaining 49 were posters. 92 of the oral presentations were with physical presence, while the remaining 70 were online. With respect to the geographical origin of the presentations, 90 came from Greece, while the remaining 121 were from abroad, with the presence of 45 countries, out of the five continents.

The conference was organized by the "Design of Environmental Processes Laboratory", of the School of Chemical and Environmental Engineering, Technical University of Crete. It was co-funded by the European LIFE Programme and by the Green Fund, under the framework of the project entitled: "New concept for energy self-sustainable wastewater treatment process and biosolids management (LIFE B2E4Sustainable-WWTP)".

The conference aimed to encourage the exchange of knowledge between academicians, scientists and engineers on hot issues and current developments in chemical and environmental engineering through sustainable perspective. The participants had the opportunity to present their recent research findings on an extended spectrum of conference topics and be informed about new challenges, future trends, and technological innovations on sustainable processes following the principles of circular economy.

One of the primary aims of the conference was to communicate to the public, and to the relative stakeholders, the findings of the LIFE B2E4Sustainable-WWTP project. Also, the conference participants had the opportunity to visit the demo site of the aforementioned LIFE project, at Rethymno municipal wastewater treatment plant.

May I thank our sponsors and supporters (PREFECTURE OF CRETE, HELECTOR, KAOUSSIS, MOTOR OIL, SEKA, DEDISA, EDEYA, SYCHEM, LIDSEN, PLASTIKA KRITIS, PANGAEA, ECOTEC, ESDAK, DEYAR, FODSA KM) for their valuable contribution for the materialization of the conference.

The abstracts/full papers presented at SUSTENG 2022 have been included in the present Conference Proceedings Book.

The Conference Chair

Petros Gikas

Professor

Head of the "Design of Environmental Processes Lab"
School of Chemical and Environmental Engineering
Technical University of Crete



TOPICS

Adsorption processes (Part I)
Circular Economy/Recycling & Reuse
Biotechnology/CO₂ Management
Air Pollution, Emissions & Quality
Microalgae
Bioremediation
Anaerobic Digestion
Municipal Solid Waste
Environmental Economics
Life Cycle Assessment
Agricultural Engineering
Waste to Energy/Energy Production
Environmental Monitoring
Adsorption Processes (Part II)
Micropollutants/Microplastics
Fuels/Biofuels
Water Resources Management
Wastewater Treatment
Policies, Regulatory & Social Acceptance
Nanomaterials
Infrastructure & Building Materials
Water Treatment
Biorefineries
Advanced Oxidation Processes
Metals/Metallurgy
Modelling



SPECIAL ISSUES

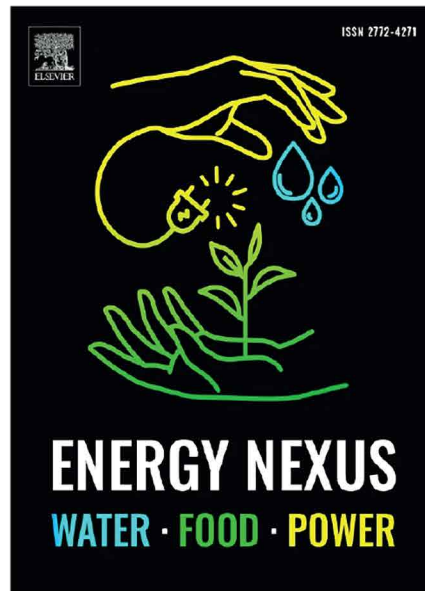


Selected abstracts may be submitted to the three following Special Issues of Scientific Journals:

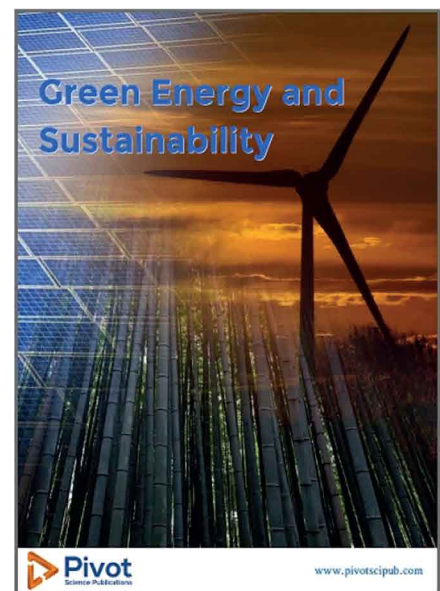


**Sustainable Solid and
Liquid Waste
Management**

*Journal of Environmental
Management
(Elsevier)*



**Sustainable
Engineering in
Circular Economy**
Energy Nexus (Elsevier)



**Selected Papers from
the 1st International
Conference on
Sustainable Chemical
and Environmental
Engineering**
*Green Energy and
Sustainability (Pivot)*

TABLE OF CONTENTS

TITLE PAGE	i
CONFERENCE REVIEW	ii
TOPICS	iii
SPECIAL ISSUES	iv
TABLE OF CONTENTS	v

ABSTRACTS

ADSORPTION PROCESSES (PART I)	1
Three-Dimensional Electrochemical Process Using Regranulated Cork Granules for the Removal of Trazodone and Sulfamethoxazole from Water	2
P. Remor, S.A. Figueiredo, V.J.P. Vilar, C. Soares, L. Correia-Sá, C. Delerue-Matos	
Activated hydrochar from grape stalk for methylene blue adsorption	4
M. Gimenez, C. Deiana	
NO ₃ ⁻ -N removal from groundwater using thermally treated palygorskite in fixed bed reactor	6
C. V. Lazaratou, S. D. Panagopoulos, D. V. Vayenas, D. Papoulis	
Biochar based sorbents to remove vanadium ions from aqueous media.....	8
J. Bak, D. Kolodynska	
Evaluation of biochar and activated carbons produced from different biomass feedstock for use as an adsorbent for pharmaceutical compounds removal in a decentralized wastewater treatment plant system ..	10
R.T. Morake, S. Septein, B.S. Martincigh, D. Lokhat	
CIRCULAR ECONOMY/RECYCLING & REUSE	12
Is circular economy the key to halting biodiversity loss?.....	13
A.E. Assogbadjo, H.G.G. Avakoudjo	
Constructed wetlands case studies for municipal and industrial wastewater management in a circular economy	15
A. Stefanakis	
Multi-purpose lignin-based benzoxazines: from hydrophobic coatings to catalyst-free vitrimers	17
A. Adjaoud, L. Puchot, C. Federico, R. Das, P. Verge	

Hydrothermal Process for Silver Leaching from Mono- and Poly-crystalline Photovoltaic Waste Panels.....	18
E. Kastanaki, E. Lagoudakis, G. Kalogerakis, A. Giannis	
Pre-processing and Leaching methods for extraction of REEs from permanent magnets: A scoping review	20
S. Papagianni, A.M. Moschovi, K.M. Sakkas, M. Chalaris, I. Yakoumis	
Technical assessment of a plant for recovery of metals from HDS catalysts	22
N.M. Ippolito, V. Innocenzi, I. D'Adamo, F. Ferella	
BIOTECHNOLOGY/CO₂ MANAGEMENT	24
Co-culture and continuous two-stage bioreactor system for the fermentation of syngas by <i>B. methylophilum</i> and <i>C. tyrobutyricum</i>	25
M. Pacheco, C. Silva, P. Moura	
Electro-conductive anaerobic membrane bioreactors for biofouling mitigation	27
S. Qi, A.D. Grossman, A. Ronen, R. Bernstein	
Effect of oxygen transfer coefficient on microbial production of lipids and carotenoids using renewable waste feedstock: batch and fed-batch mode.....	29
M.A. Villegas-Mendez, J. Montanez, J.C. Contreras-Esquivel, I. Salmeron, A. Koutinas, L. Morales-Oyervides	
Recent advances in CO ₂ to bio-oil biorefinery.....	31
A.G. Capodaglio	
Green materials-composites for CO ₂ capture and conversion- an emerging trend in sustainable CO ₂ management.....	33
M. Geetha, K.K. Sadasivuni	
Catalytic hydrogenation of CO ₂ using CuO impregnated amine-modified silica support	34
H. Onthath, M.H. Sleim, M. Geetha, K.K. Sadasivuni, A.M. Abdullah, B. Kumar	
AIR POLLUTION, EMISSIONS & QUALITY	35
Study of immobilized biomass reactors for sulfidogenic activity characterization and efficiency improvement	36
R. Castro, G. Gabriel, X. Gamisans, X. Guimera	
Analysis of PM _{2.5} and PM ₁₀ concentrations trends in selected Greek urban cities before and after the national lockdowns caused by the COVID-19 pandemic.....	38
P. Begou	

Cumulative Impact Assessments of Power Generations in Southeastern Bangladesh.....	40
M.M. Karim, N. Bindra, A. Masud	
Is there any correlation between the diabetes mellitus and atmospherical pollutants?	42
M. Koliba, D. Zmijkova, H. Raclavska	
Reducing methane emissions at gas transmission networks. Best practices literature review and case studies	44
A. Tsochatzidi, N.A. Tsochatzidis	
MICROALGAE	46
Effect of carbon concentration on the fatty acid distribution and basic FAME properties of the bio-oil of <i>Chlorella sorokiniana</i>	47
G. Papapolymerou, A. Mpesios, A. Kokkalis, D. Kasiteropoulou, M.N. Metsoviti, A. Papadopoulou	
Removal of nutrients from saline water by algae	49
S.E. Biliari, I.D. Manariotis	
Lab and photo-bioreactor scale optimization of <i>Stichococcus</i> sp. strain for CO ₂ sequestration and bio-products production.....	51
G. Makaroglou, P. Gikas	
BIOREMEDIATION	53
Separation of the α -alumina layer from a spent Three-Way-Catalyst through <i>A. thiooxidans</i> as a pre-treatment to recover PGMs	54
M. Compagnone, J.J. Gonzalez-Cortes, M.P. Yeste, D. Cantero, M. Ramirez	
Wastewater treatment coupled with <i>Synechococcus elongatus</i> PCC 7942 cultivation	56
G. Samiotis, K. Stamatakis, I. Ristanis, L. Kemmou, E. Amanatidou	
Comparative Degradation of <i>Vitis Vinifera</i> "Assyrtiko" grape pomace by two different bacteria: <i>Pseudomonas</i> sp. strain phDV1 and <i>Chlamydomonas reinhardtii</i>	58
E. Mathioudaki, M. Belenioti, D. Ghanotakis, G. Tsiotis, N. Chaniotakis	
Biodegradation of glyphosate: a Bioinformatics approach.....	60
V.L. Koumandou, M. Giannakara	

Hydrocarburoclastic fungi and bacteria to improve bioavailability and degradability of petroleum hydrocarbons in a historically contaminated soil	62
S. Di Gregorio, I. Chicca, S. Becarelli	
Aeration control using on-line calculation of oxygen uptake rate	63
K. Azis, S. Ntougias, P. Melidis	
ANAEROBIC DIGESTION	65
The role of hydrochar on the production of biogas and volatile fatty acids during anaerobic digestion of cheese whey wastewater	66
D. Liakos, G. Altiparmaki, A. Kalampokidis, S. Vakalis	
Influence of nitrate source and hydraulic residence time of the anoxic desulfurization in the bacterial consortia and the methane content of desulfurized landfill biogas	68
J.J. Gonzalez-Cortes, G. Quijano, M. Ramirez, D. Cantero	
Long-term operation of a pilot bioscrubber for landfill biogas desulfurization	70
S. Torres-Herrera, J. Palomares-Cortes, J.J. Gonzalez-Cortes, X. Gamisans, D. Cantero, M. Ramirez	
Anaerobic Co-digestion of sewage sludge and acidic cheese whey	72
F. Gkoumas, Z. Gravanis, C. Noutsopoulos, D. Mamais, S. Malamis	
The microbiology of the two stage Dark Fermentation - Metanogenic reactor, optimization of methane production	74
S. Becarelli, E. Rossi, R. Iannelli, S. Di Gregorio, I. Pecorini	
Development of a two-stage anaerobic digestion system for treating fruit and vegetable wastes from open markets	75
A. Kalogiannis, I. Vasiliadou, K. Stamatelatou	
Transition from lab to pilot scale anaerobic digestion systems: effect of the substrate composition on the process stability and repeatability	77
K. Tsigkou, D. Zagklis, P. Tsafraikidou, C.a Zafeiri, M. Kornaros	
UASB performance and microbial community during sulfate enriched hydrolyzed starch treatment	79
D. Theodosi Palimeri, A.G. Vlyssides, A.A. Vlysidis	

MUNICIPAL SOLID WASTE	81
Spatial and temporal variation of VOCs in MSW landfills	82
A. Lagoudi, K. Poullos, G. Anagnostopoulos, K. Rigas, S. Chandrinou	
An investigation on the methane gas production and emission potential from municipal solid waste dumpsites in India	84
N. Gupta, N. B.P., R. Arora, M. Karimpour	
Source-level composting of biodegradables for envisaging sustainable management of municipal solid waste in urban educational institutes – a model for developing countries.....	86
M. Shafiq	
Long-term operation of a pilot sequencing batch bioreactor for the nitrification of landfill leachates	88
S. Torres-Herrera, J. Palomares-Cortes, J.J. Gonzalez-Cortes, X. Gamisans, D. Cantero, M. Ramirez	
ENVIRONMENTAL ECONOMICS	90
Cost profile of adsorption and photocatalysis process	91
D.A. Gkika, A. Mitropoulos, G.Z. Kyzas	
Systematic and Cost Overview of Freeze Desalination utilizing Thermoacoustic Technology	93
U. Ali, H. Zhang, I. Janajreh	
Development of the IES protocol for Sustainable Blue Economy in the coastal zone	95
A. Pournara, F. Sakellariadou	
LIFE CYCLE ASSESSMENT	96
Environmental Considerations Allied with the Application and Aerobic Operation of the Fluidized Bed Bio- film Reactor (FBR).....	97
W.L. Liew, M.A. Kassim, K. Muda, S.K. Loh, M.M. Hanafiah, N.S. Zaidi	
Life cycle assessment as support tool for development of novel materials used in environmental applica- tions.....	99
G. Barjoveanu, C. Teodosiu, I. Morosanu, D. Fighir, F. Bucatariu, M. Mihai	
Life cycle assessment of chicken manure treatment options	101
G. Barjoveanu, D. Gavrilesco, P. Apopei, C. Teodosiu	
Environmental assessment of the integration of gasification into the waste management system in Reunion Island	103

J.C.I. Rabetanetiarimanana, M.H. Radanielina, H.T. Rakotondramiarana, D. Morau	
Environmental Assessment of Energy Supply Model Replacement in a Dyeing-Finishing Plant	105
M.F. Shih, J.C.T. Lin	
Biodesulfurization biorefinery using <i>Gordonia alkanivorans</i> strain 1B: Life cycle inventory of the integrated process.....	107
T.P. Silva, C. Silva, J. Tavares, S.M. Paixao, L. Alves	
Is Hemp a Sustainable Energy Resource?.....	109
E. Teirumnieka, N. Patel, K. Laktuka, I. Veidenbergs, D. Blumberga	
AGRICULTURAL ENGINEERING	111
Changes of carbon and nitrogen content in soils since 1993 to 2021 in the Krotoszyn Forest District, Poland	112
M. Konatowska, A. Mlynarczyk, P. Rutkowski, Z. Krysztofiak, A.K. Bernat	
The combination of lean manufacturing methodology and innovation in the beverage business	114
M.G. Nomikou, P. Konstantinou	
Methane production from cheese whey over longer period may be interrupted by microelements restrictions.....	116
B. Stres, A. Hatzikioseyan, P. Kousi, E. Remoundaki, L. Deutsch, K.V. Mikus, S. Kolbl-Repinc	
The effect of biogas plants on the reduction of GHG emissions on the animal production farm profile.....	118
J. Dach, W. Bojarski, J. Mazurkiewicz, A. Kowalczyk-Jusko, P. Pochwatka, A. Mazur	
Statistical Comparison of the performance of the Down-flow Expanded Granular Bed Reactor and Expanded Granular Sludge Bed Reactor train for the treatment of Poultry slaughterhouse wastewater	120
P.A. Dyosile, M. Basitere, M. Njoya, S.K.O. Ntwampe	
Comparative effects of agricultural biowaste recycling practices and inorganic fertilization on basil (<i>Ocimum basilicum</i> L.) growth and soil fertility: Modeling plant growth	122
D. Pinakoulas, V. Sotiriou, S. Grivopoulos, M. Drosos, M. Papadaki, G. Mihalakakou, E. Giannakopoulos	
Advances in avocado oil extraction replacing conventional solvent extractions with Ultrasound technique as a green technology.....	124
S.T. Mgoma, M. Basitere, V. Mshayisa	

Forest residues valorization towards wood protecting agent applications	126
L. Sillero, A. Morales, R. Fernandez-Marin, F. Hernandez-Ramos, I. Davila, X. Erdocia, J. Labidi	
WASTE TO ENERGY/ENERGY PRODUCTION	128
Hydrothermal carbonization as a pathway for co-gasification of municipal sludge and agricultural residues	129
A. Artikopoulos, G. Altiparmaki, D. Liakos, S. Vakalis	
Green pyrolysis of wine waste for hybrid supercapacitors	131
A. Mamaní, M. Gimenez, D. Barreda, S. Fabiana, R. Santamaría	
The potential of the use of reclaimed areas of transition regions for the production and accumulation of electricity as a potential to replace natural gas from risk areas	133
L. Stepanec, M. Kantor, P. Gikas, D. Juchelkova	
Gasification-energy production system for the management of wastewater primary sieved solids	135
A. Pothoulaki, A. Manali, P. Gikas	
ENVIRONMENTAL MONITORING	137
Environmental monitoring of the Balos lagoon in Western Crete for sustainable tourism development	138
M. Lilli, G. Skiniti, N. Nikolaidis, T. Tsoutsos	
Do the pathogens and antibiotic resistance genes can “ESKAPEE” from the WWTP?	140
J. Hubeny, M. Buta-Hubeny, W. Zielinski, D. Rolbiecki, S. Ciesielski, E. Korzeniewska, M. Harnisz	
Management implications in a peri-urban river under multiple stressors	142
C. Ntislidou, V. Papaevangelou, D. Latinopoulos, S. Ntougias, P. Melidis, C. Akrotos, I. Kagalou	
ADSORPTION PROCESSES (PART II)	144
Development and evaluation of magnetic tea waste based adsorbent materials for removal of cadmium from wastewater	145
M. Ervine, O. Jaiyeola, C. Mangwandi	

Converting unused concentrated metals of plating waste into novel layered double hydroxide (LDH) adsorbent for pyrophosphate removal	146
T.A. Kurniawan	
Removal of Hexavalent chromium from aqueous solution using Potato Peel waste-based adsorbent.....	147
O. Jaiyeola, C. Mangwandi	
Highly efficient removal of cadmium from waste water using eco-friendly and cost-effective aluminophosphate as adsorbents	149
O. Jaiyeola, A. Hamza, C. Mangwandi	
Olive Mill Wastewater color treatment by fibrous clay mineral.....	151
G. Panagopoulos, E. Gianni, V. Bekiari, K. Katsanou	
Comparison of rare earth elements adsorption by sodium alginate-based adsorbents	153
D. Fila, Z. Hubicki, D. Kolodynska	
Effect of conductive material addition and external voltage application on the anaerobic digestion of dairy wastewater	155
M.S. Fountoulakis, Z. Dedova, S. Lemaigre, M. Calusinska, J. Roussel	
MICROPOLLUTANTS/MICROPLASTICS	157
Influence of grain size distribution of compost from urban greenery on the distribution of microplastics and their leachability	158
H. Raclavska, J. Ruzickova, M. Safar, D. Juchelkova, B. Svedova, M. Kucbel, P. Kantor, H. Brtkova, K. Raclavsky	
Water quality analysis using physicochemical parameters and estimation of pesticides in water from various sources of Tirupati, Andhra Pradesh, India	160
S. Konda, M. Malleswari, B. Nikitha	
Photodegradation of low -and high-density polyethylene, polypropylene, polyvinyl chloride, polystyrene and nylon: evaluation by IR spectroscopy, Raman spectroscopy, DSC and SEM	162
M.P. Yeste, M.A. Cauqui, S. Bergaliyeva, M. Sendra	
One step synthesis of g-C ₃ N ₄ supported WS ₂ with enhanced photocatalytic performance.....	164
G. Mario Vino Lincy, M.M. Ghangrekar, S. Chowdhury	

Electrosynthesis of hydrogen peroxide with carbon based materials for the degradation of emerging contaminants	166
R. Dhawle, A. Ioannidi, Z. Frontistis, D. Mantzavinos	
Novel 3D MoS ₂ @graphene aerogel for enhanced photocatalytic degradation of tetracycline.....	168
R. Das, B.K. Dubey, S. Chowdhury	
Assessing the performance of a column system using zero valent iron nanoparticles for the treatment of diclofenac and bisphenol-A from wastewater	170
E. Barka, C. Noutsopoulos, A. Galani, I. Panagou, M. Kalli, E. Koumaki, D. Mamais, S. Malamis, C. Mysterioli, N. Papassiopi	
Theoretical investigation of halloysite as potential sorbent for pharmaceutical wastewaters.....	172
E. Gianni, E. Scholtzova	
FUELS/BIOFUELS	174
Optimization of a biphasic biodesulfurization system	175
T.P. Silva, S.M. Paixao, J.C. Roseiro, L. Alves	
Valorisation of crude glycerol in the production of liquefied lignin bio-polyols.....	177
F. Hernandez-Ramos, M. Gonzalez Alriols, J. Labidi, X. Erdocia	
Kinetic Study of Transesterification of Waste Cooking Oil Under Ultrasound.....	179
S. Savvopoulos, H. Hatzikirou, I. Janajreh	
Production of green hydrogen on Non-Interconnected Islands (NIIs) and combination with LNG: a modeling analysis of Lesvos (Greece).....	181
N. Perivolari, A. Dimou, S. Vakalis	
WATER RESOURCES MANAGEMENT	183
Critical insights to drive sustainable water management in process industries	184
E. Karkou, N. Savvakis, G. Arampatzis	
Assessment of groundwater contamination vulnerability using machine learning algorithms.....	186
K.H. Park, S.Y. Chung, H.E. Elzain	
Satellite-Derived Bathymetry: Machine Learning Approach in the study of water supply reservoirs.....	188
L. Coelho de Andrade, A. Amaral e Silva, I. Oliveira Ferreira, F.C. Mesquita Santos, V. Gibrim Teixeira, M.L. Calijuri	

WASTEWATER TREATMENT	190
Mechanism of polyphosphate formation and degradation in wastewater treatment plants	191
Y. Bai, L. Stout, D. Jaisi	
Advancement in waste-water treatment technologies	193
F. Dziike	
Development of a greenhouse and screw conveyor solar driers for the treatment of faecal sludge from on-site sanitation facilities	195
S. Septein, P. Naidoo, A. Ramlucken, A. Ganapathie, Y. Pather, A. Singh, J. Pocock, F. Inambao, C. McGregor	
Primary filtration systems as a viable solution to overloaded municipal wastewater treatment plants	197
K. Tsamoutsoglou, P. Gikas, N. Karamanes, M. Mavri, K. Christofinas	
POLICES, REGULATORY & SOCIAL ACCEPTANCE	199
How Productive is Waste Management? Adoption & Impact of Waste Management practices in Indian Informal MSMEs	200
L. Posti, V. Bhamoriya	
Towards Sustainable Aviation: Civil Aviation Policies in Turkey in Global Context.....	202
N.U. Temel, Y.E. Topal, B.H. Gursoy Haksevenler	
Promoting sustainability in fisheries and aquaculture through biodiplomacy	204
K. Laktuka, P. Poca, D. Blumberga	
Social Perspective of Separate Waste Collection of Municipal Waste, A Case Study for a Municipality in Istanbul, Turkey	206
B.H. Gursoy Haksevenler, A. Akpinar, B. Takta, I. Celik	
NANOMATERIALS	207
Production and Application of High-Performance Industrial Materials based on Nanocellulose	208
G. Penloglou, O. Kotrotsiou, V. Bakola, A. Pavlou, M. Sarafidou, D. Ladakis, E. Tsouko, A. Koutinas, K.T. Pappapetros, K.S. Andrikopoulos, G.A. Voyiatzis, D. Bartzialis, N.G. Danalatos, K.D. Giannoulis, E. Karagiannidis, M. Iakovlev, E. Deze, M. Papaioannou, S. Sideri, C. Kiparissides	
Investigating the effects of initial number concentration on the transport of aggregating nanoparticles	210
V.E. Katzourakis, C.V. Chrysikopoulos	

Production of cellulose nanofiber by using deep eutectic solvent and ultrasonic treatment	212
Y.Y. Chen, F.B. Mkhontfo, K.L. Chang	
Microwave-Assisted production of Cellulose nanofibers with aromatic amine	214
F. Baraka, J. Labidi	
Degradation of indigo carmine dye using magnetic ferrite nanoparticles as a heterogeneous Fenton-like catalyst: Optimization by Response surface methodology	216
A. Soufi, H. Hajjaoui, M. Khnifira, M. Abdennouri, N. Barka	
Solar Cell Elements Based on Graphene-Porphyrin Nanocomposites	217
G. Gyulkhandanyan, P. Gikas, G. Shmavonyan	
Metal Nanoparticles: eco-compatible fungicide alternatives to combat resistance	219
A. Malandrakis, N. Kavroulakis, C. Chrysikopoulos	
Synthesis and Study of starch/CeO ₂ Nanoparticle Composite Material for Removal of Hexavalent Chromium from Synthetic Wastewater Solutions.....	221
O. Jaiyeola, C. Mangwandi	
Nutmeg seed shell-based silver nanoparticle/PVA composite for the synthesis of antimicrobial food packaging films	223
T. Thomas, A.K. Thalla	
INFRASTRUCTURE & BUILDING MATERIALS	225
Risk informed decision criteria for the sustainable design of renewable energy infrastructures	226
D. Diamantidis	
Production of Phase Change Material from Waste Low Density Polyethylene for Thermal Energy Storage Applications	228
H. Akgun, A. Ozkan, Z. Gunkaya, M. Banar	
Effect on the thermal sensation of outdoor users due to the age of the granite blocks used in the coating of public areas.....	230
K. Stefanopoulos, N. Lianos, D. Polychronopoulos, S. Zoras	
WATER TREATMENT	232
Selection of method water cleaning method and qualification of demanganization temperature filter fire troubleshooting in central provision. Kedronas of DEYA Edessas.....	233

A. Mpinos, I. Chatzoglou

Improving Groundwater Quality Using Hybrid Constructed Wetland in Coastal Communities in Sub-Saharan Africa.....235

R. N. Okparanma, V. O. Ahiakwo

Methylparaben as a concerning contaminant for the proliferation of *Stenotrophomonas maltophilia*.....237

A.R. Pereira, I. Gomes, M. Simoes

Ballast water disinfection by ozone micro- and nanobubbles239

P. Seridou, E. Kotzia, K. Katris, N. Kalogerakis

The potential of OXONE as an alternative disinfectant to control drinking water biofilms.....241

I.M. Oliveira, L.C. Simoes, M. Simoes

Renewable energy desalination for island communities: Status and prospects in Greece243

G. Kyriakarakos, G. Papadakis, C.A. Karavitis

BIOREFINERIES244

Importance of the use of Multi-Criteria Analysis tools to make decisions in biorefinery.....245

A. Coz, C. Rojas, C. Rueda, R. Leonardi, J. Khawam, R.N. Comelli, T. Llano

Agro-food waste re-valorization through solid-state fermentation for hydrolytic enzymes production.....247

J.D. Sosa-Martinez, J. Montanez, J.C. Contreras, S. Gadi, L. Morales

Recycling of solid waste from the olive oil industry for various added-value products249

H.N. Abu Tayeh, Y. Gerchman, J. Asscher, H. Azaizeh

ADVANCED OXIDATION PROCESSES251

Significantly enhanced UV-A driven oxidative destruction of an organic contaminant of emerging concern from aqueous medium using nanosized catalysts252

L. Favier, A.M. Sescu, D. Lutic, M. Harja

Photoprotection of Cationic Porphyrins and Their Non-Covalent Complexes for Effective Photodynamic Therapy of Tumors.....254

L. Mkrtchyan, A. Zakoyan, T. Seferyan, P. Gikas, G. Shmavonyan, G. Gyulkhandanyan

Biochar coupled with advanced oxidation process for a novel treatment of micropollutants in effluents ...256

H. Azaizeh, G. Peer, S. Azerrad

Advanced oxidation process UV-H₂O₂ combined with biological treatment for the removal and detoxification of phenol258

M. Haj-Zaroubi, N. Bar-Niv, H. Azaizeh, E. Kurzbaum

TiO₂-assisted solar light photodegradation as a solution of the problem of spreading b-lactam resistance determinants in the environment260

M. Buta-Hubeny, E. Felis, W. Zielinski, J. Hubeny, M. Harnisz, S. Bajkacz, E. Korzeniewska

METALS/METALLURGY262

Influence of anthropogenic factors on pollution of arable soils and changes in the activity of enzymes in them263

A. Sukiasyan, Armen Kirakosyan, S. Kroyan, P. Gikas

Novel economical method for recovering valuable metals from used Li-ion batteries.....265

J. Parra Degante, S. Rojas Escobar, L.P. Jaramillo Quintero, M.A. Munive Rojas, J.A. Guevara Garcia

Beneficiation of Coal Ash for Rare Earth Elements Enrichment.....267

A. Tsachouridis, N. Kiratzis

Recovery of Pd from Pd/Al₂O₃ catalysts through a thiosulfate-copper-ammonia complex.....269

M. Compagnone, J.J. Gonzalez-Cortes, M.P. Yeste, D. Cantero, M. Ramirez

Crocin as an eco-friendly corrosion inhibitor for aluminum alloys in NaCl solution.....271

P. Pantazopoulou, S. Theohari, S. Kalogeropoulou

Anodic electrodeposition of continuous metal-organic framework films with robust adhesion by pre-anchored strategy.....273

W. Guo, X. Zhang, J. Fransaer

Hydrometallurgical recovery of Ag and Au from printed circuit boards coupled with a novel bioreactor for the treatment of wastewater: a zero-discharge scheme275

D. Vlasopoulos, P. Mendrinou, P. Oustadakis, A. Karampelas, P. Kousi, A. Stergiou, S. Karamoutsos, A. Hatziki-oseyan, P.E. Tsakiridis, S. Agatzini-Leonardou, G.N. Anastasakis, E. Remoundaki

Bayesian statistics study of a sustainable dissolution of cobalt bearing minerals from Cu-Co ores277

B. Mbuya, J. Meta Mvita, A.F. Mulaba-Bafubiandi

Investigation of the processes occurring in water of acid mine drainage during their exposure.....	278
S. Hayrapetyan, M. Chobanyan, V. Hovhannisyan, A. Kirakosyan, A. Sukiasyan, P. Gikas	
MODELLING	280
A Classification Model for Estimating Hurricane Flood Damage in Satellite Images	281
M. Gavrilesco, D. Gavrilesco	
Development of computational tools for criticality analysis of process systems, utilizing Industrial IoTs	283
T. Theodosiadis-Thomaidis, G. Panagopoulou, S. Pistikopoulos	
Modeling metal bioprecipitation in a packed-bed denitrifying bioreactor.....	285
A. Hatzikioseyan, P. Mendrinou, E. Datsika, E. Remoundaki	
Reactive Transport Model on Biogeochemical Dynamics of Colloid Associated Heavy Metal Transport	287
S.S. Sengor, K. Unlu	
The use of sensitivity analysis in ANN to determine the significance of the parameters of the anaerobic digestion process	288
P. Pochwatka, A. Kowalczyk-Jusko, A. Mazur, M. Nowak, J. Dach	
An integrated PSO – DMC framework for the identification and control of wastewater treatment plants ..	290
I. Kalogeropoulos, T. Protoulis, I. Kordatos, A. Kapnopoulos, P.L. Zervas, H. Sarimveis, A. Alexandridis	
POSTERS	292
Production of Polyhydroxyalkanoates (PHA) by Pseudomonas sp. strain phDV1 using different carbon waste sources.....	293
E. Mathioudaki, D.E. Geladas, A. Drakonaki, E. Konsolaki, N. Vitsaxakis, N. Chaniotakis, G. Tsiotis	
Food-waste management in the food service sector.....	295
M. Barbarosou, L. Evrenoglou, O. Cavoura, G. Zervas, I. Damikouka	
Removal of anthraquinone dye by hybrid modified activated carbons.....	297
A.K. Tolkou, G.Z. Kyzas	
Autotrophic and heterotrophic arsenite oxidation by a river water microcosm	299
S. Won, J. Bae, S. Lee, H. Jin, Y. Kim, H.Y. Kang	
A recycling Photovoltaic panel process by complexing reagents.....	301

P. Koulouridakis, N. Bilalis, N. Kallithrakas-Kontos

LCA studies within CREIAMO project: eco-innovation approach and environmental impact assessment	303
E. De Marco, F. Hernan Gomez Tovar, L. Mastella, A. Franzetti, M. Vaccari, S. Scaffoni	
Employment of poultry and turkey manure as fuel for small/medium scale boilers	305
C. Di Stasi, Y. Torreiro, J. Rico, R. Perez, D. Patino, A. Rodriguez-Abalde	
Cultivation of marine microalgae - Production of biomass and high value added products	307
V. Patrino, A. Daskalaki, C.N. Economou, D. Bokas, D.V. Vayenas, G. Aggelis, A.G. Tekerlekopoulou	
Use of biosolids to enhance tomato growth and assessment of metal leaching after land application	309
I. Giannakis, C. Emmanouil, M. Mitrakas, A. Lagopodi, A. Kungolos	
Biodiesel production, properties and sustainability from the biomass of <i>Chlorella sorokiniana</i> grown heterotrophically with glycerol and anaerobic digestate	311
D. Kasiteropoulou, G. Papapolymerou, A. Kokkalis, M. Metsoviti, X. Spiliotis, A. Mpesios	
The root microbiome of organically grown vegetable crops	313
N. Paranychianakis, R. Mourgela, M. Frantzeskou, N. Kavroulakis, P. Moschou	
Use of green magnetic nanoparticles (Cys-Fe ₃ O ₄) and ozone for the degradation/elimination of methylene blue in textile wastewater	315
Y.L. Ramirez Salazar, L.N. Valero-Melo, W. Marimon-Bolivar, L.P. Tejada, L. Pulgarin	
Applying solar distillation for wine lees dewatering and phenols recovery	317
P.Mastoras, S.Vakalis, M.S. Fountoulakis, A. Xenaki, D. Haralambopoulos, A.S. Stasinakis	
Heterotrophic growth of <i>Chlorella sorokiniana</i> with glycerol and anaerobic digestate: carbon uptake rate and phenolic content.....	319
D. Kasiteropoulou, G. Papapolymerou, D. Ladas, A. Mpesios, M. Metsoviti	
Influence of rejuvenating agents addition on the properties of zeolite-foamed asphalt.....	321
A. Wozuk, M. Wrobel, W. Franus	
Potential for bioenergy production from swine farms in Cyprus.....	323
A. Poullou, P. Gikas	

Challenges for public acceptance of water reuse	325
E. Gika, E.A. Fakorelli, V. Bili and P. Gikas	
A novel microbial biosurfactant/bioemulsifier: Production and characterization.....	327
T.P. Silva, S.M. Paixao, J.Tavares, L. Alves	
Mixotrophic cultivation of <i>Microchloropsis gaditana</i>	329
G. Papapolymerou, N. Katsoulas, I. Karapanagiotidis, M. Metsoviti	
Handling and Waste Management of Covid-19 Self and Rapid Tests survey: a data analysis	331
E. Panourgia, T. Daras, A. Giannis, E. Maria	
Study of the potential accumulation of pesticides in microplastics.....	332
S. Martinho, V. Cruz Fernandes, S.A. Figueiredo, C. Delerue-Matos	
A fast and effective analytical method to quantify the emulsifying activity: design and validation	334
L. Alves, J. Tavares, T.P. Silva, S.M. Paixao	
Thermodynamic characterization of Liquid-Vapor Equilibria of Propionic Acid-Water and Acetic Acid-water at atmospheric pressure	336
L. Mazzeo, V. Piemonte	
Preliminary performance evaluation for chicken manure treatment and valorization options.....	337
D. Gavrilesco, G. Barjoveanu, P. Apopei, C. Teodosiu, A. Talpalaru	
Effect of granular activated carbon (GAC) addition in a pilot-scale anaerobic digester treating sheep manure and agro-industrial wastewater	339
D. Kalantzis, I. Daskaloudis, D.F. Lekkas, T. Lacoere, J. De Vrieze, M.S. Fountoulakis	
ETV as tool dedicated to acceleration of market uptake and diffusion of green innovations. The LIFEproETV project	341
E. De Marco, S. Scaffoni, R. Preka, E. Mancuso, I. Ratman Klosinska, T. Beltrani	
Smart Water Management.....	343
E. Vgenopoulou, L. Evrenoglou, O. Cavoura, G. Zervas, I. Damikouka	
Performance of a UASB reactor treating hydrolyzed starch at various conditions.....	345

D. Theodosi Palimeri, A.G. Vlyssides, A.A. Vlysidis	
Enhancement of siloxanes biofiltration from waste air by toluene addition.....	347
J.J. Gonzalez-Cortes, P.A. Lamprea-Pineda, M. Ramirez, K. Demeestere, C. Walgraeve	
Evaluation of the Suitability of Agricultural- and Industrial-based Biochars for Soil Amendment	349
D. Vamvuka, P. Karagiannaki	
Effect of salinity and nitrogen to phosphorus ratio on the growth of the marine cyanobacterium <i>Geitlerinema</i> sp	350
S. Patsialou, C.N. Economou, S. Genitsaris, A. Rafteli, G.N. Hotos, D.V. Vayenas, A.G. Tekerlekopoulou	
Energetic potential evaluation of medical wastes for using as solid recovered fuels	352
D. Torres, M. Fonseca Almeida, S.C. Pinho	
Training A New Generation Of farmers and agricultural entrepreneurs to implement the concept of Circular economy in agriculture – The TANGO-Circular ERASMUS+ project	354
G. Papadakis, E. Dimitriou, P. Picuno, I. Plantzou, C. Stavropoulou, L. M. Closas, L. Brondelli di Brondello, A. Farrus, F. Baptista, M. E. Mur Cacaho, T. Batista, F. Cordeiro, R. Serra, D. Margout-Jantac	
Cultivation of <i>Chlorella Sorokiniana</i> in batch and sequencing batch reactors for winery wastewater treatment	356
M. Mastori, A. Xenaki, E. Zkeri, A.S. Stasinakis	
Microsieving of raw sewage at the wastewater treatment plant of Rethymno: Yield and energy content of produced biosolids	358
A. Manali, C. Kampourakis, P. Gikas	
Effect of COVID-19 lockdown on heavy metal contamination in Yamuna river water of Delhi region	360
K. Lal, M. Uttreja	
Application of ionic liquids for bacterial carotenoid extraction.....	362
F. Salgado, T.P. Silva, L. Alves, J.C. Roseiro, R.M. Lukasik, S.M. Paixao	
Process design and life cycle inventory of a syngas fermentation biorefinery	364
M. Pacheco, J. Ortigueira, P. Moura, C. Silva	
Bioremediation of cresols by <i>Pseudomonas</i> sp. strain phDV1.....	366
A. Lyratzakis, G. Valsamidis, I. Kanavaki, J.D. Langer, G. Tsiotis	

Examination of efficient harvesting and drying processes from a microalgae photo-bioreactor.....	368
E. Tsantopoulou, G. Makaroglou, P. Gikas	
CO ₂ mitigation of industrial flue gas using an attached system microalgal photo-bioreactor	370
D. Mitrogiannis, G. Makaroglou, P. Gikas	
Investigation of hydrocyclone performance to municipal wastewater treatment plants	372
A. Kehagias, K. Tsamoutsoglou, P. Gikas	
The ReCiProCo project: development of a methodology to measure and communicate the circularity of products	374
S. Scaffoni, V. Fantin	
Assessment of the contribution of an innovative biosolids microsieving-gasification system in the formation of the wastewater management legal framework.....	375
A. Syrpis, A. Manali, P. Gikas	
Isolation and determination of the energy content of grease and oil in Wastewater Treatment Plants on the island of Crete.....	377
N. Tatas, A. Manali, P. Gikas	
Treat and Reuse of high organic load wastewater with an innovative compact and modular unit	379
A. Yfantis, N. Yfantis, T. Angelakopoulou, F. Michelet, G. Giannakakis, N. Ellinakis, S. Dokianakis, E. Vasilaki, N. Katsarakis	
Resilience Water supply, sanitation service provision and hygiene in Awash Basin, Ethiopia: Sustainable Growth and multi-level governance arrangements for climate change mitigation.....	381
E. Kalapoda	

FULL PAPERS

Technical assessment of a plant for recovery of metals from HDS catalysts	385
N.M. Ippolito, V. Innocenzi, I. D'Adamo, F. Ferella	
Co-culture and continuous two-stage bioreactor system for the fermentation of syngas by <i>B. methylotrophicum</i> and <i>C. tyrobutyricum</i>	392
M. Pacheco, C. Silva, P. Moura	

Effect of oxygen transfer coefficient on microbial production of lipids and carotenoids using renewable waste feedstock: batch and fed-batch mode	398
M.A. Villegas-Mendez, J. Montanez, J.C. Contreras-Esquivel, I. Salmeron, A. Koutinas, L. Morales-Oyervides	
Study of immobilized biomass reactors for sulfidogenic activity characterization and efficiency improvement	403
R. Castro, G. Gabriel, X. Gamisans, X. Guimera	
Analysis of PM _{2.5} and PM ₁₀ concentrations trends in selected Greek urban cities before and after the national lockdowns caused by the COVID-19 pandemic	410
P. Begou	
Is there any correlation between the diabetes mellitus and atmospheric pollutants?	414
M. Koliba, D. Zmijkova, H. Raclavska	
Reducing methane emissions at gas transmission networks. Best practices literature review and case studies	420
A. Tsochatzidi, N.A. Tsochatzidis	
Effect of carbon concentration on the fatty acid distribution and basic FAME properties of the bio-oil of <i>Chlorella sorokiniana</i>	425
G. Papapolymerou, A. Mpesios, A. Kokkalis, D. Kasiteropoulou, M.N. Metsoviti, A. Papadopoulou	
Separation of the α -alumina layer from a spent Three-Way-Catalyst through <i>A. thiooxidans</i> as a pre-treatment to recover PGMs	431
M. Compagnone, J.J. Gonzalez-Cortes, M.P. Yeste, D. Cantero, M. Ramirez	
Systematic and Cost Overview of Freeze Desalination utilizing Thermoacoustic Technology	437
U. Ali, H. Zhang, I. Janajreh	
Environmental monitoring of the Balos lagoon in Western Crete for sustainable tourism development	443
M. Lilli, G. Skiniti, N. Nikolaidis, T. Tsoutsos	
Management implications in a peri-urban river under multiple stressors	448
C. Ntislidou, V. Papaevangelou, D. Latinopoulos, S. Ntougias, P. Melidis, C. Akratos, I. Kagalou	
Development and evaluation of magnetic tea waste based adsorbent materials for removal of cadmium from wastewater	454
M. Ervine, O. Jaiyeola, C. Mangwandi	

Highly efficient removal of cadmium from waste water using eco-friendly and cost-effective aluminophosphate as adsorbents	459
O. Jaiyeola, A. Hamza, C. Mangwandi	
Influence of grain size distribution of compost from urban greenery on the distribution of microplastics and their leachability	463
H. Raclavska, J. Ruzickova, M. Safar, D. Juchelkova, B. Svedova, M. Kucbel, P. Kantor, H. Brtkova, K. Raclavsky	
Water quality analysis using physicochemical parameters and estimation of pesticides in water from various sources of Tirupati, Andhra Pradesh, India	469
S. Konda, M. Malleswari, B. Nikitha	
Theoretical investigation of halloysite as potential sorbent for pharmaceutical wastewaters	477
E. Gianni, E. Scholtzova	
Kinetic Study of Transesterification of Waste Cooking Oil Under Ultrasound	483
S. Savvopoulos, H. Hatzikirou, I. Janajreh	
Critical insights to drive sustainable water management in process industries	489
E. Karkou, N. Savvakis, G. Arampatzis	
Development of a greenhouse and screw conveyor solar driers for the treatment of faecal sludge from on-site sanitation facilities	495
S. Septein, P. Naidoo, A. Ramlucken, A. Ganapathie, Y. Pather, A. Singh, J. Pocock, F. Inambao, C. McGregor	
Solar Cell Elements Based on Graphene-Porphyrin Nanocomposites	501
G. Gyulkhandanyan, P. Gikas, G. Shmavonyan	
Synthesis and Study of starch/CeO ₂ Nanoparticle Composite Material for Removal of Hexavalent Chromium from Synthetic Wastewater Solutions.....	507
O. Jaiyeola and C. Mangwandi	
Nutmeg seed shell-based silver nanoparticle/PVA composite for the synthesis of antimicrobial food packaging films	513
T. Thomas, A.K. Thalla	
Production of Phase Change Material from Waste Low Density Polyethylene for Thermal Energy Storage Applications	519

H. Akgun, A. Ozkan, Z. Gunkaya, M. Banar

Effect on the thermal sensation of outdoor users due to the age of the granite blocks used in the coating of public areas.....525

K. Stefanopoulos, N. Lianos, D. Polychronopoulos, S. Zoras

Improving Groundwater Quality Using Hybrid Constructed Wetland in a Coastal Environment in Sub-Saharan Africa531

R. N. Okparanma, V. O. Ahiakwo

Agro-food waste re-valorization through solid-state fermentation for hydrolytic enzymes production538

J.D. Sosa-Martinez, J. Montanez, J.C. Contreras, S. Gadi, L. Morales

Photoprotection of Cationic Porphyrins and Their Non-Covalent Complexes for Effective Photodynamic Therapy of Tumors.....544

L. Mkrtchyan, A. Zakoyan, T. Seferyan, P. Gikas, G. Shmavonyan, G. Gyulkhandanyan

Influence of anthropogenic factors on pollution of arable soils and changes in the activity of enzymes in them550

A. Sukiasyan, Armen Kirakosyan, S. Kroyan, P. Gikas

Beneficiation of Coal Ash for Rare Earth Elements Enrichment.....556

A. Tsachouridis, N. Kiratzis

Crocin as an eco-friendly corrosion inhibitor for aluminum alloys in NaCl solution.....562

P. Pantazopoulou, S. Theohari, S. Kalogeropoulou

Investigation of the processes occurring in water of acid mine drainage during their exposure.....568

S. Hayrapetyan, M. Chobanyan, V. Hovhannisyan, A. Kirakosyan, A. Sukiasyan, P. Gikas

Biodiesel production, properties and sustainability from the biomass of *Chlorella sorokiniana* grown heterotrophically with glycerol and anaerobic digestate574

D. Kasiteropoulou, G. Papapolymerou, A. Kokkalis, M. Metsoviti, X. Spiliotis, A. Mpesios

Heterotrophic growth of *Chlorella sorokiniana* with glycerol and anaerobic digestate: carbon uptake rate and phenolic content.....580

D. Kasiteropoulou, G. Papapolymerou, D. Ladas, A. Mpesios, M. Metsoviti

Mixotrophic cultivation of <i>Microchloropsis gaditana</i>	586
G. Papapolymerou, N. Katsoulas, I. Karapanagiotidis, M. Metsoviti	
Energetic potential evaluation of medical wastes for using as solid recovered fuels	591
D. Torres, M. Fonseca Almeida, S.C. Pinho	
CONTACT INFO	595



ADSORPTION PROCESSES (PART I)



Three-Dimensional Electrochemical Process Using Regranulated Cork Granules for the Removal of Trazodone and Sulfamethoxazole from Water

P. Remor^{1,2,3}, S.A. Figueiredo³, V.J.P. Vilar^{1,2}, C. Soares³, L. Correia-Sá³ and C. Delerue-Matos³

¹LSRE-LCM - Laboratory of Separation and Reaction Engineering – Laboratory of Catalysis and Materials, Faculty of Engineering, University of Porto, Rua Dr. Roberto Frias, Porto, Portugal.

²ALICE - Associate Laboratory in Chemical Engineering, Faculty of Engineering, University of Porto, Rua Dr. Roberto Frias, Porto, Portugal.

³Associate Laboratory REQUIMTE/LAQV, Higher Institute of Engineering of Porto (ISEP), Porto, Portugal
Corresponding author email: saf@isep.ipp.pt

keywords: *biosorption; advanced oxidation process; sulfamethoxazole; trazodone; wastewater treatment.*

Introduction

Municipal wastewater treatment plants (WWTPs) are facing an increasing number of contaminants of emerging concern (CECs), such as pharmaceuticals, chemicals used in agriculture and industry and personal care products, which represent a threat to human health. The release of CECs from WWTPs into the environment has not yet been regulated, except for Switzerland. The use of advanced treatment technologies may enhance the removal of CECs and thus minimize the spread of these contaminants into the environment.

Adsorption is an effective treatment technology widely used to remove CECs from waters. Activated carbons are common adsorbents that efficiently remove a broad spectrum of CECs; however, a circular economy encourages using more sustainable and cost-effective materials (Fernandez-Sanroman et al., 2020).

Cork, the outside bark of the cork oak tree (*Quercus suber* L.), 100% natural and sustainable, is mainly used for wine stoppers production. A large amount of cork by-products (CBPs) are generated during cork stoppers production, which are used to produce cork/rubber composites, agglomerates for wall and floor coverings, and sustainable sorbents for oil spills clean up.

Additionally, electrochemical advanced oxidation processes have been gaining interest in recent years, namely the three-dimensional (3D) processes. In this case, a third electrode in the form of particles is introduced, which act both as microelectrodes and increase the specific surface area, decreasing the distance of mass transfer and consequently improving the process's efficiency (Correia-sá et al., 2021).

In this context, this work aims to evaluate and compare the use of regranulated cork granules (RGC) and a commercial activated carbon (SARATECH[®]) as particulate electrodes in the 3D electrochemical process for the removal from water of highly consumed pharmaceuticals, trazodone (TZD) and sulfamethoxazole (SMZ), as model CECs.

Materials and methods

SMZ and TZD individual stock solutions were prepared in 50% acetonitrile and 50% methanol and stored at -10 °C. For the electrochemical experiments, a Mixed Metal Oxide (MMO) electrode (titanium-coated with RuO₂-IrO₂-TiO₂, 100×20×2 mm) was used as the anode, and stainless steel (STS) (AISI-304, austenitic grade, 100×20×2 mm) was used as the cathode. SMZ and TZD concentrations were measured in HPLC equipment (Shimadzu Corporation, Kyoto, Japan).

RGC granules (1.0-2.0 mm) were used as third electrode, provided by Corticeira Amorim (Portugal). The production of RGC granules includes the thermal treatment of raw cork granules with water vapor at 380 °C. Before usage, the RGC was dried overnight in an oven at 60 °C. The polymer-based spherical activated carbon, SARATECH[®] reference 102282, was supplied by Blücher (Germany).

The 2D electrochemical experiments were performed in an acrylic cell reactor (2x15x8 cm) with a volume capacity of 240 mL. The electrodes were placed at 7.50 cm from each other. A volume of 150 mL of an aqueous solution with 10 mg L⁻¹ of SMZ and TZD, 0.02 M NaCl (electrolyte) and with the initial pH corrected to 7, was used in the batch experiments. An airflow of 3000 cm³ air min⁻¹ was supplied to the system. The current intensity was maintained constant at 0.1 A. In the 3D experiments, the same conditions described for the 2D process were applied. In addition, 30 mg of the sorbents SARATECH[®] activated carbon



or RGC was added between the electrodes. Aliquots of the solution contained in the reactor cell were taken during the experiments (0-10 min) and filtered with a microfilter (PTFE 0.45 μm) before being injected into the HPLC. For both 2D and 3D processes, the experiments were performed in duplicate.

Results and discussion

Figure 1a shows a faster removal of TZD for the 3D electrochemical process in the presence of RGC granules. However, after 4 minutes of reaction time, all the electrochemical processes tested were able to achieve the complete removal of TZD (below the detection limit of the analytical m

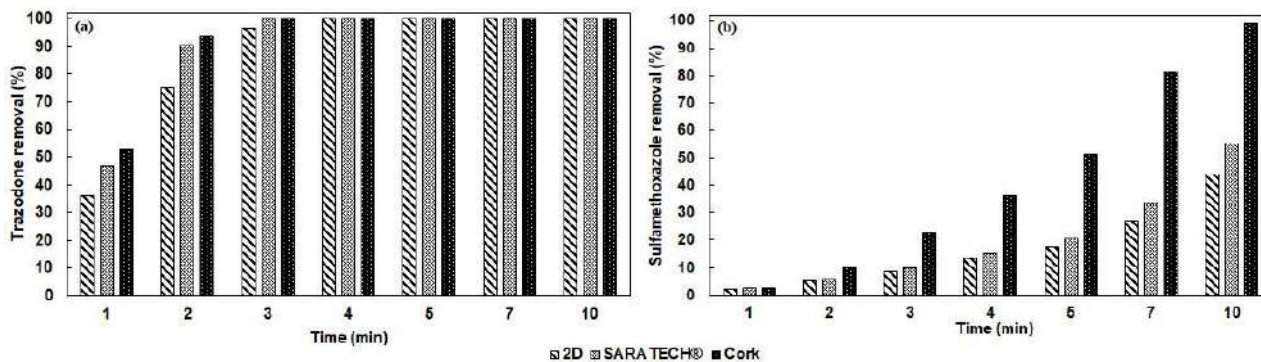


Figure 1. (a) TZD and (b) SMZ removal as a function of time in 3D (Saratech and regranulated cork granules) and 2D electrochemical processes.

For SMZ, the 2D and 3D electrochemical processes showed reaction rates at least ten times lower than those observed for TZD. The 3D electrochemical process with RGC showed the highest removal rate, 3.0 and 2.8 times higher than 2D and 3D activated carbon processes, respectively, leading to its complete removal (below the detection limit of the analytical method) after 10 min of reaction time.

The pH has a significant effect on the speciation of the pollutant species, which can directly influence its removal. During the experiments, the pH showed a slight decrease from 7.0 to around 6.5. The TZD ($\text{pK}_a = 6.7$; $\log K_{OW} = 3.21$) is a weak base with a neutral charge at pH 7.0. The SMZ ($\text{pK}_{a1} = 1.8$ and $\text{pK}_{a2} = 5.6$; $\log K_{OW} = 0.89$) is an amphoteric molecule where its protonation occurs in the amine group and ionization in the sulphonamide group. In the pH working range, the SMZ mainly exists in the anionic form as SMZ^- and the TRZ neutral species. The RGC has a pH at the point of zero charge (pHPZC) in the acid range, presenting its surface negatively charged, which can contribute to the better affinity of RGC towards the neutral TRZ species than the anionic SMZ species, moreover, the TRZ also presents a much higher hydrophobicity than SMX.

Conclusions

The 3D electrochemical process using RGC granules, a byproduct from the cork industry, as a third electrode showed a good performance for the removal of the pharmaceuticals TZD and SMZ from aqueous solutions. For TZD, the 2D and 3D electrochemical processes showed reaction rates at least 10 times higher than for SMZ, which is attributed to a better affinity of TRZ (pH working range) and also to its higher hydrophobicity. The 3D electrochemical process using RGC particles presented higher reaction rates than the 2D and 3D processes, with activated carbon, especially for SMZ, due to its ability to establish chemical interactions.

Acknowledgments: This work was financially supported by i) Associate Laboratory for Green Chemistry-LAQUV, supported by national funds through FCT/MCTES (UIDB/50006/2020); ii) Project OXI-e3D (POCI-01-0247-FEDER-039882), supported by the Program Portugal 2020, and cofunded by FEDER through POCI and iii) LA/P/0045/2020 (ALiCE), UIDB/50020/2020 and UIDP/50020/2020 (LSRE-LCM), supported by national funds through FCT/MCTES (PIDDAC). P. Remor acknowledges FCT for the Ph.D. grant (SFRH/BD/07543/2020).

References

- Fernandez-Sanroman, A., Acevedo-García, V., Pazos, M., Sanromán, M. A., Rosales, E., 2020. Removal of sulfamethoxazole and methylparaben using hydrocolloid and fiber industry wastes: Comparison with biochar and laccase-biocomposite. *J. of Cleaner Production*, 271, 122436.
- Correia-sá, L., Soares, C., Freitas, O. M., Moreira, M. M., Nouws, H.P.A., Correia, M., Paíga, P., 2021. A three-dimensional electrochemical process for the removal of carbamazepine. *Applied Sciences* 11, 6432.



Activated hydrochar from grape stalk for methylene blue adsorption

M. Gimenez¹ and C. Deiana¹

¹Instituto de Ingeniería Química/CONICET, Universidad Nacional de San Juan, San Juan, Argentina

Corresponding author email: mgimenez@unsj.edu.ar

keywords: grape stalk; hydrochar; activated carbon; adsorption.

Introduction

Viticulture is one of the main productive activities in the Cuyo Region of the Argentine Republic. Grapes are used for the production of wines, must and raisin. Around 2.6 million tons of this fruit are destined for the production of wines and musts. In these processes, wastes are generated that is not properly used, generating environmental problems. Among them is the grape stalk, which represents 6% of the total mass of processed grapes. Currently, residual materials from industrial processes are considered raw materials to generate value-added products that provide economic and environmental benefits to companies. Among the processes that are applied for these transformations are the hydrothermal carbonization and activation. Hydrochar is product obtained through hydrothermal carbonization, a process with advantages over conventional pyrolysis (Wang et al., 2018). This involves heating the biomass, between 170 and 300°C, in an oxygen-free environment, with the presence of subcritical water and autogenous pressure between 2-10 MPa (Gimenez et al., 2020). It is used in a variety of applications such as contaminant remediation, fuel, and precursors to highly porous materials, such as activated carbon, used in both energy and decontamination applications

In this work, the results of the application of hydrothermal carbonization to grape stalks, subsequent activation of hydrochar in order to obtain a highly porous material to be used as adsorbent in the removal of methylene blue, a dye generally present effluents from the textile industry. In this way, value is added to this abundant residue and contributes to the solution of environmental problems of the wine industry.

Materials and methods

Hydrothermal carbonization test was carried out in a Parr reactor, with a capacity of 1 L, heated by means of an electric furnace with temperature controller. A ratio of 0.1 grams of residual biomass/ml of distilled water was used, once the hydrocarbonization test temperature of 240 °C was reached, it was kept constant for a period of 6 h. Then the reactor was cooled to room temperature and the resulting solid-liquid mixture was filtered. Hydrochar obtained were dried at 95 °C for 24 h.

KOH Activation: Impregnation ratio, defined as activating agent mass with respect to mass of carbonaceous material, was set at a value of 2. The sample of hydrochar was impregnated in a solution at 80% w/v KOH and placed in an oven at 100°C for 24 hours. Subsequently, impregnated material was activated to 800°C for 1 h, in the absence of oxygen inside a muffle with controlled heating. The discharge product was neutralized with a 0.1M HCl solution, washed with distilled water until reaching a pH between 6 and 7 and was dried in an oven. Activated carbons obtained were denominated as SKOH.

H₂PO₃ Activation: An impregnation ratio of 0.39 was used for activation the hydrochar with phosphoric acid. Sample was impregnated with acid and kept in contact with this reagent at 110°C for 24 h until dry. Then, a heat treatment at 500°C was carried out in the absence of oxygen for 1 h. Product obtained was washed with distilled water until neutral and dried. The activated carbons were denominated as SHPO.

Material Characterization: Proximate analysis of raw biomass and hydrochar (moisture, ash, volatile matter and fixed carbon) was performed by following ASTM standards. The surfaces morphological characteristics were analyzed by scanning electron microscopy (SEM) in a JEOL JSM-6610LV (MEB) equipment. Surface functional groups were determined by Fourier transform infrared (FTIR) spectroscopy, using a Bruker Vertex 70 equipment. Textural properties of the materials were determined by adsorption-desorption isotherms of nitrogen at 77 K in a Micromeritics, ASAP 2000 Model equipment.

Methylene blue (MB) kinetic adsorption assays were performed to obtain the minimum contact time. Adsorbent samples of 30 mg were placed in sealed flasks with 30 mL of 300 mg L⁻¹ solution of MB. The suspensions were stirred at 120 rpm in a thermostatic bath at 25 °C, varying the contact time for each flask.



Results and discussion

Table 1 shows the proximate analysis of the grape stalk and the hydrochar obtained. The results indicate an increase carbon fraction fixed in the hydrochar and the decrease of about 50% of the ash.

Table 1. Proximate Analysis (%)

Material	Moisture	Ash	Volatile matter	Fixed carbon
Stalk	20.2	12.5	53.5	13.9
Hydrochar	4.97	5.1	48.87	41.06

The changes in the morphology of the grape stalk due to the hydrothermal carbonization were evaluated by SEM (figure 1). Images of the grape stalk show a cellular structure typical of lignocellulosic materials. Substantial changes in the surface morphology of hydrochar are revealed in SEM images. Numerous sphere-shaped microparticles can be observed on the surface of the hydrochar, these probably have their origin in the decomposition of cellulose during hydrothermal carbonization. In the case of lignin, due to its greater chemical stability, only partial degradation occurs and the original skeleton of the particles is mainly preserved.

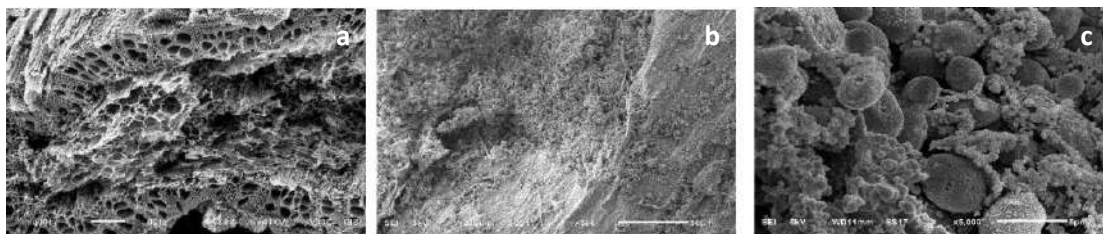


Figure 1. SEM images of the grape stalk (a) and hydrochar (b and c).

FTIR spectra of grape stalk and hydrochar show that the shape and location of spectral peaks are maintained when hydrothermal carbonization is applied, although the lower intensity for the hydrochar. The presence of chemical groups on the surface confirms the typical characteristic of the hydrochar that differentiates it from the chars obtained by conventional pyrolysis.

The determination of the BET surface area reveals an incipient development of porosity in the hydrochar, 26 m²/g, in the case of activated carbons high values were obtained, 1630 m²/g and 1880 m²/g for the SKOH and SHPO samples, respectively.

In order to evaluate the adsorbent properties of the ACs obtained, kinetic tests were carried out, using methylene blue as adsorbate. Once equilibrium is reached, the ACs remove more than 96% of the initial dye concentration. In the present study, the most used kinetic models, pseudo first order and pseudo second order models, were applied for the batch kinetic data in linear way. The results show for the SKOH sample a better fit of the pseudo second order model to the experimental data, on the contrary, for the SHPO activated carbon, the pseudo first order model presents a more appropriate fit.

Conclusions

This study demonstrated the viability of ACs prepared using KOH and HPO activated hydrochar produced from grape stalk for MB dye from aqueous solution. This new route of AC from hydrochar may open a window for waste treatment.

References

- Gimenez, M., Rodríguez, M., Montoro, L., Sardella, F, Rodríguez-Gutierrez, G., Monetta, P, Deiana, C. 2020. Two phase olive mill waste valorization. Hydrochar production and phenols extraction by hydrothermal carbonization. *Biomass and Bioenergy* 143, 105875.
- Wang, T., Zhai, Y., Zhu, Y., Li, C., Zeng, G., 2018. A review of the hydrothermal carbonization of biomass waste for hydrochar formation: Process conditions, fundamentals, and physicochemical properties. *Renew Sust Energ Rev* 90, 223.



NO₃⁻ -N removal from groundwater using thermally treated palygorskite in fixed bed reactor

C. V. Lazaratou¹, S. D. Panagopoulos², D. V. Vayenas^{2,3} and D. Papoulis¹

¹Department of Geology, University of Patras, Patras, Greece

²Department of Chemical Engineering, University of Patras, Patras, Greece

³Institute of Chemical Engineering Sciences, Foundation for Research and Technology Hellas (FORTH/ICE-HT), Patras, Greece

Corresponding author email: lchristie93@gmail.com

keywords: nitrates; adsorption; groundwater treatment; palygorskite.

Introduction

Nitrate is one of the major inorganic pollutants in groundwater systems, mostly derived from the exceeded application of N- fertilizers which leach in aquifers after irrigations and rainfalls (Lu et al., 2019). High concentration levels of NO₃⁻ -N (> 11.3 mg/L) can contribute to eutrophication and infants' disease methemoglobinemia, rendering their removal crucial (WHO and Regional, 2002). Palygorskite is a fibrous clay mineral, widely used as adsorbent of cationic pollutants. After thermal treatment (T-Pal), its pore size is getting larger, whereas more OH⁻ groups can be revealed, promoting the adsorption of voluminous anions as well (Chiari et al., 2003). Great asset on T-Pal usage, is that after its N-saturation can be exploited as 'green' fertilizer in cultivations (Lazaratou et al., 2021).

Materials and methods

For the adsorption experiments performed on fixed – bed reactors, Plexiglas tubes (columns) of laboratory scale were used. The tubes were 40.0 cm in height and 4.0 cm internal diameter, with 450 ml operational volume, equipped with four sampling valves at various heights. The column was filled with 287 g of T-Pal sample at 1.4 – 2.34 mm grain size. For the removal of NO₃⁻ -N, real groundwater sample from Neo Vouprasio (Achaia) was used with initial NO₃⁻ -N concentration 25 mg/L. The effect of continuous flow rate (15, 25, 35 and 50 ml/min) and column height were considered. Various samples were selected at various time intervals till the saturation of T-Pal was achieved and the breakthrough curve could be formed. Each sample was centrifuged at 5.500 rpm for 3 min and filtrated through Whatman filters (0.45 μm) to remove the finest suspended. The final concentration of each time interval was measured at UV-Vis spectrophotometer at 200 nm using quartz cuvette (APHA, 1998). From the data obtained, the maximum removal efficiency, adsorption capacity and liters of purified water were determined. Also, the data were applied to Clark, Yoon- Nelson and Thomas kinetic models.

Results and discussion

For the purification of Neo Vouprasio groundwater, the effect of four different continuous flow rates (10 ml/min, 25 ml/min, 35 ml/min and 50 ml/min), on T-Pal removal efficiency was examined (Figure 1). With the flow rate increase, the removal curve becomes steeper, since the rapid saturation of T-Pal is achieved, especially for 50 ml/min flow rate where curve reached the breakthrough point from almost 45 min. The flow rates of 25 ml/min and 35 ml/min presented a similar pattern, since for the T-Pal saturation 300 min were demanded, whereas the removal rate was quite common after the 30 min. At the flow rate of 15 ml/min the breakthrough curve was completed in 500 min instead of 300 min, nevertheless, the nitrate removal rate had no significant differences with 25 ml/min at the first 20 min that the effluent nitrate concentration was below the permeable limit. Concerning the column height effect (or mass effect), it was indicated that the more adsorbent mass there is, the more removal can be achieved, since for the same flow rate (35 ml/l) 1.33 L instead of 0.315 L of effluent groundwater are purified (Vw) from 287 g and 861 g of T-Pal respectively (Table 1). From the application of kinetic models very high correlation coefficients (R^2) were obtained ($R^2 > 0.91$), for all the examined flow rates. Moreover, Yoon-Nelson and Thomas models found to better describe the procedure, due to the higher R^2 value of 0.96072 instead of the 0.96068 obtained from the Clark model at 25 ml/min flow rate, and at the other examined flow rates as well. The Yoon -Nelson model is associated with Langmuir isotherm which, was indicated the most appropriate for NO₃⁻ -N interactions with T-Pal at previous batch studies as well, verifying the monolayered nitrate adsorption on T-Pal (Lazaratou et al., 2021).



Table 1. Operational parameters for NO₃⁻-N adsorption on T-Pal and liters of purified water (V_w).

Q (mL /min)	m (g _{T-Pal})	V _w (L)
15	287	0.360
25	287	0.525
35	287	0.315
50	287	0.400
35	861	1.330

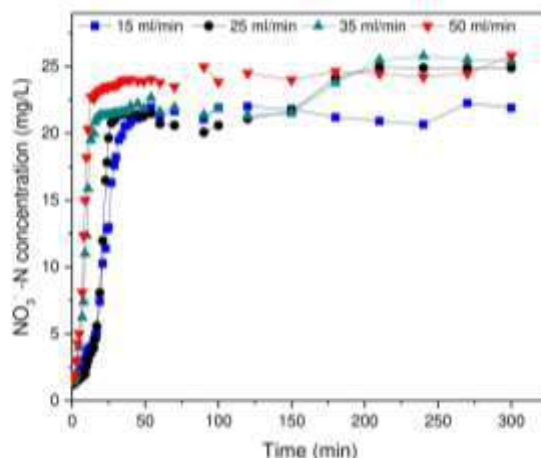


Figure 1. Effect of 15, 25, 35 and 50 ml/min flow rates for 25 mg NO₃⁻-N /L removal.

Conclusions

Summarizing, moderate flow rates of 25-35 ml/min found to be efficient for NO₃⁻-N removal from groundwater on T-Pal within 30 min, rendering this adsorption rapid, which could be a promising alternative for pre- treatment of nitrate polluted groundwaters.

References

- APHA, AWWA, WPCF.1998. Standard Methods for the Examination of Water and Wastewater, 20th edn. Washington, DC.
- WHO, W.H., Regional, O. 2002. Water and health in Europe. A joint report from the European Environment Agency and the WHO Regional Office for Europe. In: WHO Reg Publ Eur Ser 7. Vol. III–XXIII. pp. 1–222.
- Chiari, G.; Giustetto, R.; Ricchiardi, G. 2003. Crystal Structure Refinements of Palygorskite and Maya Blue from Molecular Modelling and Powder Synchrotron Diffraction. Eur. J. Mineral 2003, 15, 21–33.
- Lazaratou, C.V. Triantaphyllidou, I.E., Spyridonos, I., Pantelidis, I., Kakogiannis, G., Vayenas, D.V., Papoulis, D. 2021. NO₃⁻-N Removal from Water Using Raw and Modified Fibrous Clay Minerals and Their Potential Application as Nitrogen Fertilizers in Hydroponic Lettuce Cultivations. Environ. Tech. Innovation, 24, 102021
- Lu, J., Bai, Z., Velthof, G.L., Wu, Z., Chadwick, D., Ma, L. 2019. Accumulation and leaching of nitrate in soils in wheat-maize production in China. Agric. Water Manag., 212, 407–415.



Biochar based sorbents to remove vanadium ions from aqueous media

J. Bąk¹ and D. Kołodzyńska¹

¹Department of Inorganic Chemistry, Institute of Chemical Sciences, Faculty of Chemistry, Maria Curie-Skłodowska University, Lublin, Poland

Corresponding author email: justyna.bak@mail.umcs.pl

keywords: vanadium ions; removal; biochar; hydroxyapatite; aqueous media.

Introduction

Vanadium is an element of the fifth group which occurs in +3, +4 and +5 oxidation states in aqueous media and the +5 oxidation state is the most stable in oxic solution. Vanadium has been recognized as potentially dangerous pollution in the same class as lead, mercury and arsenic. Maximum concentrations of this element in drinking water must be within the range from about 0.2 to 100 µg/L with typical values ranging between 1 to 6 µg/L.

Because of ease dissolution of vanadium at high temperatures, this metal is added to the steel to improve resistance to cracking and abrasion as well as increasing the harness. Additionally, vanadium is commonly used in many others industries including mining, oil refinery, pigments and automobile industries. A wide application of vanadium compounds can produce huge amounts of wastes which are discharged into the environmental waters. Especially toxic for humans health is vanadium in the +5 oxidation state which can cause damage to the respiratory, gastrointestinal and central nervous system as well as increase the risk of lung cancer. Therefore, removal of vanadium (V) from industrial wastes issignificant importance for environmental protection.

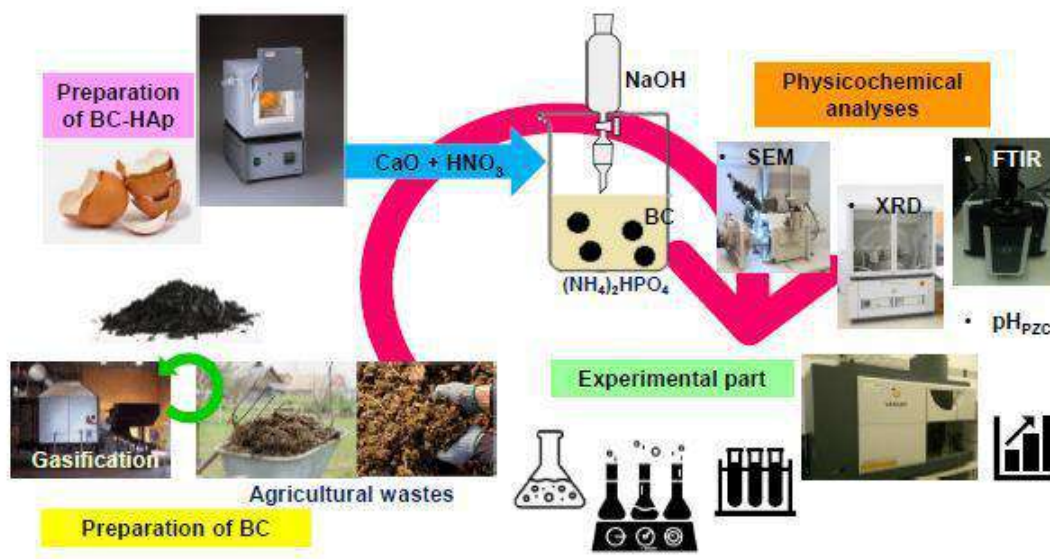
In order to remove V(V) from aqueous solutions, various methods such as chemical precipitation, ion exchange, membrane filtration, biosorption and adsorption were used. Adsorption proved to be the most effective method because of its low cost, higher uptake capacity of vanadium (V) as well as faster and easier recovery which makes the search for new sorbents of significant importance.

These needs are met by sorbents based on biochar. Biochar is the so-called charcoal produced by heating biomass in an oxygen-restricted environment. The production of biochar takes place with the use of broadly understood biomass, both primary biomass of bioenergy importance and waste biomass. Biochar is characterized by the presence of functional groups, porous structure, thermal stability, high specific surface area and high carbon content. The availability of biochar and the ease of modifying their surface encourage the use of new, natural ingredients for this purpose. Hydroxyapatite is an example of a modifier used in the research.

Synthetic hydroxyapatite (HAp) with the formula $\text{Ca}_{10}(\text{PO}_4)_6(\text{OH})_2$ is considered a natural, non-toxic, environmentally friendly material and the main inorganic component of bones and teeth. HAp plays a unique role in the regeneration of damaged bone due to its bioactivity, which makes it used as an orthopedic and dental implant. HAp has been extensively researched for biomedical applications in the form of powders, composites and even coatings. The well-defined crystal structure of HAp, which gives it the ability of ion exchange, low solubility in water, thermal stability, porosity and high adsorption affinity to many pollutants, make it one of the most effective materials for removing cationic and anionic impurities from polluted water.

Materials and methods

The research on the efficiency of sorption of vanadate (V) ions from aqueous media was carried out using the static method in 100 mL conical flasks by adding 0.1 g of sorbent and shaking with 50 mL of the solution at 180 rpm and 293 K. The first step in determining the process conditions was to examine the effect of pH in the range from 2 to 6. In the next step, the effect of the phase contact time was determined from 1 to 240 minutes and the concentration of the initial solution from 10 to 100 mg/L was determined. The scheme of obtaining hydroxyapatite modified biochar is presented below.



Results and discussion

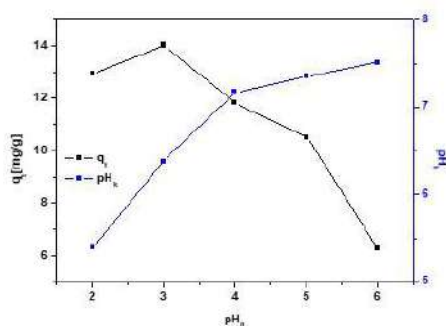


Figure 1. Dependence of the equilibrium capacity on the initial pH for the sorption of V(V) ions on BC-HAp (t 240 min, C_0 50 mg/L, 180 rpm, 293 K).

On the basis of preliminary studies, it was found that the highest q_e values were obtained for pH 3. Thus, this values was found for further research.

According to the research on the effect of the phase contact time and the initial concentration of the solution on the sorption process, it was shown that the amount of adsorbed increases with the increase of the interaction time and concentration of the solution until it reaches a plateau. At lower concentrations, it reaches equilibrium faster. After 240 minutes. the amount of adsorbed ions is: 4.69; 8.82; 13.68 and 27.45 mg/g for the concentrations of 10, 25, 50 and 100 mg/L, respectively.

Conclusions

The obtained satisfactory amounts of adsorbed vanadate (V) ions on the hydroxyapatite modified biochar confirm that this sorbent can be used for water and wastewater treatment.

References

- Gomes, H.I., Jones, A., Rogerson, M., Greenway, G.M., Lisbona, D.F., Burke, I.T., Mayes, W.M., 2017. Removal and recovery of vanadium from alkaline steel slag leachates with anion exchange resins, *J. Environ. Manage.*, 187, 384-392.
- Ahmad, M., Rajapaksha, A.U., Lim, J.E., Zhang, M., Bolan, N., Mohan, D., Vithanage, M., Lee, S.S., Ok, Y.S., 2014. Biochar as a sorbent for contaminant management in soil and water: a review, *Chemosphere*, 99, 19-33.
- Dai, L., Fan, L., Liu, Y., Ruan, R., Wang, Y., Zhou, Y., Zhao, Y., Yu, Z., 2019. Catalytic fast pyrolysis of torrefied corn cob to aromatic hydrocarbons over Ni-modified hierarchical ZSM-5 catalyst, *Bioresour. Technol.*, 272, 407-414.
- Oun, A.A., Kamal, K.H., Farroh, K., Ali, E.F., Hassan, M.A., 2021. Development of fast and high-efficiency sponge-gourd fibers (*Luffa cylindrica*)/hydroxyapatite composites for removal of lead and methylene blue, *Arab. J. Chem.*, 14, 103281.



Evaluation of biochar and activated carbons produced from different biomass feedstock for use as an adsorbent for pharmaceutical compounds removal in a decentralized wastewater treatment plant system

R.T. Morake¹, S. Septein¹, B.S. Martincigh² and D. Lokhat³

¹WASH R&D Centre, University of KwaZulu-Natal, Durban, South Africa

²Chemistry Discipline, University of KwaZulu- Natal, Durban, South Africa

³Chemical Engineering Discipline, University of KwaZulu- Natal, Durban, South Africa

Corresponding author email: 216005246@stu.ukzn.ac.za

keywords: *biochar; activated carbon; pyrolysis.*

Introduction

Water contamination caused by compounds of emerging concern, such as pharmaceuticals compounds, serves as an obstacle for water reuse, which amplifies the water crisis in South Africa. Pharmaceuticals are designed to interact with living systems by timelessly producing a pharmacological response at trace levels making detection and monitoring difficult. Pharmaceutical compounds pose an important risk to the environment because the compounds are unregulated and commonly found at ultra-trace levels in the environment, making removal in wastewater treatment plants difficult (Wang & Wang, 2016). Pharmaceuticals are stable and not easily degradable thus may exist in the environment for a longer period leading to pseudo-persistence (Bu et al., 2016). These pollutants find their way into the environment through various pathways including treated and untreated wastewater. There have been reports globally that conventional wastewater treatment systems (WWTPs) are not successful in the complete removal of these compounds during the treatment process, this further leads to contamination of surface water (Madikizela et al., 2017). As a result, the search and development of low-cost materials for the removal of pharmaceuticals in wastewater treatment have recently gained interest. This study aims to evaluate varying biochar and activated carbon produced from different feedstock for use as an adsorbent in wastewater treatment plants, with the aim to offer a solution for pharmaceutical removal. These carbon materials are intended to be used in a demonstration decentralized wastewater treatment plant systems (DEWATS) based in Durban Newlands-Mashu which receives effluents from 83 households.

Materials and methods

In this study, biochar was produced from three renewable feedstock namely eucalyptus, black wattle, and horse manure through the process of pyrolysis. The biochar was further chemically activated and will be used for the removal of pharmaceuticals from wastewater through the mechanism of adsorption. The biomass was pyrolyzed to produce the biochar at varying temperatures of 350 °C and 700 °C. Each biochar was studied in three different forms, pristine biochar (PB), modified by potassium hydroxide (AC-KOH) and modified by phosphoric acid (AC- H₃PO₄). Batch adsorption tests were carried out using tartrazine dye as a proxy to determine the effect of initial concentration on the adsorption process. To understand the physicochemical properties that are relevant for application as adsorbent material, the biochar and activated carbon samples will be characterized by Brunauer-Emmet-Teller surface area analysis (BET), Fourier transform infrared spectroscopy (FT-IR), scanning electron microscopy (SEM), transmission electron microscopy (TEM), thermogravimetric analysis (TGA), point of zero charge (pHpzc) and Boehm titration.

Results and discussion

The biochar yield was dependent on the pyrolysis temperature and feedstock type. The biochar yield was seen to decrease at 700 °C compared to 350 °C for all three feedstocks. Horse manure generated a lower biochar yield compared to Black wattle and Eucalyptus. The high biochar yield can be linked to the higher carbon content found in the wood material. The general trend indicates that material containing higher lignin content generates a higher biochar yield. Chemical activation of carbon led to a great mass loss of biochar for all the different feedstocks.



For the effect of feedstock type and the pyrolysis temperature on the removal of tartrazine dye. Both feedstock type and pyrolysis temperature indicated a strong influence on the adsorption efficiency. The surface area and pore size increased proportionally with the pyrolysis temperature. Furthermore, an increase in adsorption efficiency was witnessed with an increase in pyrolysis temperature irrespective of the type of feedstock. The Activated carbon offered a higher adsorption efficiency compared to the biochar in all three feedstocks. Activation can thus be utilized to generate biochar with improved physicochemical and adsorption properties. The characterization test results supported this as biochar produced at higher temperatures showed more distinct pores and a greater surface area. Chemical activation increased the pore size and surface area of the biochar, leading to an increase of adsorption sites, which facilitates more adsorption to occur.

Conclusions

The present study shows that biochar and activated carbon generated from a low-cost material, Black wattle, horse manure, and Eucalyptus could result efficient in the removal of pharmaceuticals from wastewater. The biochar properties are highly dependent on the feedstock type and pyrolysis temperature. The highest % yield was observed at 350 °C for all feedstocks. Chemical activation and pyrolysis temperature enhance the chemical and physical properties of biochar leading to better adsorption capacity

Acknowledgements: The authors would like to thank the Swedish Research Council for the funding, the collaborators from this project (Umea University, University Mohammed V, Polytechnic University of Mohamed VI), and the administrative and technical staff from the WASH R&D Centre (in particular: Thabiso Zikalala, Kerry Philp, Nombuso Bridget Mtshali, Lungile Ndlela).

References

- Bu, Q., Shi, X., Yu, G., Huang, J., & Wang, B. (2016). Assessing the persistence of pharmaceuticals in the aquatic environment: Challenges and needs. *Emerging Contaminants*, 2(3), 145–147. <https://doi.org/10.1016/J.EMCON.2016.05.003>
- Madikizela, L. M., Tavengwa, N. T., & Chimuka, L. (2017). Status of pharmaceuticals in African water bodies: Occurrence, removal and analytical methods. In *Journal of Environmental Management* (Vol. 193, pp. 211–220). Academic Press. <https://doi.org/10.1016/j.jenvman.2017.02.022>
- Wang, J., & Wang, S. (2016). Removal of pharmaceuticals and personal care products (PPCPs) from wastewater: A review. *Journal of Environmental Management*, 182, 620–640. <https://doi.org/10.1016/J.JENVMAN.2016.07.049>



SUST
ENG
2022



CIRCULAR ECONOMY/RECYCLING & REUSE



Is circular economy the key to halting biodiversity loss?

A.E. Assogbadjo¹ and H.G.G. Avakoudjo¹

¹Laboratory of Applied Ecology, Faculty of Agronomic Sciences, University of Abomey-Calavi, Republic of Benin

Corresponding author email: assogbadjo@gmail.com

keywords: *circular economy; biodiversity loss; waste recycling; sustainable development.*

Introduction

World population is projected to rise from 7.7 billion to 9.7 billion by 2050. Moreover, an estimated 2°C rise in global temperature by the end of the century may lead to the extinction of a third of all life on the planet. In such context, there is more advocacy to shift from linear to circular economy by creating industrial systems that are restorative by design ensuring sustainable development (Morseletto 2020) by restoring natural habitats and conserving biodiversity. This will enable to build a resilient, low carbon and sustainable economy.

Materials and methods

In this study online and offline resources (research paper, video, press article, web site, book, report, factsheet) were examined in addition to the field visits to understand how circular economy model can improve the effort of biodiversity conservation in the world. Case studies and success stories from West Africa were used to highlight how the production system based on circularity works.

Results and discussion

The traditional economy system (linear) is characterized by produce, consume, throwaway while circular economy is rather characterized by repair reuse and recycle. Circular economy is a model of economic, social and environmental production and consumption that aims to build a sustainable society based on a circular model (ICLEI Africa 2021). Based on three principles driven by design, the model enables economies and societies in general to become more autonomous, sustainable and in tune with the issue of environmental resources. The goal is to make the economy as circular as possible, by thinking to new processes and solutions for the optimization of resources, decoupling reliance on finite resources (Ellen Macarthur Foundation 2021). Therefore, it is an industrial economy that is restorative by intention, using renewable energy, eliminating the use of toxic chemical and eradicating, or promoting reduction of waste.

Biodiversity refers to the diversity of life on earth at different levels that are genes, species, and ecosystems. Mankind gets a lot of benefit from biodiversity. Indeed, they benefit from the consumptive value (food/drink, fuel, medicine, better crop varieties, industrial material) and the non-consumptive value (recreation, education and research, traditional value) of the biodiversity. However, human population growth and many human activities present real threats to biodiversity preservation. In his wake, habitat modification / fragmentation, overexploitation of selected species, innovation by exotic species, pollution, hunting, global warming and climate change and agriculture can be mentioned. To these anthropogenic threat causes can be added the natural ones such as narrow geographical area, low population, low breeding rate and natural disasters.

Among other advantages of the circular economy its role in the protection of environment and biodiversity and that of tackling global warming and climate change can be mentioned. As of the environment and biodiversity protection this system enable: several long-term positive externalities (usage of farm waste to produce sustainable energy using biomass or the use of such remnants as fertilizer for crops); reduce reliance on harmful chemicals; increase organic and healthy crops production; enable production of cheap electricity; reduce soil degradation; sustain wildlife and their habitats; reduce overconsumption; provide more natural environment for flora and fauna to thrive; create stable businesses and jobs and increase living standards and quality of life. As sustainable model for protecting future generations, circular economy tackles global warming and climate change.



Findings showed that for circular economy integration into biodiversity conservation policies, it is important to optimize the uses of biodiversity, matter and energy and limit consumption and wastage. According to Ellen MacArthur Foundation (EMF), the key concepts about biodiversity associated with the circular economy loop are biomimicry, ecosystem service valuation, bioeconomy and renewable energy. Since nature has ability to efficiently use waste in a perfectly closed natural system (Phipps, 2019), biomimicry consists in the practice of modelling human-made designs after ecological and biological interactions observed in nature (Benyus, 1997). The ecosystem service valuation is defined through economic and social benefits to humans (MEA, 2005). These services can be ranged from cultural, regulating, supporting, to provisioning. In the EMF's representation of circular economy theory, bioeconomy essentially represents the "biological nutrients" (EMF, 2015). As of the fourth key (renewable energy) under the circular economy framework, energy should ideally be of a regenerative-renewable nature (EMF, 2015). Renewable energy represents an opportunity for society to become less dependent on fossil fuels and, in some cases, promote social and economic justices (Owusu and Asumadu-Sarkodie, 2016). Thus, for a perfect integration of the circular economy into biodiversity conservation policies, it will be necessary to work on the three areas and seven pillars of the circular economy. The first area is composed of four pillars which are: sustainable extraction/exploitation and purchasing, eco-design (products and processes), industrial and territorial ecology and functional economy. The two pillars of the second area which is consumer demand and behavior are responsible consumption (purchasing, collaborative consumption, use) and extension of the period of use (reemploy, repair, reuse). The third area is about waste management and concerns recycling of matter and organic.

Among others, practical actions to be taken to limit biodiversity loss in the frame of circular economy include production systems amelioration, plastic collection, and recycling, raising awareness about changing consumption behavior, water reuse and recycling and changing the way of thinking agriculture. Regarding the latter, an ecofriendly production model called "Songhai model" developed in Benin and spreading throughout Africa shows that the circular economy contributes to biodiversity preservation. Indeed, Songhai implements 'integrated and sustainable agriculture' with "Organic Generation" and "Total Production Zero Waste". The pillars of this model are bio-production, bioprocessing, bio-consumption, and bioenergy. The waste management system at Songhai is called: Waste to wealth. In this system, livestock by-products generated (litter and droppings) are transformed into compost for soil maintenance and food production. The water used to clean the concrete and earthen ponds where fish are raised is recycled and used to irrigate crops. Plant, animal, and fish production, residues are raw material for producing energy (bioenergy) in the form of domestic biogas used for cooking, lighting, and heating without the risk of polluting the environment or damaging eco-systems. Hence, at Songhai, environment and nature are key allies treated with respect.

Conclusions

The circular economy can be a model that can help save the planet, however, it cannot be seen in isolation. The circular model is far more complex than the linear approach and requires a global workforce that is educated and able enough to use it and improve upon the current mechanisms of the model to make it as efficient and environmentally friendly as possible. As always, the attraction of a single, simple and magical answer is a mirage, possibly nefarious; the circular economy cannot do everything, see everything, foresee everything. It can only be truly beneficial for all if those who promote it explicitly recognize its limits and work with complementary approaches, thus allowing a holistic approach to the challenges of sustainability.

References

- Benyus, 1997. *Biomimicry: Innovation inspired by nature*, New York, Morrow.
- Ellen MacArthur Foundation, 2015a. *Delivering the Circular Economy—A Toolkit for Policymakers*. Isle of Wight: Ellen MacArthur Foundation.
- Ellen MacArthur Foundation, 2021. *Towards the Circular Economy: an economic and business rationale for an accelerated transition*. p. 24. Accessed 2021-11-21.
- ICLEI Africa, 2021 *Circular development pathway*. Accessed 2021-11-21.
- Millennium Ecosystem Assessment, 2005. *Ecosystems and Human Well-being: Synthesis*.
- Morseletto, P., 2020. "Restorative and regenerative: Exploring the concepts in the circular economy". *Journal of Industrial Ecology*. 24 (4): 763–773. doi:10.1111/jiec.12987. ISSN 1530-9290. S2CID 203500060.
- Owusu, P.A. and Asumadu-Sarkodie, S., 2016 *A Review of Renewable Energy Sources, Sustainability Issues and Climate Change Mitigation*. *Cogent Engineering*, 3, 1-14.



Constructed wetlands case studies for municipal and industrial wastewater management in a circular economy

A. Stefanakis¹

¹School of Chemical and Environmental Engineering, Technical University of Crete, Chania, Greece
Corresponding author email: astefanakis@tuc.gr

keywords: *constructed wetlands; nature-based solutions; circular water economy; municipal wastewater; industrial wastewater.*

Introduction

We realize today that the unsustainable way that our societies grow, consume, and waste natural resources. While resources such as water, fossil fuel, and nutrients are becoming scarce, climate change is progressing. Sustainable development implies the need to identify tools to properly manage our water resources. However, the challenge is to understand the interconnections and synergies between technical and non-technical/social/management and economic aspects. Circular economy appears today as an alternative economic model that can guarantee the economic growth while minimizing – or ideally eliminating – the climate change impacts. It dictates that new solutions are required to deal with waste; in fact, waste is no longer considered as waste rather than as a valuable input to another process. This new approach demands new solutions that will not generate an environmental impact themselves while solving another issue.

In this context, Nature-based solutions (NBS) are widely recognized as important tools in climate action, in addressing societal challenges, protecting, and restoring ecosystems and supporting biodiversity conservation (Stefanakis et al., 2021). NBS represent an attractive toolbox for sustainable strategies that can play a key role in the implementation of the European Green Deal. The use of NBS such as the green technology of Constructed Wetlands (CW) is gaining increasing global attention and popularity. This technology typically has few mechanical parts, limited maintenance needs, limited or even no need for specialized staff, minimized use of non-renewable materials (concrete, steel etc.), design flexibility and replicability, reduced greenhouse gas emissions, minimum energy consumption, and no harmful by-products. Furthermore, the use of NBS for wastewater management enables the reuse of the treated effluents, e.g., for irrigation of crops or recycling in an industrial process, closing this way the loop of water and promoting circularity aspects and practices in the industry.

This paper presents two case studies that demonstrate the feasibility, scalability and opportunities provided by CW technology for wastewater management and reuse of different wastewater sources: municipal wastewater management in the Czech Republic and oily produced water management in Oman.

Case studies description

The first case study from the Czech Republic deals with a full-scale hybrid CW that is intermittently loaded with high volumes of moderately-polluted mixed wastewater from a hotel, a restaurant and a brewery and the sequential reuse of the treated effluent for the irrigation of various types of crops (Šereš et al., 2021). The system consists of 5 stages: (i) a septic tank, (ii) a horizontal CW (HF), (iii) a vertical CW (VF), (iv) a combined CW consisting of an unsaturated vertically-flowed part and a saturated horizontally flowed part (HVF) and (v) stabilization pond (SP). The calculated maximal treatment capacity of the system is 150 population equivalent with a maximal daily wastewater inflow of 16.5 m³/day. The system is in full operation since early 2018. In the experimental irrigation field (49 m²), two sources of water were used, i.e., fresh water from a well and treated wastewater from the CW, while the irrigated crops were tomatoes (*Solanum lycopersicum* L.), potatoes (*Solanum tuberosum*), and lettuces (*Lactuca sativa* L.).

The second case study from Oman and has to do with the management of oily produced water from oilfields. Produced water is the water produced during the exploration and production of oil and gas and represents one of the largest industrial waste streams worldwide. One of the largest CW systems in the world is found in Oman for the treatment of oily produced water (Stefanakis et al., 2018). The system started its operation in end-2010 and after three expansion phases (Stefanakis, 2020), the treatment capacity today



reaches 175,000 m³/day. This treatment plant consists in 490 hectares of free-water surface CWs and 780 hectares of evaporation ponds (Stefanakis, 2020). Furthermore, a first large study was carried out in an irrigation field of 22 hectares (Stefanakis et al., 2018), where various salt tolerant plants with market value such as biofuels, cotton, forage grass, among others, were irrigated with the treated effluent (Echchelh et al., 2021). To further close the materials cycle, a compost trial that was also carried out using the reed biomass from the wetlands as main substrate. Following the same approach, another study investigates the potential to use the reed biomass for biogas production, that will be used to cover the minimum energy demand of the facility.



Figure 1. Left: the constructed wetland system in the Czech Republic. Right: the constructed wetland system in Oman.

Conclusions

Identifying sustainable management ways for wastewater effluents is a key factor towards expanding and implementing the circular economy principles. New, green technologies are needed to enhance the sustainable character of wastewater management, especially in the industrial sectors, but also new initiatives to close the materials cycle and promote water reuse and recycling. Nature-based solutions such as the green technology of Constructed Wetlands can provide these desired characteristics. The two case studies presented here from different wastewater sources and different climatic conditions demonstrate that the dual goals set of implementing sustainable technologies and circular practices is technically and economically feasible at various scales. The use of Constructed Wetlands for wastewater allows the recycling of the treated effluent in the industrial process reducing this way the freshwater consumption. It also enables the reuse and exploitation in irrigation to produce valuable crops. These examples of wastewater management indicate the potential to close the loop of water and promote circularity aspects and practices in the wide water management sector.

References

- Echchelh, A., Hess, T., Sakrabani, R., Prigent, S., Stefanakis, A.I., 2021. Towards agro-environmentally sustainable irrigation with treated produced water in hyper-arid environments. *Agricultural Water Management* 243, 106449.
- Šereš, M., Innemanová, P., Hnátková, T., Rozkošný, M., Stefanakis, A.I., Semerád, J., Cajthaml, T., 2021. Evaluation of Hybrid Constructed Wetland Performance and Reuse of Treated Wastewater in Agricultural Irrigation. *Water* 13(9), 1165, <https://doi.org/10.3390/w13091165>.
- Stefanakis, A.I., 2020. Constructed Wetlands for Sustainable Wastewater Treatment in Hot and Arid Climates: Opportunities, Challenges and Case Studies in the Middle East. *Water* 12 (6), 1665, <https://doi.org/10.3390/w12061665>.
- Stefanakis, A.I., 2018. Constructed Wetlands case studies for the treatment of water polluted with fuel and oil hydrocarbons, in: Ansari, A.A., Gill, S.S., Gill, R., Lanza, G., Newman, L. (Eds.), *Phytoremediation*, Vol. 6, Springer International Publishing, Switzerland, pp 151-167.
- Stefanakis, A.I., Calheiros, CSC, Nikolaou, I., 2021. Nature-Based Solutions as a Tool in the New Circular Economic Model for Climate Change Adaptation. *Circular Economy and Sustainability* 1, 303-318, <https://doi.org/10.1007/s43615-021-00022-3>.



Multi-purpose lignin-based benzoxazines: from hydrophobic coatings to catalyst-free vitrimers

A. Adjaoud^{1,2}, L. Puchot¹, C. Federico¹, R. Das^{1,2} and P. Verge¹

¹ Luxembourg Institute of Science and Technology, Hautcharage, Luxembourg

² University of Luxembourg, Esch-sur-Alzette, Luxembourg

Corresponding author email: pierre.verge@list.lu

keywords: lignin; polybenzoxazine; vitrimer; flame-retardant; hydrophobic coating; sustainability.

The meaningful concept of circular economy and tighter environmental legislation to phase out single-use plastics have prompted the scientific community to transform the polymer industry toward bio-based and recyclable materials. Lignin, the second largest natural polymer produced on Earth, epitomized the main source of phenolic compounds for the conception of bio-derived materials. Strategies toward lignin valorization flourished as lignin can be incorporated as fillers for composites, depolymerized into high-valued added chemicals, or modified to produce lignin-based materials¹. Polybenzoxazines (PBZs) emerged as a promising alternative to phenolic and epoxy resins thanks to their competitive features such as superior mechanical properties and thermal stability². The exceptional design versatility of their chemical structure is at the root of the growth of research works related to their synthesis from lignin-depolymerization chemicals. As unmodified lignin macromonomer meets few reactivity toward benzoxazine chemistry, we have reported a promising green and eco-friendly approach to enhance the reactivity of lignin³. A technical soda lignin was esterified in solvent-free condition with phloretic acid, a naturally occurring compound extracted from the leaves of apple trees. This sustainable synthetic route grants technical lignin with ester bonds and an increased number of phenolic reactive sites.

Therefore, this enriched platform of *ortho*-free phenolic rings was employed for the design of a series of lignin-based benzoxazines (LBZs)⁴. The properties of the monocomponent bio-based resins can be easily tuned depending on the amine used to close the benzoxazine ring. Bio-based amines synthons such as long-alkyl chain stearylamine confers hydrophobicity to LBZs coatings (= 96 °), while furfurylamine, derived from furfural, furfurylamine provide LBZs resin with high-Tg (Tg= 197 °C) and high thermal stability (CR800= 45.8 %) well adapted for fire-retardancy applications. Ethanolamine grants recyclability to the cross-linked lignin-vitrimers thanks to the internally catalyzed transesterification dynamic exchanges^{4,5}. This presentation will highlight the versatility of LBZs materials in terms of application (Figure 1).

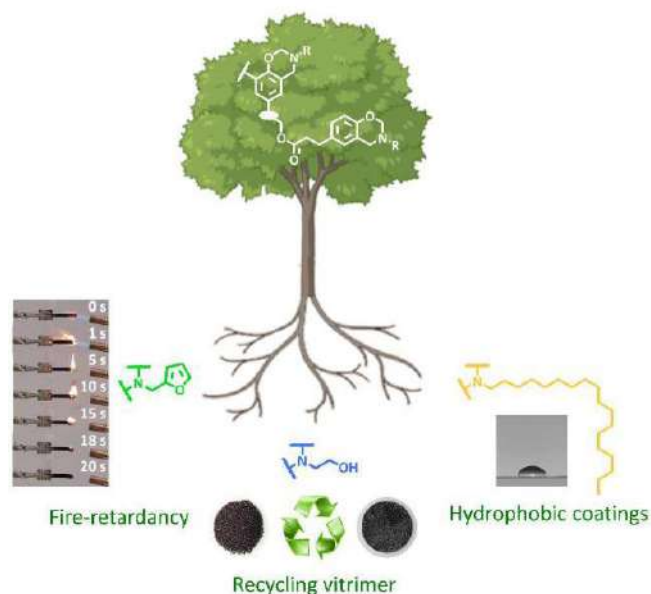


Figure 1 Multi-purpose applications of LBZs materials

Acknowledgements: The authors would like to thank the FNR for the funding of the project LIGNOBENZ (C18/MS/12538602).

References

- Kai, D.; Tan, M. J.; Chee, P. L.; Chua, Y. K.; Yap, Y. L.; Loh, X. J., *Green Chem.*, 18, 5 (2016).
Ishida, H., *Handbook of Benzoxazine Resins*, Elsevier: Amsterdam (2011).
Adjaoud, A.; Dieden, R.; Verge, P., *Polymers*, 13, 4 (2021).
Adjaoud, A.; Puchot, L.; Federico, C.; Das, R.; Verge, P., submitted in *Chem. Eng. J.* (2022).
Adjaoud, A.; Trejo-Machin, A.; Puchot, L.; Verge, P., *Polym. Chem.*, 12, 3276-3289 (2021).
Adjaoud, A.; Puchot, L.; Verge, P., *ACS Sustainable Chem. Eng.*, 10, 594-602 (2022).



Hydrothermal Process for Silver Leaching from Mono- and Poly-crystalline Photovoltaic Waste Panels

E. Kastanaki¹, E. Lagoudakis¹, G. Kalogerakis¹ and A. Giannis¹

¹School of Chemical and Environmental Engineering, Technical University of Crete, Chania, Greece.

Corresponding author email: ekastanaki@tuc.gr

keywords: *crystalline silicon photovoltaic panels; silver; recycling; e-waste; response surface methodology.*

Introduction

The New Green Deal in Europe sets the basis for energy decarbonisation in member countries and the promotion of renewable sources to meet their energy needs. Member countries have committed to a total of 338.3 GW Photovoltaic (PV) installations by 2030, almost triple than 2019, thus huge amounts of PV waste are anticipated in the future. Waste recycling is crucial to recover valuable materials from PV waste. Economic sustainability is largely dependent on the fraction and the quality of materials that can be recovered by the proposed recycling processes. Silver concentration in U.S. resources must surpass 700 g/t when mined to be commercially extracted as a primary product. As a result, Ag recovery from solar panel waste is becoming increasingly important. It is shown that the silver content in crystalline silicon photovoltaic modules reaches 600 g/t.

The purpose of this study was to investigate silver leaching from monocrystalline and polycrystalline silicon PV panel waste by hydrothermal treatment using mild HNO₃ solutions. The process parameters examined were: solid to liquid ratio (S/L), HNO₃ molarity, time (t) and temperature (T) of the hydrothermal treatment. After preliminary tests, the tested HNO₃ molarity was set in the range of 1-2 N, in an attempt to establish a low polluting process. In order to investigate the influence of these parameters on silver leaching, the Response Surface Methodology and the Box-Behnken design was used to plan the experiments. The results revealed that in the range of 1-2N HNO₃ under study, the processing time was the most important factor, followed by HNO₃ molarity and S/L ratio, while the temperature of the process (100-140 °C) was not a statistically significant. Silver leaching from monocrystalline and polycrystalline PV waste exhibited similar behavior while XRF characterization revealed that Ag concentration was higher in monocrystalline PV panel.

Materials and methods

The raw materials in this research were EoL mono-crystalline (m-Si) and poly-crystalline silicon (p-Si) PV panels, collected from local PV trading/installation companies located in reece, as described by Savvilotidou and Gidarakos (2020). After dismantling and removal of the white backsheet, the panels were thermally treated for the removal of the EVA layer in order to facilitate the separation of the main parts of the PVs i.e. glass, silicon cells, metal ribbons at 600 °C for 30 min. After the thermal treatment of the Si PV panels, the separated cells and the metal electrodes were milled with a pulverisette 19 FRITCH mill equipped with a sieve of 0.5 mm and subjected to X-ray fluorescence analysis (XRF, Rigaku Primus IV) to determine their chemical composition.

The hydrothermal leaching stage was performed in cylindrical steel reactors internally coated with PTFE and was treated at 100-140 °C for 0.5-2 h, L/S: 10-20 without stirring. The resulting product was allowed to cool down and then a sample was filtered with a 0.45µm syringe filter for subsequent analysis in the Inductively Coupled Plasma-Mass Spectrometry (7500 cx ICP-MS, Agilent).

Results and discussion

The hydrothermal leaching of Ag experiments revealed that for the conditions tested the time of reaction was the most important factor, followed by the concentration of HNO₃. The Pareto charts of the significant terms of factors and their interactions for explaining the response (leaching efficiency) are



shown in Figure 1. The significant terms are above the dotted red line, whereas the non-significant ones are below the red line. The S/L ratio was the least significant factor in the case of both m-Si and p-Si panels. Also the temperature was not a significant factor in both samples (m-Si and p-Si) and there were not significant interactions between the parameters.

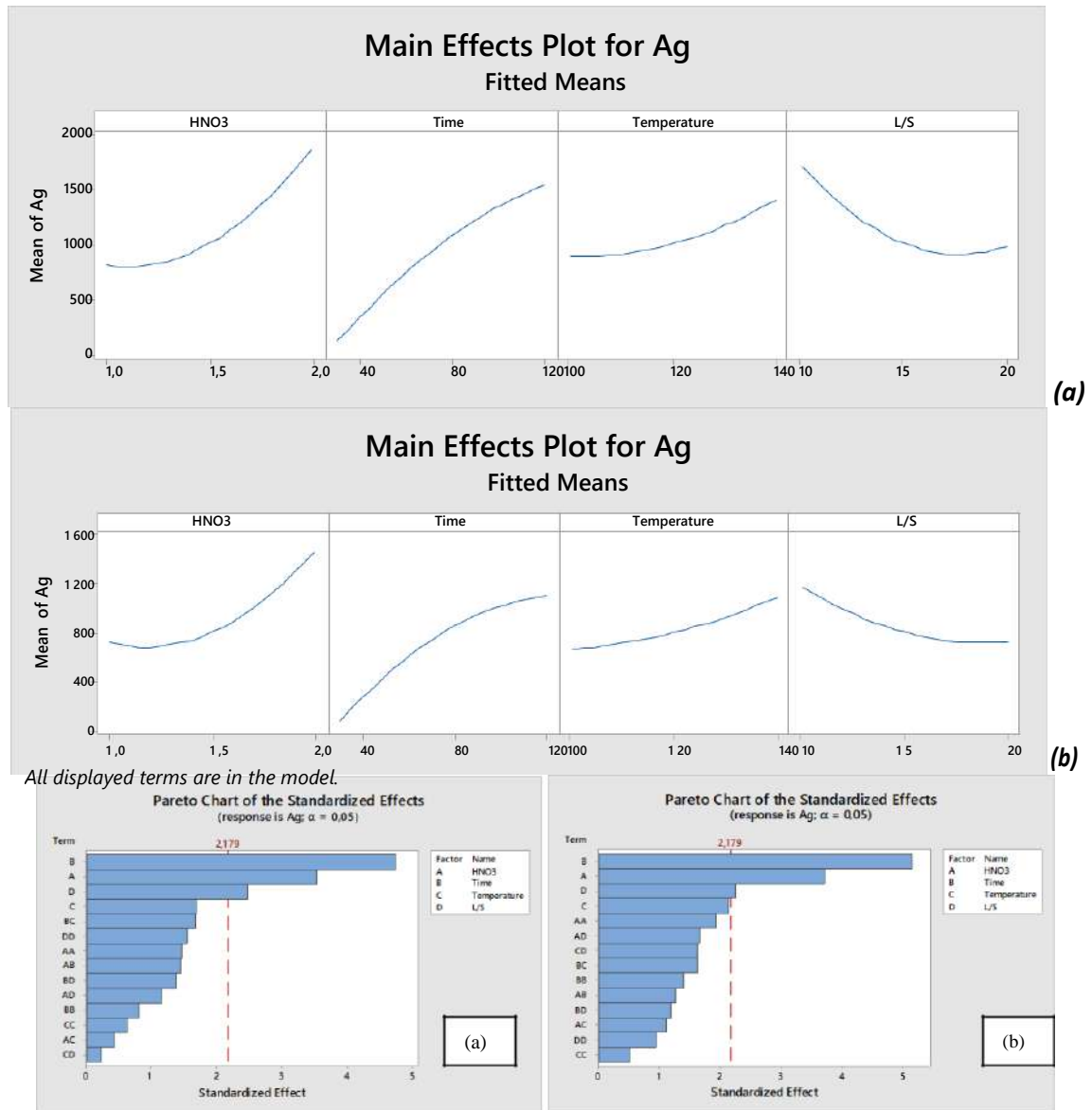


Figure 1. Main Effects Plot for parameters under study on silver leaching from monocrystalline and polycrystalline PV waste (a) and (b) Pareto Chart of Effects (a) monocrystalline and (b) polycrystalline PV waste.

Conclusions

According to the optimization through the experimental design the optimized conditions to maximize Ag leaching (100%) through hydrothermal treatment are 140 °C, 2h leaching, S/L: 1/10 and HNO₃ 2N. The efficient hydrothermal leaching of Ag is possible at a low HNO₃ concentration, thus eliminating the hazardous waste.

References

Savvilitidou, V., Gidaracos, E. (2020). Pre-concentration and recovery of silver and indium from crystalline silicon and copper indium selenide photovoltaic panels, Journal of Cleaner Production, 250, art. no. 119440. doi: 10.1016/j.jclepro.2019.119440



Pre-processing and Leaching methods for extraction of REEs from permanent magnets: A scoping review

S. Papagianni^{1,2}, A.M. Moschovi¹, K.M. Sakkas³, M. Chalaris² and I. Yakoumis¹

¹MONOLITHOS Catalysts & Recycling, Polygono, Athens, Greece

²Department of Chemistry, School of Science, International Hellenic University (IHU), Agios Loucas, Kavala, Greece

³Enalos Research and Development PC, Chalandri, Greece

Corresponding author email: yakoumis@monolithos-catalysts.gr

keywords: permanent magnets; REEs; NdFeB; preprocessing; leaching.

Introduction

The following study focuses on the in-depth analysis of the state-of-the-art preprocessing techniques of the Rare Earths Elements (REEs) magnets as well as the extraction of REEs incorporating different processes. Several investigations have aimed at the extraction of REEs from permanent magnets due to the meager world's recycling percentage (1%).

Materials and methods

Permanent magnets incorporate Critical Raw Materials, especially, rare-earth elements (REEs), such as neodymium, iron, boron (Nd-Fe-B) and Samarium and Cobalt (SmCo). These types of magnets are used in several emerging sectors, which are crucial to Europe's energy sustainability. Examples are electric vehicles (EVs), wind turbines and a multitude of domestic applications.

Results and discussion

These technologies are being rapidly developed, resulting in a growing demand for magnets and REEs. However, the primary production and supply of REEs are not capable of covering the world's demand for these metals. Further, since mining primary sources are placed almost exclusively in China, which accounts the nearly 98% of the world's REEs production and, at the same time, consumes 67% of produced REEs in the internal market. Meanwhile, the European industry is totally dependent on imported REEs, as less than 1% is recycled at the European Level.

Therefore, the dominance of third countries in REEs production and the increase of their demand in Europe creates a gap between the supply and demand of these metals, which can be decoupled by recycling the End-Of-Life Materials.

However, an industrially sound technology presenting high recovery efficiency and at the same time being techno-economically sustainable has not been developed yet.

In the following literature review the steps of the demagnetization and milling, in powder form, have been reviewed considering that the literature data are limited because of the challenging properties of the magnets, which complicate their handling. The flammability of the magnets under shredding/milling creates a challenging balance between safety and economical sound processes.

Moreover, in the specific research, the extraction of REEs will be described in detail using either a direct extraction method or a combination of methods based on the pyro- or hydrometallurgical processing. The main methods are based on dry digestion, acid baking processes, high acid hydrometallurgical methods and high temperature (pyrometallurgy) routes aiming at higher REE extractions compared to the existing methods.

Conclusions

An insight into the recycling methods for recovering critical raw materials of REEs from permanent magnets will be presented, offering a sustainable perspective of handling, storing and preprocessing the latter materials. The need for decoupling from imports from the East will be described and validated.



1st International Conference on Sustainable Chemical and Environmental Engineering
31 Aug – 04 Sep 2022, Rethymno, Crete, Greece

Acknowledgments: This study is supported by the PHEIDIAS project. The PHEIDIAS project (PA 20220) has received funding from the European Institute of Innovation and Technology (EIT), a body of the European Union, under the HORIZON 2020, the EU Framework Programme for Research and Innovation.



Technical assessment of a plant for recovery of metals from HDS catalysts

N.M. Ippolito¹, V. Innocenzi¹, I. D' Adamo² and F. Ferella¹

¹Department of Industrial and Computer Engineering and Economics, University of L'Aquila, L'Aquila, Italy

²Department of Computer, Control and Management Engineering, Sapienza University of Rome, Rome, Italy

Corresponding author email: francesco.ferella@univaq.it

keywords: HDS; catalysts; molybdenum; vanadium; recycling.

Introduction

The paper is focused on a techno-economic analysis for a plant that recycles spent hydrodesulfurization (HDS) catalysts. HDS catalysts usually are made of MoS₂, Ni, or Co sulfides supported by porous alumina. During the heavy oil or diesel refining by HDS catalysts, a significant amount of transition metals are deposited on the catalyst surface in addition to carbon and sulfur. Accumulation of such elements leads to the deactivation of HDS catalysts. Although the organic deactivation can be recovered by burning off the carbon and sulfur elements, deactivation through transition metal deposition is irreversible, leading the catalyst to the end of its life. The recycling process is based on a double thermal pre-treatment stage, followed by a series of hydrometallurgical steps that allows recovering Mo and V, as well as a Ni concentrate that needs further refining for separation and recovery of the metals.

Some spent catalysts are wet, i.e., containing residual naphtha or other hydrocarbon fractions, in a 5-13% concentration range. Others, instead, are dried and dusty, mostly containing coke and sulfur. Some are based on active metals like Ni-Mo, others on Co-Mo.

Few industrial processes are currently available to recycle HDS catalysts, particularly the pyrometallurgical and hydrometallurgical ones. This paper considered the hydrometallurgical approach, including a double-stage thermal pre-treatment required to oxidize residual hydrocarbons, coke, and sulfur. The plant is based on a process whose pre-treatment thermal stages were tested on a pilot scale by the University of L'Aquila, whereas the hydrometallurgical section was studied at a laboratory scale in the last years.

Materials and methods

The plant is divided into several sections, listed and described in the sub-paragraphs. Only dry Ni-Mo catalysts containing vanadium from the oil fractions treated in refineries were used as the plant's feedstock. The plant's capacity was set at 6000 tons/year in 7/24 continuous operation mode for a working period of 300 days/year.

In this study, the thermal treatment is carried out in two sequential roasting stages: this choice allows to have a pregnant cleaner solution, i.e., free of Na₂SO₄, that results in a higher grade of the Mo and V salts precipitated in the downstream stages.

The flue gas section heat & material balance (H&M) was carried out by Chemcad 7 (Chemstation) and Microsoft Excel. The centralized flue gas plant treats the gas coming from rotary kiln 1 (catalyst oxidation), rotary kiln 2 (roasting with soda ash), rotary kiln 3 (calcination of AMV), rotary kiln 4 (calcination of molybdic acid), EAF 1 (melting of Ni/alumina solid residue) and EAF 2 (melting of powdered vanadium pentoxide).

The material coming from the second kiln is composed of large flakes that need to be milled before leaching as the extraction yield increases with the smaller particle size of the solid. Hence, a ball mill reduces the particle size to < 2 mm. The hydrometallurgical section was simulated using the software package SuperPro Designer 9.5 (Intelligen). The leaching phase is divided into three stages in series, where three aliquots of catalysts are leached by the same hot water at 85°C for 2 h each after filtration; this process arrangement is used to concentrate the metal to recover, i.e., Mo and V.

The pregnant solution is contaminated by arsenic and phosphorous salts, that has to be removed because they reduce the quality of steel, where Mo and V are added for special alloys. This is why such

impurities have to be removed; otherwise, it is rather difficult to sell Mo and V oxide of low quality. Thus, ammonium vanadate and molybdc acid are recovered by selective precipitation.

In the 3rd rotary kiln, NH_4VO_3 is decomposed into V_2O_5 and NH_3 , and the 4th rotary kiln performs the thermal decomposition of H_2MoO_4 into MoO_3 and H_2O . Moreover, the 1st EAF melts the alumina/nickel solid residue coming from the leaching stage, and the 2nd EAF melts the powdered vanadium pentoxide to get V_2O_5 flakes.

Results and discussion

The plant is considered to be built in an Eastern European country (e.g., Poland, Croatia, Slovenia, Hungary, Czech Republic, Slovakia), and the level of taxation is set at 25%. Total CAPEX and OPEX are determined by the H&M balance of the entire plant, with the current prices for equipment, electric energy, natural gas, personnel, chemicals, etc.

The recycling plant, with a capacity of 6000 tons/year of spent HDS catalysts, can produce 1272 tons/year of V_2O_5 98 %wt, 239 tons/year of MoO_3 57 %wt (both commercial grade), and 227 tons/year of Ni/V/Mo alloy with an approximate composition of 72/25/3%wt, respectively.

As far as the first two products are concerned (V_2O_5 98% min and MoO_3 57% min), a commercial-grade is considered. Instead, for the other product (NiVMo alloy - 72/25/3%), a weighted price was chosen, considering the percentage of V, Ni, and Mo and the fact that such a material has to be refined further.

The CAPEX is around 51 M€, including the indirect costs like engineering, procurement and construction, and supervision. The total OPEX is nearly 22.6 M€/y, including the annual loan payment of 7.59 M€/y with an annually compounded interest rate of 3% (10 years as a return period). The project lifetime is foreseen to be 20 years. The cost of the equipment, electrical energy, and natural gas is for the post-Covid19 period. The main profitability indexes that do not consider the time value of money were calculated and are listed in Table 1.

Table 1. Main economic parameters

Item	
TOTAL INVESTMENT	59.084.160 €
REVENUES	36.141.580 €/y
ANNUAL OPERATING COST	22.527.063 €/y
GROSS PROFIT	13.614.517 €/y
TAXES (25%)	3.403.629 €/y
NET PROFIT	14.213.846 €/y
GROSS MARGIN	37,7 %
RETURN ON INVESTMENT	24,1 %
PAYBACK TIME	4,2 years

Conclusions

The techno-economic analysis showed that the recycling of spent HDS catalysts is a profitable activity to invest in. In particular, the investment is highly profitable, with a plant capacity of at least 6000 tons/year of catalyst feedstock. The net profit is greater than 14 M€/y with an ROI of 24.1% and a payback time of 4.2 years.

References

- Ferella, F., Ognyanova, A., De Michelis, I., Taglieri, G., Vegliò, F., 2011. Extraction of metals from spent hydrotreating catalysts: Physico-mechanical pre-treatments and leaching stage. *J. Hazard. Mater.*, 192, 176-185.
- Peters, M.S., Timmerhaus, K.D., West, R.E., 2004. *Plant Design and Economics for Chemical Engineers*, fifth ed., Mc Graw-Hill, New York.



BIOTECHNOLOGY/CO₂ MANAGEMENT



Co-culture and continuous two-stage bioreactor system for the fermentation of syngas by *B. methylotrophicum* and *C. tyrobutyricum*

M. Pacheco^{1,2}, C. Silva² and P. Moura¹

¹Unidade de Bioenergia e Biorrefinarias, LNEG – Laboratório Nacional de Energia e Geologia, Lisboa, Portugal

²Instituto Dom Luiz/Faculdade de Ciências, Universidade de Lisboa, Lisboa, Portugal

Corresponding author email: patricia.moura@lneg.pt

keywords: Synthesis gas fermentation; acetogenic bacteria; acetic acid; butyric acid

Introduction

The fermentation of industrial off-gases and synthesis gas (syngas) produced by gasification of low-cost or waste biomass represents an extremely versatile technology that is based on the use of a carbon rich gaseous feedstock as substrate for microbial metabolism, for the synthesis of chemical building blocks and biofuels. Besides the decarbonizing potential offered by the conversion of CO₂-rich gas streams, syngas fermentation has the advantage of enabling the recovery of the chemical energy stored in all parts of the biomass, and thus the subsequent bioconversion of otherwise inaccessible fractions (Daniell et al., 2012).

Carboxydrotrophic bacteria are able to use CO and CO₂+H₂ as carbon and energy source for the production of different short chain organic acids and alcohols. One of such bacteria is *Butyribacterium methylotrophicum* (BBM), a carboxydrotrophic acetogen that uses the Wood-Ljungdahl pathway (WLP) to produce acetic and butyric acid from those gaseous substrates (Pacheco et al., 2021). Even though not as interesting as a product as butyric acid, acetic acid is a very flexible compound that can be easily metabolized by bacteria and yeasts to produce chain-elongated compounds with appropriate characteristics to be used as platform chemicals. *Clostridium tyrobutyricum* (CTB) is a saccharolytic clostridia that is able to assimilate acetate and produce high concentrations of butyric acid, but also ethanol and 2,3-butanediol. The combination of acetogenic and carboxylic microorganisms in a flexible biocatalytic process has the potential to harness the carbon content of waste gases to produce economically relevant molecules.

This study aimed at the implementation of a small-scale co-culture system of *B. methylotrophicum* and *C. tyrobutyricum* to assess the potential of CO, CO₂ and acetate metabolism to C₄-products, and the upscaling of the process in a continuous two-stage bioreactor.

Materials and methods

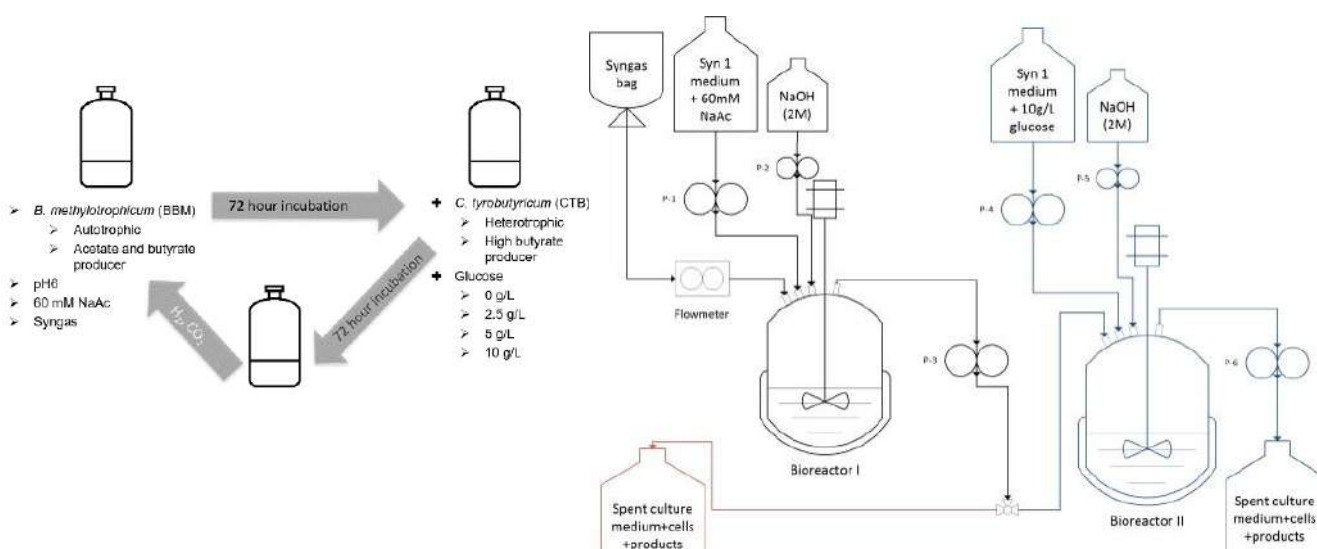


Figure 1. Schematic representation of (A) the small-scale co-culture system of *B. methylotrophicum* and *C. tyrobutyricum* and (B) the continuous single-stage (black+red) and two-stage (black+blue) bioreactor set-up.



The microbial strains used in this study were *Butyribacterium methylotrophicum* strain Marburg DSM 3468 (DSMZ, Germany) and *Clostridium tyrobutyricum* P9 (LNEG isolate). The strains were cultured anaerobically in Syn1 medium (Pacheco et al., 2021) at 37 °C, as depicted in **Figure 1**.

Analytical procedures for biomass, gas and products were performed as described in Pacheco et al., 2021.

Results and discussion

The co-culture of BBM and CTB in serum flasks was able to successfully metabolize acetate, producing 20.7 and 2.2 times more butyrate when compared with the production obtained in single cultures of BBM and CTB, respectively.

The results obtained from the continuous culture of BBM are depicted in **Table 1**. Cells grown at 0.02h⁻¹ were metabolically more active than the cells grown at 0.01 h⁻¹. However, the later were able to metabolize more acetate, producing similar amounts of both butyrate and 2,3-butanediol, while consuming less syngas. A similar trend was already observed in Pacheco et al., 2021, where BBM was able to metabolize acetate. When present in high concentration in the culture medium, acetate can be re-integrated into the WLP and converted to butyrate or 2,3- butanediol.

Table 1. Experimental results obtained from the continuous culture of *B. methylotrophicum* in bioreactor.

Parameter	Dilution rate	
	0.01 h ⁻¹	0.02 h ⁻¹
Syngas consumed [NL/g _{CDW} /d]	0.56	1.22
CDW [g/L/d]	0.05±0.00	0.07±0.00
Y _(acetate) [mmol/L/g _{CDW} /d]	-25.83±3.45	-19.32±0.03
Y _(butyrate) [mmol/L/g _{CDW} /d]	0.48±0.05	0.81±0.03
Y _(2,3-butanediol) [mmol/L/g _{CDW} /d]	3.66±1.64	3.91±0.31

Y_(acid or alcohol) [mmol/L/g_{CDW}/d], specific production/consumption rate: concentration (mmol/L) produced/consumed per g cell dry weight (CDW) per day
NL, volume of syngas in L at standard conditions of temperature and pressure—temperature of 25 °C (293.15 K) and absolute pressure of 1.0 × 10⁵ Pa

In the continuous two-stage culture, BBM was maintained at a dilution rate of 0.01 h⁻¹ in bioreactor I whereas CTB was grown at 0.08 h⁻¹ in bioreactor II. The biomass production rate in bioreactor II was 5.04 g_{CDW}/L/d and three products were detected, butyrate, ethanol and 2,3-butanediol. Acetate was metabolized by CTB at a specific rate of 1.96 mmol/L/g_{CDW}/d, 14 times lower than the rate determined with BBM at 0.01 h⁻¹. The specific production rates of butyrate, ethanol and 2,3-butanediol were 6.74, 2.66 and 6.70 mmol/L/g_{CDW}/d, respectively. These production rates were significantly higher than those obtained with BBM exclusively in bioreactor I. Upon further optimization, the developed sequential system might be a flexible bio-based production system to upgrade C2-acids to C4-acids and alcohols.

Conclusions

This work showed that the production of C4-products from CO and CO₂ was increased by integrating the culture of BBM and CTB in a continuous two-stage system. Additional optimization of the system includes the possibility of recirculating the H₂ produced by CTB, to enrich the syngas fed to bioreactor I.

Acknowledgements: AMBITION Project, an ECRIA project was funded by the European Union's Horizon 2020 research and innovation program, under grant agreement No. 731263; Operational Program for Competitiveness and Internationalization (PORTUGAL 2020), Lisbon Portugal Regional Operational Program (Lisboa 2020) and North Portugal Regional Operational Program (Norte 2020) under the Portugal 2020 Partnership Agreement, through the European Regional Development Fund (ERDF). M. Pacheco was supported by FCT through PhD grant DFA/BD/6423/2020. This work was funded by the Portuguese Fundação para a Ciência e a Tecnologia (FCT) I.P./MCTES through national funds (PIDDAC) – UIDB/50019/2020.

References

- Daniell, J., Köpke, M., and Simpson, S. D., 2012. Commercial biomass syngas fermentation. *Energies*, 5 (12).
- Pacheco, M., Pinto, F., Ortigueira, J., Silva, C., Gírio, F., and Moura, P., 2021. Lignin syngas bioconversion by *Butyribacterium methylotrophicum*: Advancing towards an integrated biorefinery. *Energies*, 14 (21).



Electro-conductive anaerobic membrane bioreactors for biofouling mitigation

S. Qi¹, A.D. Grossman¹, A. Ronen¹ and R. Bernstein¹

¹Zuckerberg Institute for Water Research, The Jacob Blaustein Institutes for Desert Research, Ben-Gurion University of the Negev, Sede-Boqer Campus, Israel

Corresponding author email: avnerr@bgu.ac.il

keywords: electrochemical anaerobic membrane bioreactor (EC-AnMBR); electroconductive membranes (ECMs); biofouling mitigation; bacterial inactivation; pH gradient.

Introduction

Membrane fouling, particularly biofouling, presents a great challenge in adopting anaerobic membrane bioreactors (AnMBRs) for wastewater treatment. A promising direction for mitigating biofouling is by applying an external charge on electroconductive membranes (ECMs). Reactive oxygen species (ROS) production at the ECM surface is usually considered one of the main mechanisms attributed to its antibacterial abilities. In particular, as carbon-based ECMs can only be used as cathodes to prevent anodic oxidation, hydrogen peroxide (H₂O₂) is considered the main ROS involved in biofouling mitigation. However, as electrochemical production of H₂O₂ requires dissolved oxygen, ROS concentration on cathode ECMs under anaerobic conditions is low. This research investigated bacteria inactivation mechanisms and biofouling mitigation in an anaerobic membrane bioreactor equipped with a carbon-based ECM membrane (EC-AnMBR).

Materials and methods

To this end, an EC-AnMBR mimetic system with three electrodes was designed with an ECM as the cathode, a platinum plate as a counter electrode, and an Ag/AgCl as a reference electrode. To decouple the reactions on each electrode, the anode and cathode were separated by a cation exchange membrane. The bacteria inactivation in the anode and cathode compartments was estimated under varying cathodic potentials (0-2.5 V vs. Ag/AgCl). ROS formation and changes in the pH values in each compartment were monitored. Specifically, the effect of pH on bacterial inactivation was evaluated by measuring changes in bacterial concentration in solution with pH values similar to the ones recorded in each compartment under the applied potentials experiments. Then, biofouling formation under the different applied potentials was assessed by following the changes in the transmembrane pressure during 48 hours of filtration, and the biofilm formed on the ECM after 48 hours was analyzed.

Results and discussion

Our results show that bacterial inactivation and biofouling mitigation in EC-AnMBR occurs mainly at a cathodic potential of -2.5 V and are mainly a result of extreme local pH conditions developed by hydrogen evolution at the cathode, while in the anode compartment, bacterial inactivation is a result of pH change and ROS formation. In addition, CLSM images (Fig.1) show that very limited biofilm and EPS has developed on the charged ECM (-2.5 V) in comparison to the control ECM with no applied potential.

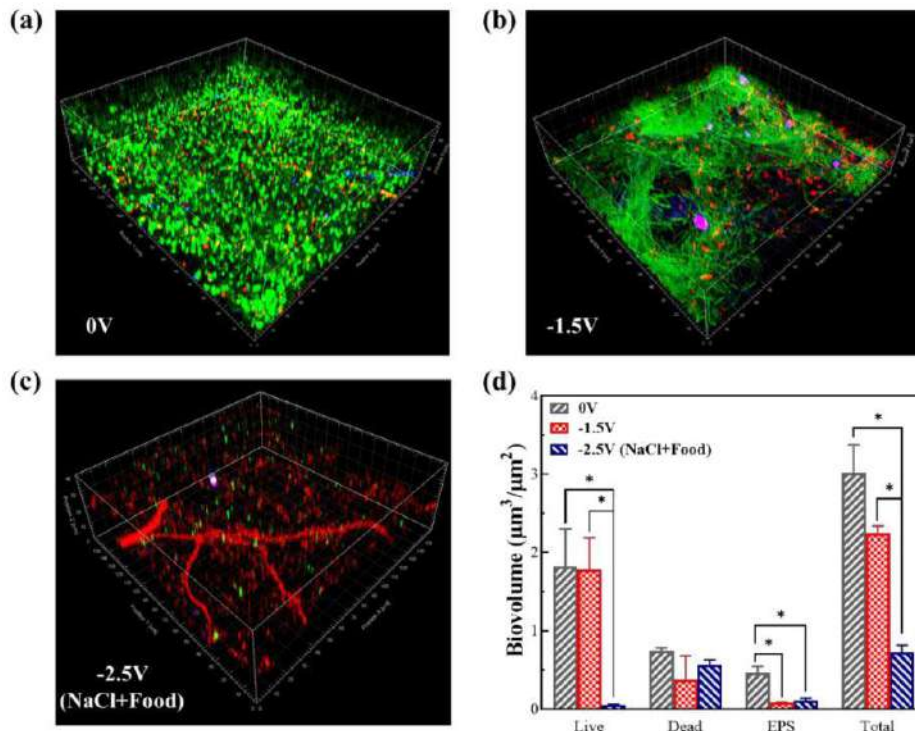


Figure 1. (a-c) 3D images of biofilm; and (d) biovolume of fouled CNT membranes at 0, -1.5, and -2.5V vs. Ag/AgCl) cathodic potential (statistically significant as $p < 0.05^*$)

Conclusions

This study demonstrated that ECMs have excellent anti-biofouling properties when used as cathodes in EC-AnMBR systems. The antibiofouling activity was mainly shown at cathodic potentials of -2.5 V(vs. Ag/AgCl). In addition, this work addresses the mechanisms involved in biofouling mitigation of externally charged ECMs, which could be a promising approach, leading to applying anaerobic membranes bioreactors in wastewater treatment.

Acknowledgements: The project was supported by the USAID Middle East Regional Cooperation (MERC) Program, M35-024 (to R.B). A.D.G acknowledges the support of Kreitman School of Advanced Graduate Studies BGU through the Negev fellowship for Ph.D. studies. The authors acknowledge Dr. Reviatl Sharon for her help with the SEM images.



Effect of oxygen transfer coefficient on microbial production of lipids and carotenoids using renewable waste feedstock: batch and fed-batch mode

M.A. Villegas-Mendez¹, J. Montañez¹, J.C. Contreras-Esquivel¹, I. Salmeron², A. Koutinas³ and L. Morales-Oyervides¹

¹Facultad de Ciencias Químicas, Universidad Autónoma de Coahuila, Unidad Saltillo, Coahuila, Mexico.

²School of Chemical Science, Autonomous University of Chihuahua, Chihuahua, Mexico.

³Department of Food Science and Human Nutrition, Agricultural University of Athens, Athens, Greece.

Corresponding author email: lourdesmorales@uade.edu.mx

keywords: oxygen transfer; agro-waste hydrolysate; oleaginous yeast; lipids; carotenoids.

Introduction

Present-day environmental research is focused on mitigating the environmental damage caused by waste gathering since statistical foresight indicates that more than 1.5 billion tons of organic waste will be generated by agro-industrial activity (Tomás-Pejó et al., 2021). In this regard, agro-industrial byproducts valorization as a feedstock for the bioproduction of high-value products has demonstrated to be a feasible alternative to handle the waste environmental impact (Tomás-Pejó et al., 2021; Stylianou et al., 2021; Deeba et al., 2022).

Oleaginous yeasts are promising cell factories for the industrial production of lipids and carotenoids, which can be developed using agro-waste feedstock (Tomás-Pejó et al., 2021; Deeba et al., 2022). Since oleaginous yeasts are aerobic microorganisms, studying the volumetric oxygen transfer coefficient (kLa) could facilitate the scale-up and operation of bioreactors to grant the biocompounds' industrial availability (Stylianou et al., 2021). Therefore, evaluating the oxygen influence in bioprocess development is a key factor for increasing production yields and establishing the power consumption rates. This study aims to assess the scale-up strategy in the simultaneous production of lipids and carotenoids by oleaginous yeast using renewable waste feedstock.

Materials and methods

The yeast *Sporobolomyces roseus* CFGU-S005 was used for the scale-up experiments to produce lipids and carotenoids simultaneously. Fermentations were performed in a 7 L benchtop bioreactor (Applikon, The Netherlands) using a working volume of 4.1 L at constant aeration (1.5 vvm). Three agitation speed levels were evaluated (150, 250, and 350 rpm) to vary kLa (16.16, 22.44, 32.16 h⁻¹). An agro-industrial waste hydrolysate was obtained by the crude enzymatic hydrolysis of pasta processing waste (Villegas-Méndez et al., 2022). The hydrolysate was adjusted to 20 g/L of total sugar and supplemented with the following salts (g/L): KH₂PO₄ (7.0), Na₂HPO₄ (2.5), MgSO₄ (1.5), CaCl₂·2H₂O (0.15), FeCl₃·6H₂O (0.15), ZnSO₄·7H₂O (0.02), MnSO₄·H₂O (0.06). Initial pH was adjusted to 5 and was uncontrolled during the experiments at 25 °C for 120 h. In Fed-batch experiments, hydrolysate pulses of ~4 g/L of total sugars were added to the bioprocess to evaluate the effect on the production yields. Carotenoids and lipids were assessed at the end of the process (Villegas-Méndez et al., 2022).

Results and discussion

The kLa values provided a scale-up strategy to determine a correlation between metabolites production (microbial oil and carotenoids) and oxygen supply in the bioprocess of the yeast *S. roseus*. Oxygen availability in the fermentation affected the simultaneous production of metabolites, in which we found that the increase in oxygen supply enhanced carotenoids but slightly decreased lipids synthesis.

Figure 1 shows the kinetic profiles regarding biomass growth, lipids, and carotenoid production in the batch (Fig. 1a, b, and c) and fed-batch (Fig. 1d) modes. The highest production of lipids (3.42 g/L) was attained using the kLa value of 22.44 h⁻¹, while higher carotenoid accumulation of 2 mg/L resulted when agitation speed was increased to 350 rpm (kLa 32.16 h⁻¹). Furthermore, the fatty acid composition was affected among evaluated aerations (Table 1). On the other hand, the fed-batch mode (Fig. 1d) enhanced the simultaneous production of lipids and carotenoids using a kLa of 22.44 h⁻¹ up to 6.6 g/L and 3.4 mg/L, respectively. Also, it can be emphasized that fatty acid composition was similar to that obtained in the



batch mode. The results obtained in this study agree that increasing kLa values in scale-up does not always positively affects the metabolites' production (Stylianou et al., 2021).

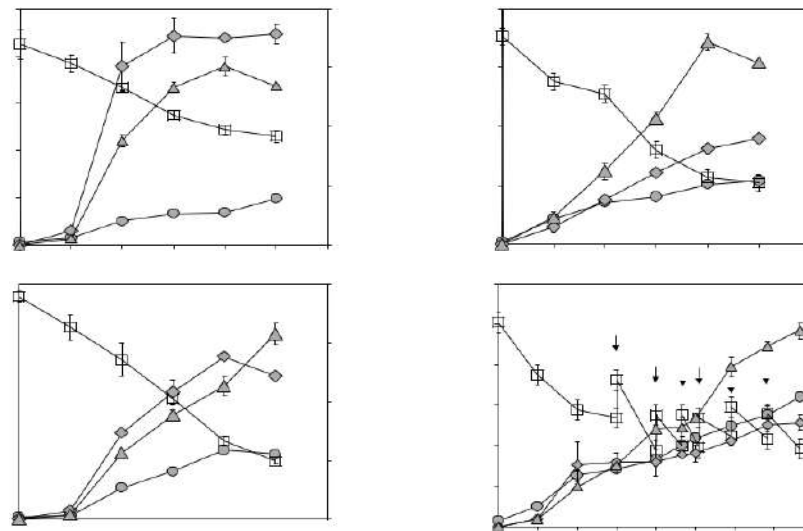


Figure 1. Kinetic studies in the assessed bioreactor kLa values a) 16.16 h^{-1} b) 22.44 h^{-1} c) 32.16 h^{-1} . d) Fed-batch fermentation using agro-waste hydrolysate at 22.44 h^{-1} , arrows represent sugar pulses $\sim 4\text{ g/L}$. Biomass (B, circles), lipid production (L, triangles), carotenoid production mg/L (P, diamonds), total sugar g/L (TS, squares).

Table 1. Fatty acid obtained from bioreactors

Fatty acid	Composition, %			
	16.16 h^{-1}	22.44 h^{-1}	32.16 h^{-1}	22.44 h^{-1} Fed-batch
MUFAs	57	65	29	64
PUFAs	2	11	34	14
SFAs	41	24	26	22

MUFAs, monounsaturated fatty acids; PUFAs, polyunsaturated fatty acids; SFA, saturated fatty acids.

Conclusions

This study showed the scale-up potential of the strain *S. roseus* in the further obtention of microbial oil and carotenoids by bioprocess development by the valorization of agro-industrial byproducts as a carbon source. The oxygen availability affected the yields of lipids and carotenoids as well as the fatty acid profile. Also, the fed-batch mode operation 2-folded the lipid and carotenoid yield without affecting the fatty acid composition.

Acknowledgments: Author M.Á.V.-M. (750450-2019) acknowledges CONACyT-Mexico for the financial support provided for conducting his doctoral studies.

References

- Tomás-Pejó, E.; Morales-Palomo, S.; González-Fernández, C. 2021. Microbial Lipids from Organic Wastes: Outlook and Challenges. *Bioresour. Technol*, 323, 1-12.
- Stylianou, E.; Pateraki, C.; Ladakis, D.; Damala, C.; Vlysidis, A.; Latorre-Sánchez, M.; Coll, C.; Lin, C.S.K.; Koutinas, A. 2021. Bioprocess Development Using Organic Biowaste and Sustainability Assessment of Succinic Acid Production with Engineered *Yarrowia Lipolytica* Strain. *Biochem. Eng. J*, 174, 1-10.
- Deeba, F.; Kiran Kumar, K.; Ali Wani, S.; Kumar Singh, A.; Sharma, J.; Gaur, N.A. 2022 Enhanced Biodiesel and β -Carotene Production in *Rhodotorula Pacifica* INDKK Using Sugarcane Bagasse and Molasses by an Integrated Biorefinery Framework. *Bioresour. Technol*, 351, 1-9.
- Villegas-Méndez, M.Á.; Montañez, J.; Contreras-Esquivel, J.C.; Salmerón, I.; Koutinas, A.; Morales-Oyervides, L. 2022. Coproduction of Microbial Oil and Carotenoids within the Circular Bioeconomy Concept: A Sequential Solid-State and Submerged Fermentation Approach. *Fermentation*, 8, 1-19.



Recent advances in CO₂ to bio-oil biorefinery

A.G. Capodaglio¹

¹Department of Civil Engineering & Architecture, University of Pavia, Italy
Corresponding author email: capo@unipv.it

keywords: carbon dioxide; microalgae; bioelectrochemical systems; biooil; biorefinery.

Introduction

Several biological methods for carbon dioxide sequestration and conversion are being studied today. Microbial electrosynthesis (MES) technologies are emerging as a promising field in microbial electrochemistry: bio-electro CO₂ recycling can convert this greenhouse gas into multi-carbon molecules, added value chemicals and biofuels.

One possible strategy involves bioconversion of CO₂ into medium and short-chain fatty acids, acetic acid being the most common product. Process technologies have been investigated to expand the portfolio of potential products since chain elongation requires multiple-step processes.

Bioelectrochemical systems (BES) are biochemical systems characterized by a pair of electrodes working concurrently with redox reactions, microbially catalyzed at one or both electrodes. Reaction can be spontaneous, with the generation of an electron flow from anode to cathode, or induced by providing an external current (or potential), to supply bacteria with the necessary reducing equivalents to promote non-spontaneous bioconversion reactions.

Coupling BES technology with microalgae organisms is being explored, whereby integrated photo-bioelectrochemical (IPB) reactors with microalgae inserted into the cathode of a microbial fuel cell can be used for electricity generation and nutrient removal from wastewater.

Heterotrophic microalgae, such as *Auxenochlorella protothecoides*, can use acetate and other short chain VFAs for growth in the presence of oxygen, and require no direct light exposure. They can therefore function as oxygen scavengers in MESs and be subsequently exploited for their properties, since many valuable products can be obtained from microalgae biorefinery. Liquid biofuels, e.g. biodiesel, bioethanol, biobutanol and jet fuels, are the most likely outcomes of algal biorefining.

This paper summarizes the most recent advances in biorefinery conversion of CO₂ to biooil and illustrates results from an experimental study on the overall conversion process from CO₂ to bio-oils via MES-mediated VFA production, and their subsequent conversion into fuel through heterotrophic microalgae biorefinery.

Materials and methods

MES reactors were assembled and operated with a suitable growth medium (synthetic wastewater) to simulate microalgae renewal from an autotrophic cultivation unit in an integrated system; CO₂ was insufflated as the only carbon source, saturating the cathodic chamber where production of volatile fatty acids (VFAs) and alcohols occurred. Methacrylate photobioreactors (1 L each) were built to grow microalgae *Chlorella vulgaris* and *Auxenochlorella protothecoides* using VFAs (acetate) produced in biocathodes as substrate.

Oil extraction from algae was then performed after mechanical cell disruption and phase separation (pellet, residual water and n-hexane with dissolved lipids).

Results and discussion

Biocathodes operated under thermophilic conditions (50 °C) produced acetate from carbon dioxide at max production rate 28 g/m²d, with maximum titre of 5250 mg/L, under mesophilic conditions (25 °C) VFA production was lower.

After microalgae collection and concentration, oil extraction yielded an average of 20 ± 2% w/w (algae dry weight), in line with other literature results. Approximately 1.11 kg dry algae per kg acetate was obtained, from which 0.207 kg of lipids were extracted and further processed for biodiesel production by transesterification process, with product properties complying with EU fuel specifications.



Microalgae biomass yield is strictly dependent on the cultivation technique and strain chosen, with concentration values ranging from 0.1 to 8 g/L (dry weight). Autotrophic microalgae can capture CO₂ directly to synthesize new biomass: 1 kg (dry) microalgae *Chlorella vulgaris* may capture 1.83 kg CO₂ with fixation rate of 0.73 to 2.22 g/L d but, less in open air raceway ponds, since part of the fed CO₂ is lost to the atmosphere. The combined process herein presented allowed almost 100% CO₂ capture and conversion. Additionally, heterotrophic cultures can generate biomass in larger cultivation volumes (ponds exceeding 100 000 L have been reported), and are not strictly dependent on the presence of sunlight. Thus, the heterotrophic process is less expensive than the autotrophic one in the long period, and allows the possibility of using a waste stream (e.g. treated wastewater effluent) as organic carbon source instead of the synthetic medium used in this study.

Conclusions

This study shows that MES-produced acetate can achieve bio-oil production from algae cultures. This proof-of-concept study demonstrates direct reuse of acetate produced in biocathodes from CO₂ as feed for heterotrophic microalgae is possible, highlighting the feasibility of a microalgae electro-biorefinery. Microalgal oil production was assessed, however other conversion possibilities could be explored. For example, the solid residue from the extraction process could be pyrolyzed to biochar, a valuable recovery material. Recovery of other valuable compounds such as proteins, pigments or other commodity chemicals may be considered to improve the economics of the process and overcome microalgae separation and oil extraction costs that represent relevant expenses components of this process.



Green materials-composites for CO₂ capture and conversion- an emerging trend in sustainable CO₂ management

M. Geetha¹ and K.K. Sadasivuni¹

¹Center for Advanced Materials, Qatar University, Doha, Qatar

Corresponding author email: mithra.geetha@qu.edu.qa

Keywords: CO₂ capture and utilization; CO₂ management; green materials; energy sustainability.

Carbon neutrality is gaining momentum as atmospheric CO₂ levels rise, worsening climate change. Sustainable CO₂ management based on its capture and conversion has garnered significant interest due to its role in resolving emission control and energy supply limitations. However, due to the challenges associated with this approach, research efforts have been directed toward developing green materials that can capture and convert CO₂ into value-added products. The present review focuses on the progress in fabricating green materials for CO₂ management in terms of catalytic conversion (electrochemistry, photochemistry, thermochemistry, and possible combinations), capture, direct utilization, and emerging integrated conversion capture and conversion based on artificial intelligence. Specifically, insights spanning multiple approaches to material research are presented, ranging from mechanistic pool reactions to rational design and specific manipulation of key materials (green polymers) to industrial application. This review concludes by discussing major challenges and future potential for utilizing advanced new materials and technologies in sustainable CO₂ management, emphasizing their stability and regeneration. Researchers working in this potentially game-changing field may benefit from this work for developing carbon dioxide capture and conversion materials.



Catalytic hydrogenation of CO₂ using CuO impregnated amine-modified silica support

H. Onthath¹, M.H. Sleim¹, M. Geetha¹, K.K. Sadasivuni¹, A.M. Abdullah¹, B. Kumar²

¹Center for Advanced Materials, Qatar University, PO Box 2713, Doha, Qatar

²Department of Technology, Elizabeth City State University, Elizabeth City, USA

Corresponding author email: mithra.geetha@qu.edu.qa

Keywords: *nanocomposite; cyclic voltammetry; electrochemical.*

Increasing CO₂ emissions from industry has disastrous consequences for the environment. Effective utilization of CO₂ as a carbon source can therefore address the environmental challenges and the energy crisis caused by fossil fuel consumption. Electrochemical conversion of CO₂ is a promising method that has recently gained widespread popularity. Its high productivity, however, remains a major challenge. This work involved a novel preparation of a suitable Mesoporous Si-CuO nanocomposite (NC) to reduce CO₂ into useful fuels effectively. Hydrothermal synthesis was used to synthesize the NC. Structure, morphology, and elemental analysis of the synthesized NC were evaluated using XRD, Raman spectroscopy, SEM, and TEM. ICP-OES analysis was performed to quantify Cu particles in the MS-Cu composite. The cyclic voltammetry method has been used to study the electrochemical activity of NC for CO₂ reduction. Additionally, the NMR & GC-MS analyses were performed to identify the product. In terms of CO₂ reduction, the NC performed greatly better. In addition, the NC exhibits high structural stability and durability, demonstrating its potential to reduce CO₂ into fuels.



SUST
ENG
2022



AIR POLLUTION, EMISSIONS & QUALITY



Study of immobilized biomass reactors for sulfidogenic activity characterization and efficiency improvement

R. Castro¹, G. Gabriel^{2,3}, X. Gamisans¹ and X. Guimerà¹

¹Department of Mining, Industrial and ICT Engineering, Universitat Politècnica de Catalunya, Barcelona, Spain

²Instituto de Microelectrónica de Barcelona, IMB-CNM (CSIC), Barcelona, Spain

³CIBER, de Bioingeniería, Biomateriales y Nanomedicina (CIBER-BBN), ISCIII

Corresponding author email: rebeca.ignacia.castro@upc.edu

keywords: sulfidogenic reactor; sulfate reducing sludge; polyvinylalcohol; immobilization.

Introduction

Flue gases, such as SO_x, are a result of combustion of sulfur-containing fuels by industrial and energetic sectors that generate air pollution and can be deposited in the environment. SONOVA is a process developed for combustion gases treatment and their valorization as elemental sulfur. This process consists of a first step where SO_x is absorbed using a slightly alkaline solution, a biological step where absorbed SO_x (as a mixture of sulfate and sulfite) is anaerobically reduced to sulfide, using glycerol as electron donor, and an aerobic sulfide oxidation step to obtain elemental sulfur (Mora et al., 2020).

Several challenges have been reported for the improvement of sulfate reduction process in anaerobic reactors, mainly related to maintaining a long-term efficiency and avoiding process failure caused by the inhibition of the biomass by Volatile Fatty Acids (VFAs) accumulation, sulfide toxicity, and oxygen presence (Fernandez-Palacios et al., 2019). Moreover, reactor configuration can strongly affect mass transfer resistance and long-term operation, reducing H₂S production (Lens et al., 2003).

On the other hand, immobilization of biomass using polymers has been positioned as a promising alternative for biomass performance improvement due to the generation of a protecting matrix that allows a decrease in starting up period and a fast adaptation to new conditions (Zhang et al., 2016).

In the present study, a new approach for sulfate reducing efficiency improvement was analyzed using immobilized sludge. For this purpose, the operation of two reactors under the same operating conditions (hydraulic residence time, sulfate load, C/S and biomass volume) was assessed. Both reactors were inoculated using PVA-sludge granules.

Materials and methods

Inoculum was obtained from an anaerobic UASB reactor from Aigües de Manresa wastewater treatment plant. Sulfate-reducing activity was enhanced through sealed flask culture using anoxic mineral medium described by Mora et al. (2020). Granules were prepared using a PVA solution (13,6% w/w of PVA) that was blended (1:1) with concentrated sludge (3,78 g VSS/L). Mixture was frozen at -15°C and cut as 5 mm granules. A column reactor (CR) and continuous stirred tank reactor (CSTR) of 500 mL were inoculated with 100 mL of artificial PVA-sludge granules and fed using mineral medium described by Mora et al. (2020). Sulfate load was increased over time, keeping C/S ratio. Sulfate was measured using spectrophotometry (HACH, Spain), VSS and chemical oxygen demand COD were analyzed using Standard methods. VFAs concentration were obtained by HPLC with an ICsep ICE-CPREGEL 87H3 column and a wavelength detector at 210 nm. H₂S monitoring was performed using electrochemical sensor (SULF-NP, UNISENSE, Aarhus, Denmark).

Results and discussion

CR and CSTR were operated at the same time and under the same conditions (Figure 1). Sulfate reduction is almost complete from 0,2 until 3 kg/m³d. When sulfate load was set at 4 kg/m³d, CR and CSTR decrease a 50% sulfate removal. However, CR regained a high removal efficiency in 7 days, in contrast with CSTR. This difference can be explained by accumulation of H₂S and VFAs that could have a toxic effect in biomass. CSTR decreased mass transfer resistance (Lens et al., 2003) exposing granules to inhibitors. Values of COD



removal, H₂S, Total VFAs and outlet VSS concentration (accumulated) at different periods are presented in Table 1. These results correspond to periods under a low sulfate load (day 20), a high sulfate load (day 75) and at the end of experiment. COD removal efficiency (RE) in CR was similar were all the experimental period. However, CSTR presented an unstable activity and low COD removal at high sulfate loads. H₂S and VFAs concentration in CR were higher than CSTR, demonstrating an enhanced sulfate reducing activity. Moreover, CSTR presented a significant loss of biomass that can explain low performance. Mechanical strength of PVA granules depends on immobilization method and concentration of PVA used. It is possible to use higher PVA concentration for increasing the density of polymer matrix but that can be detrimental for mass transfer capacity (El-Naas et al., 2013).

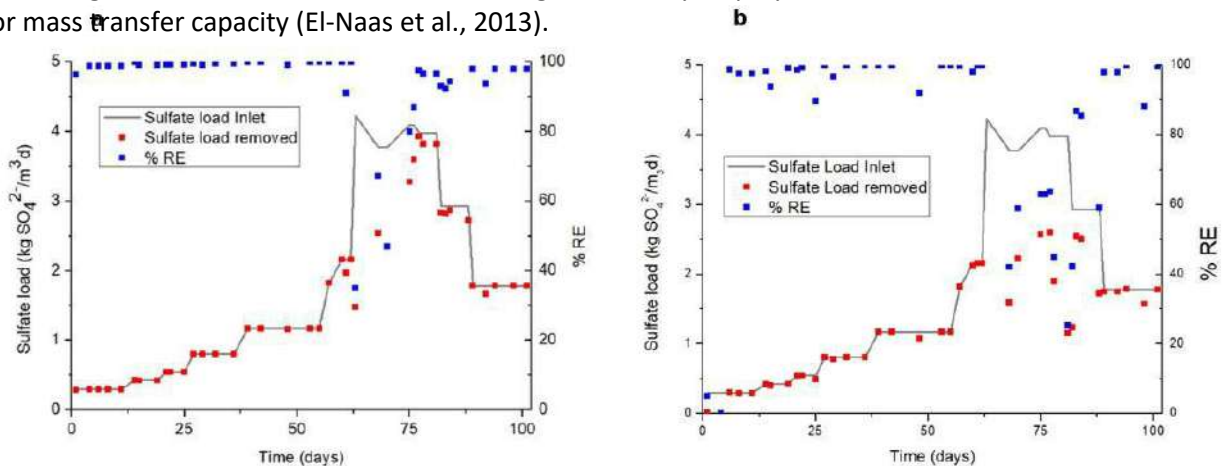


Figure 1. Sulfate removal log-term performance in a) CR and b) CSTR.

Table 1. Values of COD removal, H₂S, Total VFAs and Accumulated VSS concentration obtained for CR and CSTR.

	CR			CSTR		
Day of experiment	20	75	101	20	75	101
%RE COD	66,16	60,13	64,33	79,22	43,61	56,96
H ₂ S (mM)	0,094	0,8814	0,23	0,003	0,692	0,517
Total VFAs (mg/L)	0,028	1,083	0,742	0,061	0,862	0,429
Accumulated VSS (g/L)	0,009	0,022	0,023	0,015	0,072	0,0785

Conclusions

CR reactor filled with PVA-sludge granules presented a high stability at high sulfate load and in presence of toxic compounds such as H₂S and VFAs, compared to CSTR. Therefore CR could be an interesting option for future studies.

Acknowledgements: Authors acknowledge the Spanish Government through the project RTI2018-099362-B-C22 MINECO/FEDER, EU, for the financial support provided to perform this research.

References

- El-Naas, M. H., Mourad, A. H. I., & Surkatti, R. (2013). Evaluation of the characteristics of polyvinyl alcohol (PVA) as matrices for the immobilization of *Pseudomonas putida*. *International Biodeterioration and Biodegradation*, 85, 413–420. <https://doi.org/10.1016/j.ibiod.2013.09.006>
- Fernández-Palacios, E., Lafuente, J., Mora, M., Gabriel, D. (2019) Exploring the performance limits of a sulfidogenic UASB during the long-term use of crude glycerol as electron donor. *Science of the Total Environment*, 688, 1184–1192. <https://doi.org/10.1016/j.scitotenv.2019.06.371>
- Lens, P. N. L., Gastesi, R., & Lettinga, G. (2003). Use of sulfate reducing cell suspension bioreactors for the treatment of SO₂ rich flue gases. *Biodegradation*, 14(3), 229–240. <https://doi.org/10.1023/A:1024222020924>
- Mora, M., Fernández-Palacios, E., Guimerà, X., Lafuente, J., Gamisans, X., & Gabriel, D. (2020). Feasibility of S-rich streams valorization through a two-step biosulfur production process. *Chemosphere*, 253, 126734. <https://doi.org/10.1016/j.chemosphere.2020.126734>
- Zhang, M., Wang, H., & Han, X. (2016). Preparation of metal-resistant immobilized sulfate reducing bacteria beads for acid mine drainage treatment. *Chemosphere*, 154, 215–223. <https://doi.org/10.1016/j.chemosphere.2016.03.103>



Analysis of PM_{2.5} and PM₁₀ concentrations trends in selected Greek urban cities before and after the national lockdowns caused by the COVID-19 pandemic

P. Begou¹

¹Laboratory of Meteorology and Climatology, Department of Physics, University of Ioannina, Ioannina, Greece

Corresponding author email: p.begou@uoi.gr

keywords: Greek urban areas; urban air pollution; air quality; particulate Matter; PM₁₀; PM_{2.5}.

Introduction

The ambient air pollution is a major environmental concern in the urban areas of Greece. In the highly urbanized cities of Greece such as Athens, Thessaloniki and Patra two types of air pollution have been identified, the photochemical smog and particulate matter pollution (Valavanidis et al., 2015). Although there has been good progress in the implementation of the ambient air quality legislation in Greece, the high population density and the economic activities in the urban areas contribute to the high levels of air pollution. The air pollution problems are often exacerbated by factors that favour the accumulation of air pollutants over the cities, such as the urban landscape and the topography changes based on the urbanization progress and the urban sprawl (e.g., build-up areas, bare land, lack of vegetation, narrow and deep street canyons). Other factors such as adverse meteorological conditions, temperature inversions, low wind speed, high ambient temperature and intense sunshine duration worsen the air quality and cause air pollution episodes (Sindosi et al., 2019). Moreover, Saharan dust events are often associated with the high levels of PM₁₀ concentrations. On the other hand, vehicular traffic and residential heating are major sources of PM. Emissions from the combustion of fossil fuel or wood burning, heat stoves and fireplaces produce much of the PM_{2.5} ambient air pollution (Valavanidis et al., 2015).

During the lockdowns periods due to COVID-19 pandemic, the air quality in some places improved and the ground-based and satellite observations showed a decline in the concentrations of air pollutants emitted from the anthropogenic activities and the vehicular traffic (Varotsos et al., 2021; Zerefos et al., 2021).

The objective of this study is to assess and evaluate the PM_{2.5} and PM₁₀ concentrations in selected Greek urban cities during the lockdown periods. For this purpose, we use the data on PM_{2.5} and PM₁₀ concentrations from air quality monitoring stations in Athens (Aristotelous street, station name: ARI), Thessaloniki (Agia Sofia, station name: AGS) and Patra (station name: PAll).

Materials and methods

The data on PM_{2.5} and PM₁₀ concentrations were derived by the air quality monitoring stations of the National Air Pollution Monitoring Network (NAPMN) which is operated by the Air Quality Department of the Ministry of Environment. The air pollution data is available online in the Ministry's official website (www.yopen.gov.gr). The 24-hour PM_{2.5} and PM₁₀ concentrations data were collected from air quality monitoring stations in Athens, Thessaloniki and Patra, from the 1st of January 2017 to the 31st of December 2020. We chose to include stations which have been installed at areas characterized as "Urban-traffic" sites. The analysis of the PM_{2.5} and PM₁₀ concentrations was performed in the computer software "R" by using the package "openair", which is an open-source tool for analyzing air pollution data (Carslaw and Ropkins, 2012).

Results and discussion

In order to evaluate the effect of COVID-19 pandemic lockdowns on air quality, we split the PM_{2.5} and PM₁₀ concentrations data into two time periods, before and after January 2020. The monthly PM_{2.5} concentrations before January 2020 indicate the mean monthly values over the period 2017-2019, while the monthly PM_{2.5} concentrations after January 2020 consists of the measurements over the period from 1st of January 2020 to 31st of December 2020. At ARI, AGS and PAll air quality monitoring stations, both PM_{2.5}



and PM₁₀ mean monthly concentrations showed a significant decrease during the lockdown periods in 2020 attributed to the reduction of the anthropogenic activities and the human mobility restrictions (Figure 1).

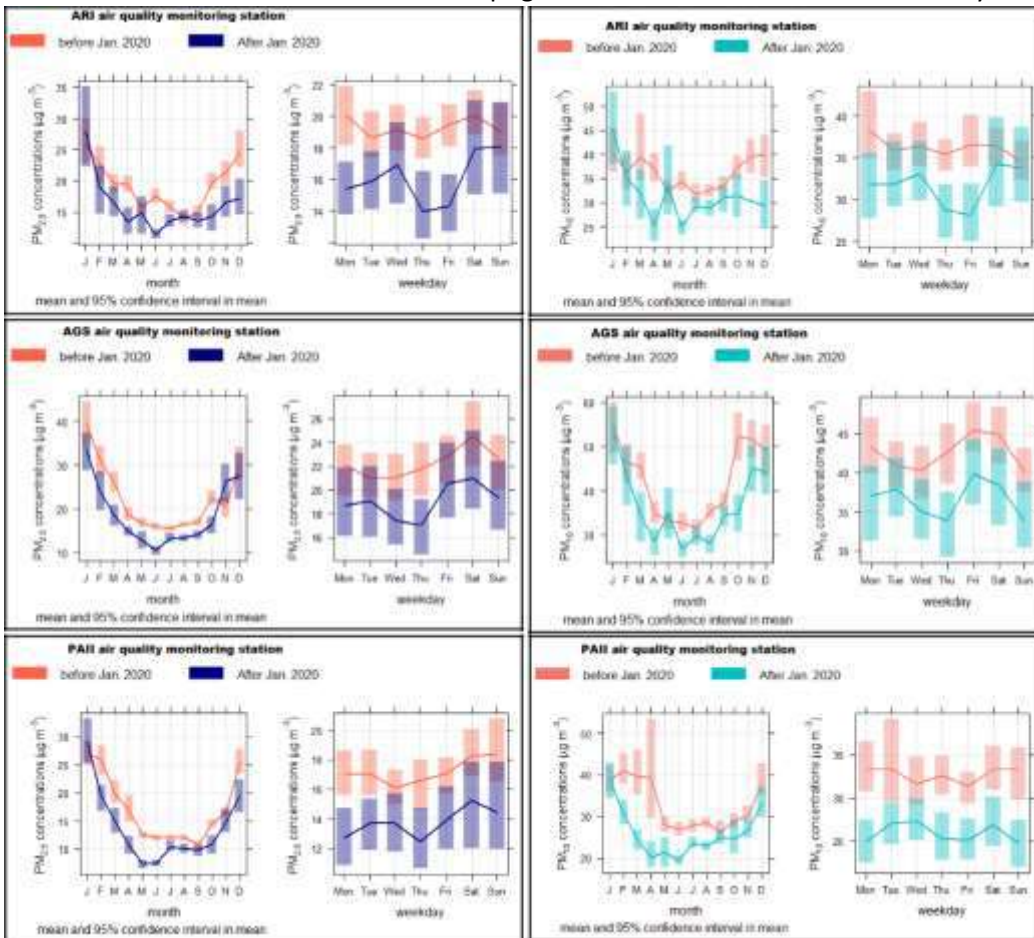


Figure 1. The average monthly PM_{2.5} and PM₁₀ concentrations ($\mu\text{g}/\text{m}^3$) in the air quality stations ARI, AGS and PAII before January 2020 (mean monthly values for the period 2017–2019) and after January 2020.

Conclusions

The purpose of this study was to investigate the air quality improvement during the lockdowns using PM_{2.5} and PM₁₀ concentrations data from air quality monitoring stations in Athens, Thessaloniki and Patra. We found that the average monthly PM_{2.5} and PM₁₀ concentrations declined during the shutdown compared to the long-term records of the airborne particulate pollution over the period 2017–2019.

References

- Carslaw D. and Ropkins K. (2012). openair - An R package for air quality data analysis. Environmental Modelling & Software. Volumes 27–28, January–February 2012, Pages 52–61.
- Sindosi O.A., Markozannes G., Rizos E., Ntzani E. (2019). Effects of economic crisis on air quality in Ioannina, Greece. Journal of environmental science and health. Part A, Toxic/hazardous substances & environmental engineering, 54(8), 768–781.
- Valavanidis A., Vlachogianni Th., Loridas S., Fiotakis C. (2015). Atmospheric Pollution in Urban Areas of Greece and Economic Crisis. Trends in Air Quality and Atmospheric Pollution Data, Research and Adverse Health Effects. Department of Chemistry, University of Athens. 1. 1–27. www.chem.uoa.gr.
- Varotsos C., Christodoulakis J., Kouremadas G.A., Fotaki E.F. (2021). The Signature of the Coronavirus Lockdown in Air Pollution in Greece. Water, air, and soil pollution, 232(3), 119.
- Zerefos C.S., Solomos S., Kapsomenakis J., Poupkou A., Dimitriadou L., Polychroni I.D., Kalabokas P., Philandras C.M., Thanos D. (2021). Lessons learned and questions raised during and post-COVID-19 anthropopause period in relation to the environment and climate. Environment, development and sustainability, 23(7), 10623–10645.



Cumulative Impact Assessments of Power Generations in Southeastern Bangladesh

M.M. Karim¹, N. Bindra² and A. Masud³

¹Engconsult Ltd., 108 Earlsbridge Blvd., Brampton, Ontario, Canada

²Ontario Power Generation, Pickering, Ontario, Canada

³Department of Health Studies, University of Waterloo, Waterloo, Ontario, Canada

Corresponding author email: info@eng-consult.com

keywords: *cumulative impact assessment; dispersion modeling; power generation; Bangladesh.*

Introduction

Cumulative assessment is a tool for project developer to try and take into consideration not only its own contribution to cumulative impacts, but also other projects and external factors that may place their developments at risk.

Materials and methods

This study assessed the cumulative impacts of air emissions from 22 major powerplants in southeast of Bangladesh planned to generate 21,550 MW of electricity. It also includes anticipated growth in small to medium size industries, brick fields, highway traffic, inland water transport, transhippers, jetty, and vessel transports used for transporting fuel resources for these power plants. A 50 km by 50 km airshed is considered for air quality modeling.

Results and discussion

Cumulative analysis indicate that predicted maximum ground level concentrations (MGLCs) of NO₂ and CO are complying with both Bangladesh National Ambient Air Quality Standards (NAAQS) and World Bank Group (WBG) Guidelines. Daily average MGLC of PM_{2.5} (62.45 µg/m³) from all sources complies with NAAQS, however, exceeds the WBG Guidelines. Annual PM_{2.5} concentration (15.45 µg/m³) exceeds NAAQS and WBG Guidelines. The PM₁₀ concentration complies with the NAAQS for both 24-hr and annual averaging times. Annual average concentration (23.12 µg/m³) exceeds WBG Guidelines. Daily average SO₂ concentration (102.49 µg/m³) complies with the NAAQS however exceeds the WBG guideline values. High concentrations of PM_{2.5} and SO₂ are due to the contribution of transboundary emission and secondary pollutants in the atmosphere. This dispersion modeling outcome can be used by the policy makers for the pollution reduction strategy.

Table 1 presents the output of cumulative impacts on the air quality for all existing, project and future sources up to 2036. For NO₂, maximum ground level concentrations were modeled for 1-hour and annual averaging periods to compare with national standards (DOE 2005) and WBG Guidelines. For short-term compliance modeling (i.e., 1-hour averaging period), percentiles are used to account for unusual/extreme metrological conditions and avoid overestimation of predicted concentrations.

USEPA Tier-1 approach assumes 100% conversion of NO_x emissions into NO₂, this approach tends to drastically overestimate results. In the Tier-2 (Ambient Ratio Method, ARM) approach, the predicted ground level concentrations are multiplied by an ambient NO₂/NO_x ratio to get more realistic and accurate results. The ARM uses an ambient equilibrium NO₂/NO_x ratio which is empirically derived based on regional monitoring data (Hanrahan 1999).

When site specific data is unavailable, the EPA exposure assessment guidelines recommend using a default ambient equilibrium NO₂/NO_x ratio of 0.75, based on a study by Chu and Meyer, 1991. According to data from Narayanganj CAMS monitoring station of DOE (CEGIS 2015) an ambient equilibrium NO₂/NO_x ratio of 0.65 was calculated. However, this ratio is dependent on many regional factors such as sunlight, climate etc. and Narayanganj is about 200 km from the project site. Therefore, as per practice of modeling for worst-case scenario, the 0.75 value is used in this study.

A Tier-3 approach was used to model the NO₂ concentrations in this study (USEPA 1992). In a Tier-3 approach, along with using ambient equilibrium ratio, background ozone levels are also considered, to get realistic results for fate of NO₂ in the atmosphere. Once NO_x enters the atmosphere, several potential



chemical reactions that can occur, depending on the relative amounts of NO and NO₂, the total NO_x, the ambient meteorological conditions, and other atmospheric trace gasses available for reaction. In most cases, the fastest and most important reactions of NO_x involve O₃ (Karim and Ohno 2000, USEPA 2015) as per the

following equation: $\text{NO} + \text{O}_3 \rightarrow \text{NO}_2 + \text{O}_2$

Table 1: Predicted Maximum Concentrations of Cumulative Case

Pollutant	Averaging Time	Concentration ($\mu\text{g}/\text{m}^3$)			Coordinates of Max Point (UTM)	
		ECR 1997 (as amended, 2005)	WBG Guidelines	Max Value	East (m)	North (m)
NO ₂	1-hr	N/A	200	168.95	393621	2381307
	Annual	100	40	22.06	393621	2413807
CO	1-hr	40,000	N/A	4,185.67	393621	2413807
	8-hr	10,000	N/A	1,818.89	393621	2413807
PM _{2.5}	24-hr	65	75 (IT-1)	62.45	403616.2	2386482
	Annual	15	15 (IT-3)	15.45	403616.2	2386482
PM ₁₀	24-hr	150	150 (IT-1)	104.07	403616.2	2386482
	Annual	50	30 (IT-3)	23.12	403616.2	2386482
SO ₂	24-hr	365	125 (IT-1)	102.49	396121	2396307
	Annual	80	-	14.78	396121	2396307

Conclusions

Cumulative air quality assessment was made to assess the capacity of the airshed for all planned and forceable future development in two major energy producing hubs of southeastern Bangladesh. The study result is extremely useful for the policy makers to exercise an informed decision on the future development in the area. The outcome can be applied for policy decisions to other parts of the country and the region. The results of this cumulative assessment can be a useful tool to assess the future air quality and make policy decisions for the current development. Once information is available about the state of air quality after the implementation of the first round of projects in 2025 and the pressures on it, and the regional criteria have been determined. It is then possible to quantify the emission reductions required from different sources (both operating and planned for the years 2030 and 2036) to achieve the criteria or guideline value.

Acknowledgements: Authors wish to confer thanks to Electricity Generation Company Bangladesh for providing support during the whole study period.

References

- CEGIS (2015); Environment Impact Assessment (EIA) for the Unit 4 Repowering of Ghorashal Thermal Power Plant, Bangladesh Power Development Board.
- Chu, S. and Meyer, E.L. (1991); Use of Ambient Ratios to Estimate Impact of NO_x Sources on Annual NO₂ Concentrations. In Proceedings of the 84th Annual Meeting & Exhibition, Air & Waste Management Association: Pittsburgh, PA; Paper 91-180.6.
- Department of Environment (DOE) (2005) Amended Environmental Conservation Rules of 1997, Government of Bangladesh.
- Hanrahan, P (1999); The Plume Volume Molar Ratio Method for Determining NO₂/NO_x Ratios in Modeling— Part I: Methodology, Journal of the Air & Waste Management Association, 49:11, 1324-1331, DOI: 10.1080/10473289.1999.10463960
- Karim, M. M. and Ohno, T. (2000); Air Quality Planning and an Empirical Model to Evaluate SPM Concentrations, Journal of Environmental Engineering, American Society of Civil Engineers, 126(12), 1116-1124. DOI: 10.1061/(ASCE)0733-9372(2000)126:12(1116)
- USEPA (1992); Guidelines for Exposure Assessment, United States Environment Protection Agency.
- USEPA (2015) Health <https://www.epa.gov/no2-pollution>, page visited on May 19, 2020.



Is there any correlation between the diabetes mellitus and atmospheric pollutants?

M. Koliba^{1,2,3}, D. Zmijková⁴ and H. Raclavská⁵

¹Diabetic and podiatric clinic, Vratimov, Czech Republic

²Department of Internal medicine, University Hospital Ostrava, 708 52 Ostrava, Czech Republic

³Department of Internal Studies, Faculty of Medicine, University of Ostrava, 703 00 Ostrava, Czech Republic

⁴Faculty of Mechanical Engineering, Czech Technical University in Prague, Prague 6-Dejvice, Czech Republic

⁵Centre ENET, VŠB-Technical University of Ostrava, Ostrava-Poruba, Czech Republic

Corresponding author email: mrkoliba@seznam.cz

keywords: *diabetes mellitus; diabetic complications; atmospheric pollution.*

Introduction

Diabetes mellitus has been considered a disease without any evident relationship to the quality of the environment for a relatively long time. Nowadays, some authors suppose a significant role of selected environmental factors in the etiopathogenesis of diabetes and its complications. The biological agents in the form of selected viruses were the first environmental factors connected with the occurrence of diabetes mellitus in the population (Nečas, 2003). During the next time period, it was found that some air pollutants could be responsible for the growing number of people with diabetes. According to Dales et al. (2012), air pollution (carbon monoxide, ground ozone, sulphur dioxide, nitrogen oxides, PM₁₀, PM_{2.5}) appears to increase the risk of acute complications of diabetes requiring hospitalisation. Ikenna et al., 2014 mention that long-term air pollution exposure (PM₁₀, nitrogen dioxide) is associated with type 2 diabetes. The association can be observed at concentrations below air quality guidelines. Thiering and Heinrich (2014) document that diabetic patients may be more vulnerable to ambient air pollution exposure effects. Balti et al. (2014) mention a significant association between increased risk for type 2 diabetes and nitrogen dioxide and PM_{2.5}.

The basic aim of this study was an evaluation of the possible relationship (association) between the abundance (frequency) of diabetes mellitus or its complications and atmospheric pollutants. Via this paper, three fundamental questions mentioned lower should be answered:

1. Are there any air pollutants that impact the distribution and frequency of diabetes mellitus in the population?
2. Is there any connection between atmospheric contamination and the rate of diabetic complications?
3. Is it possible to prevent diabetes mellitus and its complications by improving ambient air quality?

Materials and methods

Essential health data were obtained from the International Diabetes Federation and the Institute of Health Information and Statistics database of the Czech Republic. Necessary environmental data were provided by Czech Hydrometeorological Institute and European Environment Agency. Correlation analysis was applied to assess the association between the frequency of diabetes 2 type and its complications and the level of some atmospheric pollutants (particulate matter PM₁₀, particulate matter PM_{2.5}, nitrogen oxides, ground ozone and benzo(a)pyrene). Correlation analysis was realized using the software OriginPro 2021.

Results and discussion

Based on this paper, it is possible to assume a significant association exists between the frequency of diabetes mellitus or its complications and air pollution. Through the mediation of correlation analysis, a significant association was found between the occurrence of type 2 diabetes and air concentration of PM_{2.5} ($r=0.33$; $p=0.05$) and ground ozone ($r=0.49$; $p=0.01$) in the European region and Turkey in 2010. The other significant dependence was identified between mortality of diabetics and atmospheric concentration of PM₁₀ ($r=0.52$; $p=0.05$), ground ozone ($r=0.42$; $p=0.05$) and benzo(a)pyrene ($r=0.48$; $p=0.05$) in 2010 in European countries and Turkey. In 2019, the findings were similar – significant relationship between the number of deaths and



the following air pollutants – PM₁₀ (r=0.38; p=0.01), ground ozone (r=0.42; p=0.05), and benzo(a)pyrene (r=0.6; p=0.05) was detected.

In relationship to the occurrence of diabetes mellitus, the accessible resources mention particularly the following spectrum of atmospheric pollutants – i. e., some fractions of suspended air particles (PM₁₀, PM_{2.5}) (Dales et al., 2012, WHO, 2021, Yang et al., 2020), ground ozone (O₃) (Dales et al., 2012, Jerrett et al. 2017), nitrogen oxides (NO_x) (Dales et al., 2012, Liu et al., 2019), sulphur dioxide (SO₂) (Dales et al., 2012), carbon monoxide (CO) (Dales et al., 2012) and selected chemical compounds present on the surface structure of particulate matter (polycyclic aromatic hydrocarbons, toxic compounds) (Srivastava et al., 2021). According to the results of this paper and the studies carried out so far (Dales et al., 2012), it is possible to expect a reduction in the prevalence of diabetic cases and the frequency of diabetes complications in the condition of persistent improvement of air quality.

Table 1. Results of correlation analysis between parameters of type 2 diabetes and concentration of atmospherical pollutants in the years 2010 and 2019 in the European region and Turkey.

Atmospheric pollutant	2010		2019	
	abundance	mortality	abundance	mortality
PM ₁₀	r =0.68; p=0.05	r=0.52; p=0.05	-	r=0.38; p=0.1
PM _{2.5}	r=0.33; p=0.05	-	-	r=0.38; p=0.1
ground O ₃	r=0.49; p=0.01	r=0.42; p=0.05	-	r=0.42; p=0.05
BaP	r=0.38; p=0.1	r=0.48; p=0.05	-	r=0.6; p=0.05
NO _x	r=0.3; p=0.1	-	r=0.3; p=0.1	-

Explanations: PM₁₀ – particulate matter with diameter lower than 10 µm, PM_{2.5} – particulate matter with diameter lower than 2.5 µm, O₃ – ozone, BaP – benzo(a)pyrene, NO_x – nitrogen oxides, red highlights – statistically significant correlation, blue highlights – statistically insignificant correlation

Conclusions

Based on the results of this paper and other research works, diabetes mellitus can be considered a disease with altogether significant participation of some air pollutants (PM₁₀, PM_{2.5}, ground ozone, benzo(a)pyrene) in the etiopathogenesis. Atmospheric pollutants are primarily associated with type 2 diabetes and its complications. In future studies, it will be necessary to verify and determine the role and the portion of partial air pollutants in the etiopathogenesis of diabetes mellitus or diabetic complications.

References

- Dales, E.R., Cakmak, S., Vidal, C.B. and Rubio, M.A., 2012. Air pollution and hospitalization for acute complications of diabetes in Chile. *Environ. Int.* 46, 1–5.
- Liu, F., Chen, G. and Huo, W., 2019. Associations between long-term exposure to ambient air pollution and risk of type 2 diabetes mellitus: A systematic review and meta-analysis. *Environ. Pollut.* 252, 1235–1245.
- Nečas, E., 2003. *Pathological physiology of organ systems (part II)*. Charles University, Prague, Czech Republic.
- Srivastava, S. 2021. Effects of environmental polycyclic aromatic hydrocarbon exposure and pro-inflammatory activity on Type 2 Diabetes Mellitus. *MedRxiv*.3, 10.08.21264766.
- Thiering, E. and Heinrich, J., 2015. Epidemiology of air pollution and diabetes. *Trends Endocrinol. Metab.* 26 384–394.
- WHO, 2021. *WHO global air quality guidelines: particulate matter (PM_{2.5} and PM₁₀), ozone, nitrogen dioxide, sulfur dioxide and carbon monoxide: executive summary*. World Health Organization, 2021.
- Yang, J., Zhou, M., Zhang, F., Yin, P., Wang, B., Guo, Y., Wang, H., Zhang Ch., Sun, Q., Song, X. and Liu, Q., 2020. Diabetes mortality burden attributable to short-term effect of PM₁₀ in China. *Environ. Sci. Pollut. Res.* 27, 18784–18792.
- Jerrett, M., Brook, R., White, L.F., Burnett, R.T., Yu, J., Su, J., Seto, E., Marshall, J., Palmer, J.R., Rosenberg, L. and Coogan, P.F., 2017. Ambient ozone and incident diabetes: A prospective analysis in a large cohort of African American women. *Environ. Int.* 102, 42–47.



Reducing methane emissions at gas transmission networks. Best practices literature review and case studies.

A. Tsochatzidi¹ and N.A. Tsochatzidis²

¹Department of Chemical Engineering, Aristotle University of Thessaloniki, Greece

²Hellenic Gas Transmission System Operator (DESFA) SA, Greece

Corresponding author email: n.tsochatzidis@desfa.gr

keywords: methane emissions; gas network; greenhouse gases.

Introduction

Methane, the main component of natural gas, is one of the most important contributor to climate change and plays a dominating role in how fast the climate warms. Climate policies heavily emphasize actions that benefit the climate in the long-term such as decarbonization and reaching net-zero emissions (Ocko et al., 2021). Methane contributes to at least 25% of today's climate warming, and its concentration in the atmosphere continues to rise rapidly, in large part from anthropogenic sources (GMA, 2021).

Gas transmission operators, worldwide, are carrying out intensive programs on the quantification of the total methane emissions in their activities and are designing mitigation measures for methane emissions reduction. This paper presents a literature survey on this topic. Also, characteristic case studies from gas companies and from DESFA, the Hellenic gas transmission system operator, are discussed. Methane emissions of each case study are quantified to serve as quick reference for similar applications.

Materials and methods

The Oil & Gas Methane Partnership 2.0 (OGMP, 2020) is a multi-stakeholder initiative launched by United Nations Environment Programme and the Climate and Clean Air Coalition, as a voluntary initiative to help companies reduce methane emissions in the oil and gas sector. Through participation in the OGMP associated reporting, companies were provided with a credible mechanism to systematically and responsibly address their methane emissions, and to demonstrate this systematic approach and its results to stakeholders. DESFA has adhered to this partnership with 80 well known enterprises worldwide, of the oil & gas business.

The methodologies for evaluating the methane emissions from the gas systems are based on statistic approaches using specific 'activity factors' (the emitting equipment population) and 'emission factors' (the frequency of emitting events). Lately direct measurements of methane emissions are used to increase confidence of estimation. Methane emissions are divided in three macro categories (Marcogaz, 2019):

- Fugitive emissions
- Vented emissions (including pneumatic emissions)
- Emissions from incomplete combustion (unburnt)

The transmission segment of a natural gas system comprises the transmission pipeline networks, the compressor stations and the metering and pressure-regulating stations. Among the available methane emissions abatement technologies are: leak detection and repair surveys, convert gas pneumatic controls to instrument air, reinjection of methane, lower gas line pressure before maintenance, replace continuous gas vent, replace wet seals with dry seals in centrifugal compressors (Yusuf et al., 2012).

Results and discussion

Leak detection and repair (LDAR) refers to the process of locating and repairing fugitive leaks. LDAR encompasses several techniques and equipment types (IR cameras, sniffers, etc.). According to Ravikumar et al. (2020) the total methane emissions reduced by 44% after one LDAR survey at natural gas facilities, combining a reduction in fugitive emissions of 22% and vented emissions by 47%. Furthermore, more than 90% of the leaks found in the initial survey were not emitting in the re-survey, suggesting high repair effectiveness. However, fugitive emissions reduced by only 22% because of new leaks that occurred between the surveys. This indicates a need for frequent, effective, and low-cost LDAR surveys to target new leaks.

Replace continuous gas Vent with nitrogen. At large gas facilities emergency Vent lines are continuously purged with gas to prevent air introduction to the pipes. Nitrogen can be used instead of gas for this purging.



Figure 1 depicts the Vent stack of DESFA's Sidirokastro border metering station of a height 10 m, vent tip length 2 m and width 0,2 m. This Vent stack has a design purge gas consumption 0,51 Nm³/h, which results to methane emissions of 3200 kg/y, a released methane quantity that can be avoided with the replacement of gas with nitrogen.

Replace gas with air at gas operated control Valves. The gas consumption of a 24" ANSI 600 pressure / flow control valve, gas operated with spring opening piston actuator, is 1,3 m³/hr for the valve positioner at 7 barg supply. Also for the I/P converter the gas consumption is 0,16 m³/hr and for one complete stroke (open to close) of this valve, the gas consumption is 0,038 m³. When a continuous operation of this valve is considered, the maximum yearly methane emissions are estimated to 9200 kg/y, which can be avoided using instrument air instead of gas for the valve operation. Indeed, some years ago, DESFA replaced such gas operated valves at Sidirokastro border metering station with air operated valves (Figure 2) to reduce methane emissions.

Replace Wet seals with Dry seals at compressors. Centrifugal compressors have seals along their shaft to keep gas from escaping. Wet, or oil-lubricated, seals by design result in substantial methane leakages. Dry seals operate mechanically without seal ring lubrication, which in its turn reduces gas leakage.



Figure 1. Continuous Vent stack



Figure 2. Air operated flow control valve

Conclusions

Application of best practices may result in a significant reduction of methane emissions in a gas transmission system. A literature survey on this topic along with a number of case studies are presenting in this paper. Quantification of methane emissions reduction at the case studies offers a quick estimation for similar cases at gas networks. This analysis aims to contribute in better understanding of methane emissions sources and the adoption of methane emissions reduction measures at gas transmission systems.

References

- Ocko, I.B. et al., 2021. 'Acting rapidly to deploy readily available methane mitigation measures by sector can immediately slow global warming', *Environ. Res. Lett.* 16, 054042.
- Global Methane Assessment. Benefits and Costs of Mitigating Methane Emissions, 2021. *United Nations Environment Programme*, ISBN: 978-92-807-3854-4.
- OGMP, 2020. Mineral Methane Initiative OGMP2.0 Framework, 19 November, 2020
https://www.eenews.net/assets/2020/11/23/document_ew_06.pdf.
- Marcogaz, 2019. WG_ME-485, Assessment of methane emissions for gas Transmission and Distribution system operators.
- Yusuf, R.O. et al., 2012. Methane emission by sectors: A comprehensive review of emission sources and mitigation methods, *Renew. Sust. Energ. Rev.*, 16, 5059-5070.
- Ravikumar, A.P. et al., 2020. Repeated leak detection and repair surveys reduce methane emissions over scale of years, *Environ. Res. Lett.*, 15, 034029.



SUST
ENG
2022



MICROALGAE



Effect of carbon concentration on the fatty acid distribution and basic FAME properties of the bio-oil of *Chlorella sorokiniana*

G. Papapolymerou¹, A. Mpesios¹, A. Kokkalis³, D. Kasiteropoulou¹, M. N. Metsoviti¹
and A. Papadopoulou¹

¹Dept. of Environmental Studies, University of Thessaly, Gaiopolis, Larissa, Greece

²Department of Agrotechnology, University of Thessaly, Gaiopolis, Larissa, Greece

³GRINCO S.A., Industrial Area of Larisa, Makrychori Larisas, Greece

Corresponding author email: papapoly@uth.gr

keywords: *chlorella sorokiniana*; heterotrophic; glycerol; anaerobic digestate; FAME properties.

Introduction

Microalgae are unicellular photosynthetic organisms that use light and carbon dioxide, with higher photosynthetic efficiency than plants, for the production of biomass. Some microalgae species can also grow and multiply heterotrophically in the absence of light if an organic carbon source becomes available (Mata et al., 2010). The main advantage of heterotrophic growth is higher biomass growth rates and biomass production because, unlike autotrophic growth, heterotrophic growth is not limited by light transmission through the growth medium. Another advantage of heterotrophic growth is the potential of achieving higher lipid content and, as a result, higher lipid productivities can be obtained. A number of review papers focus on the heterotrophic growth of several microalgal species and the trend is that heterotrophic growth enhances both the biomass and lipid productivity (Bumbak et al., 2011; Perez-Garcia & Bashan, 2015). In the heterotrophic growth, industrial by-products or waste streams containing dissolved organic carbon, macronutrients and micronutrients can be used in terms of nutrient recovery, waste minimization and cyclic economy. Anaerobic digestate (AD) is a rich source of macro and micronutrients while, crude glycerol has a very high content in organic carbon. The aim of this work is to examine the effect of the initial concentration of organic carbon from glycerol on the carbon uptake rate, the lipid and protein content and the fatty acid distribution and basic FAME (Fatty Acid Methyl Ester) properties of the biomass and bio-oil of *Chlorella sorokiniana*. Glycerol is used as the main source of organic carbon and AD is used to provide macro and micronutrients.

Materials and methods

The cultivation of *C. sorokiniana* was carried out in glass orthogonal bioreactors of 42L capacity each that were filled to 75% of their volume. Air was continuously provided to each bioreactor through a perforated network of piping placed at the bottom of the bioreactor tank. The temperature of the cultures was kept at 28 ± 0.5 °C and the pH was held constant at 7 ± 0.3 . The bioreactors, the glass tubing and the culture medium were sterilized before use. The microalgae species *C. sorokiniana* (SAG strain 211-31) was obtained from Culture Collection of Algae from the University of Göttingen in Germany (EPSAG). Glycerol and AD were obtained from local biodiesel and biogas plants. AD was filtered, centrifuged and sterilized before use. The concentration of initial nitrogen was 110 mg/l in all five cultivations. The initial concentration of nitrogen was held constant in all bioreactors and the initial carbon concentration was varied from 1.98 g/l to 17.50 g/l. A cultivation without anaerobic digestate was carried out as a blank. The composition of the samples was determined according to AOAC methods. For the determination of organic carbon, the method of Walkley–Black was used. The total lipid content was determined with extraction using co-solvents of n-hexane/isopropanol in the microalgal biomass in accordance with the method of Bian et al (2018). The saponification number (SN) and the iodine value (IV) were calculated theoretically from the Fatty Acid (FA) distribution (Azam et al. 2005). Similarly, the cetane number (CN) was evaluated from the theoretical equations (Demirbas 1998).

Results and discussion

As the initial carbon concentration (C_0) was increased the lipid content increased while the protein content decreased.



As the initial carbon concentration increased the protein content ranged from 36.6% to 19.1% while the respective lipid content ranged from 20.8% to 39.7%. The biomass yield increased as the initial carbon concentration increased and ranged from 1 gr/l to 3.5 gr/l. Fatty acids (FA) from C10: 0 to C24: 1 were produced. The carbon uptake rate was affected by the initial carbon concentration and increased from 0.37 gr/(l-d) to 0.73 gr/(l-d). The cultivation without the use of AD gave a carbon uptake rate, for the same Co, about 15% lower than the cultivation using AD and the same Co. However, the fatty acids that are found in the highest percentage are C16: 0, C16: 1, C18: 0, C18: 1 and C18: 2. The ratio C18: 1/C18: 2 ranges from about 2.5:1 to 7.8: 1. In most vegetable oils and seed oils C18: 2 is higher than C18: 1 while in *Chlorella sorokiniana* the opposite is observed. With respect to saturation, monosaturated FA were predominant in all treatments constituting from about 48% to 56% of the total FA, while significant percentages of saturated FA were produced ranging from about 29% to about 43%. With respect to the chain length medium chain FA (C16-C18) predominated constituting from 72.9% to 92.1% of the total FA. The basic three FAME properties namely, the iodine value (IV), the cetane number (CN) and the higher heating value (HHV) were estimated from validated empirical equations and were found to be within acceptable limits. Also, the saponification number (SN) for the bio-oil was within acceptable values. Cetane numbers were equal to 56.8, 61.4, 58.0 and 56.3 for initial carbon concentrations equal to 1.98, 3.79, 7.29 and 17.50 gr/l respectively while, for the cultivation where no anaerobic digestate was used with an initial carbon concentration equal to 7.24 gr/l the cetane number is equal to 55.6. The HHV ranged from 39.9 MJ/Kg to 42.0 MJ/kg.

Conclusions

Glycerol is easily absorbed and utilized by *Chlorella sorokiniana*. The biomass yields as well as the lipid content increased with increasing Co. However, the biomass productivities increased from 0.15 gr/(l-d) to 0.22 gr/(l-d) because longer cultivation times were needed as the Co increased. Lipid productivities increased from 32.9 mg/(l-d) to 86.8 mg/(l-d). The distribution of FA was predominant in monounsaturated and medium chain FA. The basic FAME properties were within acceptable limits. Cetane numbers were equal to 56.8, 61.4, 58.0 and 56.3 for Co values equal to 1.98, 3.79, 7.29 and 17.50 gr/l respectively while, for the cultivation where no anaerobic digestate was used with an initial carbon concentration equal to 7.24 gr/l the cetane number is equal to 55.6. The anaerobic digestate is a good source for the formulation of growth media for cultivating microalgae heterotrophically and possibly autotrophically. It provides macro and micronutrients and some carbon from undigested organic material thus, reducing the cost of the growth media for microalgal cultivation and also contributes to the recycling of important nutrients such as phosphorus and potassium. The bio-oil of *Chlorella sorokiniana* is appropriate for use in biodiesel production however, lipid productivities need to improve for a commercial application for biodiesel production. The remaining biomass can be utilized, for example, as a supplement to animal feed.

Acknowledgements: The study was co-financed by the European Regional Development Fund of the European Union and Greek national funds through the Operational Program Competitiveness, Entrepreneurship and Innovation, under the call RESEARCH – CREATE - INNOVATE (project code: T1EDK-01580).

References

- Azam, M.M.; Waris, A.; Nahar, N.M. Prospects and potential of fatty acid methyl esters of some non-traditional seed oils for use as biodiesel in India. *Biomass Bioenergy* 2005, 29, 293–302.
- Bian, X.; Jin, W.; Gu, Q.; Zhou, X.; Xi, Y.; Tu, R.; Han, S.; Xie, G.; Gao, S.; Wang, Q. Subcritical n-hexane / isopropanol extraction of lipid from wet microalgal pastes of *Scenedesmus obliquus*. *World J. Microbol. Biotechnol.* 2018, 34, 39.
- Bumbak, F., Cook, S., Zachleder, V., Hauser, S., Kovar, K. (2011). Best practices in heterotrophic high-cell-density microalgal processes: achievements, potential and possible limitations. *Applied microbiology and biotechnology*, 91(1), 31-46.
- Demirbas, A. Fuel properties and calculation of higher heating values of vegetable oils. *Fuel* 1998, 77, 1117– 1120.
- Mata, T. M., Martins, A. A., Caetano, N. S. (2010). Microalgae for biodiesel production and other applications: a review. *Renewable and sustainable energy reviews*, 14(1), 217-232.
- Perez-Garcia, O., Bashan, Y. (2015). Microalgal heterotrophic and mixotrophic culturing for bio-refining: from metabolic routes to techno-economics. *Algal biorefineries*, 61-131.



Removal of nutrients from saline water by algae

S.E. Biliiani¹ and I.D. Manariotis¹

¹Environmental Engineering Laboratory, Department of Civil Engineering,
University of Patras, Patras, Greece

Corresponding author email: idman@upatras.gr

keywords: saline water; nutrients; macroalgae.

Introduction

Microalgae can grow in different environments from fresh to seawater even in sewage. Many microalgae species can grow under autotrophic, mixotrophic and heterotrophic conditions. The water type of the medium also affects the microalgae growth and the content of lipids of the biomass (Tsavatopoulou et al., 2019). Algal species differ in their adaptability to salinity and other stress conditions (Biliiani and Manariotis, 2021). Marine algal strains that could grow in brackish water or seawater have clear advantages over freshwater algae concerning water use, and could be a more economic feedstock alternative for algal-based biodiesel production (Shih-Hsin Ho et al., 2014). Wastewater particularly in coastal areas may have high electric conductivity due to seawater intrusion into the sewer network (Biliiani and Manariotis, 2021). Nutrient removal from seawater by marine algal strains is examined at different initial biomass concentration.

Materials and methods

Algal biofilm was collected from the Patras shoreline near the new port and placed in a 1 L Erlenmeyer flasks. The experiment was performed in two periods. In the beginning of each period the concentration of phosphates was 5 mg P/L and the concentration of nitrates 10 mg NO₃/L. The 1st cycle lasted from Day 0 to 22 and the 2nd period from Day 23 to 55. At the end of the 1st period, algal biomass was removed. The Erlenmeyer flasks were placed in an incubation room at a temperature of 15±2°C for 55 days with continuous light (130 μmol/m²s) and stirring (10 rpm).

Total solids (TSS) were determined gravimetrically (APHA et al., 2012). Chl-a was measured in the supernatant and the mixed liquor via a spectrophotometric method (APHA et al., 2012). Soluble total phosphorus (STotal-P) was measured by the persulfate method and ascorbic colorimetric technique (APHA et al., 2012). Nitrates concentration was determined by the sodium salicylate method (Fresenius et al., 1988).

Results and discussion

Biomass was expressed as TSS concentration in the culture, and was increased during the operation period. At the beginning of the 2nd period (day 22) 500 mg/L of the biomass were removed. The biomass concentration during the 1st period was increased in two steps, while in the 2nd period its increase was linear (**Figure 1a**). Although biomass concentration was the same in both periods, in the 2nd period chl-a concentration was higher. Chl-a concentration followed a similar pattern as TSS concentration (**Figure 1b**), and was 160 and 395 mg/m³ at the end of the 1st and 2nd period, respectively.

Nitrates and phosphates concentration was 10 mg NO₃/L and 5 mg P/L, respectively at the beginning of each period. On Day 22 biomass was withdrawn and nutrients were spiked in to bottle in order to reach the same concentration as in the beginning of the 1st period.

The biomass withdrawal led to 2.3 times increase of the time required in order macroalgae to completely consume nitrates **Figure 1c**. Nitrates consumption in both periods was faster than the phosphates. The consumption of sTotal-P was 25% lower in the 2nd period compared to the 1st period **Figure 1d**. Complete consumption of both nutrients was achieved after 22 days in both periods.

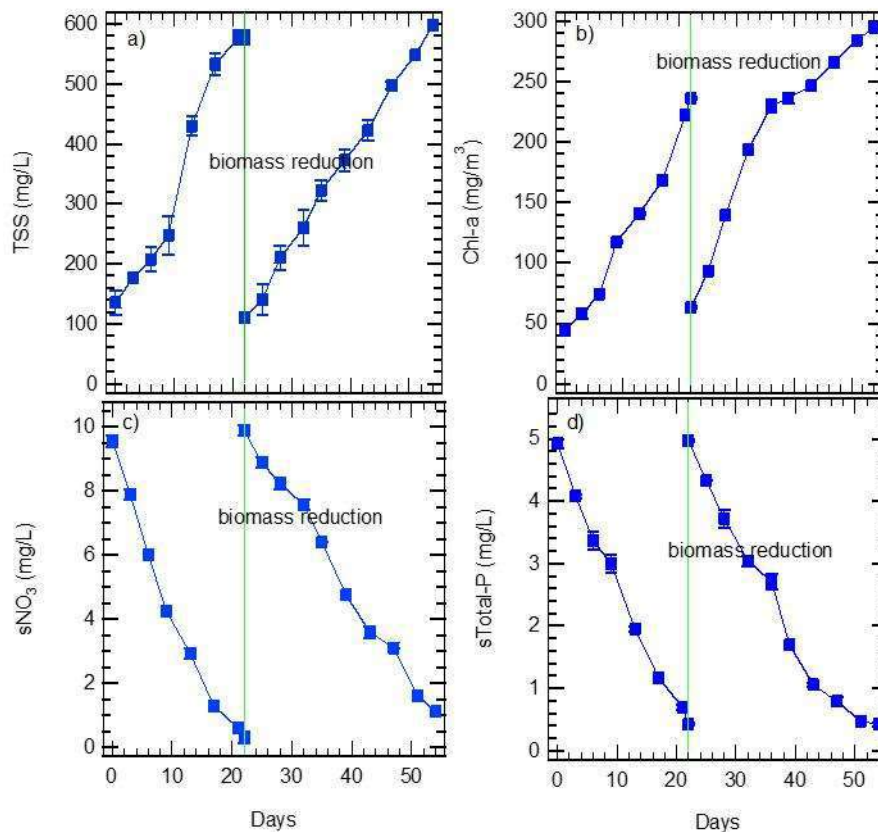


Figure 1. Concentration of a) TSS, b) chl-a, c) NO₃ and d) sTotal-P in the liquid of macroalgae cultures.

Conclusions

Macroalgae can grow in different environments from freshwater to seawater and remove nutrients. Even though 83% of the biomass was removed from the reactor, macroalgae responded very well into the new operating conditions indicating their potential for the treatment of saline waters.

Acknowledgements: This work was supported by EEA and Norway Grants 2014-2021 through the project "BLUE-GREENWAY: Innovative solutions for improving the environmental status of eutrophic and anoxic coastal ecosystems", (project number 2018-1-0284, Support for Regional Cooperation).

References

- APHA, WEF, AWWA, 2012. Standard methods for the examination of water and wastewater: 20th ed, Choice Reviews Online. Washington, D.C. <https://doi.org/10.5860/choice.37-2792>
- Biliani, S.E., Manariotis, I.D., 2021. Sodium chloride and nitrogen effects on *Chlorella vulgaris* growth and biocommodities production 237, 159–169. <https://doi.org/10.5004/dwt.2021.27729>
- Fresenius, W., Quentgen, K.E., Schneider, W., Others, 1988. Water analysis; a practical guide to physico-chemical, chemical and microbiological water examination and quality assurance.
- Shih-Hsin Ho, Nakanishi, A., Ye, X., Chang, J.-S., Hara, K., Hasunuma, T., Kondo, A., 2014. Optimizing biodiesel production in marine *Chlamydomonas* sp. JSC4 through metabolic profiling and an innovative salinity-gradient strategy. *Biotechnol. Biofuels* 7, 1–16. <https://doi.org/10.1186/1754-6834-7-97>
- Tsavatopoulou, V.D., Aravantinou, A.F., Manariotis, I.D., 2019. Biofuel conversion of *Chlorococcum* sp. and *Scenedesmus* sp. biomass by one- and two-step transesterification. *Biomass Convers. Biorefinery*. <https://doi.org/10.1007/s13399-019-00541-y>



Lab and photo-bioreactor scale optimization of *Stichococcus* sp. strain for CO₂ sequestration and bio-products production

G. Makaroglou¹ and P. Gikas¹

¹Design of Environmental Processes Laboratory, School of Chemical and Environmental Engineering,
Technical University of Crete, Chania, Greece
Corresponding author email: pgikas@tuc.gr

keywords: microalgae; photo-bioreactors; CO₂ fixation; optimization; high added value products.

Introduction

Microalgae are a promising source of biofuels and biochemical substances with high added value. Such products are proteins, lipids, carbohydrates, pigments etc. (Dolganyuk et al., 2020). Microalgae and their bio-products have a great potential in cosmetics, nutraceuticals, medicine, animal food, wastewater treatment (Costa et al., 2019) and they could be also used for CO₂ sequestration, by consuming from fossil fuel powered electric energy generation plants, combined with the parallel production of valuable products (Maghzian et al., 2022).

Materials and methods

Two *Stichococcus* sp. microalgae strains (wild and mutant) were cultivated in lab and photo-bioreactor scale. The mutant strain notes greater biomass and lower total chlorophyll productivity, compared to the wild strain. Regarding lab scale experiments, cultures were cultivated in beaker vessels with 150 mL of Bold's Basal Medium, whereas in larger scale experiments, a flat-panel photo-bioreactor was used, with 15 L of growth medium.

Different levels of salinity, CO₂, nitrogen concentration, nitrogen starvation and illumination were examined as growth parameters. In both scales, the strains were grown attached on sandblasted glasses, placed at the bottom of the containers and the photo-bioreactor. After 21 days of cultivation, biomass, lipids, proteins, carbohydrates and pigments production were measured.

Results and discussion

The strains of *Stichococcus* sp. were cultivated in atmosphere with CO₂ enriched air (5% v/v), producing biomass up to 40.70 g m⁻² for the wild strain (Fig. 1A) and 45.71 g m⁻² for the mutant (Fig. 1B) under constant light conditions and high nitrogen concentration. As for bio-products production, when nitrogen-rich conditions were applied, there was an increase in the content of proteins, carbohydrates, lipids, total chlorophyll and β-carotene, respectively up to 103% / 88%, 142% / 162%, 121% / 122 %, 500% / 487% and 408% / 220%, for the wild / mutant strain, respectively. The corresponding maximum contents respectively were: 10.25 g m⁻² / 8.87 g m⁻², 16.90 g m⁻² / 18.99 g m⁻², 9.23 g m⁻² / 10.39 g m⁻², 0.33 g m⁻² / 0.29 g m⁻² and 0.083 g m⁻² / 0.082 g m⁻² for the wild / mutant strain. The maximum total bio-product content was 33.95 (Fig. 2A) and 34.98 g m⁻² (Fig. 2B) for the wild and mutant strain, respectively. Three-day nitrogen starvation prior to biomass harvesting, resulted to increase in lipids production up to 63% / 71%, for the wild / mutant strain, respectively (Fig. 2A, 2B). Wild strain was also cultivated in photo-bioreactor scale, noting 49.17 g m⁻² of biomass and 41.70 g m⁻² of total bio-products (Fig. 3A, 3B).

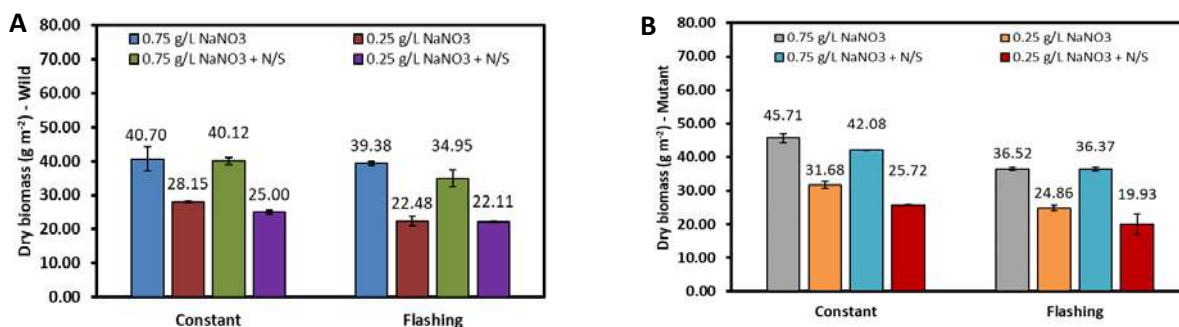


Figure 1. Biomass production of Wild (A) and Mutant (B) *Stichococcus* sp. strain in lab scale.

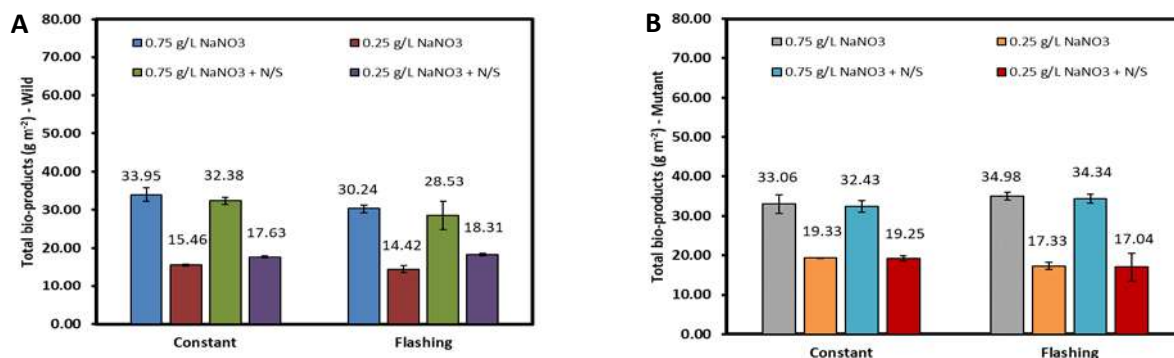


Figure 2. Bio-products production of Wild (A) and Mutant (B) *Stichococcus* sp. strain in lab scale.

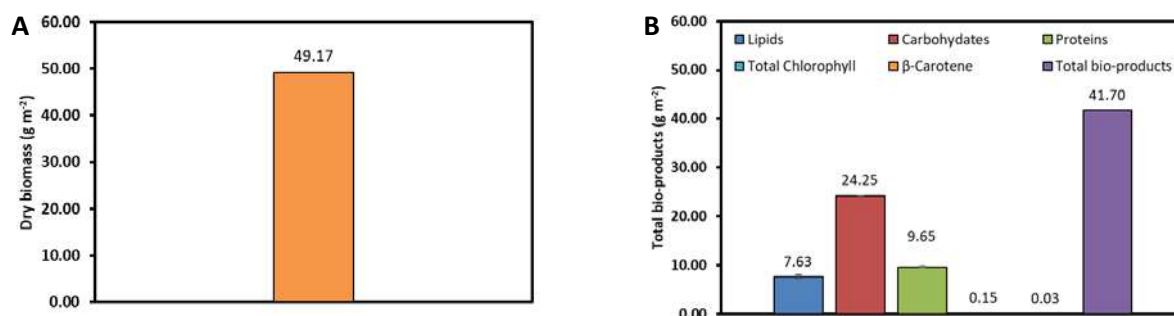


Figure 3. Biomass (A) and bio-products (B) production of Wild *Stichococcus* sp. strain in photo-bioreactor.

Conclusions

In conclusion, *Stichococcus* sp. strain was successfully cultured in both laboratory and pilot photo-bioreactors. The results showed that the aforementioned microalgae strain can be used in 3rd generation biorefinery to produce high value-added bio-products (i.e., proteins, carbohydrates, lipids, pigments), with the simultaneous capturing of CO₂ from the atmospheric air or flue gas.

Acknowledgements: This study is co-financed by the European Regional Development Fund of the EU and Greek national funds through the Operational Program Competitiveness, Entrepreneurship and Innovation, under the call “Research-Create-Innovate” (project code: T1EDK-02681). Project title: “Bioconversion of CO₂ into high-added value bioproducts through sustainable microalgae cultivation processes (CO₂-BioProducts)”.

References

- Costa, J., Freitas, B., Lisboa, C., Santos, T., Bruschi, L. and Morais, M., 2019. Microalgal biorefinery from CO₂ and the effects under the Blue Economy. *Renewable and Sustainable Energy Reviews*, 99, 58-65.
- Dolganyuk, V., Belova, D., Babich, O., Prosekov, A., Ivanova, S., Katserov, D., Patyukov, N. and Sukhikh, S., 2020. Microalgae: A Promising Source of Valuable Bioproducts. *Biomolecules*, 10(8), 1153.
- Maghjian, A., Aslani, A., Zahedi, R., 2022. Review on the direct air CO₂ capture by microalgae: Bibliographic mapping. *Energy Reports*, 8, 3337-3349.



SUST
ENG
2022



BIOREMEDIATION



Separation of the α -alumina layer from a spent Three-Way-Catalyst through *A. thiooxidans* as a pre-treatment to recover PGMs

M. Compagnone¹, J.J. González-Cortés^{1,2}, M.P. Yeste³, D. Cantero¹ and M. Ramírez¹

¹Department of Chemical Engineering and Food Technologies, Wine and Agrifood Research Institute (IVAGRO), Faculty of Sciences, University of Cadiz, Cadiz, Spain

²Department of Green Chemistry and Technology, Ghent University, Ghent, Belgium

³Department of Material Science, Metallurgical Engineering and Inorganic Chemistry, Institute of Research on Electron Microscopy and Materials (IMEYMAT), Faculty of Sciences, University of Cadiz, Cadiz, Spain

Corresponding author email: mariacristina.compagnone@uca.es

keywords: bioleaching; *A. thiooxidans*; TWCs; PGMs.

Introduction

Platinum Group Metals (PGMs) are included in the list of Critical Raw Materials for the EU. The automotive industry represents the principal consumer of PGMs. Catalytic converters contain PGMs in a considerably higher concentration than the natural ores, thus they stand as the richest secondary source. The most common car catalytic converters are the three-way catalysts (TWCs), honeycomb-type cordierite monoliths with a highly porous α -alumina wash-coat on the inner surface ($2\text{Al}_2\text{O}_3 \cdot 2\text{SiO}_2 \cdot 5\text{MgO}$).

The technologies to recover PGMs require various chemical, physical or mechanical pre-treatment steps that leach out the alumina support, altering PGMs into more soluble species. The main disadvantages of this stage are the high temperatures and the consumption of hazardous gases and chemicals which cause the production of pollutant wastes. Recently, the bioleaching treatments have been improved significantly, but they commonly still need pyro-metallurgical pre-reduction steps to reach significant results (Yakoumis et al., 2021). This study employs an environmentally friendly technique to separate the γ -alumina layer from a TWC, preventing the use of hazardous and polluting chemicals. Furthermore, we monitored *A. thiooxidans* ability to grow despite the presence of spent TWC.

Materials and methods

Pure inocula of *Acidithiobacillus thiooxidans* DSM 11478 were prepared. Biologically produced sulfur obtained from a desulfurization bioreactor (González-Cortés et al., 2020) was used as energy source.

TWC was pulverized using a cryogenic ball mill (MM400, Retsch GMBH, Germany). Then its content in Aluminium (Al) and PGMs was estimated. Aliquots of 5%, 30% and 60% w/v of milled TWC were added to (i) centrifuged biogenic acid, (ii) H_2SO_4 , (iii) *A. thiooxidans* in its exponential phase and (iv) in its stationary phase. The solutions were incubated in a rotary shaker (Comecta 2102, Selecta, Spain) at 180 rpm and $30 \pm 1^\circ\text{C}$. We monitored the change in pH and bacterial proliferation at the different pulp densities of TWC for 14 days.

To evaluate the leaching and separation of the γ -alumina layer, we measured the content of Al in the liquid medium with the analytical test kit 114825 Aluminum Test Method: photometric 0.020 - 1.20 mg/l Al Spectroquant® (Merck Millipore, Germany). A Quanta FIE 200 electron microscope (Philips) coupled to qualitative Energy Disperse X-ray analyzer (EDX) was used to obtain scanning electron microscopy (SEM) images and to identify the elemental composition of biological residues after treatment.

Results and discussion

The addition of TWC instantly increased the pH of the solutions in all four cases proportionally to the concentration of TWC due to the reaction with the alumina phases and to the ion exchange characteristics of silicates present in the TWC. The solutions with bacteria buffered the pH variation over time compared to biogenic acid and H_2SO_4 . This response is probably due to the metabolic activity of *A. thiooxidans*. Microbial proliferation and acid production were most likely stimulated by sulfur residues generally present in a spent TWC. The triggering effect of metals on microorganisms and EPSs production ability has been previously addressed (Chu et al., 2021). Complementarily, Fig. 1A and 1B show how microbial growth rates increased in proportion to the TWC pulp density. The microscope images document that on day 14, at approximately 2



minutes from agitation, the free-living bacteria were completely attached to the TWC. The acid solution with *A. thiooxidans* in its stationary phase and TWC at 5% w/v reached the highest Al extraction rate with a 57.1% of lixiviation (Fig. 1C). SEM images showed that, after treatment, microbial solution presented seemingly biological globules-like particles (Fig. 1D). Elemental composition revealed both globules and bacteria presented up to 24.8% of Al and 0.4% of Pt.

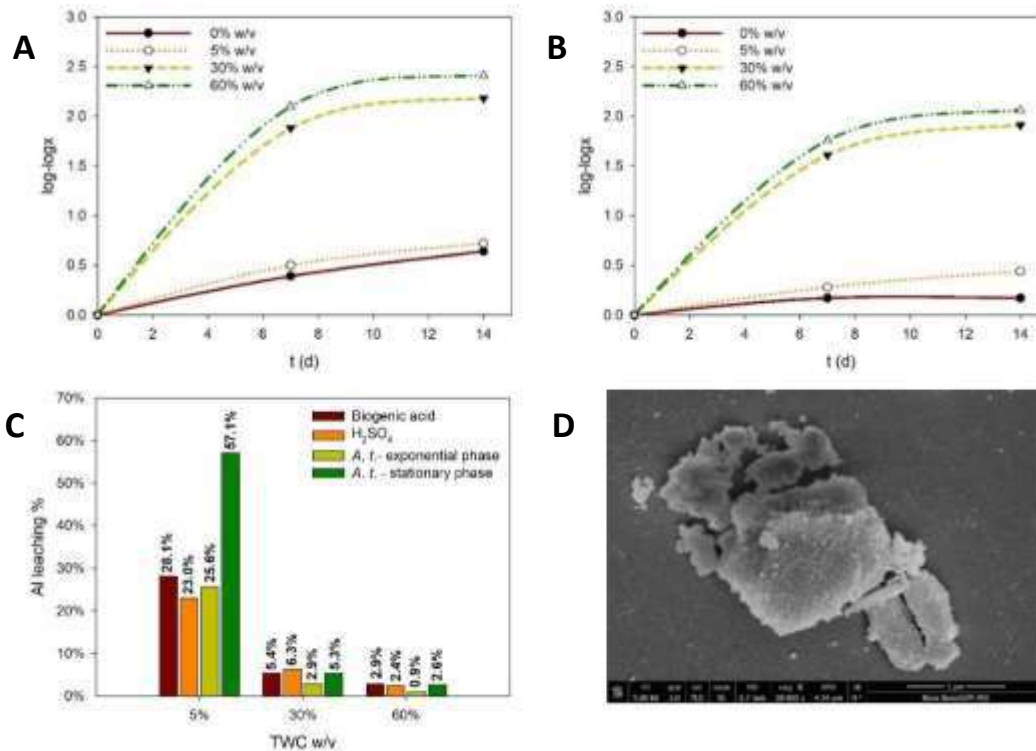


Figure 1. (A) Growth of *A. thiooxidans* inoculated in exponential phase and (B) inoculated in stationary phase, in presence of TWC; (C) leaching rate of Al from TWC; (D) SEM image of *A. thiooxidans* after TWC treatment.

Conclusions

The synergic action of using biogenic acid in presence of living *A. thiooxidans* resulted in higher extraction rates of metals compared to using chemical H₂SO₄ or bacteria-free biogenic acid.

Acknowledgements: This work has been co-financed by the 2014-2020 ERDF Operational Programme and by the Department of Economy, Knowledge, Business and University of the Regional Government of Andalusia. Project reference: FEDER-UCA18-106138.

References

- Chu, H., Wang, J., Tian, B., Qian, C., Niu, T., Qi, S., Yang, Y., Ge, Y., Dai, X., & Xin, B. (2021). Generation behavior of extracellular polymeric substances and its correlation with extraction efficiency of valuable metals and change of process parameters during bioleaching of spent petroleum catalyst. *Chemosphere*, 275, 130006. <https://doi.org/10.1016/j.chemosphere.2021.130006>
- González-Cortés, J. J., Torres-Herrera, S., Almenglo, F., Ramírez, M., & Cantero, D. (2020). Hydrogen Sulfide Removal from Biogas and Sulfur Production by Autotrophic Denitrification in a Gas-Lift Bioreactor. *ACS Sustainable Chemistry and Engineering*, 8(28), 10480–10489. <https://doi.org/10.1021/acssuschemeng.0c02567>
- Yakoumis, I., Panou, M., Moschovi, A. M., & Palias, D. (2021). Recovery of platinum group metals from spent automotive catalysts: A review. *Cleaner Engineering and Technology*, 3, 100112. <https://doi.org/10.1016/j.clet.2021.100112>



Wastewater treatment coupled with *Synechococcus elongatus* PCC 7942 cultivation

G. Samiotis¹, K. Stamatakis², I. Ristanis¹, L. Kemmou and E. Amanatidou¹

¹Department of Chemical Engineering/, University of Engineering, Kozani, Greece

²Institute of Biosciences and Applications, NCSR 'Demokritos', Athens, Greece

Corresponding author email: waterlab2@uowm.gr

keywords: cyanobacteria; nutrients removal; wastewater valorization; industrial wastewater; hydroponic wastewater.

Introduction

Wastewaters can be used as substrate for cyanobacteria cultivation, a sustainable feedstock to produce biofuels and added value products. This creates the opportunity for the development of processes that can offer tertiary wastewater treatment and CO₂ equivalent mitigation, while the generated biomass can be utilized in downstream valorization processes. The cultivation of cyanobacterium *Synechococcus elongatus* PCC 7942 monocultures in wastewater substrates is considered appealing, since does not produce cyanotoxins and can be used as a more sustainable feedstock alternative for the production of fuels, food and chemicals (Samiotis et al., 2021; Samiotis et al., 2022a). Furthermore, *Synechococcus elongatus* PCC 7942 exposed to saline conditions enhances its intracellular sucrose synthesis leading to bioethanol production, or/and metabolic biohydrogen production (Vayenos et al., 2020). However, cultivation of cyanobacteria monocultures in wastewater substrate and determination of fundamental design and operational characteristics is a challenge for full scale application (Samiotis et al., 2022b).

In this regard, this work (a) studies *Synechococcus elongatus* PCC 7942 cultivation in different wastewater substrates properly disinfected via low-cost techniques and (b) presents critical operational data and photobioreactor (PBR) volume calculation.

Materials and methods

Synechococcus elongatus PCC 7942 cultivation photobioreactors were setup using sterilized glass flasks with sterile cotton caps for uninhibited air transfer inside the PBR and protection from airborne biological contamination. For control setups, BG11 cultivation media was used as substrate, whereas for test setups three types of biologically treated wastewater were used. Cultivation was made at continuous agitation (200 rpm) and lighting (5 – 30 $\mu\text{mol-photon m}^{-2} \text{s}^{-1}$), at set temperatures ranging from 16°C to 37°C. The disinfection techniques of filtration and chemical disinfection using NaClO or H₂O₂ or hexavalent iron (ferrates), which is considered a novel and environmentally friendly disinfectant, were evaluated individually or as a synergetic couple. *Synechococcus elongatus* PCC 7942 growth rate calculated on the basis of chlorophyll *a* concentration and converted to volatile suspended solids (VSS), while nutrients removal via assimilation was calculated and expressed in terms of nitrogen or phosphorous biomass content.

Results and discussion

The results showed that upon proper disinfection of the evaluated wastewater media, which were obtained from the secondary biological treatment stage of a dairy industry and a snack industry, as well as from the drainages of an open and a closed hydroponic system, *Synechococcus elongatus* PCC 7942 can efficiently proliferate and remove nitrates and phosphates via assimilation (Figure 1). Proper disinfection is achieved through filtration coupled with chemical disinfection, preferably using ferrates that have been generated in-situ via a Fe⁰/Fe⁰ electrochemical cell in alkaline solution. Temperature and salinity oppose thresholds for *Synechococcus elongatus* PCC 7942 cultivation. Nevertheless, it is able to proliferate at a temperature range of 16°C to 32°C and at salinities up to 450 mmol NaCl L⁻¹.

The study revealed that salinity in particular, which in many wastewater streams may be as high as the threshold value, positively correlates with nitrogen assimilation into *Synechococcus elongatus* PCC 7942



biomass. Moreover, higher nutrient concentrations in cultivation media not only trigger luxury phosphorus uptake, but also increase nitrogen assimilation into the cyanobacteria (Figure 2).

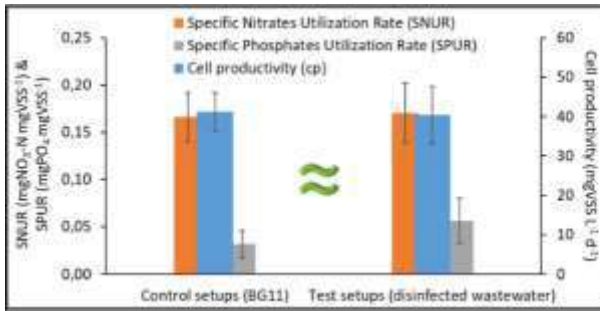


Figure 1. Assessment of *Synechococcus elongatus* PCC 7942 cultivation in wastewater media.

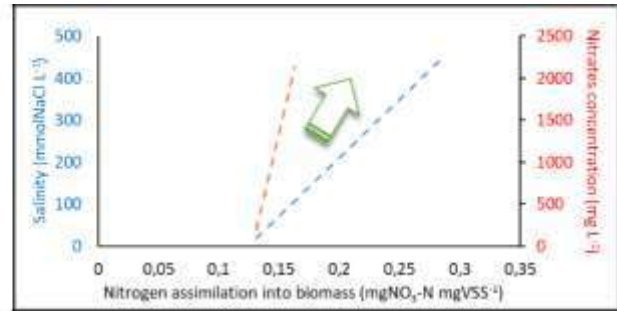


Figure 2. Effect of salinity and nutrient content on nitrogen assimilation.

These findings have significant implications on dimensioning of a photobioreactor for the treatment of high strength and relatively saline wastewater, whose treatment constitutes a challenge in common biological wastewater treatment processes. Based on the proposed by this study photobioreactor dimensioning equation (Eq. 1), which takes into account nitrate-nitrogen load (N_{Denitr} , kgNO₃-N d⁻¹), specific nitrates utilization rate ($SNUR$, kgNO₃-N kgVSS⁻¹) and cell productivity (kgVSS L⁻¹ d⁻¹), a photobioreactor (V_{PBR} , m³) volume can be of comparable volume to a common biological denitrification bioreactor. The key element for reactor volume minimization is cell productivity enhancement via bioreactor design and control of operational conditions.

$$VPBR = \frac{N_{Denitr}}{SNUR * cell\ productivity} \quad \text{Eq. 1}$$

Moreover, the study revealed that a photoautotrophic-based process can offer the only biotechnological answer to the challenge of treating nutrient-rich wastewater with low organic compounds content, in which activated sludge process cannot be applied.

Conclusions

Therefore, a *Synechococcus elongatus* PCC 7942-based wastewater treatment process can be adapted as a supplementary or an alternative treatment stage to the widely applied biological denitrification processes towards the minimization of wastewater treatment plant's ecological footprint and obtaining of added value products or/and energy.

Acknowledgements: This work was supported by the University of Western Macedonia Research Committee in the framework of Operational Programme Competitiveness, Entrepreneurship and Innovation 2014-2020 (EPANek), project code MIS 5047197.

References

- Samiotis, G., Stamatakis, K., Amanatidou, E., 2021. Assessment of *Synechococcus elongatus* PCC 7942 as an option for sustainable wastewater treatment. *Water Sci. Technol.* 84:1438. <https://doi.org/10.2166/wst.2021.319>
- Samiotis, G., Stamatakis, K., Amanatidou, E., 2022. Dimensioning of *Synechococcus elongatus* PCC 7492 cultivation photobioreactor for valorization of wastewater resources. *Chem Eng. J.* 435:134895. <https://doi.org/10.1016/j.cej.2022.134895>
- Samiotis, G., Ziaгова, M. G., & Amanatidou, E., 2022. Wastewater substrate disinfection for cyanobacteria cultivation as tertiary treatment. *Environmental Science and Pollution Research* <https://doi.org/10.1007/s11356-022-20369-w>
- Vayenos, D., Romanos, Em.G., Papageorgiou, G.C., Stamatakis, K., 2020. The freshwater cyanobacterium *Synechococcus* sp. PCC7942 under salt stress: A cell factory for sucrose and hydrogen production. *Photosynth Res* 146:235-245. <https://doi.org/10.1007/s11120-020-00747-6>



Comparative Degradation of *Vitis Vinifera* “Assyrtiko” grape pomace by two different bacteria: *Pseudomonas sp.* strain phDV1 and *Chlamydomonas reinhardtii*

E. Mathioudaki¹, M. Belenioti¹, D. Ghanotakis¹, G. Tsiotis¹ and N. Chaniotakis¹

¹Department of Chemistry, University of Crete, Voutes, Greece
Corresponding author email: eirini.mathiou@gmail.com

keywords: grape pomace; biodegradation; *Pseudomonas sp.* strain phDV1; *Chlamydomonas reinhardtii*.

Introduction

Grape pomace from *Vitis Vinifera Assyrtiko* is an important waste product of the Greek wine industry, and its disposal is a serious issue with negative environmental impacts [1]. Grape pomace is rich in bioactive compounds, such as sugars and polyphenols and its utilization for alternative uses has been of considerable interest [1]. It has been shown, for example, that it can be used as a carbon source in various biotechnological processes. Here, we utilize two different bacteria; *Pseudomonas sp.* strain phDV1 and *Chlamydomonas reinhardtii*, to study their ability to biodegrade *Vitis Vinifera Assyrtiko* grape pomace in order to produce environmentally friendly and commercially useful products.

Materials and methods

The main focus of this study is to optimize the reduction of the phenolic content of the grape pomace. For this purpose, we evaluated *Pseudomonas sp.* strain phDV1 and *Chlamydomonas reinhardtii*, for their ability to utilize polyphenols as their carbon source. The total phenolic content before and after cultivation, in different time points under controlled experimental conditions is monitored using the Folin Ciocalteu Assay. *Pseudomonas sp.* strain phDV1 and *Chlamydomonas reinhardtii* was cultivated in autoclaved grape pomace extract for 4 days and 9 days respectively, whilst their growth was monitored in different time points.

Results and discussion

In this work we show that both bacteria were able to biodegrade the polyphenols of *Vitis Vinifera* “Assyrtiko” grape pomace very efficiently. Specifically, four days after the beginning of cultivation, *Pseudomonas sp.* decreased the total polyphenols at a rate of 91%, while *Chlamydomonas reinhardtii* decreased it at a rate of 43% nine days after cultivation.

Conclusions

Both *Pseudomonas sp.* strain phDV1 and *Chlamydomonas reinhardtii* appear to biodegrade polyphenols of *Vitis Vinifera Assyrtiko* grape pomace, laying the basis for alternative uses of wine industry wastes, such as fertilizers [2], food supplements [3] or feed [4].

Acknowledgements: This research has been co-financed by the European Regional Development Fund of the European Union and Greek national funds through the Operational Program Competitiveness, Entrepreneurships and Innovation, under the call RESEARCH- CREATE- INNOVATE (project code: T2EDK-00523).





References

- Dwyer, K.; Hosseinian, F.; Rod, M.R. The market potential of grape waste alternatives. *J. Food Res.* 3, 91 (2014).
- T Manios. The composting potential of different organic solid wastes: experience from the island of Crete. *Environment International.* 29, 8, (2004).
- Ana M. González-Paramás, Sara Esteban-Ruano, Celestino Santos-Buelga, Sonia de Pascual-Teresa, and Julián C. Rivas-Gonzalo. Flavanol Content and Antioxidant Activity in Winery Byproducts. *Journal of Agricultural and Food Chemistry.* 52 (2004).
- Myrto-Panagiota Zacharof. Grape Winery Waste as Feedstock for Bioconversions: Applying the Biorefinery Concept. *Waste and Biomass Valorization.* 8 (2017).



Biodegradation of glyphosate: a Bioinformatics approach

V. L. Koumandou¹ and M. Giannakara¹

¹School of Applied Biology and Biotechnology, Agricultural University of Athens, Greece
Corresponding author email: koumandou@aua.gr

keywords: Bioinformatics; enzymes; pollutants; biodegradation; glyphosate.

Introduction

Bioremediation is a low-cost, sustainable and technologically simpler clean-up method for ecosystems. The abundance and the presence of microorganisms in different and even extreme environmental conditions, render them a constant source of study and research, aiming at their recruitment for the biodegradation of contaminants. Bioinformatics analysis can contribute to the identification of novel microorganisms, which biodegrade contaminants, or of participating proteins and enzymes, and the elucidation of the complex metabolic pathways involved in biodegradation. Our aim is to study enzymes capable of degrading pollutants, which can be used for further scientific research on the biodegradation of industrial and agricultural waste and with the potential to be used in bioremediation programs. Glyphosate, a widely used broad-spectrum herbicide (e.g. active ingredient of Roundup™). It is a synthetic amino acid and analogue of glycine, which inhibits aromatic amino acid biosynthesis in plants. We present our findings on the glyphosate-degrading enzymes C-P lyase and Glyphosate Oxidoreductase (GOX).

Materials and methods

1. Literature-search for organisms and enzymes participating in glyphosate biodegradation.
2. Sequence collection using the database KEGG for C-P lyase and BLASTp searches for GOX.
3. Multiple alignments with MUSCLE.
4. Mapping of conserved residues on the 3D structure of the enzymes using PyMOL.
5. Computation of the 3D structure of GOX using I-TASSER and AlphaFold, comparison of results with bibliography results based on Phyre2.

Results and discussion

• C-P lyase:

By collecting and comparing sequences from all prokaryotic lineages, more conserved residues were observed than in literature. The variability in the conservation among the proteins shows a correlation with their function in the enzyme complex (Fig. 1).

It is important to investigate the potential role of the additional conserved areas of the enzyme complex, as some questions regarding the function of the enzyme have not been answered yet.

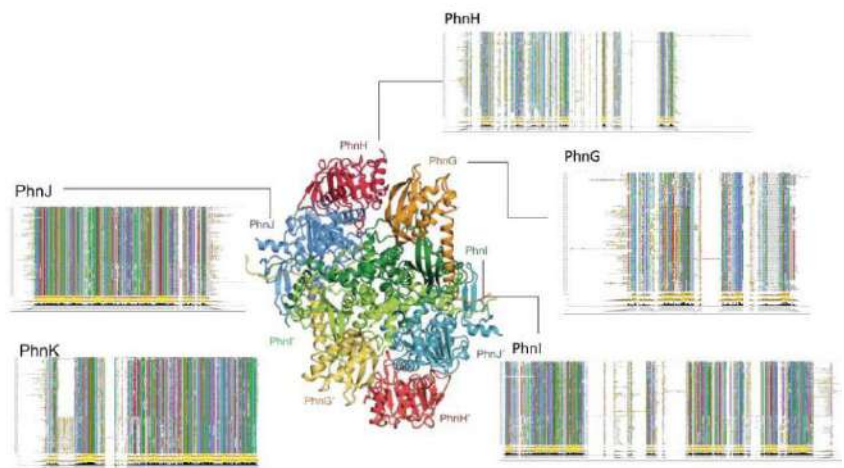


Figure 1: The multiple alignment results of each part of the C-P lyase complex (Image of C-P lyase: Seweryn et. al, 2015).



- GOX

Only 5 annotated GOX proteins were found using the BLASTp search. The remaining hits were annotated as:

- o FAD-dependent/binding oxidoreductases (same as GOX)
- o D-amino acid dehydrogenases
- o Glycine oxidases (GO)

Significant differences have been identified between the computed structures of GOX:

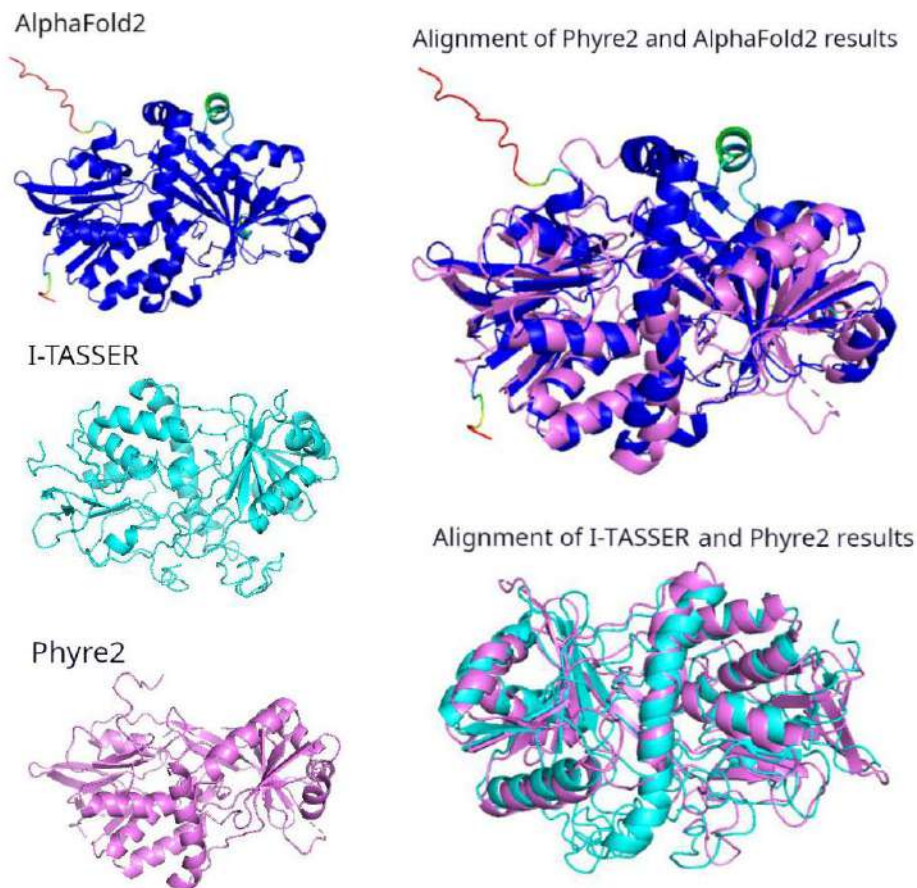


Figure 2: The computed structures of GOX using Homology Modeling (Phyre2, I-TASSER) and AI (AlphaFold2) approaches.

Future steps include (i) molecular docking of glyphosate on the computed structures and (ii) search for novel enzymes with a similar function based on the structure of the potential active site of GOX.

References

- Arora NK., Bioremediation: a green approach for restoration of polluted ecosystems. *Environ Sustain.* 2018;1(4):305-307
- Bhatt P. et al., "Binding interaction of glyphosate with glyphosate oxidoreductase and C-P lyase: Molecular docking and molecular dynamics simulation studies," *J. Hazard. Mater.* 2021;409, p. 124927.
- Hove-Jensen B. and Zechel D.L., "Utilization of Glyphosate as Phosphate Source : Biochemistry and Genetics of Bacterial Carbon-Phosphorus Lyase". 2014;78(1):176–197
- Seweryn P. et al., "Structural insights into the bacterial carbon-phosphorus lyase machinery," *Nature.* 201; 525(7567): 68–72.



Hydrocarburoclastic fungi and bacteria to improve bioavailability and degradability of petroleum hydrocarbons in a historically contaminated soil

S. Di Gregorio¹, I. Chicca¹ and S. Becarelli^{1,2}

¹Department of Biology University of Pisa, Pisa, Italy

²BD Biodigressioni Srl, Pisa. Italy

Corresponding author email: simona.digregorio@unipi.it

keywords: *mycoremediation; generalist bacterial species; specialist bacterial species; predictive functional metagenomics.*

A *Ciboria* sp. strain (Phylum Ascomycota) was isolated from Total petroleum hydrocarbon polluted soil (8538 mg/kg) of an abandoned oil refinery in Italy. The strain was able to utilize diesel oil as a sole carbon source for growth and was used in laboratory-scale experiments to evaluate the use of this fungal strain for remediation. Mesocosms soil experiments were inoculated with the fungal strain at 1% or 7%, on a fresh weight base ratio. After 90 days of incubation, the depletion of TPH contamination was of 78% with the 1% inoculant, and 99% with the 7% inoculant. 16S rDNA and ITS metabarcoding of the bacterial and fungal communities was performed in order to evaluate the potential synergism between fungi and bacteria in the bioremediation process. The functional metagenomic prediction indicated *Arthrobacter*, *Dietzia*, *Brachybacterium*, *Brevibacterium*, *Gordonia*, *Leucobacter*, *Lysobacter* and *Agrobacterium* sps. as generalist actinobacterial saprophytes, active in the first 30 or 60 days. These species were correlated also to the presence of a-specific extracellular enzymes as Dye -decolourizing peroxidase which primed the later depletion of hydrocarbons by increasing their bioavailability. This first action allows the onset of hydrocarbonoclastic specialist bacterial species, identified as *Streptomyces*, *Nocardoides*, *Pseudonocardia*, *Solirubrobacter*, *Parvibaculum*, *Rhodanobacter*, *Luteiomonas*, *Planomicrobium* and *Bacillus* sps., involved in the Total Petroleum Hydrocarbon depletion.



Aeration control using on-line calculation of oxygen uptake rate

K. Azis¹, S. Ntougias¹ and P. Melidis¹

¹Laboratory of Wastewater Management and Treatment Technologies,
Department of Environmental Engineering, Democritus University of Thrace, Greece.

Corresponding author email: pmelidis@env.duth.gr

keywords: *intermittent aeration; aeration control; oxygen uptake rate; real time monitoring.*

Introduction

Respirometry is defined as a technique to estimate the microbial activity and specifically the metabolism rate of microorganisms by oxygen uptake rate (OUR) (Hayet et al., 2016). Commonly OUR will be applied to assess the activity of microorganisms in the mixed liquor. Significant insight into the activated sludge oxidation processes are provided measuring OUR in a continuous basis.

Puig et al. (2005) implemented a control strategy to improve the removal of carbon and nitrogen in an SBR system, using OUR and redox potential (ORP) to determine the end of the aerobic and anoxic phases, respectively. The minimum value of OUR profile in most cases was considered as the end point of the aerobic processes and the system entered the endogenous respiration conditions. Dries (2016) reported the end of aerobic processes, by defining either the completion of nitrification or the oxidation of the organic carbon, at the point where oxygen uptake rate was lesser than 15 mgO₂/L.h, considering a small difference between two consequent OUR values, lower than 1 mg O₂/L.h. According to Martin de la Vega and Moran (2018), OUR values between 6 and 12 mg O₂/L.h indicates a residual amount of organic matter and ammonia charge in the bioreactor, while values lower than 6 mg O₂/L.h indicate their complete consumption.

The present study examined the validity of Oxygen Uptake Rate (OUR) as an aeration control parameter in an intermittent aeration process treating domestic wastewater (Suescun et al., 1998). A time-dependent OUR profile could be used to detect the end point of the organic carbon and ammonia nitrogen oxidation in order to adjust the aeration phase length to the influent characteristics (Hagman and Jansen, 2007).

The aim of this study was the real time monitoring of oxygen uptake rate and the evaluation of the OUR profiles, in an intermittent operating activated sludge system, in order to develop an activated sludge aeration strategy to maximize the organic carbon and ammonium nitrogen oxidation and reduce energy consumption and operating costs (Leu et al., 2009).

Materials and methods

The pilot-unit, which comprised of a 40 L feeding tank, a 100 L main reactor and an 80 L external membrane unit, was operated using intermittent aeration. The cycling feeding at the beginning of the anoxic phase improved the simultaneous removal of nutrients (C, N and P). Ammonia nitrogen concentration into the bioreactor was measured online using the ion selective electrode ISE VARiON® Plus 700 IQ AmmoLyt® Plus, and OUR calculated by measuring dissolved oxygen consumption using the optical sensor FDO® 700 IQ. The association of the decrease in DO concentration over time is normally found to be linear and OUR was determined by calculating the slope of the curve. The pilot unit including OUR respirometer and OUR measurement cell scheme is illustrated in Figure 1.

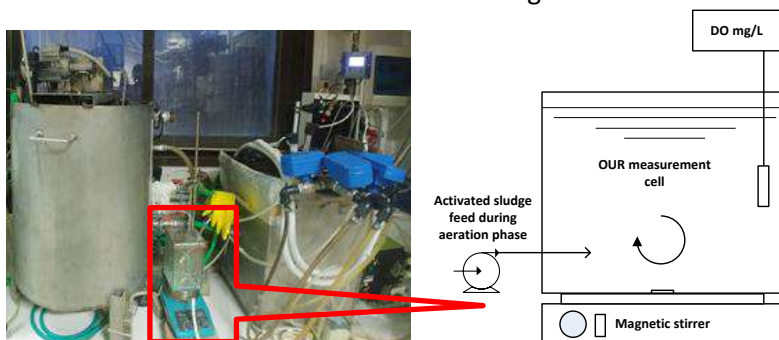


Figure 1. Pilot unit, including OUR respirometer and OUR measurement cell.



Results and discussion

Intermittent aeration consists of aeration and non-aeration cycles. In order to calculate OUR, aerated activated sludge was transferred from the biological reactor to the OUR cell. Heterotrophic and autotrophic bacteria consume the dissolved oxygen of the mixed liquor during a limited period of time, ca 10 min and the decrease in oxygen concentration was recorded. OUR values were calculated from the slope of the DO curve formed during oxygen concentration decline. In the same aeration phase, due to the ammonia nitrogen oxidation, the corresponding profile declines, until reaching the lowest value at the end of the aeration period. OUR values and ammonia nitrogen concentration profiles correlates well, indicating the effective application of OUR for activated sludge aeration process control (Fig.2). The small difference between two consequent OUR values could be used to switch to the next operation phase.

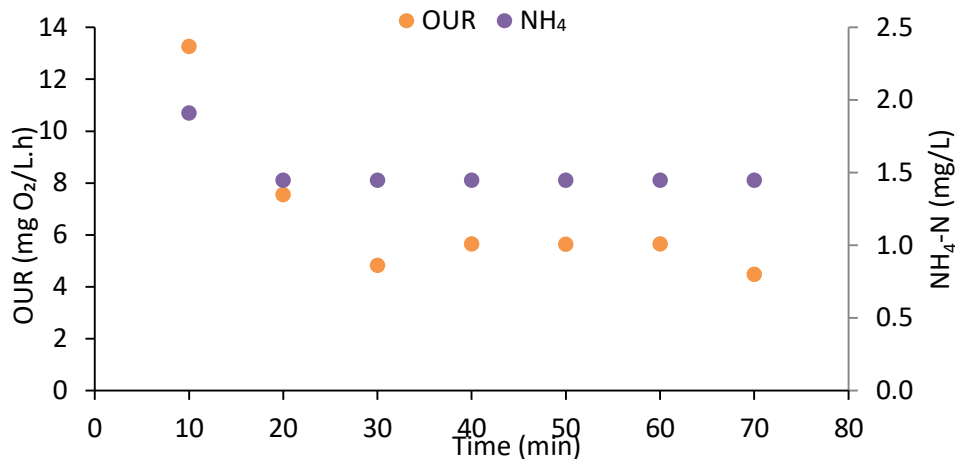


Figure 2. NH₄⁺-N and OUR profiles during a typical aeration phase.

Conclusions

On-line OUR measurements appears to be a useful tool in wastewater treatment plants in order to control the aeration phase, where organic carbon and ammonia nitrogen are oxidized. Indeed, it consists of low-cost application, where the obtained data could be used for process control.

Acknowledgements: There is no funding associated with the work featured in this article.

References

- Dries, J. (2016). Dynamic control of a nutrient-removal from industrial wastewater in a sequencing batch reactor, using common and low-cost online sensors. *Water Science Technology* 73, 740-5.
- Martín de la Vega, P., & Jaramillo-Morán, M. (2018). Multilevel Adaptive Control of Alternating Aeration Cycles in Wastewater Treatment to Improve Nitrogen and Phosphorous Removal and to Obtain Energy Saving. *Water*, 11(1), 60.
- Puig, S., Corominas, Ll., Vives, M.T., Balaguer M.D. and Colprim, J. (2005). Development and Implementation of a Real-Time Control System for Nitrogen Removal Using OUR and ORP as End Points. *Ind. Eng. Chem. Res.* 44, 3367-3373.
- Suescun, J., Irizar, I., Ostolaza, X., & Ayesa, E. (1998). Dissolved oxygen control and simultaneous estimation of oxygen uptake rate in activated-sludge plants. *Water Environment Research*, 70(3), 316–322.
- Leu, S.-Y., Rosso, D., Larson, L. E., & Stenstrom, M. K. (2009). Real-Time Aeration Efficiency Monitoring in the Activated Sludge Process and Methods to Reduce Energy Consumption and Operating Costs. *Water Environment Research*, 81(12), 2471–2481.
- Hagman, M. and Jansen, J.L.C. (2007). Oxygen uptake rate measurements for application at wastewater treatment plants. *Vatten*. 63. 131-138.



SUST
ENG
2022



ANAEROBIC DIGESTION



The role of hydrochar on the production of biogas and volatile fatty acids during anaerobic digestion of cheese whey wastewater

D. Liakos¹, G. Altiparmaki¹, A. Kalampokidis² and S. Vakalis¹

¹Energy Management Laboratory, Department of Environment, University of the Aegean, University Hill, Mytilene, Greece

²Waste Management Laboratory, Department of Environment, University of the Aegean, University Hill, Mytilene, Greece

Corresponding author email: vakalis@aegean.gr

keywords: *hydrothermal carbonization; anaerobic digestion; volatile fatty acids; biogas; Gas chromatography.*

Introduction

The food production industry is one of the main pillars of economic development for Lesvos island. However, this also is correlated to the simultaneous production of a large amount of liquid biowaste such as olive mill wastewater (OMWW), cheese whey wastewater and wine sludge. On a second level there are thousands of tons of municipal sludge from the biological treatment of the island. This study presents the applications of hydrothermal treatment in Lesvos and focuses on the production of hydrochar from high-phenolic sources, i.e., olive mill wastewater and wine sludge. Subsequently, the produced phenolic hydrochar is utilized in anaerobic digestion of cheese whey wastewater in order to study the effect on the production of biogas and volatiles fatty acids (VFAs). The co-utilization strategies of various different food waste sources support the concept of Circular Economy and provides alternative pathways in the field of waste valorization.

Materials and methods

OMWW and wine sludge underwent hydrothermal carbonization in a 4570A Parr hydrothermal reactor for a residence time of 2 hours, temperature of 250 °C and pressure of 55 bars. BMP tests were implemented for anaerobic co-digestion (at 35 °C) of cheese whey wastewater/ sludge mixtures (1:2 ratio) with various added hydrochar amounts i.e., 50 g, 100 g and 250 g respectively. This study implemented mass balances of the hydrothermal carbonization of OMWW and wine sludge, measured the biomethane potential of the co-digestion BMP tests and assessed the quality of the final digestate. In particular, the final digestate was assessed for the content in VFAs by means of a GC - BID with a specialized column (MEGA-624). The biogas quality was assessed with the same GC - BID with a Restec ShinCarbon ST Micropacked Column. Analysis also included the TS/ VS content, COD and Total Phenolic Content (Folin – Ciocalteu method).

Results and discussion

The produced hydrochars had a significant heating value, i.e. 28.05 MJ/ kg for wine sludge and 26.55 MJ/ kg for OMWW. BMP tests were used to produce biogas and the highest biogas production was measured for the samples with 100 and 250 mg of wine sludge hydrochar. The addition of hydrochar from OMWW performed also well but the addition of HC from 100 to 250 mg had a mitigating effect on biogas production. Also in all cases, the addition of OMWW hydrochar reduced the methane content. The produced ml biogas per g VS is presented in Fig. 1.

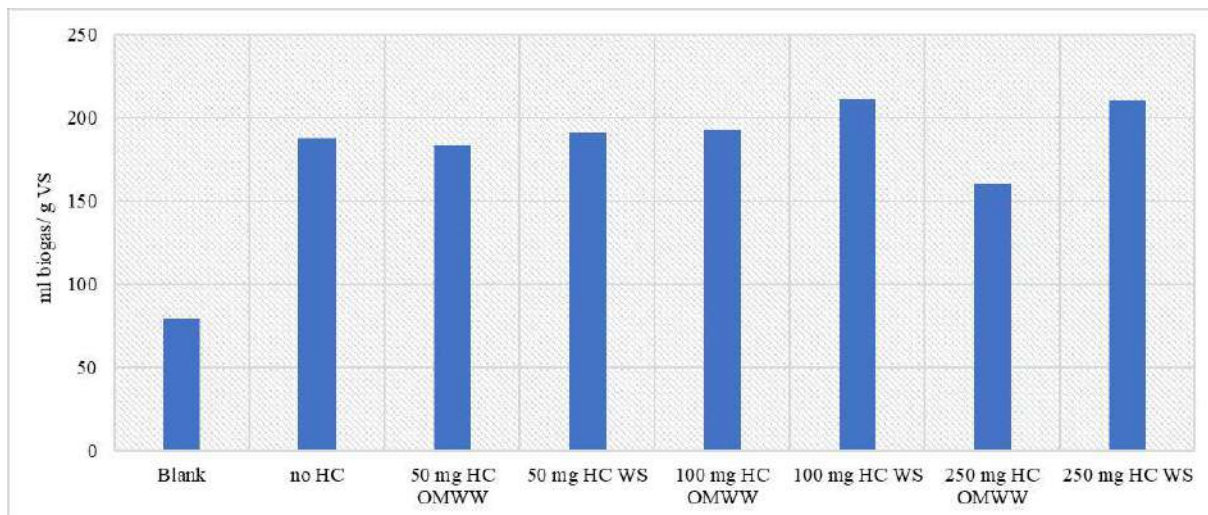


Figure 1. Average biogas potential per g VS. HC: hydrochar, WS: wine sludge

The final Total Phenolic Content of the digestates from the BMP tests were increased with the addition of hydrochar both from wine sludge and OMWW. The samples with no added hydrochar had an average 90.4 mg/ L, while with the addition of 100 ml of wine sludge hydrochar a maximum value of 1389 mg/ L. But by far the most interesting outcome of this study is that the addition of hydrochar assisted the production of medium-chain VFAs, i.e., isocaproic, caproic and heptanoic acid. The most straightforward case is the production of isocaproic acid, where the ANOVA analysis deduced the null hypothesis with a p value $< 10^{-4}$. The results are also supported by the reduced biogas (total production) and methane % production in the samples with the highest content of VFAs.

Acknowledgements: We acknowledge support of this work by the project “Center of Sustainable and Circular Bioeconomy [Aegean_BIOECONOMY]” (MIS 5045851) which is implemented under the Action “Reinforcement of the Research and Innovation Infrastructure”, funded by the Operational Programme “Competitiveness, Entrepreneurship and Innovation” (NSRF 2014-2020) and co-financed by Greece and the European Union (European Regional Development Fund).

References

- M. A. Vasileiadou, G. Altiparmaki, K. Moustakas, S. Vakalis (2022). Quality of Hydrochar from Wine Sludge under Variable Conditions of Hydrothermal Carbonization: The Case of Lesvos Island. *Energies* 15(10), 3574; <https://doi.org/10.3390/en15103574>
- S. Vakalis, Anargyros Georgiou, Konstantinos Moustakas, Michail Fountoulakis (2022). Assessing the effect of hydrothermal treatment on the volatile solids content and the biomethane potential of common reed (*phragmites australis*), *Bioresource Technology Reports* 17, 100923, <https://doi.org/10.1016/j.biteb.2021.100923>.



Influence of nitrate source and hydraulic residence time of the anoxic desulfurization in the bacterial consortia and the methane content of desulfurized landfill biogas

J.J. González-Cortés^{1,2}, G. Quijano³, M. Ramírez¹ and D. Cantero¹

¹Department of Chemical Engineering and Food Technologies, Wine and Agrifood Research Institute (IVAGRO), Faculty of Sciences, University of Cadiz, Cadiz, Spain

²Department of Green Chemistry and Technology, Ghent University, Ghent, Belgium

³Instituto de Ingeniería, Unidad Académica Juriquilla, Universidad Nacional Autónoma de México, Querétaro, México.

Corresponding author email: joaquin.gonzalez@uca.es

keywords: Anoxic Desulfurization; Biogas; Methane.

Introduction

The use of biogas is essential to reduce greenhouse gas emissions (GHGs) and our current dependence on fossil fuels. Biogas is mainly composed of CH₄ (45-75%) and CO₂ (20-50%). However, there are several minor compounds like H₂, O₂, N₂, NH₃, H₂S, volatile organic compounds (VOCs), siloxanes, etc. Despite some of them are not significantly harmful, others such as hydrogen sulfide (H₂S) are undesirable because it causes corrosion and SO₂ emissions. Biological desulfurization has been proven to be more cost-efficient and environmentally friendly than physical-chemical techniques. Specially the anoxic process, which uses nitrate or nitrite as electron acceptor instead of oxygen, has attracted the attention of researchers. Even when the number of studies referring to this technology are significant, the impact of the biological assimilation of methane in its final concentration in the treated biogas has not been widely addressed. Moreover, the effect of O₂ in the gas effluent is highly interesting. Despite its low concentration, the low gas residence times (GRTs) applied in biogas desulfurization bioreactors make significant the total oxygen supply. In order to consider this, air was mixed with methane to obtain an effluent similar to real biogas as possible to feed the bioreactor.

Hence, in the present study, the impact of different nitrate sources and hydraulic retention times (HRTs) on the methane oxidation activity and the microbial population is determined.

Materials and methods

Experiments were performed in a continuous stirred tank bioreactor (CSTBR) with a working volume of 0.8 L, magnetically stirred (150 rpm) and fed with a mixture of CH₄, N₂, H₂S and air to a final concentration of CH₄=60%, H₂S = 1,300 ppmv, O₂ = 2% and balance to N₂. The bioreactor was continuously fed with mineral medium (Gonzalez-Cortes, 2021). The CSTBR was inoculated with biomass from a pilot-scale anoxic bioscrubber (M1) fed with real biogas and nitrified landfill leachate (Gamisans et al, 2021). The bioreactor was operated under a HRT of 10 and 1.5 days ($D= 0.0042$ and 0.0278 h^{-1}) using NaNO₃ as nitrate source which led to the formation of two different microbial consortia; M2 and M3, respectively.

The microbial community shifts that occur under different HRTs and NO₂⁻ and NO₃⁻ sources were determined by 16S metagenomics analysis.

The methane oxidation capacity of the biomass obtained under different conditions was determined using serum bottles of 0.1 L. The bottle was filled with 20 mL of biomass from the bioreactor and diluted with mineral medium without NaNO₃, leaving the remaining bottle volume as headspace. The effect of different electron acceptors (O₂, NO₂⁻ and NO₃⁻) was studied for 24h.

Results and discussion

The CSTBR was successfully operated to remove the H₂S from biogas showing an average EC of $28.42 \pm 0.87 \text{ g S-H}_2\text{S m}^{-3} \text{ h}^{-1}$ (RE=91.9 ± 2.8%) and $30.56 \pm 0.37 \text{ g S-H}_2\text{S m}^{-3} \text{ h}^{-1}$ (RE=98.8 ± 1.2%) at the steady-state conditions under HRTs of 1.5 and 10 days, respectively. Fig.1a shows the relative abundances at genus levels of the three different microbial consortia studied in the present work. Bacteria capable of oxidizing reduced sulfur compounds were found as predominant in all samples being the most abundant OTUs of the



Thiomicrospira (11-25%) genus followed by *Sulfurimonas* (0-18%) genus. Furthermore, different bacteria which have been reported to be capable of metabolize methane were found in the three samples. Among these, the presence of *Halomonas* (0-17%), *Marteella* (2-8%) and *Methylophaga* (0-0.2%) genera were remarkable and as well as the family *Methylophilacea* (0-0.1%). Finally, it is worth highlighting the presence of bacteria in M1 which is frequently found in methanogenic consortia like OTUs belonging to the *Lentimicrobium* genus which were identified with a relative abundance of 9.7%.

Methane variation obtained in the batch tests by the three microbial consortia is presented in Fig 1b. It can be seen that methane concentration decreased in most tests highlighting the presence of CH₄ degrading bacteria in all the microbial consortia. While greater CH₄ removals were found by M2 using NO₂⁻ and NO₃⁻ (4.4 ± 0.2% [EC=50.1 ± 2.7 g CH₄ m⁻³ h⁻¹] and 3.0 ± 0.2% [EC=34.0 ± 2.24 g CH₄ m⁻³ h⁻¹], respectively), O₂ was found to lead to higher CH₄ removal in M3 (3.5 ± 0.1% [EC=33.1 ± 1.3 g CH₄ m⁻³ h⁻¹]). An increase in CH₄ (6.1±0.7%) was found using M1 under aerobic conditions where CH₄ increased by 6.1 ± 0.7%. This methane generation can be explained by the existence of organic matter from the landfill leachate which served as a potential substrate for biogas production.

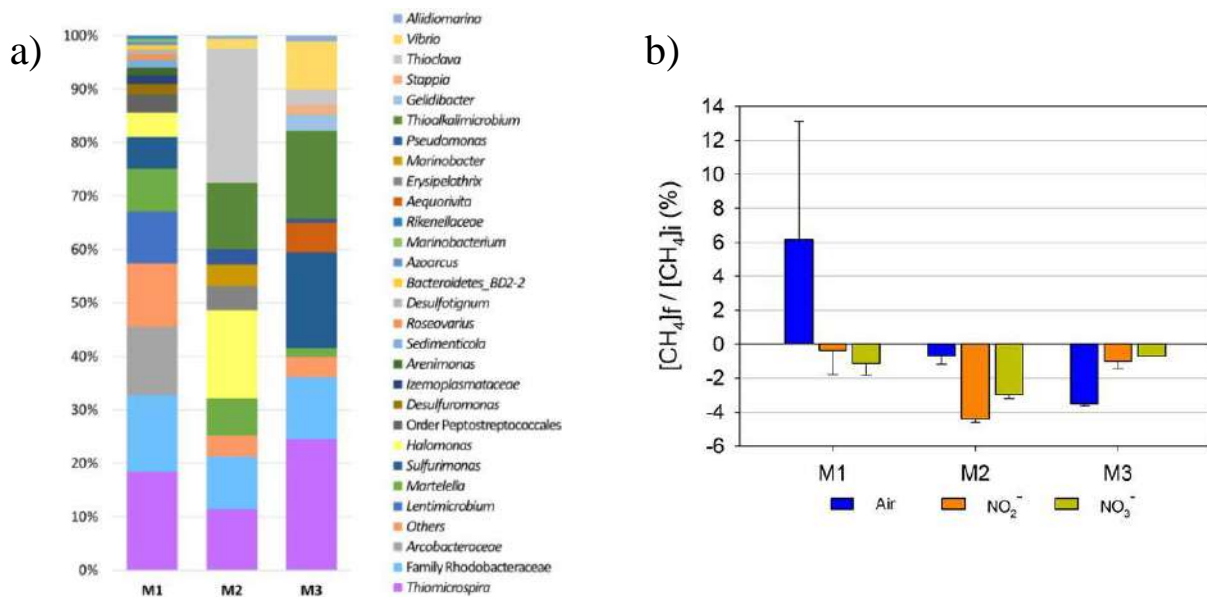


Figure 1. (a) Relative abundances at genus level of M1 (Initial conditions), M2 (HRT of 10 days) and M3 (HRT of 1.5 days) samples (b) Variation of CH₄ found in the headspace using different electron acceptor (oxygen from air, nitrite and nitrate) and the different microbial consortia.

Conclusions

The present study demonstrated the scarce impact of the anoxic desulfurization process on the CH₄ content of landfill biogas standing this technology as a reliable technique for biogas desulfurization.

Acknowledgements: This study is supported by the Department of Economy, Knowledge, Business and Universities of the Regional Government of Andalusia. Project reference: FEDER-UCA18-106138 and the European Union through the NextGenerationEU funds (UCA/R155REC/2021).

References

- González-Cortés, J.J., Torres-Herrera, S., Almenglo, F., Ramírez, M., Cantero, D., 2021. Anoxic biogas biodesulfurization promoting elemental sulfur production in a continuous stirred tank bioreactor. *J. Hazard. Mater.* 401.
- Gamisans, X., Chaguacede, I., Cantero, D., Ramírez, M., Moustakas, K., Malamis, S., Ortega, J., Prado, O., Ramírez, C., 2021. Bioprocess for simultaneous biogas landfill desulfurization and nitrogen removal from leachate in a pilot plant, in: 8th International Conference on Sustainable Solid Waste Management. Athens, pp. 1–2.



Long-term operation of a pilot bioscrubber for landfill biogas desulfurization

S. Torres-Herrera¹, J. Palomares-Cortés¹, J.J. González-Cortés¹, X. Gamisans², D. Cantero¹ and M. Ramírez¹

¹Department of Chemical Engineering and Food Technologies, Wine and Agrifood Research Institute (IVAGRO). Faculty of Sciences. University of Cadiz, Cadiz, Spain

²Department of Mining Engineering and Natural Resources, Faculty of Biosciences Engineering, Universitat Politècnica de Catalunya, Manresa (Barcelona), Spain

Corresponding author email: sandra.torres@uca.es

keywords: *biodesulfurization; biogas; anoxic; hydrogen sulfide; pilot-scale.*

Introduction

Biogas is a renewable energy source produced from the anaerobic digestion of biodegradable organic matter. The composition of biogas is mainly dependent on the origin of this organic matter. It mainly consists of a mixture of methane and carbon dioxide. Biogas also has other harmful minor components such as hydrogen sulfide (H₂S) whose presence hinders its valorization for most purposes. The aerobic or anoxic desulfurization process uses oxygen (O₂) or nitrate/nitrite (NO₃⁻/NO₂⁻) as electron acceptors, respectively, to oxidize H₂S to elemental sulfur and/or sulfate. Biotrickling filters (BTF) have been extensively investigated for H₂S removal from biogas, showing high sulfide elimination capacities (EC), cost-effectiveness, low maintenance requirements and robustness (Almenglo et al., 2019; López et al., 2016). Nevertheless, in BTFs for biogas desulfurization, column clogging can arise due to the accumulation of sulfur and/or biomass on the packing material, which in turn leads to flooding and system shutdown. A possible alternative to overcome these shortcomings would be the use of suspended growth bioreactors. González-Cortés et al. (2021) achieved high H₂S ECs using a continuous stirred tank bioreactor (CSTBR) in anoxic conditions. The BIOGASNET technology proposes to integrate an anoxic bioscrubber with a nitrification reactor. In this work, the long-term operation of a pilot scale anoxic bioscrubber fed with landfill biogas and nitrified effluent from a nitrification step is shown, as well as the optimal operating conditions of the equipment.

Materials and methods

The BIOGASNET prototype was implemented in the Miramundo-Los Hardales landfill located in Cádiz (Spain). The pilot plant consisted of an anoxic bioscrubber fed by nitrified effluent from the nitrification bioreactor and biogas from the landfill wells. The desulfurization stage was performed in an anoxic bioscrubber which consisted of 3 units: (i) a washing tower (working volume of 0.8 m³) for the H₂S absorption from biogas to the liquid phase, (ii) a stirred tank reactor for oxidizing H₂S into sulfate and/or sulfur (maximum working volume of 1 m³) and, (iii) a settler where the elemental sulfur is separated. Other components of the system were a biogas blower, and a set of pumps for liquid recirculation, nitrate feeding, pH control and antifoam-nutrients addition. A H₂S and O₂ sensor was used to determine their concentration in the biogas stream.

The inoculum was obtained from the sewage treatment plant of Rota (Cádiz, Spain). The start-up of the anoxic bioreactor was carried out with 100 L of inoculum, 1.6 kg of Na₂CO₃, 2.1 kg of NaNO₃, 0.8 of NH₄Cl, 3.75 of NPK 6-4-6 fertilizer (Ciemhus universal fertilizer, Infertosa S.A) and filled with tap water up to 761 L.

During this first stage, the bioreactor was fed using Na₂S to an IL of 6 gS-H₂S m⁻³ h⁻¹. After two weeks, the IL was doubled to 12 gS-H₂S m⁻³ h⁻¹ in order to increase the biomass concentration. From week 13 onwards, the bioreactor was fed with biogas which had an average initial concentration of H₂S and O₂ of 146.1 ± 54.2 ppm_v and 1.77 ± 0.91%, respectively.

Results and discussion

Fig. 1a summarizes the biogas flow rate and IL applied to the system and its H₂S RE since real biogas was fed to the system (week 13). An average biogas flow rate of 43.0 ± 12.2 m³ h⁻¹ has been treated during the operation time resulting in a total of 274,801 m³ of desulfurized biogas during the 38 weeks.

Weeks 13-15 correspond to the start-up of the prototype with landfill biogas. Initially, a biogas flow rate of 11.6 m³ h⁻¹ was established, corresponding to an IL of 2.1 ± 1.0 gS-H₂S m⁻³ h⁻¹ and an RE of 98 ± 1%. During



these weeks, a total amount of 850 g N-NO₃⁻ was treated by the system. In weeks 23-41, the biogas flow rate was increased to 42.6 m³ h⁻¹ achieving an IL of 11.4 ± 4.7 gS-H₂S m⁻³ h⁻¹ with an RE of 81 ± 7%. From week 31 onwards, nitrate consumption dropped to 13 g N-NO₃⁻. Finally, in weeks 47-61, a new blower was installed, which allowed reach the pre-established biogas flow rate in the project (54.1 m³ h⁻¹). Even so, the IL remained at values of 11.3 ± 3.7 gS-H₂S m⁻³ h⁻¹ due to the low H₂S concentrations at the inlet during that season (127 ± 41 ppm_v). An H₂S RE of 77 ± 11% was achieved, however, the consumption of nitrate dropped to 2 g N-NO₃⁻, probably by the oxygen content in the inlet biogas stream.

Aiming to improve the H₂S mass transfer from the gas to the liquid phase, the recirculation flow rate was increased (week 56). The mid-term effect of this change is shown in Fig. 1b. Here, a recirculation flow rate of 20.4 m³ h⁻¹ was kept constant under a biogas flow rate of 55 m³ h⁻¹. Under these conditions, an average outlet H₂S concentration of 3.0 ± 1.2 ppm_v (RE=97.1 ± 1.1%; EC=9.6 ± 0.5 gS-H₂S m⁻³ h⁻¹) was found which were the best results in terms of RE were obtained.

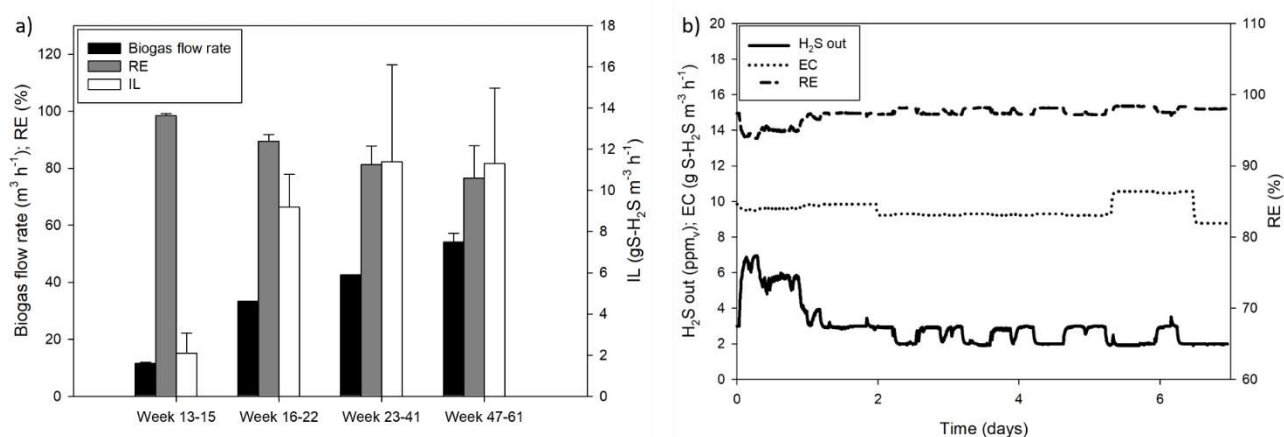


Figure 1. (a) Summary of the main operating conditions during long-term operation, and (b) results obtained during the study of the mid-term effect of increasing the recirculation flow rate.

Conclusions

The desulfurization of real biogas has been successfully carried out on a pilot-scale standing as a feasible alternative to the current physical-chemical processes. Low H₂S concentration and high O₂ concentration at the inlet biogas stream caused a decrease in nitrate demand, leading to aerobic H₂S oxidation, which rises as the recirculation flow rate increases.

Acknowledgements: This study is supported by the Green Fund and the LIFE project (EC): “Sustainable biogas purification system in landfills and municipal solid wastes treatment plants (LIFE BIOGASNET)”, LIFE18 ENV/ES/000426.

References

- Almenglo, F., Ramírez, M., Cantero, D., 2019. Application of response surface methodology for H₂S removal from biogas by a pilot anoxic biotrickling filter. *ChemEngineering* 3, 1–12. <https://doi.org/10.3390/chemengineering3030066>
- González-Cortés, J.J., Torres-Herrera, S., Almenglo, F., Ramírez, M., Cantero, D., 2021. Anoxic biogas biodesulfurization promoting elemental sulfur production in a Continuous Stirred Tank Bioreactor. *J. Hazard. Mater.* 401, 123785. <https://doi.org/10.1016/j.jhazmat.2020.123785>
- López, L.R., Bezerra, T., Mora, M., Lafuente, J., Gabriel, D., 2016. Influence of trickling liquid velocity and flow pattern in the improvement of oxygen transport in aerobic biotrickling filters for biogas desulfurization. *J. Chem. Technol. Biotechnol.* 91, 1031–1039. <https://doi.org/10.1002/jctb.4676>



Anaerobic Co-digestion of sewage sludge and acidic cheese whey

F. Gkoumas¹, Z. Gravanis¹, C. Noutsopoulos¹, D. Mamais¹ and S. Malamis¹

¹Sanitary Engineering Laboratory, Department of Water Resources and Environmental Engineering / School of Civil Engineering, National Technical University of Athens, Zografou, Athens, Greece

Corresponding author email: gkoumasfil@yahoo.com

keywords: Anaerobic co-digestion; Agro-industrial waste; Acidic cheese whey; Biochar; BMP.

Introduction

Anaerobic Digestion (AD) is widely used in the valorization of waste because of its ability to produce biogas, which belongs to the biofuel category. However, mono -digestion has significant disadvantages, such as instability of the digestion process, limited availability of a particular feedstock, presence of heavy metals and low efficiency of biogas/methane production ¹. Anaerobic co -digestion (AcoD) is the simultaneous AD of two or more substrates and is a potentially promising option to overcome mono-digestion's disadvantages and improve AD plants' economics through higher methane production. In particular, AcoD can enhance biogas production by 25% to 400% compared to the mono-digestion of the same substrates. Numerous studies have been focused on the co-digestion of sewage sludge (SS) with different types of wastes and in this context, cheese whey (CW) has been proposed as a suitable co-substrate ². Given the above, this study aims to investigate the co-digestibility of SS and Acidic CW (ACW) by conducting AD batch experiments. In this sense, the biomethane potential (BMP) of ACW, SS, waste activated sludge (WAS) and mixtures was determined and compared with SS mono-digestion with three consecutive series of BMP tests. In addition, biochar, a known conductive material produced from the pyrolysis process, was supplemented in the bulk anaerobic liquid to evaluate its influence on the AD process ³.

Materials and methods

The experiments were carried out with a compact BMP unit consisting of a heated bath maintaining a constant temperature at 35 ± 1 ° C. The working volume of each bottle is 400 to 700 mL. The biogas produced passes through a scrubber of NaOH 2M solution to separate CH₄ from other gases. The volume of CH₄ is automatically measured and recorded in the BMP unit control panel. The substrate to inoculum ratio (SIR) was 1:2 in the first and second series and 1:1 in the third series. The duration of each series was 30 d and the tests were performed in duplicate, with inoculum-only reactors also selected in each series. The methodology followed was in accordance with Angelidaki et al. 2009 ⁴. SS, WAS and inoculum were obtained from the Psytalia Wastewater Treatment Plant (WWTP) and were blended before the characterization. The ACW was obtained from a dairy industry in Patra, Greece. The biochar was supplied by Novocarbo (Dörth, Germany).

Results and discussion

Table 1 summarizes the results of the three BMP series compared to the SS mono-digestion. The findings from the first BMP series show that the inclusion of WAS in the SS digestion has a small, yet notably positive effect (3%) on methane yield compared to SS mono-digestion. In the second BMP series, ACW as a co-substrate to the SS showed a slight increase (1%) in methane yield at a ratio (SS-ACW) of 80:20. However, the methane yield was 8% and 18% lower compared to SS mono-digestion with increased ACW compared to SS with a ratio of SS: ACW at 60:40 and 50:50, respectively. After completion of the 30-day digestion, alkalinity was not significantly reduced and pH was maintained in a desired range. Therefore, in the third series of BMP tests, the SIR was changed to 1:1 and higher SS: ACW ratios were applied. Furthermore, the reactor with SS: ACW at a 95:5 ratio was found to enhance the methane yield compared to SS mono-digestion. Co-digestion experiments of SS and ACW in continuous flow anaerobic reactors in another study revealed an increase in biogas production compared to SS mono-digestion, but a negative effect was observed on the biogas composition ⁵. The lower methane content in the biogas yield could explain the reduced methane yield. In addition, the reactors with the same ratio of SS: ACW, which were enriched with biochar (5 g/L), showed a positive effect on methane yield, which was 7% and 4% higher than the SS mono-digestion and the non-



amended with biochar reactors, respectively. Interestingly, the methane yield of the biochar enriched reactors with a ratio of SS: ACW at 95:5 was higher than the SS: ACW at a 95:5 ratio. Although biochar has been shown to improve the performance of AD in many ways ⁶, further research is needed on the associated mechanisms and the effect of conductive materials on AD.

Table 1. Methane yield of the three BMP series compared to SS mono-digestion

BMP Tests mixtures used		Methane yield variation	
		NmL CH ₄ g ⁻¹ VS _{sub}	%
First Series	SS 80% - WAS 20%	354.6	3
SIR 1:2	SS 100%	343.1	0
	WAS 100%	110.8	-68
Second Series	SS 80% - ACW 20%	388.2	1
	SS 100%	383.9	0
	SIR 1:2	353.6	-8
Third Series	SS 50% - ACW 50%	342.7	-18
	SS 95% - ACW 5% Biochar (5 g/L)	381.5	7
	SS 90% - ACW 10% Biochar (5 g/L)	373.7	5
	SIR 1:1	366.8	3
	SS 100%	355.2	0

Conclusions

In this study, the effect of co-substrates on the performance of AD was investigated, with a particular interest in the co-digestion of SS and ACW and the determination of the most appropriate ratio of co-substrates. In addition, biochar's effect on AD was also investigated, although not to a great extent, with preliminary results showing that it has a favorable effect on AD's performance. In particular, methane yield of SS and ACW was increased compared to SS mono -digestion when the ratio SS: ACW was 80:20 and higher. Methane yield was further increased when the bulk anaerobic liquid was enriched with biochar. Finally, increasing SIR to 1:1 did not affect the performance of the AD process and the methane yield of the SS mono-digestion tests was relatively similar in terms of NmL CH₄ g⁻¹ VS_{sub} among the three BMP series.

Acknowledgements: This study was carried out within H2020 project "Accelerating Water Circularity in Food and Beverage Industrial Areas around Europe (H2020 AccelWater)", Project number: 958266.

References

- Hagos, K.; Zong, J.; Li, D.; Liu, C.; Lu, X. Anaerobic Co-Digestion Process for Biogas Production: Progress, Challenges and Perspectives. *Renew. Sustain. Energy Rev.* **2017**, *76* (September), 1485–1496. <https://doi.org/10.1016/j.rser.2016.11.184>.
- Fernández, C.; Blanco, D.; Fierro, J.; Judith Martínez, E.; Gómez, X. Anaerobic Co-Digestion of Sewage Sludge with Cheese Whey under Thermophilic and Mesophilic Conditions. *Int. J. Energy Eng.* **2014**, *2014* (2), 26–31. <https://doi.org/10.5923/j.ijee.20140402.02>.
- Yang, S.; Chen, Z.; Wen, Q. Impacts of Biochar on Anaerobic Digestion of Swine Manure: Methanogenesis and Antibiotic Resistance Genes Dissemination. *Bioresour. Technol.* **2021**, *324* (January), 124679. <https://doi.org/10.1016/j.biortech.2021.124679>.
- Angelidaki, I.; Alves, M.; Bolzonella, D.; Borzacconi, L.; Campos, J. L.; Guwy, A. J.; Kalyuzhnyi, S.; Jenicek, P.; Van Lier, J. B. Defining the Biomethane Potential (BMP) of Solid Organic Wastes and Energy Crops: A Proposed Protocol for Batch Assays. *Water Sci. Technol.* **2009**, *59* (5), 927–934. <https://doi.org/10.2166/wst.2009.040>.
- Maragkaki, A. E.; Fountoulakis, M.; Kyriakou, A.; Lasaridi, K.; Manios, T. Boosting Biogas Production from Sewage Sludge by Adding Small Amount of Agro-Industrial by-Products and Food Waste Residues. *Waste Manag.* **2018**, *71*, 605–611. <https://doi.org/10.1016/j.wasman.2017.04.024>.
- Altamirano-Corona, M. F.; Anaya-Reza, O.; Durán-Moreno, A. Biostimulation of Food Waste Anaerobic Digestion Supplemented with Granular Activated Carbon, Biochar and Magnetite: A Comparative Analysis. *Biomass and Bioenergy* **2021**, *149* (April). <https://doi.org/10.1016/j.biombioe.2021.106105>.



The microbiology of the two stage Dark Fermentation - Metanogenic reactor, optimization of methane production

S. Becarelli¹, E. Rossi², R. Iannelli², S. Di Gregorio¹ and I. Pecorini²

¹Department of Biology University of Pisa, Pisa, Italy ²Department of Energy, Systems, Territory and Construction Engineering, Pisa

Corresponding author email: isabella.pecorini@unipi.it

keywords: *dark fermentetion; hydrogen; metanogenesis; predictive functional metagenomics.*

Dark fermentation (DF) is an efficient technology for hydrogen production by the valorization of various organic wastes, exploited as reactor feedstock. In particular, the organic fraction of the municipal solid waste is an easily gathered fermentation substrate, providing high yields in biogas and value-added organic compounds, such as Volatile Fatty Acids. Dark fermentation, however, produces hydrogen at relatively low yield: its potential can be improved by coupling DF reactor stages with different bioreactor assets. In this study a two stage DF-metanogenic reactor was conducted and monitored by optimizing the Hydraulic Retention Time to maximize methane production, obtaining a corresponding increment of 51.7 % A focus on functional inference based on NGS metabarcoding analysis and comparison of microbial communities that populate each reactor stage will be discussed.



Development of a two-stage anaerobic digestion system for treating fruit and vegetable wastes from open markets

A. Kalogiannis¹, I.A. Vasiliadou¹ and K. Stamatelatou¹

¹Department of Environmental Engineering, Democritus University of Thrace, Xanthi, Greece
Corresponding author email: astamat@env.duth.gr

keywords: Biogas; dry anaerobic digestion; two-stage system; fruit and vegetable wastes.

Introduction

The Organic Fraction of Municipal Solid Waste (OFMSW) is considered a high potential feedstock for biogas production via anaerobic digestion (AD) (Abudi et al., 2016). Open market wastes are a category of municipal solid wastes of organic nature, devoid of pathogens usually present in manures and suitable for producing a high-quality digestate besides biogas via AD technology. Valorising the wastes from open markets, which are popular in Mediterranean countries, is the subject of the European co-funded project "CEOMED". Papirio et al. (2022) found that, despite the variable composition of the open market waste mixture throughout the year, its main biochemical and physicochemical characteristics remained within a narrow range of variation. The present study demonstrates a two-stage AD system developed to treat open market wastes. The system consisted of a Leach Bed Reactor (LBR) coupled with an Upflow Anaerobic Sludge Bed (UASB) reactor. The use of an LBR is an alternative option as a first stage for the hydrolysis of high solid wastes due to its simple and economical construction. LBR operates at a high solid content (dry AD) minimising the system's requirements for water. The leaching process in LBRs results in the extraction of organic matter into the liquid (leachate) which can be fed in a conventional continuous stirred tank reactor (CSTR) or a high-rate UASB reactor. Moreover, a bulking agent such as wood chips is necessary for the LBRs to avoid clogging problems. The two-stage system has been operated for almost one year, treating different open market waste mixtures, and its performance in terms of methane yield has been evaluated.

Materials and methods

Fruits and vegetables were purchased from local markets to simulate the waste mixtures of open municipal markets in two Mediterranean countries, Jordan and Tunisia (Papirio et al 2022). The waste mixtures corresponding to different seasons throughout the year are denoted as season 1 (for autumn/winter), season 2 (for spring) and season 3 (for summer).

An LBR (glass column of 1.9 and 1.3 L total and operating volume, respectively) was connected with a UASB reactor (2.35 and 2.1 5L of total and operating volume, respectively) and operated as a two-stage bench-scale system (Figure 1). First, the waste mixture (33.75 g volatile solids; VS) was mixed with wood chips at a ratio of 0.34 g Total Solids (TS) wood chips per gTS of the waste mixture and was loaded from the top, while the digested waste was removed from the lower part of the LBR to keep the volume of the waste bed in the LBR constant. This procedure occurred three times per week, setting the feeding rate at ca. 7 gVS d⁻¹. The leachates of the LBR were collected in a stirred chamber (1L). The leachate was recirculated in the LBR at a rate of 18 L d⁻¹, aiming to facilitate the leaching process, and was fed to the UASBR at rates ranging from 0.09 to 1.45 L L⁻¹ d⁻¹ (corresponding to an HRT of 11 and 0.69 days respectively). The UASB reactor was inoculated with 1 L of granules from a full-scale UASB reactor treating dairy wastes. The upflow velocity was 3.5 m h⁻¹ and was sustained through a recirculation imposed on the UASB reactor. Besides the UASB recirculation, the effluent supernatant was added to the LBR.

The TS, VS and Chemical Oxygen Demand concentration were measured according to the Standard Methods. The biogas composition was analysed using a GC (Shimadzu GC-2014), equipped with a thermal conductivity detector (TCD).

Results and discussion

The operating parameters of the system were (a) the VS loading rate (organic loading rate; OLR) and (b) the leachate feeding rate from the LBR to the UASB and the equivalent UASB supernatant recirculation from



the UASB reactor to the LBR (or else, the hydraulic retention time; HRT). Initially, the system was acclimatised to the waste mixtures, which were successively loaded. The OLR was first 5-7 g VS d⁻¹ (0-92 d) and then 9-12 g VS d⁻¹. The HRT in the UASB reactor was set to 11 days (0-18days) and was further reduced to 5.5 days and, finally, to 0.69 days.

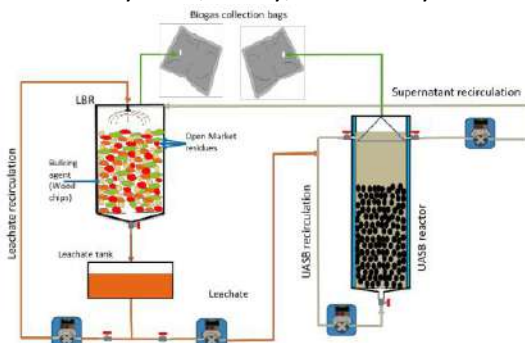


Figure 1. Experimental set-up of LBR-UASB system.

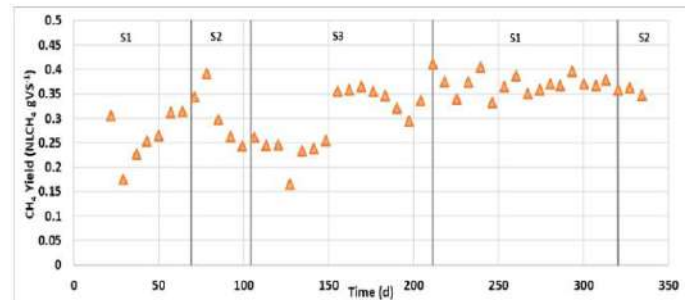


Figure 2. System's methane yield. S1-S3 denote the waste mixture fed to the system.

The COD concentration of the leachate varied from 4 to 28 gL⁻¹. It was influenced by each new loading, which increased the leached organic matter and the supernatant recirculation of the UASB to the LBR, which enhanced the methanogenic activity in the LBR. Since the UASB supernatant contained microorganisms, there was a transfer of methanogens to the LBR as the feeding rate of the leachate to the UASB and, equivalently, the recirculation rate of the UASB supernatant to the LBR was increased. This was indicated by the decreased COD concentration of the leachate (4.7 g L⁻¹) and the increased methane production (0.48 NL d⁻¹) when the feeding rate of the leachate was increased to 0.3 L L⁻¹d⁻¹ (HRT of 5.5 d).

The total methane yield (MY) from the LBR and the UASB varied initially, but it stabilised between the 246th and 334th days. The maximum MY was 0.41 NL gVS⁻¹ when the system's OLR was 8.31 gVS d⁻¹ (or 6.39 gVS L_{LBR}⁻¹d⁻¹) and the LBR was loaded with the Season 1 mixture (on the 211th day of operation). The MY recorded at the continuously operated two-stage system was close to the biochemical methane potential (BMP) of the waste mixtures 402-429 NL gVS⁻¹ (Papirio et al., 2022).

Conclusions

The LBR-UASB reactor two-stage system for treating the solid waste mixtures of fruit and vegetable waste from open markets was studied under various organic loading rates. It was found that the variation in mixture wastes throughout the year did not influence the methane yield (0.34-0.38 NL gVS⁻¹), which is very close to the maximum levels recorded via BMP tests conducted on the same waste mixtures (402-429 NL gVS⁻¹). This means that the two-stage configuration is an efficient alternative to the conventional CSTR-based systems requiring less volume and negligible addition of water.

Acknowledgements: This research has been carried out with the financial assistance of the European Union under the ENI CBC Mediterranean Sea Basin Programme.

References

- Abudi, Z. N., Hu, Z., Sun, N., Xiao, B., Rajaa, N., Liu, C., et al. (2016). Batch anaerobic co-digestion of OFMSW (organic fraction of municipal solid waste), TWAS (thickened waste activated sludge) and RS (rice straw): influence of TWAS and RS pretreatment and mixing ratio. *Energy*, 107, 131-140.
- Ma, J., Duong, T. H., Smits, M., Vestraete, W., and Carballa, M. (2011). Enhanced biomethanation of kitchen waste by different pretreatments. *Bioresour. Technol.*, 102, 592-599.
- Papirio, S., Trujillo Reyes, A., Scotto di Perta, A., Kalogiannis, A., Kassab, G., Khoufi, S., Sayadi, S., Frunzo, L., Eposito, G., Feroso, F.G., Stamatelatu K. (2022). Exploring the Biochemical Methane Potential of Wholesale Market Waste from Jordan and Tunisia for a Future Scale Up of Anaerobic Digestion in Amman and Sfax. *Waste and Biomass Valorization*. doi.org/10.1007/s12649-022-01790-1



Transition from lab to pilot scale anaerobic digestion systems: effect of the substrate composition on the process stability and repeatability

K. Tsigkou¹, D. Zagklis¹, P. Tsafrakidou², C. Zafeiri² and M. Kornaros¹

¹Lab. of Biochemical Engineering & Environmental Technology (LBEET), Dept. of Chemical Engineering, University of Patras, Patras, Greece

²Green Technologies Ltd, Patras, Greece

Corresponding author email: kornaros@chemeng.upatras.gr

keywords: anaerobic digestion; lab scale; pilot scale; two-stage systems; feedstock composition.

Introduction

The anaerobic digestion (AD) process has been extensively used for energy production through waste management and valorization. The fact that AD is a complex four-step process, in which various microorganisms are involved for several reactions accomplishment, leads to extensive study needs, aiming at efficiency maximization. The inoculum is usually inhibited by several factors (toxic compounds or environmental conditions), so for this reason the optimization of the operation parameters at lab scale systems prior to scale up tests is considered as mandatory.

Two streams of the municipal solid wastes characterized by high organic content, are the food waste and the hygiene products, focusing on the used nappies. In case of food waste there are carbohydrates, proteins and lipids, while concerning the used nappies, the organic content is mainly carbohydrates, followed by the biodegradable part of excreta and urine. Currently, for both waste streams no specific waste management strategies and regulations are pursued. The aim of this study was the valorization of two different mixtures of the aforementioned substrates, namely one consisted of fruits and vegetables wastes (carbohydrates) as well as used nappies, and a second mixture comprised of various food waste (carbohydrates, proteins and lipids) combined with used nappies. The test of such mixtures with significantly different composition is able to lead to useful conclusions about the performance of the reactors, their stability and the repeatability of the results in higher scale systems.

Materials and methods

Concerning the substrates, two mixtures were tested, namely the mixture 1 was consisted of Fruits/Vegetables and used disposable nappies hydrolysate (4:6 w/w) (Tsigkou et al., 2020) while the more complex mixture 2 was consisted of Bread, meat and fruits/vegetables and used disposable nappies hydrolysate (1:9.7 w/w). The experimental configuration in lab and pilot scale studies comprised by an acidogenic and a methanogenic reactor. The working volumes were 0.75L and 180L for the acidogenic reactor as well as 4L and 1800L for the methanogenic reactor respectively, at mesophilic conditions. In all systems the applied operational conditions were hydraulic retention time (HRT) of 2d and 20d respectively in each reactor.

Results and discussion

Even if in both cases the mixtures were successfully valorised in lab scale reactors, significant difference was presented in pilot scale operation for mixture 2, as described in Figure 1. More specifically, the mixture 1 reached the lab scale yields after 60d of operation (Tsigkou et al., 2021), while for mixture 2, the lab scale yield met the pilot scale after 30d of operation and a constant decrease followed. This was attributed to the fact that the lab and pilot scale mixtures 2 exhibited significantly different proteins/lipids ratio, leading to inoculum inhibition and thus instability of the process.

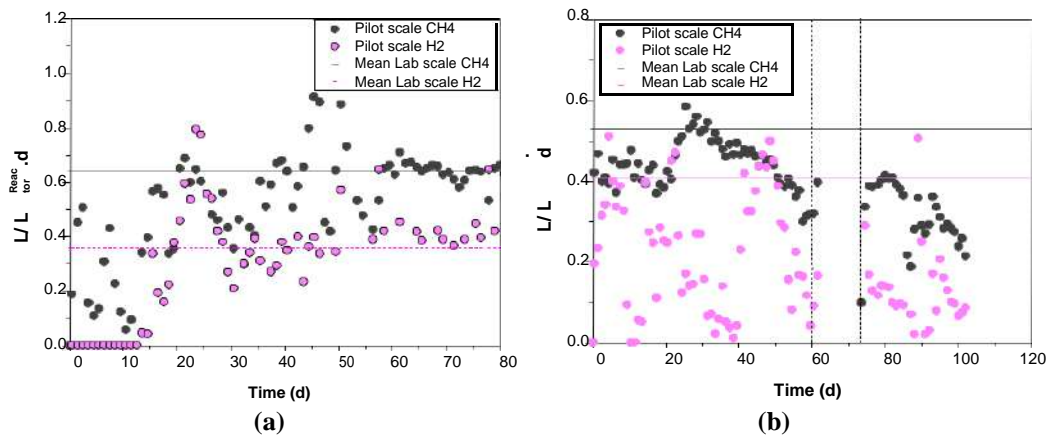


Figure 1. Biogas production of mixture 1 (a) and 2 (b) under lab and pilot scale operation.

Conclusions

The utilization of a more complex substrate in terms of organic compounds group could lead to variance of the substrate composition and thus instability of the process. On the other hand, non-complex mixtures are able to lead to repeatable results during the transition of the lab to the pilot scale.

Acknowledgements: This work was funded by the European Project WASTE4THINK (H2020 - GA 688995) “Moving towards Life Cycle Thinking by integrating Advanced Waste Management Systems”, while the travel expenses were covered by the “Sustainability Travel award 2022”, by MDPI.

References

- Tsigkou, K., Tsafrakidou, P., Kopsahelis, A., Zagklis, D., Zafiri, C., Kornaros, M., 2020. Used disposable nappies and expired food products valorisation through one- & two-stage anaerobic co-digestion. *Renew. Energy* 147. <https://doi.org/10.1016/j.renene.2019.09.028>
- Tsigkou, K., Tsafrakidou, P., Zagklis, D., Panagiotouros, A., Sionakidis, D., Zontos, D.M., Zafiri, C., Kornaros, M., 2021. Used disposable nappies and expired food products co-digestion: A pilot-scale system assessment. *Renew. Energy* 165, 109–117. <https://doi.org/10.1016/j.renene.2020.11.013>



UASB performance and microbial community during sulfate enriched hydrolyzed starch treatment.

D. Theodosi Palimeri¹, A.G. Vlyssides¹ and A.A. Vlysidis^{1,2}

¹School of Chemical Engineering, National Technical University of Athens, Athens, 15780, Greece

²School of Chemical and Environmental Engineering, Technical University of Crete, Chania, 73100, Greece

Corresponding author email: avlysidis@isc.tuc.gr

keywords: UASB; sulfate; starch; methane; microbial community.

Introduction

Anaerobic digestion is considered an efficient technology for wastewater treatment and energy production. Among anaerobic processes, Upflow anaerobic sludge blanket (UASB) reactor is one of the most widely used and has been applied for many types of wastewater such as those contained high concentration of sulfate. Granular sludge of UASB is the main factor for its successful operation performance. There is a large amount of different kind of bacteria inside the granule that interact effectively for the conversion of substrate. Moreover, it is reported that granules which degrade carbohydrates have a layered distribution and are resistant to toxicity from hydrogen sulfide (Fang, 2000). However, wastewater with high content of sulfate can inhibit methane production during anaerobic digestion since sulfate reducing bacteria (SRB) compete methanogenic bacteria for organic carbon and produce sulfide from sulfate reduction which is toxic for anaerobic bacteria (Jing et al., 2013). Hence, the COD/SO₄²⁻ ratio could affect the microbial community and subsequently the performance of the reactor (Lu et al., 2018). Although many studies have been focused on sulfate reduction, more research is needed regarding the methane production from sulfate-rich wastewater.

The aim of this study is to investigate the effect of sulfate presence in anaerobic digestion. For this reason, a UASB reactor has been constructed and operated using hydrolyzed starch as feed together with the addition of sulfate. The removal of TOC, iron, and sulfate, as well as the methane production under different Organic Loading Rates (OLRs) was studied. Furthermore, the difference between the microbial communities before and after the addition of sulfate was examined.

Materials and methods

A lab-scale UASB reactor, made of Plexiglas and with an effective working volume of 12 L was constructed and continuously operated at 35 ± 2°C for 165 days. The reactor was inoculated with 3 L anaerobic sludge from a UASB of a potato processing industry in Athens. Starch hydrolyzed by Fenton reagents was used as influent for the first 85 days of operation containing 46-69 mg N/L, 0.075 mg P/L, COD 1-1.4 g/L, Fe 4-8 mg/L, while sulfate concentration was less than 6 mg/L. The HRT examined at different values: 35 h, 32 h and 16 h with corresponding OLR values equal to 0.54, 0.66 and 2.00 g COD/L_{UASB}-day, respectively. On day 86, sulfate was added to the influent in the form of sulfuric acid at various concentrations ranging from 190 to 373 mg/L while COD was 1.5-3 g/L, TP 0.15 mg/L, TN 69-138 mg/L and Fe 8-10 mg/L. At this stage (i.e. 86-165 days), the HRT was varied from 16 h to 11 h, 22 h and back to 16 h again, with respective OLR values equal to 2.00, 3.00, 3.78, and 5.20 g COD/L_{UASB}-day, respectively. The COD/SO₄²⁻ ratio was varying from 14.8 to 3.2.

During the whole period of the experiment COD, sulfate, Fe, VFAs and alkalinity, NH₄⁺, TOC and TN in the influent and effluent were measured. The amount of biogas produced per day was recorded on a PLC and the percentage of CH₄, CO₂ and H₂ in the total biogas was measured with a biogas analyzer.

On days 85 and 150, samples of the anaerobic sludge were collected from the bottom of the reactor and the microbial communities were analyzed by 16S rRNA sequencing. The total DNA was extracted using Nucleo-Spin @ Soil Kit (MACHEREY-NAGEL) according to the kit manual procedure. The purity of the isolated DNA was quantified using nano-drop method and the extract was delivered to Novogene Bioinformatics Technology Co., Ltd. (Beijing, China.) for amplicon pyrosequencing on the Illumina MiSeq platforms. V3-V4 region of the bacterial 16S rRNA genes were amplified by PCR using the primer pair 341F/806R.

Results and discussion



At the first 85 days, TOC removal was ranging from 67.1% to 85.5%, and the percentage of methane in biogas was varying from 45.7 to 64.0%. The highest methane production was 0.24 ± 0.05 L CH₄/L_{UASB}-day when HRT was 16 h and OLR 2 g COD/L_{UASB}-day. At this period, no sulfate was observed in the effluent.

After the addition of sulfuric acid to the influent, TOC removal efficiency was varying from 70.1% to 94.9%. At HRT 16 h, the OLR, Fe and COD/ SO₄⁻² ratio were equal to 2 g COD/ L_{UASB}-day, 8 mg/L and 3.5, respectively, while the methane production was 0.267 ± 0.05 L CH₄/L_{UASB}-day. At HRT 11 h, OLR was increased at 3 g COD/ L_{UASB}-day, Fe and COD/ SO₄⁻² ratio stayed the same while the methane production increased at 0.496 ± 0.002 L CH₄/L_{UASB}-day. The methane production was further increased at 0.615 ± 0.009 L CH₄/L_{UASB}-day when the HRT, OLR, Fe and COD/ SO₄⁻² ratio were equal to 22 h, 2.78 g COD/ L_{UASB}-day, 9 mg/L and 9-15, respectively.

During the last days of UASB operation, the HRT returned to 16 h, the OLR was increased at 5 g COD/ L_{UASB}-day, Fe also increased at 10 mg/L and the COD/ SO₄⁻² ratio slightly decreased to 8.5. The methane production under these conditions was found to be 0.807 ± 0.002 L CH₄/L_{UASB}-day. Moreover, the percentage of methane in total biogas was remained relative stable at around 71%, for the whole period. The correlation between methane production and SO₄⁻² in the effluent could be described by the following equation:

$$Y = 1.07 \times X^{-8.05} \quad (R^2 = 0.942),$$

where Y is the methane production (L CH₄/L_{UASB}-day) and X is the concentration of SO₄⁻² in the effluent (mg/L).

After 16S rRNA gene sequencing the relative abundance of dominant bacteria in the two samples was investigated. At genus level, the predominant archaea before and after sulphate addition in the substrate, were *Methanosaeta* with relative abundance 27.5% and 32.3%, respectively. This genus uses only acetate as energy source for methane production. After the addition of sulphate, *Methanosarcina*, *Methanospirillum* and *Methanobacterium* species were decreased from 0.5% to 0.0%, from 0.5% to 0.1% and from 3.3% to 2.3%, respectively. The competition between SRB and methanogenic bacteria that use hydrogen can explain the increase of *Methanosaeta* abundance (Jin et al., 2020). For the bacteria community, *Ruminococcus* predominates, accounting for 20.2%, while it was just 0.5% before the addition of sulphate. *Desulfovibrio* which belongs to SRB, accounted for 9.9% while before sulfate addition was only 1.7%. *Desulfovibrio* species utilize hydrogen as electron donors for sulfate reduction, however some of them have iron reduction abilities. Furthermore, *Syntrophomonas*' relative abundance was increased from 0.3 to 4%. This genus produces acetate from fatty acids and associates with methanogenic bacteria and bacteria that utilize hydrogen. In addition, *Propionivibrio* which produce propionate from sugars' fermentation was decreased from 9.8% to 0.2%. The syntrophic relationship between iron reducing bacteria and methanogens by direct interspecies electron transfer could explain the methane production enhancement (Jin et al., 2020).

Conclusions

The suitable presence of sulfate in the substrate during anaerobic digestion, promotes the acetoclastic methanogenesis and improves UASB performance when Fe occurs in the system.

Acknowledgements: This research is co-financed by Greece and the European Union (European Social Fund-ESF) through the Operational Programme «Human Resources Development, Education and Lifelong Learning» in the context of the project “Strengthening Human Resources Research Potential via Doctorate Research” (MIS-5000432), implemented by the State Scholarships Foundation (IKY).

References

- Fang, H. 2000. Microbial distribution in UASB granules and its resulting effect. *Water Sc. & Tech.* 42, 201-208.
- Jin, Z., Zhao, Z., & Zhang, Y. 2020. Insight into ferrihydrite effects on methanogenesis in UASB reactors treating high sulfate wastewater: Reactor performance and microbial community. *Environmental Science: Water Research and Technology*, 6(7), 1794–1803.
- Jing, Z., Hu, Y., Niu, Q., Liu, Y., Li, Y. Y., & Wang, X. C. 2013. UASB performance and electron competition between methane-producing archaea and sulfate-reducing bacteria in treating sulfate-rich wastewater containing ethanol and acetate. *Bioresource Technology*, 137, 349–357.
- Lu, X., Ni, J., Zhen, G., Kubota, K., & Li, Y. Y. 2018. Response of morphology and microbial community structure of granules to influent COD/SO₄⁻² ratios in an upflow anaerobic sludge blanket (UASB) reactor treating starch wastewater. *Bioresource Technology*, 256, 456–465.



MUNICIPAL SOLID WASTE



Spatial and temporal variation of VOCs in MSW landfills

A. Lagoudi¹, K. Poullos², G. Anagnostopoulos¹, K. Rigas¹ and S. Chandrinou¹

¹Terra Nova Ltd, Environmental Engineering Consultancy, Athens, Greece

²Regional Association of Solid Waste Management Agencies of Central Macedonia, Thessaloniki, Greece

Corresponding author email: lagoudi@terranova.gr

keywords: landfill; municipal solid waste, landfill gas; VOCs; odour; air quality.

Introduction

The main compounds that contribute to the odour presence in landfills are hydrogen sulfide, organic sulfides, specific Volatile Organic Compounds (VOCs), and ammonia. Volatile organic compounds emitted in a landfill are numerous. More than 100 VOCs have been identified in air samples from different landfill sites [1]. Some of these compounds are odorous, while there is a number of VOCs that are considered hazardous air pollutants. VOCs are generated from the aerobic and anaerobic processes of organic waste biodegradation in landfills [2, 3]. The VOCs found in a landfill differ significantly depending on the position of measurements [4, 5], the waste composition, the activities taking place in the landfill as well the age of the landfill. A VOCs monitoring campaign (air sampling and analysis) was performed in a number of landfill sites in Greece over 3 years. An evaluation of the VOCs concentrations measured is presented in this paper.

Materials and methods

VOCs monitoring was performed in 11 landfill sites in Greece during different periods of the year, over 2-3 years. VOC measurements were performed in the landfill gas, the gas migration monitoring wells, the active working face and in the ambient air in the landfill.

Air sampling was performed using air sampling pumps and appropriate absorbent tubes (charcoal sorbent tubes (SKC 226-01)). Analysis of target VOC compounds as well as VOC with the highest concentration was performed using Gas Chromatography / Mass Spectrometry by EN ISO/IEC 17025 accredited laboratories. Sampling was performed according to EN 13649 in the pipes and EPA TO-2 /MDHS 96 in the monitoring wells and landfill area.

Results and discussion

VOCs found in the landfill gas show variation over time as well as between landfills and sampling site within each landfill. The most frequently detected VOCs found in landfill gas collection pipes were toluene (0.09 – 25.50 mgm⁻³), xylenes (0.03 – 34.75 mgm⁻³), octane (0.11 – 2.74 mgm⁻³), ethylbenzene (1.01 – 10.84 mgm⁻³), benzene (0.03 – 0.59 mgm⁻³), heptane (0.05 – 1.38 mgm⁻³), limonene (0.98 – 55.50 mgm⁻³) and decane (0.65 – 67.83 mgm⁻³). The compounds with the higher concentrations were butane (354.50 mgm⁻³), 1-Methyl-4-(1-methylethyl) benzene (248.42 mgm⁻³), isopropyltoluene (243.57 mgm⁻³), cymene (158.14 mgm⁻³), decane (67.83 mgm⁻³) and limonene (55.50 mgm⁻³).

The concentrations of VOCs in the monitoring wells and in the ambient air of the landfill sites were quite lower than the levels found in the landfill gas. The most frequently detected VOCs found in the ambient air of the landfill sites measured in the active tipping areas where waste disposal is performed, were toluene (0.003 – 7.476 mgm⁻³), xylenes (0.003 – 11.536 mgm⁻³), limonene (0.021 – 2.211 mgm⁻³), ethylbenzene (0.004 – 3.386 mgm⁻³) and dichloromethane (0.011 – 2.226 mgm⁻³). The most frequently detected VOCs found in monitoring wells of the landfill sites were toluene (0.022 – 0.107 mgm⁻³), xylenes (0.016 mgm⁻³) and cymene (0.164 mgm⁻³).



Conclusions

After a landfill gas sampling campaign, results show a significant variation in concentrations of VOCs and odorous substances in MSW landfills of differing age and in different spots within each landfill.

References

- Davoli, E., Gangai, M.L., Morselli, L. and Tonelli, D., 2002. *Chemosphere*, Characterization of odorants emissions from landfills by SPME and GC/MS., 51, 357–368.
- Yang, L., 2002. *PhD Thesis*, An Investigation of Volatile Organic Compounds in Landfill Gas, School of Life Sciences and Technology, Victoria University, Melbourne.
- Fang, J. J., Yang, N., Cen, D. Y., Shao, L. M. and He, P. J., 2012. *Waste Management*. Odor compounds from different sources of landfill: Characterization and source identification, 32
- Yue, D., Han, B., Yue S., and Yang, T., 2014. *Waste Management*. Sulfide emissions from different areas of a municipal solid waste landfill in China, 34, 1041-1044.
- Jiang, J., Wang, F., Wang, J., and Li, J., 2021. *Waste Management and Research*. Ammonia and hydrogen sulphide odour emissions from different areas of a landfill in Hangzhou, China, 39 (2), 360-367.



**An investigation on the methane gas production and emission potential
From municipal solid waste dumpsites in India**

N. Gupta¹, N. B.P¹, R. Arora¹ and M. Karimpour²

¹Department of Civil Engineering, Amity University Haryana, India

²School of Civil Engineering, Iran University of Science and Technology (IUST)

Corresponding author email: niharika46247@gmail.com

keywords: landfill gas; LANDGEM; methane generation; solid waste;

Introduction

MSW is a significant contributor of landfill gas (LFG), which is an important source of Green House Gases (GHG). The current study aims to estimate the methane gas emission from landfills in the metropolitan cities (IPCC) Default model, First order decay model and LandGEM.

Methods

Three models were used for calculation of CH₄ emissions at the three landfills.

IPCC Default method	$CH_4 \text{ emissions Gg/y} = \{MSW_T \times MSW_F \times MCF \times DOC \times DOC_f \times F \times (16/12 - R) \times (1 - OX)\}$
IPCC First Order Decay Model	$Q_{CH_4} = L_0 \times R \times (e^{-Kc} - e^{-Kt})$
USEPA model: landGEM	$Q_{CH_4} = \sum_{i=1}^{10} \sum_{j=0.1}^{10} KL_0 [M_i/10] e^{-kt_{ij}}$

Where all the parameters have their usual meaning as per IPCC 2006 and LandGem.

Table 1. Landfill site details

Sno	Landfill site	City	State	Area (Hectares)	Year of starting	MSW T/day
1	Ghazipur	Delhi	Delhi	29.62	1984	2700
2	Bhalaswa	Delhi	Delhi	26.22	1994	4500
3	Okhla	Delhi	Delhi	22.89	1996	3600
4	Deonar	Mumbai	Maharashtra	12.19	1950	5500
5	Mavallipura	Bangalore	Karnataka	40.46	2007	4500
6	Kodungaiyur	Chennai	Tamil Nadu	104	1986	2600
7	Dhapa	Kolkata	West Bengal	35	1941	4500
8	Jawaharnagar	Hyderabad	Telangana	121	1950	5000

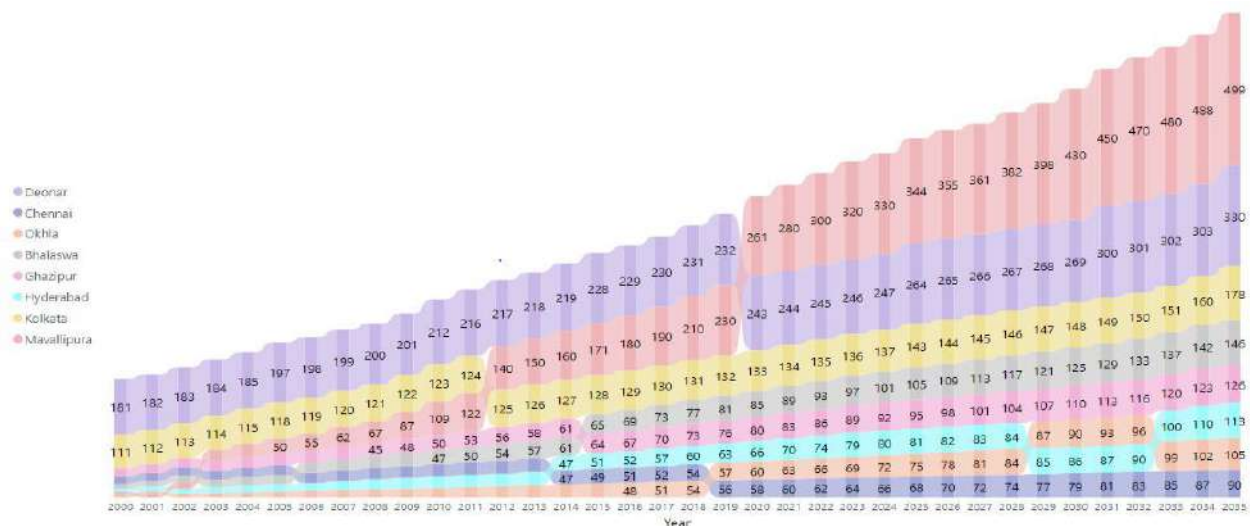


Figure 1. Estimation of methane in cities by IPCC FOD method.

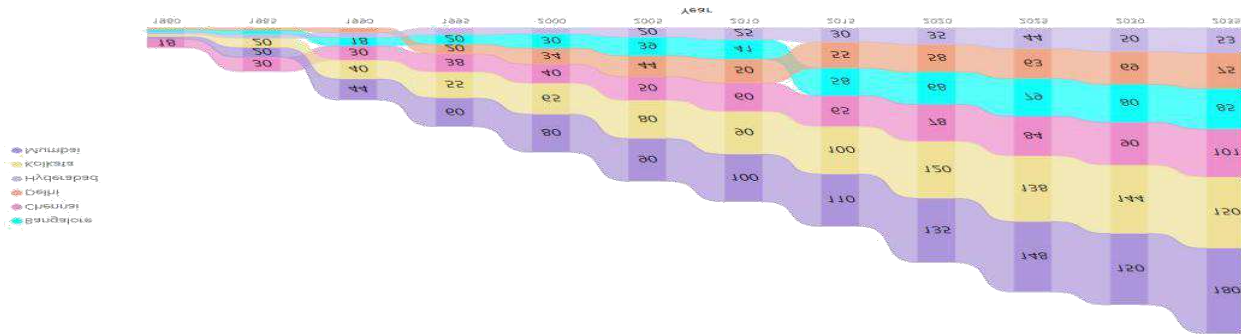


Figure 2. Estimation of methane in cities by LandGem method

Results and discussion

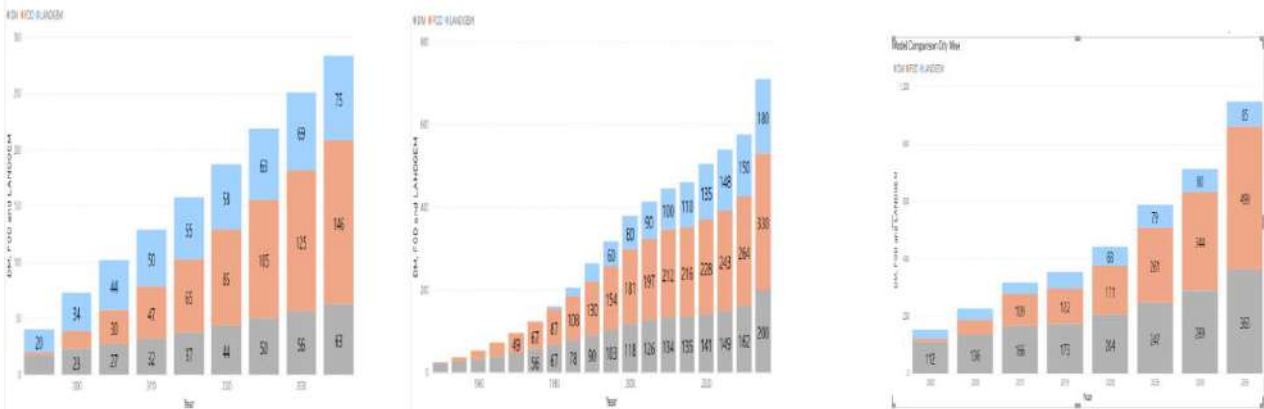


Figure 3. Few examples: City-wise distribution of methane emission by three models Delhi, Mumbai and Bangalore.

IPCC FOD model showed higher emission percentage as compared to other two models as per the final analysis done city-wise. Estimation using Default method showed that Mavallipura in Bangalore has the highest emission rates of 7969 Gg. till 2035 and Delhi's landfill sites showed least emissions with the value 1645 Gg. FOD model showed Mumbai landfill site contributing maximum i.e 10722 Gg over the years followed by Mavallipura, Bangalore and Jawaharnagar site displayed least emission rate of 2123 Gg. Mavallipura surpassed all the cities in emission rate after the year 2008 and increased drastically over the years.

Conclusions

The overall growth of the population, urbanization and economy of India has increased the amount of municipal solid waste generated in the country. Large amount of LFG i.e methane is being emitted to the atmosphere from all the Indian metro cities. Mavallipura in Bangalore and Deonar in Mumbai are highest contributor whereas Hyderabad is the least contributor. As observed from the results, variation in the estimated methane by different models is inevitable as input parameters are highly uncertain and pertains large variability according to MSW composition, disposal conditions and sometimes unrealistic assumptions.

References

- Intergovernmental Panel on Climate Change, Good practice guidance and uncertainty management in National greenhouse gas inventories, 2000.
- Babbar P., Verma S. et al. 2017, Groundwater Contamination From Non-Sanitary Landfill Sites – A Case Study on The Ghazipur Landfill Site, Delhi (India), IJAES, ISSN 0973-6077 Volume 12, Number 11 (2017)
- Srivastava A and Chakma S. 2020, Quantification of landfill gas generation and energy recovery estimation from MSW landfill sites, Delhi India, <https://doi.org/10.1080/15567036.2020.1754970>



Source-level composting of biodegradables for envisaging sustainable management of municipal solid waste in urban educational institutes – a model for developing countries

M. Shafiq¹

¹Environmental Biotechnology Laboratory (F4), Institute of Botany, University of the Punjab, Lahore, Pakistan

Corresponding author email: mshafiq.botany@pu.edu.pk

keywords: socio-economic constraints; GHGs; baseline data; circular economy; calorific value.

Introduction

The reciprocation of municipal solid waste (MSW) generation with population increase has been witnessed globally (World Bank, 2022) while being in severe disagreement with its sustainable management in most of the developing countries due to multiple socio-economic constraints. Being economic motive and waste ownership core elements of any MSW management system (MSWMS), targeting an educated and responsible community pie assured with circularity capital could prospect generating ripple of two prongs of beneficial ownership amongst the overall population of the developing countries. One of the two prongs being circular economic prospect and the other, being succinct outcome of the former, in the form of ripple of awareness amongst the communities driven by the economic assurance. Based on the UNESCO (United Nations Educational, Scientific and Cultural Organization) global education for sustainable development in the developing countries (UNESCO, 2020 & 2021), communities in urban educational institutes could be preferable adapt the sustainability practices related to composting based MSWMS. Hence, targeting community pie of the total population from higher and lower educational institutes could be preferable for initiating sustainability education. As most of the educational institutes are in urban areas of the developing countries, areas already succumbing to despair over space for MSW disposal at open dumps or landfills, preferring urban educational institutes would be more workable. The current study is aimed at assessing role of source-level composting of biodegradables in sustainable management of MSW in urban educational institutes as a model for developing countries of the world.

Materials and methods

The current was based on data collected from 350 institutes (200 Higher Education Institutes (HEIs) and 150 Elementary Schools (ES) of major cities of Punjab, Pakistan with main experimentation in Lahore, a pioneer city with modern MSWMS. From the two prongs of beneficial ownership of MSW amongst the overall population based on community pie of educational institutes, the circularity capital prospect of source level composting based MSWMS was compared with centralized MSWMS to assess: i) reduction in collection, handling, and transportation cost of MSW; ii) improvement in the calorific value of the combustible fraction of MSW for waste-to-energy (WtE); iii) revenue generation potential of the educational institutes for enhancing financial self-sufficiency; iv) reducing MSW burden on landfills as well as on designated and non-designated open dumps; and reduction in GHGs emissions of MSW. The role of composting based MSWMS model in sustainability education of the urban educational communities was assessed based on online questionnaire with 7-point Likert scale. Benefits of the established composting based MSWMS taken as independent variable: i) adaptation motivation level of respondents (dependent variable) was assessed for practicing composting based MSWMS in HEIs and ES; and ii) perceived environmental responsibility of the residents in sororities and fraternities (dependent variable) was assessed for spreading composting based MSWMS benefits in their hometowns based on scales given by Lee and Kamen (2008). The data for circularity capital prospect was applied with descriptive statistics and mean significance difference. The adaptation motivation and perceived environmental responsibility data were tested for reliability by using Cronbach's α followed by confirmatory factor analysis.

Results and discussion

The circularity capital prospect of composting based MSWMS is given in Figure 1 (A-D). The composting based MSWS rendered significant reduction in collection, handling, and transportation cost of MSW (Figure 1A).

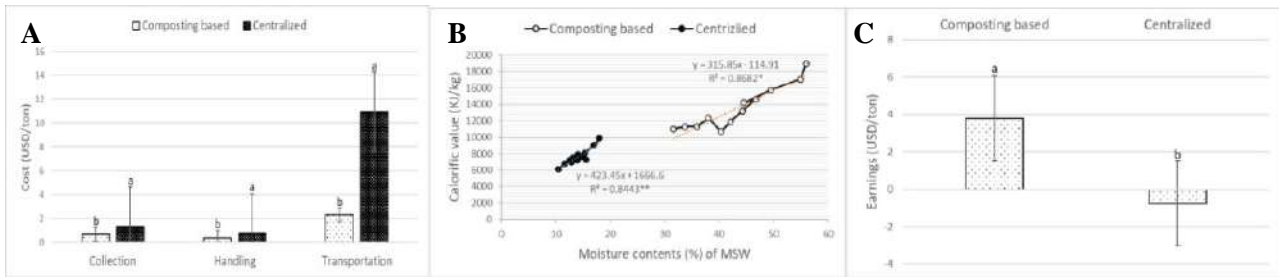


Figure 1: A) reduction in collection, handling and transportation cost; B) improvement in calorific value of the combustible fraction of MSW; C) comparison of revenue generated; D) reduction in GHGs emission from MSW

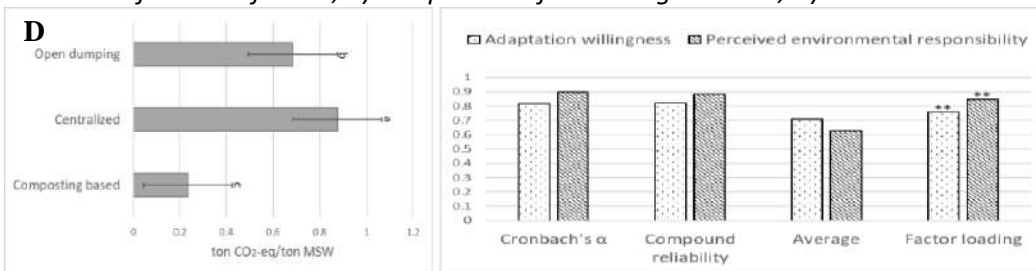


Figure 2. Sustainability education effectiveness of the composting based MSWMS amongst communities in HEIs and ES.

The calorific value of the combustible fraction of MSW was significantly increased in composting based MSWMS creating prospect of its improved demand for WtE (1B). The high transportation cost (US\$11) of MSW with ≥ 65 % biodegradables having ≥ 80 moisture contents (cumulative ≥ 50 % moisture contents in MSW) had always yielded negative benefit-to-cost ration contrary to the positive ratio achieved for composting based MSWMS (1C). Compared to the disposal of MSW at designated and non-designated open dumps, as well as, dumping in the landfill (a common practice under centralized MSWMS); there was significant reduction in the GHGs burden of the MSW when it was subjected to composting based MSWS at source level (1D). The aerobic decomposition of ≥ 50 % biodegradable of the MSW in composting based MSWMS had averted emission of CH₄ which was high unlikely in the case of open dumping and landfilling (Kennedy et al., 2010). The adaptation willingness and perceived environmental responsibility for spreading sustainability education based on composting-based MSWMS in the hometowns of the respondents from urban HEIs and ES indicated reliability based on Cronbach's α (Figure 2) with high convergent validity (>0.6) and average (>0.5).

Conclusions

The current study concludes that composting based MSWMS has strong prospect of circular economy based on multiple economic and environmental indicators observed in the selected HEIs and ES. The positive economic prospect could promote sustainability education in population of the developing countries from both ends i.e. through communities residing in the urban HEIs and ES owing for being at basic and advanced educational levels respectively, and belonging to the diversified hometowns from all corners of the country.

Acknowledgements: This study was funded by the HEC NRP2020 Project No. 12703 and PURC Project No. 300 (Fiscal Year 2021-22).

References

- Chiu, C. M., Hsu, M. H., Wang, E. T. G., 2006. Understanding knowledge sharing in virtual communities: An integration of social capital and social cognitive theories, *Decision Support Systems*, 42(3): 1872-1888.
- Kennedy, C., Steinberger, J., Gasson, B., Hansen, Y., Hillman, T., Havranek, M., Pataki, D., Phdungsilp, A., Ramaswami, A., Mendez, G.V., 2010. Methodology for inventorying greenhouse gas emissions from global cities. *Energy Policy*, 38, 4828e4837. <http://dx.doi.org/10.1016/j.enpol.2009.08.050>. Special Section on Carbon Emissions and Carbon Management in Cities with Regular Papers.
- UNESCO [63123], 2020. *Education for sustainable development: a roadmap*, ISBN: 978-92-3-100394-3., pp 66.
- UNESCO [63123], 2021. *Learn for our planet: a global review of how environmental issues are integrated in education*, ISBN: 978-92-3-100451-3., pp 48.
- World Bank., 2019. Solid Waste Management-Brief., https://www.worldbank.org/en/topic/urban_development/brief/solid-waste-management#:~:text=In%202020%2C%20the%20world%20was,3.88%20 billion%20tonnes%20in%202050, (Viewed on: June 21, 2022).



Long-term operation of a pilot sequencing batch bioreactor for the nitrification of landfill leachates

S. Torres-Herrera¹, J. Palomares-Cortés¹, J.J. González-Cortés¹, X. Gamisans², D. Cantero¹ and M. Ramírez¹

¹Department of Chemical Engineering and Food Technologies, Wine and Agrifood Research Institute (IVAGRO). Faculty of Sciences. University of Cadiz, Cadiz, Spain

²Department of Mining Engineering and Natural Resources, Faculty of Biosciences Engineering, Universitat Politècnica de Catalunya, Manresa (Barcelona), Spain
Corresponding author email: domingo.cantero@uca.es

keywords: Nitrification; Landfill leachate; Salinity; Long-term operation.

Introduction

Nitrification is an aerobic process consisting of two steps. Firstly, ammonia-oxidizing bacteria (AOB) oxidize ammonium to nitrite, and in a second step, Nitrite-oxidizing bacteria (NOB) oxidize this nitrite to nitrate. Landfill leachate varies significantly depending on the type of waste and the season of the year, presenting a high ammonium content, as well as a large number of toxic and non-biodegradable compounds (Show et al., 2019). Although autotrophic nitrifying bacteria are known to have a high sensitivity to pH, dissolved oxygen, temperature and other toxic compounds, landfill leachate can be used as an ammonium source. González-Cortés et al. (2021) found an experimental ammonium oxidation rate of 9.0 and 1.3 mg N-NH₄⁺ g TSS⁻¹ h⁻¹ using biomass adapted to intermediate and mature-intermediate landfill leachate, respectively. BIOGASNET technology integrated the nitrification of ammonium-rich effluents with anoxic biogas desulfurization. In this study, the main bottlenecks and their solutions over a long-term operation in the nitrification stage are shown.

Materials and methods

The BIOGASNET prototype was implemented in the Miramundo-Los Hadales landfill located in Cádiz (Spain). The pilot plant consists of two main parts; (i) a nitrification bioreactor that was fed with landfill leachate and (ii) an anoxic bioscrubber that was fed with the effluent of the nitrification bioreactor and the biogas from the landfill wells. The nitrification was performed in a sequencing batch bioreactor (SBR) with a maximum working volume of 1 m³, an air compressor, a storage tank of nitrified effluent, a pump for leachate feeding, and two pumps for pH control and antifoam addition.

The inoculum was obtained from the sewage treatment plant (STP) of Rota (Cádiz, Spain). The start-up of the nitrification bioreactor was carried out with 100 L of inoculum, 68 L of landfill leachate (ammonium concentration of 1,779 mg N-NH₄⁺ L⁻¹) and filled with tap water up to 536 L.

The prototype was operated for 61 weeks, and a total leachate volume of 8,929 L was fed. The leachate employed had a conductivity of 53.6 ± 6.1 mS cm⁻¹, chemical oxygen demand (COD) of 32,209 ± 10,242 mg L⁻¹ and an ammonium concentration of 1,410 ± 362 mg N-NH₄⁺ L⁻¹.

Results and discussion

For the first few weeks of system start-up, the conditions were pH 8.1, N-NH₄⁺ concentration above 200 mg L⁻¹ and temperature of 20°C. This led to an accumulation of up to 508 mg N-NH₄⁺ L⁻¹ (Figure 1). To avoid further ammonium accumulation, the pH was decreased to 7.5 and the N-NH₄⁺ concentration was maintained below 50 mg L⁻¹. In the intervals between weeks 19-28 and 51-53 there was another accumulation of ammonium, which was due to failures in the pH probe, causing pH values to reach 9.5.

As shown in Figure 1, the main final oxidation product was nitrate from weeks 13 to 19, 31 to 41 and 47-61. The maximum leachate feeding was reached on week 40, with a total volume of 588 L. In this week, maximum ammonium inlet load (161 g N-NH₄⁺ m⁻³ d⁻¹), nitrate concentration (534 mg N-NO₃⁻ L⁻¹) and



62. volumetric ammonium oxidation rate ($161 \text{ mg N-NH}_4^+ \text{ m}^{-3} \text{ d}^{-1}$) were also reached. Under the best operational conditions, a nitrate mass flow rate between $61\text{-}84 \text{ g N-NO}_3^- \text{ d}^{-1}$ (weeks 36 to 41) was obtained.

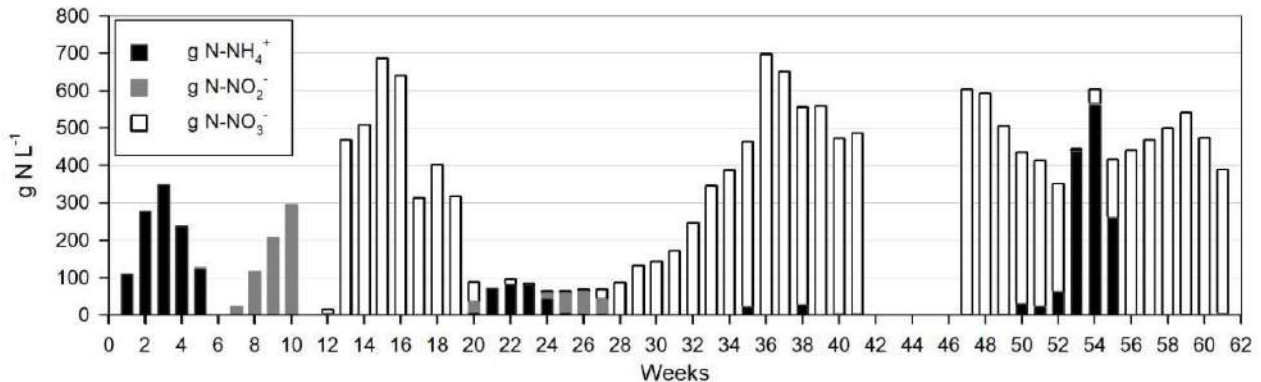


Figure 1. Ammonium, nitrate and nitrite in the nitrification bioreactor.

The initial conductivity found in the bioreactor was 7.4 mS cm^{-1} (salinity of 0.45%). As shown in Fig. 2, over the first 17 weeks, the conductivity increased up to 41 mS cm^{-1} (salinity of 2.46%). Zhang et al. (2017) considered that conductivities near 47.8 mS cm^{-1} (salinity of 3%) fully inhibited the nitrification process. For this reason, a 1:2 dilution of the leachate with tap water was used to reduce its salinity between $21.3\text{-}35.5 \text{ mS cm}^{-1}$.

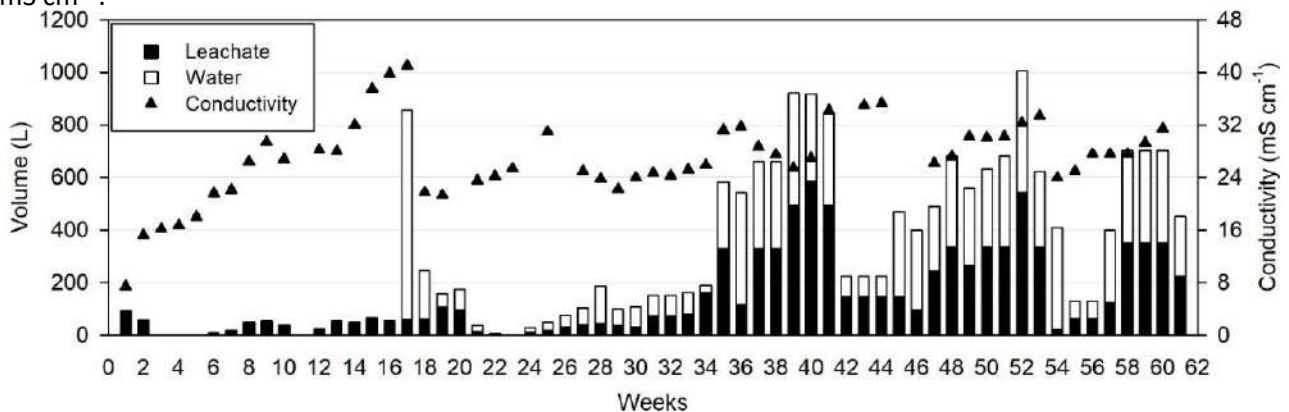


Figure 2. Volume of water and leachate added to the reactor, and reactor conductivity per week.

Conclusions

The salinity of the leachate affects the nitrification process which was minimized using a 1:2 dilution ratio with tap water which in turn was determined as the optimum ratio. Maintaining an optimum pH was determinant to obtaining a successful nitrification rate. The maximum nitrate production was $84 \text{ g N-NO}_3^- \text{ d}^{-1}$ under the best operational conditions.

Acknowledgements: This study is supported by the Green Fund and the LIFE project (EC): “Sustainable biogas purification system in landfills and municipal solid wastes treatment plants (LIFE BIOGASNET)”, LIFE18 ENV/ES/000426.

References

- González-Cortés, J.J., Almenglo, F., Ramírez, M., Cantero, D., 2021. Effect of two different intermediate landfill leachates on the ammonium oxidation rate of non-adapted and adapted nitrifying biomass. *J. Environ. Manage.* 281, 111902. <https://doi.org/10.1016/j.jenvman.2020.111902>
- Show, P.L., Pal, P., Leong, H.Y., Juan, J.C., Ling, T.C., 2019. A review on the advanced leachate treatment technologies and their performance comparison: an opportunity to keep the environment safe. *Environ. Monit. Assess.* 191. <https://doi.org/10.1007/s10661-019-7380-9>
- Zhang, Y., Jiang, W.L., Xu, R.X., Wang, G.X., Xie, B., 2017. Effect of short-term salinity shock on unacclimated activated sludge with pressurized aeration in a sequencing batch reactor. *Sep. Purif. Technol.* 178, 200–206. <https://doi.org/10.1016/j.seppur.2017.01.048>



ENVIRONMENTAL ECONOMICS



Cost profile of adsorption and photocatalysis process

D.A. Gkika¹, A.C. Mitropoulos¹ and G.Z. Kyzas¹

¹Department of Chemistry, International Hellenic University, Kavala, Greece
Corresponding author email: dgkika@chem.ihu.gr

keywords: adsorption; photocatalysis; advanced oxidation processes; cost models; total cost of ownership.

Introduction

Water pollution is a significant environmental issue that negatively affect both natural ecosystems and human daily lives. Hazard pollutants might be escaped during various biological processes that cannot be contained through traditional approaches. Advanced Oxidation Processes (AOPs) can be utilized in the removal of toxic organic pollutants from wastewater, by separating them into water and carbon dioxide. Among them, photocatalytic and adsorption methods are the most attractive ones, although studies corroborated from literature both highlight the necessity using these processes in a financially sustainable manner [1], [2]. These reactions occur through complicated and diverse pathways that are sensitive to experimental parameters. As a result, the cost process might be negatively affected by a series of factors, thus additional research identifying the critical attributes and analyzing their financial potential is crucial. The article describes the total cost of ownership (TCO) model settings, equations and input data as well as the result and discussions.

Materials and methods

There is an abundance of research works trying to implement an activity-based approach to determine and calculate costs [3]–[5], which is a commonly accepted method [6] of getting a first draft of the Total cost of ownership (TCO). The TCO methodology is an activity-based concept, attempting to analyze and evaluate all the relevant process costs [5].

A thorough financial assessment requires for the calculation of indirect costs, considering they impose a significant economic burden. Figure 1 depicts the typical steps of photocatalysis and adsorption cycles. For photocatalysis, those include light absorption, charge separation, carbon dioxide adsorption, surface redox reaction, and product desorption. For the adsorption cycle, those steps (and their costs) are the actual adsorption, regeneration, desorption, acid wash and material recovery.

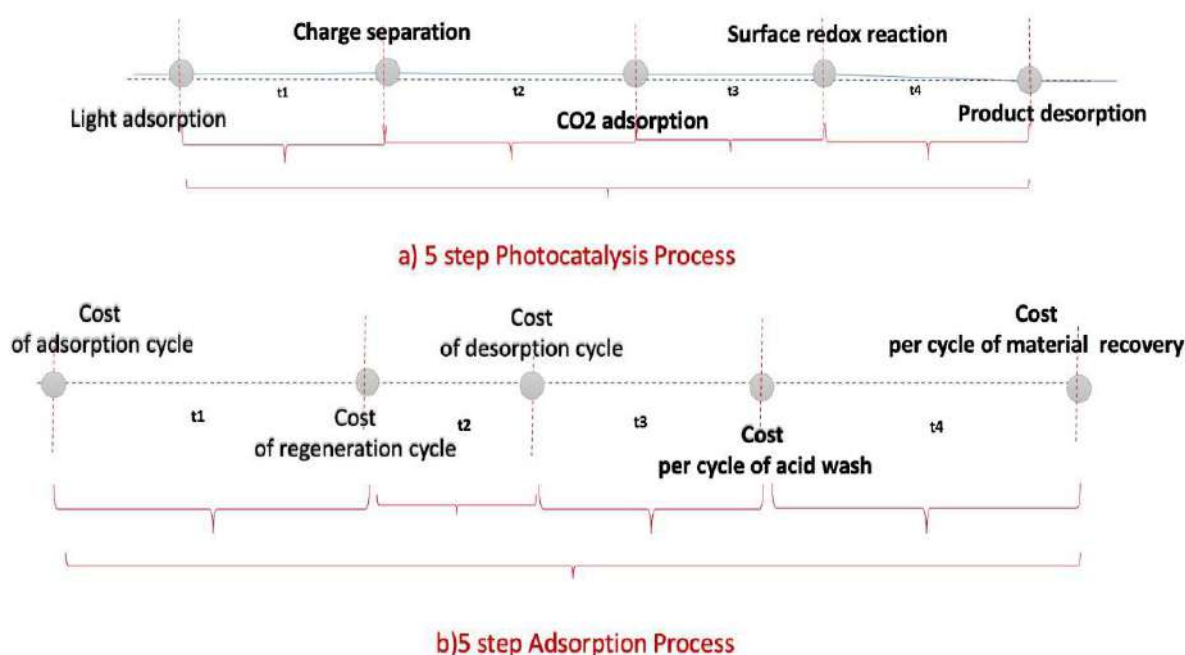


Figure 1. The basic steps and costs of the photocatalysis and adsorption process.



Results and discussion

The TCO Cost Models for the Adsorption and Photocatalysis processes *are* described below:

The TCO model takes into account various parameters that have been factored into the result.

$$\text{TCOAd/Photocatalysis} = \text{CR} + \text{CE} + \text{CL} + \text{CM} + \text{CD} + \text{CA} \quad (1)$$

where

TCOSP is the total cost of ownership adsorption/photocatalysis process

CR - Raw Material Cost

CE - Energy Cost

CL - Labor Cost

CM - Maintenance Cost

CD - Depreciation of apparatus and equipment

CA - Accident Cost

Conclusions

The TCO methodology has been deemed as suitable for the assessment of the total cost of the adsorption and photocatalysis processes, considering that this method takes into account multiple parameters, incorporating a variety of known and unforeseen not easy to estimate costs in the decision-making process. Such a detailed evaluation may be very beneficial during the decision making process. This work contributed to the current knowledge on the total cost of adsorption and photocatalysis processes by uncovering any knowledge gaps and highlighting the steps and data required to evaluate the total cost of these processes.

Acknowledgements: This research was funded by the Greek Ministry of Development and Investments (General Secretariat for Research and Technology) through the research project “Research-Create-Innovate”, with the topic “Development of an integration methodology for the treatment of micropollutants in wastewaters and leachates coupling adsorption, advanced oxidation processes and membrane technology” (Grant no: T2EDK-04066).

References

- E. V. Liakos, D. A. Gkika, A. C. Mitropoulos, K. A. Matis, and G. Z. Kyzas, “On the combination of modern sorbents with cost analysis: A review,” *J. Mol. Struct.*, vol. 1229, p. 129841, Apr. 2021, doi: 10.1016/j.molstruc.2020.129841.
- D. Gkika *et al.*, “Cost Estimation of Polymeric Adsorbents,” *Polymers*, vol. 11, no. 5, Art. no. 5, May 2019, doi: 10.3390/polym11050925.
- E. Atzeni *et al.*, “Additive manufacturing as a cost-effective way to produce metal parts,” in *High Value Manufacturing: Advanced Research in Virtual and Rapid Prototyping*, P. da Silva Bártolo, A. de Lemos, A. Pereira, A. Mateus, C. Ramos, C. Santos, D. Oliveira, E. Pinto, F. Craveiro, H. da Rocha Terreiro Galha Bártolo, H. de Amorim Almeida, I. Sousa, J. Matias, L. Durão, M. Gaspar, N. Fernandes Alves, P. Carreira, T. Ferreira, and T. Marques, Eds. CRC Press, 2013, pp. 3–8. doi: 10.1201/b15961-3.
- M. Schröder, B. Falk, and R. Schmitt, “Evaluation of Cost Structures of Additive Manufacturing Processes Using a New Business Model,” *Procedia CIRP*, vol. 30, pp. 311–316, 2015, doi: 10.1016/j.procir.2015.02.144.
- M. Baumers, C. Tuck, R. Wildman, I. Ashcroft, E. Rosamond, and R. Hague, “Transparency Built-in: Energy Consumption and Cost Estimation for Additive Manufacturing,” *J. Ind. Ecol.*, vol. 17, no. 3, pp. 418–431, Jun. 2013, doi: 10.1111/j.1530-9290.2012.00512.x.
- L. Ellram, “Total Cost of Ownership: Elements and Implementation,” *Int. J. Purch. Mater. Manag.*, vol. 29, no. 3, Art. no. 3, Sep. 1993, doi: 10.1111/j.1745-493X.1993.tb00013.



Systematic Overview of Freeze Desalination utilizing Thermoacoustic Technology

U. Ali¹, H. Zhang¹ and I. Janajreh¹

¹Department of Mechanical Engineering, Khalifa University of Science and Technology, Abu Dhabi, UAE
Corresponding author email: isam.janajreh@ku.ac.ae

keywords: *freeze desalination; thermoacoustic cooling; energy conversion; renewable energy.*

Introduction

Clean drinkable water is the basic need of humanity, and life cannot be sustained without water. World freshwater demand is on the rise, and it is predicted that 3.9 billion people in more than 75% of countries will live under water scarcity by 2050 [1, 2]. Seawater desalination industry accounts for 16,000 plants with near 95 million m³/day by 2019 [3]. Reverse osmosis (RO) and thermal distillation (TD) are the dominant technologies due to technology maturity and reasonable cost. Still facing several challenges, i.e., large energy consumption, corrosion and membrane fouling, and inability of handling high concentrated saltwater. This paper looks into the deployment of freeze desalination (FD) unit powered by thermoacoustic technology to meet the freshwater demand of a small settlements in remote locations. FD can resolve the corrosion, being conducted at low temperature, only involves heat of fusion which is 1/7 of latent heat of evaporation, and can treat highly concentrated waste brine including those rejected by RO and TD plants [4]. Himawan [5] claimed a 60% energy saving if eutectic freezing crystallization is used for recovering ice from an industrial waste stream compared to evaporative crystallization. Using solar energy or industrial waste heat to operate thermoacoustic engine and refrigerator (TAE/R) decreases the cost of FD as thermoacoustic has no moving parts and is maintenance free with direct and tandem conversion [6]. This direct and tightly coupled integration shall be recognized as complete green and environmentally safe technology. TAE/R can reach energy conversion efficiency equivalent to those attained via chemical to mechanical in the diesel engine. Remote areas pose a unique challenge for power production and delivery, as well as for the freshwater supply. Here we are considering an island with small population of 100 people, such as Pitcairn Island. The mainland grid connection is unviable option, and the cost of a small power plant driven by gas or steam is economically not feasible. Also, the renewable energy like photovoltaic solar and wind are deemed not possible either economically or logistically. Therefore, the ultimate electric power option of such islands is via diesel engine powered generators and the freshwater is unsatisfied by rainwater or seasonal streams/ponds. Diesel engines usually operate at 35% efficiency and most of the energy of fuel is lost as heat. This waste energy can be recovered by operating Tandem TAE/TAR to produce acoustic energy that needed to generate the cooling required by the FD. Here we proposal a sustainable freshwater supply and perform an economic feasibility analysis of a coupled thermoacoustic-FD system. Three scenarios are presented based on the average daily consumption of freshwater per person according to the world health organization (WHO), i.e., 50 L, 70 L, and 100 L per day [7]. The analysis is done based on internal rate of return (IRR), net present value (NPV), breakeven, payback period, and cashflow diagrams.

Materials and methods

A small community of approximately 100 individuals inhabiting a distant island is considered. The freshwater demand of this community is forecasted for a year. To meet the energy demand, standalone diesel generators are considered as the baseline to analyze the cost of electricity and freshwater production. The capital cost of diesel generators is neglected and only the running cost is considered assuming the island is already equipped with diesel generators. Table 1 shows the summary of electricity cost which will affect the cost of freshwater production. The energy demands is satisfied by using 10 Caterpillar diesel generators DE200 GC operating at 75% load and with accumulative fuel consumption of 34.2 L/hr [8].

Table 1. Electricity requirement and cost

Annual Energy Requirement per Capita	4500 kWh [9] (12.3 kWh/day)
Number of people	100
Total energy needed per day	1230 kWh



Diesel price	\$1.36/L
Fuel consumption per generator	34.2 L/hr
Diesel Required per day for 10 generators	8208 L
Cost of diesel per day	\$11,162.88

The systematic design of TAE/R powering FD is rather direct and avoids the conversion to electricity to produce freshwater for deserted islands. The module can be scaled up or down based on the available thermal energy source. The waste heat from the diesel engines is harnessed to drive the TAE/R module that provides the freezing conditions of the sea water (35g of NaCl/liter). As this cold temperature is secured, the FD module reduces the brine temperature to trigger ice crystallization near its freezing point. The growing ice crystal automatically rejects the salt impurities. The crystallized ice is collected, washed, and melted to obtain lower salinity brine. This can be successively repeated 4 to 5 times to produce a potable grade freshwater

[10]. The holistic design is shown in Fig. 1. The amount of freshwater that can be desalinated using the waste heat from the diesel generators is summarized in Table 2. Initial Results suggested that the generated freshwater are more than the required (> 10,000 liters/day). Therefore, the proposed system has a good potential for deployment in remote islands. The economical details will be discussed and analyzed next.

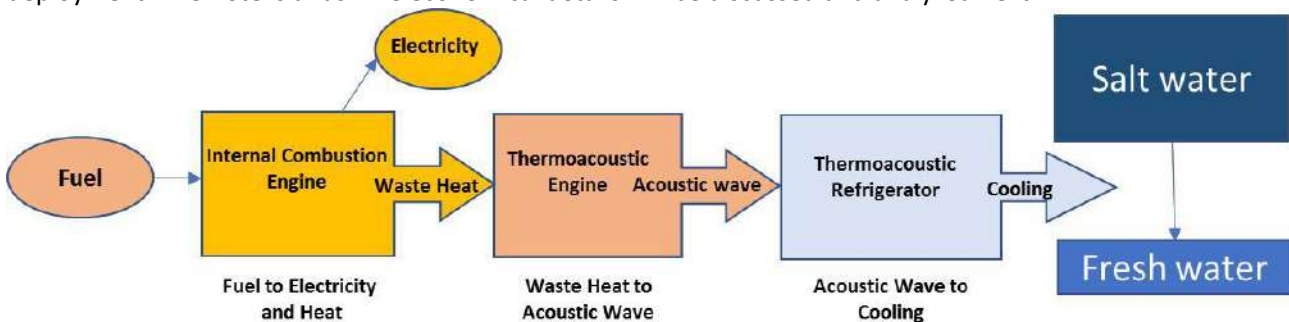


Figure 1. Freeze desalination system integrated to the TAE/TAR and Diesel Engine

Table 2. Amount of water produced using FD powered by waste heat utilizing TAE/R

Heat rejected by 1 generator /day	140.3 kW
Total heat rejected by 10 generators / day	1403 kW = 121×10^9 J
Conversion of heat to acoustic work in TAE	30.3×10^9 J (25% conversion efficiency)
Heat removed by TAR using acoustic wave	45.46×10^9 J (COP = 1.5)
Heat rejection required to produce 1L of water	2.74×10^6 J/L
Total volume of water produced	16,590 L

References

- N. Ghaffour, S. Soukane, J. G. Lee, Y. Kim, and A. Alpatova, "Membrane distillation hybrids for water production and energy efficiency enhancement: A critical review," *Applied Energy*, vol. 254, p. 113698, Nov. 2019, doi: 10.1016/J.APENERGY.2019.113698.
- U. W. W. A. Program, *The United Nations world water development report 2020: water and climate change*, vol. 1. UNESCO publishing, 2020.
- E. Jones, M. Qadir, M. T. H. van Vliet, V. Smakhtin, and S. Kang, "The state of desalination and brine production: A global outlook," *Science of The Total Environment*, vol. 657, pp. 1343–1356, 2019, doi: <https://doi.org/10.1016/j.scitotenv.2018.12.076>.
- D. Khawaji, I. K. Kutubkhanah, and J.-M. Wie, "Advances in seawater desalination technologies," *Desalination*, vol. 221, no. 1–3, pp. 47–69, 2008.
- C. Himawan, Characterization and population balance modelling of Eutectic Freeze Crystallization. PhD Thesis. Technical University of Delft, The Netherlands, 2005.
- U. Ali, I. Janajreh, M. Islam and S. Abedrabbo, Numerical Simulation Of Thermoacoustic Refrigerator Coupled With Thermoacoustic Engine, *15th International Conference On Heat Transfer, Fluid Mechanics And Thermodynamics Proceedings (HEFAT 2021)*, Pg. 1666-1671.
- https://www.un.org/waterforlifedecade/pdf/human_right_to_water_and_sanitation_media_brief.pdf
- https://www.cat.com/en_US/products/new/power-systems/electric-power/diesel-generator-sets/107851.html
- <https://www.eia.gov/todayinenergy/detail.php?id=49036>
- H. Zhang, I. Janajreh, M. I. Hassan Ali, and K. Askar, "Freezing desalination: Heat and mass validated modeling and experimental parametric analyses," *Case Studies in Thermal Engineering*, vol. 26, p. 101189, Aug. 2021, doi: 10.1016/j.csite.2021.101189.



Development of the IES protocol for Sustainable Blue Economy in the coastal zone

A. Pournara¹ and F. Sakellariadou¹

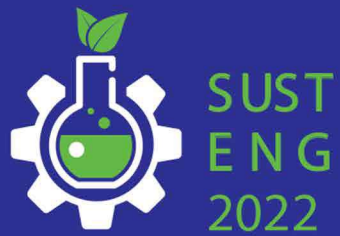
¹Department of Maritime Studies, University of Piraeus, Piraeus, Greece

Corresponding author email: anthpour@gmail.com

keywords: *Sustainable Blue Economy; coastal zone; industry; protocol.*

During the last decade a growing demand has prevailed for environmental protection and application of sustainability principles in the coastal environment. The consequences of climate change and sea-level rise on coastal systems include various biophysical and related socio-economic impacts. Humans should plan and implement their economic activities in the coastal zone with care, balancing the need to improve their living standards and to sustain a healthy coastal ecosystem. What started as Blue Growth, is now translated into Sustainable Blue Economy, offering a pathway to addressing some of the multiple socioeconomic and environmental challenges in the marine environment. Under this scheme, the integrated coastal zone management is a precious tool that contributes to the confrontation of the problems that occur due to climate change, providing at the same time a way to avoid any conflict might appear in land uses and allotment of wealth and supplies. The concept of Sustainable Blue Economy can now be expressed through the ecosystem services management framework, as their study transfuses a holistic approach of the ecosystem. Aim of the present study is to form a protocol for Sustainable Blue Economy in the coastal zone, that could be implemented for the definition of the current capacity and the boundaries of a coastal ecosystem with the specific characteristics of industrial activity, cultural heritage and protected natural environment. The protocol is based on a three-step analysis, while its name originates from the acronym Indicators Ecosystem Services (IES), as its major components are the indicators and the ecosystem services. Through this protocol, it's analyzed how and in what extend do the existing activities comply with the Sustainable Blue Economy. Case study of this research is the Gulf of Elefsis, a special sea basin in the eastern Mediterranean located in a short distance from Athens metropolitan area. The Gulf of Elefsis is characterized by a developed coastal zone which includes intense industrial activity, the ancient historical sights of Elefsis, the environmentally protected wetland of lake Koumoundourou, the town of Elefsis, a trade port and growing shipbuilding activity. Through the IES protocol, a table of indicators for Sustainable Blue Economy in a coastal zone with coexistence of industry, cultural heritage and natural environment is developed, that can be used for the analysis of such coastal ecosystems.

Acknowledgments: The study was financially supported by the Research Centre of the University of Piraeus, Greece.



LIFE CYCLE ASSESSMENT



Environmental Considerations Allied with the Application and Aerobic Operation of the Fluidized Bed Biofilm Reactor (FBR)

W.L. Liew^{1,2}, M.A. Kassim³, K. Muda⁴, S.K. Loh⁵, M.M. Hanafiah⁶ and N.S. Zaidi⁴

¹Department of Chemical and Environmental Engineering, Malaysia-Japan International Institute of Technology (MJIT), Universiti Teknologi Malaysia, Jalan Sultan Yahya Petra, Kuala Lumpur, Malaysia

²Disaster Preparedness and Prevention Centre (DPPC), Malaysia-Japan International Institute of Technology (MJIT), Universiti Teknologi Malaysia, Jalan Sultan Yahya Petra, Kuala Lumpur, Malaysia

³Azman Hashim International Business School (AHIBS), Universiti Teknologi Malaysia, Jalan Sultan Yahya Petra, Kuala Lumpur, Malaysia

⁴School of Civil Engineering, Faculty of Engineering, Universiti Teknologi Malaysia, Johor Bahru, Malaysia

⁵Energy & Environment Unit, Engineering & Processing Research Division, Malaysian Palm Oil Board, No 6, Persiaran Institusi, Bandar Baru Bangi, Kajang, Malaysia

⁶School of Environmental and Natural Resource Sciences, Faculty of Science and Technology, Universiti Kebangsaan Malaysia, Bangi, Malaysia

Corresponding author email: wlliew@utm.my

keywords: aerobic; energy consumption; fluidized bed biofilm reactor; life cycle assessment; oil palm.

Introduction

The practice of sustainability assessment or environmental considerations earns favorable public relations through the portrayal of green image of the industry, besides attaining a cost-saving and more efficient operation. Also, there are increasing legislative pressure and public awareness to include environmental considerations in product design and development. Hence, the incorporation of sustainability check in the establishment of an aerobic upflow bioreactor system of fluidized bed process (AUBS-FBR) in this study was conducted.

Materials and methods

Impact assessment is an important step in measuring the environmental impacts in LCA. GaBi comes with a large number of standard impact assessment method. In this study, Tool for the Reduction of Chemical and Other Environmental Impacts (TRACI) method was used for life cycle impact assessment using GaBi 6.0 software.

A calculation of energy use by each device and the entire AUBS-FBR was described to depict the quantity of electricity use and the associated costs. Also, energy use and cost necessary for palm oil mill effluent (POME) treatment using different processes or technologies were described and compared.

Results and discussion

The result of the impact assessment of this study is shown in **Table 1** below. Energy consumption, materials used for the construction of FBR, chemical consumption for the purpose of trace elements dosage, water use in the bioreactor system, in addition to the POME treatment process were among the five evaluated areas. As normalization and weighting of units in different impact categories was not done, a general conclusion on the dominating environmental impact as a result of the operation of the oxygenic FBR process was not made.

Table 1. Impact results of the aerobic fluidized bed biofilm reactor (FBR) (all values expressed per 13.8 ml min⁻¹ average discharge flowrate of treated effluent).

Criterion	Unit	Potential Impact Value
Acidification (Air)	kg SO ₂ -Equiv.	1.20E-04



Ecotoxicity	CTU _{eco}	-9.83E-03
Eutrophication (Air)	kg N-Equiv.	1.39E-02
Eutrophication (Water)	kg N-Equiv.	5.63E-05
Global Warming (Air)	kg CO ₂ -Equiv.	2.64E-02
Human Health Particulate (Air)	kg PM _{2.5} -Equiv.	1.16E-05
Human Toxicity (Cancer)	CTU _h	1.53E-13
Human Toxicity (Non-cancer)	CTU _h	-5.36E-13
Ozone Depletion (Air)	kg CFC 11-Equiv.	2.86E-09
Resources (Fossil Fuels)	MJ Surplus Energy	2.41E-02
Smog (Air)	kg O ₃ -Equiv.	1.10E-03

The costs associated with the above-mentioned energy use by the bioreactor system was calculated in accordance with the rate specified by Tenaga Nasional Berhad (Malaysian multinational electricity company). Information obtained through a questionnaire survey have identified that the palm oil processing mills are charged under the Tariff D – Low Voltage Industrial Tariff. Based on the calculation, the continuous operation of AUBS-FBR have induced an electricity cost of RM 565.69 per month. It was observed that the highest energy use was caused by the thermostatic heater unit in the heated water bath. It was installed to maintain the bioreactor within a working environment of 35 °C (actual measurements within the reactor column were in the range of 31.2 to 33.9 °C) to simulate a tropical outdoor temperature. The second highest energy use was contributed by the variable speed drive home booster pump to recirculate the combined influent and recycle liquid stream upward into the FBR column through the bed of biomass coated-carrier materials (BCCM).

Conclusions

Experimental data obtained from the bioreactor operation were used to accomplish the life cycle inventory (LCI) analysis, and the following impact categories were highlighted in this study: climate change, ozone depletion, freshwater ecotoxicity, freshwater eutrophication, fossil depletion, and metal depletion. Besides, energy consumptions and cost implications of the AUBS-FBR were calculated and discussed. The system has an energy consumption of 1,310.4 kWh per month, which results in an electricity cost of RM 565.69 monthly.

Acknowledgements: The authors would like to gratefully acknowledge Universiti Teknologi Malaysia (UTM) and Ministry of Education for their financial support through the Research University Grant (GUP), cost center numbers Q.J130000.2508.01H53 and Q.J130000.2611.17J14; and the Flagship Grant, cost center number Q.J130000.2411.03G28.

References

- Kargi, F. and Eyiisleyen, S. (1995). Batch Biological Treatment of Synthetic Wastewater in a Fluidized Bed Containing Wire Mesh Sponge Particles. *Enzyme and Microbial Technology*. 17: 119-123.
- Loh, S.K., Mohd Ehiwan, N. and Sukiran, M.A. (2011). Management of Palm Oil Mill Effluent. In Wahid, M.B., Choo, Y.M. and Chan, K.W. (Ed.) *Further Advances in Oil Palm Research (2000-2010)*. (Volume 2) (pp. 610-627). Malaysia: Malaysian Palm Oil Board.
- Pandey, S.K. (2010). *CFD Simulation of Hydrodynamics of Three Phase Fluidized Bed*. Master of Technology. National Institute of Technology, India.
- Sokol, W. and Korpál, W. (2006). Aerobic Treatment of Wastewaters in the Inverse Fluidised Bed Biofilm Reactor. *Chemical Engineering Journal*. 118(2006): 199-205.
- Tchobanoglous, G., Burton, F.L. and Stensel, H.D. (2004). *Wastewater Engineering, Treatment and Reuse*. (4th ed.) New York: McGraw-Hill.
- von Sperling, M. (2007). *Wastewater Characteristics, Treatment and Disposal*. UK, London: IWA Publishing.



Life cycle assessment as support tool for development of novel materials used in environmental applications

G.Barjoveanu¹, C. Teodosiu¹, I.Morosanu¹, D. Fighir¹, F. Bucatariu^{1,2} and M. Mihai^{1,2}

¹Department of Environmental Engineering and Management, “Gheorghe Asachi” Technical University of Iasi, Romania

²Department of Functional Polymers, “Petru Poni” Institute for Macromolecular Chemistry, Iasi, Romania
Corresponding authors' email: cteo@tuiasi.ro

keywords: *life cycle assessment; nano-composites; heavy-metal ions; sorption, eco-design.*

Introduction

Priority pollutants generate environmental impacts, as well as engineering challenges for their removal from water or wastewater. In consequence, there is an increased need to design more efficient materials for water/wastewater purification technologies, but these efforts usually provide additional costs and environmental impacts.

In this context, besides the structural and behavioural properties of nanomaterials, current practices in material development and engineering must include environmental criteria related to the synthesis, production, use and post-use phases of these novel materials. Life cycle assessment gained attention among various instruments used to evaluate environmental impacts, and it has been recognized as a valuable tool for the evaluation of engineered nano-materials due to the complex environmental profiles which can be used in (eco)-design and product optimization.

The objective of this study is to evaluate the technical and environmental performances (by means of LCA) of a series of synthesis strategies used to obtain nano-structured materials containing polyethyleneimine(PEI)-coated silica particles (organic/inorganic nanocomposites) to be used in environmental applications, i.e. Cd²⁺ ions removal from aqueous solutions. The life cycle assessment considers the very early stages in the product development, and it has focused on the synthesis and initial testing phases in order to develop an early environmental profile which further will enable the investigation of several scenarios related to the eco-design of these materials.

Materials and methods

With respect to the materials synthesis, the sorbents synthesis process involves an innovative method which consists of “one-pot” interpolyelectrolyte coacervate precipitation onto the inorganic Daisogel-type silica core surface.

In this study, the coacervate is a combination of polyethyleneimine (PEI) and polyacrylic acid PAA or with poly(sodium methacrylate) PMAA. The in-situ precipitation of the coacervate is followed by a chemical cross-linking reaction (in presence of glutaraldehyde) and then by the polyanion extraction from the cross-linked organic shell in strong basic medium. The composite microparticles have been cross-linked at two different molar ratios between the aldehyde and amino groups which yielded two cross-linking degrees. Considering the two polyanions and the two reticulation ratios used, 4 composite materials have been synthesized.

These nanocomposites were subjected to various characterization methods: thermogravimetric and EDAX measurements were carried out to evaluate the organic content deposited onto the silica core. SEM images have confirmed the spherical shape of all modified microparticles, and the role of the crosslinking reaction in individualizing the material to unique spheres, after the clustering obtained during the one-pot synthesis.

These materials were then tested in single-element sorption experiments which targeted the removal of Cd²⁺ ions from aqueous solutions. The influence of different parameters was investigated. Initial Cd²⁺ concentration experiments have enabled the estimation of the maximum sorption capacity and regeneration experiments were realized to investigate the reuse potential of these composites.

With respect to the life cycle assessment, the analysis has used a cradle-to-gate approach which includes the following foreground processes: lab-scale operations and material inputs for the synthesis of inorganic/organic composites, as well as testing processes for the removal of Cd²⁺ ions from synthetic



solutions. The background system has included processes for chemicals and energy production. The functional unit of the study was chosen as 1 mg Cd^{2+} ions removed from aqueous solution to account for the product utility. Life cycle impact assessment has included the classification and characterization steps according to the ISO recommendations by using the ReCiPe 2016 method at midpoint for the characterization of environmental impacts which contains 18 impact categories.

Results and discussion

Considering all aspects presented above, the environmental profiles using the LCA methodology were calculated and have shown the contribution of different materials and processes to obtain the inorganic / organic composites. For all syntheses routes, most of the environmental impacts are due to the support particle mainly because it has the majority in the overall mass of the composite material.

A comparison which considers 1 mg Cu^{2+} ions removed is presented in figure 1 for the 4 types of materials which were tested in similar conditions. This shows that the best environmental performance (expressed as the lowest impacts) is demonstrated by the IS/(PEI-PMMA) $r=1$ composite which is obtained with Poly(sodium methacrylate and for greatest CHO: NH_2 ratio during the crosslinking process. By comparison, the more composite obtained with polyacrylic acid (PAA) has yielded much higher environmental impacts for the same GA to NH_2 ratio.

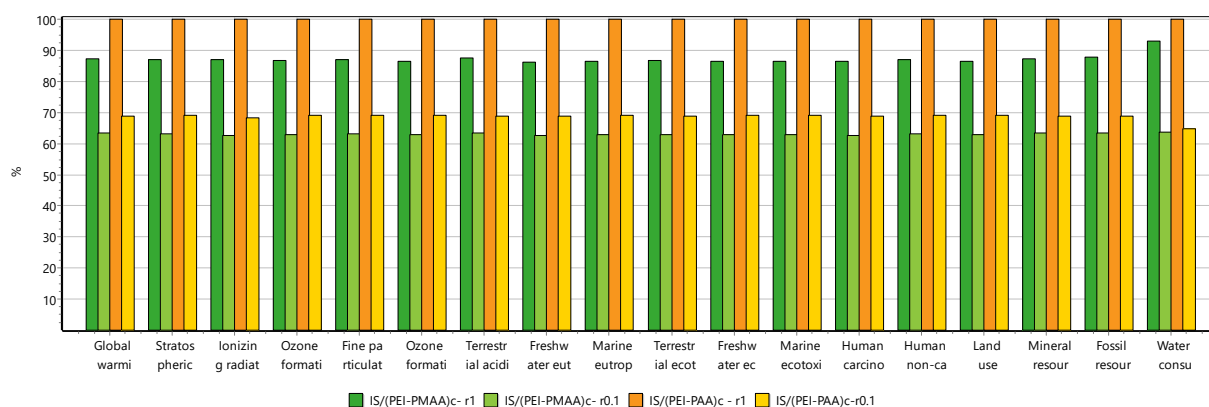


Figure 1. Environmental performance comparison for different nanocomposites used to remove 1 mg Cd^{2+} ions

Conclusions

In conclusion, the LCA analysis has enabled the identification the environmental hotspots that are associated to syntheses processes of innovative materials with environmental applications. This demonstrates the utility and necessity of this instrument to evaluate the potential environmental impacts from the earliest product & technology development process. Based on these initial findings, several eco-design measures (related to materials substitution and minimization) will be investigated. Furthermore, it is important to note that great care is needed when developing and defining several crucial LCA elements to capture the product functionality in a correct manner and to consider data availability and uncertainty when interpreting the results.

Acknowledgements: This work was supported by a grant of the Ministry of Research, Innovation and Digitization, CNCS/CCCDI–UEFISCDI, project number PN-III-P4-ID-PCE-2020-1199, within PNCDI III, contract PCE 56/2021, “Innovative and sustainable solutions for priority and emerging pollutants removal through advanced wastewater treatment processes” (SUSTINWATER).



Life cycle assessment of chicken manure treatment options

George Barjoveanu¹, Daniela Gavrilescu¹, Petru Apopei¹ and Carmen Teodosiu¹

¹Department of Environmental Engineering and Management, “Gheorghe Asachi” Technical University of Iasi, Romania

Corresponding author email: dcaile@tuiasi.ro

keywords: *chicken manure; composting; anaerobic digestion; life cycle assessment; process modeling.*

Introduction

One of the challenges of circular economy is to close the life cycle of most products. This means that new technologies have to be developed and applied to waste streams in order to valorize them from a material or energetic point of view. Wastes coming from bio-processes like animal rearing are becoming important candidates for valorization because of the quantities and periodicity with which they are produced, but also because of their characteristics. Chicken manure is one of these agricultural waste streams which pose challenges for its proper management due to high generation rates and strict elimination rules, but at the same time it provides good opportunities for valorization considering its high quantities of nutrients (nitrogen, phosphorus and potassium) which makes it a very suitable material to obtain fertilizers from. In most cases, current elimination for chicken manure is landfilling, but technologies like composting and anaerobic digestion are promising in transforming this waste into a valuable fertilization product. The biological degradation of chicken manure, be it anaerobic in the case of digestion, or aerobic as in the case of composting, poses some serious engineering challenges and some additional environmental impacts. It is important to evaluate these environmental impacts in order to understand if the new valorization technologies do more (environmental) harm than good.

In this context, this paper aims at investigating the environmental impacts induced by two waste treatment technologies: in vessel and windrow composting and anaerobic digestion. The analysis is focused on a 80000 chicken farm which produces approximately 10,000 kg/day chicken manure. Environmental impacts are determined by using life cycle assessment which is performed according to the ISO 14040 standard. This methodology considers the whole life cycle of a product, but in our case, the analysis only focuses on the waste treatment phase and is intended to evaluate impacts in some 18 impact categories which include climate change, land occupation, toxicity or resources intensity use, to name just a few.

Materials and methods

Our research methodology is based on chicken manure characterization data (composition, generation, etc.) and lab-scale experiments in-vessel composting which were performed to determine an optimal additional carbon source that would support and sustain the composting process from 4 variants of substrate-filler materials (saw-dust, wheat-straw, charcoal and lignite). These initial data was then used to model a scale-up for windrow composting and anaerobic digestion for which equipment was dimensioned and operational parameters determined based on which process inputs and outputs were calculated. This whole process data was then used to create a life cycle inventory which was submitted to the life cycle evaluation. The functional unit of the study was chosen 10 t of chicken manure (which equates to the daily waste production). The life cycle inventory was modeled in SimaPro by partially sourcing data from the EcoInvent 3.3. data base for some of the input/output entries in the inventory. The scope of the evaluation and the inventory has included the infrastructure development (with a 25 years life span), process inputs like electricity, diesel (for windrow turning and compost manipulation), additional reactivities (water, filler materials), as well as outputs (a small amount of leachate and air emissions like ammonia, etc.). Life cycle impact assessment (LCIA) has included the classification and characterization steps according to ISO 14040:2006 recommendations by using the ReCiPe 2016 method at midpoint for the characterization of



Results and discussion

In figure 1 a comparison of environmental impacts of two chicken manure technology options is presented. It may be observed that for most categories, the anaerobic digestion generates higher impacts than the composting technology. Exceptions are the Terrestrial acidification (TA) category and the marine eutrophication where the direct emissions of ammonia during the composting process generate much higher emissions than the anaerobic digestion. Furthermore, water consumption is higher in the case of composting, as is the land occupation, due to the much bigger space needed to perform the composting process. On the other hand, the anaerobic digestion generates higher impacts in the air-related categories, like climate change (CC), ozone depletion (OD), Ozone formation (OF-HH and OF-ECO), and the toxicity related categories. These higher values are generally associated with the heat generation needed to support de anaerobic digestion. In case of the toxicity-related categories, the much higher impact values associated to the anaerobic digestion are due to treatment of the digestate sludge at the end of the process.

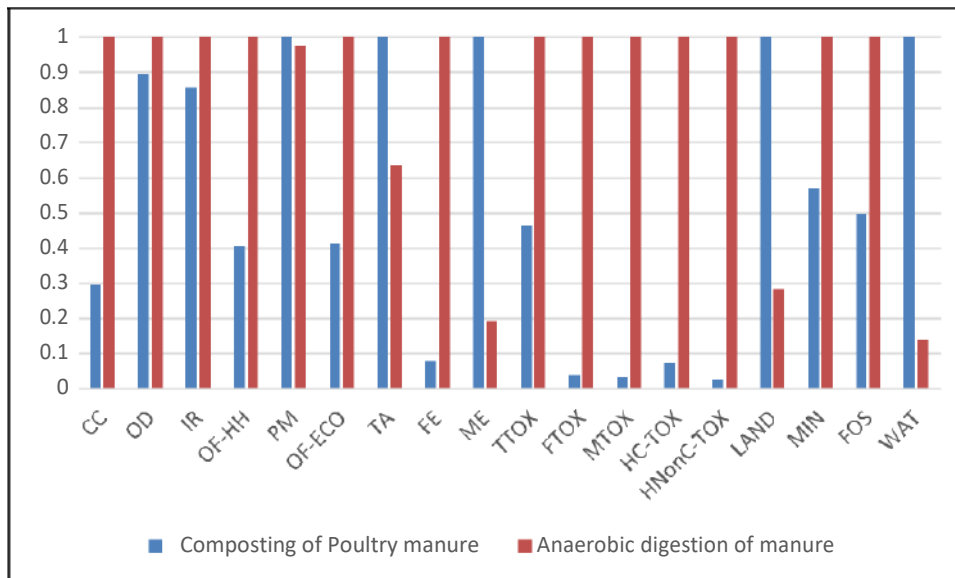


Figure 1. Environmental performance comparison of chicken manure valorization options.

When comparing the different composting mixes, the wheat straw has generated the highest environmental impacts, due to its lowest technical performance (and this in turn is due to its low bulk density which translate to very big waste volumes, despite its cheapest economical costs), while the lignite has had the best technical performance and the lowest environmental impacts.

Conclusions

This work has employed life cycle assessment to compare different technological options for the treatment of chicken manure. Our analysis has compared 2 technologies (aerobic composting versus anaerobic digestion) and 4 types of different waste mixes. Given the preliminary results, some advantages and disadvantages of these technologies and options could be identified, but further investigations are required to select the most suitable treatment option, because several other parameters need to be considered.

Acknowledgements: This work was supported by a grant funded by the Regional Operational Program 2014-2020, POR/1/1.1/OS 1.2/1, project number 136527, contract no: 7288/2021, “Integrated solutions for chicken manure waste management”- Chicken Waste.



Environmental assessment of the integration of gasification into the waste management system in Reunion Island

J.C.I Rabetanetiarimanana¹, M.H. Radanielina¹, H.T. Rakotondramiarana² and D. Morau¹

¹PIMENT Laboratory, University of Reunion Island, Le Tampon-Reunion, France

²Institute for the Management of Energy (IME), University of Antananarivo, Antananarivo, Madagascar

Corresponding author email: jordy-charly-isidore.rabetanetiarimanana@univ-reunion.fr

keywords: Life Cycle Assessment (LCA); Life Cycle Impact Assessment (LCIA); waste management; Reunion Island; multi-sectoral approach; circular economy.

Introduction

Solid waste increases and becomes more complex; therefore, current waste management based on reusing, recycling and biological treatment must be updated [1]. The waste management system in Reunion Island is based on landfill. However, the two non-hazardous waste storage facilities will reach saturation by 2022. To deal with this issue, five waste management scenarios based on the current regulations and especially on the database from last waste characterization in Reunion Island have been developed. This work aims at supporting planners' decision, providing an overall view of waste management and comparing the environmental profile of the proposed scenarios. In order to achieve the objectives, a life cycle assessment (LCA) was used. A life cycle impact assessment (LCIA) is carried out using Simapro and Ecoinvent database.

Materials and methods

According to the waste composition in Reunion, four different waste management scenarios were produced in this survey. The first scenario is a business as usual (BAU) scenario, the others are scenarios that are based on multi-sectoral approach based on different types of waste treatment such as recycling, landfill, anaerobic digestion (AD), composting, gasification and incineration. Table 1. presents a summary of the proposed scenarios. In scenario 2-a and 2-b, gasification is used for energy recovery. However, incineration is used in scenario-3.

Table 1. Numerical representation of scenarios.

Type of recovery	Scenario 1 [t]	Scenario 2-a & 3 [t]	Scenario 2-b [t]
Recycling	70 348	222 029	118 023
Energy recovery	0	50 397	192 359
AD	0	71 767	0
Composting	109 828	115 440	87 206.6
Landfill	331 574	52 117	114 161.4

Results and discussion

Fig 1. presents the results of the GWP and Cumulative Energy Demand (CED). The results found are consistent with those in the literature [1]–[3]. The results show that, scenario 1 and 2-b have a significant impact on global warming. In scenario 2-b, gasification represents 80.1% of the impact. Moreover, the scenario 3 where incineration is used as energy recovery process has the lowest impact on global warming. Besides, by comparing scenarios 2-a and 2-b, we noticed that recycling are the better way for plastics treatment. On the other hand, the results of CED indicate that scenario 1 consumes more energy than the other scenarios and gasification consumes less energy than incineration. From the results of the ReCiPe midpoint with characterization (Fig.2), it can be noted that gasification is associated with: Ozone Depletion, Photochemical oxidant formation and Metal depletion. Landfill contributes significantly to: Marine Eutrophication, Human Toxicity, Freshwater ecotoxicity, Marine ecotoxicity, Urban land occupation and Natural land transformation. Incineration is associated with: Freshwater eutrophication, Terrestrial ecotoxicity. Anaerobic digestion has a significant impact on the agricultural land occupation. Composting and recycling have a significant impact on Terrestrial acidification and fossil depletion respectively. Moreover, for the category "human toxicity, non-cancer", scenario 1 has a higher score.

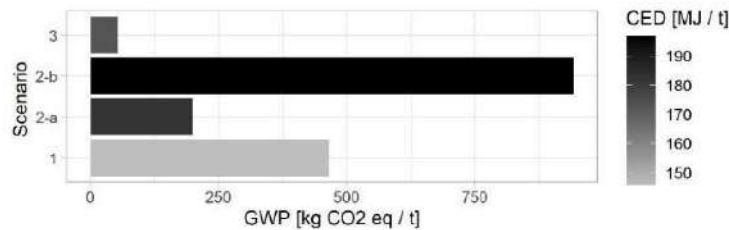


Figure 1. Results from IPCC GWP100a and Cumulative Energy Demand V1.08.

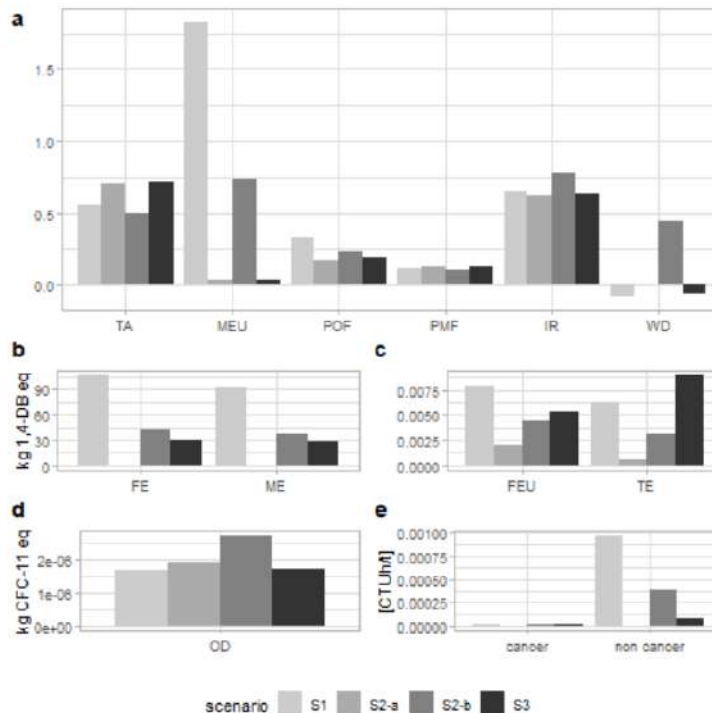


Figure 2. a-d: impact categories from ReCiPe midpoint, e: human toxicity from USEtox.

FE: Freshwater Ecotoxicity FEU: Freshwater Eutrophication IR: Ionizing Radiation MEC: Marine Eutrophication OD: Ozone Depletion
PMF: Particulate Matter Formation POF: Photochemical Oxidant Formation TA: Terrestrial Acidification TE: Terrestrial Ecotoxicity WD: Water Depletion ME: Marine Ecotoxicity

Conclusions

Indeed, it can be said that scenario 2-a based on the new national regulation is the optimal scenario in terms of emissions and preservation of human health. It is therefore important to adopt a multi-sector approach where: Extension of sorting instructions, liquid food packaging, extension of the sorting instructions for textiles, linen and shoes, furniture elements waste, wood and special household waste are recycled, green wastes including wood are composted, organic wastes are digested anaerobically, refuse from sorting are gasified and the remains of the collected wastes are landfilled. Finally, a good agreement between the results presented here and the literature was observed.

Acknowledgements: This study is supported by Région Réunion and Fonds européen de développement régional (FEDER).

References

- U. Arena, F. Ardolino, and F. Di Gregorio, "A life cycle assessment of environmental performances of two combustion- and gasification-based waste-to-energy technologies," *Waste Manag.*, vol. 41, pp. 60–74, 2015, doi: 10.1016/j.wasman.2015.03.041.
- S. Manfredi, D. Tonini, and T. H. Christensen, "Environmental assessment of different management options for individual waste fractions by means of life-cycle assessment modelling," *Resour. Conserv. Recycl.*, vol. 55, no. 11, pp. 995–1004, 2011, doi: 10.1016/j.resconrec.2011.05.009.
- H. H. Khoo, "Life cycle impact assessment of various waste conversion technologies," *Waste Manag.*, vol. 29, no. 6, pp. 1892–1900, 2009, doi: 10.1016/j.wasman.2008.12.020.



Environmental Assessment of Energy Supply Model Replacement in a Dyeing-Finishing Plant

M.F. Shih¹ and J.C.T. Lin²

¹Center of University Social Responsibility, Feng Chia University, Taichung City, Taiwan

²Department of Environmental Engineering and Science, Feng Chia University, Taichung City, Taiwan

Corresponding author email: jlin0623@gmail.com

keywords: Life cycle assessment; Dyeing mill; Water-Energy Nexus; Carbon footprint; Water footprint.

Introduction

In response to the need for global net-zero emissions, multinational trading companies have an even more urgent need for carbon reduction in their supply chains. A dyeing-finishing textile manufacturing plant in north Taiwan was gradually built an implementation blueprint for energy conservation and carbon reduction through internal energy structure adjustment and monitoring since 2011. The purpose of this case study was to evaluate the changes and performance of the carbon footprint, water footprint, and environmental impact assessment of this plant before and after replacing the steam supply sources and the water-energy nexus was addressed.

Materials and methods

The case analyzed in this study locates in northern Taiwan. It is responsible for the dyeing and finishing stage of the midstream of the textile industry, including multiple units such as pre-treatment, dyeing, setting, and finishing—the boundary and scopes, as shown in Figure 1.

The impact assessment methods used in this study include IPCC 2013 GWP 100a (IPCC, 2013) to assess the carbon footprint; the water footprint includes the Water Consumption Index (WDI) proposed by Berger et al. (2014); CML-IA [The freshwater and marine ecotoxicity (FAETP/MAETP) and eutrophication (EP) in were used to assess the deterioration of water quality. The environmental impact assessment adopts the CML-IA baseline (Guinée et al., 2001) method. The weighted evaluation results of the ReCiPe2016 Endpoint (Huijbregts et al., 2016) method are used as the analysis basis for the water-energy nexus. The LCA tools used are SimaPro Software v.8.4 (PRè Sustainability Consultant, 2017) and Ecoinvent database v.3 (Weidema et al., 2013), which the laboratory has established.

Results and discussion

The evaluation results found that after adopting the new measures, the study cases' carbon emissions and total fuel calorific value consumption rates decreased year by year, and the achievement of the annual production remained above 96% on average.

The water scarcity footprint (WSF) declined from 376,767.4 m³ to 302,510.2 m³ in the four consecutive years, with an average reduction rate calculated as 10.4% per year. The decreasing trend of WSF is consistent with annual water consumption, wastewater discharge, and water depletion index (WDI), as shown in Figure 2. Figure 3 shows the relationship trends of raw material consumption, annual production yield, monitored air pollutant emissions, carbon emission, and annual fuel cost. With the change in fuel

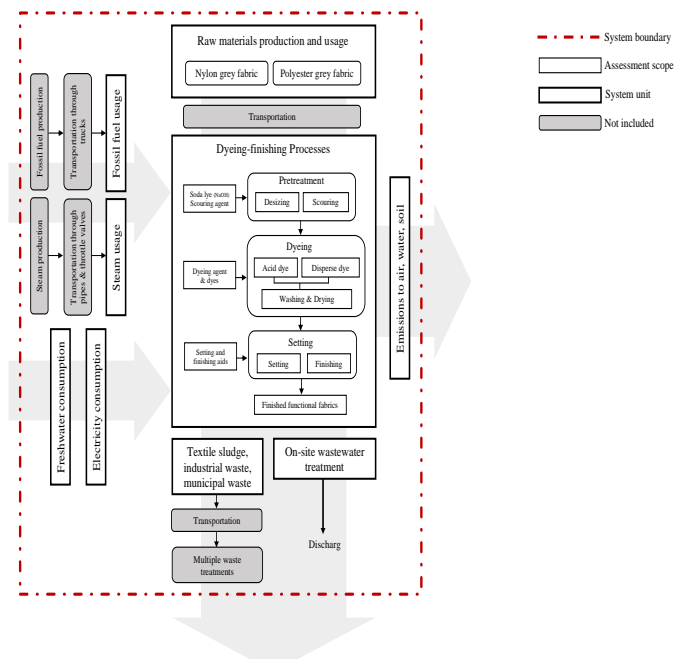


Figure 1. Boundary and scopes of this study.



types and supply methods year by year, fuel costs and carbon emission index had also fallen. Overall, it is a very enlightening practical example for regional energy network planning in the future.

The water scarcity footprint (WSF) declined from 376,767.4 m³ to 302,510.2 m³ in the four consecutive years, with an average reduction rate calculated as 10.4% per year. The decreasing trend of WSF is consistent with annual water consumption, wastewater discharge, and water depletion index (WDI), as shown in Figure 2. Figure 3 shows the relationship trends of raw material consumption, annual production yield, monitored air pollutant emissions, carbon emission, and annual fuel cost. With the change in fuel types and supply methods year by year, fuel costs and carbon emission index had also fallen. Overall, it is a very enlightening practical example for regional energy network planning in the future.

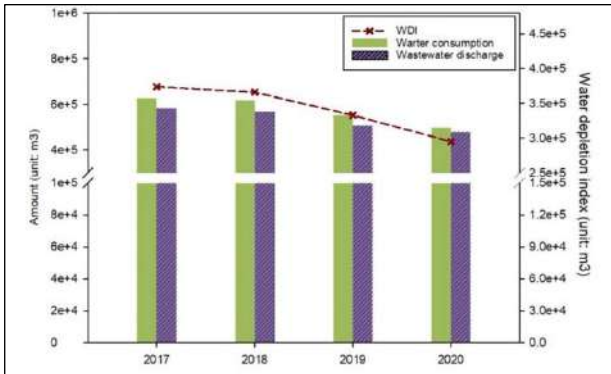


Figure 2. Different impact categories showed the textile mill's water availability and water deterioration each year.

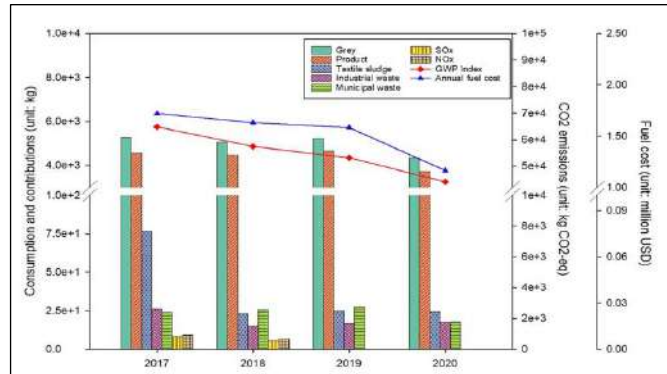


Figure 3. The relationship of raw material consumption, annual production, monitored pollutant emissions, carbon emission index, and annual fuel cost.

Conclusions

In this case study, the result said the carbon footprint, water footprint, and environmental impact results have all improved: the annual carbon footprint can be reduced by 19% in the discharge rate, and the water consumption footprint and water quality deterioration footprint can be reduced by 18% and 15%, respectively. In addition, the chemical substances used in the process significantly impact the deterioration of water quality, of which the pretreatment stage has the most significant impact. In evaluating energy recovery and reuse, it was found that this measure has considerable advantages in reducing environmental damage, annual fuel costs, and air pollution prevention. In this study, the water-energy nexus provides strong evidence of the correlation between electricity consumption and related damage indicators.

References

- IPCC, 2013: Climate Change 2013: The Physical Science Basis. Contribution of Working Group I to the Fifth Assessment Report of the Intergovernmental Panel on Climate Change [Stocker, T.F. et al. (eds.)]. Cambridge University Press, Cambridge, U.K. and New York, NY, USA, 1535 pp.
- Berger, M., van der Ent, R., Eisner, S., Bach, V., Finkbeiner, M., 2014. Water accounting and vulnerability evaluation (WAVE): considering atmospheric evaporation recycling and the risk of freshwater depletion in water footprinting. *Environmental Science & Technology*, 48(8), 4521-4528.
- Guinée, J.B., et al., 2001. Life Cycle Assessment-An Operational Guide to the ISO Standards: Characterization and Normalization. Ministry of Housing, Spatial Planning and the Environment, Centre of Environmental Science, Leiden, The Netherlands.
- Huijbregts, M.A.J., et al., 2017. ReCiPe2016: a harmonized life cycle impact assessment method at midpoint and endpoint level. *The International Journal of Life Cycle Assessment*, 22, 138–147.
- PRè Sustainability Consultant, 2017. SimaPro v.8.4 software, PRè Consultant: Amersfoort, The Netherlands.
- Weidema, B.P., et al., 2013. Overview and methodology. Data quality guideline for the ecoinvent database version 3. Ecoinvent Report 1(v3). St. Gallen, The ecoinvent Centre, Switzerland.



**Biodesulfurization biorefinery using *Gordonia alkanivorans* strain 1B:
Life cycle inventory of the integrated process**

T.P. Silva^{1,2}, C. Silva², J. Tavares¹, S.M. Paixão¹ and L. Alves¹

¹Unidade de Bioenergia e Biorrefinarias/LNEG – Laboratório Nacional de Energia e Geologia IP,
Lisboa, Portugal

²Instituto Dom Luiz/Faculdade de Ciências, Universidade de Lisboa, Lisboa, Portugal

Corresponding author email: susana.alves@lneg.pt

keywords: *biodesulfurization; Gordonia alkanivorans strain 1B; biorefinery; LCA.*

Introduction

High sulfur concentrations are a problem common to fossil fuels and derivatives (such as oil and coal), as well as many new generation fuels and biofuels (such as pyrolysis oils, syngas, biogas or even biodiesel). If the sulfur present in these fuels is released into the atmosphere it can result in SO₂/SO_x emissions, leading to environmental damage, and health issues. Transportation fuels have sulfur limits that go below 5000 ppm in ships, 3000 ppm in airplanes and 10 ppm in cars, and without treatment fuels can have several thousand ppm of sulfur. As such, they must be submitted to desulfurization, typically through a thermochemical process known as hydrodesulfurization, in which H₂ is combined with the fuel at high temperatures and pressures, in the presence of metal catalysts. However, this process has significant environmental impacts. Usually, it depends on hydrogen and heat/steam produced from natural gas, totaling 4.17 kg natural gas per 2.89 kg sulfur removed. It also involves high electricity and water consumption (approximately 2.9 kWh and 86.9 kg, respectively, per 2.89 kg sulfur removed). Furthermore, these impacts are greater for lower sulfur demands (Burgess & Brennan, 2001). Thus, there has been a search for alternative/complementary processes, one of which is biodesulfurization (BDS). It consists of the use of microorganism that consume the sulfur present in the fuels, at ambient temperature and pressure, without the need for metal catalysts. BDS still presents several bottlenecks, common to many microbial processes, such as low conversion rates and high production costs for the microbial biocatalyst. To surpass these limitations researchers have pursued different strategies: minimization/optimization of culture medium and culture conditions; employment of cheaper alternative nutrient sources; exploitation of added value products.

Gordonia alkanivorans strain 1B is a bacterium known for its biodesulfurization properties. It has demonstrated several characteristics which make it interesting: it can perform BDS of different compounds, several of which extremely recalcitrant for the thermochemical process; it has very low nutritional needs; it can be cultivated on several alternative carbon sources; it has been shown to produce two different types of added value products: carotenoids and biosurfactants (Alves et al., 2015; Silva et al., 2020, 2022). Therefore, *G. alkanivorans* strain 1B is the ideal candidate for a biodesulfurization biorefinery, that simultaneously removes sulfur from fuels and produces carotenoids and biosurfactants.

To correctly assess the overall environmental impact of the BDS biorefinery, it becomes fundamental to perform a life cycle assessment (LCA). According to ISO 14040, LCA is a technique for the assessment of environmental impacts of a product or process. It depends on the correct compilation of a process inventory, accounting for all the relevant inputs and outputs of the production system; the evaluation of the environmental impacts of each individual step of the process; the interpretation of the results within the goal and scope of the study. Through LCA it becomes possible to assess a product's impact throughout its life, from the production process to its disposal, or from any two points in between.

The present work is an initial life cycle assessment study on a biodesulfurization biorefinery, in which the process system will be defined, an inventory will be elaborated, and inputs and outputs will be accounted for. The goal of this study is to evaluate the CO_{2eq} emissions resulting from a biodesulfurization biorefinery using the bacterium *G. alkanivorans* strain 1B, to better understand its potential as a more sustainable alternative to the current thermochemical processes.



Materials and methods

Life cycle methodology: The present work follows the methodology defined by the ISO 14040 (ISO 14040–14044), composed of four major steps: (1) definition of goal, scope and boundaries; (2) elaboration of inventory (Life Cycle Inventory, LCI); (3) assessment of impacts (Life Cycle Impact Assessment, LCIA); (4) analysis. In the present study only the 1st and 2nd steps will be addressed.

Data source: The data was collected from bench scale assays, performed under the scope of the project GreenFuel (PTDC/EAM-AMB/30975/2017).

Microorganism: The microorganism used in this work was the bacterium *Gordonia alkanivorans* strain 1B, isolated in our lab from samples of hydrocarbon contaminated soils (Alves et al., 2005).

Results and discussion

The LCI of the BDS biorefinery process was performed, from the moment the sulfur rich fuel enters the biorefinery, to its conversion to a low-sulfur fuel. This process encompasses three major steps: Production of bacteria with biodesulfurization; Separation of the oil from the biocatalyst; Valorization of the spent biocatalyst and spent culture medium, through carotenoid and biosurfactant extraction.

In the first step the major inputs considered were the sulfur rich fuel, the components of the medium needed to cultivate the bacteria and the energy needed for sterilization and maintenance of the ideal growth and biodesulfurization conditions (ex: temperature 30°C and constant agitation). In the second step, inputs were mostly the energy needed for the separation process, namely through centrifugation. In the final step, the inputs considered were the organic solvents needed to extract the added value products and the energy spent in the extraction process and separation of the products of interest from the solvents.

In terms of outputs, 5 major outputs were identified: low-sulfur fuel, carotenoids, biosurfactants, biogenic CO₂-rich air and spent bacterial biomass. The CO₂ rich gas stream can be used as a carbon source to cultivate autotrophic microalgae, which can then be combined with the spent bacterial biomass and be converted through hydrothermal liquefaction into a biofuel.

Conclusions

The results obtained in this work will guide the development of future strategies to improve the sustainability of the biodesulfurization biorefinery, helping to identify which steps should be eliminated/optimized. Furthermore, the LCA resulting from this data, will help to determine if the integrated biodesulfurization approach is superior/less pollutant, than the benchmark hydrodesulfurization contributing towards future decision making.

Acknowledgements: This work was financed by national funds through FCT (Fundação para a Ciência e a Tecnologia) in the scope of the project GreenFuel (PTDC/EAM-AMB/30975/2017). Tiago P. Silva also acknowledges FCT for his PhD financial support (SFRH/BD/104977/2014). Part of LCA work was also funded by FCT/MCTES through national funds (PIDDAC) – UIDB/50019/2020.

References

- Alves, L., Salgueiro, R., Rodrigues, C., Mesquita, E., Matos, J. and Gírio, F.M., 2005. Desulfurization of dibenzothiophene, benzothiophene, and other thiophene analogs by a newly isolated bacterium, *Gordonia alkanivorans* strain 1B. *Appl. Biochem. Biotechnol.* 120(3), 199–208.
- Alves, L., Paixão, S.M., Pacheco, R., Ferreira, A.F. and Silva, C.M., 2015. Biodesulphurization of fossil fuels: energy, emissions and cost analysis. *RSC Adv.*, 5(43), 34047–34057.
- Burgess, A.A. and Brennan, D.J., 2001. Desulfurisation of gas oil: A case study in environmental and economic assessment. *J. Clean. Prod.*, 9(5), 465–472.
- Silva, T.P., Alves, L. and Paixão, S.M., 2020. Effect of dibenzothiophene and its alkylated derivatives on coupled desulfurization and carotenoid production by *Gordonia alkanivorans* strain 1B. *J. Environ. Manage.*, 270, 110825.
- Silva, T.P., Paixão, S.M., Tavares, J., Gil, C.V., Torres, C.A.V., Freitas, F. and Alves, L., 2022. A new biosurfactant/bioemulsifier from *Gordonia alkanivorans* strain 1B: Production and characterization. *Processes*, 10(5):845.



Is Hemp a Sustainable Energy Resource?

E. Teirumnieka, N. Patel, K. Laktuka, I. Veidenbergs and D. Blumberga

Riga Technical University, Faculty of Electrical and Environmental Engineering, Institute of Energy Systems and Environment, Riga, Latvia

Corresponding author email: dagnija.blumberga@rtu.lv

keywords: agrofuel; hemp pellets; ash; ash melting; multicriteria analysis; life cycle analysis.

Given the world's growing demand for energy from renewable sources and more ambitious climate targets, biomass for energy is seen as a possible solution. There is increasing competition for wood, with a preference for its use in products and materials with higher added value and a substitute for fossil resources. The availability of energy wood is becoming limited and alternative sources of solid biofuels for energy use are being sought. Industrial hemp is considered as an alternative because it is fast-growing and low demanding in terms of cultivation. A way to optimise the solid biomass fuel value chain is to pelletise or briquetting the feedstock. Pellets have advantages such as high energy density, homogeneous physical properties, easy handling and efficient transport. During the study, two methodologies are used: multicriteria analysis (MCA) and life cycle analysis (LCA) of hemp for energy applications. MCA is implemented for 10 products from hemp. LCA was carried out and compared with the characteristics of other fuels. The life cycle analysis showed that the use of hemp for energy is not sustainable, although the current geopolitical situation and the increase in energy prices seem to suggest otherwise. Nonetheless, the authors suggest that this apparent benefit of using hemp for energy will be short-lived and not beneficial in the long term, as it is more environmentally damaging than other energy sources such as peat as a fossil fuel or wood.

Introduction

According to the worldwide rising energy demand and the increased ambitious climate protection targets, the use of biomass for combustion will gain even more critical than it already has. Since wood is getting scarcer caused by the growing demand for material and energy use, alternative solid biofuels experience a growing interest in energy utilization.

For hemp as energy resource is important that:

1. in terms of Cannabis energy use: the green crop yield from hemp is, in range of, 14 -15 t/ha (calculated on the dry matter), of which 70–75% are hemp shives (by-products of hemp processing), which are usually left in the field, constituting an organic fertilizer [1]. It means that around 10 - 11 t/ha of raw material can be used for energy reasons;
2. cannabis biomass shows a substantial deviation in properties of energy resource: heat value, ash content, ash softening temperature which depend on the harvest season [2]. It is observed that hemp harvested in spring and winter has higher heat value - 19.1 MJ/kg than collected in autumn - 18.4 MJ/kg.

The hemp biomass tested was characterized by comparable technical and chemical characteristics with the results of tests presented by other researchers assessing the usefulness of this plant for energy purposes. Significantly, the content of volatiles at the level of 69% and relatively high, comparable to that for wood, combustion heat with an average value of 18,089 MJ/kg and a low ash content at the level of 2.5%. Regarding the parameters assessed, these values were also among the best biomass species for energy purposes [3,4], while the high content of volatile organic compounds indicated during research can improve the energy conversion efficiency.

Materials and methods

Two methodologies were carried out to compare hemp resources and products produced:

- multicriteria analysis (MCA) of products from hemp were used by use of six criteria: resource availability; technological; economical; environmental; climate change and circular economy aspects;
- life cycle analysis (LCA) of hemp for energy applications includes assessment of hemp combustion to produce bioenergy, data collection an analysis. Life cycle impact assessment was conducted using characterization factors by using IMPACT 2002+ methodology.



Results and discussion

MCA results are presented in Fig.1.

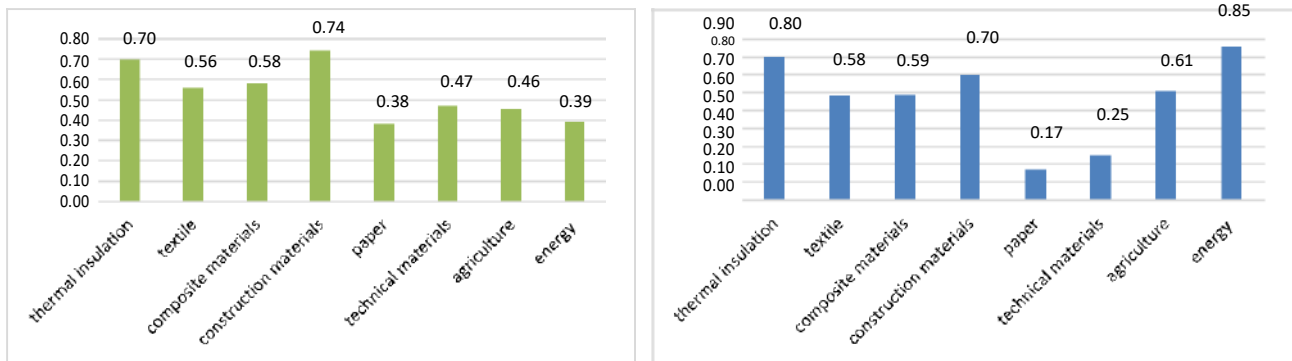


Figure 1. Before energy crisis (green graph on the left) and during energy crisis (blue graph on the right).

LCA is presented in Fig.2.

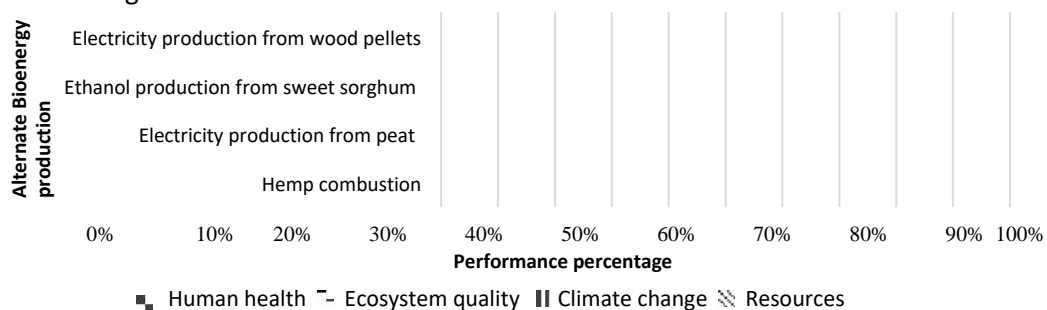


Figure 2: Comparison of damage assessment for hemp, peat, wood pellet, and sweet sorghum biomass.

Electricity production from wood biomass has a 100% contribution to ecosystem quality, whereas human health, climate change, and resources have a 21%, 15%, and 16% damage contribution, respectively. Overall, hemp combustion has a more significant damage impact than peat, wood pellets, and sweet sorghum biomasses.

Conclusions

Pelletizing or briquetting of the raw material from biomass seems to be the best way to optimize the value chain of solid biomass fuels. Pellets have advantages like high energy density, homogeneous physical characteristics, easy handling, and efficient transportation. However, biomass use for energy production has to be sorted and carefully selected. Hemp as energy resource application is short term solution (only during economic crisis). Life cycle analysis showed that hemp combustion has a more significant damage impact than other energy sources, for example, wood and other biomasses and even peat as fossil fuel.

Acknowledgements: This project has received funding from the European Union's Horizon 2020 research and innovation programme under Grant Agreement No. 862699.

References

- [1] Schluttenhofer C., Yuan L. Challenges towards Revitalizing Hemp: A Multifaceted Crop. *Trends Plant Sci.* 2017, 22, 917–929.
- [2] Prade T., Finell, M., Svensson SE, Mattsson, JE. Effect of harvest date on combustion related fuel properties of industrial hemp. *Fuel* 2012, 102, 592–604.
- [3] Daya Ram Nhuchhen, P. Abdul Salam. Estimation of higher heating value of biomass from proximate analysis: A new approach. *Fuel* 99 (2012), 55–63.
- [4] Eisenbies, MH; Volk, TA; Patel, A. Changes in feedstock quality in willow chip piles created in winter from a commercial scale harvest. *Biomass Bioenergy* 2016, 86, 180–190.



SUST
ENG
2022



AGRICULTURAL ENGINEERING



Changes of carbon and nitrogen content in soils since 1993 to 2021

M. Konatowska¹, A. Młynarczyk², P. Rutkowski¹, Z. Krysztofiak³ and A.K. Bernat³

¹Faculty of Forestry and Wood Technology/ Poznań University of Life Sciences, Poznań, Poland²Faculty of Geographic and Geological Sciences/Adam Mickiewicz University, Poznań, Poland³Bureau of Forest Management and Geodesy, Poznań, Poland
Corresponding author email: redebede@wp.pl

keywords: organic carbon; total nitrogen; oak forests; plant cover; climate change.

Introduction

The carbon and nitrogen cycle in soil and atmosphere is one of the most important research topic, important for understanding nature and environmental changes. Due to the changing research methods, there are few studies comparing soil changes over the decades. The results of the research presented below, comparing the content of carbon and nitrogen in soils at an interval of nearly 30 years, should therefore constitute a significant contribution to the understanding of the carbon and nitrogen cycle in nature.

Materials and methods

The study was carried out on 15 permanent research plots located in the Krotoszyn Forest District, Poland, in oak stands over 100 years old. The scope of the research included analyzes of soil samples, plant cover description and the analysis of climatic data between 1993 and 2021. In order to ensure the comparability of the results for the analysis of organic carbon and total-nitrogen content, the same methods were used in 2019-2021 as in 1993. Organic carbon was determined using the Tiurin method, total nitrogen using the Kjeldahl method.

Results and discussion

Table 1. Changes of content of C_{org} (%) in the oak litter and upper soil horizons between 1993 and 2021.

No.	Content of C_{org} (%) in the oak litter				Content of C_{org} (%) in upper soil horizon			
	1993.04	2019.10	2020.10	2021.04	1993.04	2019.10	2020.10	2021.04
1	34.924	34.959	36.937	37.508	4.572	2.311	2.118	3.152
2	40.188	27.459	34.135	40.743	1.914	1.607	1.187	3.133
3	38.793	35.745	37.936	38.760	3.963	2.134	2.009	2.892
4	37.802	37.866	28.680	37.469	1.194	1.366	1.206	1.639
5	39.691	28.285	34.761	37.127	4.438	2.483	2.770	4.540
6	41.847	34.845	38.856	38.325	8.033	2.879	2.824	4.102
7	38.107	31.205	30.975	39.047	7.885	1.348	1.557	1.808
8	41.297	36.546	35.171	40.052	4.449	1.342	1.118	1.326
9	16.757	32.373	27.413	42.338	6.731	3.347	4.974	8.106
10	40.865	29.745	38.880	39.181	2.855	3.086	4.110	12.586
11	34.907	34.775	35.253	35.147	2.811	2.118	2.326	4.951
12	38.470	30.118	37.609	38.971	4.577	2.623	2.722	3.996
13	37.627	30.639	30.426	37.915	1.709	3.020	4.500	4.949
14	37.330	30.168	32.154	35.420	4.169	2.231	2.352	2.943
15	40.331	29.631	30.655	29.170	3.594	2.496	2.083	2.716
Av	37.2624	32.2906	33.9894	37.8115	4.1929	2.2927	2.5237	4.1893



Table 2. Changes of content of N_{total} (%) in the oak litter and upper soil horizons between 1993 and 2021.

No.	Content of N_{total} (%) in the oak litter				Content of N_{total} (%) in upper soil horizon			
	1993.04	2019.10	2020.10	2021.04	1993.04	2019.10	2020.10	2021.04
1	1.554	1.687	1.442	1.631	0.196	0.126	0.096	0.126
2	1.666	1.547	1.624	1.820	0.091	0.084	0.068	0.112
3	1.316	1.687	1.645	1.687	0.178	0.089	0.084	0.107
4	1.575	1.869	1.659	2.058	0.068	0.077	0.063	0.070
5	1.827	1.645	1.547	1.939	0.149	0.166	0.215	0.273
6	2.072	1.981	1.666	1.715	0.399	0.207	0.275	0.200
7	1.568	1.351	1.512	1.827	0.416	0.074	0.082	0.081
8	2.002	1.652	1.799	2.128	0.150	0.074	0.065	0.081
9	1.036	1.792	1.701	1.729	0.609	0.257	0.306	0.541
10	1.946	1.603	1.757	2.149	0.158	0.200	0.235	0.746
11	1.512	1.988	1.813	2.065	0.266	0.191	0.189	0.352
12	1.918	1.855	2.016	1.771	0.259	0.145	0.187	0.189
13	1.813	1.771	1.631	2.254	0.089	0.194	0.259	0.238
14	1.694	1.736	1.687	1.659	0.182	0.098	0.149	0.112
15	1.918	1.449	1.659	1.575	0.262	0.172	0.123	0.123
Av	1.6945	1.7075	1.6772	1.8671	0.2315	0.1436	0.1597	0.2234

Stronger total nitrogen fluctuations in the measurement periods are related to the soil moisture level - higher in spring and lower in autumn. They may also depend on changing meteorological conditions in individual years. Therefore, the meteorological factor was also taken into account in the research. The season of the year also determines the carbon content in the forest litter - higher in spring, after carbon accumulation due to leaf fall in autumn and their decomposition from spring to autumn, which leads to a lower organic matter content in the litter in autumn.

Conclusions

The organic carbon content between 1993 and 2021 remained at a similar level for the same sampling period. However, changes in the content of organic carbon between spring and autumn were shown. The content of total nitrogen is more strongly variable, showing an increase between the years 1993-2021. The increase in nitrogen content, with a relatively constant carbon content, increased the C / N ratio, which should be interpreted as an improvement in the efficiency of carbon and nitrogen circulation in the tested oak stands.



The combination of lean manufacturing methodology and innovation in the beverage business

M.G. Nomikou¹ and P. Konstantinou²

¹Department of Wine, Vine & Beverage Sciences, University of West Attica, Athens, Greece

²Department of Graphic Design and Visual Communication, University of West Attica, Athens, Greece
Corresponding author email: mnomikou@uniwa.gr

keywords: *innovation; lean; manufacturing; improvement.*

Introduction

The beverage business consists of many individual parts; the central part is the consumers who expect quality, development, on-time delivery, compliance, safety, value, satisfaction, and environmental sustainability. According to the literature, the ways to meet these needs are multifactorial and multicritical. However, continuous improvement of companies is a critical point, as innovation is one of the success factors for productivity (Utterback & Abernathy, 1975). Lean production leads to eliminating waste and manufacturing products with a production process practice that considers that spending resources for any purpose other than creating value for the end customer is waste (Inmana & Green, 2018). So, LM (lean Manufacturing) is a critical component of innovation with a pillar of continuous improvement as an organizational innovation where value is added (Singh & Singh, 2009) (Verrier et al., 2014). The great competition due to the variety of products on the market and its constantly changing requirements need continuous improvements in the company's operations in applying the principles and tools of LM lean manufacturing, which extend beyond direct profits to productivity. Process innovation can be defined as using a new or significantly improved production or delivery method, including changes in techniques, equipment, or software (OECD, 2005). LM is a philosophy of the practical output appropriated by all members/departments and followed to manage the work. Toyota's production strategy has established all the setbacks that currently make up Lean production, Just in Time, and Total Quality Management. New technologies and organizational structures can help a company to evolve or survive. Lean production, six sigma, and business process reengineering are tools that can obtain these principles. The beverage business production team is trying to increase their mass production, but this contradicts the basic principles of Lean Manufacturing. Mass production results in huge stocks, large receipts, batches of production, product waiting and high costs, etc. By using tools and techniques in specific conditions and points of the production process, companies can have better results and better organization with measurable sizes and data. Table 1. shows the tools and methods that represent \ describe a production system (Veža et al., 2011).

Table 1. Lean concept principles, tools, and methods (Veža, et al., 2011).

Principles, methods, and tools in building lean concept procedures			
Pull/Kanban	JIT	Flow continue	TPM
SMED	Batch Reduction	TQM	7 waste
Layout	Visual systems	5S	5 why
Value Stream Mapping			
Work teams, high motivated workers, customer orientation			



According to Lopes et al., there is a low application of LM practices in the food and beverage industry, while most occur in the automotive sector (Lopes, Freitas, & Sousa, 2015). The systemic approach to improving customer-centric processes is the key to business excellence. Building an efficient organization with an emphasis on all parts of production can lead to cost reduction, delivery time, and quality improvement. When it comes to profitability through excellence and LM, it is not a simple improvement of a process but a waste reduction. As a result, time is reduced, so more products are produced with less fuel, which leads to the financial benefit of the company and higher levels of customer satisfaction. However, it should be noted that in addition to the successful practice of lean manufacturing, there are some risks. Such as resistance to change, lack of time, installation of new computer systems for better organization and financial burden. However, every company is different, so it cannot adopt the same practices. It depends on the organizational characteristics, the right design for the implementation of simple production and its maintenance (Sousa & Voss, 2008) (Lopes, Freitas, & Sousa, 2015). Lean principles are used by a few companies in the food and beverage industry, with a success rate of 25% to 30% (Kezia, Kumar, & Sai, 2017). Thus, by reducing the supply chain or production cost, the quality is increased, or new or significantly improved products are produced (OECD, 2005). The simple construction starts with optimizing the processes and can highlight waste that may not have been observed. And by improving production efficiency, improving product quality, decreasing production costs, reducing waste, adding value and innovate the procedure. It is a new philosophy that leads production to a change at all stages of the production process and that requires communication, coordination, and organization to achieve a larger market share (Kezia et al., 2017).

Conclusions

Through the literature research, we could conclude that the successful change of processes through Lean Manufacturing are two interrelated parts based on the definition of innovation. First, companies often need to innovate and evolve to maintain their competitive position. They should not be left in the past, as consumer needs change due to technology and competitors. For a winemaker, vineyard, or wine, the time is significant. In this way emerges in a barrel. Therefore, as a comparison between Lean Manufacturing and time, beverage businesses can save some time and have a better-quality wine by investing in this innovation.

Acknowledgements: The authors declare that they have no conflict of interest.

References

- Utterback, J. M. & Abernathy, W. J., 1975. A dynamic model of process and product innovation. *Omega*, 3, pp. 639-656.
- Inmana, R. A. & Green, K. W., 2018. Lean and green combine to impact environmental and operational performance. *International Journal of Production Research*, Vol. 56, No. 14, p. 4802–4818.
- OECD, 2005. OSLO manual, guidelines for collecting and interpreting innovation data. *3rd Edition*. OECD. , p. 49.
- Veža, I., Gjeldum, N. & Celent, L., 2011. Lean Manufacturing Implementation Problems in Beverage Production Systems. *International Journal of Industrial Engineering and Management (IJIEEM)*, Vol. 2 No 1, pp. 21-26.
- Lopes , R. B., Freitas, F. & Sousa, I., 2015. Application of Lean Manufacturing Tools in the Food and Beverage Industries. *Journal of Technology Management & Innovation* vol.10 no.3.
- Sousa, R. & Voss, C., 2008. Contingency research in operations management practices. *Journal of Operations Management*, 26.
- Kezia, P., Kumar, K. S. & Sai, B., 2017. Lean Manufacturing in food and beverage industry. *International Journal of Civil Engineering and Technology (IJCIET) Volume 8, Issue 5*, p. 168–174.
- Verrier, B., Rose, B., Caillaud, E. & Rem, H., 2014. Combining organizational performance with sustainable development issues: the Lean and Green project benchmarking repository. *Journal of Cleaner Production* 85, pp. 83-93.



Methane production from cheese whey over longer period may be interrupted by microelements restrictions

B. Stres^{1,2}, A. Hatzikioseyan³, P. Kousi³, E. Remoundaki³, L. Deutsch², K.V. Mikuš⁴ and S. Kolbl-Repinc¹

¹Department of Environmental Civil Engineering / Faculty of Civil and Geodetic Engineering, University of Ljubljana, Ljubljana, Slovenia

²Department of Animal Science, Group for Microbiology and Microbial Biotechnology / Biotechnical Faculty, University of Ljubljana, Ljubljana, Slovenia

³Laboratory of Environmental Science and Engineering, School of Mining and Metallurgical Engineering National Technical University of Athens (NTUA), Athens, Greece

⁴Department of Biology, Chair of Botany and Plant Physiology / Biotechnical Faculty, University of Ljubljana, Ljubljana, Slovenia

Corresponding author email: sabina.kolbl-repinc@fgg.uni-lj.si

keywords: anaerobic digestion; sludge; cheese whey; cow manure; microelements; AMPTS; modelling.

Introduction

Biogas is the main product of the anaerobic digestion and presents an alternative to fossil fuels. Cheese whey (CW) is a by-product from cheese production and presents one of those energy-rich products that can improve biogas production. The yearly production of CW is more than 40.5 million tons globally. According Eurostat in year 2020 56.493.720 tons of cheese whey was produced in the EU.

In this work the feasibility of using CW in anaerobic co-digestion of mixtures of wastewater sludge (WWS) and cow manure (CM) by estimating the benefits or adverse effects on methane production is explored. Further a simple kinetic model to simulate methane production for the mixtures of WWS, CW and CM was created, calibrated, tested and validated. The model is simple, easily extensible and can be adapted and used in research and industrial practice.

Materials and methods

The upgraded 5 L Automatic Methane Potential Test unit (AMPTS II; Bioprocess Control, Sweden) was used for the semi-continuous experiment (Kolbl et al., 2014) of mixture of cheese whey from two different batches of cheese production (CW1 – cheese whey 1 and CW2 – cheese whey 2), CM and WWS. Seven different combinations of substrates (CW, CM, WWS) with different organic loadings and hydraulic retention times were used. Measurements of physicochemical parameters such as pH, ammonia nitrogen, COD, trace elements (XRF), VOA/TIC ratio) were performed. After 50 days of stable methane production, we doubled the CW concentration (until day 65).

The simple kinetic model with five parameters: three kinetic equations (k_f , k_s , k_{int}) and two yield coefficients ($Y_{P/A}$, $Y_{P/B}$) was used. The model was implemented and solved in Mathematica (Wolfram). The WhenEvent option was used in NDSolve function to take into account the periodic replacement of the substrate.

Results and discussion

After the first 50 days of anaerobic digestion, 1682±204 mL of methane (cumulative) was produced in reactor I that received only WWS (Figure 1A). A daily supplement of 55 mL CW increased the cumulative production by approximately 16000 mL (reactor IV). The additional daily supplement of 10 mL of cow manure further increased production by 20000 mL (reactor VIII). Doubling the volume of added CW increased the methane production in range from 33% to 53%. Most of the methane was produced in the reactor VIII where the volumetric ratio of WWS: CW: CM was 70:55:10 (70:110:55 after 50 days).

Concentrations of SCVFA were decreasing up to day 50 in all reactors. After doubling CW daily addition, it started to increase again. The pH in reactor where the CW was added was constantly decreasing. CW was the



main source of SCVFA and contributed to the increase in methane production. Reactors that had higher alkalinity all received CM, which is evident that this is the main source of higher buffer capacity. Simple kinetic model was able to simulate the daily methane production (Figure 1 B).

Reactors that received only WWS failed to operate, showing that the addition of CW and CM prevented the failure of reactors. Strong positive linear correlation between selected microelements (Fe, Cu, Zn, Mn) was found. These microelements started to decrease in the co-digestion anaerobic reactors. Forward projection (Figure 1C) showed that concentration of these microelements would in long time period (after 100 to 270 days) be in deficiency.

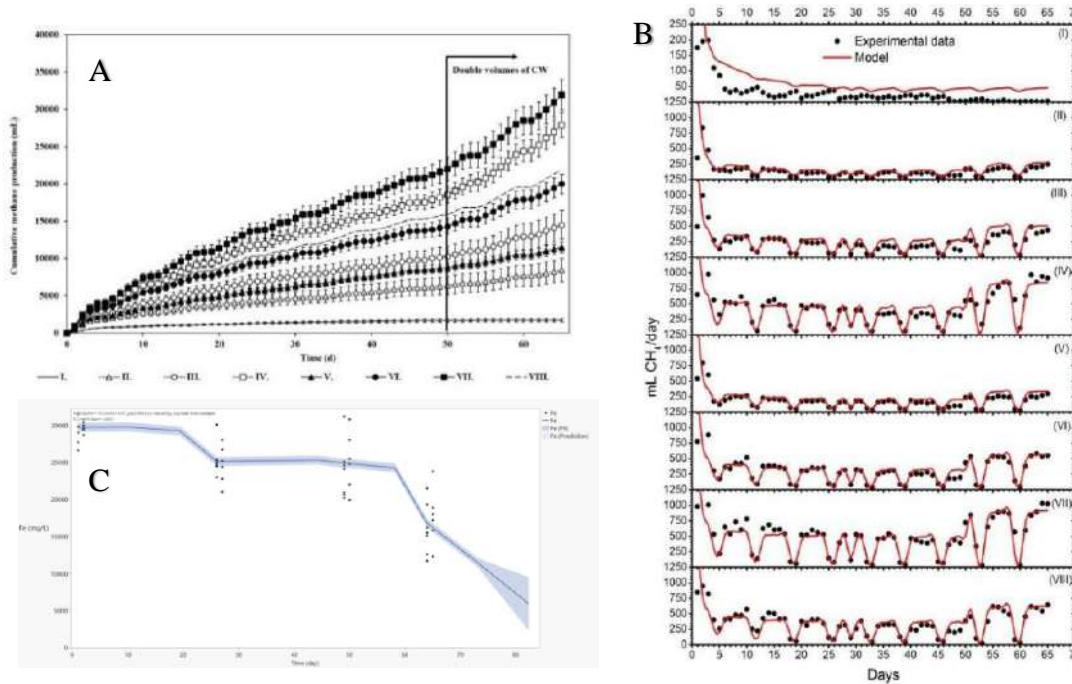


Figure 1. Cumulative methane production for eight set of reactors with different substrate mixture (A), model simulation results compared to the experimental data of methane production for different reactors (B) and forward projection of TE (Fe) washout of reactors (C).

Conclusions

Co-digestion of CW with WWS and CM is a promising alternative for the utilization of milk by-products for waste minimization and energy recovery. Co-digestion of WWS, CW and CM was successful without any signs of inhibition. Irregular feeding of reactors also did not influence on methane production or the stability of the process. There is slight possibility of the inhibition of the process, because of constant dilution of the digestive mixture with fresh liquid substrates. Decrease in concentration of important microelements that are needed for normal functioning of methanogenic *Archaea*, could expose reactors to the susceptibility in microelements deficiency. This can lead to the inhibition or failure of the process. Model successfully simulates methane production of co-digestion complex mixtures. For each additional COD source (substrate), the developed model requires only the definition of one additional parameter for the fast biodegradable fraction (f).

Acknowledgements: The modeling part of this work has been financially supported STSM of Leon Deutsch at NTUA in the frame of COST Action ES1302. This project has been co-financed by ARRS programme P2-0180 and project J2-3056.

References

Kolbl, S., Palocz, A., Panjan, J., Stres, B., 2014. Addressing case specific biogas plant tasks: Industry oriented methane yields derived from 5L AMPTS in batch or semi-continuous tests using realistic inocula, substrate particle sizes and organic loading. *Bioresour. Technol.* 153, 180–188.
<https://doi.org/10.1016/j.biortech.2013.12.010>



The effect of biogas plants on the reduction of GHG emissions on the animal production farm profile

J. Dach¹, W. Bojarski¹, J. Mazurkiewicz¹, A. Kowalczyk-Juśko², P. Pochwatka² and A. Mazur²

¹Department of Biosystems Engineering, Poznań University of Life Sciences, Poznań, Poland²Department of Environmental Engineering and Geodesy, University of Life Sciences in Lublin, Lublin, Poland

Corresponding author email: jacek.dach@up.poznan.pl

keywords: *farmyard manure; GHG emissions; energetic and economic balance; dairy farm.*

Introduction

Climate change resulting from human activities is increasingly affecting the natural environment, weather phenomena, and, consequently, society. In particular, the emission of greenhouse gases (GHG) is a disadvantage (Boyce and He 2022). Agriculture is one of the main sources of two greenhouse gas emissions: methane (a gas with a greenhouse effect 25 times greater than CO₂) and nitrous oxide (N₂O has a greenhouse effect 298 times greater than CO₂) (Pochwatka et al. 2020). Livestock farms that produce manure are particularly strong sources of methane and nitrous oxide emissions. Poland is currently the largest producer of manure in the EU (over 100 million Mg annually), and the emissions of CH₄ alone from manure piles are estimated at as much as 0.5 million Mg annually (Kozłowski et al. 2019).

The emissions origination mechanism is related to the usual manure pile formation practices. This fertilizer is dumped, but kneading operations are not commonly performed. Consequently, the oxygen in the manure is used by the bacteria to decompose the organic matter initially, and as a result, heat is released. This phenomenon raises the pile's temperature to even 40-60°C within several dozen hours. During this time, conditions are created for the anaerobic decomposition of organic matter. When this breakdown occurs, bacteria release energy in a chemical form – that is, methane (Mazurkiewicz 2022).

The study aims to show how the CH₄ and N₂O emissions will decrease in a situation where, instead of traditional manure storage for several months, it is used as a substrate for a biogas plant immediately after it is removed from a dairy cow barn. The energetic and economic balance of a model farm with dairy farming without a biogas plant and with a biogas plant using manure as a substrate was also made.

Materials and methods

The study compares two farm variants with livestock production: a variant with traditional manure storage in piles and a variant with a biogas plant, which processes freshly produced manure. For the calculations in variant I, research data was used to determine the average emission of CH₄ and N₂O per 1 Mg of stored manure to determine the amount of uncontrolled GHG emission on the farm. In variant II, the results of studies on the biogas efficiency of manure from dairy cows were used, and then the energetic and economic effect of the manure utilization biogas plant was calculated. Then, the economic efficiency of both technologies was compared, taking into account the GHG emission cost calculated according to the exchange prices of CO_{2-e} emission allowances.

Results and discussion

Variant II (investment in a biogas plant that converts manure into energy) was found to be much more economically effective than Variant I (traditional manure management). This difference is particularly pronounced in the case of using or selling heat from cogeneration.

It has also been shown that if obligatory fees cover the agricultural sector for greenhouse gas emissions, the investment in a biogas plant will be necessary to maintain a positive economic balance of farming operations.

Conclusions

Investments in biogas plants at livestock farms may be necessary in the face of increasing criticism of the livestock sector as a strong source of GHG emissions. It should also be emphasized that the electricity and



heat generated in biogas plants (processing manure) have a very high environmental value as energy carriers with negative emissions.

Acknowledgements: This study was created in the framework of 2018 Joint Call FACCE ERA-GAS, SusAn and ICT-AGRI2 on “Novel technologies, solutions and systems to reduce greenhouse gas emissions in animal production systems” of the project “Decision support system for sustainable and GHG optimized milk production in key European areas” No. ICT-AGRI-3 ID 39288, Acronym MilKey, realized at Poznań University of Life Sciences. The work was created in the framework of the National Center for Research and Development project "Mitigating emissions from livestock systems", Acronym: MELS; FACCE ERA-GAS, SusAn and ICT-AGRI2.

References

- Boyce, S. and He F., 2022. Political governance, socioeconomics, and weather influence provincial GHG emissions in Canada. *Energy Policy*, 168, 113019.
- Pochwatka, P., Kowalczyk-Juśko, A., Sołowiej, P., Wawrzyniak, A., Dach, J. 2020. Biogas Plant Exploitation in a Middle-Sized Dairy Farm in Poland: Energetic and Economic Aspects. *Energies*, 13, 6058.
- Kozłowski, K., Dach, J., Lewicki, A., Malińska, K., Do Carmo, I.E.P., Czekala, W. 2019. Potential of biogas production from animal manure in Poland. *Arch. Environ. Prot.*, 45, 99–108.
- Mazurkiewicz, J. 2022. Energy and Economic Balance between Manure Stored and Used as a Substrate for Biogas Production. *Energies*, 15, 413.



Statistical Comparison of the performance of the Down-flow Expanded Granular Bed Reactor and Expanded Granular Sludge Bed Reactor train for the treatment of Poultry slaughterhouse wastewater

P. A Dyosile¹, M. Basitere², M. Njoya² and S.K.O Ntwampe³

¹ Bioresource Engineering Research Group (*BioERG*), Department of Chemical Engineering, Cape Peninsula University of Technology, Cape Town, South Africa

² Academic Support Programme for Engineering in Cape Town (*ASPECT*) & Water Research Group, Department of Civil Engineering, University of Cape Town, Rondebosch, Cape Town, South Africa

³ Centre of Excellence in Carbon-based Fuels, School of Chemical and Minerals Engineering, North West University, Potchefstroom, South Africa

Corresponding author email: moses.basitere@uct.ac.za

keywords: Down-Flow Expanded Granular Bed Reactor (DEGBR); Expanded Granular Sludge Bed (EGSB); High Rate Anaerobic Bioreactors (HRAB); Low Rate Anaerobic Bioreactor (LRAB); Poultry Slaughterhouse Wastewater (PSW).

Introduction

The poultry industry is one of the largest industries within the South African (SA) agricultural sector (Basitere et al., 2017; Davids & Meyer, 2017). During bird slaughtering and processing operations, SA poultry industries consume a substantial quantity of potable water in order to maintain the high hygienic standards required for the production of poultry products (DARD, 2009). The treatment of the large quantities of high-strength poultry slaughterhouse wastewater (PSW) generated has proven to be a challenge for SA poultry industries due to the wastewaters' high chemical oxygen demand (COD), suspended solids, colloidal matter (i.e. fats, carbohydrates and proteins), nutrients (i.e. nitrogen and phosphorous), and the prevalence of pathogenic organisms (Debik & Coskun, 2009). The treatment of PSW prior to discharge is therefore crucial in order for poultry industries to achieve compliance with municipal discharge standards and to avoid discharge penalties as per the "polluter pays" principle implemented by local authorities. This study will statistically compare the performance of two multi-integrated system train consisting of enzyme based pre-treatment, Expanded Granular bed reactor and Downflow Expanded Granular bed reactor each coupled with Membrane bioreactor system to treat poultry slaughterhouse wastewater.

Materials and methods

Poultry slaughterhouse wastewater was collected from a poultry slaughterhouse in the westerncape Province, South Africa. The raw PSW was analyzed for TSS, pH, turbidity, FOG, protein concentration, COD, VFAs and toxicity prior to the addition of the PSW to the pretreatment tank. The PSW was pretreated by mixing 20 ml Eco-Flush mixed into 20 liters of raw PSW. The mixture was aerated for 24 hours. The Product of the pre-treatment was then split between the train containing EGSB reactor and the DEGBR reactor each coupled membrane bioreactor (see Figure 1). The system was then run continuously over a period of 120 days continuously.



Figure 1: Multi integrated system treating poultry slaughterhouse wastewater.

Results and discussion

This study aims to evaluate the efficiency of pre-treated up-flow versus down-flow reactor through a performance review and statistical analysis of the EGSB and DEGBR. Furthermore, due to limitations associated with reactor performance this study also evaluates the respective pretreatment- reactor-post-treatment chains. Overall system removal for the reactors and their respective chains included a COD, TSS and FOG removal of 53,9%, 68,4% and 66,9% for the EGSB reactor; 87%, 92,5 and 89,4% on the DEGBR; 97,8%, 99% and 96,9% for the Pretreatment-EGSB-MBR chain and lastly 99,1%, 99,8% and 99,4% respectively on the Pretreatment-DEGBR-MBR. In addition, a statistical paired T-test was used to determine whether the difference in performance of these reactors is genuine or could just have been chance. The results showed a p-value less than 5% for COD, TSS and FOG removal which confirms the difference in performance between the reactors.

Conclusions

Overall system removal for the DEGBR reactor train was better compared to the EGSB reactor train. Furthermore, the validity of the results was quantified by t-stat vales of 10,9, 4,4 and 3,8 over a t-crit. of 2,1 for COD, TSS and FOG respectively across the reactors. On the systems chains, Pre-treatment-DEGBR-MBR and Pre-treatment-EGSB-MBR, results validity was substantiated by t-stat vales of 8,9, 4,1 and 4,6 over a t-crit. of 2,1 for COD, TSS and FOG respectively. With P-values at $7,8 \times 10^{-09}$, $4,1 \times 10^{-4}$ and $1,6 \times 10^{-3}$ for COD, TSS and FOG on the reactors and $1,4 \times 10^{-07}$, $8,6 \times 10^{-4}$ and $2,7 \times 10^{-4}$ on the system chains for COD, TSS and FOG respectively. From this, it was concluded that the DEBGR and the PT-DEGBR-MBR chain outperformed the EGSB and the PT-EGSB-MBR. Furthermore, from this study it was gathered that the addition of the Eco-enzyme dosed pre-treatment and MBR units, the resultant effluent of the of both the PT-EGSB/DEGBR-MBR meeting the set-limit of effluent discharge.

Acknowledgements: This study was is supported by the National Research Foundation Thuthuka Funding, Grant No: 138173.

References

- Basitere, M., Rinquest, Z., Njoya, M., Sheldon, M.S., Ntwampe, S. K. O. (2017) . Treatment of poultry slaughterhouse wastewater using a static granular bed reactor (SGBR) coupled with ultrafiltration (UF) membrane system. *Water Science & Technology*, 76(3), 106-114.
- Davids, T., Meyer, F. H. (2017). Price formation and competitiveness of the South African broiler industry in the global index. *Agrekon*, 56(2), 123-138.
- Debik, E., Coskun, T. (2009). Use of the Static Granular Bed Reactor (SGBR) with anaerobic sludge to treat poultry slaughterhouse wastewater and kinetic modeling. *Bioresource Technology*, 100, 2777-2782.
- DARD (Department of Agriculture and Rural Development) (2009). Guideline manual for the management of abattoirs and other waste of animal origin. Department of Agriculture and Rural Development, Gauteng Provincial Government, South Africa. Available: <https://www.dgard.gov.za>, [2015, August 17].



Comparative effects of agricultural biowaste recycling practices and inorganic fertilization on basil (*Ocimum basilicum* L.) growth and soil fertility: Modeling plant growth

D. Pinakoulas¹, V. Sotiriou², S. Grivopoulos², M. Drosos^{2,3}, M. Papadaki⁴, G. Mihalakakou⁵ and E. Giannakopoulos²

¹*School of Science and Technology, Hellenic Open University, Patra, Greece*

²*Department Biosystems & Agricultural Engineering, School of Agricultural Sciences, University of Patras, Mesologhi, Greece*

³*Institute of Resource, Ecosystem and Environment of Agriculture (IREEA) Nanjing Agricultural University, Nanjing, China*

⁴*Department of Environmental Engineering, University of Patras, Agrinio, Greece* ⁵*Department of Mechanical Engineering and Aeronautics, University of Patras Rio, Greece*

Corresponding author email: v.giann@yahoo.com

Introduction

In modern societies, the disposal of ever more increasing biowaste is a serious threat [1]. Furthermore, the exploitation of soils that are unsuitable for cultivation (poor in nutrients due to intensive cultivation or polluted with organometallic pollutants) is an ongoing challenge [2]. One green and sustainable solution seems to be the disposal of biowaste, a rich source of nutrients, which might be exploited to produce biofertilizers in these soils [3-4]. The use of these organic amendments in agriculture is a common practice due to their ability to increase crop productivity, enhance soil health and improve soil physicochemical properties [5-6].

Methods

This study investigates the effects of organic soil amendments with: compost from plants; chickens' manure; sewage sludge; as well as a chemical fertilizer on basil (*Ocimum basilicum* L.) growth and soil fertility, whilst the expected effects of the abiotic and biotic environment, including effects of organic soil amendments, on plant growth were modelled using a Richards growth model [7].

Results

The results showed that the best plant growth was achieved in the sludge-modified soils, whilst the poorest plant growth was noted in the chemical fertilizer-modified soil (Fig. 1). Moreover, the results of foliar diagnostics indexes showed that the plants of organic soil amendments with chemical fertilizer have low values, at the level of malnutrition, in several elements such as Phosphorus (P) and Copper (Cu) (Table 1).

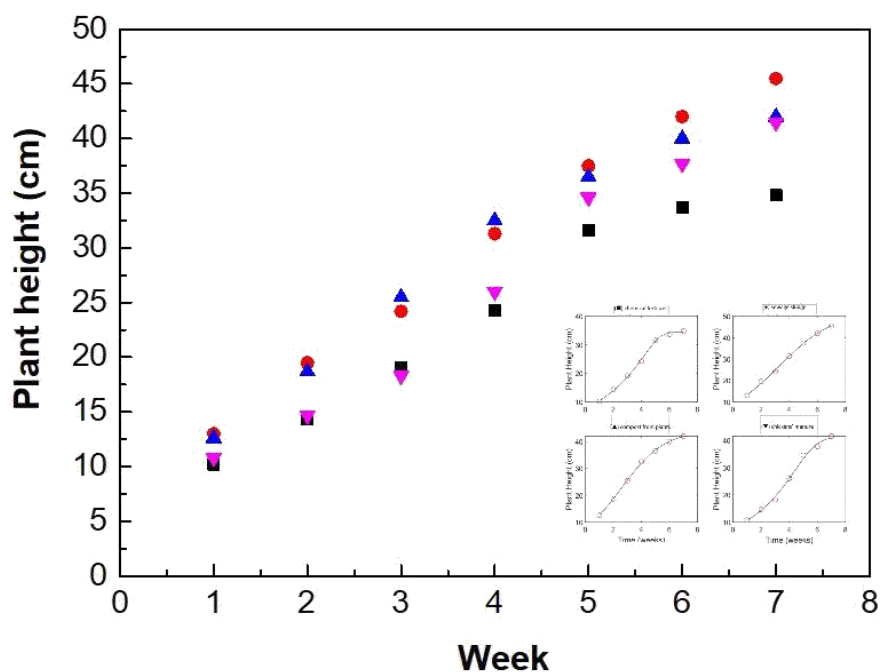


Fig.1. Developmental effects on basil growth from different organic soil amendments by use of: (■) chemical fertilizer, (●) sewage sludge, (▲) compost from plants and (▼) chickens' manure. (Insert: Theoretical fit (solid line) using Richards growth model)

Table 1: Foliar diagnostic results

Modified soil	Foliar Diagnosis Indexes				
	N (% w/w)	P(% w/w)	K (% w/w)	Cu (mg/kg DW)	Zn (mg/kg DW)
Chemical fertilizer	3.49 ± 0.05	0.05 ± 0.05	4.20 ± 0.02	< 1	17.79 ± 0.02
Sewage Sludge	3.10 ± 0.04	0.28 ± 0.02	2.31 ± 0.03	8.76 ± 0.03	45.22 ± 0.03
Compost	2.24 ± 0.03	0.16 ± 0.01	5.25 ± 0.04	8.65 ± 0.01	66.88 ± 0.02
Chickens' manure	2.86 ± 0.05	0.17 ± 0.03	3.25 ± 0.07	6.72 ± 0.02	39.54 ± 0.05
Nutrient-Limited Plant Growth	< 1.40	< 0.07	< 0.40	< 5.00	< 5.00

Conclusions

This work confirms that the organic soil amendments generally result in beneficial effects with regard to plant growth and other soil properties. Our findings are significant for sustainable agriculture regarding the sustainable use of organic wastes in problematic soils.

Acknowledgments: A part of the research project was co-funded by the University of Patras, in the framework of the program "MEDIKOS".

References

- Giannakopoulos, E., et al., (2017). Jour. Environmental Management, 195,186-194.
- Ahmad, R., et al., (2007). Annals of Microbiology 57, 471-479.
- Khadem, S.A., et al., (2010). Australian Journal of Crop Science, 4, 642-647.
- Mullins, G.L., et al., (1996). Techn. Publication No. 424-034, Virginia State University, Blackburg, VA, USA. [5]Pervez, M.A., et al., (2000). International Journal of Agriculture and Biology, 2, 1-2.
- Farrag, K., et al. (2016). Clean-Soil Air Water, 44 (9), 1174-1183.
- Damgaard, C. (2004). Comptes Rendus Biologies,327(3),255-260.



Advances in avocado oil extraction replacing conventional solvent extractions with Ultrasound technique as a green technology

S.T. Mgoma¹, M. Basitere² and V. Mshayisa³

¹Department of Chemical Engineering, Cape Peninsula University of Technology, Bellville, South Africa

²Academic Support Programme for Engineering (ASPECT), Center for Higher Education Development, University of Cape Town, Rondebosch, Cape Town, South Africa

³Department of Food Science and Technology, Cape Peninsula University of Technology, Bellville, South Africa

Corresponding author email: moses.basitere@uct.ac.za

Keywords: green technology; ultrasound technique; avocado oil; extraction.

Introduction

The growth in the health awareness of the population has led to an increase in demand of healthy diet worldwide (Iqbal et al., 2021). Furthermore the growth in demand of natural ingredients is not only for food but also for the cosmetic industry (Fonseca-Santos et al., 2015). Avocado oil production has been growing to be used as culinary oil and as an essential oil. With this increased demand, industries have been focusing on processes that will improve the yield and quantity of the oil extracted; however extraction processes should not only focus on the quantity of the oil produced but also on the quality of the oil (Reddy et al., 2012). The current oil production industries that produce oil in high quantities have solid-liquid based processes using organic solvents. Therefore as part of the effort to help contribute to the aims and targets of the sustainable development goals set out by the United Nations (UN); with SDG 9 which aims to make industries sustainable, increased resource use efficiency greater and adoption of clean and environmentally sound technologies and industrial processes. A continuation of the optimization study to extract oil from dried avocado pulp was done with the aim of using ultrasound assisted extraction as one of the green extraction techniques to replace the conventional solid-liquid solvent extraction techniques used in the previous study and by current industries.

Materials and methods

Avocado fruits were sourced from local informal fruit and vegetable market in Limpopo. The avocado pulp was grounded and dried in an oven at 70°C for 36 hours. Oil was extracted from the dried pulp with Ultrasound technique for 10, 20 and 30 minutes using water as solvent at ambient temperature of 28°C; with power of 750 Watts and intensity of 50% Amplitude. Another extraction was done using 30% aqueous hexane for 10 minutes at ambient temperature of 28°C; with power of 750 Watts and intensity of 50% Amplitude. The samples were centrifuged after ultrasound processing and the oil was separated from the water and the pulp. For the aqueous hexane extraction, the hexane was flushed with nitrogen.

Results and discussion

The technique managed to produce oil yields of 91.4 g/Kg, 101.2 g/Kg, and 102.6 g/Kg dry weight for water extractions and 353.2 g/Kg dry weight for aqueous hexane respectively. The results of the ultrasound technique were compared with the conventional techniques and both were critically discussed. The conclusion of the discussion found that green technology showed superior advantages over conventional techniques. The comparison was done with results of the study that analysed the effects of processing time, solid to liquid ratios and amount of solvent used against the oil yield.



The study found that comparing 10 minutes of aqueous hexane with ultrasound against 2, 4 and 6 hours of conventional extraction; ultrasound still produced a yield higher than that of 2 hours and only 18% less than the yield of 4 hours processing. The solid to liquid ratios compared at 4 hours of processing found that the ratios of 1:1 and 1:3 had lower yields than that of ultrasound which was extracted using the same amount of solvent as 1:1 ratio. The study of the amount of solvent used to the oil yield compared to the ultrasound technique found that ultrasound used the same amount of hexane as the lowest solid to liquid ratio but ultrasound produced an oil yield of over 30% more with 230 minutes (3 hours 50 minutes) less processing time than the conventional technique.

The water extractions have shown that ultrasound technique has the potential to do oil extraction without the use of non-polar organic solvents. Although the results are still showing a low yield but do present an opportunity to explore optimizing the technique with different parameters like amplitude, frequency and power of the ultrasound.

Conclusions

This study have proven the advantages of green technology being able to do extractions with use of very low or no organic solvents, have low energy consumption like non-thermal techniques (e.g. Ultrasound) and also requires less operation/extraction time. These advantages together with the results have proven the potential to replace conventional extraction techniques with the sustainable green extraction techniques like ultrasound assisted technique. The results of this study will be used to do a scale-up conceptual design using Aspen plus simulation and further do a techno-economic analysis. The conceptual design and economic analysis will help overcome the major challenge for the ultrasound technique, which is the adoption of this green technology at an industrial scale.

References

- Fonseca-Santos, B., Antonio Corrêa, M. & Chorilli, M. 2015. Sustainability, natural and organic cosmetics: Consumer, products, efficacy, toxicological and regulatory considerations. *Brazilian Journal of Pharmaceutical Sciences*, 51(1): 17–26.
- Iqbal, J., Yu, D., Zubair, M., Rasheed, M.I., Khizar, H.M.U. & Imran, M. 2021. Health Consciousness, Food Safety Concern, and Consumer Purchase Intentions Toward Organic Food: The Role of Consumer Involvement and Ecological Motives. *SAGE Open*, 11(2).
- Mgoma, S.T., Basitere, M. & Mshayisa, V. 2019. Effects of Different Extraction Methods and Process Conditions in the Yields of Avocado Oil. , (November).
- Reddy, M., Moodley, R. & Jonnalagadda, S.B. 2012. Fatty acid profile and elemental content of avocado (*Persea americana* Mill.) oil -effect of extraction methods. *Journal of Environmental Science and Health - Part B Pesticides, Food Contaminants, and Agricultural Wastes*, 47(6): 529–537.



Forest residues valorization towards wood protecting agent applications

L. Sillero¹, A. Morales¹, R. Fernández-Marín¹, F. Hernández-Ramos¹, I. Dávila¹, X. Erdocia² and L. Labidi¹

¹Chemical and Environmental Engineering Department. University of the Basque Country UPV/EHU. Plaza Europa, 1, 20018 San Sebastian, Spain.

²Department of Applied Mathematics. University of the Basque Country UPV/EHU. Rafael Moreno "Pichichi", 3, 48013 Bilbao, Spain.

Corresponding author email: leyre.sillero@ehu.eus

keywords: wood; extractives; antioxidant; antifungal; protecting agent.

Introduction

The use of wood in construction is back on trend thanks to the growing demand for a sustainable construction sector that has one of its bases in the use of renewable materials. According to the wood's final use, it requires a variety of treatments to improve their properties, for which up to now, petroleum-based compounds have been used. Nevertheless, in recent years, mainly due to the rising environmental concerns of today's society, and the depletion of fossil fuels, research towards the substitution of these compounds by other natural resources has been intensified.

Lignocellulosic biomass is considered one of the most promising feedstocks. This is not only due to its chemical composition, but also because it is a renewable, accessible, affordable, and carbon-neutral raw material. Apart from lignin, cellulose and hemicelluloses, wood also has other interesting non-structural components, especially extractives. They are a mixture of different compound families, including polyphenols, to which properties such as antioxidant and antimicrobial capacities are attributed. Due to the complexity of the lignocellulosic structure, the extraction process must be carefully selected. One of the most studied methods that provides good extraction yields is the conventional solid-liquid extraction process. However, the main drawbacks of this technique is the use of volatile organic compounds (VOCs), which have a great negative impact on the environment. However, the use of ethanol/water mixture as a solvent provides a green solvent alternative solution, which can efficiently extract the valuable polyphenols.

Therefore, in this work, the extraction of polyphenolic compounds from different wood residues generated in the forest of the Basque Country, and their later application as wood protecting agents, has been investigated.

Materials and methods

Wood samples were harvested by Basoekin Ltd. during the summer of 2020 in the forests of the Basque Country. The selected tree wood species were *Betula pubescens, var celtiberica* (Iberian white birch), *Quercus robur* (common oak) and *Robinia pseudoacacia* (black locust). Wood samples were debarked and grounded prior to their use. The chemical characterization of the samples confirmed that they are rich in extractives: 4.49 wt.% Iberian white birch (IWB), 4.49 wt.% Black locust (BL) and 6.32 wt.% Common oak (CO) (Sillero et al. 2021).

Each of the materials was submitted to an extraction in a temperature-controlled orbital shaker (Heidolph Unimax 1010 with Heidolph Incubator 1000), using EtOH/H₂O (50/50 (v/v)) as solvent, following the methodology optimized by Sillero et al. (2018). After extraction, the solid and liquid fractions were separated by filtration, and the supernatant was characterized. First, the extraction yield was measured gravimetrically, and then, the extracts were analyzed for total phenolic content (TPC), antioxidant capacities (DPPH, FRAP, ABTS) (Sillero et al. 2018) and antimicrobial capacity (Sillero et al. 2021), assessing growth intensity using ISO 846 standard. Finally, 1.8 x 2 x 1 cm pine wood samples were impregnated with the obtained extracts by maceration at room temperature during 1 week, previously the samples were dried and autoclaved (Salem et al. 2016). Once prepared, the impregnated woods were tested against *Trametes versicolor* following the methodology described by Salaberria et al. (2017).



Results and discussion

The maceration of the woods using an EtOH/H₂O mixture as solvent resulted in a competitive method for the extraction of polyphenols as shown in Table 1. The highest extraction yield was obtained for BL, but this extraction was not very selective, since the TPC of this extract was the lowest, as well as its antioxidant capacities. IWB extracts showed the highest TPC, as well as the highest antioxidant capacities. In general, a direct correlation was observed between the TPC and the antioxidant capacities of the extracts, the higher the TPC, the higher the antioxidant capacities (Kainama et al., 2020). Regarding the antifungal capacity against the *Trametes versicolor* fungus, all the extracts had a GI of 4. This suggests that the extracts can be used for wood preservative applications.

Table 1. Results of the characterization of wood extracts and the test of impregnated woods against *Trametes versicolor*

ID	Extraction yield (%)	TPC (mg GAE/g DM)	DPPH (mg TE/g DM)	ABTS (mg TE/g DM)	FRAP (mg TE/g DM)	Average concentrations (cells/mL sample)
IWB	1.8 ± 0.2	474 ± 30	394 ± 28	978 ± 171	262 ± 20	8.05 × 10 ⁵
BL	4.5 ± 0.3	142 ± 17	54 ± 8	246 ± 31	62 ± 5	6.58 × 10 ⁵
CO	3.3 ± 0.2	302 ± 22	228 ± 14	642 ± 37	213 ± 11	10.1 × 10 ⁵

In order to confirm this, research was carried out on the improvement of the impregnated wood against the *Trametes versicolor* fungus. For this purpose, the woods were first impregnated with the extracts, obtaining yields of 0.11% for CO, and 0.22% for IWB and BL; then, they were tested against the fungus. As shown in Table 1, all the extracts were able to reduce fungal growth on pine wood, but none of them were able to prevent the growth. The best antimicrobial results were obtained for BL, which was able to reduce fungal growth by up to 45% compared to the blank (12 × 10⁵ cells/mL sample). These results are promising, although further study is needed to achieve the desired fungal growth inhibition.

Conclusions

Extractions of bioactive compounds from three different woods were successfully carried out. These extracts were proven to be rich in phenolic compounds as well as having good antioxidant and antifungal properties. By testing impregnated wood against the fungus *Trametes versicolor*, it has been confirmed that extracts obtained from forest residues can be directly used to improve the wood's properties.

Acknowledgements: Authors would like to express their gratitude to the Department of Economic Development and Infrastructures of the Basque Government and to the European Agricultural Fund for Rural Development (00030-COO2019-30), as well as to the University of the Basque Country UPV/EHU for financially supporting this research. L.S. would also like to thank to the Spanish Ministry of Universities for the Margarita Salas fellowship financed by the European Union-Next Generation EU.

References

- Sillero L., Morales A., Fernández-Marín R., Hernández-Ramos F., Dávila I., Erdocia X. and Labidi J., 2021, Study of Different Extraction Methods of Bioactive Molecules from Different Tree Species, *Chemical Engineering Transactions*, 86, 31-36.
- Sillero L., Prado R., Labidi J., 2018, Optimization of Different Extraction Methods to Obtaining Bioactive Compounds from Larix Decidua Bark, *Chemical Engineering Transactions*, 70, 1369–1374.
- Salem M. Z. M., Zidan Y.E., Hadidi N.M.N., Masour M.M.A. and Abo Elgat W.A.A., 2016, Evaluation of usage three natural extracts applied to three commercial wood species against five common molds, *International Biodeterioration & Biodegradation*, 110, 206-226.
- Salaberria A.M., Diaz R.H, Andrés M.A., Fernandes S.C.M. and Labidi J., 2017, The Antifungal Activity of Functionalized Chitin Nanocrystals in Poly (Lactid Acid) Films, *Materials*, 10, 546.
- Kainama, H., Fatmawati, S., Santoso, M., Papilaya, P.M., Ersam, T., 2020, The Relationship of Free Radical Scavenging and Total Phenolic and Flavonoid Contents of Garcinia lasoar PAM. *Pharmaceutical Chemistry Journal*, 53, 1151–1157.



SUST
ENG
2022



WASTE TO ENERGY/ENERGY PRODUCTION



Hydrothermal carbonization as a pathway for co-gasification of municipal sludge and agricultural residues

A. Artikopoulos¹, G. Altiparmaki¹, D. Liakos¹ and S. Vakalis¹

¹Energy Management Laboratory, Department of Environment, University of the Aegean, University Hill, Mytilene, Greece

Corresponding author email: vakalis@aegean.gr

keywords: hydrothermal carbonization; solar distillation; co-gasification; agrowaste.

Introduction

Lesvos island has approximately 11 million olive trees and agricultural biowaste/ pruning have not been properly managed so far. At the same time, sustainable management of municipal sludge is an unresolved issue for several regions of Greece, including North Aegean. This study utilizes hydrothermal carbonization for the conversion of municipal sludge into hydrochar and hydrothermal liquor by means of state-of-the-art HT reactor. On the one hand, the liquid fraction is removed by means of solar distillation. For this purpose, a solar still that is constructed and operating in the Energy Management Laboratory of the University of the Aegean. On the other hand, the plan is the co-gasification of the produced hydrochar with biomass residues from agricultural operations, especially olive tree pruning. A state-of-art biomass gasifier will be installed on the island within the next year and this study has the scope of investigating the feasibility of this endeavor.

Materials and methods

Municipal sludge and waste activated sludge from the HYDROUSA site underwent hydrothermal carbonization in a 4570A Parr hydrothermal reactor for a various residence times, temperatures and evolved pressures. The mass balances of the products were implemented along with the TS/ VS content, COD and Total Phenolic Content of the digestate (Folin – Ciocalteu method) of the liquid phase. HHV analysis of the hydrochar was done in a Parr 6400 calorimeter. This study used the Multi-Box model for modeling the gasification of biomass in a Joos gasifier and assessed co-gasification scenarios of hydrochar and woody biomass, and the simulate composition is presented. Preliminary results are presented for the utilization of a solar still for the evaporation of the hydrothermal liquor with a focus on the energy demand, the evaporation time, and the recovery of phenols.

Results and discussion

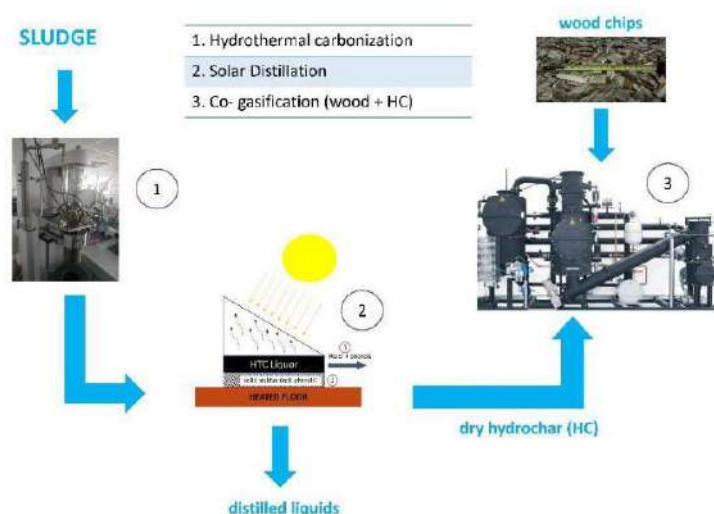


Figure 1. The integrated idea of combining hydrothermal carbonization, solar distillation and co-gasification of hydrochar with wood chips.



Figure 1 presents the integrated idea of combining hydrothermal carbonization, solar distillation and co-gasification of hydrochar with wood chips. The utilization of solar distillation overcomes the necessity for energy-intensive drying processes that need to be applied for removing the water from the produced hydrochars. The production of hydrochar ranged from 20.7% up to 34.4% of the total sludge input, while the heating value of the produced hydrochars ranged from 19.27 to 23.87 MJ/ kg and are presented on Figure 2.

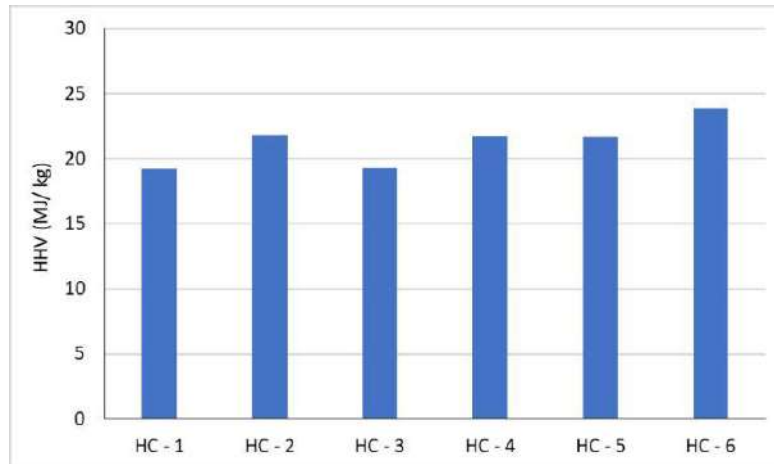


Figure 2. HHV analysis of various hydrochars (HC) from sludge sampled from Lesvos island.

The solar distillator has an integrated heated floor for optimizing the evaporation, and utilizes two pumps that operate for 8 hours (pump 1) and 24 hours (pump 2). The total energy consumption is 1.23 kWh daily and initial experiments show that approximately 200 kWh of electricity would be consumed for the distillation of 1 m³ of HTC liquor. Finally the utilization of the Multi-Box model simulated the co-gasification process and predicted the production of syngas with high molar contents of carbon monoxide (>19%) and hydrogen (>17%). It should be stated that the percentage of added hydrochar may alter the final simulated syngas content since thermodynamic modeling is influenced significantly for the initial composition of the input.

Acknowledgements: We acknowledge support of this work by the project “Center of Sustainable and Circular Bioeconomy [Aegean_BIOECONOMY]” (MIS 5045851) which is implemented under the Action “Reinforcement of the Research and Innovation Infrastructure”, funded by the Operational Programme “Competitiveness, Entrepreneurship and Innovation” (NSRF 2014-2020) and co-financed by Greece and the European Union (European Regional Development Fund).

References

- S. Vakalis, F. Patuzzi, M. Baratieri (2016). Thermodynamic modeling of small scale biomass gasifiers: Development and assessment of the "Multi-Box" approach. *Bioresource Technology* 206; 173-179. <https://doi.org/10.1016/j.biortech.2016.01.060>
- M. A. Vasileiadou, G. Altiparmaki, K. Moustakas, S. Vakalis (2022). Quality of Hydrochar from Wine Sludge under Variable Conditions of Hydrothermal Carbonization: The Case of Lesvos Island. *Energies* 15(10), 3574; <https://doi.org/10.3390/en15103574>



Green pyrolysis of wine waste for hybrid supercapacitors

A. Mamani^{1,3}, M. Giménez^{1,3}, D. Barreda², S. Fabiana^{1,3} and R. Santamaría²

¹ Instituto de Ingeniería Química, Facultad de Ingeniería, Universidad Nacional de San Juan, San Juan, Argentina

² Instituto Nacional del Carbón, INCAR-CSIC, Oviedo, España

³ Consejo Nacional de Investigaciones Científicas y Técnicas (CONICET), Buenos Aires, Argentina

Corresponding author email: mamani@unsj.edu.ar

keywords: grape stalk; hydrothermal; hydroquinone; hybrid performance; circular economy.

Introduction

Wine production is one important sector worldwide, 72 countries produce an estimated production of more than 29 million tons of wine (Food and Agriculture Organization of the United Nations, 2018). A large amount of waste including vine shoots, grape bagasse, grape stalks and wine less, are generated as a consequence. Grape stalk is one of the main biowaste during agronomic practice. According to data from the International Organization of wine, every 100 kg of processed grapes, 25% of grape stalks are generated.

The increasing production of biowaste is becoming a major environmental issue. For sustainable development, biowaste management must be taken from a circular economy perspective. Biowaste can be converted into value-added products, reducing the cost of disposal and environmental burden while generating additional revenues. Hydrothermal carbonization (HTC) is a useful green process to produce carbon materials from biowastes, which require a subsequent activation step to develop porosity. Biomass-derived activated carbons are a cheap carbonaceous material with high porosity and large surface area that have attracted attention as electrode materials in supercapacitors. The supercapacitors are promising energy storage devices due to their high-power density, large capacitance, good recyclability, high charge–discharge efficiency and excellent recharging capability with good long stability. Some studies have reported the incorporation of redox active molecules into the electrolyte as an alternative to improve the energy stored in supercapacitors. Roldan et. al, demonstrated the efficiency of the incorporation of hydroquinone into the aqueous electrolyte significantly increasing the capacitance of an activated carbon used as supercapacitor electrode (Roldan et. al, 2011).

The aim of this work is to evaluate a wine biowaste-derived activated carbon as a supercapacitor active material electrode and its performance with and without hydroquinone added as part of the aqueous electrolyte.

Materials and methods

Grape stalks were provided by Bodegas Callia and were processed as received.

Pyrolysis and activation

Hydrothermal carbonization (HTC) was carried out in a 1-liter Parr reactor, heated by means of an electric furnace with a temperature controller. Water and grape stalk maintained a solid: liquid ratio of 1:1, it was kept at constant temperature (240°C) for 6 hours, working at the corresponding autogenous steam pressure. Afterwards, the reactor was cooled to room temperature and the resulting solid-liquid mixture was filtered. The solid obtained (hydrochar) was dried at 100 °C for 24 h. As an activating agent KOH was employed according to optimization conditions (Giménez et. al, 2020).

Electrode material preparation and electrochemical characterization

The electrode was prepared from a pressured mix of 90 wt. % activated carbon, 5 wt. % of Teflon and 5 wt. of carbon black in the form of pellets of 12 mm in diameter with an approximate weight of 30 mg. The electrochemical system was assembled at a Swagelok cell employing gold disks as current collectors and glassy fibrous paper as separators. The electrochemical determinations were performed using a VPM (Biologic) multichannel generator; every measurement was carried out to the system with (Hybrid supercapacitor) and without (Symmetric supercapacitor) hydroquinone. Galvanostatic charges/discharges in two and three electrode configurations were performed at 0.2 A/g as current density, between a potential from 0V to 1V. The term cycling behavior was evaluated after 250 cycles.



Results and discussion

Using two and three electrode configurations in galvanostatic charges and discharges assays allowed us to evaluate the influence of the hydroquinone as part of the electrolyte, showing what happens into every electrode. As can be seen in Figure 1, the anode has a different behavior. As a symmetric supercapacitor, the overall voltage is distributed uniformly in both electrodes, exhibiting the typical symmetric triangle. On the other hand, the hybrid system, it means with hydroquinone into the electrolyte, conducted to different behavior both in anode and cathode. First of all, the anode showed an almost constant potential, characteristic of faradaic process, which must be attributed to the potential of the Q/HQ redox reaction developed on the electrode surface. On the contrary, the cathode displayed a capacitor-type charge/discharge shape, and as this electrode operated toward more negative potential values as consequence of redox reaction in the other electrode, hydrogen evolution could occur in the cathode (Roldán et. al, 2011). Table 1 shows the capacitance in each electrolyte system; hybrid supercapacitor has a Cs ten times higher than symmetric one. After 250 cycles, the symmetric system had a decrease in the initial capacitance much lower than the hybrid one, of 94% vs. 48%, respectively.

Table 1. Comparison of storage capacity of supercapacitors.

-	Cs (F/g) symmetric	Cs (F/g) hybrid
initial capacitance	165	1809
after 250 cycles	155	878

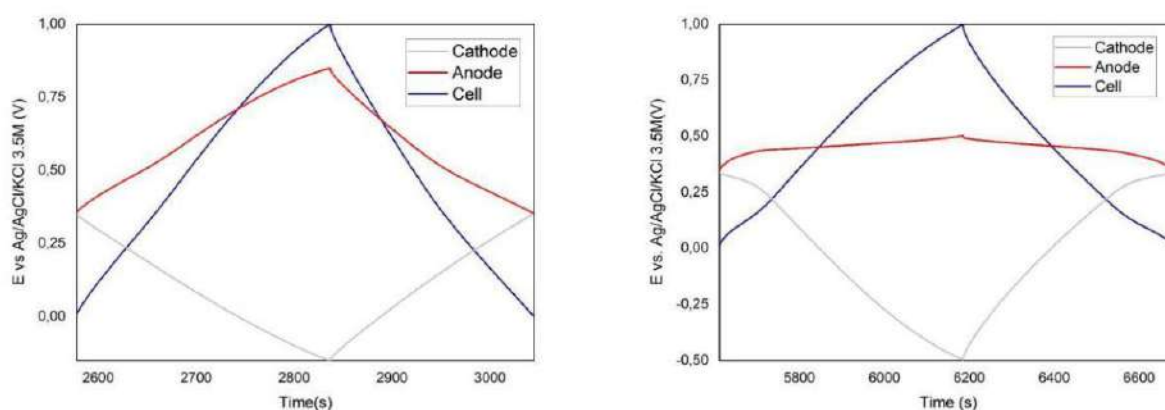


Figure 1. Galvanostatic cycle at 1V of Symmetric and hybrid supercapacitor at 0.2 A/g.

Conclusions

Using a redox active molecule led to changes in the energy storage mechanism of supercapacitor electrodes, made of grape stalk activated carbon. The anode became a battery-type electrode due to redox reactions on its surface and the cathode maintained the capacitor-type behavior. As a consequence of the asymmetric redistribution of voltage, evolution of hydrogen also occurred. Moreover, the anode capacitance increased 10 times with respect to the only symmetric supercapacitor. This work means a contribution to the circular economy concept applied to a biowaste valorization and its use as a special material for technological exploitation routes.

References

- Roldan Silvia, 2011. Mechanisms of Energy Storage in Carbon-Based Supercapacitors Modified with a Quinoid Redox-Active Electrolyte. *J. Phys. Chem. C* 2011, 115, 17606–17611.
- Roldan Silvia, 2011. Towards a Further Generation of High-Energy Carbon-Based Capacitors by Using Redox-Active Electrolytes. *Angew. Chem. Int. Ed.* 2011, 50, 1699–1701.
- Giménez, 2020. Two phase olive mill waste valorization. Hydrochar production and phenols extraction by hydrothermal carbonization, 4th ed.; *Biomass and Bioenergy* 143 (2020) 105875.



The potential of the use of reclaimed areas of transition regions for the production and accumulation of electricity as a potential to replace natural gas from risk areas

L. Štěpanec¹, M. Kantor², P. Gigas³ and D. Juchelková¹

¹Technical University of Ostrava, Ostrava, Czech Republic

²University of Jan Evangelista Purkyně, Ústí nad Labem, Czech Republic

³Technical University of Crete, Chania, Greece

Corresponding author email: dagmar.juchelkova@vsb.cz

keywords: *hydropower; electricity production; reliability; efficiency; accumulation; special installations*

Introduction

The energy potential of large watercourses is almost exhausted in several countries, for their further use it is necessary to look for innovative / new methods that were not viable with standard concepts. From this point of view, small hydroelectric power plants appear to be promising, which are power plants with an installed capacity up of 100 kW.

A lot of knowledge was collected on a laboratory model and subsequently verified in practice.

The possibility of accumulating energy will bring more possibilities, especially in remote locations, for subsequent distribution, increasing the reliability of electricity supply and thus increasing the share of RES in the energy mix. Innovative solutions for the accumulation of electricity in the form of underground storage facilities and new DC link technology will allow further expansion of potential locations.

A key area of concern for the use of small hydroelectric power plants in remote locations is also their management so that the power plant is productive in the longest possible time of the year.

Materials and methods

Small hydropower plants on watercourses with highly variable flow require the use of elements that eliminate the disadvantage of variable water flow through the power plant. As turbines with adjustable blades make the solution considerably more expensive, the concepts of small hydropower plants with variable turbine speeds and thus of an electricity generator are required. In this situation, it is necessary to convert the variable frequency and voltage from the generator to constant voltage and mains frequency. The standard element used for this conversion is a four-quadrant indirect voltage-type frequency converter, which operates in the given application in the inverse mode, i.e. the Generator side inverter operates as a pulse rectifier and the Grid side inverter operates as a fixed grid frequency inverter. In this case, the quality and parameters of the energy supplied to the grid are determined by the characteristics of the grid converter.

The amount of supply to the network is determined by the amount of energy at the DC input of the network converter from the DC intermediate circuit. To stabilize this energy, or. To cover peak energy consumption from the mains, a rechargeable battery can be connected to the DC intermediate circuit, which can compensate for the differences between the amount of energy produced in the generator and the need for energy consumption from the mains.

Results and discussion

The basic problem of connecting the DC intermediate circuit of the inverter to the battery is to find the mutual compatibility of both of these systems. Depending on the type and material of the storage elements, the battery has the parameters and characteristics that must be ensured during its operation. (No-load voltage, maximum charging / discharging current, maximum discharge depth, internal resistance, charging cycle time distribution, operating temperature, etc.) These conditions must be observed by the inverter. There are basically two connection options and the corresponding ways to ensure these conditions for battery operation:

- a) Direct connection of the rechargeable battery to the DC link terminals



In this case, the system of both inverters, both on the generator side and on the network side, must be very precisely and dynamically controlled so that the entire system of a small hydroelectric power plant, ie. the sum of its production, network consumption and energy supplied / consumed to / from accumulation was zero at all times. The advantages of this solution are the simplicity of the inverter power scheme, smaller losses associated with accumulation (only losses in the accumulator battery and losses in the main inverters) and power limitation of the charging / discharging current of the storage unit limited only by sizing the switching components of main inverters.

The disadvantages are: - the need for very precise and dynamically demanding control of both the generator itself and its inverter, as well as equally precise and dynamically demanding control of the inverter on the grid side,

- finding control algorithms that will be able to control a system with relatively small time constants of the generator and network and a significant time constant of the charging processes of the storage unit,
- finding the compatibility of the working voltage range of the DC intermediate circuit from the point of view of the functionality of the converters with the working range of the accumulator battery voltage (range given by the max. charging voltage and its max. discharge voltage)

It is obvious that the focus of this method will be on the development of suitable control algorithms, which, in addition to the above, ensure maximum efficiency of mechanical-electrical energy conversion in the generator at different turbine speeds.

b) Connection of the accumulator battery to the DC intermediate circuit terminals via a suitable coupling converter

The main advantage of this concept is the adaptation of the parameters from the DC intermediate circuit to the requirements and characteristics of the accumulator battery by means of a coupling converter. The DC link voltage can fluctuate within limits, there are no critical time requirements for its stability. The operating conditions of the accumulator as well as the energy balance between the produced and consumed energy must be ensured by the coupling converter of the accumulator battery and its control.

The disadvantage of the concept is:

- the need to use an additional two-quadrant DC converter, which must provide coupling over a wide range of battery currents and the voltage difference between the DC link voltage and the battery,
- incurrance of losses in the coupling converter,
- limiting the battery charging / discharging currents by dimensioning the switching components of the inverter,
- the need to link drive control algorithms with master drive control.

The focus of this method is the development of a suitable coupling converter and its control algorithms, which will ensure suitable operating conditions of accumulators in various energy states of the system of a small hydroelectric power plant with accumulation.

Within the research of structures of small hydropower plants with variable turbine speed and accumulation, both structures were modeled in parts, then realized in the form of laboratory samples and verified their properties in different operating conditions on a physical model of a small hydropower plant.

Conclusions

Within this paper will be indicate especial the

- Capacity, emission saving potential of hydropower, especially small hydropower in the energy transition regions
- repeatability at different regions (bordering conditions)
- new machine design
- and specially the new topology (Accumulation, electricity production effectiveness, environmental friendly design, new control and prediction methods)



Gasification-energy production system for the management of wastewater primary sieved solids

A. Pothoulaki¹, A. Manali¹ and P. Gikas¹

¹Design of Environmental Processes Laboratory, School of Chemical and Environmental Engineering,
Technical University of Crete, Chania, Greece

Corresponding author email: pgikas@tuc.gr

keywords: biosolids gasification; syngas; syngas conditioning; energy production.

Project outline

Nowadays, energy consumption for wastewater treatment is an issue of concern. Novel processes for energy neutral or even energy positive Wastewater Treatment Plants (WWTPs) are under examination (Gikas, 2017). A novel integrated process for the management of biosolids along with energy production is currently under installation at the WWTP of Rethymno, Crete, Greece (www.biosolids2energy.eu). The industrial-scale pilot plant consists of a microsieve followed by a dryer and a gasification-internal combustion engine (ICE). The aim of the project is to remove biosolids upstream of the aeration tank, so to reduce the energy requirements for downstream treatment at the aeration tank. Also, the removed biosolids, following drying, are to be used as feedstock to a downdraft gasification system, while the produced syngas is to be combusted in an ICE for the production of thermal and electric energy. The project is coordinated by the “Design of Environmental Processes Laboratory”, School of Chemical and Environmental Engineering, Technical University of Crete, which has also designed the gasification-energy production system (Figure 1) of the abovementioned pilot plant.

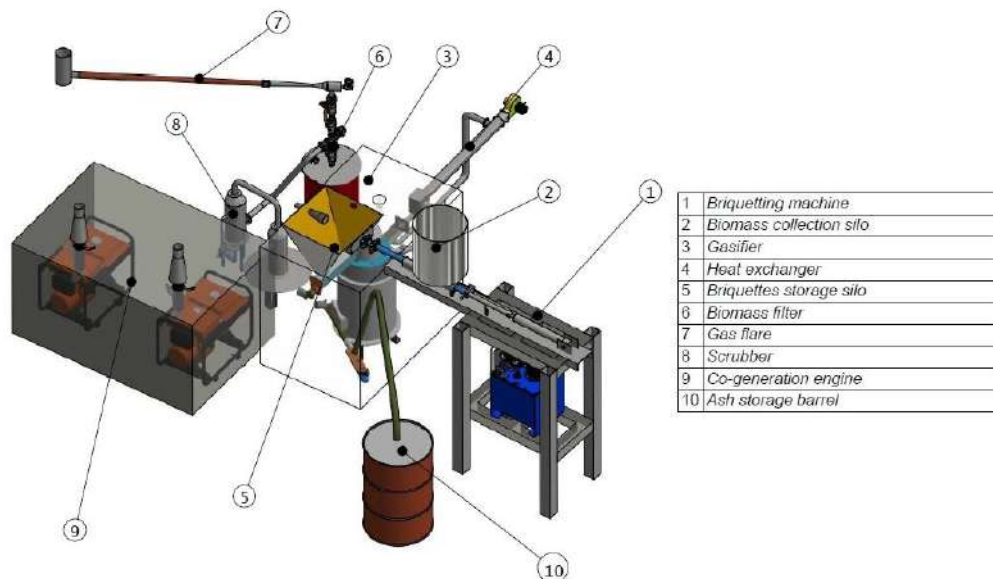


Figure 1. 3D illustration of the gasification-energy production system (left).

Gasification-energy production system description

The main steps of the process are illustrated in Figure 2. In detail, the dried solids exiting the dryer will enter the gasification system. Noted that the dried solids contain about 10-15% of moisture, which is beneficial for the gasification process. As the downdraft gasifier requires the formation of a porous bed, so to progress the gasification process, the dried biosolids will go through a briquetting machine and the briquetted biosolids will drop directly into the gasifier.

The main process of gasification will take place in a downdraft gasifier, which consists of the following zones: the drying zone, the pyrolysis zone, the combustion zone, the reduction zone, and the ash pit (for the removal of the ash without affecting the process of the gasification) (Puig-Arnavat et al., 2010). The required air for the gasification reactions will be injected into the system.

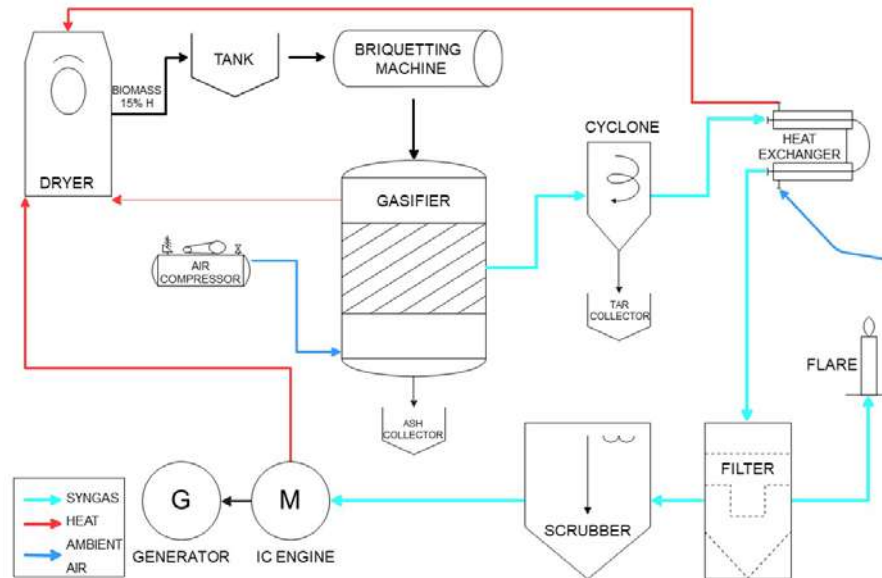


Figure 2. Flow diagram of the gasification-energy production process.

The produced syngas will primarily consist of CO, H₂, and CH₄, but also contaminants, such as: solid particles, tar, sulfur, nitrogen, and chlorine. The treatment of the raw syngas for the removal of contaminants, before entering the co-generation engine, will follow the “cold route” consisting of the following parts in sequence (Woolcock and Brown, 2013): (i) cyclone for the removal of solid particles and tar, (ii) straight tube heat exchanger for the cooling of syngas, (iii) granular biomass filter for the removal of solid particles and tar, (iv) caustic or limestone scrubber for the removal of sulfur and chlorine, and (v) water scrubber for the removal of sulfur, ammonia and tar. Following the gas treatment, a syngas analyzer and a flowmeter will be installed to record the composition and flowrate of the treated syngas. In addition, a syngas distribution will be installed between the cyclone and the heat exchanger to enable distribution of syngas to the following directions: the combustion flare for the combustion of excess/unsuitable syngas, the dryer for direct combustion, and the syngas cleaning-conditioning apparatus. All air inlets and gas outlets to and from the gasifier, including the fuel supply section, cyclone, and combustion flare are equipped with a series of non-return valves. Also, there are emergency deactivation measures, including the interruption of biosolids supply to the gasifier, the interruption of gasifier air supply, and the direction of syngas to the combustion flare, in case of malfunction. Primary sieved solids gasification-energy production system as well as the rest pilot plant components are expected to have an overall positive environmental footprint, as the process will enhance the performance of the WWTP, reducing simultaneously the production of municipal sludge.

Expected results

The thermodynamically required thermal energy to dry the biosolids is 20 kW, while the gasification-energy production system is expected to supply the dryer with 34 kW, which is significantly higher. However, the estimation of the real energy requirements of the dryer are expected to be at the same range as the thermal energy supply.

Acknowledgements: This study is supported by the Green Fund and the LIFE project (EC): “New concept for energy self-sustainable wastewater treatment process and biosolids management (LIFE B2E4sustainable-WWTP)”, LIFE16 ENV/GR/000298.

References

- Gikas, P., 2017. Towards energy positive wastewater treatment plants. *J. Environ. Manage.*, 203, 621–629.
- Puig-Arnavat, M., Bruno, J.C. and Coronas, A., 2010. Review and analysis of biomass gasification models. *Renew. Sustain. Energy Rev.*, 14, 2841–2851.
- Woolcock, P.J. and Brown, R.C., 2013. A review of cleaning technologies for biomass-derived syngas. *Biomass and Bioenergy*, 52, 54–84.



ENVIRONMENTAL MONITORING



Environmental monitoring of the Balos lagoon in Western Crete for sustainable tourism development

M. Lilli¹, G. Skiniti², N. Nikolaidis¹ and T. Tsoutsos²

¹Laboratory of Hydrogeochemical Engineering and Remediation of Soil, School of Chemical and Environmental Engineering, Technical University of Crete, Chania, Greece

²Renewable and Sustainable Energy Systems Laboratory, School of Chemical and Environmental Engineering, Technical University of Crete, Chania, Greece

Corresponding author email: gskiniti@tuc.gr

keywords: *environmental monitoring; environmental quality; physicochemical characterization; indicators; sustainable development; sustainable tourism; carrying capacity.*

Introduction

Balos lagoon is a famous, high tourism-attracted beach and even though it is meant to be protected under the Natura 2000 initiative, it is recently facing environmental degradation issues rooted mostly in these high intense touristic activities (Skiniti et al., 2022). Therefore, aiming to identify the human pressure on the area, the environmental monitoring of quality status as one parameter of addressing the region's carrying capacity was necessary, in order to achieve the creation of a strategy based on the region's sustainable development (Skiniti et al., 2022). The analysis was based on a sampling protocol in order to: a) determine the indicators that identify the environmental status of the lagoon, and b) propose ways of management that will contribute to its sustainable tourism development.

Materials and methods

A total of ten samplings were conducted (June, July, August, September, October 2021 and May, June, July, August, September 2022) in the Balos lagoon. In each sampling, two composite samples were taken from the seawater, two from the sediment and two from the sand. The sampling was designed to be taken place in two cross-sections (Figure 1) located in the lagoon area where it is more touristy (between umbrellas and bathers). A total of 60 samples were analyzed in relation to hydrocarbons (TPH), physicochemical parameters, heavy metals, microbiological parameters, microplastics etc. As a sampling unit for sand and sediment samples, a 40 × 40 cm frame was used, deployed in each transect. This frame was inserted 5 cm into the substrate of each sampling



Figure 1. Sampling design. Cross-sections (A and B) used for sand, sediment and seawater sampling.

unit. A sample of approximately 500g is taken from this frame for all analyses except the microplastics analysis. Specifically for microplastics, all sand/sediment of the frame is taken, placed in a metal container with water, from where by floating, the lightest pieces are obtained. Then, with the help of sieves (2mm and 53µm), these pieces are separated. For seawater sampling, 1L of water is taken for all analyses except microplastics analysis. Specifically for microplastics, 50L of seawater is passed through sieves (2mm and 53µm), and the corresponding samples are taken. The laboratory analyses were conducted in the "Hydrogeochemical Engineering and Remediation of Soils" laboratory of the Technical University of Crete.

Results and discussion

The results of the physicochemical characterization of the samples showed that the values are typical of coastline.



As for the results presented the density of plastic fragments and pellets calculated in different samplings, in sand samples per sampling were found on average 19 n/m² and 15 n/m² of microplastics of >2mm and >53µm size, respectively, in sediment samples were found on average 5 n/m² and 9 n/m² of microplastics of >2mm and >53µm size, respectively, and in seawater samples 0.004 and 0.014 n/L of microplastics of >2mm and >53µm size, respectively. All of the above results were compatible with the literature. Samplings in greek beaches of the Aegean island revealed microplastics (2–4 mm) densities in the top 3 cm of the subsurface ranging between 10 and 602 items/m² (Kaberi et al., 2013; Karkanorachaki et al., 2018).

The only indicator that it is important to take into consideration is the existence of large amounts of tar balls or residues (sticky remnants of oil) onto the sand, sediment and sea water (Figure 2). Marine tar residues originate from natural and anthropogenic oil releases into the ocean environment and are formed after liquid petroleum is transformed by weathering, sedimentation, and other processes (Warnock et al., 2015).



Figure 2. Tar balls on the sand of Balos beach.

Conclusions

The environmental monitoring of the quality of the Balos lagoon in Crete was conducted over a period of 2 tourist seasons, in order to determine the indicators that are important and need to be addressed with the ultimate goal of sustainable development of the area. The only indicator that it is important to take into consideration is the existence of large amounts of tar balls or residues onto the sand, sediment and seawater. Further studies are required to identify the origin of the tar residues in the Balos lagoon in order to find solutions to address it.

Acknowledgements: This publication was supported by the European Commission under the INTERREG V-A Greece-Cyprus 2014-2020 programme, within the framework of the project CROSS-COASTAL-NET initiative, Development of a Cross-Border Network for the Promotion of Sustainable Coastal Tourism ", Project MIS code: 5050612. The sole responsibility for the content of this paper lies with the authors. The European Commission is not responsible for any use that may be made of the information contained therein.

References

- Kaberi, H., Zeri, C., Mousdis, G., Papadopoulos, A., Streftaris, N., 2013. Microplastics along the shoreline of a Greek island (Kea isl., Aegean Sea): types and densities in relation to beach orientation, characteristics and proximity to sources. In: Proc. 4th Int. Conf. Environ. Manag. Eng. Plan. Econ. SECOTOX Conf. Mykonos island, Greece. June 24-28, 197–202.
- Karkanorachaki, K., Kiparissis, S., Kalogerakis, G.C., Yiantzi, E., Psillakis, E., Kalogerakis, N., 2018. Plastic pellets, meso- and microplastics on the coastline of Northern Crete: Distribution and organic pollution. Marine Pollution Bulletin 133, 578-589
- Skiniti, G., Skarakis, N., Tsoutsos, T., Nikolaidis, N., Tournaki, S., Kosmas, P., Antoniou, L., 2022, Sustainable planning for tourism in sensitive coastal regions. A case study of Balos beach in Western Crete, 3rd Symposium on Circular Economy and Sustainability, Chania, 27th -29th of June.
- Skiniti, G., Tsoutsos, T., 2022, Society in energy transition and justice, Social acceptance and contribution in Wind energy projects In Oncel S., A Sustainable Green Future - Perspectives on energy, economy, industry, cities and environment, Springer Nature.
- Warnock, A.M., Hagen, S.C. Passeri, D.L, 2015. Marine Tar Residues: a Review. Water Air Soil Pollut 226, 68. <https://doi.org/10.1007/s11270-015-2298-5>



“Do the pathogens and antibiotic resistance genes can “ESKAPEE” from the WWTP?”

J. Hubeny¹, M. Buta-Hubeny¹, W. Zieliński¹, D. Rolbiecki¹, S. Ciesielski², E. Korzeniewska¹ and M. Harnisz¹

¹Department of Water Protection Engineering and Environmental Microbiology, Faculty of Geoengineering, University of Warmia and Mazury in Olsztyn, Olsztyn, Poland

²Department of Environmental Biotechnology, Faculty of Geoengineering, University of Warmia and Mazury in Olsztyn, Olsztyn, Poland

Corresponding author email: jakub.hubeny@uwm.edu.pl

keywords: antibiotic resistance; *escapee*; resistance genes; wastewater; river water.

Introduction

Antibiotics play a fundamental role in the treatment of bacterial infections. However, the number of antibiotics able to stop a developing infection is becoming increasingly scarce due to the spread of the phenomenon of antibiotic resistance among bacteria. While this phenomenon is traditionally associated with public health/medical facilities, reports indicate that animal husbandry, aquaculture and urban facilities are also associated with the spread of antibiotic resistance. Wastewater treatment plants (WWTPs) are a particular threat through the discharge of antibiotic-resistant bacteria (ARBs), antibiotic resistance genes (ARGs) and residual concentrations of antibiotics into downstream aquatic and terrestrial environments. ESKAPEE bacteria (*Enterococcus faecium*, *Staphylococcus aureus*, *Klebsiella pneumoniae*, *Acinetobacter baumannii*, *Pseudomonas aeruginosa*, *Enterobacter* spp., and *Escherichia coli*) are increasingly being linked to antibiotic resistance phenomena that threaten public health. The World Health Organization (WHO) in 2017 published a list of antibiotic-resistant 'priority pathogens' that pose a serious threat to human health - all bacteria belonging to the ESKAPEE group are on this list. The possession of resistance genes by these bacteria results in the inability of essential antibiotics such as vancomycin, methicillin, broad-spectrum beta-lactam antibiotics, carbapenems, fluoroquinolones, aminoglycosides to work effectively.

Therefore, the aim of this study was a metagenomic quantitative analysis of the occurrence of ESKAPEE group bacteria and antibiotic resistance genes associated with this group in municipal wastewater and river water.

Materials and methods

Environmental samples were collected from WWTP located in the region of Warmia and Mazury in Northern-East part of Poland (Europe). Mentioned treatment plant uses mechanical and biological wastewater treatment systems. Additionally, WWTP receives wastewater from four hospitals, which accounts for 2% of the total treated wastewater. Samples of untreated wastewater (UWW), treated wastewater (TWW), as also river water collected upstream (URW) and downstream (DRW) from the wastewater discharge point were collected to the study in June (2018), November (2018), and March (2019). DNA of metagenome was extracted from wastewater and river water samples using the Power Water kit (MoBio Laboratories Inc., CA, United States) following the manufacturer's instructions. The obtained environmental DNA from the collected samples was used for Illumina TruSeq deep sequencing analysis. We focused on the results of species belonging to the ESKAPEE group, as well as the 400 antibiotic resistance genes (specifying resistance to beta-lactams, fluoroquinolones and aminoglycosides) associated with this group of microorganisms.

Results and discussion

Taxonomic analysis of the studied samples showed dominance at the species level of *Acinetobacter baumannii* bacteria along with *Escherichia coli*. Numberger et al. (2019) indicated a more abundant occurrence of bacteria from the family *Moraxellaceae* compared to the prevalence of bacteria from the family *Enterobacteriaceae* in influent and effluent samples from the WWTP. The literature determining the taxonomic structure of bacteria in wastewater showed the genus *Acinetobacter* as the most abundant. The



obtained results allow us to conclude that the analyzed resistance genes were present in the highest numbers in the untreated wastewater samples. The most abundant genes in these samples were *bla*GES (2.36 ppm), *bla*OXA-58 (1.93 ppm), *bla*TEM (0.72 ppm), *qnr*B (0.25 ppm), and *qnr*S (1.08 ppm). The literature describes the occurrence of these genes as very common in wastewater. Wang et al. (2020) found that the *bla*TEM, *bla*OXA, and *qnr*S are commonly detected in European countries as well as in USA or Canada in municipal wastewater. The application of a biological-mechanical wastewater treatment system using activated sludge in WWTPs resulted in a reduction of the abundance of species analyzed within the ESKAPEE group, on average by 81% (UWW vs. TWW). The literature described that the efficiency of a WWTP treatment system can depend significantly on the type of wastewater inflow and the fluctuations in the performance of the plant itself. The results of own research indicate that the WWTP enabled more than a 90% reduction of the analyzed resistance genes. The obtained result of reduction of ARGs in WWTP treated wastewater is supported by literature. A very important result of the study is the demonstration of the river water contamination collected after the discharge of treated wastewater with *A. baumannii* and *E. coli* bacteria and genes determining resistance to beta-lactam antibiotics (*bla*VEB-1, *bla*IMP-1, *bla*GES, *bla*OXA-58, *bla*CTX-M, and *bla*TEM) and fluoroquinolones (*qnr*S). The literature presents WWTPs as a potential source of both *Escherichia coli* (Osińska et al., 2017) and *Acinetobacter baumannii* (Maravić et al., 2016) in a natural environment such as river water. Moreover, Sabri et al. (2020) in their work presented a similar phenomenon of river water contamination with resistance genes after the discharge of treated wastewater. It should be noted that the inflow of analyzed WWTP in the present work contains 2% of hospital wastewater, coming from 4 urban hospitals. It is determined that hospitals play a serious role in the spread of ARBs and ARGs (Paulus et al., 2019).

Conclusions

Performed studies confirmed that WWTPs poses as an important role in dissemination of important ARGs and ESKAPEE bacteria to the natural environment. In spite of obtaining a very high percentage of reduction of the analyzed bacteria or ARGs, the results indicate the contamination of river water sampled downstream of the treated wastewater discharge with bacteria of the species *Acinetobacter baumannii* and *Escherichia coli*, which are important pathogens characterized by a rich resistome. Presence of ESKAPEE bacteria with such features in the aquatic environment raises the issue of public health risk.

Acknowledgements: This study was supported by grant No. 2017/M/NZ9/00071 from the Polish National Science Centre. Jakub Hubeny has received a scholarship from the Interdisciplinary Doctoral Program in Bioeconomy (POWR.03.02.00-00-1034/16 00) funded by the European Social Fund.

References

- Maravić, A., Skočibušić, M., Fredotović, Ž., Šamanić, I., Cvjetan, S., Knezović, M. and Puizina, J., 2016. Urban riverine environment is a source of multidrug-resistant and ESBL-producing clinically important *Acinetobacter* spp. *Environ. Sci. Pollut. Res.* 23, 3525–3535.
- Numberger, D., Ganzert, L., Zoccarato, L., Mühlendorfer, K., Sauer, S., Grossart, H.-P. and Greenwood, A.D., 2019. Characterization of bacterial communities in wastewater with enhanced taxonomic resolution by full-length 16S rRNA sequencing. *Sci. Rep.* 9, 9673.
- Osińska, A., Korzeniewska, E., Harnisz, M. and Niestępski, S., 2017. The prevalence and characterization of antibiotic-resistant and virulent *Escherichia coli* strains in the municipal wastewater system and their environmental fate. *Sci. Total Environ.* 577, 367–375.
- Paulus, G.K., Hornstra, L.M., Alygizakis, N., Slobodnik, J., Thomaidis, N. and Medema, G., 2019. The impact of on-site hospital wastewater treatment on the downstream communal wastewater system in terms of antibiotics and antibiotic resistance genes. *Int. J. Hyg. Environ. Health* 222, 635–644.
- Sabri, N.A., Schmitt, H., Van Der Zaan, B., Gerritsen, H.W., Zuidema, T., Rijnaarts, H.H.M. and Langenhoff, A.A.M., 2020. Prevalence of antibiotics and antibiotic resistance genes in a wastewater effluent-receiving river in the Netherlands. *J. Environ. Chem. Eng.* 8, 102245.
- Wang, J., Chu, L., Wojnárovits, L. and Takács, E., 2020. Occurrence and fate of antibiotics, antibiotic resistant genes (ARGs) and antibiotic resistant bacteria (ARB) in municipal wastewater treatment plant: An overview. *Sci. Total Environ.* 744, 140997.



Management implications in a peri-urban river under multiple stressors

C. Ntislidou¹, V. Papaevangelou², D. Latinopoulos², S. Ntougias³, P. Melidis³, C. Akratos² and I. Kagalou²

¹Department of Zoology/School of Biology, Aristotle University of Thessaloniki, Thessaloniki, Greece

²Department of Civil Engineering/School of Engineering, Democritus University of Thrace, Xanthi, Greece

³Department of Environmental Engineering /School of Engineering, Democritus University of Thrace, Xanthi, Greece

Corresponding author email: ikagkalo@civil.duth.gr

keywords: *Laspias river; pollutants; pressures; benthic macroinvertebrates; ecological quality.*

Introduction

Most aquatic ecosystems are exposed simultaneously to several stressors with, most usually, synergistic effect. Some stressors, such as water scarcity, pollution and contamination, can limit biodiversity and economic activities in entire regions. Water scarcity especially in regions such as the Mediterranean basin can amplify the effects of water pollution as warmer temperatures and reduced river flows will likely increase the physiological burden of pollution on the aquatic biota. The effects of these stressors are very relevant for the chemical and ecological status of water bodies as well as for ecosystem services' sustainability. The European Union water policy integrates in a balanced way the dimensions of sustainability focusing on the water management as a framework against pollution, extreme events and climate change. Sustainable water management, including of wastewater receptors, can further contribute to mitigation measures.

Herein, a Mediterranean case study located in Greece (Laspias river basin), frequently exhibits pollution events. The objective of our paper is to pinpoint the most polluted areas and to assess the effects of synergistic stressors to biota. Specifically, we evaluate its physicochemical characteristics engaged with its ecological quality through monitoring benthic macroinvertebrates.

Materials and methods

Laspias River is located in Xanthi Prefecture, Thrace, Greece. The surface area of the basin is 212 km², while the river's length is approximately 30 km consisting of Heavily Modified Water Bodies (HMWBs). It discharges in a protected area of environmental importance (Ramsar Convention, Natura 2000 site, National Park). Geomorphologically, it is a mountainous-agricultural area. Both point and diffuse pollution sources are found in the watershed. The major point sources are the wastewater treatment plant (WWTP) of the city, the industrial area of Xanthi and several livestock units, while agricultural runoff is the main non-point source.

Samplings were conducted at dry and wet period (spring and autumn 2021) from seven sites within the framework of the Eye4Water Project (www.eye4water.com). Dissolved Oxygen (DO, mg/l), Water Temperature (T, °C), Electrical Conductivity (EC, µS/cm), Salinity (SAL, ppt) and pH were measured in situ. Concentrations of Biochemical and Chemical Oxygen Demand (BOD₅ & COD, mg/l), Total Solids (dissolved and suspended, TDS & TSS, mg/l), Total Kjeldahl Nitrogen (TKN, mg/l), Total Phosphorus (TP, mg/l) and chlorophyll-a (Chl-a, µg/l) in water samples were analyzed according to standard methods (Baird et al. 2017). Benthic macroinvertebrates were sampled using a D-shaped net according to the semi quantitative 3-min kick/sweep method (Armitage and Hogger 1994) plus 1-min in the bank vegetation, when existed (Wright 2000). Specimens were identified mainly to family level and abundance of each taxon was noted. Finally, the Hellenic Evaluation System 2 (HESY2) (Lazaridou et al. 2018) was used for estimating the ecological quality in sites. A Principal Component Analysis (PCA) (Primer 6: Clarke and Gorley 2006) was applied to explore environmental gradients and identify the explanatory variables.

Results and discussion

The monitoring routine was able to track the variety of pressures posed on the system and revealed the burdened character of the river. In both periods, during 2021, the ecological assessment resulted in poor and bad ecological quality (Figure 1a). Specifically, the physicochemical properties and common pollutant analysis demonstrated values exceeding the legislation limits in many cases (91/271/EEC, 2006/44/EC, GG 356/B/26-2-2009). Indicators describing the pollutant loads as the oxygen related ones (DO, BOD₅, COD), nutrient



related ones (TKN, TP) and solids (TDS, TSS) revealed a hostile water system for aquatic life in about half the sampling sites, especially those in the downstream part. To this compliment, the benthic macroinvertebrate community, characterized by the dominance of tolerant to organic pollution taxa (i.e., Chironomidae, Oligochaeta), the low biodiversity and the absence of sensitive taxa highlighted the synergistic effect on both chemical and biological quality. Searching for a spatial pattern (Figure 1b), it seems like the river receives an excess of loads from the landfill (L6) and gets worse after the inclusion of the WWTP effluents (L5). The situation is aggravated following the industrial area and animal farms (L4A and 4B). Then, the ecological quality seems to be ameliorated in site L3.5 after the inclusion of discharges from an adjacent basin and then one weir (L2) retains water for flood control and acts as sink for pollutants, overflowing and oxygenating the river water course up to the estuary (L1). In the PCA analysis, the samplings sites were arranged following axis I, with BOD₅, TKN and TS being the most significant factors for the classification (72.2%) and axis II with TDS, TP and EC (10.9%), respectively (Figure 1b). There is no or little seasonal pattern with augmented flows assisting the pollutants' dilution effect.

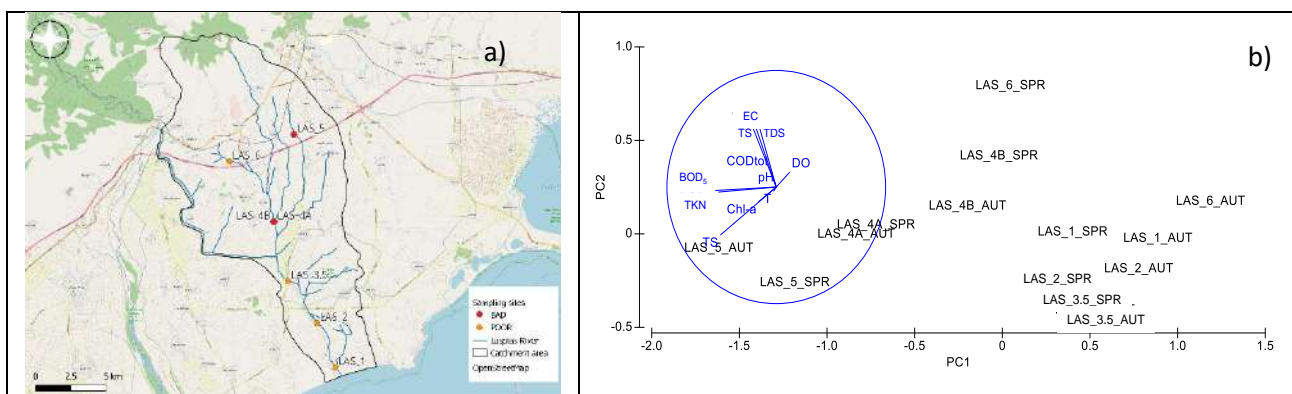


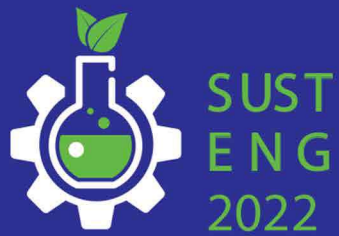
Figure 1. a) Map of Laspias basin with ecological quality. b) PCA plot with physiochemical and nutrients parameters from Laspias River during wet and dry period (sp: spring, au: autumn).

The overall picture of Laspias is characteristic of a mismanaged river receiving an excess of pollution loads, and in several cases partially or fully untreated. It is evident that the multiplicity effect of pollutants surpasses the river self-purification ability and the sustainable water use should be more promoted, including advanced nutrients' treatment and remediation measures coupled with stricter enforcement framework and awareness raising. These findings should be regarded as an alert for the sustainability of the entire area's production system (agricultural and industrial) and the national park's prosperity.

Acknowledgements: Produced for Eye4Water project, MIS 5047246, Co-financed by Greece and the European Union - European Regional-Development Fund.

References

- Armitage, P.D. and Hogger, J., 1994. *Invertebrates Ecology and Methods of Survey*, 1st ed.; RSPB Sandy: Bedfordshire, UK.
- Baird, R.B., Eaton, A.D. and Rice, E.W., 2017. *Standard Methods for the Examination of Water and Wastewater*, 23th ed.; American Public Health Association, American Water Works Association & Water Environment Federation: Washington, DC, USA.
- Directive 2006/44/EC of the European Parliament and the Council of 6 September 2006 on the quality of fresh waters needing protection or improvement in order to support fish life.
- Directive 91/271/EEC of 21 May 1991 concerning urban waste-water treatment.
- Government Gazette 356 / B / 26-2-2009 Bathing water quality and management measures, in accordance with the provisions of Directive 2006/7/EC on the management of bathing water quality and repealing Directive 76/160 / EEC of the European Parliament and of the Council of 15 February 2006.
- Lazaridou, M., Ntislidou, C., Karaouzas, I. and Skoulikidis, N., 2018. Harmonization of a new assessment method for estimating the ecological quality status of Greek running waters. *Ecol. Indic.*, 84, 683–694.
- Wright, J.F., 2000. *An introduction to RIVPACS*, 1st ed.; Freshwater Biological Association: Ambleside, UK.



ADSORPTION PROCESSES (PART II)



Development and evaluation of magnetic tea waste based adsorbent materials for removal of cadmium from wastewater

M. Ervine¹, O. Jaiyeola¹ and C. Mangwandi¹

¹School of Chemistry and Chemical Engineering, Queen's University Belfast, Belfast BT9 5AG,
Northern Ireland, UK

Corresponding author email: c.mangwandi@qub.ac.uk

keywords: *cadmium; adsorption; magnetic teawaste; experimental design; iron chloride.*

In this research, a new low-cost bio sorbent material for application in heavy metal removal focusing on cadmium removal from wastewater. Previous research into tea waste, showed that modification of the surface via bleach and iron (II) chloride has a positive impact on the adsorbent capacity. A full adsorption study was completed by using the optimum MBTW (Magnetic Bleached Tea Waste) from the initial experiment. This experiment differs due to cadmium removal being the focus of the experiment. The Freundlich isotherm was the optimum fit for the experimental data for the three temperatures studied. For the kinetics of the experiment, the most accurate fit was the pseudo second-order kinetics model by Lagergren. Fourier transform infrared (FT-IR) analysis of the MBTW was before and after adsorption which shows the functional groups which changed due to adsorption of cadmium. All the results reported strongly applied the potential of MBTW as an economic bio adsorbent for removal of cadmium from contaminated waters.



Converting unused concentrated metals of plating waste into novel layered double hydroxide (LDH) adsorbent for pyrophosphate removal

T.A. Kurniawan¹

¹College of Environment and Ecology, Xiamen University Fujian, PR China

Corresponding author email: toni@xmu.edu.cn

keywords: electroplating; circular economy; low-cost adsorbents; resource recovery; zero-waste.

This work incorporated technological values into Zn₂Cr-layered double hydroxide (LDH), synthesized from unused resources, for removal of pyrophosphate (PP) in electroplating wastewater. To adopt a resource recovery for the remediation of the aquatic environment, the Zn₂Cr-LDH was fabricated by co-precipitation from concentrated metals of plating waste that remained as industrial by-products from metal finishing processes. To examine its applicability for water treatment, batch experiments were conducted at optimum M^{+2}/M^{3+} , pH, reaction time, and temperature. To understand the adsorption mechanisms of the PP by the adsorbent, the Zn₂Cr-LDH was characterized using Brunauer-Emmett-Teller (BET), X-ray diffraction (XRD), Fourier-transform infrared spectroscopy (FT-IR), scanning electron microscopy/energy dispersive X-ray spectroscopy (SEM/EDS), transmission electron microscopy (TEM), and X-ray photoelectron spectroscopy (XPS) analyses before and after adsorption treatment. An almost complete PP removal was attained by the Zn₂Cr-LDH at optimized conditions: 50 mg/L of PP, 1 g/L of adsorbent, pH 6, and 6 h of reaction. Ion exchange controlled the PP removal by the adsorbent at acidic conditions. The PP removal well fitted a pseudo-second-order kinetics and/or the Langmuir isotherm model with 79 mg/g of PP adsorption capacity. The spent Zn₂Cr-LDH was regenerated with NaOH with 86% of efficiency for the first cycle. The treated effluents could comply with the discharge limit of <1 mg/L. Overall, the use of the Zn₂Cr-LDH as a low-cost adsorbent for wastewater treatment has contributed to national policy that promotes a zero-waste approach for a circular economy (CE) through a resource recovery paradigm.

Acknowledgements: This is supported by TWAS Fellowship for Visiting Expert (FR3240322700).



Removal of Hexavalent chromium from aqueous solution using Potato Peel waste-based adsorbent

O. Jaiyeola and C. Mangwandi¹

¹School of Chemistry and Chemical Engineering, Queen's University Belfast, Belfast, United Kingdom

Corresponding author email: c.mangwandi@qub.ac.uk

keywords: adsorption; biochars; pyrolysis; hexavalent chromium; potato peel waste.

Introduction

Wastewater from industrial operations is often polluted with heavy metals that can cause damage to aquatic life and cause further health problems to human beings through accumulation in the food chain. Chromium is one of the heavy metals of concern and its pollution sources include electroplating, tanning, paint and paint industries. In aqueous solutions, chromium exists as either hexavalent chromium (Cr(VI)) or tri-valent chromium (Cr(III)); Cr(VI) is about 100 times more toxic in comparison to Cr(III). Prolonged exposure to Cr(VI) can lead to several health issues such as dyspnea, abdominal pains, vomiting, gastrointestinal diseases and even genetic mutations. Therefore, removal of hexavalent from wastewater is crucial before wastewater is discharged into natural water bodies.

There are several technologies that can be used to remove heavy metals from wastewater namely precipitation, ionic exchange, electrochemical reduction, membrane filtration and adsorption. Among these adsorptions remains one of the most economical and widely used due to its simplicity in design and low operational costs.

Different biomass based materials have been used for the adsorption of Cr(VI), coffee grounds, date pit, potato peels, fruit peelings and leaves (Mutongo, Kuipa, and Kuipa 2014; Albadarin et al. 2013; Cherdchoo, Nithettham, and Charoenpanich 2019; Chen et al. 2022). This study investigated the use of potato peels which are widely available in many countries as a biosorbent for a low cost Cr(VI) removal technology.

Materials and methods

Potato peel waste collected from a local fish & chips shops was washed thoroughly in tap water and then dried at room temperature. The dried potato peels were then milled into fine powder (to be referred as potato peel powder (PPP) here forth, using a coffee grinder (Shardor CG63B, Shardor USA). PPP was stored in sealed airtight bags until further use. In the chemical and thermal activation step the PPP was mixed with potassium hydroxide, the chemical activation agent in different mass ratios of 1: 0.75, 1:1 and 1: 1. About 20 grams of the PPP/KOH mixtures were carefully weighed into 3 separate ceramic crucibles. A similar mass of PPP (without KOH) was carefully weighed into the 4th crucible. The Carbolite Muffle furnace was then preheated to 500 °C. Once the desired temperature was achieved the crucibles were placed in the furnace. The temperature was allowed to stabilize back to the desired temperature before a timer was for monitoring the hold temperature was initiated. At the expiry of the hold temperature the crucibles were taken out to cool to room temperature. The resultant biochars were then washed in distilled water to a neutral pH and then dried in an oven at 105C before storing them in seal vials for future analysis and use. The following nomenclature was use for naming the samples PPP_KOH_xx, where XX represents the percentage by mass of potassium hydroxide used in the preparation of sample, for example sample with a mixing ratio of 1:1 would be PP_KOH_50 and that without KOH would be named as PP_KOH_00.

In the evaluation of the adsorptive properties of the adsorbents, the samples were contacted with synthetic aqueous solutions of hexavalent chromium of know concentration for a constant dosage and contact time. The concentration of Cr(VI) remaining in solution at the end of contact time was determined with UV-VIS spectrophotometry using method previously described by (Albadarin et al. 2013).

The percentage removal of the Cr(VI) was calculated using the equation:

$$Y = \frac{C_0 - C_e}{C_0} \times 100 \quad (1)$$



where C_o and C_e are the initial and final concentrations of the solution respectively, m is mass of the adsorbent sample used and V is the volume of the solution.

The amount of the adsorbate loaded onto the sample was calculated from the equation:

$$q_e = \frac{C_o - C_e}{m} V \quad (2)$$

Results and discussion

The results from a preliminary study to compare the effect of chemical and thermal treatment of the potato peel powder are shown in Figure 1. On comparing the raw potato peel (PPP) with thermally treated adsorbent without addition of KOH (sample PPP_KOH-00) after a contact time of 300 minutes, results show that the pristine material performed better than adsorption efficiency decrease from around 40 to 10 %. Using potassium hydroxide as the chemical activation agent significantly improved the adsorption capacity, for example removal efficiency increased from 10% (PPP_KOH-00) to ~ 45% for the PPP_KOH_43 sample. Increasing the composition of KOH added to the formulation increase the adsorption efficiency.

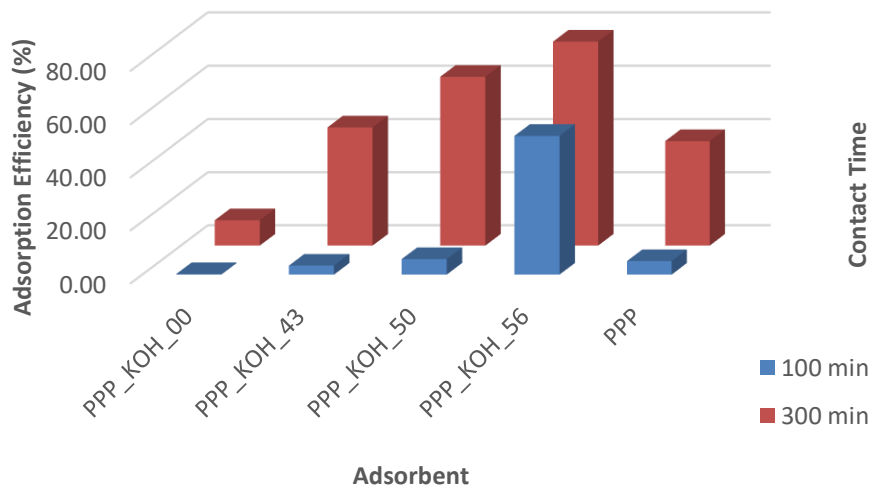


Figure 1. Comparison of the adsorption efficiencies of the different adsorbent samples.

Conclusions

Potato peel powder was successfully converted to a biochar which can be used as an adsorbent material. It can be concluded that chemical and thermal modification of potato peel powder improves the adsorption capacity of the powder peel powder.

References

- Albadarin, Ahmad B., Chirangano Mangwandi, Gavin M. Walker, Stephen J. Allen, Mohammad N. M. Ahmad, and Majeda Khraisheh. 2013. 'Influence of solution chemistry on Cr(VI) reduction and complexation onto date-pits/tea-waste biomaterials', *Journal of Environmental Management*, 114: 190-201.
- Chen, Haili, Zhouyang Huang, Jiahong Wu, and Chirangano Mangwandi. 2022. "Enhancing the Chromium Removal Capacity of Banana Peel Wastes by Acid Treatment." In, 317-20. Cham: Springer International Publishing.
- Cherdchoo, Wachiraphorn, Srisuda Nithettham, and Jittima Charoenpanich. 2019. 'Removal of Cr(VI) from synthetic wastewater by adsorption onto coffee ground and mixed waste tea', *Chemosphere*, 221: 758-67.
- Mutongo, Farai, Olga Kuipa, and Pardon K. Kuipa. 2014. 'Removal of Cr(VI) from Aqueous Solutions Using Powder of Potato Peelings as a Low Cost Sorbent', *Bioinorganic Chemistry and Applications*, 2014: 973153.



Highly efficient removal of cadmium from waste water using eco-friendly and cost-effective aluminophosphate as adsorbents

O. Jaiyeola¹, A.Hamza^{1,2} and C. Mangwandi¹

¹School of Chemistry and Chemical Engineering, Queen's University Belfast, Northern Ireland, UK

²Department of Chemistry, University of Lancaster, Bailrigg, Lancaster LA 4YB

Corresponding author email: c.mangwandi@qub.ac.uk

keywords: cadmium; aluminophosphate; sodium silicate; adsorption.

Introduction

In recent years, with the fast development of industrialization and agriculture, the heavy metal cadmium pollution has received extensive attention. Cadmium has the features of high migration rate, persistence and easy accumulation, which can be migrated to the environment through run-off, irrigation, sediment deposition, etc., and can also be transferred to the human body by the food chain (Luo et al.,2020). Several technologies have been used to remove heavy metal ions from effluents, including chemical co-precipitation, ion exchange, membrane filtration, coagulation, adsorption and others. Amongst them, the adsorption technology is known as a high-efficiency method due to its effectiveness, simplicity, low cost, and regenerable adsorption capacity.

The study focuses on removing heavy metals using aluminum phosphate. The heavy metal being targeted is cadmium. This project assesses the potential of silicate bonded aluminophosphate composite material as an adsorbents for removal of cadmium from synthetic aqueous solutions. The removal capacity alongside the effect of the presence of silicate and other conditions such as contact time and temperature were evaluated.

Materials and methods

20g of Aluminium nitrate and 3.611mls of phosphoric acid in a 1:1 mol ratio were weighed and added to 400 ml of distilled water. Ammonia was added dropwise to adjust the solution pH to between 7 and 7.5. The resultant solution was left on the stirrer for 2 hours, excess moisture was filtered out and the adsorbent was dried in the oven for 6 hours at 60°C.

A known mass of the adsorbent material was calcined at 300°C for 5 hours. The following nomenclature was use for naming the samples SiAlPO(xx) where (xx) represents the percentage by mass of silicon used in the preparation of sample. For example sample with a mixing ratio of 0:1 with no silicate present would be AlPO₄ and that with a ratio of (0.975:0.025) with 2.5% silicate would be named as SiAlPO(2.5).

The previous steps were repeated with the inclusion sodium silicate in different ratios to introduce the presence of silicate in the adsorbent material. The ratios used were (0.05:0.95), (0.075:0.925) and (0.10:0.90). For SiAlPO(2.5)(ratio 0.975:0.025), 0.16g sodium silicate, 19.31g of aluminum nitrate and 3.611ml of phosphoric acid were added to 400ml of distilled water.

To evaluate the performance of the different adsorbent samples, 50 mg of the adsorbent material was added to 20 ml, 100 ppm cadmium solutions and agitated on the shaker for a period of 6 hours. The concentration of Cd remaining in solution at the end of adsorption study was determined by withdrawing 1ml from each vial sample was taken and added to 9ml of water to make up a dilution factor of 10. The resultant samples were analysed by ICP (Inductively Coupled Plasma optical emission spectrometry) to give the final concentration of cadmium ions. The cadmium concentration in solid phases was calculated from the equation:

$$Q_e = \frac{(C_i - C_e) V}{m}$$

Where C_i and C_e are the liquid-phase concentrations of cadmium initially and at equilibrium respectfully and both measured in mg/L. Volume of solution (L) and m is the mass of dry adsorbent used for the experiment in grams.



Results and discussion

From Figure 1(a) the comparison of the effect of the presence of the silicate and the non-presence of the silicate (AlPO) was compared to select the best adsorbent ratio. It was seen that adsorbent material SiAlPO(7.5) had the highest percentage removal of cadmium ions. The trends observed here are similar to other results reported in literature (Chen et al. 2019). The improvement in the removal capacity could be due changes in the surface structure of adsorbent material when silicate is introduced. The variations of the Cd²⁺ removal efficiency with contact time for the SiAlPO(7.5) adsorbent material were shown in figure 1 (b). The rate of removal of cadmium removal is higher at the beginning, this is largely due to the larger surface area of the adsorbent being available at the beginning for the adsorption of cadmium.

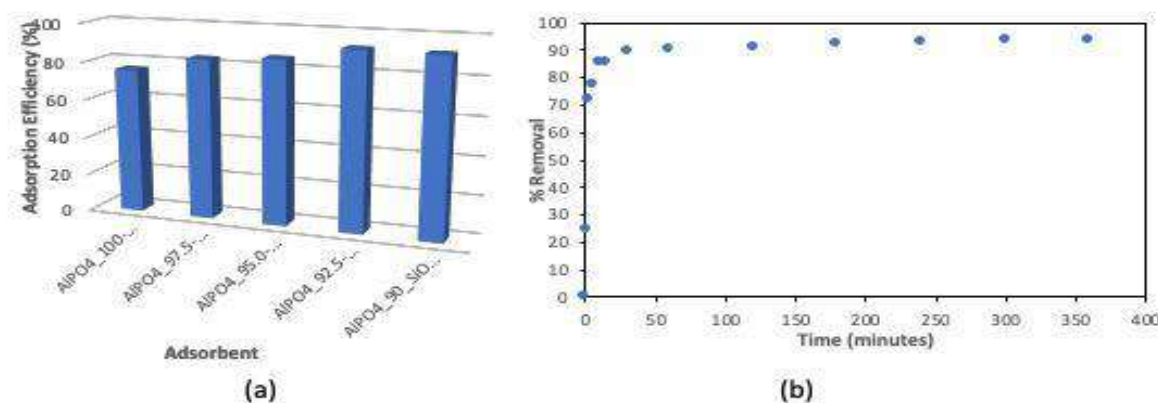


Figure 1. comparison of the different adsorbent materials. (a) kinetics of the cadmium loading on SiAlPO(7.5) adsorbent sample(b). All experiments were done using cadmium solutions with initial concentration of 100ppm and adsorbent dosage of 2.5g/L.

Conclusions

In this study, aluminophosphate adsorbent showed a high capacity in the removal of Cd²⁺ from aqueous solutions, and the detailed study showed that the adsorption process followed the pseudo second order kinetic model and Langmuir isotherm. The adsorbent which performed best of all ratios SiAlPO(7.5) had the maximum removal capacity of 52.63 mg/g. Therefore, the mechanisms of Cd²⁺ removal by aluminophosphate could possibly due to a combination of chemical precipitation, ion exchange and surface complexation with oxygen functional groups. The new adsorbent developed in this work show great potential for heavy metal removal. Future studies will focus on evaluating its performance in a continuous system.

References

- Choi, C. H. *et al.* Tuning selectivity of electrochemical reactions by atomically dispersed platinum catalyst. *Nat. Commun.* 7:10922 doi: 10.1038/ncomms10922 (2016).
- J. Luo, W.X. He, S.H. Qi, J. Wu, X.S. Gu. A novel phytoremediation method assisted by magnetized water to decontaminate soil Cd based on harvesting senescent and dead leaves of *Festuca arundinacea*. *J. Hazard Mater.*, 383 (2020), p. 121115



Olive Mill Wastewater color treatment by fibrous clay mineral

G. Panagopoulos¹, E. Gianni², V. Bekiari³ and K. Katsanou⁴

¹Department of Mechanical Engineering, University of the Peloponnese, 263 34, Patras, Greece²Centre for Research and Technology, 15125 Hellas (CERTH), Greece

³Department of Crop Science, University of Patras, 30200 Messolonghi, Greece

⁴Department of Water Resources and Ecosystems, IHE Delft Institute for Water Education, 8 Westvest 7, 2611 AX Delft

Corresponding author email: gpanagopoulos@go.uop.gr

keywords: *discoloration; sorption; fibrous clay mineral; batch experiments; olive mill wastewater.*

Introduction

Olive oil production is very common in Mediterranean area, with two main produced wastes; the wet solid “olive husk” and the aqueous “olive mill wastewater (OMW)” (Tsagaraki et al. 2007). OMW is more complex and harmful in comparison with other industrial wastes. The discoloration of such pollutant is crucial for its safe disposal. Until now, different physicochemical and biological techniques (Kiril Mert et al. 2010, Fezzani and Ben Cheikh 2010) aiming to the polyphenols removal with subsequent color reduction had been tested. Sorption is characterized as one of the most promising methods for the removal of organic compounds, that maintains the low-cost of the procedure. A fibrous clay mineral, palygorskite, is proposed in the present study as a discoloration media for the treatment of OMW. The already known sorption properties of palygorskite, the abundant and non-toxic nature as well as the low-cost of the material make it a promising sorbent for the discoloration of industrial wastes aiming in their safe disposal to the environment.

Materials and methods

A raw palygorskite sample from Grevena/Western Macedonia, Greece produced by Geohellas S.A., was used for the performance of batch kinetic experiments investigating the discoloration of OMW. A range of diluted samples of OMW were prepared for the examination of the effect of initial concentration, and different sorbent dosages of palygorskite were tested for its discoloration. The optimal palygorskite dosage of 40 g/L was further used based on maintaining low cost due to the small amount of palygorskite in combination with its effective action in such a quantity. The effect of pH, temperature, and contact time were also examined. The experiments were carried out in triplicate, and the results are reported as color removal efficiency (Nandi and Patel, 2017). True color was measured with a DR3900 spectrophotometer (Hach®) with the Platinum-Cobalt Standard Method.

Results and discussion

Palygorskite was an efficient material for the discoloration of OMW, with higher than 58.9% color removal percentages for all the tested concentrations (Fig. 1a). The higher effectiveness of palygorskite was for initial concentration of 2010 mg/L Pt-Co where the removal rate reached 78.8%. In concentrations higher than 2010 mg/L Pt-Co, the free space in the structure of palygorskite is fulfilled and hence palygorskite has the tendency to desorb the molecules. The minimum tested dosage of palygorskite (10 g/L) acts effectively in the discoloration of OMW with 44.3% removal (Fig. 1b). By doubling the dose (20 g/L) the efficiency reached the 71.4%. After further increasing of the palygorskite, from 40 to 320 g/L, the color removal efficiency ranged from 78.8% to 80.5%, respectively. At those dosage ranges, the effectiveness of palygorskite is almost stable and the removal rates differ at the error limits. Taking into consideration both the maintenance of low cost and the minimal waste of material, the usage of 40 g/L is proposed as the optimum dosage for the discoloration of OMW.

The most effective discoloration was observed in extremely acidic conditions, pH=2, where the value reached 78.8%. The more acidic the environment, the more effective the color removal (Fig. 2a). It is observed that discoloration efficiency is inversely proportional to the temperature (Fig. 2b). At 16°C the discoloration value reached the 68.8%, while at 63°C is only 39.6%. As the differences in the discoloration



efficiency between 16°C (68.8%) and 25°C (63.8%) are on the verge of error, room temperature is preferred to maintain low cost as the changes of the temperature require high levels of energy. The discoloration process of OMW by palygorskite was a rapid procedure with percentages higher than 75% for the first 2 min. The color removal continuously increased for the first 60 min (80.2% discoloration efficiency), while after that, the rhythm of the reaction was reduced due to the fulfilment of the active sites of the mineral.

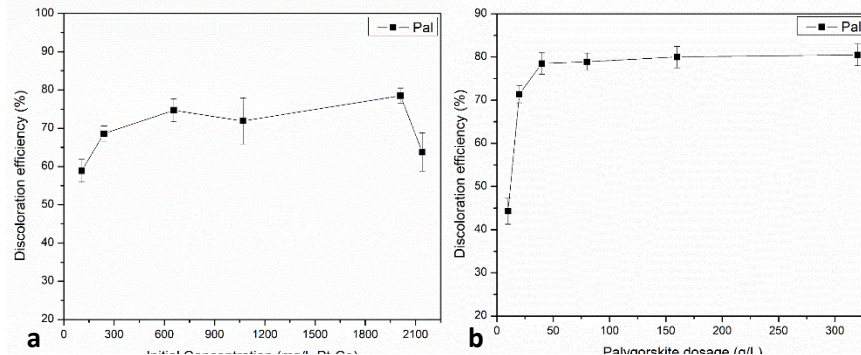


Figure 1. a. Effect of initial concentration for discoloration of OMW by 40 g/L palygorskite and b. Effect of palygorskite dosage for discoloration of 2,010 mg/L Pt-Co OMW at pH=2, room temperature and equilibrium contact time 30 min.

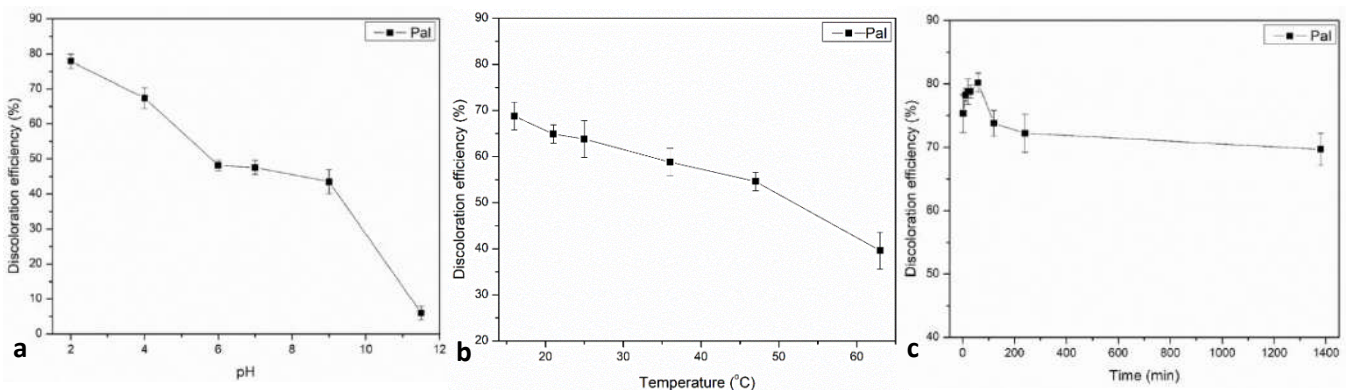


Figure 2. a. Effect of pH for discoloration of 2010 mg/L Pt-Co OMW by 40 g/L palygorskite at room temperature, b. Effect of temperature for the discoloration of 1380 mg/L Pt-Co OMW by 40 g/L palygorskite at pH=2 and equilibrium contact time 30 min, and c. Effect of contact time for discoloration of 2,010 mg/L Pt-Co OMW by 40 g/L palygorskite at pH=2 and room temperature.

Conclusions

Palygorskite is proposed for the discoloration procedure of OMW using the cost-effective adsorption process. The color removal reached 78.8% under 30 min of contact time, extremely acidic conditions of pH=2, that can be easily achieved as the nature of OMW is also acidic, and room temperature which requires no energy. The optimal palygorskite dosage was 40 g/L, which is quite affordable based on palygorskite's abundance. The mineral could be used as an ideal sorbent for the pre-treatment or the last step of OMWs treatment.

References

- Fezzani, B. and Ben Cheikh, R., 2010. Two-phase anaerobic codigestion of olive mill wastes in semi-continuous digesters at mesophilic temperature. *Bioresour. Technol.*, 101,1628–1634.
- Kiril Mert, B., Yonar, T., Yalili Kilie, M. and Kestioglu, K., 2010. Pretreatment studies on olive oil mill effluent using physicochemical, Fenton and Fenton-like oxidations processes. *J. Hazard. Mater.*, 174, 122–128.
- Nandi, B.K. and Patel, S. (2017). Effects of operational parameters on the removal of brilliant green dye from aqueous solutions by electrocoagulation. *Arab. J. Chem.*, 10(2), S2961-S2968.
- Tsagaraki, E., Lazarides, H.N. and Petrotos, K.B., 2007. Olive Mill Wastewater Treatment. In: Oreopoulou V, Russ W (eds) *Utilization of By-Products and Treatment of Waste in the Food Industry*. Springer, pp 133-157.



Comparison of rare earth elements adsorption by sodium alginate-based adsorbents

D. Fila¹, Z. Hubicki¹ and D. Kołodźńska¹

¹Department of Inorganic Chemistry, Institute of Chemical Sciences, Faculty of Chemistry, University of Maria Curie-Skłodowska, Lublin, Poland

Corresponding author email: dominika.fila@mail.umcs.pl

keywords: adsorbents; alginate; efficiency; rare earths.

Introduction

Rare earth elements (REEs) are a valuable material resource for a wide range of high-tech applications. They are distinguished by their optical, electronic, and metallurgical properties, which enable them to be used in the production of a wide range of sophisticated devices such as computer memories, batteries, smartphones as well as digital versatile discs [1]. Because of their importance, a variety of technologies for recovery and separation have been developed, including ion exchange, solvent extraction, adsorption, precipitation, and liquid membranes [2]. Unfortunately, the recovery and separation of REEs from waste products is a difficult process due to their similar physicochemical characteristics. As a result, several studies have focused on the development of sustainable and cost-effective methods for their recovery from discarded electronic devices and various waste streams. Adsorption has emerged as an effective strategy for improving separation efficiency for REEs among these separation methods. The adsorbents may efficiently remove REEs from aqueous solutions by using sodium alginate, chitosan, zeolite, silica, and cellulose as raw materials.

Sodium alginate is a well-known natural anionic polysaccharide extracting from brown algae. High biocompatibility, biodegradability, and renewable are just a few of the sodium alginate advantages. Furthermore, the alginate structure's abundance of carboxyl and hydroxyl groups made it useful for the adsorption of heavy metals, dyes, pharmaceutical contaminants, radionuclides, and rare earth elements from aqueous media. Sodium alginate, on the other hand, has a low mechanical strength, stability, and heat resistance. As a result, physical or chemical modification is frequently used to improve its suitability for metal adsorption. Surface grafting, cross-linking, and composite with other materials are the most common modification methods used in sodium alginate-based adsorbents. Activated carbon, graphene oxide, inorganic or carbonaceous materials, and different other polymers have been encapsulated inside alginate-based hydrogels in order to improve their mechanical and thermal stability and efficiency for environmental applications [3].

The overall purpose of this study was to characterize the lanthanum(III) adsorption performance of alginate-based adsorbents crosslinked by calcium chloride. Specific objectives were to determine lanthanum(III) uptake kinetics, adsorption capacities, and thermodynamic characteristics of rare earth elements binding to modified adsorbents.

Materials and methods

In the study, sodium alginate from Carl Roth (Germany), cellulose phosphate from Serva (Germany), Bayoxide E33 from Lanxess (Germany), Lewatit S1080 from Merck KGaA (Germany), and calcium chloride from Chempur (Poland) were used. The composites in which sodium alginate was the matrix and cellulose phosphate, Bayoxide E33 and Lewatit S1080 were used as additives were synthesized. The preparation procedure of alginate-based composites was similar to that described in the paper [4].








All batch adsorption experiments were performed under speed shaking of 180 rpm. The effect of pH solutions (pH from 1 to 7), interaction time (from 1 to 1440 minutes), temperature (from 293 to 333 K) and initial metal concentration (from 25 to 500 mg/dm³) on lanthanum(III) removal was studied. The adsorption was evaluated in terms of equilibrium (using Langmuir, Freundlich, Temkin, and Dubinin-Raduschkevich isotherms) as well as pseudo-first order, pseudo-second order, Weber-Morris, Boyd, and Dumwald-Wagner kinetic models. Thermodynamic parameters and desorption abilities of composites were also evaluated. The synthesized composites were characterized by ATR/FT-IR spectroscopy and pH_{PZC} measurements.



Results and discussion

The drift method was used to determine the pH_{PZC} of biosorbents. This parameter was evaluated for prepared alginate-cellulose phosphate, alginate-bayoxide 33, and alginate-lewatit S1080 composites and then the results were compared with raw alginate, cellulose phosphate, Bayoxide e33, and Lewatit S1080. Table 1 presents the obtained pH_{PZC} values.

Table 1. The appearance and pH_{PZC} measurements of biosorbents.

Type of biosorbents	Appearance	Functional groups	pH_{PZC}
Calcium alginate		Carboxyl, hydroxyl	6.14
Cellulose phosphate		Hydroxyl, carbonyl, ether, phosphate	5.10
Bayoxide E33		α -Ferric oxide hydroxide	7.32
Lewatit S1080		Sulfonic	1.98
Alginate-cellulose phosphate		Carboxyl, hydroxyl carbonyl, ether, phosphate	5.81
Alginate-Bayoxide E33		Carboxyl, hydroxyl, α -Ferric oxide hydroxide	6.50
Alginate-Lewatit S1080		Carboxyl, hydroxyl, sulfonic	2.55

The sorption of lanthanum(III) ions was dependent on the pH of the solution. Higher solution pH values resulted in more metal ions adsorbed on alginate-based composites. Sorption was most effective for pH = 5, with a composite mass of 0.05 g, and at 333 K. The sorption equilibrium time varied and depended on the initial La(III) ions concentration used. According to the kinetic and equilibrium studies, the sorption process followed the pseudo-second order kinetic model and the Langmuir isotherm model.

Conclusions

The study showed that the synthesized alginate-based composites have high adsorption capacity towards La(III) ions. Alginate with the Lewatit S1080 addition was characterized by the highest sorption capacity.

Acknowledgements: This study is supported by the National Science Centre in accordance with decision No. 2019/35/N/ST8/01390.

References

- Elbashier, E., Mussa, A., Hafiz, M., Hawari, A.H., 2021. Recovery of rare earth elements from waste streams using membrane processes: An overview. *Hydrometallurgy*, 204, 105706.
- Xiaoqi, S., Huimin, L., Mahurin, S.M., Rui, L., Xisen, H., Sheng, D., 2017. Adsorption of rare earth ions using carbonized polydopamine nano carbon shells. *J. Rare Earths*, 34, 77-82.
- Rizwan, K., Rasheed, T., Bilal, M., 2022. Chapter 21 - Alginate-based nanobiosorbents for bioremediation of environmental pollutants, *Nano-Biosorbents for Decontamination of Water, Air, and Soil Pollution*, Elsevier, Amsterdam, Netherlands, pp. 479-502.
- Fila, D., Hubicki, Z., Kołodyńska, D., 2022. Applicability of new sustainable and efficient alginate-based composites for critical raw materials recovery: General composites fabrication optimization and adsorption performance evaluation, *Chem. Eng. J.*, 446, 137245.



Effect of conductive material addition and external voltage application on the anaerobic digestion of dairy wastewater

M.S. Fountoulakis¹, Z. Dedova², S. Lemaigre², M. Calusinska² and J. Roussel²

¹Department of Environment, University of the Aegean, Mytilene, Greece ²Environmental Research and Innovation Department, Luxembourg Institute of Science and Technology, Belvaux, Luxembourg
Corresponding author email: fountoulakis@env.aegean.gr

keywords: *activated carbon; magnetite; methane; biogas; direct interspecies electron transfer.*

Introduction

The application of anaerobic treatment requires long hydraulic retention times (HRTs) for stable operation, negatively affecting the economic feasibility of anaerobic digestion plants (Ahring et al., 2003). The main reason for these long HRTs is the slow conversion of soluble organic acids to methane by syntrophic microorganisms. Specifically, the indirect interspecies electron transfer (IIET) between methanogens and fatty acid-oxidizers with the use of hydrogen or formate as electron carriers is the most important step for the stability of the process (Baek et al., 2018). If the partial pressure of hydrogen increased the fatty acid oxidation via IIET will not be thermodynamically feasible resulting in digester souring and failure.

Recent studies shown that the addition of electrically conductive materials (Gahlot et al., 2020) or the application of external voltage (Sun et al., 2020) promote the direct interspecies electron transfer (DIET). In that case, the multiple enzymatic steps for the production of electron carriers (hydrogen, formate etc) are not required as the electrons from the degradation of organic matter could be directly captured and utilized by methanogens (Baek et al., 2018). Despite the significant number of studies conducted mainly during last 5 years on the enhancement of DIET in anaerobic digesters there are still many questions which have not been clearly answered such as the effect of the application on real wastewater, the characteristics of conductive materials, the effect of external voltage on the process and the identification of microorganisms which are responsible for DIET.

In this context, the aim of this study was to examine for the first time the effect of magnetite or granular activated carbon (GAG) addition, external voltage application and their combination on the anaerobic digestion of real dairy wastewater.

Materials and methods

The experiment was conducted in 2-L anaerobic reactors which were operated under fed-batch mode at mesophilic conditions (35 °C). In total, three repeated batch cycles were conducted during a period of about 30 days. The inoculum used in the reactors was originated from a full-scale anaerobic digester treating sewage sludge (Schiffange, Luxembourg) while dairy wastewater was provided by a local dairy industry (LuxLait, Luxembourg). The inoculum to substrate ratio (based on VS) was 2.0. Six different configurations were examined: a) typical anaerobic digestion (AD), b) GAG addition, c) Magnetite addition, d) voltage application, e) GAG addition and voltage application and f) Magnetite addition and voltage application. GAC and magnetite were added in the reactors at a concentration of 10 g/L and 12mM Fe, respectively.

Biogas production and CH₄ content was monitored daily. The methane production over time was fitted using the modified Gompertz equation (Baek et al., 2015) to interpret the experimental results and directly compare each parameter among the different treatments:

$$B(t) = B_0 \exp \left[-\exp \left\{ \frac{R_m \times e}{B_0} (\lambda - t) + 1 \right\} \right]$$

where, B(t) is the accumulated methane production at time t, B₀ is the maximum methane potential (ml/g VSS/d), R_m is the maximum methane production rate (ml/gVSS/d), e is the Euler's number (2.718) and λ is the lag phase (d).



Results and discussion

The parameters estimated by modified Gompertz equation during the third batch cycle are presented in Table 1. Results shown that the addition of GAC and the addition of GAC in combination with the external voltage application increase the maximum methane production rate (R_m) at 11.9% and 13.7%, respectively, in comparison with the typical anaerobic digestion of dairy wastewater. In contrast, the addition of magnetite with or without the combination of external voltage had less positive effect (2-3%) on the maximum methane production rate. The maximum methane potential (BO) was found slightly higher (2-5%) in the digesters contained GAC or magnetite in comparison with the typical AD. The lag phase was found quite low (<0.35) for all digesters indicating the acclimatization of microbial communities. It is mentioned that the addition of GAC seems to reduce the time of lag phase at a percent around 30%.

Table 1. The parameters estimated by modified Gompertz model.

Reactors	B_o (ml/g VS/d)	R_m (ml/g VS/d)	λ (d)
Typical AD	594.1 ± 30.9	185.4 ± 1.2	0.35 ± 0.01
GAC	607.7 ± 0.1	207.4 ± 4.2	0.24 ± 0.03
Magnetite	618.8 ± 2.4	188.9 ± 1.6	0.35 ± 0.01
GAC + Voltage	611.8 ± 2.7	210.9 ± 1.5	0.25 ± 0.01
Magnetite + V	623.4 ± 5.2	190.7 ± 1.0	0.31 ± 0.01
Voltage	618.5 ± 17.3	186.8 ± 5.6	0.30 ± 0.01

The findings of this study are in accordance with previous works found that the addition of conductive materials could enhance the anaerobic digestion process. Specifically, there are several works examined the addition of GAC in doses ranged from 1 to 50 g/L. Most of them reported an increase of methane production yield and methane production rate ranged from 0 to 390%. In this work the increase of methane production rate observed (11-14%) was in the lower limits of previous reported. This could be related with the use of real wastewater as substrate. Xu et al. (2015) concluded that GAC can accelerate the degradation of simple organic compounds, but it can utilize complex materials such as proteins and carbohydrates. It is known that dairy wastewater contains significant amounts of proteins and carbohydrates. He et al. (2021) reported that the addition of carbon materials in anaerobic digesters treating waste activated sludge and grease led to an increase of methane production rate between 13-22% similar with this study.

Conclusions

The addition of GAC in the anaerobic digesters treating dairy wastewater increases the methane production rate. Furthermore, the application of external voltage in combination with GAC addition seems to improve further the overall performance. In contrast, magnetite addition had less positive effect on the methane production.

References

- Ahring, B.K., Angelidaki, I., de Macario, C.C., Gavala, H. et al. 2003. *Biomethanation* I. Springer, New York.
- Baek, G., Kim, J., Kim, J., Lee, C., 2018. Role and potential of direct interspecies electron transfer in anaerobic digestion. *Energies* 11, 107.
- Gahlot, P., Ahmed, B., et al. 2020. Conductive material engineered direct interspecies electron transfer (DIET) in anaerobic digestion: Mechanism and application. *Environ. Technol. Innov.* 20, 101056.
- Baek, G., Kim, J., Cho, K., Bae, H., Lee, C., 2015. The biostimulation of anaerobic digestion with (semi) conductive ferric oxides: their potential for enhanced biomethanation. *Appl. Microbiol. Biotechnol.* 99 (23), 10355–10366.
- Xu, S., He, C., Luo, L., Lu, F., He, P., Cui, L., 2015. Comparing activated carbon of different particle sizes on enhancing methane generation in upflow anaerobic digester. *Bioresour. Technol.* 196, 606–612.



SUST
ENG
2022



MICROPOLLUTANTS/MICROPLASTICS



Influence of grain size distribution of compost from urban greenery on the distribution of microplastics and their leachability

H. Raclavská¹, J. Růžičková¹, M. Šafář¹, D. Juchelková², B. Švédová¹, M. Kucbel¹, P. Kantor¹, H. Brťková¹
and K. Raclavský¹

¹Centre ENET, VŠB-Technical University of Ostrava, Ostrava-Poruba, Czech Republic

² Department of Electronics, VŠB-Technical University of Ostrava, Ostrava-Poruba, Czech Republic

Corresponding author email: michal.safar@vsb.cz

keywords: *compost; microplastics; additives; Py-GC/MS.*

Introduction

The lack of mineral fertilizers and their ever-increasing cost force farmers to look for other sources of nutrients to ensure soil fertility that is more economically affordable and yet safe for humans and the ecosystem. There is the possibility of using compost. Truly biodegradable plastics should not be visible in compost since it is specified that these plastics should not be visible after 12 weeks in the composting process, and 90% should be mineralised after six months (Amery et al., 2020). However, parts can still be present in the compost as micro and nano plastics.

The increased biodegradation of fine-grained PET particles was demonstrated by Farzi et al. (2020). The article deals with the identification of the proportion of chemical compounds that identify microplastics and additives and their ability to release them into the aqueous environment depending on the size of the compost particles and the choice of measures to limit their migration.

Materials and methods

Research on microplastics and additives released from them was carried out at the OZO Ostrava composting plant. OZO Ostrava uses only municipal green waste from the maintenance of urban greenery and brown bins containing biowaste from individual housing in Ostrava (Czech Republic) as feedstock. The composting plant processes up to 15,000 tonnes of biowaste/year. Composts were collected during 2022. Microplastics and additives were monitored both in the matured compost (after six months) and during the composting process in the input material and after six weeks of maturation.

Microplastics were determined by pyrolysis chromatography with mass detection, which allows the analysis of individual components forming plastics and their additives in the dry matter and in the aqueous leachate. Analyses were carried out for individual granular grades of compost, which were prepared by sieve analysis according to EN 15428 "Soil improvers and growing media – determination of particle size distribution". In addition, phytotoxicity tests were carried out to assess the effect of microplastics and their additives on plant growth, and a germination index (Pane et al., 2015) for watercress and white mustard was determined. In addition, leachable nutrient forms (N-NH₄⁺, K⁺) were determined in the aqueous leachate according to ISO 14911:2019 and dissolved organic carbon (DOC) and nitrogen according to ISO 20236:2018.

Results and discussion

Matured composts made from urban greenery contain microplastics (PET – polyethylene terephthalate, PE – polyethylene, PP – polypropylene, and PS – polystyrene) in a concentration of 40 – 80 mg/kg and additives in a concentration of 50 – 100 µg/kg. The input material for composting contains 500 – 800 mg/kg of microplastics and 186 – 320 µg/mg of additives. The following plastics have been identified in the most considerable quantities in matured compost: PET > PS > PE > PP.

PET relics are present in the highest amount in composts, which make up 50% of microplastics; approximately 20% are PE and polystyrene PS. The highest concentration of microplastics was found in the grain size class of 0.31 – 0.63 and 0.63 – 1.25 mm. The highest concentration of additives was found in class 0.31 – 0.63 mm, which is also about 1.8 times higher than the concentration in the total sample. The highest yield by weight of 20% was found in the grain size class 1.25 – 2.50 mm and 19% in the class 2.50 – 5 mm.



A maximum of 15% of the total content of chemical compounds identified in the dry matter passes into the aqueous leachate. Most PET compounds are released into the aqueous environment, the smallest amount of compounds is leached from PE (0.5 – 5%). The relationship between carbon content in compost and microplastics has not been demonstrated. The mechanism of decomposition of biogenic organic matter and microplastics is different.

The leaching analysis has not confirmed that the leaching ability of additives and microplastics is affected by grain size. The leachability of additives ranges from 1 to 33%. Some additives have shown a statistically significant dependence between the content in dry matter and the leachability (7,9-Di-tert-butyl-1-oxaspiro(4,5)deca-6,9-diene-2,8-dione, butylated hydroxytoluene, n,n dibutyl formamide, and for phthalates, only diisobutyl phthalate). The leaching of additives is affected by the leaching of soluble organic carbon. A statistically significant dependence has been shown to confirm that higher leachability of DOC reduces the leachability of additives. The presence of humic acids (the main component of DOC) limits the leaching of additives.

A germination index of 68% was found for compost sampled in March 2022 with a total microplastics content of 4,000 mg/kg, and for composts (May 2022) with a total microplastics content of 2,400 mg/kg, the germination index for watercress was higher (87%), which characterises the better properties of the compost.

Conclusions

Repeated analyses have found that during the composting process, the highest accumulation of microplastics occurs in the 0.63 – 1.25 mm grain size class. No relationship between the extractability of additives and the grain size has been demonstrated, but for some compounds, a statistically significant relationship between the concentration in dry matter and the extractability has been demonstrated. For identified phthalates (endocrine disruptors), this relationship has only been confirmed for diisobutyl phthalate.

Acknowledgements: This paper was supported by the research project of the Ministry of Education, Youth and Sport of the Czech Republic: The Doctoral grant competition VŠB-Technical University of Ostrava (Reg. No. CZ.02.2.69/0.0/0.0/19_073/ 0016945) within the Operational Programme Research, Development and Education, under the project (DGS/TEAM/2020-012) “Optimization of decomposition processes of major components of waste biomass ensuring requirements of phytotoxicity”.

References

- Amery, F., Vandaele, E., Körner, I., Loades, K., Viaene, J., Vandecasteele, B. and Willekens, K., 2020. Compost quality indicators. SoilCom. Aarslev, Denmark.
- Farzi, A., Dehnad, A. and Fotouhi, A.F., 2019. Biodegradation of polyethylene terephthalate waste using *Streptomyces* species and kinetic modelling of the process. *Biocatal. Agric. Biotechnol.*, 17, 25–31.
- Pane, C., Celano, G., Piccolo, A., Vilecco, D., Spaccini, R., Palese, A.M. and Zaccardelli, M., 2015. Effects of on-farm composted tomato residues on soil biological activity and yields in a tomato cropping system. *Chem. Biol. Technol. Agric.*, 2:4, 1–13.



Water quality analysis using physicochemical parameters and estimation of pesticides in water from various sources of Tirupati, Andhra Pradesh, India

Dr.K.Swathi¹, M. Malleswari¹ and B. Nikitha¹

¹ Institute of Pharmaceutical Technology, Sri Padmavati Mahila Visvavidyalayam, Tirupati, Andhra Pradesh India.

Corresponding author email: kswathi84@yahoo.co.in

keywords: Physico-chemical Parameters; Water Quality; Pesticide Analysis; Tirupati; GC-MS.

Introduction

Tirupati is one of the famous tourist places in India. So, safe drinking water is priority. Therefore, to handle ground water contamination and to aware the people in the area of Tirupati, in present paper, research was conducted with the goal to estimate water quality by using physico-chemical parameters and analysis of pesticides with analytical technique (GC-MS) of ground water in and around Tirumala, Tirupati located at Andhra Pradesh State of country India. For this estimation, ground water samples were collected from different locations of Tirupati i.e., Sri Padmavati Mahila Visvavidyalayam (Women's University), Mallamgunta, LB nagar, Singalagunta, SV University, Perumallapalli, Settipalli, AK palli, Srikrishna nagar, Gandhipuram, Pathalaganga, Cherllopalli areas and water quality parameters (alkalinity, pH, Total Hardness, chloride, calcium, potassium, and silica) were tested. Based on the physico-chemical parameters obtained it can be concluded that water was good like Tirumala patahlaganga were found be within the standard limits set by WHO so it is pure water without any contaminants. RO water doesn't contain any contaminants it is free from dissolved solids, ions so it is pure and clean water. Ground water sample which is collected from Tirupati area is less polluted than surface water sample so it is pure when compared with tap water. Hence, drinking water pollution should be Controlled by the proper environment management plan. Ground and surface water of this area should be treated to Make suitable for drinking and to maintain proper health Conditions of people living in this area. Among all sample which is collected from ground water from the fields of Settipalli area exceeded the standard limits set by WHO and BIS which suggests poor water quality. The present study reported the contamination status of diclorvos, methyl parathion, parathion, malathion in ground water of Tirupati in Settipalli, Andhra Pradesh, India. In agriculture, pesticides are frequently viewed as a quick, simple, and low-cost option for controlling weeds and insect pests. The results obtained from the present study shall be useful in future management of the Ground Water in Tirupati area.

Methods and results

Table 1. Experimental results for the physico-chemical parameters in study area with methods used.

S. No	Parameter and Methods used for Analysis	S1	S2	S3	S4	S5	S6
1	Colour (Visual comparison)	colourless	colourless	colourless	colourless	colourless	colourless
2	odour	odourless	odourless	odourless	odourless	odourless	odourless
3	appearance	clear	clear	clear	clear	clear	clear
4	Conductivity (Conductivity meter)	744	199.9	614	485	325	648
5	Turbidity (Turbidity meter)	21	1.6	1.7	2.2	2	1.9
6	pH (pH meter)	6.78	8.2	7.3	8.5	7.2	8.2
7	TDS	836	260	487	383	271	515
8	Dissolved oxygen	2.56	1.28	3.584	2.688	3.712	2.56



9	Acidity (Titrimetric method)	60	130	110	40	90	100
10	Alkalinity (Titrimetric method)	542	480	490	380	350	560
11	Temperature (Thermometer)	28.7	28	29.6	31.6	28.6	28.9

Table 2. List of ions and time windows used for SIMEI–MS detection, retention times and regression results for the analytes.

Compound	Starting time/min	m/z	Retention time (min)	Regression equation	r ²	Linear range (mg/l)
Dichlorvos	4	109, 79, 185, 220	4.82	$y = 1 \times 10^7x + 129629$	0.9967	0.01–2.00
Methyl parathion	8	109, 263, 125	8.85	$y = 1 \times 10^7x - 636386$	0.9820	0.01–2.00
Malathion	9	125, 93, 173, 127, 285	9.21	$y = 1 \times 10^7x + 2863160$	0.9928	0.01–2.00
Parathion	9.35	109, 125, 155, 139, 291	9.46	$y = 1 \times 10^7x + 83557$	0.9900	0.0055–1.10

Conclusions

The water of Andhra Pradesh and Tirupati region are Studies for various physico-chemical properties. The study Was carried out by collecting water ground water from this Region. Based on physicochemical analysis of ground water samples gathered in several Tirupati location.

From the observations it can be concluded that the concentration of turbidity, conductivity, total acidity content, Dissolved oxygen are within the limits but only sample which is collected at ground water in fields exceed the standard limits set by WHO and BIS which suggests poor water quality in these water sample (settipalli). The sample which is collected at Tirumala (patahlaganga) were found be within the standard limits set by WHO so it is pure water without any contaminants. RO doesn't contain any contaminants it is free from dissolved solids ,ions so it is pure and clean water. Ground water sample which is collected from Tirupati area is less polluted than surface water sample so it is pure when compared with tap water.

Hence, drinking water pollution should be controlled by the proper environment management plan. Ground and surface water of this area should be treated to Make suitable for drinking and to maintain proper health Conditions of people living in this area. The present study reports the contamination status of diclorvos, methyl parathion, parathion, malathion in ground water in Tirupati sample (settipalli), Andhra Pradesh, India. In agriculture, pesticides are frequently viewed as a quick, simple, and low-cost option for controlling weeds and insect pests. Pesticide use, on the other hand, has a huge environmental cost. Pesticides have infiltrated nearly every aspect of our ecosystem.

Acknowledgements: This study is supported by Sri Padmavati Mahila Visvavidyalayam, Tirupati, Andhra Pradesh, India.

References

- Gupta, D. P., Sunita, S.J.P. and Saharan J.P., 2009. Physiochemical Analysis of Ground Water of Selected Area of Kaithal City (Haryana) India. *Researcher*, 1(2), 1-5.
- Martins, M. L., Prestes, O. D., Adaime, M. B. and Zanella, R., 2014. Determination of Pesticides and Related Compounds in Water by Dispersive Liquid–Liquid Microextraction and Gas Chromatography–Triple Quadrupole Mass Spectrometry. *Anal. Meth.*, 6 (14), 542.



Photodegradation of low- and high-density polyethylene, polypropylene, polyvinyl chloride, polystyrene and nylon: evaluation by IR spectroscopy, Raman spectroscopy, DSC and SEM

M.P. Yeste¹, M.A. Cauqui¹, S. Bergaliyeva^{1,2} and M. Sendra³

¹Department of Materials Science, Metallurgical Engineering and Inorganic Chemistry. University of Cadiz, Cadiz, Spain

²Department of Physics and Technology. University of Al-Farabi Kazakh National, Almaty, Kazakhstan.

³Department of Biotechnology and Food Science. University of Burgos, Burgos, Spain.

Corresponding author email: pili.yeste@uca.es

keywords: plastic; UV; degradation; FTIR; RAMAN.

Introduction

Some of the most common plastic wastes are composed of high density polyethylene (HDPE), low density polyethylene (LDPE), polystyrene (PS), polyvinyl chloride (PVC), nylons and polypropylene (PP) (Dogan M. 2021). These residues are very stable and resistant to degradation due to the hydrophobic character of their polymer chains and high molecular weight. They are therefore a major environmental pollution concern.

Among the main degradation mechanisms of plastics we can mention biodegradation, photodegradation, thermal degradation and environmental erosion. Photodegradation with UV light is considered one of the most important causes of ageing in plastics (Wang C. 2020) and, in this regard, the number of publications dealing with this topic has increased significantly in recent years (Andrady A.L. 2022). However, despite the large number of reported results, there is a lack of studies analyzing the influence of extended UV radiation exposure times. In addition, most studies only analyze the degradation of one type of polymer, which prevents comparative results on the influence of ageing conditions on polymers of different nature. In this study, the effect of 7 months UV radiation aging on the chemical and morphological properties of the HDPE, LDPE, PS, PVC, nylon and PP has been analyzed in detail.

Materials and methods

HDPE, LDPE, PS, PVC, nylon and PP were procured from Sigma-Adrich. Artificial photooxidation studies were carried out with two UV-B lamps (UVB-150) with an irradiance of 0.6 mW/cm² from 0 to 7 months (**Figure 1**). According to Rafieepour A. 2015, a correlation has been made between time of artificial UV light irradiation with time of sun exposure. Polymers exposed to UV-B radiation were characterized by Fourier Transform Infrared spectroscopy (FTIR), Raman spectroscopy, Differential Scanning Calorimetry (DSC) and Scanning Electron Microscopy (SEM).

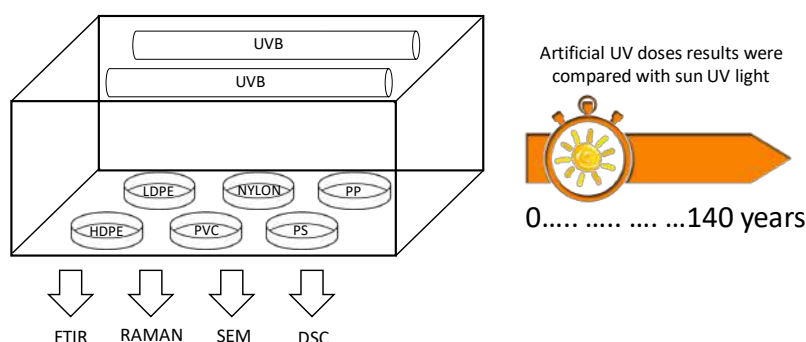


Figure 1. Photodegradation experiment setup.

Results and discussion

As an example, structural changes of HDPE were characterized by FTIR (**Figure 2**). The peaks around 2915 and 2848 cm⁻¹ show the stretching vibration of CH₂ (asymmetric and symmetric vibration respectively). The band at 1462 cm⁻¹ represent the bending vibrations of CH₂ and the band at 713 cm⁻¹ corresponds to the rocking vibrations of CH₂. The modification of the spectra during photooxidation indicate that carboxylic acids (1713 cm⁻¹) are formed at 40 years, and the formation of double bonds (1640 cm⁻¹) and hydrogen-bonded



alcohols and hydroperoxides (3420 cm^{-1}) are formed at 100 years. This is associated with a decrease in the bands at 2915 and 2848 cm^{-1} . This is in accordance with the changes of surface morphology (SEM) where the surface of treated HDPE presented rough texture from 40 years. However, there are no changes in Raman spectra, suggesting that the structural changes are not affecting the bulk structure, only the surface. For LDPE, PP, PVC and PS alterations also appear during UV irradiation in the region of $1600\text{--}1750\text{ cm}^{-1}$ (-C=C- , >C=O). In the case of nylon, it is the polymer that degrades earlier, and from the first moment, the characteristic FTIR peaks of secondary and tertiary amines disappear.

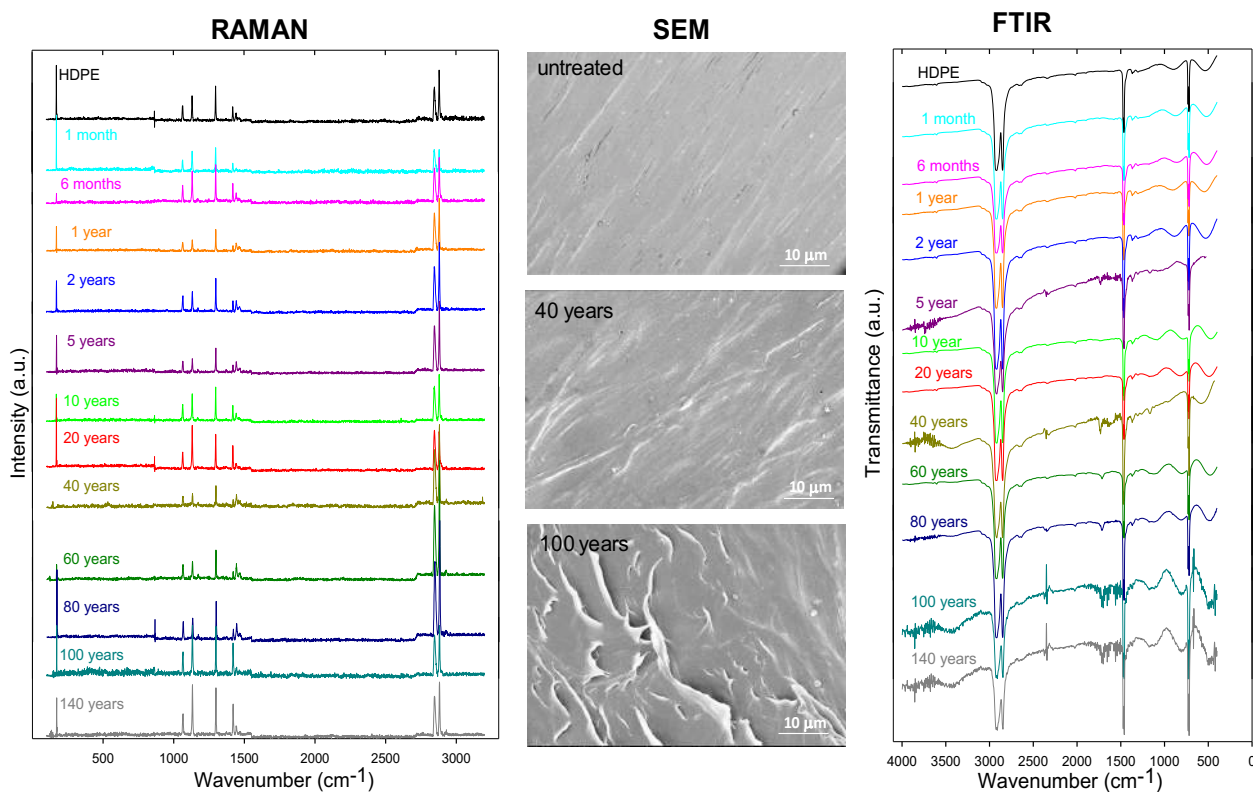


Figure 2. FTIR, RAMAN and SEM of HDPE with varying degradation time.

Conclusions

In this study, UV irradiation time of six types of conventional plastics (HDPE, LDPE, PP, PVC, PS and nylon) was carried out over a period of 7 months. The infrared spectra and the SEM results showed the characteristics of plastic degradation with time, such as fractures and pits. PP, HDPE and PVC are considered to be more stable than LDPE, PS and nylon. These results will allow scientists to identify the degradation period of plastics in the environment, therefore these results are of great interest and applicability in this field.

References

- Andrady, A.L., Law, K.L., Donohue, J. and Koongolla, B., 2022. Accelerated degradation of low-density polyethylene in air and in sea water. *Sci. Total Environ.*, 811, 151368.
- Dogan, M., 2021. Ultraviolet light accelerates the degradation of polyethylene plastics. *Micros Res Tech.*, 84, 2774-2783.
- Rafieepour, A., Ghamari, F., Mohammadbeigi, A., Asghari, M., 2015. Seasonal Variation in Exposure Level of Types A and B Ultraviolet Radiation: An Environmental Skin Carcinogen. *Ann. Med. Health. Sci. Res.*, 5, 129-133.
- Wang, C., Xian, Z., Jin, X., Liang, S., Chen, Z., Pan, B., Wu, B., Ok, Y. and Gu, C., 2020. Photo-aging of polyvinyl chloride micropastic in the presence of natural organic acid. *Water Res.*, 183, 116082.



One step synthesis of g-C₃N₄ supported WS₂ with enhanced photocatalytic performance

G. Mario Vino Lincy¹, M.M. Ghangrekar² and S. Chowdhury¹

¹School of Environmental Science and Engineering, Indian Institute of Technology, Kharagpur, West Bengal India

² Department of Civil Engineering, Indian Institute of Technology, Kharagpur, West Bengal, India

Corresponding author email: mariovino@iitkgp.in

keywords: calcination; g-C₃N₄/WS₂; photocatalysis; photocatalytic degradation; reactive oxygen species.

Introduction

In the midst of countless possibilities for exploring sustainable and highly efficient technologies for environmental remediation, heterogenous photocatalysis is widely considered as one of the most promising approaches. In particular, two-dimensional (2D) semiconductors, such as polymeric graphitic carbon nitride (g-C₃N₄), with tunable optical and electronic properties and quasi-resistance-free lateral charge transfer mechanisms, hold tremendous potential in photocatalysis. Additionally, constructing 2D/2D van der Waals heterojunction by allies of 2D carbon nitride sheets and other 2D semiconductors like tungsten disulfide (WS₂) can further promote the separation of photogenerated charge carriers, with significantly improved visible photon absorption.

Materials and methods

Melamine (99%) (C₃H₆N₆), thiourea (CH₄N₂S), sodium tungstate (Na₂WO₄), tetracycline (TC), isopropanol, sodium azide, potassium iodide were procured from Sigma Aldrich. All the chemicals were of analytical grade and used without further purification. Distilled water (DI) was used throughout the experiments.

g-C₃N₄ and g-C₃N₄/WS₂ composites were synthesized via a one-step calcination method. In brief, 10 g of melamine was exposed to a high temperature of 550°C for 4 h in a muffle furnace with a temperature ramp of 5°C/min. The obtained material (pale-yellow color) was cooled naturally and ground into a powder with the help of an agate mortar and pestle. To prepare the composite sample, different masses of Na₂WO₄ were first mixed with 5g CH₄N₂S and 60 mL distilled water and then sonicated for 30 min to prepare a uniformly-dissolved solution. The mixed solution was then dried at 105°C until complete evaporation of water. Thereafter, each precursor was uniformly ground and calcined in a muffle furnace at 550°C for 2 h at a heating rate of 15°C/min and cooled to room temperature. The cooled samples were uniformly ground and washed several times with deionized water to remove sodium ions. By keeping the concentration of g-C₃N₄ constant and altering the concentration of Na₂WO₄ in the reaction medium, four different types of g-C₃N₄/WS₂ were developed, labelled as 'g-C₃N₄/WS₂-1' (0.05), 'g-C₃N₄/WS₂-2' (0.1 g), 'g-C₃N₄/WS₂-3' (0.5 g), 'g-C₃N₄/WS₂-4' (0.7 g), and 'g-C₃N₄/WS₂-5' (1 g), respectively, depending on the mass of Na₂WO₄ used during synthesis

Results and discussion

1. Instrumental characterization

The SEM image of the as-synthesized composite materials showed stacking layers of g-C₃N₄ upon which WS₂ was loaded, as shown in **Fig.1a**. XRD peaks were observed at 2θ of 13.3° and 27.3° for gC₃N₄ and at 33.4° and 59° for WS₂, respectively (**Fig.1b**). FTIR fingerprints showed peaks from 1200 cm⁻¹ to 1600 cm⁻¹, which can be attributed to the stretching vibration modes of C-N and C=N heterocycles of g-C₃N₄ and another sharp peak at 660 cm⁻¹ representing W-S stretching vibration (**Fig.1c**). Raman spectra of the samples showed multiple peaks at 473 cm⁻¹, 581 cm⁻¹, 701 cm⁻¹, 981 cm⁻¹, 1105 cm⁻¹, 1233 cm⁻¹, 1492 cm⁻¹, 1613 cm⁻¹ of g-C₃N₄ and peaks only at 370 cm⁻¹ and 410 cm⁻¹ for WS₂ (**Fig.1d**).

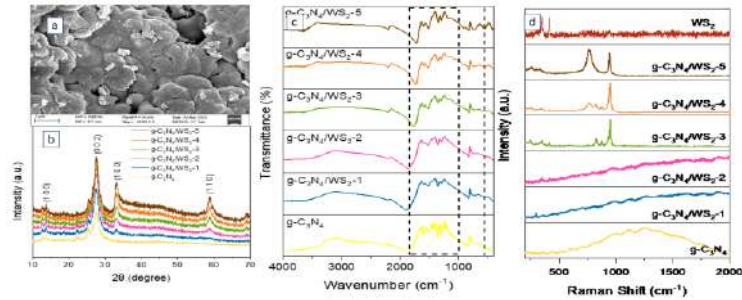


Figure 1. (a) SEM image (b) XRD patterns (c) FTIR spectra and (d) Raman spectra of g-C₃N₄/WS₂ composite.

2. Photocatalytic performance

The photocatalytic activity of the hybrid material was determined by analyzing the degradation of model pollutants like tetracycline (TC). The photodegradation efficiency under visible light of the as-synthesized nanocomposites with respect to pure g-C₃N₄ and WS₂ is shown in **Fig.2a**. After 30 minutes of adsorption-desorption equilibrium in dark, the pure g-C₃N₄ and WS₂ reported photodegradation efficiency of 63% and 65%, respectively, when the TC solution was exposed to visible light. Meanwhile, the g-C₃N₄/WS₂-5 nanocomposite attained the highest photodegradation efficiency of 90.15% after 2 h of irradiation amongst all the tested sample.

3. Reactive oxygen species (ROS) Analysis

Various scavenger additives were used to evaluate the degradation mechanism in order to identify the radicals that were involved in the degradation process (**Fig.2b**). Potassium iodide, scavenger for holes (h⁺), reduced the photodegradation efficiency to 50% while isopropyl alcohol, scavenger for hydroxy radical (OH[•]) suppressed the photodegradation efficiency to 65%. In addition, sodium azide reduced the degradation efficiency to 68% which also indicated the involvement of singlet oxygen radical (¹O₂) in the degradation process.

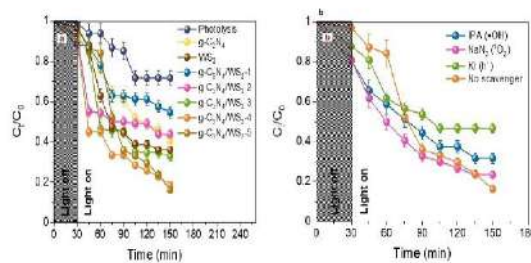


Figure 2. (a) Photocatalytic degradation of tetracycline, and (b) photocatalytic degradation of tetracycline in the presence and absence of various ROS scavenger additives by the as-synthesized g-C₃N₄/WS₂ composites.

4. Toxicity of the oxidation end products

The potential toxicity of the oxidation by-products formed during the TC photodegradation process was determined using the resazurin assay. The untreated TC solution with a concentration of 10 mg L⁻¹ showed obvious toxicity toward *E. coli*, as the blue color of resazurin remained unchanged. However, resazurin underwent florigenic change from blue to pink after photocatalytic treatment, suggesting that the TC photocatalysis by-products and derivatives did not exert considerable toxicity. The effective reduction in toxicity implies that g-C₃N₄/WS₂ may be a viable photocatalyst for treatment of TC contaminated waters.

Conclusion

In summary, a series of g-C₃N₄/WS₂ nanocomposite were prepared by a facile one-step calcination method for the removal of tetracycline. The highest photodegradation efficiency recorded was 90.15% by g-C₃N₄/WS₂-5 under visible light irradiation. The ROS species analysis indicated that the creation of holes and hydroxy radical significantly influenced the degradation rates. Besides, the ecotoxicity evaluation depicted that the end products from the photodegradation of TC were non-toxic.



Electrosynthesis of hydrogen peroxide with carbon based materials for the degradation of emerging contaminants

R. Dhawle¹, A. Ioannidi¹, Z. Frontistis² and D. Mantzavinos¹

¹Department of Chemical Engineering, University of Patras, Patras, Greece

²Department of Chemical Engineering, University of Western Macedonia, Kozani, Greece

Corresponding author email: r.dhawle@chemeng.upatras.gr

keywords: hydrogen peroxide; electrochemical; hybrid processes; micropollutants.

Introduction

In recent years, traces of different organic compounds have been increasingly detected in surface and groundwater. These compounds are called micropollutants and include various categories such as pharmaceutical compounds, personal care products, and endocrine disruptors. Conventional treatment methods have proved inadequate to minimize them, and many researchers have turned their attention to new advanced wastewater treatment methods [1].

Among new technologies, advanced oxidation processes (AOPs) are prevalent. AOPs are physicochemical technologies based on creating very active oxidizing species - radicals for decomposing organic compounds. Several of these processes, such as the Fenton reaction, produce these active species by activating well-known oxidants such as hydrogen peroxide or persulfates. However, since a) the hydrogen peroxide exists in liquid form and ii) has a relatively low lifespan, the flexibility of the peroxide-based process is limited, and it becomes difficult to use the abovementioned processes in applications such as decentralized systems [1]. Therefore, this work proposes an approach to overcome the above problems by studying the *in situ* production of hydrogen peroxide using electrochemistry and relatively inexpensive carbon-based materials in the absence of precious metals and their combination with mature technologies such as Fenton reaction or ultraviolet radiation for the destruction of emerging contaminants.

Materials and methods

Unless otherwise specified, all reagents were obtained from Sigma-Aldrich and were used as received. Carbon cloth (CC) from Fuel Cell Earth (Woburn, MA, USA), carbon black (CB) from Cabot Corporation (Vulcan XC72, Billerica, MA, USA) and Nafion N117 from Ion Power Inc (New Castle, DE 19720, USA). The electrochemical reactor was a dual-chamber cell (H type) made from PYREX with a working volume up to 120 ml for each compartment. The two compartments were separated with an ion-transfer membrane, (silica frit ROBU VitraPOR Quartz filter disc, Por. SGQ5, diameter 25 mm, thickness 2 mm, amorphous porous silica). Current-voltage measurements were performed with an Autolab potentiostat PGSTAT128N (Utrecht, The Netherlands). A graphite plate (9 cm²) served as the anode and a carbon black/carbon cloth electrode as the cathode

Construction of the CB/CC air electrode: The CB/CC electrode was made of carbon cloth, cut in pieces which provided a functional area of 9 cm², and covered on one side with a layer of mesoporous carbon. For this purpose, we prepared the following paste based on carbon black: 0.3 g of carbon black was mixed with 8 ml of distilled water by vigorous mixing in a mixer until it became a viscous paste. This paste was mixed with 0.1 ml polytetrafluorethylene (Teflon 60% wt. dispersion in water) and then applied to the carbon cloth. This has been achieved by first spreading the paste with a spatula, preheating for a few minutes at 80 °C and finally heating also for a few minutes in an oven at 340 °C. Then the above procedure was repeated once more. In this way, a hydrophobic gas diffusion layer was developed on the carbon cloth [3].

Hydrogen peroxide concentration was measured using the potassium titanium oxalate titration as described in a previous study [3], and Sulfamethoxazole was measured using Waters Alliance HPLC equipped with a Photodiode Array detector at 270 nm using a Kinetex column (C18 100A, 150 mm × 3 mm, 2.6 μm particle size) purchased from Phenomenex.



Results and discussion

In a preliminary set of experiments, the electro-synthesis of hydrogen peroxide over a carbon black/carbon cloth electrode in a dual-chamber reactor operated in batch mode was investigated using almost neutral conditions (pH 6) and 0.1 M of sodium sulfate as the electrolyte, and the results are depicted in Figure 1.

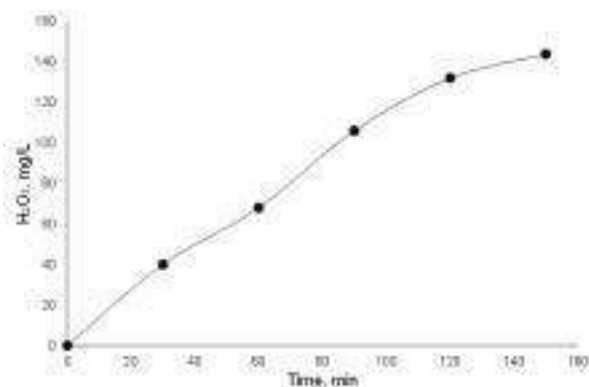


Figure 1. Production of hydrogen peroxide using Carbon Black/Carbon Cloth cathode, 0.1 M Na_2SO_4 , pH 6 and 2 V.

As shown, the system produced more than 140 mg/L of hydrogen peroxide in less than 150 minutes, while the rate of hydrogen peroxide formation decreased after 120 min. According to preliminary experiments, 100 mg/L of hydrogen peroxide in combination with a) 5 mg/L Fe^{2+} or 8 Watt UV-C lamp could degrade 500 $\mu\text{g/L}$ of the antibiotic sulfamethoxazole in less than 60 minutes; however, further optimization is needed in this direction. In future work, the system will operate in continuous mode to examine its stability, where a part of the produced hydrogen peroxide will be used for the removal of different classes of micropollutants and pathogens (disinfection).

Conclusions

The electro-production of hydrogen peroxide using cheap and abundant carbon-based material is an interesting option to allow the application of advanced oxidation processes in decentralized facilities. According to the preliminary results, the proposed system can generate peroxide in concentration relevant to the degradation of micropollutants using mature processes like Fenton reaction or UVC/ H_2O_2 . However, additional research is needed to study both the efficiency and stability of the system under continuous flow and a wide range of operating parameters

Acknowledgements: This project has received funding from the European Union's EU Framework Programme for Research and Innovation Horizon 2020 under Grant Agreement No 861369 innoveox.eu.

References

- G. Bampos, A. Petala, Z. Frontistis, Recent Trends in Pharmaceuticals Removal from Water Using Electrochemical Oxidation Processes, *Environments*. 8 (2021) 85.
- R. Dhawle, Z. Frontistis, D. Mantzavinos, P. Lianos, Production of hydrogen peroxide with a photocatalytic fuel cell and its application to UV/ H_2O_2 degradation of dyes, *Chemical Engineering Journal Advances*. 6 (2021) 100109.
- R. Dhawle, D. Mantzavinos, P. Lianos, UV/ H_2O_2 degradation of diclofenac in a photocatalytic fuel cell, *Applied Catalysis B: Environmental*. 299 (2021) 120706.



Novel 3D MoS₂@graphene aerogel for enhanced photocatalytic degradation of tetracycline

C. Das,¹ B.K. Dubey² and S. Chowdhury¹

¹School of Environmental Science and Engineering, Indian Institute of Technology Kharagpur, West Bengal India

²Department of Civil Engineering, Indian Institute of Technology Kharagpur, West Bengal

Corresponding author email: daschinmayee94@gmail.com

keywords: Graphene aerogel; molybdenum disulfide; photocatalysis; photodegradation; tetracycline.

Introduction

Graphene aerogels (GAs) are receiving widespread scientific attention for various environmental applications in recent years. This can be credited to their inherent hydrophobicity, superlative mechanical features, precise and physically linked permeable networks, enormous surface area, and profound porosity, amongst others. However, the absence of a sizeable band gap in their 2D nanoscale building blocks as well as their randomly oriented pores grossly minimize the application potential of graphene aerogels. In order to overcome the limitations of GAs, the in situ deposition of 2D semiconductors, like molybdenum disulfide (MoS₂), can result in improved performance due to the synergistic effect. Herein, we therefore anchor 2D MoS₂ nanostructures on the 3D interconnecting networks of graphene aerogel and evaluate the photodegradation ability of the resulting mixed-dimensional hybrid aerogel towards a model pharmaceutical pollutant (i.e., tetracycline) under visible light irradiation.

Materials and methods

Graphite powder (< 20 μm), sulfuric acid (98 wt.%, H₂SO₄), phosphoric acid (85 wt.%, H₃PO₄), potassium permanganate (KMnO₄), hydrogen peroxide (30 wt.%, H₂O₂), sodium molybdate dehydrate (Na₂Mo₄.2H₂O), and L-cysteine (C₃H₇NO₂S) were used as obtained from the supplier without any further purification. Deionized water was used throughout the experiments.

MoS₂@GA were synthesized through a facile one-pot hydrothermal method. In a typical procedure, a desired amount of GO, synthesized via modified Hummer's method, was taken to prepare GO aqueous dispersion (5 mg mL⁻¹) and sonicated for 60 min. Thereafter, a weighed amount of Na₂Mo₄.2H₂O and C₃H₇NO₂S were added sequentially under stirring for 30 min. The resulting homogenous mixture was sealed in a 100 mL Teflon-lined stainless-steel autoclave and hydrothermally treated at 180 °C for 12 h. The as-obtained MoS₂@GA was washed repeatedly with water to remove any residual chemicals and finally freeze-dried for 24 h. For comparison, pristine graphene aerogel (denoted as "GA") was also produced using the same method but without adding any Na₂Mo₄.2H₂O or C₃H₇NO₂S.

The as-synthesized material was thereafter characterized using a wide range of state-of-the art microscopy, spectroscopy, and surface analytical techniques.

The photocatalytic efficiency of the as-synthesized MoS₂@GA materials was examined for degradation of tetracycline (TC) at room temperature (25 °C) in a 250 mL quartz triple-jacketed water-cooled immersion-type photochemical reactor under visible light irradiation. The reaction mixture of MoS₂@GA suspended onto TC solution was illuminated using 250 W high-pressure mercury lamp fitted with UV cut-off filter (λ < 420 nm). During irradiation, aliquots were withdrawn at pre-fixed time intervals and the residual TC concentration was quantified using a UV/VIS spectrophotometer at λ_{max} = 490 nm. The transient reaction intermediates and end products were identified using a matrix assisted laser desorption ionization/time of flight (MALDI-TOF) equipment. A series of controlled experiments were also conducted in the presence of different reactive oxygen species (ROS) scavengers in order to probe the photodegradation mechanism of TC over the as-developed MoS₂@GA material. The potential toxicity of the oxidation byproducts formed during the photodegradation of TC over the MoS₂@GA materials was analyzed by monitoring the viability of the Gram-negative bacterium *Escherichia coli* (*E. coli*) using the Alamar Blue assay.



Results and discussion

1. Instrumental characterization

The microstructure of the as-prepared MoS₂@GA material was examined through SEM. MoS₂@GA possessed a well-developed continuously interconnected network of randomly oriented crinkly graphene sheets, with pore sizes ranging from hundreds of nanometers to several micrometers (Fig. 1, left panel). Subsequently, the degree of lattice distortion in the MoS₂@GA material was investigated by Raman spectroscopy. The Raman spectra of MoS₂@GA presented two prominent peaks at approximately 1340 and 1570 cm⁻¹ (Fig. 1, middle panel), corresponding to the well-documented D band and G band, respectively. More importantly, the ratio of D to G bands integrated intensities (I_D/I_G) was found to be 1.12. The successful loading of MoS₂ onto the 2D nanoscale building blocks of the MoS₂@GA was further confirmed by FTIR. The FTIR spectra of the MoS₂@GA displayed absorption bands associated with C=C=O, C=C, C–O, and Mo–S stretching vibrations, validating the successful fabrication of the anticipated novel materials. In order to assess the light absorption characteristic of MoS₂@GA, its diffuse reflectance spectra were recorded. The band gap energy (E_g) of the MoS₂@GA for direct interband transition, was estimated applying the Kubelka–Munk method and the band gap was found to be 1.26 eV (Fig. 1, right panel).

2. Photocatalytic performance

The photocatalytic properties of the as-synthesized MoS₂@GA were tested under visible light irradiation by choosing TC as a model pollutant. Before initiating the photoreaction, the TC solution along with the photocatalyst was stirred in the dark for 30 min in order to establish adsorption–desorption equilibrium. A substantial amount of TC was adsorbed within the first 30 min. After 2 h exposure to visible light, the TC photodegradation efficiency of the synthesized GA was 35% and MoS₂@GA was 91%.

3. Radical scavenging experiments and photocatalytic mechanism

A series of controlled experiments were also conducted in the presence of different ROS scavengers in order to probe the photodegradation mechanism of TC over MoS₂@GA. Isopropyl alcohol (IPA), potassium iodide (KI) and sodium azide (NaN₃) were used as scavengers for •OH, hole and singlet oxygen (¹O₂) respectively. When IPA was spiked into the reaction mixture, the photocatalytic process was more severely suppressed, resulting in a fairly low photodecomposition efficiency of 36%. These findings conclusively emphasize that photodegradation of TC over MoS₂@GA was primarily driven by •OH radicals.

4. Toxicity of the photooxidation byproducts

The potential toxicity of the oxidation byproducts formed during the TC photodegradation process was determined using the resazurin assay. The untreated TC solution with a concentration of 5 mg L⁻¹ showed obvious toxicity toward *E. coli*, as the blue color of resazurin remained unchanged. However, resazurin underwent florigenic change from blue to pink after photocatalytic treatment, suggesting that the TC photocatalysis byproducts and derivatives did not exert considerable toxicity.

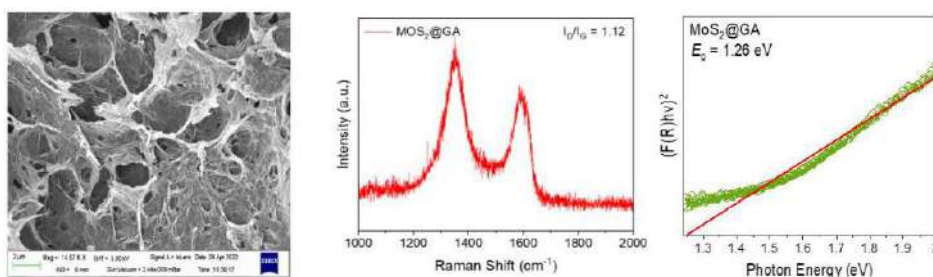


Figure 1. SEM image (left panel), Raman spectroscopic signature (middle panel) and Kubelka–Munk plot (right panel) of the as-synthesized MoS₂@GA.

Conclusions

The photocatalytic degradation of the as-synthesized MoS₂@GA towards pharmaceutical TC was found to be 91%. Moreover, the oxidation byproducts formed during TC photodegradation was non-toxic in nature as evidenced from resazurin assay.



Assessing the performance of a column system using zero valent iron nanoparticles for the treatment of diclofenac and bisphenol-A from wastewater

E. Barka¹, C. Noutsopoulos¹, A. Galani¹, I. Panagou¹, M. Kalli¹, E. Koumaki¹, D. Mamais¹, S. Malamis¹, C. Mystrioti² and N. Papassiopi²

¹Sanitary Engineering Laboratory, Department of Water Resources and Environmental Engineering, School of Civil Engineering, National Technical University of Athens, Athens, Greece

²School of Mining and Metallurgical Engineering, Athens, Greece

Corresponding author email: Ebarka8@gmail.com

keywords: *contaminants of emerging concern; nano zero valent iron; green tea extract; advanced wastewater treatment; advanced oxidation processes.*

Introduction

Contaminants of Emerging Concern (CECs) have raised scientific awareness worldwide in recent decades, because they can have toxic effects on ecosystems and human health. Many chemical products used in daily life contain CECs. These include pharmaceuticals and personal care products, plasticizers, food additives, etc. One of the main sources of their release into the aquatic environment is wastewater, as conventional techniques are unable to mitigate them. Therefore, advanced treatment processes have come to the fore, including adsorption on activated carbon [1] or biochar [2], photocatalysis and Fenton processes [3] and persulfate activation by transition metals [4]. Among transition metals, nano zero valent iron (nZVI) is promising as it not only has the ability to act as a catalyst for radicals' generation, but also has reducing and adsorptive capabilities. In addition, the small particle size contributes to its high reactivity. The objective of the present study is to evaluate the performance of a nZVI column system with respect to the removal of diclofenac (DCF) and bisphenol-A (BPA).

Materials and methods

The fabrication of the nanocomposite material (R-nFe) is based on the method developed by Toli et al., 2018 [5]. The main idea is the adsorption of trivalent iron into the resin due to electrostatic attraction and the subsequent reduction of iron to the elemental state by the action of polyphenols derived from green tea extract. Column experiments were conducted to investigate various operating parameters such as contact time, initial pollutant concentration, initial pH of the wastewater matrix, synergistic effect of an oxidative reagent, namely sodium persulfate (PS) and the effect of concentration of PS. In the first period of operation, the columns were connected in series to test the effects of four different contact times (2.2, 4.4, 6.6 and 8.8 min) and initial concentration (1 and 5 µg/L). In the second period of operation, where the columns were working in parallel, the effect of the initial pH set at the acidic value of 3.5 and the effect of adding PS at two different concentrations (1 and 5 mM respectively) were studied. The wastewater matrix was tertiary effluent with a flowrate of 26 L/d, while the flowrate of the sodium persulfate solution was 1.2 L/d.

Results and discussion

The results showed that the initial concentration of the target compounds plays an important role in the removal efficiency of DCF, as the increase from 1 to 5 µg/L contributed to lower removal rates and the earlier occurrence of breakthrough. In contrast, this was not the case for BPA, as the removal efficiency increased with the higher concentration, showing that saturation of the active sites has not yet been reached.

The contact time appeared to have a small positive effect on the removal efficiency of the target compounds and even at the highest contact time tested of 8.8 min, the longevity of the treatment process could not be established as breakthrough occurred after 3 days for DCF and 8 days for BPA (results not shown). Adjusting the pH of the influent wastewater matrix to the acidic value of 3.5, showed improved behavior of the system (Fig. 1), as the Fenton mechanism could take place due to the availability of H⁺ and enhanced iron corrosion. However, this modification was also limited to a few days of operation and the addition of an oxidative reagent seemed necessary. Sodium persulfate together with nZVI can generate



sulfate radicals which have a high redox potential ($E_0=2.5-3.1$ V) and can oxidize the recalcitrant compounds tested. In addition, both PS concentrations tested, 1 and 5 mM respectively, showed high removal rates of the target compounds (Fig. 1), leading to the conclusion that 1 mM might be the optimal concentration from a technical point of view. The application of 1 mM PS at a contact time of 2.2 min, ensured the successful long-term performance of the system, which achieved removal efficiencies of 61-93% for BPA and 70-95% for DCF during 30 d of continuous operation, showing that this combined technology could be a promising solution for the elimination of CECs from wastewater.

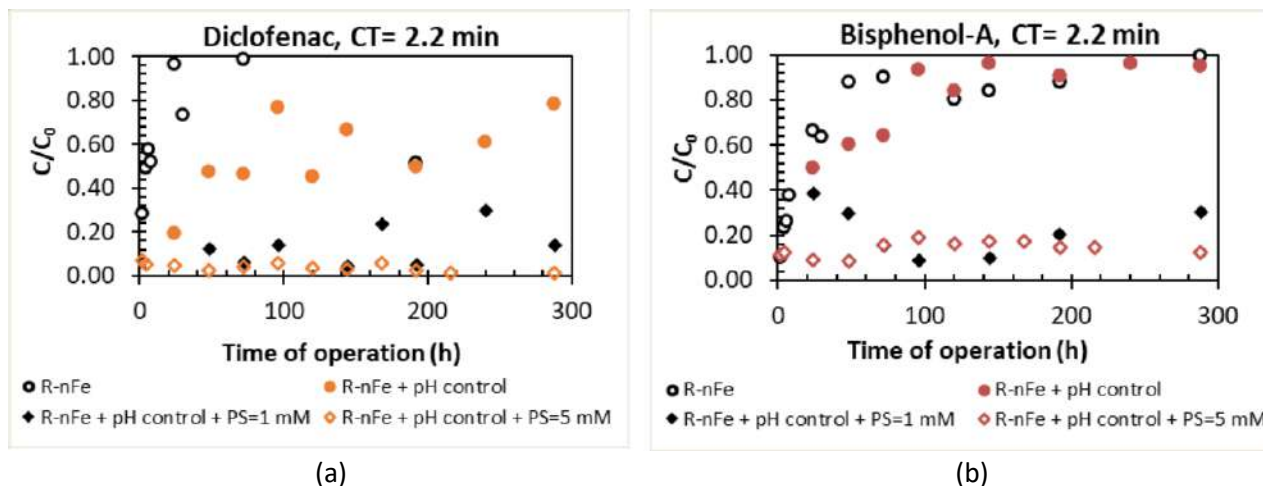


Figure 1: The effect of pH adjustment to the acidic value of 3.5 and the effect of PS concentration on the removal efficiency of Diclofenac (a) and Bisphenol-A (b).

Conclusions

The synergistic effect of R-nFe with sodium persulfate under acidic conditions could be a promising post-treatment for the elimination of CECs from wastewater. Not only the safe discharge into the aquatic environment, but also the safe reuse of the reclaimed water according to the principles of circular economy is an important issue that should be addressed.

Acknowledgements: This study was carried out within the project “Safe and Sustainable Solutions for the Integrated Use of Non-Conventional Water Resources in the Mediterranean Agricultural Sector (FIT4REUSE)” which has received funding from the Partnership on Research and Innovation in the Mediterranean Area (PRIMA) under grant agreement No 1823. PRIMA is supported by the European Union’s Horizon 2020 research and innovation program.

References

- Ahmed, M.J. Adsorption of Non-Steroidal Anti-Inflammatory Drugs from Aqueous Solution Using Activated Carbons: Review. *Journal of Environmental Management* 2017, 190, 274–282, doi:10.1016/j.jenvman.2016.12.073.
- Rosales, E.; Meijide, J.; Pazos, M.; Sanromán, M.A. Challenges and Recent Advances in Biochar as Low-Cost Biosorbent: From Batch Assays to Continuous-Flow Systems. *Bioresource Technology* 2017, 246, 176–192, doi:10.1016/j.biortech.2017.06.084.
- Villanueva-Rodríguez, M.; Bello-Mendoza, R.; Hernández-Ramírez, A.; Ruiz-Ruiz, E.J. Degradation of Anti-Inflammatory Drugs in Municipal Wastewater by Heterogeneous Photocatalysis and Electro-Fenton Process. *Environmental Technology* 2019, 40, 2436–2445, doi:10.1080/09593330.2018.1442880.
- Gao, F.; Li, Y.; Xiang, B. Degradation of Bisphenol A through Transition Metals Activating Persulfate Process. *Ecotoxicology and Environmental Safety* 2018, 158, 239–247, doi:10.1016/j.ecoenv.2018.03.035.
- Toli, A.; Varouxaki, A.; Mystrioti, C.; Xenidis, A.; Papassiopi, N. Green Synthesis of Resin Supported Nanoiron and Evaluation of Efficiency for the Remediation of Cr(VI) Contaminated Groundwater by Batch Tests. *Bull Environ Contam Toxicol* 2018, 101, 711–717, doi:10.1007/s00128-018-2425-2.



Theoretical investigation of halloysite as potential sorbent for pharmaceutical wastewaters

E. Gianni^{1,2} and E. Scholtzová²

¹Centre for Research and Technology, Hellas (CERTH), Marousi, Greece

²Institute of Inorganic Chemistry, Slovak Academy of Science, Bratislava, Slovakia

Corresponding author email: eva.scholtzova@savba.sk

keywords: halloysite; CPT-11; drug removal; hospital wastewaters; *ab initio* DFT.

Introduction

The presence of antitumoral drugs is dominant in municipal and hospital wastewaters with a major impact on the natural environment. CPT-11 (Irinotecan, Fig 1) is a chemotherapeutic agent which can be used for various cancer types and has been extensively studied in the last years (Gianni et al., 2019). Therefore, 45-63% is excreted as a parent drug by the human body, concluding to wastewater and further the groundwater (Slatter et al., 2000). On the other hand, halloysite is a clay mineral that has been extensively tested for its sorption properties due to its nanotubular morphology, the combination of negative outer (octahedral, O) surface and positive inner (tetrahedral, T) surface charge of its crystals, its high specific surface area and the low cost (Gianni et al., 2019). In the present study, the adsorption energy and interactions among the halloysite and all forms of CPT-11 (neutral, anionic and cationic) (Di Nunzio et al., 2018) were investigated by the *ab initio* Density Functional Theory (DFT) method for the potential use of this mineral as a sorption medium for drug removal from wastewaters.

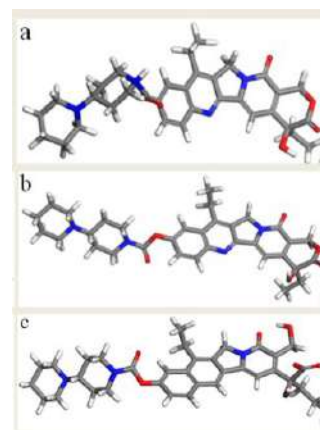


Figure 1. (a) Cationic, (b) Neutral and (c) Anionic form of CPT-11.

Materials and methods

Halloysite model was created as $3a \times 2b \times 1c$ of the elementary cell published by Mehmel (1935). To keep the neutral charge of the whole system, the substitutions were done if necessary ($\text{Si}^{4+}/\text{Al}^{3+}$ for the negative surface of halloysite and $\text{Al}^{3+}/\text{Ti}^{4+}$ for the positive one). Six initial models were created (Fig 2): 1. Negative T sheet interacted with the cationic form of the drug, 2. Neutral O sheet of halloysite interacted with the aromatic ring of the neutral drug molecule, 3. Neutral O interacted with the carboxylate group of the neutral drug molecule, 4. Neutral T interacted with the aromatic ring of the neutral drug molecule, 5. Neutral T interacted with the carboxylate group of the neutral drug molecule, and 6. Positive O interacted with the anionic form of the drug. It must be highlighted that these periodic models represent 'a planar structure of halloysite' or a curved structure with infinite radius.

The study of models was performed using the *ab initio* DFT method involving dispersion corrections using D3 scheme (Grimme et al., 2010) implemented in the VASP program (Kresse&Hafner, 1993) first time. The computational cells were fully optimized.

The adsorption energy (ΔE_{ads}) of the models was calculated according to the reaction scheme:

$$\Delta E_{ads} = E_{Total} - (E_{Hal+Wat} + E_{Irin})$$

where E_{Total} -total energy of the system, $E_{Hal+Wat}$ -total energy of halloysite and water molecules excluding irinotecan molecule and E_{Irin} -total energy of irinotecan molecule.

Results and discussion

Table 1. Total and adsorption (ΔE_{ads}) energies of the optimized models [kJ/mol].

Model	1	2	3	4	5	6
Total energy	-188381	-188145	-188181	-188183	-188279	-189675
	-573	-54	-85	-37	-138	-320



The energetically preferred system (6) includes the anionic form of CPT-11 interacting with the O surface of the halloysite (-189675 kJ/mol). The anionic form of the drug exists only in strong alkaline pH environments. The total energy of the cationic CPT-11 (1) interacting with the outer T surface of halloysite is also low (-188381 kJ/mol), and this system is due to mutual electrostatic interactions more stable than systems containing the neutral form of the drug (2-5). When the drug is in the neutral form, it preferably interacts through its carboxylate group with the octahedral surface of the halloysite (-188279 kJ/mol).

Based on the adsorption energy (Table 1), the most stable system is when the drug is in the cationic form (1/-573 kJ/mol), which is the most common form in neutral and acidic conditions. The high stability is caused by the presence of C-H...Ob H-bonds (Ob - basal oxygen) that are stronger than every other type, and they directly interact with the T surface of the halloysite. Moreover, the presence of very strong "non-direct" hydrogen bonds, which support the anchoring of drugs on the halloysite surface, is crucial for the stability of the system. Model 6 also has high adsorption energy (-320 kJ/mol) due to electrostatic interactions, weak C-H...Oo bonds (Oo - oxygen of O sheet), strong "non-direct" H-bonds and strong Oo-H...Oi bonds (Oi-oxygen of irinotecan) which probably enhance the interactions in the system. In the case of a neutral drug, weaker interactions exist in the systems. However, this is not a problem as in nature, drug tends to convert into ion depending on the conditions of the surrounding environment. Although, when a neutral drug interacts with halloysite, the carboxylate group of CPT-11 is the one that interacts with the mineral and is preferable with the octahedral surface of halloysite.

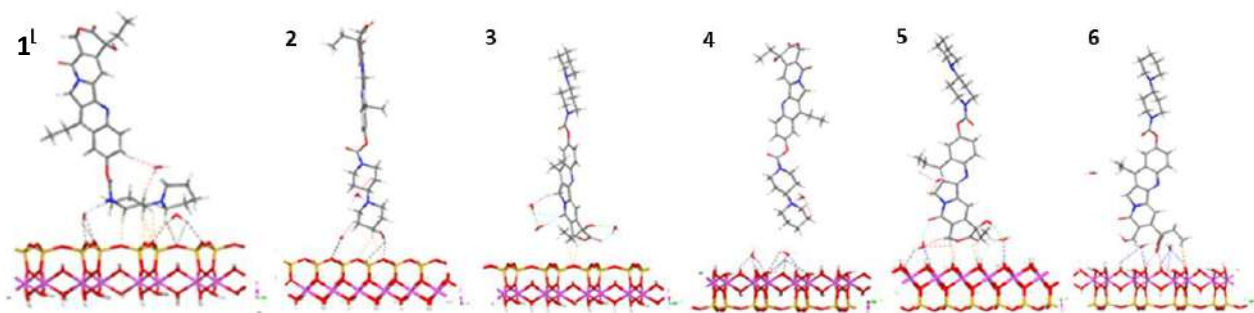


Figure 2. Optimized models.

Conclusions

The analysis of the calculated results revealed that halloysite mineral is suitable sorbent for treatment of wastewater polluted by CPT-11. Based on the values of adsorption energies, all potential forms of the CPT-11 drug (anionic, cationic and neutral) produce stable systems with halloysite. The cationic drug is the most stable, thus the halloysite can be an ideal sorbent for acidic and neutral waste waters.

Acknowledgement: ES is grateful for the financial support by the Scientific Grant Agency VEGA (2/0021/19).

References

- Gianni, E., Avgoustakis, K., Pšenička, M. and Pospíšil, M., 2019. Halloysite nanotubes as carriers for irinotecan: Synthesis and characterization by experimental and molecular simulation methods. *J. Drug Deliv. Sci. Technol.*, 52, 568–576.
- Slatter, J.G., Schaaf, L.J., Sams, J.P., Feenstra, K.L., ... , Pesheck, C.V. and Lord, R.S., 2000. Pharmacokinetics, metabolism, and excretion of irinotecan (CPT-11) following I.V. infusion of [14C] CPT-11 in cancer patients. *Drug Metab. Dispos.*, 28, 423e433.
- Di Nunzio, M.R., Douhal, Y., Organero, J.A. and Douhala, A., 2018. Structural and photodynamic properties of the anti-cancer drug irinotecan in aqueous solutions of different pHs. *Phys. Chem. Chem. Phys.*, 20, 14182-14191.
- Mehmel, M., 1935. Über die Struktur von Halloysit und Metahalloysit. In: E., Antipov, E.V., Boldyreva, K., Friese, H., Huppertz, S., Jahn, E.R.T. Tiekink (Eds.) *Zeitschrift für Kristallographie - Crystalline Materials* (pp. 35-43), Volume 90(1-6).
- Grimme, S., Antony, J., Ehrlich, S. and Krieg, S., 2010. A consistent and accurate ab-initio parametrization of density functional dispersion correction (dft-d) for the 94 elements H-Pu. *J. Chem. Phys.*, 132, 154104.
- Kresse, G. and Hafner, J., 1993. Ab-initio molecular-dynamics for open-shell transition-metals. *Phys. Review B*, 48, 13115-13118.



SUST
ENG
2022



FUELS/BIOFUELS



Optimization of a biphasic biodesulfurization system

T.P. Silva¹, S.M Paixão¹, J.C. Roseiro¹ and L. Alves¹

¹LNEG – Laboratório Nacional de Energia e Geologia, IP, Unidade de Bioenergia e Biorrefinarias; Estrada do Paço do Lumiar, Lisboa, Portugal

Corresponding author email: luis.alves@lneg.pt

keywords: *biodesulfurization; model fuel; biorefinery.*

Introduction

Many of the new generation fuels, although more sustainable, share some of the problems inherent to fossil fuels. Depending on the biomass/material that originated them, they can present different contaminants that can lead to environmental problems. Sulfur is one of the most common and problematic contaminants in fuels. It is released into the atmosphere in the form of SO_x, leading to the formation of acid rains, which cause drastic environmental and infrastructural problems, as well as several types of health issues. High sulfur concentrations in fuels also result in a loss of efficiency of motors and energy generation systems, mostly due to corrosion and catalyst poisoning.

The current thermochemical desulfurization process, hydrodesulfurization (HDS), is energy demanding, pollutant and has low efficiency against more complex organosulfur molecules. This led researchers to look for new alternatives. Biodesulfurization (BDS), is, as the name implies, the biological removal of sulfur from fuels using microorganisms as living biocatalysts. If correctly employed this process could be more efficient and less pollutant, since microorganisms directly target the sulfur atoms, even those present in complex molecular structures, such as dibenzothiophene (DBT). Moreover, microbial activity occurs at much lower temperatures and pressures, without the need for metal catalysts, resulting in a lower energy demand.

While BDS is a promising technology, it is still at a low development stage, mostly due to some bottlenecks, which have been hindering its large-scale application. Similarly, to other biotechnological processes, it presents lower reaction rates, when compared to HDS, since it depends on the use of living organisms as catalysts. Furthermore, it must be performed under conditions that allow the microorganisms to maintain biological activity, limiting the range of applications. These conditions vary greatly depending on the microorganism selected, and their optimization can significantly increase the biodesulfurization activity of a biocatalyst.

Traditionally, most optimization work has been performed under conditions ideal for bacterial growth, without taking into consideration the conditions that the biocatalysts will be subjected to when in contact with actual fuels in a refinery environment. To better understand microbial behavior and increase BDS activity, it becomes fundamental to study how these microorganisms respond in biphasic systems, if high hydrocarbon ratios and lower water availability are tolerable, and how to compensate for any metabolic activity loss.

Gordonia alkanivorans strain 1B is a bacterium that has demonstrated great potential to be used in a BDS biorefinery. Not only can it remove sulfur from complex compounds, but it seems to increase its efficiency with more complex molecules, such as DBT and its derivatives (Silva et al., 2020). Furthermore, it can simultaneously produce high added value products (carotenoids and surfactants) and can be cultivated with agro-industrial residues as nutrient sources. To this date, most works published with this strain were performed in aqueous medium. This work focusses on the optimization of biodesulfurization conditions in a biphasic system with n-heptane as a model fuel. Using the Doehlert distribution for two factors (X₁: n-heptane:water ratio and X₂: initial cell concentration) an experimental design was performed and evaluated in terms of biodesulfurization activity.

Materials and methods

Microorganism and culture medium: This work was performed using the bacterium *Gordonia alkanivorans* strain 1B, cultivated in a SFMM medium with fructose (Alves et al., 2005; Pacheco et al., 2019).



Experimental design methodology: Following a Doehlert uniform shell design, an experimental distribution for two factors was used to produce response surfaces (Doehlert, 1970). Seven conditions were tested in duplicate, varying the ratio of n-heptane: water (X_1) between 0.1 and 0.9 and initial cell concentration (X_2) between 5 and 20 g/L (dry cell weight). Response was evaluated in terms of 2-HBP produced (the result of DBT biodesulfurization) in μM and results were collected at 3 and 6 h. The model used to express this response was a second-order polynomial model: $Y_i = \beta_0 + \beta_1 X_1 + \beta_2 X_2 + \beta_{12} X_{12} + \beta_{11} X_{12} + \beta_{22} X_{22}$ where Y_i , is the response from experiment i , β are parameters of the polynomial model and X is the experimental factor level (coded units).

Biodesulfurization assays: Cells were collected and centrifuged to obtain a concentrated cell suspension, which was then diluted in the supernatant to obtain different concentrations. n-Heptane was used as a model fuel with a concentration of 1.13 mM of DBT. Cells and n-heptane were placed in 30 mL screw cap tubes, at different ratios and the tubes were placed in an incubator at 30°C and 150 rpm.

Analytical methods: Cell concentration was evaluated through dry cell weight and 2-HBP concentration was determined through HPLC.

Results and discussion

G. alkanivorans strain 1B was able to desulfurize regardless of the ratio of n-heptane it was subjected to, indicating a significant resistance to solvents, which is fundamental for this bioprocess.

In terms of biodesulfurization activity, results demonstrate that both factors tested had a significant influence, but only for n-heptane: water ratios below 50% (0.5), with higher ratios the influence of these factors was greatly reduced. For ratios between 0.1 and 0.5, n-heptane: water ratio was the most influential factor, regardless of cellular concentration. This factor showed a clear negative influence, since any increase resulted in a loss of desulfurization activity. Conversely, within the same interval, any increase in cell concentration had a positive influence on the response, resulting in a biodesulfurization increase. Time was also shown to have a positive influence on most results, since desulfurization increased from 3 h to 6 h, with the exception of the 10% (0.1) ratio where the 1.13 mM of DBT were completely desulfurized in first 3 h. This indicates that, with an aqueous phase of at least 50%, it is possible to compensate for an increment in the fuel ratio by increasing cell concentration, and that this effect is greater for lower fuel ratios. According to this experimental design the best conditions for biodesulfurization are 10 % fuel (0.1 ratio) with 20 g/L biocatalyst and 3 h of biodesulfurization.

Conclusions

This work demonstrates that by increasing cell concentration it is possible to use greater fuel:water ratios maintaining high desulfurization activities, thus reducing reaction times and increasing process efficiency. Further optimization work is still needed, however, this gives important clues for the development of a large scale biodesulfurization process.

Acknowledgements: This work was financed by national funds through FCT (Fundação para a Ciência e a Tecnologia) in the scope of the project GreenFuel (PTDC/EAM-AMB/30975/2017). Tiago P. Silva also acknowledges FCT for his PhD financial support (SFRH/BD/104977/2014).

References

- Alves, L., Salgueiro, R., Rodrigues, C., Mesquita, E., Matos, J. and Gírio, F.M., 2005. Desulfurization of dibenzothiophene, benzothiophene, and other thiophene analogs by a newly isolated bacterium, *Gordonia alkanivorans* strain 1B. *Appl. Biochem. Biotechnol.*, 120(3), 199–208.
- Doehlert, D.H. (1970). Uniform Shell Designs. *J. R. Stat.*, 19(3), 231-239.
- Pacheco, M., Paixão, S.M., Silva, T.P. and Alves, L., 2019. On the road to cost-effective fossil fuel desulfurization by: *Gordonia alkanivorans* strain 1B. *RSC Adv.*, 9, 25405-25413.
- Silva, T.P., Alves, L. and Paixão, S.M., 2020. Effect of dibenzothiophene and its alkylated derivatives on coupled desulfurization and carotenoid production by *Gordonia alkanivorans* strain 1B. *J. Environ. Manage.*, 270, 110825.



Valorisation of crude glycerol in the production of liquefied lignin bio-polyols

F. Hernández-Ramos¹, M. González Alriols¹, J. Labidi¹ and X. Erdocia²

¹Chemical and Environmental Engineering Department. University of the Basque Country UPV/EHU, San Sebastian, Spain

²Department of Applied Mathematics. University of the Basque Country UPV/EHU, Bilbao, Spain
Corresponding author email: fabio.hernandez@ehu.eus

keywords: bio-polyol, organosolv lignin, crude glycerol, liquefaction.

Introduction

Polyurethanes (PUs) are one of the most relevant synthetic materials nowadays. PUs are formed by the polyaddition reaction between isocyanates and polyols which are usually petroleum-derived. However, the use of renewable resources, such as lignin are gaining relevance to produce polyols for PU. Lignin can be considered the most abundant renewable phenolic polymer on earth and due to its phenolic nature and its renewable raw material status, it has become an ideal resource for obtaining high-added-value chemicals, such as polyols (Hernández-Ramos et al., 2021). But despite its big potential lignin is treated as a waste and is employed as fuel in paper mills where it is produced. Despite this low value application, lignin can be directly used in small quantities without any modification in the polymer industry, however, mainly due to its low reactivity resulting from the steric hindrance of many of its hydroxyl groups, lignin is often modified to make these hydroxyl groups more accessible. Among others, liquefaction employing polyhydric alcohols such as, polyethylene glycol (PEG) and glycerol (Gly) as solvents, is one of the most studied methods to synthesise lignin based bio-polyols (Xue et al., 2015). In this process, technical grade glycerol is used, which can be obtained from both, the petroleum industry and the biodiesel industry. Nevertheless, glycerol from the biodiesel industry requires to be purified and this process is not economically viable since the cost of the process (50.85 \$/kg) is higher than the value of the final product (1-15 \$/kg) (Kumar et al., 2021). Therefore, in this work, *Eucalyptus globulus* and *Pinus radiata* organosolv lignins were liquefied employing PEG and crude glycerol from used vegetable oil employing microwave irradiation technology. The reaction conditions to obtain polyols for rigid and elastic PUs were optimised in a previous work

Materials and methods

Eucalyptus globulus and *Pinus radiata* organosolv lignins (EOL and POL respectively) were obtained following the procedure described in our previous work (Hernández-Ramos et al., 2021). EOL showed a molecular weight (Mw) and polydispersity index (PI) of 2837 g/mol and 3.196, while POL's Mw was 2924 g/mol and its PI 3.209.

The vegetable oil employed to obtain the crude glycerol was supplied by the restaurant of the Faculty of Engineering of Gipuzkoa in Eibar. The crude glycerol was obtained through a transesterification reaction employing methanol in a molar ratio of 6:1 (methanol:oil). KOH (1 %wt of oil) was employed as catalyst. The reaction was conducted at 60°C with constant stirring for 120 min under reflux. After that, the crude glycerol was separated from the biodiesel. The lignin liquefaction reaction was carried out employing a CEM Microwave Discover System Model, the solid liquid ratio was 1:6 and the reaction time was 5 min with sulphuric acid as catalyst. The optimised reaction conditions are summarised in Table 1.

Table 1. Liquefaction reaction conditions.

	Rigid bio-polyol		Elastic bio-polyol	
	EOPR	POPR	EOPE	POPE
Cat (% wt.)	0	0	5	3.86
T (°C)	161	159	180	160
PEG/Gly	3/1	3/1	7.75/1	7.34/1



Bio-polyols were characterised to determine the molecular weight distribution employing gel permeation chromatography (GPC)- The hydroxyl number (IOH) (mg KOH/g) and the acidic number (An) (mg KOH/g) were obtained using the ASTM D4274 and ASTM D974 standards, respectively. The functionality (f) of bio-polyols and yield were also determined.

Results and discussion

A summary of the results obtained from the characterisation of the bio-polyols is shown in Table 2.

Table 2. M_n and M_w (g/mol), PI, IOH and An (mg KOH/g) and functionality.

Sample	M_n	M_w	PI	IOH	An	f
EOPR	442 ± 34	1742 ± 275	4.25 ± 0.55	554±4	1.91 ± 0.06	4.16 ± 0.10
EOPE	941 ± 30	8818 ± 127	9.38 ± 0.16	228 ± 36	20.94 ± 2.75	3.51 ± 0.68
POPR	453 ± 24	1431 ± 362	3.14 ± 0.63	383±8	4.21 ± 0.90	3.14 ± 0.16
POPE	780 ± 20	5530 ± 131	7.10 ± 0.31	173 ± 16	25.09 ± 2.59	2.08 ± 0.27

Depending on the final application of bio-polyols, the M_w , IOH and the f should be between certain values. Thus, bio-polyols for rigid PU must have a M_w between 300-1000 (g/mol), an IOH between 200-1000 (mg KOH/g) and a f between 3-8. While for elastic PU these values are between 300-1000 (g/mol), 28-160 (mg KOH/g) and 2-3 respectively. Considering the above, the bio-polyols EOPE and POPE showed an appropriate M_w and f to be used in the manufacture of elastic PUs, however, the IOH was slightly beyond the desired values. On the other hand, the IOH and the f of EOPR and POPR bio-polyols were suitable to be used in the synthesis of rigid PUs, even though the M_w was somewhat higher than the desired values. It can also be observed that the catalyst had a significant relevance since the higher the catalyst concentration the higher the An and the lower the IOH (Lee et al., 2000). The higher M_w can be explained since in presence of an acid catalyst the repolymerisation reactions are favoured. The yield was also influenced by the catalyst due to the repolymerisation reactions, which increased the solid residue and therefore reduced the yield. Accordingly, EOPR and POPR showed yields above 90% while EOPE and POPE had yields between 70-80%.

Conclusions

Crude glycerol from vegetable oil were successfully employed together with PEG to produce bio-polyols through the liquefaction of organosolv lignins from *Eucalyptus globulus* and *Pinus radiata*. Although the IOH values of EOPE and POPE and the M_w of EOPR and POPR were slightly above that the desired values, the bio-polyols resulted suitable in the synthesis of PUs.

Acknowledgements: Authors would like to express their gratitude for the financial support of the University of the Basque Country (project COLAB20/04). F. Hernández-Ramos would like to acknowledge the Grant received from the Environmental Department of the Diputación Foral de Gipuzkoa.

References

- Hernández-Ramos, F., Alriols, M.G., Calvo-Correas, T., Labidi, J., Erdocia, X., 2021. Renewable Biopolyols from Residual Aqueous Phase Resulting after Lignin Precipitation. ACS Sustain. Chem. Eng. <https://doi.org/10.1021/acssuschemeng.0c09357>
- Kumar, L.R., Kaur, R., Tyagi, R.D., Drogui, P., 2021. Identifying economical route for crude glycerol valorization: Biodiesel versus polyhydroxy-butyrates (PHB). Bioresour. Technol. 323, 124565. <https://doi.org/10.1016/j.biortech.2020.124565>
- Lee, S.H., Yoshioka, M., Shiraiishi, N., 2000. Liquefaction of corn bran (CB) in the presence of alcohols and preparation of polyurethane foam from its liquefied polyol. J. Appl. Polym. Sci. 78, 319–325. [https://doi.org/10.1002/1097-4628\(20001010\)78:2<319::AID-APP120>3.0.CO;2-Z](https://doi.org/10.1002/1097-4628(20001010)78:2<319::AID-APP120>3.0.CO;2-Z)
- Xue, B.L., Wen, J.L., Sun, R.C., 2015. Producing lignin-based polyols through microwave-assisted liquefaction for rigid polyurethane foam production. Materials (Basel). 8, 586–599. <https://doi.org/10.3390/ma8020586>.



Kinetic Study of Transesterification of Waste Cooking Oil with Ultrasound

S. Savvopoulos¹, H. Hatzikirou¹, and I. Janajreh²

¹Department of Mathematics, Khalifa University of Science and Technology, Abu Dhabi, UAE

²Department of Mechanical Engineering, Khalifa University of Science and Technology, Abu Dhabi, UAE

Corresponding author email: isam.janajreh@ku.ac.ae

keywords: *ultrasound; biodiesel; transesterification; chemical kinetics; conversion metrics.*

Introduction

Biodiesel is a biofuel made from animal or vegetable fats including waste cooking oils that all referred as triglycerides. According to the chemistry, biodiesel consists of monoalkyl esters of saturated and unsaturated long-chain fatty acids. Stoichiometrically, one mole of triglyceride (TG) reacts with three moles of alcohol (AL: methanol or ethanol) to produce three moles of biodiesel and one biproduct model of crude glycerol. However, the main reaction is multiple steps with diglycerides (DG) and monoglycerides (MG) appearing as intermediates. Due to immiscibility of the reactants, stirring and excess alcohol molar ratio up to 12:1 have been used. This results in high waste yield and compromising the process metrics. Nevertheless, biodiesel is considered as a renewable, non-toxic, biodegradable, oxygenated, sulfur-free, and widely available fuel. Transesterification is the most prevalent method of producing biodiesel (Šánek et al. 2019). To stay with 1:3 molar ratio, we investigate the effect of the acoustic conditions in the biodiesel conversion using both numerical simulation and experimental analysis. One of the benefits of ultrasound is the generated cavitating bubbles and as they implode the reaction rates are intensified. Sonication is utilized in chemical manufacturing process of crystals and pharmaceuticals as well as nanomaterial synthesis, waste-water treatment, and biofuel production, oil-related applications and desalination (Janajreh et al. 2015, 2021).

Materials and methods

Restaurant franchises provided a variety of waste cooking oil samples. Five liters of McDonald waste oil samples were collected over five weeks period, mixed in a large 5 liter beaker and then heated under sun temperature to about 45 °C and subjected to 20 μ m paper filtration from suspended solid residues. The filter 5liter sample was then heated until 105°C for 8 hours under continuous stirring to get rid of any moisture. Two types of transesterification experiments then carried out: with and without sonication. The methoxide consists of mixture of granular of potassium hydroxide (sigma Aldrich) as the catalyst (at 1% oil ratio) and GCMS methanol grade 99.99% (sigma Aldrich) prepared using a magnetic stirring heating pad set at 50 °C and 250 rpm. The two different experiments were carried out in a closed 350 mL borosilicate glass beaker and each lasted for 100min and repeated three times (Hussain and Janajreh 2018). In each experiment, the beaker was filled with 200 mL of the filtered and dried waste cooking oil and the stipulated amount of methoxide, i.e., oil to methoxide molar ratio of 1:3, and 1:6 for sonication and regular stirring, respectively. The sonicating probe (horn) was submerged into the beaker that filled by mixture (see Fig. 1). Using 2.5ml sampling straws, 20 samples were collected from the beaker during each experiment that immediately stored in cold ice bath to stop sample reaction and thereafter used for GCMS five species (TG, DG, MG, Al, ester, and Glycerol) analyses.

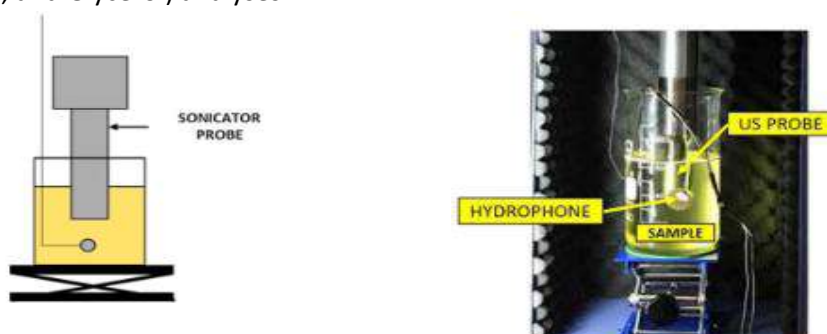


Fig. 1: Experimental setup.



Results and discussion

All the measurements were collected for model parameter estimation by applying Particle Swarm Optimizer (PSO). Fig. 2 shows how well the model fits the experimental data at 60°C in both conventional stirring sonicated conditions. The data measured were the concentrations of triglycerides (TG), diglycerides (DG), monoglycerides (MG), biodiesel (E), glycerol (GL), and alcohol (AL). The data reveals the effectiveness of sonication in rapid consuming the TG and formation of the ester. This is also due to the fast formulation of the DG and MG, that otherwise seemed to occur sequentially during conventional transesterification.

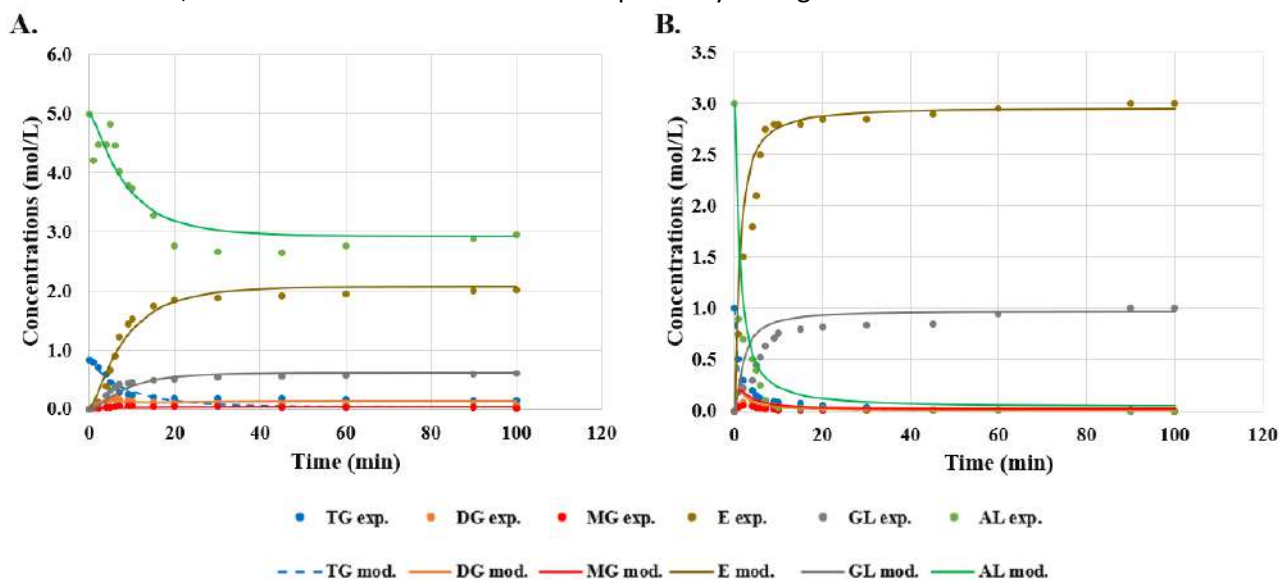


Fig. 2: Comparison of experimental data (points) and mathematical model prediction (lines) at 60 °C without ultrasound (left), and with the use of ultrasound (right).

It is noteworthy noticing the fast production of biodiesel under sonication and in reaching to the asymptotic limit earlier of nearly 10 minutes than the experiment under conventional conditions. Also, the efficiency was enhanced as the final concentration of the biodiesel was greater under sonication and at half of the molar ratio (1:3 vs 1:6). The transesterification kinetic parameters with the application of the ultrasound were calculated by fitting experiments at different temperatures. Comparisons of parameter values with or without ultrasound are to be presented, and discussed thoroughly.

Conclusions

Ultrasound in transesterification seems a promising technology in biofuel production. By using the kinetic parameters in tandem with more enlarged setups and different geometries, future research may enable a dynamic, and commercially efficient biodiesel production.

Acknowledgements: The support received by the Khalifa University of Science and Technology under Award No. RC2-2018-009 is highly acknowledged.

References

- Šánek, L., Jiří, P., Husár, J., and Kolomazník, K., 2019. Mathematical modeling of transesterification process kinetics of triglycerides catalyzed by TMAH. *MATEC Web of Conferences* (Vol. 292, p. 01027). EDP Sciences.
- Janajreh, I., ElSamad, T., AlJaberi, A. and Diouri, M., 2015. Transesterification of waste cooking oil: kinetic study and reactive flow analysis. *Energy Procedia*, 75, pp.547-553.
- Janajreh, I., Ali U., Hawwa M., 2021. Sonicated direct contact membrane distillation: Influence of sonication parameters, *Desalination* 533, 115779
- Hussain, M.N. and Janajreh, I., 2018. Acousto-chemical analysis in multi-transducer sonochemical reactors for biodiesel production. *Ultrasonics sonochemistry*, 40, pp.184-193.



Production of green hydrogen on Non-Interconnected Islands (NIIs) and combination with LNG: a modeling analysis of Lesvos (Greece)

N. Perivolari¹, A. Dimou¹ and S. Vakalis¹

¹Energy Management Laboratory, Department of Environment, University of the Aegean, Mytilene, Greece
Corresponding author email: nataperiv@gmail.com

keywords: hydrogen; non-interconnected islands; energy storage; LNG; energy analysis.

Introduction

Greece has several islands that are not interconnected to the mainland energy grid and rely on local power plants with diesel generators. Conventional renewable energy systems (RES) are also defined as VRE, (variable energy systems), and are characterized by significant fluctuations on their performance, due to their dependence on the regional climate. The national grid operator (HEDNO) has recorded 29 NIIs in Greece, and all of them have moderate RES penetration into their energy mix. The addition of storage and thermal valorization solutions can increase the RES penetration in small islands. However, bigger islands require integrated solutions and constant energy supply that can supplement the baseload and support energy intensive operations like industrial applications. In this framework, this study applied a model by Dimou and Vakalis (2021) that utilizes the energy produced by RES, considers RES excess scenarios and assesses the H₂ production for the case of Lesvos island. Lesvos is a unique case since an LNG power plant has been licensed to operate on the island. In this framework, the model found the operating times and hydrogen power generation capabilities of different Fuel Cells, while the co-combustion of NG with H₂ was assessed by means of the Wobbe Index.

Materials and methods

The RES and conventional energy generation for all NIIs have been collected by using the official published data of HEDNO. The first analysis involved the determination how many of the islands have RES, so that green hydrogen can be produced. The annual production considered only the VRE production, i.e., by photovoltaic and wind parks. The utilized model (Dimou and Vakalis, 2021) calculated the number of electrolyzers (Norsk HPE 30 & Teledyne EC-500) that can be installed on each island, the annual hydrogen mass production, and the operational times of seven different fuel cell models (including ZTEK, Ballard, Toshiba, and UTC Power). In addition, the amount of excess stored H₂ was calculated for each scenario. The Monte Carlo method was used for the sensitivity analysis of the model and in order to incorporate the fluctuation of energy production from RES. Regarding the combination of NG and H₂, the Wobbe index equation was used (Equation 1) and how its value varies if the two fuels are combined, with the percentage of each receiving values from 0 – 100% cumulatively.

Equation 1. Wobbe index equation for calculating x of LNG and H₂

$$Iw_{total} = \left(\frac{HHV_{CH_4}}{\sqrt{d_{CH_4}}} \times \frac{\% CH_4}{100} \right) + \left(\frac{HHV_{H_2}}{\sqrt{d_{H_2}}} \times \frac{\% H_2}{100} \right)$$

An additional analysis includes the use of the software RETScreen for Lesvos island, where the co-combustion of H₂, NG and biomass are considered for the reduction of the CO₂ footprint. Hydrogen fuel (ZTEK– SOFC modules) is used as the base load, natural gas (Mitsubishi Heavy Industries – MF111A) as the intermediate load and biomass (GE – JMS 320 GS-B.L) for the peak load. The latter type of fuel was proposed since Lesvos has a significant amount of biomass available for exploitation.

Results and discussion

Some of the main analysis results are represented in the following diagrams. Figure 1 shows the RES production, the number of electrolyzers and H₂ production for each large NII.

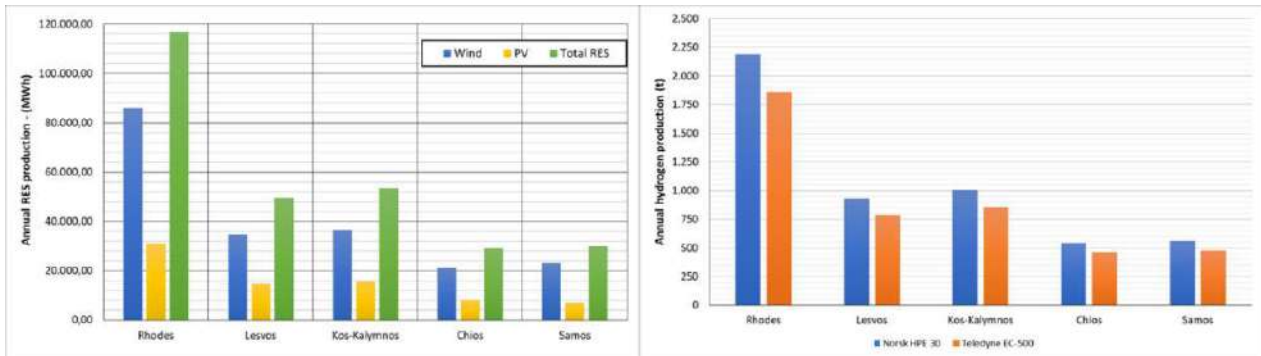


Figure 1. Number of electrolytic cells and H₂ production for each large NII.

Figure 2 shows the co-combustion of H₂, NG and biomass for Lesvos island. The chosen operating strategy is a full power capacity output in which the base load power system reaches a capacity of 2,9%, the intermediate load power system 92,6% and the peak load power system 7,8%. The modeling by RETScreen showed that approximately 1 MW of power could be produced by hydrogen fuel cells, while the co-combustion of hydrogen and natural gas is an achievable possibility with a Wobbe index that ranged within 48 – 53 MJ per cubic meter.

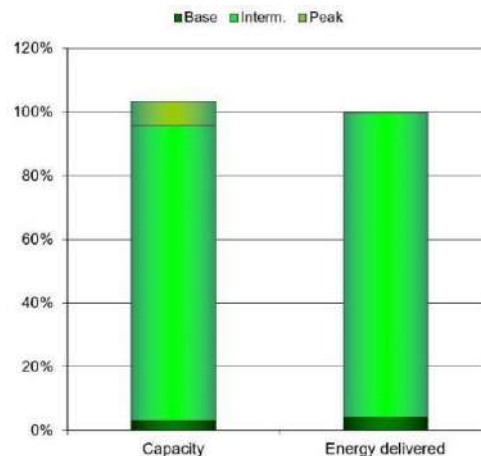


Figure 2. Co-combustion of H₂, NG and biomass for Lesvos island.

Conclusions

Bigger islands can support green H₂ production, while for smaller islands the practice is unsustainable. For these islands the model showed that there is a possibility of utilizing a certain amount of H₂. The results from H₂ production in Lesvos are optimistic, as they can support the local community in peak conditions and everyday life. The combined use of H₂ with NG show that it may be possible, which could lead to the gradual decoupling of the islands from conventional fuels and the greater penetration of RES into the energy mix.

References

- Atsonios, K., Samlis, Ch., Manou, K., Nikolopoulos, A., Sfetsioris, K., Mitsotakis, A. & Grammelis, P., 2021. Technical assessment of LNG based polygeneration systems for non-interconnected island cases using SOFC. *International Journal of Hydrogen Energy*, 46, 4827 – 4843.
- Dimou, A. and Vakalis, S., 2021. Assessing the utilization of fuels cells for the valorization of produced excess energy in isolated grids – the green transition of Agios Efstratios. *CEST 2021 – 17th International Conference on Environmental Science and Technology*. 1-4 September 2021, Athens (Greece).



SUST
ENG
2022



WATER RESOURCES MANAGEMENT



Critical insights to drive sustainable water management in process industries

E. Karkou¹, N. Savvakis¹ and G. Arampatzis¹

¹School of Production Engineering and Management, Technical University of Crete, Chania, Greece
Corresponding author email: garampatzis@tuc.gr

keywords: *water management; process industry; water reuse; circular; modelling.*

Introduction

The industry confronts water stress due to the limited availability of resources. In this regard, industrial water management needs to be enhanced to mitigate the consequences of the water crisis (Diaz, 2021). Freshwater intake reduction, water reuse and recycling practices, advanced water treatment technologies incorporation, and closed-loop water reuse technologies encompass compact solutions (Kinnunen et al., 2021).

In the process industry, wastewater treatment and reclamation of water prove the importance of sustainability by implementing the zero liquid discharge (ZLD) approach (Panagopoulos, 2022). Furthermore, the potential synergies between process industries, which operate in the same or different fields, focus on exchanging water and materials. By-products are utilized within the developed network of interrelated industries and other actors, e.g., the municipality (Ashton et al., 2022).

Previous studies have examined the technologies for wastewater treatment and resources recovery (Dutta et al., 2021), the mathematical models of advanced processes (Lindamulla et al., 2021), and the practices that interrelate with the circular economy (Mbavarira & Grimm, 2021) and the industrial symbiosis (Mohan & Katakajwala, 2021). However, no study examines sustainable water management practices in the industry and the development of models to control and optimize the system simultaneously. The purpose of this research is on the one side to help identify the core aspects of sustainable water management in the industrial sector, along with identifying the potential levels of modelling that could be applied.

Methodology

A thorough scientific literature review was carried out to identify and analyse the water management options in the industry. The developed methodology presupposes the analysis of each step to evaluate the potential outcomes and support the decision-making process:

- Definition of system boundaries and objectives
- Design of the detailed process flow diagram
- Map the water sources, reuse and recycle options
- Determination of water quality requirements
- Identification of involved actors and their interdependencies
- Selection and development of the appropriate model
- Integration and simulation of the whole system.

The case studies for demonstrating this methodology are the industries of Dow, Solvay, BASF, Agricola plant, Jems, and Tüpraş petroleum refinery company.

Results and discussion

Sustainable water management focuses on (a) decreasing the demand for water resources, (b) improving the performance of the existing treatment technologies, (c) incorporating advanced processes for water production of high quality, and (d) utilizing all by-products by preventing waste production.

It is essential to predict the water quality and the processes' performance through models. The levels of modelling emanate from the necessities of different use cases. Firstly, water can be reused within a treatment process, e.g., a membrane bioreactor, to reduce the fresh feed water, and enhance and optimize the process performance (in-process modelling). Expanding across the whole factory (in-factory modelling), water mass balance is a tool to quantify water demand and production and detect possible sources of water losses either intra-process or intra-factory closed loops. In addition, a factory may collaborate with other



industries by exchanging relevant materials, resulting in optimisation of water and valuable substances allocation (industrial symbiosis). Finally, water reuse and circular practices among different actors are modeled (systemic modelling) by incorporating the water cost and quality requirements, as well as their related interdependencies. Figure 1 depicts the levels of modelling.

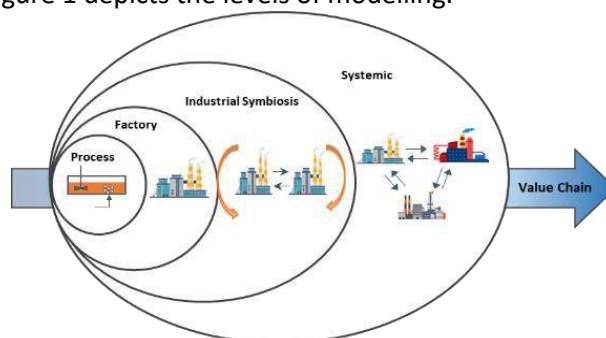


Figure 1. Levels of modelling in the equivalent sector to be deployed.

European process industries represent the demonstration sites to give prominence to the modelling. In-process modelling includes the development of mathematical models to predict the performance of advanced technologies, including granular activated carbon, ultrafiltration, advanced oxidation, and reverse osmosis. It is applied to Dow chemical company, Solvay plant, BASF, Agricola, and Tüpraş plant. In-factory modelling is demonstrated in Dow by describing water mass balances. In addition, the aforementioned industries may supply their generated wastewater to the Jems plant to recreate new added-value products. Thus, the modelling of the industrial symbiosis is deployed. Finally, Solvay interacts with the municipality and the Aretusa reclamation plant by exchanging water. Hence, a systemic model has been developed.

Conclusions

The transition to the circular economy requires the deployment of different levels of modelling based on the case-specific requirements for predicting the behavioral responses of each involved actor. Hence, fit-for-purpose closed-loop approaches are adopted to reinforce the sustainability of the industrial sector.

Acknowledgements: The research methodology and results are part of the H2020-AquaSPICE project. This project has received funding from the European Union's Horizon-2020 research and innovation program under grant agreement No. 958396. The responsibility for this publication lies only with the authors.

References

- Ashton, W. S., Chertow, M. R., & Althaf, S., 2022. Industrial Symbiosis: Novel Supply Networks for the Circular Economy. In *Circular Economy Supply Chains: From Chains to Systems*, 1st ed.; Emerald Publishing: UK.
- Diaz, L., 2021. Water footprint: A sustainability tool for industries. In *Sustainable Industrial Water Use: Perspectives, Incentives, and Tools*, 1st ed.; IWA Publishing: London, UK.
- Dutta, D., Arya, S., & Kumar, S., 2021. Industrial wastewater treatment: Current trends, bottlenecks, and best practices. *Chemosphere*, 285, 131245.
- Kinnunen, P., Obenaus-Emler, R., Raatikainen, J., Guignot, S., Guimerà, J., Citroth, A., & Heiskanen, K., 2021. Review of closed water loops with ore sorting and tailings valorisation for a more sustainable mining industry. *Journal of Cleaner Production*, 278, 123237.
- Lindamulla, L. M. L. K. B., Jegatheesan, V., Jinadasa, K. B. S. N., Nanayakkara, K. G. N., & Othman, M. Z., 2021. Integrated mathematical model to simulate the performance of a membrane bioreactor. *Chemosphere*, 284, 131319.
- Mbavarira, T. M., & Grimm, C., 2021. A systemic view on circular economy in the water industry: Learnings from a belgian and dutch case. *Sustainability*, 13, 3313.
- Mohan, S. V., & Katakajwala, R., 2021. The circular chemistry conceptual framework: A way forward to sustainability in industry 4.0. *Current Opinion in Green and Sustainable Chemistry*, 28, 100434.
- Panagopoulos, A., 2022. Brine management (saline water & wastewater effluents): Sustainable utilization and resource recovery strategy through Minimal and Zero Liquid Discharge (MLD & ZLD) desalination systems. *Chemical Engineering and Processing - Process Intensification*, 176, 108944.



Assessment of groundwater contamination vulnerability using machine learning algorithms

K.H. Park¹, S.Y. Chung¹ and H.E. Elzain¹

¹Department of Earth & Environmental Sciences, Pukyong National University, Busan, Korea
Corresponding author email: chungsy@pknu.ac.kr

keywords: groundwater contamination vulnerability; DRASTIC; SVR; RFR; statistical criteria.

Introduction

Groundwater is an important water resources for human, agricultural, and industrial activities. However, groundwater contamination is continuously increasing in the world because of many kinds of contaminants. The preservation of groundwater from the contamination is our essential task and the accurate assessment of groundwater contamination vulnerability is required in advance of acting plan.

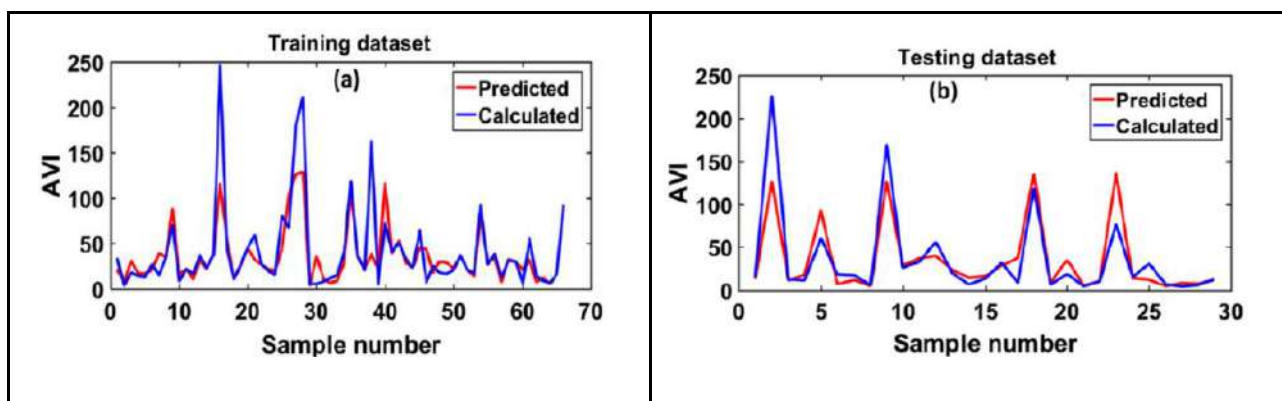
Materials and methods

Original DRASTIC method (ODM) developed by Aller et al. (1987) has been widely used for the assessment of groundwater vulnerability in the world. By the way, weights of seven factors of ODM are determined by the subjective decision of Aller et al. and the weights are not matched with the conditions of contaminated sites. Thus, many methods are developed for more effective assessment. In this research, Machine Learning Methods of Support Vector Machine (SVR) (Drucker et al., 1997) and Ensemble Random Forest (RFR) (Breiman, 2001) are used for the assessment of groundwater in Miryang City of Korea. The validation of two methods was carried out by the statistical criteria (MAE, RMSE, ρ), graphical comparisons, ROC/AUC and spatial distribution maps.

Results and discussion

Table 1. Statistical results of two machine learning methods

Model	Training Phase			Testing Phase		
	RMSE	MAE	ROC/AUC	RMSE	MAE	ROC/AUC
SVR	28.61	14.09	0.82	25.33	13.71	0.87
RFR	9.99	5.81	0.97	12.66	9.92	0.96



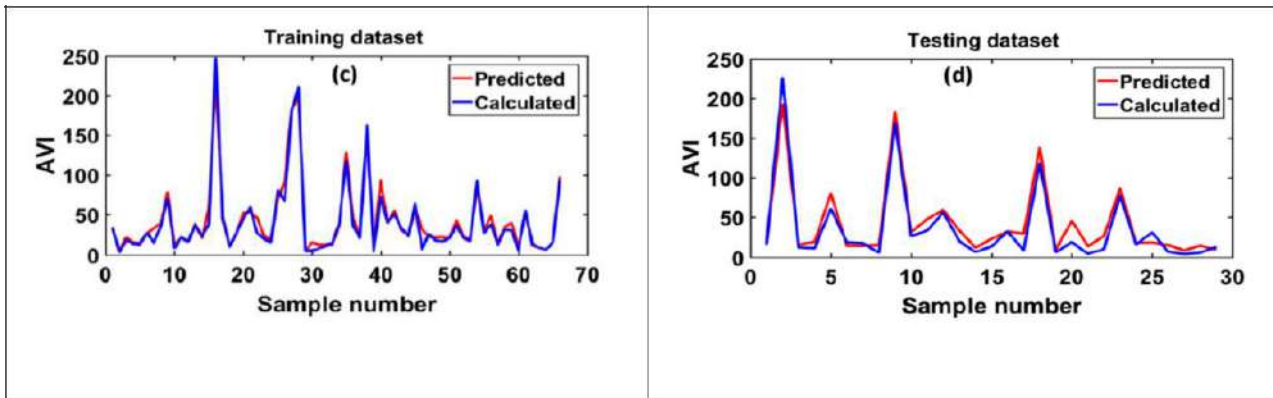


Figure 1. Predicted and calculated AVIs of SVR (a, b) and RFR (c, d) in training and testing phases.

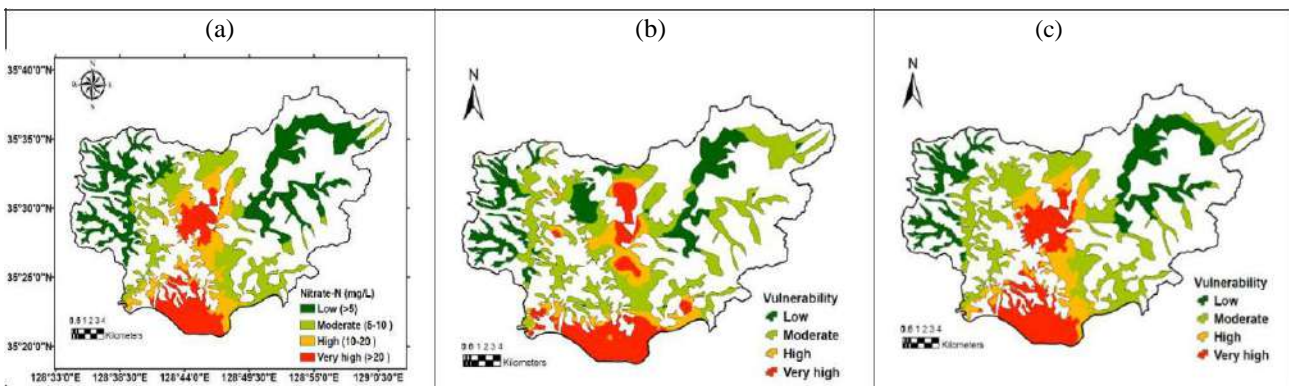


Figure 2. (a) Concentration map of nitrate, (b) Vulnerability map of SVR, (c) Vulnerability map of RFR.

Conclusions

Statistical and ROC/AUC values (Table 1) and graphical expressions (Fig. 1) showed the better performance of RFR technique. Spatial distribution maps (Fig. 2) using the predicted AVIs also represented that RFR produced the more superior result than SVR (Fig. 2b). The map of RFR (Fig. 2c) was very similar to the original nitrate concentration map (Fig. 2a). Therefore, it was understood that RFR method carried out the better performance in the evaluation of groundwater contamination vulnerability in Miryang City, Korea.

Acknowledgements: This research was supported by the Basic Science Research Program through the National Research Foundation of Korea (NRF) funded by the Ministry of Education (2019R1D1A3A03103683).

References

- Aller, L., Bennett, T., Lehr, J., Petty, R.J., Hackett, G., 1987. DRASTIC: A Standardized System for Evaluating Ground Water Pollution Potential Using Hydrogeologic Settings. US Environmental Protection Agency, Washington, DC, p. 455.
- Breiman, L., 2001. Random forests. *Mach. Learn.* 45 (1), 5–32.
- Drucker, H., Burges, C.J., Kaufman, L., Smola, A., Vapnik, V., 1997. Support vector regression machines. *Adv. Neural Inf. Process. Syst.* 9, 155–161.



Satellite-Derived Bathymetry: Machine Learning Approach in the study of water supply reservoirs

L. Coelho de Andrade¹, A. Amaral e Silva¹, I. Oliveira Ferreira¹, F.C. Mesquita Santos¹, V. Gibrim Teixeira¹ and M.L. Calijuri¹

¹Department of Civil Engineering – Federal University of Viçosa, Viçosa, Brazil
Corresponding author email: arthuramaral.e.a@gmail.com

keywords: *satellite-derived bathymetry; Machine Learning; reservoirs.*

Introduction

The use of optical remote sensing in bathymetry is notorious nowadays. The need to map locations that pose a risk to the ship's crew or those that are very shallow makes it impossible for a traditional bathymetric survey to be carried out with echo sounders and large vessels. However, the periodic calculation of reservoirs' bathymetries can show the evolution of geomorphological features and help manage water supply reservoirs.

Furthermore, the use of acoustic systems is time-consuming, expensive, and requires a great deal of experience from the operator. However, with the technological evolution, several orbital systems can provide centimetric accuracy at a lower cost than echo sounders in a different scenario.

Services such as controlling the sedimentation level of the reservoir, and checking the water quality, among other activities that directly assist in the characteristics of the reservoir, can be monitored using orbital images without the need to carry out bathymetric surveys. In addition, environmental impacts in the study area, which may interfere with the availability of water directed to the population's supply, can be studied and even mitigated with satellite monitoring.

In this context, this work aimed to evaluate the potential of CBERS 4A images in determining the bathymetry of reservoirs using the Machine Learning (ML) algorithm called Gradient Boosting Machine (GBM). A reservoir belonging to the São Francisco River Integration Program (PISF) was used as the study area, which aims to provide water supply for the population living in the northeastern arid areas.

Materials and methods

To carry out this research, the ML GBM algorithm was used in CBERS 4A images, specifically the WPM sensor (spatial resolution of 8 meters), in the Muquém reservoir, located in the state of Ceará.

The Muquém reservoir is located in the municipality of Cariús, in the state of Ceará. It has a drainage area of approximately 298 km² and a volume of 47.64 hm³. Regarding the main water demands of the reservoir in question, it has the highest demand for irrigation activities, followed by animal watering, rural, and urban supply, respectively.

To improve the training and consequently the data prediction, the NDTI (Normalized Difference Turbidity Index) and NDWI (Normalized Difference Water Index) were considered in the algorithm. Notably, 70% of the bathymetric points were used for training and 30% for testing, the algorithm was configured to perform 50 repetitions, and there was no trend in the data.

In this sense, the data from satellite-derived bathymetry were later compared with those collected traditionally, using the echo sounder. The RMSE (Root Mean Square Error) and MAE (Mean Absolut Error) estimators were used to quantify the vertical uncertainty of the estimated data. In addition, the volume generated by the two surfaces created with data from traditional bathymetry and that derived from the satellite was also compared after creating a digital model with the simple kriging interpolator.

Results and discussion

After training the data in the GBM algorithm, the bathymetry prediction was performed with the radiance pixel values of the CBERS 4A image, together with the NDWI and NDTI values for each point randomly selected for the test set. Thus, after 50 repetitions, it was possible to obtain an average vertical uncertainty of 0.47 meters for the RMSE and 0.34 meters for the MAE. In addition, after interpolating the estimated



depth and the reference bathymetry (collected with an echo sounder), it was possible to obtain the following Digital Depth Models, as shown in Figure 1.

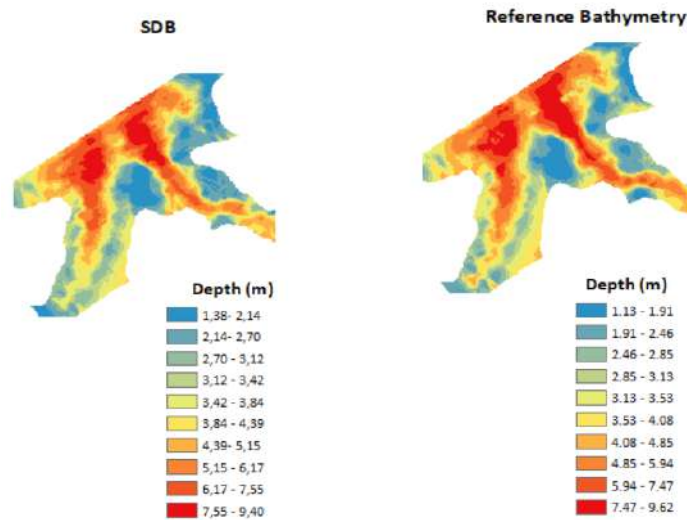


Figure 1. Digital Depth Models for SDB and Reference Bathymetry.

From these models, the volume calculation was performed, which showed a difference of 4% between the Satellite-Derived Bathymetry (SDB) and the reference. Thus, a high coercivity of the predicted data was evidenced, demonstrating reliability in using the methodology in question for the study of reservoirs. Thus, allowing the application of this method in environmental studies, the management of reservoirs, and the identification of sedimentation levels of water bodies, among others. It can also collaborate in reducing time and cost since the CBERS 4A images are available for free when compared to the traditional method of depth collection, using acoustic sensors.

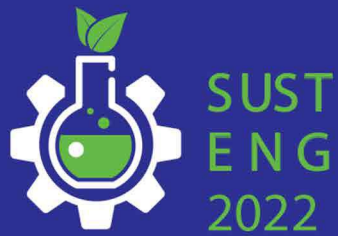
Conclusions

The study showed the potential of CBERS 4A images in conjunction with the GBM algorithm in estimating reservoirs' bathymetry, especially in collaboration with the region's preliminary environmental studies and water supply. The methodology will greatly facilitate the study of the water capacity of all the São Francisco River Integration Program reservoirs and the systematic analysis of the level of silting they are suffering. Furthermore, this way allows the identification of the impacts of anthropization in the reservoirs, not only on the PISF but also on other water bodies with similar characteristics.

Acknowledgements: This work was carried out with the support of CAPES - Financing Code 001.

References

- ANA - Agência Nacional de Águas, 2016. Reservatórios do Semiárido Brasileiro: hidrologia, balanço hídrico e operação – Muquém/CE.
- Cahalane, C., Magee, A., Monteys, X., Casal, G., Hanafin, J., & Harris, P., 2019. A comparison of Landsat 8, RapidEye and Pleiades products for improving empirical predictions of satellite-derived bathymetry. *Remote sensing of environment*, 233, 111414.
- Ferreira, Í.O., Rodrigues, D.D., Santos, G.R, 2015. Collection, processing and analysis of bathymetric data. 1^a ed. Saarbrücken: Novas Edições Acadêmicas, v. 1, 100p.



WASTEWATER TREATMENT



Mechanism of polyphosphate formation and degradation in wastewater treatment plants

Y. Bai¹, L. Stout¹, J. Li¹ and D. Jaisi¹

¹Harker Interdepartmental Science and Engineering Laboratory, University of Delaware, Newark, DE USA
Corresponding author email: jaisi@udel.edu

keywords: biological phosphorus removal; Polyphosphate; formation; degradation; phosphate oxygen isotopes; *Pseudomonas*.

Introduction

Enhanced biological phosphorus removal (EBPR) is the state-of-the-art technology in wastewater treatment plants. In the EBPR process, phosphorus (P) is removed as polyphosphate (poly-P). The P-accumulating organisms (PAOs) and thus the formation of poly-P respond strongly to oxic-anoxic conditions and P availability (Deinema et al., 1980). Despite several years of intensive research into PAOs and EBPR, the mechanism of synthesis and degradation of poly-P remain poorly known.

Materials and methods

This research investigated the mechanisms of poly-P cycling at different scales, from enzyme-substrate reaction to pure bacterial cell culture and to field study in a wastewater treatment plant. It included measurements of P speciation [orthophosphate (PO₄) and poly-P], enzyme activity, microbial gene expression, and phosphate oxygen isotopes (¹⁸OP).

Results and discussion

Enzyme reaction results show that both acidic phosphatase and alkaline phosphatase enzymes are capable of catalyzing poly-P degradation, with contrasting efficiency of > 70% and < 18%, respectively. Isotope fractionation factors during enzymatic degradation of poly-P varied from +1.6‰ to +4.4‰, a positive fractionation factor, which is uncommon and hence distinct from the degradation of many other organic P compounds. Results from pure culture experiments with *Escherichia coli* JM103 and *Pseudomonas putida* KT2440 suggest that poly-P synthesis and degradation are strongly associated with the cell growth stage: poly-P is synthesized during exponential growth, causing an apparent isotope fractionation (~+5‰) in the residual PO₄ in *E. coli* incubation (Bai et al., 2020). Degradation of poly-P in the late stationary phase, however, leads to lighter ¹⁸OP values. Poly-P cycling in treatment plants responded strongly to variations in dissolved oxygen concentrations: under oxic condition high amount of poly-P suggest poly-P synthesis, while the lighter ¹⁸OP values suggest rapid microbial P cycling potential via organic matter degradation. Under the anoxic condition, degradation of poly-P was accompanied by continued assimilation of PO₄, as suggested by a decrease in concentration and heavier ¹⁸OP values.

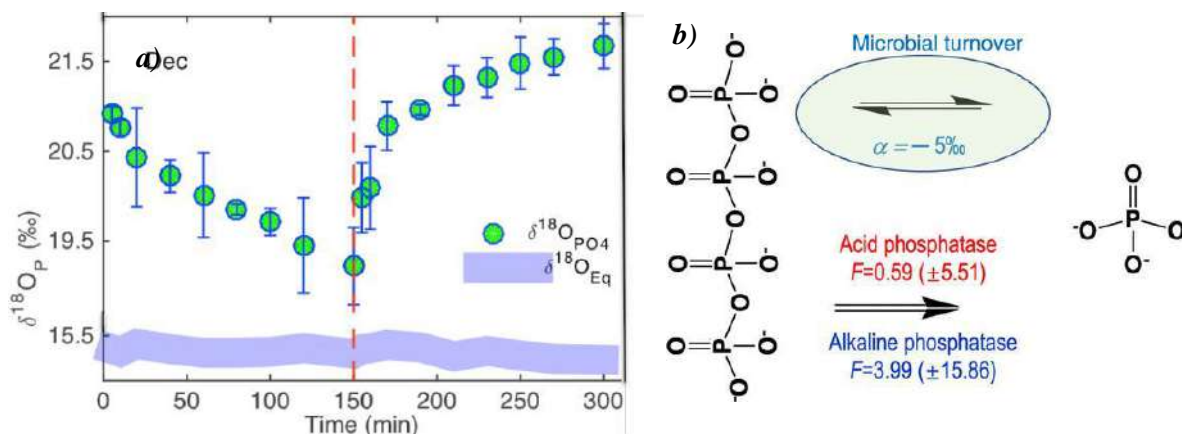


Figure 1. a) Isotope excursion in the aeration basin of a wastewater treatment facility. The vertical red dashed line represents the switching of anoxic condition (by stopping aeration) and the purple light color zone represents the calculated equilibrium values. b) Schematics of polyphosphate hydrolysis and accompanying fractionation factor.



Conclusions

The findings of this research are intriguing and indicate a potential alternative mechanism of poly-P cycling in the wastewater treatment plants that some microorganisms may continue to take up PO_4 under the anoxic condition even though degradation of poly-P and release of PO_4 are otherwise common processes under this condition. Nonetheless, specific isotope values, fractionation factors, and P dynamics during poly-P synthesis and degradation could serve as useful proxies to interpret poly-P dynamics in the environment.

Acknowledgements: This study is supported by the National Science Foundation (NSF 1709724).

References

- Bai, Y., Stout, L., Tosun, G., Li, J., and Jaisi, D., 2020. Synthesis and degradation of polyphosphate: Isotope effects in enzyme- and bacteria-catalyzed reactions. *ACS Earth and Space Chemistry*, 4, 2327-2336
- Deinema, M., Habets, L., Scholten, S., Turkstra, E., Webers, H., 1980. The accumulation of polyphosphate in *Acetobacter* spp. *FEMS Microbiology Letters* 9: 275-279.



Advancement in waste-water treatment technologies

F. Dziike¹

¹Technology Transfer and Innovation Directorate, Durban University of Technology, Durban, South Africa
Corresponding author email: FaraiD1@dut.ac.za

keywords: *nanomaterials; photocatalyst; bio-digestion; oxidation; flocculation.*

Introduction

Conventional waste-water treatment (WWT) has large carbon footprint and mostly Remove only simple organics in 2⁰ biological treatments.¹ The pain of persistent organics in water in compounded by complex organics from pharmaceutical industries, personal care products, petrochemical industry process waters, and textile industries which are not removed through the conventional WWT methods. The complex dissolved organics pose as serious environmental pollutants. There is a need for advanced 3⁰ technologies but current methods are expensive despite hundreds of advanced oxidation research groups globally trying to develop treatment technological processes that are both more innovative, cost effective, more efficient, off-grid and less maintenance.²

Materials and methods

Titania was prepared using a simple hydrothermal method of synthesis to produce electrophotocatalytic nanomaterials constructed into “dandelion-like structures called radially aligned nanorutile (RANR) nanoparticles.³ The catalyst materials were tested at laboratory scale to decompose methyl orange dye in a simulated solar electro photochemical reactor. The set up was scaled up and prototyped for an industrial scale application. An engineering process plant was assembled incorporation a bio digester for gray and black waste water treatment.

Results and discussion

Titania was successfully prepared as nano rutile nanorods (RANR) from titanium tetrachloride using a simple hydrothermal method. The nano photocatalyst material efficiently degraded methyl orange dye material dissolved in water as a control organic waste. The degradation efficiency ranged from 80 – 98 % over a 2 h time period in a parametric set up with 50 ppm organics over 50 mg catalyst materials.



Figure 1. Reaction interface of the catalyst and organic molecules during photo degradation process.

The catalyst material was successfully fitted on a fixed bed in a solar photocatalyst reactor in an engineering assembly of a solar waste water treatment plant comprising a bio digester and the novel reactor for the treatment of black and gray water for safe environmental disposal and potable purposes.



Conclusions

- The Catalytic Ozone Reduction, Regenerative Activated Carbon and UV light are processes that perform the same task
- Use of multi-components that replicate same performance task is costly, complicated and unnecessary.
- The unique nano-photocatalyst is a very powerful technique than a combination of COR, RAC and a simple UV light technique.
- COR and RAC are competing technologies to the IYHTS nano-photocatalysis treatment process that is both more innovative, cost effective, more efficient, off-grid and less maintenance.

Acknowledgements: This study is supported by the South African National Research Fund (NRF) and Durban University of technology.

References

- Hollender, J. et al. Elimination of organic micropollutants in a municipal wastewater treatment plant upgraded with a full-scale post-ozonation followed by sand filtration. *Environ. Sci. Technol.* 43, 7862–7869 (2009).
- Pei, M. et al. State of the art of tertiary treatment technologies for controlling antibiotic resistance in wastewater treatment plants. *Environ. Int.* 131, 105026 (2019).
- Bouleglimat, E. Materials for the photocatalytic treatment of recalcitrant organic waste. (2017).



Development of a greenhouse and screw conveyor solar driers for the treatment of faecal sludge from on-site sanitation facilities

S. Septien¹, P. Naidoo¹, A. Ramlucken¹, A. Ganapathie², Y. Pather², A. Singh², J. Pocock², F. Inambao³ and C. McGregor⁴

¹WASH R&D Centre, University of KwaZulu-Natal, Durban, South Africa

²Chemical Engineering Discipline, University of KwaZulu-Natal, Durban, South Africa

³Mechanical Engineering Discipline, University of KwaZulu-Natal, Durban, South Africa

⁴STERG, University of Stellenbosch, Stellenbosch, South Africa

Corresponding author email: septiens@ukzn.ac.za

keywords: *faecal sludge; on-site sanitation; solar thermal drying; temperature; drying rate.*

Introduction

Thermal drying is an important unit operation in faecal sludge treatment. It drastically reduces the mass and volume of the waste by removing its moisture and pathogen content. However, this process requires a high energy input due to the high latent heat of vaporization of pure water (2 260 kJ/kg), which can lead to high running costs due to high electricity or fuel consumption. To decrease the costs of the drying process, it is therefore imperative to find a low-cost or free source of energy, such as solar energy. Several solar thermal technologies have been developed for sewage sludge, such as greenhouse solar-type driers (Shanahan et al., 2010), solar roof dryers (Wang et al., 2019) and cabinet solar drier (Ameri et al., 2018) but almost no information has been found in literature for faecal sludge apart some isolated cases (Muspratt et al., 2014; Seck et al., 2015).

The aim of this work is to develop solar thermal drying technologies that harness the solar thermal energy in an efficient way and that are designed as a function of the sludge characteristics. Two different types of technologies were selected for their development, i.e. greenhouse-type solar drier and screw conveyor solar drier. The prototypes were built at pilot-scale to be able to process several kg of faecal sludge per day. After construction, the technologies were tested to measure their performance, find the optimum operating conditions, and identify improvement points. Based on these results, a technical-economic analysis will be performed for the upscaling and implementation of the technologies in faecal sludge treatment facilities.

Materials and methods

The greenhouse prototype consists in a solar dryer where faecal sludge will be placed in a bed and dried using solar thermal energy. The prototype offers an enclosed space where the solar thermal energy can be collected through greenhouse effect and the presence of an absorber wall. It includes a ventilation system and sludge rake system to boost the drying process. The sludge bed will stand on a suspended grid, which will let the sludge to dry also from the bottom.

In the screw conveyor solar drier prototype, the sludge will be dried during its passage through a transparent tube exposed to solar radiation (drying chamber). During this process, the sludge will absorb the solar thermal energy and use it as latent heat for moisture evaporation. An air stream will circulate inside the drying chamber to enhance the drying process. The air stream will be dehumidified and heated before introduction in the drying chamber. Reflectors will be placed next to the drying chamber to increase the amount of solar radiation received by the sludge.

The first experiments in the solar thermal drying technologies were carried out to test the individual components of the prototype and the integrated system without feedstock. Thereafter, the solar driers were tested using water (greenhouse), wet soil (screw conveyor) and synthetic faecal sludge (screw conveyor) as feedstock. The parameters measured during the tests were the temperature and relative humidity at different positions in the system, the ambient conditions (including temperature, relative humidity and solar irradiance) and the moisture content of the sample during the run. The tests were performed from 9 AM to 2 PM during the months of April and May in Durban, South Africa (corresponding to the autumn).



Results and discussion

During the tests in the greenhouse solar drier, it was observed that temperatures inside the enclosure were higher with respect to the ambient conditions (+10-15°C), leading to lower relative humidities. If the fans were turned on, the temperature in the greenhouse decreased of a few degrees, leading to a lower performance. This result suggests that the increase of ventilation leads to lower temperature rise inside the greenhouse. An evaporation rate was measured in the order of 2.5 kg/h/m² when conducting the tests with water.

The testing results from the screw conveyor prototype are promising, with the functionality tests showing that the systems functioned well together, leading to an important temperature increase (up to 45-50°C) and relative humidity decrease (below 30%) before the drying chamber. The drying tests with wetted soil resulted in a good performance with most of moisture being removed from the soil after less than 30 minutes of operation. The testing with synthetic sludge showed also positive results, with moisture removal in the region of 20% to 50% in 2 hours. The performance of the dryer was improved greatly by ensuring that the reflectors were in the optimal position. The most optimal conditions were obtained when the ventilation was operated at low air flowrate, as the maximum temperatures achieved in the system were higher (after the solar air heater), leading to a higher moisture removal from the synthetic sludge. It was also found that the sludge was extremely difficult to work with because of its high stickiness.

After the testing phase for both prototypes, improvements have been identified for the next round of iteration.

Conclusions

The testing results for the greenhouse solar-drier and screw conveyor were positive. From the first results, the greenhouse would be able to dry 0.1 m³ faecal sludge (bed of 1 m² surface area and 100 mm of thickness) from an initial moisture content of 80% (typical value for the sludge from local pit latrines) to 20% in approximately 36 h (equivalent to 5 days considering 7 hours of full sunlight per day). The screw conveyor achieves to the same result in a few hours, but the sludge stickiness is a critical problem that must be resolved to achieve sustainable long operation times.

Acknowledgements: The authors would like to acknowledge the funders from this project (Water Research Commission through the K5/2852 project and the Royal Academy of Engineering through TSP2021_100224 Grant), as well as the eThekweni municipality and the administrative and technical staff from the WASH R&D Centre (in particular, Poovalingum Govender, Thabiso Zikalala, Kerry Lee Philp, Nombuso Mtshali and Lungile Ndlela).

References

- Ameri, B., Hanini, S., Benhamou, A., and Chibane, D., 2018. Comparative approach to the performance of direct and indirect solar drying of sludge from sewage plants, experimental and theoretical evaluation. *Solar Energy*, 159, 722-732.
- Murray Muspratt, A., Nakato, T., Niwagaba, C., Dione, H., Kang, J., Stupin, L., Regulinski, J., Mbéguéré, M., and Strande, L., 2014. Fuel potential of faecal sludge: calorific value results from Uganda, Ghana and Senegal. *Journal of Water, Sanitation and Hygiene for Development*, 4 (2): 223–230.
- Seck, A., Gold, M., Niang, S., Mbéguéré, M., Diop, C., and Strande, L., 2015. Faecal sludge drying beds: increasing drying rates for fuel resource recovery in Sub-Saharan Africa. *Journal of Water, Sanitation and Hygiene for Development*, 5(1), 72-80.
- Shanahan, E. F., Roiko, A., Tindale, N. W., Thomas, M. P., Walpole, R., & Kurtböke, D. İ., 2010. Evaluation of pathogen removal in a solar sludge drying facility using microbial indicators. *International Journal of Environmental Research and Public Health*, 7(2), 565-582.
- Wang, P., Mohammed, D., Zhou, P., Lou, Z., Qian, P., and Zhou, Q., 2019. Roof solar drying processes for sewage sludge within sandwich-like chamber bed. *Renewable Energy*, 136, 1071-1081.



Primary filtration systems as a viable solution to overloaded municipal wastewater treatment plants

K. Tsamoutsoglou¹, P. Gikas¹, N. Karamanes², M. Mavri² and K. Christofinas³

¹Design of Environmental Processes Laboratory, School of Chemical and Environmental Engineering, Technical University of Crete, Chania, Greece

²Municipal Enterprise for Water Supply and Sewerage of Paros, Greece

³Sewerage Board of Kyperounda (SBK), Cyprus

Corresponding author email: pgikas@tuc.gr

keywords: wastewater treatment plant; primary filtration; energy savings; capacity increase.

Introduction

Numerous Wastewater Treatment Plants (WWTPs) operate at flow-rates or loads above to their designed capacity, leading to insufficient wastewater treatment. Primary Filtration (PF) systems are emerging technologies in wastewater treatment, providing substantial benefits to overloaded WWTPs. PFs are currently under installation at the activated sludge WWTPs of Kyperounda, Limassol (Cyprus) and Marpissa, Paros (Greece), with average hydraulic capacities of 1,800 and 2,500m³/d, respectively. Following the installation and operation of PFs, both WWTPs will be able to receive increased loadings, at reduced energy and operational costs.

Innovation

The innovation of the present study lies in the removal of suspended solids upstream of the aeration tank, using a combination of microsieves, sandfilters and lamellar settling tanks (Figure 1).

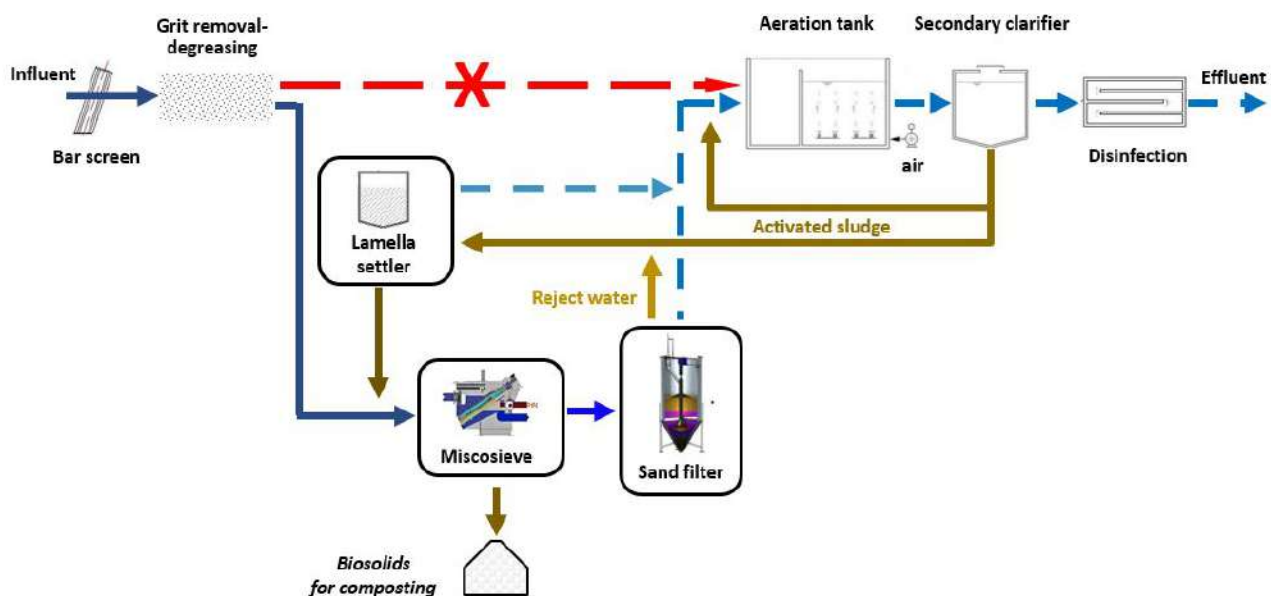


Figure 1. Flow diagram of the pilot system.

Microsieves are novel devices for separating solids from raw wastewater via a sieving process (Koliopoulos & Gikas, 2013). Microsieves have a higher suspended solids removal efficiency (between 50-80%), compared to primary clarifiers (Rusten & Odegaard, 2006). Microsieves consume less than 5% of the area required for primary clarification, and may be constructed and operated at significantly lower at capital and operating costs (Odirile et al., 2021). Suspended solids are initially filtered by gravity on a rotating filter belt, and then they are dewater by an integrated screw press. Due to the pattern of suspended solids removal from raw



wastewater, by microsieves, the texture of the solids in the produced sludge (called Primary Sieved Solids (PSS)) remains almost intact (Sarathy et al.,2015). PSS typically have solids concentrations between 40 to 45%, which is twice that of that of conventionally dewatered sludge, and following compostion may be used as soil amendment. Due to high solids content, PSS are more successive to thermal processing, compared to anaerobic digestion, for exploiting their energy content (Gikas, 2014). On the other hand, the Continuous Backwash Upflow Media Filter (CBUMF) is a continuous sand filtration process, with a self-cleaning system of the sand bed. The key advantages of the CBUMF include compact installation, uninterrupted operation and continuous concentrate removal (Feldthusen,2004).

Expected results

Based on preliminary estimations, the microsieve will remove between 40-60% of the Total Suspended Solids (TSS) and 25-40% of the incoming BOD₅ (depending on the wastewater characteristics and the type of microsieve). Following microsieving, the wastewater will go through the CBUMFs. The combined treatment is expected to reduce TSS and BOD₅ by 90 and 60% respectively. As a result, the total electricity consumption at the aeration tank of the existing WWTP is expected to be reduced by 30-35%. Due to the reduced loading, the plant capacity is expected to increase by about 40%, thus allowing for the expansion of the sewerage network of the region, without the need for additional works in the WWTP. Concurrently, the project will improve the environment, as the quality of effluent will improve, while it will release high quality effluent, which following appropriate treatment may be reused for irrigation.

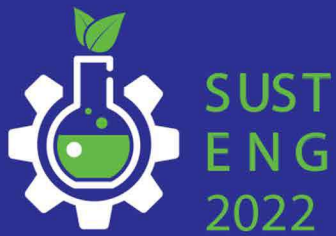
Conclusions

Installation of a microsieve followed by CBUMF in existing WWTPs will increase the loading capacity of the WWTPs, without the need for conventional expansion of the plant. The WWTP, following the installation of the microsieve- CBUMF system will operate at reduced energy expense, while it will produce high quality effluent. PSS contain 40 to 45% solids, which after composting may be used as soil amendment, or may be used as feed stock for energy production.

Acknowledgements: This study is co-financed by the European Regional Development Fund (ERDF) and national resources of Greece and Cyprus, through the of the Cooperation Program INTERREG V-A Greece - Cyprus 2014-2020: "Upgrade of WWTPs for the management of increased demands and the reduction of the operational cost" (ANELIXI).

References

- Feldthusen, F., 2004. Continuous Sand Filters - Tertiary WWT and Other Applications. In: *SAWEA Workshop*. Dammam, KSA.
- Gikas, P., 2014. Electrical energy production from biosolids: A comparative study between anaerobic digestion and ultra-high-temperature gasification. *Environmental Technology (United Kingdom)*, 35(17), 2140–2146.
- Koliopoulos, G. and Gikas, P., 2013. Fine mesh sieving of raw municipal wastewater for TSS and COD removal, *13th International Conference on Environmental Science and Technology*.
- Odirile, P. T., Marumoloa, P. M., Manali, A. and Gikas, P., 2021. Anaerobic digestion for biogas production from municipal sewage sludge: A comparative study between fine mesh sieved primary sludge and sedimented primary sludge. *Water*, 13(24).
- Rusten, B., and Odegaard, H., 2006. Evaluation and testing of fine mesh sieve technologies for primary treatment of municipal wastewater. *Water Science and Technology*, 54(10), 31–38.
- Sarathy, S., Ho, D., Murray, A., Batstone, D. and Santoro, D., 2015. Engineered fractionation of primary solids– A comparison of primary treatments using rotating belt filters and primary clarifiers. *Proceedings of the Water Environment Federation*, 2015(6), 4950–4959.



POLICES, REGULATORY & SOCIAL ACCEPTANCE



How Productive is Waste Management? Adoption & Impact of Waste Management practices in Indian Informal MSMEs

L. Posti¹ and V. Bhamoriya¹

¹ Indian Institute of Management, Kashipur, Uttarakhand-244713, India
Corresponding author email: lokesh.fpm1808@iimkashipur.ac.in

keywords: *Informal firms; Solid Waste; Liquid Waste, Waste Management; Productivity; India.*

Introduction

The paper revisits the Porter-Wagner dilemma about the association between environmental management (EM) and firm performance (FP). The discussion pertains to the environment as a strategic competitive factor where enterprises invest in the environment to reap long-term economic benefits (Porter, 1996; Porter and Linde, 1995) or the environment as a luxury good that better-performing firms only adopt (Boons and Wagner, 2009; Wegner and Bloom, 2011; Wegner, 2015).

The context of informal Micro, Small and Medium Enterprises (MSMEs) provides an interesting case since they are away from regulatory scrutiny or corporate/social obligations. The paper contributes to this emerging debate by analyzing the relationship between firm performance (FP) and waste management practices (WMPs) adopted by the informal firms. In contemporary times, where high priority is assigned to environmental concerns by governments and various business firms, this study analyses the factors that may influence the adoption of WMPs among the Indian informal firms and the resultant impact on their performance.

Materials and methods

We present the analysis of a survey covering unincorporated Non-agricultural Enterprises conducted by the National Sample Survey Office (NSSO) under the Government of India (GOI) – namely –NSS 73rd round - July 2015 - June 2016.

We model WMPs adoption as a function of rank effects, organizational structure and other environmental effects. The simple model specification is as follows;

$$WMP_i = \alpha + \beta Firm_characteristics_i + \gamma Organisational_structure_i + \theta Market_concentration_i + \mu_i \dots (2)$$

Where, WMP_i = type of WMP (categorical variable) adopted by the i^{th} firm

For addressing the second part of the study, to address the issue of the heterogeneous impact of WMPs on labor productivity we use quantile regression model. The linear regression estimates the conditional mean function but does not explain how the entire distribution of labor productivity changes in response to different WMPs. However, as we understand that there is significant heterogeneity within the informal enterprises, therefore it might be more prudent to define the relationship at different points on the conditional distribution of the outcome variable. Thus, instead of using linear regression, employing quantile regression (Koenker and Bassett, 1978) can help us to reveal the potential heterogeneous impact of WMPs on labor productivity.

$$Q_{Y_i|X_i}(\tau) = \theta_0(\tau) + \theta_1(\tau)WMP + \lambda(\tau)Z_i + \phi(\tau)Fixed_effects_i + \mu_i \dots (3)$$

Where Q = denotes conditional quantile indicating it is a random variable

τ = quantile 25th, 50th and 75th

Y_i = Ln(Labor Productivity) for the i^{th} firm

WMP_i = waste management practice adopted by the i^{th} firm



Z = control variables

X = explanatory variables

Assumption: τ^{th} conditional quantile is given as the linear function of the explanatory variables

For robustness check, we addressed the endogeneity issues, as there is an immediate concern regarding the direction of the relationship between WMPs and productivity. Assuming adoption of cleaner WMPs as a treatment/event, in the absence of any experimental data, using a counterfactual framework via propensity score matching (PSM) technique, we randomize the ex-post facto data, thus helping us adjust the selection bias and decomposition of average productivity effects of cleaner WMPs. The counterfactual analytical framework permits the estimation of potential outcomes in treated and untreated groups. Our PSM model controls majorly for observable firm-level characteristics, except for the involved human capital, due to the lack of explicit information in the dataset.

Results and discussion

We found that bigger, urban located, and female-owned firms adopt cleaner WMPs that positively impact their performance. Furthermore, the positive impact of WMPs was higher in the case of more productive firms in the quantile, indicating the relevance of the Porter-Wagner dilemma. The direction of causality was further validated using the propensity score matching technique by decomposing the average treatment effect (ATE) into average treatment effect on the treated (ATT) and average treatment effect on the untreated (ATU).

Conclusions

Waste management is directly connected with three SDGs (Sustainable Development Goals); SDG-11 (Sustainable cities and communities), SDG-12 (Responsible consumption and production), and SDG-13 (Climate Action). By understanding the waste management behavior of the informal firms, policies can be better formulated and targeted for optimum results. The positive impact of cleaner waste management on firm performance can induce policymakers to formulate policies that favor the adoption of WMPs that are not just environmentally friendly but also economically rewarding for the firm. From the results, we infer that policies that enhance financial inclusion, prioritize women-headed businesses,

Since the informal firms are hard to regulate but have a huge economic significance, a policy of inducement is best suited to minimize the regulation costs for the government and reduce regulative oversight that will allow the informal firms to voluntarily adopt cleaner WMPs and operate in a more responsible manner.

Acknowledgements: This study is not supported nor funded by any organization.

References

- Porter, M., 1996. America's green strategy. *Business and the environment: a reader*, 33, p.1072.
- Boons, F. and Wagner, M., 2009. Assessing the relationship between economic and ecological performance: Distinguishing system levels and the role of innovation. *Ecological economics*, 68(7), pp.1908-1914.
- Koenker, R. and Bassett Jr, G., 1978. Regression quantiles. *Econometrica: journal of the Econometric Society*, pp.33-50.
- Porter, M.E. and Van der Linde, C., 1995. Toward a new conception of the environment-competitiveness relationship. *Journal of economic perspectives*, 9(4), pp.97-118.
- Wagner, M., 2015. The link of environmental and economic performance: Drivers and limitations of sustainability integration. *Journal of Business Research*, 68(6), pp.1306-1317.
- Wagner, M. and Blom, J., 2011. The reciprocal and non-linear relationship of sustainability and financial performance. *Business Ethics: A European Review*, 20(4), pp.418-432.



Towards Sustainable Aviation: Civil Aviation Policies in Turkey in Global Context

N. Ü. Temel¹, Y.E. Topal² and B.H. Gürsoy Haksevenler¹

¹ Department of Political Science and Public Administration, Faculty of Political Science, Marmara University, Beykoz, Istanbul, Turkey

² Department of Economics and Science and Technology Policies Research Center (TEKPOL), Middle East Technical University, Ankara, Turkey

Corresponding author email: umrantml@gmail.com

keywords: *policy; civil aviation; sustainability; Turkey.*

Introduction

Civil aviation is defined as all aviation activities carried out for non-military purposes, such as private, sporting, or commercial. This sector has proliferated since the late 1940s globally (Addepalli et al., 2018). However, this rapid growth causes environmental degradation and brings sustainable aviation practices into the national green transition agendas (Planès et al., 2021). This paper examines the concept of sustainability in civil aviation by (i) describing the historical background of international civil aviation (in the world and in Turkey) ii) reviewing the literature on sustainability in civil aviation (emphasis on international aviation organizations designing sustainable aviation policies, i.e. ICAO) iii) elaborating the case of Air France-KLM as a best practice example (Air France-KLM, 2022). This paper evaluates the relevant breakthroughs of the global civil aviation industry, the goals of international authorities, and Turkey's approach to providing suggestions for harmonizing the Turkish civil aviation industry with the globe. In the literature, it is seen that solutions to sustainability problems are mostly sought by referring to technological developments. This study states that; integrative approaches by the sectoral and policy actors need to be produced to achieve effective results in sustainable aviation. For this purpose, we made a comprehensive literature review and content analysis of the relevant documents and reports to have a snapshot of sustainable aviation practices by analyzing the related international and national policy documents for sustainable aviation such as BM ICAO CORSIA and EU Green Deal (EC, 2022). Then, Air France KLM Example is elaborated to derive the lessons learned for improving the sustainable aviation practices in Turkey.

Materials and methods

We made a comprehensive literature review and content analysis of the secondary sources of policies, regulations, and reports. The aim is to examine the application areas of the sustainable aviation concept, the targets and policies envisaged by the international civil aviation authorities through literature review and desk research on related documents.

Results and discussion

The sector in Turkey is particularly successful in following the latest technologies and is enthusiastic about catching international trends. This success is mostly realized under the leadership of the private sector in order to increase their international competitiveness. The shortcomings focus on national legislation, incentives, and obligations, lack of resources, and environmental awareness. Sustainability policies in the sector are formed as a result of the effects of international obligations, competition, and related parties (stakeholders). The sector has a multi-actor structure and cooperation between actors is present and necessary. However, cooperation on sustainability issues needs to be increased.

Conclusions

It has been determined that the studies in the literature on sustainable aviation mostly progress on greenhouse gas emissions and noise pollution and offer solutions through developments such as fuel savings or new generation aircraft technology. However, these developments and suggestions cannot serve the targeted and needed sustainability purpose alone. This study draws attention to the inadequacy of reducing the approach to sustainable aviation to sectoral developments, that realistic and tangible solutions to the issue are only possible with a network chain which requires policymakers, institutions and



organizations in the sector, civil actors and even non-sector actors to act together with a comprehensive and integrated approach.

Acknowledgements: This study is derived from an N. Ümran Temel's unpublished MSc. Thesis entitled "Evaluation of Turkey's Civil Aviation Policy within the Scope of the Global Sustainable Aviation" From Graduate School of Social Sciences, Marmara University/ Turkey.

References:

- Addepalli S., Pagalday G., Salonitis K. ve Roy R. (2018), "Socio-economic and demographic factors that contribute to the growth of the civil aviation industry." *Procedia Manufacturing*, 19:2-9.
<https://doi.org/10.1016/j.promfg.2018.01.002>.
- Air France-KLM (2022), "Principles", Airlines.
https://www.airfranceklm.com/sites/default/files/afklm_principles_2021_en.pdf
- European Commission (2021), "Reducing emissions from aviation",
https://ec.europa.eu/clima/policies/transport/aviation_en
- Planès, T. , S.Delbecq, V.Pommier-Budinger, E.Bénard (2021). "Simulation and evaluation of sustainable climate trajectories for aviation", *Journal of Environmental Management*, 295, 113079.



Promoting sustainability in fisheries and aquaculture through biodiplomacy

K. Laktuka¹, P. Poca¹ and D. Blumberga¹

¹Riga Technical University, Faculty of Electrical and Environmental Engineering, Institute of Energy Systems and Environment, Riga, Latvia

Corresponding author email: krista.laktuka@rtu.lv

keywords: *fisheries; aquaculture; bioeconomy; biodiplomacy; communication strategy.*

Introduction

One of the objectives of the EU Bioeconomy Strategy is to produce "more with less", a concept that includes the development of sustainable and knowledge-based fisheries and aquaculture [1]. Global aquaculture production reached 80.1 million tonnes in 2017, making it the fastest-growing animal food industry globally [2]. In 2017, fisheries and aquaculture production in the EU Member States reached 6.0 million tonnes of live weight, representing 3.5% of world production [6]. In the EU 81.2% of production was from wild fisheries and 18.9% from aquaculture [2]. EU aquaculture sector accounted for around 1.4% of world production in 2017 with Spain, France and Italy as the leading aquaculture countries in the EU in terms of volume, and France, Greece and Spain in terms of value [2]. Over the last decade, the value of EU aquaculture production has increased, but the volume has declined due to environmental concerns, thus leading to an increase in cultivation of high-value species such as salmon, seabass and seabream [2].

Biodiplomacy in the context of the bioeconomy is the dialogue between stakeholders to promote the use of bioresources under internationally and nationally agreed on principles to contribute to environmental sustainability and climate neutrality [3]. Industry, organisations or any actor involved in such a dialogue must be both an expert in the bioeconomy and possess a range of other qualities to be able to find sustainable pathways and shape the strategy and form of communication to maximise the outcome.

The roots of biodiplomacy lie in the concept of biopolitics, which is part of the "Bios Theory" formulated by A. Vlavianos-Arvanitis and developed in the late 1980s [4]. Bios, which translates from Greek as "life", and the proposed theory is rooted in the belief that human beings should be able to interact harmoniously with the environment and all living beings [4]. Bioeconomy is also part of the "Bios Theory" and is seen as one of the possible salvations for the increasing number of people globally [5].

Almost 30 years later, the concept of biodiplomacy is starting to regain its relevance [6, 3] as a communication strategy to raise international public awareness of circular economy principles and more sustainable use of bioresources [6]. However, the concept of biodiplomacy has still been little explored and discussed in the literature.

The study aimed to select aquaculture or fisheries products with the highest development potential to identify the most sustainable ones through a multi-criteria analysis. Based on the results, to develop a biodiplomacy communication approach that would serve as an educational and awareness-raising material on sustainability and change in current practices in fisheries and aquaculture sectors.

Materials and methods

A mixed-methods approach was used. The research was divided into two phases. The first part consisted of literature analysis on global and EU trends in fisheries and aquaculture. Summarises and analyses the current situation in the fisheries and aquaculture sector, looking at sector averages. Assess the sustainability performance of different fisheries and aquaculture products. To carry out a multi-criteria analysis of 6 different products, 3 of fish origin and 3 of algae origin, using TOPSIS and AHP methods to determine the most sustainable of them.

The second stage involved an analysis of the literature on biopolitics and biodiplomacy, the development of a successful communication strategy on environmental issues and public awareness methods. Later, a quantitative sociological method – a questionnaire survey- was conducted to determine the public's communication habits and attitudes towards educational materials on climate change and sustainability.



Results and discussion

Multi-criteria analysis results:

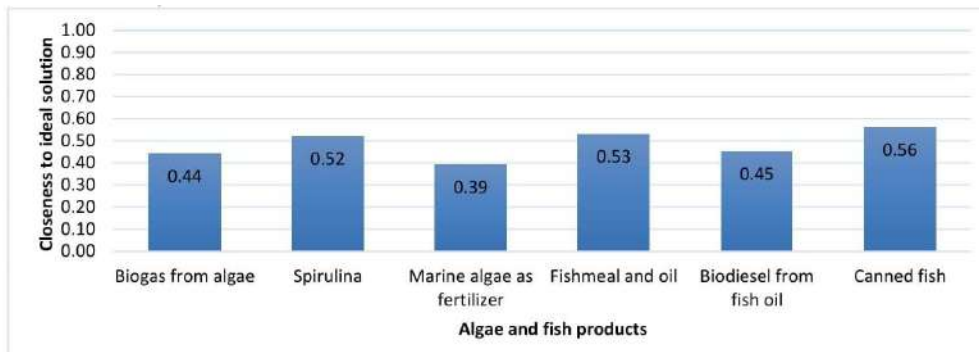


Figure 1. TOPSIS and AHP evaluation results of algae and fish products.

An electronic survey form was created in Google Forms format and distributed on Facebook to reach as many respondents as possible. One hundred forty respondents of different ages, ranging from 18 to 55 years, completed the survey. The survey results show that infographics are the most appropriate format for communication. Such visual material is easy to distribute on social networks, which are the most popular source of information according to the survey results.

Conclusions

According to the results obtained by TOPSIS and AHP, canned fish is the most sustainable of the selected aquaculture products. The results show that respondents have a strong preference for visual educational materials.

Acknowledgements: This project has received funding from the European Union's Horizon 2020 research and innovation programme under Grant Agreement No. 862699.

References

- European Commission, "A Bioeconomy for Europe," 2012. [Online]. Available: <https://op.europa.eu/en/publication-detail/-/publication/1f0d8515-8dc0-4435-ba53-9570e47dbd51>.
- European Commission's Knowledge Centre for Bioeconomy, Brief on biomass production of fisheries and aquaculture, JRC121199, 2020
- Vecina, Anita & Kalnbalķite, Antra & Zihare, Lauma & Rozakis, Stelios & Blumberga, Dagnija. (2021). Biodiplomacy Attractiveness in Bioeconomy Education. Case Study. Environmental and Climate Technologies. 25. 1205-1214. 10.2478/rtuct-2021-0091
- Vlavianos-Arvanitis, Agni, Introduction to the Bios Theory, Bio-Diplomacy And International Cooperation, Hellenic Russian Symposium 1991, Athens, December 13-14, 1991
- Vlavianos-Arvanitis, Agni. (1993). Biopolitics — a new pathway to bio-diplomacy and bio-education redefining the concept of profit. Journal of Cleaner Production - J CLEAN PROD. 1. 119-122. 10.1016/0959-6526(93)90050-L.
- Aguilar, Alfredo, Patermann, Christian, Biodiplomacy, the new frontier for bioeconomy, New Biotechnology, Volume 59, 2020, Pages 20-25, ISSN 1871-6784, <https://doi.org/10.1016/j.nbt.2020.07.001>



Social Perspective of Separate Waste Collection of Municipal Waste, A Case Study for a Municipality in Istanbul, Turkey

B.H. Gursoy Haksevenler¹, A. Akpınar² and B. Takta² and İ. Celik²

¹Marmara University, Faculty of Political Science, Department of Political Science and Public Administration, Istanbul, Turkey

² Marmara University, Faculty of Political Science, Department of Local Governments, Istanbul, Turkey
Corresponding author email: hande.gursoy@marmara.edu.tr

keywords: *social perspective, municipal waste, separate waste collection, survey analysis.*

Introduction

The increasing amount of waste and the disposal process has become one of the important international problems encountered today (UNEP 2015). Worldwide rapid population growth, change in consumption habits, urbanization and economic development are the main reasons for the increase of the waste amount (Nair et al. 2021). This brings about the inadequacy of current waste management policies, while revealing the need for a sustainable and integrated waste management policy. In developed countries such as Germany, USA and Japan, significant success has been achieved by introducing new policies with the introduction of various laws and regulations regarding waste management policies (Potdar et al. 2016). However, in developing countries such as Turkey, the importance of this issue was realized later and this caused the steps taken to lag behind. For Turkey, the search for sustainable policies regarding waste management ended with the recent policy implementation of the "Zero Waste Project" realized under the responsibility of Turkish Ministry of Environment and Urbanization. In this concept, Zero Waste Regulation was published on 12.07.2019 in Turkey and the recycling approach became mandatory for local administrations, public institutions and organizations, industrial facilities, and etc. (MoEU 2019). With Zero Waste Management (ZWM), it is not only aimed to recycle waste, it is also aimed to eliminate or minimize the amount of waste produced by changing our consumption habits. The first step of ZWM starts with separating the wastes of individuals in their own internal environment (such as home, office). For this, it is necessary to increase the awareness of individuals by increasing the practices on a local scale and to reach the global dimension of waste recycling. Municipalities have important duties in separate waste collection (SWC) in Turkey. Studies on SWC are increasingly included in the literature as it is a current topic. However, there are limited studies on the social aspect of zero waste management. In this context, Zeytinburnu Municipality in Istanbul, Turkey which conducting a project on collecting segregated waste more efficiently was selected as a pilot study. Its separated waste collection application was analyzed by its social aspect to reveal out the knowledge, attitude, behavior, expectation and tendency of the residents.

Materials and methods

In order to evaluate the social impact of separate waste collection in Municipalities, Zeytinburnu Municipality was chosen as the pilot scale in the study since a project is carried out in the Municipality. In the project, the recyclable wastes are collected by waste collection vehicle that comes to certain neighborhoods on certain days and to fixed points. The residents receive a certain amount of payment that can be used for market shopping for the recyclable waste they bring. A survey was conducted with the residents who participate in the project in 15-30 December 2021. The number of residents who separate their waste (participate in the project) were approximately 10,000. Considering the 5% margin of error and 95% confidence interval, the sample was determined as 370 participants (RAOSOFT 2021). The questions evaluated within the scope of the study were asked to the participants on a 3-point Likert. The questions asked were aimed at evaluating the knowledge, attitude, behavior, expectation and tendency of the participants.



SUST
ENG
2022



NANOMATERIALS



Production and Application of High-Performance Industrial Materials based on Nanocellulose

G. Penloglou¹, O. Kotrotsiou¹, V. Bakola¹, A. Pavlou¹, M. Sarafidou², D. Ladakis², E. Tsouko², A. Koutinas², K.T. Papapetros³, K.S. Andrikopoulos³, G.A. Voyiatzis³, D. Bartzialis⁴, N.G. Danalatos⁴, K.D. Giannoulis⁴, E. Karagiannidis⁵, M. Iakovlev⁶, E. Deze⁶, M. Papaioannou⁶, S. Sideri⁶ and C. Kiparissides¹

¹Centre for Research and Technology Hellas (CERTH/CPERI), 57001 Thermi, Thessaloniki, Greece

²Dept. of Food Science and Human Nutrition, Agricultural University of Athens, 11855 Athens, Greece

³Foundation for Research and Technology Hellas (FORTH-ICEHT), 26504 Rio Patras, Greece

⁴University of Thessaly, Dept. of Agriculture Crop Production and Rural Environment, 38446 Volos, Greece

⁵CHIMAR HELLAS SA, 57001 Thermi, Thessaloniki, Greece

⁶API Europe MEPE, Research & Experimental studies in Biotechnology, 15342 Athens, Greece

Corresponding author email: costas.kiparissides@certh.gr

keywords: nanocellulose; lignocellulosic biomass; packaging; composite materials; wood products.

Introduction

The continuous pursuit of sustainable and environmentally friendly materials indicates today nanocellulose (NC) as a very promising candidate for diverse applications, e.g. plastic composites, food packaging, wood additives, biomedical applications, 3D printing (Kingshuk et al., 2021). This derives from the excellent properties of NC, such as reduced size and high specific surface area, high tensile strength, crystallinity and transparency. Moreover, additional characteristics of NC like abundance, renewability and biocompatibility fully comply with the contemporary needs for “green” materials and applications (Trache et al., 2020).

Nonetheless, significant techno-economic constraints, e.g. large energy demands and production costs, presently hinder the wider application of NC. In this sense, the scope of the present study *-in the framework of the HIPERION research project-* is to intensify already existing value chains and develop innovative routes for NC-based products. Existing technologies are optimized to minimize their environmental impact, and new sustainable processes are adopted to produce NC in a cost-effective manner. NC products are also evaluated for their effectiveness as fillers in plastic composites, and as additives in packaging and wood products.

Production technologies

Different types of NC are produced: microfibrillated (MFC), nanofibrillated (CNF) and nanocrystalline (NCC) cellulose, as well as bacterial nanocellulose (BNC). Four different plants, cultivated in dedicated crops, are used as biomass sources: *Phalaris aquatica* L. (harding grass), *Cynara cardunculus* (cardo), *Panicum virgatum* (switchgrass) and *Cannabis sativa* (hemp). The experimental design consists of 3&4 different levels of irrigation and 3&4 levels of fertilization (N-P-K) (according to the cultivation) and is applied to compare the different crops and identify the most appropriate lignocellulosic source for NC production.

Biomass samples from the above 4 crops (upon harvesting, drying and milling), as well as additional residues and wastes, are converted to NC by three major pathways (and their variants) (Figure 1):

(i) A thermo-chemical technology for NCC production (Figure 2), based on the sequential treatment of biomass in alkali, bleaching and hydrolysis process steps. This technology is optimized to minimize the number and duration of steps, as well as decrease their severity (in terms of temperatures, presence of chemicals, etc.). An additional goal is to combine the hydrolysis step with a milder ball milling step.

(ii) An innovative, though simple and cost-efficient, 2-step thermo-mechanical technology for CNF production that includes hot water pretreatment of biomass and novel mechanical disintegration of derived pulp using a Masuko grinder or ball milling treatment. CNF will be produced from alternatively sources of biomass, such as wood chips or board/paper packaging residues. The objective is to identify the optimum pretreatment conditions and a single material to be used as an additive in “brown” packaging and food packaging products, as well as in adhesives for wood products.

(iii) A bio-chemical technology based on the hydrolysis of cellulose and hemicellulose contained in biomass, the production of a sugar-rich hydrolysate used as a C-source for microbial production of bacterial cellulose by *K. sucrofermentans*, and finally hydrolysis for BNC production (Figure 2). The saccharification step has been optimized using own-produced enzymes via solid-state fermentation (SSF) of *A. awamori*.

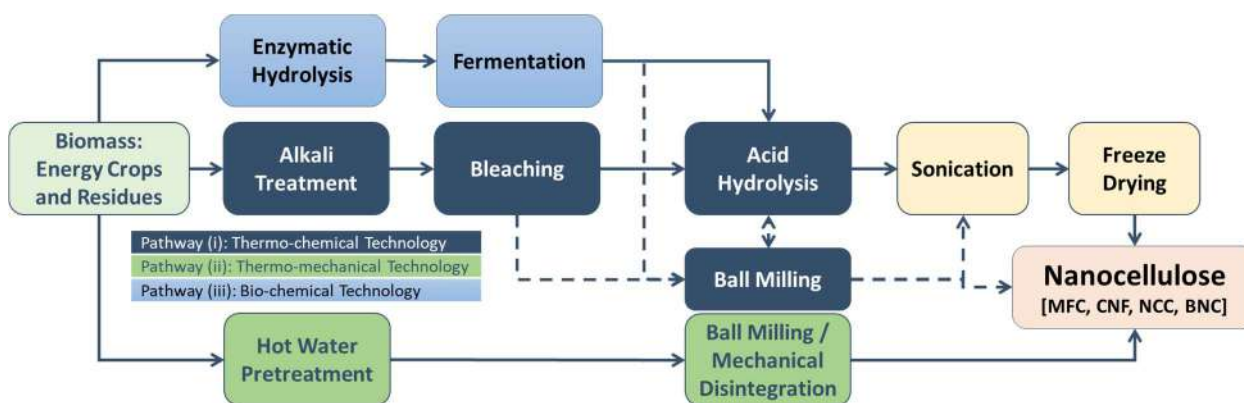


Figure 1. Nanocellulose production value chains: variants of processes and products.

Applications of nanocellulose

The produced nanocellulose samples are exploited for the development:

(a) *“Brown” paper packaging products*: preparation of pulps for corrugating medium, linerboard and mixtures, with and without CNF and commercial papermaking additives. Characterization tests are applied to compare the mechanical strength of pulp sheets with the addition of different NC contents (TAPPI).

(b) *Plastic food packaging products*: developed by film casting, using water soluble polyvinyl alcohol (PVA) and/or biodegradable chitosan as polymeric matrices. The structures of both matrices and fillers are studied at molecular (Raman and FTIR) and macroscopic (SEM, DSC and XRD) scales. Following the relevant EU regulations, the composites are tested in accredited migration cells (UV-Vis and SERS).

(c) *Adhesives/binders for wood products*: the potential of NC to strengthen commercial synthetic resins is evaluated in urea-formaldehyde (UF) and melamine-UF (MUF) resins. The physicochemical, thermal and molecular properties of the resins are measured. Particleboard (PB) and fiberboard (MDF) are prepared and their physico-mechanical properties are evaluated, according to EU standards.

(d) *Surface coatings for wood products*: NC is tested as a coating for wood products, as the means to control formaldehyde release from their surface. Two types of wood panels are prepared, i.e., particleboard (PB) and fiberboard (MDF). Formaldehyde release from the boards is examined according to EU standards.

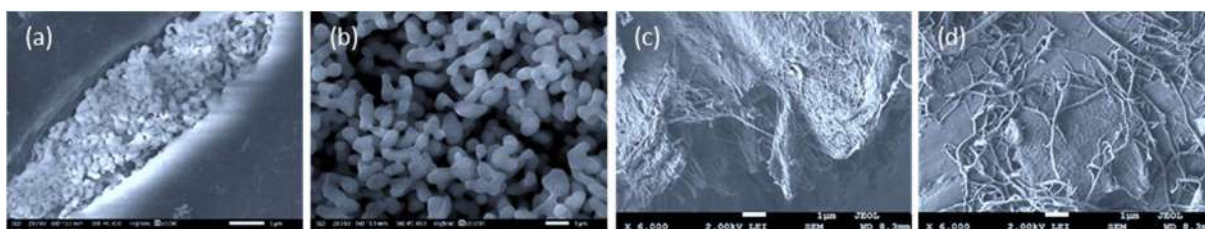


Figure 2. SEM images of rod-shaped NCC (a) and (b), and fiber-shaped BNC (c) and (d).

Conclusions

As research on nanocellulose (NC) is accelerating fast, the proposed here technologies will lead to sustainable scalable processes and “green” products with controlled characteristics. Based on the multi-functionality of the different NC types, intensified or newly developed value chains with ease of applicability, and significant positive economic and environmental impact will be developed, demonstrated and evaluated.

Acknowledgements: This research has been co-financed by the European Regional Development Fund of the European Union and Greek national funds through the Operational Program Competitiveness, Entrepreneurship and Innovation, under the call RESEARCH – CREATE – INNOVATE [Project code and title: T2EDK-01394 – HIPERION: High Performance Industrial Materials based on Nanocellulose].



References

Kingshuk Dhali, K., Ghasemlou, M., Daver, F., Cass P., Adhikari B., 2021. *Sci. Total Environ.*, 775, 145871.
Trache, D., Tarchoun, A.F., Derradji, M., ... , N., Brosse, N., and Hussin, M.H., 2020. *Front. Chem.*, 8, 392.



Investigating the effects of initial number concentration on the transport of aggregating nanoparticles

V.E. Katzourakis¹ and C.V. Chrysikopoulos¹

¹School of Environmental Engineering, Technical University of Crete, Greece

Corresponding author email: billiskatz@yahoo.gr

keywords: migration; nanoparticles; transport; aggregation; porous media.

Introduction

Recently nanotechnology has attracted the strong interest of the scientific community due to its applications in various fields including materials science, medicine, environmental protection, pharmacy and agriculture. However nanoparticles due to their small size may enter the human bloodstream through the skin or epithelial and endothelial barriers and reach internal organs. Experiments have shown the toxicity of nanoparticles for the human body may cause thrombosis by enhancing platelet aggregation. Unfortunately humans can be exposed to nanoparticles through drinking water obtained from underground aquifers. Nanoparticles may enter underground aquifers through inappropriate disposal of nanomaterials or through wastewater coming industrial sources which are not properly treated.

An important process when considering the nanoparticle migration, is aggregation. Colliding particles may attach to each other and form cluster of particles with different physicochemical characteristics. However the common particle transport models often overlook this and instead may employ conventional colloid filtration theory (CFT), surface blocking, depth-dependent retention approaches or use simplifying, empirical reaction rates to model particle attachment. Methods which may not always capture the physicochemical mechanisms that that nanoparticles experience during their migration.

In the present study the developed model of Katzourakis and Chrysikopoulos, 2021 that describes the transport of aggregating nanoparticles in a water saturated, homogeneous 1D- aquifer, was used to investigate the effects of initial particle number concentration on the nanoparticle migration. Due to the nature the Smoluchowski population balance equation (PBE) used to model the aggregation process, it is evident that the particle collisions increase rapidly as the initial injected number of particles increases N_0 . Therefore it is expected that the effects of aggregation to be more pronounced as the N_0 increases. To validate this expectation two model simulations were performed with two different N_0 being injected instantaneously upstream an 1d- aquifer. The breakthrough normalized concentration curves seen in Figure 1.

Mathematical Modelling

The nanoparticle aggregation process is assumed can be represented by the Smoluchowski population balance equation (PBE):

$$\left(A_n \right)_k = \frac{dn_k}{dt} = \frac{1}{2} \sum_{i=1}^{k-1} b_{i,k-i} n_i n_{k-i} - n_k \sum_{i=1}^{\infty} b_{k,i} n_i \quad (1)$$

where n_i [npk/L³] is the number of particle concentration of cluster k .



Results and discussion

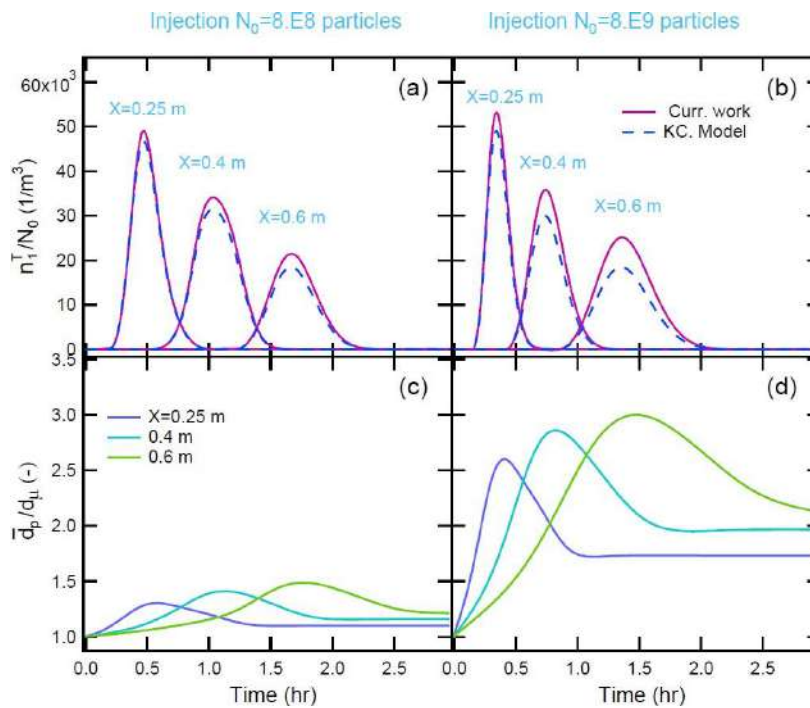


Figure 1: Breakthrough concentration curves for two cases of initial number particle injection, along with the normalized average particle diameter. Aquifer size $L_x=0.6$ m. Injection location $L_x=0.1$ m. Finally KC. Model neglects aggregation.

Conclusions

- 1) Increased initial particle injection (see Figure b,d) produces increased aggregate diameter (see Figure 1d) and pronounces further the overall aggregation process.
- 2) The formation of aggregate clusters Figure 1c,d changes the average attachment of particles onto the solid matrix, producing higher breakthrough curves.



Production of cellulose nanofiber by using deep eutectic solvent and ultrasonic treatment

Y.Y. Chen¹, F.B. Mkhontfo¹, B.Y. Chen¹, Q.T. Huynh¹ and K.L. Chang¹

¹ Institute of Environmental Engineering, National Sun Yat-Sen University, Kaohsiung, Taiwan
Corresponding author email: klchang@mail.nsysu.edu.tw

keywords: *deep eutectic solvent; ultrasonic crusher; cellulose nanofiber.*

Introduction

Cellulose nanofiber (CNF) has a high diameter ratio and has been produced in nanometer sizes. Therefore, CNF has been used in various ways, which can improve the material's extreme, tearing, waterproof, and wear-resistant effects. Therefore, in recent years, they are mostly used for tensile strength (Jiao et al., 2016). They find out that after adding 0.05%~0.4% CNF to the cement, the compressive and bending resistance of the cement get higher. The results showed that the more CNF was added, the longer the cement set time, which is precisely because of its heat release and set time. Influenced by the reason, the molecular arrangement and combination in the cement are more stable, resulting in an increase in its compressive and flexural resistance. The addition of 0.15% CNF improves the compressive and flexural resistance of the cement after it has completely solidified in the ground for 28 days. Due to environmental protection, humans are committed to reducing plastic and actively looking for alternatives. Adding CNFs can improve the hydrophobicity and resistance of paper, so the demand for CNFs will not be underestimated in the future.

At present, industry has used the method of acid treatment to produce the CNFs, but the method will cause secondary pollution due to its spent acid. Since the deep eutectic solvent (DES) has the effect of softening lignin (Chen & Wan, 2018), it is hoped that the deep eutectic solvent can be used as a pretreatment so that the biomass material can be easily broken by a ultrasonic crusher in a physical way, thereby producing CNFs. In this experiment, rice straw was used as biomass material, and 1 g was taken to the beaker and heated with the DES in different concentrations (5–10%) and different heating times (0.5–4 hours). After the step, add water to the biomass material to observe the sonic fragmentation for 0.5 to 4 hours, and use the result occurrence method to analyze the optimal reaction conditions.

Materials and methods

- (1) Prepare the DES with glycerin and methyl carbonate.
- (2) Mix glycerin and methyl carbonate together with a mole ratio 4:1 in the beaker.
- (3) Heat the beaker with the oil bath to 80°C for an hour.
- (4) Put 1 gram of rice straw in a 200 ml beaker and add 5 ml; 7.5 ml; and 10 ml of DES with 95 ml; 92.5 ml; 90 ml di water together.
- (5) Heat the liquid to 80°C for 30 minutes, 135 minutes, and 240 minutes.
- (6) After heating, recycle the DES. Allow the sample to pass through the filter with a different aperture filter paper. Size range from 7 µm to 5 µm to 1 µm.
- (7) Use DI water to wash the biomass three to four times.
- (8) Put the biomass into a 200 ml beaker with 100 ml of water and set it in the ultrasonic crusher (750 watts; 20 kHz) for 30 minutes; 135 minutes (rest 15 minutes per 30 minutes); 240 minutes (rest 15 minutes per 30 minutes).
- (9) Let the sample over the filter with the filter paper whose aperture is 1 µm.
- (10) Using the pipe to take out 1 mL of liquid from the sample. Put it into the particle analyzer.
- (11) Let the remaining liquid be frozen by the freeze drier.
- (12) Weigh the powder and calculate the yield.
- (13) Using the Response Surface methodology for calculating the best experimental conditions.



Results and discussion

Through the analysis of the particle size analyzer, it can be seen that there was a significant difference between the biomass materials pre-treated with DES and without DES after passing through the ultrasonic crusher. Without DES pretreatment, it was difficult to produce a particle size that was smaller than 1 μm despite using ultrasonic disintegration. However, the biomass material which was pre-treated with DES can easily be destroyed to a particle size smaller than 1 μm and arrive at 200 nm in length. Figure 1 showed the result of biomass material that has not been pre-treated by DES and just used the ultrasonic crusher for an hour. Conversely, figure 2 showed the biomass material which was pre-treated by DES for 30 minutes before using the ultrasonic crusher for an hour.

Compare the Fig. 1 and Fig. 2, the biomass material in Fig. 2 obviously cannot see the original fibers. In comparison, the fibers in Fig. 1 were clearly visible. Otherwise, the results of the particle size analyzer. The biomass material was pretreated and crushed by ultrasonic broadcast, and its average particle size distribution was 408 nm. The same ultrasonic fragmentation time, without pretreatment, figure showed that the particle size distribution was 2,404 nm.

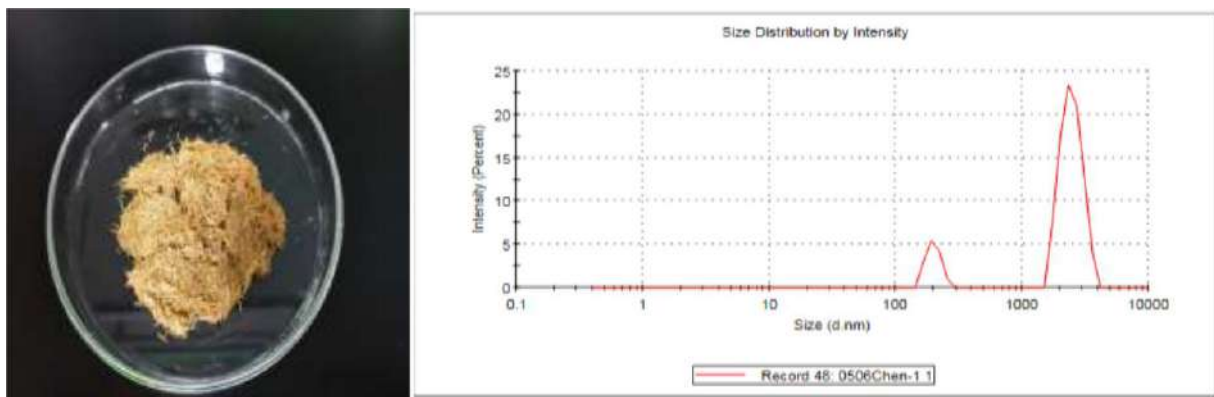


Figure 1. Biomass with using ultrasonic crusher for 1hr.

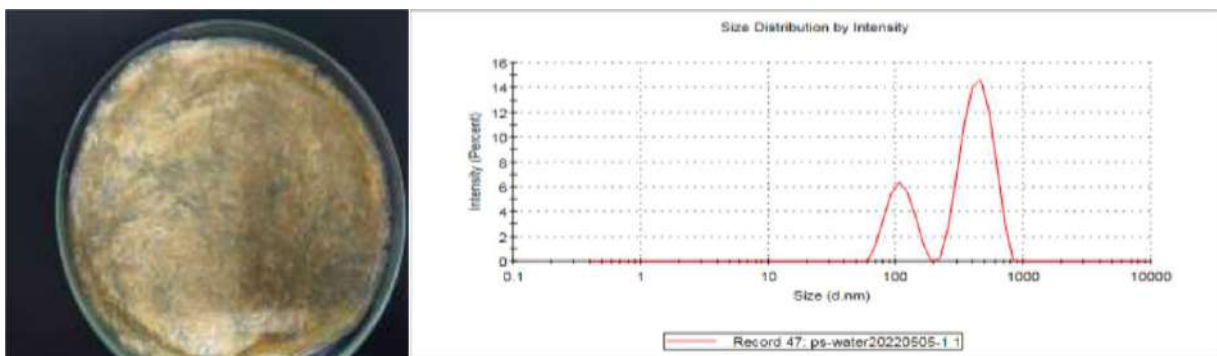


Figure 2. Biomass pretreated with 5% DES 1hr and using ultrasonic crusher for 1hr.

Conclusions

The results prove that DES does make fibers more easily broken after pretreatment. This was similar to the literature Zhu Chen and Caixia Wan wrote. (Chen & Wan, 2018). They used DES and microwave at the same time and found out that the method can let significant amounts of lignin and xylan dissolve in the pretreatment liquor, which means DES can make lignin easier to destroy.

References

- Chen, Z., & Wan, C. (2018). Ultrafast fractionation of lignocellulosic biomass by microwave-assisted deep eutectic solvent pretreatment. *Bioresource Technology*, 250, 532-537.
- Jiao, L., Su, M., Chen, L., Wang, Y., Zhu, H., & Dai, H. (2016). Natural Cellulose Nanofibers As Sustainable Enhancers in Construction Cement. *PLOS ONE*, 11(12), e0168422.



Microwave-Assisted Sustainable of Cellulose nanofibers with aromatic amine

F. Baraka¹ and J. Labidi¹

¹Biorefinery Processes Group, Chemical and Environmental Engineering Department, Engineering Faculty of Gipuzkoa, University of the Basque Country UPV/EHU, Donostia, Spain

Corresponding author email: farida.baraka@ehu.eus

keywords: sterification; CNF; aromatic amine.

Introduction

Valorization of nanocellulosic material is an extensive subject. This abundant biopolymer offers an attractive set of properties such as renewability, biocompatibility, and tunable surface chemistry. Therefore, it allows its use as a sustainable platform for the development of green functional materials. Nowadays, various surface modifications have been reported allowing a wide range of applications [1].

Among these modifications, esterification aims to introduce ester groups by using acylating agent that reacts with the hydroxyl groups present on the surface of cellulose nanofibers. Several reagents have been employed over years to esterified CNF hydroxyl groups such as acid anhydrides [2], carboxylic acid [3] or more recently acylchlorides [4]. However, it is well known that the esterification of CNF usually involves long and complicated procedures, which hinders green production and thereby limits its scope of application.

In this communication, we describe a sustainable chemical pathway developed for the esterification of cellulose nanofibers using para-aminobenzoic acid (PABA), an aromatic carboxylic acid biologically produced from glucose. The reaction was performed under microwave energy (MW) leading to a rapid, efficient, and instantaneous heating process. Fourier transform infrared confirmed the grafting of aromatic amines on the CNF surface by the appearance of new peak associated to the ester group. Thermal analysis demonstrated a significant increase of the char yield.

Materials and methods

Local producer (Papeleria Guipuzcoana de Zicuñaga) kindly provided cellulose pulp extracted from Eucalyptus. All other chemicals were purchased from Sigma-Aldrich and used without further purification. The cellulose fibers were subjected to a homogenization process to obtain CNFs. For this purpose, a fiber suspension (10 wt.% in water) was prepared and then defibrillated using a GEA Niro Soavi equipment.

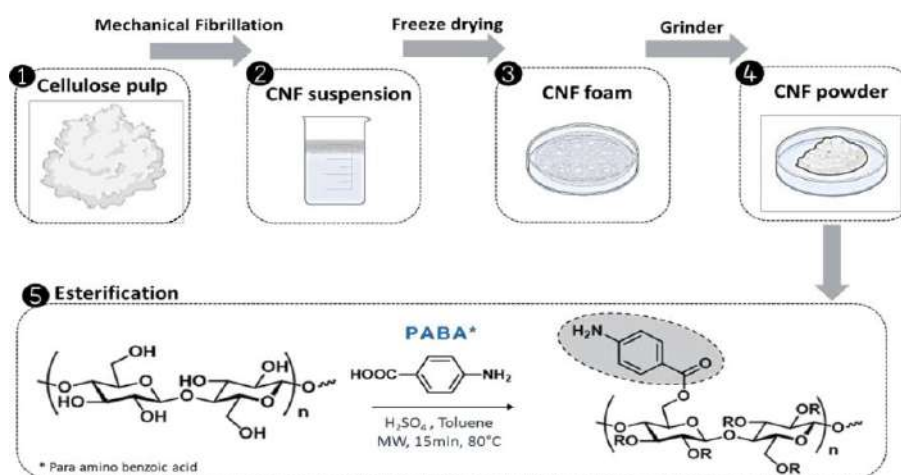


Figure 1. Methodology of the extraction and esterification of CNFs.



The extracted CNFs were then esterified in the presence of toluene and catalytic amount of sulfuric acid (H₂SO₄). The ratio of 4-amino-benzoic acid (para-amino-benzoic acid, PABA) to fiber was set to 2:1 (w/w ratio). The mixture was heated at 80 °C for 15 minutes at 300 W microwave power. Unreacted PABA was removed by washing the product with ethanol and filtered under Buchner. Finally, the product was dried at 50 °C for 48 hours and then analyzed. Fourier transform infrared spectra of native and esterified samples were acquired on a PerkinElmer Spectrum. TGA thermograms were recorded on a TGA/SDTA 851 Mettler Toledo (10 °C.min⁻¹ under N₂).

Results and discussion

The effects of grafting PABA on CNFs were examined by FTIR spectroscopy and presented in Figure 1. The native nanofibers shown band at 3340 cm⁻¹ assigned to the O-H vibration resulted from the hydrogen bonds in cellulose I. This peak has completely disappeared after the MW esterification, leading to the emergence of the stretching band at 1695 cm⁻¹ associated to ester connected to the aromatic group. The presence of this band indicates the successful formation of acetyl groups resulting from the esterification of hydroxyl groups.

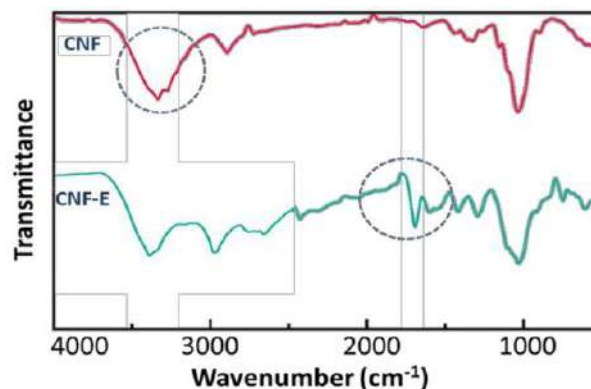


Figure 2. FTIR spectrum of native (red) and esterified CNFs (green).

In addition to the structural analysis, the thermal properties of the esterified CNFs were investigated by TGA analysis. A slight loss of thermal stability is observed in Table 1. The onset of thermal degradation is 256 °C lower (Td= 205 °C) for the esterified nanofibers. However, the later also shows a better char yield (from 10.6 % to 37.5 %) associated to the formation of the aromatic ester.

Table 1. Thermal proprieties of CNF: cellulose nanofibers and CNF-E: esterified cellulose nanofibers.

Sample	H2O content (%)	Tonset (°C)	Tmax,1 (°C)	Tmax,2 (°C)	Char (%)
CNF	3.5	256	n.a.	336	10.6
CNF-E	1.8	205	223	309	21.7

Conclusions

A sustainable esterification of cellulose nanofibers was successfully developed under microwave irradiation (MW) with para-aminobenzoic acid (PABA) as naturally occurring aromatic acid. Esterified CNF exhibited aromatic ester groups and demonstrates a higher char yield.

Acknowledgements: The authors would like to thank the funding from the University of the Basque Country (PIFG20/13).

References

- Missoum, K., Belgacem, N., & Bras, J. Nanofibrillated Cellulose Surface Modification : A Review. *Materials*, (2013), 6(5), 1745-1766.
- Aloulou, F., Boufi, S., & Labidi, J. Modified cellulose fibres for adsorption of organic compound in aqueous solution. *Separation and Purification Technology*, 2006, 52(2), 332-342.
- Ramírez, J., Suriano, C., Cerrutti, P., & Foresti, L. Surface esterification of cellulose nanofibers by a simple organocatalytic methodology. *Carbohydrate polymers*, 2014, 114, 416-423.
- Chhaged, M., Yadav, C., Agrawal, A., & Maji, P. Esterified superhydrophobic nanofibrillated cellulose based aerogel for oil spill treatment. *Carbohydrate Polymers*, 2019, 226, 115286.



Degradation of indigo carmine dye using magnetic ferrite nanoparticles as a heterogeneous Fenton-like catalyst: Optimization by Response surface methodology

A. Soufi¹, H. Hajjaoui¹, M. Khnifira¹, M. Abdennouri¹ and N.Barka¹

¹MRI Lab, Research Group in Environmental Sciences and Applied Materials (SEMA), Sultan Moulay Slimane University, Beni Mellal, Morocco

Corresponding author email: soufiamal94@gmail.com

keywords: *catalytic wet peroxide oxidation; magnetic nanoparticles; recyclable catalyst; Box–Behnken design.*

In the present study, heterogeneous Fenton-like process was applied for the treatment of indigo carmine dye. The copper ferrites nanoparticles synthesized by co-precipitation method were applied during Fenton-like process. The NPs were characterized by X-ray diffraction (XRD), Fourier transform infrared spectroscopy (FTIR), scanning electron microscopy (SEM) and energy dispersive X-ray (EDX). The response surface methodology based on Box–Behnken design was applied to evaluate and optimize the interactive effects of three operating variables including copper nanoferrite dosage, initial concentrations of indigo carmine and H₂O₂ concentration on the indigo carmine degradation rate in Fenton-like process. A significant quadratic model (p-value= 0.0003, R² = 0.98) was derived using analysis of variance (ANOVA). The desirability function was applied to determine the best process parameters and predict the responses. The predicted degradation rate under the optimum conditions as determined by the proposed model was 99.58%. Confirmatory tests were carried out and the degradation rate of 98.20 % was observed under the optimum conditions, which agreed well with the model prediction. The recyclability of copper ferrite was also investigated after five successive runs, in which the catalyst remains stable after five times recovery and reuse. Based on the experimental results, possible mechanism for the degradation of indigo carmine was proposed. Hence, magnetic copper ferrite can be used as effective catalysts for the destructive removal pollutants in wastewater.



Solar Cell Elements Based on Graphene-Porphyrin Nanocomposites

G. Gyulkhandanyan¹, P. Gikas² and G. Shmavonyan³

¹Laboratory of Bioengineering, Institute of Biochemistry of the NAS of Armenia, Yerevan, Armenia,

²Laboratory of Design of Environmental Processes, Technical University of Crete, Rethymno, Crete, Greece,

³Laboratory of 2D materials Engineering and Nanotechnology Innovation, National Polytechnic University of Armenia, Yerevan, Armenia

Corresponding author email: gshmavon@yahoo.com

keywords: solar cell; porphyrins; graphene; nanocomposites; photobleaching.

Introduction

Photovoltaic systems (cells) convert sunlight directly into electricity through the photovoltaic effect. The following three processes determine the conversion of solar energy: (I) light harvesting and exciton diffusion, (II) charge separation, and (III) carrier transport (Hasobe, 2010). The absorption of light and the subsequent transfer of an electron through an excited state are important processes for the final energy conversion (Hasobe, 2013). The design of any solar cell requires a light-absorbing material to absorb photons and generate free electrons by the photovoltaic effect (Mao, et al., 2021). The third generation is a step beyond the single-junction cells that include not only multijunction cells but also polymer and organic and dye-sensitized solar cells (DSSCs) (Dragonetti and Colombo, 2021). As such elements, photosensitizing dyes (mainly of a porphyrin structure), which have absorption in both the ultraviolet and visible regions of the spectrum, have now begun to be widely used.

As photosensitizers, porphyrins are widely used in biophotonics, in particular, for photodynamic therapy of tumors, as well as in phototherapy of microorganisms and viruses. In solar batteries, one of the most important processes is the most efficient capture/absorption of solar energy in a wide range of the light spectrum and the efficient transfer process (the first nodal element of the solar battery) for further conversion into electricity. The first and most important nodal element of a solar battery is a nanocomposite consisting of porphyrins/metalloporphyrins (an effective element for absorbing solar energy) and graphene (a binding element and effectively transferring energy without loss to the next nodal element, the semiconductor part of the battery) (Mao, et al., 2021). The aim of the study is to develop and obtain a new structure of the key and most important element of the third generation solar battery, consisting of a nanocomposite based on new nanostructures of graphene and porphyrins with a high solar energy conversion efficiency. Porphyrins as photosensitizers can convert solar energy according to the first of three processes, namely - (I) light harvesting and exciton diffusion. A simple synthesis pathway, a high molar extinction coefficient, and a lower fabrication cost compared to other photosensitizers give to porphyrin sensitizers a big advantage (Armel, et al., 2011). Graphene, which has a high conductivity and unique electronic properties, can convert solar energy by the second of three processes - (II) charge separation. These two substances, porphyrin and graphene, forming a nanocomposite, turned out to be extremely promising and effective in terms of converting solar energy into electrical energy without loss of light energy (Mao, et al., 2021; Ge, et al., 2015).

Materials and methods

1. Porphyrins. As a component of nanocomposites will be used meso-substituted cationic 3- and 4-pyridylporphyrins and metalloporphyrins with various peripheral functional groups (butyl-, hydroxyethyl-, allyl-, and metallyl-) synthesized in Armenia and in UK in accordance with the procedures of (Tovmasyan, et al., 2008). The initial preparations (powders) of porphyrins and metalloporphyrins and other photosensitizers (Al-phthalocyanine) are dissolved in an appropriate organic solvent (dimethyl formamide, dimethyl sulfoxide or acetonitrile), as well as to control distilled water at a concentration of 10^{-3} M one hour before the experiment. All solutions are stored at room temperature or at 6-8°C in the dark.

2. Graphene. Graphene is obtained manually (homemade) or mechanically (for mass production) by rubbing graphite on dielectric, semiconducting and other substrates at atmospheric pressure conditions, as well as the requirements to both the substrates and material being rubbed (layered bulk powder, highly ordered pyrolytic graphite (HOPG)) (Shmavonyan, et al., 2017).



Results and discussion

In order to obtain nanocomposites, we investigated firstly a number of cationic and anionic porphyrins to study the phenomenon of photobleaching, since this phenomenon can lead to a decrease in the efficiency of collecting sunlight by the porphyrin molecule, as well as eventually to damage to the solar battery. The study were carried out in aqueous solutions with cationic porphyrins both metal-free and containing a central Zn atom, as well as with an anionic photosensitizer Al-phthalocyanine in a wide range of concentrations from 10^{-6} to 10^{-4} M for 1 to 24 hours in bright sunlight (about 70 mW/cm²). The results showed a significant dependence of photobleaching of all cationic porphyrins on the concentration of the preparation in solution, while Al-phthalocyanine in the whole concentration range from 10^{-6} to 10^{-4} M was subject to photobleaching within 24 hours less significantly. The study of photobleaching of porphyrins (both cationic and anionic) in bright sunlight, immobilized and dried on a glass substrate, gave much more optimistic results: photobleaching for cationic porphyrins also depended on the concentration of the applied preparation, but photobleaching occurred to a much lesser extent (up to 15 % within 24 hours) than in solutions; for anionic porphyrin, photobleaching was even less significant, up to 5%. This result can be explained by the fact that reactive oxygen species (ROS) (and, in particular, singlet oxygen) are formed in solutions, leading to the photodegradation of photosensitizers (porphyrins), while in the dry immobilized state, this phenomenon is apparently insignificant (formation of the ROS in air is insignificantly due to the low presence of water vapor in the air in dry weather).

To achieve a homogeneous (equable) incorporation (interaction) of porphyrin molecules with graphene, we studied the solubility of the studied photosensitizers in various organic solvents, for which the solubility of graphene was previously studied: acetonitrile, dimethyl formamide, and dimethyl sulfoxide. All studied compounds of photosensitizers showed good solubility in these solvents in a wide range of concentrations. Severally, we also studied the production of new graphene nanostructures in the same organic solvents by the previously developed substrates rubbing method (Shmavonyan, et al., 2017).

Conclusions

To obtain stable and long-lasting components of solar cells, it is necessary to strictly study the stability (photobleaching) of the applied photosensitizers.

References

- Armel, V.; Pringle, J. M.; Wagner, P.; Forsyth, M.; Officer, D.; MacFarlane, D. R. Porphyrin Dye-Sensitised Solar Cells Utilising a Solid-State Electrolyte. *Chem. Commun.* 2011, 47, 9327. doi:10.1039/c1cc13205a
- Dragonetti, C.; Colombo A. Recent Advances in Dye-Sensitized Solar Cells. *Molecules* 2021, 26(9), 1-3, 2461. doi:10.3390/molecules26092461
- Ge, R.; Wang, X.; Zhang, C.; Kang, S.-Z.; Qin, L.; Li, G.; Li, X. The influence of combination mode on the structure and properties of porphyrin–graphene oxide composites. *Colloids Surf. A*, 2015, 483, 45-52.
- Hasobe, T. Supramolecular Nanoarchitectures for Light Energy Conversion. *Phys. Chem. Chem. Phys.* 2010, 12, 44–57.
- Hasobe, T. Porphyrin-Based Supramolecular Nanoarchitectures for Solar Energy Conversion. *The Journal of Physical Chemistry Letters* 2013, 4(11), 1771–1780. doi:10.1021/jz4005152
- Mao, B.; Hodges, B; Franklin, C.; Calatayud, D. G.; and Pascu, S. I. Self-Assembled Materials Incorporating Functional Porphyrins and Carbon Nanoplatfoms as Building Blocks for Photovoltaic Energy Applications. *Front Chem* 2021, 9, 1-36, 727574. doi: [10.3389/fchem.2021.727574](https://doi.org/10.3389/fchem.2021.727574)
- Shmavonyan, G. Sh.; Vázquez-Vázquez, C.; and López-Quintela, M. A. Single-step rubbing method for mass production of large-size and defect-free 2D materials. *Trans. Mater. Res.* 2017, 4(2), 025001. doi: <https://doi.org/10.1088/2053-1613/aa783d>
- Tovmasyan, A. G.; Babayan, N. S.; Sahakyan, L. A.; Shahkhatuni, A. G.; Gasparyan, G. H.; Aroutiounian, R M.; and Ghazaryan, R. K. Synthesis and in vitro anticancer activity of water-soluble cationic pyridylporphyrins and their metallocomplexes. *J. Porphyrins Phthalocyanines* 2008, 12, 1100-1110.



Metal Nanoparticles: eco-compatible fungicide alternatives to combat resistance

A. Malandrakis¹, N. Kavroulakis² and C. Chrysikopoulos¹

¹ School of Environmental Engineering, Technical University of Crete, Chania, Greece.

² Hellenic Agricultural Organization “Dimitra”, Institute for Olive Tree, Subtropical Plants and Viticulture, Agrokipio-Souda, Chania, Greece.

Corresponding author email: tasmal@aua.gr

keywords: Nanofungicides; Ag-NPs; Cu-NPs; ZnO-NPs; synergy; fungicide resistance.

Introduction

Chemical control via the use of synthetic fungicides remains the most cost-efficient disease management strategy so far ensuring food sustainability and safety. This valuable asset of the plant protection arsenal is seriously threatened by high environmental footprints, toxic effects to non-target organisms, increasing costs on RnD and registration and the loss of fungicide effectiveness due to resistance development. The risk of environmental pollution and especially contamination of the aquifer by misuse of pesticides, have forced the EU to implement strict regulations resulting in the withdrawal of a great number of older fungicide active ingredients and a restrain in the development of new ones. This fact has rendered fungicide resistance management even more difficult highlighting the necessity for alternative disease management agents for controlling resistant pathogens in a more environmentally safe way.

Nanotechnology has the potential to be an important part of modern agriculture by providing novel means for improving crop production and protection in the form of nano-fertilizers, nano-pesticides or nano-carriers for biologically important active ingredients. Metal nanoparticles (MNPs) possess unique physico-chemical properties enabling them to control a number of plant pathogens both sensitive and fungicide-resistant. Lower than their ionic counterparts' doses required for anti-microbial action and their potential to be synthesized by green methods (utilizing plants or microorganisms) render MNPs eco-friendly alternatives to synthetic fungicides. Under this light, this study aimed to: (a) evaluate the effectiveness of silver, copper, and zinc oxide NPs against sensitive and fungicide resistant *Alternaria alternata*, *Botrytis cinerea* and *Monilia fructicola* isolates, (b) investigate the potential of metal-NPs to be used in mixtures with fungicides against fungal phenotypes both *in vitro* and *in vivo*, and (c) provide insights on the mechanisms underlying the fungitoxic mode of action and synergy profiles of MNPs with fungicides.

Materials and methods

Nanoparticles, fungicides and their mixture suspensions were characterized by measuring zeta potential and hydrodynamic diameter using a Zetasizer (Nano ZS90, Malvern Instruments, Southborough, MA).

Fungal isolates were screened *in vitro* for resistance to commercial fungicides by fungitoxicity tests utilizing the poison agar assay. Resistance mutations of respective phenotypes were identified at a molecular level by target gene amplification and sequencing.

The potential of metal NPs to control sensitive and fungicide-resistant fungal isolates alone or in combination with fungicides, was evaluated by fungitoxicity tests both *in vitro* and *in vivo*. Fungitoxicity was expressed as percent relative inhibition of isolates grown on PDA amended with appropriate concentrations of the antifungal active ingredients.

Results and discussion

Metal NPs could effectively inhibit mycelial growth in a dose-dependent way in both sensitive and fungicide resistant isolates. The fungitoxic effect of NPs against the pathogens was significantly enhanced when combined with a number of fungicides boscalid, thiophanate-methyl and fluazinam compared to the individual treatments in most phenotype cases both *in vitro* and *in vivo* (Fig.1a).

Indications for possible mechanisms explaining the fungitoxic effect of metal NPs were found to include metal-ion release, nanoparticle interference on cellular ion homeostasis mechanisms and a potential “capping” effect contributing to an enhanced NP membrane penetration. A possible role of ATP-dependent ion efflux mechanism and ROS production in the mode of action of metal NPs was also identified (Fig. 1b,c).

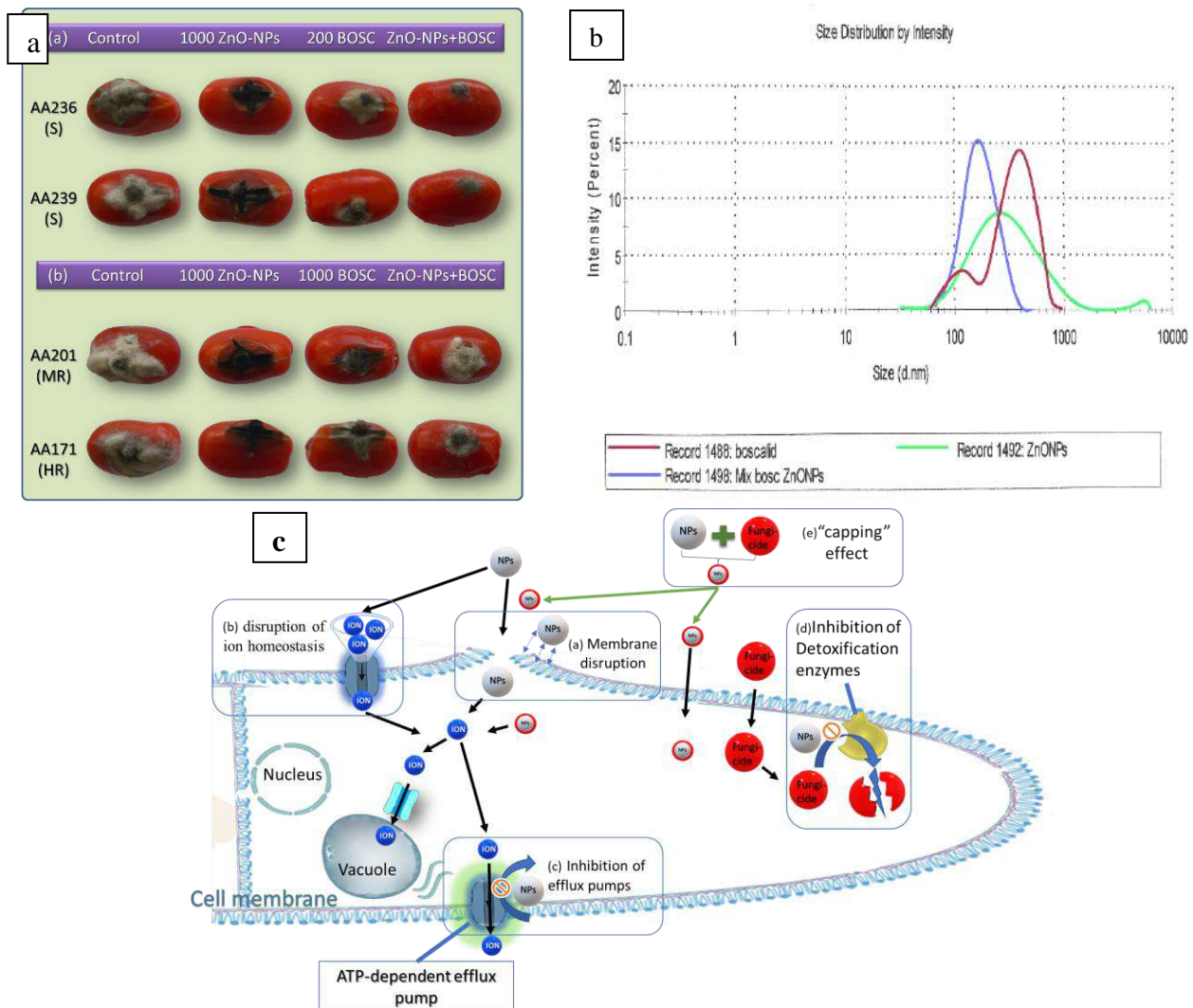


Figure 1. (a) Synergistic activity of ZnO-NPs in combination with boscalid against representative sensitive or highly boscalid-resistant *Alternaria alternata* isolates; (b) Mean size distribution of boscalid (10 µg/mL), ZnO-NPs (300 µg/mL) particles and their mixture measured by Dynamic Light Scattering; (c) Potential fungitoxicity mechanisms of metal NPs.

Conclusions

Silver, copper and zinc oxide NPs exhibit a great potential and can be effectively used against plant pathogens both alone or in combination with conventional fungicides, providing tools for combating fungicide-resistance and reducing the environmental footprint of synthetic fungicides.

References

- Malandrakis, A.A., Kavroulakis, N., Chrysikopoulos, C.V., Use of copper, silver and zinc nanoparticles against foliar and soil-borne plant pathogens. *Science of the Total Environment* 670: 292-299 (2019).
- Malandrakis, A.A., Kavroulakis, N., Chrysikopoulos, C.V. Zinc nanoparticles: Mode of action and efficacy against boscalid-resistant *Alternaria alternata* isolates *Science of the Total Environment* 829: art. no. 154638 (2022).
- Slavin, Y.N., Asnis, J., Häfeli, U.O., Bach, H. Metal nanoparticles: Understanding the mechanisms behind antibacterial activity *Journal of Nanobiotechnology* 15: art. no. 65 (2017).
- Jamdagni, P., Rana, J.S., Khatri, P., Comparative study of antifungal effect of green and chemically synthesised silver nanoparticles in combination with carbendazim, mancozeb, and thiram. *IET Nanobiotechnology* 12: 1102-1107 (2018).



Synthesis and Study of starch/CeO₂ Nanoparticle Composite Material for Removal of Hexavalent Chromium from Synthetic Wastewater Solutions

O. Jaiyeola¹ and C. Mangwandi¹

¹School of Chemistry and Chemical Engineering, Queen's University Belfast, Northern Ireland, UK

Corresponding author email: c.mangwandi@qub.ac.uk

keywords: chromium; starch, biosorption; starch cerium oxide, isotherm.

Introduction

Hexavalent chromium is known to be very toxic to humans and animals due to its ability to diffuse freely across cell membranes and its high oxidation potential (Mona et al., 2011). The common methods used for the chromium removal from wastewater include precipitation, ion exchange, membrane filtration, reverse osmosis and adsorption. Precipitation process is usually favoured, but the major drawback is sludge formation. Biosorption however, is an innovative method that uses biomaterials which are either inexpensive or highly available, for instance; olive oil industry waste (Malkoc et al., 2006). This study uses the biomaterial starch-based as an adsorbent material for the removal of Cr(VI) ions. In this project the new adsorbent material starch/cerium oxide nanocomposite was produced as low-cost adsorbents for complete removal of chromium (hexavalent/trivalent) from synthetic aqueous solutions. The effect of pH, temperature and dosage were evaluated.

Materials and methods

A dispersed solution of starch was prepared by mixing 3.0g of starch in 100ml of deionised water. 3.0 grams of citric acid (the crosslinking agent) and 1.5g of the sodium hypophosphite monohydrate catalyst (NaH₂PO₂·H₂O) was dissolved in the starch solution for cross-linking (M. Naushad et al.2016). The resulting starch suspension was continuously stirred at 60°C for 2 hours, then left to cool to room temperature.

To prepare the hydrous cerium oxide, 0.02 moles of sodium hydroxide powder was dissolved in 100 mL of ethanol (absolute) to prepare 0.2 M sodium hydroxide/ethanol solution. 0.005 moles of Ce(NO₃)₃·6H₂O powder was dissolved in 100 mL of ethanol (absolute) to prepare 0.05 M Ce(NO₃)₃/ethanol solution. The sodium hydroxide/ethanol solution was then added into the Ce(NO₃)₃/ethanol solution at ambient temperature under vigorous stirring.

After the two solutions were mixed, the colour of the precipitates was white in just 20 minutes after continuous stirring. Precipitate was collected by centrifugation, rinsed with deionised water and ethanol (absolute) three to four times and then dried in an oven at 60°C for 12 hours to obtain Starch/CeO₂ adsorbent. Finally, the dried product was crushed using a mortar and pestle into fine particles of uniform size and shape (Ronghui Li et al.2012). The Cr(VI) concentration in solid phases was calculated from the equation:

$$Q_e = \frac{(C_i - C_e) V}{m}$$

where C_i and C_e are the liquid-phase concentrations of chromium initially and at equilibrium respectfully and both measured in mg/L. Volume of solution (L) and m is the mass of dry adsorbent used for the experiment in grams. A colour reagent was synthesized using methods reported by (Albadarin et al. 2013) by adding 0.25g of 1,5-diphenylcarbohydrazide to 50mL methanol, 14mL sulfuric acid and 500mL deionised water. To determine Cr(VI) concentration after treatment using the nanocomposites 6mL of the solution was added to 2mL of the colour reagent for each sample.

Results and discussion

pH studies were carried out and it was confirmed that low pH values favour adsorption onto the starch/CeO₂ nanocomposites (Albadarin et al. 2013). The highest removal was achieved at pH 2 and the removal decreased as the pH was increased. The general interpretation of the influence of pH on Cr (VI) metal adsorption is based



on the functional group as well as the ionic composition that is present in the nanocomposite adsorbent. The high percentage removal at low pH is related to the composition of the Cr and the starch nanocomposite surface. In acidic conditions the dominant species of Cr present is $\text{Cr}_2\text{O}_7^{2-}$ (M.S. Alfa-Sika et al.2010). To determine the adsorption capacity of the material different isotherms were fitted to the data. The Langmuir isotherm provide the best fit to the data.

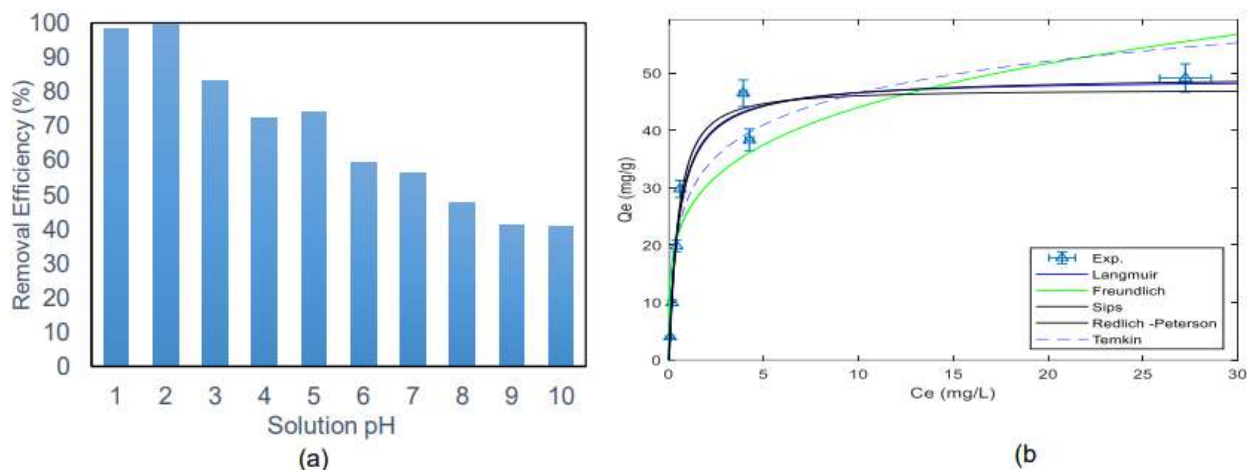


Figure 1. pH Test: The effect of solution pH on Removal % with initial concentration of 100ppm and adsorbent dosage of 2.5g/L. (a) Isotherm models comparison for Cr(VI) removal from solution by CeO_2 starch nanocomposite adsorbent with constant pH 2 and adsorbent dosage of 2.5g/L (b).

Conclusions

In conclusion, there was a successful synthesis of starch/ CeO_2 nanocomposites via the sol-gel method and its use for the removal of Cr(VI). The optimum pH for this study was pH 2. The detailed adsorption study shows that increasing the dosage, decreasing the initial Cr(VI) concentrations, increasing the contact time and temperature resulted in better removal percentages. The detailed adsorption study also showed that starch cerium oxide nanocomposite material had Cd removal capacity (48.54 mg/g) which is competitively high when compared to other adsorbent materials reported in literature. The new adsorbent developed in this work show great potential for removal of hexavalent chromium. Future studies will focus on evaluating its performance in a continuous system.

References

- M. Naushad, T. Ahamad, G. Sharma, A. a. H. Al-Muhtaseb, A. B. Albadarin, M. M. Alam, Z. A. Alothman, S. M. Alshehri and A. A. Ghfar, *Chemical Engineering Journal*, 2016, 300, 306-316.
- Ronghui Li, Qi Li, Shian Gao, Jian Ku Shanga (2012) 'Exceptional arsenic adsorption performance of hydrous cerium oxide nanoparticles: Part A. Adsorption capacity and mechanism', *Chemical Engineering Journal*, 246(1), pp. 127-135
- A. B. Albadarin, C. Mangwandi, G. M. Walker, S. J. Allen, M. N. M. Ahmad and M. Khraisheh, *Journal of Environmental Management*, 2013, 114, 190-201.
- M.S. Alfa-Sika, F. Liu, H. Chen Optimization of key parameters for chromium(VI) removal from aqueous solutions using activated charcoal *J Soil Sci Environ Manage*, 1 (2010), pp. 55–62
- S. Mona, A. Kaushik, C.P. Kaushik Biosorption of chromium(VI) by spent cyanobacterial biomass from a hydrogen fermentor using Box-Behnken model. *International Biodeterioration & Biodegradation*, 65 (2011), pp. 656-663.
- E. Malkoc, Y. Nuhoglu, M. Dunder. Adsorption of chromium(VI) on pomace-an olive oil industry waste: batch and column studies. *Journal of Hazardous Materials*, 138 (2006), pp. 142-151.



Nutmeg seed shell-based silver nanoparticle/PVA composite for the synthesis of antimicrobial food packaging films

T. Thomas¹ and A.K. Thalla¹

¹Center for sustainable development, National Institute of Technology Karnataka, India

Corresponding author email: teemathomas111@gmail.com

keywords: Nutmeg seed shell; Aqueous extract; PVA; Antimicrobial property.

Introduction

Increasing the application of polyvinyl alcohol (PVA) films for food packaging and other applications, it is vital to enhance its mechanical and antibacterial properties. PVA added with silver nanoparticles (AgNP) enhances the antimicrobial property. The green synthesis of silver nanoparticles from their metal precursor can be done by adopting an apt reducing and capping agent. Nutmeg seed shell is an agricultural waste which has a high content of these reducing agents and capping agents in terms of flavonoids, myristicin, polyphenols and tannins.

Materials and methods

Preparation of nutmeg seed shell aqueous extract

The aqueous extract from the nutmeg seed shell is prepared by adding 10 g, 105 μ m size nutmeg seed shell powder into 100 mL deionized water and boiled for 1 hour and then centrifuged to separate the supernatant at 5000 rpm for 5 min.

Preparation of polymer films

In-situ preparation of polymer film is carried out by adding 5 mL of nutmeg seed shell aqueous extract to 95 mL of 1mM silver nitrate solution then, 10 g of PVA is added and continuously stirred at 1000 rpm at 90°C for One hour. The solution is poured into a Petri dish and dried for 6 hours in a hot air oven to prepare films.

The polymer films were cast with 1 mM, 2 mM, 3 mM, 4 mM, and 5 mM concentrations of silver nitrate solution and control as only PVA for further analysis.

Antimicrobial property

The antibacterial property of films is determined by inhibition zone analysis. Escherichia coli and Bacillus subtilis were used as model bacteria to evaluate the antibacterial properties of the PVA-AgNP films prepared in this study, and the standardized agar disk diffusion plate test method was used. The nutrient broth is poured into each sterilized petri dish and microbes are uniformly spread onto it. Plates were incubated for 24 h at 37°C immediately after placing the test specimens with 5 mm circular diameter PVA-AgNP films on the agar. The bacterial growth was then checked (Maruti Kesava Kumar et al. 2015).

XRD analysis and mechanical analysis

Crystalline nature and components in the polymer composite are analyzed by X-ray diffraction analysis at a 2θ range of 10° - 80° with monochromatic Cu K α radiation ($\lambda = 0.1540598$ nm). Tensile tests of the films were performed using an electromechanical universal testing machine according to the ISO 527-3-2018 standard method (ISO 527-2, Plastic) to determine the mechanical properties.

Results and discussion

Antimicrobial property analysis with gram-positive and gram-negative bacteria shows that with respect to PVA films PVA-AgNP polymer composite shows better antimicrobial character and it is evident from the inhibition zone analysis (Table 1). The inhibition of cell growth of microorganisms is due to the distortion of cytoplasm by silver nanoparticles (Yahia et al. 2022). The distortion of microbe can be attained by two mechanisms: it will attach to the proteins that contain sulphur and result in the cell malfunctioning. The other mechanism is attachment or penetration through the cell wall, resulting in cell degradation (Haider and Kang 2015).



Table 1. Inhibition zone diameter for silver nanoparticles embedded film against bacterial strains

Microbes	Inhibition zone (mm)			
	1 mM silver nitrate	Nutmeg seed shell extract	PVA	PVA-AgNP
E coli rosetta	6	6	0	10
Bacillus subtilis	0	6	0	11

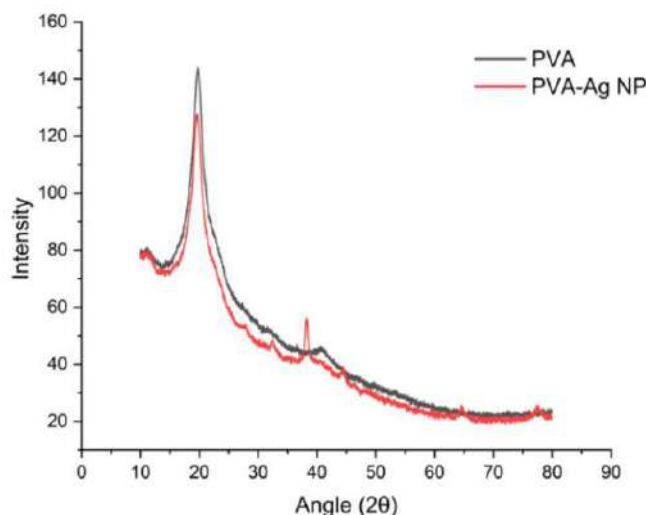


Figure 1. XRD analysis for polymer sheet with and without Ag NP.

As can be seen from figure 1, the AgNPs were well crystallized and showed sharp peaks at 2θ angles of 37.5° , 45° , 63.8° and 76° . These were assigned to the (111), (022), (220) and (131) planes of the Ag and confirm that the AgNP crystals were successfully prepared (Aravind et al. 2021). The tensile strength of the CNC-PVA-AgNP nanocomposite films increased from 42.4 MPa to 81 MPa for 10% PVA and 10% PVA with 5 mM silver nitrate solution and 5 mL extract.

Conclusions

PVA films are mostly used as food packaging material which is having less antimicrobial potential. In this study agricultural waste: nutmeg seed shell-based nanoparticle infusion into PVA films in a one-step process is implemented successfully with better antimicrobial properties to both gram-positive and gram-negative bacteria along with better tensile strength property. The work done shows that agricultural waste as nutmeg Seed shell and its extract can act as reducing and capping agent to support the formation of silver nanoparticles and helps to improve the properties of packaging material with higher mechanical properties and antimicrobial property.

Acknowledgements: The authors express their heartfelt gratitude to the Center for sustainable development NITK Surathakal (UV-visible spectrophotometer and centrifuge), the Department of Metallurgy NITK Surathakal (XRD,) and the Department of chemistry (FTIR) for providing the instrumental analysis for this research work. **Funding:** Authors didn't receive any funding from any organization.

References

- Aravind, M., Ahmad, A., Ahmad, I., Amalanathan, M., Naseem, K., Mary, S. M. M., Parvathiraja, C., Hussain, S., Algarni, T. S., Pervaiz, M., and Zuber, M. (2021). "Critical green routing synthesis of silver NPs using jasmine flower extract for biological activities and photocatalytic degradation of methylene blue." *J. Environ. Chem. Eng.*, 9(1), 104877.
- Haider, A., and Kang, I. K. (2015). "Preparation of silver nanoparticles and their industrial and biomedical applications: A comprehensive review." *Adv. Mater. Sci. Eng.*, 2015.
- Maruti Kesava Kumar, C., Yugandhar, P., and Savithamma, N. (2015). "Adansonia digitata leaf extract mediated synthesis of silver nanoparticles; characterization and antimicrobial studies." *J. Appl. Pharm. Sci.*, 5(8), 82–89.
- Yahia, R., Owda, M. E., Abou-Zeid, R. E., Abdelhai, F., Gad, E. S., Saleh, A. K., and El-Gamil, H. Y. (2022). "Synthesis and characterization of thermoplastic starch/PVA/cardanol oil composites loaded with in-situ silver nanoparticles." *J. Appl. Polym. Sci.*, 139(3).



SUST
ENG
2022



INFRASTRUCTURE & BUILDING MATERIALS



Risk informed decision criteria for the sustainable design of renewable energy infrastructures

D. Diamantidis¹

¹Ostbayerische Technische Hochschule Regensburg, Germany

Corresponding author email: Dimitris.Diamantidis@oth-regensburg.de

keywords: design, infrastructures, reliability, renewable energy, risk.

Introduction

Project funding in clean energy need to be increased considerably in the coming years to support growth under climate change conditions. Significant public investments have been recently made worldwide leading to an expansion of the green energy production and of the associated supporting structures such as wind turbines, ground or roof mounted photovoltaics, storage systems of biomass or of wood pellets. At present limited guidelines on the design of such structures are available and therefore standards for the design of normal buildings are frequently applied. However, the design of clean energy structures significantly differs from common structural design due to: a) lower design lifetime (20-25 years) which in many cases is defined; b) failure is usually not associated with the loss of human life; c) resistance uncertainties need attention due to new materials involved; d) extreme actions such a wind are dominating structural reliability as associated with a large scatter. To provide economically, environmentally, and socially sustainable design solutions risk informed decision criteria have to be provided and embedded in related standards. The scope of this contribution is to discuss such criteria based on experience from other industrial domains e.g. the chemical or the transportation industry and to illustrate their implementation in case studies.

Methodology

The basics of risk assessment are presented first, see for a discussion Trbojevic (2005), Diamantidis (2017). The risk combined with a hazard is a combination of the probability of occurrence of this hazard and the consequences in case that it occurs. The simplest function relating the two constituents of risk R is therefore used by multiplying the probability of failure (of the structure) p_F by the consequences of failure C_F and represents the expected value E of the failure consequences:

$$R = p_F \times C_F = E[C_F]$$

The failure probability is calculated based on data and computation techniques. Three major types of potential consequences are considered: a) direct and indirect economic losses reflecting the resilience of the wider system, b) environmental impacts due to pollution, c) human consequences. The consequences can be monetized by assigning values to the various types of losses. By applying a cost-benefit approach, risk acceptability criteria have been implemented in industrial domains and related projects by evaluating the costs and benefits of each possible investment into safety.

The most important parameter obtained from such analyses affecting sustainability in construction is the optimum target level of reliability based on probabilistic optimization (Rackwitz, 2000) considering sustainability parameters including construction costs and failure consequences.

Results and conclusions

It is shown that the derived reliability levels may be lower for energy related infrastructures due to lower consequences of failure in case of limited human losses.



Two case studies are considered:

- a) Ground mounted photovoltaic constructions subjected to dead and wind load, s. Fig. 1.
- b) Storage rooms for wood pellets (Fig. 2) subjected to blow overpressure and static silo pressure.

In both cases it is shown that the optimum target reliability level to be used in design is lower than the one used for normal constructions and that sustainability in construction of energy related structures and infrastructures can be effectively achieved by saving material costs.



Figure 1. Ground mounted photovoltaic structure.



Figure 2. Storage construction for wood pellets (sbz-online.de).

Acknowledgements: This study has been supported by the Regensburg Centre of Energy and Resources (RCER) of the Ostbayerische Technische Hochschule Regensburg (OTH Regensburg) and the Technology- and Science Network Oberpfalz (TWO).

References

- Diamantidis, D., 2017. A critical view on environmental and human risk acceptance criteria. *International Journal of Environmental Science and Development*, Vol. 8, No.1.
- Rackwitz, R., 2000. Optimization - the basis of code-making and reliability verification. *Structural Safety*, Vol. 22, pp. 27-60.
- Trbojevic, V.M., 2005. Risk Criteria in the EU. *Proceedings of ESREL 05*. Rotterdam: Balkema.



Production of Phase Change Material from Waste Low Density Polyethylene for Thermal Energy Storage Applications

H. Akgun¹, A. Ozkan¹, Z. Gunkaya¹ and M. Banar¹

¹Environmental Engineering Department of Eskisehir Technical University, Eskisehir, Turkey
Corresponding author email: hasretakgun@eskisehir.edu.tr

keywords: LDPE, PCM, TES, waste plastic.

Introduction

After the petroleum crises experienced in recent years, thermal energy storage (TES) by using heat transfer media such as phase change materials has become an increasingly important research area (Peng et al., 2021). Latent heat thermal energy storage (LHTES) is the most interesting method in TES technologies recently. Phase change materials (PCMs) used in LHTES have a compound annual growth rate (CAGR) which is 16 % (http 1, 2021). PCMs are special materials that can store a high amount of heat as energy during phase change at constant temperature and are classified as organics, inorganics, and eutectic (Abdelrazeq, 2016). Paraffins, as PCMs among organic materials, are the substances that have shown the most interest by researchers (Acar, 2014; George et al., 2020). Paraffins provide high energy storage density relative to their low mass and exhibit favorable melting and solidification with negligible supercooling, are very chemically stable, and do not react with most chemicals. However, since the phase changes of paraffin waxes are between solid and liquid phases, they cannot be used directly in applications. Paraffin waxes can be mixed with polymers to prevent the PCM's tendency to leak after melting and loss of the liquid phase. Low density polyethylene (LDPE) is considered as a suitable polymer to be mixed with paraffin waxes due to its significant share in plastic waste in the global plastic demand (17.4%), its structural and chemical compatibility with wax and prevention of wax leakage (Sobolciak et al., 2015; Abdelrazeq et al., 2016; http 2, 2021). Unfortunately, as a result of the use of LDPE, the amount of waste also increases (Stan et al., 2019).

In this study, it was aimed to obtain paraffin wax by pyrolysis of LDPE packaging wastes and to use it as a PCM. (Jeswani et al., 2020).

Materials and methods

In the first stage, the decomposition temperature of LDPE packaging waste was determined by thermogravimetric analysis (TGA). According to the results obtained from the literature review, the pyrolysis process was carried out according to the temperature and heating rates at which the expected maximum wax product yield would be obtained. LDPE wastes were pyrolyzed at 450°C and a heating rate of 10°C/min. Elemental analysis, TGA, and differential scanning calorimetry analysis (DSC) of the liquid product (PE-Wax) were performed. Additionally, for the comparison, these analyzes were performed for waste LDPE and commercial wax too.

In the second stage, composite PCMs were produced by mixing PE-Wax and waste LDPEs at 10, 20, 30, 40, and 50% PE-Wax ratios by twin screw extrusion process. The extrusion has a screw diameter of 16 mm, and an initial temperature of 130 °C, the other 7 zones are 140 °C, and screw speed 35 rpm. In addition to this, mixing processes were performed using commercial paraffin wax. Elemental contents of composite PCM samples were determined by elemental analysis, decomposition temperatures and weight loss percentages were determined by TGA, and melting temperatures were determined by DSC analysis. For the comparison, DSC analysis was performed for commercial wax composites too.

Results and discussion

Elemental analysis results are given in Table 1. According to these results, the carbon content of the product obtained by the pyrolysis of waste LDPE decreases compared to waste LDPE. On the other hand, elemental content of pyrolysis wax was found to be very close to commercial wax.

Table 1. Elemental analysis results

%	C	H	O	N
Waste LDPE	87.9	10.5	1.1	0.5
PE-Wax	55.6	9.2	34.4	0.8



Commercial wax	57.6	9.4	32.3	0.7
Waste LDPE + %50 PE-Wax	82.9	10.3	6.1	0.7

TGA-DTA and DSC analysis results are shown in Figure 1(a-b).

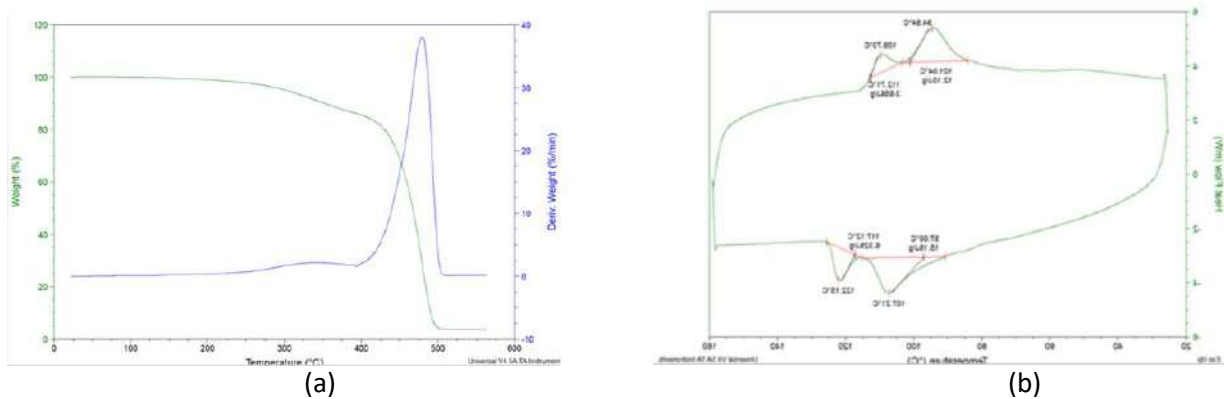


Figure 1. a) TGA-DTA curve of PCM produced with 50% PE-Wax + waste LDPE, **b)** DSC curve of PCMs produced with 50% PE-Wax + waste LDPE.

Conclusions

In this study, wax was produced from waste LDPE as an alternative to paraffin wax (produced from crude oil), which is a low-cost thermal energy storage material in a certain temperature range with good thermal stability and suitable latent heat and used as PCM.

Acknowledgements: This study was supported by Eskişehir Technical University Scientific Research Projects Commission under the grant number 22DRP156 and 22ADP097.

References

- Abdelrazeq, H., W., 2016. Heat Absorbers Based on Recycled Polyethylene and Paraffin Wax for Energy Storage. Master's Thesis, Qatar University, College of Arts and Sciences.
- Acar, S. Ş., 2014. Phase change materials and applications. Master thesis. Firat University
- Europe, P., 2020. Plastics-the Facts 2020 An analysis of European plastics production, demand and waste data. Available on the website: <http://www.plasticseurope.org>.
- George, M., Pandey, A. K., Abd Rahim, N., Tyagi, V. V., Shahabuddin, S., & Saidur, R., 2020. A novel polyaniline (PANI)/paraffin wax nano composite phase change material: Superior transition heat storage capacity, thermal conductivity and thermal reliability. *Sol. Energy*, 204, 448-458.
- http 1, 2021. Global Phase Change Materials Market - Segmented by Product Type, End-User, Encapsulation Technology and Geography - Growth, Trends and Forecasts (2018 - 2023) (accessed 18.06.2021).
- http 2, 2021. <https://www.mordorintelligence.com/industry-reports/low-density-polyethylene-market> (Accessed 27.10.2021)
- Jeswani, H., Krüger, C., Russ, M., Horlacher, M., Antony, F., Hann, S., & Azapagic, A., 2021. Life cycle environmental impacts of chemical recycling via pyrolysis of mixed plastic waste in comparison with mechanical recycling and energy recovery. *Sci. Total Environ.*, 769, 144483.
- Peng, H., Wang, J., Zhang, X., Ma, J., Shen, T., Li, S., & Dong, B., 2021. A review on synthesis, characterization, and application of nanoencapsulated phase change materials for thermal energy storage systems. *Appl. Therm. Eng.*, 185, 116326
- Sobolčiak, P., Abdelrazeq, H., Ouederni, M., Karkri, M., Al-Maadeed, M. A., & Krupa, I., 2015. The stabilizing effect of expanded graphite on the artificial aging of shape stabilized phase change materials. *Polym. Test.*, 46, 65-71.
- Stan, F., Stanciu, N. V., Fetecau, C., & Sandu, I. L., 2019. Mechanical Recycling of Low-Density Polyethylene/Carbon Nanotube Composites and Its Effect on Material Properties. *J. Manuf. Sci. Eng.*, 141(9), 091004.



Effect on the thermal sensation of outdoor users due to the age of the granite blocks used in the coating of public areas

K. Stefanopoulos¹, N. Lianos¹, D. Polychronopoulos¹ and S. Zoras²

¹Dept. of Architectural Engineering, Democritus University of Thrace, Xanthi, Greece

²Dept. of Environmental Engineering, Democritus University of Thrace, Xanthi, Greece

Corresponding author email: kstefanopoulo@gmail.com

keywords: *granite; blocks; coating; outdoor; public area; urban; temperature; thermal sensation, comfort conditions.*

Introduction

The aim of this work is the study of the differentiation of responses among newer materials compared to the same but older materials that have been used and exposed for a longer period of time.

The old town of Xanthi is located at the north-eastern edge of Greece in the homonymous prefecture and the Region of Eastern Macedonia and Thrace. After the catastrophic earthquake of 1829 with which the city of Xanthi was levelled, the new period of its reconstruction began with particular prosperity due to the tobacco trade from 1870-1910. Reconstruction and economic prosperity stopped in 1912 with the start of the Balkan Wars. To this day, the traditional character of the old town of Xanthi has been preserved and is a protected settlement. The streets of the old city have always had as a paving material the dark grey granite blocks that are placed with a special technique and due to their great durability are kept for many years in very good condition.

Materials and methods

The difference in climatic conditions between the city and its periphery is greatly influenced by the response of sunlight that falls and is trapped in the ground, in the coating materials and in the various general constructions (Chrysomallidou N., Theodosiou Th., Tsikaloudaki K., 2002). This response also depends on other factors concerning the paving materials of public areas. The comparison is made between different points in the urban fabric of the old town of Xanthi, which are paved with grey granite cobblestones. These areas are important road intersections, squares but also parking lots. These points have been reconstructed in different periods of time, which we know from an archive of the Municipality of Xanthi with projects carried out from 1992 until today. During the day the selected areas are exposed to the sun as well as they are in the shadow caused by vegetation or buildings, due to the course of the sun.

An effort has been made to demonstrate whether newer or older coating materials behave better in the comfort conditions of their users and especially the thermal sensation. For this purpose, the temperature was recorded at the height of a person, above specific areas that are covered with grey granite blocks, during the warm period of the year. The comparison was made between the means of the temperature measurements recorded at each point. The measurements were made hours of the day when the sun most influences the response of the materials and specifically at 12.00pm, 15.00pm and 18.00pm.

Results and discussion

A comparison was made between points that were reconstructed in the same year and specifically in 1998, such as points 4 and 14. In addition, the comparison was made between points that were reconstructed in close years, such as points 4 and 10 with respective reconstructions years of 1998 and 1995 (Figure 1). It was made at the same time of the day as well as the measurements were made when the two points that compared were both exposed to the sun or in the shadow. This choice was necessary so the worst case of sun exposure not to affect the outcome. During this comparison it was found that the two points compared to each other were very close to the temperatures measured. They have a difference less than 1,0°C at points 4 and 14 at the same time. This can be justified due to the riparian location of the point 14 in comparison with the point 4 located in the heart of the settlement with the narrow streets and a larger number of buildings.



In the comparison between points that were reconstructed at long intervals between each other and specifically before 1992 and 2003 and points 3 and 8, the measurements were made for the same time of the day. That time was chosen when both of the points were exposed to the sun or in the shadow, so that the worst case of sun exposure not to affect the result once again (Figure 1). During this comparison it was found that the two points compared to each other had a deviation in the temperatures measured. There was a difference of more than 1,0°C at points 3 and 8 at the same time. Both points are located in the old town of Xanthi in similar morphologically areas or even if they are affected by other conditions. The highest temperatures were measured in the older granite cobblestone coatings.



Figure 1. Measurement points and years of cobblestone reconstruction.

Conclusions

The comparison was made between points that were reconstructed in the same year or in nearest years as well as the comparison between points that were reconstructed in distant years. Also was made for the same time of the day, that is, 12.00pm, 15.00pm and 18.00pm. The measurements were made when the two points that compared were both exposed to the sun or in the shadow.

The results of the comparison were found that the two points which compared with the nearest years of reconstruction, were very close to the temperatures measured, with a difference less than 1,0°C. The comparison between points that were reconstructed in distant years had a deviation in the temperatures measured, with a difference of more than 1,0°C. The same conclusions were found in the comparison of other points with similar conditions.

As we have seen, the highest temperatures were measured in the older granite cobblestone coatings. This leads us to the conclusion, that the newer grey granite blocks respond better in terms of comfort conditions to users of the outdoor public areas where they have been coated. The temperature difference between the newer and the older granite blocks is more than 1,0°C.

References

Chrysomallidou N.- Theodosiou Th.- Tsikaloudaki K. ,2002. Sustainable development of free spaces in an urban environment, paragraph 5.1., Conference: Bioclimatic design in urban outdoor space.



SUST
ENG
2022



WATER TREATMENT



**Selection of method water cleaning method and qualification of demanganization temperature
filter fire troubleshooting in central provision.
Kedronas of DEYA Edessas**

A. Mpinos¹ and I. Chatzoglou²

¹Diploma Engineering of Production and Management, PhD, Technical Department DEYA Edessas, Greece

²President of Municipal Enterprise, Board of directors of DEYA Edessas, Greece

Corresponding author email: mpinosan@yahoo.gr

keywords: *pyrolusite filters; water analysis; ironing; demanganization.*

Introduction

The purpose of this study is to examine the water produced in Kedrona Edessa as well as to find the best techno-economic method of treatment to be characterized as suitable for drinking. The study was carried out with the aim of producing 50 m³ / d of water. The technical study presents the laboratory analyzes that were performed and the treatment methods that were piloted and finally the method that was selected and used was selected. In the present study, the laboratory measurements of the produced water are presented, which highlight its high content of turbidity, mud and iron and the optimal way of its treatment is proposed.

Materials and methods

The flocculation method was studied in order to reduce the turbidity and parameters that are outside the law. This method combines the use of various chemical additives and engineering to remove contaminants in the form of sediment. The use of flocculants such as iron chloride, aluminum sulfate, iron sulfate in combination with organic polymers such as polyelectrolytes has been considered. Although these methods seem to have very good results, they have led to high cost and maintenance unit design and have therefore been rejected.

After a thorough study of such industrial applications, use of appropriate computer tools and after laboratory verification, the use of turbidity filters (pyrolusite sand filters) in combination with iron removal filters is able to process and successfully produce drinking water at the lowest possible cost. maintenance, operation as well as initial investment.

Results and discussion

The system water regeneration cycle is activated when a predetermined volume of water passes through the filter. 10% sodium hypochlorite solution is used as a means of regenerating manganese black oxide. The regeneration function requires an initial reverse wash to remove residual substances such as iron hydroxides, manganese or other suspended solids. The filtration bed is then drained and then refilled with water (at room temperature) with a predetermined dose of sodium hypochlorite. The filtration bed is left flooded for a predetermined time. After this operation, the reverse wash of the filter is completed.

Prior to restarting the filter in normal operation, a thorough rinsing is performed to eliminate possible sodium hypochlorite residues and to rearrange the filtration bed.

Conclusions

The proposed solution was selected as the most optimal for reasons of low cost of purchase and installation as well as low cost of use due to lack of consumables. In addition, the installation of a fully automated operating device with telemetry elements that will be analyzed in the next article make the solution of these filters a value for money option.

References

Stumm, W. Chemistry of the Solid-Water Interface: Processes at the Mineral-Water and Particle-Water Interface in Natural Systems; John Wiley & Sons: New York, NY, USA, 1992.



- Macioszczyk, A. Hydrogeochemia; Wyd. Geologiczne: Warszawa, Poland, 1987.
- Jędrzychowska, S. Możliwości Wykorzystania Spektroskopii Ramanowskiej w Branży Naftowej, cz. I.; Nafta-Gaz: Kraków, Poland, 2012.
- Anschutz, P.; Dedieu, K.; Desmazes, F.; Chaillou, G. Speciation, oxidation state, and reactivity of particulate manganese in marine sediments. *Chem. Geol.* 2005, 218, 265–279. [CrossRef]
- Szybowicz, M.; Koralewski, M. Micro-Raman spectroscopy of natural and synthetic ferritins and their mimetics. *Acta Phys. Pol. A* 2015, 127, 534–536. [CrossRef]
- Julien, C.; Massot, M.; Baddour-Hadjean, R.; Franger, S.; Bach, S.; Pereira-Ramos, J.P. Raman Spectra of birnessite manganese dioxides. *Solid State Ion.* 2003, 159, 345–356. [CrossRef]
- Julien, C.M.; Massot, M.; Poinsignon, C. Lattice vibration of manganese oxides. Part I Periodic structure. *Spectrochim. Acta* 2004, 60, 689–700
- Gikas, P., 2017. Towards energy positive wastewater treatment plants. *J. Environ. Manage.*, 203, 621–629.
- Manali, A. and Gikas, P., 2019. Utilization of primary sieved solids for gasification and energy production, 17th *International Waste Management and Landfill Symposium*, 30 September-4 October, Sardinia, Italy.



Improving Groundwater Quality Using Hybrid Constructed Wetland in Coastal Communities in Sub-Saharan Africa

R. N. Okparanma¹ and V. O. Ahiakwo¹

¹Department of Agricultural and Environmental Engineering, Rivers State University,
Nkpolu-Oroworukwo, PMB 5080 Port Harcourt, Nigeria

Corresponding author email: okparanma.reuben@ust.edu.ng

keywords: Artificial Wetland; Groundwater Quality; Groundwater Remediation; Heavy Metals; Developing Economies.

Introduction

The provision of potable water is arguably one of the most important municipal services any government can provide for its residents. It is widely known that achieving a well-functioning and sustainable water treatment facility is capital intensive. Consequently, providing this all-important municipal service to its teeming residents has continued to elude many low-income economies including Nigeria in sub-Saharan Africa. This has left residents with little or no option other than self-help with a huge financial burden.

In Nigeria, local groundwater sources in some crude oil-bearing coastal communities are characterized by high contents of heavy metals due to oil pollution. This makes the domestic use of such groundwater highly objectionable. Therefore, developing a simple, low-cost, and easy-to-maintain groundwater treatment facility would be beneficial to residents in coastal communities in low-income economies struggling with high contents of heavy metals in local groundwater sources.

Materials and methods

In this study, we constructed a simple, easy-to-maintain hybrid wetland with locally available materials and used it to remove Fe^{3+} and Mn^{2+} from groundwater collected from Yenagoa, a coastal city in Bayelsa State in the Niger Delta region of Nigeria (5.317°N, 6.467°E). To do this, three plastic containers (cells) of volume 70.22cm^3 were connected in series with decreasing elevation, packed with gravel and coarse aggregates in turn up to one-third of the depth, and planted with water hyacinth to enhance Fe^{3+} and Mn^{2+} removal (Figure 1). The system flow rate was 43.20 L/day with a retention time of 1.63 days. The concentrations of Fe^{3+} and Mn^{2+} in the groundwater before and during treatment, as well as pH and colour, were determined periodically for 12 days using standard analytical protocols.

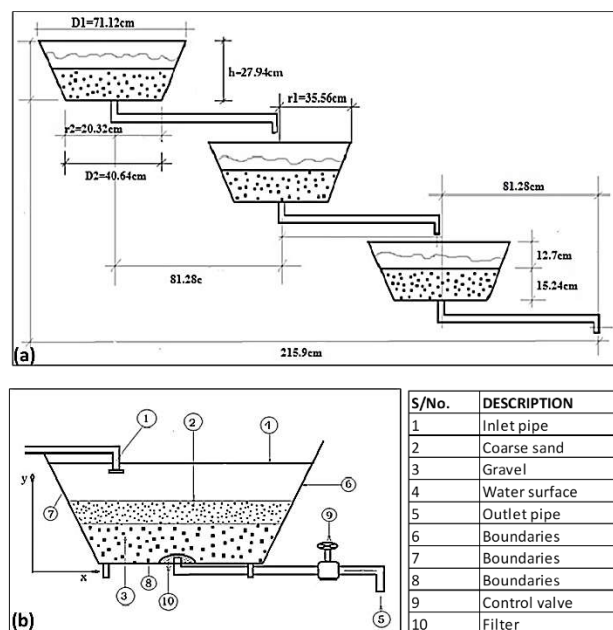


Figure 1. (a) The experimental set-up and (b) Sectional diagram of the cell without the plants.



Results and discussion

Results obtained after treatment on day 12 showed that both Fe^{3+} and Mn^{2+} were reduced to less than their respective WHO (2008) permissible limits with cell-3 outperforming cell-1 and cell-2 as expected (Table 1). Moreover, the pH across the cells dropped to within WHO's permissible range from an initial 8.94.

Table 1. Selected properties of the groundwater before and after treatment in the hybrid constructed wetland

Property	Before treatment	12 days after treatment			WHO (2008) Permissible Limit
		Cell-1	Cell-2	Cell-3	
Fe^{3+} (mg/L)	1.094	0.012	0.008	0.003	0.3
Mn^{2+} (mg/L)	1.043	0.004	0.003	0.001	0.2
pH	8.94	6.8	7.15	7.25	6.5-8.5

Similarly, the colour of the groundwater changed from an initial reddish-brown before treatment to colourless after 12 days of treatment (Figure 2).

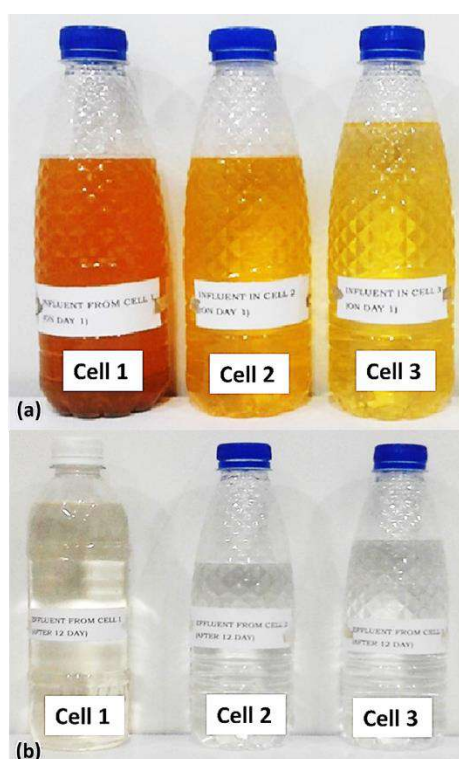


Figure 2. Colour change of the water samples on (a) day 1 and (b) day 12 of treatment in the hybrid constructed wetland.

Conclusions

From the results obtained in this study, there is the promise that the simple, low-cost, and easy-to-maintain hybrid constructed wetland could improve the quality of groundwater for domestic use, especially for washing purposes. If adopted, the treatment method would increase profitability in groundwater treatment and reduce the financial burden on coastal dwellers in low-income economies.

Acknowledgements: This study did not receive any financial assistance from any funding agency.

References

WHO (World Health Organization) (2008). *Guidelines for Drinking-Water Quality: Incorporating the First and Second, Addenda*, Volume 1 Recommendations (3rd Edition), WHO Press, 20 Avenue Appia, 1211 Geneva 27, Switzerland.



Methylparaben as a concerning contaminant for the proliferation of *Stenotrophomonas maltophilia*

A.R. Pereira^{1,2}, I. Gomes^{1,2} and M. Simões^{1,2}

¹LEPABE - Laboratory for Process Engineering, Environment, Biotechnology and Energy, Faculty of Engineering, University of Porto, Porto, Portugal

²ALICE - Associate Laboratory in Chemical Engineering, Faculty of Engineering, University of Porto, Porto, Portugal

Corresponding author email: mvs@fe.up.pt

keywords: *biofilms; drinking water; emerging pollutants; parabens; polypropylene.*

Introduction

Drinking water (DW) safety imposes high concern for public health. Despite all the strategies used to guarantee DW chemical and microbiological safe, biofilm development in drinking water distribution systems is unavoidable, being a huge problem for DW companies. DW is also affected by the presence of emerging contaminants (ECs), which are molecules present in most of the products of routine and indispensable use. Therefore, it is expected an increase in environmental contamination by ECs to worrying levels (Gomes et al., 2019). Parabens are ECs often detected in DW worldwide and represent remarkable concerns for human health (Gomes et al., 2019). Since microorganisms can adapt to environmental changes, their exposure to parabens may constitute a problem for the microbiological quality and safety of DW. The scientific community is focusing on the direct consequences from the intake of ECs for DW consumers, disregarding the effects on the DW intrinsic microbiome (Gomes et al., 2020). Despite that, there is some evidence that the presence of ECs on DW microorganisms promotes alteration on biofilm formation and on the production of virulence factors, promoting antimicrobial resistance spread (Gomes et al., 2018; Gomes et al., 2019; Gomes et al., 2019). This work focus on understanding the consequences from the exposure to parabens (methylparaben (MP), butylparaben (BP) and propylparaben (PP)) on biofilms formed by *Stenotrophomonas maltophilia* isolated from DW, helping to anticipate potential microbiological-related public health concerns.

Materials and methods

Biofilm formation and exposure to parabens

Stenotrophomonas maltophilia, isolated from DW, was grown overnight at 25 °C and under agitation (160 rpm) in R2A broth medium. Biofilms were formed in the presence and absence (control) of parabens (MP, BP, and PP) under the maximum concentration reported in DW (150 ng/L) (Gomes et al., 2020). Biofilms were developed on polypropylene (PPL) coupons (1 cm × 1 cm) in 48-wells microtiter plates. Colonized coupons were exposed to parabens for 7 days and for 26 days, according to Arruda et al. (2022) and Gomes et al. (2018), respectively. Biofilms only exposed to STW (prepared as described by Gomes et al. (2019) or to acetone at 0.005% (v/v) were used as negative control and solvent control, respectively.

Assessment of Biofilm Cellular Density and culturability

The culturability of exposed and unexposed biofilm cells was quantified in terms of CFU/cm², by plating the biofilm suspensions as well as appropriate serial dilutions in R2A agar. The plates were incubated at 25 °C for 24h for cell count. The cellular density of biofilms was quantified through 4',6-diamidino-2-phenylindole (DAPI) staining and epifluorescence microscopy.

Results and discussion

The concentrations of the selected parabens found in the environment (\approx 150 ng/L) are 1 million times lower than minimum inhibitory concentration (200–400 mg/L). Therefore, antimicrobial activity is not expectable, for the concentration tested.

For 7-days old *S. maltophilia* biofilms exposed to parabens in PPL it was noticeable that PP, BP and MIX caused a slight decrease of log CFU/cm² in relation to the control (Figure 1). Note that MIX is a triple formulation composed by MP, PP and BP at the same concentration (150 ng/L). On the other hand, MP



exposed-*S. maltophilia* biofilms have increased the number of CFU in comparison to the unexposed biofilms (STW). Specifically, an increase of 121% on the numbers of CFU was observed in MP-exposed biofilms in comparison to the unexposed counterparts ($P < 0.05$). Moreover, MP also increased the proliferation of cultivable cells from *S. maltophilia* biofilms when exposed for 26 days (Figure 1), however, at a lower extent. This situation can be explained by the fact that these cells may have the ability to adapt over time, being less susceptible to the presence of ECs. To complement this study, the production of virulence factors was also studied. The gelatinase activity was more pronounced in MP-exposed *S. maltophilia* biofilms (for 7 days) than in the unexposed counterparts. In fact, an increase of 73% was detected on the gelatinase activity halo of bacteria exposed to MP for 7 days. Furthermore, the number of total cells in biofilms seems not to be affected by the exposure to parabens, for both exposure times tested ($P > 0.05$).

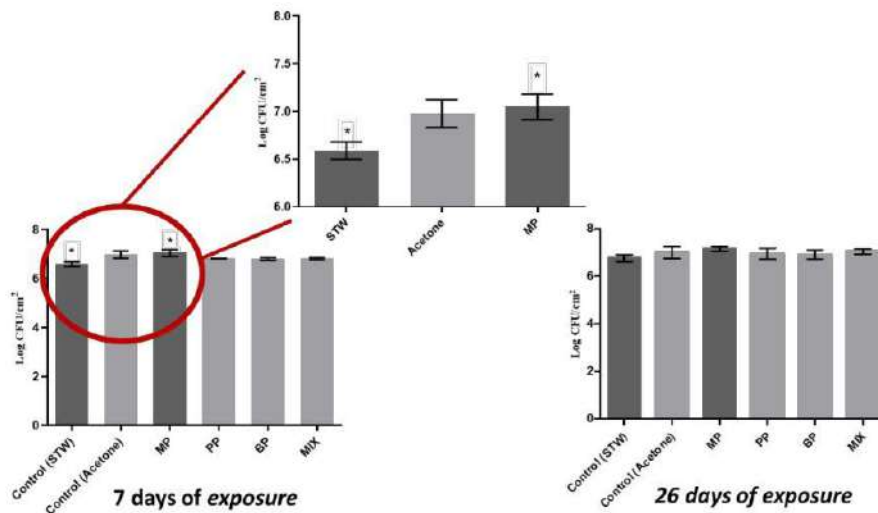


Figure 1. Log CFU/cm² of *S. maltophilia* biofilms after growing for 7 days (on the left) and 26 days (on the right) in the presence of the selected ECs (MP, PP, BP, MIX). *- samples were statistically different from unexposed bacterial biofilms (control) (Tukey's test, $P < 0.05$).

Conclusions

The exposure of parabens even in residual concentrations affects the biofilm cells and may potentiate the production of virulence factors namely gelatinase production. MP enhances the formation of biofilms in drinking water. However, PP, BP and MIX seem to slightly decrease the culturability of *S. maltophilia* biofilm cells.

Acknowledgements: This work was financially supported by LA/P/0045/2020 (ALiCE), UIDB/00511/2020, UIDP/00511/2020 (LEPABE) - FCT/MCTES (PIDDAC); by the PhD scholarship (2021.06226.BD) and HealthyWaters (NORTE-01-0145-FEDER-000069)- NORTE 2020/ERDF.

References

- Arruda, V., Simões, M., Gomes, I.B., 2022. The impact of synthetic musk compounds in biofilms from drinking water bacteria. *Journal of Hazardous Materials.*, 129185.
- Gomes, I. B., Madureira, D., Simões, L.C., Simões, M., 2019. The effects of pharmaceutical and personal care products on the behavior of *Burkholderia cepacia* isolated from drinking water. *International Biodeterioration and Biodegradation.*, 141, 87–93.
- Gomes, I.B., Maillard, J.Y., Simões, L.C., Simões, M., 2020. Emerging contaminants affect the microbiome of water systems—strategies for their mitigation. *npj Clean Water.*, 3, 39.
- Gomes, I. B., Querido, M.M., Teixeira, J.P., Pereira, C.C., Simões, L.C., Simões, M., 2019. Prolonged exposure of *Stenotrophomonas maltophilia* biofilms to trace levels of clofibric acid alters antimicrobial tolerance and virulence. *Chemosphere.*, 235, 327–335.
- Gomes, I.B., Simões, L.C., Simões, M., 2018. The effects of emerging environmental contaminants on *Stenotrophomonas maltophilia* isolated from drinking water in planktonic and sessile states. *Science of the Total Environment.*, 643, 1348–1356.



Ballast water disinfection by ozone micro- and nanobubbles

P. Seridou ¹, E. Kotzia ¹, K. Katris ¹ and N. Kalogerakis ¹

¹ School of Chemical and Environmental Engineering, Technical University of Crete, Chania, Greece
Corresponding author email: nkalogerakis@tuc.gr

keywords: ozone nanobubbles 1; ballast water 2; sea water disinfection.

Introduction

The vast majority of world cargo handling takes place by sea with suitable ships (Li, Xu and Shi, 2015). International shipping is considered a significant source of pollution derived from uncontrolled disposal of seawater, which is used as ballast (Wan *et al.*, 2021). Ballast water is a great amount of seawater stored in ballast tanks and is essential to certify ship buoyance and maneuverability. During de-ballasting, thousands of cubic meters of seawater containing invasive species can be disposed to a totally different environment (Kim, Lee and Seo, 2022). To reduce the global spread of these invasive aquatic species, international regulations has already set environmental limits in the number of organisms in ballast water discharged by ships according to Table 1 (IMO Marine Environment Protection Committee (MEPC), 2008). Ozonation has been widely used to treat the discharged ballast water, however this method is limited by the rapid consumption of ozone. Micro and nanobubbles (MNBs) have been attracted scientific interest due to the high residence time and the utilization of this technology is expected to enhance the ozone half-time and the residual concentration.

Table 1. Acceptable limit of indicator microbes according to D2 standard

Indicator Microbes		Size of microorganisms	
<i>Escherichia coli</i> (<i>E. coli</i>)	<250 cfu per 100 mL	≥50 μm	<10 viable organisms per m ³
Intestinal Enterococci	<100 cfu per 100 mL	≥10 μm and <50 μm	<10 viable organisms per mL
Toxicogenic <i>Vibrio cholerae</i>	<1 cfu per 100 mL		

Materials and methods

The ozonation experiments were conducted in batch mode. Tap water containing ozone with and without the presence of MNBs was used to conduct the disinfection experiments. A desired bacterial concentration (CFU/mL) was added to OMNB tap water and sample were collected at predetermined time intervals (1, 5 and 10 min) in sterile tubes for ozone determination and cell viability.

Results and discussion

The experimental design was divided into two phases. The first phase was designed to determine the influence of salinity and ozone dose on the ozone reaction, without the addition of bacterial inoculum. The second experimental phase includes the ozone disinfection of *Escherichia coli* in three different concentrations. In Figure 1, it can be seen that in two different ozone concentrations the trend in ozone consumption is similar. In high salinities, the ozone reaction with seawater is rapid. The residual concentration reached around 20% in the first minute of reaction.

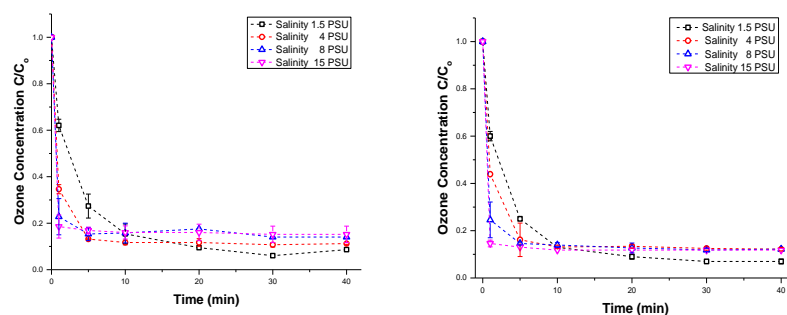


Figure 1. Ozone reaction with seawater in different salinities (left) at 0.8 ppm and (right) 1.6 ppm ozone concentration.



In three different bacterial concentration, the presence of MNBs enhanced the ozone consumption and the disinfection capacity was greater in seawater with salinity 1.5 PSU.

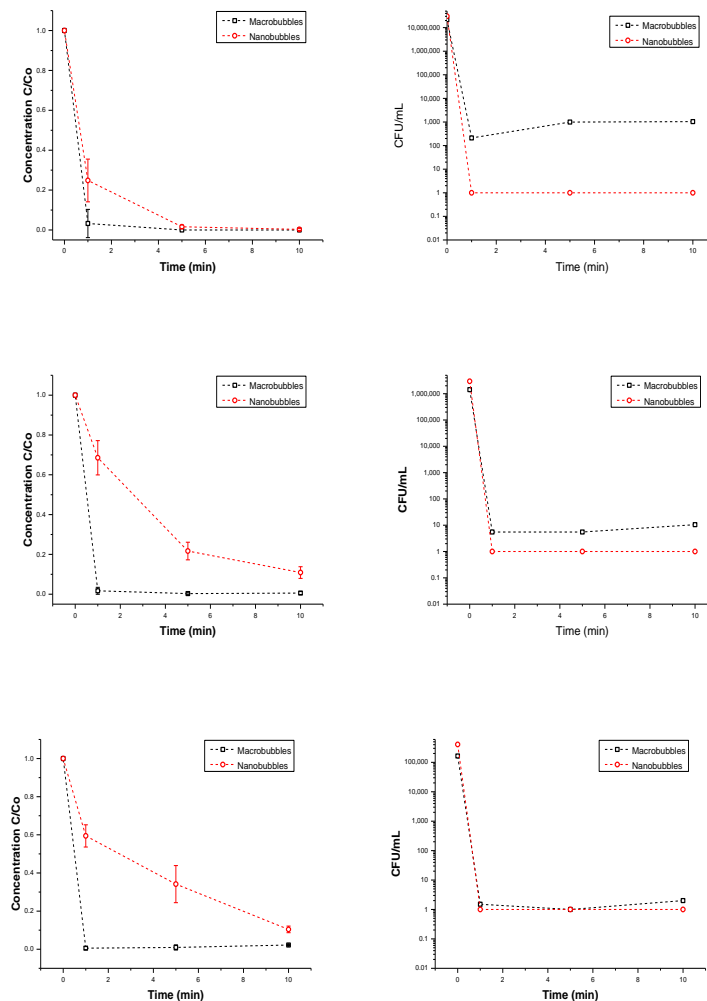


Figure 2. Ozone consumption and bacterial concentrations with and without the presence of MNBs.

Conclusions

The salinity of water has a strong impact on the residual concentration of ozone. When salinity is increased, ozone reacts rapidly with the bromide and chloride ions. The use of Nanobubbles technology exhibited greater disinfection performance.

Acknowledgements: «This research is co-financed by Greece and the European Union (European Social Fund- ESF) through the Operational Programme «Human Resources Development, Education and Lifelong Learning» in the context of the project “Strengthening Human Resources Research Potential via Doctorate Research” (MIS-5000432), implemented by the State Scholarships Foundation (IKY)».

References

- IMO Marine Environment Protection Committee (MEPC), 2008. Resolution MEPC.174(58), Guidelines for approval of ballast water management systems (G8)', *Mepc.174 (58)*, 174(October).
- Kim, A.R., Lee, S.W. and Seo, Y.J., 2022, How to control and manage vessels' ballast water: The perspective of Korean shipping companies', *Marine Policy*, 138(December 2021), p. 105007.
- Li, Z., Xu, M. and Shi, Y., 2015. Centrality in global shipping network basing on worldwide shipping areas', *GeoJournal*, 80(1), pp. 47–60. doi:10.1007/s10708-014-9524-3.
- Wan, Z. *et al.*, 2021. Risk assessment of marine invasive species in Chinese ports introduced by the global shipping network', *Marine Pollution Bulletin*, 173(PA), p. 112950.



The potential of OXONE as an alternative disinfectant to control drinking water biofilms

I.M. Oliveira^{1,2}, L.C. Simões^{3,4} and M. Simões^{1,2}

¹LEPABE – Laboratory for Process Engineering, Environment, Biotechnology and Energy, Faculty of Engineering, University of Porto, Porto, Portugal

²ALiCE – Associate Laboratory in Chemical Engineering, Faculty of Engineering, University of Porto, Porto, Portugal

³CEB – Centre of Biological Engineering, University of Minho, Campus de Gualtar, Braga, Portugal⁴LABELLS – Associate Laboratory, Braga/Guimarães, Portugal
Corresponding author email: mvs@fe.up.pt

keywords: *biofilm; disinfection; drinking water; rheometry; viscoelasticity.*

Introduction

Chlorination is the most widely used method for the disinfection of drinking water (DW) (Ellis, 1991). However, the production of toxic disinfection by-products and the occurrence of biofilms in chlorinated drinking water distribution systems (DWDS) have been frequently reported (Andersson et al., 2019; Liu et al., 2016). Biofilms are responsible for several undesirable effects on water quality and constitute a reservoir of pathogenic microorganisms (Simões and Simões, 2013).

Given the health concerns of the side reactions of chlorine compounds and the increase of microbial tolerance to conventional chlorination, new alternatives for DW disinfection are required. Therefore, the main purpose of this study was to evaluate the antibiofilm efficacy of pentapotassium bis(peroxymonosulphate) bis(sulphate) (OXONE) compared to the common free chlorine disinfection.

Materials and methods

The effects of OXONE and free chlorine from calcium hypochlorite were evaluated against 48 h-old *Stenotrophomonas maltophilia* biofilms. *S. maltophilia* was previously isolated from a DWDS in Braga (Portugal) and was selected as model microorganism given its importance as emerging pathogen. Polyvinyl chloride (PVC) and stainless steel (SS) coupons (1 × 1 cm) were used as substrata for biofilm formation and were selected as representative pipe material from DW networks. The antibiofilm activity was analyzed in terms of biofilm culturability (log (CFU/cm²)) immediately after a 30 min exposure to the disinfectants at 10 × minimum bactericidal concentration (MBC) and biofilm regrowth for 24 h after chemical exposure. The MBC of OXONE and free chlorine against *S. maltophilia* (344 and 0.8 mg/L, respectively) were already determined in a previous work (Oliveira et al., 2022).

Additionally, the changes in the viscoelastic properties of biofilms resulting from the 30 min exposure to the disinfectants were evaluated by rheometry. Colony biofilms of *S. maltophilia* were subjected to oscillatory tests performed using a parallel plate rheometer.

Results and discussion

The 30 min exposure to OXONE allowed a reduction in the biofilm culturability up to 7 log, resulting in CFU levels significantly lower than the biofilms unexposed to disinfectants ($P < 0.05$). The biofilms exposed to OXONE showed CFU numbers of 0.0 ± 0.0 and 3.6 ± 0.7 log (CFU/cm²) on SS and PVC, respectively, in contrast to unexposed biofilms with 7.2 ± 0.3 and 7.2 ± 0.1 log (CFU/cm²) on SS and PVC, respectively.

The reposition of nutrients after disinfectant exposure allowed biofilm regrowth, even in biofilms that had been exposed to OXONE or free chlorine. However, the biofilms previously exposed to OXONE showed CFU levels significantly lower than the biofilms unexposed to disinfectants ($P < 0.05$). After 24 h of biofilm regrowth, the biofilms previously exposed to OXONE presented CFU numbers of 2.6 ± 2.3 and 6.1 ± 0.5 log (CFU/cm²) on SS and PVC, respectively. In contrast, the unexposed biofilms showed CFU numbers of 7.8 ± 0.3 and 7.9 ± 0.3 log (CFU/cm²) on SS and PVC, respectively.



In both tests, the antibiofilm activity of OXONE was significantly better than the activity of free chlorine against biofilms formed on SS ($P < 0.05$). The CFU numbers on SS coupons immediately after free chlorine exposure and after 24 h of biofilm regrowth were 4.3 ± 0.9 and 6.7 ± 0.5 log (CFU/cm²), respectively.

The rheometry analysis demonstrated that independently of the disinfectant treatment the *S. maltophilia* biofilms behaved as viscoelastic solid material, with a higher elastic shear modulus (G') than viscous shear modulus (G''). Nonetheless, biofilms exposed to OXONE had complex shear modulus (G^*) significantly lower than the values of unexposed biofilms and biofilms treated with free chlorine ($P < 0.05$) (Table 1). Therefore, the 30 min exposure to OXONE reduced the stiffness of the biofilm, weakening its cohesiveness.

Table 1. Complex shear modulus (G^*) of colony *S. maltophilia* biofilms after 30 min exposure to OXONE and free chlorine at $10 \times$ MBC.

Treatment	Complex shear modulus (G^* , kPa)
Control	140 ± 29
Free chlorine	104 ± 70
OXONE	69 ± 21

Conclusions

This study demonstrated that OXONE presented significant action against *S. maltophilia* biofilms. In biofilms formed on SS, OXONE had better efficiency in reducing biofilm culturability and limiting biofilm regrowth than free chlorine. The antibiofilm activity of OXONE was related to changes in the viscoelastic properties of the biofilms, reducing their cohesiveness and promoting the disinfection of bacteria. This study reinforces OXONE as promising alternative to free chlorine for DW biofilms disinfection and highlights the importance of understanding biofilm rheology to improve biofilm control strategies.

Acknowledgements: This work was financially supported by: UIDB/04469/2020, LA/P/0045/2020 (ALiCE), UIDB/00511/2020 and UIDP/00511/2020 (LEPABE), funded by national funds through FCT/MCTES (PIDDAC); Project Biocide_for_Biofilm - PTDC/BII-BTI/30219/2017 - POCI-01-0145-FEDER-030219, funded by FEDER funds through COMPETE2020 – Programa Operacional Competitividade e Internacionalização (POCI) and by national funds (PIDDAC) through FCT/MCTES; and FCT PhD grant awarded to Isabel Maria Oliveira (SFRH/BD/ 138117/2018).

References

- Andersson, A., Harir, M., Gonsior, M., Hertkorn, N., Schmitt-Kopplin, P., Kylin, H., Karlsson, S., Ashiq, M.J., Lavonen, E., Nilsson, K., Pettersson, Å., Stavklint, H., Bastviken, D., 2019. Waterworks-specific composition of drinking water disinfection by-products. *Environ. Sci. Water Res. Technol.* 5, 861–872. <https://doi.org/10.1039/C9EW00034H>
- Ellis, K. V., 1991. Water disinfection: A review with some consideration of the requirements of the third world. *Crit. Rev. Environ. Control* 20, 341–407. <https://doi.org/10.1080/10643389109388405>
- Liu, S., Gunawan, C., Barraud, N., Rice, S.A., Harry, E.J., Amal, R., 2016. Understanding, monitoring, and controlling biofilm growth in drinking water distribution systems. *Environ. Sci. Technol.* 50, 8954–8976. <https://doi.org/10.1021/acs.est.6b00835>
- Oliveira, I.M., Gomes, I.B., Simoes, L.C., Simoes, M., 2022. Chlorinated cyanurates and potassium salt of peroxymonosulphate as antimicrobial and antibiofilm agents for drinking water disinfection. *Sci. Total Environ.* 811. <https://doi.org/10.1016/j.scitotenv.2021.152355>
- Simões, L.C., Simões, M., 2013. Biofilms in drinking water: problems and solutions. *RSC Adv.* 3, 2520–2533. <https://doi.org/10.1039/c2ra22243d>



Renewable energy desalination for island communities: Status and prospects in Greece

G. Kyriakarakos¹, G. Papadakis² and C.A. Karavitis²

¹Institute for Bio-Economy and Agri-Technology (iBO), Centre for Research and Technology–Hellas (CERTH),
Thermi, Thessaloniki, Greece

²Department of Natural Resources and Agricultural Engineering, School of Environment and Agricultural
Engineering, Agricultural University of Athens, Athens, Greece

Corresponding author email: gpap@aua.gr

keywords: *desalination, renewables, reverse osmosis, photovoltaics, wind turbines, Greek islands.*

Energy and water are two of the most important components required to ensure prosperity and sustainable development to societies. This paper aims to critically review the status of renewable energy desalination for Greek islandic communities, deployed in two axes. Under the first one it reviews the state of the art in terms of technological solutions in desalination systems, their energy needs, how renewable energy may be employed. Finally, the cost of renewable energy desalination is investigated. The second axis focuses on Greek islands per se, where the current situation is investigated, potential solutions for meeting the water needs are evaluated all leading to the proposal of a methodology towards designing an appropriate and applicable approach in addressing the water needs. Lastly, a discussion takes place on how such options might further be deployed, particularly regarding the impacts they may produce for the life hood and the future prosperity of the pertinent communities, and at the same time supporting the energy transition towards the EU Green Deal goals.

Major results and conclusions regard

Water and energy security will be top political priorities for Greece in the nearest future, following EU policy. Detailed reviews of utilized solutions for the provision of fresh water may shed light on the advantages and disadvantages of the various technologies deployed on the islands and reveal alternative management options (i.e., appropriate operation and practices) for a more efficient production. The ongoing research in improving the desalination technologies powered by renewables aims at improving operational efficiencies and the overall cost reduction. Nevertheless, interregional, and international cooperation will be required, as the challenge of providing fresh water in a sustainable manner may be too great for any country, region, and development funding body to address on its own. Water supply, in the nearest future, in the islands of central and south-eastern Aegean Sea is expected to use desalination combined with solar and/ or wind energy, instead of fossil fuels, in full alignment with the EU Green Deal.

Acknowledgements: This study was supported by the European Bank for Reconstruction and Development (EBRD). We would like to acknowledge the support provided by the rest of the team working on this EBRD project, Graydon Jeal, Nathan Visvanathan, George Davies, Steve Hodgson, and Erica Mitsi, as well as David Tyler at EBRD. Moreover, we would like to acknowledge the support of Orfeas Mavrikios (CEO of Watera Hellas) in providing valuable insights regarding commercial desalination plants.



SUST
ENG
2022



BIOREFINERIES



Importance of the use of Multi-Criteria Analysis tools to make decisions in biorefinery

A. Coz¹, C. Rojas¹, C. Rueda¹, R. Leonardi², J. Khawam², R.N. Comelli² and T. Llano¹

¹Chemistry and Process & Resources Engineering Department. University of Cantabria, Santander, Spain

²Departamento de Medio Ambiente, Fac. de Ingeniería y Ciencias Hídricas (FICH), Univ. Nacional del Litoral (UNL), Santa Fe, Argentina

Corresponding author email: alberto.coz@unican.es

keywords: *biorefinery; MCA; decision tools.*

Introduction

Biorefinery has been defined by the International Energy Agency as the sustainable processing of biomass into a spectrum of marketable products and energy (IEA, 2019). Lignocellulosic materials represent one of the most promising sources of renewable raw material under the bioeconomy, giving useful biobased chemicals and fuels, due to their low economic value and high availability (Coz et al., 2016). Lignocellulosic biomass has a complex structure consisting of three major fractions: cellulose (35%–50% dry weight), hemicelluloses (15%–35%), and lignin (10%–25%) (Huang et al., 2008); and all of them can be used in different applications. Depending on the final product, the conversion of lignocellulosic materials requires the separation or not of the material into its components. In addition, different processes as physico-chemical and biological methods can be used to produce the final products and to purify them.

Due to the different alternatives, scales, products and so on, different tools for making decisions about the best options need to be studied. In this sense, Multi-Criteria Analysis (MCA) tools can be a good option in order to take into account not only the technical and economic aspects but also the environmental and social issues. MCA is a decision-making tool applied to a wide range of environmental management problems, including renewable energy planning and management (Vassoney et al., 2017). In addition, these tools can be used in all steps of the process in biorefinery applications. In this work, MCA has been used in different cases within the biorefinery concept.

Materials and methods

The MCA analysis has been performed using the DEFINITE 3.1 software which includes a weighted summation MCA algorithm to obtain the results. The weighted summation can be used to address problems that involve a finite and discrete set of alternatives that must be evaluated based on conflicting objectives (Beinat and Nijkamp, 2007).

The process to be followed to carry out weighted summation is further detailed: (1) alternatives definition that will be compared against each other; (2) selection and definition of criteria identifying the most relevant indicators for the decision; (3) assessment of scores for each alternative by assigning values to each indicator for all the alternatives; (4) standardisation of the scores to make the criteria comparable with each other; (5) weighting of criteria to assign priorities to them; and (6) ranking of the alternatives. Finally, a sensitivity analysis needs to be done.

Results and discussion

Four different cases have been studied. On the one hand, the evaluation of specific processes within the biorefinery process, in this case, the evaluation of different detoxification processes in a spent sulfite liquor have been studied considering that can be adapted to a wide variety of fermenting scenarios and using previous experimental data. Technical, economic, environmental, and social criteria have been studied. Total inhibitors, removal, phenolics removal, acetic acid removal, lignosulfonates removal, total sugar losses, fixed capital invested, manufacturing costs, waste toxicity, social acceptance, and employment have been chosen. Different scenarios with only technical criteria, technoeconomic criteria and adding the environmental and social aspects have been studied. Figure 1 shows the results considering all the criteria.

Taking into account the previous results and using the results of modelling and simulation at industrial scale, three different alternatives of production of xylitol, furfural and ethanol have been studied. In this case, only technical and economic criteria have been considered because of the importance of the use of these alternatives in a real company. Total production, market price, fixed capital invested, manufacturing costs,



and return period have been used. Sensitivity analysis was also studied. Xylitol is the best alternative almost in the whole weight range except for the market where ethanol becomes the best alternative when the weight of market is above 30 %.

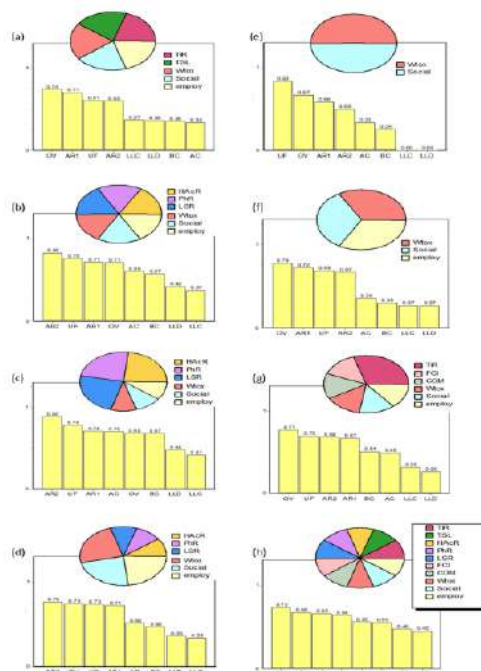


Figure 1. Results of the rankings for the techno-economic and socio-environmental alternatives.

Finally, in order to increase the impact in small companies and rural areas, two different cases have been studied: (i) essential oil production from waste local biomass, and (ii) the production of lactic acid using different regional feedstocks and analysing three purification strategies.

Conclusions

Multi-Criteria Analysis are good alternatives for making decisions about the best biorefinery options because of the diversity of waste materials, processes, and products, and not only in large biorefineries but also for small areas.

Acknowledgements: This study is supported by the CELISE project (<https://celise.unican.es>) from the European Union's Horizon 2020 research and innovation programme under the Marie Skłodowska-Curie grant agreement No 101007733.

References

- Beinat, E. and Nijkamp, P., 2007. *Multicriteria Analysis for Land-Use Management*, second ed., Springer, New York.
- Coz, A., Llano, T., Cifrián, E., Viguri, J., Maican, E. and Sixta, H., 2016. Review Physico-Chemical Alternatives in Lignocellulosic Materials in Relation to the Kind of Component for Fermenting Purposes, *Mat.*, 9, 574.
- Huang, H.-J., Ramaswamy, S.H., Tschirner, U.W. and Ramarao, B.V., 2008. A review of separation technologies in current and future biorefineries. *Sep. Purif. Technol.*, 62, 1–21.
- IEA, 2019. IEA Bioenergy Annual Report 2009. Available online: <http://www.ieabioenergy.com/wp-content/uploads/2013/10/IEA-Bioenergy-2009-Annual-Report.pdf>
- Vassoney, E., Mochet, A.M. and Comoglio, C., 2017. Review Use of multicriteria analysis (MCA) for sustainable hydropower planning and management. *J. Environ. Manage.*, 196, 48-55.



Agro-food waste re-valorization through solid-state fermentation for hydrolytic enzymes production

J. Sosa-Martínez¹, J. Montañez¹, J.C. Contreras¹, S. Gadi² and L. Morales¹

¹Facultad de Ciencias Químicas. Universidad Autonoma de Coahuila. Unidad Saltillo. Saltillo, Coahuila, México

²Facultad de Ingeniería Mecánica y Eléctrica. Universidad Autonoma de Coahuila. Unidad Torreón. Torreón, Coahuila, México

Corresponding author email: lourdesmorales@uadec.edu.mx

keywords: agro-industrial waste, hydrolytic enzymes, solid-state fermentation.

Introduction

Nowadays, harnessing agro-food wastes through a revalorization approach has become a promising alternative to promote a circular economy. One potential alternative is producing fungal enzymes through solid-state fermentation (SSF). Agro-industrial waste is made up of cellulose, hemicellulose, and lignin; they also contain phenolic compounds, proteins, lipids, and trace elements (Barcelos et al., 2020) that microorganisms can use without the need to provide another nutritional element. The nature of agro-industrial waste plays a critical role in the SSF process for enzyme synthesis. Material's chemical composition will affect the microorganism growth and the desired product yield. Determining the ideal materials for SSF will allow the development of bioprocesses for synthesizing enzymes such as xylanase, cellulase and pectinase. Multi-enzyme extracts produced by SSF have the potential to be used in several industrial processes, given the high demand for enzymes for the manufacture of food products and the pretreatment of raw materials. In addition, enzymes are also used for assisted extraction to obtain value-added compounds. The agro-industrial waste characterization and fungal screening to obtain hydrolytic enzymes by SSF are strategies proposed in this work to generate an efficient and profitable bioprocess.

Materials and methods

Agro-food wastes were obtained from different agricultural activities, food processing and commercial activities, which were subjected to a proximal and physicochemical characterization. The substrates used were apple pomace (AP), brewery spent grain (BSG), corn cob (CC), cotton seed (CS), carrot waste (CW), grapefruits peels (GfP), grape pomace (GP), orange peel (OP), peanut shell (PS), pasta residue (PR), soybean waste (SW), wheat bran (WB).

Five fungal strains (A5, A13, B1, D1 and G5) isolated from maize silage were used to examine their qualitative xylanolytic, cellulolytic and pectinolytic activities. The three best strains, according to their ability to degrade polysaccharides (xylan, cellobiose and pectin), were used to perform solid fermentation using the twelve agro-wastes as support-substrate. The growth parameters were determined through the fast-acceleration/slow-deceleration model (Mitchell et al., 2004), which describes filamentous fungi growth in solid culture.

The selected strain and residues were further evaluated for enzyme production. Statistical optimization was used for optimal production of xylanase, cellulase and pectinase. The evaluated factors were substrate ratio (75/25, 80/20 and 85/15), moisture (40, 50 and 60 %) and pH (4, 4.5 and 5), which were optimized using a central composite design using the response surface methodology (CCD-RSM).

Results and discussion

The proximate chemical analysis of the agro-industrial wastes shows the agro-food wastes' potential to be used as a source of nutrients and an inducer of enzymatic activity (Table 1). It is well reported that the composition is a decisive factor for stimulating enzyme secretion by microorganisms (Barcelos et al., 2020). The physico-chemical parameters are plotted in Fig. 1. WAI (water absorption index) determines the ability to absorb water; WHC indicates how much water is retained by the material. A high percentage of WAI is desirable for support-substrate used in solid fermentation. This material's parameters are directly related to the interaction of the water molecules with the non-cellulosic cell wall polysaccharides, mainly pectins and xylan (Du et al., 2018). CHP is an important parameter because it indicates the critical moisture



percentage for the system. Since SSF is carried out with humidity ranging from 40 to 80 %, the CHP should not exceed 30 % (Torres-León et al., 2019).

Strains B1, D1 and G5 were able to degrade the highest number of substrates. B1 failed to degrade CMC and D1 xylan and cellobiose, while G5 degraded all substrates. The highest enzymatic activity for xylanase was in BSG (481.45 ± 4.39 U), pectinase in AP (47.88 ± 7.09 U), and cellulase in AP (41.25 ± 3.85 U). Based on the growth parameters obtained and the ability to produce hydrolytic enzymes on the substrates, the G5 strain and the BSG and AP residues were selected.

CCD-RSM allowed determining various settings of optimal conditions to maximize the production of each hydrolytic enzyme. The activity was increased by 20, 69 and 28 % for xylanase, cellulase and pectinase respectively.

Table 1. Proximal chemical composition of lignocellulosic materials

	AP	BSG	CW	CC	CS	GfP	GP	OP	PR	PS	SW	WB
Protein	10.46 ^e	16.41 ^d	10.59 ^e	3.86 ^h	21.47 ^b	7.22 ^g	19.18 ^{bc}	7.57 ^{fg}	9.83 ^{ef}	7.67 ^{fg}	45.69 ^a	17.84 ^{cd}
Lipids	3.16 ^g	3.96 ^{ef}	2.72 ^g	3.71 ^f	13.50 ^a	4.98 ^d	5.41 ^d	9.02 ^b	6.40 ^c	1.96 ^h	5.31 ^d	4.28 ^e
Carbohydrates	65.05 ^a	29.41 ^c	30.11 ^c	14.25 ^e	0.55 ^h	52.60 ^b	5.77 ^g	23.38 ^d	8.93 ^f	12.39 ^e	9.61 ^f	6.60 ^g
Hemicellulose	9.88 ^{de}	19.16 ^b	3.17 ^{fg}	44.16 ^a	11.95 ^c	5.44 ^e	7.03 ^e	6.32 ^{ef}	8.65 ^e	13.11 ^{cd}	ND	14.22 ^c
Lignin	ND	3.55 ^{de}	ND	9.73 ^{cd}	21.61 ^b	16.84 ^{cd}	13.83 ^c	13.33 ^c	3.48 ^e	52.74 ^a	ND	ND
Cellulose	12.86 ^{ef}	4.78 ^g	11.78 ^{ef}	40.57 ^c	48.09 ^b	15.70 ^{de}	10.23 ^f	23.98 ^d	0.01 ^h	63.85 ^a	4.69 ^g	8.00 ^f

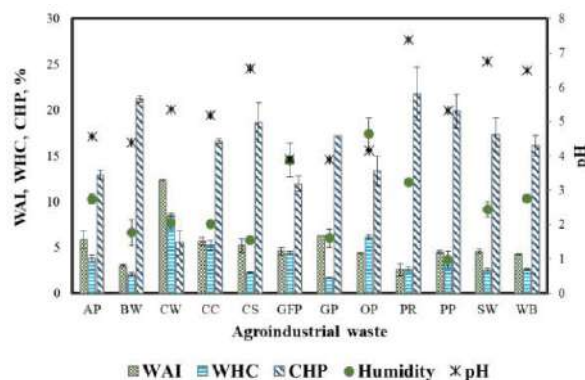


Figure 1. Physico-chemical parameters of agro-industrial wastes.

Conclusions

Studying the properties and composition of agro-industrial wastes allowed the understanding of the growth and production of enzymes by microorganisms. The G5 strain demonstrated the ability to biosynthesize xylanase, cellulase and pectinase of the five strains studied. It was possible to gain process knowledge about the simultaneous production of xylanase, cellulase and pectinase, which will allow adjusting process conditions to maximize a single enzyme or mixture of enzymes depending on the application.

Acknowledgements: CONACyT-México for the financial support provided for conducting J. Sosa-Martinez PhD studies.

References

- Barcelos, M.C.S., Ramos, C.L., Kuddus, M., Rodriguez-Couto, S., Srivastava, N., Ramteke, P.W., Mishra, P.K., Molina, G., 2020. Enzymatic potential for the valorization of agro-industrial by-products. *Biotechnol. Lett.* 42, 1799–1827.
- Du, J., Cheng, L., Hong, Y., Deng, Y., Li, Z., Li, C., Gu, Z., 2018. Enzyme assisted fermentation of potato pulp: An effective way to reduce water holding capacity and improve drying efficiency. *Food Chem.* 258, 118–123.
- Mitchell, D.A., Meien, O.F. Von, Krieger, N., Diba, F., Dalsenter, H., 2004. A review of recent developments in modeling of microbial growth kinetics and intraparticle phenomena in solid-state fermentation. *Biochem. Eng. J.* 17, 15–26.
- Torres-León, C., Ramírez-Guzmán, N., Ascacio-Valdés, J., Serna-Cock, L., dos Santos Correia, M.T., Contreras-Esquivel, J.C., Aguilar, C.N., 2019. Solid-state fermentation with *Aspergillus niger* to enhance the phenolic contents and antioxidative activity of Mexican mango seed: A promising source of natural antioxidants. *Lwt* 112, 108236.



Recycling of solid waste from the olive oil industry for various added-value products

H.N. Abu Tayeh^{1,2}, y. Gerchman^{1,3}, J. Asscher^{4,5} and H. Azaizeh^{2,6}

¹Faculty of Natural Sciences, University of Haifa, Haifa, Israel

²The Galilee Society Institute of Applied Research, University of Haifa, Shefa-Amr, Israel.

³Oranim academic college, Tivon, Israel

⁴Department of Quality and Reliability Engineering, Kinneret College on the Sea of Galilee, Israel

⁵Faculty of Industrial Engineering and Management, Technion - Israel Institute of Technology, Haifa, Israel

⁶Tel Hai college, Department of Environmental Science, Upper Galilee, Israel

Corresponding author email: hebaabutayeh@yahoo.com

keywords: olive mill solid waste; bioenergy; lignocellulose; experiment design; biosolids management and valorization.

Introduction

Olive oil production is a common agro-industry in the Mediterranean region producing a large amount of solid wastes (OMSW) with each ton of olives processed resulting in 0.6 tons of solid. The solid fraction consisted of varying fractions of the three major structural components: lignin (20-43%), cellulose (16.6-37%), and hemicellulose (14.4-36.6%). As of today, OMSW is considered an environmental nuisance without proper solutions. With the increasing interest in renewable energy, there is a rise in the interest in the use of lignocellulose biomass as feedstock for ethanol and biogas production in addition to other added-value products.

Materials and methods

We have explored ways to utilize this waste as feedstock for the production of ethanol and added-value products.

Utilization of agriculture waste rich in cellulose, releasing the glucose from the cellulose, and using it as feedstock for ethanol production could solve this issue, but this conversion is often hampered by the complex nature of the waste, requiring complex pretreatment before enzymatic saccharification.

The effect of different microwave (MW) and organic acid (OA) pretreatments on the production of bioethanol from OMSW was investigated using a statistical design of experiments. Four pretreatment factors (MW temperature, MW time, OA type, and OA concentration) were investigated as well as enzyme amount and Tween 80 additive concentration, concluding 64 experimental runs, and allowing identification of interactions between the six factors. Response variables tested were loss of sugars from hemicellulose, production of fermentation inhibitors in the pretreatment process, cellulose saccharification efficiency in the hydrolysis, and ethanol production by fermentation.

The remnant after bioethanol production was used for either biogas production by anaerobic digestion (AD) or for the removal of heavy metals from contaminated water.

An extra experiment has been conducted for the OMSW, for producing lactic acid. The lactic acid fermentation has been performed with *Bacillus coagulans* bacteria, following the pretreatment with chemical microwave with formic acid or maleic acid at 180°C for 10 min, and followed by enzymatic hydrolysis with Cellic CTec2 (Novozyme) and Accelerase BG, 50°C, and pH 5.

Results and discussion

Saccharification and ethanol production ranged from 17 - 94%, and 6 -15 g/L, respectively. Results analysis demonstrated that the MW temperature had the largest positive effect on ethanol production, followed by OA type, with an interaction between them. MW time beyond 4 minutes had no effect, suggesting much energy can be saved by shortening heating.

Microwave with water resulted in the best sorbent, followed by microwave with formic acid.



The biochemical methane potential results fitted the modified Gompertz model. No influence of pretreatment was observed on the maximum methane production. A clear difference was observed in the kinetic constant and in the lag phase. The maleic acid pretreatment showed the highest energy conversion efficiency of 71.0% and the energy yield for the combined ethanol production and biomethane production was 12.92 GJ fuel per ton of dry weight of substrate (10.3 MJ/kg from methane and 2.6 MJ/kg from ethanol).

Pretreatment with formic acid was the best condition for lactic acid production.

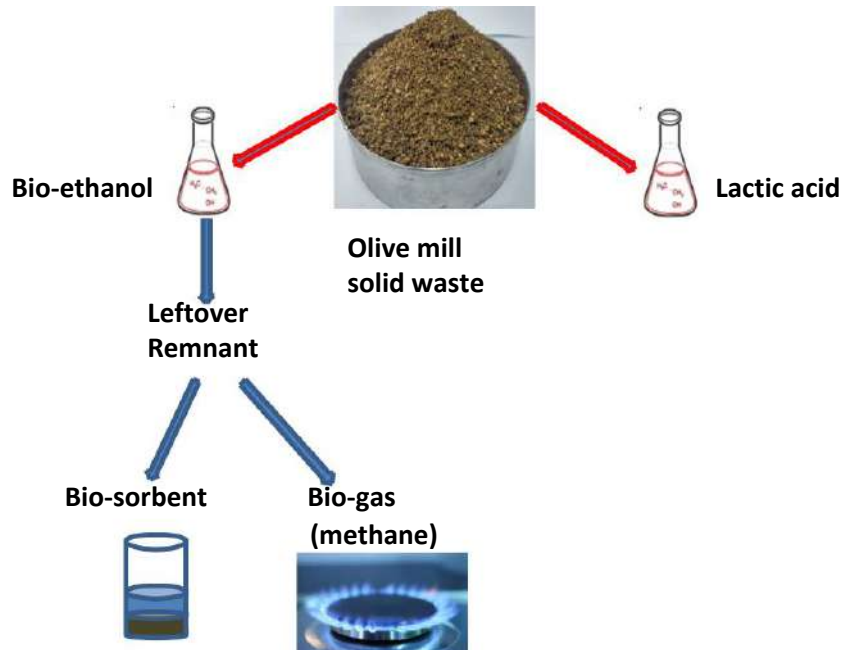


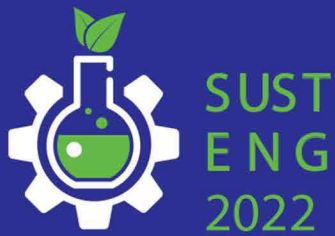
Figure 1. Added value products produced from Olive mill solid waste (OMSW).

Conclusions

This study shows that the synergy between bioethanol production and AD process could exploit the OMSW - energy nexus.

The results of this work study could facilitate the conversion of lignocellulosic biomass to added values, enhance the economic viability, and obtain the maximum value of OMSW, which is our major goal. The gap in the OMSW management could be achieved by applying the circular economy model to this solid biomass.

Acknowledgements: This research was supported by the Israeli Ministry of Science and Technology; grant number 3-13270 and the Israeli Ministry of Environmental Protection, project number 132-3-3.



ADVANCED OXIDATION PROCESSES



Significantly enhanced UV-A driven oxidative destruction of an organic contaminant of emerging concern from aqueous medium using nanosized catalysts

L. Favier¹, A.M. Sescu², D. Lutic³ and M. Harja²

¹Univ Rennes, Ecole Nationale Supérieure de Chimie de Rennes, CNRS, F-3500 Rennes, France

²Faculty of Chemical Engineering and Environmental Protection/ Department of Chemical Engineering/
“Gheorghe Asachi” Technical University of Iasi, Iasi, Romania

³ Faculty of Chemistry/“Alexandru Ioan Cuza” University of Iasi, Iasi, Romania

Corresponding author email: lidia.favier@ensc-rennes.fr

keywords: AOPs; pharmaceuticals; photocatalysis; oxidation; mineralization.

Introduction

The elimination of organic pollutants from the aquatic system is considered today as a subject of environmental primary concern. Due to their carcinogenicity or mutagenicity these water contaminants are recognized today for their negative effects on biota (Lutic et al., 2022; Sescu et al., 2020a). Most of them are considered as emerging water contaminants because they are not regulated yet by the water framework directive but they may be taken into account in future, depending on the researches data on risk assessment (Favier et al., 2016). Also are so-called contaminants of emerging concern (CECs) and include pharmaceuticals and personal care products. Among them, sartans are a class pharmaceuticals which are frequently detected in the water bodies due to their increased consumption over the world as well as to the rapid development of the pharmaceutical industry. This confirms that the conventional sewage treatment plants are not able to efficiently remove such kind of molecules.

Advanced oxidation processes (AOPs) are a group of chemical processes exploiting the high reactivity and non-specificity of hydroxyl radicals in driving degradation of a wide range of organic pollutants to non toxic intermediates such as carbon dioxide and water via oxidation reactions, thus limiting the generation of secondary contaminants (Sescu et al., 2020b; Favier et al., 2016). Among these processes, heterogeneous photocatalysis using metal oxide semiconductors received an increased interest in environmental decontamination because of its destructive efficiency for persistent pollutants. Specifically, this technique is considered as a convenient option for water detoxification because of its high degradation and mineralization ability, mild operation conditions and low cost (Harja et al., 2020).

Therefore, this study focuses on the evaluation of the photodegradation efficiency of an emergent water pollutant belonging to sartans family using TiO₂ catalysts and UV-A irradiation conditions. The model pollutant considered in this work is the antihypertensive losartan (LS) which was recently detected in many WWTPs around the world. It is important to mention that up to now the photodegradation of this molecule was rarely studied. In this context, the contribution of different process parameters and of reactive oxygen species was studied to have a better understanding on their effect on the process efficiency and on the mechanism involved in the transformation of the considered molecule. In addition, degradation kinetics were also evaluated in different water matrices to study the practical application of the considered process.

Materials and methods

A series of photocatalytic experiments were systematically designed to investigate the degradation and mineralization efficiency of the photocatalytic process in the elimination of the target molecule. The tests were performed at room temperature in a glass reactor (1L of working volume) functioning in batch mode. Irradiation was provided by an UV-A mercury vapor lamp (emitting at 365 nm) placed in the center of the reactor. In all photocatalytic experiments prior to the irradiation phase, the aqueous suspensions were magnetically stirred in dark for 2h to reach the adsorption/desorption equilibrium. Samples were taken at designated time intervals, filtered (0.45 μm PTFE Millipore syringe filter) and then analyzed directly by high performance liquid chromatography (HPLC) to evaluate the progress of the photocatalytic reaction. In



addition, dissolved organic carbon (DOC) was measured by using a Shimadzu TOC-5050 analyser to determine the mineralization rate of losartan.

Results and discussion

Different commercially available titanium dioxide (TiO₂) samples were investigated for their photocatalytic efficiency in the elimination of the target molecule. The best activity was achieved when TiO₂ AEROXIDE® P25 was used as a catalyst. Adsorption and direct photolysis experiments were also conducted to determine the contribution of these phenomena on the removal of this contaminant. Accordingly, for these tests a no significant change in the elimination efficiency was found. On the other hand, the photodegradation experiments performed in this study clearly provided that the LS removal and its mineralization rate strongly depends on the considered operating factors. It was observed that the LS elimination and mineralization were enhanced by increasing the catalyst concentration and light intensity. Also, a significant removal yield (99%) was achieved after 10 min. of reaction when the initial pollutant concentration was reduced from 60 mg/L to 5 mg/L. Under these conditions, a high mineralization rate of 87% was obtained. Accordingly, the measured removal rate was higher than the percentage of elimination of DOC, which can be due to the formation of organic intermediates. To further investigate the effect of water matrix on the degradation kinetics of the target molecule, different natural water samples were spiked with 10 mg/L pollutant. It was clearly observed that the degradation extent of LS decreases in the natural water samples, which may be due to a competition effect between pollutant and dissolved organic matter naturally present in the real water samples.

Conclusions

In summary, this work demonstrates that UV-A/TiO₂ photocatalysis is very efficient for the transformation and mineralization of this drug of the satins family recently detected in many WWTPs. Moreover, results clearly showed that the photocatalytic removal and mineralization efficiencies are affected by the considered operating conditions. The DOC removal rate was significantly enhanced (about 87% within 2h of reaction) confirming the excellent efficiency of the investigated process. The next step of this study is to identify the reaction intermediates generated during this oxidation process.

References

- Favier, L., Harja, M., Simion, A.I., Rusu, L., Kadmi, Y., Pacala, M.L., Bouzaza, A., 2016. Advanced Oxidation Process for the Removal of Chlorinated Phenols in Aqueous Suspensions, *J. Environ. Prot. Ecol.*, 17, 1132-1141.
- Harja, M., Sescu, A. M., Favier, L., and Lutic, D., 2020. Doping titanium dioxide with palladium for enhancing the photocatalytic decontamination and mineralization of a refractory water pollutant. *Rev. Chim.*, 71, 145-152.
- Lutic, D., Sescu, A. M., Siamer, S., Harja, M., and Favier, L., 2022. Excellent ambient oxidation and mineralization of an emerging water pollutant using Pd-doped TiO₂ photocatalyst and UV-A irradiation. *C. R. Chim.*, 25, 1-13.
- Sescu, A. M., Harja, M., Favier, L., Berthou, L.O., Gomez de Castro, C., Pui, A., and Lutic, D., 2020b. Zn/La mixed oxides prepared by coprecipitation: Synthesis, characterization and photocatalytic studies. *Materials*, 13, 4916.
- Sescu, A.M., Favier, L., Lutic, D., Soto-Donoso, N., Ciobanu, G., and Harja, M., 2020a. TiO₂ doped with noble metals as an efficient solution for the photodegradation of hazardous organic water pollutants at ambient conditions. *Water*, 13, 19.



Photoprotection of Cationic Porphyrins and Their Non-Covalent Complexes for Effective Photodynamic Therapy of Tumors

L. Mkrtchyan¹, A. Zakoyan¹, T. Seferyan², P. Gikas³, G. Shmavonyan⁴ and G. Gyulkhandanyan^{1,4}

¹Laboratory of Bioengineering, Institute of Biochemistry of the NAS of Armenia, Yerevan, Armenia,

²Laboratory of Biomedical research, Institute of Biochemistry of the NAS of Armenia, Yerevan, Armenia,

³Laboratory of Design of Environmental Processes, Technical University of Crete, Rethymno, Crete, Greece,

⁴Laboratory of 2D materials Engineering and Nanotechnology Innovation, National Polytechnic University of Armenia, Yerevan, Armenia

Corresponding author email: mkrtchyanlusine709@gmail.com

keywords: porphyrins; photodynamic therapy; photobleaching; folic acid; cancer.

Introduction

PDT is a treatment technique based on the combination of photosensitizing molecules (PS), PS-specific excitation wavelength light, and intracellular oxygen. The combination of these three factors will generate cytotoxic reactive oxygen species (especially singlet oxygen $^1\text{O}_2$) capable of inducing cancer cell death (Baydoun, et al., 2020). A strategy for improving the efficiency of PDT is to increase the selectivity towards tumor cells in order to reduce the adverse side-effects caused by normal cell injury. It is known that numerous cancer cell lines (on prostate, brain, lung, nose, ovary, colon, cancer cells) over-express FA receptors because of their fast growth and cell division (Stallivieri, et al., 2017). Considering this, we perform non-covalent complexation of folic acid and cationic porphyrins. One of the characteristics of PS's is the photobleaching, which is the loss of absorption or emission intensity that is caused by light (Khaled, et al., 2011). The aim of this work was to gain stable complexes and enhance the effectiveness of PDT by reducing the photobleaching of FA, cationic porphyrins, and non-covalent complexes. The stable complexes were obtained: we chose 20 % glycerin as stabilizing agent for complexation and enhancement of photostability. The study of PS's and complexes photobleaching in presence of known quenchers (L-histidine as a singlet oxygen quencher and D-mannitol as a free radicals' quencher (Khaled, et al., 2011)) was also performed.

Materials and methods

The cationic porphyrins and metalloporphyrins are as follows: 1) zinc meso-tetra [4-N- (2'-oxyethyl) pyridyl] porphyrin (Zn-TOEt4PyP), 2) zinc-meso-tetra [3-N-butyl pyridyl] porphyrin (Zn-TBut3PyP), 3) TOEt4PyP.

FA and PS were mixed in a ratio of 5/1 and incubated for 24 hour, in the dark, at 25°C. Glycerin was added to the mixture of FA and PS to make it 20% in the final volume. After additional 24 hour incubation with glycerin, the unbounded components were purified by using Al₂O₃ (aluminum oxide) column chromatography with 0.1 M PBS containing 20 % glycerin as eluent. The absorption spectra of porphyrins and their complexes with FA were recorded on Agilent co. (USA), Cary 60 spectrophotometer, in the range 200-700 nm. Fluorescence spectra of complexes were recorded on Agilent co. (USA), Cary Eclipse Fluorescence spectrophotometer.

Photostability studies were conducted by illuminating under similar conditions and following the absorbance changes over time of the PS's and their complexes with FA. PS's, FA and non-covalent complexes (PS+FA) were irradiated by tungsten lamp with a range of a wavelength 380 - 1000 nm using an irradiance of 30 mW/cm², to a total of 30 minute duration. The absorptions for samples were recorded during the irradiation and after irradiation for 0 min, 5 min, 15 min, and 30 min. The studies of the effect of histidine's, mannitol's concentrations on photobleaching were performed too.

Results and discussion

FA forms non-covalent stable complexes with ZnTOEt4PyP, ZnTBut3PyP, and TOEt4PyP with different ratio of components for targeted PDT. Stable complexes were obtained in presence of 20 % glycerin as it is known that by replacing water by glycerin, the stability of compounds improves. The addition of 20 %



glycerin led to the less photobleaching of porphyrins (2 times) and photolysis of FA than for samples without glycerin. Considering this, further the complexation and photostability studies with quenchers were performed in presence of glycerin.

Different concentrations of quenchers were tested and it was shown that the D-mannitol concentration (0.8 mM) that is needed for effective quenching and for decrease of photobleaching rate after 30 min of illumination by tungsten lamp is 10 times higher than the concentration for L-histidine (0.08 mM). It is also noted that further increase of quenchers' concentration to 10 mM for D-mannitol and to 1 mM for histidine has the reverse effect as the photobleaching was more intense. L- Histidine was more effective quencher for Zn-TBut3PyP and for its complex with FA. D-Mannitol was shown to be more effective for TOEt4PyP and Zn-TOEt4PyP than L-histidine. The more effective photoprotection by L-histidine for Zn-TBut3PyP is correlated with higher singlet oxygen quantum yield of this PS ($\gamma_{\Delta}=0,98$) compared with other two PS's ($\gamma_{\Delta}=0,7$ for TOEt4PyP and $\gamma_{\Delta}=0,84$ for Zn-TBut3PyP). It should be noted that both quenchers has a protective effect, thus indicating that both singlet oxygen and free radicals play a crucial role in the photobleaching mechanism of these cationic porphyrins.

Conclusions

FA forms non-covalent stable complexes with cationic porphyrins in presence of 20 % glycerin. The advantage of gaining this type of complexes is the simplicity of method.

By using singlet oxygen quencher L-histidine and free radicals' quencher D-mannitol, it was concluded that the use of quenchers with optimal concentration can led to the reduction of photobleaching rate and thus the enhancement of PDT efficiency.

Acknowledgements: This study is supported by the Foundation of Basic Research of the Republic of Belarus as well as by the State Committee of Science of the Ministry of Education and Science of the Republic of Armenia (Grant No 21SC-BRFFR-1F007). The authors thank to Dr. Robert Ghazaryan from Yerevan State University for providing of cationic porphyrins and metalloporphyrins.

References

- Baydoun, M.; Moralès, O.; Frochot, C.; Ludovic, C.; Leroux, B.; Thecua, E.; Ziane, L.; Grabarz, A.; Kumar, A.; de Schutter, C.; Collinet, P.; Azais, H.; Mordon, S.; Delhem, N., 2020. Photodynamic therapy using a new folate receptor-targeted photosensitizer on peritoneal ovarian cancer cells induces the release of extracellular vesicles with immunoactivating properties. *J. Clin. Med.*, 9, 1185.
- Khaled, A., Khalid, O., Mohamad, J., 2011. Photobleaching of Sn(IV) chlorine e6 dichloride trisodium salt in different environments. *African Journal of Biotechnology*, 10 (45), 9137.
- Stallivieri, A., Colombeau, L., Jetpisbayeva, G., Moussaron, A., Myrzakhmetov, B., Arnoux, P., Frochot, C., 2017. Folic acid conjugates with photosensitizers for cancer targeting in photodynamic therapy: Synthesis and photophysical properties. *Bioorganic & Medicinal Chemistry*, 25(1), 1–10.



Biochar coupled with advanced oxidation process for a novel treatment of micropollutants in effluents

H. Azaizeh^{1,2,3}, G. Peer^{1,2} and S. Azerrad^{4,5}

¹ Tel Hai College, Department of Environmental Science, Upper Galilee, Israel

² Institute of Applied Research, The Galilee Society, Israel

³ Department of Natural Resources & Environmental Management, University of Haifa, Haifa, Israel

⁴ Shamir Research Institute, University of Haifa, Qatzrin, Israel

⁵ The Natural Resources and Environmental Research Center-NRERC, University of Haifa, Haifa, Israel

Corresponding author email: hazaizeh@yahoo.com

keywords: biochar; advanced oxidation process; micropollutants; wastewater treatment; olive mill solid waste.

Introduction

Agricultural waste is generated in large amounts annually in the form of by-products in agriculture and crop residues. One of the strategies in sustainable waste management is a proper treatment of the waste to produce value-added products and minimize environmental pollution. Olives are the leading commercial tree crop in the Mediterranean region where more than 97% of the global olive production is concentrated in the Mediterranean region. The solid waste from oil extraction is called olive mill solid waste (OMSW).

The overall aim of the current research was to test the scientific and technical feasibility of the reuse of OMSW to produce biochar (BC), an added value product, for its application in water treatment prior irrigation. Reuse of treated effluents for irrigation in agriculture is a good alternative to deal with the consequences of climate change such as water scarcity. However, micropollutants (e.g., pharmaceuticals, hormones) should be removed from effluents to avoid their accumulation in crops to prevent their negative effects on the consumer's as well as their widespread into the environment.

Materials and methods

Biochar was produced from the pyrolysis of OMSW at different temperatures (400-600 °C), furthermore BC was activated physically in using an oven at 900 °C under a nitrogen atmosphere as well as modified chemically with transition metals Fe/Zn or with basic solution KOH. The modified BC activates persulfate (PSF), a chemical agent, generating sulfate radicals which oxidize pollutants in water since sulfate radical ($\text{SO}_4^{\bullet-}$) and hydroxyl radical ($\bullet\text{OH}$) have a high oxidative potential to breakdown various compounds. Acetaminophen (AMP, pain reliever) was used as a model compound due its chemical properties - the molecule is neutral at the pH of water treatment ($\text{pK}_a = 9.38$), and it is considered relatively hydrophilic ($\text{pK}_{ow} = 0.34$). These properties make acetaminophen a suitable model compound for testing different types of BC prepared in terms of adsorption, oxidation in the water solution as well as oxidation on the BC surface. Acetaminophen was spiked into the water matrixes used, tertiary effluents and buffer phosphate at 4 mg/L initial concentration. AMP measurements were performed using a HPLC-DAD.

Results and discussion

Our results showed that the effectiveness of BC for adsorption and oxidation of AMP increases along with the pyrolysis temperature; however, after 5h treatment less than 10% overall removal (adsorption + oxidation) in all the temperatures tested was achieved. Physical activation significantly enhanced the AMP removal, 84% overall removal was achieved after 20 min treatment whereas the contribution of adsorption was only 32% as can be observed in Fig. 1. Similar results were achieved for overall removal under chemical modification with Zn/Fe or KOH. However, modification with Zn/Fe enhanced the AMP adsorption achieving 72% in the first 20 min while BC under KOH modification achieved 35% in the same timeframe.

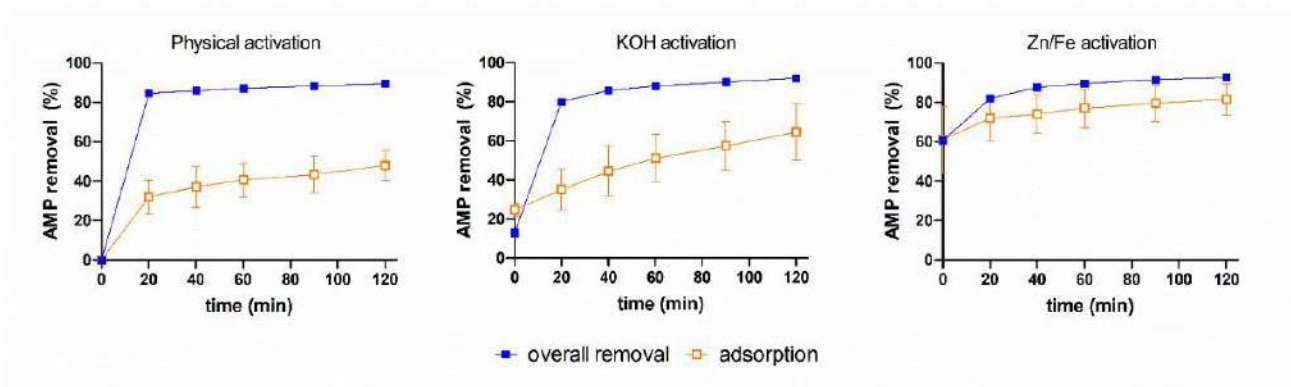


Figure 1. Removal of Acetaminophen in water by activated biochar.

Reuse of BC after the treatment was assessed during three water cycles with slightly decrease in the overall removal (persulfate system successfully removed ACM from water in the three types of activated biochar tested). Activation of BC should be performed undoubtedly in order to allow modification in BC functional groups, which are responsible for the electron transfer from the BC to the receiving persulfate. Application of agriculture waste-based BC coupled with persulfate for oxidation of micropollutants in water is a relatively new topic. Our results indicate that this may be a promising direction in the field of water treatment for a circular economy of agricultural waste and the production of economical products.

Conclusions

Application of agricultural waste-based BC combined with physical or chemical activation coupled with persulfate for oxidation of micropollutants in water is a unique approach to remove micropollutants such as pharmaceuticals.

References

Abdelhadi, O. S., Dosoretz, G. C., Rytwo, G., Gerchman, Y., Azaizeh, H. 2017. Production of biochar from olive mill solid waste for heavy metal removal. *Bioresource Technology* 244:759-767. doi: <http://dx.doi.org/10.1016/j.biortech.2017.08>



Advanced oxidation process UV-H₂O₂ combined with biological treatment for the removal and detoxification of phenol

M. Haj-Zaroubi^{1,2}, N. Bar-Niv³, H. Azaizeh^{1,2,3} and E. Kurzbaum^{3,4,5}

¹Institute of Applied Research, The Galilee Society, Shefa-Amr, Israel

²Department of Natural Resources & Environmental Management, University of Haifa, Israel

³Tel Hai College, Department of Environmental Science, Upper Galilee, Israel

⁴Shamir Research Institute, University of Haifa, Qatzrin, Israel

⁵Department of Geography and Environmental Studies, University of Haifa, Haifa, Israel

Corresponding author email: ekurzbaum@univ.haifa.ac.il

keywords: phenols; wastewater treatment; advanced oxidative processes; biological treatment; biodegradation; *Artemia*.

Introduction

Phenol is one of the first substances included on the list of toxic substances with high priority for treatment due to health problems arising in response to increased exposure to such substances. Furthermore, phenolic compounds have been listed by the United States Environmental Protection Agency (USEPA) and the European Union (EU) as pollutants of priority concern (Mohamad Said et al., 2021). High concentrations of phenol and phenolic compounds may be found in wastewater from industries such as textile, plastic, paper, medicines, oil refining, coal processing, and more (Benit et al., 2022). Advanced oxidative processes (AOP) uses ozone, hydrogen peroxide (H₂O₂), UV radiation, titanium oxide (TiO₂), and other substances that are able to produce free radicals for phenol oxidation have been reported previously. However, the main disadvantage of this method is the high cost of the process when aiming to achieve total mineralization of the substances. Furthermore, AOP produces by-products that may be more toxic than the original substances, as reported elsewhere.

The current study examined the degradation of a high, toxic concentration of phenol using a combined approach: AOP pre-treatment (combining UV radiation and H₂O₂) followed by biological treatment. Each process was also examined separately to determine the potential of each treatment alone and in combination. AOP—combining UV radiation and H₂O₂ was performed as a pretreatment, assuming that this process would make the contaminant easier to degrade biologically. The second step was biological treatment with the bacterium *Acinetobacter* EMY, which had been previously isolated in our laboratory and found to have the ability to degrade phenolic compounds. The study monitored the decomposition products produced by the system using HPLC and the concentration of organic matter (total organic carbon, TOC). Toxicity tests on *Artemia* brine shrimp were performed to determine the toxicity.

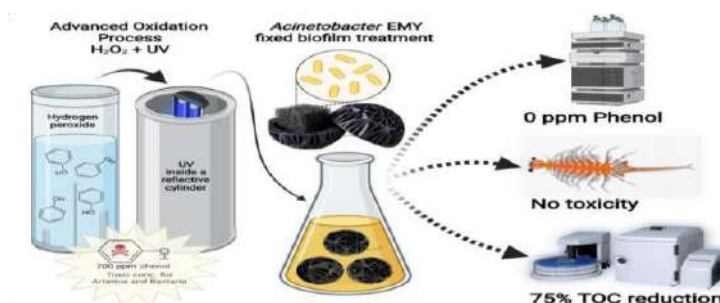


Figure 1. Graphical abstract of phenol degradation using a combined approach: AOP pre-treatment (combining UV radiation and H₂O₂) followed by biological treatment.

Materials and methods

This study used the bacterium, *Acinetobacter* EMY, for the preparation of microbial culture. This bacterium has the ability for rapid production of a resistant biofilm and demonstrated long-term activity on various surfaces. The bacterium was identified by 16S ribosomal RNA; its serial number is MT410617. After exposure and acclimatization of *Acinetobacter* EMY to high phenol concentrations, they were fixed inside



Sterile biocarriers (bioMérieux BioBalls) as a biofilm and were used in the experiments. The amount of bacterial biomass on the biofilm, measured by protein concentration, was determined using the Bradford method.

The synthetic wastewater (phenol) used throughout the study contained relevant nutrients and carbon sources and was used as the medium of the bacterium. Toxicity test of the treatment mediums was performed at the end of each experiment using *Artemia* brine shrimp.

The concentration of phenol and decomposition products was tested by using HPLC, TOC. Hydrogen peroxide residues was tested by using a commercial test kit (Macherey-Nagel).

The following treatments were performed on the original medium containing 700 ppm phenol: 1) biological treatment alone; 2) AOP treatment alone; 3) serial combination of AOP and biological treatment; and 4) a control system, including the experimental medium with phenol, but without any treatment, to determine whether spontaneous degradation of phenolic compounds occurs in the experimental system.

Results and discussion

The combination of UV-H₂O₂ and biological treatment may provide an economical solution for the industrial sector. The results of phenol concentration in the different treatments (Figure 2) show that the separate treatments (biological or AOP) did not lead to significant decomposition results. Biological treatment did not affect the phenol concentration over time due to its toxicity. Oxidation reduced the phenol concentration by 29% in the first 3 h; this value remained until the end of the experiment (20 h). The phenol was fully degraded only when biological treatment and AOP were combined: after 3 h of AOP, 29% of the phenol was removed; another 13 h of biological treatment were required to remove the remaining 71% phenol. However, we note that no further phenol could be removed after AOP without the biological treatment.

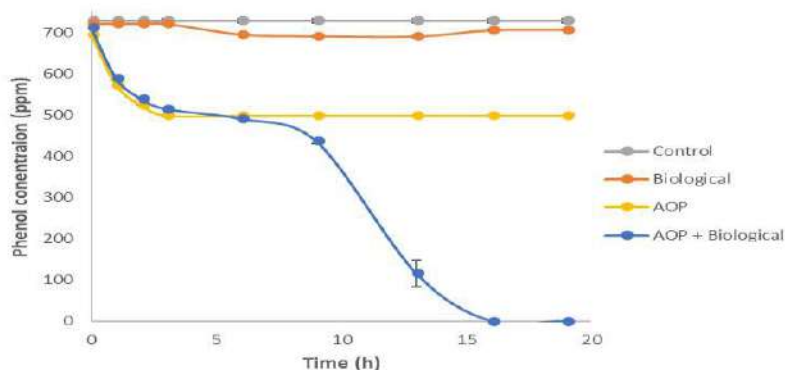


Figure 2. Change in phenol concentration with time in the four different treatments: AOP+Biological—combined treatment (blue); Biological—biological treatment alone (orange), Control (sterile phenol, grey), AOP—UV-H₂O₂ alone (yellow). The test was performed in triplicates; error bars indicate standard deviations.

Conclusions

This study shows that the combination of AOP and biological treatments has great potential for removing contaminants that are not readily biodegradable, by reducing their concentrations and their decomposition products, and preventing the accumulation of toxic by-products. Hence, it is a more economical solution for pollutants, and the significant reduction of the level of the medium toxicity increases the safety profile of water for reuse or return to nature.

Acknowledgements: This study was supported by the Israeli Ministry of Science, Space and Technology (Grant no. 3-16806).

References

- Benit, N., Lourthuraj, A. A., Barathikannan, K., Mostafa, A. A.-F., Alodaini, H. A., Yassin, M. T., & Hatamleh, A. A. (2022). Immobilization of *Halomonas halodurans* and *Bacillus halodurans* in packed bed bioreactor for continuous removal of phenolic impurities in waste water. *Environmental Research*, 209, 112822.
- Mohamad Said, K. A., Ismail, A. F., Abdul Karim, Z., Abdullah, M. S., & Hafeez, A. 2021. A review of technologies for the phenolic compounds recovery and phenol removal from wastewater. *Process Safety and Environmental Protection*, 151, 257–289.
- Parker, A. M., Lester, Y., Spangler, E. K., von Gunten, U., & Linden, K. G. 2017. UV/H₂O₂ advanced oxidation for abatement of organophosphorous pesticides and the effects on various toxicity screening assays. *Chemosphere*, 182, 477–482.



TiO₂-assisted solar light photodegradation as a solution of the problem of spreading β -lactam resistance determinants in the environment

M. Buta-Hubeny¹, E. Felis^{2,3}, W. Zieliński¹, J. Hubeny¹, M. Harnisz¹, S. Bajkacz^{3,4} and E. Korzeniewska¹

¹Department of Water Protection Engineering and Environmental Microbiology, Faculty of Geoengineering, University of Warmia and Mazury, Olsztyn, Poland

²Silesian University of Technology, Faculty of Power and Environmental Engineering, Environmental Biotechnology Department, Gliwice, Poland

³Silesian University of Technology, Centre for Biotechnology, Gliwice, Poland

⁴Silesian University of Technology, Faculty of Chemistry, Department of Inorganic Chemistry, Analytical Chemistry and Electrochemistry, Gliwice, Poland

Corresponding author email: martyna.but@uwm.edu.pl

keywords: antibiotic resistance determinants; mobile genetic elements; wastewater; photodegradation; solar light.

Introduction

The overuse of antimicrobial drugs in human and veterinary medicine has become a serious environmental threat. Drugs unmetabolized by the body enter surface waters and groundwaters, and cause serious risks due to their biological activity in nature and limited biodegradability. Additionally, the presence of excessive amounts of antimicrobial drugs promote the generation of drug-resistant bacteria, resulting in the transmission of resistant genes in different environmental compartments. The highest antimicrobial drug consumed in 2018 in Poland consisted of beta-lactam antibiotics and penicillin's (6.4 DDD), while the smallest were sulfonamides (0.5 DDD). The main cause of antimicrobial drugs occurrence in surface waters arises from the discharge of wastewater after the technological treatment process into natural water bodies. Municipal wastewater, as well as wastewater from the pharmaceutical industry and hospitals, is contaminated with large amounts of drugs, as well as antibiotic resistance genes (ARGs). Most applied wastewater treatment technologies only partially degrade selected drugs allowing their introduction into the environment. Treated wastewater is also a source of ARGs in the environment, because they are not completely removed in the treatment processes, and the conditions in wastewater treatment plants contribute to the multiplication of bacteria that can transmit information on antibiotic resistance via horizontal gene transfer. Hence, the final wastewater discharged per day may contain up to 10¹⁸ ARGs.

Materials and methods

Object of the study was wastewater after a technological treatment process obtained from a wastewater treatment plant (WWTP) located in Olsztyn, Poland. This region is located in a warm-transitional temperate climate zone. The wastewater constituted a medium and the effects of solar-light-driven processes were examined.

Treated wastewater samples (after the secondary step of treatment) were collected as 24 h composite samples. Analyses of the photochemical degradation of selected genes were carried out using a Solarbox 1500 photoreactor (Coformega, Italy). The solar light radiation was produced by an air-cooled xenon lamp and the irradiance was constantly controlled. Uniform distribution of the light on the samples surface was ensured by appropriate shape of the chamber (parabolic mirror) and location of the xenon lamp. The experiments were carried out at 500 W/m², which is the average annual irradiance of countries located at 52nd northern parallel. In the case of solar-driven photolysis, 500 mL of treated wastewater sample and a magnetic stirrer were placed in a beaker and inserted into the photoreactor. The samples were continuously mixed during the irradiation process. The process was conducted under controlled temperature, which did not exceed 30°C for 3 h. During solar photocatalysis, the experimental procedure was the same as above, except TiO₂ was used as the photocatalyst at 500 mg/L concentration. Pure anatase TiO₂ ($\geq 99\%$) was used for the experiments. The control sample was treated sewage that was not subjected to photolysis and photocatalysis.



In order to quantify selected ARGs (*bla*TEM, *bla*OXA, *bla*SHV – β -lactam resistance genes and first, second class integrase genes (*int*11, *int*12) belonging to mobile genetic elements (MGEs) and 16S rRNA gene characteristic of prokaryotic organisms, a series of qPCR (quantitative Real-Time PCR) reactions were performed on the control and tested samples with the use of primers appropriately selected for each gene.

All experiments have been prepared in triplicates.

Results and discussion

According to the literature, genes selected for this study can constitute a proxy for anthropogenic pollution and present a scale of antibiotic resistance spread. In the environmental matrix, high concentrations of selected tested ARGs in the range of 6.4×10^4 gene copies/mL (*bla*TEM) – 1.8×10^6 gene copies/mL (*bla*OXA) and mobile genetic elements (MGEs) in the range of 2.9×10^5 gene copies/mL (*int*12) – 1.7×10^6 gene copies/mL (*int*11) were noticed. It is important to emphasize that the presence of *int*11 in the environment has been proposed as an indicator of pollution associated with human activities. Among all studied genes, only *bla*SHV gene was not detected. Removal of the tested genes by both methods was very high and ranged from 76% to 98%. Both methods were effective in degradation of 16S rRNA gene at level up to 98%. The most susceptible to degradation was *bla*TEM and *int*11, which were removed in 97% and 98% respectively in the photocatalysis process and in more than 93% in the solar light-driven photolysis. In general, the removal ratio of all detected genes was always higher after using photocatalysis with TiO₂ (88%-98%) than solar light-driven photolysis (76%-93%).

Conclusions

The results of the study have confirmed that solar light-driven processes can be effective in the removing of selected emergent pollutants as β -lactam resistance genes and MGEs. Further research on the effectiveness and optimization of the genes removal from the wastewater matrix will allow to create an ecological system that minimizes or even completely removes the threat that stems from the transferal of ARGs into the environment.

Acknowledgements: This study was supported by grant No. 2017/27/B/NZ9/00267 from the National Science Centre (Poland). Martyna Buta-Hubeny, Wiktor Zieliński and Jakub Hubeny are recipients of a scholarship from the Programme Interdisciplinary Doctoral Studies in Bioeconomy (POWR.03.02.00 00 1034/16 00), which is funded by the European Social Funds.

References

- Amarasiri, M., Sano, D. and Suzuki, S., 2020. Understanding human health risks caused by antibiotic resistant bacteria (ARB) and antibiotic resistance genes (ARG) in water environments: Current knowledge and questions to be answered. *Crit. Rev. Environ. Sci. Technol.* 50, 2016–2059.
- Chen, H., Huang, M., Wang, Z., Gao, P., Cai, T., Song, J., Zhang, Y. and Meng, L., 2020. Enhancing rejection performance of tetracycline resistance genes by a TiO₂/AgNPs-modified nanofiber forward osmosis membrane. *Chem. Eng. J.* 382, 123052.
- Gillings, M.R., Gaze, W.H., Pruden, A., Smalla, K., Tiedje, J.M. and Zhu, Y.G., 2015. Using the class 1 integron-integrase gene as a proxy for anthropogenic pollution. *ISME J.* 9, 1269–1279.
- León, D.E., Zúñiga-Benítez, H., Peñuela, G.A. and Mansilla, H.D., 2017. Photocatalytic Removal of the Antibiotic Cefotaxime on TiO₂ and ZnO Suspensions Under Simulated Sunlight Radiation. *Water, Air, Soil Pollut.* 228, 361.
- Manaia, C.M., Rocha, J., Scaccia, N., Marano, R., Radu, E., Biancullo, F., Cerqueira, F., Fortunato, G., Iakovides, I.C., Zammit, I., Kampouris, I., Vaz-Moreira, I. and Nunes, O.C., 2018. Antibiotic resistance in wastewater treatment plants: Tackling the black box. *Environ. Int.* 115, 312–324.
- Poulopoulos, S.G., Yerkinova, A., Ulykbanova, G. and Inglezakis, V.J., 2019. Photocatalytic treatment of organic pollutants in a synthetic wastewater using UV light and combinations of TiO₂, H₂O₂ and Fe(III). *PLoS One* 14, e0216745.
- Sanganyado, E. and Gwenzi, W., 2019. Antibiotic resistance in drinking water systems: Occurrence, removal, and human health risks. *Sci. Total Environ.* 669, 785–797.



SUST
ENG
2022



METALS/METALLURGY



Influence of anthropogenic factors of arable soil pollution on changes in the activity of enzymes in them

A.Sukiasyan¹, A. Kirakosyan¹, S. Kroyan² and P. Gikas³

¹Chair General chemistry and chemical technology,
National Polytechnic University of Armenia, Yerevan, Armenia

²National University of Architecture and Construction of Armenia, Yerevan, Armenia

³Technical University of Crete, School of Chemical and Environmental Engineering, Chania, Greece

Corresponding author email: sukiasyan.astghik@gmail.com

keywords: transition heavy metals; soil; total pollution index; humus; catalase; amylase; urease; invertase.

Introduction

Irrational human activities as well as greedy exploitation of natural resources have destabilized the biosphere. These phenomena have become cause-and-effect pushes that require increased attention in order to mitigate the effects of technogenic environmental problems. The problem of deterioration of soil biological properties is relevant against the background of uncontrolled environmental pollution by a wide range of pollutants (Huang et al., 2020; Sukiasyan and Kirakosyan, 2020). In this context, multi-component studies may be the then necessary information, allowing us to connect the impact of adverse factors on the biota and human economic activity. In view of the above, the aim of this work is to combine biochemical and geocological approaches to determine the degree of anthropogenic load on soils, taking into account the activity of some hydrolytic and oxidoreductase enzymes for a comparative assessment of bioremediation of arable soils near the industrial zone of Hrazdan town. There are the Hrazdan Thermal Power Station (HTPS) and Hrazdan Cement Plant (HCP) as well as other important enterprises which formed a large industrial area.

Materials and methods

The sample soil from point-area Hrazdan1 was near HTPS and HCP. Considering that the wind was blowing in a south-westerly direction, the second experimental point-site Hrazdan 2 was located at a distance of 380-400 m from the first one. The third experimental point-area for collecting soil samples Hrazdan 3 was located in the same direction at a distance of 800-850 m from the industrial zone. The objects of study were chemical elements of the fourth periodicity (scandium (Sc), titanium (Ti), vanadium (V), chromium (Cr), manganese (Mn), iron (Fe), cobalt (Co), nickel (Ni), copper (Cu) and zinc (Zn)). The obtained soil sample was grounded to a powdery mass in a ceramic mortar, transferred into a 32 mm diameter closed container under special pressure and "XRF Sample Cups" made of polypropylene film. Soil samples were examined under direct exposure to X-rays using a Termo Scientific™Niton™ XRF Portable Analyser. Determination of humus in soils was carried out by Tyurin's method modified by GOST 26213 - 91. The activities of all of enzymes (catalase, amylase, urease, and invertase) in soil samples were carried out according to the method by Khziev's methods. To characterize the processes of accumulation of chemical elements in soil samples, the total pollution index (Z_c) was calculated according background content of chemical elements in the soil.

Results and discussion

The d-elements forming the group known as transition heavy metals (THMs) were considered in soil samples located at different distances of about 350-400 m from each other were determined. The elements Sc and Co were detected in trace amounts among the HTMs, regardless of the location of the point zones. Fe and Ti differed in the highest concentration values by an order of magnitude compared to other elements of HTMs. Then, the calculations of Z_c based on the values of THMs concentrations in soil samples showed that soil contamination in all investigated points-areas is within dangerous. In the middle point-area (Hrazdan 2) the value of reduced total pollution index was on 15% lower compared to the extreme points of soil sampling (Table 1).



Table 1. Concentrations of some transition metals (mg/kg) and value of in arable soil samples near industrial zone of Hrazdan.

The elements of the d-block (valence electron configuration)	The soil sampling from point-area		
	Hrazdan 1	Hrazdan 2	Hrazdan 3
Sc (4s23d1)	trace	trace	trace
Ti (4s23d2)	3702.4±5.9	3408.1±81.8	4675.6±112.2
V (4s23d3)	130.1±2.7	104.4±2.7	143.3±4.0
Cr (4s13d5)	120.5±2.9	88.4±1.9	98.1±2.4
Mn (4s23d5)	717.3±32.6	974.7±26.3	883.8±23.9
Fe (4s23d6)	27850.0±668.4	29417.0±991.0	31030.2±899.9
Co (4s23d7)	trace	trace	trace
Ni (4s23d8)	63.2±0.8	71.9±1.5	62.2±1.3
Cu (4s13d10)	66.3±1.1	57.7±0.5	51.4±1.3
Zn (4s23d10)	129.0±2.7	99.1±1.5	101.8±2.4
Total pollution index (Zc)*	63	56	66

Such "non-standard" distribution of THMs in soil samples was also duplicated in biochemical parameters (Table2). Thus, according to the activity of invertase and amylase enzymes, it is well seen that their activity in the point-area of Hrazdan 2 differs from the activity in other point-areas. Invertase activity in Hrazdan 2 was on average 30% lower than in soil samples from Hrazdan 1 and Hrazdan 3. As the distance from the industrial zone from point-area Hrazdan3 towards point-area Hrazdan 1 against the background of a gradual increase in pH in soil samples up to 7%, a significant increase in humus up to 25% was found. On the activity of catalase near the industrial zone, high activity was noted, which decreases by 60% as the distance from the source of pollution decreases.

Table 2. Biochemical analysis of soil samples.

The soil sampling from point-area	Humus (%)	pH	Enzyme activity			
			Catalase (1.11.1.6) (O ₂ cm ³ in one g of soil per one min)	Invertase (3.2.1.26) (mg of glucose in one g of soil per one day)	Amylase (3.2.1.1) (mg of maltase in one g of soil per one day)	Ureaza (3.5.1.5) (mg NH ₃ in one g of soil per one day)
Hrazdan 1	3.13±0.01	7.66	4.37±0.06	10.62±0.29	3.38±0.27	2.63±0.09
Hrazdan 2	2.23±0.03	7.47	9.93±0.21	7.67±0.16	6.06±0.61	2.39±0.21
Hrazdan 3	2.34±0.02	7.19	10.87±0.15	11.13±0.43	3.71±0.17	2.39±0.05

Conclusions

A peculiar anomaly was detected in the general pattern of element distribution near the middle point-area (Hrazdan 2). There was a decrease in the value of the total pollution index was 15% lower compared to the extreme points of soil sampling. The pool of soil hydrolytic and oxidoreductase enzymes is involved in all stages of transformation of organic compounds entering anthropogenically contaminated soil.

Acknowledgements: This study is supported by the by the Science Committee of RA, in the frames of the research project № 21T-2H216.

References

- Huang, H., Luo, L., Huang, L., Zhang, J., Gikas, P. and Zhou, Y., 2020. Effect of manure compost on distribution of Cu and Zn in rhizosphere soil and heavy metal accumulation by Brassica juncea. *Water, Air, & Soil Pollution*, 231(5), 1–10.
- Sukiasyan, A. and Kirakosyan, A., 2020. Ecological evaluation of heavy metal pollution of different soil-climatic regions of Armenia by biogeochemical coefficients. *DRC Sustainable Future: Journal of Environment, Agriculture, and Energy*, 1(2), 94–102, doi: 10.37281/DRCSF/1.2.2.
- Tyurin, I., 1951. On the method of analysis for comparative study of the composition of soil humus or humus. *Proceedings of Soils, Institute after Dokuchaev*, 38, p. 5–21.
- GOST 26213-91 *Soils. Methods for determination of organic matter*. Standards Publishing, 1992.
- Khaziev, F., 1990. *Methods of soil enzymology*. Mi: Science, 189 p.



Novel economical method for recovering valuable metals from used Li-ion batteries

J. Parra Degante¹, S. Rojas Escobar², L.P. Jaramillo Quintero¹, M.A. Munive Rojas¹ and J.A. Guevara-García¹

¹Fac. de Ciencias Básicas, Ingeniería y Tecnología. Universidad Autónoma de Tlaxcala, Campus Apizaco, Tlaxcala, México

²Fac. de Agrobiología, Cs. Ambientales. Tlaxco, Tlaxcala, México
Corresponding author email: jaguevarag@garzas.uatx.mx

keywords: Li-ion; economical; cobalt; organic acids; Mexico.

Introduction

The high demand for portable electronic devices increases the consumption of batteries, which are replaced by new ones at the first failure. Recycling practices for Lithium-Ion Batteries (LIB's) in Mexico are almost nil, they end up in landfills or are simply thrown away irresponsibly, causing metal contamination of the soil and groundwater bodies (Guevara-García, J. A., & Montiel-Corona, V., 2012). It is estimated that there are 46,620,000/year LIB's in Mexico that can potentially be recycled (Parra Degante *et al.* 2019).

Reports in the literature on the recovery of metals from used LIB's contemplate the passivation of the components of the cathode material as a previous step (Velázquez-Martínez *et al.* 2019). In this work, the the energy coming from the hydration of Li⁺ ions were used to carry out the digestion of the material and release of metals, mainly cobalt; with energy savings avoiding processes such as calcination, heating, and reagents for initial passivation.

Materials and methods

The LIB's were collected in a campaign carried out in 2019 at the Faculty of Basic Sciences, Engineering and Technology of the Autonomous University of Tlaxcala. Batteries that were not inflated and that presented a voltage of 0 V were used, proceeding to recover each of their components (cathode, anode, and separator). Leaching experiments were performed using a 500 mL three-neck round-bottom flask with an upright condenser and thermometer, on a temperature-controlled hot plate. A volume of 250 mL of a 6% hydrogen peroxide solution and one of three organic acids (acetic acid, 4.5 M, citric acid, 1 M, or lactic acid 1.5 M) was placed in each reactor. The solution was placed under constant stirring and 5 g of the cathode material recovered from the LIB's was added little by little.

Content of Li, Co, Mn, Ni, and Al of the initial cathodic material and of the solutions resulting from the leaching were analyzed by ICP, according to the USEPA Method 6010B (USEPA, 1996). The thermal behavior of the cathode material was determined by TGA, in a heating process from 20 to 500 °C, with a ramp of 20 °C/min. While the identification of the oxidation state of Co in the leachates was performed by UV-Vis.

Results and discussion

The anticipated exothermic effect did not happen only with stirring of the reaction mixture; some time and a temperature of about 40 °C were needed. Once started, the temperature reached values above 100 °C, even in an ice bath, with abundant release of bubbles.

It was observed that citric acid is the best leaching agent (Table 1), achieving the dissolution of 98.4% of the cobalt present, according to ICP analysis. It is evident that organic acids exert the metal leaching process selectively.

Table 1. Percentage of recovery of cobalt by different acid leachates after analysis by ICP.

Acid	Percentage recovery (%)
citric	94.80
acetic	65.83
lactic	83.39

Figure 1 shows the TGA profile of the initial cathode material and the UV-Vis spectra of the leached solutions. The first thermal process observed in the TGA profile corresponds to the different types of water,



which averages 126 °C. A second set of processes has a mean temperature of 385 °C, here mainly occurs the reduction of Co_3O_4 to give CoO (Natarajan *et al.* 2018). A third set of thermal processes begins before 500 °C and ends above 600 °C, to immediately trigger the processes of greater weight loss, which end in the residue or ash.

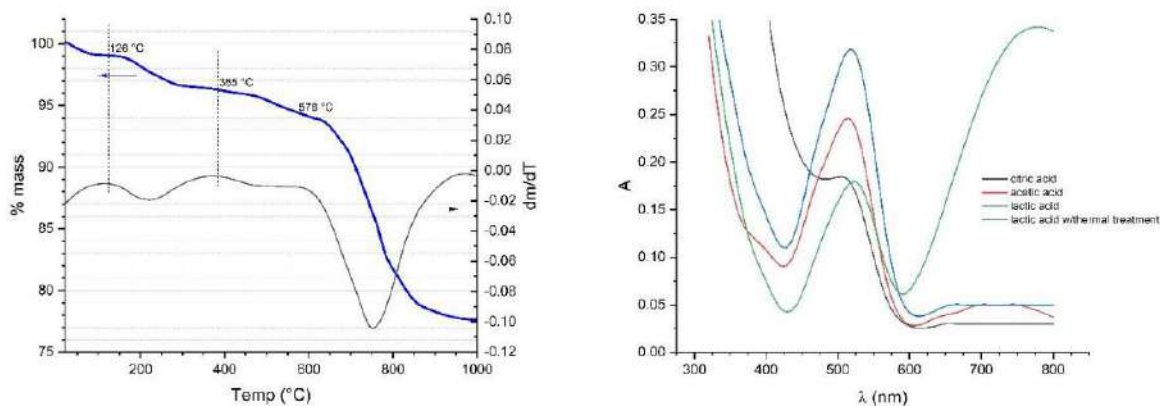


Figure 1. Left: Mass TGA profile of the starting cathode material; right, UV-Vis spectra of the leached solutions.

The UV-visible spectroscopy (right plot in Figure 1) confirms that the oxidation state of the cobalt ion in the leachates is Co^{2+} , in the state of low spin and octahedral geometry. Identified by means of by its charge transfer band in the region 470-200 nm, and the electronic transition, $2\text{Eg} \rightarrow 2\text{T}_{1g}$, observed above 500 nm.

Conclusions

The recycling of Li-ion batteries generates several benefits: environmental, economic, and social. In the environmental aspect, considered the total LIB's that can potentially be recycled in Mexico, this gives 832,500 kg CO_2 -eq/Kg/year of emissions savings. In the economic aspect, the commercial value of the recovered metals is close to 2.8/year million USD. While electric energy savings of 0.8/year million USD can be achieved by using the thermal effect as the energy source.

At the social level, recycling alleviates entropic pressure in extraction sites, recovering of ecosystems and improving the living conditions of the inhabitants of the places where the extraction of metals and raw materials is carried out. In the national context, the generation of recycling technologies enables the creation of companies, generating jobs, activating the economy, and enabling the conditions of technological, political, and economic independence.

References

- Guevara-García, J. A., & Montiel-Corona, V., 2012. Used battery collection in central Mexico: Metal content, legislative/management situation and statistical analysis. *J. Environ. Manage.*, 95, S154-S157.
- Parra Degante, J., Hernández, J, Mendoza, G., Guevara, J. A., 2019. Reciclado de pilas y baterías III. Recuperación de metales y manejo sustentable, *Colección Memorias de los Congresos de la Sociedad Química de México. 54° Congreso Mexicano de Química 38° Congreso Nacional de Educación Química. Trabajos estudiantiles y profesionales de Química Ambiental (QSUS), 18-39.*
<https://sqm.org.mx/wp-content/uploads/2021/04/CMC-SM-2019.pdf>
- Natarajan, S., Boricha, A.B., Bajaj, H.C., 2018. Recovery of value-added products from cathode and anode material of spent lithium-ion batteries. *Waste Manage.* <https://doi.org/10.1016/j.wasman.2018.04.032>
- USEPA (1996). 6010B - 1. Revision 2. December 1996. METHOD 6010B. INDUCTIVELY COUPLED PLASMA-ATOMIC EMISSION SPECTROMETRY.
- Velázquez-Martínez, O., Valio, J., Santasalo-Aarnio, A., Reuter, M., & Serna-Guerrero, R., 2019. A critical review of lithium-ion battery recycling processes from a circular economy perspective. *Batteries*, 5(4), 68.



Beneficiation of Coal Ash for Rare Earth Elements Enrichment

A. Tsachouridis¹ and N.Kiratzis¹

¹Department Of Mineral Resources Engineering/School of Engineering, University of Western Macedonia,
Kozani, Greece

Corresponding author email: nkiratzis@uowm.gr

keywords: Coal ash; Rare Earth Elements; Beneficiation; Size Separation; Magnetic Separation.

Introduction

Rare Earth Elements consist an important family of metallic elements that are vital components for hundreds of industrial applications. This family of metals includes the lanthanides plus scandium and yttrium and they are generally denoted as REY. They can be classified as Heavy(H) and Light(L), based on their atomic number, with the L.REY being the elements from La to Sm (Atomic number 57 → 62) and the H.REY from Eu to Lu (Atomic Number 63 → 71) [1]. Furthermore, REY be categorized as Critical (Nd, Eu, Tb, Dy, Y, Er), Uncritical (La, Pr, Sm, Gd) and Excessive (Ce, Ho, Tm, Yb, Lu) [2] with respect to their economic value. For further characterization of any given material, the Outlook Coefficient and the Critical Percentage indexes have been introduced and described by the equations below (w/w):

$$C_{outlook} = \frac{(Nd + Eu + Tb + Dy + Er + Y)/\sum REY}{(Ce + Ho + Tm + Yb + Lu)/\sum REY} \quad (1)$$

$$Critical \% = \frac{(Nd + Eu + Tb + Dy + Er + Y)}{\sum REY} \times 100 \quad (2)$$

Materials and methods

A large quantity of coal fly (CFA) and bottom (CBA) ash was collected every day, for five days, from the active thermal power plant of PPC Meliti, Florina. The material was thoroughly mixed and subjected to coning and quartering so as to produce two final samples of fly and bottom ash, representative of the material that the power plant produces on weekly basis.

The two ash samples were subjected to thermogravimetric analysis (TGA) for their Loss on Ignition (LOI) content. The major and minor elements composition of the samples was examined by X-Ray fluorescence (XRF), while their REY content was determined by Inductively Coupled Plasma – Mass Spectroscopy (ICP-MS). CFA had the higher REY content and was selected for further examination. Its mineralogical composition was determined by XRD.

Particle size separation showed the following size ranges: +50 Mesh (>297 μm), 50-120 Mesh (297-125 μm), 120-200 Mesh (125-75 μm), 200-325 Mesh (75-44 μm), 325-400 Mesh (44-37 μm) and -400 Mesh (<37 μm). Wet magnetic separation followed, at two different magnetic fluxes (4200 Gauss & 8420 Gauss). As feed material the <400 Mesh size fraction was selected due to its higher REY yield. For the slurry, 120 gr of the material were mixed with 480 ml of water (solid-to-liquid ratio 1:4) and the mixture was subjected to magnetic separation. The REY distribution in the resulting fractions was determined.

Results and discussion

The REY recovery (%) and the enrichment factor (EF) were defined following Lin et al. [3] where REY_i is the concentration in the i fraction and W_i is the mass percentage of that fraction. Fig. 1 shows the major chemical composition and the LOI content of the various size fractions, while table 1 summarizes the results of the two beneficiation processes.

$$REY \text{ recovery } (\%) = \frac{REY_i W_i}{(\sum_i^n REY_i W_i)} \times 100 \quad (3)$$

$$EF_i = \frac{REY_i}{REY_f} \quad (4)$$

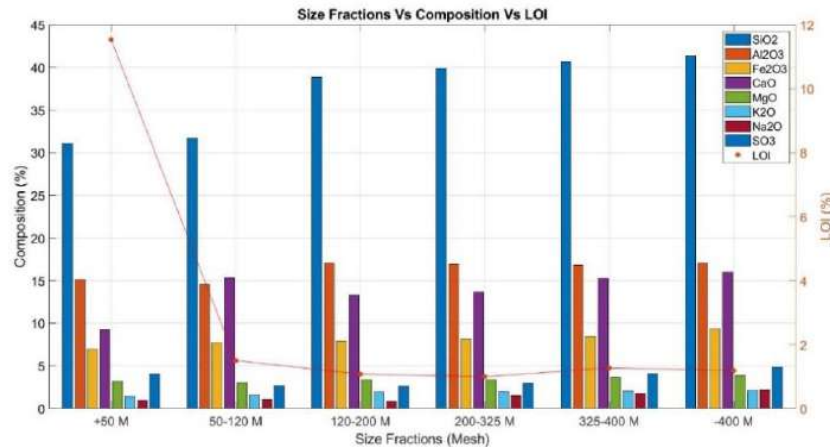


Figure 1. Chemical composition and LOI content of the various size fractions.

Table 1. Size and magnetic separation results.

Size Fraction	REY Conc. (ppm)	E.F.	Recovery (%)	Critical (%)
+50 Mesh	254.95	1.001	4.07	34.22
50-120 Mesh	257.9	1.013	14.59	34.63
120-200 Mesh	256.27	1.006	14.17	35.71
200-325 Mesh	255.82	1.005	18.24	36.57
325-400 Mesh	242.04	0.951	11.31	36.61
-400 Mesh (↓)	247.21	0.971	37.62	36.89
Fraction/M. Flow	REY Conc. (ppm)	E.F.	Recovery (%)	Critical (%)
Magn. 8420 G.	273.86	1.108	52.36	37.4
Non-Magn. 8420 G.	227.7	0.921	47.64	38.04
Magn. 4200 G.	283.99	1.149	45.77	36.98
Non-Magn. 4200 G.	225.22	0.911	54.23	38.49

Conclusions

Fly and bottom ash samples from the active thermal power plant of PPC Meliti, Florina were evaluated as potential REY sources. It was confirmed that the fly ash contained higher concentrations of REY and it was selected for further beneficiation. It was found that size separation did not significantly enrich REY content in a specific size fraction. Almost 40% of the material resulted in the finest fraction (-400 Mesh) a fact that led to a 37.62% recovery. The Critical REY (%) was also found being highest in that size fraction. Magnetic separation resulted in REY enrichment in both flows tested. The 4200 G magnetic fraction exhibited the higher REY content (283.99 ppm), but the REY recovery (%) was relatively low (45.77%), since the majority of the feed material resulted in the non-magnetic fraction. In contrast, the 8420 G. fraction showed both a high REY content (273.86 ppm) and recovery (52.36%). The Critical (%) of all the resulting fractions of the magnetic process was increased compared to that of the -400 Mesh feed material.

Acknowledgements: The authors are indebted to Prof. K. Komnitsas and his team at the School of Mineral Resources Engineering, Technical University of Crete, for the magnetic separation experiments.

References

- M. Simoni, E. P. Kuhn, L. S. Morf, R. Kuendig, and F. Adam, "Urban mining as a contribution to the resource strategy of the Canton of Zurich," *Waste Management*, vol. 45, pp. 10–21, Mar. 2015, doi: 10.1016/j.wasman.2015.06.045.
- V. V. Seredin and S. Dai, "Coal deposits as potential alternative sources for lanthanides and yttrium" *International Journal of Coal Geology*, vol. 94. Elsevier, pp. 67–93, May 01, 2012. doi: 10.1016/j.coal.2011.11.001.
- R. Lin, B. H. Howard, E. A. Roth, T. L. Bank, E. J. Granite, and Y. Soong, "Enrichment of rare earth elements from coal and coal by-products by physical separations," *Fuel*, vol. 200, pp. 506–520, Jul. 2017, doi: 10.1016/j.fuel.2017.03.096.



Recovery of Pd from Pd/Al₂O₃ catalysts through a thiosulfate-copper-ammonia complex.

M. Compagnone¹, J.J. González-Cortés^{1,2}, M.P. Yeste³, D. Cantero¹ and M. Ramírez¹

¹Department of Chemical Engineering and Food Technologies, Wine and Agrifood Research Institute (IVAGRO). Faculty of Sciences. University of Cadiz, Cadiz, Spain;

²Department of Green Chemistry and Technology, Ghent University, Ghent, Belgium;

³Department of Material Science, Metallurgical Engineering and Inorganic Chemistry, Institute of Research on Electron Microscopy and Materials (IMEYMAT), Faculty of Sciences, University of Cadiz, Cadiz, Spain.

Corresponding author email: martin.ramirez@uca.es

keywords: *Platinum group metals; leaching; thiosulfate-copper-ammonia; catalysts; Palladium.*

Introduction

Palladium (Pd) as a Platinum Group Metal (PGM) is considered both a precious and critical metal due to its scarcity and wide application. PGMs are essential in modern industry due to their unique physical and chemical properties. In the last decades, the demand for PGMs has kept increasing which raises concerns about sustainability issues. Ore grades contain very low concentrations of PGMs, from 3 to 8 g/t, while secondary sources of these metals keep accumulating as industrial waste. It is estimated that recycling 2 mg of spent automotive catalysts equals the mining of 150 kg PGM ores. Hence, the need to convert the abundant hazardous wastes originating from PGM's industry (automotive catalysts, superalloys, electronics, space materials, jewelry, etc.) into an opportunity for metal recycling becomes urgent. Today, every technology used for PGMs recovery involves pyrometallurgical treatments. The major problem with these traditional processes is the environmental costs due to the high temperatures required and the high pollution level of the generated wastes.

With this work, the recovery of Pd from a Pd/Al₂O₃ catalyst through a thiosulfate-copper-ammonia complex is proposed. This environmentally friendly process is considered an alternative method to the use of cyanide for gold recovery (Xu et al., 2017) but it has been scarcely studied for Pd recovery.

Materials and methods

Experiments were performed at a working volume of 50 mL with 15% w/v of Pd/Al₂O₃ milled catalyst in liquid solutions at different concentrations of (NH₄)₂SO₄; CuSO₄·5H₂O; Na₂S₂O₃·5H₂O and Na₂SO₃. The pH of the solutions was adjusted to the desired value right before starting the tests by adding 1M NaOH solution. The solutions were immediately agitated at a constant speed of 300 rpm, and heated to keep temperatures constant. When required, samples were aerated with 0.5 L/min. The pH value of the leaching systems was kept steady by readjustment every 30 min for leaching times of 48 h. When the reaction was completed, the solutions were centrifuged at 1,610 x g for 10 min and the solid phase was dried in an oven at 80°C for 24 h.

The Plackett-Burman (PB) analysis was performed using different experimental variables at different levels (temperature [25-60 °C], airflow [0-0.5 L/min], thiosulfate concentration [0.6-1.2M], ammonia concentration [0.5-1.5M], sulfite concentration [0-0.1M] and pH [8-12]).

Additional tests were performed considering the PB's results (Table 1). Each variable was increased or decreased based on its positive or negative effect on the process. The temperature was kept constant at 60°C while aeration was eliminated due to its negative effect on the process.

Table 1. Study of the effect of the main factors in the leaching process.

Samples	Thiosulfate (M)	Copper (M)	Ammonia (M)	Sulfite (M)	pH
1	2.4	0.030	1.5	0.1	8.0
2	1.2	0.015	1.5	0.1	8.0
3	1.2	0.030	3.0	0.1	8.0
4	1.2	0.030	1.5	0.2	8.0
5	1.2	0.030	1.5	0.1	6.0



The Pd present in the liquid solutions was measured by induction-coupled plasma atomic emission spectroscopy (ICP-AES) (Iris Intrepid, Thermo Scientific).

Results and discussion

The PB experimental design was successfully used to evaluate the effect on the Pd leaching rate of different experimental variables. Fig. 1A showed the standardized effect of the studied variables and their positive or negative effect on the leaching process. Aeration of the process negatively affected the leaching process probably because it led to faster evaporation of the liquid phase affecting the % w/v of pulp density. The same can be seen for the higher value of pH and copper. Excess of NaOH in the reaction can be responsible for the deposition of inorganic solid residues on the catalyst surface, inhibiting the active sites (Cobo et al., 2008). Moreover, copper is the most unstable element of this process and high concentrations of this heavy metal can result in the oxidation of thiosulfate (Xu et al., 2017). Copper stabilization can be obtained through the use of inorganic additives which motivated the decision to test the effect of adding Na₂SO₃ to the solutions. Fig 1A shows that sulfite has a positive effect on the process. The same happens for thiosulfate and for ammonia which reduces thiosulfate decomposition. In line with the literature, high temperatures also make Pd dissolution faster. The highest leaching percentage of Pd obtained using the PB design was 26%. The Pd leaching rate of these new tests is shown in Fig 1B. The maximum percentage of leaching was obtained in test 4 (32.4%) in which sulfite concentration was doubled from 0.1 to 0.2M. In test 1 the percentage of leaching was similar (30.6%), however, the concentration of thiosulfate was double that in test 4. Test 5 shows the remarkably negative impact of low pH, with only 0.6% of Pd recovery at pH 6.0.

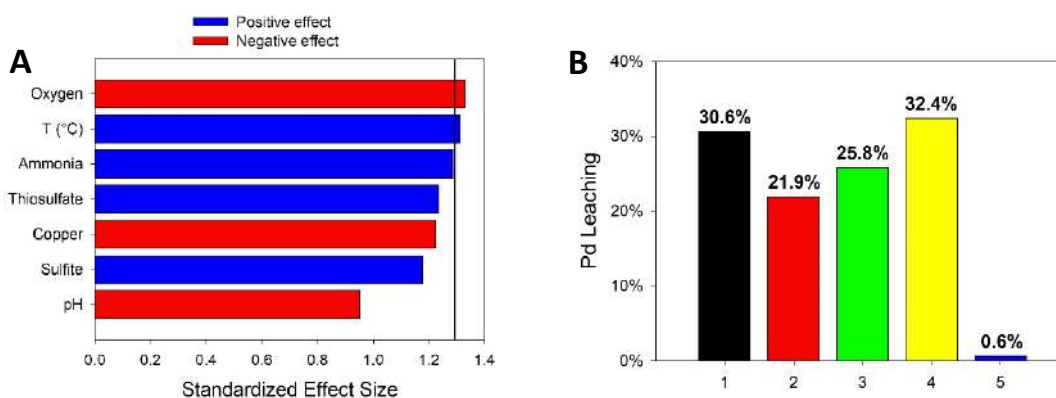


Figure 1. (A) Standardized effect size of Plackett-Burman ($\alpha = 0.25$); **(B)** Effect of modifying the experimental variables on the leaching process.

Conclusions

Thiosulfate-copper-ammonia leaching method is viable in the recovery of Pd from Pd/Al₂O₃ catalysts. The maximum leaching percentage was 32.4% reached throughout the significantly effective addition of sulfite. However, there is room for improvement so further research is needed.

Acknowledgments: This work has been co-financed by the 2014-2020 ERDF Operational Programme and by the Department of Economy, Knowledge, Business and University of the Regional Government of Andalusia. Project reference: FEDER-UCA18-106138.

References

- Cobo, M., Conesa, J. A., & Montes de Correa, C. (2008). Effect of the reducing agent on the hydrodechlorination of dioxins over 2 wt.% Pd/ γ -Al₂O₃. *Applied Catalysis B: Environmental*, 92(3–4), 367–376. <https://doi.org/10.1016/j.apcatb.2009.08.016>
- Xu, B., Kong, W., Li, Q., Yang, Y., Jiang, T., & Liu, X. (2017). A review of thiosulfate leaching of gold: Focus on thiosulfate consumption and gold recovery from pregnant solution. *Metals*, 7(6). <https://doi.org/10.3390/met7060222>



Crocin as an eco-friendly corrosion inhibitor for aluminum alloys in NaCl solution

P. Pantazopoulou¹, S. Theohari² and S. Kalogeropoulou¹

¹ Department of Electrical and Electronic Engineering, University of West Attica, Athens, Greece² Graphic Design and Visual Communication Department, University of West Attica, Athens, Greece

Corresponding author email: parpant@uniwa.gr

keywords: aluminum corrosion; sodium chloride environment; eco-friendly inhibitors; Crocin; electrochemical and gravimetric methods.

Introduction

Corrosion inhibition of aluminum and its alloys is crucial for economic and environmental reasons and conservation of natural resources, energy and materials. Various organic substances have been used as inhibitors, but many of them are toxic with hazardous effects on living beings. Within the research for eco-friendly inhibitors, Crocin, a natural organic substance from the Greek plant *Crocus sativus*, is examined against corrosion of AA 1050, 5083, 5754 and 6082 aluminum alloys in a highly corrosive environment such as sodium chloride solution. Crocin is a water-soluble carotenoid forming an orange-colored solution with protective antioxidant function against free radicals. Linear and Tafel polarization, mass loss measurements and Scanning Electron Microscopy were used for the study of the effectiveness of Crocin against corrosion.

Materials and methods

Specimens of aluminum alloys with %wt composition as displayed in Table 1 were tested. The corrosive environment was either a solution of 0.01M NaCl p.a. (reference solution) or a solution of 0.01M NaCl with 1.25mM Crocin (inhibiting solution). Crocin or 8,8-diapo-8,8-carotenoid acid (C₄₄H₆₄O₂₄) was supplied from Sigma-Aldrich.

Table 1. Composition (%wt) of aluminum and aluminum alloys.

Type	Si	Fe	Mn	Mg	Cu	Ti	Cr	Zn	Al
1050	0.168	0.245	0.003	0.001	0.001	0.006	0.002	0.013	balanced
5083	0.133	0.318	0.523	4.698	0.061	0.015	0.061	0.117	balanced
5754	0.125	0.273	0.142	2.939	0.017	0.014	0.052	0.008	balanced
6082	0.900	0.430	0.460	0.800	0.080	0.030	0.020	0.050	balanced

Linear and Tafel Polarization measurements were performed by a Gamry Interface 1000 Potentiostat/Galvanostat/ZRA and DC105 Corrosion Software. Inhibition efficiency of Crocin was calculated from Tafel curves by the equation $IE (\%) = [(I_{corr,R} - I_{corr,I}) / I_{corr,R}] \times 100$, where $I_{corr,R}$ and $I_{corr,I}$ are the corrosion currents in the reference and inhibiting solutions, respectively.

Mass loss of aluminum alloy samples was monitored weekly for a total immersion period of 13 weeks in the test solutions. Prior to weighing, corrosion products were removed according to ISO 8407.

Observation and analysis of the specimens' surface were carried out by Stereomicroscopy via an Olympus SZ61 Stereo Microscope equipped with a camera (Image Pro Plus - Infinity Capture) and by Scanning Electron Microscopy (SEM) equipped with Energy Dispersive Spectroscopy (EDS) (JEOL JSM-6510 LV - EDAX / Oxford Instruments, 10 mm² Silicon Drift Detector - x - act).

Results and discussion

Mass loss of specimens vs. immersion time in the reference and inhibiting solutions is presented in Figure 1a. The positive influence of Crocin is obvious, notably for specimens 5083, where the protective performance of Crocin was as high as 95%, whereas for the other specimens it ranged between 80 and 90%. These results are in good accordance with the findings derived from the electrochemical measurements (Figure 2a), confirming the beneficial effect of Crocin on aluminum surface, which is attributed to the creation of a shielding film against the aggressive chloride ions of the solution.

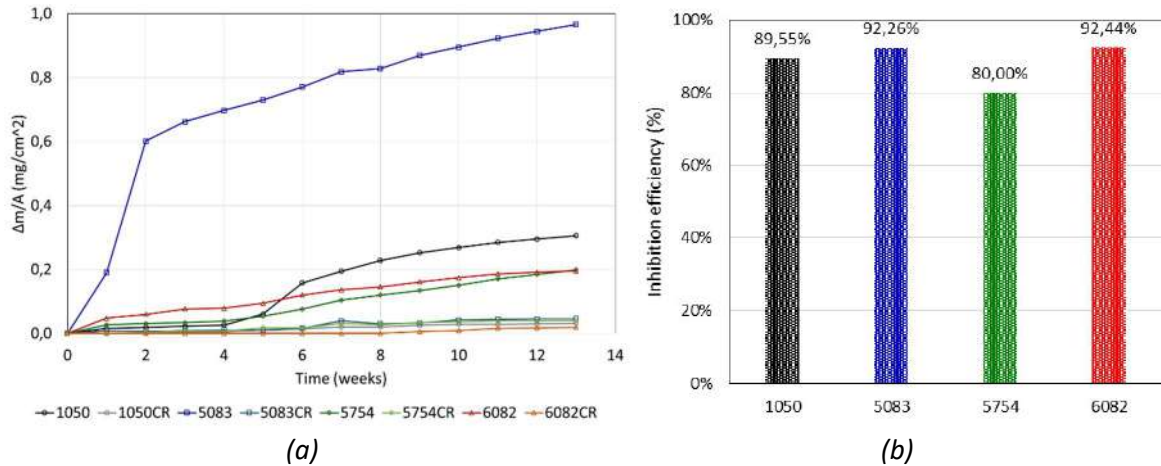


Figure 1. (a) Mass loss of the specimens vs. immersion time and (b) Inhibition efficiency (%) of Crocin obtained from corrosion currents.

Specimens immersed in the inhibiting solution with Crocin for 13 weeks present less corroded surface, without any signs of localized pitting corrosion, as shown in Figure 2. These results validate the favorable influence of Crocin as corrosion inhibitor and confirm the findings of the electrochemical corrosion tests and mass loss measurements.

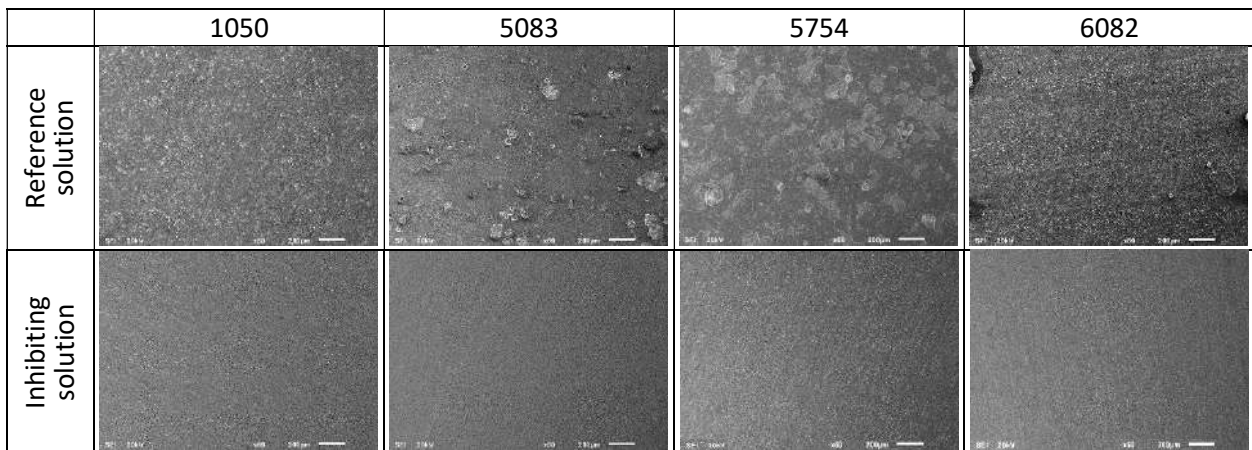


Figure 2. SEM micrographs (X60) of specimens' surfaces after immersion in test solutions for 13 weeks.

Conclusions

This study evidences the effectiveness of Crocin as an eco-friendly corrosion inhibitor for aluminum alloys in the eroding environment of NaCl. Crocin was found to retard the dissolution of the natural protective aluminum oxide layer, obstruct pitting corrosion and reduce the formation of corrosion products.

References

- Badawi, A.K. and Fahim, I.S., 2021. A critical review on green corrosion inhibitors based on plant extracts: Advances and potential presence in the market. *Int. J. Corros. Scale Inhib.*, 10, 1385–1406.
- Natishan, P.M. and O'Grady, W.E., 2014. Chloride Ion Interactions with Oxide-Covered Aluminum Leading to Pitting Corrosion: A Review. *J. Electrochem. Soc.*, 161, C421-C432.
- Pantazopoulou, P.; Theohari, S.; Kalogeropoulou, S., 2021. Organic dyes as corrosion inhibitors of commercial AA1050 aluminum alloy in sodium chloride environment. *MATEC Web of Conference* 349, 02017, ICEAF-VI 2021.
- Verma, C., Ebenso, E., Quraishi, M.A., Hussain, C.M., 2021. Recent developments in sustainable corrosion inhibitors: design, performance and industrial scale applications. *Mater. Adv.*, 2, 3806-3850.
- Xhanari, K., Finšgar, M., Hrnčič, M.K., Maver, U., Knez, Z., Seiti, B., 2017. Green corrosion inhibitors for aluminium and its alloys: a review. *RSC Adv.*, 7, 27299-27330.



Anodic electrodeposition of continuous metal-organic framework films with robust adhesion by pre-anchored strategy

W. Guo¹, X. Zhang¹ and J. Fransaer¹

¹Department of Materials Engineering, KU Leuven, Leuven, Belgium

Corresponding author email: Jan.Fransaer@Kuleuven.be

keywords: *Metal-organic frameworks; films; anodic electrodeposition; modified electrodes.*

Introduction

As porous materials with high surface area, metal-organic frameworks (MOFs), comprising coupling units (metal ions or metal-oxo cluster) coordinated by organic ligands, have received a lot of attention since first reported in the 1990s by Yaghi and Li ^[1]. Their diverse structures and tunable properties (including pore size, metal center, and functional linkers) provide a lot of opportunities for a broad range of applications ^[2]. Some applications such as gas storage and drug release, are based on MOFs in powder form. However, for many other applications (e.g. sensors, catalysis, electronic devices, optoelectronics, membranes and energy storage and conversion devices.), MOF layers/films are preferred.

Electrosynthesis is a promising method to prepare MOF films owing to mild synthesis conditions, short synthesis time, real-time monitoring capability, low cost and the possibility for scale-up ^[3]. However, the deposition of continuous and thick MOF films by anodic electrodeposition still remains elusive. The major problem is the detachment of MOF during synthesis. In the anodic deposition, the dissolution of the metal substrate creates voids at the MOF-substrate interface that gradually weakens the adhesion of the MOF films, and eventually leads to their detachment^[4]. Therefore, the thickness of anodic deposited MOF films is usually limited to a few microns, which excludes these films from applications requiring high mass loading of MOFs or strong film adhesion (such as MOF-based water adsorption-driven heat reallocation systems).

In this work, a strategy is proposed that improves the adhesion between anodically precipitated MOF films and the substrate to such an extent that it allows the synthesis of MOF films with a thickness ≥ 40 μm . Instead of dissolving a metal substrate inside an electrolyte that contains MOF linkers, this strategy involves two-steps. Firstly, HKUST-1 particles are partly embedded in a copper layer by electrodeposition using pulse reductive current by adding prepared MOF particles to a copper deposition electrolyte. Subsequently, the anodic deposition technique is applied on the prepared electrode to form the MOF films. Due to the “anchor effect” of the pre-deposited MOF particles, the adhesion strength of the deposited MOF films increases dramatically, the detachment can be effectively mitigated, and the growth of thick MOF films becomes possible. Because of the well-developed experience of the electrodeposition of metal, this facile modified pre-embedded strategy can be extended to other conductive substrates and other kinds of MOFs, providing an applicable route for MOF films toward practical applications like sorption-based heat transformation.

Materials and methods

1,3,5-Benzenetricarboxylic acid (H_3BTC , Alfa Aesar, Germany, 98%), methyltributylammonium methyl sulfate (MTBS, ChemCruz, USA), copper (II) sulfate pentahydrate (Sigma-Aldrich, 98%) and ethanol (absolute ethanol, Fisher Chemical, 99.8%) were used as received without further purification.

The electrosynthesis process was carried out using an Autolab PGSTAT 302N electrochemical workstation at ambient temperature. The copper wafers were used both as anode and cathode.

Results and discussion

The surface and cross-section morphology of the modified electrode with the electrodeposition proceeding are studied by optical microscopy and SEM. It is noticeable that new HKUST-1 crystals prefer to grow onto the previously embedded HKUST-1 particles, forming islands or clusters (red circles in Fig. 1a II) rather than nucleate on the bare copper. With the synthesis time prolonged, the HKUST-1 islands that grow attached to the pre-embedded MOF particles expand and intergrown with each other (Fig. 1b I). The thickness and the coverage of the films increase with the deposition time. Due to the anchor effect of the pre-embedded MOF particles, a high-quality HKUST-1 film with an average thickness of ~ 42 μm can be obtained after 500 min of deposition instead of detachment from the substrate.

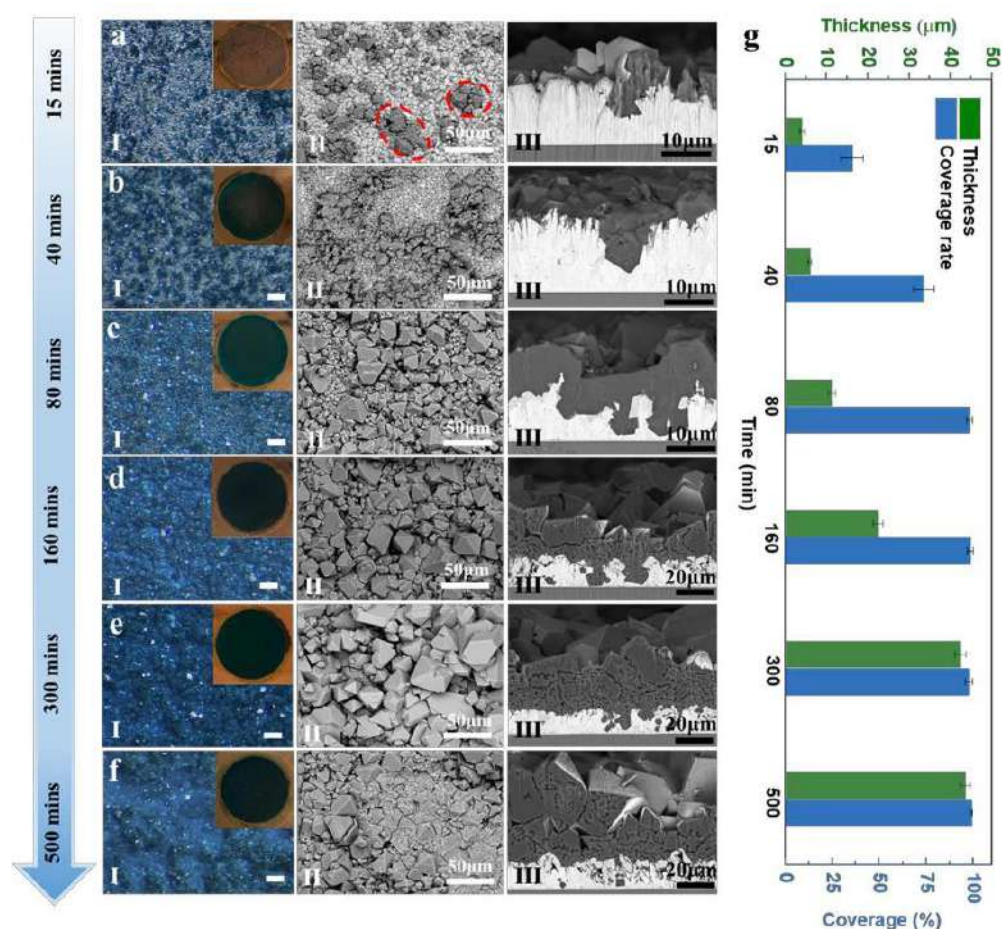


Figure 1. (I) Optical micrographs (insert: photograph of the electrode surface), (II) SEM images of the surface, and (III) SEM images of the cross section of the electrode after reaction for: (a) 15 mins; (b) 40 mins; (c) 80 mins; (d) 160 mins; (e) 300 mins; (f) 500 mins; (g) the coverage and thickness as a function of time for HKUST-1 film on the electrode (determined by ICP). 2 g of H_3BTC and 1 g of MTBS per 100 mL solution ($EtOH/H_2O$ 67:33vol%) at a current density of 0.64 mA cm^{-2} . The scale bar in optical micrographs is $100 \mu\text{m}$ and the diameter of the working electrode in the photograph is 20 mm.

Conclusions

In summary, our results demonstrated a convenient pre-embedded MOF particles strategy to improve the MOF-substrate adhesion and achieve extreme thick MOF films ($\geq 40 \mu\text{m}$) for the in-situ synthesis of MOF films. The scratch results imply that the pre-deposited MOF particles play an important role in avoiding the detachment of the MOF film in the anodic electrodeposition process and increase the film-substrate adhesion by the anchoring effect.

Acknowledgements: The authors are grateful for the FWO (12ZV320N) and NNSF (22005250). W.G is grateful to the China Scholarship Council.

References

- Yaghi, O. M., Selective binding and removal of guests in a microporous metal-organic framework. *Nature* 1995, 378 (6558), 703-706.
- Furukawa, H., The chemistry and applications of metal-organic frameworks. *Science* 2013, 341 (6149), 1230444.
- Zhang, X., Electrochemical deposition of metal-organic framework films and their applications. *J. Mater. Chem. A* 2020, 8(16), 7569-7587.
- Campagnol, N., On the electrochemical deposition of metal-organic frameworks. *J. Mater. Chem. A* 2016, 4 (10), 3914-3925.



Hydrometallurgical recovery of Ag and Au from printed circuit boards coupled with a novel bioreactor for the treatment of wastewater: a zero-discharge scheme

D. Vlasopoulos¹, P. Mendrinou¹, P. Oustadakis¹, A. Karampelas¹, P. Kousi¹, A. Stergiou², S. Karamoutsos², A. Hatzikioseyan¹, P.E. Tsakiridis¹, S. Agatzini-Leonardou¹, G.N. Anastasakis¹ and E. Remoundaki¹

¹School of Mining and Metallurgical Engineering, National Technical University of Athens (NTUA), Zografou, Greece

²Ecoreset S.A., Thessi Agios Georgios, Aspropyrgos, Greece

Corresponding author email: remound@metal.ntua.gr

keywords: printed circuit boards; silver; gold; hydrometallurgy; denitrification.

Introduction

Waste Electrical and Electronic Equipment (WEEE) ranks among the fastest growing waste streams in the world. The global generation of e-waste grew to 53.6 Mt in 2019 with the perspective to reach 74.7 Mt by 2030 (Forti *et al.*, 2020). Among e-waste, printed circuit boards (PCBs) consist of 30% of base and precious metals (copper and iron: 10%-20%, gold, silver, platinum) as well as rare earths. Their metal content is much higher than the natural ores, making metal recovery from PCBs a worldwide priority for circular economy (Işıldar, 2018).

Hydrometallurgical processing can be established in local WEEE recycling industries permitting the decentralized “green” production of pure metals (Tuncuk *et al.*, 2012; Tunsu *et al.*, 2016). These processes involve essentially two steps: (a) leaching of metals, which is generally achieved by means of strong acids such as nitric, hydrochloric and their mixtures (aqua regia); and (b) separation/selective extraction of the metals of interest from the leachate. Thus, the effluents from the separation and recovery stages contain residual anions such as NO³⁻, Cl⁻ as well as residual metal ions which have not been recovered. Neutralization of these streams removes part of the soluble metal species by precipitation without altering the content of nitrate and chloride. Therefore, to satisfy the requirement for minimum discharge, nitrate and residual metals removal from wastewater with high chloride content, can also be addressed via a microbially-mediated process. Heterotrophic denitrification has been demonstrated feasible and efficient for the treatment of wastewater which is characterized by elevated nitrate and chloride concentrations and presence of soluble metal species such as Fe, Ni, Cu, and Zn (Mendrinou *et al.*, 2021).

This work presents an integrated process for the hydrometallurgical treatment of PCBs for the recovery of silver and gold coupled with a downstream packed-bed biofilm reactor for the removal of residual nitrate and soluble metals from highly saline effluents.

Materials and methods

The PCB material was filter dust produced during crushing of PCBs in a recycling facility. The non-metallic fraction was removed from the material by treatment in a shaking table. The metallic part was used in all experiments. The metal content of the dust was determined via dissolution after eutectic fusion at 1000 °C. The metals in leachates and effluents were determined by Atomic Absorption Spectrometry (AAS). X-ray Diffraction (XRD) and Scanning Electron Microscopy (SEM) gave additional information about the different characteristics of the metallic content of the solids.

Results and discussion

The material grain size is < 250 µm and contains: Sn: 3.9%, Fe:16.5%, Cu: 14.9%, Ag: 0.4%, Au: 0.03%, Ni: 1.7% and Zn: 6.2%.

The proposed multi-stage process is as follows:

- Initially, the metallic part of the PCB material is leached with 6 M HCl in order to remove other metals and enrich the fraction in copper. The leached residue is the raw material for copper recovery.



- Copper is extracted with HCl-H₂O₂ and recovered via solvent extraction with ACORGA M5640 (Vlasopoulos *et al.*, 2021). After this second stage, silver and gold remain in the solid residue which is free from other metals, such as Sn, Fe, Zn, Ni and Cu.
- During leaching with HCl, silver remains in the solid residue as AgCl and cannot be further dissolved and separated from gold. Silver may be reduced quantitatively upon direct contact of the solid material with hydrazine-NaOH solution and then quantitatively extracted via leaching with HNO₃. Soluble silver may then be quantitatively recovered by both precipitation or electrowinning.
- Gold is leached with aqua regia (HCl/HNO₃ 3:1) and quantitatively recovered upon reduction by hydrazine.
- The wastewater generated during the various leaching steps, is rich in chloride and nitrate and contains residual soluble metals. This is fed into the denitrifying bioreactor after neutralization and appropriate mixing. The concentrations of Fe, Ni, Cu, Zn and Pb in the feed solution do not exceed 10 mg/L. Biological denitrification is achieved in the bioreactor for initial nitrate and chloride concentrations of 5 g/L and 8 g/L, respectively. Denitrification proceeds through the formation of nitrite as intermediate which is sequentially reduced completely into nitrogen. The presence of metals, such as Fe, Zn, Cu and Ni at concentrations up to 50 mg/L, does not affect the denitrification process and these are sequestered from solution via bioprecipitation (Mendrinou *et al.*, 2021).

Conclusions

The main advantages of the process are:

- Extraction of base and precious metals by only two leaching agents: HCl and HNO₃.
- Selective separation and recovery of silver and gold.
- Efficient reduction of silver and gold by hydrazine avoiding reductant residues.
- Microbial denitrification in presence of metals at ppm level in a packed-bed biofilm reactor is an interesting alternative for the treatment of the produced wastewater.

Acknowledgements: This research has been co-financed by the European Regional Development Fund of the European Union and Greek national funds through the Operational Program Competitiveness, Entrepreneurship and Innovation, under the call RESEARCH – CREATE – INNOVATE (project code: T1EDK-00219).

References

- Forti, V., Baldé, C.P., Kuehr, R. & Bel, G. (2020). The global e-waste monitor 2020: quantities, flows and the circular economy potential. Bonn/Geneva/Rotterdam: United Nations University (UNU)/United Nations Institute for Training and Research (UNITAR) – co-hosted SCYCLE Programme, International Telecommunication Union (ITU) & International Solid Waste Association (ISWA), 120 pp.
- Işıldar, A. (2018). 10 - Biotechnologies for metal recovery from electronic waste and printed circuit boards. in: Vegliò, F. & Birloaga, I. (Eds.), *Waste Electrical and Electronic Equipment Recycling*. Woodhead Publishing, pp. 241-269.
- Mendrinou, P., Hatzikioseyan, A., Kousi, P., Oustadakis, P., Tsakiridis, P. & Remoundaki, E. (2021). Simultaneous Removal of Soluble Metal Species and Nitrate from Acidic and Saline Industrial Wastewater in a Pilot-Scale Biofilm Reactor. *Environmental Processes* 8(4): 1481-1499.
- Tuncuk, A., Stazi, V., Akcil, A., Yazici, E.Y. & Deveci, H. (2012). Aqueous metal recovery techniques from e-scrap: Hydrometallurgy in recycling. *Minerals Engineering* 25(1): 28-37.
- Tunsu, C. & Retegan, T. (2016). Chapter 6 - Hydrometallurgical processes for the recovery of metals from WEEE. in: Chagnes, A., Cote, G., Ekberg, C., Nilsson, M. & Retegan, T. (Eds.), *WEEE Recycling*. Elsevier, pp. 139-175.
- Vlasopoulos, D., Oustadakis, P., Agatzini-Leonardou, S., Tsakiridis, P. & Remoundaki, E. (2021). A Hydrometallurgical Process for Cu Recovery from Printed Circuit Boards. *Materials Proceedings* 5(1): 56.



Bayesian statistics study of a sustainable dissolution of cobalt bearing minerals from Cu-Co ores

B. Mbuya^{1,2}, J. Meta Mvita² and A.F. Mulaba-Bafubiandi^{2,3}

¹ Department of Metallurgy, Faculty of Engineering, University of Likasi, Likasi, Democratic Republic of Congo

² Mineral Processing and Technology Research Centre, Department of Metallurgy, School of Mining, Metallurgy and Chemical Engineering, Faculty of Engineering and The Built Environment, University of Johannesburg, Doornfontein, South Africa

³ Department of Mining Engineering, School of Engineering and Technology, College of Science, Engineering and Technology, University of South Africa, Florida, South Africa

Corresponding author email: mbuya.bienvendu@gmail.com

keywords: Co-leaching; Cu-Co ore; Bayesian statistics; DOE; conditional probability.

The present paper discusses the dissolution of cobalt bearing minerals from a copper-cobalt mixed ore using probabilistic models where a priori and a posteriori knowledges on leaching is used to predict the dissolution of cobalt bearing minerals in a sulfuric acid medium in the presence of a reducing agent. Priorily, the dissolution of cobalt bearing minerals depends on their mineralogy, leading to the use of FeSO₄ as a reducing agent of the trivalent (Co³⁺) form of cobalt [Co(Fe)OOH]. A posteriori, the dissolution of Co³⁺ is improved by the presence of ferrous ions resulting from the dissolution of Fe-bearing minerals, including Fe from Co(Fe)OOH. The results showed that the predictive oriented probabilistic graphic models based on the Bayesian approach, in combination with the design of experiments data, made it possible to model the leaching of cobalt bearing minerals. The results from the design of experiment using the experimental tree methodology associated with the optimization of the multiple responses , in a multiple input for a multiple output set – up derived the following optimised parameters: 60°C for the temperature (T), 850 rpm for the agitation, 40% for the solid percentage, 1.5 for the pH and 4 g/L for the concentration of the Fe²⁺ ion. The cobalt dissolution yield obtained was 89.95% . The analysis of the dependence between the random variables only (P(Fe²⁺|T), P(pH|T), P(Fe²⁺|pH)), of the dependence between the random variables and the responses (P(Co-yield|pH,Eh)) allowed the construction of two Bayesian networks, respectively with and without posterior knowledge. For the Bayesian network with hindsight, the {5-2} structure was found as the most appropriate arrangement. The model predicted cobalt yield value and the experimental value indicated a correlation coefficients (R²) of 0.861.



Investigation of the processes occurring in water of acid mine drainage during their exposure

S. Hayrapetyan¹, M.Chobanyan¹, V. Hovhannisyan¹, A. Kirakosyan², A. Sukiasyan² and P. Gikas³

¹ Faculty of Chemistry of Yerevan State University, Yerevan, Armenia

²Chair General chemistry and chemical technology, National Polytechnic University of Armenia, Yerevan, Armenia

³Technical University of Crete, School of Chemical and Environmental Engineering, Chania, Greece

Corresponding author email: sukiasyan.astghik@gmail.com

keywords: acid mine drainage; metals; total suspended solid; pH.

Introduction

The most actual environmental problem currently faced by the coal and metal mining industry is acid mine drainage (AMD). The formation of drainage with low pH increases the dissolution of heavy metals in the AMD waters (AMDW). Adsorbent filtration is widely used as an effective treatment strategy for removing organic and inorganic pollutants from storm water. The mining industry is a major producer of AMD systems, and both active and abandoned mines are affected. Of all the pollutants in drains, AMD is perhaps one of the most serious because of its nature, scale, and difficulty of remediation. Therefore, the treatment of AMDW samples is primarily needed to avoid large-scale environmental contamination of surface waters. The aim of this work is to study a number of physicochemical properties of AMDW, which will serve as a basis for the development of new competitive approaches to their purification.

Materials and methods

Drainage water of ten days' exposure in the laboratory was studied. During this period, a certain amount of ions precipitated in the water. Total suspended particles (TSS) was estimated in situ, using turbid metric measurements and calculated by formula: $\ln(TSS) = 0.979 \ln(\text{Turb.}) + 0.574$. Portable Turbid meter HI 98713 ISO (HANNA Instruments, USA) was used to determine turbidity or the suspended particles in the supernatant using FTU as a unit of measurement. It was calibrated with 0.10, 10, 100, 1000 and 10000 FTU standard solutions. Batch experiments were carried out by sampling and measuring pH. The pH was then adjusted (with 1 M H₂SO₄, when necessary) in order to study the following pH range: 1.0; 1.5; 2.0; 2.5; 3.0; 4.0; and 5.0. Each solution was equilibrated by agitation for 2 h at room temperature (23±1°C). All chemicals were analytical grade reagents and were supplied by Panreac Química SLU. Distilled water was used to correct the sample volumes. Triplicate experiments were performed in order to increase the accuracy of the results. Thus, data are reported as the mean ± standard deviation of triplicate determinations.

Results and discussion

The content of a number of chemical elements (Al, Ca, Cd, Cu, Fe, Mg, Mn, Na, Pb, S, and Zn) in AMDW samples after its 10-day exposition at room temperature in an open container was determined. The main component of the precipitated sediment is iron – 64.01 wt. %, (61.53 mg, which is 49.07 wt % of the total iron concentration in AMDW). The calcium content in the sediment is 8.05 wt % (7.59 g, which is 2.44 wt % of the total calcium content in AMDW), the mechanism of precipitation which is probably connected with the formation of its insoluble sulfates. It is assumed that the precipitation of other metals and sulfate ions occurs as a result of the adsorption of iron hydroxide due to the significant active surface. It was of particular interest the process of transition of sodium ions to the precipitate since they do not form insoluble compounds. The only possible explanation for this process can be adsorption. For sulfur, there is 17.35 wt % (16.67 g, which is 1.24 wt % of the total sulfur content in AMDW). In this case, our calculations show that the amount of precipitated sulfur in the form of gypsum is only 34.99 wt % of the total mass of sulfur contained in the precipitate. The removal of sulfur in the form of sulfate ions is associated not only with the formation of gypsum since only 19.32 mg/l is precipitated in the form of gypsum, but in the case when 17.69 mg of sulfur (which corresponds to 53.07 mg of sulfate ion), i.e. 53.07-19.32 = 33.75 mg sulfate



ions do not have a gypsum character. The gypsum nature of sulfate ions is only 1/3 of the precipitated sulfate ions (34.99 wt.%). The remaining 65.01 wt.% part of sulfate ions is apparently deposited adsorbed on the surface of iron hydroxide. From the main physical and chemical indicators of AMDW, we have chosen determination its turbidity and pH. The samples of water taken directly from the source had a turbidity of 5 ± 0.4 FTU and a pH of 3.48. Being in an open vessel, water underwent certain qualitative changes. By 30 hours of standing water, the formation of a precipitate with a predominance of $\text{Fe}(\text{OH})_3$ was visually observed as a result of the oxidation of ferrous iron to ferric. The values both of turbidity and TSS of AMDW increase during its exposure. With an increase in the time of water exposure up to 10 days, simultaneously with a decrease in pH, the values of turbidity and TSS increase, which we tend to associate with the formation of $\text{Fe}(\text{OH})_3$. It should also be noted that, in addition to iron hydroxide, 18.22 mg of gypsum (CaSO_4) is also formed in the precipitate, which is comparable to the calcium content. Actually, the turbidity of the water is due to iron hydroxide with adsorbed metals and gypsum. It turned out that with decreasing pH, turbidity increases almost linearly (figure). This shows that the formation of $\text{Fe}(\text{OH})_3$ during the decrease in pH (according to $\text{Fe}^{3+} + 3\text{H}_2\text{O} \rightarrow \text{Fe}(\text{OH})_3 + 3\text{H}^+$) is directly proportional to the number of hydrogen ions formed. With the termination of the process of lowering the pH, the formation of $\text{Fe}(\text{OH})_3$ also stops, and an equilibrium state is established at a certain pH value.

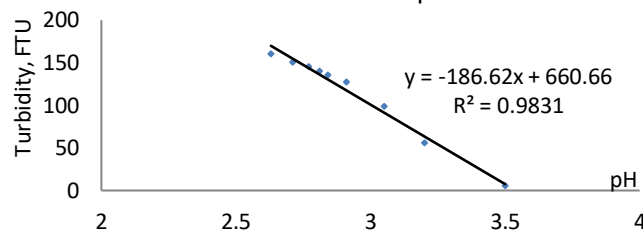


Figure. Functional dependence of turbidity of acid mine drainage water samples on pH value.

Conclusions

The processes that occur in AMDW samples during their long exposure under normal conditions lead to changes in such characteristics as pH, TSS, turbidity, and metal content. It has been reliably established that as the pH decreases, the turbidity of the source water increases, which has a linear character. The main, but not the only, component of the precipitate is $\text{Fe}(\text{OH})_3$, while its share in terms of Fe^{3+} is 64.01 wt %. Calcium precipitates in the form of insoluble sulfates, and in the case of other metals, precipitation occurs with iron hydroxide in adsorbed form. In the case of transition of sodium and magnesium to the precipitate, they are precipitated with iron hydroxide in adsorbed form. The gypsum nature of sulfate ions in the sediment is about 1/3 of the total sulfur content in the sediment. The rest of the sulfate ions are precipitated with iron hydroxide in adsorbed form.

Acknowledgements: This study is supported by the by the Science Committee of RA, in the frames of the research project № 21T-2H216.

References

- Sounthararajah, D., Loganathan, P., Kandasamy, J., Vigneswaran, S., 2015. Effects of Humic Acid and Suspended Solids on the Removal of Heavy Metals from Water by Adsorption onto Granular Activated Carbon. *Int. J. Environ. Res. Public Health*. 12, 10475–10489. doi:10.3390/ijerph120910475.
- Glover-Kerkvilet, J., 1995. Environmental assault on immunity. *Environ. Health Persp.*, 103, 236–237.
- Roesner, L., Charles, R., 1996. National storm water quality regulations and standards. *J. Hydraul. Res.* 34, 841–856.
- Strosnider, W., Llanos, F., Marcillo, C., Callapa, R., Nairn, R., 2014. Impact on tributaries of the Pilcomayo River by additional pollutants from mine acid drainage from Cerro Rico de Potosí-Bolivia. *Adv. Sci. Eng.* 5, 1–17.
- Johnson, D., Hallberg, K., 2005. Acid mine drainage remediation options: a review. *Science of the Total Environment*, 338 3– 14.
- Alyaseri, I., Morgan, S., Retzlaff, B., 2007. Using Turbidity to Determine Total Suspended Solids in Storm-Water Runoff from Green Roofs. *J. Environmental Engineering*. 139(6), 822–828. doi:10.1061/(ASCE)EE.1943-7870.0000685.



SUST
ENG
2022



MODELLING



A Classification Model for Estimating Hurricane Flood Damage in Satellite Images

M. Gavrilescu¹ and D. Gavrilescu²

¹Faculty of Automatic Control and Computer Engineering, “Gheorghe Asachi” Technical University of Iasi, Romania

²“Cristofor Simionescu” Faculty of Chemical Engineering and Environmental Protection, “Gheorghe Asachi” Technical University of Iasi, Romania

Corresponding author email: marius.gavrilescu@academic.tuiasi.ro

keywords: hurricane damage; convolutional neural network; damage assessment

Introduction

The significant changes in global climate from recent decades have caused several regions of the world to experience systematic abnormal meteorological phenomena, of which the most destructive are hurricanes. These pose a significant health and safety risk for the population and cause significant property damage. In regions affected by hurricane damage, it is imperative that damage assessment and rescue teams intervene as fast as possible in order to minimize casualties and reduce the impact caused by hurricane destruction. However, in most such situations the damage is widespread, making it necessary to prioritize areas where there is higher risk to human safety or greater damage to the respective property. This is especially true for flooding damage, which tends to cover extensive areas and cause the most severe long-term negative effects. Commonly, damage and risk assessment are carried out either on foot, which is the most reliable but by far the slowest approach, or by manually inspecting satellite imagery, which is tedious and inaccurate. These limitations significantly impact the reaction times of rescue / damage control personnel, and as such greatly increases the risk of extensive damage or loss of human life. Consequently, our contribution is a classification model that automatically assesses whether a region is affected by flooding damage caused by hurricanes and allows for the rapid inspection of large regions for areas which pose greater risk and require more rapid intervention.



Figure 1. Examples of images from the training dataset: (top row) images labels as being affected by flooding damage; (bottom row) images labels as not having flooding damage.

Classification model

Our model is based on a convolutional neural network trained with satellite images containing small regions labeled as being affected and unaffected by flooding damage (Figure 1). The images are taken from a region of Texas which was stuck by hurricane Harvey, causing partial flooding of affected neighborhoods. The dataset consists in 10000 training images, 2000 validation images and 2000 test images, each split equally between the two classes (damages / undamaged). In order to determine the best neural network architecture, we perform a hyperparameter search focusing on finding the optimal kernel counts and sizes



for four sequential convolutional layers, intermixed with maxpooling layers. We performed a grid search combined with 5-fold validation in order to determine the optimal layer configuration, which is shown in Table 1.

Table 1. Architecture of the optimal model.

Layer type	Number of channels, kernel size
Input	3, -
Conv1	32, 11x11
MaxPool + ReLU	-
Conv2	64, 7x7
MaxPool + ReLU	-
Conv3	96, 7x7
MaxPool + ReLU	-
Conv4	128, 3x3
AdaptiveMaxPool	16, -
FullyConnected	136
Output	1, -

Results

Using the aforementioned model we achieved a maximum accuracy of 99.3% on the test images. Training, validation and testing took approx. 5 hours on a GTX 2070 Super GPU. Subsequently, we use the trained model on a larger satellite image covering a wider area in order to predict subregions which exhibit significant damage and thus pose significant risk. An example is shown in Figure 2, which shows the results of running the classification model on each 128x128 subregion and estimating the level of damage as the sigmoid-transformed values of the output logits of the neural network. The resulting probabilities are normalized and color mapped using a logarithmic scale. Figure 2(a) shows the original, unaltered image, while Figure 2(b) shows the predicted damaged areas using a red-scale colormap overlay. Consequently, the redder regions are estimated to show more significant damage and thus are good candidates for urgent intervention.



Figure 2. Predictions of our model of a large satellite image: (a) original image; (b) the image with a red overlay showing areas exhibiting increased damage

References

- Cao, Q. D. and Choe, Y. 2020. Building damage annotation on post-hurricane satellite imagery based on convolutional neural networks. *Nat. Haz.* 103, 3357-3376.
- Guo, W., Yang, W., Zhang, H., Hua, G. 2018. Geospatial Object Detection in High Resolution Satellite Images Based on Multi-Scale Convolutional Neural Network, *Remote Sens.*, 10, 131.
- Mateusz de Souza, M., de Santiago, V.A., Körting, T.S., Leonardi, R., de Freitas, M.L. 2021. Deep Convolutional Neural Network for Classifying Satellite Images with Heterogeneous Spatial Resolutions, *Computational Science and Its Applications – ICCSA 2021*, 12955, 519-530.



Development of computational tools for criticality analysis of process systems, utilizing Industrial IoTs

T. Theodosiadis-Thomaidis¹, G. Panagopoulou² and S. Pistikopoulos³

¹Future Technology Systems sa A' Industrial Area, Volos, Greece

²Pangaea.sa, Volos, Greece

³Chemical Engineering, Director, Texas A&M Energy Institute, Texas,

Corresponding author email: theo.thom.tom@gmail.com

keywords: Computational algorithm; Effective Risk Assessment; Fault Trees, FMEA; Directed Functional AND/OR Logic Digraphs; NASA's Fault-Tree Diagnosis System FTDS; Flexibility; Reliability; Criticality; Process Systems; Predictive Maintenance; Industrial-IoTs.

Introduction

Traditional sensitivity analysis based on reliability models, such as logic-tree or fault-tree analysis, together with existing FMECA techniques, are powerful and well established methods for the identification of critical parts of equipment / events affecting the system functionality and safety. However, they share a common limitation since they do not explicitly take into account process models and process interactions; this may overestimate the real system efficiency and provide misleading information regarding rating critical components or events. This paper presents, in a uniform framework, computational tools and algorithms for criticality analysis of process systems, which embodies: system logic via DFLD/ Fault-Tree Diagnosis System FTDS, explicit process and safety models, equipment reliability data and occurrence probabilities of external events/utilizing sets of data collected via Industrial IoTs. The criticality analysis framework is used as a guide for improvements towards safer and more efficient systems design and/or condition-based maintenance activities whereas the proposed computational toolset is based considering process and equipment interactions, equipment failure, stochastic process variations and external events related to process operations and safety. Important extensions are also presented for the use of such criticality analysis tools for safety and maintenance considerations. A module for rating all the equipment, operations and events according to the associated criticality index is utilized, coupled with a condition based maintenance framework for enhancing overall system efficiency and safety. The computational tools and the algorithms are demonstrated via case studies. The developed software and methodology coupled with valuable sets of information from dedicated Industrial-IoTs is applied in order to rank the criticality of the parts/subsystems/systems/events and then to propose a maintenance/safety policy which fulfills certain efficiency and safety targets.

Criticality Analysis of Process Systems

The objective of the criticality analysis module is to identify the relative importance of equipment (un)availability (or other external events affecting the process operations) over a time horizon by taking into account process interactions, reliability models, parameter variations and operational characteristics of a process system. Criticality analysis comprises: size reduction of the system state space, translation of process flow-sheet into DFLD(automatic generation of fault-trees/n-order cut sets); Estimation of state probabilities as a function of time and system's efficiency; Estimation of a system criticality index as a function of time; Estimation of a combined flexibility-reliability-criticality index for each part of equipment or event; Criticality based maintenance.

Follows the description of the fundamental computational modules:

MODULE GRAPHS: - SYSTEM AGGREGATION, DFLDs and FAULT-TREE GENERATION

An aggregation utility is employed in order to cope with complex large-scale systems reducing the size of the corresponding state space while guaranteeing the upper and lower bounds of system performance indexes. Here, Directed Functional Logic AND/OR Digraph representations are employed that can automatically be transformed into fault-trees/ minimal cut set, bounding easily reliability and criticality indexes for complex system.



MODULE CRI: CRITICALITY RATING OF PROCESS SYSTEMS

In this module the quantitative metrics of *combined flexibility-reliability index FR* and *combined flexibility-reliability criticality index, FRC* are estimated for measuring the expected level of critical operation of process systems taking into account interactions between process undesired critical operations (as a result of systems malfunctioning, equipment degradation or even the occurrence of certain events based on IIoT information sets) while a *relative criticality index CRI* is ranking all equipment or events according to their relative importance (sensitivity) for system's operations. The results from such a relative ranking can guideline preventive maintenance planning and scheduling.

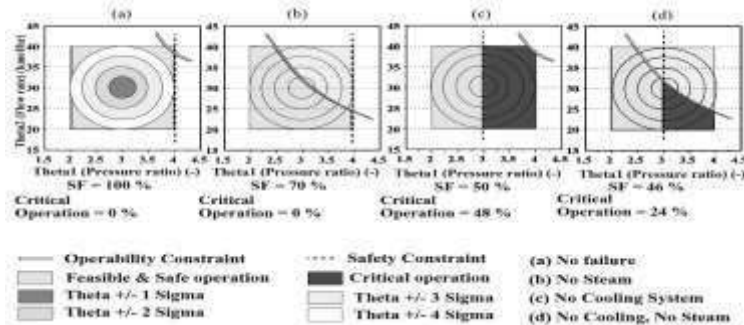


Figure 1. Feasible Region of operation and Regions of Critical Operation.

MODULE MAINTENANCE: CONDITION-BASED and PREVENTIVE MAINTENANCE

In this module, we developed algorithms and tools for the planning and execution of preventive and condition-based maintenance. The algorithms rely on the criticality analysis as it is performed by module CRI; additionally, it requires quantitative information regarding maintenance resources and logistics (number of service crews, man hours/job, personnel availability, job durations etc) and maintenance tasks (equipment maintenance specifications, list of scheduled preventive maintenance activities).

Results and discussion

While the criticality analysis computational tools developed in this work predict variable information regarding the overall system expected critical operations, the relative importance of the equipment to the process and identification of process and/or reliability bottlenecks, utilizing Industrial Internet of Things (IIoT) as they have been developed NITLAB and tested on the real field by Pangaea R&D interfacing/monitoring external events, advocating labor and material-saving as well as safety advantages for processes and operators in the field. However, as it is shown via case studies, the proposed methodology could be an efficient tool for the proper balance of preventive and condition based maintenance activities and the prediction of their impact to process operational decisions.

Acknowledgements: This study is supported by FED4Fire/HORIZON2020/Field Research With LoRa (PAWL) and the NITOS/LoRa (Low Power Wide Area Network) testbed of NITLAB (Network Implementation Testbed Laboratory), Department of Electrical and Computer Engineers, University of Thessaly.

References

- Andrews J., 1990 'Applications on the digraph method of fault tree construction to a complex control configuration', *Reliability Eng. And Systems Safety*, vol. 28, pp. 357-384.
- Boyes H. et. al., 2018, *The industrial internet of things (IIoT): An analysis framework*, *Computers in Industry*, Volume 101, Pages 1-12
- Iverson D.L., 1992, 'Automatic Translation of Digraph to Fault-Tree Models', *Proceeding Annual Reliability and Maintainability Symposium*, pp.354-362.
- Paulsen C. et. al., 2018, "Criticality Analysis Process Model Prioritizing Systems and Components, NISTIR 8179 Sisinni E. and Jennehag U, 2018, *Industrial Internet of Things: Challenges, Opportunities and Directions*, *IEEE TRANSACTIONS ON INDUSTRIAL INFORMATICS*, VOL. 14, NO. 11
- Straub D. A. and Grossmann I. E., 1993, 'Design optimization of stochastic flexibility', *Comp. Chem. Engng.* 17(4), pp. 339-354.
- Thomaidis T.V. and Pistikopoulos E.N., 1995, 'Optimal Design of Flexible and Reliable Process Systems', *IEEE Trans. on Reliability*, 44(2), pp. 243-250.



Modeling metal bioprecipitation in a packed-bed denitrifying bioreactor

A. Hatzikioseyan¹, P. Mendrinou¹, E. Datsika¹ and E. Remoundaki¹

¹School of Mining and Metallurgical Engineering, National Technical University of Athens (NTUA),
Heron Polytechniou 9, 157 80, Zografou, Greece

Corresponding author email: artin@metal.ntua.gr

keywords: denitrification; metal bioprecipitation; model; AQUASIM.

Introduction

The hydrometallurgical processing of the end of life (EoL) printed circuit boards (PCBs), utilizes mineral acids such as HNO₃ or mixtures of HNO₃ and HCl acids (aqua regia) for the dissolution of base (e.g., Cu, Zn, Ni, Pb, Sn) and precious metals (e.g., Au, Ag). Target metals are recovered from these metal-laden acidic streams by various methods among which the selective extraction with organic solvents and electrowinning (e.g., Cu) or reductive precipitation (e.g., Au, Ag).

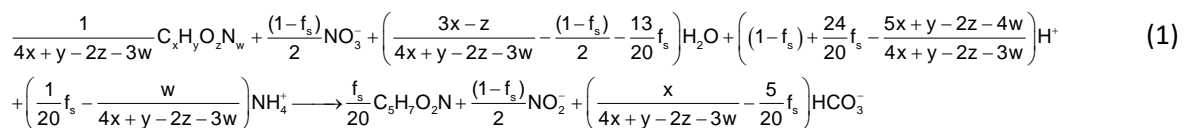
The wastewater should be treated to remove nitrate and metals, often in presence of chloride. Conventional wastewater treatment includes neutralization for metals precipitation and other techniques (e.g., reverse osmosis, ion exchange) for nitrate and chloride removal. In previous research, we have shown that the nitrate content of these solutions is amenable for biological denitrification in presence of dissolved metal species at ppm level which could potentially be considered toxic to the microorganisms (Mendrinou et. al. 2021). In this work we develop a model to study the biotic and abiotic processes taking place in the bioreactor in order to determine the kinetics of biological denitrification and elucidate the mechanisms regulating metal bioprecipitation in a packed-bed bioreactor.

Materials and methods

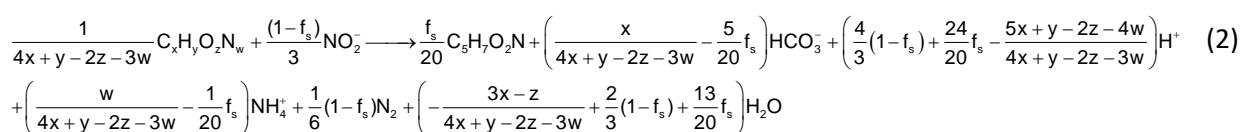
A heterotrophic denitrification model in presence of metal ions was created in AQUASIM (Reichert, 1994). AQUASIM (<https://www.eawag.ch/en/department/siam/software/>) is a freely available versatile software which can simulate biological (biotic) and chemical (abiotic) processes in mixed and biofilm reactor compartments.

In our model, the simulation of the microbiological activity is based on the principles of bioenergetics as presented by Rittmann and McCarty (Rittmann and McCarty, 2020). The methodology is based on the combination of three semi-reactions namely: (a) the electron donor reaction (R_d); (b) the electron acceptor reaction (R_a); and (c) the cell synthesis reaction (R_c). Electrons released from the oxidation of the organic substrate (electron donor) are captured by the electron acceptors (i.e. NO₃⁻, NO₂⁻) and the biomass synthesis reaction. The overall biological action can be written by combining these three semi-reactions. The biotic part of the model consists of the two most important biological actions:

(a) the reduction of nitrate (NO₃⁻) to nitrite (NO₂⁻) as shown in equation 1:



(b) the reduction of nitrite (NO₂⁻) to elemental nitrogen (N₂) as shown in equation 2:



where C_xH_yO_zN_w is a generalized formula for the organic substrate which serves as carbon source and electron donor, C₅H₇O₂N is a "typical" formula used for the biomass in wastewater applications and f_s is the fraction



of electrons captured for biomass synthesis. The values of f_s depend on the nature of the organic substrate and indicative values for heterotrophic denitrification ranges between 0.50-0.65 (Rittmann and McCarty, 2020).

The kinetic terms of the model consist of mixed Monod type equations involving the limiting substances i.e. carbon source, and electron acceptors NO_3^- , NO_2^- as:

$$\frac{dX}{dt} = \mu_{\max, \text{NO}_3} \cdot \frac{C_{\text{org}}}{K_{\text{sorg}} + C_{\text{org}}} \cdot \frac{C_{\text{NO}_3}}{K_{\text{NO}_3} + C_{\text{NO}_3}} \cdot X \quad (3)$$

$$\frac{dX}{dt} = \mu_{\max, \text{NO}_2} \cdot \frac{C_{\text{org}}}{K_{\text{sorg}} + C_{\text{org}}} \cdot \frac{C_{\text{NO}_2}}{K_{\text{NO}_2} + C_{\text{NO}_2}} \cdot X \quad (4)$$

where μ_{\max, NO_3} and μ_{\max, NO_2} are the maximum specific growth rates for the reactions (1) and (2) respectively, C_{org} , C_{NO_3} and C_{NO_2} are the concentrations of the organic substrate, the nitrate and the nitrite respectively, K_{sorg} , K_{NO_3} and K_{NO_2} are the half saturation constant of the organic substrate, the nitrate and the nitrite respectively, and X is the biomass concentration.

Reactions (1) and (2) quantitatively determine the changes in the concentration of the chemical species $\text{NH}_4^+_{(\text{aq})}$, $\text{HCO}_3^-_{(\text{aq})}$ and $\text{H}^+_{(\text{aq})}$ in the environment of the cells as the denitrification progresses. Acid-base equilibria between these species are included in the model namely the hydrolysis of $\text{NH}_4^+_{(\text{aq})}$, $\text{HCO}_3^-_{(\text{aq})}$ and the dissociation of water in order to simulate the increase of the pH in the treated wastewater. In the presence of metal ions such as Fe^{2+} , Cu^{2+} , Ni^{2+} and Zn^{2+} the model predicts the precipitation of the metals in the form of $\text{Me}(\text{OH})_{2(\text{s})}$ and/or $\text{MeCO}_{3(\text{s})}$ depending on their corresponding solubility product constants and the abundance of OH^- and HCO_3^- as the pH and the alkalinity of the wastewater increases.

Results and discussion

The model parameters have been calibrated with different sets of experimental data obtained from pilot scale studies in a batch reactor (Mendrinou et. al. 2021). The model adequately simulates the concentration profiles of nitrate/nitrite reduction and carbon source consumption. In addition, it can predict the fate of the metal ions in the reactor environment.

Conclusions

In this work we attempt to quantify and elucidate the mechanisms of metal bioprecipitation during biological denitrification for an acidic industrial wastewater containing nitrate and elevated concentrations of metal ions. The model provides the necessary infrastructure to study in combination biotic and abiotic processes.

Acknowledgements: The experimental part of this study has been co-financed by the European Regional Development Fund of the European Union and Greek national funds through the Operational Program Competitiveness, Entrepreneurship and Innovation, under the call RESEARCH – CREATE – INNOVATE (project code: T1EDK-00219).

References

- Mendrinou, P., Hatzikioseyan, A., Kousi, P., Oustadakis, P., Tsakiridis, P. & Remoundaki, E. 2021. Simultaneous Removal of Soluble Metal Species and Nitrate from Acidic and Saline Industrial Wastewater in a Pilot-Scale Biofilm Reactor. *Environ. Process.* 8, 1481–1499. <https://doi.org/10.1007/s40710-021-00536-w>.
- Reichert, P., 1994. AQUASIM - A tool for simulation and data analysis of aquatic systems, *Water Sci. Tech.*, 30(2), 21-30.
- Rittmann, B. E., & McCarty, P. L. 2020. Environmental biotechnology: principles and applications. McGraw-Hill Education, 2nd Edition.



Reactive Transport Model on Biogeochemical Dynamics of Colloid Associated Heavy Metal Transport

S.S. Şengör¹ and K. Ünlü¹

¹Department of Environmental Engineering, Middle East Technical University, Ankara, Turkey

Corresponding author email: ssengor@metu.edu.tr

keywords: heavy metals; colloids; reactive transport; modeling; subsurface sediments.

Introduction

Colloid particles are widely distributed in the environment and they have recently been gaining significant attention due to their unique characteristics in environmental remediation pertaining to degradation, transformation and immobilization of contaminants in soils and aquifers. On the other hand, once mobilized by runoff and/or subsurface water flow, colloids may pose risks to surface water and groundwater quality as they are effective “carriers” of a variety of common contaminants found in water and soils. Fe (hydr)oxide colloidal compounds are naturally occurring and have large surface areas and high reactivity, which can lead to spontaneous adsorption of various contaminants. Understanding the transport mechanisms of colloids and incorporation of colloidal transport processes in reactive transport models are crucial for successful applications of many remediation efforts in the subsurface.

Materials and methods

The impact of colloid-facilitated transport of Fe(hydr)oxide minerals on the mobility of heavy metals (Pb and Zn) undergoing natural biogeochemical processes is presented using Lake Coeur d’Alene (LCdA) sediments as an example site for demonstration.

Numerical simulations are carried out with the reactive transport code PHREEQC. The considered transport processes include advective transport with multispecies diffusion, colloidal Fe(hydr)oxide phase transport with electrical double layer treatment of Fe(hydr)oxide surfaces. Advective velocity ranges representative of low flow subsurface systems are calculated corresponding to Pe number ranges between 0.02 – 0.0006. The input parameters of inorganic and microbially-mediated reaction network is based on previous works for the LCdA system including microbially mediated iron and sulfate reduction in suboxic and anoxic zones in the benthic sediment system (Li and Sengor 2020).

Results and discussion

The results of the study reveal that when the potential transport of sorbed contaminants with colloidal particles are ignored, the contaminant concentrations in aqueous environments might be underestimated especially under low flow velocity conditions (around 10^{-8} or 10^{-9} m/s). Microbially mediated reductive dissolution of Fe(hydr)oxide phases is observed to result in enhanced control of iron reduction in the case of immobile Fe(hydr)oxide mineral surfaces; whereas abiotic reductive dissolution of Fe(hydr)oxide phases are shown to result in enhanced impact of sulfate reduction in the anoxic zone.

Conclusions

The sensitivity of the colloidal transport of heavy metals under low flow velocity conditions illustrate the significance of colloidal transport processes to be considered in reactive transport models for successful (bio)remediation applications in the subsurface, as well as contaminant transport in low velocity systems.

Acknowledgements: This study is supported by the 2236 Co-Funded Brain Circulation Scheme2 (CoCirculation2) of TÜBİTAK (Project No:120C053).

References

Li, J. and Şengör, S.S., 2020. Biogeochemical cycling of heavy metals in lake sediments: Impact of multispecies diffusion and electrostatic effects. *Computational Geosciences*, 24(4), pp.1463-1482.



The use of sensitivity analysis in ANN to determine the significance of the parameters of the anaerobic digestion process

P. Pochwatka¹, A. Kowalczyk-Juśko¹, A. Mazur¹, M. Nowak² and J. Dach²

¹Department of Environmental Engineering and Geodesy, University of Life Sciences in Lublin, Lublin, Poland

²Department of Biosystems Engineering, Poznań University of Life Sciences, Poznań, Poland
Corresponding author email: patrycja.pochwatka@up.lublin.pl

keywords: neural modeling; biogas plant; artificial neural networks; methane efficiency.

Introduction

Poland currently has just over 130 agricultural biogas plants (KOWR 2022). However, the biogas potential of the Polish agri-food sector is assessed by specialists from the Poznań University of Life Sciences (PULS) at over 3.5 GW of electricity or 8 billion m³ of biomethane per year (excluding additional energy crops). Since Russia cut off natural gas exports in April 2022 – Poland must quickly develop new ways to gain energy independence from Russia. One of those ways is an investment in the biogas sector. Therefore, one should expect a swift development of the number of biogas installations in the next decade.

Meanwhile, however, the existing biogas plants are operating at a far from optimal level. Anaerobic digestion is a very complex biochemical process consisting of 4 main phases (hydrolysis, acidogenesis, acetogenesis, and methanogenesis) carried out by consortia of bacteria and archaea composed of millions of strains, most of them still unidentified. Due to a vast number of physical and chemical parameters and a huge number of interactions between these factors and microorganisms – the entirety of processes taking place in biogas fermenters are called "black box" by specialists (Dach et al. 2016). Many scientific teams around the world conduct research on the determination of these relationships and try to resolve the impact of individual parameters on the biogas (especially methane) production process (Nikpey et al. 2014; Flores-Asis et al. 2018). Most often, however, these are preliminary studies without covering the entire fermentation process.

As a result of quite limited knowledge, the operation of biogas plants is at a relatively low level of energy efficiency. Assuming that 1 MW of installed electric power can theoretically produce 8,760 MWh per year (it is a theoretical value, impossible to obtain), then the average electricity production in Poland, according to the data of the Ministry of Energy (2019), was only 5250 MWh / MW installed. This means that the electrical efficiency of biogas plants in Poland was less than 60%, slightly higher than the efficiency of offshore windmills (somewhat over 50%). In the case of Germany, which has the largest biogas market in Europe (over 9,000 installations), the average electricity production efficiency is 6,300 MWh / MW installed annually, which gives the installation an electrical efficiency of 71.9%. This value is still much lower than expected because there are modern installations in Poland under the PULS technological care, the production of which reaches 8,500 MWh / MW, installed, which exceeds 95% of electrical efficiency. One of the reasons for the very high efficiency is the detailed analysis of the process taking place in the fermenters of biogas plants, using as much data as possible. Artificial Neural Networks (ANN) are particularly suitable for this type of analysis of nonlinear phenomena (and such are the anaerobic digestion processes). They enable the modeling of biogas production processes and, thanks to the sensitivity analysis, the assessment of the significance of the influence of the tested parameters on the biogas and biomethane production process (Kowalczyk-Juśko et al. 2020). The study aimed to analyze the possibility of determining the significance of the impact of physical and chemical parameters on the efficiency of biogas/biomethane production based on the already conducted studies described in the literature and to propose a solution for the use of sensitivity analysis (with the use of ANN) to optimize the operation of agricultural biogas plants.

Materials and methods

In order to achieve the aim of the work, a knowledge base of the results of publications related to the research on the fermentation process with the use of neural networks was built, especially those works



where the sensitivity analysis of process parameters was carried out. Then, the parameters taken into account in the research were analyzed, and the ranking of their significance in the context of biogas/biomethane production was determined.

Results and discussion

The analysis of the research carried out so far has shown that numerous physical and chemical parameters of both the substrates used and the anaerobic digestion process itself were taken into account in the neural modeling and the sensitivity analysis. These parameters include: the content of dry matter, organic dry matter, total and mineral nitrogen, carbon, pH level, conductivity, as well as temperature (including the type of process: meso or thermophilic fermentation), OLR (Organic Loading Rate), fermentation time, and FOS / TAG.

Conclusions

Based on the conducted analysis, it was found that the research conducted so far does not allow for an unambiguous determination of which of the analyzed parameters are the most important for the effectiveness of the anaerobic digestion process. This is due to the too narrow scope of the research conducted so far. However, it should be emphasized that most of the works stress the role of dry matter level, organic matter content, and decomposition time as the most important production parameters.

Acknowledgements: This study was created in the framework of the Young Scientists project “Application of artificial intelligence techniques in modeling the biogas production process” TKD/MN-2/IŚGiE/21 realized at University of Life Sciences in Lublin, Poland. The work was created in the framework of the National Center for Research and Development project "Mitigating emissions from livestock systems", Acronym: MELS; FACCE ERA-GAS, SusAn and ICT-AGRI2.

References

- Dach, J., Koszela, K., Boniecki, P., Zaborowicz, M., Lewicki, A., Czekąła, W., Skwarcz, J., Qiao, W., Piekarska-Boniecka, H., Biało-brzewski, I., 2016. The use of neural modelling to estimate the methane production from slurry fermentation processes. *Renew. Sustain. Energy Rev.*, 56, 603–610.
- Flores-Asis, R., Méndez-Contreras, J.M., Juárez-Martínez, U., Alvarado-Lassman, A., Villanueva-Vásquez, D., Aguilar-Lasserre, A.A., 2018. Use of artificial neuronal networks for prediction of the control parameters in the process of anaerobic digestion with thermal pretreatment. *J. Environ. Sci. Heal. - Part A Toxic/Hazardous Subst. Environ. Eng.*, 53, 883–890.
- Kowalczyk-Juśko, A., Pochwatka, P., Zaborowicz, M., Czekąła, W., Mazurkiewicz, J., Mazur, A., Janczak, D., Marczuk, A., Dach, J., 2020. Energy value estimation of silages for substrate in biogas plants using an artificial neural network. *Energy*, 202, 117729.
- KOWR, 2022. Register of agricultural biogas producers (in Polish), Available online: <https://www.kowr.gov.pl/odnawialne-zrodla-energii/biogaz-rolniczy/wytworcy-biogazu-rolniczego/rejestr-wytworcow-biogazu-rolniczego>.
- Ministry of Energy, 2019. The scenario of the energy and climate policy (PEK). Assessment of the effects of planned policies and measures. Annex 2 (in Polish). Available online: <https://www.gov.pl/attachment/a8db078d-535b-4b1b-bfe5-bda64df73778>.
- Nikpey, H., Assadi, M., Breuhaus, P., Mørkved, P.T., 2014. Experimental evaluation and ANN modeling of a recuperative micro gas turbine burning mixtures of natural gas and biogas. *Appl. Energy*, 117, 30–41.



An integrated PSO – DMC framework for the identification and control of wastewater treatment plants

I. Kalogeropoulos^{1,2}, T. Protoulis³, I. Kordatos³, A. Kapnopoulos³, P.L. Zervas⁴, H. Sarimveis¹ and A. Alexandridis³

¹School of Chemical Engineering, National Technical University of Athens, Zografou, Greece²Systemica - G.Vangelatos & Co L.P., Dafni, Athens, Greece

³Department of Electrical and Electronic Engineering, University of West Attica, Aigaleo, Greece

⁴Entrade SA, Athens, Greece

Corresponding author email: alex@uniwa.gr

keywords: *Dynamic matrix control; PSO; system identification; wastewater treatment plants.*

Introduction

Wastewater treatment plants (WWTPs) can be considered as important components in the design and implementation of a circular economy model, because they allow the maximum amount of water to be reused. Automatic control of WWTPs is a challenging problem due to the complexity of the multiple biological processes which are involved (Shen et al., 2009), the high energy consumption of the plant and the increasingly strict environmental regulations. In this work, we propose a combined system identification and control scheme for WWTPs; the system is suitable for real world applications, as it is based on a data driven approach to construct a dynamic model of the system, which is then integrated in the process of developing and validating the controller. More specifically, system identification is performed by applying the particle swarm optimization (PSO) method (Alexandridis et al., 2017) on plant dynamic data, in order to estimate the parameters in the COST/IWA Benchmark Simulation Model No. 1 (BSM1) and produce dynamic step test models, which are subsequently employed as predictive models in a dynamic matrix control (DMC) setting.

Materials and methods

BSM1 is a generic dynamic model of WWTPs, which includes default fixed values for all the kinetic parameters involved in the mass balance equations. These parameters can be affected and altered by the conditions where a specific WWTP operates and therefore it is of particular importance to estimate their values in a real WWTP operational environment. In this work, the task of parameter identification is accomplished by formulating a nonlinear optimization problem where the objective function to be minimized is the mean squared error (MSE) between the BSM1 model responses and the actual dynamic plant data at discrete time instances. We solve this nontrivial optimization problem using the PSO algorithm (Alexandridis et al., 2017), due to its simple yet efficient structure. PSO is a metaheuristic search method based on a population of potential solutions called particles, which explore the search space, trying to approach the optimal solution.

The plant-specific dynamic model is employed next to derive suitable for DMC step response models between the input and the controlled variables, where input variables include both manipulated variables and measured disturbances. To be more specific, two manipulated variables, namely the oxygen transfer coefficient of the last aerated tank and the internal recirculation flow rate, and two measured disturbances, namely the influent ammonia concentration and the influent flow rate, were used. The control variables of the prediction model are the nitrate and nitrite concentration of the last anoxic tank, the nitrate and nitrite concentration of the last aerated tank and the ammonia concentration of the last aerated tank.

The multi-input multi-output (MIMO) DMC algorithm formulates and solves at each time instant a quadratic optimization problem over a future time horizon, known as the prediction horizon. The objective function to be optimized, contains the deviations of the process outputs (as predicted from the step response models) from the desired set points and the incremental changes on the future values of the manipulated variables. In a receding horizon manner, only the first inputs are actually applied to the plant, and then the quadratic optimization problem is reformulated and solved again in the next time instant.

Results and discussion

The proposed integrated PSO-DMC is applied in a simulation environment, where pseudorandom binary sequences are applied first on the BSM1 model input variables. The output variables are collected at discrete



time instances. These sets of input-output values are the data which are fed to the PSO algorithm for estimating the kinetic parameters of the BSM1 model. The resulting model is compared with the original model in dynamic simulations and the dynamic responses present a very good match. Indicatively, Fig.1 compares the nitrate nitrogen and the ammonia concentration dynamic profiles of the original BSM1 model and the model where the kinetic parameters have been estimated by the PSO algorithm.

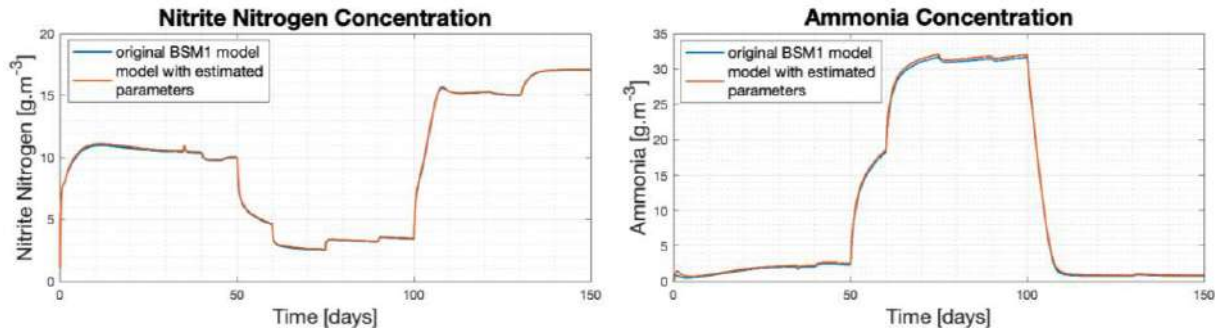


Figure 1. Nitrite Nitrogen and Ammonia Concentration Profiles for original BSM1 model and the model with estimated parameters.

The BSM1 model with the estimated parameters is employed next to derive step response models, and use them in the DMC algorithm. The resulting DMC controller was applied on the original BSM1 model to test its robustness. In particular, a case study employing the dry weather influent profile was used for performance evaluation of the controller. The simulation procedure was performed as suggested by Alex et al. Table 1, provides the simulation results and compares them with the results of the default BSM1 control strategy which uses two PI controllers. The results indicated that using the DMC approach we can achieve an improved effluent quality (EQ) index, due to the lower nitrogen oxide concentration ($SN_{O,eff}$) in the effluent stream, albeit at the cost of slightly increased ammonia concentration ($SN_{H,eff}$). In parallel, the aeration energy consumption (AE) is reduced and the pumping energy (PEQ_a) is increased, but overall, the cost index (CI) is improved compared to the default PI.

Table 1. Performance metrics of the control strategies.

Controller Type	(g N.m ⁻³)	(g N.m ⁻³)	(kWh.d ⁻¹)	(kWh.d ⁻¹)	(kg.d ⁻¹)	(kWh.d ⁻¹)
Default PI	2.54	12.42	854.39	74.23	6123.23	928.62
DMC	2.96	10.57	734.97	171.88	6004.73	886.86

Conclusions

The proposed integrated PSO-DMC framework managed to successfully control the WWTP in terms of improving the effluent quality and reducing the energy costs. Future plans include applying the method in a real WWTP environment.

Acknowledgements: This research has been co-financed by the European Regional Development Fund of the European Union and Greek national funds through the Operational Program Competitiveness, Entrepreneurship and Innovation, under the call RESEARCH – CREATE – INNOVATE (project code: T2EAK-02191).

References

- Alex, J., Benedetti, L., Copp, J. B., et al. (2008). Benchmark simulation model no. 1 (BSM1). *Report by the IWA Taskgroup on benchmarking of control strategies for WWTPs, 1*.
- Alexandridis, A., Paizis, E., Chondrodima, E., & Stogiannos, M. (2017). A particle swarm optimization approach in printed circuit board thermal design. *Integrated Computer-Aided Engineering, 24*(2), 143–155.
- Shen, W., Chen, X., Pons, M. N., & Corriou, J. P. (2009). Model predictive control for wastewater treatment process with feedforward compensation. *Chemical Engineering Journal, 155*(1–2), 161–174.



SUST
ENG
2022



POSTERS



Production of Polyhydroxyalkanoates (PHA) by *Pseudomonas sp.* strain phDV1 using different carbon waste sources

E. Mathioudaki¹, D.E. Geladas¹, A. Drakonaki¹, E. Konsolaki¹, N. Vitsaxakis¹, N. Chaniotakis¹ and G. Tsiotis¹

¹Department of Chemistry, University of Crete, Voutes, Greece
Corresponding author email: chemp1147@edu.chemistry.uoc.gr

keywords: grape pomace; PHAs; *Pseudomonas sp.* Strain phDV1; biodegradation.

Introduction

Grape wine is one of the most popular alcoholic beverages, and its consumption is increasing every year. Wine production produces waste in several steps; the most important of which is the grape pomace, the solid residues after the extraction of the grape juice. Grape pomace from *Vitis vinifera Assyrtiko* is an important sub-product of the Greek wine industry. Grape pomace is a substrate rich in bioactive compounds, such as sugars and polyphenols and its utilization for alternative uses has been a focus of research [1]. Meanwhile, *Pseudomonas* strains have a variety of potential uses in bioremediation and biosynthesis of biodegradable plastics. *Pseudomonas sp. strain phDV1*, a Gram-negative phenol degrading bacterium, has been found to utilize monocyclic aromatic compounds as sole carbon source via the meta-cleavage pathway [2], [3]. The degradation of aromatic compounds comprises an important step in the removal of pollutants [2]. The present study aimed to investigate the ability of the *Pseudomonas sp. strain phDV1* to produce polyhydroxyalkanoates (PHAs) in different carbon sources, specifically in grape pomace and in several concentrations of phenol, and comparing the degradation ratio of phenol in these conditions.

Materials and methods

We investigated the growth of *Pseudomonas sp. strain phDV1*, providing as a carbon source three different concentrations of phenol, 200 mg/L, 400 mg/L and 600 mg/L. In the same concentrations the phenol degradation ratio was determined by measuring the optical density (OD) in 270 nm, and Fluorescence Microscopy was performed in three different time points 24, 48 and 72 hours. In order to characterize the produced biopolymer, homonuclear ¹H-¹H 2D gCOSY NMR experiment was performed by recording in CDCl₃ solution at 500.13 MHz, for the 600 mg/L concentration, with 128 scans on a Bruker Avance III 500 NMR spectrometer. Meanwhile, similar experiments took place using *Vitis Vinifera Assyrtiko* as a carbon source for the cultivation of *Pseudomonas*. Specifically, *Pseudomonas sp. strain phDV1* was cultivated in 1% autoclaved grape pomace extract, while we monitored its growth in different time points. At the same time, its ability to consume polyphenols as a carbon was tested by the Folin–Ciocalteu Assay, while the total sugars concentration was measured as well. In order to detect PHAs production, optical fluorescence microscopy took place using Nile Red (BioReagent) as a dye.

Results and discussion

Using ¹H-¹H 2D gCOSY NMR spectrum we managed to confirm that the produced PHA is the 3-β-hydroxybutyric acid, also known as PHB. In addition, *Pseudomonas* cultivation in grape pomace extracts indicated that the bacterium is able to grow while using polyphenols as a carbon source. At the same time, PHAs production took place in all tested time points, with 48h after cultivation to exhibit the maximum production as optical fluorescence microscopy demonstrate.

Conclusions

Here we were able to conclude that the bacterium *Pseudomonas sp. phDV1* can utilize phenol and polyphenols as a sole carbon sources and produce PHAs. This finding suggest that *Pseudomonas sp. phDV1* is very efficient in its ability to biodegrade waste carbon sources such as phenol and wine industry wastes, making this bacteria a very promising candidate for bioremediation processes.



References

- Dwyer, K.; Hosseinian, F.; Rod, M.R. The market potential of grape waste alternatives. *J. Food Res.* 2014
- Kanavaki I, Drakonaki A, Geladas ED, Spyros A, Xie H, Tsiotis G. Polyhydroxyalkanoate (PHA) Production in *Pseudomonas* sp. phDV1 Strain Grown on Phenol as Carbon Sources. *Microorganisms.* 2021
- Lyratzakis A, Valsamidis G, Kanavaki I, Nikolaki A, Rupprecht F, Langer JD, Tsiotis G. Proteomic Characterization of the *Pseudomonas* sp. Strain phDV1 Response to Monocyclic Aromatic Compounds. *Proteomics.* 2021



Food-waste management in the food service sector

M. Barbarosou¹, L. Evrenoglou¹, O. Cavoura¹, G. Zervas¹ and I. Damikouka¹

¹Department of Public Health Policy, School of Public Health, University of West Attica, Athens, Greece
Corresponding author email: idadamikouka@uniwa.gr

keywords: catering; restaurant sector; food waste management; food waste reduction.

Introduction

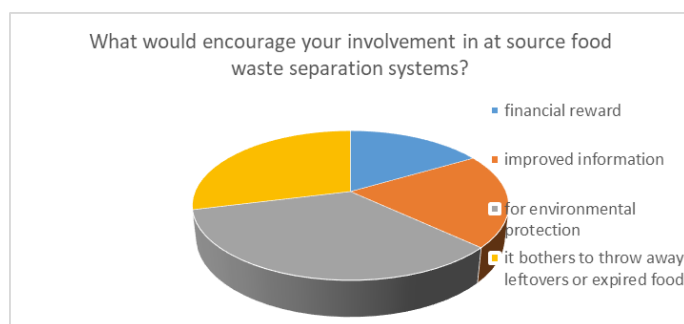
Food-waste mitigation is essential both for the reduction of food poverty and for the sustainable management of natural resources, particularly land, water and energy. While approximately 70% of global freshwater is consumed in the agricultural sector for food production (UNESCO, 2003), it is estimated that approximately 88 million tonnes of food waste are disposed of every year in the European Union (Beretta and Hellweg, 2019) and that globally one quarter of produced food is lost in the different stages of the food supply chain (Kummu et al. 2012). After household and processing, the food service sector is a key contributor to food-waste generation (Stenmark et al. 2016). Therefore, an understanding of the specific causes of food waste in the food service sector (Dhir et al. 2020) focusing on the attitudes and practices amongst employees in the industry is fundamental for the improvement of food management practices.

Materials and methods

The levels of knowledge and understanding of catering and restaurant staff in East Attica, Greece, regarding issues related to food-waste mitigation and management were assessed by means of an anonymous questionnaire. The questionnaire consisted of four (4) basic sections: a) demographic elements, b) opinions and attitudes, c) applied food-waste management practices, and d) causes of surplus quantity of food-waste generation. The collected questionnaires were analyzed with descriptive statistics.

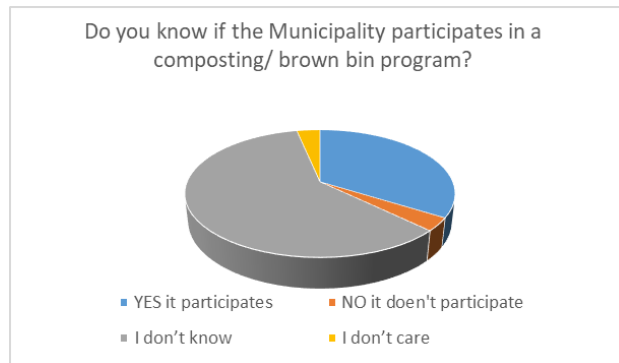
Results and discussion

Regarding employee involvement in at-source food waste separation and collection systems, the majority (34%) responded that a desire for environmental protection would encourage their participation, 29% answered that participation would result from a dislike of throwing away left over or expired food, 20% answered that improved information would encourage their participation in at-source waste separation systems and 17% answered that their participation could be encouraged by financial reward or relief (Graph 1).



Graph 1. Response rates to question 'What would encourage your involvement in at source food waste separation and collection systems?'.
34% for environmental protection, 29% it bothers to throw away leftovers or expired food, 20% improved information, 17% financial reward.

The majority of employees were unaware if the Municipality participated in an at-source food waste separation and collection system (Graph 2), and believed that improvements in the organization of the kitchen supply chain such as scheduling and planning of orders would contribute to the purchase of appropriate quantity of food and to food waste reduction.



Graph 2. Response rates to question 'Do you know if the Municipality participates in a brown bin program?'.



Graph 3. Response rates to question 'Will improvements in organizing kitchen supply chain contribute to food waste reduction?'.

Conclusions

According to the research results, employees would be willing to participate in at-source food waste separation systems, motivated primarily by a desire for environmental protection and to a smaller degree by economic reward, indicating a positive attitude to the adoption of new practices. Most participants believed that improvements in kitchen supply chain organization like schedule and planning of orders would contribute to the purchase of right/appropriate quantity of food and to food-waste reduction. There is a need for employee training and information dissemination regarding food-waste reclamation and mitigation practices in food service sector. A well-designed and a well-executed informative campaign could develop environmental awareness and raise participation not only of food service sector employees but also of the Municipality citizens, in an at-source food recycling scheme.

References

- Beretta, C. and Hellweg, S., 2019. Potential environmental benefits from food waste prevention in the food service sector. *Resources, Conservation & Recycling*, 147, 169-178
- Dhir, A., Shalini Talwar, S., Kaur, P. and Malibari, A., 2020. Food waste in hospitality and food services: A systematic literature review and framework development approach. *Journal of Cleaner Production*, 270,
- Kummu, M., Moel, H., Porkka, M., Siebert, S., Varis, O. and Ward, P.J., 2012. Lost food, wasted resources: Global food supply chain losses and their impacts on freshwater, cropland, and fertiliser use. *Science of The Total Environment*, 438, 477-489.
- Stenmarck, Å., Jensen, C., Quedsted, T. and Moates, G., 2016. Estimates of European food waste levels, FUSION EU project <http://edepot.wur.nl/378674>
- UNESCO, 2003. Water for people, water for life. UNESCO



Removal of anthraquinone dye by hybrid modified activated carbons

A.K. Tolkou¹ and G.Z. Kyzas¹

¹Department of Chemistry, International Hellenic University, Kavala, Greece
Corresponding author email: kyzas@chem.ihu.gr

keywords: Remazol Brilliant Blue R; adsorption; activated carbon; anthraquinone Dye.

Introduction

Dyes have become one of the major pollutants to the environment due to the high amount of discharge of wastewater, lost in the dyeing process, without any further treatment and containing high concentrations of dye. Anthraquinone dyes are one of the major water pollutants due to their stability and persistence in the aquatic system (Yeow, Wong, and Hadibarata 2021). Various methods, including physical and chemical treatments, have been used to remove these dyes from the wastewater. Adsorption on activated carbon has been found to be a very efficient technique for removal of dyes from wastewater (El Maguana et al. 2020) and the modification of activated carbon with the oxides and hydroxides of metals have been used to increase its surface area (Tolkou et al. 2022).

Materials and methods

The present study describes the use of activated carbon produced from coconut shells, modified with a mixture of metals and metalloids, such as magnesium, silicate, lanthanum and aluminum (AC-Mg-Si-La-Al), as an adsorbent to remove reactive anthraquinone dye Remazol Brilliant Blue R (RBBR) from its aqueous solution. The effect of the adsorbent's dosage, pH value, contact time and initial RBBR concentration was examined with respect to RBBR removal.

Results and discussion

In batch experiments, the effect of the adsorbent's dosage and the initial solution pH were studied to determine the feasibility of AC-Mg-Si-La-Al for RBBR removal. As illustrated in Fig. 1, with the increase of the adsorbent's dosage, the percentage removal of RBBR is increased in all examined pH values. Especially, in pH 9, the removal rate increases with the use of low dose (0.2 g/L) reaching 100% by 0.5 g/L.

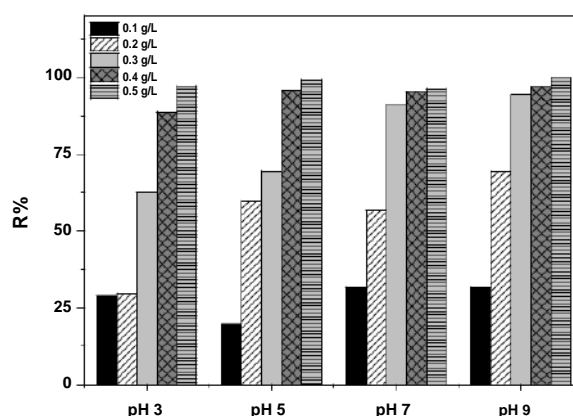


Figure 1. Effect of dosage and effect of RBBR initial solution pH, $T=25\pm 1$ °C, contact time 24 h.

Fig. 2a presents the effect of RBBR initial concentration in the range of 50-250 mg/L. The adsorption capacity of AC-Mg-Si-La-Al was found to increase at pH value 9, from 1.25 to 4.9 mg/g for initial RBBR concentration 50 and 250 mg/L, respectively.

Another key factor in the adsorption process is the kinetic behavior of the adsorbents, thus, the effect of contact time from 5 to 1440 (24 h) min was then studied, keeping all other parameters constant. The results (Fig. 2b) showed that in order to increase the removal rate of RBBR and the relative cost



-effectiveness of adsorption, 4h (240 min) were selected as the optimal contact time for batch experiments.

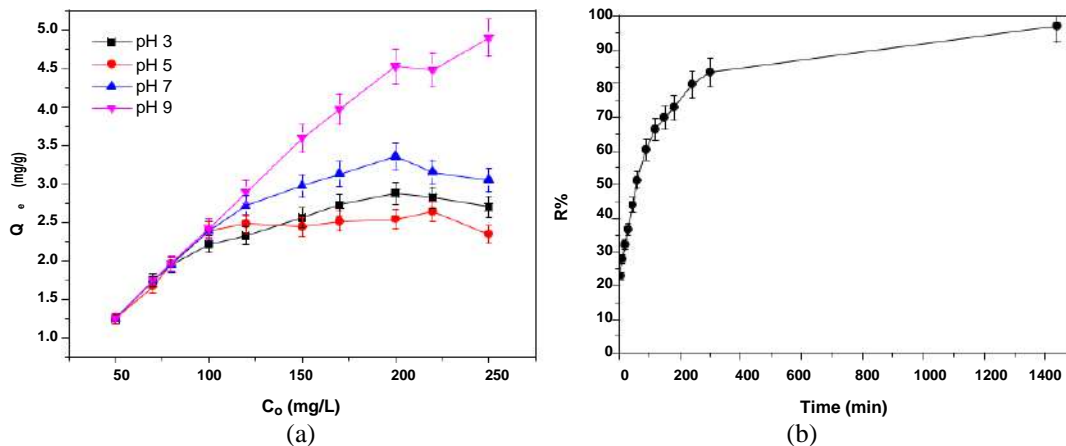


Figure 2. Effect of initial RBBR concentration, and contact time; dose 0.4 g/L, $T=25\pm 1$ °C.

Conclusions

The optimal dose of 0.4 g/L and pH 9 are selected, which leads to 99% removal of RBBR and the adsorption capacity of AC-Mg-Si-La-Al was found to increase. So as to increase the cost-effectiveness of adsorption, 4 h (240 min) of contact time were selected as optimal time for batch experiments.

Acknowledgements: This research was funded by the Greek Ministry of Development and Investments (General Secretariat for Research and Technology) through the research project “Research-Create-Innovate”, with the topic “Development of an integration methodology for the treatment of micropollutants in wastewaters and leachates coupling adsorption, advanced oxidation processes and membrane technology” (Grant no: T2EDK-04066).

References

- Maguana, Y. El, N. Elhadiri, M. Benchanaa, and R. Chikri. 2020. “Activated Carbon for Dyes Removal: Modeling and Understanding the Adsorption Process.” *Journal of Chemistry* 2020. <https://doi.org/10.1155/2020/2096834>.
- Tolkou, Athanasia K, Sultana Trikalioti, Olina Makrogianni, Maria Xanthopoulou, Eleni A Deliyanni, George Z Kyzas, and Ioannis A Katsoyiannis. 2022. “Lanthanum Modified Activated Carbon from Coconut Shells for Chromium (VI) Removal from Water.” *Nanomaterials* 12 (7): 1–18. <https://doi.org/10.3390/nano12071067>.
- Yeow, Peck Kah, Sie Wei Wong, and Tony Hadibarata. 2021. “Removal of Azo and Anthraquinone Dye by Plant Biomass as Adsorbent – a Review.” *Biointerface Research in Applied Chemistry* 11 (1): 8218–32. <https://doi.org/10.33263/BRIAC111.82188232>.



Autotrophic and heterotrophic arsenite oxidation by a river water microcosm

S. Won^{1,2}, J. Bae¹, S. Lee¹, H. Jin¹, Y. Kim¹ and H.Y. Kang¹

¹Department of Microbiology, Pusan National University, Busan, Republic of Korea

²Microbiological Resource Research Institute, Pusan National University, Busan, Republic of Korea

Corresponding author email: khanhvn88@pusan.ac.kr

Keywords: heterotrophic bacteria; autotrophic bacteria; freshwater; arsenic; microbial oxidation.

Introduction

Arsenic (As) is a toxic element to human health, which was thoroughly studied worldwide to establish various guidelines to react to the effect of As contamination on human beings (Mandal and Suzuki, 2002). The popular use of As in modern industry has resulted in the increasing accumulation of As in surrounding environments. Therefore, this has attracted much attention of scientific community to remediation technology for treatment of As contamination in the environment.

There are various techniques for remediation of As contaminated in the environment including chemical, physical, and biological treatments. Among them, biological methods were proved to be more economical and eco-friendly. In biological remediation of As, the microbial oxidation of arsenite [As(III)] to arsenate [As(V)] is considered a primary detoxification strategy because it would help reduce As toxicity and change its mobility in the environment.

This study aims to investigate both the autotrophic and heterotrophic oxidation of As(III) to As(V) by the microcosm obtained from Nakdong river water to evaluate the potential self-detoxification mechanism in the river system. The As(III) oxidation was also tested with various contaminant concentrations to estimate the kinetics of the microbial As(III) oxidation reaction.

Materials and methods

The water sample was collected from Nakdong river and the microcosm was obtained through filtration using sterilized filter paper. The microcosm was inoculated into the culture media and incubated in a shaking incubator at 25°C and 200 rpm. The minimal medium (Santini et al., 2000) containing 0.1 g/L NH₄Cl, 0.1 g/L KH₂PO₄, 0.012 g/L CaCl₂·2H₂O, 0.05 g/L KCl, 1 ml/L vitamin solution (Gamborg's vitamin solution 1000×, Merck KGaA, Darmstadt, Germany), and 1 mL/L mineral solution. As(III) was added to the culture from the stock solution of NaAsO₂. Bicarbonate (as 0.5 g/L NaHCO₃) was supplied as an inorganic carbon source for autotrophic growth, whereas acetate (as 1 g/L CH₃COONa) was added as an organic carbon source for heterotrophic growth. Both autotrophic and heterotrophic As(III) oxidation were investigated at a concentration of 1 mM, 2 mM, 5 mM, and 10 mM As(III).

The enrichment culture was then spread on the agar plate containing the same ingredients. Selected colonies found on agar plates were continuously streaked on fresh agar plates until a pure culture was obtained. The pure isolates were re-cultured in liquid media and tested for As(III) oxidation ability. Newly isolated bacteria were determined through 16S rRNA sequencing. The phylogenetic relationship of the newly-isolated bacteria with their closest relatives and previously reported As(III)-oxidizing bacteria were analyzed using MEGA X.

The cell growth in each culture was estimated by measuring the optical density of the culture medium at a wavelength of 600 nm using a spectrophotometer (UV-Vis Double Beam Model UVD-3200, Labomed Inc., Los Angeles, CA, USA). The As(III) and As(V) concentrations were determined using a DionexUltiMate 3000 high-performance liquid chromatography system (Thermo Fisher Scientific Inc., Waltham, MA, USA) as described in our previous studies (Nguyen et al., 2017). The total soluble As in the culture was calculated as the sum of As(III) and As(V).

Results and discussion

Experimental data indicated that As(III) can be oxidized to As(V) under both heterotrophic and autotrophic conditions. However, As(III) was oxidized at a much higher rate under heterotrophic conditions than under



autotrophic conditions. It could be due to the higher cell growth and cell density of the heterotrophic condition compared to the autotrophic condition. At the high concentration of As(III) (10 mM), the autotrophic As(III) oxidation was not completed even with a long extent of incubation time, which might be due to the inhibition effect of high contaminant concentration on the growth of bacteria. Representative pure isolates were also obtained from both heterotrophic and autotrophic enrichment cultures and show substantial As(III) oxidation potential for further applications.

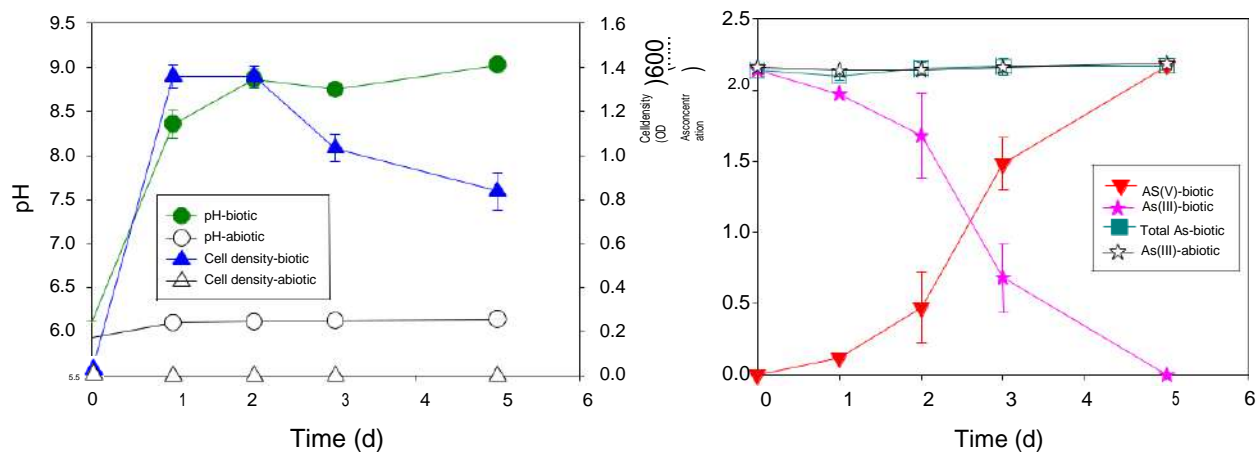


Figure 1. Heterotrophic As(III) oxidation by the river water microcosm.

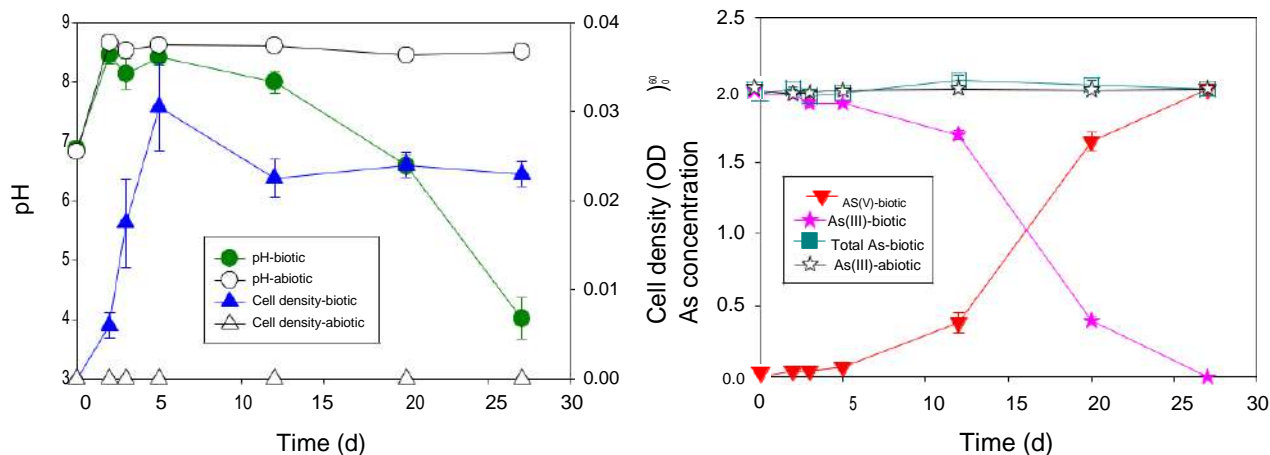


Figure 2. Autotrophic As(III) oxidation by the river water microcosm.

Conclusions

This study successfully proved the ability of a river microcosm to oxidize As(III) to As(V) under both heterotrophic and autotrophic conditions. This indicated the potential self-detoxification of the river system. The newly isolated bacterial strains could be further studied for future applications in As remediation systems. However, it requires clarifying the pathway of As transformation in these systems for appropriate application.

Acknowledgements: This research was supported by the Basic Science Research Program through the National Research Foundation of Korea (NRF) funded by the Ministry of Education (NRF-2020R1I1A3068585)

References

- Mandal, B.K., Suzuki K.T., 2002. Arsenic round the world: A review, *Talanta*, 58, 201–235.
- Santini J.M., Sly L.I., Schnagl R.D., Macy J.M., 2000. A New Chemolithoautotrophic Arsenite-Oxidizing Bacterium Isolated from a Gold Mine: Phylogenetic, Physiological, and Preliminary Biochemical Studies, *Appl. Environ. Microbiol.*, 66, 92–97.
- Nguyen V. K., Tran H. T., Park Y., Yu J., Lee T., 2017. Microbial arsenite oxidation with oxygen, nitrate, or an electrode as the sole electron acceptor, *J. Ind. Microbiol. Biotechnol.* 44, 857–868.



A recycling Photovoltaic panel process by complexing reagents

P. Koulouridakis¹, N.Bilalis¹ and N.Kallithrakas-Kontos²

¹School of Production Engineering and Management, Technical University of Crete, Chania, Greece

²School of Mineral Resources Engineering, Technical University of Crete, Chania, Greece

Corresponding author email: pavloskoul@gmail.com

keywords: recycling; photovoltaic; reagents; x-rays.

Introduction

Our aim is to use complex reagents in the field of Cd-Te recycling PV panels and to recover elements such as cadmium. For this purpose we measure the ability of these reagents to bond with cadmium.

Materials and methods

We filtered a solution of 10 ppm Cadmium in tap water with two set ups. At the first one we soaked the filter paper with the reagent ammonium pyrrolidine-dithiocarbamate and the second one without any reagent. The final collected Cd concentration from the two types of filters were measured by X-Ray Tube Ag (Amptek) and X-123 Amptek detector.

Results and discussion

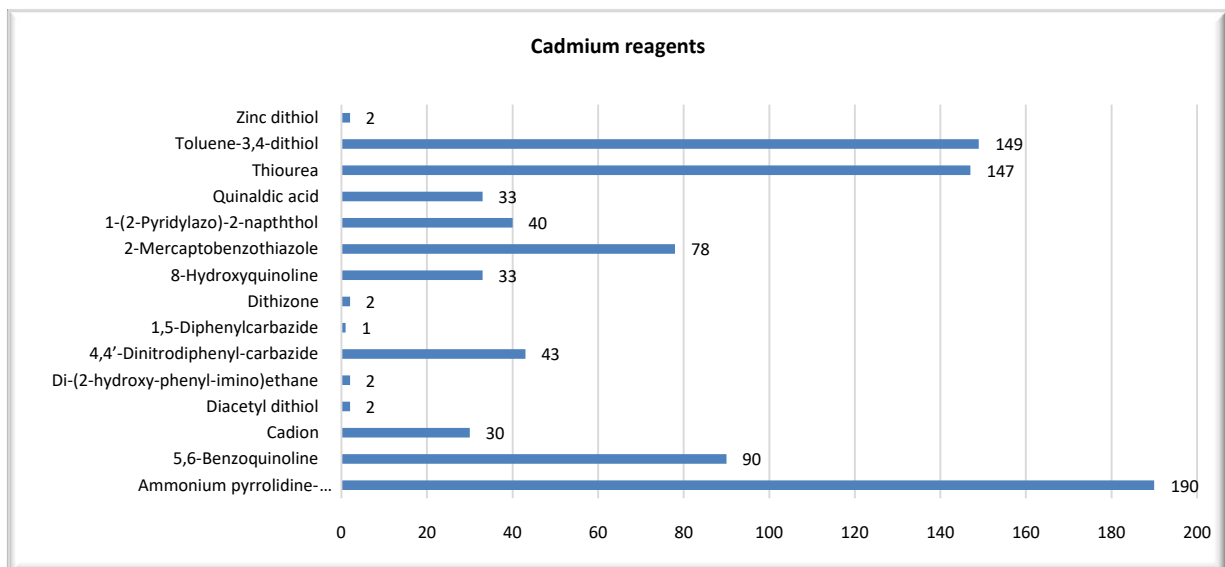


Figure 1. Comparison of various complexing reagents for Cadmium found in PV cells as determined in the Index of Chemical Reagents.

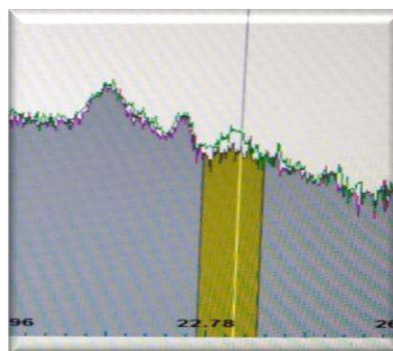


Figure 2. Typical X-Ray Spectra from the two different filters. The above green spectrum shows the concentration of Cadmium at the filter with the complex reagent.



Conclusions

Filtering process finished after 40 minutes approximately. The filter without the reagent had no cadmium concentration. So cadmium cannot be collected only with filtered paper. The filter with the reagent binds 100% the cadmium from the solution. That shows that selectivity of the reagent ammonium pyrrolidine-dithiocarbamate can completely separate cadmium from solution.

References

- Koulouridakis, P. and Kallithrakas-Kontos, N., 2004. Selective Mercury Determination after Membrane Complexation and Total Reflection X-Ray Fluorescence Analysis, *Analytical Chemistry*, 76, 4315-4319.
- Koulouridakis, P., Domazos, E., Galani-Nikolakaki, S. and Kallithrakas-Kontos, N., 2004. Low Level Lead Determination after Membrane Complexation and TXRF Analysis, *Microchimica Acta*, 146, 245-250.
- Rentoumis, M., Athanailidis, I., Koulouridakis, P., Katsigiannis, Y. and Bilalis, N., June 2015. Development of a three dimension industrial production line simulation for crystalline silicon photovoltaic panel recycling, *4th International Symposium & 26th National Conference on Operational Research, Chania –Crete, Greece.*



LCA studies within CREIAMO project: eco-innovation approach and environmental impact assessment

E. De Marco¹, F. Hernan Gomez Tovar², L. Mastella³, T. Beltrani¹, R. Vahizadeh², A. Franzetti⁴, M. Vaccari² and S. Scaffoni¹

¹ RISE (Resource Valorisation) Laboratory, ENEA, Rome, Italy

² DICATAM, University of Brescia, Brescia, Italy

³ BtBs, University of Milano-Bicocca, Milano, Italy

⁴ DISAT, University of Milano-Bicocca, Milano, Italy

Corresponding author email: emanuela.demarco@enea.it

keywords: *eco-innovation; impact assessment; biosurfactant; soil remediation; laboratory scale.*

Introduction

This contribution focuses on project activities related to environmental assessment through the LCA methodology within the Creiamo project, funded by CARIPLO Foundation, aimed at identifying and promoting new destinations and economic opportunities for by-products and waste deriving from the olive and wine sectors, under a circular economy perspective.

This contribution summarizes the main results of the experiments conducted in the laboratory for the production of biosurfactants from olive oil and wine production waste (WP2) and the subsequent preliminary studies for the treatment of soils contaminated by hydrocarbons using different bioremediation techniques and biosurfactants produced in experimental phase (WP3). The assumption of the results achieved in the experimental phases constitutes the basis for Life Cycle Assessment study (WP4) and at the same time defines a framework of scenarios to be validated on the basis of the comparison of the results. In general, the study aims to evaluate the environmental impact and the related advantages in the production and use of innovative products created in the experimental phase compared to traditionally used products.

Materials and methods

The results produced in the experiments conducted in WP2 and WP3 have been incorporated as basic data to conduct the environmental assessment in WP4, the aim of which is to verify that the biosurfactants produced have a better environmental impact assessment than the products they are replacing. The improvement will therefore be assessed considering the total balance of global impacts, on the consumption of resources, on human health, on ecosystems and on emissions into the atmosphere. An in-depth study of the impact assessment methods and the indicators considered will be explained to justify the appropriateness of the method used with compared to the objectives of the evaluation study.

The evaluation based on the LCA methodology allows to obtain data that allow to make comparisons between conventional and innovative scenarios. Specifically, two distinct evaluation phases were carried out. The first evaluation phase (LCA 1) concerns the production of biosurfactants from the residues of oil and wine production. In this phase, the impacts of three scenarios are compared. These scenarios differ in the type of organic waste used (unfermented marc and pomace) and in the use of the bacterium for fermentation (pathogenic bacterium and non-pathogenic bacterium). The second evaluation phase (LCA 2) was conducted on the basis of four scenarios, which envisage the treatment of the soil contaminated by hydrocarbons with two different techniques tested in the project (soil washing and biopile), and with the use of the best biosurfactant produced in the first phase of evaluation in comparison with surfactants traditionally used for soil decontamination. (Figure 1)

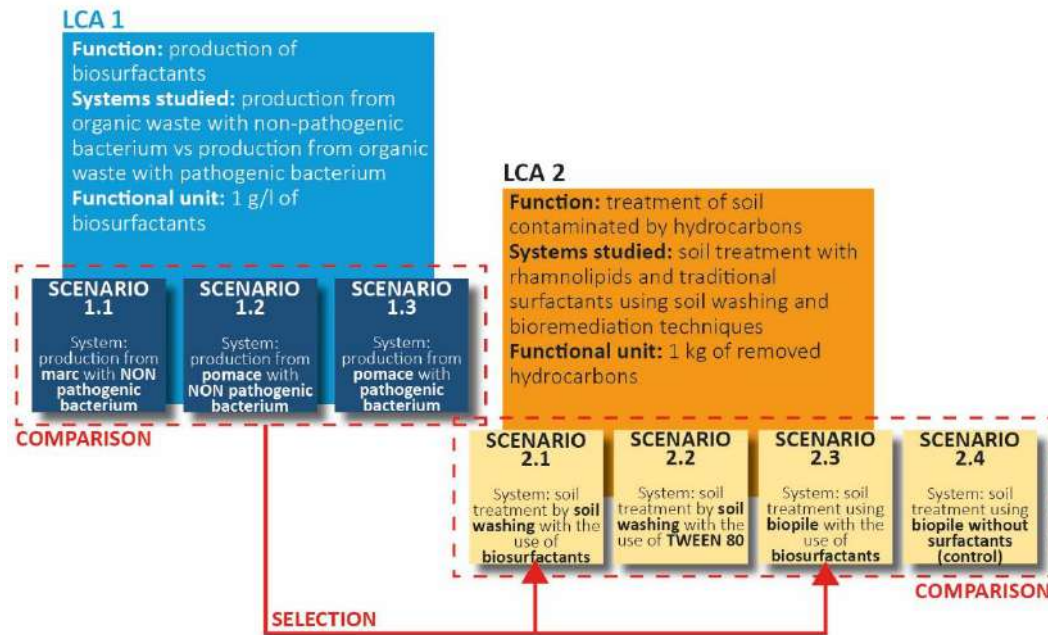


Figure 1. Structure of the assessment study.

Results and discussion

From the results of the comparative analysis of LCA1 conducted between new products/processes and conventional products/processes, it is possible to state that the production of rhamnolipids from marc is the most sustainable process for the impacts analyzed;

From the results of the comparative analysis of the LCA2 conducted between the new products/processes and conventional products/processes, it is possible to state that the treatment of contaminated soils with the soil washing technique and the use of rhamnolipids is the most sustainable process for the impacts analyzed.

Conclusions

The potential benefits of innovative solutions and scenarios compared to conventional systems are evident from the LCA study, and the critical points of the synthesis process and the treatment of contaminated soils emerge;

A subsequent study of the environmental impacts at a pilot plant scale would make it possible to optimize the environmental advantages that emerged in this preliminary phase of the study regarding the treatment of contaminated soils with bio surfactants, with a view to possible commercial production.

Acknowledgements: The authors are thankful to "Fondazione Cariplo" for funding the project "Creiamo - Circular economy in olive oil and wine sectors. Valorisation of by-products and residues through innovative processes and new business models" (D76C19000230007). Details on the project are available on www.creiamocirculareconomy.com.

References

- UNI EN ISO, 2006. ISO 14040:2006 - Environmental management — Life cycle assessment — Principles and framework.
- Chebbi, A., M. Tazzari, C. Rizzi, F. H. G. Tovar, S. Villa, S. Scaffoni, M. Vaccari and A. Franzetti (2021). "Burkholderia thailandensis E264 as a promising safe rhamnolipids' producer towards a sustainable valorization of grape marcs and olive mill pomace." *Applied microbiology and biotechnology*, 105 (9), 3825-3842.



Employment of poultry and turkey manure as fuel for small/medium scale boilers

C. Di Stasi¹, Y. Torreiro¹, J. Rico², R. Pérez², D. Patiño² and A. Rodríguez-Abalde¹

¹Centro Tecnológico EnergyLab, Edificio CITEXVI, Fonte Das Abelleiras, Vigo, Pontevedra, Spain

²E.T.S. Ingenieros Industriales, Universidad de Vigo, Lagoas-Marcosende s/n, Vigo, Pontevedra, Spain

Corresponding author email: christian.distasi@energylab.es

keywords: poultry manure; biofuels; renewable energy; farming; poultry litter.

Introduction

During 2016, the 89% of the total poultry meat production was represented by chickens [1]. This market is responsible for significant greenhouse gases (GHG) emissions, which in this sector can be ascribed to the production of the feed, to the management and storage of manure, to the direct energy consumption and to the activities of the facility itself [2]. For this reason, poultry manure (chicken and turkey) represents one of the most abundant and problematic wastes in the poultry sector.

The AVIENERGY project promotes a more efficient use of resources in the poultry sector by applying a strategy based on the fundamentals of circular bioeconomy. This strategy focuses on the recovery of the manure generated in poultry farms (meat and egg production), to be employed as a source of renewable energy in situ, reducing the dependence from other energy sources and reducing the costs and the GHG emission derived by the management of the manure. Furthermore, due to their inherent composition, the ashes generated by the combustion of this residue could be employed as soil amendment to improve the fertility of the soil. Hence, the proposed solution aims to become an efficient and environmentally sustainable tool to contribute to the reduction of GHG while improving the competitiveness of the sector.

In this work, chicken and turkey broilers manure were characterized in order to evaluate their feasibility for being employed as solid fuel for small/medium boilers.

Materials and methods

The chicken and turkey broiler manure (Figure 1a and 1b, respectively) analyzed in this work were provided by two Spanish farms involved in the AVIENERGY project. The manure samples characterization in terms of proximate analysis (moisture, ash, volatile matter and fixed carbon content), elemental composition (carbon, hydrogen, oxygen, sulfur and chlorine content), ashes melting behavior, high and low heating value (HHV and LHV) were carried out according to the corresponding UNE-EN ISO standards.



Figure 1. Samples characterized in this work: (a) Chicken manure; (b) Turkey manure.

Results and discussion

In Table 1 the results of the proximate analysis of the samples studied in this work are summarized. Similar values obtained with a reference fuel (woody chips) are included for comparison purpose. The results show that both samples studied have a high moisture content (which was expected considering their nature) and, therefore, they should undergo a drying process before their employment as fuel.

The relatively high ash content may represent a problem for the correct operation of the boiler. Those results make mandatory the study of the melting point of the ashes. A high ash content and a low melting point of those ashes can cause slagging during combustion process. The sintering temperature of the ashes achieves values < 850 °C for both samples, which implies the need for an exhaustive combustion control and, if necessary, the placement of a continuous ash removal system.



The elemental analysis of the two poultry samples (Table 2) reveals a high content of nitrogen, sulfur, and chlorine. The presence of more than 1 wt.% of chlorine implies that, to avoid the production of hydrochloric acid and dioxins, the combustion must be carried out at temperatures above 1.100 °C [3]. The content of sulfur and nitrogen could lead to NO_x and SO_x emissions [4,5] which, depending on the boiler size, must not exceed a certain threshold determined by law or regulations.

Polluting gaseous emissions could be mitigated in part by implementing cleaning measures in the outlet gas. This task will be carried out in later stages of AVIENERGY project.

Finally, in Table 3 the heating values of both samples are reported. The results of this characterization indicate that, among the two studied samples, the chicken manure represent the best fuel. Nevertheless, the relatively LHV of these fuels is relatively low if compared with the traditional fuels (i.e., wood chips). A possible solution is represented by the combustion of poultry manure along with another fuel with higher heating value (co-combustion) [6].

Table 1. Proximate analysis.

	Moisture wt%	Ash	Volatile wt _{dry} %	Fixed Carbon
Chicken manure	27,82 ± 0,46	11,40 ± 0,14	74,77 ± 2,81	13,83
Turkey manure	30,85 ± 0,29	19,59 ± 0,40	66,91 ± 0,46	13,50
Wood chips	12,18	1,65	75,08	23,27

Table 2. Elemental composition.

	wt _{dry} %				
	C ^a	H ^a	N ^a	S ^b	Cl ^b
Chicken manure	41,92	4,27	2,62	1,915	2,659
Turkey manure	38,31	3,96	4,96	2,702	2,887
Wood chips	51,90	6,10	1,04	0,056	0,012

^a UNE-EN ISO 16948:2015

^b UNE-EN ISO 16994:2017

Table 3. High heating value and low heating value.

	HHV MJ kg _{dry} ⁻¹	LHV MJ kg _{dry} ⁻¹
Chicken manure	17,61 ± 0,45	11,35 ± 0,45
Turkey manure	16,04 ± 0,03	9,74 ± 0,03
Wood Chips	19,95	16,45

Conclusions

The high moisture content along with low values of LHV, suggested that the feedstocks should be submitted to a preliminary drying process. As already suggested by other authors, the co-combustion of poultry manure with another types of waste such as forest and wood waste or municipal solid waste should be considered to convert this waste in a feasible alternative energy source.

Acknowledgements: This study was funded for the 80% by European Agricultural Fund for Rural Development (EAFRD) and for the 20% by Ministerio de Agricultura, Pesca y Alimentación, within the framework of the Programa Nacional de Desarrollo Rural 2014-2020.

References

- FAO. 2019.
- MacLeod, et al. 2013. Greenhouse gas emissions from pig and chicken supply chains – A global life cycle assessment. Food Agric Organ United Nations.
- Directive 2000/76/EC of the European Parliament and of the Council of 4th December 2000 on the incineration of waste.
- Sartor K, Restivo Y, Ngendakumana P, Dewallef P. 2014. Prediction of SO_x and NO_x emissions from a medium size biomass boiler. Biomass and Bioenergy 2014;65:91–100.
- Turzy T, Kluska J, Karda D. 2022. Study on chicken manure combustion and heat production in terms of thermal self-sufficiency of a poultry farm. Renew Energy 2022;191:84–91.
- Quiroga G, et al. 2010. Physico-chemical analysis and calorific values of poultry manure. Waste Manag;30:880–4.



Cultivation of marine microalgae - Production of biomass and high value added products

V. Patrino¹, A. Daskalaki², C.N. Economou³ D. Bokas⁴, D.V. Vayenas³, G. Aggelis² and A.G. Tekerlekopoulou¹

¹Department of Environmental Engineering, University of Patras, Agrinio, Greece

²Department of Biology, University of Patras, Patras, Greece

³Department of Chemical Engineering, University of Patras, Patras, Greece

⁴PLAGTON S.A., Thesi Konaki Skentou, Municipality of Xiromero, Aitolokarnania, Greece

Corresponding author email: atekerle@upatras.gr

keywords: *Nannochloropsis* sp.; *Nannochloropsis oculata*; *Isochrysis galbana*; *Tetraselmis striata*; substrate optimization.

Introduction

Marine microalgae are considered versatile cellular factories that produce a plethora of metabolic compounds. The high value added components they produce is a broad category containing mainly lipids, carbohydrates and proteins (Ma et al., 2020). Lipids from marine microalgae are significant as they are a major source of important poly-unsaturated fatty acids (PUFAs) such as omega-3 [EPA (C20:5), DHA (C22:6), α -Linolenic (C18:3(n-3))] and omega-6 (Dammak et al., 2016). Additionally, extracted high value products can be utilized in many different commercial applications including biofuels, health food supplements, aquafeeds, cosmetics, and pharmaceuticals. The addition of microalgal biomass into fish diets is beneficial for fish as it leads to improved growth and fillet quality, increased deposition of proteins in muscle tissue, improved resistance to disease, and higher fatty acid content (Shah et al., 2018).

In this work, four marine microalgae were studied (*Nannochloropsis* sp., *Nannochloropsis oculata*, *Isochrysis galbana* and *Tetraselmis striata*). Each is currently of high interest for aquafeeds and has the potential to produce important lipids. The aim was to select the most suitable microalga for full-scale production. The strains were cultivated in drilling seawaters, and specific growth rate and biomass productivity were the determining parameters for the selection of the optimum microalga. Growth medium optimization was then performed for the selected strain. Subsequent fatty acid analysis revealed significant EPA and PUFAs contents when the microalga was cultivated in the optimized growth medium.

Materials and methods

Dry cell biomass and lipid content were determined gravimetrically (mg L^{-1}) as Total Suspended Solids (TSS) according to Standard Methods (1998). Biomass productivity expressed in $\text{mg L}^{-1} \text{d}^{-1}$ was calculated following Gonçalves et al. (2016), while maximum specific growth rate (d^{-1}) was calculated following Tsolcha et al. (2017). Lipid extraction was carried out following Folch (1957) and the fatty acid profile was determined according to AFNOR (1984).

Results and discussion

The microalgal strains were cultivated in 38 ‰ drilling waters originating from the commercial fish farm PLAGTON S.A. (Western Greece). The seawaters had no nutrient load and nutrient supplementation was essential to sustain growth. Only N and P, at a ratio of about 5:1, were added to the drilling waters, with the aim of reducing production costs in potential future full-scale cultivations. *Tetraselmis striata*, the Chrysophyceae *Isochrysis galbana* and the two *Nannochloropsis* species, were cultivated under conditions of continuous illumination of $56 \mu\text{mol m}^{-2} \text{s}^{-1}$, and unregulated temperature and pH. The biomass efficiencies achieved for the different strains are presented in Table 1.

The *Nannochloropsis* strains presented the lowest biomass productivities and specific growth rates. Although *Isochrysis galbana* exhibited the highest biomass productivity it was not selected as the optimum species, because of the difficulty in maintaining the culture's purity. Microscopic observations showed that the strain was susceptible to contamination even in laboratory-scale experiments and thus it was not considered suitable for full-scale cultivations. Therefore, *Tetraselmis striata* was selected as the optimum



species, as it presented satisfactory biomass yields under conditions of high salinity and low nutrient availability.

Table 1. Biomass productivities and specific growth rates obtained from the four marine microalgae.

Strain	Biomass productivity (mg L ⁻¹ d ⁻¹)	Specific growth rate (d ⁻¹)
<i>Nannochloropsis</i> sp.	23.2	0.073
<i>Nannochloropsis oculata</i>	27.0	0.077
<i>Tetraselmis striata</i>	40.2	0.101
<i>Isochrysis galbana</i>	95.2	0.366

Substrate optimization was performed to further enhance growth. A medium of double N:P ratio (12:1) was studied in 38 ‰ and 29 ‰ seawaters. The highest biomass productivity (47.6 mg L⁻¹d⁻¹) was recorded in the 29 ‰ medium indicating that *T. striata* prefers lower salinities. The effect of medium composition on growth was also evaluated in 29 ‰ seawater by further enriching the medium with the commercial fertilizer Nutri-Leaf (30% TN, 10% P, 10% K) together with NaHCO₃. Using Nutri-Leaf significantly enhanced the recorded biomass productivity (79.8 mg L⁻¹d⁻¹ with a corresponding growth rate of 0.266 d⁻¹), while the produced biomass also contained high lipid contents of up to 27.8% dry weight.

Finally, fatty acid analysis of the biomass generated under the optimum cultivation conditions showed that *T. striata* produced high EPA (27.6%) and PUFAs (33.2%) contents.

Conclusions

The results of this study indicate that the marine microalgae *T. striata* is suitable for full-scale applications and can achieve significant biomass yields. Additionally, the strain is an important Pufa producer and its high nutritional value shows its suitability for incorporation into aquafeeds.

Acknowledgements: The project "Large-scale cultivation of microalgae and utilization of the biomass produced as alternative raw material in fish feed - AlgaFeed4Fish" (MIS 5045858, FK 80916), was co-funded by European (European Regional Development Fund) and National Resources (General Secretariat for Research and Technology).

References

- American Public Health Association. *Standard Methods for the Examination of Water and Wastewater*, 20th ed.; American Public Health Association: Washington D.C., USA, 1998.
- Association Francaise de Normalisation. *Collection of French Standards for Fats, Oleaginous Grains and Derived Products*, 3rd ed.; French Association for Standardization, Paris (AFNOR): Paris, France, 1984; pp. 95.
- Dammak, M., Haase, S.M., Miladi, R., Ben Amor, F., Barkallah, M., Gosset, D., Pichon, C., Huchzermyer, B., Fendri, I., Denis, M., Abdelkafi, S., 2016. Enhanced lipid and biomass production by a newly isolated and identified marine microalga. *Lipids Health Dis.*, 15, pp. 1–13.
- Folch, J., Lees, M., Sloane-Stanley, G.A., 1951. A simple method for the isolation and purification of total lipids from animal tissues. *J. Biol. Chem.*, 226, pp. 497–509.
- Gonçalves, A.L., Pires, J.C.M., Simões, M., 2016. Wastewater polishing by consortia of *Chlorella vulgaris* and activated sludge native bacteria. *J. Clean. Prod.*, 133, pp. 348–357.
- Ma, R., Wang, B., Chua, E.T., Zhao, X., Lu, K., Ho, S.H., Liu, L., Xie, Y., Lu, Y. and Chen, J., 2020. Comprehensive utilization of marine microalgae for enhanced co-production of multiple compounds. *Mar. Drugs*, 18, pp. 1–26.
- Shah, M.R., Lutz, G.A., Alam, A., Sarker, P., Kabir Chowdhury, M.A, Parsaeimehr, A., Liang, Y., Daroch, M., 2018, Microalgae in aquafeeds for a sustainable aquaculture industry. *J. Appl. Phycol.*, 30, pp. 197–213.
- Tsolcha, O.N., Tekerlekopoulou, A.G., Akratos, C.S., Aggelis, G., Genitsaris, S., Moustaka-Gouni, M., Vayenas, D.V. (2017). Biotreatment of raisin and winery wastewaters and simultaneous biodiesel production using a *Leptolyngbya*-based microbial consortium. *J. Clean. Prod.*, 148, pp. 185–193.



Use of biosolids to enhance tomato growth and assessment of metal leaching after land application

I. Giannakis¹, C. Emmanouil², M. Mitrakas³, A. Lagopodi⁴ and A. Kungolos¹

¹Department of Civil Engineering, School of Engineering, AUTH

²Department of Spatial Planning and Development, School of Engineering, AUTH

³Department of Chemical Engineering, School of Engineering, AUTH

⁴Department of Agriculture, School of Agriculture Forestry and Natural Environment, AUTH

Corresponding author email: kungolos@civil.auth.gr

keywords: *biosolids; plant growth; metal leaching; environmental risk; circular economy.*

Introduction

Waste management is nowadays a worldwide problem (Torri & Cabrera, 2017). In this context, sewage sludge is a waste which however may be utilized for raw material or for energy extraction and as such it can become a “product” (Pradel et al., 2016). Biosolids (BS) derive from processed sewage sludge, and they may be applied to soil as fertilizers (Torri et al., 2017). It should be noted however that leaching of toxic metals may also take place from BS (Batziaka et al., 2008) and therefore, limits for the use of biosolids in agriculture have been set in 86/278/EEC.

Materials and methods

Mixtures of soil (sandy S or clay C) and BS were made at predetermined concentrations (0, 20 και 40 tn/ha) in cornfields. Samples of the mixtures were taken right before corn seed planting from soil mixed with the BS one year earlier and a bit after corn seed planting from soil just mixed with the BS again. The mixtures were subjected to the NEN 7341 availability test (NEN 7341, 1995) and Zn, Ca, Mg, Cu, Ni, Cd and Pb were measured in the leachates according to Pantazopoulou et al. (2015).

At the same time, tomato seedlings “ACE 55” were planted into soil (S or C) at concentrations corresponding to 0, 80 και 160 tn/ha, and plant development parameters were measured at 5 and at 7 weeks after planting. Differences between the tested groups were compared via two-way ANOVA with the LSD criterion.

Results and discussion

It was clearly shown that leachates of Ni, Cd, Pb, Zn, Cu, but also leachates of Ca and Mg contained very low concentrations of these elements (for Cu the concentrations were always lower than the 0.2 mg/kg d.w. limit). The NEN 7341 is quite good for simulation of low pH range (3-5) which is also the most dangerous condition for soil metal leaching (van der Sloot et al., 2003). In any case the results were at least 10fold or lower than the limits (for acid digestion) for metals set in 86/278/EEC. At the same time, there was a beneficial effect for all plant development parameters after use of BS, which was also dose dependent. This was also noted in the study of Wang et al. (2008) on *Zoysia japonica*.

Conclusions

It was shown that incorporation of BS into two types of agricultural soil (S and C) improved all plant development parameters in a dose dependent manner. Furthermore, low risk due to toxic metal leaching was noted, again for all the concentrations tested. These concentrations (especially 80 or 160 tn /ha) are quite realistic for common cultivations (Sharma et al., 2017).

Acknowledgements: Mr Giannakis’ scholarship: «This research is co-financed by Greece and the European Union (European Social Fund- ESF) through the Operational Programme «Human Resources Development, Education and Lifelong Learning» in the context of the project “Strengthening Human Resources Research Potential via Doctorate Research” (MIS- 5000432), implemented by the State Scholarships Foundation (IKY)»



References

- Batziaka, V., Fytianos, K. and Voudrias, E. 2008. *Leaching of nitrogen, phosphorus, TOC and COD from the biosolids of the municipal wastewater treatment plant of Thessaloniki*. Environmental Monitoring and Assessment, 140: 331-338.
- Council Directive 86/278/EEC of 12 June 1986 on the protection of the environment, and in particular of the soil, when sewage sludge is used in agriculture
- NEN 7341 (1995). *Leaching tests, Determination of the Availability of Inorganic Components for Leaching. In Leaching Characteristics of Solid Earthy and Stony Building and Waste Materials*. Netherlands Standards, Delft, Netherlands.
- Pantazopoulou, E., Zebiliadou, O., Noli, F., Mitrakas, M., Samaras, P. and Zouboulis, A. 2015. *Utilization of phosphogypsum in tannery sludge stabilization and evaluation of the radiological impact*. Bulletin of Environmental Contamination and Toxicology, 94(3): 352-357.
- Pradel, M., Aissani, L., Villot, J., Baudez, J.C. and Laforest V. 2016. *From waste to added value product: Towards a paradigm shift in life cycle assessment applied to wastewater sludge - A review*. Journal of Cleaner Production, 131(10): 60-75.
- Sharma, B., Sarkar, A., Singh, P. and Singh, R.P. 2017. *Agricultural utilization of biosolids: A review on potential effects on soil and plant grown*. Waste Management, 64: 117-132.
- Torri, S.I., Correa, R.S. and Renella, G. 2017. *Biosolid Application to Agricultural Land—a Contribution to Global Phosphorus Recycle: A Review*. Pedosphere 27(1): 1–16.
- Torri, S.I. and Cabrera, M.N. 2017. *The environmental impact of biosolids' land application*. In Organic Waste: Management Strategies, Environmental Impact and Emerging Regulations. Nova Science Publishers, NY, USA.
- van der Sloot, H.A., Comans, R.N.J., Meeussen, J.C.L. and Dijkstra, J.J. 2003. *Leaching methods for soil, sludge and treated biowaste*. ECN – Environmental Risk Assessment, Final Report Horizontal-23Wang, X., Chen, T., Ge, Y. and Jia, Y. 2008. *Studies on land application of sewage sludge and its limiting factors*. Journal of Hazardous Materials, 160(2–3): 554–558.



Biodiesel production, properties and sustainability from the biomass of *Chlorella sorokiniana* grown heterotrophically with glycerol and anaerobic digestate

D. Kasiteropoulou¹, G. Papapolymerou¹, A. Kokkalis², M. N. Metsoviti¹, X. Spiliotis¹ and A. Mpesios¹

¹Dept. of Environmental Studies, University of Thessaly, Gaiopolis, Larissa, Greece

²GRINCO S.A., Industrial Area of Larisa, Makrychori Larisas, Greece

*Corresponding author email: dkasiter@uth.gr

keywords: *bio-oil, biodiesel; Chlorella sorokiniana; heterotrophic, glycerol; anaerobic digestate.*

The bio-oil and biodiesel production process from the bio-oil of *Chlorella sorokiniana* biomass is reported. The bio-oil extraction parameters from the biomass of *Chlorella sorokiniana* were examined and two successive base-catalyzed transesterifications were carried out. Bio-oil, biodiesel and glycerin yields were determined and basic bio-oil and biodiesel properties were measured. Also, maximum biomass yields were estimated in order that biodiesel production using glycerol as a carbon source be competitive, from an energy point of view, to the anaerobic production of biogas from glycerin. Optimum extraction parameter values are a solvent to biomass ratio 20:1 (v/w), an extraction time of 48 hours and an extraction temperature 40 °C but, in any potential industrial application the combination of these parameters may be different. Biodiesel conversion efficiency (w/w) is 96% and all basic bio-oil and biodiesel properties measured were within acceptable ranges. Biomass yields of about 11 gr/l with a minimum lipid content of 35% and a carbon yield coefficient of 0.40 are needed in order for the biodiesel produced per ton of glycerin be comparable to the electrical energy produced from biogas from the anaerobic digestion also of 1 ton of glycerin.

Materials and methods

The cultivation of *C. sorokiniana* carried out in 42L cylindrical glass bioreactors of 42L filled to 75% of their volume. Air was continuously provided to each bioreactor through perforated steel tubing placed at the bottom of the bioreactors at a rate of about 40 L/(L-h). The bioreactors, the glass tubing and the culture medium were sterilized before use. At the end of each experiment, and specifically at the stationary growth phase, the biomass was collected by centrifugation, it was rinsed with distilled water and was re-centrifuged. Finally, it was dried in an air circulation oven at 45 °C until constant weight. Prior to lipid extraction, the biomass was pulverized using a planetary ball mill at 200 rpm for 10 minutes (FRITSCH, Idar-Oberstein, Germany). The total lipid content was determined with extraction using co-solvents of n-hexane/isopropanol in a 3:2 ratio according to the Bian method (Bian et. al., 2018). Extraction of the bio-oil was carried out in a horizontal extraction apparatus (tehtnica ZELEZNIKI EV-402) at 300 rpm. Following extraction, the biomass was filtered out and the solvent was evaporated. The bio-oil was subjected to transesterification via a double classical transesterification procedure. The microalgal species *Chlorella sorokiniana* (SAG strain 211-31) was obtained from Culture Collection of Algae from the University of Göttingen in Germany (EPSAG). Glycerin and anaerobic digestate (AD) were obtained from local biodiesel and biogas plants. AD was filtered, centrifuged and sterilized before use.

Results and discussion

In this work for the extraction of bio-oil from microalgae, the following procedure was used: a) concentration of the biomass, b) centrifugation, c) drying, d) milling, e) extraction of the solid phase with a mixture of solvents, f) filtration and g) evaporation of the solvents. The percentage of oil extraction that can be achieved using this technique is almost 95-96% while up to about 4-6% bio-oil are expected to remain within the biomass. The bio-oil extraction yield depends on the following factors: a) the grinding method (manually or using a planetary ball mill), b) the time speed of grinding, c) the extraction time, d) the ratio of biomass to solvent mixture and e) the extraction temperature. This technique may be suitable for use in processing large amounts of microalgal biomass if suitably modified for a large-scale application. The main points that this technology should focus to be cost-efficient for use on a large scale are: 1) the effective concentration of the culture solution of the microalgae to a percentage of solids above 50%-60%, 2) A second concentration step



to a percentage more than 80% solids content with as little energy consumption as possible and the subsequent drying of the biomass, 3) the grinding of microalgae biomass with a small percentage of moisture (up to about 3-5%), 4) extraction with a solvent mixture and 5) efficient recovery of the solvent so as to minimize the operating cost of this material.

After the biomass was concentrated and dried, as microalgae have rigid cell walls and lipids are located within these cell walls, a planetary ball mill type setup with zirconium oxide beads was used for grinding in order to rupture the cell wall of the microalgae and make the lipids accessible to the solvent mixture. Grinding was done with constant and equal amounts of dry biomass in each of the four containers of the planetary ball mill for a period of 10 min and with a rotation speed of 200 rpm. Afterwards, the oil was extracted from the dry biomass of the microalgae with a conventional extraction device (tehtnica ZELEZNIKI EV-402) at 300 rpm, using a solvent mixture of hexane and isopropanol in a ratio of 3:2. The following three parameters were investigated in order to determine the optimal conditions for oil extraction performance: a) solvent to biomass ratio (v/w), b) extraction time and c) extraction temperature. The methodology-procedure was to subject quantities of microalgal biomass from the same cultivation treatment to homogenization and grinding, then to obtain batches of biomass and divide them in equal amounts and study them comparatively in order to determine the effect of the aforementioned three extraction parameters on the amount of bio-oil extracted. Each time, one of the three extraction parameters was varied while the other two were held constant.

Conclusions

Bio-oil extraction from the biomass of *Chlorella sorokiniana* via a combination of mechanical pre-treatment in a planetary ball mill and solvent extraction has an extraction efficiency over 93%. Increasing the solvent/biomass ratio from 5:1 to 10:1, the extraction time from 24 hours to 48 hours and the extraction temperature from 25°C to 40°C and the increases the extraction efficiency by 27%, 9.6% and 5.5% respectively. The efficiency of bio-oil to biodiesel conversion via two successive base-catalyzed transesterifications is 96%. 14% (w/w) of the bio-oil-methanol reactive mixture was converted to glycerin. The bio-oil of *Chlorella sorokiniana* cultivated heterotrophically with glycerol and anaerobic digestate is appropriate for use for biodiesel production as all basic bio-oil and biodiesel properties measured are within acceptable ranges. In order for the biodiesel produced from the cultivation of *Chlorella sorokiniana* to be competitive, from an energy point of view, to the biogas produced from the anaerobic digestion of an equal amount of glycerin a biomass yield of 21.6 gr/l with a 35% lipid content is needed. Semi-batch mode or mixotrophic mode cultivation, a combination of the two, use of genetically modified microalgae may achieve this.

Acknowledgements: The study was co-financed by the European Regional Development Fund of the European Union and Greek national funds through the Operational Program Competitiveness, Entrepreneurship and Innovation, under the call RESEARCH – CREATE - INNOVATE (project code: T1EDK-01580).



The root microbiome of organically grown vegetable crops

N. Paranychianakis¹, R. Mourgela¹, M. Frantzeskou¹, N. Kavroulakis² and P. Moschou³

¹School of Chemical and Environmental Engineering, Technical University of Crete, Chania, Crete, Greece

²ELGO-DIMITRA, Institute for Olive Tree, Subtropical Crops and Viticulture, Chania, Crete, Greece

³Department of Biology, University of Crete, Heraklion, Greece

⁴Institute of Molecular Biology and Biotechnology, Foundation for Research and Technology - Hellas, Heraklion, Greece

Corresponding author email: nparanychianakis@tuc.gr

keywords: *root microbiome; soil; sustainability.*

Introduction

There is a growing concern in recent years to improve our understanding on the drivers shaping soil and root microbiomes in agroecosystems. Such knowledge could be potentially exploited to maximize provisioned services, like higher crop yields, improve use efficiency of resources, boost C sequestration, improved tolerance to (a)biotic stressors, and alleviating environmental impacts. In greenhouses the effect of applied management practices on soil and crop microbiome attributes (diversity, stability, functioning) remains, however, largely unknown. To address this knowledge gap, we sampled several organic production greenhouses in the island of Crete that differed in the intensity of soil management and the cultivated crops. Employing 16S rRNA amplicon sequencing, we test specific hypotheses, including:

- i) The positive effect of organic farming on microbial communities will intensify with the passage of time since the transition to the new farming system;
- ii) The intensity of management practices will affect soil and crop microbiomes specific attributes and this effect will be mediated by soil properties (SOM, pH, nutrients);
- iii) Crop type (or sequence of crops) can mediate the structure of soil microbial communities in greenhouse crops.

Materials and methods

Eleven greenhouses were sampled (three replicates/greenhouse) and bulk soil and rhizosphere samples were taken from the 0-20 cm soil depth. DNA was extracted with the DNeasy PowerSoil Pro kit following the manufacturer's instructions. The universal prokaryotic primer set 515f/806r was used to amplify the V4 hyper-variable region of the 16S rRNA gene. Amplicon sequencing was performed in a MiSeq platform (Illumina) at the NOVOGENE UK Facilities. Raw reads were processed with the DADA2 (v. 1.22) pipeline following the typical workflow described by authors. Different metrics were used to estimate the α -diversity (Shannon, Pielou's J, Faith's PD) and β -diversity (Bray-Curtis dissimilarity, UniFrac distances) of microbial communities. Network construction and analysis was performed with the Molecular Ecological Network Analysis Pipeline and differential abundance with the DESEQ2 package. All the bioinformatic and statistical analyses were performed in the R environment using the packages phyloseq, microbiome, microeco, vegan, and ade.

Results and discussion

Our findings revealed high values of α -diversity in greenhouses, particularly in the bulk soil compared to the rhizosphere. Significant differences in the α -diversity were also detected between crops, with greenhouses planted with pepper to show the highest values. Significant differences in β -diversity among the crops were detected only in the rhizosphere compartment. Although soil and root microbiomes shared a significant fraction of microorganisms, up to 85% (core microbiome), a significant fraction was also unique in the different crops and soils implying a strong effect of crops to shape soil microbiome. Our analysis also revealed strong links between soil and root microbiome, environmental variables, and applied practices with important implications in the sustainable management of the agro-ecosystems.



Conclusions

This is one of the few studies to provide insights on the soil and root microbiome of greenhouse organically-grown crops. Our findings provide important implications for the sustainable management of greenhouses through the engineering of soil and root microbiome. On-going work focusing on the isolation of bacterial strains which promote plant growth and provide protection against pathogens and engineered plant genotypes will allow us to further test the robustness of our approach.

Acknowledgements: This study is financed by the Project “Application of Emerging Biotechnological Methods in Biological Grown Vegetable Crops” (code: T2EDK-00597), that is supported by the EU Regional Development Fund and Greek national funds through the Operational Program Competitiveness, Entrepreneurship, and Innovation, under the call RESEARCH–CREATE-INNOVATE.



Use of green magnetic nanoparticles (Cys-Fe₃O₄) and ozone for the degradation/elimination of methylene blue in textile wastewater

Y.L. Ramirez Salazar¹, L.N. Valero Melo¹, W. Marimon-Bolivar¹, L.P. Tejada² and L. Pulgarín¹

¹Gestión y tecnología para la sustentabilidad de las comunidades – GRIIS, Facultad de Ingeniería, Universidad Católica de Colombia, Bogotá, Colombia

²Chemical Engineering Program, Process Design and Biomass Utilization Research Group, Universidad de Cartagena, Cartagena, Colombia

Corresponding author email: wmarimon@ucatolica.edu.co

Keywords: magnetite Nanoparticles; ozonation; methylene blue.

Introduction

In this research, an improvement of advanced oxidation by means of ozonation with magnetite catalyst was studied, where the percentage removal of methylene blue (MB) in a synthetic sample of textile wastewater was analyzed.

The case study of methylene blue dye removal was selected due to its impact on water pollution resulting from activities in the textile industry, since it is a problem that increases proportionally to population growth since consumption generates greater demand for the use of water resources, either for production and/or for cleaning garments. The accumulation of residues of the agents present in these processes causes direct damage to ecosystems, the greenhouse effect, and, especially, water sources (Wu and Vaneeckhaute, 2022).

The dye is a soluble organic component that provides permanent color in its direct application, resists conventional treatments, and if it is in solution in the triplet state, it is allowed to form superoxide radicals with the ability to oxidize DNA, some lipids, and polysaccharides. As mentioned above, the chemical process of ozonation belonging to advanced oxidation was enhanced and improved, which presents some advantages such as the affordability of the compounds, the easy removal of excess ozone, avoids sludge formation, collaborates in the control of turbidity and odor and, in comparison with the other methods, is more economical. The efficiency of using ozone and the magnetite catalyst was evaluated to generate a combination of nanoparticles that would increase the extent of ozone and thus optimize time and costs.

Materials and methods

For this purpose, green magnetite (Fe₃O₄) nanoparticles (Cys@MNPs) were synthesized, although magnetite is a potential catalyst due to its abundance in the earth's crust and effectiveness in organic synthesis since it provides active sites without modifying the surface, thanks to its oxide-reductive properties. In addition, one of its most incredible benefits is its reusability due to its superparamagnetism, which facilitated using a magnetic field to recover it.

Likewise, they were characterized by XRD analysis: for their crystallography based on the identification of the crystalline planes of the inverse spinel and polycrystals in the different Miller indices of the diffractogram. By means of magnetic properties analysis: it was obtained through a magnetic saturation curve of the nanoparticles synthesized at room temperature, where a value of 82.67 emu/g, it was evidenced a successful decrease of iron (III) to iron (II) atoms with adequate molar ratio for a precipitation reaction and, therefore, a suitable ordering of the magnetic moments and the absence of a magnetic hysteresis loop indicated that the remanence and coercivity were zero, which defined the material as superparamagnetic and with a high separability; These characteristics were verified by approaching an external magnetic field (magnet) to the container containing the solution where the MNPs were attracted and which, when removed, produced a uniform dark brown dissociation. Fourier Transform Infrared Spectroscopy (FTIR): It was used to identify in the fingerprint of the magnetite material the functional groups present in it, as well as the stretches of its bonds; Infrared adsorption length tables (which are represented in the bands) were used as a guide in the curve performed in cm⁻¹ for its recognition, observing bands corresponding to the N-H stretching bond of the amine group (~2994 cm⁻¹) the vibration bond of C=O (~1151 cm⁻¹) the stretching bond of Fe and O corresponding to the presence of magnetic (~229 cm⁻¹) finally the absence of the free bond of Thiol (~2500



cm^{-1}) indicated that the SH in the cysteine is responsible for creating the bond with the particle (Marimón-Bolívar and González, 2018; Marimon-Bolívar, Tejeda-Benítez, et al., 2019).

After preparing the synthetic wastewater, adsorption and removal tests were performed where the initial concentration of the solution was 2 mg/L with a maximum adsorption capacity of 0.008647751 mg/g obtained with linear modeling of the pseudo-second-order models (adsorption kinetics) and Temkin a Langmuir derived equation (adsorption isotherms).

Results and discussion

The former presented higher R^2 and indicated that the adsorption kinetics of methylene blue on Cys@MNPs with an adsorption velocity (between adsorbate and surface) is dominated by chemisorption and that the interactions are located at the so-called active sites. The model's slope and intersection were used to calculate the rate constant (K) 23.54 min^{-1} and the adsorption capacity (q_e) 0.033 mg/g. And the second one with an equilibrium constant (K_0) 0.5425 describes that the binding energy is related to the heat of adsorption comprised of all existing molecules in a layer, which decreases linearly due to the interaction between sorbate and sorbent, respectively.

It was found that the pH was an essential parameter during all the tests because it helps the ionization processes to be carried out. In this case, the one that most favors adsorption is the pH at calcium 9.5. The pH at the point of zero charges (pHPCC) for synthetic magnetite is 7.9, and the pH of the solution with methylene blue was maintained in a range of 5.0- 10. To carry out the process, cysteine (Cys) $\text{CH}_2\text{-CHNH}_2\text{-COOH}$ was used; an amphoteric sulfur amino acid where the acid pH causes a protonation in the amino group and, a basic pH generates a loss of protons in the carboxyl group; therefore, Cys had a positive surface charge favoring the adsorption of cations and a negative surface charge that favored the adsorption of anions. To regulate it, sodium hydroxide (NaOH) and hydrochloric acid HCl were used.

Finally, the percentage removal of methylene blue from synthetic water for this project was 60.7%, using an initial concentration of 2 mg/L and a final concentration of 0.786 mg/L from the adsorption kinetics test in which the time was varied and a 40 mL water sample with 1.5 mL of Cys@MNPs was used. Also, it is corroborated that the higher the ozone concentration, the higher the removal percentage. Since the ozone concentration cannot be controlled, it is adjusted concerning the amount of ozone supplied each time. The condition for this case was 250 mL of wastewater with 10 mL of nanoparticles and 60 minutes of the jar test at 20 RPM.

References

- Marimón-Bolívar, W. and González, E. E. (2018) Green synthesis with enhanced magnetization and life cycle assessment of Fe_3O_4 nanoparticles. *Environmental Nanotechnology, Monitoring and Management*, **9**, 58–66.
- Marimon-Bolívar, W., Tejeda-Benítez, L. P., Núñez-Avilés, C. A., and De León-Pérez, D. D. (2019) Evaluation of the in vivo toxicity of green magnetic nanoparticles using *Caenorhabditis elegans* as a biological model. *Environmental Nanotechnology, Monitoring and Management*, **12**.
- Wu, H. and Vaneckhaute, C. (2022) Nutrient recovery from wastewater: A review on the integrated Physicochemical technologies of ammonia stripping, adsorption and struvite precipitation. *Chemical Engineering Journal*, **433**, 133664.



Applying solar distillation for wine lees dewatering and phenols recovery

P. Mastoras¹, S. Vakalis¹, M.S. Fountoulakis¹, A. Xenaki¹, D. Haralambopoulos¹ and A.S. Stasinakis¹

¹Department of Environment, University of the Aegean, Mytilene, Greece
Corresponding author email: pmastoras@env.aegean.gr

keywords: wine lees; solar still; dewatering; Phenols.

Introduction

Wine lees are a by-product of winemaking, consisting of dead and living yeast that settle at the bottom of the wine tanks at the end of alcoholic fermentation (Felix et al., 2021). It can be described as a sludge-looking material with high organic matter content, where treatment is essential before disposal of to the environment. This by-product has not been extensively studied for the recovery of valuable materials such as yeast, tartaric acid, phenolic compound, and other organic compounds (De Iseppi et al., 2021).

Solar still is an environmentally friendly device that use solar energy to treat saline water and wastewater. Also, solar still has been used for the recovery of phenolic compounds for olive mill wastewater and for the dewatering of sewage sludge (Jaradat et al., 2019).

In this study we used an active pilot solar still for the dewatering of wine lees and the recovery of phenolic compounds in distillates and the solid residual remained at the end of the experiments.

Materials and methods

Wine Lees were collected from a local winery at Lesvos Island. They were examined for pH, conductivity, total solids, COD, total phenols, antioxidant activity and for the existence of specific phenolic compounds.

The active pilot solar still (**Figure 1**) consisted of 1.5 m² single slope solar still unit covered with glass in inclination 22°. The under-floor heating system consisted of vacuum tubes solar collectors, heating storage unit and the solar kit.



Picture 1. Schematic diagram of the pilot solar still unit.

Two experiments cycles were conducted. At every cycle the distillate was collected once per day and it was analyzed for pH, conductivity, COD, total phenols, antioxidant activity and for the specific phenolic compounds. At the end of each cycle, the solid residual was also collected for the examination of its water



content and calorific value. Additionally, it was extracted with 40% methanol/water and the extract was analyzed for the total phenolic content and the presence of specific phenolic compounds.

During the experiments the environmental conditions and the temperatures at the solar still were recorded.

Results and discussion

The basic chemicals characteristics of the wine lees that were used in each cycle are presented in **Table 1**.

Table 1. Chemical characteristics of wine lees.

Parameter	1 st cycle	2 nd cycle
COD (mg/L)	261,167 ± 7,751	290,333 ± 10,017
Total Phenols (mg/L)	4,908 ± 148	4,946 ± 617
TSS (mg/L)	686.3 ± 186.7	865.8 ± 18.3

The average reduction of the COD in the distillates was equal to 74.6% with measured average concentrations, at the first cycle equal to 58,640 mg/L and at the second 82,555 mg/L. The total phenolic content of the distillates was equal to 4.4 mg/L at the first cycle and 10.7 mg/L at the second. The antioxidant activity was estimated in Trolox equivalent. In the first cycle it was measured at 28.1 mg/L while at the second at 39.2 mg/L. The chemical extraction of the solid residuals showed that the concentration of total phenols were equal to 3,504 and 4,203 mg/DW Kg at the first and second experimental cycle, respectively. Finally, the average calorific value of the solid residual was measured to 28.25 MJ/DW KJ.

Conclusions

The solar still achieved an important removal of COD; however, the collected distillates do not meet the criteria for safe release to the environment and need further treatment. Concerning the phenolic content of the solid residual, it was revealed that this material could be potentially used for the recovery of phenols. Alternatively and taking into account its high calorific value, it could be used as an alternative fuel.

Acknowledgements: This work was partially funded by the project “FoodOmicsGR_RIComprehensive Characterization of Foods” (MIS 5029057, <http://foodomics.gr/>) which is implemented under the Action “Reinforcement of the Research and Innovation Infrastructure”, funded by the Operational Program Competitiveness, Entrepreneurship, and Innovation (NSRF2014–2020) and co-financed by Greece and the European Union (European Regional Development Fund). The construction of the pilot solar still was funded by the Region of North Aegean (Greece) through the project “Research Infrastructures for the development of novel olive and vine products in Region of North Aegean: RI-Food-Aegean” (MIS: 5021542).

References

- Felix, M., Martínez, I., Sayago, A., Recamales, M.Á.F., 2021. Wine lees: From waste to O/W emulsion stabilizer. *Innovative Food Science and Emerging Technologies*. 74.
- De Iseppi, A., Marangon, M., Vincenzi, S., Lomolino, G., Curioni, A., Divol, B., 2021. A novel approach for the valorization of wine lees as a source of compounds able to modify wine properties. *LWT* 136.
- Jaradat, A., Gharaibeh, S., Altarawneh, K., Hatamleh, R., 2019. Optimum design parameters of solar still unit operating toward olive mill wastewater management. *Jordan Journal of Civil Engineering*. 13.



Heterotrophic growth of *Chlorella sorokiniana* with glycerol and anaerobic digestate: carbon uptake rate and phenolic content

D. Kasiteropoulou¹, G. Papapolymerou¹, D. Ladas¹, A. Mpesios¹ and M.N. Metsoviti¹

¹Dept. of Environmental Studies, University of Thessaly, Gaiopolis, Larissa, Greece

Corresponding author email: dkasiter@uth.gr

keywords: *chlorella sorokiniana*; heterotrophic; glycerol; anaerobic digestate; FAME properties.

Introduction

Microalgae are unicellular photosynthetic organisms and some microalgae species can also grow and multiply heterotrophically in the absence of light if an organic carbon source becomes available and several advantages of heterotrophic growth are discussed and reviewed by Bumbak et al., (2011) and Perez-Garcia & Bashan, (2015). In the heterotrophic growth, industrial by-products or waste streams containing dissolved organic carbon, macronutrients and micronutrients can be used in terms of nutrient recovery, waste minimization and cyclic economy. Anaerobic digestate (AD) is a rich source of macro and micronutrients while, crude glycerol has a very high content in organic carbon. The biomass of microalgae is also reported to contain antioxidant compounds (Coulombier, N. 2021). The aim of this work is to examine the effect of low percentages of anaerobic digestate in the growth medium on the carbon uptake rate using glycerol as the main source of organic carbon and also examine the biomass of *Chlorella sorokiniana* grown with low percentages of anaerobic digestate and glycerol for its content in antioxidants, namely phenolic compounds.

Materials and methods

The cultivation of *C. sorokiniana* carried out in 5L cylindrical glass bioreactors as well as in orthogonal glass bioreactors of 42L. Air was continuously provided to each bioreactor at a rate of about 40 L/(L-h). The bioreactors, the glass tubing and the culture medium were sterilized before use. The microalgae species *C. sorokiniana* (SAG strain 211-31) was obtained from Culture Collection of Algae from the University of Göttingen in Germany (EPSAG). Glycerol and AD were obtained from local biodiesel and biogas plants respectively. AD was filtered, centrifuged and sterilized before use. Biomass was collected via centrifugation at 4000 rpm. For the determination of organic carbon, the method of Walkley–Black was used. An extraction method with the use of innovative vacuum microwave extraction technology (MAW) was used under the following conditions: 60 °C temperature, 1:10 ratio of solid material to solvent and 30 min extraction time. These conditions proved to be optimum for the extraction of phenolic compounds. The polyphenolic content was determined using the Folin-Ciocalteu method (Singleton, et. al. 1999).

Results and discussion

a) Effect of low percentages of AD on the carbon uptake rate

Figure 1 shows the reduction in organic carbon as a function of culture time of *Chlorella sorokiniana* for the initial carbon concentrations as shown and for AD percentages in the four growth media equal to 0% (blank), 4%, 8% and 16%. The carbon uptake rate is obtained from the average slope in the exponential phase. The anaerobic digestate affects the organic carbon uptake rate above 8% AD. The increase is 6% and 13% at AD percentages of 8% and 16% respectively.

b) Phenolic content of the biomass of *Chlorella sorokiniana* using glycerol and AD

The phenolic content of four samples of biomass of *Chlorella sorokiniana* grown heterotrophically with glycerol and anaerobic digestate was analyzed. For the extraction, the use of innovative microwave assisted extraction (MAE) technology was used under the following conditions: a) 60 °C temperature, b) 1:10 ratio of solid to solvent and c) 30 min extraction time. The samples were obtained from four cultivation experiments in which took place in 42-liter bioreactors. The initial concentration of ammonium nitrogen was varied in the four cultivations and it was equal to 108.2 mg/l, 300 mg/l, 800 mg/l and 2000 mg/l while the initial concentration of carbon which, was provided by glycerin, was held nearly constant and equal to 14±0.1 g/l. 12% anaerobic digestate was used. Table 1 summarizes the values of total phenolic compounds measured.

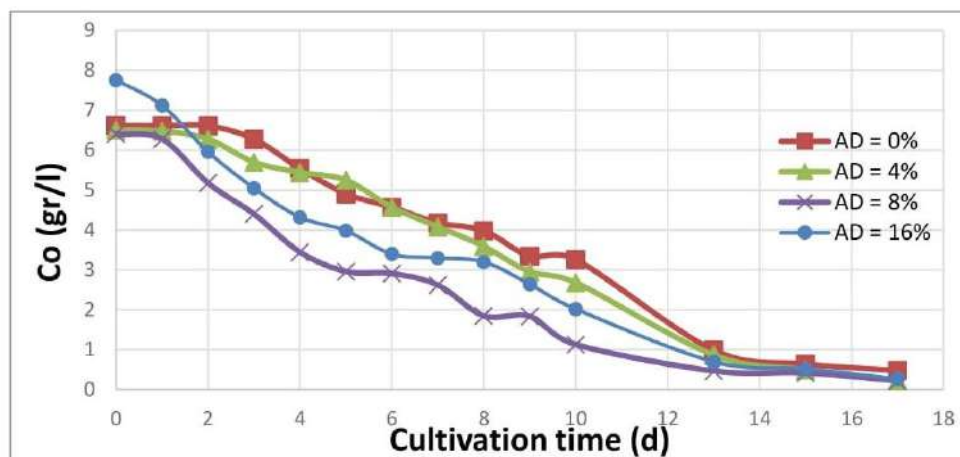


Figure 1. the reduction in organic carbon as a function of culture time of *Chlorella sorokiniana*.

Table 1. Concentration of polyphenols (expressed in mg of gallic acid / g dry weight) of *Chlorella sorokiniana* extracts (cultured with a nitrogen concentration gradient of 108-2000 mg / l), 100 mg of dry matter / ml H₂O, extraction at 30 ° C min, microwave intensity 100W.

N →	108 mg N/l	300 mg N/l	800 mg N/l	2000 mg N/l
Polyphenols (mg/l) →	3.6	2.8	3.4	2.3

We note that in these preliminary measurements a significant amount of polyphenols is measured in the biomass of *Chlorella sorokiniana* grown heterotrophically.

Conclusions

Glycerol is easily absorbed and utilized by *Chlorella sorokiniana*. The anaerobic digestate is a good source for the formulation of growth media for cultivating microalgae heterotrophically and possibly autotrophically. It provides macro and micronutrients and some carbon from undigested organic material thus, reducing the cost of the growth media for microalgal cultivation and also contributes to the recycling of important nutrients such as phosphorus and potassium. At 16%, it increases the carbon uptake rate by 13%. The biomass of *Chlorella sorokiniana* grown heterotrophically is rich in polyphenols. Their concentration ranges from 2.3 mg/l to 3.6 mg/l.

Acknowledgements: The study was co-financed by the European Regional Development Fund of the European Union and Greek national funds through the Operational Program Competitiveness, Entrepreneurship and Innovation, under the call RESEARCH – CREATE - INNOVATE (project code: T1EDK-01580).

References

- Bian, X.; Jin, W.; Gu, Q.; Zhou, X.; Xi, Y.; Tu, R.; Han, S.; Xie, G.; Gao, S.; Wang, Q. Subcritical n-hexane / isopropanol extraction of lipid from wet microalgal pastes of *Scenedesmus obliquus*. *World J. Microbol. Biotechnol.* 2018, 34, 39.
- Bumbak, F., Cook, S., Zachleder, V., Hauser, S., Kovar, K. (2011). Best practices in heterotrophic high-cell-density microalgal processes: achievements, potential and possible limitations. *Applied microbiology and biotechnology*, 91(1), 31-46.
- Coulombier, N.; Jauffrais, T.; Lebouvier, N. Antioxidant Compounds from Microalgae: A Review. *Mar. Drugs* 2021, 19, 549.
- Perez-Garcia, O., Bashan, Y. (2015). Microalgal heterotrophic and mixotrophic culturing for bio-refining: from metabolic routes to techno-economics. *Algal biorefineries*, 61-131.
- Singleton L., V., Orthofer, R., Lamuela-Raventós M., R., Singleton, V.L., Orthofer, R., Lamuela-Raventós, R.M., 1999. Analysis of total phenols and other oxidation substrates and antioxidants by means of folin-ciocalteu reagent. *Oxid. Antioxidants Part A Volume* 299, 152–178.



Influence of rejuvenating agents addition on the properties of zeolite-foamed asphalt

A. Wozzuk¹, M. Wróbel¹ and W. Franus¹

¹ Civil Engineering and Architecture Faculty, Lublin University of Technology, Lublin, Poland
Corresponding author email: a.wozzuk@pollub.pl

keywords: asphalt; zeolite; foamed asphalt.

In recent years, accelerated degradation of road pavements and increasing the amount of reclaimed asphalt pavement (RAP) has been a major problem occurring in many countries [1]. On the other hand, the use of reclaimed asphalt pavement in the asphalt mix is limited due to the altered properties in the aging process of the asphalt. In order to improve the mechanical properties of asphalt mix containing RAP it is necessary to use either softer binder, rejuvenators or bitumen modified with synthetic polymers, while limiting the asphalt aging process is possible through the use of warm mix asphalt technology [2,3]. This paper presents an evaluation of the properties of zeolite foamed asphalts with used engine oil (WEO). In this research, synthetic zeolite NaP1 and natural clinoptilolite soaked with water were used. On the basis of tests of properties of asphalts (dynamic viscosity and penetration) with WEO and zeolites in concentrations of 0, 3, 5, 7%, the optimal amount of zeolite material was determined. Then, water and frost resistance of the asphalt mixture with 20% addition of RAP was determined. The analysis of the results indicates the possibility of using zeolite-foamed asphalt technology with WEO addition.

Materials and methods

The hard road bitumen was used in the tests: 20/30 asphalt penetration grade and waste engine oil from a local car service. The applied additive included: clinoptilolite natural zeolite and NaP1-type synthetic zeolite obtained from fly-ash. In order to improve the "foaming effect", zeolite materials were soaked with water. The water saturation of zeolite in relation to dry mass was 75% in relation to NaP1 and 50% in relation to clinoptilolite. Both materials were added to the bitumens in the amount of 3, 5 and 7% in relation to mass.

Asphalt concrete mixture for subbase course AC 16 P was used as a reference material (tab. 1).

Table 1. Composition of the mix asphalt.

Type of aggregate	Composition of [%]	
	Mineral	Mix
Dolomite 0/2	17.0	16,2
Dolomite 2/8	25.0	23.9
Dolomite 8/11	17.0	16.2
Dolomite 8/16	20.0	19.2
Mineral filler	1.0	0.8
RAP	20.0	19.1
25/55-60 asphalt		3.32
asphalt from the		1.18
Total	100	100

The dynamic viscosity tests were performed using a Brookfield's viscometer according to ASTM D 4402 standard.

The softening point tests were performed according to PN-EN 1427:2009 standard.

The penetration tests were performed in accordance to PN-EN 1426:2009 standard.

Water and frost resistance tests with the result of indirect tensile strength ratio (ITSR) were performed according to EN 12697-12:2018 standard.



slightly lower penetration. This is caused by the effect of bitumen stiffening after adding a solid in the form of dust. Based on the results of bitumen viscosity and penetration tests, a 7% additive calculated for the weight of bitumen contained in the RAP was used in the tests of asphalt mixtures.

Table 2. The results of viscosity tests for 20/30 asphalt with the addition of WEO and zeolites.

addition	7% NaP1	5% NaP1	3% NaP1	7% CLIN	5% CLIN	3% CLIN
Viscosity [mPa·s]						
7% WEO	209	211	212	210	191	179
5% WEO	250	245	231	244	235	236
3% WEO	292	289	274	275	274	267

Table 3. The results of penetration tests for 20/30 asphalt with the addition of WEO and zeolites.

addition	7% NaP1	5% NaP1	3% NaP1	7% CLIN	5% CLIN	3% CLIN
Penetration [0,1 mm]						
7% WEO	49.0	48.2	47.5	44.0	40.4	44.7
5% WEO	37.5	37.0	36.9	36.5	37.8	35.9

The results of the strength properties together with water and frost resistance testing are presented in fig. 1. The reference asphalt mix had the highest average tensile strength values of 1,268 kPa for dry and 1,026 kPa for wet specimens, respectively. After application of the WEO rejuvenator, the strength decreased in both NaP1 zeolite and clinoptilolite samples.

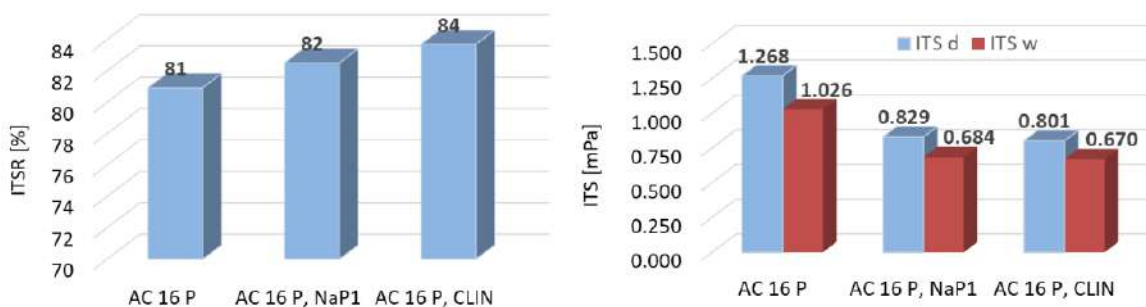


Figure 1. The results of ITSR, ITS_w and ITS_d mix asphalts.

The asphalt mix with synthetically modified asphalt was characterized by the lowest in water and frost resistance with an ITSR value of 81%. Whereas in the other two mixtures made foamed asphalt technology with zeolite, the water and frost resistance was 82% and 84% respectively. The observed ITSR value increase confirms the high effectiveness in using the WEO as a rejuvenator for mix asphalt with RAP produced at a reduced temperature with the addition of zeolite materials.

Acknowledgements: This research was funded by the National Centre for Research and Development of Poland grant number LIDER/5/0013/L-9/17/NCBR/2018

References

- Zhu, Y., Dave, E.V., Rahbar-Rastegar, R., Daniel, J.S., Zofka, A., 2017. Comprehensive evaluation of low-temperature fracture indices for asphalt mixtures, *Road Mater. Pavement Des.* 18 (sup4),467–490.
- Silva, H. Oliveira, J. Jesus, C., 2021. Are totally recycled hot mix asphalts a sustainable alternative for road paving?, *Resour Conserv Recycl*, 60, 38–48.
- Wróbel, M., Wozuk, A., Ratajczak, M., Franus, W., 2021. Properties of reclaimed asphalt pavement mixture with organic rejuvenator. *Construc Building Mater*, 271, 121514.
- Mamun, A.A.; Al-Abdul Wahhab, H. I, 2018. Evaluation of Waste Engine Oil-Rejuvenated Asphalt Concrete Mixtures with High RAP Content, *Adv Mater Science Eng*, 6, 1-8.
- Wozuk, A., 2018, Application of fly ash derived zeolites in warm-mix asphalt technology. *Materials*, 11, 1542.



Potential for biogas production from swine farms in Cyprus

A. Poullou¹ and P. Gikas^{1,2}

¹School of Science and Technology, Hellenic Open University, Patras, Greece

²School of Chemical and Environmental Engineering, Technical University of Crete, Chania, Greece

Corresponding author email: pgikas@tuc.gr

keywords: pig farm; swine farm waste; anaerobic digestion; biogas; Cyprus.

Anaerobic digestion is commonly used for the management of animal manure. Anaerobic digestion improves the quality of manure as fertilizer, while reduces odors and greenhouse gas emissions. The main product of anaerobic digestion, apart from the digestate, is biogas, a mixture of methane (2/3-3/4), carbon dioxide (1/4-1/3) and trace gaseous compounds, which may be used as a fuel for the production of heat, or in Combined Heat and Power units (CHP) for the cogeneration of thermal and electric energy. CHP units have efficiencies between 80-90%, with average thermal and electric energy yields of about 65% and 35%, respectively. Trace amounts of hydrogen sulfide should be effectively removed prior to combustion to avoid engine damage and environmental implications. In practice, 1.0 m³ of biogas may produce the equivalent amount of energy as about 0.5 kg of diesel, contributing to the reduction of 2.6 kg of CO₂.

Swine farm waste is liquid or semi-liquid and is collected almost entirely using drainage channels. It is characterized by a high concentration of suspended solids, which is evident during storage, due to the formation of sedimented matter and scum at the bottom and surface, respectively. It has increased salinity and often high boron concentration, and it is treated at onsite Wastewater Treatment Plants (WWTP). Swine farm waste is an ideal feedstock for anaerobic digesters, as it is rich in organics and in nutrients. The biodegradable fraction in swine slurry has been measured between 32% to 70%, with biogas yields (approximately 65% CH₄) from 5 Nm³/t to 18.1 Nm³/t, corresponding to 0.062 Nm³CH₄/kgCOD to 0.210 m³CH₄/kgCOD, respectively. The observed large spectrum in yield may be attributed to the storage time prior to digestion, thus, it is not efficient to use aged manure slurries for biogas production.

Cyprus has 65 swine farms with about 360,680 pigs and sows, producing about 1.3 million tons of swine farm waste per annum. Swine farm waste management and disposal is particularly demanding, while getting an environmental permit for the establishment of a new unit is complicated. As a result, large swine farms are commonly established next to each other, which imposes problems to neighboring villages, particularly due the emission of unpleasant odors. There are 11 licensed anaerobic digesters utilizing about 477 tones swine farm waste per year (often with up to 10-20% additional organic wastes, such as poultry or cattle waste). In total, about 21.5 GWh of electric energy were exported to the grid, due to biogas production from swine farm waste (2020 data).

The most important environmental legislations that determine the best waste management of Cypriot pig farms are: a) Laws 2002 and 2006, on Water Pollution Control (issuance of Waste Disposal Permits), b) Law 187(I)/2002, on the Control of Atmospheric Pollution, c) Law 56(I)/2003, for Integrated Pollution Prevention and Control, d) Code of Good Agricultural Practice (407/2002).

The present study, focuses on energy consumption and production in three swine farms: Tersefanou and Xylotymbou (Andreou Piglets LTD) at the wider area of Larnaca, and Lagos Farm unit (S. & P. LAGOS FARMA LTD) at the wider area of Nicosia. The total energy-fuel consumptions and energy production for the year 2020 for the studied pig farms are shown below:



Table 1. Electric energy and fuel consumption by the studied farms and electric energy production from biogas, for the year 2020

Parameter	Tersefanou farm	Xylotymbou farm	Lagos farm
Electric energy consumption by the piggery (kWh/yr)	954,400	400,815	510,320
Electric energy consumption by the WWTP (kWh/yr)	128,741	104,590	118,361
	5,713	2,949	22,265
Fuel (diesel) consumption by the WWTP (L/yr)	48,743	37,977	131,673
Electric energy production from biogas (kWh/yr)	3,172,668	2,684,176	4,423,434
Thermal energy production from biogas (kWh/yr)	3,645,215	3,083,265	5,082,274

In 2022, pig farms in Cyprus are experiencing demanding challenges due to the very significant cost increase for pig feed and for electricity. However, pig farms equipped with anaerobic deservers and electric energy production facilities are likely to overcome the financial difficulties with less implications, in compassion with the ones which do not bear such facilities. If all swan farm waste would be utilized for biogas production, it is expected that the electric energy exports to the grit shall increase from 21.5 to over 50 GWh per annum.

References

- Andreou Piglets LTD, 2020. Annual Analytical Report 2020 (Waste Disposal Permit). Xylotymbou-Tersefanou Pig Farms, Cyprus.
- Theofanous, E., Kythreotou, N., Panayiotou, G., Florides, G A., 2014. Energy production from piggery waste using anaerobic digestion: Current status and potential in Cyprus. *Renewable Energy*. 71:263-270.
- www.cea.org.cy, www.iaco.com.cy, www.agroenergy.gr, www.bioenergynews.gr



Challenges for public acceptance of water reuse

E. Gika¹, E.A. Fakorelli¹, V. Bili¹ and P. Gikas¹

¹ School of Chemical and Environmental Engineering, Technical University of Crete, Chania, Greece
Corresponding author email: pgikas@tuc.gr

keywords: water reuse; public acceptance; reclaimed water.

Introduction

Water reuse is a reliable and environmentally friendly option, in water deficient areas, and definitely it lies within the frame of circular economy. Indeed, recent technological advances are mature to provide high quality reclaimed water from wastewater, for almost any type of application: from restricted irrigation to potable uses. However, most water reclamation applications are focusing on either agricultural or recreational applications (potable applications are limited, but they are gradually increasing, especially in areas which are exercising severe water scarcity). Nowadays, the main bottleneck for water reuse is not technology limitations, but the acceptance by the public. Public acceptance is a slow process, which is built with time and with focused efforts of the authorities (central or local), scientists, environmental organizations and individuals educated on the benefits of water reuse (Al-Saidi, 2021).

A number of political, economic, social and institutional factors affect the degree of public acceptance for the use of reclaimed water. In many instances, expensive water reuse facilities have been abandoned due to the lack of willingness by the public to use reclaimed water. The present study aims to identify and discuss the main challenges which affect the public acceptance for water reuse.

Public concerns for water reuse

The main factors affecting the public acceptance for water reuse are outlined below:

- The **degree of contact** with the reclaimed water is of high importance for the persons who use the reclaimed water. The water consumers feel safer when the reclaimed water is not meant for direct use. For example, they may have no problem if the reclaimed water is used for drip agricultural irrigation, while they may feel not comfortable if it is used for sprinkler irrigation, or for irrigating green loans. Needless to say that direct potable reuse raises the highest negative emotions.
- The **time and special conjunctures** occurring during water reuse strongly affects the public opinion. It is accustomed that the social acceptance increases in times of water scarcity, which sometimes may lead in accepting the use of reclaimed water even for potable applications.
- There is **lack of experience and research** specializing on public acceptance for water reuse. Relatively few scientific studies have been conducted on this particular field. As a result, the authorities which plan and implementing water reuse projects, do not have reliable scientific guidance about how to handle the public concerns (Smith *et al.*, 2018).
- The **public's perception of risk**, which is often referred as the “yuck factor”, is often based on vague perceptions. Often the public believes that the reclaimed water contains large amounts of microbes and harmful substances. However, natural water used for irrigation or even for urban water supply may not be of higher quality, compared to reclaimed water. It is thus wise that the public be educated about the high quality standards enforced in water reclamation and distribution processes (Smith *et al.*, 2018).
- **Social, economic and demographic** factors have been found to affect the acceptance of water reuse. In general, educated persons and persons with higher income tend to have a more positive opinion about water reuse. Moreover, the increased concern and sensitivity about the status of the environment, is a further reason driving to the acceptance of water reuse.
- **Public campaigns** definitely affect the attitude of the public towards water reuse. It is important that positive campaigns should involve early the public and the various stakeholders to the decision making processes, so to prevent the formulation of negative opinion by the public (which may be the result of negative campaigns by the opponents for water reuse). It has been documented that often the main



reason for negative campaigns is not the concern for the public health, but political or financial interests may hide behind the motivation of the campaign leaders.

- **Cost** is certainly critical when it comes to the use of reclaimed water. The prevailing public opinion is that reclaimed water should be significantly cheaper, compared to the natural one. If the natural water is offered at relatively low price, then subsidization of the reclaimed water may be required (at least during the beginning of the reclaimed water supply), so to act as a motivation for the use of reclaimed water. Obviously, the higher the level of treatment, the higher the cost of reclaimed water can be expected. On the other hand, the public often expects that the agricultural products grown on reclaimed water should also be significantly cheaper, compared with the ones grown on natural water. In such case it is important that the public is informed about the contribution of water cost to the final cost of the agricultural products (which in almost all cases is marginal, compared with the rest of the costs).

Acceptance of water reuse by various stakeholders

The main sectors who potentially may use reclaimed water are farming, industry and tourist industry. Water reuse for industrial applications is specific to the type of industry, while reclaimed water may not be used in some industrial applications, such as the food industry. The acceptance for the utilization of reclaimed water by the farming and tourist industry is outlined below.

Farmers are most likely to use reclaimed water, compared with other professionals. Due to factors such as water scarcity, high cost of natural irrigational water, or even high cost for the conveyance of natural water, the use of reclaimed water often looks as an attractive alternative. Research has indicated that more than 50% of the farmers would agree to pay for reclaimed water, only if the cost of reclaimed water is less than half the price of the natural irrigational water. Less than 50% of the farmers supported that they would deny the use of reclaimed water even if there is no sufficient supply of irrigational water. On the other hand, just a few farmers are willing to use reclaimed water at a price marginally lower than that of irrigational water. In all cases, farmers have expressed concerns about the potential for the transmission of diseases due to pathogens and about the potential presence of toxic or harmful substances in the reclaimed water. Certainly, campaigns to educate the farmers about the quality of reclaimed water and the benefits from its use, would have a positive impact in improving their perception for water reuse.

Undoubtedly, the **tourist industry** has a much smaller footprint for water consumption, compared to the agricultural and industrial sectors. The increased demand for water in water scarcity areas creates problems in its supply (especially during the summer months). Often there is not enough water to sustain use by the tourists (for personal hygiene), for swimming pools, fountains, watering of green loans, air conditioning, ventilation systems and for cleaning; thus water reuse may often assist to close the water balance. It is worth noting that wastewater production in tourist areas maximizes during the session for high water demand, which eliminates the need for expensive water storage facilities (Gikas and Tchobanoglous, 2009).

Conclusions

A number of factors restricting public acceptance for the use of reclaimed water by the public have been identified in the present study. In order to enhance public acceptance for water reuse, the authorities should primarily emphasize in educating the public regarding the safety of reclaimed water and the environmental benefits rising from its use. Cost is a significant factor, but if the issue would be seen only from the financial point of view, it would not convince the public to reuse water. The study concluded that the early involvement of stakeholders, who will potentially use reclaimed water, to the decision processes for the development of water reuse projects will enhance the public acceptance for reclaimed water use.

References

- Al-Saidi, M., 2021. From Acceptance Snapshots to the Social Acceptability Process: Structuring Knowledge on Attitudes Towards Water Reuse. *Front. Environ. Sci.*, 9.
- Gikas, P. and Tchobanoglous, G., 2009. Sustainable use of water in the Aegean Islands. *J. Environ. Manage.*, 90, 2601–2611.
- Smith, H.M, Brouwer, S., Jeffrey, P. and Frijns, J., 2018. Public responses to water reuse - Understanding the evidence. *J. Environ. Manage.*, 207, 43-50.



A novel microbial biosurfactant/bioemulsifier: Production and characterization

T.P. Silva¹, S.M. Paixão¹, J. Tavares¹ and L. Alves¹

¹LNEG-Laboratório Nacional de Energia e Geologia, IP, Unidade de Bioenergia e Biorrefinarias, Lisboa, Portugal
Corresponding author email: susana.alves@lneg.pt

keywords: biosurfactants; bioemulsifiers; *Gordonia alkanivorans* strain 1B.

Introduction

Currently there is an immediate need for new and more sustainable production methods in most industries. The detergent industry, frequently associated with negative environmental impacts, is also in need of new alternatives, such as biosurfactants/bioemulsifiers (BS/BE). These are naturally synthesized compounds, classified as amphiphilic, for having both hydrophobic and hydrophilic properties. Their application results in a reduction of the surface tension between two immiscible phases, facilitating the mixture of different substances such as water and oil, or water and air (Tavares et al., 2021).

BS/BE present several advantages over conventional detergents, they have lower toxicity and greater biodegradability, resulting in lower negative impacts to both consumers and ecosystems. Furthermore, these compounds present antibiotic, antiviral and antioxidant properties. They can be used in a broad range of pH, temperature and salinity and are effective at small concentrations. This makes them interesting for many other industries, such as food, cosmetics, pharmaceutical and chemical.

BS/BE are commonly produced by microorganisms found in particular environments such as oil wells, hydrocarbon contaminated soils and solid waste lixiviates. These compounds facilitate the access to hydrophobic nutrient sources abundant in these environments, while also increasing the resistance of the microorganisms to such toxic environments.

Gordonia alkanivorans strain 1B, is a bacterium with significant biotechnological potential, which was isolated from oil contaminated soils (Alves et al., 2005). It is mostly known for its biodesulfurizing properties, carotenoid production and broad catabolic range (Silva et al., 2016). The present work focuses on the potential of this strain to produce BS/BE compounds, initial purification and characterization.

Materials and methods

Microorganism and culture media: All assays were performed using the bacterium *Gordonia alkanivorans* strain 1B, isolated in our laboratory, cultivated in a sulfur-free mineral (SFM) medium (Alves et al., 2005).

Preliminary assays: *G. alkanivorans* strain 1B was cultivated with three different individual carbon sources, fructose and glucose, simple sugars commonly used and easily consumed by the bacteria, and olive oil a known hydrophobic inducer. Two different sulfur sources were also tested for their influence on BS/BE production, sodium sulfate (Na_2SO_4) and dibenzothiophene (DBT). Fructose and glucose solutions and olive oil were filter sterilized and added to the medium to obtain 10 g/L of carbon source. Na_2SO_4 or DBT were added as sulfur source to an initial concentration of 300 mg/L and 300 μM respectively. After the growth ended cells were separated through centrifugation and cell-free supernatants were used in emulsification assays (E24) to determine BS/BE production.

BS/BE cellular activity: Bacteria were cultivated with fructose and SO_4 , separated through centrifugation and resuspended in ultra-pure water, to obtain different concentrations of cell suspension. These were used in emulsification tests (E24) to determine cellular BS/BE activity.

BS/BE production and concentration: Bacteria were cultivated with fructose and SO_4 and cell free supernatants were obtained through centrifugation. The cell-free liquids were then mixed with n-heptane in a 4:1 ratio, shaken vigorously and left to rest overnight. After observing the separation of three phases, the middle layer containing the BS/BE was collected, and freeze-dried to obtain a raw BS/BE powder, used in the characterization assays.

Emulsification assays (E24): Cell-free supernatants were mixed with olive oil in a 1:1 ratio in 20 ml tubes, shaken for 60 s and left to rest for 24 h. Emulsification activity was detected by the presence of a layer containing a mixture of water and oil, an emulsion. Relative quantification was obtained by measuring the height of the emulsion and comparing it to the total height of the liquids.



Critical micelle concentration (CMC): Several solutions of crude BS/BE powder were prepared with ultra-pure water, to obtain concentrations between 1.37 mg/L and 841.2 mg/L. These were then taken to a Kruss K12 Mk6 tensiometer and used to determine the influence of the BS/BE concentration on the surface tension (ST) of water. Results obtained in mN/m were plotted and used to calculate CMC for the crude BS/BE. The process was repeated with SDS (0.024–4.723 g/L) and Tween 80 (0.18 and 106.24 mg/L), as benchmark to correctly evaluate the results obtained.

Chemical characterization: Using the raw powder, chemical characterization by CHNS elemental analysis was performed following the ISO 16967:2015.

Results and discussion

The initial screening revealed that strain 1B can produce extracellular substances with emulsifying properties with different degrees of activity depending on culture conditions. The best results were observed using hydrophobic inducers such as olive oil or DBT, while the worst results were obtained combining glucose and sulfate. Nonetheless, activity was detected for every condition tested, with the highest being obtained for fructose and DBT at an E24 of 55.6% with complete emulsification of the hydrophobic layer.

In the assays with bacterial biomass, the highest concentration tested was able to generate an E24 of 95%, with complete emulsification of the aqueous phase. Even when diluted 16 times, a strong emulsion with an E24 of 77% was still observed. This clearly attests to the emulsifying properties of the cells, demonstrating the presence of BS/BE substances not just released to the culture medium, but also adhered to the cells.

Based on the preliminary results, the strain 1B was cultivated in a larger volume, and a method was developed to extract/concentrate the BS/BE compounds, resulting in raw BS/BE powder. This powder was resuspended at different concentrations and taken to a tensiometer, where it was able to lower the surface tension of water from 71.71 to 45.92 mN/m, with only 33.28 mg/L, reaching a CMC of 16.94 mg/L. Even in an unpurified form, these results are similar to what was obtained for Tween 80 (CMC= 6.4 mg/L) and superior to SDS (CMC= 1836.9 mg/L), indicating the potential of this extract.

Finally, the raw powder was taken to an elemental analyzer to access its CHNS composition, revealing that it was mostly constituted by carbon and hydrogen (41.5% and 8.3% respectively) followed by nitrogen (3.4%) and only residual sulfur (<0.3%). These results were within what would be expected and point to a protein content of 21.25%, indicating they are not the main component.

Conclusions

Results show that the strain 1B can produce extracellular and cell-bound compounds with BS/BE properties, even without the presence of hydrophobic inducers. Further work still needs to be performed towards purification and characterization of these substances, however an unpurified extract clearly demonstrated properties equal/superior to some conventional surfactants, proving its potential as a future sustainable alternative to these substances.

Acknowledgements: This work was financed by national funds through FCT (Fundação para a Ciência e a Tecnologia) in the scope of the project GreenFuel (PTDC/EAM-AMB/30975/2017). Tiago P. Silva also acknowledges FCT for his PhD financial support (SFRH/BD/104977/2014).

References

- Alves, L., Salgueiro, R., Rodrigues, ., Mesquita, E., Matos, J. and Gírio, F.M., 2005. Desulfurization of dibenzothiophene, benzothiophene, and other thiophene analogs by a newly isolated bacterium, *Gordonia alkanivorans* strain 1B. *Appl.Biochem. Biotechnol.* 120(3), 199–208.
- Silva, T.P., Paixão, S.M. and Alves, L., 2016. Ability of *Gordonia alkanivorans* strain 1B for high added value carotenoids production. *RSC Adv.*, 6(63), 58055–58063.
- Tavares, J., Alves, L., Silva, T.P. and Paixão, S.M., 2021. Design and validation of an expeditious analytical method to quantify the emulsifying activity during biosurfactants/bioemulsifiers production. *Colloids Surf. B*, 208, 112111.



Mixotrophic cultivation of *Microchloropsis gaditana*

G. Papapolymerou¹, N. Katsoulas², I. T. Karapanagiotidis³ and M. N. Metsoviti¹

¹Dept. of Environmental Studies, Univ. of Thessaly, Gaiopolis, Larissa, Greece

²Dept. of Agriculture, Crop production and Rural Development, University of Thessaly, Volos, Greece

³Dept. of Ichthyology and Aquatic Environment, University of Thessaly, Volos, Greece

Corresponding author email: papapoly@uth.gr

keywords: *microchloropsis gaditana*; mixotrophic; heterotrophic; autotrophic; biomass yield.

Introduction

It is well accepted that microalgae have excellent nutritional properties, as they contain high amounts of proteins, lipids, antioxidants, vitamins (such as A, B1, B2, B6, B12, C, E, biotin, folic acid), minerals (phosphorus, zinc, iron, calcium, selenium, magnesium) and are rich in pigments such as chlorophylls, carotenoids and phenols (Lubián 2000). Some species of microalgae are rich sources of lipids with significant amounts of DHA, EPA and arachidonic acid (AA) that are essential in the diet of fish. Protein content in microalgae varies depending on the species, but also on the growing conditions. The same applies to the content in lipids. Significant amounts of polyunsaturated fatty acids (HUFAs), which are essential in the diet of fish, are also found in the biomass of microalgae (Huerlimann et. al. 2010). Some microalgae species can also grow and multiply heterotrophically in the absence of light if an organic carbon source becomes available (Mata et al., 2010). Mixotrophic cultivation combines autotrophic and heterotrophic growth. The aim of this study is to study the mixotrophic growth of the microalgal species *Microchloropsis gaditana* using four different initial carbon concentrations (C_0) and to compare the biomass yield and biomass productivities with those of the autotrophic and heterotrophic growth.

Materials and methods

The cultivations were carried out in cylindrical bioreactors each of 10L capacity that were filled up to 6L. Air was continuously passed through the solution in each bioreactor at 150 L/hr through 2 mm glass tubing positioned at the tip of a magnetic bar and the air bubbles were dispersed with the magnetic bar at the bottom of the glass flasks at a rotational speed of 500 rpm. The carbon dioxide feed rate corresponds to 0.062 L CO₂ h⁻¹ or 0.026 mole CO₂ h⁻¹. The experiments were performed in the greenhouse of the University of Thessaly under the same conditions of temperature, light intensity, orientation and aeration each time. The pH in all six bioreactors was fixed at 8.5 ±0.3 with the addition of a weak base or weak acid. Crude glycerol, the source of organic carbon, was obtained from a local biodiesel manufacturing plant. Its composition was approximately 86% glycerol, 0.5% methanol, 4% free fatty acids and 7.5% H₂O. Initial nitrogen concentration was fixed in all six bioreactors at 100 mg/l. In the four mixotrophic cultivations and in the heterotrophic cultivation the carbon was supplied from glycerol and the macro and micronutrients from inorganic salts. In the autotrophic cultivation, the macro and micronutrients were supplied by inorganic salts. In the four mixotrophic cultivations all concentrations, except carbon, were equal. Initial carbon concentration was varied and was equal to 2.87 g/l, 2.92 g/l, 3.69 g/l and 4.96 g/l. In the heterotrophic cultivation the initial carbon concentration was equal to 2.24 g/l. The initial nitrogen concentration was equal in all six cultivations and equal to 77.1 mg N/l as ammonium nitrogen and the potassium concentration, 138.7 mg/l, was also equal in all six cultivations. For the determination of organic carbon, the method of Ciavatta et al. was used (1991). The biomass, at the end of the cultivation period, was collected via centrifugation at 4000 rpm for 5 minutes and was dried in an air circulation oven at 45 °C.

Results and discussion

The mode of cultivation and the initial carbon to nitrogen ratio influenced both the time necessary for the organic carbon to be utilized and the rate of carbon uptake. The heterotrophic cultivation required less than 15 days for completion while, the mixotrophic cultivations with C_0/N_0 equal to 37.2 and 37.8 required about



25 days. The carbon uptake rate was higher for the heterotrophic growth and equal to 0.14 g/(l-d) compared to 0.10, 0.12 and 0.09 g/(l-d) for Co/No=37.8, 47.9 and 64.3 respectively for the mixotrophic growth. This is probably due to the fact that in the mixotrophic growth, during the day, organic carbon is not utilized as efficiently because carbon from CO₂ is also used by the *Microchloropsis gaditana*. Also, the biomass yield differed in these cultivations. In the mixotrophic cultivations as the Co/No ratio increased the biomass yield, expressed per gr of organic carbon added to the growth medium, for Co/No=37.2, 37.8 and 47.9 were nearly the same and equal to 1.1, 1.1 and 1.0 gr/(l-gr of C) respectively, declining to 0.85 for Co/No=64.3. For the heterotrophic growth for Co/No=29 the yield was higher and equal to 1.3 gr/(l-gr of C). The autotrophic cultivation gave a yield of 2.8 g/l. The biomass productivity was equal to 0.087, 0,044, 0,044 and 0.034 gr/(l-d-gr of C) for the heterotrophic and the four mixotrophic cultivations respectively. The productivity is much higher for the heterotrophic growth because of the higher yield and shorter cultivation period required. For the autotrophic growth the biomass productivity was 0.086 g/(l-d). At the end of the cultivation period carbon utilization was 76%, 66% and 37% for the mixotrophic cultivations with Co equal to 2.92, 3.69 and 4.96 gr/l respectively while, for the heterotrophic growth with a Co=2.24 gr/l after 15 days 96% of the carbon had been utilized.

Conclusions

The species *Microchloropsis gaditana* can grow in a variety of modes since it absorbs and utilizes glycerol efficiently. The mode of cultivation of the microalgal species *Microchloropsis gaditana* affects the kinetics of carbon reduction as well as the carbon uptake rate. The biomass productivity for the autotrophic growth is 0.086 g/(l-d). Heterotrophic growth appears to be superior if the biomass productivity is expressed in gr/(l-d-gr of carbon supplied). Excess carbon, 4.96 gr/l, in the mixotrophic growth leads to a decrease in biomass productivity per gr of carbon and also decreases the kinetics of carbon reduction because, after 30 days of cultivation only about 37% of the carbon supplied is utilized. This is to compare with a 66% and 76% reduction for 2.92 gr/l and 3.69 gr/l carbon added. For the heterotrophic growth at the end of the cultivation with 2.24 gr/l carbon added 96% of the carbon had been utilized. Therefore, other modes of heterotrophic or mixotrophic cultivation such as heterotrophic semi-batch or mixotrophic semi-batch, in which carbon is added in small amounts, may lead to higher productivities.

Acknowledgements: This study was part of the project coded MIS 5045804 that has been co-financed by Greece and EU under the "Operational Programme Competitiveness, Entrepreneurship and Innovation - EPAnEK 2014-2020".

References

- Ciavatta C., Govi M., Antisari L. V. and Sequi P., Determination of organic carbon in aqueous extracts of soils and fertilizers. *Commun. Soil Sci. Plant Anal.*, 22(9-10) (1991) 795-807.
- Huerlimann R., de Nys R., Heimann K. (2010). Growth, lipid content, productivity, and fatty acid composition of tropical microalgae for scale-up production. *Biotechnol. Bioeng.* 107 (2), 245–257.
- Lubián L. M., Montero O., Moreno-Garrido I., Huertas I. E., Sobrino C., González-Del Valle M., Parés G., (2000). *Nannochloropsis* (Eustigmatophyceae) as source of commercially valuable pigments. *J. Appl. Phycol.* 12 (3–5), 249–255.
- Mata, T. M., Martins, A. A., Caetano, N. S. (2010). Microalgae for biodiesel production and other applications: a review. *Renewable and sustainable energy reviews*, 14(1), 217-232.



Handling and Waste Management of Covid-19 Self and Rapid Tests survey: a data analysis

E. Panourgia¹, T. Daras¹, A. Giannis¹ and E. Maria¹

¹School of Chemical and Environmental Engineering, Technical University of Crete, Chania, Greece.

Corresponding author email: epanourgia@tuc.gr

keywords: *questionnaire; Covid-19; self-tests; rapid tests; perception.*

During the Covid-19 pandemic, precautionary measures were imposed worldwide to minimize virus spread affecting a major part of our lives. For the detection of virus and the return to normalcy, medical tests (named self and rapid tests) were used massively causing new health and environmental challenges. The waste produced by these tests would have been properly handled, stored, and managed because of their probable infectious and hazardous characteristics.

A structured questionnaire was designed to facilitate the assessment of the situation of the waste relevant to self and rapid tests. The purpose was to investigate the social perception and awareness level regarding the disposal and management of such waste. In total, 600 anonymous questionnaires were collected to enable the assessment and reveal possible correlations w.r.t. sex, age, educational level etc.

The questionnaire included 26 questions, and it was divided into 3 sections. The first section referred to the demographic profile of the respondents (gender, age, educational level, type of employment, housing size, income, etc.). The second section examined the diagnostic's screening tests use frequency, the reason of their use etc. The respondents were also asked whether they believe that the results of self and rapid tests are being reliable. The third section focused on the handling and the waste management of the tests. The respondents were asked about the storage and disposal procedure of the waste generated. Moreover, a further information regarding the guidance issue of the Ministry of Environment and Energy about Covid-19 diagnostic tests safe disposal, was given to the interviewees via the survey.

One of the results of the data analysis was that the respondents were not aware about the proper management of the waste of self and rapid tests. The public was not properly informed about safe handling and sorting of such a waste based on the Ministry's guidance. The majority answered that they disposed the used tests together with the household waste regardless of their hazardous and infectious nature. It is highlighted that more than 50% of the interviewees did not know that when the result of a test is positive, the kit should be considered as hazardous and infectious waste. However, the public was willing to separate the waste kits and place them in special bins for safe collection and disposal.

Although the perception and knowledge about proper management of the waste of self and rapid tests is inadequate, the public is also willing to cooperate and communicate with the local waste management authorities aiming to a more efficient and safe waste handling.



Study of the potential accumulation of pesticides in microplastics

S. Martinho¹, V. Cruz Fernandes¹, S.A. Figueiredo¹ and C. Deleure-Matos¹

¹REQUIMTE/LAQV – Instituto Superior de Engenharia do Porto do Instituto Politécnico do Porto 4200-072
Porto, Portugal

Corresponding author email: VirginiaCruz@grag.isep.ipp.pt

keywords: microplastics; pesticides; adsorption; waters.

Introduction

Synthetic polymers, currently known as plastics, have been one of the most used materials in the world. They became a source of pollution all over the world due to their uncountable applications and widespread use. Even though recycling has been growing in the last few years, approximately 50% of plastics have single-use disposable applications, which leads us to an accumulation of plastics in the environment. They will suffer transformations, such as fragmentation and degradation, that lead to the formation of different sizes of plastics, from nano to microplastics (MP). The plastic lifetime is a concern since on one hand good durability allows extended use, and is considered a good material choice, but on the other hand, the resistance to degradation of the plastic wastes is problematic. It is estimated that 10% of the plastics produced end up in the oceans, where they persist, accumulate and are a way of transporting pollutants. There are more microplastics in the soils than in the oceans (4 to 23 times), representing a significant environmental risk. MP are considered a threat to the equilibrium of the environment and human health, not only due to their intrinsic characteristics but also due to their role as carriers for other environmental contaminants. Their reduced dimension, high specific surface area and low density favor the adsorption of other contaminants (e.g. pesticides, pharmaceuticals) and their dissemination in the environment.

Materials and methods

The analytical standard of α -Endosulfan with high purity ($\geq 98\%$) was obtained from Sigma Aldrich-Merck. The chromatograph grade n-hexane was purchased from Merck. The microplastic Low-density Polyethylene (LDPE) (300 μm) was supplied by Goodfellow. Distilled (pH 5.95) and tap water (6.98) samples, collected in REQUIMTE/LAQV laboratory in Porto, Portugal (GPS 41.1815, -8.5937), and river Douro water (pH 7.22), in Portugal (GPS 41.1401, -8.6167), were collected in glass bottles and used in adsorption studies to prepare the α -Endosulfan solutions. The river water sample was previously filtered (pore size 0.45 μm) to eliminate suspended solids.

Batch equilibrium studies were carried out by adding LDPE weighted, with concentrations from 0.30 to 1.40 g L^{-1} , into the glass Erlenmeyer flasks of 50 mL, to 10.0 mL of aqueous solutions of α -Endosulfan, with a concentration of 150 $\mu\text{g L}^{-1}$ (prepared in the previous day). Two aliquots of 1 mL were collected as initial samples. Then the Erlenmeyer flasks were stirred (orbital shaking at 110 rpm) for 48h, which was the equilibrium time (previously determined). Before the collection of samples, the glass Erlenmeyer flasks were agitated in a vortex for 1 minute. The α -Endosulfan was extracted from water using liquid-liquid extraction with n-hexane, in a proportion of 1:1. The mixture was vigorously shaken on the vortex agitator for 30 seconds and then rested for 5 minutes. An aliquot of 500 μL of the extraction solvent (upper layer) was transferred to a glass flask and filtered with a nylon filter of 0.22 μm . The extract was injected, in triplicate, into a gas chromatograph (GC-2100) to determine the α -Endosulfan concentration.

Results and discussion

The Freundlich and Langmuir models were used to fit the results of the equilibrium studies of α -Endosulfan on the LDPE microplastic using different aqueous matrixes (distilled, tap and river waters). The fitted parameters and the statistical analysis for each model are shown in Table 1. Analyzing the results, it is possible to conclude that the Freundlich model presented a better fit for distilled and tap water and Langmuir's model is the best fit for river water.



Table 1. Isotherm model parameters for the sorption of α -Endosulfan on LDPE with the different types of water.

Model	Water	Parameters				
Freundlich		$k_F (\mu\text{g}\cdot\text{g}^{-1} (\text{L}\cdot\mu\text{g}^{-1})^{1/n})$	n	R^2_{adj}	χ^2_{Red}	SSE
	Distilled	89.0 ± 14.0	2.67 ± 0.38	0.955	609.2	3046.2
	Tap	89.1 ± 27.1	5.72 ± 3.74	0.851	498.1	2490.7
	River Douro	100.0 ± 36.3	4.38 ± 2.35	0.908	801.2	2403.6
Langmuir		$k_L (\text{L}\cdot\mu\text{g}^{-1})$	$q_m (\mu\text{g}\cdot\text{g}^{-1})$	R^2_{adj}	χ^2_{Red}	SSE
	Distilled	0.18 ± 0.06	366.4 ± 39.4	0.919	1109.9	5549.7
	Tap	0.71 ± 0.79	157.4 ± 22.3	0.818	607.4	3037.1
	River Douro	0.26 ± 0.19	246.8 ± 38.4	0.912	762.1	2286.2

Despite the best fit model, the statistical difference between them is not significant, so the maximum adsorption capacity ($q_m (\mu\text{g}\cdot\text{L}^{-1})$) estimated by Langmuir's model may be used to compare the LDPE adsorption capacity to α -Endosulfan. LDPE presents a higher adsorption capacity in distilled water, followed by the river water (filtered) and then the tap water (respectively, 366 ± 39 , 247 ± 38 , $157\pm 22 \mu\text{g}\cdot\text{g}^{-1}$). Considering the underlying hypothesis of each model it is possible that for distilled and tap water the interactions between LDPE and α -Endosulfan may occur in a multilayer coverage. Yurtsever et al, 2020 also considered that the Freundlich model could be the best model fit for interactions between LDPE (500 μm)/ α -Endosulfan, although with a lower maximum adsorption capacity ($0.011 \mu\text{g}\cdot\text{g}^{-1}$). The use of different particle sizes has a significant impact on the adsorption capacity, as low is the particle size as higher is expected to be the specific surface area of MP and therefore its adsorption capacity. For the river water, Langmuir's model was considered the best fit, suggesting the occurrence of adsorption in a monolayer's coverage. The research for the equilibrium studies of LDPE is not widely explored to provide comparisons for the adsorption capacities obtained in tap water. However, LDPE has already shown a high capacity to absorb different pollutants, such as PAHs (Fries et al 2012) and PCBs (Allen et al 2018).

Conclusions

In this study, the adsorption of α -Endosulfan onto LDPE was studied in different aqueous matrices (distilled, tap and river waters). Comparing the maximum adsorption capacities estimated for the different types of waters it was possible to observe different behaviors, higher adsorption capacities were observed in distilled water followed by filtered river water and then tap water, which might be related to the lower complexity of the matrix and the lower pH. Pesticides and microplastic particles coexist ubiquitously in soils, being possible the contact with water and therefore the occurrence of interactions between them, such as the adsorption, as demonstrated in this study.

Acknowledgements: This research was funded by the Associate Laboratory for Green Chemistry-LAQV, which received financial support from UIDB/50006/2020, UIDP/50006/2020, and LA/P/0008/2020 by the Fundação para a Ciência e a Tecnologia (FCT)/Ministério da Ciência, Tecnologia e Ensino Superior (MCTES) through national funds. The research was funded also by FCT and BiodivRestore Joint Call 2020–2021—European Union's Horizon 2020 research and innovation programme under grant agreement No 101003777-BiodivRestore-406/DivRestore/0002/2020-BioReset- "Biodiversity restoration and conservation of inland water ecosystems for environmental and human well-being". Virgínia Cruz Fernandes thanks FCT for the financial support through a postdoctoral fellowship (SFRH/BPD/109153/2015).

References

- Fries, E. and Zarfl, C., 2012. Sorption of polycyclic aromatic hydrocarbons (PAHs) to low and high density polyethylene (PE). *Environ Sci Pollut Res Int.*, 19, 1296-1304.
- Allen, T. Farley, S., Draper, J., Clement, C. and Polidoro, B., 2018. Variations in Sorption of Organochlorine Pesticides and PCBs across Six Different Plastic Polymers. *J Environ Toxicol Stud* 2(1).
- Yurtsever, M., Oz, N., Aksu, A., Balkis, N., Altug, G. and Taskin, O. S., 2020. Hydrophobic Pesticide Endosulfan ($\alpha + \beta$) and Endrin Sorption on Different Types of Microplastics. *J.Chem.Soc.Pak.*, 42, 789-797.



A fast and effective analytical method to quantify the emulsifying activity: design and validation

L. Alves¹, J. Tavares¹, T. P. Silva¹ and S.M. Paixão¹

¹LNEG – Laboratório Nacional de Energia e Geologia, IP, Unidade de Bioenergia e Biorrefinarias,
Lisboa, Portugal

Corresponding author email: luis.alves@lneg.pt

keywords: analytical method; emulsifying activity; emulsification unit.

Introduction

Biosurfactants (BS) and bioemulsifiers (BE) are amphiphilic molecules that are produced by a wide range of microorganisms. According to Willumsen and Karlson [1], BS/BE are both surface active biomolecules, but while the surfactants play the role of surface tension reduction, emulsifiers are involved in formation and stabilization of emulsions. However, some biomolecules possess both surfactant and emulsifying properties, which contributes to their unique features, including high biodegradability, low toxicity, effectiveness at extremes of temperature, pH and salinity, and special biological activities (e.g., antimicrobial, antiviral, anticancer, etc). These attributes make them an alternative to their chemical counterparts and allows them to have key roles in several fields [2, 3].

In fact, the chemical composition of BS and BE is different, and this may contribute to their specific roles in nature and biotechnological applications; however, both BS/BE have recognized emulsifying properties, which are the focus of this study. The idea of quantifying the emulsifying activity rather than quantifying the emulsifiers and/or surfactants themselves has been studied before [4]. The concept that stands out is the emulsification index (E24: % emulsification after 24 h) proposed by Cooper and Goldenberg [4], which is still applied, and some of its adaptations such as the one proposed by Trebbau de Acevedo and McInerney [5]. These authors have defined one unit of emulsifying activity as the amount of emulsifier that results in an emulsification (E24) of 20%. Although theoretically simple, these approaches require considerable sample volume, have a long wait (24 h) and are lengthy. Moreover, they can be subjective, since two substances might induce complete emulsion at 24 h, with one resulting in a much denser emulsion. This may indicate more BS/BE activity; however, it is not easily comparable, or demonstratable. Furthermore, due to nature of emulsions and the factors that influence them, small differences in test conditions, such as shape or size of the tubes, or nature of the hydrophobic layer, can generate drastic differences, which hinders reproducibility between authors.

In this context, it is crucial to have a reliable method that not only allows for an accurate evaluation of the BS/BE emulsifying activity during its production conditions, but also that constitutes a valid parameter, which can be consistently comparable for different BS/BE. Therefore, the main goal of this study was the development and validation of a simple, expeditious and inexpensive analytical method to detect, quantify and compare the emulsifying activity of microbial culture broths or BS/BE solutions. Hence, a quantitative assay was developed to measure the emulsifying activity (EA) of any water-soluble compound, based on its ability to form and stabilize emulsion with n-heptane, in a fast, sensitive and reproducible manner.

Materials and methods

Microorganism and BS/BE production - The microorganism used in this work was the bacterium *Gordonia alkanivorans* strain 1B, isolated on our laboratory [6] and kept at a culture collection of microorganisms (CCM at LNEG, Portugal, Lisbon). The BS/BE production by strain 1B was performed as described by Silva et al. [7].

Emulsifying activity (EA) test design and its validation - For the method development and validation, several synthetic surfactants (Tween 80, Tween 20, Triton X-100, SDS and STC), and industrial/domestic dishwashing detergents (Magilar[®] S100 and Fitipol[®], Ultra Pro[®], Super Pop[®], and Fairy[®]) were tested in parallel with the crude BS/BE produced by strain 1B. The preparation of aqueous solutions for synthetic surfactants, industrial/domestic detergents and for crude BS/BE was made by dissolving the different products in ultrapure water to obtain a set of specific known increasing concentrations for each one. After, for each test product concentration, an aliquot (e.g. 10 µL) was diluted in water, up to 1 mL aqueous fraction



in 4 mL screw cap glass tubes (10x75 mm, ND10 caps with PTFE septum), and then 1 mL of n-heptane was added and mixed by vortexing at high speed for 2 min. Lastly, the tubes were left resting vertically for 10 minutes for emulsion detection. A set of emulsification tests with increasing volumes of test product solutions were carried out until 100% emulsion was obtained in the organic phase. One emulsification unit (1 U) consists of the minimum volume of product (volume of emulsifier/surfactant = Vol_{min}) needed to form and maintain 100% emulsion in 1ml of n-heptane. Thus, the corresponding EA value is presented in U/mL and calculated as: $EA(\text{product}) = 1 U/Vol_{min}(\text{mL})$.

Results and conclusions

In this study, a new and simple method to assess the emulsifying activity (EA) was developed and further validated both for BS/BE and for synthetic surfactants/commercial detergents. It is an easy test that enables the obtention of a quantitative value within 10 minutes, by mixing 1 mL of an aqueous solution, containing the product with emulsifying properties (e.g., BS/BE or synthetic surfactants), with 1 mL of n-heptane as the organic phase. In this analytical approach, the EA can be evaluated through the quantification of emulsification units per mL (U/mL), with one emulsification unit (1 U) defined as the minimum amount of test product (volume, up to 1 mL) needed to form and maintain 100% emulsion of 1 mL of n-heptane. So, for the crude BS/BE (0.352 g/L solution), 1 U = 350 μ L and the corresponding EA = $1/0.350 = 2.86$ U/mL, while for Tween 80 (0.289 g/L solution), 1 U = 30 μ L and the correspondent EA = $1/0.065 = 15.38$ U/mL.

In this test method a rapid and stable emulsion is obtained, and, moreover, the sample amount required is usually very small. These features are an advantage towards a quick quantification of the EA for a great number of samples, primarily for screen/monitoring assays of products with emulsifying properties (BS/BE).

Furthermore, the specific emulsifying activity (SEA in U/g) for each product tested can be estimated through correlation analysis (linear regression) between volumetric emulsifying activity (U/mL) and product concentration (g/L) allowing actual data comparison between different products with emulsifying properties (BS/BE or synthetic surfactants/detergents).

In overall, the novel analytical method proposed seems to be a fundamental tool for at-line quantification/estimation of emulsifying activity required for the prospecting of new microbial sources of BS/BE and monitoring the production of these natural compounds within microbial cultivation process.

Acknowledgments: This work was financed by national funds through FCT (Fundação para a Ciência e a Tecnologia) in the scope of the project GreenFuel (PTDC/EAM-AMB/30975/2017). Tiago P. Silva also acknowledges FCT for his PhD financial support (SFRH/BD/104977/2014).

References

- Willumsen, P.A. and Karlson, U., 1997. Screening of bacteria, isolated from PAH-contaminated soil, for production of biosurfactants and bioemulsifiers. *Biodegradation*, 7, 415–423.
- Jahan, R., Bodratti, A.M., Tsianou, M. and Alexandridis, P., 2020. Biosurfactants, natural alternatives to synthetic surfactants: Physicochemical properties and applications. *Adv. Colloid Interface Sci.*, 275, 102061.
- Uzoigwe C., Burgess, J.G., Ennis, C.J. and Rahman, P.K.S.M., 2015. Bioemulsifiers are not biosurfactants and require different screening approaches. *Front. Microbiol.*, 6:245.
- Cooper, D. and Goldenberg, B., 1987. Surface-active agents from two *Bacillus* species. *Appl. Environ. Microbiol.* 53(2), 224-229.
- Trebbau de Acevedo, G. and McInerney, M.J., 1996. Emulsifying activity in thermophilic and extremely thermophilic microorganisms. *J. Ind. Microbiol.*, 16, 1–7.
- Alves, L., Salgueiro, R., Rodrigues, C., Mesquita, E., Matos, J. and Gírio, F.M., 2005. Desulfurization of dibenzothiophene, benzothiophene and other thiophene analogues by a newly isolated bacterium, *Gordonia alkanivorans* strain 1B. *Appl. Biochem. Biotechnol.*, 120, 199–208.
- Silva, T.P., Paixão, S.M., Tavares, J., Gil, C.V., Torres, C.A.V., Freitas, F. and Alves, L., 2022. A new biosurfactant/bioemulsifier from *Gordonia alkanivorans* strain 1B: Production and characterization". *Processes*, 10(5):845.



Thermodynamic characterization of Liquid-Vapor Equilibria of Propionic Acid-Water and Acetic Acid-water at atmospheric pressure

L. Mazzeo¹ and V. Piemonte¹

¹Department of Engineering, University Campus Biomedico of Rome, Rome, Italy

Corresponding author email: l.mazzeo@unicampus.it

keywords: Acetic Acid; Propionic Acid; Vapor Liquid Equilibrium; NRTL.

Introduction

Propionic acid is a Volatile Fatty Acid (VFA) which global market is projected to reach the size of US\$1.8 Billion by 2027 [1]. Such molecule finds its main application as a food preservative which account for nearly 78% of its total consumption. Propionic acid it is also employed in the food industry (as aroma additive, food additive and flavoring) and in the pharmaceutical industry (for pharmaceuticals and solvents formulation). The price of Propionic Acid was estimate to be 2000-2500 €/ton [2]. Although the main production of Propionic Acid occurs by means of ethylene carbonylation, oxidation of propanal and direct oxidation of hydrocarbons [3], nowadays increasing attention is given to the production of such molecule by means of Anaerobic Digestion [4]. As a matter of fact, currently it was investigated the potential of AD as an environmentally friendly alternative for the production of bulk chemicals such as Volatile Fatty Acids (VFAs)

[5]. In this context rises the necessity to analyze different methods for the possible recovery of VFAs from fermentation broth in which water and Acetic acid (among all the other VFAs) are abundant. This works sets a first step on this path studying the Vapor-liquid equilibrium of the mixture Propionic acid-water and Acetic acid-water at 1 atm. The aim of his work is then to increase the literature data for the liquid vapor equilibrium at 1 atm for the binary systems Propionic Acid-Water and Acetic Acid-Water and to evaluate the goodness of NRTL model in describing the liquid phase deviations from ideality.

Materials and methods

Analytical grade Propionic acid (C₃H₆O₂) and Acetic Acid (C₂H₄O₂) reagent were purchased from Sigma Aldrich (United States) and used without any further purification together with distilled water. The measured Refractive Indexes (RI) of both components are shown in Table 1.

Table 1. Refractive index of pure compounds at 25°C.

Compound	RI measured
Acetic Acid	1.3705 ± 0.0005
Propionic Acid	1.3843 ± 0.0005
Water	1.3340 ± 0.0005

The experimental runs were carried out in a modified Gillespie vapor recirculation still already used in other works [12]. Details of the apparatus are reported elsewhere [13]. The condenser of the still was open to the atmosphere in order to keep the system at atmospheric pressure. The equilibrium temperature was measured by means of an Hg thermometer with an accuracy of ± 0.1 °C. Isobaric liquid-vapor equilibrium data were collected once no changes in the measured temperature were observed. Such condition was reached after 30 – 45 minutes from the beginning of each test. The liquid samples at equilibrium (liquid phase and the condensed vapor phase) were analyzed using a Bawch and Lomb Abbe-3L precision refractometer.

Results and discussion

In Figure 1 were reported the equilibrium curves for both Propionic Acid-water (Figure 1a) and Acetic Acid-water (Figure 1b) systems. The experimental data collected in this work are in good agreement with literature ones, in particular for the system Propionic Acid-water the data were compared with the ones of Dakshinamurty et al. [6] and Ito & Yoshida [7] while for the system Acetic Acid-water they were compared with the ones of Sebastiani et al. [8] and Ito & Yoshida [7]. The non-ideal behavior of the vapor phase was



Preliminary performance evaluation for chicken manure treatment and valorization options

D. Gavrilescu¹, G. Barjoveanu¹, P. Apopei¹, C. Teodosiu¹ and A. Talpalaru¹

¹Department of Environmental Engineering and Management, Gheorghe Asachi Technical University of Iasi, Romania

Corresponding author email: gb@tuiasi.ro

keywords: chicken manure; composting; performance evaluation; process modeling.

Introduction

In view of the new European paradigm of the circular economy which calls for closing the life cycles of most waste streams, this study presents a preliminary evaluation of several technological options which can be employed for the valorization of chicken manure. This type of waste represents a major challenge for poultry farms because of the high generation rates and the strict rules for its management. On the other hand, chicken manure is a high humidity material, it has acidic pH values and contains high quantities of nutrients (nitrogen, phosphorus and potassium) which makes it a very suitable material to obtain fertilizers from. The vast majority of the poultry waste is currently landfilled, but technologies like anaerobic digestion and composting are promising in transforming this waste into a valuable fertilization product. The biological degradation of chicken manure, be it anaerobic in the case of digestion, or aerobic as in the case of composting, poses some serious engineering challenges, as compared to other similar waste streams, due to its particular characteristics: high acidity which limits the type and activity of specialized microbial consortia, low C:N ratio which impedes biological processes start-ups.

The main objective of this study is to investigate a series of technological options and different substrate mixes from a technological, environmental and economical point of view, to ensure the treatment of chicken manure coming from a poultry farm with 80000 chicken, producing 10000 kg of manure/day.

Materials and methods

Our research strategy, as presented in figure 1 considers two technologies, namely anaerobic digestion and composting, and for the latter one we investigate two different technological variants: windrow (classic) composting and an in-vessel forced-aeration composting. Furthermore, we investigate 4 substrate mixes: (chicken manure plus, saw-dust, wheat straw, charcoal and lignite respectively).

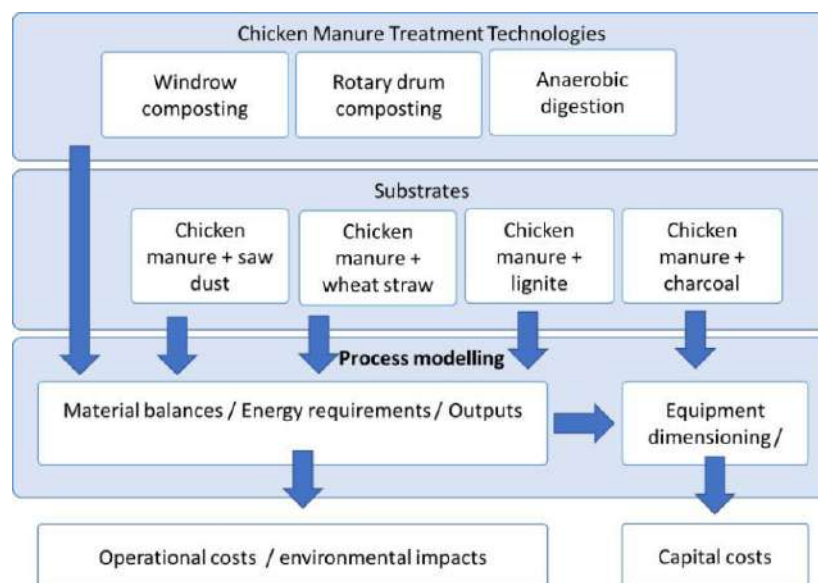


Figure 1. Research methodology.



The four substrates are mixes of chicken manure and another material which has the purpose of raising the C:N ration to a targeted value of 30:1, as only the manure has a C:N ratio of only 9:1. The other objective of using a different material is to create and maintain a mixture in which the air, liquid and solid phases are evenly distributed so as the biological processes occur at a high and controllable pace.

In the next step, chicken manure and filler material composition data were used as inputs into a modeling process in which aeration and energy requirements were calculated, as well as final compost mix. This data was then used to calculate the dimensions of equipments which subsequently was analyzed against a set of performance criteria. In order to achieve the main objective of the study, preliminary criteria were selected to analyze the suitability of a treatment technology for these waste mixtures. These criteria refer to: area requirements, greenhouse gas emissions, energy impacts and economic costs. The area requirements were calculated by considering the most common composting options: windrow composting (in different geometric configurations: triangular, trapezoidal and semicircle) and in-vessel composting in rotary drum; and anaerobic digestion for small and medium scale biogas installations (classic fixed dome, as well as Deenbandhu and Chinese models, floating drum and balloon types, according to the IRENA 2016 classification). The greenhouse gas emissions generation, expressed as tones CO₂e/year, the energy (GJ/year) and economic impact (RON/year, in wages and taxes and employment hours/year) from each waste management option, were calculated according to the US EPA WARM 2020 methodology.

Results and discussion

The area requirements results indicate that from the composting options, in-vessel composting in rotary drums, needs the minimum space. Compared to all anaerobic digestion installations, the in-vessel composting gives similar results with the balloon digesters, while the other anaerobic digestion options have less space requirements, because most installations are vertical.

In terms of greenhouse gas emission reductions, compared to the reference scenario, chicken manure drying and landfilling, the best results are obtained in the case of anaerobic digestion with digestate direct land application, followed by composting and anaerobic digestion with digestate curing. In terms of energy impact, the best option would be anaerobic digestion based on CH₄ production and further usage, while the in-vessel composting has the highest energy impact. In terms of economic impact, composting and landfilling have approximately the same employment hours/year and composting registers minimum wages and taxes. The in-vessel composting generates the highest income, while the anaerobic digestion generates the highest capital costs.

When comparing the different composting mixes, the wheat straw has generated the lowest technical performance (despite its cheapest economical costs), while the lignite has had the best technical performance and the most promising economical advantages.

Conclusions

This work has considered different technological options for the treatment of chicken manure which is a particularly difficult animal waste type to treat. Our analysis has investigated 2 technologies and 4 types of different waste mixes. Given the preliminary results, some advantages and disadvantages of these technologies and options could be identified, but further investigations are required to select the most suitable treatment option, because several other parameters need to be considered.

Acknowledgements: This work was supported by a grant funded by the Regional Operational Program 2014-2020, POR/1/1.1/OS 1.2/1, project number 136527, contract no: 7288/2021, “Integrated solutions for chicken manure waste management”- Chicken Waste.



Effect of granular activated carbon (GAC) addition in a pilot-scale anaerobic digester treating sheep manure and agro-industrial wastewater

D. Kalantzis¹, I. Daskaloudis¹, D.F. Lekkas¹, T. Lacoere², J. De Vrieze² and M.S. Fountoulakis¹

¹Department of Environment, University of the Aegean, Mytilene, Greece

²Center of Microbial Ecology and Technology (CMET), University of Ghent, Gent, Belgium

Corresponding author email: fountoulakis@env.aegean.gr

keywords: agro-industrial wastewater, anaerobic digestion, granular activated carbon, methane, circular economy.

Introduction

It is an undeniable fact that climate change has been and will continue to be one of the most prominent global issues that humanity faces. One of the most ambitious climate targets, is the transition to energy sources characterized by low carbon footprint, such as renewable energy sources. At the same time, there are unsolved serious issues like the unproperly management of many waste types. One way to deal with these problems is the utilization of waste with anaerobic digestion, where the treatment of waste accompanied with biogas production, that can be used as a replacement of fossil fuels in activities like transport, heating, and power production (Hublin et al., 2014).

Recent studies shown that the addition of electrically conductive material such as activated carbon, biochar, carbon cloth and graphite in anaerobic digesters could a) reduce lag time for methane formation between 10-75%, b) increase methane formation rate by 79-300% and c) improve the resistance of anaerobic digesters to low pH condition and high ammonia concentration (Park et al., 2018). However, these promising results were obtained mostly from lab-scale experiments. Therefore, it is important to validate the benefits of conductive material addition at pilot-scale.

In this context, the scope of this work was to examine the effect of granular activated carbon (GAC) addition into a pilot-scale anaerobic digester treating sheep manure and agro-industrial wastewater. Furthermore, the effect of GAC addition on downstream process (membrane bioreactor) was monitored.

Materials and methods

The pilot-scale wastewater treatment plant used in the experiment is presented in Figure 1. A 180-L anaerobic CSTR reactor fed with agro-industrial wastewater and sheep manure was operated for 222 days at mesophilic conditions. The hydraulic retention time applied in the anaerobic digester was 56 d for the first 104 days and then reduced to 25 days. At the final phase of the experiment, GAC (10g/L) was added in the digester. During the 7.5 months of operation, samples were collecting every 2 days per week and analyzed for pH, Total Solids (TS), Volatile Solids (VS) and Chemical Oxygen Demand (COD). All physicochemical parameters were measured according to Standard Methods (ALPHA, 1999). Biogas flow was measured using a drum-type gas meter (TG 0.5, Ritter), while biogas composition was analyzed using an Agilent 6890N gas chromatograph. The pH, TS, VS and COD content of feedstock was 5.9 ± 0.8 , 11.5 ± 2.5 g/L, 8.0 ± 2.4 g/L and 20.9 ± 7.9 g/L respectively.

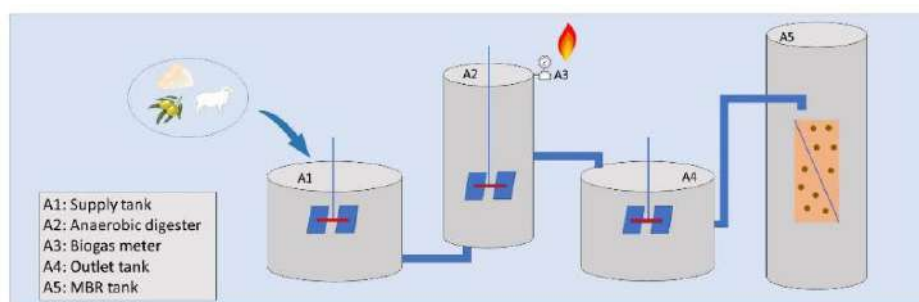


Figure 1. Schematic presentation of pilot-scale treatment unit.



Results and discussion

Figure 2 shown the daily average biogas production prior (last month) and after the addition of GAC. Biogas production rate increased from 26.6 L/d to 35.9 L/d after the addition of GAC. Moreover, methane content increased from 61-62% to 67-70%. The quality of the MBR effluent was almost the same (COD: 152 mg/L, turbidity: 1.5 NTU) during the experiment indicating that GAC had no negative effect on downstream process. Results obtained in this study validate the positive effect of GAC addition in the anaerobic digestion process. Lab-scales experiments in the past found that GAC addition in doses ranged from 1 to 50 g/L could increase biogas production rate from -15 to 390% (Kutlar et al., 2022). In this study an increased of about 35% was recorded. This increase could be probably correlated with the promotion of direct interspecies electron transfer (DIET) as reported in the previous works (Gahlot et al., 2020).

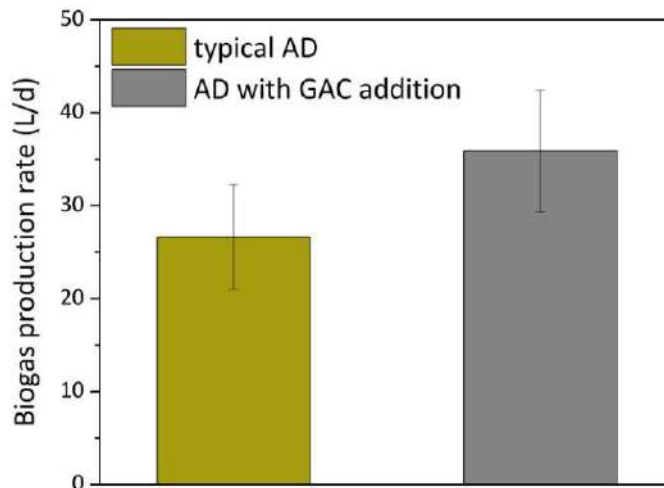


Figure 2. Average biogas production rate in pilot-scale anaerobic digester prior and after the addition of GAC.

Conclusions

The addition of GAC in a pilot-scale anaerobic digester treating sheep manure, olive mill wastewater and dairy wastewater increases biogas production rate and methane content. The presence of GAC in the digestate had no negative effect on the effluent quality of an aerobic membrane bioreactor.

Acknowledgements: We acknowledge support of this work by the project “Center of Sustainable and Circular Bioeconomy [Aegean_BIOECONOMY]” (MIS 5045851) which is implemented under the Action “Reinforcement of the Research and Innovation Infrastructure”, funded by the Operational Programme “Competitiveness, Entrepreneurship and Innovation” (NSRF 2014-2020) and co-financed by Greece and the European Union (European Regional Development Fund).

References

- American Public Health Association (APHA) (1999). Standard methods for the examination of water and wastewater. 20th Edition, APHA, Washington DC, 1268 p.
- Gahlot, P., Ahmed, B., et al. 2020. Conductive material engineered direct interspecies electron transfer (DIET) in anaerobic digestion: Mechanism and application. *Environ. Technol. Innov.* 20, 101056.
- Hublin, A., Schneider, D. R., & Džodan, J. 2014. Utilization of biogas produced by anaerobic digestion of agro-industrial waste: Energy, economic and environmental effects. *Waste Management & Research: The Journal for a Sustainable Circular Economy*, 32(7), 626–633.
- Kutlar, F.E. Tunca, B. Yilmazel Y.D. 2021. Carbon-based conductive materials enhance biomethane recovery from organic wastes: a review of the impacts on anaerobic treatment. *Chemosphere* 133247
- Park, J.H. Kang, H-J., et al. 2018. Direct interspecies electron transfer via conductive materials: a perspective for anaerobic digestion applications *Bioresour. Technol.*, 254, 300-311



ETV as tool dedicated to acceleration of market uptake and diffusion of green innovations. The LIFEproETV project

E. De Marco¹, S. Scaffoni¹ and R. Preka¹, E. Mancuso¹, I. Ratman-Kłosińska² and T. Beltrani¹

¹RISE (Resource Valorisation) Laboratory, ENEA, Rome, Italy

²Institute for Ecology of Industrial Areas, Department of international Cooperation, Katowice, Poland
Corresponding author email: emanuela.demarco@enea.it

keywords: *environmental technologies; verification; promotion; innovation; scheme.*

Introduction

Despite an increasing demand for green innovations due to challenges posed by the EU with the New Green Deal, their market still remains a challenge to developers and providers. The barriers encountered in the market entry of green innovations lead to missed opportunities for addressing the innovation challenge of sustainable transitions offered by these technologies. To eliminate this barrier, it is necessary to promote and build strong market acceptance and recognition of tools that deliver sufficient and trustful proofs about the performance of green innovations and make the benefits of their application obvious to users. One of these tools is the EU Environmental Technology Verification (ETV), a voluntary environmental scheme dedicated to help new environmental technologies enter the market.

However, ETV has not gained strong market acceptance and recognition as a brand representing new reliable technical solutions with environmental added value to effectively fulfill its role, so its ETV potential is greatly underused at EU level and of the Member States.

LIFEproETV project promotes, provides knowledge, develops skills, capacities and enables the political environment to create strong acceptance and recognition of environmental technology verification as a voluntary scheme to support market adoption of innovative environmental technologies.

The objective of this contribution is to identify and explore the drivers for boosting the ETV potential for market acceptance and recognition.

Materials and methods

The activities of the LifeProETV project have focused on the definition of the key reasons for low ETV market uptake and consequent addressing of these reasons while defining actions needed to boost the ETV potential for market acceptance and recognition at EU and national level.

The LIFEproETV project therefore intends to promote the ETV scheme and create strong brand awareness, market acceptance and recognition of ETVs on the European market.

The actions implemented will contribute to the creation of a political environment favorable for the ETV to its use in public procurement, as well as to the knowledge and promotion of the ETV scheme through the organization of workshops, guidance and coaching activities to develop skills, competences and understanding of ETV among technology providers, buyers, policy makers and other stakeholders. Life pro ETV projects aims also to provide an ETV Knowledge Platform with information materials, guidance and tools, to improve access to ETV information by creating an ETV Knowledge Centers network.

Results and discussion

The research done has regarded a thorough analysis of the context of ETV at EU and national level (6 partner countries) considering value perception of the scheme, policy framework, financial factors, ease of access of the scheme, compatibility, infrastructure, ETV awareness etc. After consultation with the stakeholders panel and direct interviews to potential beneficiaries of the scheme, key contributors to boost factors determining the ETV market uptake and recognition have been defined and explored.



Finally, extended objectives and scope, a strengthened credibility and certainty as well as a collaborative institutional framework through concrete actions, will enforce the ETV uptake and improve the environmental technologies market.

Demonstrating the added value of ETV and building its operational links with the EU Green Deal and national/regional policies should help promote and adopt the scheme as a tool to support policies relevant to sustainable industrial processes, zero pollution targets and green financing.

Promoting the use of ETV in public procurement should enhance the competitive advantage of ETV and foster procurement practices of buyers. Information tools for technology providers should help them prepare more effectively for ETV. The promotion of ETV through the involvement of Business Support Organizations as information and promotion centers should increase the reach of ETV and contribute to a better awareness of this useful tool to support innovation.

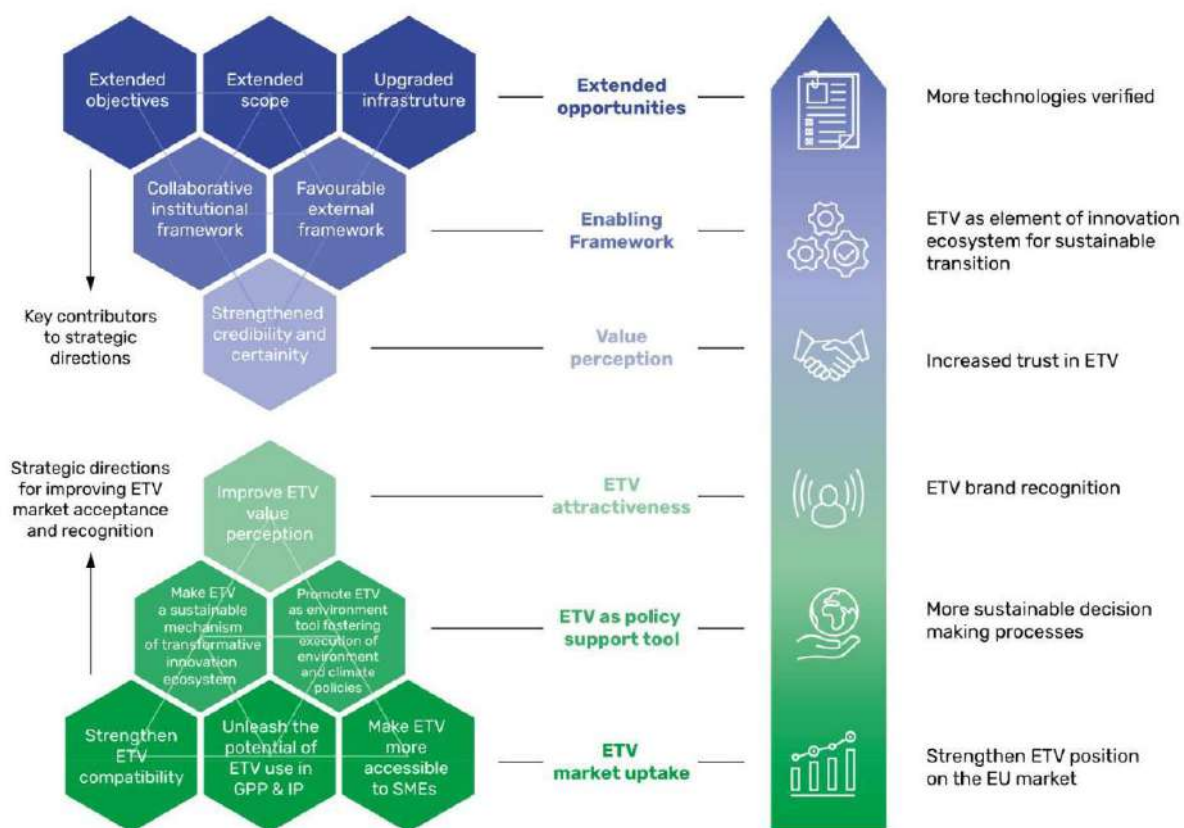


Figure 1. Contributors and strategic directions: building a mutually supportive framework for increasing the market acceptance and recognition of ETV.

Acknowledgements: This study is supported the LIFE project (EC): “Promotion and implementation of ETV as an EU voluntary scheme for verifying performance of environmental technologies”, LIFE19 GIE/PL/000784. LIFEproETV project has received funding from the European Union’s LIFE Programme and is co-financed by the National Fund for Environmental Protection and Water Management, Poland and the Ministry of Agriculture, Hungary

References

- European Commission, Environment General Directorate, 2018. Support study for the evaluation of the EU ETV pilot programme including an ex-ante assessment of possible options for the future of an EU ETV scheme: final report, Publications Office, 2018, <https://data.europa.eu/doi/10.2779/041303>
- Commission Staff Working Paper, 2011. The Environmental Technology Verification (ETV) initiative Helping Eco-Innovations to reach the Market, Accompanying the document, Communication from the Commission to the European Parliament, the Council, The European Economic and Social Committee and the Committee of the Regions Innovation for a sustainable Future - The Eco-innovation Action Plan (Eco-AP), https://ec.europa.eu/environment/ecoap/sites/default/files/etvfiles/documents/sec_2011_1600_f1_other_staff_working_paper_en_v3_p1_674169.pdf



Smart Water Management

E. Vgenopoulou¹, L. Evrenoglou¹, O. Cavoura¹, G. Zervas¹ and I. Damikouka¹

¹Department of Public Health Policy, School of Public Health, University of West Attica, Athens, Greece
Corresponding author email: idadamikouka@uniwa.gr

keywords: *water pressures; water safety; real time control; smart monitoring systems.*

Introduction

Water plays a leading role in sustainable development. However, it is subject to great pressures due to an imbalance between supply and demand (Ding & Ghosh, 2017). Population growth, intensive urbanization and climate change are affecting its quantity and quality, causing global concern, as the lack of adequate clean and safe water is a major cause of morbidity and mortality (Su et al., 2020). A sustainable future requires adequate water management to meet the challenges and the needs of present and future generations (Li et al., 2020). Awareness of this need combined with the achievements of evolving technology, has contributed to the development of Smart Water Management (SWM) and the implementation of various projects within it, aimed at addressing emerging challenges (Su et al., 2020). Using technology, water resources can be managed sustainably and preserved for future use.

Materials and methods

Technological developments in water management are presented and in particular, based on the international literature, innovative technologies are examined within the framework of SWM, which contribute to the reduction of water losses and the assurance of its quality. In addition, technological solutions related to rainwater management, efficient irrigation and desalination, that contribute to the development of a sustainable environment are explored.

Results and discussion

The implementation of smart solutions and the conversion of data into active information in real time, improves decision-making and contributes to the optimization of water management with a view to their safety, a key factor in achieving sustainable development. Applied tools like sensors, smart meters, geographic information systems, etc., offer improved levels of monitoring, early warning, automatic control and operational efficiency in a wide range of applications:

- SMART WATER LOSS MANAGEMENT: allows timely management of water loss through the detection of leaks and immediate response, providing the possibility of improved system operation and sustainable water use. In addition, a balance between supply and demand is achieved, as is timely information dissemination to the public about the consumption, raising awareness about use.
- SMART WATER QUALITY MONITORING: allows early warning of reduced water quality, suggests appropriate corrective actions and can predict future events. The combination of smart monitoring and risk assessment contributes to a rapid and reliable strategy to improve drinking water quality and protect public health.
- SMART RAINWATER MANAGEMENT: allows the dynamic management of the quantity and quality of rainwater, as the current conditions of the system and any predicted inputs are considered in order to make decisions (Shishegar et al., 2019). Real-time control prioritizes infrastructure maintenance, improves system resilience, enables up-to-date climate change adaptation decisions, and helps ensure a sustainable future.
- SMART IRRIGATION MANAGEMENT: allows the efficient utilization of water, through the determination of crop specific irrigation time and water quantity. In addition to water savings of up to 72%, better crop yields, higher quality in the final product and reduction of agricultural costs can be achieved, while farmers can be informed in real time. Intelligent irrigation techniques can also be extended to conserve rainwater, increase groundwater, protect crops from unpredictable rainfall, reuse irrigation water, and sustain water resources (Masseroni et al., 2020).



- SMART DEALTION MANAGEMENT: allows early identification of water quality issues, prevention of pipeline corrosion and timely response (Alshehri et al., 2021).

Many countries have adopted such smart approaches in tackling pressures and improving water resource management, achieving many of the Sustainable Development Goals (SDGs), while providing the framework for effective SWM implementation (eg extreme floods in Korea, reduced water usage and leaks). However, standardization and the development of best practices, cross-sectoral policies and good governance are essential. More incentives for funding and research need to be provided. Training, public awareness and data encryption are required. With political will, collective planning, participation and the exchange of information, SWM systems can be developed to address global water issues. However, only a holistic response can address the complexity of water management in urban environments.

Conclusions

Sustainable access to safe water is one of the biggest challenges and will become even greater in the future. Intensive urbanization is exacerbating water pressures associated with rapid population growth and the effects of climate change. SWM with real-time remote monitoring, ensures their management with accuracy and efficiency. The development of smart systems promotes sustainability and needs to be further explored and implemented as part of broader strategic approaches to meet the demands of the present and the future. Through smart system implementation, automated control, improved decision-making and water monitoring and management can be realized, ensuring both water quality and public health, while maintaining the vision of safe, clean water for all.

References

- Alshehri, M., Bhardwaj, A., Kumar, M., Mishra, S. & Gyani, J., 2021. Cloud and IoT based smart architecture for desalination water treatment. *Environmental Research*, 195, 110812
- Ding, K., Ghosh, S., 2017. Sustainable Water Management. A strategy for Maintaining future water resources. *Encyclopedia of Sustainable Technologies, University of Technology Sydney, Ultimo, NSW, Australia*.
- Li, X., Wang, T., Sun, H., Xu, N., Bao, F., 2020. Strengthening monitoring and supervision of water supply utilities in rural areas: Research and practices. *China Water Resour.*, 5, 15-17
- Masseroni, D., Arbat, G., de Lima, P., 2020. Editorial managing and planning water resources for irrigation systems for providing sustainable agriculture and maintaining ecosystem services. *Water*, 12 (1), 263.
- Shishegar, S., Duchesne, S., Pelletier, G., 2019. A smart predictive framework for system-level stormwater management optimization. *Journal of Environmental Management*, 278, 111505.
- Su, Y., Gao, W., Guan, D., Zuo, T., 2020. Achieving urban water security: a review of water management approach from technology perspective. *Water resources management, Springer Nature B.N.*, 34: 4163-4179.



Performance of a UASB reactor treating hydrolyzed starch at various conditions.

D. Theodosi Palimeri¹, A.G. Vlyssides¹ and A.A. Vlysidis^{1,2}

¹School of Chemical Engineering, National Technical University of Athens, Athens, 15780, Greece

²School of Chemical and Environmental Engineering, Technical University of Crete, Chania, 73100, Greece

Corresponding author email: avlysidis@isc.tuc.gr

keywords: Fenton oxidation; starch; UASB reactor; methane; methanogenic sludge activity.

Introduction

Wastewater generated from potato processing industries usually has a high starch concentration that can cause operational problems in the industry's equipment due to its low solubility and high viscosity (Li et al. 2020) and for this reason is separated from the wastewater stream. This by-product can be pretreated and used as substrate to an anaerobic digestion process for biogas production due to its high organic content. Fenton oxidation process has been confirmed to be an effective approach in the treatment of potato starch (Pietrzyk et al. 2007). After oxidation, the hydrolysed starch solution is amenable to biodegradation and can be treated in an anaerobic digester.

Among anaerobic options, upflow anaerobic sludge blanket reactor (UASB) is the most widely used system for treatment of high strength food processing wastewater and specifically for wastewater with high content of carbohydrates (Daud et al. 2018) due to its high energy generation in the form of methane and the ability to treat high organic loads. Many studies have been focused on treatment of starch wastewater using UASB reactors, however only few studies have investigated the operation of UASB utilizing only starch as carbon source because of the low pH and high sugar content (Lu et al. 2015). Further research is needed to evaluate the long-term performance of UASB which is fed only with starch and to optimize all operational parameters.

The approach of this study was to investigate the effect of some of the operational parameters on UASB performance and methane production after feeding with hydrolyzed starch. For this reason, starch was hydrolyzed by adding Fenton reagents' and fed in UASB reactor which was constructed and operated for more than a year. Organic loading rate (OLR) was increasing under various HRTs ranging from 11 to 82 hours and various TOC concentrations. Moreover, in order to examine the biodegradability of substrate, the specific methanogenic activity (SMA) of granular sludge after feeding with hydrolyzed starch was also determined.

Materials and methods

For starch hydrolysis, 31 g dry weight of starch collected from a potato processing industry in Athens, were suspended in 1 L of distilled H₂O. The Fenton reagents', FeSO₄·7H₂O and H₂O₂, were added at concentrations 1 g/L and 0.53 g/L, respectively and the suspension was set to 70°C under stirring for 3 hours. After oxidation, the solution was diluted and urea and molasses were added at various concentrations to improve the growth of anaerobic microorganisms.

For the anaerobic treatment of starch, a UASB reactor was constructed in the laboratory and inoculated with 3 L anaerobic granular sludge from a full-scale UASB reactor of a potato processing industry in Athens. UASB was cylindrical, made of Plexiglas, with an effective working volume of 12 L and internal diameter of 12 cm. The temperature inside the reactor was kept constant at 35°C and the upflow velocity was about 1 m/h. The reactor operated continuously for more than 200 days under various HRTs ranging from 11 h to 82 h, while the TOC of the influent varied from 185 mg/L to 1850 mg/L and OLR from 0.50 g COD/L_{UASB}-day to 6.65 g COD/L_{UASB}-day. Furthermore, in order to examine the impact of the organic load, the UASB operated at a constant HRT of 72 h and the OLR was increased gradually by increasing the TOC concentration in the substrate from 1 g/L to 11.65 g/L.

The total solids (TSS), volatile solids (VSS), chemical oxygen demand (COD), the total amount of VFAs and the alkalinity of the influent and effluent were monitored in accordance with Standard Methods (Rodger et al., 2017). The TOC of the solid starch, the organic carbon in the starch solution and the Total Nitrogen (TN) in the substrate, were measured with a TOC analyzer (Shimadzu, SSM-5000A, Shimadzu, TOC-L, TNL-M analyzer). The pH and REDOX potential were measured continuously using a pH electrode (HI 3214P Hanna Instruments, Co.) and an ORP electrode (H1 2114P, Hanna Instruments, Co.), respectively. The total amount



of biogas produced per day was recorded on a PLC and the biogas composition was checked with the biogas analyzer (Gas analyzer, GFM 406 series). Specific methanogenic activity (SMA) test of granular sludge after feeding with 50 mg COD of hydrolyzed starch was determined according to (Miller and Wolin 1974) in serum bottle of 500 mL containing 4 g VSS of sludge.

Results and discussion

After oxidation with Fenton reagents, the starch solution was composed of 13.5 g TOC/L and the efficiency of hydrolysis was 99.3%. Specific methanogenic activity test was used to investigate the biodegradability of the hydrolysates and the maximum SMA was found to be 0.333 ± 0.02 g COD_{methane}/g VSS_{sludge}-day which is higher compared to other studies that investigated the SMA after feeding sludge with starch (Lu et al. 2015).

During the operational period of UASB under various HRTs, the OLR was gradually increased from 0.62 ± 0.09 to 5.2 ± 0.182 g COD/L_{UASB}-day and the UASB performance was stabilized after 30 days. The reduction-oxidation potential was ranging from -247 to -465 mV and the pH was kept relatively constant in the range of 6.2 to 7.2. However, at HRTs of 20 h, 24 h and 14.4 h with OLR exceeding 4.2 COD/L_{UASB}-day, pH was decreased at lower levels between 5.5 - 5.9. At HRT 24 h and OLR 3.9 g COD/L_{UASB}-day, TOC removal efficiency was $95.32\% \pm 2.28$ with respective methane yield equal to 0.255 L CH₄/g COD_{removed} and methane percentage of the total biogas equal to 68.5%.

During the period that HRT was kept constant at 72 h, the OLR was increased from 1.4 to 9.8 g COD/L_{UASB}-day with TOC removal varying from 65.0% to 96.2%. It is observed that when OLR increased to 7.6 g COD/L_{UASB}-day, VFAs were accumulated in the UASB while pH was reduced. When OLR reached 9.8 g COD/L_{UASB}-day, methane yield was found to be 0.223 L CH₄/g COD_{removed}, TOC removal equal to 91.1% and methane percentage in the total biogas equal to 59.2%. Further increase in OLR, caused deterioration of UASB performance, since TOC removal decreased rapidly and VFAs accumulated further in the system. The reactor recovered by applying a lower OLR of 2.17 g COD/L_{UASB}-day.

Conclusions

Industrial starch after its hydrolysis is a suitable substrate for bioenergy production, with UASB showing a good performance. The methane yield and TOC removal efficiency could reach 0.223 L CH₄/g COD_{removed} and 91% respectively, under the high OLR of 10 g COD/L_{UASB}-day and 72-h HRT.

Acknowledgements: This research is co-financed by Greece and the European Union (European Social Fund-ESF) through the Operational Programme «Human Resources Development, Education and Lifelong Learning» in the context of the project “Strengthening Human Resources Research Potential via Doctorate Research” (MIS-5000432), implemented by the State Scholarships Foundation (IKY).

References

- Daud, M. K. Rizvi, H., Akram, M.F., Shafaqat A., Rizwan, M., Nafees, M., Jin, Z.S. 2018. Review of Upflow Anaerobic Sludge Blanket Reactor Technology: Effect of Different Parameters and Developments for Domestic Wastewater Treatment. *Journal of Chemistry*, vol. 2018, Article ID 1596319.
- Pietrzyk S., Fortuna T., Raś Ł. 2007. THE INFLUENCE OF PH AND Fe(II) IONS ON PHYSICOCHEMICAL PROPERTIES OF OXIDISED POTATO STARCH. *ELECTRONIC JOURNAL OF POLISH AGRICULTURAL UNIVERSITIES*, 10 (4), 1-8.
- Li, J., Zhou, M., Cheng, F., Lin, Y., Shi, L., Zhu, P. 2020. Preparation of oxidized corn starch with high degree of oxidation by fenton- like oxidation assisted with ball milling. *Mater. Today Commun.* 22, 100–793
- Lu, X., Zhen, G., Estrada, A.L., Chen, M., Nic, J., Hojo, T., Kubota, K., Li, Y-Y. 2015. Operation Performance and Granule Characterization of Upflow Anaerobic Sludge Blanket (UASB) Reactor Treating Wastewater with Starch as the Sole Carbon Source. *Bioresource Technology* 180, 264–73.
- Miller, T L, and M J Wolin. 1974. A Serum Bottle Modification of the Hungate Technique for Cultivating Obligate Anaerobes. *Applied microbiology* 27 (5), 985–87.
- Rodger, B., and Bridgewater, L. 2017. *Standard Methods for the Examination of Water and Wastewater. 23rd edition.*; American Public Health Association, Washington.



Enhancement of siloxanes biofiltration from waste air by toluene addition

J.J. González-Cortés^{1,2}, P.A. Lamprea-Pineda¹, M. Ramírez², K. Demeestere¹ and C. Walgraeve¹

¹Research group EnVOC, Department of Green Chemistry and Technology, Faculty of BioscienceEngineering, Ghent University, Ghent, Belgium

²Department of Chemical Engineering and Food Technologies, Wine and Agrifood Research Institute (IVAGRO), Faculty of Sciences, University of Cadiz, Cádiz, Spain

Corresponding author email: JoseJoaquin.GonzalezCortes@UGent.be

keywords: *volatile methylsiloxanes; biofiltration; toluene; biofilter; L3; D4.*

Introduction

Cyclic and linear volatile methylsiloxanes (VMS) are chemicals widely used as carriers in personal care products. Furthermore, they are used as intermediates in the production of silicone fluids, elastomers or resins which have a wide variety of industrial and consumer applications. The large production volume of these products (estimated to reach 2.8 million tons by 2023) and the high environmental persistence of VMS are causes of concern, especially in the environment surrounding silicone factories, oil fields and paper production facilities. The interesting properties of these chemicals make their usage expected to grow, so appropriate management of environmental emissions is required (Horii et al., 2020).

Traditionally, the elimination of these compounds from waste gas streams has been carried out in a physical-chemical way (e.g. activated carbon). However, the use of biological technologies that offer a lower operational cost and are more environmentally friendly, has been attracting the interest of researchers in the last decade, particularly for the removal of siloxanes from biogas. The main challenge for biodegrading these compounds is, however, their poor mass transfer due to the hydrophobicity of VMS, which hinders their transfer from the gaseous stream to the liquid phase that contains the microbial population and their poor biodegradability. In this work, the use of biofilters (BFs) is investigated for the removal of VMS (octamethyltrisiloxane (L3) and octamethylcyclotetrasiloxane (D4)) from waste air for the very first time. L3 and D4 were selected because they can be used as model compounds of the linear and cyclic siloxanes groups, respectively, and their presence has been reported in petroleum refineries and silicon manufacturing sites. It is evaluated if the simultaneous addition of an easy degradable carbon source like toluene might enhance the removal of the VMS in biofilters. To the best of our knowledge, this has not been investigated before.

Materials and methods

Experiments were performed in two different BFs with a working volume of 14 L, and packed with a mixture of woodchips and compost (WC, BF 1) (80:20 % v/v) and perlite (PER, BF 2), respectively. Both BFs were inoculated with activated sludge from a municipal wastewater treatment plant (Ossemeersen, Ghent). The BFs were fed with an airstream polluted with L3, D4 and toluene using a mass-flow controlled home-made generation system. Both BFs were operated for more than 140 days. In Stage I, they were started-up for 54 days at an inlet load (IL) of 1.8 g VMS m⁻³ h⁻¹ (0.9 g D4 m⁻³ h⁻¹ and 0.9 g L3 m⁻³ h⁻¹) at an empty bed residence time (EBRT) of 15 min. In Stage II, the EBRT was increased to 28 min, and both BFs were operated at a constant VMS IL of on average 0.81 ± 0.19 g VMS m⁻³ h⁻¹ (0.36 ± 0.04 g L3 m⁻³ h⁻¹ and 0.47 ± 0.18 g D4 m⁻³ h⁻¹). In Stage III, the VMS IL remained equal to stage II and both BFs were fed with an increasing IL of toluene (ILs 0.6 - 2 g toluene m⁻³ h⁻¹) aiming to enhance the removal of VMS. The effect of lowering the EBRT stepwise from 28 min to 7 min was investigated under all three stages. A gas chromatograph coupled to a flame ionization detector (GC-FID) was used to determine the concentration of the VMS and toluene in the air stream. CO₂ production was measured using a CO₂ probe (MI70, Vaisala, Finland).



Results and discussion

The average removal efficiency (RE) of D4 and L3 in both biofilters at steady-state conditions both before and after feeding toluene is shown in Fig. 1. D4 shows to be more biodegradable than L3, as noticed also by other authors (Pascual et al., 2021). Adding toluene as an easily biodegradable VOC helps the removal of the very recalcitrant L3 and D4 from an air stream. Indeed, the addition of $0.6 \pm 0.1 \text{ g toluene m}^{-3} \text{ h}^{-1}$ improved the average VMS RE in both BFs by a factor of 2.5. Hence, the total VMS elimination capacity (EC) increased from an average of $0.03 \pm 0.01 \text{ g VMS m}^{-3} \text{ h}^{-1}$ to $0.13 \pm 0.02 \text{ g VMS m}^{-3} \text{ h}^{-1}$ (WC biofilter) and from $0.02 \pm 0.01 \text{ g VMS m}^{-3} \text{ h}^{-1}$ to $0.11 \pm 0.02 \text{ g VMS m}^{-3} \text{ h}^{-1}$ (PER biofilter). Toluene was completely removed in both BFs 7 days after the start of its feeding. As a novelty of this work, our results thus highlight the potential of BF to remove VMS from an air stream with significant ECs that are in line with other bioreactors reported in the literature. For example, Santos-Clotas et al. (2019) operated an anoxic biotrickling filter (BTF) packed with lava rock and achieved a maximum VMS EC of $0.17 \text{ g VMS m}^{-3} \text{ h}^{-1}$ (RE= 13-37%; EBRT 15 min). In our BF experiments, the type of packing material does not indicate a huge effect on the removal of VMS, but a much higher CO_2 production is found in the WC BF compared to the PER one most probably because of the biodegradability and mineralization of the WC packing material.

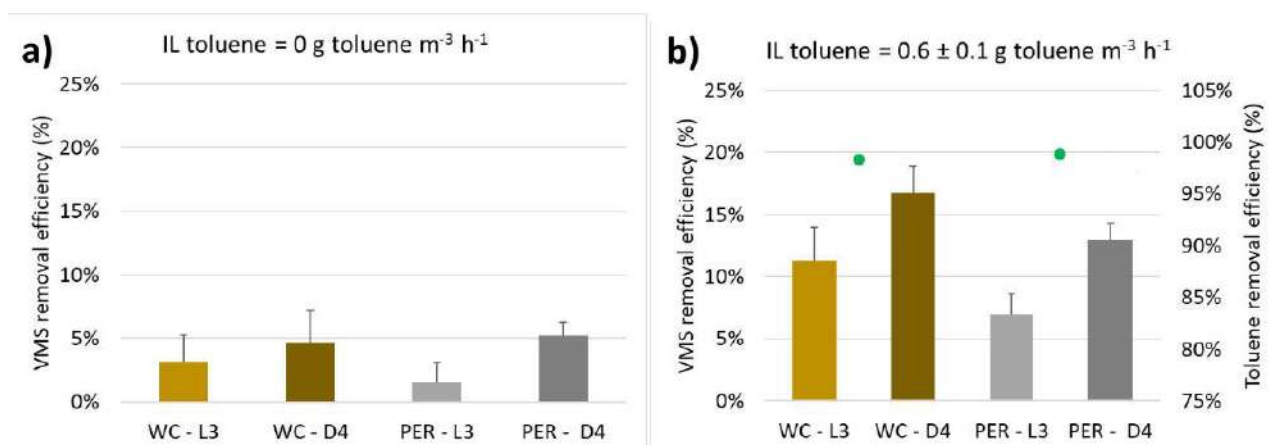


Figure 1. L3 and D4 removal efficiency by the biofilters packed with woodchips + compost (WC) and perlite (PER), operated at a constant VMS IL of $0.36 \pm 0.04 \text{ g L3 m}^{-3} \text{ h}^{-1}$ and $0.47 \pm 0.18 \text{ g D4 m}^{-3} \text{ h}^{-1}$ (a) before toluene addition and (b) after feeding $0.6 \pm 0.1 \text{ g toluene m}^{-3} \text{ h}^{-1}$. VMS RE is represented by bars and toluene RE is represented by green dots.

Conclusions

L3 and D4 are very recalcitrant siloxane compounds whose removal by biofiltration is challenging but possible. The addition of toluene improved the removal of L3 and D4. Although the type of packing material investigated did not have a great influence on VMS removal, a difference in CO_2 production is noticed.

Acknowledgements: This study is supported by UGENT BOF 2019005701 and the European Union through the NextGenerationEU funds (UCA/R155REC/2021).

References

- Horii, Y., Kannan, K., 2020. Main Uses and Environmental Emissions of Volatile Methylsiloxanes. *Handb. Environ. Chem.* 89, 33–70.
- Pascual, C., Cantera, S., Muñoz, R., Lebrero, R., 2021. Siloxanes removal in a two-phase partitioning biotrickling filter: Influence of the EBRT and the organic phase. *Renew. Energy* 177, 52–60.
- Santos-Clotas, E., Cabrera-Codony, A., Boada, E., Gich, F., Muñoz, R., Martín, M.J., 2019. Efficient removal of siloxanes and volatile organic compounds from sewage biogas by an anoxic biotrickling filter supplemented with activated carbon. *Bioresour. Technol.* 294, 122136.



Evaluation of the Suitability of Agricultural- and Industrial-based Biochars for Soil Amendment

D. Vamvuka¹ and P. Karagiannaki¹

¹Department/School of Mineral Resources Engineering, Technical University of Crete, Chania, Greece
Corresponding author email: vamvuka@mred.tuc.gr

keywords: *biochar; wastes; soil; leaching; amendment.*

Introduction

Biochars are carbon-rich porous materials, which can be used as fuels, as carbon sink in soils for thousands of years, as adsorbents of various contaminants from soil and waste waters, or as soil fertilizers. Present study aimed at evaluating two biochars, generated from agricultural and industrial wastes, for their suitability for amendment of a Mediterranean type soil and their combined application with a swine sludge.

Materials and methods

Biochars were produced from pyrolysis of raw materials at 350°C in a fixed bed system. Column leaching experiments were carried out simulating field conditions in South European countries. Solids were characterized by chemical and mineralogical analyses, while liquid effluents for pH, electrical conductivity, chemical oxygen demand (COD), nitrates, phosphates, phenols, nutrients and heavy metals.

Conclusions

Application of biochars to the soil improved its water holding capacity, increased the pH, while reduced the electrical conductivity and COD values of the leachates. Application of swine sludge to the soil increased the COD values of water extracts and promoted leaching of nitrates and phosphates. Addition of biochars to the soil/swine sludge mixture allowed the slower release of nitrates, phosphates and nutrient elements except potassium, the extractability of which was enhanced. For all soil combinations, the amount of phenols released in liquid effluents was very low. Also, heavy metal levels were low and below legislation limits, whereas in the presence of biochars in soil blends they were significantly reduced.



Effect of salinity and nitrogen to phosphorus ratio on the growth of the marine cyanobacterium *Geitlerinema* sp.

S. Patsialou¹, C. N. Economou², S. Genitsaris³, A. Rafteli², G. N. Hotos⁴, D. V. Vayenas^{2,5} and A.G. Tekerlekopoulou¹

¹Department of Environmental Engineering, University of Patras, Agrinio, Greece

²Department of Chemical Engineering, University of Patras, Patras, Greece

³Section of Ecology and Taxonomy, School of Biology, National and Kapodistrian University of Athens,

⁴Department of Animal Production, Fisheries & Aquaculture, University of Patras, Messolonghi, Greece

⁵Institute of Chemical Engineering Sciences (ICE-HT), Patras, Greece

Corresponding author email: atekerle@upatras.gr

keywords: *Geitlerinema* sp.; marine cyanobacteria; salinity stress; nutrient removal; phycocyanin.

Introduction

The production of high value-added products from cyanobacteria (blue-green algae) has currently attracted intense interest from both research and industry field. Cyanobacteria under specific growth conditions are able to produce a wide range of bioactive compounds such as proteins, carbohydrates and pigments (e.g., chlorophyll-a, carotenoids and phycocyanin) that could be used either in the food and pharmaceutical sector [1,2], as building blocks for high-value products, or in the energy sector as biofuels [3]. Bioactive compounds production is stimulated by various factors, such as salinity level, nutrients availability, light intensity, temperature and differs between cyanobacterial strains and experimental conditions [4,5].

Filamentous cyanobacterium *Geitlerinema* sp. belongs to marine blue-green algae and can accumulate high-value bioproducts, like carbohydrates and pigments [6]. This study investigated the biomass production from cyanobacterium *Geitlerinema* sp. under different salinity conditions (5, 10, 20, 30, 40, 50, 60, 70‰) and nitrogen to phosphorus (N/P) ratios (5, 6, 7.5) aiming to determine the optimum conditions for maximizing biomass concentration. The biomass carbohydrate and phycocyanin contents as well as removal of nitrates (N-NO₃⁻) and phosphates (P-PO₄³⁻) were also studied.

Materials and methods

Sample of the cultivation were analyzed to determine biomass concentration (mg/L), as total suspended solids (TSS), as well as N-NO₃⁻ and P-PO₄³⁻ removal according to Standard Methods [7]. The phycocyanin content was determined by extraction method in a 10% CaCl₂ solution [8]. The carbohydrate content was estimated using the phenol-sulfuric acid method according to Dubois et al [9]. All experiments were performed in lab-scale photobioreactors of 1L working volume under continuous illumination (2000 lux) and mechanical aeration, using artificial seawater medium [10]. The range of salinity was achieved either with dilution with deionized water or with addition of NaCl.

Results and discussion

Experiments were initially performed to investigate the resistance of the culture to different salinity conditions. The culture was acclimatized at 40‰ sterilized seawater, obtained from the sea near Rio, city of Patras, using the modified Walne's medium [10]. Salinities from 5‰ to 70‰ were examined to determine the impact of the salinity stress to *Geitlerinema* sp. and its capability to produce biomass. The final biomass concentration, biomass carbohydrate content and nutrient removal during sixteen days cultivation period is presented in Table 1. It was observed that *Geitlerinema* sp. has strong tolerance to low and high salinity media up to 60 ‰, without any significant preference for its growth concerning the salinity. However, the



40‰ salinity was selected for the next experimental sets as it presented satisfactory biomass yield, carbohydrate content and high nutrient percentage removal, without the need for correction of salinity.

Table 1. Final biomass concentration, carbohydrate content and nutrient removal for various salinities tested

Salinity (‰)	5	10	20	30	40	50	60	70
Biomass concentration (mg/L)	500	570	560	550	500	460	495	395
Carbohydrate content (%)	21.5	22.9	25.1	23.5	23.9	29.7	22.4	29.6
N-NO ₃ ⁻ removal (%)	96	91	87	88	95	96	92	92
P-PO ₄ ³⁻ removal (%)	48	28	59	64	67	87	98	96

Furthermore, the effect of N/P ratio (5, 6 and 7.5) on biomass concentration was examined at salinity of 40‰. The phycocyanin concentration (mg/g) was also estimated to determine the impact of nitrogen content on phycocyanin production. According to Table 2 there was a slight increase on the biomass concentration from ratio of 5 to 7.5 after 16 days of cultivation, but the noteworthy outcome was that P-PO₄³⁻ removal was enhanced at higher N/P ratios (without increasing the amount of phosphorus) indicating that N/P ratio of 7.5 was the optimum for the growth of *Geitlerinema* sp.

Table 2. Final biomass concentration, carbohydrate and phycocyanin contents, and nutrient removal for various N/P ratios tested

N/P	5	6	7.5
Biomass concentration (mg/L)	500	580	550
Phycocyanin concentration (mg/g)	23.9	44.7	43.9
Carbohydrate content (%)	20.9	25.9	29.1
N-NO ₃ ⁻ removal (%)	95	93	95
P-PO ₄ ³⁻ removal (%)	67	79	97

Conclusions

This study demonstrated that the marine filamentous cyanobacterium *Geitlerinema* sp. is capable to adapt in a variety of salinities, thus it could be used for biotechnological studies, like wastewater treatment, regardless the salt concentration. Overall, the high biomass carbohydrate and phycocyanin contents suggests that the biomass formed could be used for biofuel or food production.

References

- García, A.B., Longo, E., Bermejo, R., 2021, *J Appl Phycol* 33, 3059–3070.
- Renugadevi, K., Nachiyar, C.V., Sowmiya, P., Sunkar. S., 2018, *Biocatalysis and Agricultural Biotechnology*, 16, 237–242.
- Arashiro, L.T., Ferrer, I., Pániker, C.C, Gómez-Pinchetti, J.L., Rousseau, D.P.L., Van Hulle, S.W.H., Garfí, M., 2020. *ACS Sustainable Chemistry & Engineering*, 8 (29), 10691-10701.
- D'Alessandro, E.B., Soares, A.T., de Oliveira D'Alessandro, N.C., Filho, N.R.A., 2019. *Bioprocess Biosyst Eng*, 42, 2015–2022.
- Kenekar, A.A., Deodhar, M.A., 2013, *Biotechnology* 12 (3), 146-154.
- Anagnostidis, K., 1989, *Pl. Syst. Evol.*, 164, 33-46.
- APHA/AWWA/WEF, Standard Methods for the Examination of Water and Wastewater, 2012. Stand. Methods.
- Chentir, I., Doumandji, A., Ammar, J., Zili, F., Jridi, M., Markou, G., Ouada, H. B., 2018. *Journal of Applied Phycology*, 30, 1563–1574.
- Dubois, M., Gilles, K.A., Hamilton, J.K., Rebers, P.T., Smith, F., 1956. *Anal. Chem.* 28, 350–356
- Walne, P.R., 1970. *Fish. Invest.* 26, 162.



Energetic potential evaluation of medical wastes for using as solid recovered fuels

D. Torres¹, M. Fonseca Almeida¹ and S. C. Pinho¹

¹LEPABE, Laboratory for Process Engineering, Environment, Biotechnology and Energy, Faculty of Engineering, University of Porto

Corresponding author email: scpinho@fe.up.pt

keywords: *medical wastes; solid recovered fuels; alternative fuel.*

Introduction

The growth of medical waste production and the need for a specific treatment made those responsible for managing such wastes look for new and more efficient ways to treat them. Over the last decades, incineration and autoclaving have been the most commonly used technologies for treating medical wastes (Sukandar et al., 2006). However, the microwave shows solid indications of becoming more common for treating medical waste, since it achieves a high volume reduction, an important characteristic for wastes which continue to be deposited in landfills after treatment. In the last years, the use of alternative fuel (such as refuse derived fuel, tire derived fuel, sewage sludge, and municipal solid wastes) has shown to be ecologically and economically profitable (Chatziaras and Psomopoulos, 2016). The utilization of wastes that have the potential of being used to recover energy could be an option to consider. Nevertheless, current laws only recognize nonhazardous wastes as potential solid recovered fuels (SRF), which does not include hazardous medical wastes. Since microwave technology shows a high efficiency on microbial inactivation (Zimmermann, 2017), and, after treatment, medical wastes are equated to nonhazardous wastes, it could be possible to produce SRF from these wastes. The objective of this study was to evaluate the energetic potential of using medical wastes as SRF, analyzing the parameters set as mandatory by the European standards.

Materials and methods

The three samples of medical waste samples used in this study were collected in a microwave treatment unit in three different months to prevent possible changes in the constitution of medical wastes that may exist in different periods. Medical wastes are mainly constituted by plastics (33 %), paper (24 %), absorbents (34 %), glass (3 %), metals (2 %) and others (2 %) (Alvim-Ferraz and Afonso, 2005). Figure 1 shows the sample of medical waste, looking *fluff*, after microwave treatment. The gross calorific value was obtained at 25 °C in a bomb calorimeter model Parr 1672 according to EN 15400:2011. The chlorine was determined according to CEN/TS 15408:2011 and total carbon according to EN 13137 (2001). The ash content and the moisture content followed the CEN/TS 15403:2011 and CEN/TS 15414-1: 2011 standards, respectively. For metals quantification, the samples were subjected to chemical attack with aqua regia, according to the ISO 11466:1995 standard and the solutions were analyzed by Atomic Absorption Spectrometry (AAS).



Figure 1. *Sample of medical waste after microwave treatment.*



Results and discussion

Table 1 reports the values of the mandatory specification parameters obtained on the medical wastes. As expected, the total carbon content was high as well as the calorific value, and the content of mercury was low. The chlorine in the samples is from plastic components made of polyvinyl chloride, such as transfusion tubes and/or collection bags. The ISO 21640:2021 standard uses a classification system for SRF based on three parameters: an economic parameter (net calorific value), a technical parameter (chlorine content), and an environmental parameter (mercury content). Each parameter is divided into five classes (described in table 2 of the standard), and the class code consists on the combination of the three classifications. The net calorific value of the medical waste obtained was greater than 25 MJ/kg, therefore, it is in class 1; the chlorine content was 0.84 %, which corresponds to class 3. The median mercury content was 0.0082 mg/MJ and the 80th percentile value was 0.0092 mg/MJ, thus corresponding to class 1. Therefore, the medical waste analysed having the characteristics above described has the following classification code: PCI 1; Cl 3; Hg 1.

Table 1. Mandatory specification parameters

Parameter	Value
Total carbon, %	68.7
Ash content, %	6.0
Moisture content, %	12.5
Gross calorific value, MJ/kg	33.40
Net calorific value, MJ/kg	31.02
Chlorine, %	0.84
Mercury [mg/MJ]	0.0082
Median 80 th percentile	0.0092
∑ Heavy metals (mg/kg)	335.98

Conclusions

The heat of combustion determined for the samples show the potential of using this waste as one more alternative for solid recovered fuels. This ability is supported by its classification according to the ISO 21640:2021 standard, which, in terms of net calorific value and of mercury content ranks this waste in class 1, and in class 3 regarding chlorine content. In terms of economic and environmental parameters it is class 1, the best value provided by the standard.

Indeed, based on the analyzed hospital waste's characteristics, energy production can be an asset in its management both from an environmental and economic point of view.

Acknowledgements: This work was financially supported by LA/P/0045/2020 (ALiCE), UIDB/00511/2020 and UIDP/00511/2020 (LEPABE), funded by national funds through FCT/MCTES (PIDDAC).

References

- Alvim-Ferraz, M. C. M., Afonso, S. A. V., 2005. Incineration of healthcare wastes: management of atmospheric emissions through waste segregation. *Waste Management*, 25(6), 638-648.
- Chatziaras, N, Psomopoulos, C. S., 2016. Use of waste derived fuels in cement industry: a review. *Management of Environmental Quality: An International Journal*, 27, 178-193
- Sukandar S., Yasuda K., Tanaka M., Aoyama I., 2006. Metals leachability from medical waste incinerator fly ash: A case study on particle size comparison. *Environmental Pollution*, 144, 726–735.
- Zimmermann, K. (2017). Microwave as an emerging technology for the treatment of biohazardous waste: A mini-review. *Waste Management & Research*, 35(5), 471-479.



Training A New Generation Of farmers and agricultural entrepreneurs to implement the concept of Circular economy in agriculture – The TANGO-Circular ERASMUS+ project

G. Papadakis¹, E. Dimitriou¹, P. Picuno², I. Plantzou³, C. Stavropoulou⁴, L.M. Closas⁵, L. Brondelli diBrondello⁶, A. Farrus⁷, F. Baptista⁸, M.E. Mur Cacuo⁹, T. Batista¹⁰, F. Cordeiro¹¹, R. Serra¹², D. Margout-Jantac¹³

¹Agricultural University of Athens, Greece

²University of Basilicata, Italy, Project coordinator

³EUROTRAINING, Athens, Greece

⁴INASO-PASEGES, Athens, Greece

⁵University of Lleida, Spain

⁶ENAPRA-Confagricoltura, Italy

⁷Federació de Cooperatives Agraries de Catalunya, Spain

⁸University of Evora, Portugal

⁹IPCENA, Spain

¹⁰Comunidade Intermunicipal do Alentejo Central, Portugal

¹¹Associação dos Jovens Agricultores de Portugal, Portugal

¹²Unione delle Province Italiane – Regione Puglia, Italy

¹³University of Montpellier, France

Corresponding author email: gpap@aua.gr

keywords: agriculture; circular economy; Farmers; training.

Introduction

A very promising way to reduce the impact of agriculture on the environment, passes through the valorization of crop residues, agricultural by-products and other materials such as plastics used for crop cultivation and animal production currently considered as wastes. Farmers consider such materials an economic burden. However, if properly managed, they can become a source of income while at the same time protect the environment. Hence, for a sustainable agriculture and under the perspective of circular economy, it is necessary to address the issue of properly managing such agricultural residues and by-products as also other materials considered as “waste”. Education of farmers on such issues of circular economy is imperative for environment protection and economy enhancement.



Figure 1. Agricultural by-product, co-product and waste management hierarchy.

Objectives

- Training 1000 farmers in EU.
- Stimulate new entrepreneurship in the field of collecting, transporting and re-using biomass.
- Boosting innovation through developing and implementing new multidisciplinary approaches to teaching and learning.
- Developing a sense of initiative and entrepreneurial mind-sets, competences and skills.



- Stimulating the flow and exchange of knowledge between higher education, VET, enterprises and research, in the framework of a Quadruple-Helix approach.
- Identifying resilience-related, market needs and emerging professions.
- Develop and implement new multidisciplinary curricula for the valorisation of agricultural wastes in the framework of a Circular Economy.
- Development of 4 Rural Living Labs.
- Compilation, selection, and optimal configurations of state-of-the-art technologies.
- Political, Economic, Social and Technical (PEST) analysis.
- Training Needs Validation and Curriculum Design.
- Identification of new skills for future professionals.
- Identify alternative business models for waste collection and treatment based on farmer needs, as input to public policies.

Methodology

The TANGO-Circular Project follows a well-defined methodology for the preparation, design and delivery of the training programme:

- Analysis of the skills acquired by agricultural workers based on the latest research in the scientific bibliography, to provide a good scientific basis.
- Providing a training programme that is comprehensive and detailed in all its parts.
- Strengthening of the users' curricula, and provide strong capacity to the user being trained.
- Development of smart skills so that they can be used by the final operator.

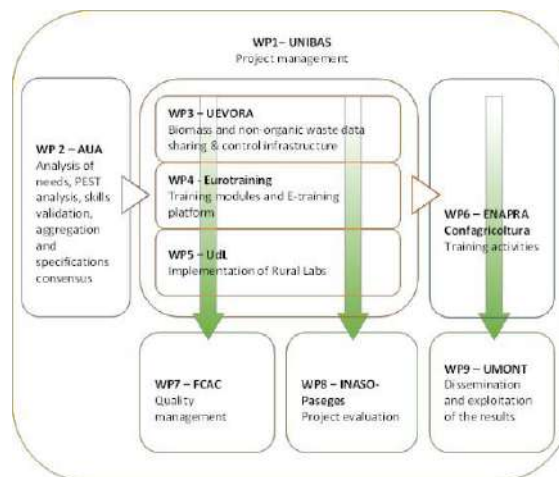


Figure 2. Overall work plan structure.

Training programme

The TANGO-Circular training programme will be organized into the following nine (9) training modules:

1. Classification of agricultural biomass.
2. Valorization of agricultural biomass.
3. Valorization of agro-food co-products, byproducts and organic residuals.
4. Classification of agricultural plastic waste.
5. Collection, transportation and recycling of Agricultural Plastic Waste.
6. De-contamination and valorization of Agricultural Plastic Packaging Waste.
7. Waste/Biomass legislation.
8. Environmental, territorial and economic planning, associated with each form of valorization.
9. Advantages and disadvantages associated with each possible form of valorization.

Acknowledgements: The TANGO-Circular project is Co-funded by the Erasmus+ Programme of the European Union.



Cultivation of *Chlorella Sorokiniana* in batch and sequencing batch reactors for winery wastewater treatment

M. Mastori¹, A. Xenaki¹, E. Zkeri¹ and A.S. Stasinakis¹

¹Department of Environment, Water and Air Quality Laboratory, University of the Aegean,
University Hill, Greece

Corresponding author email: astas@env.aegean.gr

keywords: winery wastewater; microalgae; *Chlorella Sorokiniana*; removal of pollutant.

Introduction

During the last decade, considerable interest has been focused on utilizing microalgae to remove pollutants from wastewater originated from different industrial activities (Amenorfenyo et al., 2019; Zkeri et al., 2021). The wine industry is producing a large quantity of wastewater which is characterized by high concentrations of organic compounds, and low pH value (Brito et al., 2007).

Previous studies have shown that the microalgae *Chlorella sorokiniana* can achieve satisfactory removal of organic load, and total nitrogen from several categories of wastewater. It has also been shown that the biomass produced is characterized by high nutritional, and economic value (López -Sánchez et al., 2022; Kusmayadi et al., 2022).

The main objective of the current research was to draw some initial conclusions about the effectiveness of the use of *Chlorella sorokiniana* for winery wastewater treatment. The biomass protein content was also measured to investigate possible future valorization options for the biomass.

Materials and methods

Winery wastewater was collected from a winery located in Lesbos Island (Greece). They were characterized by low pH value (4.5-5.0), the electrical conductivity of 681 $\mu\text{S cm}^{-1}$, Total Phosphorous (TP) concentration equal to 10 mg L^{-1} and COD concentrations that ranged between 4400 mg L^{-1} and 6800 mg L^{-1} . No ammonium nitrogen was detected in the collected samples.

During this research, three different experiments were carried out under batch or sequencing batch conditions using diluted winery wastewater.

The Batch experiment included four reactors in parallel. In the first two reactors, *Chlorella sorokiniana* had been previously acclimatized in medium, and the effect of the presence or absence of 40 mg L^{-1} N-NH₄ was examined in Reactor 1, and Reactor 2, respectively. Similar experiments were conducted in Reactors 3, and 4 with the difference that microalgae had been previously acclimatized to municipal wastewater. The duration of these experiments was 14 days, and the temperature was stable at 25°C.

The first SBR experiment consisted of two bioreactors, the SBR1, and the SBR2 that were connected in series. SBR1 was fed on diluted winery wastewater while at the end of each experimental cycle, the effluent of SBR1 was transferred to SBR2 for further treatment. Different experimental cycles were carried out. In all experimental cycles, NH₄ -N was added to achieve an initial concentration of 40 mg L^{-1} in the influent wastewater of SBR1. The pH was adjusted to 7 during the experiments, and the HRT was equal to 3 days. Mixotrophic conditions (16 h light/8 h dark) were applied.

In the second SBR experiment, the winery wastewater were biologically pretreated in an anaerobic Moving Bed Biofilm Reactor, and the effluents of this system were used as feeding of a SBR containing *Chlorella sorokiniana*. The HRT, and the light conditions in this experiment were similar to the previous SBR experiment.



Wastewater samples were collected at the beginning, and at the end of each cycle in each experiment, and from each bioreactor for the analysis of COD, and ammonium nitrogen. Daily measurements of temperature, pH, and Optical Density (OD) were also performed.

Results and discussion

According to the results, in batch experiments with the addition of $\text{NH}_4\text{-N}$, the concentrations of COD and $\text{NH}_4\text{-N}$ were reduced by 80% in diluted winery wastewater. In batch experiments without the addition of $\text{NH}_4\text{-N}$, COD removal was equal to 78%. Characterization of *Chlorella sorokiniana* biomass at the end of the Batch experiment showed that its protein content was equal to 58.8%.

In the first SBR experiment, COD was reduced by 29.4% in SBR1, and 31.1% in SBR2. The $\text{NH}_4\text{-N}$ removal was equal to 50.5%, and 31.1% in SBR1, and SBR2, respectively. Concerning the biomass's protein content, it was equal to 46.8%. The results of the second SBR experiment showed increased COD, and ammonium nitrogen removal comparing to the first one.

According to the results, *Chlorella sorokiniana* can grow efficiently in winery wastewater achieving, in parallel, important removal of major pollutants. The produced biomass seems to be a profitable source of proteins, indicating the potential for future use of *Chlorella sorokiniana* as animal feed or as food supplements.

Acknowledgments: We acknowledge support of this work by the project «FoodOmicsGR Comprehensive Characterisation of Foods» (MIS 5029057, <http://foodomics.gr/>) which is implemented under the Action “Reinforcement of the Research, and Innovation Infrastructure”, funded by the Operational Programme “Competitiveness, Entrepreneurship and Innovation” (NSRF 2014–2020), and co-financed by Greece, and the European Union (European Regional Development Fund).

References

- Amenorfenyo, D. K., Huang, X., Zhang, Y., Zeng, Q., Zhang, N., Ren, J., & Huang, Q. (2019) Microalgae brewery wastewater treatment: potentials, benefits, and the challenges. *International Journal of Environmental research and public health*, 16(11), 1910.
- Brito, A. G., Peixoto, J., Oliveira, J. M., Oliveira, J. A., Costa, C., Nogueira, R., & Rodrigues, A. (2007) Brewery and winery wastewater treatment: some focal points of design and operation. In *Utilization of by-products and treatment of waste in the food industry* (pp. 109-131). Springer, Boston, MA.
- Kusmayadi, A., Lu, P. H., Huang, C. Y., Leong, Y. K., Yen, H. W., & Chang, J. S. (2022) Integrating anaerobic digestion and microalgae cultivation for dairy wastewater treatment and potential biochemicals production from the harvested microalgal biomass. *Chemosphere*, 291, 133057.
- López-Sánchez, A., Silva-Gálvez, A. L., Aguilar-Juárez, Ó., Senés-Guerrero, C., Orozco-Nunnally, D. A., Carrillo-Nieves, D., & Gradilla-Hernández, M. S. (2022) Microalgae-based livestock wastewater treatment (MbWT) as a circular bioeconomy approach: Enhancement of biomass productivity, pollutant removal and high-value compound production. *Journal of Environmental Management*, 308, 114612.
- Zkeri, E., Iliopoulou, A., Katsara, A., Korda, A., Aloupi, M., Gatidou, G., Fountoulakis, M.S., Stasinakis, A.S. (2021) Comparing the use of a two-stage MBBR system with a methanogenic MBBR coupled with a microalgae reactor for medium-strength dairy wastewater treatment. *Bioresource Technology* 323, 124629.



Microsieving of raw sewage at the wastewater treatment plant of Rethymno: Yield and energy content of produced biosolids

A. Manali¹, C. Kampourakis¹ and P. Gikas¹

¹Design of Environmental Processes Laboratory, School of Chemical and Environmental Engineering, Technical University of Crete, Chania, Greece
Corresponding author email: pgikas@tuc.gr

keywords: *microsieving; wastewater treatment; biosolids; calorific value; energy content.*

Introduction

Microsieving is a novel process for the removal of suspended solids from wastewater, upfront of the aeration tank (Gikas, 2017). Microsieves remove suspended particles from raw wastewater, resulting to the reduction of energy requirements in the downstream aeration tank. The produced microsieved biosolids are characterized by high solids content and high Higher Heating Value (HHV) (Manali and Gikas, 2019). In extended aeration Wastewater Treatment Plants (WWTPs), usually there is no primary clarification, so raw wastewater enters directly into the aeration tank following pretreatment processes. The absence of primary clarification drives to increased energy consumption in the aeration tank, as solids that would have been removed by sedimentation have to be degraded by aerobic microorganisms.

The present study aimed to examine, at industrial scale, the efficiency of the microsieving process on the removal of suspended solids from pretreated wastewater and the energy content of the produced biosolids.

Materials and methods

An industrial microsieve, with capacity of up to 5,000 m³/d of incoming wastewater and belt width of 110cm, has been installed at the WWTP of Rethymno. This microsieve is the first stage of an integrated pilot plant for biosolids management, followed by a dryer and a gasification-energy production system (Figure 1).

Several performance tests were carried out with the microsieve, concluding that the most efficient operational conditions were with 350µm pore opening belt filter, with incoming wastewater supply of 200m³/h, without the addition of coagulants and with the integration of a collection-recirculation system of the washing water and leachate of the microsieved biosolids, for the recovery of solids.



Figure 1. Inlets-outlets of microsieving process (left); Microsieve installed at Rethymno WWTP (right).

Results and discussion

Based on analyses of the Rethymno WWTP's laboratory, the average TSS inlet concentration during the last five years (2017-2021) was 229 ± 102 mg/L, however a significant reduction of the concentration has been observed from 2019 onwards, as the average annual TSS concentrations were 273, 342, 203, 146, and 180 mg/L for 2017, 2018, 2019, 2020, and 2021, respectively (Figure 2).

Under the abovementioned operational conditions of the microsieve, the average solids removal reached 30% (Figure 3), while the hourly production rate of biosolids on a dry basis measured as 7.7kg/h.

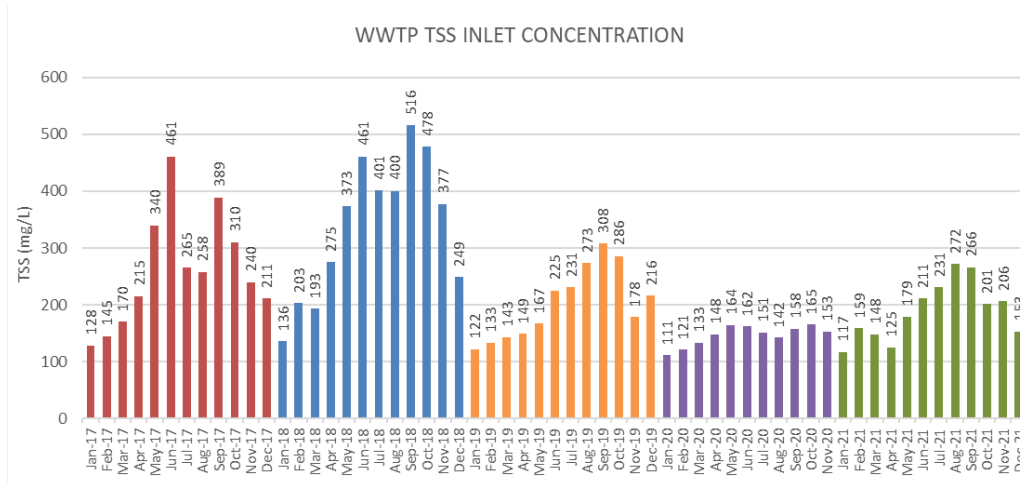


Figure 2. Inlet TSS concentration of Rethymno WWTP.

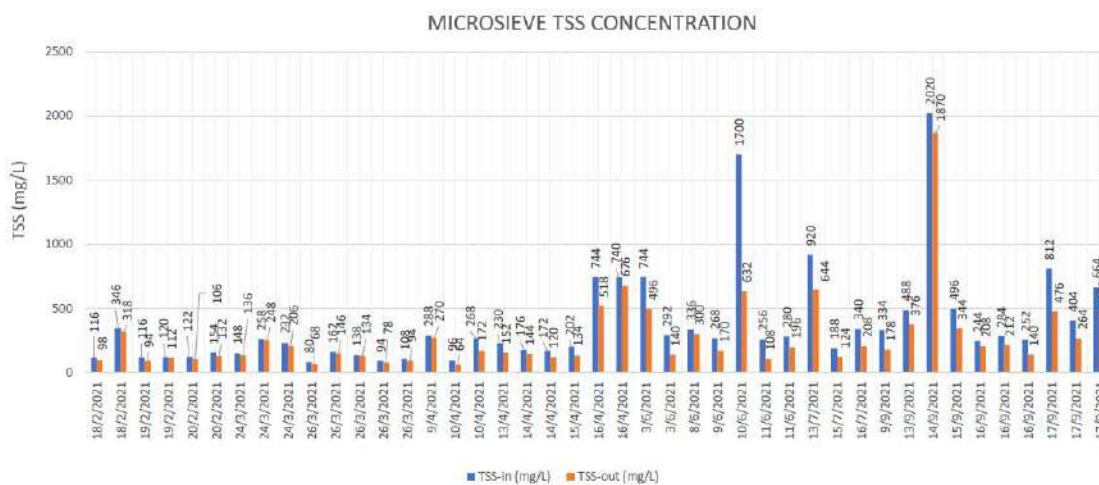


Figure 3. Inlet-outlet TSS concentration of microsieve.

Lab analyses showed that the TS content of biosolids was $36 \pm 3\%$, with VS content of $90 \pm 1\%$, indicating high solids content rich in organics, which reduces the energy requirements of the downstream aeration stage. Also, the HHV of the microsieved biosolids was measured as 21.5 ± 1.4 MJ/kg (dry basis), which indicates that their energy content is considerably higher from all other types of biosolids.

Conclusions

The microsieve is a fully functional industrial scale apparatus, able to remove about 30% of TSS (at 350nm pore size). It may treat up to 200 m³/d, producing between 9-10kg/h of biosolids on a dry basis or even higher, depending on wastewater characteristics.

Acknowledgements: This study is supported by the Green Fund and the LIFE project (EC): “New concept for energy self-sustainable wastewater treatment process and biosolids management (LIFE B2E4sustainable-WWTP)”, LIFE16 ENV/GR/000298.

References

- APHA-AWWA-WEF, 2012. Standard Methods for the Examination of Water and Wastewater, 22nd ed; American Water Works Association, Washington D.C., USA.
- Gikas, P., 2017. Towards energy positive wastewater treatment plants. *J. Environ. Manage.*, 203, 621–629.
- Manali, A. and Gikas, P., 2019. Utilization of primary sieved solids for gasification and energy production, 17th International Waste Management and Landfill Symposium, 30 September-4 October, Sardinia, Italy.



Effect of COVID-19 lockdown on heavy metal contamination in Yamuna river water of Delhi region

K. Lal¹ and M. Uttreja¹

¹Environment and Health, The Energy and Resources Institute, New Delhi, India
Corresponding author email: kanhaiyatiitb@gmail.com

keywords: Heavy metals; COVID-19; Environmental monitoring; Natural treatment; River pollution; Yamuna.

Introduction

An unprecedented twenty-one-day nationwide lockdown was imposed on March 24, 2020, at midnight by the Government of India as a preventive approach to contain the COVID-19 spread, which was further extended up to May 31, 2020, in three more phases. The total lockdown led to the complete closure of the industries, thus ceasing the economic activities in the nation. This hindered the speed of the flow of resources used in the production process and the goods produced, and the waste discharged into the environment. As a result, industrial effluents are reduced, and measurable data support the clearing of pollutants from the atmosphere, soil, and water compartments (Invest India 2020). Amidst the global gloom of COVID-19 causing severe damage to health, the economy, and general societal well-being, the lockdown has provided a unique opportunity to monitor the baseline pollution levels in several environmental matrices, particularly in the cities facing severe anthropogenic pollution issues.

The Yamuna is the longest and the second largest tributary of the Ganga river, originating from the Yamunotri glacier of the Himalayas (38°59'N, 78°2'E), which is situated in the Uttarkashi district of Uttarakhand, India (Sehgal et al. 2012). It carries sewage, agricultural runoff, and industrial discharge from unidentified sources. The Yamuna water is also supplied for household purposes in Delhi, which has about 200 million population.

The present water pollution monitoring study aimed to investigate the effect of lockdown on the heavy metal concentrations of the Yamuna river flowing in the Delhi region. The lockdown imposed to restrain COVID-19 has provided a unique opportunity for environmental monitoring under an ideal scenario with the complete shutdown of industrial activities. The evidence gathered from this study can help plan necessary steps for the Yamuna pollution abatement and frame the policy decisions for its rejuvenation.

Materials and methods

For three consecutive days, the surface water sampling and onsite monitoring were conducted during the COVID-19 lockdown period (May 13 - 15, 2020). Due to the strict travel restrictions imposed by central and state governments as a precautionary measure, we could collect only limited surface water samples (one from each sampling location for three consecutive days). The water samples were then analyzed using ICP-MS (Agilent ICP-MS 7700 series) in an ISO, and NABL accredited laboratory in Delhi.

Results and discussion

In the present study, heavy metals/metalloids such as chromium (Cr), nickel (Ni), copper (Cu), zinc (Zn), arsenic (As), lead (Pb), and mercury (Hg) were found below the detection concentration, which was reported in significantly higher concentrations in our earlier monitoring study (Sehgal et al. 2012) as well as in other studies conducted afterward (Bhattacharya et al. 2015; Bhardwaj et al. 2017; Yadav and Khandegar 2019).

The above discussion clearly shows the dilution effect of heavy metals in the Yamuna water due to the COVID-19 lockdown. The closure of point sources (industrial activities) and non-point sources (diffuse discharge) of the Yamuna river has most likely prevented the industrial release into the water, thereby reducing heavy metal pollution. The present study's findings provide evidence of the anthropogenic origin of toxic heavy metals (Cr, Ni, Cu, Zn, Cd, and Pb) in Yamuna water.

The manganese (Mn) and iron (Fe) concentrations in the river water get lowered as we moved downstream from the Wazirabad barrage (entry point of Yamuna in Delhi) to Okhla barrage (exit point of



Yamuna in Delhi). At the entry point, both Mn and Fe had the highest concentrations in the river water above the permissible limit (0.3 mg/l). As we moved downstream, Mn was measured below the permissible limit, while Fe was still found to be above the permissible limit in river water at all five sampling points. These two metals were consistently found in high concentrations at all thirteen sampling points in our earlier monitoring studies (Sehgal et al. 2012), with no decreasing trend observed in the concentrations of Mn and Fe. Also, the maximum concentration of Fe in this study was found to be about eight times lesser than our previous study (Sehgal et al., 2012). From the above discussion, the source of Fe and Mn in Yamuna river water seems to be geogenic (naturally) during the lockdown period, which may arise from the interaction of iron-bearing mineral and groundwater (Sarkar and Shekhar 2018).

Conclusions

The COVID-19 pandemic forced the authorities to shut down the industries completely. Thus, a rare opportunity opened to monitor the baseline levels of heavy metal pollution in the Yamuna. This study provides strong evidence for the anthropogenic origin of at least six heavy metals (Cr, Ni, Cu, Zn, Cd and Pb) causing pollution in the water of Yamuna, Delhi. However, the less toxic metals, iron and manganese, are of mostly geogenic origin. Natural treatment using suitable heavy metal accumulating plants is suggested as a preventive measure.

Acknowledgments: The authors acknowledge the TERI field team members (Mr. S. S. Negi and Mr Gaurav) for onsite monitoring and water sampling. This study didn't receive financial assistance from any external institution/organization.

References

- Invest India (2020). How is COVID-19 impacting the environment around us? <https://www.investindia.gov.in/team-india-blogs/how-covid-19-impacting-environment-around-us> (accessed June 28 2020).
- Sehgal, M., Garg, A., Suresh, R., & Dagar, P. (2012). Heavy metal contamination in the Delhi segment of Yamuna basin. *Environmental Monitoring and Assessment*, 184(2), 1181–1196. <https://doi.org/10.1007/s10661-011-2031-9>.
- Bhattacharya, A., Dey, P., Gola, D., Mishra, A., Malik, A., & Patel, N. (2015). Assessment of Yamuna and associated drains used for irrigation in rural and peri-urban settings of Delhi NCR. *Environmental Monitoring and Assessment*, 187(1). <https://doi.org/10.1007/s10661-014-4146-2>.
- Bhardwaj, R., Gupta, A., & Garg, J. K. (2017). Evaluation of heavy metal contamination using environmetrics and indexing approach for River Yamuna, Delhi stretch, India. *Water Science*, 31(1), 52–66. <https://doi.org/10.1016/j.wsj.2017.02.002>.
- Yadav, A., & Khandegar, V. (2019). Dataset on assessment of River Yamuna, Delhi, India using indexing approach. *Data in Brief*, 22, 1–10. <https://doi.org/10.1016/j.dib.2018.11.130>
- Sarkar, A., & Shekhar, S. (2018). Iron contamination in the waters of Upper Yamuna basin. *Groundwater for Sustainable Development*, 7(January), 421–429. <https://doi.org/10.1016/j.gsd.2017.12.011>



Application of ionic liquids for bacterial carotenoid extraction

F. Salgado¹, T.P. Silva¹, L. Alves¹, J.C. Roseiro¹, R.M. Lukasik¹, S.M. Paixão¹

¹LNEG – Laboratório Nacional de Energia e Geologia, IP, Unidade de Bioenergia e Biorrefinarias,
Lisboa, Portugal

Corresponding author emails: susana.alves@lneg.pt

keywords: bacterial carotenoids; ionic liquids; extraction method.

Introduction

One of the ways to make microbial bioprocesses more economically viable is to enhance valorization of high added value products resulting from the biomass, like carotenoids, which have a high market value. To recover these pigments from microbial biomass a good extraction method is required. Solvent extraction is one of the methods commonly used to extract carotenoids, however, solvent extractions are both material and time-consuming, and moreover also present some health and safety concerns [1].

Ionic liquids (ILs) are a promising step forward to tackle some of these problems, even with their high price, and has been tested for the extraction of microorganism's components [2]. These "molten salts" are a group of compounds that have been known for a long time, but only in the last decades they have been attracting more attention from both researchers and industry. ILs are solvents that have a high solvation power for a wide range of molecules [3]. ILs are salts with a melting point below 100°C, which possess unique properties that depend on both the cation and anion present, high thermal and chemical stability, a large electrochemical window, great solvent power, non-flammability, and a negligible vapor pressure. Their versatility is one of their most attractive features, making them adaptable to many technologies [2]. Therefore, ILs can be used to facilitate chemical reactions, extraction and separation, biotransformation, and can be used in biorefineries and other processes.

As shown in previous works, *Gordonia alkanivorans* strain 1B has the capacity to produce carotenoids, however, since it was originally isolated from hydrocarbon rich environments, it is highly resistant to different organic solvents commonly used in extraction protocols. This makes the process slow and laborious, lowering yields and increasing solvent spending [4, 5]. As such, new extraction protocols must be developed and tested to obtain higher pigments yield. So, herein, the potential of ILs for carotenoids extraction was evaluated, since these compounds have been described as a good option to extract pigments produced by microorganisms.

In this context, a preliminary screening of 19 ILs, chosen based on their properties, was performed to ascertain which, if any, had potential to be used for carotenoid extraction from cells of *G. alkanivorans* strain 1B, in combination with ethyl acetate (EAc) as co-solvent. After the selection of an IL that highly increases extraction efficiency, the novel extraction process was optimized through a surface response methodology based on a Doehlert distribution for two factors (volume of IL and EAc)

Materials and methods

Ionic liquids – #1: 1-Ethyl-3-methylimidazolium bis(trifluoromethylsulfonyl)imide; #2: 1,3-Dimethyl imidazolium Dimethyl Phosphate; #3: Trihexyltetradecylphosphonium bis(trifluoromethylsulfonyl) amide; #4: 1-Butyl-3-methylimidazolium bis(trifluoromethylsulfonyl)imide; #5: 1-Hexyl-3-methylimidazolium bis(trifluoromethylsulfonyl)imide; #6: 1-Ethyl-3-Methylimidazolium hydrogensulfate; #7: Triisobutyl methyl phosphonium tosylate; #8: 1-Ethyl-3-Methylimidazolium thiocyanate; #9: 1-Butyl-3-Methylimidazolium thiocyanate; #10: 1-Butyl-3-Methylimidazolium tetrachloroferrate (III); #11: 1-Butyl-3-Methylimidazolium dicyanamide; #12: 1-Butyl-3-Methylimidazolium triflate; #13: 1-Ethyl-3-Methylimidazolium dihydrogen phosphate; #14: 1-Ethyl-3-methylimidazolium trifluoromethanesulfonate; #15: 1-Ethyl-3-Methylimidazolium methanesulfonate; #16: Didecyl-dimethyl-ammonium nitrate; #17: 2-hydroxyethyl ammonium formate; #18: Tributyl(ethyl)phosphonium Diethyl Phosphate; #19: Methylimidazolium bis(trifluoromethylsulfonyl)imide.

Bacterial biomass - The biomass used in this study was obtained from the cultivation of *Gordonia alkanivorans* strain 1B [6] in a sulfur free mineral medium [4, 5] and fructose as C-source. Afterwards, cells



were centrifuged (8600 x g at 4°C, 20 min) and concentrated until obtaining the quantity of cells necessary (cells concentration: ≈50 g/L dry cell weight) for further extraction.

Preliminary Carotenoid extraction method - a protocol was adapted from Ruiz et al. [7], in which biomass of strain 1B was extracted with EAc mixed with each tested IL (#1 to #19). For each extraction, 400 μL of biomass, 300 μL of IL and 300 μL of EAc were put in a 1.5 mL Eppendorf tube and mixed in an overhead shaker, at room temperature, overnight. After centrifugation (15000 x g, 15 min), the results of carotenoid extraction were evaluated, visually and/or quantitatively through spectrophotometer analysis [4, 5].

Results and discussion

To evaluate the potential of ILs to increase the efficiency of carotenoid extraction from strain 1B biomass, a set of assays was carried out to test 19 ILs combined with EAc, a solvent known for its high extraction capacity. Out of the 19 ILs tested (#1 to #19), only 10 were able to form a biphasic system and extract carotenoids. Total carotenoids in the more colorful extracts were quantified using a spectrophotometer. Based on the value of total carotenoids obtained, the two ILs that generated the highest extractions were selected: IL#2, which extracted 2.79 μg, and IL#18, which extracted 3.43 μg. These results contrast with the value of the extracted carotenoids using EAc as sole solvent (0.92 mg). Moreover, subsequent tests confirmed the greater efficiency of IL#18 as a co-solvent to extract carotenoids demonstrating the advantages of this novel method towards a faster and enhanced extraction. The good results obtained for IL#18 were expected, since the IL#18 belongs to the group of ILs which could be acting as lipidic membrane permeabilizer. IL#18 permeates the cell membrane facilitating ethyl acetate penetration thus increasing carotenoid extraction. Further optimization of the extraction method using IL#18/EAc was carried out using a surface response methodology, based on the Doehlert uniform shell design [9] for two factors (X1 = volume IL#18 volume; X2 = volume EAc). The results obtained point out for 50 μL of IL#18 with 1125 μL of AcE, as the best condition for high carotenoid extraction from biomass of *G. alkanivorans* strain 1B.

Acknowledgments: This work was financed by national funds through FCT (Fundação para a Ciência e a Tecnologia) in the scope of the project GreenFuel (PTDC/EAM-AMB/30975/2017). Tiago P. Silva also acknowledges FCT for his PhD financial support (SFRH/BD/104977/2014).

References

- Orr, V.C.A., Plechkova, N.V., Seddon, K.R. and Rehmann, L., 2016. Disruption and wet extraction of the microalgae *Chlorella vulgaris* using room-temperature ionic liquids. *ACS Sustain. Chem. Eng.*, 4(2), 591–600.
- Eppink, M.H.M., Ventura, S.P., Coutinho, J.A.P. and Wijffels, R.H., 2021. Multiproduct microalgae biorefineries mediated by ionic liquids. *Trends in Biotechnol.*, 39(11), 1131–1143.
- Chiappe, C., Malvaldi, M. and Pomelli, C.S., 2009. Ionic liquids: Solvation ability and polarity. *Pure and Appl. Chem.*, 81(4), 767–776.
- Silva, T.P., Paixão, S.M. and Alves, L., 2016. Ability of *Gordonia alkanivorans* strain 1B for high added value carotenoids production. *RSC Adv.*, 6(63), 58055–58063.
- Fernandes, A.S., Paixão, S.M., Silva, T.P., Roseiro, J.C. and Alves, L., 2018. Influence of culture conditions towards optimal carotenoid production by *Gordonia alkanivorans* strain 1B. *Bioprocess Biosyst. Eng.*, 41, 143–155.
- Alves, L., Salgueiro, R., Rodrigues, C., Mesquita, E., Matos, J. and Gírio, F.M., 2005. Desulfurization of dibenzothiophene, benzothiophene and other thiophene analogues by a newly isolated bacterium, *Gordonia alkanivorans* strain 1B. *Appl. Biochem. Biotechnol.*, 120, 199–208.
- Ruiz C.A.S., Kwaijtaal, J., Peinado, O.C., van den Berg, C., Wijffels, R.H. and Eppink, M.H.M., 2020. Multistep fractionation of microalgal biomolecules using selective aqueous two-phase systems. *ACS Sustain. Chem. Eng.*, 8 (6), 2441-2452.
- Doehlert, D.H., 1970. Uniform Shell Designs. *J. R. Stat. Soc., C: Appl. Stat.*, 19(3), 231–239.



Process design and life cycle inventory of a syngas fermentation biorefinery

M. Pacheco^{1,2}, J. Ortigueira¹, P. Moura¹ and C. Silva²

¹Unidade de Bioenergia e Biorrefinarias, LNEG – Laboratório Nacional de Energia e Geologia, Lisboa, Portugal

²Instituto Dom Luiz/Faculdade de Ciências, Universidade de Lisboa, Lisboa, Portugal

Corresponding author email: camsilva@fc.ul.pt

keywords: thermochemical and biological process integration; circular economy; platform chemicals.

Introduction

Sustainability is one of the main pillars of new policies in Europe and over the world. The transition from a linear economy to a circular form requires sustainable waste management policies, focusing on waste minimization, reuse, and recycling. These are main priorities of the European Environmental Agency, in the Action Program 2020 (di Maria et al., 2020).

One of the technologies used to transform otherwise untreated residues is gasification. This thermochemical process allows the transformation of hard-to-treat carbonaceous residues, e.g., lignin from forestall biomass residues used in bioethanol biorefineries, into energy and synthesis gas (syngas). Syngas is mainly composed by carbon monoxide (CO), carbon dioxide (CO₂) and hydrogen (H₂), and in lower amounts by methane (CH₄), short chain hydrocarbons (C_nH_m), ammonia (NH₃) and hydrogen sulfide (H₂S). Syngas is normally burnt in a gas turbine for energy retrieval (heat and electricity) or used to produce liquid fuels through the Fisher-Tropsch process, however, both these “ends” either produce more hard-to-treat residues or are highly expensive due to the utilization of rare metal catalysts. Syngas fermentation is an alternative biological process which uses carboxydrotrophic microorganisms that are able to consume the CO and the CO₂+H₂ present in syngas as carbon and energy sources, producing short chain acids and alcohols. *Butyribacterium methylotrophicum* (*B. methylotrophicum*) is one of such microorganisms, being able to produce acetic and butyric acids from syngas. These molecules are considered platform chemicals, and are essential to several industries like food, feed, pharmaceutical and cosmetic, while also serving as precursors to biofuels (Pacheco et al., 2021).

Life cycle assessment (LCA) and techno-economic assessment (TEA) studies are necessary to evaluate prospective industrial biorefineries and for the acceleration of the syngas fermentation technology. LCA is a methodology used to evaluate the environmental impacts of a product or process from its origin (cradle) to its final disposal (grave). This methodology has been widely used in assessing waste management systems since it compares the environmental performances of different options and is a valuable tool for decision makers (di Maria et al., 2020). Since there are few LCA studies focused on syngas fermentation, the objective of this work is to perform an initial process design defining the boundaries to be used in the LCA and the life cycle inventory (LCI) of a syngas fermentation biorefinery using *B. methylotrophicum*, based on syngas produced by the gasification of low-grade technical lignin generated as a by-product in a second-generation (2G) ethanol biorefinery. All the biorefinery prospective products are identified.

Materials and methods

Life cycle methodology: The methodology used in this analysis is based on the ISO 14040 (ISO 14040–14043) LCA directives. Herein, goal, scope and boundaries were defined, and the LCI (inputs and outputs inventory) was performed, based on the bench-scale data.

Goal, scope and boundaries: The goal of this study was to analyze the global warming potential (GWP) of a syngas fermentation biorefinery. A cradle-to-gate analysis was performed, and the process boundaries are limited to the syngas fermentation biorefinery itself.

Experimental data: Using the gasification yield of 1.2 m³ of syngas produced from 1 kg of dry lignin, determined by (Pinto et al., 2019), calculations for the carbon emissions of the gasification process were performed using 1 ton of biomass as functional unit. The syngas fermentation data used for the calculations



and LCI in this study are published in Pacheco et al., 2021, and were based on the batch fermentation of lignin syngas by *B. methylotrophicum* in a bench-scale bioreactor.

Process schematic: The process schematic (**Figure 1**) depicts all the inputs and outputs from cradle-to-gate, and the defined boundaries for this study.

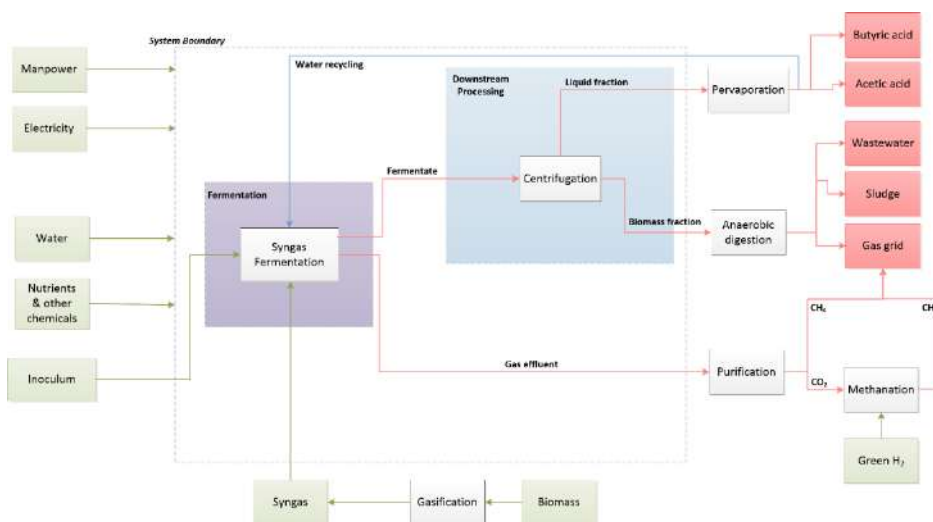


Figure 1. Process schematic of the syngas fermentation process. Marked as green are the inputs and marked as red are the outputs of the system.

Results and discussion

The syngas produced by 1 ton of lignin contained 297.5 kg of CO, 590.8 kg of CO₂, 46.1 kg of H₂, 99.6 kg of CH₄ and 45.32 kg of C₂H₄. The bioconversion of this syngas by *B. methylotrophicum* produced, as outputs, 2.6 kg of CO₂, and 3.1 kg of CH₄ and 0.7 kg of C₂H₄, whereas 96.9 kg of acetic acid, 0.7 kg of butyrate and 35.1 kg of biomass were formed per ton of lignin. All the available CO was converted to products and biomass simultaneously with a slight accumulation of CO₂ and CH₄ in the bioreactor headspace (Pacheco et al., 2021).

Conclusions

This study allowed to identify mass balances in a future syngas biorefinery at an industrial scale and access potential improvements in order to decrease the GWP of the overall process.

Acknowledgements: This research was performed under the framework of the AMBITION Project, an ECRIA project funded by the European Union's Horizon 2020 research and innovation program, under grant agreement No. 731263, and the Operational Program for Competitiveness and Internationalization (PORTUGAL 2020), Lisbon Portugal Regional Operational Program (Lisboa 2020) and North Portugal Regional Operational Program (Norte 2020) under the Portugal 2020 Partnership Agreement, through the European Regional Development Fund (ERDF). M. Pacheco was supported by FCT through PhD grant DFA/BD/6423/2020. This work was funded by the Portuguese Fundação para a Ciência e a Tecnologia (FCT) I.P./MCTES through national funds (PIDDAC) – UIDB/50019/2020.

References

- Di Maria, A., Eyckmans, J. and van Acker, K., 2020. Use of LCA and LCC to help decision-making between downcycling versus recycling of construction and demolition waste. In *Advances in Construction and Demolition Waste Recycling* (pp. 537–558). Elsevier, Amsterdam, Netherlands.
- Pacheco, M., Pinto, F., Ortigueira, J., Silva, C., Gírio, F. and Moura, P., 2021. Lignin syngas bioconversion by *Butyribacterium methylotrophicum*: Advancing towards an integrated biorefinery. *Energies*, 14(21).
- Pinto, F., André, R., Marques, P., Mata, R., Pacheco, M., Moura, P. and Gírio, F., 2019. Production of syngas suitable to be used in fermentation to obtain biochemical added-value compounds. *Chem. Eng. Trans.*, 76, 1399–1404.



Bioremediation of cresols by *Pseudomonas* sp. strain phDV1

A. Lyratzakis¹, G. Valsamidis¹, I. Kanavaki¹, J. D. Langer² and G. Tsiotis¹

¹Department of Chemistry University of Crete, Iraklion, Greece

²Max Planck Institute for Biophysics, Frankfurt am Main, Germany

Corresponding author email: alexlamp2008@gmail.com

keywords: *Bioremediation; Shotgun Proteomics; Transmission Electron Microscopy; PHA.*

Introduction

Aromatic compounds in wastewaters are harmful pollutants which originate as by-products from several industries and are toxic to aquatic micro-organisms. Here, *Pseudomonas* sp. strain phDV1, a gram-negative bacterium that is selected for its ability to degrade aromatic compounds is studied. This strain was isolated from an enriched mixed culture from samples of petroleum-contaminated soil in Denmark. In order to understand how the aromatic compounds and their degradation products are reintroduced in the metabolism of the bacteria and the systematic/metabolic response of the bacterium to the new carbon source, the proteome of this strain is analyzed in the presence of succinate, phenol, and o-, m-, and p-cresol as the sole carbon source. Hence, the bacteria are grown in succinate and then compared with the respective proteomes of bacteria grown on phenol and different cresols. The carbon source affects the synthesis of enzymes related to aromatic compound degradation and in particular the enzyme involved in the meta-pathway of monocyclic aromatic compounds degradation. In addition, proteins involved in the production of polyhydroxyalkanoate (PHA), an attractive biomaterial, and show higher abundance in the presence of monocyclic aromatic compounds. This study will be a valuable resource for researchers working on the degradation of aromatic compounds.

Materials and methods

Growth Conditions: The overnight culture was used to inoculate M9 minimal medium containing 10 mM succinate, 2.2 mM phenol, and 1.9 mM cresols, respectively. The cultures were grown at 32 °C and the growth was monitored by measuring the optical density at 600 nm. Optical spectra were recorded on a dual wavelength UV2700 UV vis spectrophotometer (Shimadzu) The consumption of aromatic compounds was monitored by 275 nm and the consumed compound was resupplied.

Mass spectrometry and Data Analysis: The samples were prepared using the Filter Aid Sample preparation and the Peptides eluting from the analytical column were ionized online using a Bruker Captive Spray ESI-source and analyzed in a Bruker Impact-II mass spectrometer. The raw files were loaded into MaxQuant (version 1.5.3.8) and analyzed using the Andromeda search engine.

Transmission Electron Microscopy (TEM): The formation of PHA was examined using TEM. Samples from *Pseudomonas* sp. phDV1 grown phenol at 72 h were centrifuged and the cell pellet was fixed in Thin sections of 70–100 nm were prepared using an LKB 2088 UltratomeV, stained with 2% uranyl acetate and finally samples were observed using a JEM-2100 Electron Microscope at 80 kV.

Results and discussion

Overall, 2295 proteins were identified using the data set of *Pseudomonas* sp. phDV1 strain, which represent more than 50% of the predicted genes. Using only proteins detected in 2 of 3 technical and 3 of 3 biological replicates, 1356 proteins were detected in all samples, representing the core proteome present in the different carbon source. Hierarchical clustering revealed a high correlation between biological replicates of the same condition. Finally, the transition from succinate to monocyclic aromatic phenols was associated with the significant ($p < 0.01$) change in the abundance of 76 proteins for phenol, 109 proteins for o-cresol, 154 proteins for m-cresol, and 160 proteins for p-cresol.

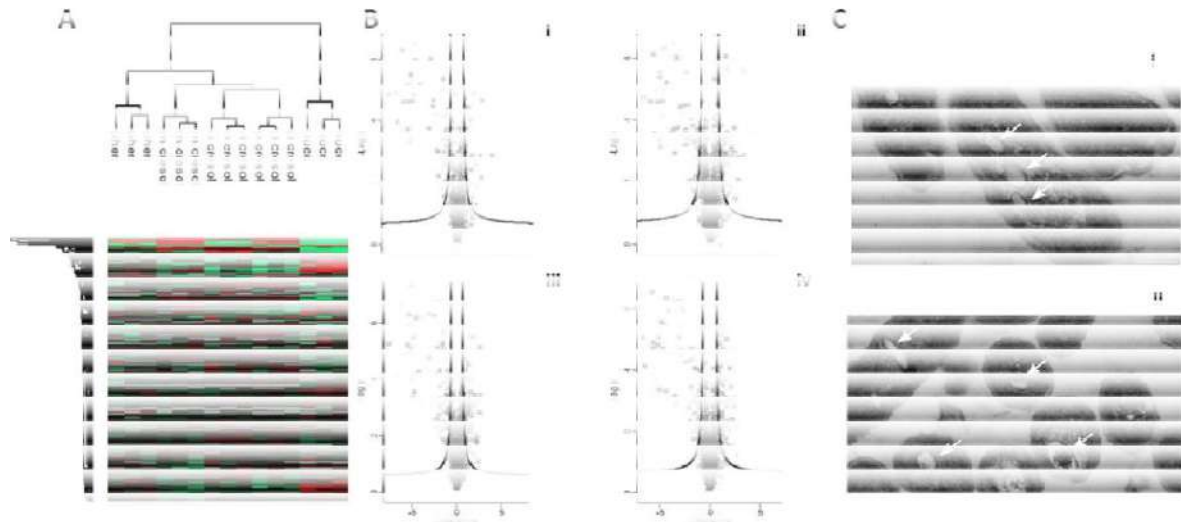


Figure 1. A) Hierarchical clustering B) Volcano plot (*t* test result) comparing succinate with i) phenol, ii) *o*-cresol, iii) *m*-cresol iv) and C TEM images showing the PHAs.

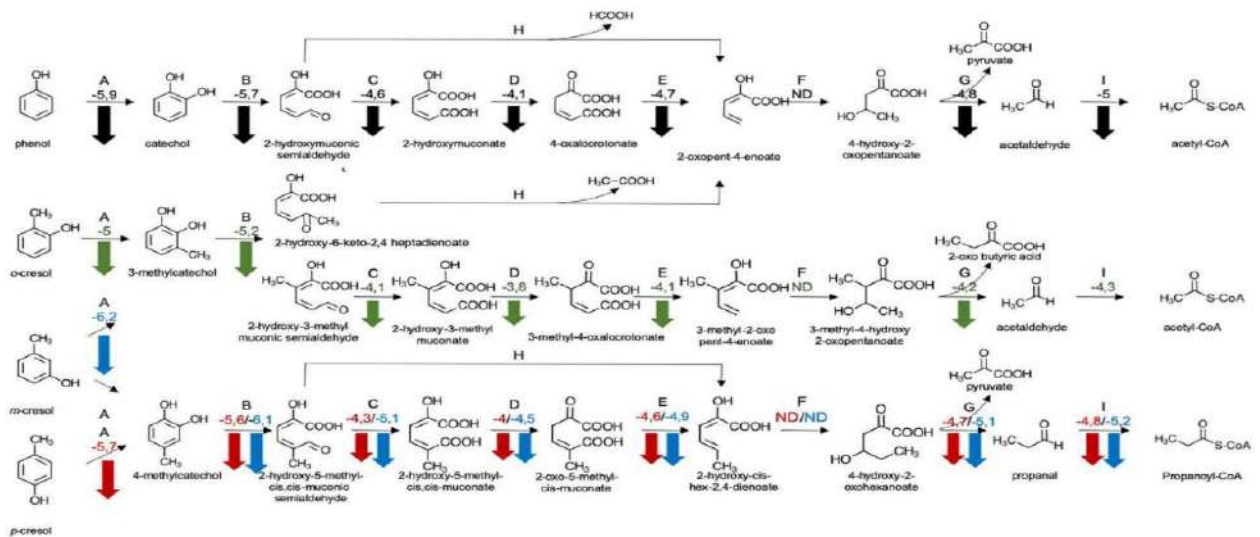


Figure 2. Proposed phenol, *o*-, *m*-, *p*-cresol degradation pathways in *Pseudomonas* phDV1 strain. A) Phenol hydroxylase; B) Catechol 2,3-dioxygenase; C) 2-Hydroxymuconic semialdehyde dehydrogenase; D) 4-Oxalocrotonate tautomerase; E) 2-Oxo-3-hexenedioate decarboxylase; F) 2-Keto-4-pentenoate hydratase; 4-Hydroxy 2-oxovalerate aldolase; H) 2-Hydroxymuconate-semialdehyde hydrolase; I) Acetaldehyde dehydrogenase; Numbers indicate fold change of regulation. Negative difference down regulated in control: ND, not detected. Phenol, black; *o*-cresol, green; *m*-cresol, blue; *p*-cresol, red. Numbers indicate fold of change of regulation abundance.

Conclusions

This study is the first comprehensive analysis of the proteome of *Pseudomonas* sp. phDV1 using quantitative, nano-ESI-LCMS/MS-based proteomic. Our analyses further showed a strong repression in the genes involved in the degradation of aromatics when the cells were grown on succinate. In addition, we have observed that phenol and *o*-cresol as well as *m*- and *p*-cresol are degraded by similar pathways. Lastly, the aromatic substrates on the central carbon metabolism were directly reflected in the decreased abundance of glycolysis and gluconeogenesis enzymes and the increased abundance of the key enzymes of PHA synthesis. These changes denote energy-deprived cells, which replenish the energy needed using the aromatic compounds as carbon sources.

References

- C. Masque, M. Nolla, A. Bordons, *Biotechnol. Lett.* 1987, 9, 655.
- P. N. Polymenakou, E. G. Stephanou, *Biodegradation* 2005, 16, 403.
- A. Lyrtzakakis, G. Tsiotis, *PROTEOMICS* 2021, 21, 2000003.



Examination of efficient harvesting and drying processes from a microalgae photo-bioreactor

E. Tsantopoulou¹, G. Makaroglou¹ and P. Gikas¹

¹Design of Environmental Processes Laboratory, School of Chemical and Environmental Engineering,
Technical University of Crete, Chania, Greece

Corresponding author email: pgikas@tuc.gr

keywords: *Stichococcus sp.*; photo-bioreactors; biomass separation; biomass dehydration; high added value products.

Introduction

Microalgae have been identified as one of the new feedstocks for renewable energy production. Commercial conversion of microalgae into various valuable products has been significantly increasing in the last decade (Kurniawan et al., 2022). Microalgae are rich in proteins, carbohydrates, lipids and pigments, which may be affected during the drying stages of the recovery process (Min et al., 2022). A number of microalgae harvesting methods have been used including flocculation, filtration and centrifugation, while for biomass drying have been used solar drying, spray drying, freeze drying and convective drying (Chen et al., 2015).

The present study focuses on the development of novel processes for microalgal biomass. The conventional processes of filtration, centrifugation and flocculation (using chitosan as flocculant) have been compared with the biomass scraping process, for microalgae growing attached on flat surface photo-reactors.

Materials and methods

Stichococcus sp. microalgae cultivation took place both in small and larger scale photo-bioreactors. Cultures were cultivated in beaker vessels, representing small scale, with 150 mL of Bold's Basal Medium. Larger scale experiments were conducted in a flat-panel photo-bioreactor filled with 15 L of growth medium and a batch photo-bioreactor filled with 1.5 L of growth medium. Moreover, the drying processes of convective- (@60 °C), freeze- and solar-drying (@~55 °C), so to reveal most efficient process for bio-products recovery.

Results and discussion

Experiments indicated that biomass scraping from the glass surfaces (Fig. 1A) showed lower recovery, compared to the rest of the methods applied. The microalgae growing in suspension in the biomedium, which accounted for about 35% of the total biomass, were also pumped out along with the culture media; however, the biomedium (with the suspended microalgae) may be used as an inoculum for the following cultures, alleviating the operation of a biomass feeding unit. Biomass manual scraping proved as a cost-effective method. Based on calculations, the proposed process per kg of water removed requires energy of about 0.7 kWh, while filtration or centrifugation require about 12.0 kWh or 10.0 kWh, respectively. On the other hand, the combination of flocculation/centrifugation or flocculation/filtration require about 2.5 kWh or 2.0 kWh, respectively.

With respect to drying processes, experiments performed using 21 g of biomass, with moisture content 39%. I took about 5, 6.5 and 8 h, for drying the aforementioned amount of biomass, by oven drying, solar drying and freeze drying, respectively. Furthermore, oven drying and freeze drying required approximately 58.5 and 49.7 kWh/kg for complete removal of moisture, while no energy addition (apart from solar energy) required for passive solar drying. Production of proteins and carbohydrates were maximized when implementing oven drying, noting 0.45 and 0.19 g/g of dry biomass, respectively (Fig. 1B). The maximum recovery yields of lipids, total chlorophyll, and β -carotene were found to be 0.26, 6.99 and 1.44 mg/g of dry biomass, under freeze-drying dehydration.

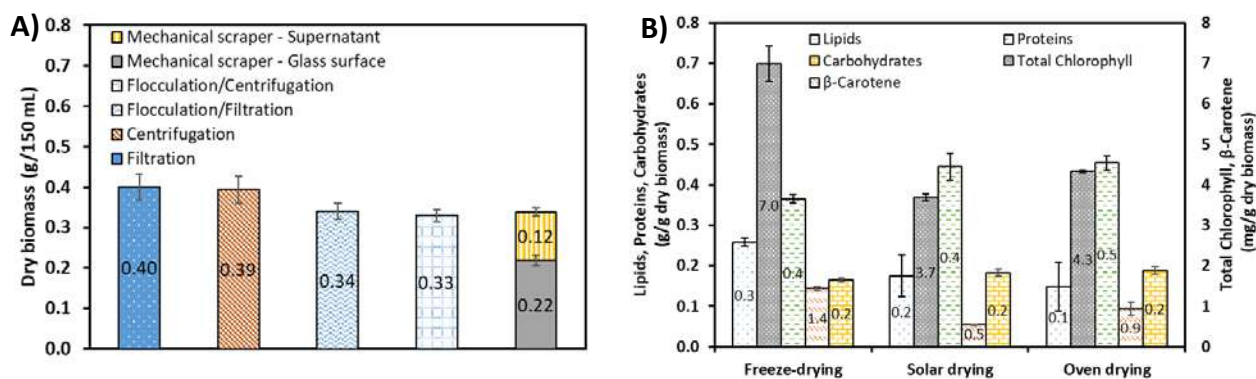


Figure 1. A) Biomass harvesting by: mechanical scraping, filtration, centrifugation, flocculation/vacuum filtration, and flocculation/centrifugation. **B)** Bio-products recovery through freeze drying, solar drying, and oven drying.

Conclusions

This study evaluated the effectiveness of various processes for algal biomass harvesting and drying, taking into account the relative environmental impacts. The study indicated that biomass scraping from an immobilized-cell cultivation system is more efficient, compared with conventional processes. Oven drying was proved as the faster process for the removal of moisture from algal biomass, but it was the most energy consuming process, followed by freeze drying. Solar drying is the most energy effective process, but it is affected by weather conditions. The selection of the most beneficial harvesting and drying processes may significantly reduce production costs, maximizing the revenue from added value products.

Acknowledgements: This study is co-financed by the European Regional Development Fund of the EU and Greek national funds through the Operational Program Competitiveness, Entrepreneurship and Innovation, under the call “Research-Create-Innovate” (project code: T1EDK-02681). Project title is “Bioconversion of CO₂ into high-added value bioproducts through sustainable microalgae cultivation processes (CO₂-BioProducts)”.

References

- Chen C. L., Chang, J. S., Lee, D. J., 2015. Dewatering and Drying Methods for Microalgae. *Sludge Drying and Dehydration*, 33(4), 443-454.
- Kurniawan, S. B., Ahmad, A., Imron, M. F., Abdullah, S. R. S., Othman, A. R., Hasan, H. A., 2022. Potential of microalgae cultivation using nutrient-rich wastewater and harvesting performance by bio-coagulants/bio-flocculants: Mechanism, multi-conversion of biomass into valuable products, and future challenges. *Journal of Cleaner Production*, 365, 132806.
- Min, K. H., Kim, D. H., Ki, M. R., Pack, S. P., 2022. Recent progress in flocculation, dewatering, and drying technologies for microalgae utilization: Scalable and low-cost harvesting process development. *Bioresour. Technol.*, 344, Part B, 126404.



CO₂ mitigation of industrial flue gas using an attached system microalgal photo-bioreactor

D. Mitrogiannis¹, G. Makaroglou¹ and P. Gikas¹

¹Design of Environmental Processes Laboratory, School of Chemical and Environmental Engineering,
Technical University of Crete, Chania, Greece

Corresponding author email: pgikas@tuc.gr

keywords: *Stichococcus sp.*; photo-bioreactors; flue gas; CO₂ fixation; high added value products.

Introduction

CO₂ is the end product of any combustion process. Its emission to the atmosphere is controlled, as it has been classified as greenhouse gas. On the other hand, CO₂ is necessary for vegetal and algal growth. A number of useful biochemical products, food supplements, cosmetics and animal feed may be produced from microalgae. Combining CO₂ reduction with the production of high added value products is an ideal situation, especially if CO₂ comes from large facilities, such as power plants (Molitor et al., 2020).

Most microalgal species grown in artificial environments for the production of high added value products have been isolated from natural streams, lakes or oceans. Microalgae growth may be enhanced, if grown under CO₂ rich environment, but very high CO₂ concentrations may affect negatively microalgal growth. Post-combustion flue gas streams typically contain between 4-14% or beyond CO₂ concentration (v/v) and possibly toxic compounds (such as: SO_x, NO_x, trace elements) at high temperature (80-120 °C or above). Thus, microalgae should be able to tolerate the harsh flue gas conditions in order to capture CO₂. Microalgal CO₂ bio-fixation is a complex biochemical process; for a given specie, it is influenced by physicochemical and other cultivation parameters (such as CO₂ concentration, pollutants in the flue gas, initial inoculation density, culture temperature, light, nutrients and pH) and hydrodynamic parameters (for example, flow, mixing and mass transfer). Microalgae growth on flue gas from coal combustion facilities is significantly more challenging, compared to flue gas from natural gas facilities (Zhang, 2015).

The purpose of the present study is use of microalgae for the removal of CO₂ from the flue gas of a power plant operating on natural gas, and the production of high added value products.

Materials and methods

The study is carried out at the Lavrio, Greece, natural gas power plant, owned by the Public Power Corporation (PPC) Group. Microalgae are growing immobilized on sandblasted glass, in a 15 L closed type photo-bioreactor, installed inside a thermostatic enclosure to provide protection from weather conditions and from other limiting factors. *Stichococcus sp.* is used throughout the experiments. Flue gas containing mainly CO₂ (3.5%), N₂, O₂ and NO_x is conveyed into the photo-bioreactor at a rate of 1 L min⁻¹. Cultures are illuminated by LED lamps (5500 lux), while the temperature is controlled by an A/C unit at 25 ± 1 °C. The cultivation conditions were selected based on a previous study (Makaroglou et al., 2021). *Stichococcus sp.* is cultivated in artificial seawater + Bold's Basal Medium, containing 35 g L⁻¹ and 0.75 g L⁻¹ NaCl and NaNO₃, respectively. Nitrogen starvation is implemented 3 days prior to biomass harvesting, in order to increase lipids production. At the end of the cultivation period, the collected biomass shall be used for the extraction of high added value products (i.e., carbohydrates, lipids, pigments and proteins), to assess the potential of *Stichococcus sp.* to be used in 3rd generation biorefineries. A typical flow chart of the experimental set-up is shown in Figure 1.

Results and discussion

Preliminary data of the experiment indicated that *Stichococcus sp.* biomass yield is approximately 45 ± 5 g m⁻² dry basis, following the abovementioned growth parameters. The CO₂ that was converted into microalgae biomass in the present study, was calculated to be 82 ± 0.5 g m⁻². By processing the harvested biomass, there is an 85-94 % recovery of bio-products. Specifically, carbohydrates account for up to 48%, while proteins 26 %. Lipids are maximized through the implementation of nitrogen starvation prior to biomass recovery, noting



up to 29 % of biomass. The concentration of photosynthetic pigments is 0.4 and 0.1% of total chlorophyll and β -carotene, respectively.

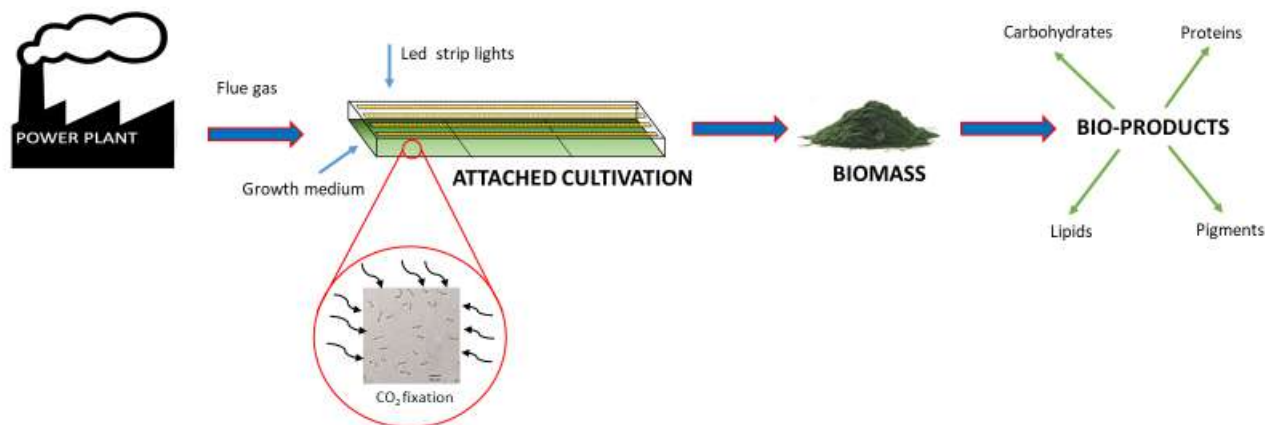


Figure 1. Microalgae cultivation flow chart.

Conclusions

According to the study, *Stichococcus* sp. is successfully grown under real-time industrial flue gas produced from a power plant operation on natural gas. Microalgae has effectively used for CO₂ removal from flue gases before they are released into the atmosphere, while the produced biomass was efficiently harvested and processed for the production of high added value products. In conclusion, large scale microalgae photo-bioreactors, where microalgae grown immobilized, may be employed for CO₂ capture (mitigating the greenhouse effect), with parallel production of high added value bioproducts.

Acknowledgements: This study is co-financed by the European Regional Development Fund of the EU and Greek national funds through the Operational Program Competitiveness, Entrepreneurship and Innovation, under the call “Research-Create-Innovate” (project code: T1EDK-02681). Project title: “Bioconversion of CO₂ into high-added value bioproducts through sustainable microalgae cultivation processes (CO₂-BioProducts)”.

References

- Makaroglou, G., Pavlou, A., Kompogennitaki, R., Penloglou, G., Gikas, P., Kalogerakis, N., Kiparissides, C., 2021. Optimization of *Stichococcus* sp. cultivation in lab and pilot scale photo-bioreactors for efficient CO₂ fixation and bio-products production, *3rd Online International Conference on Environmental Sustainability and Climate Change*, 15-16 November 2021.
- Molitor, H. R., and Schnoor, J. L., 2020. Using simulated flue gas to rapidly grow nutritious microalgae with enhanced settleability. *ACS Omega* 5, 42, 27269–27277.
- Zhang, X., 2015. Microalgae removal of CO₂ from flue gas. *IEA Clean Coal Centre*, London, United Kingdom.



Investigation of hydrocyclone performance to municipal wastewater treatment plants

A. Kehagias¹, K. Tsamoutsoglou¹ and P. Gikas¹

¹Design of Environmental Processes Laboratory, School of Chemical and Environmental Engineering,
Technical University of Crete, Chania, Greece
Corresponding author email: pgikas@tuc.gr

keywords: wastewater treatment plant; hydrocyclone; solid–liquid separation.

Introduction

Solids separation is an important process for wastewater treatment applications. Sedimentation tanks and filtration processes are commonly employed for the removal of suspended solids from various wastewater streams, especially in municipal wastewater treatment applications (Ali-Zade et al., 2008). Hydrocyclones have been used effectively for the removal of solids suspended in water (Souza et al., 2000). A hydrocyclone consists of a conic end linked to a cylindrical body, at the top of which there is a tangential entrance for the feeding suspension (Figure 1). When the feeding suspension is introduced into the hydrocyclone, the centrifugal motion separates the solids based on their density. A fraction of the liquid and the heavier particles are discharged through a concentrated underflow drain and the remaining liquid and lighter particles are discharged throughout the diluted overflow exit (Flintoff et al., 1987). Separation of suspended solids by hydrocyclones is a cost effective process with minimal need for installation and maintenance, and at low energy consumption (Wei et al., 2017). However, the use of hydrocyclones for the removal of solids in municipal wastewater has not been sufficiently exploited. The present study aims to investigate the performance of hydrocyclone for the removal of solids from the overflow of the primary clarifier at the municipal Wastewater Treatment Plant (WWTP) of Chania, Greece.

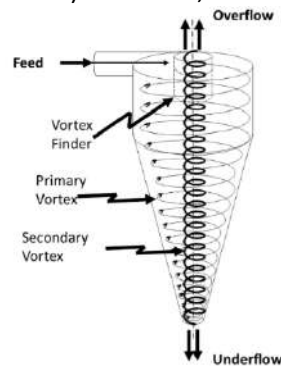


Figure 1. Fluid-flow inside hydrocyclone (Khatri et al., 2020).

Materials and methods

A hydrocyclone was installed at the Chania WWTP downstream of the primary clarifier in order to evaluate its efficiency for separating suspended solids. The hydrocyclone has an overall height of 1.079m and an inlet diameter of 172mm. The primary clarifier effluent was pumped into the hydrocyclone using a submersible pump with a horsepower of 1.5 Hp, at flowrate of 21 m³/h. Biochemical Oxygen Demand (BOD₅), Chemical Oxygen Demand (COD), and Total Suspended Solids (TSS) were measured twice per week over a one-month period. All tests accomplished according to the standard method for water and wastewater examination (Federation and Association, 2005). The sampling points of the system are depicted in Figure 2.

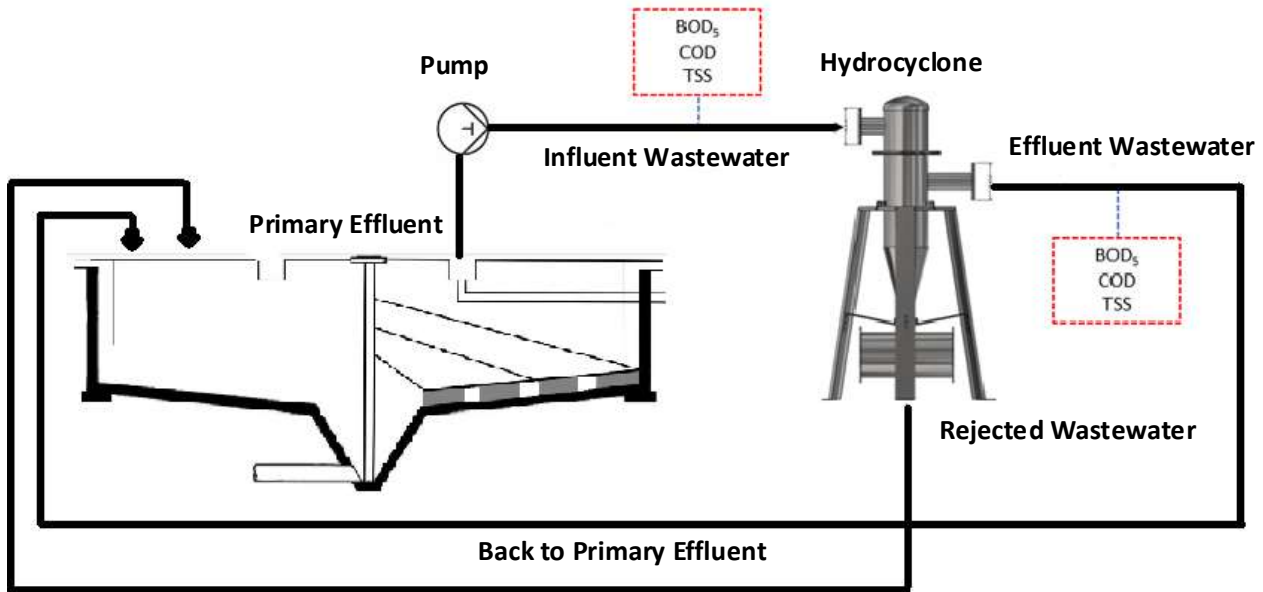


Figure 2. A schematic illustration of the system's sampling points.

Results and discussion

During the experiments the flowrate was fixed at 21m³/h. TSS, BOD₅, and COD concentrations of the primary clarified effluent were measured as 222 ± 24 of TSS, 601 ± 33 of COD and 428 ± 9 mg/L of BOD, respectively, while hydrocyclone effluent were determined as 147 ± 13, 539 ± 29 and 283 ± 22mg/L, respectively. Based on the experimental results, the hydrocyclone removed approximately 34% of TSS, 24% of BOD₅, and 10% COD, reactively, which is a significant amount, taking into account that the wastewater had already been processed through a clarifier. Additional experimentation should be conducted to investigate the effect of flowrate to the solids removal rate. Also, further experiments should be carried out to investigate the efficiency of the hydrocyclone on raw wastewater, upstream of the primary clarifier.

Conclusions

Hydrocyclones are a low-capital-and-operational-cost option for removing TSS from WWTPs. The hydrocyclone was demonstrated to be capable of removing up to 34%, 24% and 10% of TSS, BOD₅ and COD, respectively, at flowrate of 21 m³/h downstream of the primary clarifier.

References

- Ali-Zade, P., Ustun, O., Vardarli, F. and Sobolev, K., 2008. Development of an electromagnetic hydrocyclone separator for purification of wastewater. *Water Environ. J.* 22, 11–16.
- Federation, W.E. and Association, A., 2005. *Standard methods for the examination of water and wastewater*, Am. Public Heal. Assoc. Washington, DC, USA 21.
- Flintoff, B.C., Plitt, L.R. and Turak, A.A., 1987. *Cyclone modelling: a review of present technology*, CIM Bull.:(Canada) 80.
- Khatri, N., Khatri, K.K. and Sharma, A., 2020. Enhanced energy saving in wastewater treatment plant using dissolved oxygen control and hydrocyclone. *Environ. Technol. Innov.* 18, 100678.
- Souza, F.J., Vieira, L.G.M., Damasceno, J.J.R. and Barrozo, M.A.S., 2000. Analysis of the influence of the filtering medium on the behaviour of the filtering hydrocyclone. *Powder Technol.* 107, 259–267.
- Wei, W., Jiu-yang, Y., Xiao-tao, Z., Xia, L. and Wei, L., 2017. A New Method for Predicting the Hydrocyclone Efficiency with the Light Dispersed Phase. *Energy Procedia* 105, 4428–4435.



The ReCiProCo project: development of a methodology to measure and communicate the circularity of products

S. Scaffoni¹ and V. Fantin²

¹Department SSPT, ENEA - National Agency for New Technologies, Energy and Sustainable Economic Development, Rome, Italy

²Department SSPT, ENEA - National Agency for New Technologies, Energy and Sustainable Economic Development, Bologna, Italy

Corresponding author email: silvia.scaffoni@enea.it

keywords: *circular economy measurement; circularity communication; construction sector; textiles sector; paper sector.*

Introduction

The RECIProCo Project is carried out by ENEA in the framework of the agreement with the Italian Ministry for Economic Development on the "Implementation of tools and initiatives on circular economy for the benefit of consumers".

One of the objectives of the project is the execution of a feasibility study for the development of a voluntary environmental communication system for non-food and non-energy products, based on 2 types of indicators: a set of mandatory circularity indicators and a set of optional indicators on the use of water resources. The final goal, in addition to communicating the circularity of a product in a complete and adequate way, is to support companies in identifying areas for environmental improvement (e.g. through eco-design), also in a supply chain approach.

Materials and methods

A life cycle approach was followed, therefore considering the materials the product is made of (e.g. percentage of recycled materials, percentage of by-product), the phase of use (e.g. duration of product, reparability) and the end of life (e.g. percentage of material destined for recycling). A measurement / verification method was identified for each indicator.

Results and discussion

A set of indicators (about 20 qualitative and quantitative indicators) was identified and selected among the ones already present in the environmental labels / certifications, in some main national and European directives and regulations, in the technical specification UNI/TS 11820 "Circularity Measurement - Methods and indicators for measuring circular processes in organizations", currently being published. An IT tool available for the companies was developed, based on the circularity indicators selected. The indicators and the tool were tested on selected products and supply chains in collaboration with companies in the construction, textile, and paper sectors. Such sectors were identified in agreement with MiSE and the consumers' associations, as they are relevant for the Italian production and industrial system as well for the consumers.

In addition, a QR code system will also be developed which will help communicate the results of the circularity indicators to the consumer, as well as to companies, in a B2B perspective.

Acknowledgements: This study received funding from the Ministry of Economic Development in implementation of art. 5, paragraph 1 of the decree of 10 August 2020.



Assessment of the contribution of an innovative biosolids microsieving-gasification system to the formation of the wastewater management legal framework

A. Syrpis¹, A. Manali¹ and P. Gikas¹

¹Design of Environmental Processes Laboratory, School of Chemical and Environmental Engineering,
Technical University of Crete, Chania, Greece
Corresponding author email: pgikas@tuc.gr

keywords: *wastewater management; legislation; biosolids; microsieving; gasification.*

Project outline

Activated sludge Wastewater Treatment Plants (WWTPs) require large amounts of electric energy for proper wastewater treatment, with the aeration tank alone consuming over 70% of the supplied energy (Siatou et. al, 2020). Moreover, WWTPs produce significant amounts of biosolids, a nuisance material requiring further treatment and proper disposal. Thus, wastewater treatment and biosolids management should be viewed in a new light: Wastewater treatment should be redesigned so to achieve significant energy savings (without compensating to effluent quality), while the energy content of biosolids should be exploited. Such a novel process (LIFEB2E4sustainable-WWTP) is currently under development at the WWTP of Rethymno, Greece, where an innovative biosolids management pilot plant is being installed. The pilot plant, with capacity of approximately 5,000m³/d of incoming wastewater, consists of the following processes in sequence: microsieving (removal of biosolids upstream of the aeration tank using a rotating belt filter), drying (moisture removal), gasification (syngas production) and syngas combustion in co-generation engine (thermal and electric energy production). However, successful demonstration of novel approaches in wastewater treatment and biosolids management, even if the novel process is absolutely beneficial, would not lead to process adoption in new projects. New norms and legislative initiatives should be implemented, so the new process to be applied.

The present study aims in mapping the relevant legislations, regulations and directives, in frame of the development of the aforementioned novel wastewater and biosolids management process. The study will also examine the project's contribution to the transformation of the existing regulatory and legal framework related to wastewater management.

Wastewater management regulatory and legal framework

The most relevant to the project regulatory and legal framework are EU policies/directives related to wastewater, waste, water, and sewage sludge management, wastewater engineering and energy efficiency. In detail, the project objectives are related to the following policies and directives:

- Directive 2000/60/EC establishing a framework for the community action in the field of water policy (EU Water Framework Directive).
- Directive 91/271/EEC concerning urban wastewater treatment.
- Directive 86/278/EEC on the protection of the environment, and in particular of the soil, when sewage sludge is used in agriculture.
- Directive 1999/31/EC on the landfill of waste.
- Directive 2012/27/EU on energy efficiency.
- CEN/TC 165 on standardization in the field of wastewater engineering in the European Union.
- European Innovation Partnership on Water for addressing major European and global water challenges.

The project will contribute to achieve the goals and follow the standards set in the abovementioned regulations, including raising awareness of the benefits of the proposed process and opportunities for integrating this into wider wastewater management projects, proving its environmental and social acceptability. Also, global policy frameworks will be studied, in order to record the existence of any relevant



global standards to the treatment of wastewater to assure the project partners to ensure that the technology will be compliant.

Expected results

After the completion of the project, the main outcomes are expected to be the driving force for the enactment of new regulations/directives regarding the wastewater treatment with a sustainable perspective. Also, the new legislation will be adapted to the proposed system, so to encourage the wide application of new technologies.

Acknowledgements: This study is supported by the Green Fund and the LIFE project (EC): “New concept for energy self-sustainable wastewater treatment process and biosolids management (LIFE B2E4sustainable-WWTP)”, LIFE16 ENV/GR/000298.

References

- Council Directive 1999/31/EC on the landfill of waste (1999), 26 April. <https://eur-lex.europa.eu/eli/dir/1999/31/oj>
- Council Directive 86/278/EEC on the protection of the environment, and in particular of the soil, when sewage sludge is used in agriculture (1986), 12 June. <https://eur-lex.europa.eu/eli/dir/1986/278/oj>
- Council Directive 91/271/EEC concerning urban waste-water treatment (1991), 21 May. <https://eur-lex.europa.eu/eli/dir/1991/271/oj>
- Directive 2000/60/EC of the European Parliament and of the Council, establishing a framework for Community action in the field of water policy (2000), 23 October. <https://eur-lex.europa.eu/eli/dir/2000/60/oj>
- Directive 2012/27/EU of the European Parliament and of the Council on energy efficiency, amending Directives 2009/125/EC and 2010/30/EU and repealing Directives 2004/8/EC and 2006/32/EC Text with EEA relevance (2012), 25 October. <https://eur-lex.europa.eu/eli/dir/2012/27/oj>
- Siatou, A., Manali, A. and Gikas, P. 2020. Energy consumption and internal distribution in activated sludge wastewater treatment plants of Greece", *Water*, 12, 1-16.



Isolation and determination of the energy content of grease and oil in Wastewater Treatment Plants on the island of Crete

N. Tatas¹, A. Manali¹ and P. Gikas¹

¹Design of Environmental Processes Laboratory, School of Chemical and Environmental Engineering, Technical University of Crete, Chania, Greece
Corresponding author email: pgikas@tuc.gr

keywords: wastewater treatment plants; degreasers; fats and oils; extraction; calorific value.

Introduction

Food preparation in households and in restaurants generates significant quantities oil and grease (O&G), which often end up at the Wastewater Treatment Plant (WWTP). Crete is not an exception to the above rule, with O&G maximizing during summer, due to the increase of tourists. Even if there are companies collecting O&G in Crete, and most municipalities in Crete have enforced the use of degreasing facilities at the restaurants (prior to wastewater discharge into the sewer), large amounts of O&G are entering the sewers. The O&G separated at the WWTPs are usually disposed, however they could be used as raw materials to produce alternative fuels such as biofuel (biodiesel) (Srivastava et al., 2018). The present study aims in estimating the production of O&G in the island of Crete, and determining their energy content, by measuring their heating value.

Materials and methods

O&G samples were collected from the degreasing facilities of the three largest WWTPs of Crete, treating the wastewater of municipalities of Chania, Rethymno and Heraklion. Although the sampling points were always the same for each WWTP, the samples had large heterogeneity, so they were managed as liquid or solid depending on their composition. Three samples had been collected between September 2021 and January 2022. All the studied WWTPs are equipped with aerated degritting/degreasing facilities, located downstream of the screening facilities.

O&G were extracted from the samples using the 5520 Standard Method (APHA, 2017), using Gerhardt's Soxtherm apparatus, with petroleum ether as solvent. The Higher Heating Value (HHV) of O&G was determined by the XRY-1A Oxygen Bomb Calorimeter.

Results and discussion

The average O&G content in liquid samples was measured as: 23.1 ± 8.4 , 19.4 ± 5.1 and 7.9 ± 3.4 g/L for the WWTPs of Heraklion, Rethymno and Chania, respectively (Figure 1). According to previous studies, the concentration of fats and oils in raw municipal wastewater ranges from 0 to 15 g/L (APHA, 2017; Williams et al., 2017). However, the O&G concentrations measured from the WWTPs of Heraklion and Rethymno were measured above the concentrations reported by the literature, which is probably due to inadequate removal of O&G by the onsite degreasers.

Solid samples had been collected only from the Chania and Rethymno WWTPs, resulting to an average O&G content of 490.6 ± 246.4 and 122.2 ± 7.7 mg/g, respectively (Figure 2). No solid sample was collected from the WWTP of Heraklion.

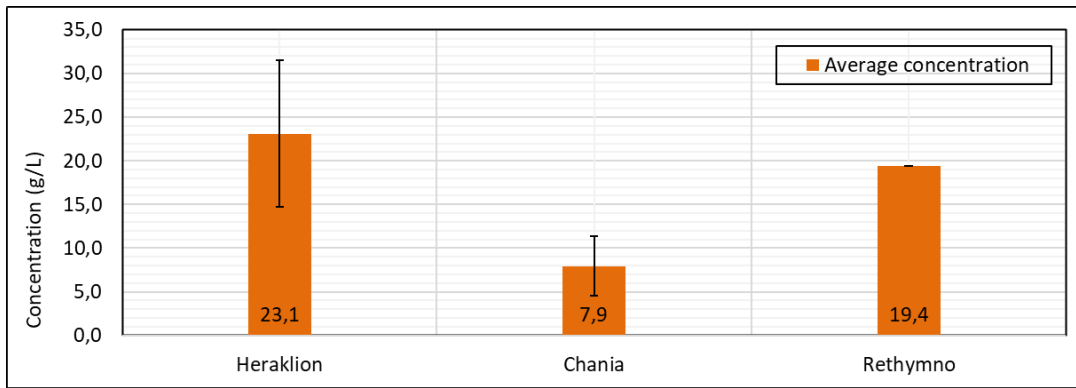


Figure 1. Average concentrations in liquid samples of O&G at WWTPs in Crete.

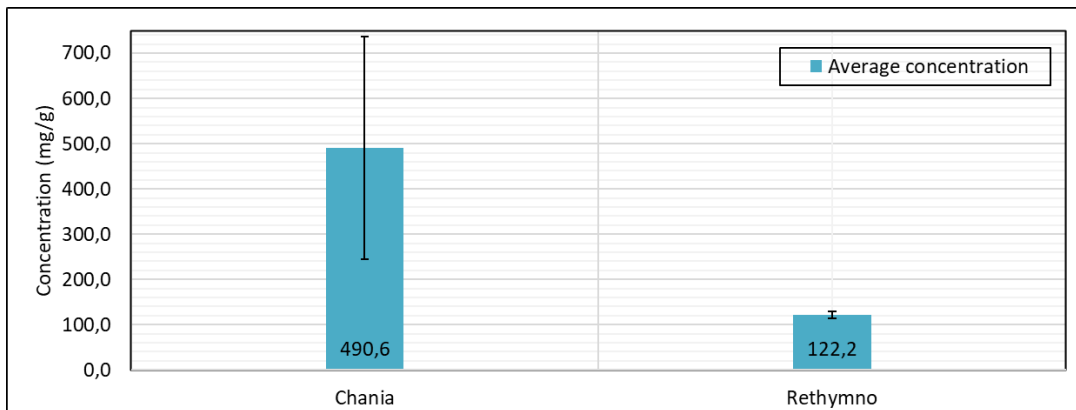


Figure 2. Average concentrations in solid samples of O&G at WWTPs in Crete.

The HHVs of the O&G isolated from the samples were measured as: 43.6 ± 0.7 , 42 ± 1.8 and 40.2 ± 3.2 MJ/kg, for the WWTPs of Heraklion, Chania and Rethymno, respectively. HHV values of other typical oils, such as oil from corn, soybean, sunflower, olive, and eucalyptus, range from 37 to 43 MJ/kg, which is quite similar with the values found for O&G.

Despite the differences monitored in O&G concentrations in the samples, the HHVs are quite similar. This may be because the chemical composition of fats and oils is similar no matter the source. Also, the high energy content of the isolated fats and oils shows that they can be used as raw material to produce alternative fuels, such as biodiesel, by following the process of esterification/transesterification. The produced biodiesel is valuable for the coverage of the energy needs of WWTPs, and particularly for the aeration process, which is responsible for 45-90% of the total energy consumption of a WWTP (Rosso et al., 2008).

Conclusions

The O&G concentrations in the samples found to be quite different, ranging from 7.9 to 23.1 g/L for the liquid samples, and from 122.2 to 490.6 mg/g for the solid samples. Despite the large heterogeneity of the samples (liquid or solid), their HHV values, and therefore their energy content, found to be quite similar, varying between 40.2 to 43.6 MJ/kg.

References

- APHA, 2017. *Standard Methods for the Examination of Water and Wastewater*, 23rd Edition.
- Rosso, D., Stenstrom, M.K. and Larson, M.K. 2008. Aeration of large-scale municipal wastewater treatment plants: state of the art. *Water Sci. Technol.*, 57 (7), 973–978.
- Srivastava, N., Srivastava, M. and Gupta, V.K., 2018. Recent development on sustainable biodiesel production using sewage sludge. *Biotech*, 8, 245.
- Williams, J.B., Clarkson, C., Mant, C., Drinkwater, A. and May, E., 2012. Fat, oil and grease deposits in sewers: Characterisation of deposits and formation mechanisms. *Water Research*, 46 (19), 6319-6328.



Treat and Reuse of high organic load wastewater with an innovative compact and modular unit

A. Yfantis¹, N. Yfantis¹, T. Angelakopoulou¹, F. Michelet¹, G. Giannakakis¹, N. Ellinakis¹, S. Dokianakis², E. Vasilaki² and N. Katsarakis²

¹Sychem Advanced Water Technologies s.a., Heraklion, Greece

²Center of Materials Technology and Photonics, Hellenic Mediterranean University,
Heraklion, Crete, Greece

Corresponding author email: katsan@hmu.gr

keywords: wastewater; innovative; high organic load; modular unit; compact; mbr.

Introduction

High organic load wastewaters are widely used as potential resources for producing energy via biogas from anaerobic digestion (AD). AD is considered as one of the best technologies for treating high strength wastewaters (Mata-Alvarez et al., 2000), thing that led to a significant development of these units around the world. According to a recent statistical report from European Biogas Association (EBA,2020) the number of biogas plants reached up to 19,000 in Europe in 2020 producing 15.8 bcm. This number will continue to grow, since the price of fossil natural gas has risen to a previously unimaginable height in recent years. These installments also produce liquid and solid digestate that need to be treated prior to disposal in order to avoid nutrient infiltration into the groundwater, soil acidification and the eutrophication of the surface waters (Jurgutis et al., 2021). It would be of significant added value to create an end-product that can treat these kind of wastewaters, in order to solve important wastewater management problems encountered either by government agencies or companies operating in this field. The aim of our study was to manufacture an industrial standard of a pre-assembled, modular, high organic load wastewater treatment unit which will serve as a demonstration model. This unit could adjust the tolerance and function parameters, based on the assessment of measurements and results, so that the effluent of the wastewater treatment system is pure irrigation water that meets all relevant standards. It would also guarantee the flexibility in using the pre-assembled wastewater standard unit for a wide range of applications with competitive manufacturing and operating parameters. The proposed facility is an innovative compact, modular process units with particularly low operating costs, which combine membrane reactor technologies (MBR) and bioaugmentation, advanced photocatalytic oxidation, as well as reverse osmosis processes (Fig 1.), aiming at clean water production for safe disposal and / or irrigation. The modular type of this unit gives the advantage to have the capability of treat a widely range of wastewaters, according to the effluent standards that the end user is willing to meet. Furthermore in this study a working scenario will be presented by using a liquid digestate from an industrial scale AD facility that treats high strength wastes (pig manure, food waste, cheese whey and slaughterhouse).



Figure 1. Innovative process for the treatment of digestate.

Materials and methods

Industrial Unit is consisted of:

- Balance tank of 155 m³ which is separated in two compartments (25 and 135 m³) for anoxic treatment and denitrification.
- Aeration tank of 78 m³ made of polypropylene
- Ultrafiltration unit that is capable for being used in compact units with 2 membranes of PVDF and 11 m² area (each)
- Photocatalysis unit that is used in a batch mode with 2 m³ working volume in which the wastewater (with the added catalyst TiO₂) is recirculated under UV-Light.
- Reverse Osmosis Unit that can treat up to 60 m³ of wastewater in two stages.



- Disinfection unit with a MDPE tank of 100 l

Liquid Digestate was obtained from an industrial scale AD facility installed in Heraklion Crete, which treats high strength wastes and wastewaters.

Chemical Analyses. The following parameters were examined: pH, chemical oxygen demand (COD), BOD₅, Total (TS) solids, total (TSS) suspended solids, total nitrogen (TN), ammonium nitrogen, total coliforms and acute toxicity.

Results and discussion

Concerning the presented process the liquid digestate was first added to the balance tank and then moved to the aeration tank. Effluent of the aeration tank was moved to the membrane bioreactor consisted of ceramic membranes. Reverse osmosis followed the MBR process. In parallel a small quantity of the MBR treated wastewater was used as influent to the photocatalytic batch reactor.

Characteristics of the liquid digestate are presented in Table 1 . An average value of measurements is presented in Table 1 for the determined parameters for the different processes that were used for the treatment of the digestate. It should be mentioned that the effluent of each process was used as influent to the next one as presented in Fig. 1.

Table 1. Reverse Osmosis efficiency.

	pH	Cond. (µS/cm)	TS (g/L)	TSS (g/L)	BOD ₅ (mg/L)	t-COD (mg/L)	TN (mg/L)	NH ₄ ⁺ (mg/L)	NO ₃ ⁻ (mg/L)	Total Col.
Digestate	8.16	33380	93	42	n.m.	59300	7610	4750	n.m.	n.m.
Influent MBR	8.08	20460	78	35	n.m.	51359	4850	3429	87.8	n.m.
Effluent MBR	8.07	24240	9.2	0.012	268	3845	3860	2680	80.1	n.m.
Effluent UV-TiO ₂ *	7.59	26200	9.1	0.012	241	2791	3425	2635	78.4	n.m.
Influent RO	7.25	25700	10.4	0.010	212	2668	3272	2587	82	n.m.
Final Effluent	5.43	433	0.29	0.001	9.9	15	55	45.6	3.9	n.d.

n.d. not detected, n.m. not measured, *photocatalysis process run in a batch mode independently.

All the monitored parameters were significantly decreased as it is demonstrated in table 1.

Conclusions

Based on the results of this study, it has been demonstrated that the proposed process is a sustainable method to treat high strength wastewaters. Moreover the final effluent meets the standards according to legislation for irrigation.

Acknowledgements: This research has been co-financed by the European Regional Development Fund of the European Union and Greek national funds through the Operational Program Competitiveness, Entrepreneurship and Innovation, under the call RESEARCH – CREATE – INNOVATE (project code:T1EDK-01633).

References

- Mata-Alvarez, J., Macé, S., Llabrés, P., (2000). Anaerobic digestion of solid wastes. An overview of research achievements and perspectives. *Bioresource Technology* 74, 3–16.
- European Biogas Association (EBA) Annual Report 2020
- Jurgutis, L.; Šlepėtiene, A.; Šlepėtys, J.; Cesevičienė, J. (2021) Towards a Full Circular Economy in Biogas Plants: Sustainable Management of Digestate for Growing Biomass Feedstocks and Use as Biofertilizer. *Energies*, 14, 4272



International trends in the formation of water tariffs policy for the supply of reclaimed water for reuse purposes

P. Pliatsika¹, A. Manali¹ and P. Gikas¹

¹Design of Environmental Processes Laboratory, School of Chemical and Environmental Engineering,
Technical University of Crete, Chania, Greece
Corresponding author email: pgikas@tuc.gr

keywords: *water tariff; pricing policy; pricing methodology; reclaimed water; wastewater reuse.*

Introduction

Despite the fact that water is abundant in the earth surface, less than 2% may be used directly from humans. In arid and semi-arid regions water balances are negative, thus water transportation from far away is often selected. On the other hand, large amounts of treated wastewater are disposed to the environment, with no beneficial use. Lately, new legislations and policies have been enacted, to allow for water reuse, primarily for non-potable applications (Apostolidis et al., 2011). However, even if there is relative a global common line, regarding the quality characteristics of reclaimed water, in relation to the final application, the tariff policy for reclaimed water varies significantly, even between neighboring regions. The present study aims to examine the international trends regarding water tariffs policy for the supply of reclaimed water for reuse.

Background

Reclaimed water is used for agricultural and landscape irrigation, for the restoration of the environment, for industrial applications and for groundwater aquifer recharge, while in extreme cases high quality reclaimed water is also used for direct or indirect potable applications (Asano et al., 2007). Guidelines for quality criteria for water reuse have been issued by international organizations, (such as the World Health Organization (WHO) and the Food and Agriculture Organization of the United Nations (FAO)), while many countries and regions have issued their own regulations (Papadaskalopoulou, 2013).

The recent EU Regulation 2020/741 is expected to be effective from June 2023, however the aforementioned Regulation deals only with the qualitative characteristics – not with the applied water tariffs. Directive 2000/60/EC (WFD) is the main directive for water management in EU, providing (among others) guidance on the pricing of water services based on total cost recovery where the following parameters are controlled (Voivontas and Asimakopoulos, 2002) (Figure 1):

- Economic costs, including investment, operation and maintenance costs, management and administrative costs and other direct economic costs.
- The cost of natural resources representing the loss of benefits due to the limitation of available water resources to a degree greater than their natural rate of renewal.
- Environmental costs representing the cost of the damage caused by water use to the environment and aquatic ecosystems.

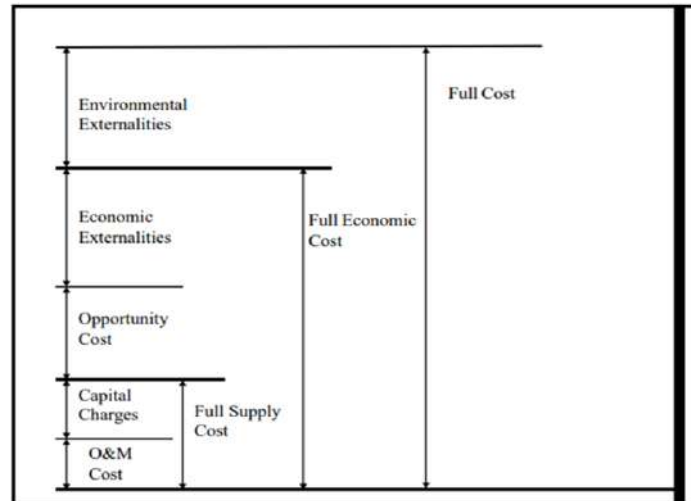


Figure 1. General principles for cost and value of water (Rogers et al., 2002).

However, each water/wastewater company in the world sets water tariffs. Often, reclaimed water is subsidized either from the water companies or from the municipalities, in order to promote its use, while in a number of cases reclaimed water for agricultural irrigation is provided free of charge for an initial period of time, so to be attractive for farmers to try its use.

In order to result to a complete costing and pricing of the reclaimed water, the economic cost (which includes capital, maintenance, operating and administration costs), the environmental cost and the resource cost have to be considered. Some general guidelines/choices for the formation of the reclaimed water pricing policy are the followings:

- No charge.
- Price based on supply cost.
- Fixed percentage on the price of drinking water.
- Fixed percentage on the price of irrigation water.
- Price adjusted to users' willingness to pay.
- Same pricing for conventional and reclaimed water.
- Pricing based on the recovery of environmental and resource costs.

Conclusions

Each water/wastewater company or organization should determine the water tariff based on the conditions prevailing in the area of interest, without forgetting to consider the environmental cost.

References

- Apostolidis, N., Hertle, C. and Young, R., 2011. Water Recycling in Australia. *Water*, 3, 869-881.
- Asano, T., Burton, F. L., Leverenz, H. L., Tsuchihashi, R. and Tchobanoglous, G., 2007. *Metcalf and Eddy: Water Reuse: Issues, Technologies, and Applications*; McGraw Hill: New York, NY, USA, 3 (1), 36-46.
- Directive 2000/60/EC of the European Parliament and of the Council, establishing a framework for Community action in the field of water policy (2000), 23 October. <https://eur-lex.europa.eu/eli/dir/2000/60/oj>
- Papadaskalopoulou, M., 2013. Investigation of metal removal from biomass filtrate by the combined use of ultrafiltration membranes and different adsorbent materials, NTUA, Athens, Greece.
- Regulation (EU) 2020/741 of the European Parliament and of the Council on minimum requirements for water reuse (2020), 25 May. <http://data.europa.eu/eli/reg/2020/741/oj>
- Rogers, P., Silvab, R. and Bhatia, R., 2002. Water is an economic good: How to use prices to promote equity, efficiency, and sustainability, *Water Policy*, 4, 1-17.
- Voivontas, D. and Asimakopoulos, D., 2002. Cost recovery and water pricing in the context of Directive 2000/60, NTUA, Athens, Greece.



**Resilience Water supply, sanitation service provision and hygiene in Awash Basin, Ethiopia:
Sustainable Growth and multi-level governance arrangements for climate change mitigation**

E. Kalapoda¹

¹Department of Architecture & Urban Design/Graduate School of Architecture Planning & Preservation,
Columbia University, City of New York, United States
Corresponding author email: ek3130@columbia.edu

keywords: *urban sanitation; waste-water treatment; sustainable development; climate change mitigation; Addis Ababa.*

Introduction

Water supply, sanitation provision, and hygiene in Addis Ababa, Ethiopia are grossly deficient, as in most cities in sub-Saharan Africa: the combination of the emergent water scarcity due to climate change and the chronic lack of adequate sanitation infrastructure is now threatening the resiliency of the low-income households and the informal settlements of the Addis Ababa's periphery. Struggling between the perception of the grassroots who identify the access to safe water and urban sanitation as a right, and the government's development agenda that sees Addis Ababa as the center for the country's economic expansion, the city's infrastructure is at high risk when assessed for resilient urban sanitation and water supply provision to its inhabitants. This paper builds upon the recent Addis Ababa's Resilience Strategy to focus on the Addis Ababa Water and Sewerage Authority's plan (aiming to build 3,000 shared sanitation facilities as the country's first sewage grid) to identify how these perceptions intertwine between the communities and the government, to examine how just and inclusive the AAWSA's urban sanitation and water supply provision plan is and explore the overall qualitative and quantitative impact of improving the urban water flows in and out of the city in Addis Ababa. Drawing on the recent City Water Resilience Approach (CWRA), integrated with spatial analysis, interviews, and policy documents reviews, I conclude that both grassroots and top-down (growth-centric) approaches do not successfully provide sustainable, accessible, and more just urban sanitation livelihoods in Addis Ababa. This mainly occurs because the conventional approaches to urban sanitary improvement at the city level do not address the dual context of Addis Ababa, that being both a city of informality and the capital of Africa's largest expanding market. But rather, focus on altering the city's water-production-consumption cycle benefitting in most cases the more affluent, well-connected, service-oriented, and resilient city-center communities at the expense of the low-income, fragmented, agriculture-oriented peripheral communities where informality, urban displacement and lack of climate-mitigation infrastructure historically occurs. Building up on the Addis Ababa City Water Resilience Approach (CWRA), I ended up suggesting that a more inclusive coordination of a multi-scalar governance approach would optimize the supply and promote sustainable demand side management practices as workable climate change adaptation measures for a water-scare city such as the Addis Ababa.

References

- Addis Ababa Water and Sewerage Authority (AAWSA), 2015 Addis Ababa Water and Sewerage Authority Growth and Transformation Plan (2015-2020), Addis Ababa, Ethiopia
- AAWRM&P Framework Preparation task force. 2016. Addis Ababa-Adama resources management and protection framework. Addis Ababa, Ethiopia.
- Addis Ababa City Administration and Resilient Cities Network. 2020. Addis Ababa Resilience Strategy. The Resilience Shift. 2019. "City Water Resilience Approach (CWRA)." City Water Resilience Approach (CWRA) (blog). 2019. <https://www.resilienceshift.org/tool/city-water-resilience-approach-cwra/>.
- Proclamation No. 574/ 2008, Federal Democratic Republic of Ethiopia (FRDE). Urban Planning Proclamation, Negarit Gazeta. Year 14, No.29



SUST
ENG
2022



FULL PAPERS



Technical assessment of a plant for recovery of metals from HDS catalysts

N. M. Ippolito¹, V. Innocenzi¹, I. D'Adamo² and F. Ferella¹

¹Department of Industrial and Computer Engineering and Economics, University of L'Aquila, L'Aquila, Italy

²Department of Computer, Control and Management Engineering, Sapienza University of Rome, Rome, Italy

Corresponding author email: francesco.ferella@univaq.it

ABSTRACT

The paper aims to present a techno-economic analysis to recover nickel, molybdenum, and vanadium from spent hydrodesulfurization (HDS) catalysts. The plant, with a 6000 tons/year capacity, is based on a industrial process with pre-treatment thermal stages tested on a pilot scale. In contrast, the hydrometallurgical section was studied at the University of L'Aquila. The simulations were carried out using lab- and pilot-scale experimental data. Only wet Ni-Mo catalyst was used as the plant's feedstock, producing 1272 tons/year of V₂O₅ 98%wt, 239 tons/year of MoO₃ 57%wt, and 227 tons/year of Ni-V-Mo alloy with an approximate composition of 72-25-3%wt, respectively. The investment is highly profitable, with a net profit of around 14.1 MEUR/year, gross margin of 37.2%, return on investment equal to 23.9%, and a payback time slightly greater than 4 years.

Keywords: HDS; catalysts; molybdenum; vanadium; recycling.

1. INTRODUCTION

Refinery and petrochemical plants are based on catalyzed processes. Hydrotreating, hydrocracking, reforming, isomerization, alkylation, and fluid catalytic cracking are unit operations in petroleum refining using different catalysts to get high-quality products (Furimsky, 1996; Kim et al., 2009; Wang et al., 2021).

Hydrodesulfurization (HDS) catalysts play a crucial role in producing low-sulfur fuels to match the strict environmental regulations on car emissions. HDS catalysts usually are made of MoS₂, with the addition of Ni or Co sulfides supported by porous alumina (Ruiz et al., 2011). During the heavy oil or diesel refining, a significant amount of transition metals are deposited on the HDS catalyst surface in addition to carbon and sulfur. One of these is vanadium, an essential metal that can be recovered together with those active in the catalysis. Nevertheless, the accumulation of such elements leads to the deactivation of the catalysts that have to be regenerated. Sulfur, coke, and soot can easily be removed by a thermal treatment, but metal poisoning is not. Hence, the catalytic activity cannot be fully recovered after each treatment; thus, after some regenerations, the entire amount has to be replaced. Spent HDS catalysts are classified as hazardous materials: their disposal causes environmental threats because of the potential release of heavy metals into the soil and the groundwater table (Ferella et al., 2011; Park et al., 2012; Krishnan et al., 2021; Le and Lee, 2021). Apart from that, these catalysts contain exploitable amounts of metals like Mo, Ni, Co, and V, in concentrations much higher than that they have in primary ores. Several leaching strategies are used to bring valuable metals into the solution (Beolchini et al., 2009; Pradhan et al., 2010).

Few industrial processes are currently available to recycle HDS catalysts, particularly the pyrometallurgical and hydrometallurgical ones. In the hydrometallurgical route, one or two-stage thermal pre-treatment is required to remove hydrocarbons, coke, and sulfur and then oxidize the active metals. After the leaching stage, which can be carried out in several steps, metals are usually recovered from the pregnant solution by standard techniques like precipitation, solvent extraction, adsorption, ion exchange, and electrolysis.

This paper considered the hydrometallurgical approach, including a double-stage thermal pre-treatment required to oxidize residual hydrocarbons, coke, and sulfur.



2. PROCESS AND PLANT DESCRIPTION

The plant is divided into several sections. Only wet Ni-Mo catalysts containing vanadium from the oil fractions were used as feedstock. The plant's capacity was set at 6,000 tons/year of sole Ni-Mo catalyst, in 7/24 continuous operation mode, 300 days/year. The catalyst is impregnated with residual naphtha. The process flow-sheet is shown in Figure 1. Nevertheless, in other recycling plants, wet catalysts are usually mixed with the dry ones containing Ni or Co to lower the low heating value (LHV). The composition of the catalyst is listed in Table 1. It was calculated as average values from the ICP-OES, CHNS, and XRF analyses of many catalysts samples worked at the laboratory. HDS catalysts are based on an alumina carrier (spheres and cylinders) with a high specific surface area, on which the active metals are dispersed.

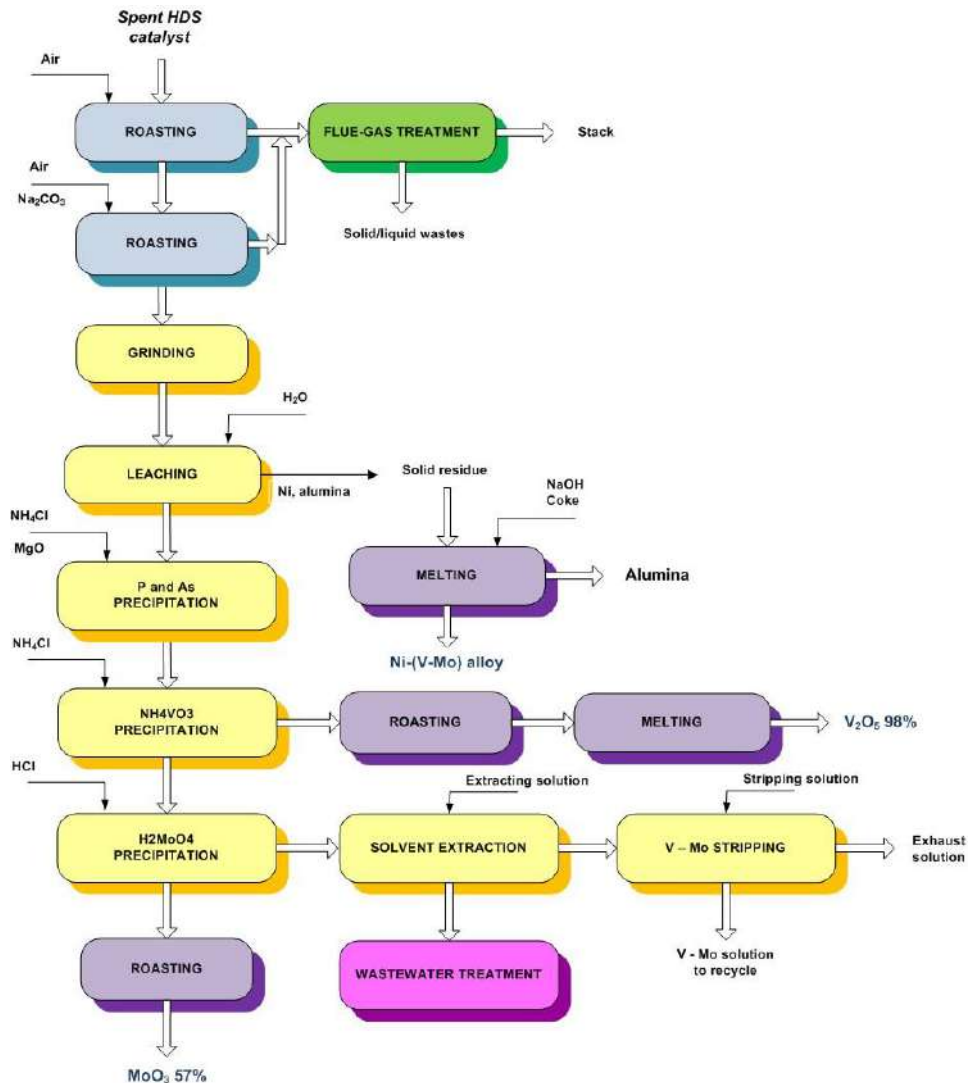


Figure 1. Flow-sheet of the recycling process.

2.1. Catalyst pre-treatment

HDS catalysts require a thermal pre-treatment to remove carbon and sulfur compounds and simultaneously oxidize the metals to recover, i.e., Mo, Ni, and V. The thermal treatment is carried out in two sequential roasting stages: this leads to a pregnant cleaner solution, i.e., free of Na_2SO_4 , that results in a higher grade of the Mo and V salts precipitated in the downstream stages. That is why using a double roasting stage is crucial, although with more disadvantages than the single-stage treatment. In the first kiln, the metal sulfides are converted into the corresponding oxides, mainly oxidizing sulfur into SO_2 , whereas a minimum fraction oxidizes further to SO_3 . Coke and hydrocarbons are oxidized into carbon dioxide and water, supposing a complete conversion yield of 100%. But the conversion rate is usually lower, and, in addition, many



intermediates form like VOC and CO. Nonetheless, the complete oxidation makes all the calculations easier and releases the entire LHV of the catalyst mixture, around 13,400 kJ/kg. In the second stage, Na₂CO₃ is added to convert Mo and V into sodium molybdate and vanadate, which are water-soluble; nickel does not react with carbonate but oxidizes into NiO and partially into Ni₂O₃, thus remains in the solid residue. A representative compound, i.e., tetradecane, was used to simulate naphtha, a mixture of hydrocarbons.

Table 1. Ni-Mo catalyst composition.

Compound	Flow-rate (kg/h)
MoS ₂	41.6
V ₂ S ₃	219.9
NiS	35.7
Coke	116.6
Naphtha	127.4
P	2.5
As	1.5
Al ₂ O ₃	287.5
Total	832.7

The first roasting is carried out in a rotary kiln at 850°C for 3 h, with a catalyst capacity of 3.6 tons/batch, L = 12.00 m, and inner D = 1.40 m. 30% excess air excess was chosen to keep the temperature constant and supply enough oxygen for the oxidation reactions.

Once roasted, the catalyst is partially cooled down and mixed with soda ash in +5%wt to the required stoichiometric amount and loaded into the second rotary kiln. The second roasting is carried out at 800°C for 2 h. The catalyst/soda ash load is 1.9 tons/batch, and the estimated sizes are L = 7.50 m and inner D = 1.25 m. Each of the two rotary kilns is equipped with all the necessary auxiliaries like weighting hoppers, conveyors, and cooling devices. The roasting section was simulated by Chemcad 7 (Chemstation).

2.2. Flue gas section

This section treats six gas streams, i.e., from rotary kiln 1 (catalyst oxidation), rotary kiln 2 (roasting with soda ash), rotary kiln 3 (calcination of AMV), rotary kiln 4 (calcination of molybdic acid), EAF 1 (melting of Ni/alumina solid residue) and EAF 2 (melting of powdered vanadium pentoxide). The plant includes the following stages:

- post-combustion chamber;
- selective non-catalytic reduction (SNCR) of NO_x;
- cooling of the flue gas;
- dry removal of SO_x and other acidic gases;
- wet removal of SO_x.

The post-combustion chamber heats the flue gas to 900°C for a sufficient time to oxidize all the hazardous compounds like CO, hydrocarbons, oxidation intermediates, furans, and dioxins. The flue gas rate in the PCC was calculated to be around 78,000 m³/h. In this process, a catalyst is not required for the non-catalytic conversion (SNCR) of the NO_x. The temperature is suitable for a non-catalytic reduction of NO_x using dry ammonia. An inline injection carries out the reduction with a downstream mixing chamber.

With a total flow rate of 19,359 kg/h at 900°C, the flue gas is cooled down in a heat exchanger, where 5,310 kg/h of water at 15°C and 2 bar cool down the flue gas to 250°C. Water changes phase into superheated steam at 2 bar and 150°C: this steam is used for heating the leaching and molybdenum precipitation reactors in the hydrometallurgical section. The great amount of SO_x (around 128 kg/h of SO₂ and 20 kg/h of SO₃) is



reduced by a dry system, where Na_2CO_3 with a high specific area is injected inline. According to the data for such a technique in industrial plants, the conversion yields were set to 80% and 75%, respectively. The injection of a small amount of powdered activated carbon (PAC) could be required together with soda ash to capture micro-pollutants like dioxins and furans. This will depend on the flue gas analysis. Sodium sulfate, mixed with unreacted sodium carbonate and some black particulate matter in the flue gas, is separated in bag filters and collected at the bottom. This solid is mainly composed of Na_2SO_4 ($\approx 98\%$ wt) but is contaminated, so it cannot be sold as salt and shall be disposed of. The flue gas undergoes a wet removal of SO_x that was not completely removed in the dry stage: the scrubber contains a 25%wt NaOH solution that can remove 97% and 95% of SO_2 and SO_3 , respectively. The treated gas is thus released through the stack at a temperature of at least 140-150°C to avoid condensation of acid gases. If needed, such treated gas can be re-heated with steam to ensure the correct flow. The flue gas treatment produces two waste streams, one solid and the other liquid. The latter is treated in the WWTP, but sodium sulfate represents the most significant amount of waste to dispose of.

2.3. Hydrometallurgical stages

The SuperPro Designer software package was used to simulate the hydrometallurgical operations. The calcined material from the second kiln is composed of large flakes that need to be milled to enhance the leaching extraction yield. The leaching phase is divided into three stages in series, where three aliquots of catalysts are leached by the same hot water at 85°C for 2 h each after filtration. This process arrangement concentrates the metal to recover, i.e., Mo and V. Na_2MoO_4 and NaVO_3 are dissolved in the water without any chemical reaction. Na_2HPO_4 , Na_2HAsO_4 , soda ash, and some Na_2SO_4 are also leached during this stage. The unreacted solid, mainly composed of alumina, nickel oxide, and a few ppm of unleached Mo and V salts, is separated from the pregnant solution by a plate and frame (P&F) filter. The pregnant solution is contaminated by arsenic and phosphorous salts, which must be removed because they reduce the quality of steel, where Mo and V are added for special alloys. Thus, As and P are precipitated by adding a magnesium salt, usually MgO or MgCl_2 , and concentrated ammonium chloride solution (NH_4Cl). The solid precipitated is removed from the solution by a vacuum Nutsche filter. A pump transfers the solution to the mixing reactor, where the NH_4Cl is added together with HCl to adjust the pH to the correct value required to enhance vanadium's precipitation rate. After filtration, A pump transfers the solution to the following reactor, where SO_2 is injected into the solution to reduce V^{5+} to V^{4+} ions and avoid co-precipitation with molybdenum. Afterward, concentrated HCl is added to acidify the solution's set-up value. At high temperatures, the precipitation of molybdic acid (H_2MoO_4) occurs. More than 95% of Mo is precipitated in this stage. The spent solution is put in contact with the organic extractant, Aliquat 336, dissolved in kerosene and decanol. This operation is carried out in mixers & settlers in series. The spent solution is stored and treated in the wastewater treatment plant (WWTP). Instead, the organic solution is stripped with an alkaline solution that, in several stages, extracts Mo and V. Such a solution is recycled back to the reactor, where arsenic and phosphorous are precipitated. The spent organic solution is stored and reused for further solvent extraction, with the addition of a small makeup of extracting solution.

2.4. Other sections

The recycling plant includes the 3rd rotary kiln, where NH_4VO_3 is decomposed into V_2O_5 and NH_3 , and the 4th rotary kiln that performs the thermal decomposition of H_2MoO_4 into molybdenum trioxide MoO_3 and H_2O . Moreover, the 1st EAF melts the alumina/nickel solid residue from the leaching stage, and the 2nd EAF melts the powdered vanadium pentoxide to get V_2O_5 flakes. All the waste streams, i.e., wash water and spent solutions, coming from all the other sections of the recycling plant, are stored in a tank; downstream of it, there is the wastewater treatment equipment. The majority of the treated water is recycled back into the plant. The plant also includes all the equipment to support the operations: one compressor for technical and instrument air, one cooling tower, one emergency boiler (500 kWth) in case steam produced from the cooling of electric furnaces and kilns cannot temporarily be used for heating of reactors, one diesel generator with a



power of 125 kVA in case of failure of the energy supply and a firefighting system. Considering all the equipment and their working time per day, the total installed electric power is 6.2 MW.

3. ECONOMIC ANALYSIS

The H&M balance of the entire plant was carried out by Microsoft Excel, using the data from SuperPro Designer and Chemcad simulations. The H&M balance is crucial to estimate reagents, product streams, energy consumption, and all the other running cost throughout the year.

The economic analysis was developed according to Peters et al. (2004). The analysis considered a postcovid19 scenario, with increased equipment, natural gas, and electrical energy prices, but also the selling price of products (metal oxides) and generally all other services. Moreover, this analysis was developed for refineries and petrochemical companies that own the spent HDS catalysts. Other companies can also invest in recycling, but the HDS catalysts must be found and collected from the market. When the metal prices are relatively low, the petrochemical companies need to pay to dispose of their catalysts because of the treatment costs; instead, in periods like the current one, when the prices are very high, petrochemical companies sell the catalysts on the market. Hence, the purchase of spent catalysts represents an additional and significant annual operating cost that must be considered when performing the profitability analysis of the recycling plant. The plant has an estimated useful life of at least 20 years, a construction time of 12 months, and the opportunity cost of capital quantified at 5%. Capital received from third parties is considered, with a 10-year loan and an interest rate of 3%. The plant is supposed to be built in an Eastern European country and the total level of taxation is set at 25%. The depreciation period for a recycling plant is usually set at 10 years. The equipment purchase cost was estimated using direct request of an offer to suppliers and estimation from indirect methods Peters et al. (2004). The equipment purchase cost (EPC) is nearly 20.5 MEUR, including auxiliary equipment (secondary pumps and conveyors, forklifts, etc.), reusable drums and big bags for packaging of products, and laboratory instruments. Auxiliary and unlisted equipment were calculated as a percentage of the EPC. The total plant direct cost is 40,680,470 EUR, whereas the engineering, procurement & construction, supervision and contingencies amount to 9,356,508 EUR: thus, the direct fixed capital (DFC) invested on the project is 50,036,978 EUR. The depreciation is 4,002,601 EUR/year, considering the DFC, a recovery period of 10 years, and a salvage value of 20%. Regarding OPEX, they are listed in Table 2.

Table 2. Operating costs.

Item	(EUR/year)
Raw Materials	2,913,341
Labor-Dependent	713,805
Facility-Dependent	5,013,566
Laboratory/QC/R&D	60,000
Consumables	485,000
Waste Treatment/Disposal	1,038,600
Utilities (electric energy + gas)	4,231,436
Transportation	65,000
Miscellaneous	80,000
Running Royalties	500,000
Loan payment	7,588,407
Annual operating costs	22,689,155



The main utilities used in the plant are electrical energy and natural gas. The price of the electrical energy was set at 150 EUR/MWh, whereas the natural gas was at 0.424 EUR/Nm³. The facility-dependent cost was calculated as the sum of maintenance & repairs, insurance, and depreciation. The total consumption of electrical energy is 25,841 MWh/year. Natural gas is required to heat all the rotary kilns and the emergency boiler, the latter when used. The total consumption is 838,210 Nm³/year. Other utilities consist of technical and instrument compressed air, steam, and cooling water, but they are produced on-site. Consumables includes oil, grease, membranes, carbon electrodes, gaskets, etc.

Royalties take into account the exploitation of the process' patent. The loan payment was calculated in 10 years with an annually compounded interest (rate of 3%).

Table 3. Profitability summary.

Item		
Direct Fixed Capital	50,036,978	EUR
Working Capital	8,977,182	EUR
Start-up cost	20,000	EUR
Up-front R&D	50,000	EUR
Total Investment	59,084,160	EUR
Revenues	36,141,580	EUR/year
Annual Operating Costs	22,689,155	EUR/year
Gross Profit	13,452,425	EUR/year
Taxes	3,363,106	EUR/year
Net Profit	14,092,277	EUR/year
Gross Margin	37.2	%
ROI	23.9	%
Payback Time	4.2	years

The revenues were calculated according to the market prices of metal commodities: V₂O₅ 98%wt min. 9.8 USD/lb, MoO₃ 57%wt min. 17.3 USD/lb, Ni-alloy 5.5 USD/kg (Vanadium price, 2022; Trading Economics, 2022a,b). The plant revenues are 1272 tons/year of V₂O₅ 98%wt, 239 tons/year of MoO₃ 57%wt, and 227 tons/year of Ni/V/Mo alloy with an approximate composition of 72/25/3%wt, respectively. Vanadium and molybdenum oxides are both of commercial grade. Working capital is the investment in temporary or consumable materials, i.e., tied-up funds required to operate the business. It is based on the contributions from labor, raw materials, utilities, waste treatment and disposal, and miscellaneous (process validation and overhead-type expenses).

The tax rate is 25% of the gross profit (gross profit = revenues - operating costs). Net profit = gross profit - taxes + depreciation (Peters et al., 2004). The profitability indexes, that do not take into account the time value of money, are calculated as:

$$\text{Gross margin} = \frac{\text{Gross profit}}{\text{Revenues}} \quad (1)$$

$$\text{ROI} = \frac{\text{Net profit}}{\text{Total investment}} \quad (2)$$

$$\text{Payback time} = \frac{\text{Total investment}}{\text{Net profit}} \quad (3)$$



Overall, the economic analysis highlights the outstanding profitability of the catalyst recycling business. Considering the economy of scale, the indexes calculated above even enhance with the increase of the plant's capacity.

4. CONCLUSIONS

The present paper was focused on the techno-economic analysis of a plant that recycles spent HDS catalysts. The analysis was developed for a capacity of 6,000 tons/year. The technical analysis was based on an industrial process whose main stages were tested on lab- and pilot-scale. The profitability analyses demonstrated the overall benefit of investing in such a recycling business with very positive economic indexes, i.e. a net profit of 14.1 M EUR/year, ROI equal to 23.9%, and a payback time of around 4 years.

REFERENCES

- Beolchini, F., Fonti, V., Ferella, F., Centofanti, M. and Vegliò, F., 2009. Bioleaching of nickel, vanadium and molybdenum from spent refinery catalysts. *Adv. Mat. Res.*, 71-73, 657-660.
- Ferella, F., Ognyanova, A., De Michelis, I., Taglieri, G. and Vegliò, F., 2011. Extraction of metals from spent hydrotreating catalysts: Physico-mechanical pre-treatments and leaching stage. *J. Hazard. Mater.*, 192, 176-185.
- Furimsky, E., 1996. Spent refinery catalysts: Environment, safety and utilization. *Catal. Today*, 30, 223-286.
- Kim, H.I., Park, K.H. and Mishra, D., 2009. Influence of sulfuric acid baking on leaching of spent Ni-Mo/Al₂O₃ hydro-processing catalyst. *Hydrometallurgy*, 98, 192-195.
- Krishnan, S., Zulkapli, N.S., Kamyab, H., Taib, S.M., Din, M.F.B.M. and Abd Majid, Z., S. Chaiprapat, S., Kenzo, I., Ichikawa, Y., Nasrullah, M., 2021. Current technologies for recovery of metals from industrial wastes: An overview. *Environ. Technol. Innov.*, 22, 101525.
- Le, M.N. and Lee, M.S., 2021. A Review on Hydrometallurgical Processes for the Recovery of Valuable Metals from Spent Catalysts and Life Cycle Analysis Perspective. *Min. Proc. Ext. Met. Rev.*, 42, 335-354.
- Park, K., Kim, H.I., Parhi, P., Mishra, D., Nam, C., Park, J. and Kim, D., 2012. Extraction of metals from Mo-Ni/Al₂O₃ spent catalyst using H₂SO₄ baking-leaching-solvent extraction technique. *J. Ind. Eng. Chem.*, 18, 2036-2045.
- Peters, M.S., Timmerhaus, K.D. and West, R.E., 2004. *Plant Design and Economics for Chemical Engineers*, 5th ed.; Mc Graw-Hill: New York, NY, USA.
- Pradhan, D., Kim, D.J., Ahn, J.G., Chaudhury, J.R. and Lee, S.W., 2010. Kinetics and statistical behavior of metals dissolution from spent petroleum catalyst using acidophilic iron oxidizing bacteria. *J. Ind. Eng. Chem.*, 16, 866-871.
- Ruiz, V., Meux, E., Diliberto, S. and Schneider, M., 2011. Hydrometallurgical Treatment for Valuable Metals Recovery from Spent CoMo/Al₂O₃ Catalyst. Improvement of Soda Leaching of an Industrially Roasted Catalyst. *Ind. Eng. Chem. Res.*, 50, 5295-5306.
- Trading Economics, 2022a. <https://tradingeconomics.com/commodity/molybden>, accessed 14th June 2022.
- Trading Economics, 2022b. <https://tradingeconomics.com/commodity/nickel>, accessed 14th June 2022.
- Vanadium price, 2022. <https://www.vanadiumprice.com/>, accessed 14th June 2022.
- Wang, J.Z., Du, H., Olayiwola, A., Liu, B., Gao, F., Jia, M.L., Wang, M.H., Gao, M.L., Wang, X.D. and Wang, S.N., 2021. Recent advances in the recovery of transition metals from spent hydrodesulfurization catalysts, *Tungsten*, 3, 305-328.



1st International Conference on Sustainable Chemical and Environmental Engineering
31 Aug – 04 Sep 2022, Rethymno, Crete, Greece

Co-culture and continuous two-stage bioreactor system for the fermentation of syngas by *B. methylotrophicum* and *C. tyrobutyricum*



This study focused on the implementation of a small-scale co-culture system of *B. methylotrophicum* and *C. tyrobutyricum* to assess the potential of CO, CO₂ and acetate metabolization to C₄ products, and the upscaling of the process in a continuous two-stage bioreactor.

2. MATERIALS AND METHODS

2.1. Microorganisms, culture media and syngas composition

The microbial strains used in this study were *Butyribacterium methylotrophicum* strain Marburg DSM 3468 (Deutsche Sammlung von Mikroorganismen und Zellkulturen, Braunschweig, Germany) and *Clostridium tyrobutyricum* P9 (isolated at LNEG). Both bacteria were cultured anaerobically in Syn1 medium, as described in Pacheco et al. (2021) with minor adaptations. *B. methylotrophicum* used a commercial syngas mixture (Table 1) as carbon and energy source, while 10 g/L of filter sterilized glucose were supplemented in the *C. tyrobutyricum* culture. Both strains were inoculated at 2% (v/v), every 2 (*C. tyrobutyricum*) or 4 (*B. methylotrophicum*) days and incubated at 37°C, 150 rpm in an orbital shaker.

Table 1. Commercial syngas compositions used in the serum flasks and bioreactor experiments.

Syngas compound	Syngas A	Syngas B
CO (vol%)*	30	26
CO ₂ (vol%)*	20	19
H ₂ (vol%)*	30	18
N ₂ (vol%)*	20	37
CO:H ₂	1	1.4

*, Values are at standard conditions of temperature and pressure—temperature of 25°C (293.15 K) and absolute pressure of 1.0x10⁵ Pa.

2.2. Experimental set-up

In the small-scale co-culture experiment, *B. methylotrophicum* was cultured anaerobically in 20 mL of Syn1 medium at pH 6.0 with Syngas B, in 120 mL serum flasks, with supplementation of 60 mM sodium acetate. Incubation was performed at 37 °C and 150 rpm for 72 hours. After this first incubation stage, filter sterilized glucose or water were added to the serum flasks to reach a concentration of 2.5, 5 or 0 g/L glucose, and the media were inoculated with 2% (v/v) *C. tyrobutyricum*. A positive control with 10 g/L of glucose was also prepared. The flasks were incubated under the same conditions for more 72h. All the experiments were performed in triplicate and at each sampling time three flasks were collected for processing.

In the continuous bioreactor experiments (depicted in **Figure 1**), *B. methylotrophicum* was cultured using Syngas A and Syn1 medium supplemented with 60 mM sodium acetate, while *C. tyrobutyricum* was cultured in Syn1 medium supplemented with 10 g/L glucose, in two 0.5 L IO 1000 bioreactors (Solaris, Lombardy, Italy), herein named Bioreactor I and II, respectively. Both bioreactors were equipped with pH and redox sensors and all the necessary inlets/outlets for pH control, gas sampling, pressure measurement (LabQuest2 with gas pressure sensor, Vernier, Oregon, USA), syngas feed (Bioreactor I) and inline flowmeter (μflow, Bioprocess Control, Stockholm, Sweden), liquid sampling/inoculum addition and culture media inlet/outlet. Syngas A was fed on demand to Bioreactor I from a H₂ gas tight sampling bag (SKC 263-03 Standard FlexFoil® series with stainless steel fittings, Pennsylvania, USA) as described by Pacheco et al., 2021. Temperature and stirring were kept at 37°C, 400 rpm for Bioreactor I and 37°C, 150 rpm for Bioreactor II. The pH was set to 6.0 in both bioreactors.

Bioreactor I was initially kept at a constant dilution rate of 0.02 h⁻¹, using an entry/exit flow of 0.006 L/h with a working volume of 300 mL. In a second test, the dilution rate was lowered to 0.012 h⁻¹, maintaining the entry/exit flow rate but increasing working volume to 500 mL (**Figure 1**, black+red). After reaching steady state (at least 3 turnovers of the working volume inside the reactor), the culture media outlet was connected to Bioreactor II (**Figure 1**, black+blue), which was kept at a constant dilution rate of 0.08 h⁻¹ until steady state. Samples were collected during the steady state periods for analysis.

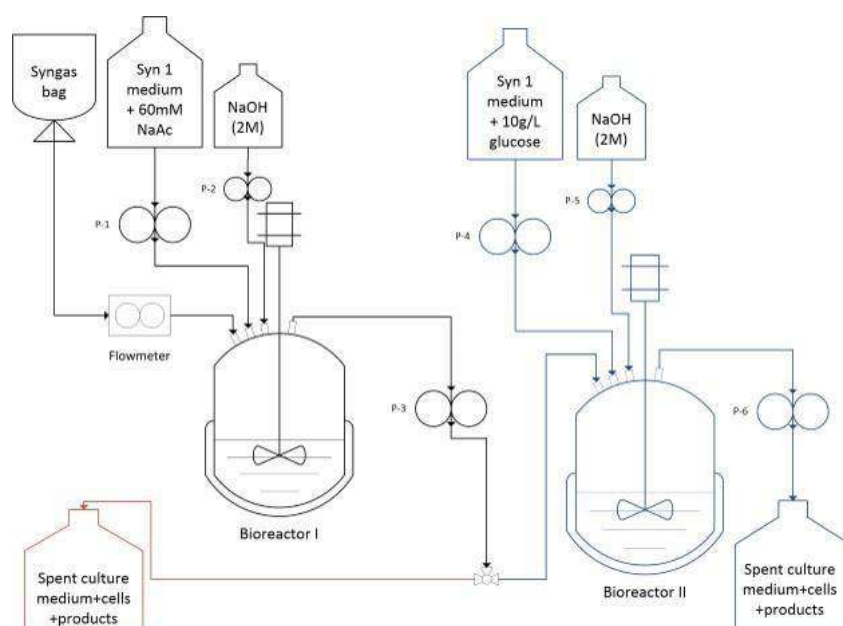


Figure 1. Schematic representation of the continuous single-stage (black+red) and two-stage (black+blue) bioreactor set-up for syngas fermentation by *B. methylotrophicum* and *C. tyrobutyricum*.

2.3. Analytical methods

The analytical methods used are described in Pacheco et al., 2021. Microbial growth was monitored by optical density at 600 nm (Thermo Fisher Scientific spectrophotometer, Genesys 20, Massachusetts, USA) and cell dry weight (CDW), which was quantified according to official methods of analysis (AOAC, 2019). Acetate and butyrate were quantified by High-Performance Liquid Chromatography (HPLC) with a Biorad Aminex HPX-87H column (Bio-Rad Laboratories, California, USA) at 35°C, using a LaChrom L-7490 (Merck, Darmstadt, Germany) chromatographer equipped with a differential refractive index detector. The liquid phase was 0.5 mM H₂SO₄, at a flow rate of 0.4 mL/min. Solutions of glucose, carboxylic acids and alcohols were used as external standards. Gas samples were analyzed through gas chromatography (GC) in an Agilent/HP 6890 gas chromatograph equipped with a gas sampling valve, two filling columns (Molecular Sieve 5A and Porapak Q) and two detectors (Thermal Conductivity Detector and Flame Ionization Detector) mounted in series. Each injected sample was heated to 40°C for 17 min and then up to 185°C for 43 min, with a heating rate of 15°C/min. The carrier gas used was argon at a constant flow of 18.5 mL/min. The molar concentration of CO, H₂ and CO₂ were estimated from the GC analysis using the Peng–Robinson equation (Ortigueira et al., 2015).

In the experiments where the culture medium was supplemented with sodium acetate, the acetate production was determined as the difference between the concentration in the samples collected from the supplemented culture medium at each time-point and the concentration determined immediately after the supplementation occurred.

3. RESULTS AND DISCUSSION

3.1. *B. methylotrophicum* and *C. tyrobutyricum* co-culture in serum flasks

The sequential culture of *B. methylotrophicum* (BBM) and *C. tyrobutyricum* (CTB) was firstly tested in a small-scale assay wherein serum flasks. At a first stage, the Syn 1 medium in the serum flasks was inoculated with BBM, for the conversion of Syngas B in acetic and butyric acid. At 72 hours, the medium was inoculated with CTB and supplemented with 0, 2.5 or 5 g/L glucose, or 10 g/L as positive control. The fermentation proceeded for more 72 hours (totalizing 144 hours of fermentation). The results obtained in this experiment are depicted in **Figure 2**.

After the first 72 hours of growth, BBM was able to completely consume the supplied CO and H₂ but only 8.2 vol% of CO₂, since the H₂ concentration was not sufficient for total CO₂ conversion. The culture achieved a cell dry weight (CDW) of 1.1 g/L and produced 21.8 mmol/L acetate and 3.4 mmol/L butyrate. These results were similar to 20.2 mmol/L acetate and 5.7 mmol/L butyrate obtained by Pacheco et al. (2021) for BBM under the same culture conditions but using Syngas A with a CO:H₂ ratio of 1 as carbon and energy source.



After the inoculation of CTB, glucose was depleted between 86 and 96 hours and the culture achieved a maximum CDW of 2.5 g/L, 1.9 g/L, 1.7 g/L and 1.21 g/L when Syn1 was supplemented with 10, 5, 2.5 or 0 g/L glucose, respectively (**Figure 2(a)**).

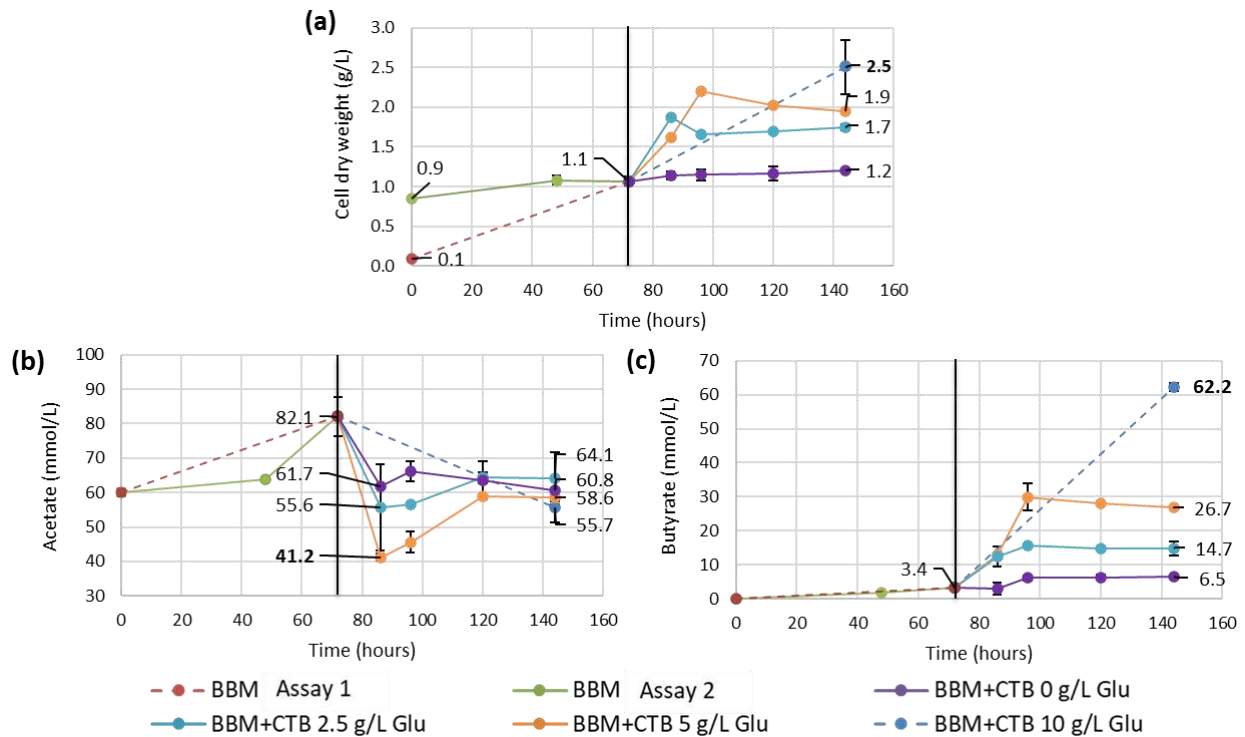


Figure 2. Variation of cell dry weight **(a)**, acetate **(b)** and butyrate **(c)** concentrations during the co-culture of *B. methylophilum* (BBM) and *C. tyrobutyricum* (CTB). The vertical line represents 72 hours of BBM growth using syngas B as carbon and energy source, time after which the Syn1 medium was inoculated with CTB and supplemented with 0, 2.5 and 5 g/L of glucose. The dashed lines represent the positive control supplemented with 10 g/L of glucose.

As can be observed in **Figure 2 (a)**, **(b)** and **(c)**, even when cellular growth was residual, from 72 to 86 hours a steep decrease in acetate from 82.1 mmol/L to 41.2 mmol/L, 55.6 mmol/L and 61.7 mmol/L occurred, accompanied by an increase in butyrate concentration. The metabolization of acetate with production of butyrate is possible due to the presence of the enzyme butyryl-CoA:acetyl-CoA transferase in certain acetogens (Jaros et al., 2013; Millat et al., 2014). The simultaneity of low pH and excess acetic acid concentrations in the culture medium enables the re-incorporation of some acids into the acetogenic pathway to produce metabolites less toxic to the cell (Jaros et al., 2013). Acetate concentration started to gradually increase again between 86 and 120 hours, while butyrate concentration increased proportionally with the glucose concentration (**Figure 2(c)**) showing the effectiveness of the BBM and CTB co-culture to increase the production of C4 products from syngas.

Overall, the balance of acetate by the co-culture of BBM+CTB from 72-144 hours was a decrease of 26.4, 23.5, 21.3 and 18.0 mmol/L when the medium was supplemented with 10, 5, 2.5 and 0 g/L glucose, respectively. However, when considering the net balance of acetate from 0-144 hours, it was observed that a glucose supplementation below 5 g/L resulted in an accumulation of up to 4.1 mmol/L acetate (**Figure 2(b)**). Using glucose as carbon and energy source, CTB not only produces organic acids but also H₂ and CO₂ (Michel-Savin et al., 1990). In co-culture, this additional H₂ represents a potential for the BBM to fix more CO₂ and resume growth. This was observed after 86 hours, when acetate started to accumulate again (**Figure 2(b)**) due to the preference of BBM to produce acetic acid over butyric acid (Pacheco et al., 2021; Park et al., 2017). The effectiveness of the co-culture in increasing the butyrate titers is therefore highly dependent on the ability of CTB to impose itself on BBM in the 2nd fermentation stage.



3.2 Continuous two-stage culture of *B. methylotrophicum* and *C. tyrobutyricum*

To test further the potential of the sequential culture of BBM and CTB, a two-stage continuous culture setting was implemented. In Bioreactor I BBM was grown in continuous culture, using Syngas A as carbon and energy source fed on demand. The dilution rates (D) 0.02 and 0.012 h^{-1} were selected, which would enable the maximum conversion of the carbon present in the gas. The results obtained from the continuous culture of BBM in Bioreactor I are depicted in **Table 2**.

Table 2. Cell growth and specific productivities achieved in the continuous culture of BBM in Bioreactor I.

Parameter	Dilution rate	
	0.012 h^{-1}	0.02 h^{-1}
Biomass [g/L]	0.24 \pm 0.03	0.15 \pm 0.01
Biomass production rate [g/L/d]	0.06 \pm 0.01	0.07 \pm 0.00
Q_(syngas) [NL⁺/g_{CDW}/d][*]	0.4	0.5
Q_(acetate) [mmol/g_{CDW}/d]^{**}	36.0 \pm 6.24	14.7 \pm 7.95
P_(butyrate) [mmol/g_{CDW}/d][†]	0.7 \pm 0.08	0.8 \pm 0.03
P_(2,3-butanediol) [mmol/g_{CDW}/d][†]	5.2 \pm 2.47	3.9 \pm 0.31

⁺, NL, volume of syngas in L at standard conditions of temperature and pressure—temperature of 25 °C (293.15 K) and absolute pressure of 1.0×10^5 Pa

^{*}, Q_(syngas) [NL/g_{CDW}/d], specific consumption rate: volume (NL) consumed per g cell dry weight (CDW) per day

^{**}, Q_(acetate) [mmol/g_{CDW}/d], specific consumption rate: amount (mmol) consumed per g cell dry weight (CDW) per day

[†], P_(acid or alcohol) [mmol/g_{CDW}/d], specific production rate: amount (mmol) produced per g cell dry weight (CDW) per day

The specific productivities obtained from both steady states show that at $D=0.02 \text{ h}^{-1}$ the cells were able to consume more syngas and produce more butyrate (**Table 2**). However, by lowering D to 0.012 h^{-1} , an increase in biomass production, and in the specific acetate consumption rate and 2,3-butanediol production rate was observed, meaning that at $D=0.02 \text{ h}^{-1}$ the cell residence time was too low for the cells to fully consume the carbon available in the syngas. At a lower dilution rate, the residence time inside the reactor increases, rising the carbon availability to the cells, while also increasing contact time of the cells with the acetate supplemented to the culture medium. This improved the metabolization of acetate and the butyrate and 2,3-butanediol production, increasing the C4 production rate from 0.7 mmol/L/d at $D=0.02 \text{ h}^{-1}$ up to 1.1 mmol/L/d at $D=0.012 \text{ h}^{-1}$, during steady state.

Since $D=0.012 \text{ h}^{-1}$ yielded the best results in terms of carbon and acetate conversion, while achieving the highest C4 productivity, this dilution rate was selected for the two-stage continuous culture of BBM and CTB. To enable total glucose consumption and facilitate acetate conversion in Bioreactor II a $D=0.08 \text{ h}^{-1}$ (0.012 h^{-1} from Bioreactor I plus fresh culture medium at a rate of 0.068 h^{-1}) was selected. The results obtained during the steady state of Bioreactor II are depicted in **Table 3**.

Table 3. Cell growth and specific productivities achieved in the continuous two-stage culture of BBM and CTB determined in Bioreactor II.

Parameter	Dilution rate
	0.08 h^{-1}
Biomass [g/L]	2.64 \pm 0.00
Biomass production rate [g/L/d]	0.06 \pm 0.01
Q_(glucose) [mmol/g_{CDW}/d][*]	40.5 \pm 0.06
P_(acetate) [mmol/g_{CDW}/d][†]	38.3 \pm 2.06
P_(butyrate) [mmol/g_{CDW}/d][†]	6.7 \pm 0.34
P_(ethanol) [mmol/g_{CDW}/d][†]	2.5 \pm 0.49
P_(2,3-butanediol) [mmol/g_{CDW}/d][†]	6.1 \pm 0.20

^{*}, Q_(glucose) [mmol/g_{CDW}/d], specific consumption rate: amount (mmol) consumed per g cell dry weight (CDW) per day

[†], P_(acid or alcohol) [mmol/g_{CDW}/d], specific production rate: amount (mmol) produced/consumed per g cell dry weight (CDW) per day



The co-culture of BBM and CTB in Bioreactor II produced butyrate, 2,3-butanediol and ethanol. Acetate balance was also positive, reaching a specific production rate of 38.3 mmol/g_{CDW}/d, similar to the amount consumed by the single culture of BBM in Bioreactor I at D=0.012 h⁻¹. Ethanol was an additional product in this two-stage and was produced at a specific production rate of 2.5 mmol/g_{CDW}/d. The specific butyrate and 2,3-butanediol production rates in Bioreactor II were 9.6 and 1.2 times higher than that observed in Bioreactor I, respectively. The C4 products butyrate and 2,3-butanediol in Bioreactor II amounted to 17.7 and 16.2 mmol/L/d, respectively, during steady state. This value largely exceeded the production obtained only in Bioreactor I at D=0.012 h⁻¹. The accumulation of acetate that occurred in Bioreactor II increased its concentration to levels where the cells were able to convert it to C4 acids and alcohols, showing that the use of the BBM and CTB co-culture can be highly interesting to produce longer chain products.

4. CONCLUSIONS

This work showed that the production of C4 products from CO and CO₂ was increased by integrating the culture of BBM and CTB in a continuous two-stage system. The specific production rate of butyrate and 2,3-butanediol increased 9.6 and 1.2 times, respectively, and 2.5 mmol/g_{CDW}/d of ethanol were additionally produced when compared to BBM in Bioreactor I. Nonetheless, further optimization of the process is still necessary. In future works, continuous supply of syngas into the bioreactor to increase the gas/liquid mass transfer rate should be tested, so as a wider array of dilution rates to maximize the process productivity and C4 product recovery.

5. ACKNOWLEDGEMENTS

This research was performed under the framework of the AMBITION Project, ECRIA project funded by Horizon 2020 EU, grant agreement No. 731263, and the Operational Program for Competitiveness and Internationalization (PORTUGAL 2020), Lisbon Portugal Regional Operational Program (Lisboa 2020) and North Portugal Regional Operational Program (Norte 2020) under the Portugal 2020 Partnership Agreement, through the European Regional Development Fund (ERDF). M. Pacheco was supported by FCT through PhD grant DFA/BD/6423/2020. This work was funded by the Portuguese Foundation for Science and Technology (FCT) I.P./MCTES through PIDDAC funds (UIDB/50019/2020).

REFERENCES

- Adhikari, S. P., Zhang, J., Guo, Q., Unocic, K. A., Tao, L. and Li, Z., 2020. A hybrid pathway to biojet fuel via 2,3- butanediol. *Sustain. Energy Fuels*, 4(8), 3904–3914.
- AOAC, 2019. *Official methods of analysis of AOAC International*; 21st ed.; AOAC International.
- Daniell, J., Köpke, M. and Simpson, S. D. 2012. Commercial biomass syngas fermentation. *Energies*, 5 (12), 5372–5417.
- Jaros, A. M., Rova, U. and Berglund, K. A., 2013. Acetate adaptation of *Clostridia tyrobutyricum* for improved fermentation production of butyrate. *Springerplus*, 2 (47), 1–8.
- Karlson, B., Bellavitis, C. and France, N., 2021. Commercializing LanzaTech, from waste to fuel: An effectuation case. *J. Manag. Organ.*, 27 (1), 175–196.
- Kiefer, D., Merkel, M., Lilge, L., Henkel, M. and Hausmann, R., 2021. From acetate to bio-based products: Underexploited potential for industrial biotechnology. *Trends Biotechnol.*, 39 (4), 397–411.
- Kumar Panda, S., Sahu, L., Kumar Behera, S. and Ray, R. C., 2019. Research and production of organic acids and industrial potential. *Bioprocessing for Biomolecules Production* (pp. 195–209). Wiley.
- Michel-Savin, D., Marchal, R. and Vandecasteele, J. P., 1990. Control of the selectivity of butyric acid production and improvement of fermentation performance with *Clostridium tyrobutyricum*. *Appl. Microbiol. Biotechnol.*, 32(4), 387–392.
- Millat, T., Voigt, C., Janssen, H., Cooksley, C. M., Winzer, K., Minton, N. P., Bahl, H., Fischer, R. J. and Wolkenhauer, O., 2014. Coenzyme A-transferase-independent butyrate re-assimilation in *Clostridium acetobutylicum*—evidence from a mathematical model. *Appl. Microbiol. Biotechnol.*, 98(21), 9059– 9072.
- Ortigueira, J., Alves, L., Gouveia, L. and Moura, P., 2015. Third generation biohydrogen production by *Clostridium butyricum* and adapted mixed cultures from *Scenedesmus obliquus* microalga biomass. *Fuel*, 153, 128–134.
- Ortigueira, J., Leite, T., Pereira, J., Serafim, L. S., Silva, C., Moura, P. and Lemos, P. C., 2021. A biorefinery approach for the simultaneous production of biofuels and bioplastics. *17th International Conference on Renewable Resources and Biorefineries*, 6 September-8 September, Aveiro, Portugal.
- Pacheco, M., Pinto, F., Ortigueira, J., Silva, C., Gírio, F. and Moura, P., 2021. Lignin syngas bioconversion by *Butyribacterium methylotrophicum*: Advancing towards an integrated biorefinery. *Energies*, 14(21).
- Park, S., Yasin, M., Jeong, J., Cha, M., Kang, H., Jang, N., Choi, I. G. and Chang, I. S., 2017. Acetate-assisted increase of butyrate production by *Eubacterium limosum* KIST612 during carbon monoxide fermentation. *Bioresour. Technol.*, 245, 560–566.



Effect of oxygen transfer coefficient on microbial production of lipids and carotenoids using renewable waste feedstock: batch and fed-batch mode

M.A. Villegas-Mendez¹, J. Montañez¹, J.C. Contreras-Esquivel¹, I. Salmeron², A. Koutinas³ and L. Morales-Oyervides¹

¹Facultad de Ciencias Químicas, Universidad Autónoma de Coahuila, Unidad Saltillo, Coahuila, Mexico.

²School of Chemical Science, Autonomous University of Chihuahua, Chihuahua, Mexico.

³Department of Food Science and Human Nutrition, Agricultural University of Athens, Athens, Greece.

Corresponding author email: lourdesmorales@uadec.edu.mx

ABSTRACT

Agro-industrial by-products valorization as a feedstock for the bioproduction of high-value products has demonstrated a feasible alternative to handle the environmental impact of waste. Oleaginous yeasts are promising cell factories for the industrial production of lipids and carotenoids. Since oleaginous yeasts are aerobic microorganisms, studying the volumetric mass transfer (k_{La}) could facilitate the scale-up and operation of bioreactors to grant the biocompounds' industrial availability. Scale-up experiments for the simultaneous production of lipids and carotenoids using the yeast *Sporobolomyces roseus* CFGU-S005 and comparing the yields in batch and fed-batch mode cultivation using agro-waste hydrolysate. The results indicate that oxygen availability in the fermentation affected the simultaneous production of metabolites. The highest production of lipids (3.42 g/L) was attained using the k_{La} value of 22.44 h⁻¹, while higher carotenoid accumulation of 2 mg/L resulted when agitation speed was increased to 350 rpm (k_{La} 32.16 h⁻¹). The adapted fed-batch mode in the fermentation increased the production yields two times without affecting the fatty acid profile of lipids. This study showed the scale-up potential of the strain *S. roseus* in the further obtention of microbial oil and carotenoids by bioprocess development by the valorization of agro-industrial byproducts as a carbon source.

Keywords: agro-waste valorization, yeast, lipids, carotenoids, oxygen transfer, fed-batch.

1. INTRODUCTION

Present-day environmental research is focused on mitigating the environmental damage caused by waste gathering since statistical foresight indicates that more than 1.5 billion tons of organic waste will be generated by agro-industrial activity (Tomás-Pejó et al., 2021). In this regard, agro-industrial byproducts valorization as a feedstock for the bioproduction of high-value products has demonstrated to be a feasible alternative to handle the waste environmental impact (Tomás-Pejó et al., 2021; Stylianou et al., 2021; Deeba et al., 2022).

Biobased additives production through microbial platforms contributes to green manufacturing development, which can be emphasized in the research on food additives. Lipids synthesized by microorganisms can be used to produce microbial oils whose manufacturing costs have been estimated between 2.4 - 5.8 US \$/kg (Bonatsos et al., 2020). Similarly, microbial pigments such as carotenoids can be placed in the pigment market segment which is projected to surpass US \$ 2 billion in the forthcoming years (Foong et al., 2021). The research in microbial platforms to obtain food additives highlight substituting chemically produced pigments and reducing the water and land utilization for oilseed crops (Sen et al., 2019). Thereby, the main advantages of biobased production of lipids and carotenoids include minimal land usage, lower susceptibility to climatic conditions, and high antioxidant capacity for carotenoids (Braunwald et al., 2016; L. R. Kumar et al., 2020).

Oleaginous yeasts are promising cell factories for the industrial production of lipids and carotenoids, which can be developed using agro-waste feedstock (Tomás-Pejó et al., 2021; Deeba et al., 2022). Since oleaginous yeasts are aerobic microorganisms, studying the volumetric oxygen transfer coefficient (k_{La}) could facilitate the scale-up and operation of bioreactors to grant the biocompounds' industrial availability (Stylianou et al., 2021). Therefore, evaluating the oxygen influence in bioprocess development is a key factor for increasing production yields and establishing the power consumption rates. This study aims to assess the



scale-up strategy in the simultaneous production of lipids and carotenoids by oleaginous yeast using renewable waste feedstock.

2. MATERIALS AND METHODS

The yeast *Sporobolomyces roseus* CFGU-S005 was used for the scale-up experiments to produce lipids and carotenoids simultaneously. Fermentations were performed in a 7 L benchtop bioreactor (Applikon, The Netherlands) using a working volume of 4.1 L at constant aeration (1.5 vvm). Three agitation speed levels were evaluated (150, 250, and 350 rpm) to vary k_{La} (16.16, 22.44, 32.16 h^{-1}). An agro-industrial waste hydrolysate was obtained by the crude enzymatic hydrolysis of pasta processing waste (Villegas-Méndez et al., 2022). The hydrolysate was adjusted to 20 g/L of total sugar and supplemented with the following salts (g/L): KH_2PO_4 (7.0), Na_2HPO_4 (2.5), $MgSO_4$ (1.5), $CaCl_2 \cdot 2H_2O$ (0.15), $FeCl_3 \cdot 6H_2O$ (0.15), $ZnSO_4 \cdot 7H_2O$ (0.02), $MnSO_4 \cdot H_2O$ (0.06). Initial pH was adjusted to 5 and was uncontrolled during the experiments at 25 °C for 120 h.

In Fed-batch experiments, hydrolysate pulses of ~4 g/L of total sugars were added to the bioprocess to evaluate the effect on the production yields. Carotenoids and lipids were assessed at the end of the process (Villegas-Méndez et al., 2022). Lipids obtained from bioreactor experiments were transesterified using methanolic KOH solution (5 w/v) and mixed for 90 min at 55 °C. Fatty acid methyl esters were recovered by hexane and filtered prior to gas chromatography-mass spectrophotometer (GC-MS) detection.

The yeast growth kinetics can be calculated using a logistic model, which allows the calculation of fermentation parameters of biological and geometrical significance by sigmoid profiles independent of substrate concentration. Equation 1 was used for modeling yeast growth:

$$X(t) = \frac{X_0 e^{\mu t}}{[1 - (X_0/X_{max})(1 - e^{\mu t})]} \quad (\text{Eq. 1})$$

where $x(t)$ is the biomass growth (g/L) at time (t, h), x_0 is the initial biomass (g/L), x_{max} is the maximum growth (g/L) and μ is the growth rate (h^{-1}). The product formation (lipids and carotenoids) in yeast fermentation was described by Luedeking-Piret equation. The product formation can be classified into three types; the linear relationship between microbial growth and metabolites production (class 1), microbial growth and product formation partially associated (class 2), and metabolite production and microbial growth non-associated (class 3). Thus equation 2 can describe lipids and carotenoids formation in the fermentation:

$$P(t) = P_0 + \alpha X_0 \left\{ \frac{e^{\mu t}}{[1 - (X_0/X_{max})(1 - e^{\mu t})]} - 1 \right\} + \beta \frac{X_{max}}{\mu} \ln [1 - (X_0/X_{max})(1 - e^{\mu t})] \quad (\text{Eq. 2})$$

where P and P_0 are the concentration of lipids (units) or carotenoids (units) at time (t, h) and at the beginning of the process, respectively. α is product's formation coefficient, and β is non-growth correlation coefficient (Yang et al., 2011). X_0 , x_{max} and μ are the same parameters in equation 1. Both models were jointly fitted by minimizing the sum of squares residuals between the predicted and experimental results using solver (Microsoft Excel). The measured responses were carotenoid production (P , mg/L), carotenoid yield (Y_x , $\mu\text{g/g}$ dry biomass weight), lipid production (L , g/L) and lipid content ($Y_{L/x}$, % w/w).

3. RESULTS AND DISCUSSION

The k_{La} values provided a scale-up strategy to determine a correlation between metabolites production (microbial oil and carotenoids) and oxygen supply in the bioprocess of the yeast *S. roseus*. Oxygen availability in the fermentation affected the simultaneous production of metabolites, in which we found that the increase in oxygen supply enhanced carotenoids but slightly decreased lipids synthesis.

Table 1 displays the model parameters μ and α as well as the production yields obtained by the operational conditions performed in the bench-scale experiments. The kinetic model was able to describe microbial growth and product formation. The μ obtained in the mathematical model describes the slight difference between the growth rates. The agitation speed of 150 rpm with 1.5 vvm resulted in a higher growth rate. On



the other hand, the product's formation coefficient implies that the metabolites are grown associated; thus, the yeast synthesis of lipids and carotenoids increases along with the biomass growth.

Carotenoids' yield per gram of dry biomass resulted higher when using 150 rpm (lower k_{La} value); however, it was the lower volumetric production of carotenoids (1.7 mg/L). On the other hand, higher carotenoid production was observed in the higher oxygen supply (32.16 h⁻¹). The higher availability of oxygen in bioreactors, such as lower volume or high agitation speeds, has been pointed out that it enhances carotenoid production (Parreira et al., 2015). Carotenoids are molecules that contrast the oxidative stress that the free oxygen radicals might cause; in such a case, the yeast might increase the synthesis of carotenoids. Nonetheless, the increased oxygen transfer did not have a positive effect in the lipid synthesis. The highest value of lipid production was obtained in the intermediate value which could be attributed to lipids oxidation in the cell (Lopes et al., 2018). On the other hand, other reports pointed out that the high oxygen availability in the system is beneficial for the concomitant synthesis of carotenoids and lipids (Parreira et al., 2015).

The fatty acid profile of the lipids produced by *S. roseus* in the bioreactor experiments is shown in Table 2. The content of monounsaturated fatty acids (MUFAs) was around 60 % when 150 and 250 rpm were used, also, oleic acid was the most abundant in these conditions. Polyunsaturated fatty acids (PUFAs) were 34 %, which is higher than MUFAs (29 %) when agitation speed was increased (350 rpm). In literature has been reported the oleic acid content in microbial oil from oleaginous yeast (Bansal et al., 2020; Boviatsi et al., 2020; Chaiyaso et al., 2019). The effect of increased aeration was most visible in the fatty acid profile at 350 rpm, where MUFAs were slightly decreased and PUFAs percentage increased, meaning that the oxygen also affected the fatty acid composition.

Table 1. Kinetic parameters of *S. roseus* fermentation varying aeration in bioreactor.

Parameter	k_{La} value, h ⁻¹		
	16.16	22.44	32.16
Biomass, μ	0.05	0.08	0.06
Carotenoids, α	0.51	0.15	0.30
Lipids, α	0.41	0.15	0.17
Y_x , mg/g	0.50	0.30	0.30
P, mg/L	1.70	1.80	2.00
$Y_{L/x}$, %	45	48	35
L, g/L	1.50	3.40	2.40

Fed-batch is an adopted strategy in fermentation to avoid high concentration substrate inhibition, thus, the correct feed delivery in fermentation is a key parameter to increasing productiveness in the process (Singh et al., 2020). Figure 1 shows the kinetic profiles regarding biomass growth, lipids, and carotenoid production in the fed-batch mode performed at a k_{La} value of 22.44 h⁻¹. In the adopted strategy of total sugar feed pulses of ~4 g/L at 12 h intervals resulted in 2-fold production of lipids and carotenoids (up to 6.6 g/L and 3.4 mg/L, respectively). The development of the fed-batch mode in this study compares to other research using wastes as feedstock where it was obtained a lipid content of 70 % in oleaginous strain *Rhodospiridium toruloides*, 50 % of lipid content in *Yarrowia lipolytica* (Singh et al., 2020; Kumar et al., 2021). Regarding the carotenoids production is similar to that obtained in fed-batch fermentation of the strain *Xanthophyllomyces dendrorhous* (Villegas et al., 2021). Also, the fed-batch mode did not affect the fatty acid profile (Table 2), which demonstrates the bioprocess's robustness and the *Sporobolomyces roseus* CFGU-S005 potential for industrial implementation.

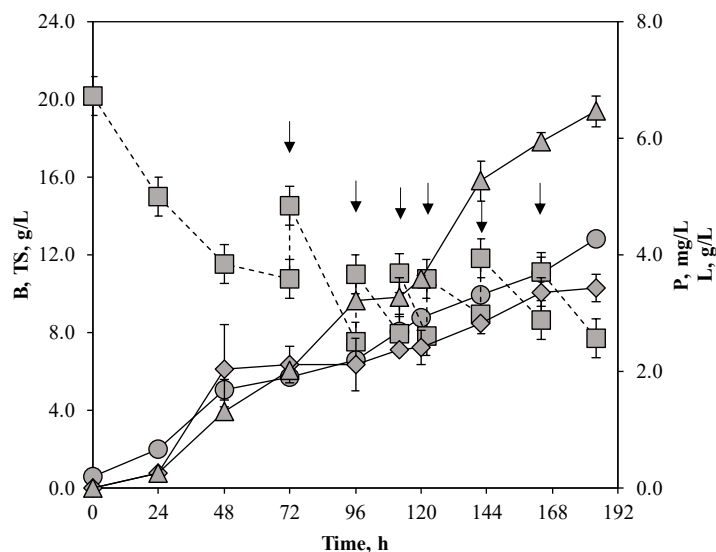


Figure 1. Kinetic studies in the assessed bioreactor fed-batch fermentation using agro-waste hydrolysate at 22.44 h^{-1} , arrows represent sugar pulses $\sim 4 \text{ g/L}$. Biomass (B, circles), lipid production (L, triangles), carotenoid production mg/L (P, diamonds), total sugar g/L (TS, squares).

Table 2. Fatty acid obtained from $k_L a$ experiments and fed-batch mode in bioreactors.

Fatty acid	Composition, %			
	16.16 h^{-1}	22.44 h^{-1}	32.16 h^{-1}	Fed-batch 22.44 h^{-1}
MUFAs	57	65	29	64
PUFAs	2	11	34	14
SFAs	41	24	26	22

MUFAs, monounsaturated fatty acids; PUFAs, polyunsaturated fatty acids; SFA, saturated fatty acids.

4. CONCLUSIONS

This study showed the scale-up potential of the strain *S. roseus* in the further obtention of microbial oil and carotenoids by bioprocess development by the valorization of agro-industrial byproducts as a carbon source. The oxygen availability affected the yields of lipids and carotenoids as well as the fatty acid profile. Also, the fed-batch mode operation 2-folded the lipid and carotenoid yield without affecting the fatty acid composition.

5. ACKNOWLEDGMENTS

Author M.Á.V.-M. (750450-2019) acknowledges CONACyT-Mexico for the financial support provided for conducting his doctoral studies.

REFERENCES

- Tomás-Pejó, E., Morales-Palomo, S. and González-Fernández, C., 2021. Microbial Lipids from Organic Wastes: Outlook and Challenges. *Bioresour. Technol*, 323, 1-12.
- Stylianou, E., Pateraki, C., Ladakis, D., Damala, C., Vlysidis, A., Latorre-Sánchez, M., Coll, C., Lin, C.S.K. and Koutinas, A., 2021. Bioprocess Development Using Organic Biowaste and Sustainability Assessment of Succinic Acid Production with Engineered *Yarrowia Lipolytica* Strain. *Biochem. Eng. J*, 174, 1-10.
- Deeba, F., Kiran Kumar, K., Ali Wani, S., Kumar Singh, A., Sharma, J., Gaur, N.A., 2022. Enhanced Biodiesel and β -Carotene Production in *Rhodotorula pacifica* INDKK Using Sugarcane Bagasse and Molasses by an Integrated Biorefinery Framework. *Bioresour. Technol*, 351, 1-9.
- Bonatsos, N., Marazioti, C., Moutousidi, E., Anagnostou, A., Koutinas, A., Kookos, I.K., 2020. Techno-Economic Analysis and Life Cycle Assessment of Heterotrophic Yeast-Derived Single Cell Oil Production Process. *Fuel*, 264, 1–8.



- Foong, L.C., Loh, C.W.L., Ng, H.S. and Lan, J.C.-W, 2021. Recent Development in the Production Strategies of Microbial Carotenoids. *World J. Microbiol. Biotechnol.*, 37, 1-12.
- Sen, T., Barrow, C.J. and Deshmukh, S.K., 2019. Microbial Pigments in the Food Industry—Challenges and the Way Forward. *Front. Nutr.*, 6, 1-14.
- Braunwald, T., French, W.T., Claupein, W. and Graeff-Hönninger, S., 2016. Economic Assessment of Microbial Biodiesel Production Using Heterotrophic Yeasts. *Int. J. Green Energy*, 13, 274–282.
- Kumar, L.R., Yellapu, S.K., Tyagi, R.D. and Drogui, P., 2021. Microbial Lipid and Biodiesel Production from Municipal Sludge Fortified with Crude Glycerol Medium Using pH-Based Fed-Batch Strategy. *J. Environ. Chem. Eng.*, 9, 1-9.
- Villegas-Méndez, M.Á., Montañez, J., Contreras-Esquivel, J.C., Salmerón, I., Koutinas, A. and Morales-Oyervides, L., 2022. Coproduction of Microbial Oil and Carotenoids within the Circular Bioeconomy Concept: A Sequential Solid-State and Submerged Fermentation Approach. *Fermentation*, 8, 1-19.
- Yang, J.S., Rasa, E., Tantayotai, P., Scow, K.M., Yuan, H.L. and Hristova, K.R., 2011. Mathematical Model of *Chlorella minutissima* UTEX2341 Growth and Lipid Production under Photoheterotrophic Fermentation Conditions. *Bioresour. Technol.*, 102, 3077–3082.
- Parreira, T.M., Freitas, C., Reis, A., Roseiro, J. and da Silva, T.L., 2015. Carbon Concentration and Oxygen Availability Affect Lipid and Carotenoid Production by Carob Pulp Syrup-Grown *Rhodospiridium toruloides* NCYC 921. *Eng. Life Sci.*, 15, 815–823.
- Lopes, M., Gomes, A.S., Silva, C.M. and Belo, I., 2018. Microbial Lipids and Added Value Metabolites Production by *Yarrowia Lipolytica* from Pork Lard. *J. Biotechnol.*, 265, 76–85.
- Bansal, N., Dasgupta, D., Hazra, S., Bhaskar, T., Ray, A. and Ghosh, D., 2020. Effect of Utilization of Crude Glycerol as Substrate on Fatty Acid Composition of an Oleaginous Yeast *Rhodotorula mucilagenosa* IIP132: Assessment of Nutritional Indices. *Bioresour. Technol.*, 309, 1-9.
- Boviatsi, E., Papadaki, A., Efthymiou, M.N., Nychas, G.J.E., Papanikolaou, S., da Silva, J.A.C., Freire, D.M.G. and Koutinas, A., 2020. Valorisation of Sugarcane Molasses for the Production of Microbial Lipids via Fermentation of Two *Rhodospiridium* Strains for Enzymatic Synthesis of Polyol Esters. *J. Chem. Technol. Biotechnol.*, 95, 402–407.
- Chaiyaso, T., Manowattana, A., Techapun, C., Watanabe, M., 2019. Efficient Bioconversion of Enzymatic Corn cob Hydrolysate into Biomass and Lipids by Oleaginous Yeast *Rhodospiridium paludigenum* KM281510. *Prep. Biochem. Biotechnol.*, 49, 545–556.
- Singh, G., Sinha, S., Kumar, K.K., Gaur, N.A., Bandyopadhyay, K.K. and Paul, D., 2020. High Density Cultivation of Oleaginous Yeast Isolates in 'Mandi' Waste for Enhanced Lipid Production Using Sugarcane Molasses as Feed. *Fuel*, 276, 1–11.
- Villegas-Méndez, M.Á., Papadaki, A., Pateraki, C., Balagurusamy, N., Montañez, J., Koutinas, A.A. and Morales-Oyervides, L., 2021. Fed-Batch Bioprocess Development for Astaxanthin Production by *Xanthophyllomyces Dendrorhous* Based on the Utilization of *Prosopis* sp. Pods Extract. *Biochem. Eng. J.*, 166, 1-10.



Study of immobilized biomass reactors for sulfate reducing activity characterization and improvement

R. Castro¹, G. Gabriel^{2,3}, X. Gamisans¹ and X. Guimerà¹

¹Department of Mining, Industrial and ICT Engineering, Universitat Politècnica de Catalunya, Avinguda de les Bases de Manresa 61-73, 08240 Manresa, Barcelona, Spain,

²Instituto de Microelectrónica de Barcelona, IMB-CNM (CSIC), 08193 Bellaterra, Barcelona, Spain

³CIBER, de Bioingeniería, Biomateriales y Nanomedicina (CIBER-BBN), ISCIII

Corresponding author email: rebeca.ignacia.castro@upc.edu

ABSTRACT

Immobilization of non-granular sludge is an auspicious option for sulfate reducing activity improvement. In this study, PVA-biomass granules and alginate-biomass granules were tested for mechanical stability, adsorption capacity and sulfate reduction. Moreover, two configurations of reactors, a Continuous Stirred Tank Reactor (CSRT) and a Column Reactor (CR) were operated, evaluating sulfate and glycerol consumption H₂S production in order to improve sulfate-reduction process within SONOVA process. The CR presented a stable sulfate reducing activity, higher production of H₂S and low wash out comparing to CSRT.

Keywords: sulfidogenic reactor; sulfate reducing sludge; polyvinylalcohol; alginate; immobilization.

1. INTRODUCTION

Combustion of sulfur fuels, mainly in the energy and the industrial sectors leads to the emissions of flue gases containing sulfur oxides (SO_x). Sulfur emission is responsible of air pollution and can be deposited in the environment. To this aim, SONOVA process has been developed to remove SO_x from combustion gases and their valorization as elemental sulfur. This process consists of a first step where SO_x is absorbed using a slightly alkaline solution, a biological step where absorbed SO_x (as a mixture of sulfate and sulfite) is anaerobically reduced to sulfide using glycerol as electron donor, and an aerobic sulfide oxidation step to obtain elemental sulfur (Mora et al., 2020).

Process development has highlighted that anaerobic sulfate-reduction is the process bottleneck. Several challenges have been reported for the improvement of sulfate reduction process, mainly related to maintaining a long-term efficiency and avoiding process failure caused by the inhibition of the biomass by Volatile Fatty Acids (VFAs) accumulation, sulfide toxicity, and oxygen presence (Fernandez-Palacios et al., 2019). Moreover, mass transfer resistance can be increased throughout the reactors operation, depending on their configuration. These operational limitations reduce H₂S production and thus process efficiency (Lens et al., 2003).

On the other hand, immobilization of biomass using synthetic polymers has been positioned as a promising approach for biomass immobilization. Synthetic granules improve reactors performance due to the generation of a protecting matrix that allows a decrease in starting up period and a fast adaptation to new conditions (Zhang et al. 2007). These methods can be an alternative for natural immobilization through Exopolysaccharides EPS production in cultures that have a slow production of these compounds. In addition, it has been described that polymer-biomass granules increase the mechanical strength of synthetic granules, preventing bacteria wash out (Zhang et al., 2016). These methods have been successfully used in sulfate-reduction process for acid mine draining treatment, avoiding toxicity of heavy metals and achieving high sulfidogenic activity (Selvaraj et al., 1997; Zhang et al., 2016).

Polymers used for biomass immobilization can be divided in two categories depending on the source where they have been obtained: natural or artificial polymers. Natural polymers such as alginate, chitin and carrageenan have high diffusion coefficients and low toxicity. On the other hand, synthetic polymers such as polyacrylamide, polypropylene and polyvinyl alcohol (PVA) have high mechanical strength. However, their preparation can be toxic for microorganism (Bouabidi et al., 2019).



In the present study, a new approach for sulfate reduction within SONOVA process is presented. For this purpose, two different polymers were tested for biomass immobilization, assessing sulfate adsorption, mechanical strength and removal efficiency of sulfate and chemical oxygen demand (COD). Besides, the long-term performance of both reactors operated under the same conditions (hydraulic residence time, sulfate load (HRT), C/S and biomass concentration) was evaluated using immobilized sludge as inoculum.

2. MATERIALS AND METHODS

2.1. Inoculum and cultivation

Inoculum was obtained from an anaerobic UASB reactor from Aigües de Manresa wastewater treatment plant. Sulfate-reducing activity was enhanced through sealed flask culture using anoxic mineral medium described by Mora et al. (2020).

2.2. Immobilization of sulfate reducing sludge

PVA-biomass granules were prepared using a PVA solution (13.6% w/w of PVA) that was blended (1:1) with concentrated sludge (3.78 g VSS/L). Mixture was frozen at -15 °C and cut as 5 mm granules.

Alginate-biomass granules were prepared using an alginate solution (3 %w/w of alginate) that was mixed (1:1) with concentrated sludge (also at 3.78 g VSS/L) and dropped into a CaCl₂ solution (4 %w/w) forming a 5 mm beads.

2.2.1. Adsorption and mechanical stability of immobilized biomass

Adsorption tests were performed by incubating both polymer-granules without cells for 24 h, in a sealed flask with anoxic mineral medium. Percentage of sulfate removal was calculated.

Regarding to mechanical stability, polymer-biomass granules were incubated in a sealed flask with anoxic mineral medium for 24 h, stirred at 300 rpm. Granules were counted and weighted (wet weight) at 0 and 24 h of incubation. Percentages of granules and weight loss were calculated.

2.2.2. Sulfate and COD consumption of synthetic biomass-granules and free cells

Alginate-biomass granules, PVA-biomass granules and free cells were incubated with anoxic mineral medium at 32 °C. Consumption rates were calculated measuring sulfate and COD concentration of the media every 6 hours, during 72 h.

2.3. Reactors set up and operation

A column reactor (CR) and continuous stirred tank reactor (CSTR), both of 500 mL of volume, were inoculated with 100 mL of artificial PVA-biomass granules (Figure 1). Both reactors were fed using mineral medium described by Mora et al. (2020) with an HRT of 5 h. Sulfate load was increased from 0.2 to 4 kg/m³d, keeping a C/S ratio of 6.25 mg O₂/mg SO₄²⁻. Reactors were operated during 101 days. pH, sulfate, COD, H₂S, volatile suspended solids (VSS) concentration and VFAs concentration were measured at the outlet of both reactors.

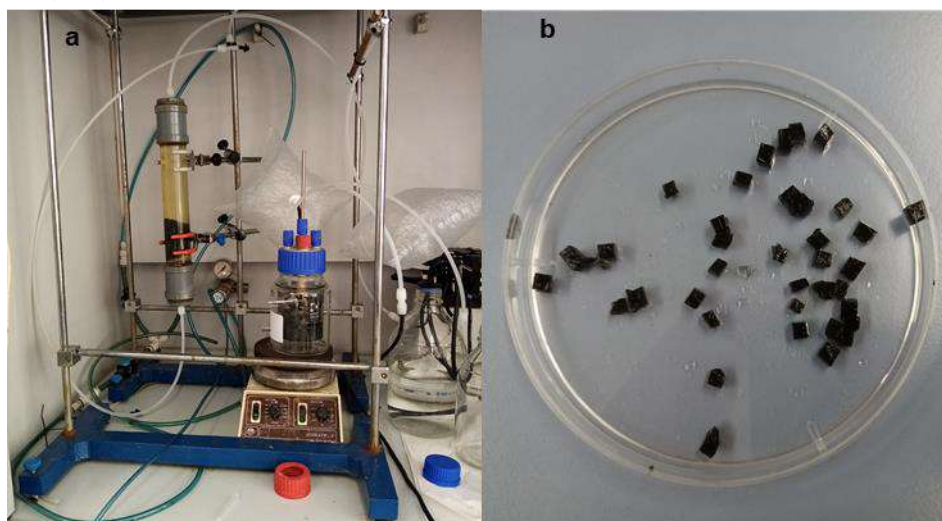


Figure 1: a) CR and CSRT reactors set-up. b) Inoculum of PVA biomass-granules.



2.4. Analytical methods

Sulfate was measured using spectrophotometry (HACH, Spain), VSS and COD were analyzed using Standard methods (APHA, 1998). VFAs concentration were obtained by HPLC with an ICsep ICE-CPREGEL 87H3 column and a at 210 nm wavelength detector. H₂S was measured using an electrochemical sensor (SULF-NP, UNISENSE, Aarhus, Denmark).

3. RESULTS

3.1. Characterization of immobilized biomass using PVA and Alginate

3.1.1. Adsorption test and mechanical strength evaluation

Alginate and PVA were used as synthetic polymer for biomass immobilization. Sulfate adsorption and mechanical stability of granules were quantified (Table 1). Adsorption tests highlighted that sulfate was not absorbed into either polymer. According to these results changes in sulfate concentration are only caused by microbial sulfate reducing activity.

Mechanical stability test presented differences between polymers (Table 2). A low degradation of PVA-biomass granules was observed at 24 h of stirred incubation. However, alginate biomass-granules were degraded up to 77%.

Table 1: Sulfate adsorption test for PVA and alginate matrix.

	PVA		Alginate	
Time (h)	0	24	0	24
Adsorbed Sulfate (mg/L)	94.7	94.7	95.1	95

Table 2: Mechanical stability test for mixtures of PVA-sludge and Alginate-sludge.

	PVA biomass-granules		Alginate biomass-granules	
Time (h)	0	24	0	24
Initial granule amount	40	38	40	2
Final granule amount	100	95	100	15
Wet weight (g)	1.6077	1.4022	1.2910	0.0309
% degraded	100	12.9	100	77.6

3.1.2. Kinetic study

Kinetic study was performed with PVA-biomass granules, Alginate-biomass granules and suspended cells (Figure 2). Regarding sulfate consumption, PVA-biomass granules presented a high consumption rate compared to alginate-biomass granules and suspended cells, removing 98% of sulfate in 15 h. These results can be explained by the diffusion capacity and the final structure of each matrix. It has been reported that immobilization allows high concentration of substrates in the matrix. Thus, free cells have a poor performance compared to synthetic biomass granules (Chen et al., 2015). However, cell density and diffusion rates of substrates and products can affect the performance of the synthetic biomass-granules (Plieva et al. 2008). Diffusion limitations have been described in alginate beads due to the high volume of the structure, generating larger diffusion distances and lower kinetic rates (Seifert & Phillips, 1997). Since PVA biomass-granules have a compact structure and a higher cell density than alginate granules, higher kinetic rates were obtained.

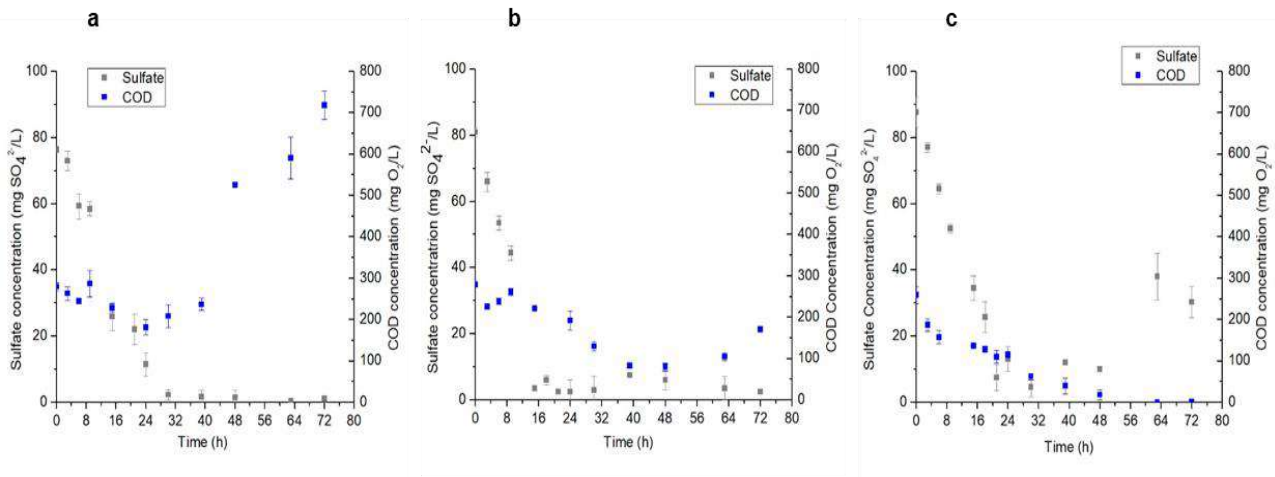


Figure 2: Kinetic study of a) Alginate-biomass granules b) PVA-biomass granules c) Free cells.

COD concentration was measured to quantify glycerol intake. Only in the assay of suspended cells, glycerol was completely depleted. In PVA-biomass-granules and alginate-biomass granules assays, an increase of COD concentration at 48 h of the experiment was observed due to degradation of polymer materials and dissolution in mineral medium. Since PVA-biomass granules showed a higher sulfate consumption rate and mechanical stability, it was selected as inoculum for reactors operation.

3.2. Long-term performance of CR and CSTR

3.2.2. Sulfate and glycerol removal

CR and CSTR were simultaneously operated under the same operational conditions (inlet sulfate concentration, C/S and HRT). Results obtained during reactors operation and monitoring are presented in Figure 3. Sulfate reduction is more than 95% when reactors were fed with sulfate loads from 0.2 to 3 kg/m³d. When sulfate load was set at 4 kg/m³d, CR and CSTR sulfate RE decreased a 50%. Nevertheless, CR regained a 97% removal efficiency in 10 days, in contrast with CSTR. This difference can be explained by accumulation of H₂S and VFAs that can be toxic for the biomass. In CSTR, lower mass transfer resistance exposed granules to inhibitors (Lens et al., 2003). Moreover, COD was not completely removed in any of the reactors. However, in CR COD RE varied between 60% and 80% and in CSTR COD RE had a decreasing trend, ranging from 90% in day 1, to 58% at the end of the experiment. It is possible to observe that sulfate reduction is not limited by glycerol concentration.

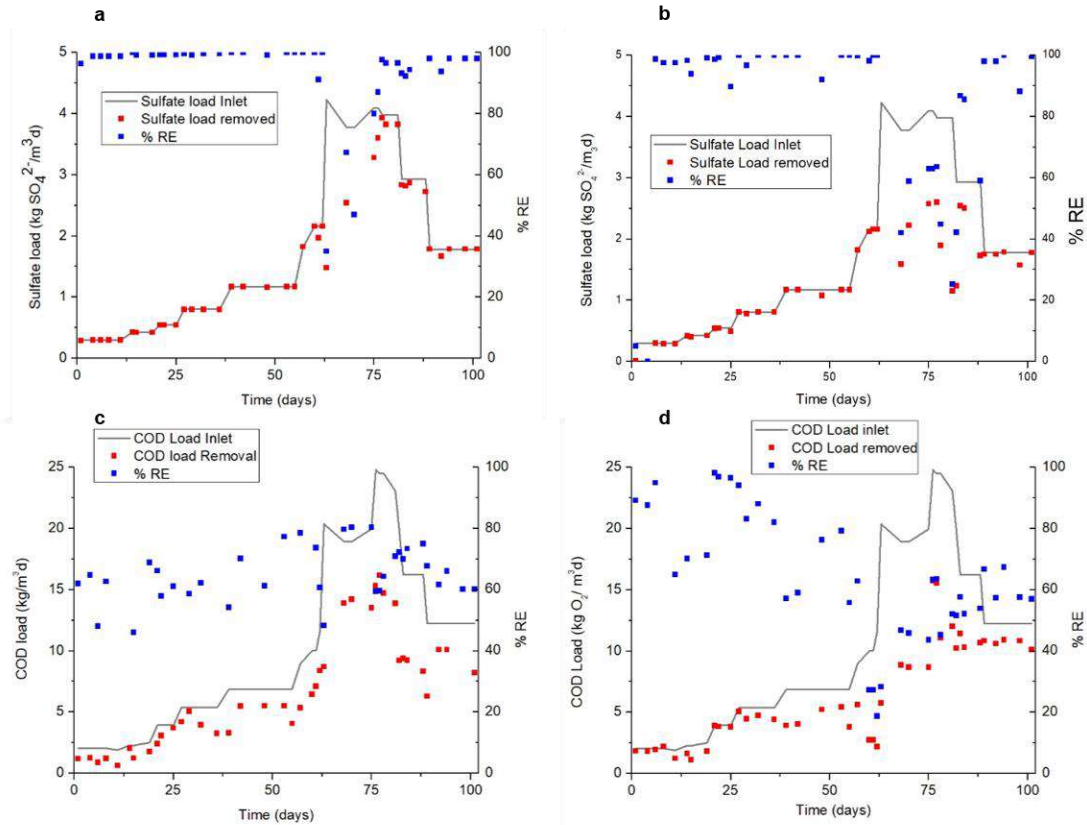


Figure 3: Long-term performance of CR and CSTR reactors. a) Sulfate removal in CR, b) sulfate removal in CSTR c) COD removal in CR, d) COD removal in CSTR.

3.3.2. H₂S production

H₂S concentration in the outlet of CR and CSTR was measured (Figure 4). It was possible to determine that H₂S concentration was higher in CR than CSTR. This is explained because H₂S stripping takes place in stirred reactor. Furthermore, H₂S concentration in both reactors increase at sulfate load of 4 kg/m³d as a consequence of a raised sulfate reducing activity.

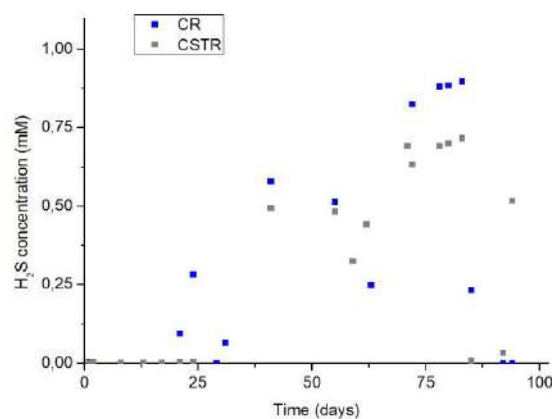


Figure 4: H₂S concentration in CR and CSTR outlets.

3.2.3. VFAs Analysis

VFAs accumulation were lower in CSTR (0.8 mg/L) than in CR (1.4 mg/L) due to gaseous compounds stripping. Besides at high loads of sulfate there is more production and accumulation of VFAs due to C/S value remained constant (Figure 5). Acetic and propionic acid accumulation demonstrated the absence of microorganism that could use these compounds as an electron donor. This trend is reported in studies of sulfidogenic reactor



operation and can trigger a process failure (Jing et al., 2013; Mohan et al., 2005). Despite VFAs accumulation, synthetic biomass granules prevent inhibition by toxic compounds and do not affect sulfate reducing activity.

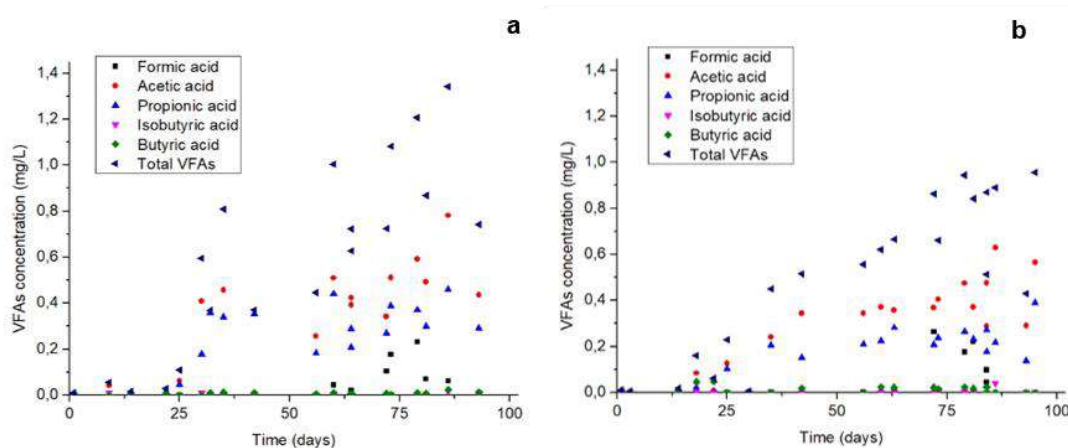


Figure 5: VFAs concentration in outlet of a) CR b) CSTR.

3.3. Granules degradation during CR and CSTR operation

VSS was determined in the outlet of CR and CSTR during all operation time (Figure 6). CSTR presented a final degradation of granules of 0.078 g VSS/L due to mechanical stirring and CR 0.023 g VSS/L. Despite of it is possible to improve PVA mechanical strength increasing the PVA concentration and the density of polymer matrix, this can be detrimental for mass transfer capacity (El-Naas et al., 2013).

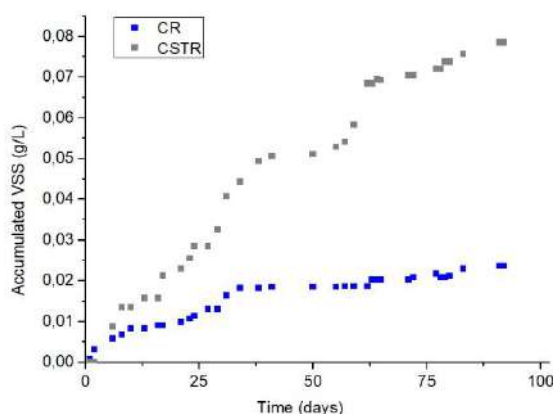


Figure 6: Biomass accumulation in the outlet of CR and CSTR.

4. CONCLUSIONS

The aim of this study was to analyze polymer-biomass granules performance for sulfate reduction process and to select a reactor configuration that allows high sulfate removal and H₂S production. PVA-biomass granules do not limit the activity of biomass and present high mechanical resistance and no adsorption of sulfate, thus can be used for scaling-up applications. Besides, CR reactor filled with PVA biomass granules presented a high stability in presence of toxic compounds such as H₂S and VFAs, therefore it could be an interesting option for future studies.

5. ACKNOWLEDGEMENTS

Authors acknowledge Ministerio de Economía y Competitividad (Spain), through the project RTI2018-099362-B-C22 MINECO/FEDER, EU, for the financial support provided to perform this research.

REFERENCES

APHA (1998). Standard methods for the examination of water and wastewater, Edition 20.



- Bouabidi, Z. B., El-Naas, M. H. and Zhang, Z., 2019. Immobilization of microbial cells for the biotreatment of wastewater: A review. In *Environmental Chemistry Letters* (Vol. 17, Issue 1, pp. 241–257). Springer Verlag.
- Chen, G., Li, J., Tabassum, S. and Zhang, Z., 2015. Anaerobic ammonium oxidation (ANAMMOX) sludge immobilized by waterborne polyurethane and its nitrogen removal performance—a lab scale study. *RSC Advances*, 5(32), 25372–25381.
- El-Naas, M. H., Mourad, A. H. I. and Surkatti, R., 2013. Evaluation of the characteristics of polyvinyl alcohol (PVA) as matrices for the immobilization of *Pseudomonas putida*. *International Biodeterioration and Biodegradation*, 85, 413–420.
- Jing, Z., Hu, Y., Niu, Q., Liu, Y., Li, Y. Y. and Wang, X. C., 2013. UASB performance and electron competition between methane-producing archaea and sulfate-reducing bacteria in treating sulfate-rich wastewater containing ethanol and acetate. *Bioresource Technology*, 137, 349–357.
- Lens, P. N. L., Gastesi, R. and Lettinga, G., 2003. Use of sulfate reducing cell suspension bioreactors for the treatment of SO₂ rich flue gases. *Biodegradation*, 14(3), 229–240.
- Mohan, S. V., Rao, N. C., Prasad, K. K. and Sarma, P. N., 2005. Bioaugmentation of an anaerobic sequencing batch biofilm reactor (AnSBBR) with immobilized sulphate reducing bacteria (SRB) for the treatment of sulphate bearing chemical wastewater. *Process Biochemistry*, 40(8), 2849–2857.
- Mora, M., Fernández-Palacios, E., Guimerà, X., Lafuente, J., Gamisans, X. and Gabriel, D., 2020. Feasibility of S-rich streams valorization through a two-step biosulfur production process. *Chemosphere*, 253, 126734.
- Plieva, F., Galaev I., Noppe, W. and Mattiason, B., 2008. Cryogel applications in microbiology. *Trends in Microbiology*, 16 (11), 543-551.
- Seifert, D. and Phillips, J., 1997. Production of small, monodispersed alginate beads for cell immobilization. *Biotechnology Progress*, 13(5), 562-568.
- Selvaraj, P. T., Little, M. H. and Kaufman, E. N., 1997. Biodesulfurization of flue gases and other sulfate/sulfite waste streams using immobilized mixed sulfate-reducing bacteria. *Biotechnology Progress*, 13(5), 583–589.
- Zhang, L.-S., Wu, W.-Z., and Wang, J.-l., 2007. Immobilization of activated sludge using improved polyvinyl alcohol (PVA) gel. *Journal of Environmental Sciences*, 19(11), 1293–1297.
- Zhang, M., Wang, H. and Han, X., 2016. Preparation of metal-resistant immobilized sulfate reducing bacteria beads for acid mine drainage treatment. *Chemosphere*, 154, 215–223.



Analysis of PM_{2.5} and PM₁₀ concentrations trends in selected Greek urban cities before and after the national lockdowns caused by the COVID-19 pandemic

P. Begou¹

¹Laboratory of Meteorology and Climatology, Department of Physics, University of Ioannina, Ioannina, Greece

Corresponding author email: p.begou@uoi.gr

ABSTRACT

The advent of the COVID-19 pandemic had a positive ecological footprint resulting in a reduction in air pollution concentration levels related to the lockdown measures were implemented worldwide in order to prevent the spread of the virus. The strict lockdowns along with the mobility restrictions and the reduced industrial, commercial and human activities caused a better air quality in many countries during the national quarantine periods. In this study, we assess and evaluate the particulate air pollution in Athens, Thessaloniki and Patra during the lockdown periods. For this purpose, we used the data on PM_{2.5} and PM₁₀ concentrations from air quality monitoring stations in Athens (Aristotelous street, station name: ARI), Thessaloniki (Agia Sofia, station name: AGS) and Patra (station name: PAII). We discriminated the PM data into two phases (pre-lockdown period (baseline period): from the 1st of January of 2017 to the 31st of December 2019 and the lockdown period: from the 1st of January of 2020 to the 31st of December 2020. The analysis revealed a reduction in the mean monthly PM_{2.5} and PM₁₀ concentrations compared to the monthly values of the period 2017-2019. As well as, we analyzed the weekday patterns PM concentrations and found a considerable reduction of both PM_{2.5} and PM₁₀ during the weekdays compared to the weekends at AGS and PAII stations except ARI station. Overall, the results demonstrated that during the lockdowns the air quality was improved significantly but temporally.

Keywords: Greek urban areas; urban air pollution; air quality; Particulate Matter; PM₁₀; PM_{2.5}.

1. INTRODUCTION

The ambient air pollution is a major environmental concern in the urban areas of Greece. In the highly urbanized cities of Greece such as Athens, Thessaloniki and Patra two types of air pollution have been identified, the photochemical smog and particulate matter pollution (Valavanidis et al., 2015). Although there has been good progress in the implementation of the ambient air quality legislation in Greece, the high population density and the economic activities in the urban areas contribute to the high levels of air pollution. The air pollution problems are often exacerbated by factors that favor the accumulation of air pollutants over the cities, such as the urban landscape and the topography changes based on the urbanization progress and the urban sprawl (e.g., build-up areas, bare land, lack of vegetation, narrow and deep street canyons). Other factors such as adverse meteorological conditions, temperature inversions, low wind speed, high ambient temperature and intense sunshine duration worsen the air quality and cause air pollution episodes (Sindosi et al., 2019). Moreover, Saharan dust events are often associated with the high levels of PM₁₀ concentrations. On the other hand, vehicular traffic and residential heating are major sources of PM. Emissions from the combustion of fossil fuel or wood burning, heat stoves and fireplaces produce much of the PM_{2.5} ambient air pollution (Valavanidis et al., 2015).

During the lockdowns periods due to COVID-19 pandemic, the air quality in some places improved and the ground-based and satellite observations showed a decline in the concentrations of air pollutants emitted from the anthropogenic activities and the vehicular traffic (Varotsos et al., 2021; Zerefos et al., 2021).

In Greece, the first strict lockdown implemented during the first COVID-19 pandemic wave on the 23rd of March 2020 and the second lockdown started on the 7th of November 2020. During these lockdowns the Greek authorities announced stringent traffic, transport, travel and industry restrictions and strict non-essential movement ban along with advise to try to stay at home and avoid contact with other people.



All these measures against the spread of pandemic revealed a marked fall in air pollution concentrations levels at several greek cities (Melidis and Tzagkarakis, 2021; Kotsiou et al., 2021; Varotsos et al., 2021; Zerefos et al., 2021).

The objective of this study is to assess and evaluate the $PM_{2.5}$ and PM_{10} concentrations in selected Greek urban cities during the lockdown periods. For this purpose, we use the data on $PM_{2.5}$ and PM_{10} concentrations from air quality monitoring stations in Athens (Aristotelous street, station name: ARI), Thessaloniki (Agia Sofia, station name: AGS) and Patra (station name: PAII).

2. DATA AND METHODOLOGY

2.1. Data

The data on $PM_{2.5}$ and PM_{10} concentrations were derived by the air quality monitoring stations of the National Air Pollution Monitoring Network (NAPMN) which is operated by the Air Quality Department of the Ministry of Environment. The air pollution data is available online in the Ministry's official website (www.ypen.gov.gr). The 24-hour $PM_{2.5}$ and PM_{10} concentrations data were collected from air quality monitoring stations in Athens, Thessaloniki and Patra, from the 1st of January 2017 to the 31st of December 2020. We chose to include stations which have been installed at areas characterized as "Urban-traffic" sites.

2.2. Methodology

The analysis of the $PM_{2.5}$ and PM_{10} concentrations was performed in the computer software "R" by using the package "openair", which is an open-source tool for analyzing air pollution data (Carslaw and Ropkins, 2012).

In order to evaluate the effect of COVID-19 pandemic lockdowns on air quality, we split the $PM_{2.5}$ and PM_{10} concentrations data into two time periods, before and after January 2020. The monthly $PM_{2.5}$ concentrations before January 2020 indicate the baseline period consisting of the mean monthly values over the period 2017-2019, while the monthly $PM_{2.5}$ concentrations after January 2020 consists of the measurements over the period from 1st of January 2020 to 31st of December 2020.

3. RESULTS AND DISCUSSION

Figures 1(a) to 1(f) show the mean monthly concentrations of $PM_{2.5}$ and PM_{10} at ARI, AGS and PAII air quality monitoring stations during two phases. The pre-lockdown period (before January 2020) corresponds to the baseline period 2017-2019 and the lockdown period (after 2020) consists of the months with the government-imposed pandemic restrictions. Both $PM_{2.5}$ and PM_{10} showed a significant decrease during the lockdown periods in 2020 attributed to the reduction of the anthropogenic activities and the human mobility restrictions (Figures 1(a) to 1(f)). During the first national lockdown, the mean monthly $PM_{2.5}$ concentrations in March 2020 and April 2020 were $16.62 \mu\text{g}/\text{m}^3$ and $13.53 \mu\text{g}/\text{m}^3$ in ARI station, $18.58 \mu\text{g}/\text{m}^3$ and $15.07 \mu\text{g}/\text{m}^3$ in AGS station and $15.06 \mu\text{g}/\text{m}^3$ and $10.80 \mu\text{g}/\text{m}^3$ in PAII station, respectively (Figures 1(a), 1(c) and 1(e)). The mean monthly PM_{10} concentrations were $31.91 \mu\text{g}/\text{m}^3$ and $25.19 \mu\text{g}/\text{m}^3$ in ARI station, $34.49 \mu\text{g}/\text{m}^3$ and $28.35 \mu\text{g}/\text{m}^3$ in AGS station and $24.62 \mu\text{g}/\text{m}^3$ and $20.06 \mu\text{g}/\text{m}^3$ in PAII station, in March 2020 and April 2020, respectively (Figures 1(b), 1(d) and 1(f)). Similarly, the monthly mean concentrations of $PM_{2.5}$ and PM_{10} during the second lockdown in November 2020 and December 2020, were also lower compared to the baseline period 2017-2019 but the remarkable difference showed at the ARI station. For instance, the mean monthly $PM_{2.5}$ concentrations registered during this period at ARI station were $16.64 \mu\text{g}/\text{m}^3$ and $17.16 \mu\text{g}/\text{m}^3$, in November 2020 and December 2020, respectively (Figure 1(a)). In general, the $PM_{2.5}$ and PM_{10} concentrations at AGS and PAII stations showed a considerable decline during the weekdays compared to the weekends. Interestingly, at ARI station both $PM_{2.5}$ and PM_{10} concentrations were at the same levels during the weekends before and during the lockdown periods.

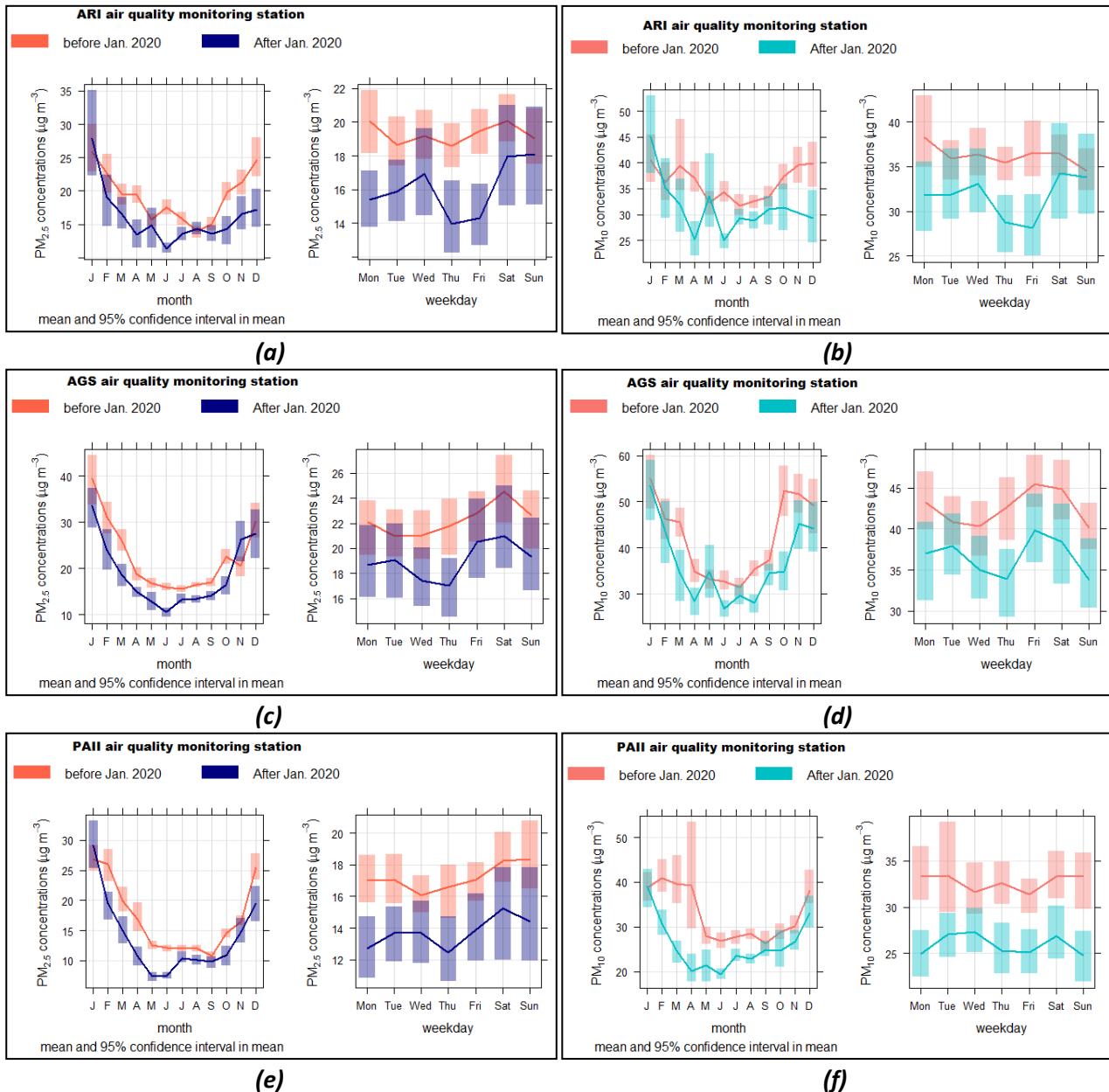


Figure 1. The mean monthly $\text{PM}_{2.5}$ and PM_{10} concentrations ($\mu\text{g}/\text{m}^3$) in the air quality stations ARI, AGS and PAII before January 2020 and after January 2020.

4. CONCLUSIONS

The purpose of this study was to investigate the air quality improvement during the lockdowns using $\text{PM}_{2.5}$ and PM_{10} concentrations data from air quality monitoring stations in Athens, Thessaloniki and Patra. We found that the average monthly $\text{PM}_{2.5}$ and PM_{10} concentrations declined during the shutdown compared to the long-term records of the airborne particulate pollution over the period 2017-2019.

REFERENCES

- Carslaw, D. and Ropkins, K., 2012. openair – An R package for air quality data analysis. *Environmental Modelling & Software*. Volumes 27–28, January–February 2012, Pages 52-61.
- Kotsiou, O.S., Saharidis, G., Kalantzis, G., Fradelos, E.C. and Gourgoulialis, K.I., 2021. The Impact of the Lockdown Caused by the COVID-19 Pandemic on the Fine Particulate Matter ($\text{PM}_{2.5}$) Air Pollution: The Greek Paradigm. *International journal of environmental research and public health*, 18(13), 6748.
- Melidis, M. and Tzagkarakis, S.I., 2021. Assessing Air Quality in Greece in Times of a Global Pandemic. *HAPSc Policy Briefs Series*, 2(1), 87–93.



- Sindosi, O.A., Markozannes, G., Rizos, E. and Ntzani, E., 2019. Effects of economic crisis on air quality in Ioannina, Greece. *Journal of environmental science and health*. Part A, Toxic/hazardous substances & environmental engineering, 54(8), 768–781.
- Valavanidis, A., Vlachogianni, Th., Loridas, S. and Fiotakis, C., 2015. Atmospheric Pollution in Urban Areas of Greece and Economic Crisis. *Trends in Air Quality and Atmospheric Pollution Data, Research and Adverse Health Effects*. Department of Chemistry, University of Athens. 1. 1-27. www.chem.uoa.gr.
- Varotsos, C., Christodoulakis, J., Kouremadas, G.A. and Fotaki E.F., 2021. The Signature of the Coronavirus Lockdown in Air Pollution in Greece. *Water, air, and soil pollution*, 232(3), 119.
- Zerefos, C.S., Solomos, S., Kapsomenakis, J., Poupkou, A., Dimitriadou, L., Polychroni, I.D., Kalabokas, P., Philandras, C.M. and Thanos, D. (2021). Lessons learned and questions raised during and post-COVID-19 anthropopause period in relation to the environment and climate. *Environment, development and sustainability*, 23(7), 10623–10645.



Is there any correlation between diabetes mellitus and atmospheric pollutants?

M. Koliba^{1,2,3}, D. Zmijková⁴ and H. Raclavská⁵

¹Diabetic and podiatric clinic, Vratimov, Czech Republic

²Department of Internal medicine, University Hospital Ostrava, Ostrava, Czech Republic

³Department of Internal Studies, Faculty of Medicine, University of Ostrava, Ostrava, Czech Republic

⁴Faculty of Mechanical Engineering, Czech Technical University in Prague, Prague 6-Dejvice, Czech Republic

⁵Centre ENET, VŠB-Technical University of Ostrava, Ostrava-Poruba, Czech Republic

Corresponding author email: mrkoliba@seznam.cz

ABSTRACT

The basic aim of this study was an assessment of the possible association between atmospheric pollution and type 2 diabetes mellitus. We evaluated the impact of chosen air pollutants (size fractions of particulate matter (PM_{2.5}, PM₁₀), nitrogen dioxides (NO_x), ground ozone (O₃), benzo(a)pyrene (BaP) on the occurrence of type 2 diabetes mellitus and mortality of diabetics. Using correlation analysis, we found out statistically significant dependence between the occurrence of type 2 diabetes mellitus and air concentration of PM_{2.5} and the concentration of ground ozone in the year 2010. Moreover, we identified a statistically significant association between mortality of diabetics and air concentrations of the following pollutants in the years 2010 and 2019 – i.e., PM₁₀, O₃, and BaP. Based on the results of our study, type 2 diabetes mellitus can be considered a disease with the participation of some air pollutants (PM₁₀, PM_{2.5}, O₃, and BaP) in the etiopathogenic process.

Keywords: diabetes mellitus; diabetic complications; atmospheric pollution; correlation analysis.

1. INTRODUCTION

Diabetes mellitus (DM) represents a leading public health problem. The International Diabetes Federation estimated that in 2019, 463 million people suffered from diabetes mellitus. The trend of the growing incidence of diabetes will also continue in the following years – the estimation of the future number of patients with diabetes mellitus is 578 million diabetics by 2030 and 700 million diabetics by 2045. This fact is alarming because, according to the Centers for Disease Control and Prevention, diabetes mellitus is the most common cause of renal impairment, non-accidental lower limb amputation, and a common cause of blindness (Centers for Disease Control and Prevention, 2022). Moreover, the therapeutic costs spent on the care of diabetics are very high, especially when diabetes mellitus is joined with complications.

For the reasons mentioned above, the interest in the causes of the permanently rising occurrence of diabetes mellitus is still increasing. In connection with an epidemic of diabetes mellitus, the attention is especially concentrated on ambient air pollution. Atmospheric pollution has been intensively studied in connection with cardiovascular and pulmonary disease. On the contrary, the association between diabetes mellitus and the level of concentrations of atmospheric pollutants has received only less attention. Diabetes mellitus was considered to be a disease without the participation of any environmental factors in etiopathogenesis. However, this trend has changed. Nowadays, there are many studies documenting the fact that environmental factors or ambient air pollution can play an important role in the etiopathogenic process of type 2 diabetes mellitus. An increased incidence of diabetes mellitus was found in persons exposed to PM₁₀ after ten years of exposition (Ikenna et al., 2014). Environmental stimuli (high concentration of PM_{2.5} and ground O₃) and endothelial dysfunction might be potential mechanisms of cardiovascular events in individuals having type 2 diabetes mellitus (Lazinger et al., 2014).

According to the accessible scientific studies (Dales et al., 2012; Ikenna et al., 2014; Lazinger, 2014), the following gaseous air pollutants are considered to be in relationship with the occurrence of type 2 diabetes mellitus – i.e., nitrogen oxides (NO_x), sulfur dioxide (SO₂), carbon monoxide (CO), and ground ozone (O₃). Some fractions (PM_{2.5}, PM₁₀) of particulate matter also have an important role in the etiology of type 2 diabetes mellitus (Dales et al., 2012; Wu et al., 2021; Yang et al., 2020).

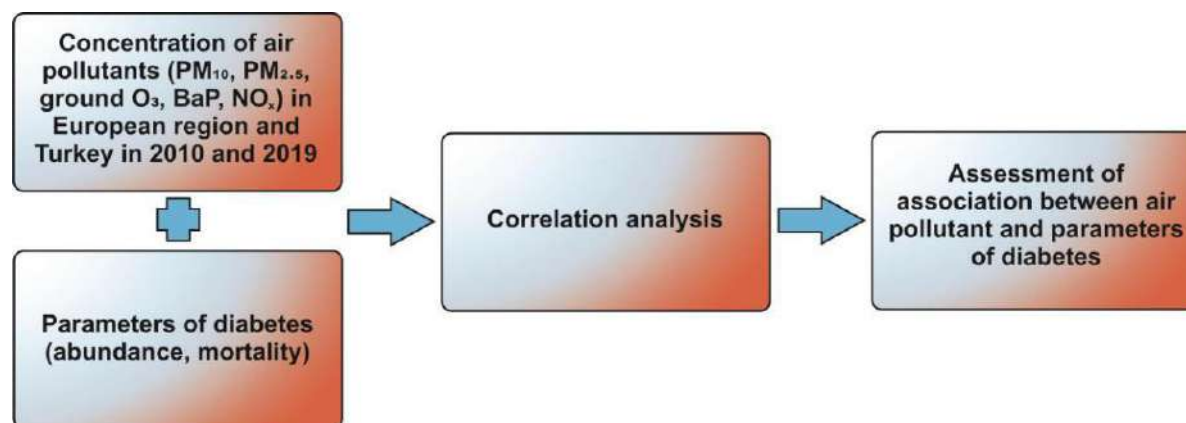


The association between air pollution (CO, ground O₃, SO₂, NO₂, PM_{2.5}, and PM₁₀) appears to increase the risk of acute complications of diabetes mellitus requiring hospitalisation, and improvement in air quality could reduce morbidity from diabetes mellitus (Dales et al., 2012).

The article aims to compare the environmental burden expressed by air pollution parameters and the evolution of the occurrence of DM disease or mortality caused by DM in EA countries and Turkey based on statistical data published by the European Environmental Agency (EEA) and databases of International Diabetes Federation (IDF).

2. MATERIALS AND METHODS

The used work procedure is demonstrated in Figure 1.



Explanations: PM₁₀ – particulate matter with a diameter lower than 10 µm, PM_{2.5} – particulate matter with a diameter lower than 2.5 µm, O₃ – ozone, BaP – benzo(a)pyrene, NO_x – nitrogen oxides

Figure 1. Diagram of work procedure.

2.1 Specification of the study area, air pollutants, and the sampling period

The assessment of the possible association between air pollution and the occurrence of diabetes mellitus or its complications was realised in European countries and Turkey (Figure 2). We monitored four atmospheric pollutants – i.e., particulate matter (PM_{2.5} and PM₁₀), nitrogen oxides (NO_x), ground ozone (O₃), and benzo(a)pyrene (BaP). For this purpose, we choose two study years (2010 and 2019) to monitor the impact of each of the pollutants. We obtained air pollution data from the European Environmental Agency (EEA) databases. Essential health data were assumed from databases of the International Diabetes Federation (IDF).

Correlation analysis was applied to assess the possible association between the frequency of type 2 diabetes mellitus or its complications and the level of monitoring air pollutants. We evaluated the effect of every pollutant separately (single-pollutant model). Outliers were tested using a boxplot and subsequently excluded from the regression analysis. Correlation analysis was realised using the OriginPro 2019 software.

3. RESULTS AND DISCUSSION

Dependencies between air pollutant concentration and abundance of diabetes mellitus and mortality in EU countries, Turkey, and Ukraine expressed per 100,000 inhabitants are shown in Table 1. The number of monitored values for individual dependencies varies, due to either missing information in databases or the exclusion of outliers. The lowest incidence of DM in 2010 was found in Iceland (1,351 per 100,000 inhabitants) and the highest in Portugal (9,512), followed by Germany (9,296 per 100,000 inhabitants). The average incidence of DM in EU countries in 2010 was $6,232 \pm 1,819$ per 100,000 inhabitants. In 2019, there was a high increase of DM in the population of Iceland; the lowest incidence of DM was found in Latvia (3,545) and the highest in Germany (11,797), followed by Portugal (10,394 per 100,000 inhabitants). In 2019, the average population with DM increased to $6,755 \pm 1,919$ per 100,000 inhabitants.



3.1 Evaluation of the impact of PM on type 2 diabetes mellitus

In 2019, the annual average concentration of PM₁₀ in the EU and Turkey ranged from 18.6 (Iceland) to 83.2 µg/m³ (Turkey), with an average value of 37.2 ± 13.6 µg/m³. Eight countries failed to meet the annual limit of 40 µg/m³. Linear dependence was found between mortality of diabetics and atmospheric concentration of PM₁₀. This dependence shows that an increase in the concentration by 10 µg/m³ leads to an increase in mortality of persons having diabetes. This dependence is statistically significant in both monitoring years. Between concentration of PM₁₀ and occurrence of type 2 diabetes mellitus, it was determined only a less significant relation in 2010. In the year 2019, any dependence was not found. An increase in PM₁₀ concentration by 10 µg/m³ above limits determined by the World Health Organization (WHO) for four to ten days causes an increase in mortality of diabetics in the interval from 0.40 to 1.03%

(Yang et al., 2020). Similar results concerning the surpassing of limit concentration are published by Orioli et al. (2018) and WHO (2021). PM₁₀ concentration provides statistically more significant dependencies between diabetes occurrence and mortality than PM_{2.5}.

The annual average concentration of PM_{2.5} in 2019 ranged from 5.6 (Finland) to 26.9 µg/m³ (Turkey) in the EU and Turkey with an average value of 13.30 ± 5.44 µg/m³. PM_{2.5} is the most important pollutant in terms of the mortality value in the exposed population and the potential development of cardiovascular disease and asthma (WHO, 2021). Therefore, in 2021, the WHO prepared new proposals to reduce the limit concentration of PM_{2.5} from 10 to 5 µg/m³ (annual average). In the year 2019, only Estonia, Finland, Iceland, Denmark, Norway, Sweden, Portugal, Spain, and Switzerland met the annual average PM_{2.5} concentration of less than 10 µg/m³. The value < 5 µg/m³ has not been achieved in any EU country. Guidelines according to Air Quality Directives 2008/50/EC in the EU are less stringent than WHO limits (Figure 2). Only Turkey and Poland do not meet these criteria for PM_{2.5} (20 µg/m³).

In the year 2010, we proved statistically significant dependence between the concentration of PM_{2.5} and diabetes prevalence. The cause of the low correlation between the concentration of PM_{2.5} and the occurrence of type 2 diabetes mellitus or mortality of diabetics can be seen from the comparison of PM_{2.5} concentration in the years 2010 and 2019 (Figure 2). The decline in concentrations of PM_{2.5} concerns all European countries; the exception represents only Turkey.

Table 1. Results of correlation analysis between parameters of type 2 diabetes and concentration of atmospheric pollutants in the years 2010 and 2019 in the European region and Turkey.

Atmospheric pollutant	2010		2019		Annual WHO Air quality guidelines (µg/m ³)		Annual EU Air quality criteria (µg/m ³)
	abundance	mortality	abundance	mortality	2005	2021	
PM ₁₀	r=0.68; p=0.05; n=29*	r=0.52; p=0.05; n=28*	insignificant	r=0.68; p=0.05; n=29*	20	15	40
PM _{2.5}	r=0.43; p=0.25; n=29**	insignificant	insignificant	r=0.38; p=0.1; n=30**	10	5	25→20
ground O ₃	r=0.49; p=0.25; n=23**	r=0.42; p=0.25; n=26**	insignificant	r=0.42; p=0.25; n=23**	ND	60 ^a	
BaP	r=0.43; p=0.25; n=25**	r=0.51; p=0.25; n=19**	insignificant	r=0.61; p=0.05; n=20*	< 0.12 ng/m ³	1 ng/m ³	
NO _x	insignificant	insignificant	r=0.38; p=0.25; n=26**	insignificant	40	10	40

Explanations: PM₁₀ – particulate matter with a diameter lower than 10 µm, PM_{2.5} – particulate matter with a diameter lower than 2.5 µm, O₃ – ozone, BaP – benzo(a)pyrene, NO_x – nitrogen oxides, * – statistically significant correlation, ** – statistically less significant dependency, p – significance level, n = number of countries. ND – not defined, ^a – Average of daily maximum 8-hour mean O₃ concentration in the six consecutive months with the highest six-month running-average O₃ concentration.

The literature informs on the intensive increase in risk of type 2 diabetes mellitus if the concentration of PM_{2.5} is higher than 2.4 µg/m³ (Li et al., 2019). Blood concentration of glycated hemoglobin HbA1c is rising with growing exposition time and growing concentration of air pollutants (Li et al., 2019). However, in this place, it is necessary to consider that most people spend the predominant part (80%) of their life indoors (Liu et al., 2019).

The emissions of PM₁₀, sulfur dioxide (SO₂), nitrogen dioxide (NO₂), and carbon monoxide (CO) are the main factors affecting the outdoor concentration of PM_{2.5}, while meteorological conditions and outdoor concentration of ground O₃ belong to secondary parameters (Zheng et al., 2019). Further reduction of PM_{2.5} concentration in the EU will be problematic as up to 54% of emissions come from domestic boilers, while



energy contributes only 2.3%, industrial production 18%, transport 12.7%, agriculture 6.3%, and waste 6.7% (EEA).

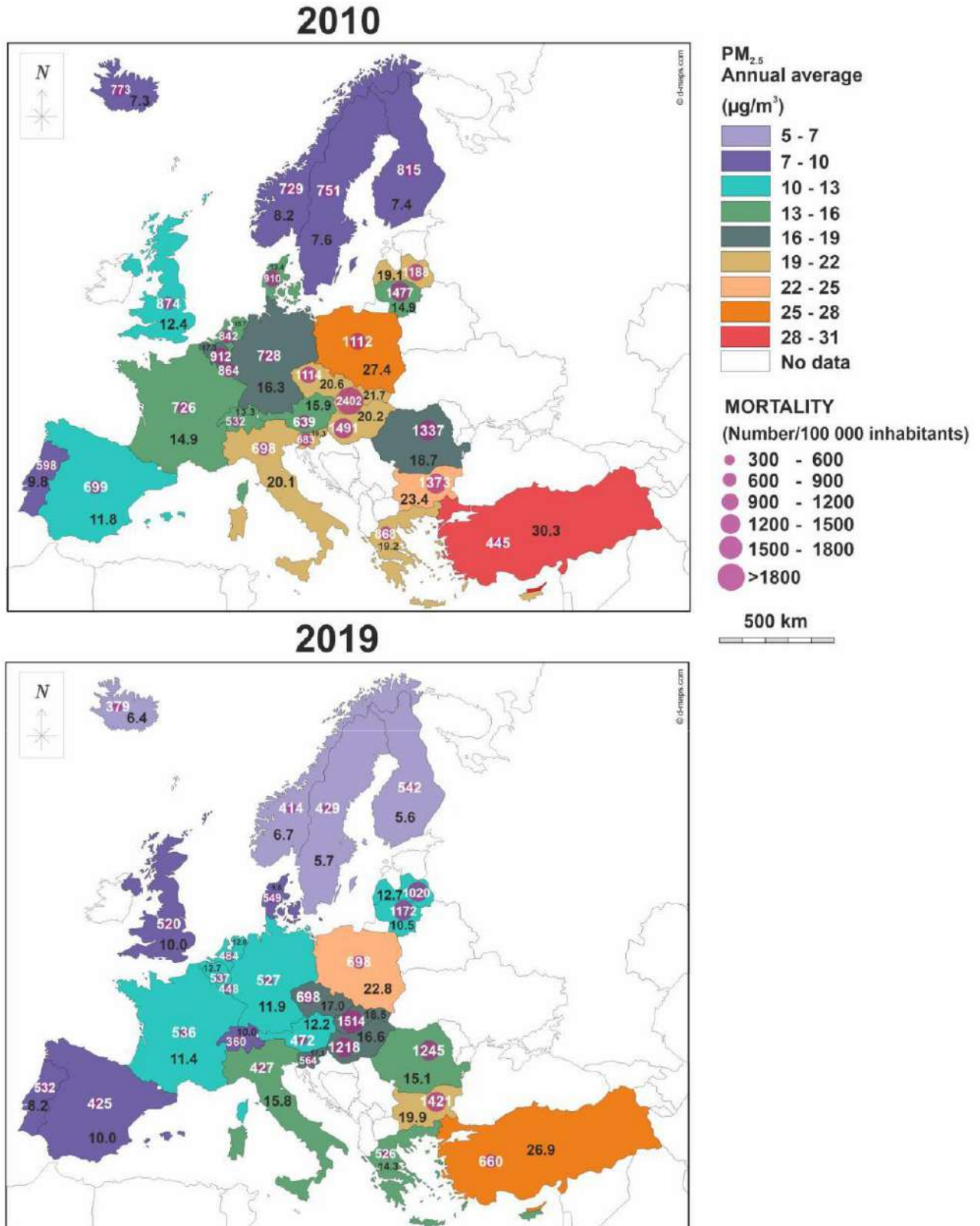


Figure 2 Average PM_{2.5} concentration in 2010 and 2019 and information on mortality caused by diabetes; in the medium average PM_{2.5} concentration, wheel diameter considers mortality.



3.2 Evaluation of the impact of ground ozone on type 2 diabetes mellitus

In 2010, we found a statistically significant dependence between diabetes occurrence and concentration of ground O₃, while in 2019, there was insignificant relation between the same parameters. In both years, a statistically significant relationship between mortality of diabetics and concentration of ground O₃ was also confirmed. The number of deaths of diabetics was rising with the growing concentration of ground O₃. There is a scarcity of works discussing the long-term impact of ground O₃ on the occurrence of type 2 diabetes mellitus. The toxicological studies show that ground O₃ causes oxidative stress and amplifies insulin resistance (Jerrett et al., 2017). Ground O₃ appears to have a similar mechanism as particulate matter PM_{2.5} (Rao et al., 2015).

3.3 Evaluation of the impact of nitrogen oxides on type 2 diabetes mellitus

In 2010, NO₂ concentrations ranged from 8.54 (Iceland) to 31.91 µg/m³ (UK), with an average value of 24.99 ± 6.06 µg/m³. In 2019, average NO₂ concentrations were lower at 20.12 ± 5.22 µg/m³. In the case of our study, we did not find any evident relationship between the number of deaths of diabetics and the level of concentration of NO_x, which is consistent with the results of Dijkema et al. (2011). The existing relationship between nitrogen oxides and the occurrence of type 2 diabetes mellitus was confirmed by Liu et al. (2019) and Unnikrishnan et al. (2017). Our data confirmed only a statistically less significant dependence between the occurrence of type 2 diabetes mellitus and the concentration of nitrogen dioxide (NO₂) in the year 2019. The reason for statistical dependency between NO_x concentration and occurrence of type 2 diabetes mellitus or mortality of diabetics can be seen in the fact that applied statistical data represent average values obtained from regions of miscellaneous nature (urban areas versus rural zones), consistent with the findings of (Hassanvand et al., 2018). Increased concentration of NO₂, which comes mainly from transport, is rather typical for large towns or urban agglomerations, where it often surpasses the limit concentrations.

3.4 Evaluation of the impact of benzo(a)pyrene on type 2 diabetes mellitus

BaP concentration in 2010 ranged from 0.093 (Sweden) to 5.76 ng/m³ (Poland), with an average value of 1.00 ± 1.28 ng/m³. EU's air quality directives (2008/50/EC) limit values were measured in six countries out of 20: Poland > Czech Republic > Slovakia > Bulgaria > Hungary > Austria. Compared to 2010, the average annual concentration of BaP in the air decreased slightly in 2019 at 0.85 ± 1.01 ng/m³. The lowest average concentration was measured in Switzerland 0.14 ng/m³, and the highest in Poland 4.27 ng/m³. In six countries, the concentration was above the limit value: Poland > Slovakia > Italy > Czech Republic > Bulgaria > Hungary.

Dependence between the occurrence of type 2 diabetes mellitus and atmospheric concentration of BaP was found only in the case of the database from 2010. A statistically significant relationship was detected between the number of deaths and concentration of BaP in both years. The impact of BaP on the occurrence of type 2 diabetes mellitus and mortality of diabetics is described in the study carried out by Srivastava (2021). An increase in polycyclic aromatic hydrocarbons (PAHs) concentration caused an increase in the occurrence of type 2 diabetes mellitus in the interval from 78 to 124%. The increase of occurrence of type 2 diabetes mellitus is especially enormous if the increased air concentration of PAHs is accompanied by the other risk factors of diabetes (obesity, hypertension, hyperlipidemia).

4. CONCLUSIONS

Based on the results of our study, some air pollutants can be considered significant factors in the occurrence of type 2 diabetes mellitus (PM₁₀, PM_{2.5}, ground O₃, and BaP) in 2010. Mortality of diabetics was influenced quite significantly in both years by concentrations of PM₁₀, ground O₃, and BaP. According to the results of this paper, it is possible to expect a reduction in the prevalence of diabetic cases and frequency of diabetes complications under the condition of continuous improvement of air quality. In addition to the quality of the environment, the incidence of diabetes mellitus is also influenced by the cost of treatment per patient and the standard of living of the population as expressed by the purchasing power standard (PPS).



5. ACKNOWLEDGEMENTS

This paper was supported by the research project of the Ministry of Education, Youth and Sport of the Czech Republic: “OP RDE grant number CZ.02.1.01/0.0/0.0/16_019/0000753 Research Centre for Low-carbon Energy Technologies”.

6. REFERENCES

- Centers for Disease Control and Prevention [WWW Document]. USA: U. S. Department of Health and Human Services, 2022. <https://www.cdc.gov/diabetes/basics/quick-facts.html> (accessed 6.10.2022).
- Dales, E.R., Cakmak, S., Vidal, C.B. and Rubio, M.A., 2012. Air pollution and hospitalization for acute complications of diabetes in Chile. *Environ. Int.*, 46, 1–5.
- Dijkema, M.B., Mallant, S.F. and Gehring, U., 2011. Long-term exposure to traffic-related air pollution and type 2 diabetes prevalence in a cross-sectional screening-study in the Netherlands. *Environ. Health*, 10, 76–84.
- European Environment Agency (EEA). *Country fact sheets*. <https://www.eea.europa.eu/themes/air/country-fact-sheets> (accessed 6.13.2022).
- Hassanvand, M.S., Naddafi, K., Malek, M., Valojerdi, A.E., Mirzadeh, M., Samavat, T., Hezaveh, A.M., Hodjatzadeh, A. and Khamseh, M.E., 2018. Effect of long-term exposure to ambient particulate matter on prevalence of type 2 diabetes and hypertension in Iranian adults: an ecologic study. *Environ. Sci. Pollut. Res. Int.*, 25, 1713–1718.
- Ikenna, C.E., Schaffner, E., Fischer, E., Schikowski, T., Adam, M., Imboden, M., Tsai, M., Carballo, D., Eckarstein, A. von, Künzli, N., Schindler, Ch., and Probst-Hensch, N., 2014. Long-term air pollution exposure and diabetes in a population-based Swiss cohort. *Environ. Int.*, 70, 95–105.
- International Diabetes Federation (IDF), 2019. *IDF Diabetes Atlas*. 9th ed.; International Diabetes Federation: Brusel, Belgium.
- Jerrett, M., Brook, R., White, L.F., Burnett, R.T., Yu, J., Su, J., Seto, E., Marshall, J., Palmer, J.R., Rosenberg, L. and Coogan, P.F., 2017. Ambient ozone and incident diabetes: A prospective analysis in a large cohort of African American women. *Environ. Int.* 102, 42-47.
- Lazinger, S., Breitner, S., Neas, L., Cascio, W., Diaz-Sanchez, D., Hinderlitter, A., Peters, A., Devlin, R.B. and Schneider, A., 2014. The impact of decreases in air temperature and increases in ozone on markers of endothelial function in individuals having type-2 diabetes. *Environ. Res.*, 134, 331–338.
- Li, N., Liu, Z., Li, Y., Li, N., Chartier, R., McWilliams, A., Chang, J., Wang, Q., Wu, Y., Xu, Ch. and Xu, D., 2019. Estimation of PM_{2.5} infiltration factors and personal exposure factors in two megacities, China. *Build. Environ.*, 149, 297–304.
- Liu, F., Chen, G. and Huo, W., 2019. Associations between long-term exposure to ambient air pollution and risk of type 2 diabetes mellitus: A systematic review and meta-analysis. *Environ. Pollut.* 252, 1235–1245.
- Orioli, R., Cremona, G., Ciancarella, L. and Solimini, A.G., 2018. Association between PM₁₀, PM_{2.5}, NO₂, O₃ and self-reported diabetes in Italy: A cross-sectional, ecological study. *PLoS ONE*, 13, e0191112.
- Rao, X., Montresor-Lopez, J., Puett, R., Rajagopalan, S., Brook, R.D., 2015. Ambient Air Pollution: An Emerging Risk Factor for Diabetes Mellitus. *Curr. Diab. Rep.*, 15, 33.
- Srivastava, S. 2021. Effects of environmental polycyclic aromatic hydrocarbon exposure and pro-inflammatory activity on Type 2 Diabetes Mellitus. *MedRxiv*. 10.08.21264766.
- Unnikrishnan, R., Pradeepa, R., Joshi, S.R. and Mohan, V., 2017. Type 2 Diabetes: Demystifying the Global Epidemic. *Diabetes*, 66, 1432–1442.
- World Health Organization (WHO), 2021. *WHO global air quality guidelines: particulate matter (PM_{2.5} and PM₁₀), ozone, nitrogen dioxide, sulfur dioxide and carbon monoxide: executive summary*. World Health Organization: Geneva, Switzerland.
- Wu, Y., Fu, R., Lei, C., Deng, Y., Lou, W., Wang, L., Zheng, Y., Deng, X., Yang, S., Wang, M., Zhai, Z., Zhu, Y., Xiang, D., Hu, J., Dai, Z., Gao, J., 2021. Estimates of Type 2 Diabetes Mellitus Burden Attributable to Particulate Matter Pollution and Its 30-Year Change Patterns: A Systematic Analysis of Data From the Global Burden of Disease Study 2019. *Front. Endocrinol.*, 12, 1–11.
- Yang, J., Zhou, M., Zhang, F., Yin, P., Wang, B., Guo, Y., Wang, H., Zhang Ch., Sun, Q., Song, X. and Liu, Q., 2020. Diabetes mortality burden attributable to short-term effect of PM₁₀ in China. *Environ. Sci. Pollut. Res.* 27, 18784–18792.
- Zheng, Y., Li, S., Zou, C., Ma, X. and Zhang, G., 2019. Analysis of PM_{2.5} concentrations in Heilongjiang Province associated with forest cover and other factors. *J. For. Res.*, 30, 269–276.



Reducing methane emissions at gas transmission networks. Best practices literature review and case studies.

A. Tsochatzidi¹ and N.A. Tsochatzidis²

¹Department of Chemical Engineering, Aristotle University of Thessaloniki, Greece

²Hellenic Gas Transmission System Operator (DESFA) SA, Greece

Corresponding author email: n.tsochatzidis@desfa.gr

ABSTRACT

Methane emissions reduction at natural gas transmission systems is studied. A literature survey on this topic is presented along with characteristic case studies. Such case studies reveal that a significant reduction of methane emissions at gas transmission systems may be achieved with application of best practices, resulting in a large impact on decarbonization and environmental protection efforts. Quantification of methane emissions reduction at the presented case studies may serve as quick reference for similar applications. The analysis aims to contribute in better understanding of methane emissions sources and the adoption of emissions reduction measures at gas transmission systems.

Keywords: methane emissions; gas network; greenhouse gases.

1. INTRODUCTION

Methane, the main component of natural gas, is one of the most important contributor to climate change and plays a dominating role in how fast the climate warms. Methane contributes to at least 25% of today's climate warming, and its concentration in the atmosphere continues to rise rapidly, in large part from anthropogenic sources (GMA, 2021). Over the past decade atmospheric concentrations of methane have been increasing much faster than previously, and in 2020 at the fastest rate since records began in the 1980s (Stern, 2022). Methane is a more potent greenhouse gas (GHG) than carbon dioxide, having a shorter atmospheric lifespan. Climate policies heavily emphasize actions that benefit the climate in the long-term such as decarbonization and reaching net-zero emissions (Ocko et al., 2021).

Gas transmission operators, worldwide, are carrying out intensive programs on the quantification of the total methane emissions in their activities and are designing mitigation measures for methane emissions reduction. Lechtenböhmer et al. (2007) reports that methane emissions from a long distance gas network (the Russian network) are approximately 0.6% of the natural gas delivered. Mitigating these emissions can not only earned carbon credits, but can also create new revenue streams for the operator in the form of reduced costs, increased gas throughput and sales.

This paper presents a literature survey on methane emissions reduction at transmission systems. Also, characteristic case studies from gas companies and from DESFA (www.desfa.gr), the Hellenic gas transmission system operator, are discussed. Methane emissions of each case study are quantified to serve as quick reference for similar applications.

2. RESULTS AND DISCUSSION

The Oil & Gas Methane Partnership 2.0 (OGMP, 2020) is a multi-stakeholder initiative launched by United Nations Environment Programme and the Climate and Clean Air Coalition, as a voluntary initiative to help companies reduce methane emissions in the oil and gas sector. This initiative is a comprehensive, measurement-based reporting framework that improves the accuracy and transparency of methane emissions reporting in the oil and gas sector. Through participation in the OGMP associated reporting, companies were provided with a credible mechanism to systematically and responsibly address their methane emissions, and to demonstrate this systematic approach and its results to stakeholders. DESFA has adhered to this partnership with 80 well known enterprises worldwide, of the oil & gas business (IMEO, Report 2021).



The methodologies for evaluating the methane emissions from the gas systems are based on statistic approaches using specific ‘activity factors’ (the emitting equipment population) and ‘emission factors’ (the frequency of emitting events). Lately direct measurements of methane emissions are used to increase confidence of estimation. Methane emissions are divided in three macro categories (Marcogaz, 2019):

- Fugitive emissions
- Vented emissions (including pneumatic emissions)
- Emissions from incomplete combustion (unburnt)

Sources of methane emissions for midstream and downstream gas segments (i.e. transmission networks, underground gas storages, LNG regasification terminals and distribution networks) are listed in the Table 1 (OGMP, 2020). The transmission segment of a natural gas system comprises the transmission pipeline networks, the compressor stations and the metering and pressure-regulating stations. Among the available methane emissions abatement technologies (Yusuf et al., 2012) are: leak detection and repair surveys, convert gas pneumatic controls to instrument air, re-injection of natural gas at maintenance and repair works, lower gas line pressure before maintenance, replace continuous gas vent, replace wet seals with dry seals in centrifugal compressors, use nitrogen instead of natural gas at seals of compressor units, replace gas operated safety block valves. Some of these abatement technologies to reduce methane emissions at transmission networks are discussed and quantified below.

Table 1. Sources of methane emissions for midstream and downstream Gas segments.

Type of emissions	Sources of methane emissions	
Fugitives	Leaks from components (loss of tightness)	
	Permeation	
Vented	Operational emissions	Purging & venting (maintenance, process, commissioning & decommissioning)
		Regular emission technical devices (pneumatic devices, gas analysers...)
		Starts & stops
	Incidents / emergency situations	
Incomplete combustion	Gas combustion devices (turbines, engines, boilers...)	
	Flaring	

2.1. Leak detection and repair (LDAR)

Leak detection and repair (LDAR) refers to the process of locating and repairing fugitive leaks. LDAR encompasses several techniques and equipment types (IR cameras, sniffers, etc.). According to Ravikumar et al. (2020) the total methane emissions reduced by 44% after one LDAR survey at natural gas facilities, combining a reduction in fugitive emissions of 22% and vented emissions by 47%. Furthermore, more than 90% of the leaks found in the initial survey were not emitting in the re-survey, suggesting high repair effectiveness. However, fugitive emissions reduced by only 22% because of new leaks that occurred between the surveys. This indicates a need for frequent, effective, and low-cost LDAR surveys to target new leaks.

2.2. Replace continuous gas Vent with nitrogen

Not neglecting the other methane emissions macro categories, the vented emissions have a significant part at the total and their mitigation measures have a direct and large impact. At large gas facilities emergency



vent lines are continuously purged with gas to prevent air introduction to the pipes. Nitrogen can be used instead of gas for this purging. Figure 1 depicts the vent stack of DESFA's Sidirokastros border metering station of a height 10 m, vent tip length 2 m and width 0,2 m. This vent stack has a design purge gas consumption 0,51 Nm³/h (Operation & Maintenance manual of DESFA's Sidirokastros station), which results to methane emissions of 3200 kg/y, a released methane quantity that can be avoided with the replacement of gas with nitrogen.

2.3. Replace gas with air at gas operated control valves

The gas consumption of a 24" ANSI 600 pressure / flow control valve, gas operated with spring opening piston actuator, is 1,3 m³/hr for the valve positioner at 7 barg supply. Also for the I/P converter the gas consumption is 0,16 m³/hr and for one complete stroke (open to close) of this valve the gas consumption is 0,038 m³. (Operation & Maintenance manual of DESFA's Sidirokastros station). When a continuous operation of this valve is considered, the maximum yearly methane emissions are estimated to 9200 kg/y, which can be avoided using instrument air instead of gas for the valve operation. Indeed, some years ago, DESFA replaced such gas operated valves at Sidirokastros border metering station with air operated valves (Figure 2) to reduce methane emissions.



Figure 1. Continuous Vent stack.



Figure 2. Air operated flow control valve.

2.4. Replace wet seals with dry seals at compressors

Compressors and compressor-related equipment are usually the largest methane emission sources at gas transmission systems (Zimmerle et al., 2015). Centrifugal compressors have seals along their shaft to keep gas from escaping. Wet, or oil-lubricated, seals by design result in substantial methane leakages. Dry seals operate mechanically without seal ring lubrication, which in its turn reduces gas leakage (Ishkov et al., 2011).

2.5. Optimize preventive maintenance program

To minimize Venting and to adopt best practices, DESFA reduced the frequency of the preventive internal inspection of the scraper traps along the gas transmission network from the initial frequency of six months to two years and recently to five years. Internal inspection requires depressurization and gas venting (Figure 3). This optimization of the maintenance plan reduced methane emissions for this specific maintenance operation by 90% as Table 2 indicates.

2.6 Re-injection of natural gas

At certain cases of maintenance or repair works at transmission networks a large section of a pipe must be depressurized. Instead of venting to the atmosphere, the gas contained in the section of pipe can be removed



to be reinjected it in a neighboring section with the help of mobile compressor unit (Methane Guiding Principles, 2020). Figure 4 illustrates such a process already followed by some gas transmission system operators (Report for the Madrid Forum, 2019).



Figure 3. Gas venting during depressurization of a scraper trap.

Table 2. Methane emissions reduction due to the optimization of scraper traps' maintenance plan.

Preventive maintenance frequency	Total Methane emissions (kg/y)	Methane emissions reduction (%)
6 months	120000	-
2 years	30000	75
5 years	12000	90

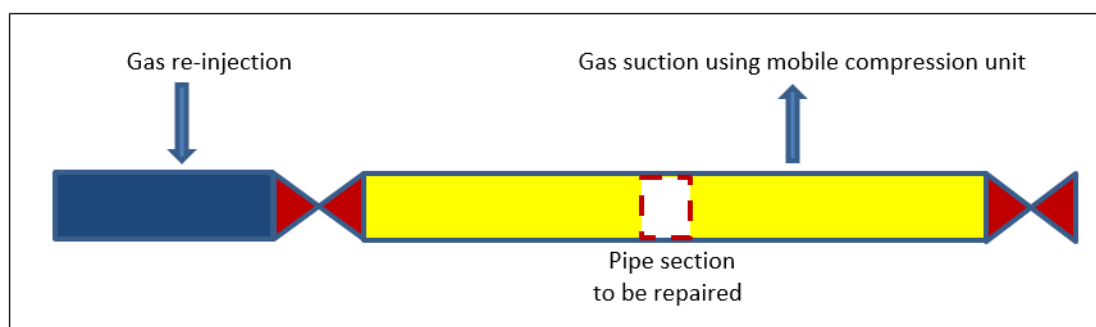


Figure 4. Re-injection of natural gas at large pipeline repair works.

3. CONCLUSIONS

Application of best practices may result in a significant reduction of methane emissions in a gas transmission system (Stern, 2022). A literature survey on this topic along with a number of case studies are presenting in this paper. Quantification of methane emissions reduction at the case studies offers a quick estimation for similar cases at gas networks. For example, the total methane emissions reduced by 44% after one LDAR



survey at natural gas facilities. Also, optimization of the maintenance plan reduced methane emissions from the operation of the gas network scraper traps inspection by 90%.

This analysis aims to contribute in better understanding of methane emissions sources and the adoption of methane emissions reduction measures at gas transmission systems.

REFERENCES

- Global Methane Assessment. Benefits and Costs of Mitigating Methane Emissions, 2021. *United Nations Environment Programme*, ISBN: 978-92-807-3854-4
- IMEO Report, 2021. An Eye on Methane, *International Methane Emissions Observatory, United Nations Environment Programme*, ISBN: 978-92-807-3893-3
- Ishkov, A. et al., 2011. Understanding methane emissions sources and viable mitigation measures in the natural gas transmission systems: Russian and U.S. experience, *International Gas Union Research Conference*, Oct. 2011
- Lechtenböhmer, S. et al., 2007. Tapping the leakages: Methane losses, mitigation options and policy issues for Russian long distance gas transmission pipelines, *International Journal of Greenhouse Gas Control*, 1, 4, 387-395.
- Marcogaz, 2019. WG_ME-485, Assessment of methane emissions for gas Transmission and Distribution system operators
- Methane Guiding Principles, 2020. Reducing Methane Emissions: Best Practice Guide Identification, Detection, Measurement and Quantification, September 2020, <https://methaneguidingprinciples.org/best-practice-guides/>
- Ocko, I.B. et al., 2021. Acting rapidly to deploy readily available methane mitigation measures by sector can immediately slow global warming, *Environ. Res. Lett.*, 16, 054042
- OGMP, 2020. Mineral Methane Initiative OGMP2.0 Framework, 19 November, 2020 https://www.eenews.net/assets/2020/11/23/document_ew_06.pdf.
- Ravikumar, A.P. et al., 2020. Repeated leak detection and repair surveys reduce methane emissions over scale of years, *Environ. Res. Lett.*, 15, 034029
- Report for the Madrid Forum, 2019. Potential ways the gas industry can contribute to the reduction of methane emissions, 5 - 6 June, https://ec.europa.eu/info/sites/default/files/gie-marcogaz_-_report_-_reduction_of_methane_emissions.pdf
- Stern, J.P., 2022. Measurement, reporting, and verification of methane emissions from natural gas and LNG trade: Creating transparent and credible frameworks, *OIES Paper: ET, No. 06, ISBN 978-1-78467-191-4*, The Oxford Institute for Energy Studies, Oxford.
- Yusuf, R.O. et al., 2012. Methane emission by sectors: A comprehensive review of emission sources and mitigation methods, *Renew. Sust. Energ. Rev.*, 16, 5059-5070
- Zimmerle, D.J. et al., 2015. Methane Emissions from the Natural Gas Transmission and Storage System in the United States, *Environ. Sci. Technol.*, 49, 9374–9383.



Effect of carbon concentration on the fatty acid distribution and basic FAME properties of the bio-oil of *Chlorella sorokiniana*

G. Papapolymerou¹, A. Mpesios¹, A. Kokkalis², D. Kasiteropoulou¹, M. N. Metsoviti¹ and A. Papadopoulou¹

¹Dept. of Environmental Studies, University of Thessaly, Gaiopolis, Larissa, T.K. 41500, Greece

²GRINCO S.A., Industrial Area of Larisa, Makrychori Larisas, TK 41303, Greece

Corresponding author email: papapoly@uth.gr

ABSTRACT

The heterotrophic cultivation of the microalgal species *Chlorella sorokiniana* using glycerol as the main organic carbon source and anaerobic digestate (AD) as the source of macro and micronutrients was studied. Five experiments were carried out simultaneously in five aerated 42 L orthogonal glass bioreactors in which the nitrogen initial concentration (No) was fixed at 110 mg/l while the initial carbon concentration (Co) was varied from 1.98 gr/l to 17.50 gr/l. 11% AD was added to four of the five bioreactors while, in one bioreactor (blank cultivation) no AD was added. The biomass yield as well as the lipid content and lipid productivity increased with Co while, the opposite was found for the protein content and protein productivity. Co also affects the distribution of fatty acids (FA) in the bio-oil extracted from the biomass both with respect to the chain length and the degree of saturation. Medium chain FA and monosaturated FA (MUFA) predominate in all treatments. As a result, the FAME properties, saponification number (SN), iodine value (IV), cetane number (CN) and higher heating value (HHV) are affected by the Co. However, for all five treatments, all four values are within the acceptable ranges.

Keywords: *Chlorella sorokiniana*; Heterotrophic; glycerol; anaerobic digestate; FAME properties.

1. INTRODUCTION

Microalgae are unicellular photosynthetic organisms that use light and carbon dioxide, with higher photosynthetic efficiency than plants, for the production of biomass. Some microalgae species can also grow and multiply heterotrophically in the absence of light if an organic carbon source becomes available (Mata et al., 2010). The main advantage of heterotrophic growth is higher biomass growth rates and biomass production because, unlike autotrophic growth, heterotrophic growth is not limited by light transmission through the growth medium. Another advantage of heterotrophic growth is the potential of achieving higher lipid content and, as a result, higher lipid productivities can be obtained. A number of review papers focus on the heterotrophic growth of several microalgal species and the trend is that heterotrophic growth enhances both the biomass and lipid productivity (Bumbak et al., 2011; Perez-Garcia & Bashan, 2015). In the heterotrophic growth, industrial by-products or waste streams containing dissolved organic carbon, macronutrients and micronutrients can be used in terms of nutrient recovery, waste minimization and cyclic economy. Anaerobic digestate (AD) is a rich source of macro and micronutrients while, crude glycerol has a very high content in organic carbon.

Anaerobic digestate (AD) produced by biogas plants is mainly used for field fertilization in various crops such as corn. When there are no adequate fields available or the land is not sufficiently flat, nitrification of underground and surface water and high soil salinity may result because excess anaerobic digestate is applied. Therefore, developing new applications for the efficient use of anaerobic digestate is needed in order to utilize the macro and micro nutrient content of the AD in the framework of circular economy. A good solution is the use of anaerobic digestate for microalgae cultivation since it is a good source of nitrogen, phosphorus and potassium, as well as a source of over 30 different micronutrients. Potassium and phosphorus availability is projected to decrease in the future.

A wide variety of organic carbon have been used for the heterotrophic growth of various microalgal species such as glucose, sucrose, fructose, mannose, glycerol, lactose or galactose (Perez-Garcia et al., 2011). Additionally, various industrial effluents and by-products, such as anaerobic digestate can be used as a carbon and nitrogen source. Studies on the heterotrophic cultivation of different microalgal species using glucose as carbon source have been published (Li et al., 2007; Xiong et al., 2008), while work on the cultivation of microalgae using glycerol is limited. It should be mentioned that studies on cultivation using industrial effluents and by-products, such as anaerobic digestate are lacking. The aim of this work is to examine the



effect of the initial concentration of organic carbon from glycerol on the carbon uptake rate, the lipid and protein content, the fatty acid distribution and basic FAME (Fatty Acid Methyl Ester) properties of the bio-oil of *Chlorella sorokiniana*. Glycerol is used as the main source of organic carbon and AD is used to provide some undigested organic carbon, macro and micronutrients.

2. MATERIALS AND METHODS

The cultivation of *C. sorokiniana* carried out in 42 L cylindrical glass bioreactors of 42 L filled to 75% of their volume. Air was continuously provided to each bioreactor through perforated steel tubing placed at the bottom of the bioreactors at a rate of about 40 L/(L-h). The bioreactors, the glass tubing and the culture medium were sterilized before use.

At the end of each experiment, and specifically at the stationary growth phase, the biomass was collected by centrifugation, it was rinsed with distilled water and was re-centrifuged. Finally, it was dried in an air circulation oven at 45 °C until constant weight. Prior to biochemical analysis and lipid extraction, the biomass was pulverized using a planetary ball mill at 180 rpm for 10 minutes (FRITSCH, Idar-Oberstein, Germany). The nutrient composition of the samples was determined according to AOAC methods (AOAC, 1995). Total nitrogen content in samples was measured with digestion using the Kjeldhal method (Rhee K.C., 20021). The total lipid content was determined with extraction using co-solvents of n-hexane/isopropanol in the microalgal biomass according to the Bian method (Bian et. al., 2018).

Extraction of the bio-oil was carried out in a horizontal extraction apparatus (tehnica ZELEZNIKI EV-402) at 300 rpm for 48 hours. A solvent mixture of n-hexane and isopropanol in a 3:2 ratio was used. The ratio of solvent to biomass was 10:1 (v/w). Following extraction, the biomass was filtered out and the solvent was evaporated. The bio-oil was subjected to transesterification and the fatty acid distribution was determined by gas chromatography. For this, 1 µl of the FAME (Fatty Acid Methyl Ester) phase was injected into an Agilent Gas Chromatographer Model 6890 N. Analysis of the FAME distribution was performed according to the EN 14103 method.

The saponification number (SN), the iodine value (IV) were calculated theoretically from the FA distribution using the equations suggested by Kalayasiri et al. (1996), validated by Azam et al. (2009). Similarly, the cetane number (CN) was evaluated from the theoretical equation suggested by Krisnangkura (1986) and the higher heating value (HHV) from the equation suggested by Demirbas (1998).

$$SN = 560 \sum_{i=1}^{i=n} \frac{\%W_i}{MW_i} \quad (1)$$

$$IV = 254 \sum_{i=1}^{i=n} \frac{N(\%W_i)}{MW_i} \quad (2)$$

$$CN = 46.3 + \left(\frac{5458}{SN} \right) - (0.225IV) \quad (3)$$

$$HHV = 49.43 - (0.041SN) - (0.015IV) \quad (4)$$

Where, %Wi is the % weight of each FA, N is the number of double bonds and MWi is the molecular weight of the respective FAME.

Table 1 shows the parameters of the five experiments that took place simultaneously in the 42 liter bioreactors.

Table 1. Variables of the experiments in the five bioreactors where the influence of the initial concentration of organic carbon was studied.

Bioreactor	% AD	No (mg/l)	Co (gr/l)	Co/No	T (±1°C)	pH (±0.3)
1	0	110	7.24	65.8	28	7
2	11	110	1.98	18.0	28	7
3	11	110	3.79	34.5	28	7
4	11	110	7.29	66.3	28	7
5	11	110	17.50	159.1	28	7

The microalgal species *Chlorella sorokiniana* (SAG strain 211-31) was obtained from Culture Collection of Algae from the University of Göttingen in Germany (EPSAG). Glycerol and AD were obtained from local biodiesel and biogas plants. AD was filtered, centrifuged and sterilized before use. The concentration of initial nitrogen was 110 mg/l in all five cultivations. The initial concentration of nitrogen was held constant in all bioreactors and the initial carbon concentration was varied from 1.98 g/l to 17.50 g/l. A cultivation without

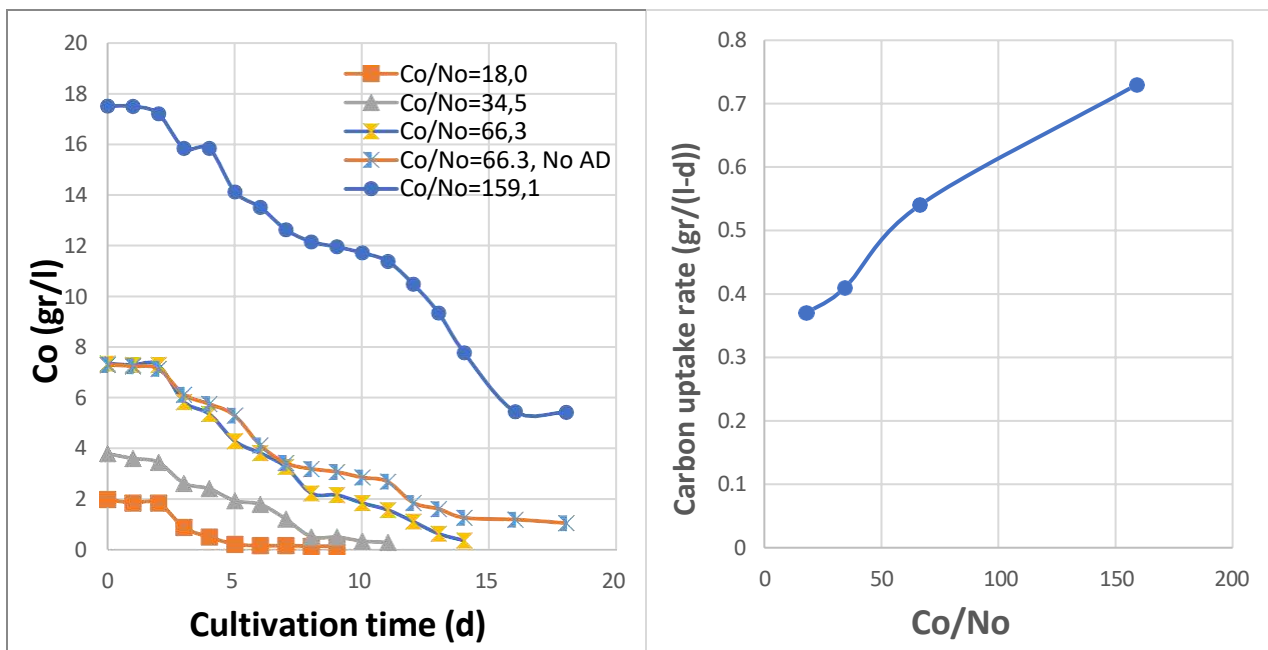


anaerobic digestate was carried out as a blank. The composition of the samples was determined according to AOAC methods. For the determination of organic carbon, the method of Walkley–Black was used. In this method, the sample is first centrifuged and then filtered. Organic carbon is then oxidized by a mixture of $K_2Cr_2O_7$ and H_2SO_4 in a ratio of 1:2. The remaining $K_2Cr_2O_7$ was titrated with 0.5 N $FeSO_4 \cdot 7H_2O$.

3. RESULTS AND DISCUSSION

3.1 Rate of Carbon uptake

Figures 1 and 2 show the rate of carbon reduction as a function of cultivation time and the rate of carbon uptake rate for the different initial carbon concentrations shown in table 1. The Co/No ratio varies from 18.0 to 159.1. The initial concentration of ammonium and the percentage of anaerobic digestate (except for the blank) were the same in all cultivations and equal to 110 mg/l and 11% respectively. It can be seen from figure 1a that cultivation time varies from about 5 days to more than 20 days. As the concentration of carbon increases so does the cultivation time. This affects the biomass productivity discussed in paragraph 3.2. However, unlike the cultivation time, the carbon uptake rate increases as the initial carbon concentration or the Co/No ratio increase. From a low 0.37 gr/(l-d) at Co/No=18.0 it increases to 0.73 gr/(l-d) at Co/No=159.1. For comparison, the rate of carbon uptake rate for the blank (without AD) cultivation for Co/No=65.8 (not shown in figure 2) is 0.47 gr/(l-d) lower by about 15% than the carbon uptake rate of similar Co/No=66.3 for the cultivation with 11% AD, which is 0.54 gr/(l-d). The anaerobic digestate (AD) is a very complex medium. It contains a great number of elements, basically all elements, as well as various organic compounds. Micronutrients present in the AD, such as cobalt, molybdenum and iron, may be affecting carbon uptake kinetics. Cobalt and molybdenum may also be affecting nitrogen uptake by the microalgal cells which the cells utilize for protein synthesis and cell growth and therefore indirectly may be involved in the carbon utilization process.



Figures 1 (left) and 2 (right). The rate of carbon reduction as a function of cultivation time and the rate of carbon uptake rate versus the Co/No ratio. Curves were drawn between data points for clarity.

3.2 Biomass, Lipid and Protein productivities

Table 2 gives the *Chlorella sorokinana* biomass yield in proteins and lipids and the productivity of biomass, proteins and lipids for the five treatments shown in table 1. As it is seen in table 2, the lipid percentage increases as the Co/No ratio increases. The reverse is true for the protein content. The biomass yield increases as No is increased however, the productivity initially increases for Co up to 3.79 gr/l but it levels off because of the increased time needed for the cultivation. Maximum lipid productivity is noted for an initial carbon concentration of 17.5 g/l.



Table 2 The content of the biomass in proteins and lipids and the biomass yield of *Chlorella sorokiniana*. The productivities in biomass (P_b), lipids (P_l) and proteins (P_p) are also shown.

Quantity	Initial Carbon Concentration (gr/l)				
	7.24*	1.98	3.79	7.29	17.50
Proteins %	28.5	36.6	32.9	26.1	19.1
Lipids %	33.9	20.8	25.8	33.2	39.7
Biomass yield (gr/l)	2.2	0.95	1.7	2.4	3.5
P_b (gr/(l-d))	0.15	0.16	0.21	0.22	0.22
P_l (mg/(l-d))	50.9	32.9	54.8	71.9	86.8
P_p (mg/(l-d))	42.8	58.6	69.1	57.4	42.0

* Blank, no anaerobic digestate added.

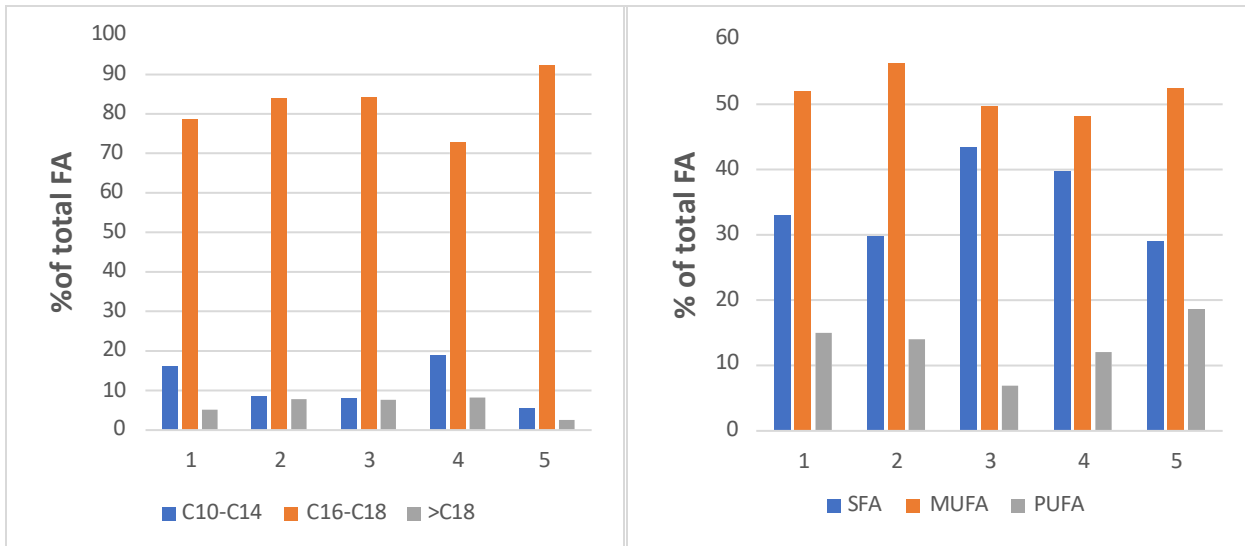
3.3 Fatty Acid distribution

Table 3 shows the distribution of methyl esters of the corresponding FAs of the biomass of *C. sorokiniana* cultivated with glycerol and biofertilizer for the four different initial carbon concentrations as well as the case where no biofertilizer was used (Table 1).

Table 3. The distribution of fatty acids for the five treatments of Table 1. In all five treatments the concentration of nitrogen (ammonia nitrogen) is equal to 110 g/L.

A/A	FATTY ACID	Co=7.24 gr/l (No AD)	Co=1.98 gr/l	Co=3.79 gr/l	Co=7.29 gr/l	Co=17.5 gr/l
		%	%	%	%	%
1	C10:0	1.31	0.12	0.71	7.86	0.20
2	C10:1	2.34	0.93	1.05	0.71	0.84
3	C12:0	2.89	1.15	2.17	1.71	1.16
4	C12:1	1.28	1.07	1.08	0.12	0.14
5	C14:0	3.70	2.76	2.11	3.52	1.29
6	C14:1	4.65	2.33	0.92	5.01	1.18
7	C14:2	-----	-----	-----	-----	0.55
8	C16:0	15.32	17.41	16.78	16.37	15.46
9	C16:1	12.37	9.68	4.81	8.57	7.44
10	C16:2	0.34	-----	0.63	0.61	0.41
11	C18:0	6.11	4.77	16.07	5.48	9.61
12	C18:1	29.94	37.93	39.73	30.43	41.60
13	C18:2	10.57	11.15	5.11	9.45	16.55
14	C18:3	4.06	2.87	1.19	1.98	1.04
15	C20:0	3.69	2.34	2.21	1.53	0.35
16	C20:1	1.43	1.86	0.72	3.32	1.03
17	C22:0	-----	0.31	-----	0.38	0.15
18	C22:1	-----	0.78	-----	-----	0.19
19	C24:0	-----	0.93	3.38	2.95	0.81
20	C24:1	-----	1.61	1.33	-----	-----

From table 3 we observe that the chain length ranges from C10: 0 to C24: 1. However, the fatty acids that are found in the highest percentage are C16: 0, C16: 1, C18: 0, C18: 1 and C18: 2. The ratio C18: 1 / C18: 2 ranges from about 2.5: 1 to 7.8: 1. In most vegetable oils and seed oils C18: 2 is higher than C18: 1 while in the microalgae *Chlorella sorokiniana* the opposite is observed. Figures 3 and 4 show the distribution of fatty acids in terms of chain length (short, medium and long chain fatty acids) and their degree of saturation (saturated, monounsaturated and polyunsaturated fatty acids) respectively.



Figures 3 (left) and 4. The distribution of fatty acids in terms of chain length C10-C14, C16-C18 & >C18) and their degree of saturation (SFA, MUFA & PUFA). The numbers 1 through 5 indicate the Co/No ratio = 65.8 (blank- no AD added), 18.0, 34.5, 66.3 and 159.1 respectively.

From Figure 3 it can be concluded that medium chain FAs are predominant and constitute from a minimum of 72.9% to a maximum of 92.1% of FA. Also, from Figure 4, the monounsaturated FAs predominate in all treatments and accounts for about 48% to 56% of total FA, while significant percentages of saturated FAs from about 29% to about 43%. % are produced.

3.4 Estimated FAME properties

Table 4 shows the SN (saponification number), IV (iodine value), CN (cetane number) and HHV (higher heating value) values of FAME, calculated from the data of Table 3 and equations 1-4. The values of the FAME properties in Table 4 can be explained based on the distribution of FA in relation to the chain length (figure 3) and the degree of saturation (figure 4). Increasing the degree of saturation leads to a decrease in the iodine value (IV). Also, increasing the average chain length, both the iodine value and the saponification number (SN) decrease and the cetane number (CN) increases. However, according to Equation 3, a decrease in SN has a more pronounced effect on CN than a decrease in IV.

Table 4. The FAME properties of the bio-oil obtained from the cultivation of *Chlorella sorokiniana* in relation to the Co/No ratio, for a constant initial nitrogen concentration of 110 mg/l (Table 1).

Property*	Co=7.24 gr/l (NO AD)	Co=1.98 gr/l	Co=3.79 gr/l	Co=7.29 gr/l	Co=17.5 gr/l
Saponification number (SN)	204.3	197.0	196.1	206.2	196.1
Iodine Value (IV)	77.6	76.5	56.9	65.8	79.4
Cetane Number (CN)	55.6	56.8	61.4	58.0	56.3
Upper Heating Value (HHV)	39.9	40.2	41.0	40.0	40.2

* Units: Iodine Value: g L/100 g FAME and HHV: MJ/kg.

The FAME values for all treatments are within acceptable limits. It is noted that low iodine values lead to higher cetane numbers due to the reduced ignition time, but very low IV, below 50-60 g l/100g FAME, cause poor flowing properties at low temperatures and this can lead to clogging of the fuel filters.

4. CONCLUSIONS

Glycerol is easily absorbed and utilized by *Chlorella sorokiniana*. The biomass yields as well as the lipid content increased with increasing Co. However, the biomass productivities increased only from 0.15 g/(L-d)



to 0.22 gr/(l-d) because longer cultivation times were needed as the Co increased. Lipid productivities increased from 32.9 mg/(l-d) to 86.8 mg/(l-d). The distribution of FA was predominant in monounsaturated and medium chain FA. The basic FAME properties were within acceptable limits. Cetane numbers were equal to 56.8, 61.4, 58.0 and 56.3 for Co values equal to 1.98, 3.79, 7.29 and 17.50 gr/l respectively while, for the cultivation where no anaerobic digestate was used with an initial carbon concentration equal to 7.24 gr/l the cetane number is equal to 55.6. The anaerobic digestate is a good source for the formulation of growth media for cultivating microalgae heterotrophically and possibly autotrophically. It provides macro and micronutrients and some carbon from undigested organic material thus, reducing the cost of the growth media for microalgal cultivation and also contributes to the recycling of important nutrients such as phosphorus and potassium. The bio-oil of *Chlorella sorokiniana* is thus appropriate for use in biodiesel production. However, lipid productivities need to be improved for a commercial application for biodiesel production. The remaining biomass can be utilized, for example, as a supplement to animal feed.

5. ACKNOWLEDGEMENTS

The study was co-financed by the European Regional Development Fund of the European Union and Greek national funds through the Operational Program Competitiveness, Entrepreneurship and Innovation, under the call RESEARCH – CREATE - INNOVATE (project code: T1EDK-01580).

REFERENCES

- Association of Official Analytical Chemists (AOAC), 1995. *Official Methods of Analysis of the Association of Official Analytical Chemists International*, 16th ed.; AOAC: Arlington, VA, USA.
- Azam, M. M., Waris, A. and Nahar, N. M., 2005. Prospects and potential of fatty acid methyl esters of some non-traditional seed oils for use as biodiesel in India. *Biomass Bioenergy*, 29, 293–302.
- Bian, X., Jin, W., Gu, Q., Zhou, X., Xi, Y., Tu, R., Han, S., Xie, G., Gao, S. and Wang, Q., 2018. Subcritical n-hexane/isopropanol extraction of lipid from wet microalgal pastes of *Scenedesmus obliquus*. *World Journal of Microbiology and Biotechnology*, 34 (3), 39.
- Bumbak, F., Cook, S., Zachleder, V., Hauser, S. and Kovar, K., 2011. Best practices in heterotrophic high-cell-density microalgal processes: achievements, potential and possible limitations. *Applied microbiology and biotechnology*, 91(1), 31-46.
- Demirbas, A., 1998. Fuel properties and calculation of higher heating values of vegetable oils. *Fuel*, 77, 1117–1120.
- Kalayasiri, P., Jayashoke, N. and Krisnangkura, K., 1996. Survey of seed oils for use as diesel fuels. *J. Am. Oil Chem. Soc.*, 73 (4), 471–474.
- Krisnangkura, K., 1986. A simple method for estimation of cetane index of vegetable oil methyl esters. *Journal of the American Oil Chemists' Society*, 63(4), 552-553.
- Li, X., Xu, H. and Wu, Q., 2007. Large-scale biodiesel production from microalga *Chlorella protothecoides* through heterotrophic cultivation in bioreactors. *Biotechnology and bioengineering*, 98(4), 764-771.
- Mata, T. M., Martins, A. A., Caetano, N. S., 2010. Microalgae for biodiesel production and other applications: a review. *Renewable and sustainable energy reviews*, 14(1), 217-232.
- Perez-Garcia, O., Escalante, F. M., De-Bashan, L. E., Bashan, Y., 2011. Heterotrophic cultures of microalgae: metabolism and potential products. *Water research*, 45(1), 11-36.
- Perez-Garcia, O. and Bashan, Y., 2015. Microalgal heterotrophic and mixotrophic culturing for bio-refining: from metabolic routes to techno-economics. *Algal biorefineries*, 61-131.
- Rhee, K. C., 2001. Determination of total nitrogen. *Current protocols in food analytical chemistry*, (1), B1-2.
- Xiong, W., Li, X., Xiang, J. and Wu, Q., 2008. High-density fermentation of microalga *Chlorella protothecoides* in bioreactor for microbio-diesel production. *Applied microbiology and biotechnology*, 78(1), 29-36.



Separation of the α -alumina layer from a spent Three-Way-Catalyst through *A. thiooxidans* as a pre-treatment to recover PGMs

M. Compagnone¹, J.J. González-Cortés^{1,2}, M.P. Yeste³, D. Cantero¹ and M. Ramírez¹

¹Department of Chemical Engineering and Food Technologies, Wine and Agrifood Research Institute (IVAGRO), Faculty of Sciences, University of Cadiz, Cadiz, Spain

²Department of Green Chemistry and Technology, Ghent University, Ghent, Belgium

³Department of Material Science, Metallurgical Engineering and Inorganic Chemistry, Institute of Research on Electron Microscopy and Materials (IMEYMAT), Faculty of Sciences, University of Cadiz, Spain

Corresponding author email: mariacristina.compagnone@uca.es

ABSTRACT

The acid bioleaching of Al by *Acidithiobacillus thiooxidans* was studied as an environmentally friendly pre-treatment to facilitate the extraction of platinum group metals from a spent three-way catalyst (TWC). The lixiviation ability of biogenic acid without bacteria and with bacteria in its exponential and stationary phase were compared using commercial H₂SO₄ as control. Tests were performed at pulp densities of 5%, 30% and 60% of milled TWC. Sulfur residues on the solid matrix enhanced microbial growth. Metal dissolution from the solid to the liquid phase triggered the spontaneous activation of survival mechanisms typical of the stationary phase resulting in the production of biological polymeric substances which were able to absorb traces of Al and Pt. The solution at 5% w/v of TWC with bacteria in the stationary phase reached an Al lixiviation rate of 57.1% whereas the bacteria in the exponential phase, abiotic acid and H₂SO₄ had Al lixiviation rates of 25.6%, 28.1% and 23.0%, respectively.

Keywords: bioleaching; *A. thiooxidans*; attachment; TWCs; PGMs.

1. INTRODUCTION

Platinum group metals (PGMs) are included in the list of Critical Raw Materials for the EU. The automotive industry represents the principal consumer of PGMs. Catalytic converters contain PGMs in a considerably higher concentration than the natural ores, thus they stand as the richest secondary source. The most common vehicle catalytic converters are the three-way catalysts (TWCs), honeycomb-type cordierite monoliths with a highly porous α -alumina wash-coat on the inner surface. The technologies to recover PGMs require various chemical, physical or mechanical pre-treatment steps that leach out the alumina support, converting the PGMs into more soluble species. The main disadvantages of this stage are the high temperatures and the consumption of hazardous gases and chemicals which cause the production of pollutant wastes. Recently, the bioleaching treatments have improved significantly, but they commonly still need pyro-metallurgical pre-reduction steps to reach significant results (Yakoumis et al., 2021). This study employs an environmentally friendly technique to separate the α -alumina layer from a TWC, preventing the use of hazardous and polluting chemicals. Furthermore, we monitored *A. thiooxidans* ability to grow despite the presence of spent TWC.

2. MATERIALS AND METHODS

2.1. Spent Three-Way Catalysts

A spent TWC was purchased from an Authorized Vehicle Treatment Center (Center “El Caimán”, Cádiz, Spain). Part of the three-way catalyst was pulverized using a cryogenic ball mill (MM400, Retsch GMBH, Germany). The catalyst composition was analyzed by XRF. The metal content (%w/w) of the spent catalyst was as follows: Al (22.5%), Pt (0.12%).

2.2. *Acidithiobacillus thiooxidans* growth

Acidithiobacillus thiooxidans DSM 11478 cultures were grown at a working volume of 100 mL in OK medium (Silverman and Lundgren, 1959) supplemented with commercially available sulfur powder (10 g/L) (Scharlab



S.L., Spain). The pH of the solution was adjusted to 2.5 with H₂SO₄ 96% (VWR International Eurolab S.L, Spain) using a pH probe (CRISON 5202, HACH Lange, S.L.U, Spain). Flasks were inoculated at 10% v/v with *A. thiooxidans* in the exponential phase. The inoculum was incubated in a rotary shaker (Comecta 2102, Selecta, Spain) at 150 rpm and 30 ± 1°C.

Bacterial growth was monitored by cell counting using a Neubauer Counting Chamber (Marienfeld Superior™, Germany) and an optical microscope (Olympus BH-2, Olympus Europa SE and Co. KG, Hamburg).

2.3. Use of commercial and biologically produced sulfur for acid production

The effect of the initial pH of the medium was studied with commercial sulfur powder and biologically produced sulfur (1% v/v) obtained from desulfurization bioreactors (González-Cortés et al., 2020).

The experiment was performed at three different starting pH values of 2.5, 5 and 7.5.

2.4. Acid solutions preparation

Flasks containing 200 mL of OK medium at pH 2.5 with 10% v/v of *A. thiooxidans* and 1% w/v of biogenic sulfur were incubated at 150 rpm and 30°C. Three different biogenic acids were obtained; (i) biogenic acid with bacteria in its exponential phase (pH 1.0), (ii) biogenic acid with bacteria in its stationary phase (pH 0.7) and (iii) bacteria-free biogenic acid (pH 0.55) (obtained by centrifugation at 1,610 x g for 10 min). Commercial H₂SO₄ (≥98%) was diluted to prepare an acid solution at a pH of 0.55 which was used as a control.

2.5. Leaching tests

TWC was treated with the 4 different acid solutions at 5%, 30% and 60% pulp densities for 14 days measuring the variation of pH and cell growth over time. The solutions were centrifuged at 1,610 x g for 10 min to separate the liquid from the solid phase. To monitor bacterial proliferation, each sample was diluted and vigorously agitated before cell counting to avoid bacterial immobilization due to cell adhesion to the catalyst. The content of Al in the liquid medium after treatment was measured with the analytical test kit 114825 Aluminum Test Method: photometric 0.020-1.20 mg/L Al Spectroquant® (Merck Millipore, Germany).

2.6. Scanning electron microscopy (SEM)

A FEI Quanta 200 electron microscope coupled to a qualitative energy disperse X-ray analyzer (EDX) was used to obtain SEM images and to identify the elemental composition of biological residues before and after treatment. The samples were fixed with glutaraldehyde and dehydrated by immersion in increasing concentrations of acetone solution (50–100%). Then, the fixed samples were dried with CO₂ to a critical point to remove the acetone and were metalized with gold (at 15 mA, 120 s, and a distance of 35 mm).

3. RESULTS

3.1. Evaluation of commercial and biologically produced sulfur for acid production

The potential benefits of using biogenic sulfur as an energy source were evaluated and compared to using commercial sulfur. Fig. 1 shows the pH variation under different initial pH values for 10 days.

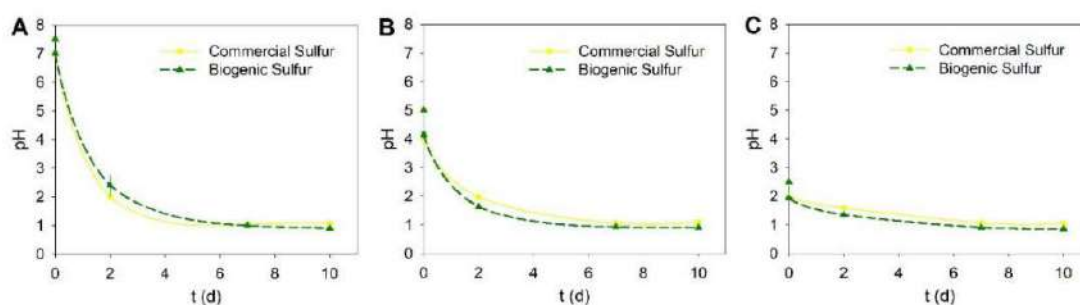


Figure 1. pH variation with commercial and biogenic sulfur under an initial pH of (A) 7.5, (B) 5 and (C) 2.5.



Both types of sulfur promoted strong acid production. All the solutions reached similar final values of pH, meaning that the initial pH of the solution does not affect the process of acid production.

Therefore, the use of biologically produced sulfur does not prejudice acid production. In fact, the bacteria with biogenic sulfur as a source of energy reached lower pH values compared to commercial sulfur highlighting that acid production is influenced by the nature of the elemental sulfur.

Sulfur globules produced by chemotrophic bacteria present a smaller and more hydrated form of S₈ rings/chains which make it hydrophilic and provide a lower density to its particles (Steudel and Eckert, 2003). Furthermore, biogenic sulfur is more bioavailable for microorganisms (Findlay et al., 2014). Thus, biogenic sulfur has a positive effect on bacteria and acid production.

3.2. Acid treatment and study of pH variation

To compare the ability of different acid solutions to leach the Al wash-coat, 4 pulp densities of TWC were treated with abiotic biogenic acid, H₂SO₄ and biogenic acid with bacteria in exponential and stationary phases (Fig. 2).

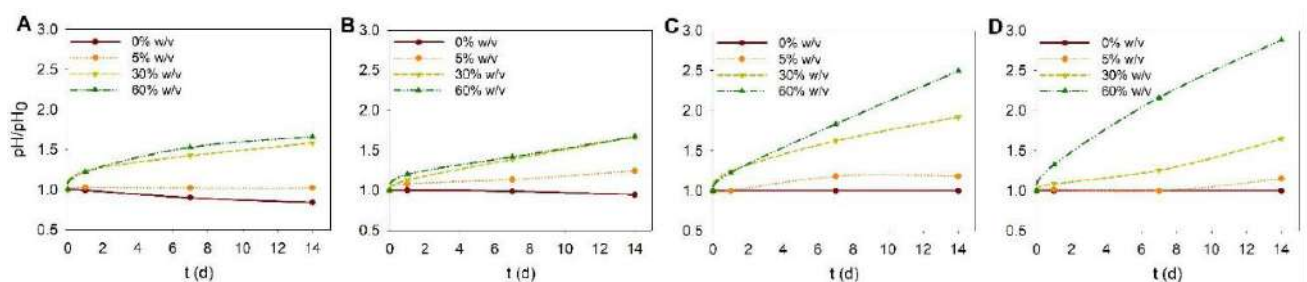


Figure 2. Normalized pH variation after treatment of different %w/v of TWC with (A) *A. thiooxidans* in its exponential phase; (B) *A. thiooxidans* in its stationary phase; (C) biogenic acid; (D) H₂SO₄.

The addition of TWC instantly changed the pH of the solutions due to the alkaline nature of the solid pulp. The higher pulp densities led to sharper pH increases as already reported by Mishra et al. (2007). During acid bioleaching or abiotic leaching processes, metal oxides are reduced to their lower valence states and are solubilized as metal sulfates resulting in the basification of the liquid solution. Thus, the pH increase was correlated to the consumption of acid which is in turn correlated to the leaching rate (Pathak et al., 2015).

Biogenic acid without bacteria and H₂SO₄ had lower values of pH throughout the whole experiment (Fig. 2A and 2B). The solutions with bacteria in the stationary phase presented very similar pH values to the bacteria-free acids despite the higher initial pH of the former (0.7) (Fig. 2C). On day 14 and with 60% pulp density, the samples reached a pH value of 2.37 resulting in a better ability to buffer the pH increase compared to the H₂SO₄. The acid solutions with bacteria in its exponential phase presented the highest values of pH for all the pulp densities tested (Fig. 2D). On day 14 and at 60% w/v, the solutions reached a pH value of 4.75 which was probably caused by the initial lower acid load. In Mikoda et al. (2020) greater extraction yields were correlated to lower values of pH. Although the bacteria-free acids report lower pH values, in Fig. 2C and 2D it can be observed that the biotic solutions, especially at 30% and 60% pulp density, better withstand the variation of pH over time compared to Fig. 2A and 2B. This response can be attributed to the metabolic activity of *A. thiooxidans* and to the unceasing acid production explained by the presence of residues of suspended sulfur, typical of spent TWCs (Wei et al., 2019).

3.3. *A. thiooxidans* growth rate in the presence of TWC

In order to gain insights into the effect of TWC on the *A. thiooxidans* growth, the cell concentration of the exponential and the stationary phase was monitored for 14 days under different pulp densities (Fig. 3A, 3B).

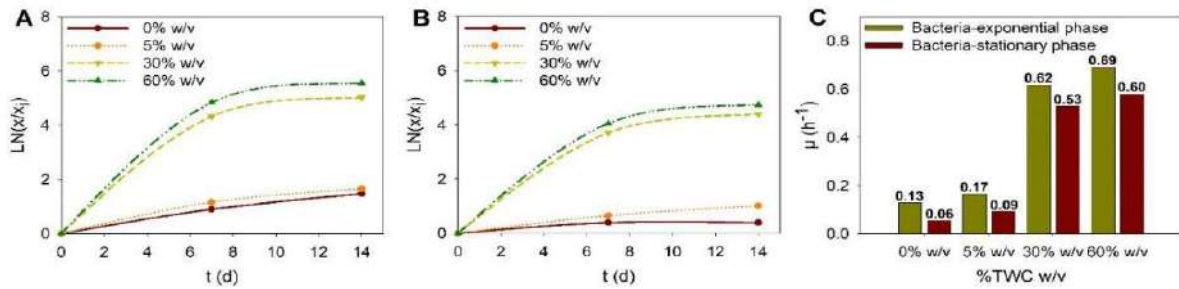


Figure 3. Bacterial growth under different % w/v of TWC. (A) *A. thiooxidans* in the exponential phase; (B) *A. thiooxidans* in the stationary phase. (C) Specific growth rate (μ) on day 7.

The cell number kept increasing over time for both solutions. It is worth mentioning that while on day 0 the bacteria and the TWC were separated and easily countable, after 24 h the images in the optical microscope exhibited that bacteria tended to attach to the TWC surface. Higher values of pulp density promoted cell growth and attraction between the cells and the TWC. On day 14, after approximately 2 minutes from the agitation, the free-living bacteria resulted completely attached to the TWC resulting in an apparent absence of cellular vitality. Fig. 3C shows the specific growth rates (μ) obtained at day 7 under different %TWC. In this way, higher pulp densities meant higher μ being the maximum specific growth rate (μ_{\max}) achieved at 60% pulp density by the bacteria at the exponential phase (0.69 h^{-1}). Therefore, the presence of TWC promoted an intensified metabolic response from *A. thiooxidans* resulting in an increased μ and cell attachment.

Seidel et al. (2001) report that the rate of leaching of Al from coal fly ash followed the rate of *A. thiooxidans* cell growth. Harneit et al. (2006) reported that strains of the genus *Acidithiobacillus* got attached to the surface of mineral coupons up to an 80% in 5 minutes from the inoculation. In that study, atomic force microscopy images revealed the presence of hardly detectable microcolonies and individual cells covered by self-produced extracellular polymeric substances (EPS). Furthermore, the EPS monolayer biofilm completely covered the entire mineral surface which mediated the cell adhesion to metal sulfide surfaces and the biofilm. Gehrke et al. (1998) reported that EPS has proven to be important for metal sulfide dissolution since the potential strongly increased with EPS-containing bacteria, thus EPSs are crucial for mineral extraction. Microbial proliferation and EPS production are most likely stimulated by sulfur residues generally present in a TWC, and its positively charged matrix surface (Kreve and dos Reis, 2021).

3.4. Separation of the α -alumina layer

The content of Al in the four leaching solutions after TWC treatment was measured to analyze the leaching percentage and hence quantify the separation of the α -alumina layer (Fig. 4).

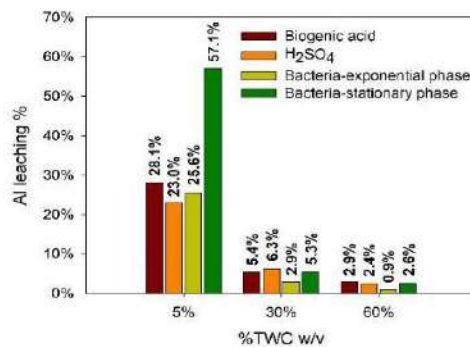


Figure 4. Percentage of Al dissolved in the acid solutions after treatment.

The highest Al lixiviation rate was achieved using biologically produced acid with the bacteria in its stationary phase with 5% w/v of TWC (57.1%). In general, lower pulp densities lead to higher leaching rates.



High solid values inhibit the bioleaching process because of the insufficient amount of liquid reactant compared to the solid pulp (Yakoumis et al., 2021). The decrease of the leaching yield with the increment of pulp density is very common in the bioleaching processes (Karim and Ting, 2021).

The solution with *A. thiooxidans* in the exponential phase was less effective than in the stationary phase, which could be a consequence of the reduced acid load of the former. However, the acid load cannot be the only influencing variable for the lixiviation process. If that were the case a lower lixiviation rate would have been generated compared to H₂SO₄ and biogenic acid which had a much lower pH.

Spontaneous activation of survival mechanisms is typical of the stationary phase. These mechanisms allow the bacteria to reprogram the gene expression pattern to adapt to different stresses (Jaishankar and Srivastava, 2017). These adaptive strategies imply physical and molecular changes that allow the cell to survive resonating with its morphology and the synthesis of EPS and proteins indispensable in nutrient-deprived conditions (Jefferson, 2004). This idea is compatible with the adhesion tendency observed in the microscopy images. The synergic action between lower pH values and *A. thiooxidans* action, as reported before (Nareshkumar et al., 2008; Sreekrishnan et al., 1995), can explain the higher extraction yield of Al in the biogenic acid solution containing *A. thiooxidans* in stationary phase.

3.5. Bacterial residues and metal biosorption

Aiming to detect potential morphological changes in *A. thiooxidans* and to establish the elemental composition of the bacteria in the stationary phase before and after treatment, an EDX analysis was performed. Fig. 5 shows the most representative images.

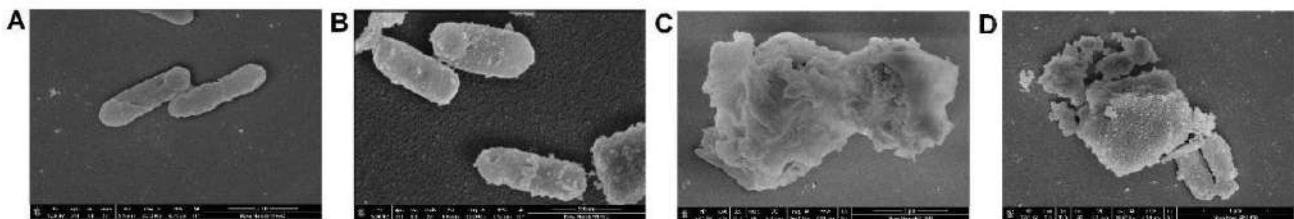


Figure 5. *A. thiooxidans* in stationary phase: (A) before treatment; (B-C) after treatment at 5% w/v TWC; (D) after treatment at 60% w/v TWC.

The cell membranes of the bacteria before the acid treatment (Fig. 5A) do not present a layer of seemingly biologically produced substances which can be noticed in cell membranes after the treatment (Fig. 5B and 5D). Globule-like structures were present within the biological residues either in the solution with 5% and 60% w/v of TWC (Fig. 5C and 5D). These aggregates are presumably single cells, pieces of cells, or agglomerates of cells covered by EPS. The analysis of the elemental composition of the biological residue solutions revealed that the globules composition included traces of Al and Pt. The globules of the former solution were composed of $12.79 \pm 11.28\%$ of Al and one also presented 0.25% of Pt. The globules of the latter solution were composed of $6.36 \pm 2.29\%$ of Al and $0.40 \pm 0.01\%$ of Pt. Additionally, the surface of one of the bacteria of the acid treatment at 60% pulp density (Fig. 5D) also had a composition of 0.38% of Pt.

Pal and Paul, (2008) state that while a large number of metals have been known to bind polysaccharides, the protein part of the EPS also plays an important role in the mechanism, providing the anionic properties of EPS. Furthermore, extracellular polymers surrounding the cells can chelate metals and link them to the cell surface (Jefferson, 2004). This extracellular complexation is nowadays used for metals biosorption as a bioremediation technique in soil or aquifer systems and some studies specifically contemplate the use of *A. thiooxidans* (Liu et al., 2003; Nguyen et al., 2016).

4. CONCLUSIONS

The acid solution with the bacteria in the stationary phase was the best buffer for the pH increase compared to the other acids during the bioleaching process of the Al wash-coat of a TWC through *A. thiooxidans*. The presence of a higher pulp density of TWC promoted bacterial proliferation. The bacteria tend to get attached



to the TWC and produce a biological matrix that absorbed both Al and Pt. The synergic action of using biogenic acid with a strong acid pH and the presence of living *A. thiooxidans* resulted in a higher extraction yield of metals compared to the other solutions and the inorganic acid control.

5. ACKNOWLEDGEMENTS

This work has been co-financed by the 2014-2020 ERDF Operational Programme and by the Department of Economy, Knowledge, Business and University of the Regional Government of Andalusia. Project reference: FEDER-UCA18-106138.

REFERENCES

- Findlay, A. J., Gartman, A., MacDonald, D. J., Hanson, T. E., Shaw, T. J. and Luther, G. W., 2014. Distribution and size fractionation of elemental sulfur in aqueous environments: The Chesapeake Bay and Mid-Atlantic Ridge. *Geochimica et Cosmochimica Acta*, 142, 334–348.
- Gehrke, T., Telegdi, J., Thierry, D. and Sand, W., 1998. Importance of Extracellular Polymeric Substances from *Thiobacillus ferrooxidans* for Bioleaching. *Applied and Environmental Microbiology*, 64(7), 2743–2747.
- González-Cortés, J. J., Torres-Herrera, S., Almenglo, F., Ramírez, M. and Cantero, D., 2020. Hydrogen sulfide removal from biogas and sulfur production by autotrophic denitrification in a gas-lift bioreactor. *ACS Sustainable Chemistry and Engineering*, 8(28), 10480–10489.
- Harneit, K., Göksel, A., Kock, D., Klock, J. H., Gehrke, T. and Sand, W., 2006. Adhesion to metal sulfide surfaces by cells of *Acidithiobacillus ferrooxidans*, *Acidithiobacillus thiooxidans* and *Leptospirillum ferrooxidans*. *Hydrometallurgy*, 83(1–4), 245–254.
- Jaishankar, J. and Srivastava, P., 2017. Molecular basis of stationary phase survival and applications. *Frontiers in Microbiology*, 8(OCT), 1–12.
- Jefferson, K. K., 2004. What drives bacteria to produce a biofilm? *FEMS Microbiology Letters*, 236(2), 163–173.
- Karim, S. and Ting, Y. P., 2021. Recycling pathways for platinum group metals from spent automotive catalyst: A review on conventional approaches and bio-processes. *Resources, Conservation and Recycling*, 170(April), 105588.
- Kreve, S. and dos Reis, A. C., 2021. Effect of surface properties of ceramic materials on bacterial adhesion: A systematic review. *Journal of Esthetic and Restorative Dentistry*, 34, 461–472.
- Liu, H.-L., Chen, B.-Y., Lan, Y.-W. and Cheng, Y.-C., 2003. Biosorption of Zn (II) and Cu (II) by the indigenous *Thiobacillus thiooxidans*. *Chemical Engineering Journal*, 97, 195–201.
- Mikoda, B., Potysz, A., Kucha, H. and Kmiecik, E., 2020. Vanadium removal from spent sulfuric acid plant catalyst using citric acid and *Acidithiobacillus thiooxidans*. *Archives of Civil and Mechanical Engineering*, 20:132.
- Mishra, D., Kim, D. J., Ralph, D. E., Ahn, J. G. and Rhee, Y. H., 2007. Bioleaching of vanadium rich spent refinery catalysts using sulfur oxidizing lithotrophs. *Hydrometallurgy*, 88(1–4), 202–209.
- Nareshkumar, R., Nagendran, R. and Parvathi, K., 2008. Bioleaching of heavy metals from contaminated soil using *Acidithiobacillus thiooxidans*: Effect of sulfur/soil ratio. *World Journal of Microbiology and Biotechnology*, 24(8), 1539–1546.
- Nguyen, T. A., Fu, C.-C. and Juang, R.-S., 2016. Biosorption and biodegradation of a sulfur dye in high-strength dyeing wastewater by *Acidithiobacillus thiooxidans*. *Journal of Environmental Management*, 182, 265–271.
- Pal, A. and Paul, A. K., 2008. Microbial extracellular polymeric substances: Central elements in heavy metal bioremediation. *Indian Journal of Microbiology*, 48(1), 49–64.
- Pathak, A., Srichandan, H. and Kim, D. J., 2015. Feasibility of bioleaching in removing metals (Al, Ni, V and Mo) from as received raw petroleum spent refinery catalyst: A comparative study on leaching yields, risk assessment code and reduced partition index. *Materials Transactions*, 56(8), 1278–1286.
- Seidel, A., Zimmels, Y. and Armon, R., 2001. Mechanism of bioleaching of coal fly ash by *Thiobacillus thiooxidans*. *Chemical Engineering Journal*, 83(2), 123–130.
- Silverman, M. P. and Lundgren, D. G., 1959. Studies on the chemoautotrophic iron bacterium *Ferrobacillus ferrooxidans*. An improved medium and a harvesting procedure for securing high cell yields. *Journal of Bacteriology*, 77(5), 642–647.
- Sreekrishnan, T. R., Tyagi, R. D., Blais, J. F., Meunier, N. and Campbell, P. G. C., 1995. Effect of sulfur concentration on sludge acidification during the SSDML process. *Water Research*, 30(11), 2728–2738.
- Studel, R. and Eckert, B., 2003. *Elemental Sulfur and Sulfur-Rich Compounds I*, Top.Curr. Chem. 230. Springer: Berlin, Heidelberg.
- Wei, X., Liu, C., Cao, H., Ning, P., Jin, W., Yang, Z., Wang, H. and Sun, Z., 2019. Understanding the features of PGMs in spent ternary automobile catalysts for development of cleaner recovery technology. *Journal of Cleaner Production*, 239, 118031.
- Yakoumis, I., Panou, M., Moschovi, A. M. and Panias, D., 2021. Recovery of platinum group metals from spent automotive catalysts: A review. *Cleaner Engineering and Technology*, 3, 100112.



Systematic and Cost Overview of Freeze Desalination utilizing Thermoacoustic Technology

U. Ali¹, H. Zhang¹ and I. Janajreh¹

¹Department of Mechanical Engineering, Khalifa University of Science and Technology, Abu Dhabi, UAE
Corresponding author email: isam.janajreh@ku.ac.ae

ABSTRACT

This paper investigates the deployment of freeze desalination (FD) coupled with thermoacoustic engine and refrigerator (TAE/R) to provide freshwater to small settlements in remote locations like small islands. It presents an economic feasibility assessment of deployment of waste energy to satisfy the freshwater requirements, as an alternative to using conventional techniques such as reverse osmosis (RO) and thermal distillation (TD) that are energy intensive. Different scenarios are presented comparing the economic feasibility of FD vs RO. The analysis is done based on the net present value (NPV), internal rate of return (IRR), selling price, and payback period using cashflow diagrams. Compared with the RO, FD powered by TAE/R turns out to be the most favorable option to produce freshwater from seawater for a small community on a far-off island due to high NPV and IRR, and low selling price and payback period.

Keywords: Freeze desalination; Thermoacoustic cooling; Energy conversion; Waste heat recovery.

1. INTRODUCTION

Clean drinkable water is the basic need of humanity, and life cannot be sustained without water (Ghaffour et al., 2019). World freshwater demand is on the rise, and it is predicted that 3.9 billion people in more than 75% of countries will live under water scarcity by 2050 (United Nations World Water Development Report, 2020). Seawater desalination industry accounts for 16,000 plants with near 95 million m³/day by 2019 (Jones et al., 2018). Reverse osmosis (RO) and thermal distillation (TD) are the dominant technologies due to technology maturity and reasonable cost. Still facing several challenges, i.e., large energy consumption, corrosion and membrane fouling, and inability of handling high concentrated saltwater. The specific energy consumption of a real-scale seawater RO plant is approximately 3.5–4.5 kWh/m³, including pre-treatment and posttreatment processes (Kim et al., 2019). However, this number is for large scale RO plants with output of 100,000 m³/day or higher. The small-scale single pass RO plants consume more energy /m³, usually 6 – 10 kWh/m³ (El Kadi et al., 2021). This paper looks into the deployment of freeze desalination (FD) unit powered by thermoacoustic technology to meet the freshwater demand of a small settlements in remote locations. FD can resolve the corrosion, being conducted at low temperature, only involves heat of fusion which is 1/7 of latent heat of evaporation, and can treat highly concentrated waste brine including those rejected by RO and TD plants (Khawaji et al., 2008). Himawan (2005) claimed a 60% energy saving if eutectic freezing crystallization is used for recovering ice from an industrial waste stream compared to evaporative crystallization. Using solar energy or industrial waste heat to operate thermoacoustic engine and refrigerator (TAE/R) decreases the cost of FD as thermoacoustic has no moving parts and is maintenance free with direct and tandem conversion (Ali et al., 2021). This direct and tightly coupled integration shall be recognized as complete green and environmentally safe technology. TAE/R can reach energy conversion efficiency equivalent to those attained via chemical to mechanical in the diesel engine. Remote areas pose a unique challenge for power production and delivery, as well as for the freshwater supply. Here we are considering an island with small population of 100 people, such as Pitcairn Islands. The mainland grid connection is unviable option, and the cost of a small power plant driven by gas or steam is economically not feasible. Also, the renewable energy like photovoltaic solar and wind are deemed not possible either economically or logistically. Therefore, the ultimate electric power option of such islands is via diesel engine powered generators and the freshwater is unsatisfied by rainwater or seasonal streams/ponds. Diesel engines usually operate at 35% efficiency and most of the energy of fuel is lost as heat. This waste energy can be recovered by operating tandem TAE/R to produce acoustic energy that is needed to generate the cooling required by



the FD. Here we propose a sustainable freshwater supply and perform an economic feasibility analysis of a coupled thermoacoustic-FD system. Six scenarios are presented based on the average daily consumption of freshwater per capita according to the world health organization (WHO), i.e., 50 L, and 100 L per day (World Health Organization, 2000). The analysis is done based on internal rate of return (IRR), net present value (NPV), breakeven, payback period, and cashflow diagrams.

2. MATERIALS AND METHODS

A small community of approximately 100 people inhabiting a distant island is considered. The energy requirement of this population is estimated for a year and for a daily basis. The life of the project is forecasted to be 20 years and the analysis is based on this assumption. To meet the energy demand, standalone diesel gensets are considered as the baseline to analyze the cost of electricity and freshwater production. The capital cost of diesel generators is neglected and only the running cost is considered assuming the island is already equipped with diesel generators. Table 1 shows the summary of electricity cost which will affect the cost of freshwater production. The energy demand is satisfied by using 10 Caterpillar diesel generators DE200 GC operating at 75% and 50% load (depending upon the energy requirement) and with a fuel consumption of 34.2 L/hr and 22.3 L/hr per engine, respectively (Caterpillar DE200 GC). The exhaust from the mentioned diesel genset is at a temperature of 491°C, whereas the onset temperature for thermoacoustic engine to produce acoustic wave can be as low as 29°C (Jin et al., 2017). The assumptions of this study are listed below.

2.1. Assumptions:

- A small population of roughly 100 persons is considered
- The island is already equipped with diesel generators as the source of energy, therefore capital expense of diesel generators is ignored
- The life of the project is forecasted to be 20 years
- Heat exchangers efficiency is assumed to be 80%
- The baseline electricity consumption of RO is considered as 8kWh/m³

Table 1. Electricity requirement and cost.

Annual Energy Requirement per Capita	4500 kWh (12.3 kWh/day) (US Energy Information Administration, 2020)
Number of people	100
Current nominal diesel price	\$1.36/L
Fuel consumption per generator	22.3 L/hr at 50% load, 34.2 L/hr at 75% load
Diesel Required per day for 10 generators	5352 L – 8208 L
Cost of diesel per day	\$7278.72 – \$11,162.88

2.2. Scenarios

The different scenarios considered in this study are presented in Table 2. The breakdown of scenarios is mainly done on the daily amount of water production (10 m³/day and 5 m³/day), the technology used (RO and FD), and the engine load (75% and 50%) as it affects the fuel consumption. The FD has higher CAPEX and OPEX than RO as pointed out by El Kadi and Janajreh (2017).

Table 2. Scenarios considered in this study.

Scenario	Water production (m ³ /day)	Technology	CAPEX (\$)	OPEX without fuel cost (\$/year)	Engine Load (%)	Required daily fuel (L)
1	10	RO	15,000	15,000	75	500
2	10	RO	15,000	15,000	50	396
3	10	FD + TAE/R	60,000	40,000	-	-
4	5	RO	15,000	15,000	75	259
5	5	RO	15,000	15,000	50	206
6	5	FD + TAE/R	60,000	25,000	-	-



2.3. Freeze desalination powered by thermoacoustic

The systematic design of TAE/R powering FD is rather direct and avoids the conversion to electricity to produce freshwater for remote islands. The module can be scaled up or down based on the available thermal energy source. The waste heat from the diesel engines is harnessed to drive the TAE/R module that provides the freezing conditions of the sea water (35g of NaCl/liter). As this cold temperature is secured, FD module reduces the brine temperature to trigger ice crystallization near its freezing point. The growing ice crystal automatically rejects the salt impurities. The crystalized ice is collected, washed, and melted to obtain lower salinity brine. This can be successively repeated 4 to 5 times to produce a potable grade freshwater (Zhang et al., 2021). The holistic design is shown in Figure 1. The amount of freshwater that can be desalinated using the waste heat from the diesel generators is summarized in Table 3. The efficiency of the heat exchangers connecting TAE to diesel engine exhaust and TAR to FD setup is assumed to be 80% (Swift, 2017). The efficiency of TAE is taken as 25% and the coefficient of performance (COP) of TAR is taken as 1.5 (Swift, 2017). From Table 3 it can be seen that the potential freshwater generation from engine waste heat is more than the required ($> 10 \text{ m}^3/\text{day}$). Therefore, the proposed system has a good potential for deployment in remote islands. The economical details are discussed in the next section.

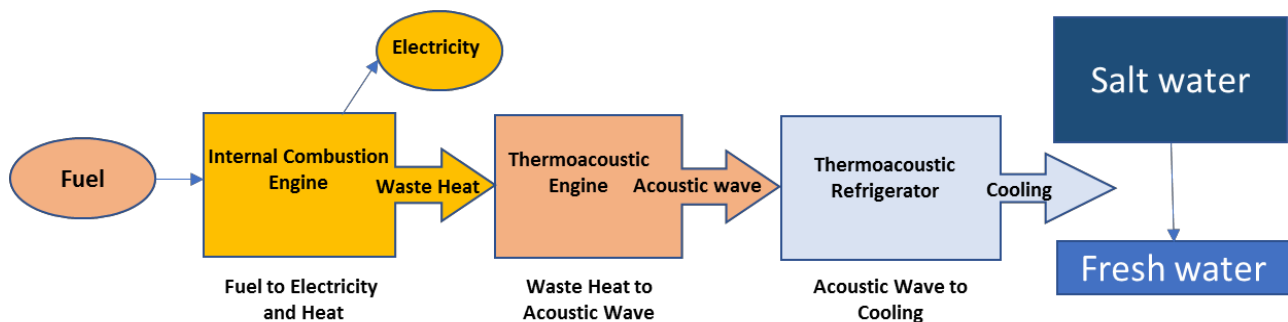


Figure 1. Freeze desalination system integrated to the TAE/R and Diesel Engine.

Table 3. Amount of water produced using FD powered by waste heat utilizing TAE/R.

Heat rejected by 1 generator / day	140.3 kW (Caterpillar DE200 GC)
Total heat rejected by 10 generators / day	1403 kW = $121 \times 10^9 \text{ J}$
Heat available to TAE	$96.8 \times 10^9 \text{ J}$ (80% heat exchanger efficiency)
Conversion of heat to acoustic work in TAE	$24.2 \times 10^9 \text{ J}$ (25% conversion efficiency)
Heat removed by TAR using acoustic wave	$36.3 \times 10^9 \text{ J}$ (COP = 1.5)
Heat absorbed by the TAE/R	$29.04 \times 10^9 \text{ J}$ (80% heat exchanger efficiency)
Heat absorption required to produce 1 L of water	$2.74 \times 10^6 \text{ J/L}$
Total volume of water produced /day	10,600 L

2.4. . Economic analysis

The economic study for all the scenarios was carried out by calculating their Net Present Value (NPV), Internal Rate of Return (IRR), and Payback Period. The discount rate was selected as 5% to calculate NPV. The economic analysis was done by taking into account two types of costs, i.e., the CAPEX and the OPEX. The CAPEX includes all the capital, initial or one-time costs. The OPEX comprises of all the costs that are incurred repeatedly (annually) which include the operational costs, maintenance, raw materials, labor, insurance, and inflation. In each case the NPV, payback period, IRR, and selling price were calculated and analyzed. The NPV was calculated according to the following equation considering a lifetime of 20 years for the project.



$$NPV = \sum_{t=1}^n \frac{R_t}{(1+i)^t}$$

where R_t is the net cash inflow-outflow during time t , n is the lifetime set as 20 years, and i is the discount rate which is set as 5% in this analysis.

The NPV is the difference of the present values of the inflows and outflows of cash over a period of time. It gives the idea whether the project will be profitable after a certain period of time. A project with larger NPV is more feasible than a project with smaller NPV. When NPV is set equal to zero during the analysis, then i corresponds to the internal rate of return (IRR), which is the rate of growth a project is expected to generate. Generally, the project is more suitable to pursue at a higher internal rate of return.

3. RESULTS

The results of the economic analysis are presented in Figure 2 and Figure 3. The net worth of the project on a year-by-year basis is depicted in Figure 2. Initially the net worth is negative for all scenarios due to the CAPEX. As the projects run, they create revenue decreasing the negative net worth and eventually reaching breakeven. The time period after reaching breakeven is the time where the project starts to make profit and the net worth enters positive values. The behavior of these diagrams depends on the CAPEX and OPEX given in Table 2, and the selling price of freshwater shown in Figure 3. It must be noted that the selling price is set different for each scenario in order to reach breakeven within the life of the project (20 years).

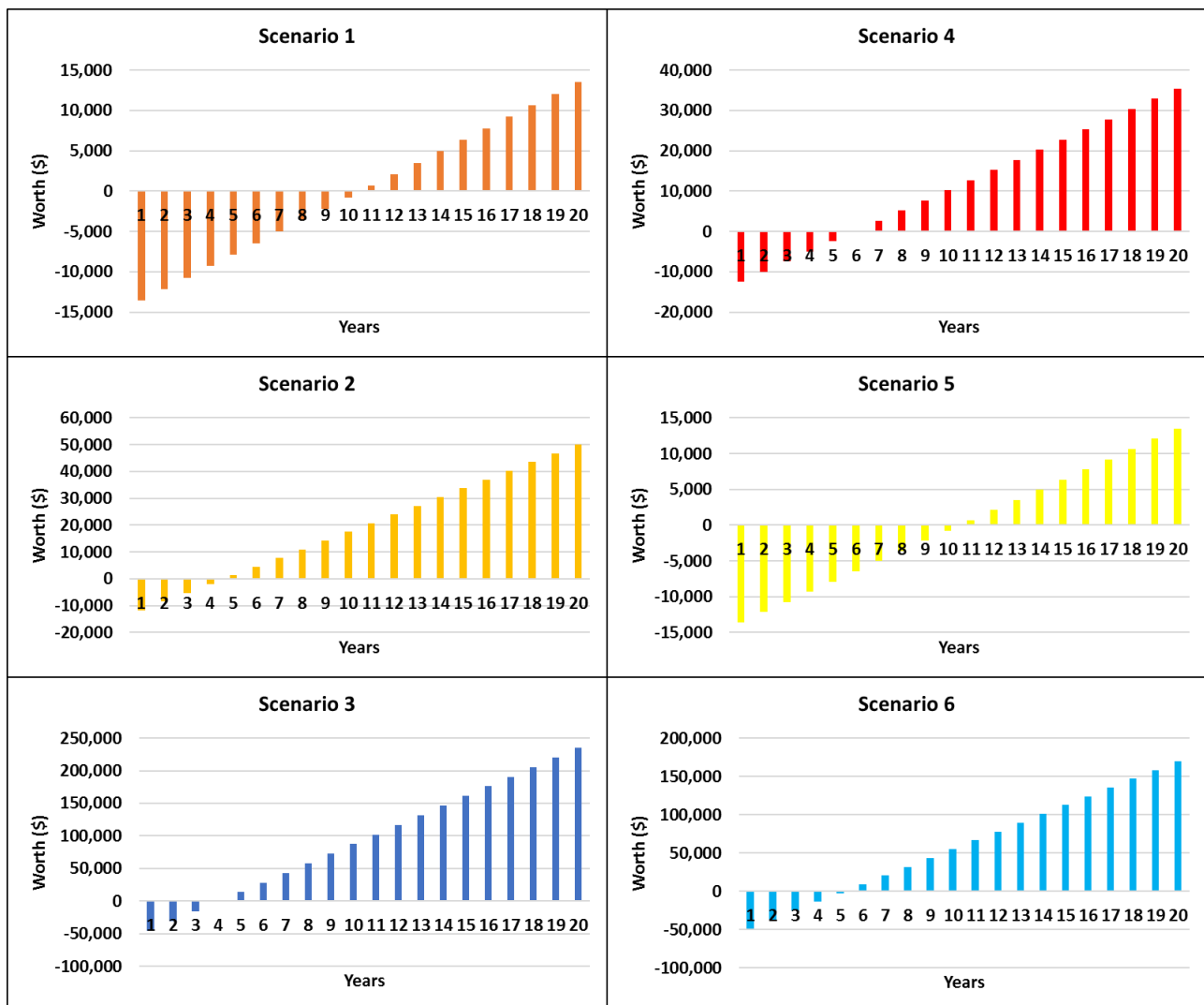


Figure 2. Cashflow diagrams for all the scenarios.



The other economic parameters (NPV, payback period, and IRR) are also shown in Figure 3. The NPV of cases 1, 2, 3, and 5 is low due to the fuel cost as RO plant is directly powered by diesel generators in these scenarios. This also leads to their low IRR and high selling price. The NPV for scenarios with FD (3 and 6) have higher NPV despite higher CAPEX and OPEX. NPV is supposed to decrease with increase in OPEX, but this is true only if the revenues generated by different scenarios are identical, which is not the case in this study as we are not considering equal selling price in the different scenarios. The selling price turns out to be the deciding factor in these scenarios as high price would not be feasible for consumers. The scenarios with RO have high selling price of freshwater due to the dependency on diesel fuel to operate RO plant. Usually, large scale production favors reduction of freshwater prices but this is not the case in this study as the RO plant is entirely fuel-dependent, leading to higher price with high production volume.

The selling price of scenarios with FD (3 and 6) are much lower than scenarios with RO, and these are much attractive options as they are most viable for the end consumers. Considering NPV, IRR, payback period, and selling price, scenarios 3 and 6 are the most economically feasible options, although they have high CAPEX and OPEX. However, it should be noted that FD+TAE/R requires large spaces to accommodate the necessary setup components.

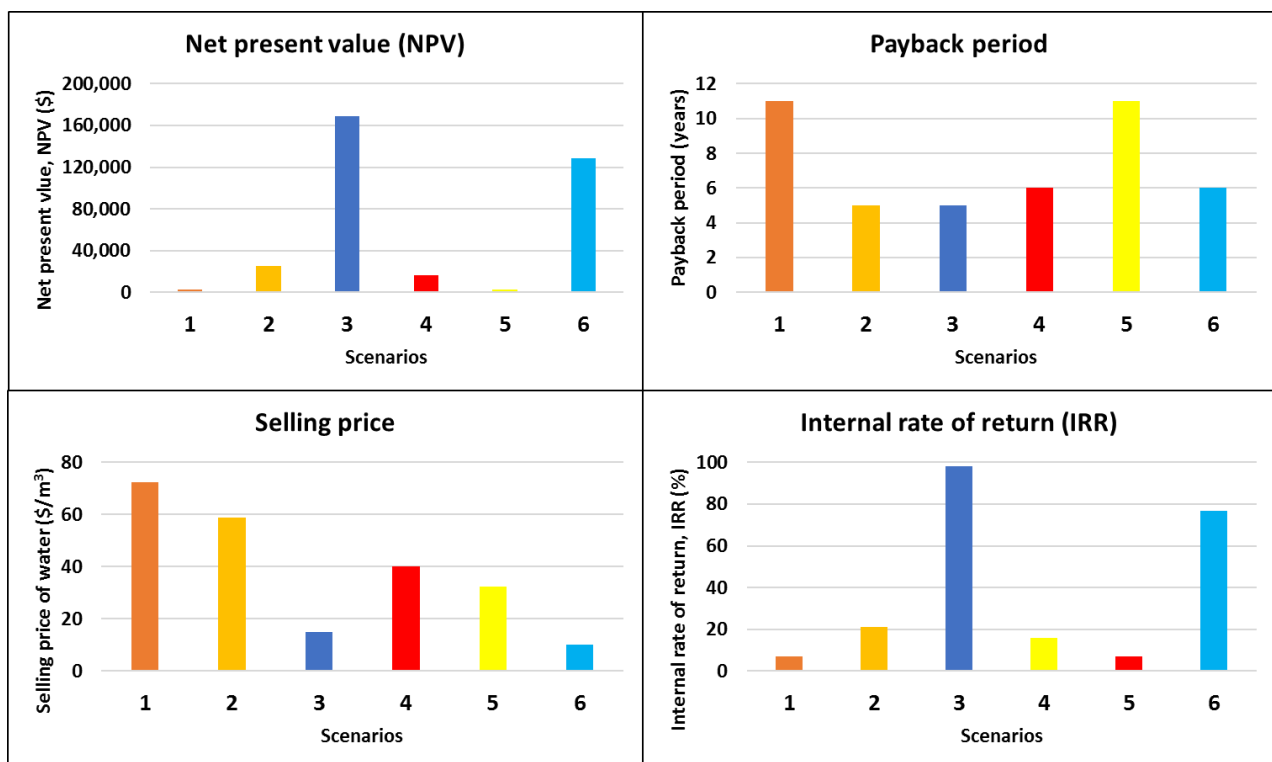


Figure 3. Economic analysis of the scenarios considered in this study.

4. CONCLUSIONS

This study was done to highlight the economic advantages of FD coupled with TAE/R operating on waste engine heat, in comparison to RO operating on diesel engines directly. Different scenarios were presented based on the daily production of freshwater and fuel consumption. The analysis was done in terms of NPV, IRR, selling price, and payback period for each scenario. The life span of the project was set as 20 years and the discount rate as 5% to evaluate the NPV. The results revealed that FD coupled with TAE/R is the most economically feasible option for remote islands to meet the freshwater supply. The FD despite its high CAPEX and OPEX turned out to be the best solution as indicated by high NPV and IRR, and low selling price which is of most concern to the end consumers.



REFERENCES

- Ali, U., Abedrabbo, S., Islam, M. and Janajreh, I., 2021. Numerical Simulation Of Thermoacoustic Refrigerator Coupled With Thermoacoustic Engine. *15th International Conference On Heat Transfer, Fluid Mechanics And Thermodynamics (HEFAT)*.
- Caterpillar DE200 GC. https://www.cat.com/en_US/products/new/power-systems/electric-power/diesel-generator-sets/107851.html
- El Kadi, K. and Janajreh, I., 2019. Desalination by Freeze Crystallization: An Overview. *International Journal of Thermal and Environmental Engineering*, 15(2).
- El Kadi, K., Adeyemi, I. and Janajreh, I., 2021. Application of directional freezing for seawater desalination: Parametric analysis using experimental and computational methods. *Desalination*, 520, 115339.
- Ghaffour, N., Soukane, S., Lee, J.-G., Kim, Y. and Alpatova, A., 2019. Membrane distillation hybrids for water production and energy efficiency enhancement: A critical review. *Applied Energy*, 254, 113698.
- Himawan, C., 2005. Characterization and Population Balance Modelling of Eutectic Freeze Crystallization. *Institutional Repository*, TU Delft.
- Jin, T., Yang, R., Wang, Y., Feng, Y. and Tang, K., 2017. Low temperature difference thermoacoustic prime mover with asymmetric multi-stage loop configuration. *Scientific Reports*, 7(1), 7665.
- Jones, E., Qadir, M., van Vliet, M. T. H., Smakhtin, V. and Kang, S., 2019. The state of desalination and brine production: A global outlook. *Science of The Total Environment*, 657, 1343–1356.
- Khawaji, A. D., Kutubkhanah, I. K. and Wie, J.-M., 2008. Advances in seawater desalination technologies. *Desalination*, 221(1–3), 47–69.
- Swift, G. W. (2017). *Thermoacoustics*. Springer International Publishing.
- United Nations World Water Development Report, 2020. *water and climate change*, vol. 1. UNESCO publishing, 2020.
- US Energy Information Administration, 2020. <https://www.eia.gov/todayinenergy/detail.php?id=49036>
- World Health Organization/United Nations International Children's Emergency Fund. WHO/UNICEF Joint Monitoring Program for Water Supply and Sanitation; Global Water Supply and Sanitation Assessment, 2000. Report; WHO/UNICEF: Washington, DC, USA.
- Zhang, H., Janajreh, I., Hassan Ali, M. I. and Askar, K., 2021. Freezing desalination: Heat and mass validated modeling and experimental parametric analyses. *Case Studies in Thermal Engineering*, 26, 101189.



Environmental monitoring of the Balos lagoon in Western Crete for sustainable tourism development

M. Lilli¹, G. Skiniti², N. Nikolaidis¹ and T. Tsoutsos²

¹Laboratory of Hydrogeochemical Engineering and Remediation of Soil, School of Chemical and Environmental Engineering, Technical University of Crete, Chania, Greece

²Renewable and Sustainable Energy Systems Laboratory, School of Chemical and Environmental Engineering, Technical University of Crete, Chania, Greece

Corresponding author email: gskiniti@tuc.gr

ABSTRACT

Balos lagoon, a Natura 2000 area located in Western Crete, is currently facing environmental degradation issues rooted mostly in the increasing phenomenon of overtourism. CROSS-COASTAL-NET initiative, Development of a Cross-Border Network for the Promotion of Sustainable Coastal Tourism, which is underneath the Interreg Greece–Cyprus program, investigates Balos in order to address this issue. Thus, aiming to identify the human pressure on the area, environmental monitoring of quality status was required as one parameter of addressing the region's carrying capacity, to design appropriate strategies for the region's sustainable development. The examination was conducted during 2 seasons, based on a sample technique to: a) determine the indicators that define the lagoon's environmental status, and b) propose management strategies that will contribute to its long-term tourism development. The only indicator important to take into consideration is the existence of large amounts of tar balls or residues. Further studies are required to identify the origin of the tar residues in the Balos lagoon in order to find solutions to address it.

Keywords: environmental monitoring; environmental quality; physicochemical characterization; indicators; sustainable development; sustainable tourism; carrying capacity.

1. INTRODUCTION

Balos lagoon is a famous, high tourism-attracted beach and even though it is meant to be protected under the Natura 2000 initiative, it is recently facing environmental degradation issues rooted mostly in these high intense touristic activities (Figure 1) (Skiniti et al., 2022). Therefore, aiming to identify the human pressure on the area, the environmental monitoring of quality status as one parameter of addressing the region's carrying capacity was necessary, in order to achieve the creation of a strategy based on the region's sustainable development (Skiniti et al., 2022). The analysis was based on a sampling protocol in order to: a) determine the indicators that identify the environmental status of the lagoon, and b) propose ways of management that will contribute to its sustainable tourism development.

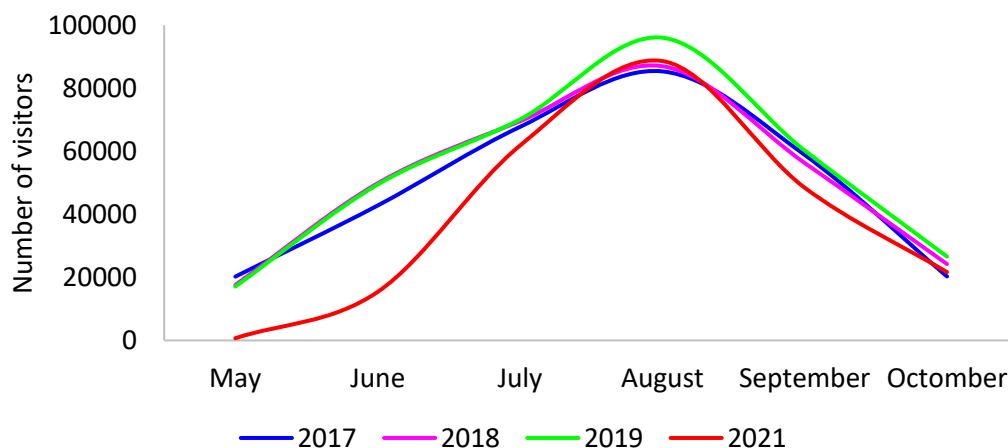


Figure 1. Tourists' flows during the years 2017, 2018, 2019 and 2021.¹



2. MATERIALS AND METHODS

A total of ten samplings were conducted (June, July, August, September, October 2021 and May, June, July, August, September 2022) in the Balos lagoon. In each sampling, two composite samples were taken from the seawater, two from the sediment and two from the sand. The sampling was designed to be taken place in two cross-sections (Figure 2) located in the lagoon area where it is more touristic (between umbrellas and bathers). A total of 60 samples were analyzed in relation to hydrocarbons (TPH), physicochemical parameters, heavy metals, microbiological parameters, microplastics etc.

As a sampling unit for sand and sediment samples, a 40 × 40 cm frame was used, deployed in each transect. This frame was inserted 5 cm into the substrate of each sampling unit. A sample of approximately 500g is taken from this frame for all analyses except the microplastics analysis. Specifically for microplastics, all sand/sediment of the frame is taken, placed in a metal container with water, from where by floating, the lightest pieces are obtained. Then, with the help of sieves (2 mm and 53 μm), these pieces are separated. For seawater sampling, 1 L of water is taken for all analyses except microplastics analysis. Specifically for microplastics, 50 L of seawater is passed through sieves (2 mm and 53 μm), and the corresponding samples are taken.

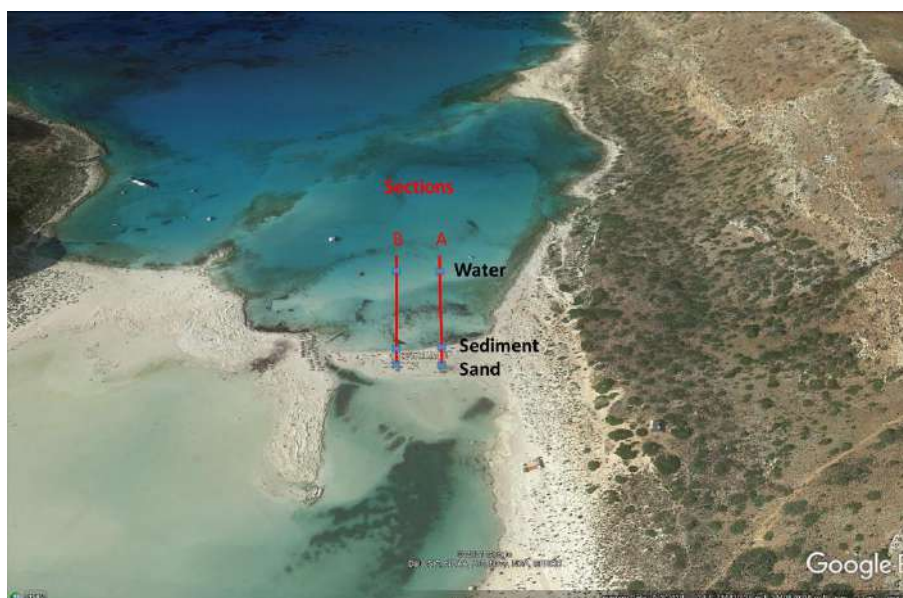


Figure 2. Sampling design. Cross-sections (A and B) used for sand, sediment and seawater sampling.

The laboratory analyses were conducted in the "Hydrogeochemical Engineering and Remediation of Soils" laboratory of the Technical University of Crete and included the determination of the concentration of nitrate, sulfate, phosphate and ammonia ions using spectrophotometry (HACH - DR 2800). Total organic carbon (TOC) was also determined by the method of thermocatalytic oxidation using appropriate equipment (multi N / C[®] 2100S Analyzer, AnalyticJena). The determination of the total metal concentration (B, Na, Mg, Al, Si, K, Ca, Cr, Mn, Fe, Co, Ni, Cu, Zn, As, Cd, Ba, Hg, Pb) of the samples was performed by Inductively coupled plasma mass spectrometry (ICP-MS, 7500cx, Agilent Technologies). The microbiological test for the presence of E. Coli was done by culturing sea water samples or leachates (sand-sediment) in a special nutrient (Hicrome E. Coli Agar) at 37°C. Respectively, enterococci (Slanetz & Bartley Medium, Membrane Enterococcus Agar) and total coliforms (Membrane Lauryl Sulfate Broth & Agar) are cultured. The detection of total petroleum hydrocarbons (TPH) was performed by gas chromatography (GC-FID, Shimatzu) of pentane extracts of the samples, according to the procedure described in method EPA 8015C. Finally, the microplastics were separated by hand using forceps. Each subcategory was then counted and weighed.

¹ 2020 was not included, as because of Covid-19 touristic activities were not representative.



3. RESULTS AND DISCUSSION

The results of the physicochemical characterization (Table 1) of the samples show that the values are typical of coastline. Co, As, Cd, Cs, Hg and U were measured below detection for all of the seawater, sand and sediment samples taken in the different samplings.

Table 1. Range of physicochemical characteristics of the data. The results are referred to both cross-sections.

Type of sample	pH	DO	N-NO ₃	P-PO ₄	TPH	TOC	SO ₄
Sea water	6.6-8.04	9.95 mg/L	2.7 mg/L	<0.01 mg/L	<DL	51-235 mg/L	2977-4522 mg/L
Sand	-	-	8.38 mg/kg	<0.01 – 0.18 mg/kg	<DL	2,9-4,4 g/kg	53-2065 mg/kg
Sediment	-	-	14.28 mg/kg	<0.01 – 0.24 mg/kg	<DL	2,2-4,1 g/kg	1050 -1611 mg/kg

Table 2 presents the density of plastic fragments and pellets calculated in different samplings. The results showed that in sand samples per sampling were found on average 19 n/m² and 15 n/m² of microplastics of >2mm and >53µm size, respectively. In sediment samples were found on average 5 n/m² and 9 n/m² of microplastics of >2mm and >53µm size, respectively, and in seawater samples 0.004 and 0.014 n/L of microplastics of >2mm and >53µm size, respectively. These results are compatible with the literature. Samplings in greek beaches of the Aegean island revealed microplastics (2–4 mm) densities in the top 3 cm of the subsurface ranging between 10 and 602 items/m² (Kaberi et al., 2013; Karkanorachaki et al., 2018).

Table 2. Abundance of microplastics in sand, sediment and sea water samples (results are referred to both cross sections)

Type of sample	Units	>2mm		>53µm	
		Range	Mean	Range	Mean
Sand	n/m ²	0-53	19	0-47	15
Sediment	n/m ²	0-20	5	0-27	9
Sea water	n/L	0-0.02	0.004	0-0.06	0.014

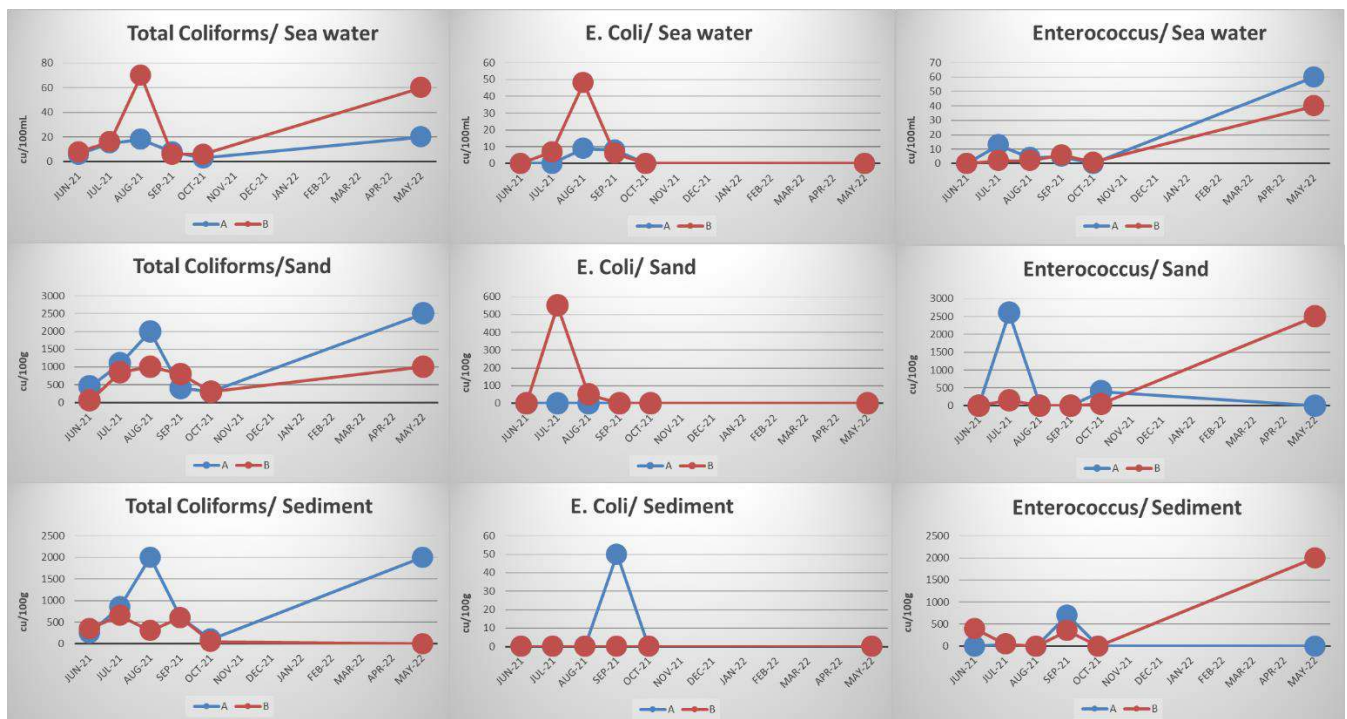


Figure 3. Temporal variability of total coliforms, Escherichia coli and enterococcus in seawater, sand and sediment samples.



Table 3. European and greek recommendations for bathing water quality. Units refer to cu/100mL.

Parameter	Water Directive 2006/7/EC			Greek guidelines	
	'excellent' classification	'good' classification	'sufficient' classification	recommended value	maximum value
Enterococcus	100	200	185	100	-
E. Coli	250	500	500	-	-
Total coliforms	-	-	-	500	10000
Fecal coliforms	-	-	-	100	500

Figure 3 presents the temporal variability of total coliforms, escherichia coli and enterococcus in seawater, sand and sediment samples. According to the European and greek recommendations for bathing water quality (Table 3), the seawater of Balos lagoon could be characterized as of "excellent" quality.

The only indicator that it is important to take into consideration is the existence of large amounts of tar balls or residues (sticky remnants of oil) onto the sand, sediment and sea water (Figure 4). Marine tar residues originate from natural and anthropogenic oil releases into the ocean environment and are formed after liquid petroleum is transformed by weathering, sedimentation, and other processes (Warnock et al., 2015).



Figure 4. Tar balls on the sand of Balos beach.

4. CONCLUSIONS

The environmental monitoring of the quality of the Balos lagoon in Crete was conducted over a period of 2 tourist seasons, in order to determine the indicators that are important and need to be addressed with the ultimate goal of sustainable development of the area. The only indicator that it is important to take into consideration is the existence of large amounts of tar balls or residues onto the sand, sediment and seawater. Further studies are required to identify the origin of the tar residues in the Balos lagoon in order to find solutions to address it.

5. ACKNOWLEDGEMENTS

This publication was supported by the European Commission under the INTERREG V-A Greece-Cyprus 2014-2020 programme, within the framework of the project CROSS-COASTAL-NET initiative, Development of a Cross-Border Network for the Promotion of Sustainable Coastal Tourism ", Project MIS code: 5050612. The sole responsibility for the content of this paper lies with the authors. The European Commission is not responsible for any use that may be made of the information contained therein.



REFERENCES

- Kaberi, H., Zeri, C., Mousdis, G., Papadopoulos, A., Streftaris, N., 2013. Microplastics along the shoreline of a Greek island (Kea isl., Aegean Sea): types and densities in relation to beach orientation, characteristics and proximity to sources. In: Proc. 4th Int. Conf. Environ. Manag. Eng. Plan. Econ. SECOTOX Conf. Mykonos island, Greece. June 24-28, 197–202.
- Karkanorachaki, K., Kiparissis, S., Kalogerakis, G.C., Yiantzi, E., Psillakis, E., Kalogerakis, N., 2018. Plastic pellets, meso- and microplastics on the coastline of Northern Crete: Distribution and organic pollution. *Marine Pollution Bulletin* 133, 578-589
- Skiniti, G., Skarakis, N., Tsoutsos, T., Nikolaidis, N., Tournaki, S., Kosmas, P., Antoniou, L., 2022, Sustainable planning for tourism in sensitive coastal regions. A case study of Balos beach in Western Crete, 3rd Symposium on Circular Economy and Sustainability, Chania, 27th -29th of June.
- Skiniti, G., Tsoutsos, T., 2022, Society in energy transition and justice, Social acceptance and contribution in Wind energy projects In Oncel S., *A Sustainable Green Future - Perspectives on energy, economy, industry, cities and environment*, Springer Nature.
- Warnock, A.M., Hagen, S.C. Passeri, D.L, 2015. Marine Tar Residues: a Review. *Water Air Soil Pollut* 226, 68. <https://doi.org/10.1007/s11270-015-2298-5>.



Management implications in a peri-urban river under multiple stressors

C. Ntislidou¹, V. Papaevangelou², D. Latinopoulos², S. Ntougias³, P. Melidis³, C. Akrotos² and I. Kagalou²

¹Department of Zoology/School of Biology, Aristotle University of Thessaloniki, Thessaloniki, Greece

²Department of Civil Engineering/School of Engineering, Democritus University of Thrace, Xanthi, Greece

³Department of Environmental Engineering /School of Engineering, Democritus University of Thrace, Xanthi, Greece

Corresponding author email: ikagkalo@civil.duth.gr

ABSTRACT

Rural and peri-urban ecosystems usually have to confront the environmental pressure deriving from the agricultural schemes. These are usually aggravated by the synergistic multiplying effect of other pressures. In the case study of Laspias basin, it is witnessed that the river is subject to a large variety of pressures ever since its springs, receiving sorts of effluents affecting both the biota and the services this river could provide. Two sampling campaigns were conducted in the wet and dry season in 2021. Water parameters were measured in situ and both sediment and water samples were further analyzed for macroinvertebrates, nutrients and other eutrophication metrics (i.e., Chl-a, BOD₅, COD). A spatial and a temporal pattern was investigated using a principal component analysis, whereas the values were compared with the legislative limits. Based on benthic macroinvertebrates, the ecological quality of Laspias river was estimated to be less than moderate in all sites failing to achieve Water Framework Directive goal. In half of the sites, abiotic parameters demonstrated values higher than the acceptable thresholds. Landfills, wastewater treatment plants, industrial effluents and primer production practices charge the heavily modified river beyond its self-purification ability, despite the fact that it receives water from an adjacent basin assisting the dilution effect.

Keywords: Laspias river; pollutants; pressures; benthic macroinvertebrates; ecological quality.

1. INTRODUCTION

During the last decades, river water quality and issues concerning the proper utilization and management of water resources have gained the interest of both scientists and policy makers. This is reflected in the sum of European Union and United Nations environmental legislation. The European Union water policy integrates in a balanced way the dimensions of sustainability focusing on the water management as a framework against pollution, extreme events and climate change. Sustainable water management, including wastewater receptors, can further contribute to mitigation measures.

The EU Water Framework Directive (WFD, 2000/60/EC) was and still remains (WFD 20+) the main legislation of water bodies complemented by sisters (Marine and Floods), daughters (Groundwater and Environmental Quality) and other (Urban, Nitrate, Bathing and Drinking) directives. The above establish a framework for community action in the water policy field and set objectives aiming to ensure achievement or maintenance of at least good ecological status. Though, most aquatic ecosystems are exposed simultaneously to several stressors with, most usually, synergistic effects. Some stressors, such as water scarcity, pollution and contamination, can limit biodiversity and economic activities in entire regions. Water scarcity, especially in areas such as the Mediterranean basin, can amplify the effects of water pollution as warmer temperatures and reduced river flows will likely increase the physiological burden of pollution on the aquatic biota. The effects of these stressors are very relevant for the chemical and ecological status of water bodies as well as for ecosystem services' sustainability.

Rivers still play a key role in receiving or transferring agricultural, industrial and municipal discharges responsible for river pollution as a long-established practice (Streeter and Phelps 1958). So, along with Europe, the main types of pressures that rivers receive are nutrients and chemical pollution, hydrological alterations and morphological modifications (Grizzetti et al. 2017). Despite the effort made by many European countries (Greece included) to decrease pollution from point sources (Skoulikidis et al. 2018), the rivers' degradation due to pollution loads remains unsolved. Findings of nutrient enrichment in rivers follow



a seasonality related to agricultural practices enhanced in cases by localized industrial activities (Stefanidis et al. 2020). The rivers' self-purification is an attribute provided by physical, chemical and biological processes that enable the improvement of water quality and the preservation of the aquatic ecosystem, depending on each river's hydrological properties and the magnitude of pollution and pressures it receives (Wei et al. 2009).

Herein, a Mediterranean case study located in Greece (Laspias river basin), frequently exhibits pollution events. The objective of our study is to pinpoint the most polluted areas and to assess the effects of synergistic stressors to biota. Specifically, we evaluate its physicochemical characteristics engaged with its ecological quality through monitoring benthic macroinvertebrates thus providing the key elements that would facilitate an integrated management plan.

2. MATERIAL AND METHODS

Laspias River is located in Xanthi Prefecture, Thrace, Greece. The surface area of the basin is 212 km², while the river's length is approximately 30 km consisting of Heavily Modified Water Bodies (HMWBs). It discharges in a protected area of environmental importance (Ramsar Convention, Natura 2000 site, National Park). Geo-morphologically, it is a mountainous-agricultural area. Both point and diffuse pollution sources are found in the watershed. The main pollutants derived from the untreated or maltreated effluents, i.e., water and sludge from the wastewater treatment plant (WWTP) of the city, the industrial area of Xanthi and several livestock units, concerning point sources, while agricultural runoff is the main diffuse source.

Samplings were conducted at dry and wet period (spring and autumn 2021) from seven sites within the framework of the Eye4Water Project (www.eye4water.com). Dissolved Oxygen (DO, mg/L), Water Temperature (T, °C), Electrical Conductivity (EC, µS/cm), Salinity (SAL, ppt) and pH were measured in situ. Concentrations of Biochemical and Chemical Demand (BOD₅ & COD, mg/L), Total Solids (dissolved and suspended, TDS & TSS, mg/L), Total Kjeldahl Nitrogen (TKN, mg/L), Total Phosphorus (TP, mg/L) and chlorophyll-a (Chl-a, µg/L) in water samples were analyzed according to standard methods (Baird et al. 2017).

Benthic macroinvertebrates were sampled using a D-shaped net according to the semi quantitative 3-min kick/sweep method (Armitage and Hogger 1994) plus 1-min in the bank vegetation, when existed (Wright 2000). During the 3-min sampling, all microhabitats were covered proportionally according to the matrix of possible river habitats (Lazaridou et al. 2018). Specimens were identified at the family level, except for Ostracoda, Hydracarina, Araneae and Oligochaeta (apart from Tubificidae) and the relative abundance of each taxon was determined. Finally, the Hellenic Evaluation System 2 (HESY2) (Lazaridou et al. 2018) was used to estimate the ecological quality. A Principal Component Analysis (PCA) (Primer 6: Clarke and Gorley 2006) was applied to explore environmental gradients and identify the explanatory variables.

3. RESULTS AND DISCUSSION

The monitoring routine was able to track the variety of pressures posed on the system and revealed the burdened character of the river. In both periods, during 2021, the ecological assessment resulted in poor and bad ecological quality (Figure 1). Specifically, the physicochemical properties and common pollutant analysis demonstrated values exceeding the legislation limits in many cases (91/271/EEC, 2006/44/EC, GG 356/B/26-2-2009) (Figure 2). Indicators describing the pollutant loads as the oxygen related ones (DO, BOD₅, COD), nutrient related ones (TKN, TP) and solids (TDS, TSS) revealed a hostile water system for aquatic life in about half the sampling sites, especially those in the downstream part.

To this complement, the benthic macroinvertebrate community is characterized by the dominance of two tolerant to organic pollution taxa (i.e., Chironomidae up to 97% of the total abundance, Oligochaeta up to 46% of the total abundance). In total, 29 families were identified, indicating low biodiversity. The absence of sensitive taxa highlighted the synergistic effect on both chemical and biological quality. Moreover, river regulation (e.g., channelization, dredging) has altered the natural spatio-temporal heterogeneity of the Laspias river, which resulted in low biodiversity.

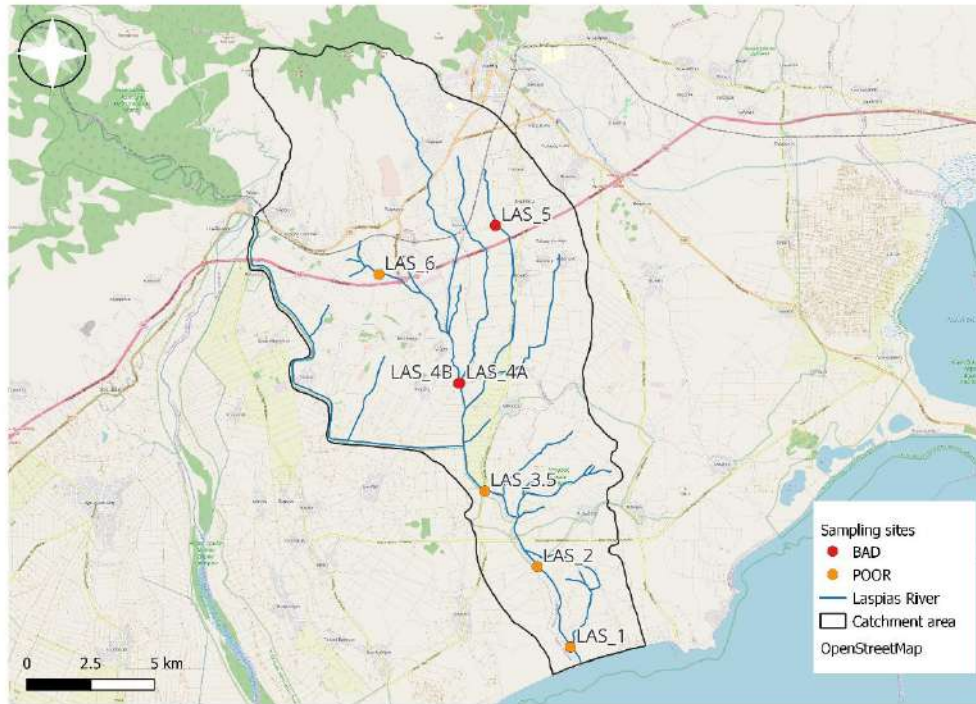


Figure 1. Map of Laspias basin with ecological quality.

Natural water systems, such as rivers, have the ability of self-purification, a process that helps aquatic systems deal with pollution and eventually recover their background conditions (Gonzales et al. 2014). However, if pollution load surpasses this ability of self-purification, then the aquatic systems cannot return to their initial water quality status and deterioration of aquatic water and eventually life begins. Organic pollution represents one of the most common forms of pollution in an aquatic system (Gonzalez et al. 2014) and it can be expressed in terms of DO depletion, COD and BOD₅ concentration. Therefore, these parameters are usually used as river's health indicators. According to the Directive 2006/44/EC, the lowest DO limit below which aquatic life is threatened is 4 mg/L. Unfortunately, almost all sites, except for site LAS_6, demonstrated DO values lower than 4 mg/L, which underlines the stress that aquatic life receives (Figure 2b). Since Laspias river constitutes a legislative WWTP recipient, it is regulated by the Directive 91/271/EEC. Therefore, COD and BOD₅ values was compared to these legislative limits. As shown in Figure 2, sites LAS_4A and LAS_5 seemed to be the most problematic (Figure 1, 2d and e), since BOD₅ and COD values exceeded the legislative limits. Specifically, at site LAS_5, located downstream of the WWTP, all values were much higher than 25 mg/L and 125 mg/L for BOD₅ and COD, respectively. Accordingly, in site LAS_4A, values reached the higher limit or even exceeded it. Overall, it can be underlined that Laspias river receives a rather significant amount of organic pollution. In terms of nutrients (ammonia and phosphorus), again the river's status is deteriorated. The legislative limits for total nitrogen and total phosphorus are 15 and 2 mg/L, respectively. As in the case of COD and BOD₅, sites LAS_4A and LAS_5, demonstrated values surpassing these limits (Figure 2g and 2h). Additionally, in site LAS_4B, TKN was also above the legislative limit (Figure 2g). Regarding TS, only TSS is illustrated in Figure 2, since this parameter is included in the Directive. Again, the permitted TSS value (35 mg/L) was exceeded in sites LAS_4A and LAS_5 (Figure 2f). LAS_5 can be classified as "sensitive" / "polluted" under the UWWT and/or Nitrates Directives.

Similar to the findings of other researchers (Canobbio et al. 2009), our results, especially those of biota-pollutants interplay, support that the pollution caused from WWTP effluents can impair the river's water quality. Moreover, the series of important hydro-morphological alterations, the seasonality and magnitude of floods and droughts events (causing agricultural wash-off, industrial spills and sewages) have a detrimental complimentary effect.

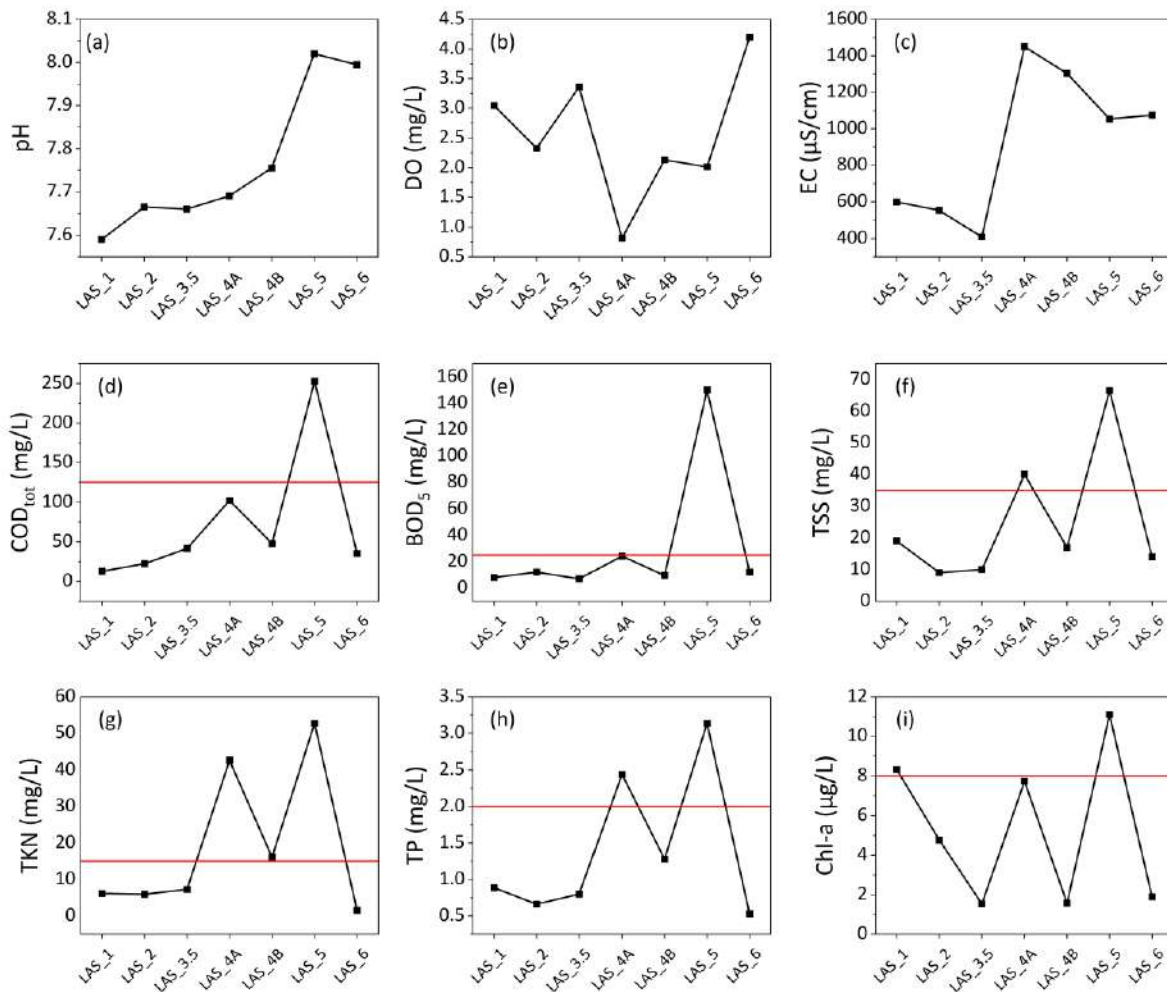


Figure 2. Average values of abiotic parameters per site with limits. Red horizontal lines indicate the legislative limits according to the 91/271/EEC Directive.

Searching for a spatial pattern (Figure 3), it seems like the river receives an excess of loads from the landfill (L6) and gets worse after the inclusion of the WWTP effluents (L5); thus, a non-proper operation might be responsible. The situation is aggravated after the industrial area and animal farms (L4A and 4B). Then, the ecological quality seems to be ameliorated in site L3.5 after the inclusion of discharges from an adjacent basin and then one weir (L2) retains water for flood control and acts as a sink for pollutants, overflowing and oxygenating the river watercourse up to the estuary (L1). In the PCA analysis, the samplings sites were arranged following axis I, with BOD₅, TKN and TS being the most significant factors for the classification (72.2%) and axis II with TDS, TP and EC (10.9%), respectively (Figure 3). There is no or little seasonal pattern with augmented flows assisting the pollutants' dilution effect.

4. MANAGEMENT IMPLICATIONS

The overall picture of Laspías is characteristic of a mismanaged river receiving an excess of pollution loads and, in several cases, partially or fully untreated. Yet, there is evidence of inadequate plant operation as well as of illegal by-pass of untreated sewages. From the results, a measure scheme for pressure alleviation at the point sources is deemed necessary and it should also be highlighted that the major pressures fit more with an urban environment supporting the watershed's particularity.

It is generally acknowledged that diffuse losses by agricultural activity are a main phosphorus and nitrogen source for river basins. Reducing diffuse nutrient losses has become a major issue since it is related with the achievement of good ecological status by 2027. Although agri-environmental measures



were introduced in Greece through the application of the Council Regulation (EEC/ No 2078/92), no specific agro-environmental measures are undertaken besides water cost accounting related to the supply, training program for the locals and extended hydrological research. In fact, in the district level tools are suggested for the rational use of water and fertilizers, but not tailor-made for the case study. A possible suggestion could be the application of good agricultural practices, along with the establishment of strictly protected zones in the basin, where at least the land cultivation should be done with ecological (organic) techniques. In this phase also an integrated modeling system at catchment level, able to evaluate the relative contribution of nutrients in association to selected driving forces and taking into consideration the stakeholders' opinions should be aimed at the effective management of different pollutants. This is actually included in an undergoing project, Eye4Water, dealing with the strengthening of the water management practices (in Thrace) through the development of innovative ICT methodologies and improvement of research infrastructures.

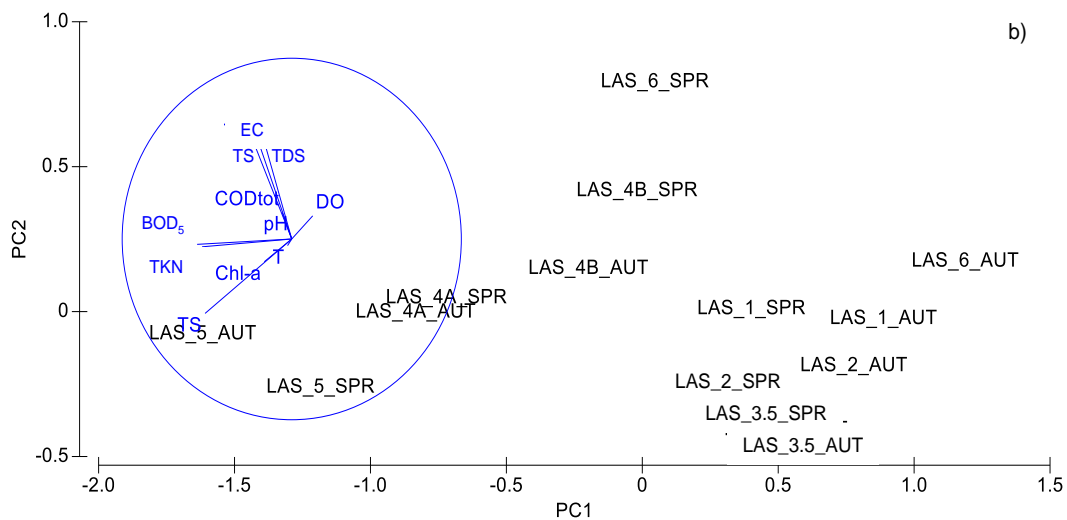


Figure 3. PCA plot with physiochemical and nutrients parameters from Laspias River during wet and dry period (sp: spring, au: autumn).

As it was reported earlier, Laspias basin and, in particular, the delta area consists of an interesting issue in terms of biodiversity, thus it should be protected and maintained in order to support the existence of the habitats and species. Increased land use changes have led, to the deterioration of the habitats, the degradation of spawning and nursery areas. The pollutants loads across the river combined with the modified riparian areas and steep slopes decrease meso-scale habitat variability. An integrated monitoring and conservation plan should be set up taking into consideration besides the traditional conservation efforts on priority habitats and endangered species, also on the whole ecosystem's functioning through the evaluation of its ecosystem services.

The Administrative infrastructure of this region (Thrace) for the river basins and further for the water resources management, following the general national pattern, includes usually competent authorities dealing with water management and in some cases their responsibilities overlap, while the active participation of the local community is weak. At this level, the enforcement of participation by stakeholders can ensure that the proposed measures would have taken into account the local knowledge, strengthening the public commitment to the management implication.

In conclusion, the need for development should be coincided with water policy avoiding overexploitation of aquatic resources. This becomes more complex at remote areas, as Thrace where the pressure for development projects is high. The impact of human activities on these seasonally water-stressed systems may be limit their future ability to survive as sustainable, self-regulated systems. The obligation to apply the environmental European policy on a regional scale, hopefully, pushes the environmental planning and awareness.

It is evident that the multiplicity effect of pollutants surpasses the river's self-purification ability and the sustainable water use should be more promoted, including advanced nutrients treatment and remediation



measures coupled with stricter enforcement framework and awareness raising. These findings should be regarded as an alert for the sustainability of the entire area's production system (agricultural and industrial) and the national park's prosperity.

5. ACKNOWLEDGEMENTS

Produced for Eye4Water project, MIS 5047246, implemented under the action: "Support for Research Infrastructure and Innovation" by the Operational Program "Competitiveness, Entrepreneurship and Innovation" in the framework of the Co-financed by Greece and the European Union-European Regional Development Fund.

REFERENCES

- Armitage, P.D. and Hogger, J., 1994. *Invertebrates Ecology and Methods of Survey*, 1st ed.; RSPB Sandy: Bedfordshire, UK.
- Baird, R.B., Eaton, A.D. and Rice, E.W., 2017. *Standard Methods for the Examination of Water and Wastewater*, 23th ed.; American Public Health Association, American Water Works Association & Water Environment Federation: Washington, DC, USA.
- Canobbio, S., Mezzanotte, V., Sanfilippo, U. and Benvenuto, F., 2009. Effect of multiple stressors on water quality and macroinvertebrate assemblages in an effluent-dominated stream. *Water Air Soil Pollut.*, 198, 359-371.
- Directive 2006/44/EC of the European Parliament and the Council of 6 September 2006 on the quality of fresh waters needing protection or improvement in order to support fish life.
- Directive 91/271/EEC of 21 May 1991 concerning urban waste-water treatment.
- Gonzales, S.O., Almeida, C.A. and Calderon, M., 2014. Assessment of the water self-purification capacity on a river affected by organic pollution: application of chemometrics in spatial and temporal variations. *Environ. Sci. Pollut. Res.*, 21: 10583-10593.
- Government Gazette 356 / B / 26-2-2009 Bathing water quality and management measures, in accordance with the provisions of Directive 2006/7/EC on the management of bathing water quality and repealing Directive 76/160 / EEC of the European Parliament and of the Council of 15 February 2006.
- Lazaridou, M., Ntislidou, C., Karaouzas, I. and Skoulikidis, N., 2018. Harmonization of a new assessment method for estimating the ecological quality status of Greek running waters. *Ecol. Indic.*, 84, 683–694.
- Grizzetti, B., Pistocchi, A., Liqueste, C., Udias, A., Bouraoui, F. and Van De Bund, W., 2017. Human pressures and ecological status of European rivers. *Sci. Rep.*, 7, 1-11.
- Phelps, E.B. and Streeter, H.W., 1958. *A study of the pollution and natural purification of the Ohio River*. US Department of Health, Education, & Welfare.
- Skoulikidis N., Dimitriou E. and Karaouzas I., 2018. *The Rivers of Greece*, 1st ed.; Springer: Berlin/Heidelberg, Germany.
- Stefanidis, K., Christopoulou, A., Poulos, S., Dassenakis, E. and Dimitriou, E., 2020. Nitrogen and phosphorus loads in Greek rivers: Implications for management in compliance with the Water Framework Directive. *Water*, 12, 1531.
- Wei, G., Yang, Z., Cui, B., Li, B., Chen, H., Bai, J. and Dong, S., 2009. Impact of dam construction on water quality and water self-purification capacity of the Lancang River, China. *Water Resour. Manag.*, 23, 1763-1780.
- Wright, J.F., 2000. *An introduction to RIVPACS*, 1st ed.; Freshwater Biological Association: Ambleside, UK.



Development and evaluation of magnetic tea waste based adsorbent materials for removal of cadmium from wastewater

M. Ervine¹, O. Jaiyeola¹ and C. Mangwandi¹

¹School of Chemistry and Chemical Engineering, Queen's University Belfast, Belfast BT9 5AG, Northern Ireland, UK

Corresponding author email: c.mangwandi@qub.ac.uk

ABSTRACT

In this research, a new low-cost bio sorbent material for application in heavy metal removal focusing on cadmium removal from wastewater. Previous research into tea waste, showed that modification of the surface via bleach and iron (II) chloride has a positive impact on the adsorbent capacity. A full adsorption study was completed by using the optimum MBTW (Magnetic Bleached Tea Waste) from the initial experiment. This experiment differs due to cadmium removal being the focus of the experiment. The Freundlich isotherm was the optimum fit for the experimental data for the three temperatures studied. For the kinetics of the experiment, the most accurate fit was the pseudo second-order kinetics model by Lagergren. Fourier transform infrared (FT-IR) analysis of the MBTW was before and after adsorption which shows the functional groups which changed due to adsorption of cadmium. All the results reported strongly applied the potential of MBTW as an economic bio adsorbent for removal of cadmium from contaminated waters.

Keywords: cadmium; adsorption; magnetic teawaste; experimental design; iron chloride.

1. INTRODUCTION

Heavy metal pollution of natural water bodies has been on the increase due to industrial activities across the world. Heavy metal pollution causes a great threat to human health due to their toxic nature. Among all the heavy metals cadmium is considered as a toxic element and potentially cause chronic toxicity even at low concentrations (Cruz, da Costa et al. 2004). The main sources of cadmium pollution into waste streams are alloy manufacturing, battery production, plastics, electroplating, mining, and refining processes (Cruz, da Costa et al. 2004). Cadmium readily accumulates in living systems. It has been reported that cadmium exposure can lead to diseases such as pulmonary oedema, anaemia, trachea- bronchitis, lung cancer and brain damage (Pal and Maiti 2019). Cadmium poisoning can also result in changes in the constitution of the liver, bone and blood (Nogawa, Kobayashi et al. 2004).

The goals of this study were to produce a magnetic adsorbent material from tea waste by treating it with iron (III) chloride at different concentrations and to thermally treat this at different temperatures and durations to find the optimum combination for cadmium removal. From this material produced, the capacity of the adsorbent to remove cadmium from wastewater was found and evaluated in different conditions such as temperature and dosage.

2. MATERIALS AND METHOD

2.1 Preparation of the adsorbents

Based on the method described in literature, bleaching the tea waste is to improve the surface oxygen groups and active sites making it more hydrophilic and enhancing the adsorption process (Saygılı et al., 2018). Household bleach (6% sodium hypochlorite) is added to a 2000 mL beaker and allowed to stir for 24 hours. Every 24 hours the bleach is removed, and new bleach is added. This process is repeated until the black tea waste is now white. This white paste is then washed until all of the bleach residue is removed, it is then spread on a flat surface and allowed to dry in an oven at 60°C. This is bleached tea waste (BTW).

This is the step which dictates the concentration of iron (III) chloride in which the BTW is in contact with. Using Design Experts, it was decided that the concentrations of iron (III) chloride used would be 0.2, 0.6 and 1 g iron (III) chloride per gram of BTW used. These mixtures were allowed to stir for 24 hours then filtered



using filter paper to remove excess iron (III) chloride. The MBTW was then placed on a glass dish and allowed to dry in an oven at 60 °C for 24 hours.

These samples are then divided up into the required size of sample for the experiment and placed in a furnace at either 200 °C, 350 °C and 500 °C for a time of 2, 3 or 4 hours. This resulted in 17 samples while varying these variables to get an accurate overview of the optimum conditions for adsorption of cadmium. Samples taken from the 17 batches were contacted with cadmium solution with an initial concentration of 190 ppm over a 24-hour period.

The residual concentration of the solution was determined using Inductively Coupled Plasma Optical Emission spectroscopy (ICP-OES). The cadmium concentration in solid phases was calculated from the equation 1:

$$Q_e = \frac{(C_i - C_e)V}{m} \quad (1)$$

Where C_i and C_e are the liquid-phase concentrations of cadmium initially and at equilibrium respectively and both measured in mg/L. Volume of solution (L) and m is the mass of dry adsorbent used for the experiment in grams.

2.2 Characterization of the adsorbent

2.2.1 FTIR Analysis

The functional groups of MBTW were determined by Fourier Transform Infrared (FTIR) Spectroscopy using a Perkin Spectrum 100 within the range 4000–400 cm^{-1} with a resolution 4 cm^{-1} . The FTIR analysis was also repeated after the adsorption.

2.2.2 Thermogravimetric analysis (TGA)

Thermogravimetric analysis allows the prediction of characteristics which can change the processability options of the material for scaling up to industrial sized production compared to lab scale. For bio sorbents, this analysis can be described as moisture removal, cellulose decomposition, and lignin decompositions due to the heating rate being below 100 °C/min. The rate used for this analysis was 20 °C/min.

3. RESULTS AND DISCUSSION

3.1 Characterization

Figure 1 FTIR analysis for samples before and after adsorption. The peak at 3400 cm^{-1} on pre and the peak at 3230 cm^{-1} corresponds to -OH bonding groups. The peaks at 2100 and 2230 cm^{-1} have been linked with $\text{C}\equiv\text{C}$ stretch. The peak at 1750 cm^{-1} could be due to carbonyl group stretching.

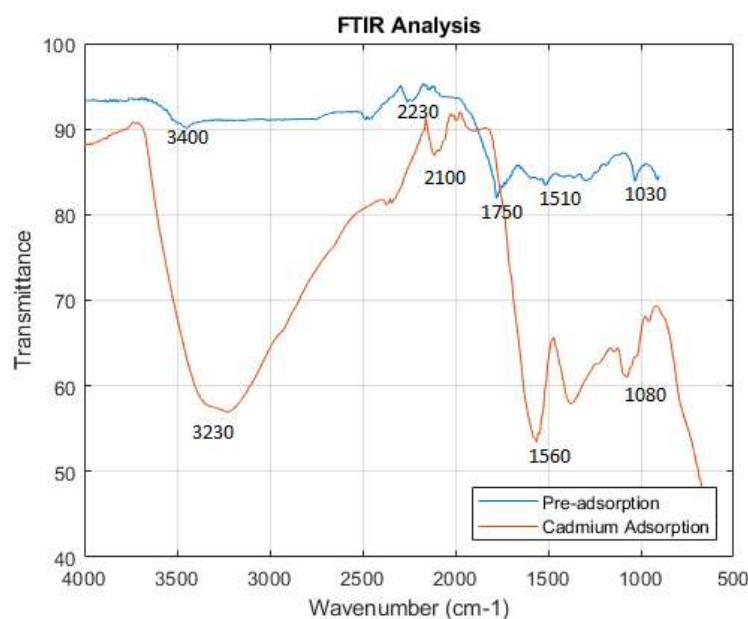


Figure 1. Comparison of the FTIR spectra of the MBTW sample before and after adsorption of cadmium.



The peaks at 1560 and 1510 cm^{-1} could correspond to the C single bond O stretching mode conjugate with the amine group. The peaks at 1030 and 1080 cm^{-1} are related to the C single bond O stretching of alcoholic groups. As can be seen from Figure 1 the peaks change after adsorption with cadmium showing an alteration in chemical structure from the adsorption. The slight change in the peaks shows the biosorption of the cadmium ions to the MBTW. This shows that the changes are within the chemical structure of the MBTW, concluding that there must be chemisorption taking place to alter these groups and to stretch bonds when adsorbing cadmium by MBTW (Wan et al. 2014).

3.2 Design Experiment

As stated above there were multiple variants of the MBTW made. The variables which were used for this were; time of pyrolysis, the concentration of iron (III) chloride within the tea and the temperature at which the pyrolysis took place. With the results, these variables were modelled to calculate the variable which affected the adsorption efficiency the most and which had the lowest impact on the adsorption efficiency. The equation which was used for this modelling is shown below.

$$q_e = \beta_0 + \sum_{i=1}^k \beta_i x_i + \sum_{i,j=1}^k \beta_{i,j} x_i x_j + \sum_{j=1}^k \beta_j x_j^2 \quad (2)$$

In equation (2) β_0 represents the residuals term β_i and β_j are coefficients for the linear and quadratic terms respectively and $\beta_{i,j}$ are coefficients for the interaction terms. x_i is the normalize process/ formulation variable (i.e., temperature, duration of pyrolysis and concentration of Fe).

The ANOVA analysis results are presented in Table 1. The P-values and F-values reported in the table show that the most influential variables are concentration of iron chloride and the pyrolysis temperature. The p-Value for the model of is reported as 0.0018 implying there is only 0.18% chance that model F-Value is due to error. The coefficient of terms of eq. (2) are reported in the last column of Table 1.

Table 1: ANOVA analysis table showing effect of process variables on Q_e values.

	Sum of		Mean	F	p-value	Coefficient
Source	Squares	df	Square	Value	Prob > F	
Model	432.96	9	48.11	35.79	0.0018	92.10
A-T	22.19	1	22.19	16.51	0.0153	-2.58
B-con	179.95	1	179.95	133.89	0.0003	+6.23
C-time	0.26	1	0.26	0.19	0.6820	+0.28
AB	42.26	1	42.26	31.44	0.0050	-4.30
AC	59.46	1	59.46	44.24	0.0027	+3.74
BC	9.14	1	9.14	6.80	0.0595	+2.00
A ²	39.15	1	39.15	29.13	0.0057	+4.42
B ²	57.25	1	57.25	42.60	0.0028	-5.67
C ²	17.10	1	17.10	12.72	0.0234	+2.92
Residual	5.38	4	1.34			
Lack of Fit	4.71	2	2.35	7.06	0.1240	
Pure Error	0.67	2	0.33			
Cor Total	438.34	13				

Figure 2 shows the variation of Cd loading on the adsorbent with the process conditions use in their production. The highest loading was obtained with the absorbent produced with a duration of thermal activation of 4 hours, pyrolysis temperature of 200 °C and with the highest concentration of iron chloride of 1.0 g/g. The worst percentage removal over the 50-hour duration of the experiment was 42.21% for MBTW



under the conditions of 500 °C for 2 hours and concentration of 0.2 g/g. At lower concentrations of Fe and lower activation temperature, the duration of thermal processing had a little effect on removal of Cd ions from solution, however at higher concentration and higher activation temperature differences in performance of the adsorbents become more significant. At short duration of activation increasing the processing temperature resulted in high reduction on the Cd loading capacity of the adsorbent material.

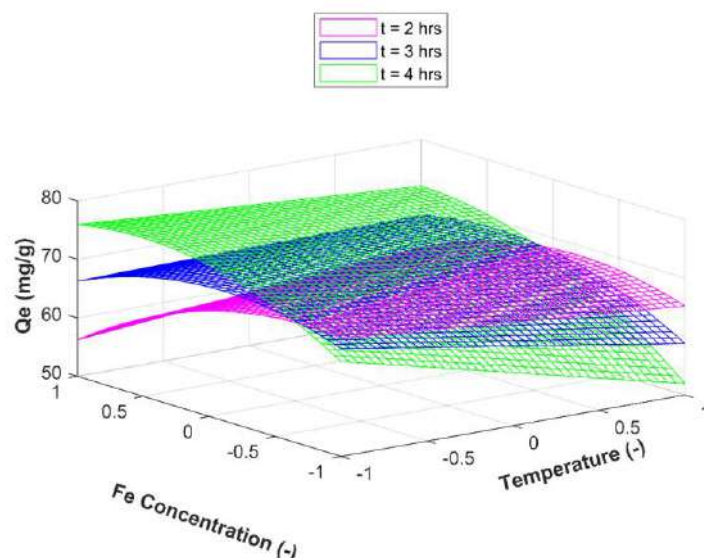


Figure 2. Effect of processing conditions on the cadmium loading on to the resultant biochar adsorbent materials. Adsorption experiments performed using dosage of 2.5 g/L and solutions with initial concentrations of 190 ppm at room temperature.

3.3 Comparison with literature

Table 2 shows a collection of Q_{max} results from various papers researching the use of tea waste in various forms to remove pollutants from aqueous solutions. The majority of papers researching the removal of cadmium have fairly low removal values. The most modified adsorbent was the use of biochar without the bleaching step. The papers which have a step which modifies the tea waste, for example alkali treated which was using sodium hydroxide which had a large removal of 430 mg/g. The paper by Saygılı et al. (2018) shows that bleaching had a very positive effect on the black tea as it improved the removal from 125 to 416 mg/g. Also shows that adding iron nanoparticles within the structure of the tea waste allows for a slightly better removal of the contaminant and easier removal of the adsorbent due to magnetic tendencies caused by the addition of the iron (III) chloride.

Table 2. Comparison of the adsorption capacity with values reported in literature.

Adsorbent	pH/T (K)	Q_{max} (mg/g)	Reference
Tea factory waste	5.5/298	11	Cay and Ozsik, 2004
Teawaste	5/328	16	Kamsonlian et al., 2011
Teawaste biochar	5/298	42.0	Pal and Maiti, 2019
Teawaste biochar	6/298	5.9	Fan et al., 2017
Saw dust	8/298	41.21	Albadarin et al. 2011
Food waste digestate granules	-/298	217	Chen et al., 2019
Jatropha Carbon	6/298	20.79	Mohammad et al., 2013
Magnetic Bleached Biochar	7-8/333	511	Current work

4. CONCLUSIONS

This can be seen visually from Figure 2 as the point that has the highest Q_e (mg/g) is the optimum variables for the MBTW. The worst percentage removal over the 50-hour duration of the experiment was 42.21% for



MBTW under the conditions of 500 °C for 2 hours and concentration of 0.2 g/g. The optimum MBTW was 1 g/g concentration, 200 °C for pyrolysis temperature and the time of pyrolysis was 4 hours. The detailed adsorption study showed that MBTW had Cd removal capacity (511 mg/g) which is competitively high when compared to other adsorbent materials reported in literature. The new adsorbent developed in this work show great potential for heavy metal removal. Future studies will focus on evaluating its performance in a continuous system.

REFERENCES

- Abdelwahab, O., Nemr, A., Sikaily, A. and Khaled, A., 2005. Use of rice husk for adsorption of direct dyes from aqueous solution: a case study of direct f. Scarlet. *Egyptian Journal of Aquatic Research*, 31(1), 1110-0354.
- Albadarin, A. B., Mangwandi, C., Walker, G. M., Allen, S. J. and Ahmad M. N., 2011. Biosorption characteristics of sawdust for the removal of Cd(II) ions: Mechanism and thermodynamic studies. *Chem. Eng. Trans.*, 24, 1297–1302.
- Çay, S., Uyanık, A. and Özaşık, A., 2004. Single and binary component adsorption of copper(II) and cadmium(II) from aqueous solutions using tea-industry waste, *Separation and Purification Technology*, 38(3), 273-280.
- Chen, H., Osman, A. I, Mangwandi, C. and Rooney, D., 2019. Upcycling food waste digestate for energy and heavy metal remediation applications. *Resources, Conservation & Recycling: X*, 3, 100015.
- Cruz, C. C. V., da Costa, A. C. A., Henriques, C. A. and Luna, A. S., 2004. Kinetic modeling and equilibrium studies during cadmium biosorption by dead *Sargassum* sp. biomass. *Bioresource Technology*, 91(3), 249-257.
- Fan, S., Li, H., Wang, Y., Wang, Z., Tang, J., Tang, J. and Li, X., 2017. Cadmium removal from aqueous solution by biochar obtained by co-pyrolysis of sewage sludge with tea waste. *Research on chemical intermediates*, 44(1), 135-154.
- Kamsonlian, S., Balomajumder, C., Chand, S. and Suresh, S., 2011. Biosorption of Cd (II) and As (III) ions from aqueous solution by tea waste biomass. *African Journal of Environmental science and technology*, 5(1), 1-71.
- Mohammad, M., Yaakob, Z. and Abdullah, S. R. S., 2013. Carbon Derived from Jatropha Seed Hull as a Potential Green Adsorbent for Cadmium (II) Removal from wastewater. *Materials*, 6(10), 4462-4478.
- Nogawa, K., Kobayashi, E., Okubo, Y. and Suwazono, Y., 2004. Environmental cadmium exposure, adverse effects and preventive measures in Japan. *BioMetals*, (5), 581-7.
- Pal, D. and Maiti, S. K., 2019. Abatement of cadmium (Cd) contamination in sediment using tea waste biochar through meso-microcosm study. *Journal of Cleaner Production*, 212, 986-996.
- Saygılı, H., Saygılı, G. A. and Güzel, F., 2018. Surface modification of black tea waste using bleaching technique for enhanced biosorption of Methylene blue in aqueous environment. *Separation Science and Technology* 53(18), 2882-2895.
- Wan, A., Ma, Z., Xue, Y., Ma, M., Xu, S., Qian, L. and Zhang, Q., 2014. Sorption of lead (II), cadmium (II) and copper (II) ions from aqueous solutions using tea waste. *Industrial & Engineering Chemistry research*, 53, 3629-3635.



Highly efficient removal of cadmium from waste water using eco-friendly and cost-effective aluminophosphate as adsorbents

O. Jaiyeola¹, A. Hamza^{1,2} and Mangwandi¹

¹School of Chemistry and Chemical Engineering, Queen's University Belfast, Belfast BT9 5AG, Northern Ireland, UK

²Department of Chemistry, University of Lancaster, Bailrigg, Lancaster LA 4YB

Corresponding author email: c.mangwandi@qub.ac.uk

ABSTRACT

This study comprehensively discusses the use of aluminophosphate with the presence of silicate as an adsorbents material for the removal of Cadmium. The effect of adding silicate to the material increased the removal capacity pf the adsorbent material up to a certain point. Adding more that 7.5% of silicate results in the reduction of removal capacity. Adsorption kinetics was done using the best adsorbent sample (adsorbent with 7.5% silicate). Results showed that more than 90% was removed within the first 30 minutes of the adsorption process. This shows that this material has great potential as an adsorbent for the removal of cadmium.

Keywords: Cadmium; Aluminophosphate; Sodium silicate; Adsorption.

1 INTRODUCTION

In recent years, with the fast development of industrialization and agriculture, the heavy metal cadmium pollution has received extensive attention. Cadmium has the features of high migration rate, persistence and easy accumulation, which can be migrated to the environment through run-off, irrigation, sediment deposition, etc., and can also be transferred to the human body by the food chain (Luo et al.,2020). Several technologies have been used to remove heavy metal ions from effluents, including chemical co-precipitation, ion exchange, membrane filtration, coagulation, adsorption and others. Amongst them, the adsorption technology is known as a high-efficiency method due to its effectiveness, simplicity, low cost, and regenerable adsorption capacity.

The study focuses on removing heavy metals using aluminum phosphate based adsorbents. Cadmium is used as a model heavy metal. This project assesses the potential of silicate bonded aluminophosphate composite material as an adsorbents for removal of cadmium from synthetic aqueous solutions. The removal capacity alongside the effect of the presence of silicate and other conditions such as contact time and temperature were evaluated.

2. MATERIALS AND METHODS

20 g of Aluminium nitrate and 3.611mls of phosphoric acid in a 1:1 mol ratio were weighed and added to 400 ml of distilled water. Ammonia was added dropwise to adjust the solution pH to between 7 and 7.5. The resultant solution was left on the stirrer for 2 hours, excess moisture was filtered out and the adsorbent was dried in the oven for 6 hours at 60°C.

A known mass of the adsorbent material was calcined at 300°C for 5 hours. The following nomenclature was use for naming the samples SiAlPO(xx) where (xx) represents the percentage by mass of silicon used in the preparation of sample. For example sample with a mixing ratio of 0:1 with no silicate present would be AlPO₄ and that with a ratio of (0.975:0.025) with 2.5% silicate would be named as SiAlPO(2.5).

The previous steps were repeated with the inclusion sodium silicate in different ratios to introduce the presence of silicate in the adsorbent material. The ratios used were (0.05:0.95), (0.075:0.925) and (0.10:0.90). For SiAlPO(2.5)(ratio 0.975:0.025), 0.16 g sodium silicate, 19.31 g of aluminum nitrate and 3.611ml of phosphoric acid were added to 400ml of distilled water.

To evaluate the performance of the different adsorbent samples, 50 mg of the adsorbent material was added to 20 ml, 100 ppm cadmium solutions and agitated on the shaker for a period of 6 hours. The



concentration of Cd remaining in solution at the end of adsorption study was determined by withdrawing 1ml from each vial sample was taken and added to 9ml of water to make up a dilution factor of 10. The resultant samples were analysed by ICP (Inductively Coupled Plasma optical emission spectrometry) to give the final concentration of cadmium ions. The cadmium concentration in solid phases was calculated from the equation:

$$Q_e = \frac{(C_i - C_e)V}{m} \quad \text{Eq.1}$$

Where C_i and C_e are the liquid-phase concentrations of cadmium initially and at equilibrium respectively and both measured in mg/L. Volume of solution (L) and m is the mass of dry adsorbent used for the experiment in grams.

3. RESULTS AND DISCUSSION

3.1 Effect of Si content

From Figure 1 the comparison of the effect of the presence of the silicate and the non-presence of the silicate (AlPO) was compared to select the best adsorbent ratio. It was seen that adsorbent material SiAlPO(7.5) had the highest percentage removal of cadmium ions. The trends observed here are similar to other results reported in literature (Chen et al. 2019). The improvement in the removal capacity could be due changes in the surface structure of adsorbent material when silicate is introduced.

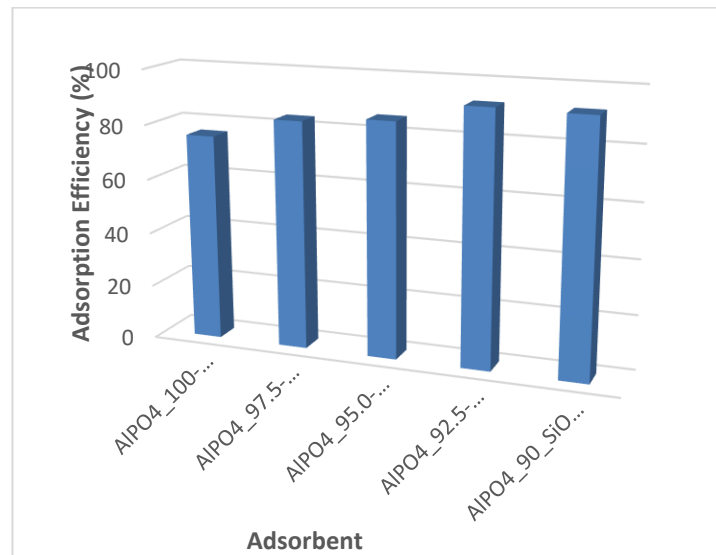


Figure 1. comparison of the different adsorbent materials. All experiments were done using cadmium solutions with initial concentration of 100ppm and adsorbent dosage of 2.5 g/L.

3.2 Adsorption Kinetics

The kinetics of Cd^{2+} removal were fitted by the pseudo first order and pseudo second order, respectively. The adsorption kinetics can be evaluated using pseudo 1st order kinetics equation which is written as:

$$q(t) = q_e[1 - \exp(-k_1 t)] \quad \text{Eq. 2}$$

where $q(t)$ is the amount of adsorbed solute at time t , q_e its value at equilibrium, and k_1 the pseudo-first-order rate constant.

According to Ho and McKay if the sorption process is 2nd order chemisorption, the sorption rate can be expressed by the equation:

$$\frac{dq_t}{dt} = k_2(q_e - q_t)^2 \quad \text{Eq. 3}$$



In Eq. (4) q_e and q_t are sorption capacity at equilibrium and at a time t respectively and k_2 is the rate constant of the pseudo order. Integrating the equation and using the boundary conditions of $q_t = 0$ at $t = 0$ and $q_t = q_t$ at $t = t$ will result in the following equation:

$$\frac{1}{(q_e - q_t)} = 1 + k_2 q_e t \quad \text{Eq. 4}$$

It can be shown that Eq. (5) can be expressed as

$$q_t = \frac{k_2 q_e^2 t}{1 + k_2 q_e t} \quad \text{Eq. 5}$$

The variations of the Cd^{2+} removal efficiency with contact time for the SiAlPO(7.5) adsorbent material were shown in Figure 2. The rate of removal of cadmium is higher at the beginning, this is largely due to the larger surface area of the adsorbent being available at the beginning for the adsorption of cadmium.

At contact time of only 15 minutes, the q_t was as high as 26 mg/g with about 86% removal of cadmium ions already. The results exhibited that Cd^{2+} ions could be rapidly immobilized on surface sites of the adsorbent. With time, the surface adsorption sites become exhausted where at this point, the uptake rate can be regarded to be controlled by the rate at which the adsorbate is transported from the exterior to the interior sites of the adsorbent particles

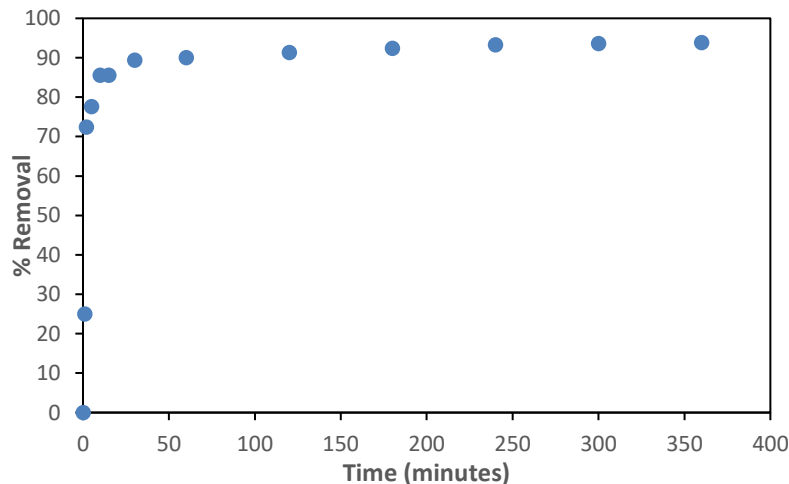


Figure 2. kinetics of the cadmium loading on SiAlPO(7.5) adsorbent sample(b). All experiments were done using cadmium solutions with initial concentration of 100ppm and adsorbent dosage of 2.5 g/L.

The kinetic parameters were listed below. As can be seen, the pseudo second order model was the best among both models to describe kinetic experimental data because of the highest correlation coefficients ($R^2 > 0.990$). The results indicated that the rate controlling step in Cd^{2+} removal was chemisorptive bonds of Cd^{2+} species and chemisorption involving valence forces through sharing or exchanging electrons between adsorbent and adsorbate.

Table 3: Kinetic parameters for the removal of cadmium.

Model	Parameter	Value
Pseudo 1 st order	K_1 (min^{-1})	3.39
	q_e (mg g^{-1})	28.52
	R^2	0.81
Pseudo 2 nd order	$K_2 \cdot 10^3$ ($\text{g}(\text{mg min})^{-1}$)	22.80
	q_e (mg g^{-1})	28.52
	R^2	0.99



4. CONCLUSIONS

In this study, aluminophosphate adsorbent showed a high capacity in the removal of Cd²⁺ from aqueous solutions, and the detailed study showed that the adsorption process followed the pseudo second order kinetic model and Langmuir isotherm. The adsorbent which performed best of all ratios SiAlPO(7.5) had the maximum removal capacity of 52.63 mg/g. Therefore, the mechanisms of Cd²⁺ removal by aluminophosphate could possibly due to a combination of chemical precipitation, ion exchange and surface complexation with oxygen functional groups. The new adsorbent developed in this work show great potential for heavy metal removal. Future studies will focus on evaluating its performance in a continuous system.

REFERENCES

- Chen, H., Osman, A. I., Mangwandi C. and Rooney, D., 2019. Upcycling food waste digestate for energy and heavy metal remediation applications. *Resources, Conservation & Recycling: X*, 3, 100015.
- Choi, C. H., Kim, M., Kwon, H. C., Cho, S. J., Yun, S., Kim, H-T., Mayrhofer, K. J. J., Kim, H. and Choi, M., 2016. Tuning selectivity of electrochemical reactions by atomically dispersed platinum catalyst. *Nat. Commun.* 7, 10922.
- Luo, J., He, W. X., Qi, S. H., Wu, J. and Gu, X. S., 2020. A novel phytoremediation method assisted by magnetized water to decontaminate soil Cd based on harvesting senescent and dead leaves of *Festuca arundinacea*. *J. Hazard Mater.*, 383, 121115.



Influence of grain size distribution of compost from urban greenery on the distribution of microplastics and their leachability

H. Brtková¹, H. Raclavská¹, J. Růžičková¹, M. Šafář¹, M. Kucbel¹, P. Gikas²,
D. Juchelková³, B. Švédová¹ and K. Slamová⁴

¹ Centre ENET, VŠB-Technical University of Ostrava, Ostrava-Poruba, Czech Republic

²School of Chemical and Environmental Engineering, Technical University of Crete, Chania, Greece

³Department of Electronics, VŠB-Technical University of Ostrava, Ostrava-Poruba, Czech Republic

⁴Institute of Foreign Languages, VŠB-Technical University of Ostrava, Ostrava-Poruba, Czech Republic

Corresponding author email: michal.safar@vsb.cz

ABSTRACT

Microplastics have been found in composts made from urban greenery: polyethylene terephthalate (PET) > polystyrene (PS) > polyethylene (PE) > polypropylene (PP). Microplastics and additives are most concentrated in composts in the 0.63–1.25 mm grain size class. Additives in dry matter of compost represent 0.11–0.13% of microplastics. A maximum of 15% of the total content of chemical compounds in the dry matter passes into the aqueous leachate. The leachability of additives from compost is higher than the leachability of chemical compounds from polymers. The leaching of additives in the 0.63-1.25 grain size class affected the germination index of the watercress.

Keywords: compost; microplastics; additives; granulometry; watercress.

1. INTRODUCTION

The lack of mineral fertilisers and their ever-increasing cost force farmers to look for other sources of nutrients to ensure soil fertility that is more economically affordable and yet safe for humans and the ecosystem. There is the possibility of using compost. Truly biodegradable plastics should not be visible in compost since it is specified that these plastics should not be visible after 12 weeks in the composting process, and 90% should be mineralised after six months (Amery et al., 2020). However, parts can still be present in the compost as micro and nano plastics. A more recent definition of microplastics follows the logical differentiation according to the standard international unit nomenclature (SI units) of microplastics = 5 mm–1 µm, and nanoplastics are smaller than 1 µm (Hartmann et al., 2019).

The environmental threats and risks of microplastics (MPs) that act in the soil environment are known. They include the release of hazardous additives, entry into the food chain, accumulation in organisms, ability to adsorption of other pollutants (sorption of hydrophobic pollutants on the surface of microplastics), and environmental persistence. In soils, MPs negatively affect the ability to form soil aggregates, but on the other hand, it increases the amounts of the soil microorganisms present and does not affect the cycling of nutrients and crop growth (Li et al., 2022). Microplastics (MPs) and nanoplastics (MNPs) reach soils mainly through the direct application of composts that are used to improve soil properties (organic carbon content, moisture, nutrients, sorption capacity, etc.), sludge from WWTPs (waste-water treatment plants), irrigation, mulching (Lehman et al., 2021) or atmospheric deposition (Cai et al., 2017). Due to the high persistency of MP (Yang et al., 2021), most plastic debris fragments into smaller pieces with time and can persist in the environment for hundreds of years (Zhang and Liu, 2018). The size of MP particles is very significant in terms of their migration and accumulation along the food chain. The increased biodegradation of fine-grained PET particles was demonstrated by Farzi et al. (2020).

MNPs can be degraded through biodegradation, oxidation, hydrolysis, and photodegradation (Watteau et al., 2018). Processes of abiotic and biotic degradation of plastic are described by Zhang et al. (2021). Several studies confirm the persistence and accumulation of small plastic residues (Bläsing and Amelung, 2018). Microplastics are incorporated in soil aggregates, and thus their further mobility in the soil environment is affected. According to Zhang and Liu (2018), up to 72% of MPs form soil aggregates, and only 28% of particles are dispersed. It can be assumed that when new organic compounds



are formed when decomposing primary organic matter (cellulose, hemicellulose, and lignin), MPs will also be incorporated into emerging aggregates. The problem with composting is the possible concentration of MPs due to the decomposition of natural organic matter, similar to other persistent organic pollutants (Gui et al., 2021).

Since methods for determining MPs are not unified, a wide range of information in the literature is not comparable. A summary of commonly used analytical techniques for the analysis of microplastics is presented by Yang et al. (2021). The advantage of thermoanalytical methods (Py-GS-MS) is that the sample is not modified before analysis. Some authors consider the disadvantage of thermoanalytical methods to be a destructive technique that does not provide information on the colour, size, and shape of MPs that may be relevant in assessing their environmental properties (Yang et al., 2021). Shapes of MPs (spheres, beads, pellets, foam, fibres, fragments, films, and flakes) depend on the original form of microplastics, the degradation and erosion processes of the residence particle surface, and plastic persistence in the environment (Zhang et al., 2020).

On the contrary, the advantage of using Py-GC-MS for MP analysis can be considered the possibility of analysing additives used to improve the properties and functionality of plastics (stabilisers, flame retardants, plasticisers, lubricants, foaming agents, biocides, etc.), colourants (pigments, azocolourants, etc.), fillers (mica, kaolin, calcium carbonate, etc.), and reinforcements (e.g., glass and carbon fibres). Additives are used in concentrations from 0.001 to 1% and in biocides in the range of 20-50% (Ügdüler et al., 2020). In many cases, they are dangerous to the ecosystem and cause health risks, e.g., phthalates, as an endocrine disruptor (Grindler et al., 2018).

Polyethylene terephthalate (PET), polypropylene (PP), polyethylene (PE), and styrene are the most common polymers in compost from rural domestic waste. $2,400 \pm 358$ particles per kg (dry weight) have been identified in compost from rural domestic waste, with more than 50% of MPs occurring in a grain size class below 1 mm (Gui et al., 2021). Despite the fact that there is much information about MPs in the environment, information about the occurrence of MPS in the form of concentration and not the number of particles is scarce and shows a considerable dispersion. Recent studies on compost contain information about the concentrations of up to 1.20 g of plastics per kg (Braun et al., 2021) and from 48.3 ± 88.8 mg/kg up to $1,358 \pm 178$ mg/kg for compost with a grain size of 1–5 mm produced from municipal solid waste (Bandini et al., 2022). The average concentration of MPs in compost in Germany is estimated at 400 mg/kg for a grain size class of 1–5 mm (Henseler et al., 2022).

Information on the distribution of MPs depending on the size of the compost particles is very limited. There is only information on the content of MPs in soils from the Valencia region, which confirms that the highest amounts of MPs occur in the grain size class 150–250 μm . Other data are from Yuannan province, China, which confirms that with a larger size of soil particles, the concentration of MPs decreases, and the highest concentration was found in the class $< 490 \mu\text{m}$ (Yang et al., 2021).

The article deals with identifying the proportion of chemical compounds that identify microplastics and additives and their ability to release them into the aqueous environment depending on the size of the compost particles and the choice of measures to limit their migration.

2. MATERIALS AND METHODS

Research on microplastics and additives released from them was carried out at the OZO Ostrava composting plant. OZO Ostrava uses only municipal green waste from the maintenance of urban greenery and brown bins containing biowaste from individual housing in Ostrava (Czech Republic) as feedstock. The composting plant processes up to 15,000 tonnes of biowaste per year. Composts were collected three times during 2022 (March, May, and June). Microplastics and additives were monitored both in the matured compost (after four months – three samples) and during the composting process in the input material and after six weeks of maturation (samples collected in June). In addition to the dry matter of the sample, MPs were also monitored in an aqueous extract to determine the migration capacity of additives and MNPs.

Microplastics were determined by pyrolysis chromatography with mass spectrometry detection, which allows the analysis of individual components forming plastics and their additives in the dry matter and in the aqueous leachate. Analyses were carried out for individual grain-size classes of compost, which were prepared by sieve analysis according to EN 15428 “Soil improvers and growing media – determination



of particle size distribution”. In addition, phytotoxicity tests were carried out to assess the effect of microplastics with their additives on plant growth. A germination index (Pane et al., 2015) for watercress and white mustard was determined. In addition, leachable nutrient forms (N-NH₄⁺, K⁺) were determined in the aqueous leachate according to ISO 14911:2019 and dissolved organic carbon (DOC) and nitrogen according to ISO 20236:2018.

3. RESULTS AND DISCUSSION

Matured composts made from urban greenery contain microplastics (PET, PE, PP, and PS) in a concentration of 1,427 ± 597 mg/kg and additives in a concentration of 1.78 ± 0.81 mg/kg.

The highest concentrations were determined for compost taken in April (green harvesting and composting during winter). MPs concentration was 2,115 mg/kg, and additives had a concentration of 2.73 mg/kg. In composts taken in spring (May and June), the MPs content was comparable, but approximately 50% lower, MPs 1,125 mg/kg and additives 1.28 mg/kg (Figure 1). Additives in compost represent 0.11-0.13% of MPs.

The following plastics have been identified in the most considerable quantities in matured compost: PET > PS > PE > PP. PET relics are present in the highest amount in composts, which make up 50% of microplastics; approximately 20% are PE and polystyrene PS.

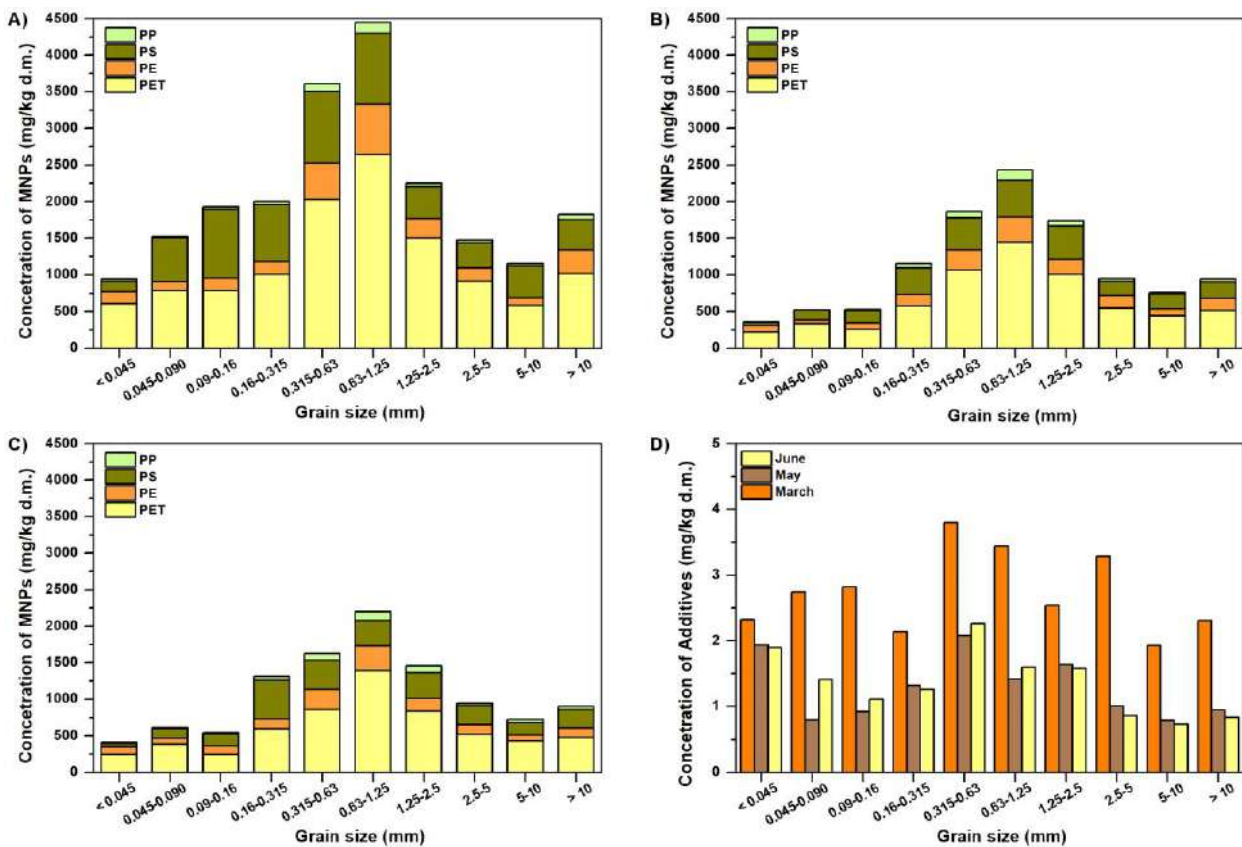


Figure 1. The distribution of MPs and additives in different grain size classes of compost: A) compost collected in March; B) compost collected in May; C) compost collected in June, and D) the distribution of additives.

The polymer type has been identified based on the occurrence of typical compounds. The PET concentration in the compost has been calculated based on the identification of the following compounds: 1,2-ethanediol, 2-ethylhexyl benzoate, 2-ethyl-1-hexanol, 2-chloroethyl benzoate, bis(2-ethylhexyl)terephthalate, 2-methylpropyl benzoate, 1,3-dioxolane, benzyl benzoate, butyl benzoate, decyl benzoate, diethylene glycol, ethyl methyl terephthalate, methyl hydrogen terephthalate, and methyl vinyl terephthalate. The PE concentration has been calculated based on the identification of 1,12-tridecadiene, 1,13-tetradecadiene, 1,14-pentadecadiene, 1,15-hexadecadiene, and hexatriacontane.



Polystyrene has been identified based on the occurrence of styrene, styrene dimer, and styrene trimer. The amount of polypropylene has been identified from 2-methyl-1-pentene (dimer), 2,4-dimethyl-1-heptene (trimer), and 2,4,6-trimethyl-1-nonene. The following compounds were identified from the additives: 2-propanol, 1-chloro-, phosphate (3:1) DM, 1,3-dioxol-2-one, 2,4-di-tert-butylphenol, 2,4,7,9-tetramethyl-5-decyn-4,7-diol, 3,5-di-tert-butyl-4-hydroxybenzaldehyde, 7,9-di-tert-butyl-1-oxaspiro(4,5)phen-6,9-diene-2,8-dione, 2,6-di-tert-nitrool (compound Bayer 28,589), benzophenone, butylated hydroxytoluene, dibutyl phthalate, diethyl phthalate, diisobutyl phthalate, isopropyl myristate, methacrylamide, n-dibutylformamide, p-terphenyl, phthalic anhydride, phthalimide, and tributyl phosphate.

The highest concentration of microplastics was found in the grain size class of 0.31–0.63 and 0.63–1.25 mm. The highest concentrations of additives were found in the grain size class 0.31–0.63 mm, which are also approximately 1.8 times higher than the concentrations in the total sample. The highest yield by weight of 20% was found in the grain size class 1.25–2.50 mm and 19% in the class 2.50–5 mm.

The highest content for all polymers was found in the 0.63–1.25 mm grain size class. Additives showed the highest concentrations in the finest < 0.045 mm grain size class and in the 0.315–0.63 mm class. In the 0.63–1.25 mm grain size class, all composts showed the highest concentration of C_{org} (June 30.07%, C_{org} concentration in the total sample 25.92%, May 28.13%, C_{org} in the total compost sample 24.87%, and for March 29.24%, the concentration in the total compost sample 25.77%). These results confirm the incorporation of MPs into the emerging natural component of compost (humic matter). However, some studies report that the presence of MPs negatively affects the humification process (Zhou et al., 2022).

A maximum of 15% of the total content of chemical compounds identified in the dry matter passes into the aqueous leachate. Most PET compounds are released into the aqueous environment, the lowest concentrations of compounds are leached from PE (0.5–5%).

The leachability of additives ranges from 1 to 33%. On average, the amounts leached from the compost in June 2022 were $195.6 \pm 60.4 \mu\text{g}$ of additives/kg, $127.1 \pm 37.6 \mu\text{g}$ of PET compounds/kg, $35.4 \pm 10.7 \mu\text{g}$ of PE compounds/kg, 22.5 ± 13.3 of PS compounds/kg, and only $10.1 \pm 6.8 \mu\text{g/kg}$ of PP compounds (the lowest leaching). Additives, which are more dangerous than the basic components contained in MPs, are the most readily leached as they are only physically bound to the polymer matrix; therefore, they are easily leached in contact with water. About 1% of the total content is transferred to leachate (Marttinen et al., 2004). The extractability of additives from OZO Ostrava composts is in accordance with data reported in the literature. Roy et al. (2018) found 17–26 μg of DEHP/L (170–260 $\mu\text{g/kg}$) in the leachate of compost prepared from municipal waste. They consider plastic bags in which waste is stored to be an important source of DEHP.

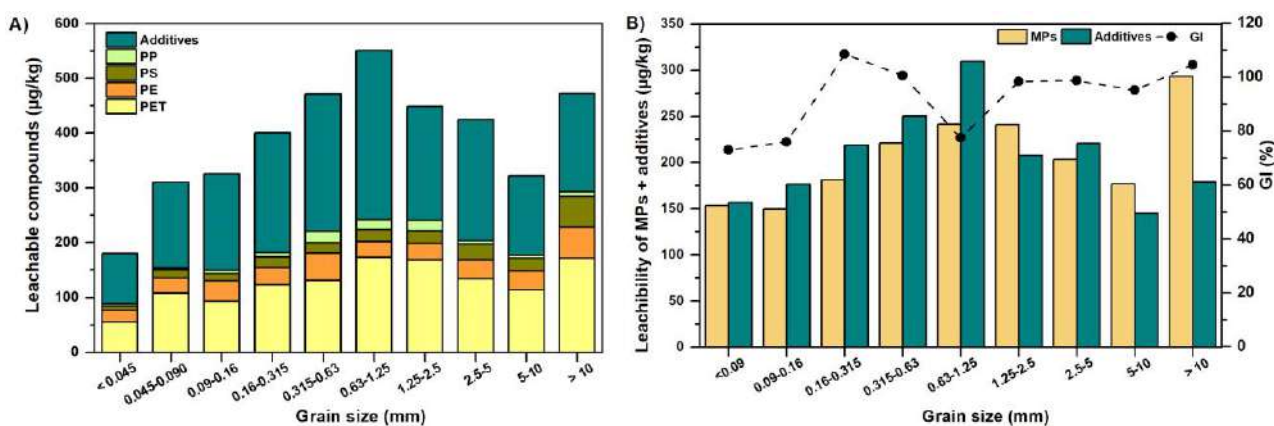


Figure 2. Leachability of MPS and additives from individual grain size class of compost (A), leachability of MPS and additives from compost in relationship to GI for watercress (B).

The leachability of additives continuously increases from the lowest grain size class to the grain size of 0.63–1.25 mm (Figure 2). The amounts leached from coarser grain size classes have no regularity. Statistically minor dependencies between the leachability of MPs and additives ($r = 0.63$, $p = 0.5$) and between the total content of additives in the dry matter and their extractability ($r = 0.61$, $p = 0.5$) were found.



The highest leachability of additives was found in the grain size class of 0.63–1.25 mm, similarly to the MPs content in the dry matter of compost. Some additives have shown a statistically significant dependence between the content in dry matter and the leachability (7,9-Di-tert-butyl-1-oxaspiro(4,5)deca-6,9-diene-2,8-dione, butylated hydroxytoluene, n,n dibutyl formamide, and for phthalates, only diisobutyl phthalate). From the additives, the most easily leached phthalates are dibutyl phthalate ($59.04 \pm 33.23 \mu\text{g}/\text{kg}$), diisobutyl phthalate ($39.77 \pm 16.82 \mu\text{g}/\text{kg}$), and 7,9-di-tert-butyl-1-oxaspiro(4,5)deca-6,9-diene-2,8-dione ($20.25 \pm 16.86 \mu\text{g}/\text{kg}$). The last one is the degradation product of IRGANOX 1010, which is part of food packaging materials (Ibarra et al., 2019).

A germination index of 68% was found for compost sampled in March 2022, with a total microplastic content of 2,115 mg/kg. For compost (May 2022), with a total microplastic content of 1,125 mg/kg, the germination index for watercress was higher (87%). The germination index was the highest (105%) for compost (June 2022), with a total microplastic content of 1,072 mg/kg. The absence of phytotoxic compounds and the maturity of the compost is confirmed by a germination index reaching the value of > 80% (Zucconi et al., 1981). Compost from March is not suitable for direct application in agriculture. For compost from June 2022, the germination index was also monitored in the individual grain classes. The lowest GI value of 78% was found for the grain size class 0.63–1.25 mm, which contained the highest concentration of MPs and additives. Unfortunately, it also contained the lowest concentration of leachable N_{tot} (4.3 g/kg), while the leachability of N_{tot} from the total sample was 8.5 g/kg.

4. CONCLUSIONS

Repeated analyses (3 times) have found that during the composting process, the highest accumulations of microplastics and also additives occur in the 0.63–1.25 mm grain size class. Additives are leached in a grain size class from 0.16 to 1.25 mm in a higher concentration than MPs (about 1.3×). The leachability from particles of size > 2.5 mm is lower than for MPs. Additives represent a bigger problem in terms of leachability than polymeric MPs particles. In the dry matter of compost and in the leachate of compost, 19 compounds have been identified which have been classified as plastic additives. On average, $15.96 \pm 6.08\%$ is leached from the dry matter of compost. Additives have been leached mostly from particles > 2.5 mm ($22.30 \pm 3.08\%$). Phthalates are compounds with the highest leachability in the group of compounds classified as additives. The germination index established for watercress has confirmed that composts from May and June 2022 do not contain phytotoxic compounds, and compost is mature and applicable in agriculture. However, certain risks are evident relating to the presence of MPs, including additives in the composting input material. These results could provide a basis for ensuring the safe application of composts on agricultural land after the addition of suitable sorbents minimising leachability or promoting the formation of soil aggregates.

5. ACKNOWLEDGEMENTS

This paper was supported by the research project of the Ministry of Education, Youth and Sport of the Czech Republic: The Doctoral grant competition V^{SB} TU-Ostrava, (Reg. No. CZ.02.2.69/0.0/0.0/19_073/ 0016945) within the Operational Programme Research, Development and Education, under the project (DGS/TEAM/2020-012) “Optimization of decomposition processes of major components of waste biomass ensuring requirements of phytotoxicity”.

6. REFERENCES

- Amery, F., Vandaele, E., Körner, I., Loades, K., Viaene, J., Vandecasteele, B. and Willekens, K., 2020. Compost quality indicators. *SoilCom*.
- Bandini, F., Taskin, E., Bellotti, G., Vaccari, F., Misci, Ch., Guerrieri, M.Ch., Cocconcelli, P.S. and Puglisi, E., 2022. The treatment of the organic fraction of municipal solid waste (OFMSW) as a possible source of micro- and nano-plastics and bioplastics in agroecosystems: a review. *Chem. Biol. Technol. Agric.*, 9.
- Bläsing, M. and Amelung, W., 2018. Plastics in soil: Analytical methods and possible sources. *Sci. Total Environ.*, 612, 15 January 2018, 422–435.
- Braun, M., Mail, M., Heyse, R. and Amelung, W., 2021. Plastic in compost: prevalence and potential input into agricultural and horticultural soils. *Sci Total Environ.*, 760, 143335.



- Cai, L., Wang, J., Peng, J., Tan, Z., Zhan, Z., Tan, X. and Chen Q., 2017. Characteristic of microplastics in the atmospheric fallout from Dongguan city, China: preliminary research and first evidence. *Environ. Sci. Pollut. Res.*, 24 (32), 24928–24935.
- Farzi, A., Dehnad, A. and Fotouhi, A.F., 2019. Biodegradation of polyethylene terephthalate waste using *Streptomyces* species and kinetic modelling of the process. *Biocatal. Agric. Biotechnol.*, 17, 25–31.
- García Ibarra, V., Rodríguez Bernaldo de Quirós, A., Paseiro Losada, P. and Sendón, R., 2019. Non-target analysis of intentionally and non intentionally added substances from plastic packaging materials and their migration into food simulants. *Food Packag. Shelf Life.*, 21, 100325.
- Grindler, N.M., Vanderlinden, L., Karthikraj, R., Kannan, K., Teal, S., Polotsky, A.J., Powell, T.L., Yang, I.V. and Jansson, T., 2018. Exposure to phthalate, an endocrine disrupting chemical, alters the first trimester placental methylome and transcriptome in women. *Sci. Rep.*, 8, 6086.
- Gui, J., Sun, Y., Wang, J., Chen, X., Zhang, S. and Wu, D., 2021. Microplastics in composting of rural domestic waste: abundance, characteristics, and release from the surface of macroplastics. *Environ. Pollut.*, 274, 116553.
- Hartmann, N.B., Hüffer, T., Thompson, R.C., Hassellöv, M., Verschoor, A., Daugaard, A.E., Rist, S., Karlsson, T., Brennholt, N., Cole, M., Herrling, M.P., Hess, M.C., Ivleva, N.P., Lusher, A.L. and Wagner, M., 2019. Are we speaking the same language? recommendations for a definition and categorization framework for plastic debris. *Environ. Sci. Technol.*, 53, 1039–1047.
- Henseler, M., Gallagher, M.B. and Kreins, P., 2022. Microplastic Pollution in Agricultural Soils and Abatement Measures – a Model-Based Assessment for Germany. *Environ. Model. Assess.*
- Lehmann, A., Leifheit, E.F., Gerdawischke, M. and Rillig, M.C., 2021. Microplastics have shape- and polymer-dependent effects on soil aggregation and organic matter loss – an experimental and meta-analytical approach. *Micropl. Nanopl.* 1.
- Li, H., Liu, L., Xu, Y. and Zhang, J., 2022. Microplastic effects on soil system parameters: a meta-analysis study. *Environ. Sci. Pollut. Res.*, 29, 11027–11038.
- Marttinen, S.K., Hänninen, K. and Rintala, J.A., 2004. Removal of DEHP in composting and aeration of sewage sludge. *Chemosphere*, 54, 265–272.
- Pane, C., Celano, G., Piccolo, A., Vilecco, D., Spaccini, R., Palese, A.M. and Zaccardelli, M., 2015. Effects of on-farm composted tomato residues on soil biological activity and yields in a tomato cropping system. *Chem. Biol. Technol. Agric.*, 2.
- Roy, D., Azaïs, A., Benkaraache, S., Drogui, P. and Tyagi, R.D., 2018. Composting leachate: characterization, treatment, and future perspectives. *Rev. Environ. Sci. Biotechnol.*, 17, 323–349.
- Ügdüler, S., Van Geem, K.M., Roosen, M., Delbeke, E.I.P. and de Meester, S., 2020. Challenges and opportunities of solvent-based additive extraction methods for plastic recycling. *Waste Manag.*, 104, 148–182.
- Watteau, F., Dignac, M.F., Bouchard, A., Revallier, A. and Houot, S., 2018. Microplastic detection in soil amended with municipal solid waste composts as revealed by transmission electronic microscopy and pyrolysis/GC/MS. *Front. Sustain. Food Syst.*, 2, 81.
- Yang, L., Zhang, Y., Kang, S., Wang, Z. and Wu, Ch., 2021. Microplastics in soil: A review on methods, occurrence, sources, and potential risk. *Sci. Total Environ.*, 780, 146546.
- Zhang, G.S. and Liu, Y.F., 2018. The distribution of microplastics in soil aggregate fractions in southwestern China. *Sci. Total Environ.*, 642, 12–20.
- Zhang, K., Hamidian, A.H., Tubić, A., Zhang, Y., Fang, J.K.H., Wu, Ch. and Lam, P.K.S., 2021. Understanding plastic degradation and microplastic formation in the environment: A review. *Environ. Pollut.*, 274.
- Zhang, Y., Kang, S., Allen, S., Allen, D., Gao, T. and Sillanpää, M., 2020. Atmospheric microplastics: A review on current status and perspectives. *Earth Sci. Rev.*, 203.
- Zhou, Y., Sun, Y., Liu, J., Ren, X., Zhang, Z. and Wang, Q., 2022. Effects of microplastics on humification and fungal community during cow manure composting. *Sci. Total Environ.*, 803, 150029.
- Zucconi, F., Forte, M., Pera, A. and de Bertoldi, M., 1981. Evaluating toxicity of immature compost. *BioCycle*, 22, 54–57.



Water quality analysis using physicochemical parameters and estimation of pesticides from various sources of Tirupati, Andhra Pradesh, India

K. Swathi¹, M. Malleswari¹ and B. Nikitha¹

¹Institute of Pharmaceutical Technology, Sri Padmavati Mahila Visvavidyalayam, Tirupati, Andhra Pradesh
India

Corresponding author email: kswathi84@yahoo.co.in

Keywords: Physico-chemical Parameters; Water Quality; Pesticide Analysis; Tirupati; GC-MS.

1. INTRODUCTION

Water plays a significant role in maintaining the human health and welfare. Clean drinking water is now recognized as a fundamental right of human beings. Around 780 million people do not have access to clean and safe water and around 2.5 billion people do not have proper sanitation. As a result, around 6–8 million people die each year due to water related diseases and disasters. Therefore, water quality control is a top-priority policy agenda in many parts of the world. Next inorganic chemicals hold a greater portion as contaminants in drinking water in comparison to organic chemicals. Inorganics mostly are in mineral form and are of heavy metals. Heavy metals tend to accumulate in human organs and nervous system and interfere with their normal functions.

Tirupati is one of the famous Tourist places in India. So, Safe Drinking water is priority. Therefore, to handle ground water contamination and to aware the people in the area of Tirupati, in Present Paper, Research was conducted with the Goal to Estimate Water Quality by using Physico-chemical Parameters and analysis of pesticides with analytical technique (GC-MS) of ground water in and around Tirumala, Tirupati Located at Andhra Pradesh State of Country India. For this estimation, Ground water Samples were collected from Different Locations of Tirupati i.e., Sri Padmavati Mahila Visvavidyalayam (Women's University), Mallamgunta, LB nagar, Singalagunta, SV University, Perumallapalli, Settipalli, AK palli, Srikrishna nagar, Gandhipuram, Pathalaganga, Cherllopalli areas and Water quality parameters (alkalinity, pH, Total Hardness, chloride, calcium, potassium, and silica) were tested. Based on the Physico-Chemical Parameters obtained it can be concluded that water was good for example some areas from present study like the sample which is collected at Tirumala patahlaganga were found be within the standard limits set by WHO so it is pure water without any contaminants. RO water doesn't contain any contaminants it is free from dissolved solids, ions so it is pure and clean water. Ground water sample which is collected from Tirupati area is less polluted than surface water sample so it is pure when compared with tap water. Hence, drinking water pollution should be Controlled by the proper environment management plan. Ground and surface water of this area should be treated to Make suitable for drinking and to maintain proper health Conditions of people living in this area.

Among all sample which is collected from ground water from the fields of Settipalli area exceeded the standard limits set by WHO and BIS which suggests poor water quality.

The present study reported the contamination status of diclorvos, methyl parathion, parathion, malathion in ground water of Tirupati in Settipalli, Andhra Pradesh, India.

In agriculture, pesticides are frequently viewed as a quick, simple, and low-cost option for controlling weeds and insect pests. Pesticide use, on the other hand, has a huge environmental cost. Pesticides have infiltrated nearly every aspect of our ecosystem.

The results obtained from the present study shall be useful in future management of the Ground Water in Tirupati area.

2. MATERIALS AND METHODS

2.1. Study area

The current study examines the quality of water in several areas in Tirupati, Chittoor district, Andhra Pradesh, in terms of physicochemical parameters. It is situated at a latitude of 13.6288 N and a longitude of 74.4192 E. Tirupati covers a total area of 27.44 km². Water is used for agriculture, residential, and fishing activities in various locations of Tirupati.



For residential and drinking purposes, people in rural areas around Tirupati rely primarily on ground water. The goal of this study was to obtain Physicochemical analysis of water in order to assess the health of the people who live in this area. According to the WHO, contaminated water causes 600 million instances of diarrhea and 46,00,000 childhood deaths per year. For drinking purposes, most Indians rely on surface and ground water.



Figure 1. Location of sample collection.

2.2. Selection of Sampling Points

As a result, 13 alternative localities in the state of Chittoor were picked based on predetermined criteria. SPMVV, lb Nagar, mallamgunta, singalgunta, Sv university, perumallapalli, settipalli, AK palli, Srikrishna Nagar, gandhipuram, pathalaganga, and cherlopalli were among the places visited. (See Table 1).

Table 1. Details of the samples with various areas of Tirumala and Tirupati.

S.No	Area in Tiumala and Tirupati	SAMPLE	Sample no
1	SPMVV	Tap water	S1
2	Mallamgunta	Bore water	S2
3	LB nagar	Bore water	S3
4	Singalagunta	Telugu ganga water	S4
5	SV University	Tap water	S5
6	Perumallapalli	Drinking water	S6
7	Perumallapalli	Bore water	S7
8	Settipalli	Pond water	S8
9	AK palli	Bore water	S9
10	Srikrishna nagar	RO water	S10
11	Gandhipuram	Tap water	S11
12	Pathalaganga	Water falls	S12
13	Cherllopalli	Bore water	S13

2.3. Sample Collection

The research region depicts a distinct composite environment comprising the rural and urban confluence of Tirupati and Tirumqla's total 13 places. Tirupati is located in the Chittoor district of Andhra Pradesh. It is situated at a latitude of 13.6288 N and a longitude of 74.4192 E. Tirupati covers a total area of 27.44 km². Water is used for agriculture, residential, and fishing activities in various locations of Tirupati.

All the sampling locations, such as restaurants and private residences, are open to the public. The samples were assigned a number between 1 and 13 based on their locations and sources (Table 1). The samples were collected in 1-liter polyethylene (PE) bottles washed with deionized water before use. These sample vials were sealed and kept in a dark environment at a constant temperature of 4–10°C to avoid contamination and the effects of light and temperature.



Each of the duplicate samples was tested in the laboratory for a number of criteria in order to assess the overall drinking water quality.

2.4. Labelling of samples

To avoid any confusion or error, each sample was properly coded and marked with a permanent marker at two locations on sampling bottles, as well as recording all of the information about the sampling site, source, and date of collection in a field book.

Table 2. Methods Used for Analysis of Physico-chemical Parameters.

Water quality test	Description	Method /Instrument
Temperature	It exerts a major influence on biological activities & growth	Thermometer
Colour	True colour of water from which turbidity removed	Visual comparison
pH	The major of acidity [hydronium ion, H ⁺] in water	pH meter
Conductivity	-	Conductivity meter
Total hardness	Measurement of Ca & Mg in water	Titrimetric method
Calcium & Mg, Cl	Measurement of Ca & Mg, Cl amount in water	Titrimetric method
Na & k	Measurement of Na & K amount in water	Flame photometer
Nitrate, Fluoride	--	Spectrophotometer
Turbidity	It is the reduction of transparency	Turbidity meter
Alkalinity	It is quantitative capacity to react with strong acid to a designated pH.	Titrimetric method
TDS	Measure of amount of total particulate solids	TDS meter

2.5. Analytical Method

Systematically, both volumetrically and using instrumental techniques, the analysis was conducted out. The pH, temperature, turbidity, dissolved oxygen, conductivity, total dissolved solid, alkalinity, and acidity of the collected water samples were all tested analytically. The tap water and ground water were used as sampling points for water samples throughout the study. To examine the nature and amount of pollution, observations and findings were regularly recorded for parameters like as pH, temperature, turbidity, conductivity, TDS, DO, alkalinity, and acidity.

Total dissolved solids, dissolved oxygen, turbidity, acidity, and alkalinity were measured according to the usual guidelines and procedures given in the guide manual and other reference materials. The gathered waste water samples can be kept without affecting the samples' biodegradation characteristics, and their biodegradation characteristics are evaluated. All of the reagents used in the experiment were of analytical quality.

2.6. Pesticides analysis in water sample Reagents, standards, and sample

- From the various sources standards malathion, methyl parathion, dichlorvos, parathion were



purchased.

- In 200 mg/l in CHCl₃ stock solution were prepared for every pesticide.
- In CHCl₃ 55 mg/l parathion and 100 mg/l methyl parathion, parathion, diclorvos, malathion concentrations were prepared.
- In the freezer all these solutions were stored.
- HPLC grade ethyl acetate solvent was purchased.

2.7. Sample

- The underground water sample was taken from the Settipalli sample from 8 fields which was done all physicochemical parameters and it exceeded the standards set by WHO so this sample was analyzed for pesticides.
- The sample filtered with 0.45 um membrane before analysis and GC-MS performed.

3. RESULTS AND DISCUSSION

Table 3. Details of the samples with various areas of Tirumala and Tirupati.

S.No	Area in Tiumala and Tirupati	SAMPLE	Sample no
1	SPMVV	Tap water	S1
2	Mallamgunta	Bore water	S2
3	LB nagar	Bore water	S3
4	Singalagunta	Telugu ganga water	S4
5	SV University	Tap water	S5
6	Perumallapalli	Drinking water	S6
7	Perumallapalli	Bore water	S7
8	Settipalli	Pond water	S8
9	AK palli	Bore water	S9
10	Srikrishna nagar	RO water	S10
11	Gandhipuram	Tap water	S11
12	Pathalaganga	Water falls	S12
13	Cherilopalli	Bore water	S13

Table 4.0. Experimental results for the Physico-Chemical Parameters in Study area.

S.No	Parameter	S1	S2	S3	S4	S5	S6
1	Colour	colourless	colourless	Colourless	Colourless	Colourless	Colourless
2	odour	odourless	odourless	odourless	odourless	odourless	odourless
3	appearance	clear	clear	clear	clear	clear	clear
4	conductivity	744	199.9	614	485	325	648
5	turbidity	21	1.6	1.7	2.2	2	1.9
6	pH	6.78	8.2	7.3	8.5	7.2	8.2
7	TDS	836	260	487	383	271	515
8	Dissolved oxygen	2.56	1.28	3.584	2.688	3.712	2.56
9	acidity	60	130	110	40	90	100
10	alkalinity	542	480	490	380	350	560



11	temperature	28.7	28	29.6	31.6	28.6	28.9
----	-------------	------	----	------	------	------	------

Table 4.1. Experimental results for the Physico-Chemical Parameters in Study area.

Parameter	S7	S8	S9	S10	S11	S12	S13
Colour	Colourless	Colourless	Colourless	Colourless	Colourless	Colourless	Colourless
odour	odourless	odourless	odourless	odourless	odourless	odourless	odourless
appearance	clear	Muddy	clear	clear	clear	clear	Muddy
conductivity	1139	1755	614	525	984	76.2	350
turbidity	0.6	8.9	2.8	1	2.4	2.2	3.1
pH	7.6	7.2	6.7	6.6	6.9	6	7
TDS	111	1260	412	716	810	29	810
Dissolved oxygen	2.432	0.000096	3.456	3.968	3.712	3.84	2.56
acidity	50	330	120	170	70	30	220
alkalinity	320	820	490	500	400	350	290
Temperature	28	28	29.8	29.9	31	30.9	29.8

3.1 Chromatographic separation

✓ Under the optimized GC–MS conditions, a baseline separation for the four OPPs was obtained. A typical chromatogram is shown in Figure 1.

✓ The identification of OPPs was made on the basis of standard solution retention times and mass spectra of the four OPPs. Figure 2 shows the mass spectra of the four OPP compounds in this study.

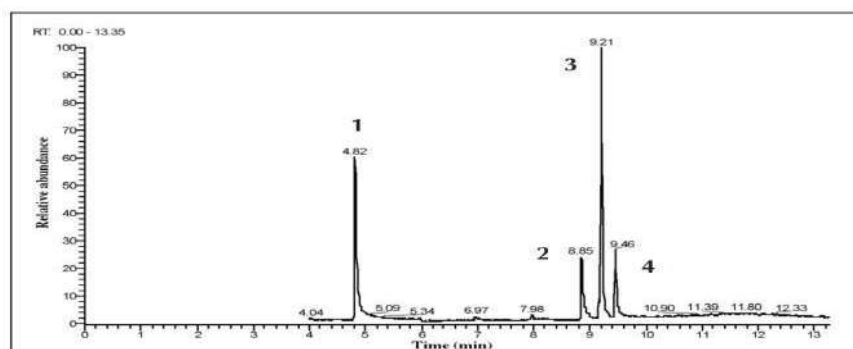


Figure 2. Total ion chromatogram (TIC) of the four OPPs. Experimental conditions: DB-5MS fused-silica column (30 m × 0.25 mm; 0.25 μm); Carrier gas (99.999% Helium) flow rate: 1.0 mL/min; Temperature program: T₀ = 50°C; T₀ – T₁, 30°C/min, T₁ = 150°C (hold, 1 min); T₁ – T₂, 30°C/min, T₂ = 210°C; T₂ – T₃, 10°C/min, T₃ = 250°C (hold, 3 min); Injection: splitless mode at 250°C; Injection volume: 1.0 μL; Solvent delay: 4.00 min; EI, 70 eV; MSD transfer-line temperature: 280°C; Ion source temperature: 230°C; Mass range: m/z 50–650. Peak identification: 1, dichlorvos; 2, methyl parathion; 3, malathion; 4, parathion.

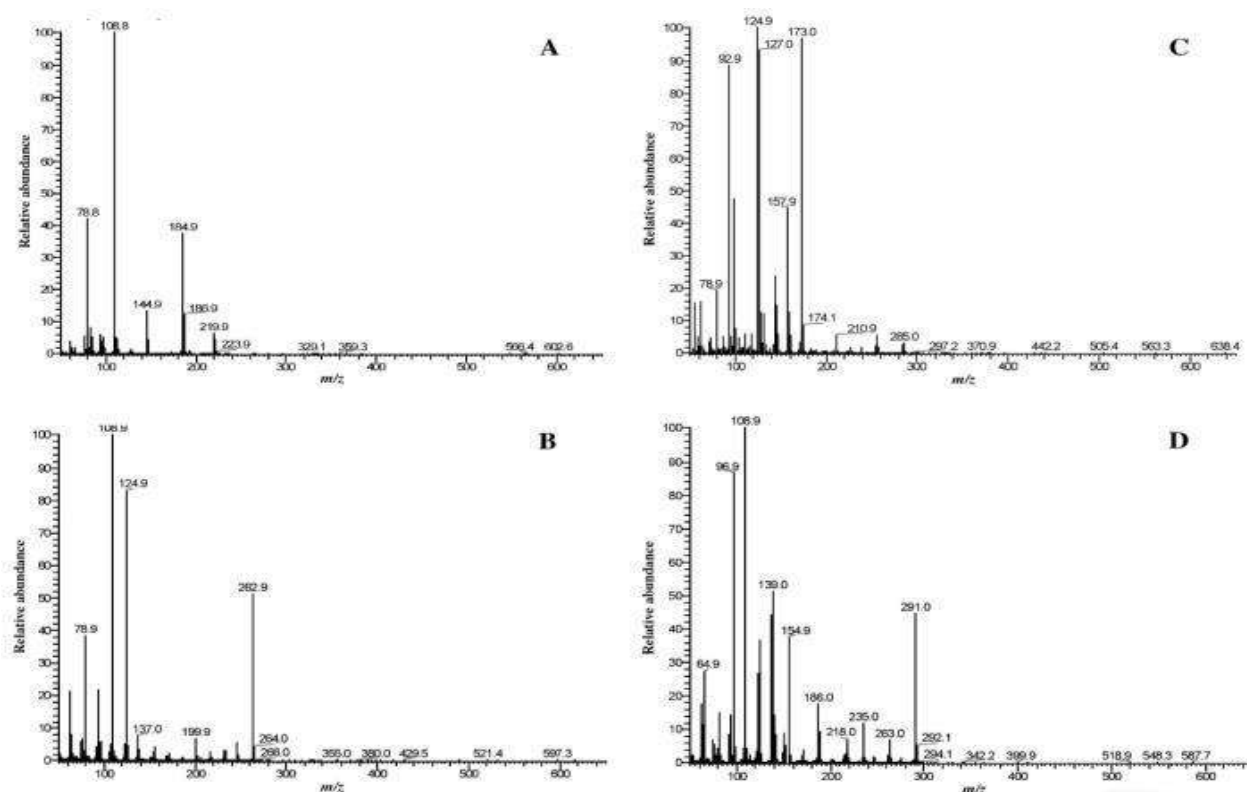


Figure 3. Mass spectra of the OPPs: mass spectrum of dichlorvos (A); mass spectrum of methyl parathion (B); mass spectrum of malathion (C); mass spectrum of parathion (D).

3.2 Calibration

- Calibration curves were obtained preparing six level concentrations for each analyte (0.01, 0.05, 0.10, 0.50, 1.00, and 2.00 mg/L) except for of parathion, for which concentrations were 0.0055, 0.0275, 0.055, 0.275, 0.55, and 1.1 mg/L.
- A mixture containing each analyte at the specified concentration was injected. Detection was performed referring to the selective ions listed in Table I. The results obtained for the regression are collected in Table 2.

Table 5. List of Ions and Time Windows used for SIMEI–MS Detection.

Compound	Starting time/min	m/z
Dichlorvos	4	109, 79, 185, 220
Methyl parathion	8	109, 263, 125
Malathion	9	125, 93, 173, 127, 285
parathion	9.35	109, 125, 155, 139, 291

Table 6. Retention Times and Regression Results for the analytes.

Analyte	Retention time (min)	Regression equation	r ²	linear range (mg/l)
Dichlorvos	4.82	$y = 1 \times 10^7x + 129629$	0.9967	0.01–2.00
Methyl parathion	8.85	$y = 1 \times 10^7x - 636386$	0.9820	0.01–2.00
malathion	9.21	$y = 1 \times 10^7x + 2863160$	0.9928	0.01–2.00



parathion	9.46	$y = 1 \times 107x + 83557$	0.9900	0.0055–1.10
-----------	------	-----------------------------	--------	-------------

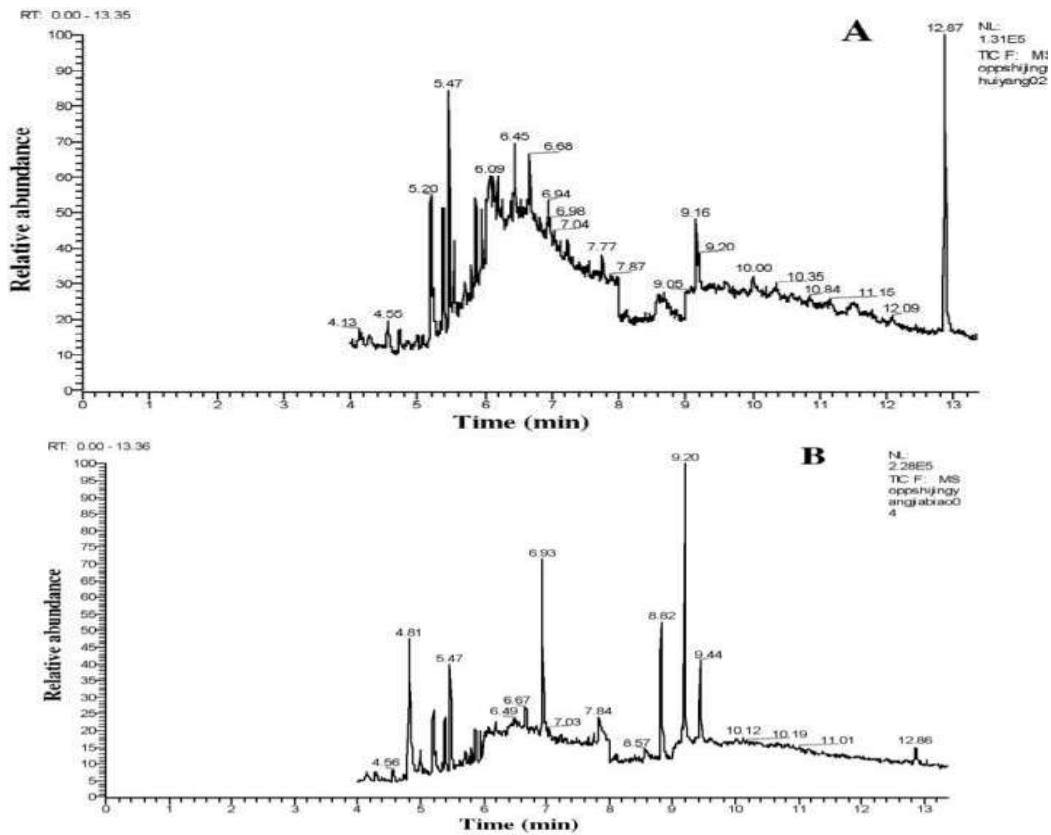


Figure 4. Chromatogram obtained by SPE-GC-MS(TIC) of unspiked underground water samples (A)underground water samples spiked with OPPs (final conc of 0.5 ug/l).peak identification :1,dichlorvos (4.81 min),2,methyl paarthion (8.82),3,malathion (9.20 min),4,parathion (9.44 min).

4. CONCLUSIONS

To handle ground water contamination and to aware the people in the area, and to giving further research this study was conducted. The study objectives are evaluation of physico chemical parameters and analysis of pesticides with analytical techniques ground water of Tirupati, Tirumala, Andhra Pradesh.

The water of Andhra Pradesh and Tirupati region are studied for various physico-chemical properties. The study was carried out by collecting ground water from this region. Based on physicochemical analysis of ground water samples gathered in several Tirupati locations. Water quality parameters (alkalinity, pH, Total Hardness, chloride, calcium, potassium, and silica) were tested in some samples.

From the observations it can be concluded that the concentration of turbidity, conductivity, total acidity content, Dissolved oxygen are within the limits but only on sample i.e., S8 the water which is collected at ground water in fields exceed the standard limits set by WHO and BIS, which suggests poor water quality in these water samples (S8 Settupalli).

The sample which is collected at Tirumala (patahlaganga) sample S12 were found to be within the standard limits set by WHO so it is pure water without any contaminants.

RO (sample 10) doesn't contain any contaminants it is free from dissolved solids, ions so it is pure and clean water.

Ground water sample which is collected from Tirupati area is less polluted than surface water sample so it is pure when compared with tap water.

Hence, drinking water pollution should be controlled by the proper environment management plan. Ground and surface water of this area should be treated to make suitable for drinking and to maintain proper health conditions of people living in this area.



The present study reports the contamination status of diclorvos, methyl parathion, parathion, malathion in ground water in Tirupati sampleS8 (Settipalli), Andhra Pradesh, India.

In agriculture, pesticides are frequently viewed as a quick, simple, and low-cost option for controlling weeds and insect pests. Pesticide use, on the other hand, has a huge environmental cost. Pesticides have infiltrated nearly every aspect of our ecosystem.

Pesticide residues can be found in the soil, air, surface water, and groundwater, among other places. OCPs, OPPs, and their derivatives are the most common pesticides found in water from various sources because they last a long time in the environment. The flow of harmful heavy metals and pesticides pollutes the rivers severely.

These toxic compounds do not decompose; they stay persistent in the environment and have the potential to bioaccumulate in the food chain, posing long-term dangers. It may be inferred that the presence of high quantities of organochloride pesticides in India may cause significant sanitary and ecological issues. To control pesticide contamination in India, better educational and control activities are required. The goal of this research is to gain a better knowledge of the causes of water quality degradation caused by pesticide residues and to create solutions to reduce the losses caused by residues.

Farmers must be aware of the problem so that excessive use can be curtailed. Strict action against suppliers of illegal or forged pesticides, as well as the adoption of integrated pest control strategies, may be viable options for reducing pesticide use in the future.

5. ACKNOWLEDGEMENTS

This study is supported by Sri Padmavati Mahila Visvavidyalayam, Tirupati, Andhra Pradesh, India.

REFERENCES

- Gupta, D., Sunita and Saharan, J. P., (2009). Physiochemical Analysis of Ground Water of Selected Area of Kaithal City (Haryana) India, *Researcher*, 1(2), pp 1-5.
- Martins, M. L., Prestes, O. D., Adaime, M. B. and Zanella, R., 2014. Determination of Pesticides and Related Compounds in Water by Dispersive Liquid–Liquid Microextraction and Gas Chromatography–Triple Quadrupole Mass Spectrometry. *Anal. Meth.*, 6 (14), 542.



Theoretical investigation of halloysite as potential sorbent for pharmaceutical wastewaters

E. Gianni^{1,2} and E. Scholtzová^{2*}

¹Centre for Research and Technology, Hellas (CERTH), 15125 Marousi, Greece

²Institute of Inorganic Chemistry, Slovak Academy of Science, Dúbravská cesta 9, 84536 Bratislava, Slovakia

Corresponding author email: eva.scholtzova@savba.sk

ABSTRACT

Antitumoral drugs are dominant in municipal and hospital wastewaters with a major impact on the natural environment. The treatment of such wastewaters is crucial for their safe disposal in the environment and the limitation of the effects on human and animal health. CPT-11 is an industrial antitumoral drug extensively studied for various cancer types. The adsorption technique is one of the most promising and low-cost methods for wastewater treatment. Halloysite clay mineral is theoretically studied in the present work for its ability to adsorb CPT-11 in its structure. *Ab initio* Density Functional Theory (DFT) method was used for the investigation of the adsorption energy and interactions among the halloysite and all forms of CPT-11. Halloysite was found to be a potential medium for drug removal from wastewater under different pH values.

Keywords: halloysite; CPT-11; drug removal; hospital wastewaters; DFT-D3.

1. INTRODUCTION

The presence of antitumoral drugs is dominant in municipal and hospital wastewaters with a major impact on the natural environment. CPT-11 (Irinotecan, Fig. 1), is a chemotherapeutic agent which can be used for various cancer types and is extensively studied the last years (Gianni et al., 2019) since is an industrial medicinal substance. Therefore, 45% to 63% is excreted as parent drug by the human body, concluding to wastewater and further the groundwater (Slatter et al., 2000). Numerous methods have been applied for drug removal from water and wastewaters, with sorption to outweigh among other methods due to the low initial cost, operational simplicity and absence of harmful byproducts (Ahmad et al., 2010). Clay minerals are considered superb when compared to other commercial adsorbents for organic pollutants (e.g., graphene oxide) since are abundant materials, cost-effective, with significant sorption capacities and surficial properties (Han et al., 2019). Halloysite is a clay mineral that had been extensively tested for its sorption properties due to its nanotubular morphology, the combination of negative outer (octahedral, O) and positive inner (tetrahedral, T) surface charge of its crystals, its high specific surface area and the low cost (Gianni et al., 2019). These properties facilitate the development of interactions between the mineral and the organic pollutants.

CPT-11 differentiates in two forms; an active lactone form and an inactive hydroxyl-acid anion form. Acidities determine the prevail of the form. Lactone prevails in an acidic to slight alkaline pH and hydroxyl acid anion form in strong alkaline pH values (Slatter et al., 2000). At a pH range of 1.11 to 9.46, the cationic and neutral form of the active substance are favored (Di Nunzio et al., 2018). In the present study, the adsorption energy and hydrogen bonds between halloysite and all forms of CPT-11 were investigated *via* Density Functional Theory (DFT) calculations for the potential use of the halloysite mineral as a sorption medium for this drug removal from wastewaters.

2. COMPUTATIONAL MODELS AND METHOD

2.1. Computational models

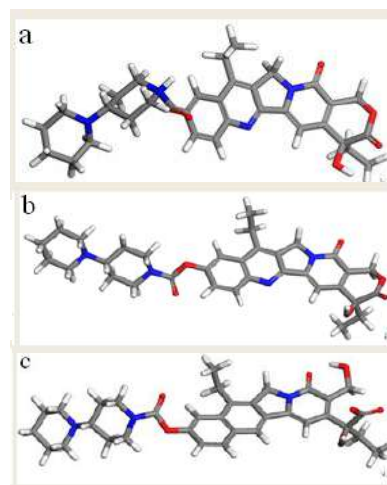


Figure 1. (a) Cationic, (b) Neutral and (c) Anionic form of CPT-11.



The elementary cell of halloysite by Mehmel (1935), was used in the present study. The missing hydrogen atoms were added into the structure according to the symmetry rules ($a = 5.151 \text{ \AA}$, $b = 8.900 \text{ \AA}$, $c = 7.570 \text{ \AA}$, $\beta = 100^\circ$) in the final $P1$ space group symmetry. Further, larger halloysite computational model was created by multiplying the elementary cell as $3a \times 2b \times 1c$ ($A = 14.919 \text{ \AA}$, $B = 17.814 \text{ \AA}$, $C = 50.000 \text{ \AA}$, $\alpha = 92.80^\circ$, $\beta = 94.43^\circ$ and $\gamma = 90.81^\circ$, 204 atoms) to fit the adsorbed drug molecule. To keep the neutral charge of the whole system, the substitutions were done if necessary ($\text{Si}^{4+}/\text{Al}^{3+}$ for the negative surface of halloysite and $\text{Al}^{3+}/\text{Ti}^{4+}$ for the positive one). In total, six initial models were created (Fig. 2): 1. Negative T sheet interacted with the cationic form of the drug, 2. Neutral O sheet of halloysite interacted with the aromatic ring of the neutral drug molecule, 3. Neutral O interacted with the carboxylate group of the neutral drug molecule, 4. Neutral T interacted with the aromatic ring of the neutral drug molecule, 5. Neutral T interacted with the carboxylate group of the neutral drug molecule, and 6. Positive O interacted with the anionic form of the drug. It must be highlighted that these periodic models represent 'a planar structure of halloysite' or a curved structure with infinite radius. Models with already known repulsive interactions were not tested as it was unnecessary (e.g. interaction of cation with the positive O surface).

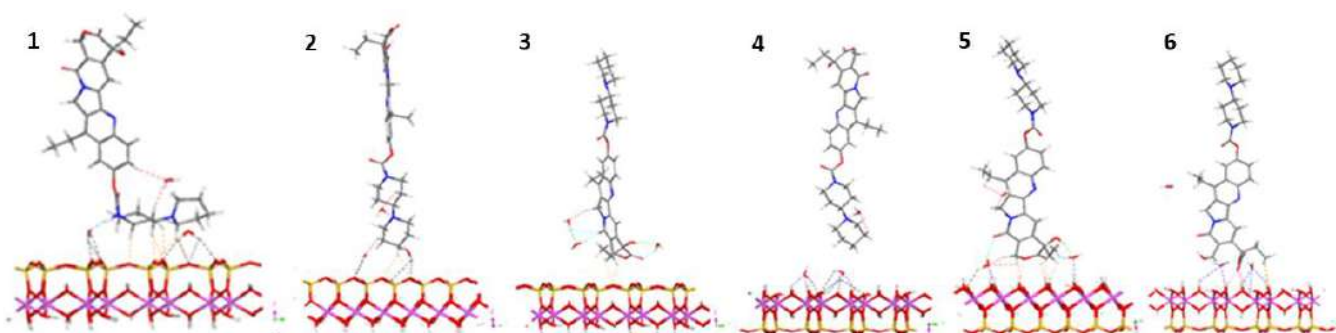


Figure 2. Optimized structural models of respective halloysite surface and drug form.

2.2 Computational method

All calculations on the models mentioned above were performed using the DFT method implemented in the VASP program (Kresse & Hafner, 1993; Kresse & Furthmuller, 1996a,b) first time. The exchange-correlation energy was described by Perdew, Burke, and Ernzerhof (PBE) functional which is based on the generalized gradient approximation (GGA) theory (Perdew et al., 1996, Grimme, 2006). The Kohn-Sham equations were calculated by the variation method with a plane-wave (PW) basis set with the kinetic energy cut-off of 500 eV in the projector-augmented-wave (PAW) method (Blochl, 1994; Kresse & Joubert, 1999). Because of the large size of the computational cells of models, Brillouin-zone sampling was restricted to the Γ point only. The computational cell was fully optimized. The relaxation criteria were 10^{-5} eV/atom for the total energy change and 0.015 eV/ \AA for the maximal allowed forces acting on each atom. Owing to the weak interactions between the layers and intercalated compounds in the structure, DFT calculations were performed with involving of dispersion corrections using D3 scheme (Grimme et al., 2010).

Hydrogen-bond interactions and also the adsorption energy (ΔE_{ads}) of the models, based on the following equation, were calculated:

$$\Delta E_{ads} = E_{Total} - (E_{Hal+Wat} + E_{Irin})$$

where E_{Total} the total energy of the system, $E_{Hal+Wat}$ the total energy of halloysite and water molecules excluding irinotecan molecule and E_{Irin} the total energy of irinotecan molecule.

3. RESULTS AND DISCUSSION

The analysis of calculated total energies of the modelled systems, hydrogen bonds formed by drug with the respective halloysite surface and present water molecules as well as adsorption energies revealed the most stable mutual constitution of halloysite surface and respective drug form.



The energetically preferred system (**6**) includes the anionic form of CPT-11 interacting with the O surface of the halloysite (-189675 kJ/mol) (see Table 1). The anionic form of the drug exists only in strong alkaline pH environment. The total energy of the cationic CPT-11 (**1**) interacting with the outer T surface of halloysite is also low (-188381 kJ/mol), and this system is due to mutual electrostatic interactions more stable than systems containing the neutral form of the drug (**2-5**). When the drug is in the neutral form, it preferably interacts through its carboxylate group with the octahedral surface of the halloysite (-188279 kJ/mol).

Table 1. Total and adsorption (ΔE_{ads}) energies of the optimized models [kJ/mol].

Model	1	2	3	4	5	6
Total energy	-188381	-188145	-188181	-188183	-188279	-189675
ΔE_{ads}	-573	-54	-85	-37	-138	-320

The analyzed and described present hydrogen bonds (Table 2) with their strength correlate well with the values of calculated adsorption energies (Table 1) for respective models. Based on the adsorption energy, the most stable system is when the drug is in the cationic form (**1**/-573 kJ/mol), which is the most common form in neutral and acidic conditions. The high stability is caused by the presence of C-H...Ob H-bonds (Ob - basal oxygen) that are stronger than every other type, and they directly interact with the T surface of the halloysite. Moreover, the presence of very strong "non-direct" hydrogen bonds, which support the anchoring of drugs onto the halloysite surface, is crucial for the stability of the system. Model **6** also has high adsorption energy (-320 kJ/mol) due to electrostatic interactions, weak C-H...Oo bonds (Oo - oxygen of O sheet), strong "non-direct" H-bonds and strong Oo-H...Oi bonds (Oi-oxygen of irinotecan) which probably enhance the interactions in the system. In the case of a neutral drug, weaker interactions exist in the systems. However, this is not a problem as in nature, drug tends to convert into ion depending on the conditions of the surrounding environment.

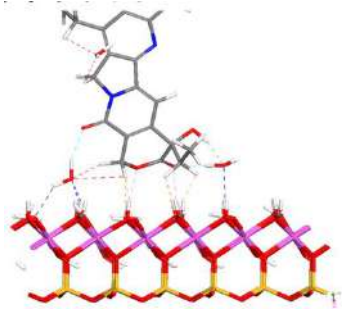
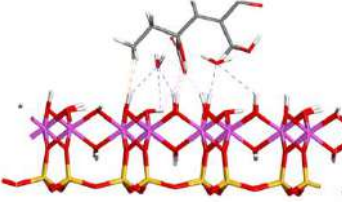
Although, when a neutral drug interacts with halloysite, the carboxylate group of CPT-11 is the one that interacts with the mineral preferably with the octahedral surface of halloysite. Both total energy and adsorption energy of Model **5** are lowest than the other tested arrangements of the drug molecule. At this favored state, there are weak C-H...Oo bonds and "non-direct" C-H...Ow bonds, while strong Oo-H...Oi bonds reducing the interaction energy (**5**/-138 kJ/mol). When the aromatic part of CPT-11 interacts with O, there is a lack of direct interactions between the mineral and the drug and thus the adsorption energy increased (**4**/-37 kJ/mol), giving non stable conditions compared with the other models. Only weak C-H...Ob bonds and weak "non-direct" bonds exist when the aromatic part of CPT-11 interacts with T (**2**/-54 kJ/mol), leading in the conclusion that aromatic part of the molecule is not the favored one for creating strong interactions with the halloysite structure. When the carboxylate part of CPT-11 interacts with T, the adsorption energy is getting lower (**3**/-85 kJ/mol), due to the weak C-H...Ob bonds, proving that carboxylate part preferable interacts with both surfaces of halloysite with preference in the octahedral one.

Table 2. Hydrogen bonds for respective models: H...A – hydrogen ... acceptor; D...A – donor ... acceptor and D-H-A hydrogen bond angle. The background color of the respective type of HB corresponds with the color of HB in the figure of model.



Type	H··A (Å)	D··A (Å)	Angle D-A (°)	Model 1	Description		
C-H··Ow	2.289	3.362	163.2		Weak and strong C-H··Ob bonds to T. One strong N-H··Ow bond between the drug and a water molecule, which is continuously connected through strong and weak Ow-H··Ob bonds to T.		
	2.510	3.578	167.8				
Ow-H··Ob	1.645	2.625	92.5				
	2.297	3.086	129.6				
C-H··Ob	3.199	3.513	162.0				
	2.162	3.231	118.7				
N-H··Ow	2.569	3.492	144.7				
	2.848	3.584	163.9				
	1.442	2.581	176.5				
Type	H··A (Å)	D··A (Å)	Angle D-A (°)			Model 2	Description
C-H··Ow	2.657	3.470	130.0				Weak C-H··Ob bonds connect the molecule with T directly. A weak C-H··Ow bond between the drug and a water molecule continuously connected to T via weak Ow-H··Ob.
	2.796	3.613	130.8				
Ow-H··N	1.835	2.827	171.2				
	2.146	3.059	98.2				
Ow-H··Ob	2.284	3.214	156.2				
	3.109	3.392	161.7				
C-H··Ob	2.663	3.511	122.8				
	2.910	3.624	133.6				
Type	H··A (Å)	D··A (Å)	Angle D-A (°)	Model 3	Description		
C-H··Ow	2.197	3.234	155.0		Weak C-H··Ob bonds connect the molecule with T.		
Ow-H··Oi	1.708	2.675	110.6				
	1.824	2.716	148.9				
Ow-H··Ow	1.796	2.778	169.4				
Oi-H··Ow	1.796	2.780	170.2				
C-H··Ob	2.571	3.471	106.0				
	3.166	3.629	138.6				
Type	H··A (Å)	D··A (Å)	Angle D-A (°)	Model 4	Description		
C-H··Ow	2.701	3.473	126.7		No H-bonds between halloysite and irinotecan molecule.		
Ow-H··N	1.843	2.830	168.9				
Ow-H··Oo	1.686	2.654	103.6				
	2.941	3.377	111.0				
Oo-H··Ow	1.944	2.796	109.7				
	1.986	2.823	142.8				
Type	H··A (Å)	D··A (Å)	Angle D-A (°)	Model 5	Description		
C-H··Ow	2.559	3.153	91.2		Weak C-H··Oo bonds and strong Oo-H··Oi bonds between irinotecan and O. Strong Oi-H··Ow and Ow-		
	2.819	3.277	106.7				
Oi-H··Ow	1.874	2.819	159.2				



Ow-H \cdots Oi	1.744 1.868	2.681 2.820	155.6 160.9		H \cdots Oi bonds and weak C-H \cdots Ow bonds connect irinotecan with water molecules which continuously connected with O via strong Oo-H \cdots Ow and strong Ow-H \cdots Oo bonds.
Oo-H \cdots Ow	1.885 1.908	2.759 2.796	143.5 153.8		
Ow-H \cdots Oo	2.002	2.844	141.9		
C-H \cdots Oo	2.403 2.753	3.229 3.388	93.9 106.8		
Oo-H \cdots Oi	1.903 2.016	2.838 2.957	161.0 162.3		
Type	H \cdots A (Å)	D \cdots A (Å)	Angle D-A (°)	Model 6	Description
C-H \cdots Ow	3.070	3.334	94.3		Weak C-H \cdots Oo bonds and weak to strong Oo-H \cdots Oi bonds exist between anionic drug and O. Weak to strong Ow-H \cdots Oi bonds and a weak C-H \cdots Ow bond connect anion with water molecules which continuously interacting with O via strong and weak Oo-H \cdots Ow bonds.
C-H \cdots Oo	3.039 3.139	3.557 3.557	103.3 109.3		
Ow-H \cdots Oi	1.676 1.855	2.685 2.804	127.9 160.2		
Oo-H \cdots Oi	1.620 2.255	2.597 2.911	104.6 131.9		
Oo-H \cdots Ow	1.805 2.493	2.733 3.244	112.3 140.7		

4. CONCLUSIONS

The *ab initio* DFT method was successfully applied onto structural models of halloysite surface and respective forms of irinotecan drug first time. The analysis of the calculated results revealed that halloysite mineral is suitable sorbent for treatment of wastewater polluted by CPT-11. Based on the values of adsorption energies, all potential forms of the CPT-11 drug (anionic, cationic and neutral) produce stable systems with halloysite. The most common form of the CPT-11, which is the cationic drug, created the most stable models when interacting with halloysite mineral. Thus, halloysite can be an ideal sorbent for acidic and neutral waste waters. As in such conditions, neutral molecules are also present, halloysite has the capacity to interact also with them by creating strong and also weak interactions between the carboxylate group of CPT-11 and the octahedral surface of halloysite. Thus, halloysite mineral is suitable for the simultaneous sorption of cationic drug in the outer part of halloysite and the sorption of neutral drug in the inner part of the mineral. When increasing the pH values, anionic drug interacts with the inner part of the mineral also giving stable complexes.

As halloysite is an abundant, low-cost clay mineral with unique characteristics, that found to be a promising adsorbent for all the states of CPT-11 drug, at least from theoretical calculations, further investigations are suggested from an experimental point of view.

5. ACKNOWLEDGEMENTS

ES is grateful for the financial support by the Scientific Grant Agency VEGA (2/0021/19).

REFERENCES

- Ahmad, T., Rafatullah, M., Ghazali, A., Sulaiman, O., Hashim, R. and Ahmad, A., 2010. Removal of pesticides from water and wastewater by different adsorbents: A review. *J. Environ. Sci. Heal. - Part C Environ. Carcinog. Ecotoxicol. Rev.*, 28, 231–271.
- Bloch, P.E., 1994. Projector Augmented-Wave Method. *Phys. Rev. B: Conde. Matter Mater. Phys.*, 50, 17953–17979.
- Di Nunzio, M.R., Douhal, Y., Organero, J.A. and Douhala, A., 2018. Structural and photodynamic properties of the anti-cancer drug irinotecan in aqueous solutions of different pHs. *Phys. Chem. Chem. Phys.*, 20, 14182–14191.



- Gianni, E., Avgoustakis, K., Pšenička, M. and Pospíšil, M., 2019. Halloysite nanotubes as carriers for irinotecan: Synthesis and characterization by experimental and molecular simulation methods. *J. Drug Deliv. Sci. Technol.*, 52, 568–576.
- Grimme, S., 2006. Semiempirical GGA-type density functional constructed with a long-range dispersion correction. *J. Comp. Chem.*, 27, 1787.
- Grimme, S., Antony, J., Ehrlich, S. and Krieg, S., 2010. A consistent and accurate ab-initio parametrization of density functional dispersion correction (dft-d) for the 94 elements H-Pu. *J. Chem. Phys.*, 132, 154104.
- Han, H., Rafiq, M.K., Zhou, T., Xu, R., Mašek, O. and Li, X., 2019. A critical review of clay-based composites with enhanced adsorption performance for metal and organic pollutants. *J. Hazard. Mater.*, 369, 780–796.
- Kresse, G. and Furthmüller, J., 1996a. Efficiency of ab-initio total energy calculations for metals and semiconductors using a plane-wave basis set. *Comput. Mater. Sci.*, 6, 15-50.
- Kresse, G. and Furthmüller, J., 1996b. Efficient iterative schemes for ab initio total-energy calculations using a plane-wave basis set. *Phys. Review B*, 54, 11169-11186.
- Kresse, G. and Hafner, J., 1993. Ab-initio molecular-dynamics for open-shell transition-metals. *Phys. Review B*, 48, 13115-13118.
- Kresse, G. and Joubert, D., 1999. From ultrasoft pseudopotentials to the projector augmented-wave method. *Phys. Review B: Cond. Matter Mater. Phys.*, 59, 1758–1775.
- Mehmel, M., 1935. Über die Struktur von Halloysit und Metahalloysit. In: E., Antipov, E.V., Boldyreva, K., Friese, H., Huppertz, S., Jahn, E.R.T. Tiekink (Eds.) *Zeitschrift für Kristallographie - Crystalline Materials* (pp. 35-43), Volume 90(1-6).
- Perdew, J.P., Burke, K. and Wang, Y., 1996. Generalized Gradient Approximation for the Exchange-Correlation Hole of a Many-Electron System. *Phys. Review B: Cond. Matter Mater. Phys.*, 54, 16533–16539.
- Slatter, J.G., Schaaf, L.J., Sams, J.P., Feenstra, K.L., Johnson, M.G., Bombardt, P.A., Cathcart, K.S., Verburg, M.T., Pearson, L.K., Compton, L.D., Miller, L.L., Baker, D.S., Pesheck, C.V. and Lord, R.S., 2000. Pharmacokinetics, metabolism, and excretion of irinotecan (CPT-11) following I.V. infusion of [14C] CPT-11 in cancer patients. *Drug Metab. Dispos.*, 28, 423e433.



Kinetic Study of Transesterification of Waste Cooking Oil Under Ultrasound

S. Savvopoulos¹, H. Hatzikirou¹ and I. Janajreh²

¹Department of Mathematics, Khalifa University of Science and Technology, Abu Dhabi, UAE

²Department of Mechanical Engineering, Khalifa University of Science and Technology, Abu Dhabi, UAE

Corresponding author email: isam.janajreh@ku.ac.ae

ABSTRACT

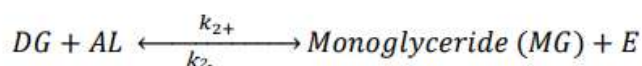
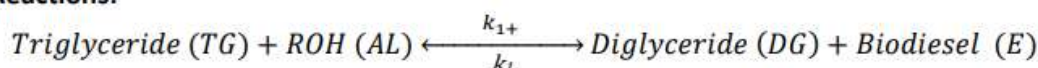
This paper investigates the effect of the acoustic conditions in biodiesel conversion using experimental analysis and numerical modeling. The raw materials used for the transesterification were waste cooking oil and methoxide. Acoustic conditions were generated with an ultrasound probe. The experiments were run at different temperatures, and the same experiments were run in silent/conventional stirring conditions. The initial ratio of methoxide to oil was lower in the setup with acoustics to highlight its advantages in achieving faster and higher conversion and resulted in less residual crude glycerol. The species of both experimental setups were measured frequently until the systems reached a steady state. The goal to evaluate the conversion kinetics is also met by conducting each process at two different temperatures. Comparing both processes (conventional and acoustic stirring), biodiesel production with ultrasound seems to be the most favorable option because it produces biodiesel faster, with larger biodiesel amount and with a lower amount of methoxide and residual glycerol.

Keywords: *ultrasound; biodiesel; transesterification; chemical kinetics; conversion metrics.*

1. INTRODUCTION

Biodiesel is a biofuel made from animal and/or vegetable fats. It's mostly made up of monoalkyl esters of saturated and unsaturated long-chain fatty acids, according to the chemistry. It is regarded as a renewable, non-toxic, biodegradable, oxygenated, sulfur-free, and widely available fuel because to its chemical composition. Transesterification is the most prevalent method of producing biodiesel (Singh and Singh 2010). Transesterification is a reversible reaction, in which triglycerides react with a short-chain alcohol (e.g., methanol methanolysis) under alkaline or acidic conditions to produce fatty acid methyl esters (FAME) and glycerol as the major by-product. The stepwise transesterification reactions and the overall reaction, are shown in Fig. 1 (Šánek et al. 2019).

Stepwise Reactions:



Overall reaction:

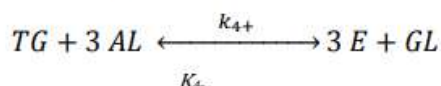


Fig. 1: Transesterification reaction with alcohol.

Although the benefits of ultrasound for biodiesel synthesis have been well documented, the current industry lacks a reliable sonochemical reactor for continuous biodiesel production. In the manufacturing of biodiesel, sonochemical reactors are the current state-of-the-art technology. The numerous physics involved in designing sonochemical reactors makes it a complex task. Ultrasound is used in a reactor to create products faster by increasing the reaction rates. It is utilized in the manufacturing of a variety of chemicals,



such as crystals, pharmaceuticals, nanomaterial synthesis, waste-water treatment, and biofuel production (Rastogi, 2011). It is also been used in other oil-related applications with great success.

Ultrasound emits waves of high-frequency flow through the reacting fluids. Internal tensions in the fluid layers are caused by these waves, resulting in fluid shearing at micro-levels. This shearing causes micro cavitation bubbles to develop, which are filled with highly active fluid vapors. In order to develop cavitation the acoustic pressure (defined in eq. 1) needs to exceed the Blake pressure threshold evaluated by eq. 2 as:

$$P_{Ac} = \sqrt{2I\rho C} \quad (1)$$

$$P_{Blake} = P_o + \frac{4}{3}\sigma \sqrt{\frac{2}{3} \cdot \frac{\sigma}{\left(P_o + \frac{2\sigma}{r_b}\right) \cdot r_b^3}} \quad (2)$$

where I is the acoustic intensity, ρ is the fluid density, and C is the acoustic speed in the fluid medium $\sim 1481\text{m/s}$, P_o is the fluid static pressure, σ is the fluid surface tension and r_b is the minimum cavitation bubble radius (which is in the order of $10\ \mu\text{m}$). The Blake threshold pressure is nearly $1.033 \times 10^5\ \text{Pa}$ (evaluated by the eq.2). In the range of Blake pressure localized cavitation bubbles are formed near the sonotrode tip in the form of short lived cloud that stream within the mixture bath (Janajreh et al. 2022). These bubbles occur in each constituent fluid of a mixture of fluids. Extremely high temperatures in the range of $5000\ \text{K}$ and pressures in the range of $1000\ \text{atm}$ are estimated in the bubbles (Hussain and Janajreh 2018; Savvopoulos et al. 2019, 2020). These cavitation bubbles, whose number is in millions, and create cavitation clouds under the ultrasonic source, are the primary cause of higher response rates in reactive systems. While increasing reaction times is a desirable issue, it has a negative side effect. The main disadvantage of the bubbles cloud generated is that it causes the acoustic wave to be hampered or attenuated. This is one of the primary disadvantages that has affected the scale-up of sonochemical reactors (Janajreh et al. 2015; 2022).

In our study, chemical kinetics of the transesterification conversion is evaluated under both conventional and sonication. The goal is to evaluate the reaction rate, activation energy as well as pre-constants. A MATLAB script file is written to carry such evaluation using the instantaneous/temporal measured GCMS data of the six species, i.e., TG, DG, MG, AL, E, and GL. The experiments carried out at two different temperatures in order to evaluate the needed reaction kinetics. The transesterification reaction is modeled at a stoichiometric molar ratio of 6:1 for methanol to oil in silent/conventional conditions, and 3:1 in sonication. These data will be used in developing high fidelity reactive flow model to capture temperature and species distribution for the design of future reactors.

2. MATERIALS AND METHODS

Restaurant franchises provided a variety of waste cooking oil samples. Five liters of McDonald waste oil samples were collected over five weeks period, mixed in a large 5 liter beaker and then heated under sun temperature to about 45°C and subjected to $20\ \mu\text{m}$ paper filtration from suspended solid residues. The filter 5 liter sample was then heated/dried at 105°C for 8 hours using heating plate under continuous magnetic stirring ($\sim 250\ \text{rpm}$) to get rid of any moisture. Two types of transesterification experiments then carried out: with and without sonication. The methoxide consists of mixture of granular of potassium hydroxide (sigma Aldrich) as the catalyst (at 1% oil ratio) and GCMS methanol grade 99.99% (sigma Aldrich) prepared using a magnetic stirring heating plate sets at 50°C and $250\ \text{rpm}$. The two different set of experiments were carried out in a closed 500 mL capacity borosilicate glass beaker and each single experiment was lasted for 100min (Hussain and Janajreh 2018). In each experiment, the 500 ml beaker was filled with 200 mL of the filtered and dried waste cooking oil (TG) and the corresponding amount of methoxide was added, i.e., oil to methoxide molar ratio of 1:3 and 1:6 for sonication and conventional stirring, respectively. The sonicating probe (horn) was also submerged into the 500 ml beaker after is filled by mixture (see Fig. 1). The sonication is applied by using Hielscher UP400S Ultrasonic apparatus with the horn positioned vertically in the beaker. The horns are subjected to an adjustable amplitude and pulse fixed frequency of $24\ \text{kHz}$. The full-scale power of the UP400S, which is $400\ \text{W}$, provides an acoustic intensity of $4.0\ \text{W/cm}^2$ (based on the horn tip cross-section area). The sonication amplitude can be varied at several operation levels reaching the full range, however all experiments ran at half range operation. Using 2.5ml solution sampling straws, 20 samples were collected from the beaker during each experiment at different time covering the 100 minutes and those are immediately stored in cold ice bath to stop sample reaction and thereafter used for GCMS six species (TG,



DG, MG, AL, ester/E, and Glycerol) analyses. The beaker were also equipped with submersible piezoelectric hydrophone to monitor and confirm the beyond Blake induced acoustic pressure. These hydrophones were positioned at the beaker's inner wall surface and at the bottom. Each experiment was run for a total of 100 minutes and all experiments were repeated in triplicate to minimize the statistical error. The analysis of the six species compositions (TG, DG, MG, FAME, GL and AL) is carried out using Thermo Scientific DSQ II GC/MSD which is equipped with a flame ionization detector. At first, the FAME column is calibrated using standard, TG, DG, MG, biodiesel and glycerol samples of Sigma-Aldrich (St. Louis, Missouri USA) to ensure precise qualitative and quantitative analysis. The breakdown of sample species composition is acquired using methods similar to those carried out by Nouredini and Zhu (1997).

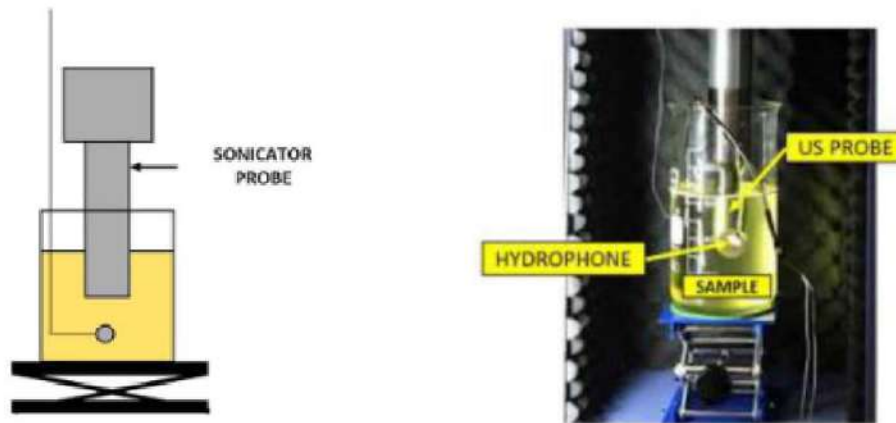


Fig. 2: Experimental setup

In reference to Fig. 1, the mathematical model is represented numerically by six ordinary differential equations (ODEs), and are expressed as (Šánek et al. 2019):

$$\frac{dTG}{dt} = -k_1 [TG][AL] + k_{1+} [E][DG] \quad (3)$$

$$\frac{dDG}{dt} = -k_{2+} [DG][AL] + k_{2-} [E][MG] + k_{1+} [TG][AL] - k_{1-} [E][DG] \quad (4)$$

$$\frac{dMG}{dt} = -k_{3+} [MG][AL] + k_{3-} [E][GL] + k_{2+} [DG][AL] - k_{2-} [E][MG] \quad (5)$$

$$\frac{dE}{dt} = k_{1+} [TG][AL] - k_{1-} [E][DG] + k_{2+} [DG][AL] - k_{2-} [E][MG] + k_{3+} [MG][AL] - k_{3-} [E][GL] \quad (6)$$

$$\frac{dGL}{dt} = k_{3+} [MG][AL] - k_{3-} [E][GL] \quad (7)$$

$$\frac{dAL}{dt} = -\frac{dE}{dt} \quad (8)$$

Concerning the k_i values $\forall i \in \{1+, 1-, 2+, 2-, 3+, 3-\}$:

$$k_i = A_{0,i} e^{-\frac{E_{\alpha,i}}{RT}} \quad (9)$$

where A_0 denotes the frequency factor of the reaction, E_α is the activation energy of the reaction, R the ideal gas constant, and T the thermodynamic temperature.



Based on the experimental data, all k_i parameters can be estimated by a nonlinear least-squares solver like *lsqcurvefit* in MATLAB (MATLAB 2022). Briefly, the nonlinear solver finds the reaction rates k (Eq. 9) that solve the problem:

$$\min_k \|F(\mathbf{k}, xdata) - ydata\|_2^2 = \min_k \sum_n (F(\mathbf{k}, xdata_n) - ydata_n)^2 \quad (10)$$

Given two sets of input data ($xdata$ and $ydata$), which may be matrices or vectors, $F(\mathbf{k}, xdata)$ is a matrix- or vector-valued function with a size equal to $ydata$. The elements of \mathbf{k} which is the vector of the reaction rates, may alternatively have lower and upper bounds, which can be either vectors or matrices. *lsqcurvefit* requires the user-defined function to compute the *vector*-valued function:

$$F(\mathbf{k}, xdata) = \begin{bmatrix} F(\mathbf{k}, xdata(1)) \\ F(\mathbf{k}, xdata(2)) \\ \vdots \\ F(\mathbf{k}, xdata(n)) \end{bmatrix} \quad (11)$$

Therefore, from the results of the *lsqcurvefit*, the activation energy (E_i) and frequency factor (A_i) for each subsequent reaction can be calculated by graphing the logarithm of the achieved reaction rates against the inverse value of the absolute temperature ($1/T$). As a result of the given technique, expression (9) is linearized, and the data can be analyzed using relatively easy linear regression as per eqs. 12 and 13.

$$E_{a,i} = -slope_i R \quad (12)$$

$$k_{0,i} = e^{intercept_i} \quad (13)$$

Generally, the work aims at understanding the changes that ultrasound causes in the production of biodiesel, and to have an insight into what changes in the kinetics comparing the species dynamically in both conventional and sonication conditions.

3. RESULTS

All the measurements were collected for model parameter estimation by applying the *lsqcurvefit* function in MATLAB. Fig. 3 shows how well the model fits the experimental data at 50°C, and 60°C in both conventional conditions, and under sonication. In conventional reaction the initial alcohol to oil molar ratio was 6:1, while in sonication that ratio was 3:1 to emphasize the effectiveness of sonochemistry in transesterification. The data measured were the concentrations of triglycerides (TG), diglycerides (DG), monoglycerides (MG), biodiesel (E), glycerol (GL), and alcohol (AL).

In Figs. 3A and 2B, the model fits the species dynamics in the same temperature but in different conditions, and in Figs. 3C and 3D, the performance of the model is still good to capture the concentrations at a relatively higher temperature. It is clear from the figures not only how fast the conversion occurs under sonication, but also its attained FAME molar concentration and the depletion of the TG. Regarding the reaction rates, their values estimated by *lsqcurvefit* in conventional and sonication conditions, and in both temperatures are shown in Table 1.

Table 1: Reaction kinetics in both conditions at 50°C, and 60°C

Parameter	Convent. at 50°C (min ⁻¹)	Convent. at 60°C (min ⁻¹)	Sonic. at 50°C (min ⁻¹)	Sonic. at 60°C (min ⁻¹)
k_{1-}	0.044953	0.045878	0.000157	0.00019
k_{2-}	0.2729	0.2729	7.59E-09	1.37E-08
k_{3-}	0.045254	0.045255	4.89E-14	9.7E-14
k_{1+}	0.026118	0.026887	0.418227	0.418274
k_{2+}	0.080985	0.083707	1.470778	1.470779
k_{3+}	0.456285	0.456285	0.837988	0.837988

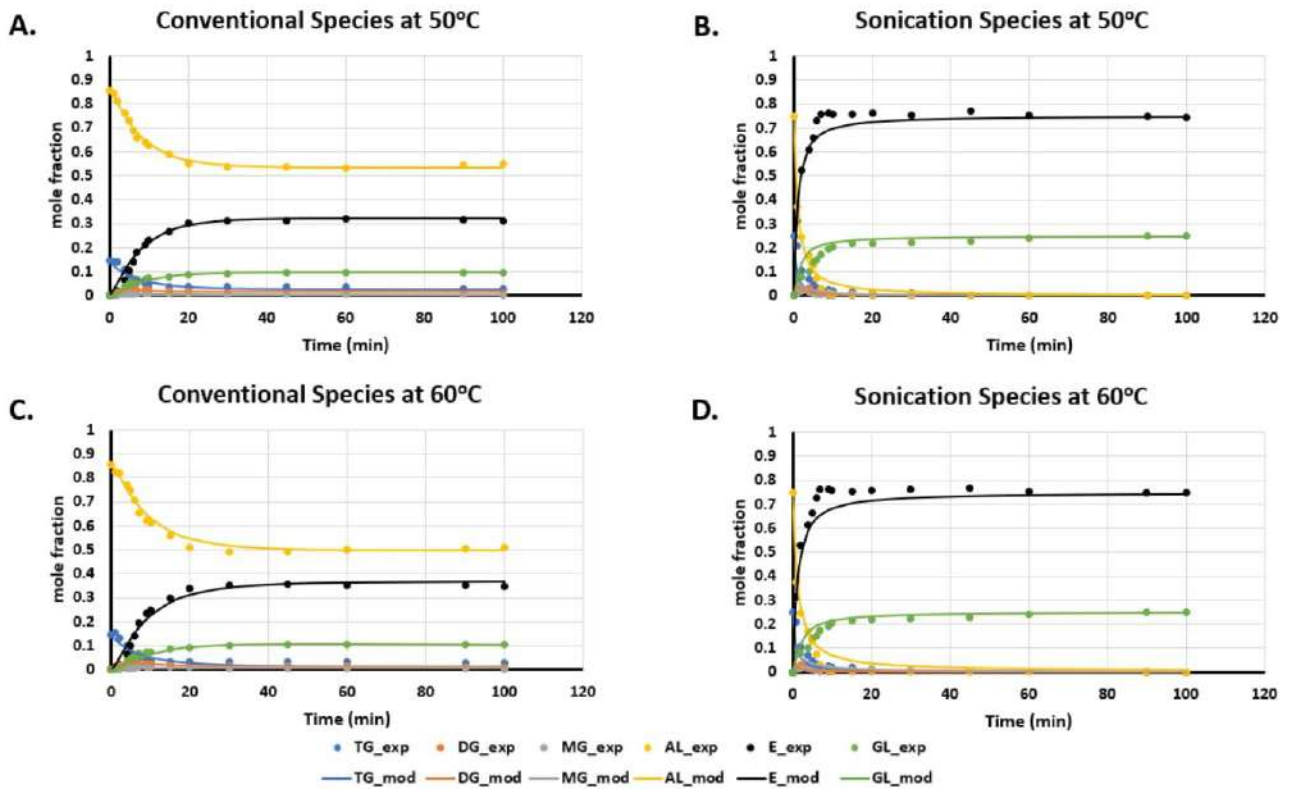


Fig. 3: Mole fractions of species at different temperature in both conventional and sonication conditions

By using the linearization, the frequency factors with the activation energies for each reaction are also evaluated and shown in Table 2.

Table 2: Frequency factors and activation energy in both conditions

Rate	Convent. Frequency Factor (min ⁻¹)	Convent. Activation Energy (J/mol)	Sonic. Frequency Factor (min ⁻¹)	Sonic. Activation Energy (J/mol)
k_{1-}	0.0886	1822.11	0.0942	17178.64
k_{2-}	0.2729	0.0031	2.5000	52668.36
k_{3-}	0.0453	2.73	0.0004	61296.00
k_{1+}	0.0687	2597.16	0.4198	10.08
k_{2+}	0.2435	2956.25	1.4708	0.04
k_{3+}	0.4563	0.09	0.8380	0.04

Firstly, the rate constants of sonicated transesterification are much higher for the forward reactions than for those in the conventional approach, and the reverse happens for the backward reactions (Tables 1 and 2). Regarding energies, the backward activation energies of sonication are significantly higher than the values of conventional circumstances, indicating that reverse reactions are more likely to occur when utilizing conventional transesterification techniques rather than sonicated conversion. More precisely, when the alcohol to oil molar ratio is 6:1, diglycerides and monoglycerides are short-lived species, as they briefly appear at both temperatures before asymptotically disappearing. There is a decent level of FAME conversion, evidenced by the fact that the amount of unreacted alcohol at 50°C, and 60°C and the FAME generation are nearly identical. At the higher temperature, greater reactivity and a greater yield of FAME are obtained. The rate constants are often larger for the forward reactions than the linked reverse reaction constants (Tables 1, and 2). In sonication conditions, the conversion is faster, and the yield is greater even if the alcohol to molar ratio is 3:1. Therefore, sonicated transesterification is regarded as more environmentally friendly conversion by leaving less residual crude glycerol and using lesser methanol.



4. CONCLUSIONS

From the current study, the transition from the conventional to sonication production of biodiesel is feasible. A comparison of conventional mixing and ultrasonic-assisted processes demonstrates the superiority of the sonication conditions in terms of accelerating forward reactions by raising reaction rates and lowering forward reaction activation energies.

5. ACKNOWLEDGEMENTS

The support received by the Khalifa University of Science and Technology under Award No. RC2-2018-009 is highly acknowledged.

REFERENCES

- Hussain, Mohammed Noorul and Isam Janajreh. 2018. "Acousto-Chemical Analysis in Multi-Transducer Sonochemical Reactors for Biodiesel Production." *Ultrasonics Sonochemistry* 40:184–93.
- Janajreh, Isam, Ussama Ali, and Muhammad Hawwa. 2022. "Sonicated Direct Contact Membrane Distillation: Influence of Sonication Parameters." *Desalination* 533.
- Janajreh, Isam, Tala Elsamad, Ahmed Aljaberi, and Mohamed Diouri. 2015. "Transesterification of Waste Cooking Oil: Kinetic Study and Reactive Flow Analysis." *Energy Procedia* 75:547–53.
- MATLAB. 2022. "Nonlinear Curve Fitting with Lsqcurvefit." Retrieved (<https://www.mathworks.com/help/optim/ug/nonlinear-curve-fitting-with-lsqcurvefit.html>).
- Noureddini, H., & Zhu, D. (1997). Kinetics of transesterification of soybean oil. *Journal of the American Oil Chemists' Society*, 74(11), 1457–1463. <https://doi.org/10.1007/s11746-997-0254-2>
- Rastogi, Navin K. 2011. "Opportunities and Challenges in Application of Ultrasound in Food Processing." *Critical Reviews in Food Science and Nutrition* 51(8):705–22.
- Šánek, Lubomír, Pecha Jiří, Jakub Husár, and Karel Kolomazník. 2019. "Mathematical Modeling of Transesterification Process Kinetics of Triglycerides Catalyzed by TMAH." *MATEC Web of Conferences* 292:01027.
- Savvopoulos, Symeon V., Mohammed N. Hussain, Tom Van Gerven, and Simon Kuhn. 2020. "Theoretical Study of the Scalability of a Sonicated Continuous Crystallizer for the Production of Aspirin." *Industrial and Engineering Chemistry Research* 59(45):19952–63.
- Savvopoulos, Symeon V., Mohammed N. Hussain, Jeroen Jordens, Steffen Waldherr, Tom Van Gerven, and Simon Kuhn. 2019. "A Mathematical Model of the Ultrasound-Assisted Continuous Tubular Crystallization of Aspirin." *Crystal Growth and Design* 19(9):5111–22.
- Singh, S. P. and Dipti Singh. 2010. "Biodiesel Production through the Use of Different Sources and Characterization of Oils and Their Esters as the Substitute of Diesel: A Review." *Renewable and Sustainable Energy Reviews* 14(1):200–216.



Critical insights to drive sustainable water management in process industries

E. Karkou¹, N. Savvakis¹ and G. Arampatzis¹

¹School of Production Engineering and Management, Technical University of Crete, Chania, Greece
Corresponding author email: garampatzis@tuc.gr

ABSTRACT

The depletion of natural resources and the constant extraction of water for the production processes within an industry make imperative the efficient management of water. In this regard, this study aims to highlight the importance of adopting a more circular and sustainable approach, which entails the incorporation of reuse and recycling practices as well as the exploitation of the produced industrial wastewater by recovering the valuable components and reusing the water. A methodology was developed in order to classify the requirements, distinguish the opportunities of the discrete use cases, indicating the most appropriate model to be applied. Regardless of the case study, the produced wastewater decreases by re-entering the industrial area as a reclaimed product. In addition, the negative impact on the environment lessens because of reduced discharge into the water recipients and more eco-friendly water treatment technologies, and sustainability is promoted through the synergies. It is necessary to model the behavioral response of the implemented circular practices, referring to the treatment processes, industries, and all the actors. Based on the prospects and involved actors, four distinct levels of modelling are emerged: process modelling, in-factory modelling, industrial symbiosis, and systemic modelling. This methodological approach is conceptually deployed to six European process industries to make noticeable its practical use.

Keywords: water management; process industry; water reuse; circular; modelling.

1. INTRODUCTION

The industry confronts severe water stress due to the limited availability of natural resources. By 2050, industrial water demand is foreseen to rise by 400%. In this regard, industrial water management needs to be enhanced to mitigate the consequences of the water crisis (Diaz, 2021). Freshwater intake reduction and more efficient water management within one or more industries encompass major goals. Water reuse and recycling practices are compact solutions. The incorporation of advanced water treatment technologies in the process industry is fundamental for achieving sustainable water management. Closed-loop water reuse practices contribute to the reduction of freshwater and other materials consumption (Kinnunen et al., 2021). In the process industry, significant amounts of wastewater are produced and discharged into the environment with inadequate or without treatment (Ezemagu et al., 2021). Efficient wastewater treatment leads to water conservation and recovery of valuable resources (Lizot et al., 2021). Water reuse and the exploitation of the extracted materials prove the importance of sustainability by implementing the zero liquid discharge (ZLD) approach within the industry's boundaries (Panagopoulos, 2022). Through circular practices, the life of water and by-products is extended as much as possible (Arora et al., 2022). Furthermore, the potential synergies between process industries, which operate in the same or different fields, focus on exchanging water and materials. By-products are utilized within the developed network of interrelated industries and other actors, e.g., the municipality (Ashton et al., 2022). In this regard, the industries become more sustainable and efficient. Hence, the identified need for sustainable water management seems achievable. Previous studies have examined the technologies for wastewater treatment and resources recovery (Dutta et al., 2021), the mathematical models of advanced processes (Lindamulla et al., 2021), and the practices that interrelate with the circular economy (Mbavarira & Grimm, 2021) and the industrial symbiosis (Mohan & Katakojwala, 2021). However, no study examines sustainable water management practices in the industry and the development of models to control and optimize the system simultaneously. The purpose of this research is on the one side to help identify the core aspects of sustainable water management in the industrial sector, along with identifying the potential levels of modelling that could be applied.



2. METHODOLOGY

A thorough scientific literature review was carried out to identify and analyse the alternative water management options in the industry. The developed methodology presupposes the analysis of each step to evaluate the contextually potential outcomes and support the decision-making process:

- Definition of system boundaries and objectives
- Design of the detailed process flow diagram
- Map the water sources, reuse and recycle options
- Determination of water quality requirements
- Identification of involved actors and their interdependencies
- Selection and deployment of the appropriate model
- Integration and simulation of the whole system.

The methodology is demonstrated in six industrial cases, studied in the course of AquaSPICE H2020 innovation action, including four chemical industries (Dow Chemical in Böhlen Germany and Terneuzen Netherlands, Solvay Rosignano in Italy, and BASF in Antwerp Belgium), one refinery (Tüpraş in Izmit Turkey), a meat production industry (AGRICOLA in Bacau Romania), and a waste-to-fuel transformation plant (JEMS in Ljubljana, Slovenia).

3. RESULTS AND DISCUSSION

To adopt the reduce-reuse-recycle concept, innovative strategies need to be implemented. Sustainable water management focuses on (a) decreasing the demand for water resources, (b) improving the performance of the existing treatment technologies, (c) incorporating advanced processes for water production of high quality, and (d) utilizing all by-products by preventing waste production.

Freshwater consumption has the potential to be minimised through intra-process or intra-factory water reuse. Instead of discharging the produced wastewater into the recipient waters, it could be treated and reused in the production processes of the industry. As a result, it substitutes for a share of raw water. Also, the effective monitoring and prediction of an individual or a series of processes lead to the accurate calculation of water demand. Hence, the water in the inlet of the system may decrease up to a certain level. The development of models to predict the process performance facilitates the reduction of freshwater intake and the enhancement of the process yield. The reactions that take place within a reactor are modeled and possible sources of water losses are detected. Furthermore, the capability of predicting the quality characteristics of the effluent streams contributes to the decision-making for the most appropriate way to recycle them in order to comply with the relevant quality requirements. Contemporary eco-friendly water treatment technologies, which apply to a wide range of industrial applications, may be considered to produce water of precise criteria. Then, the recovery of water and its utilization for reuse and recycling purposes are feasible. Advanced model-based tools assess water reuse practices and determine cost-efficient solutions. At the same time, industries could have insights into the opportunities for synergies with other companies, which operate in the same or different sectors. Minimization of waste production by exchanging by-products, lower environmental impact and enhancement of circularity and sustainability constitute decisive benefits in a broader industrial collaboration.

It is essential to predict the water quality and the processes' performance through model-based tools in order to accelerate change in industrial water management. The levels of modelling emanate from the different use cases and their necessities. European process industries represent the demonstration sites to give prominence to the modelling. Firstly, mathematical modelling of a treatment process, e.g., a membrane bioreactor, an ultrafiltration membrane, enables the enhancement and optimization of the process performance (in-process modelling). Expanding across the whole factory (in-factory modelling), water mass balance is included to quantify water demand and production, and detect possible sources of losses either in-process closed loops or intra-factory loops. In addition, a factory may collaborate with other industries by exchanging water and other relevant materials. In this case, modelling of industrial symbiosis optimizes water and valuable substances allocation. Finally, reuse and circular practices among different actors are modeled (systemic modelling) by incorporating the water cost, quality requirements, and actors' interdependencies. Closed water loop systems can be deployed at different levels based on the accessible water sources, reuse purposes and actors' capabilities. The levels of modelling and the applied systems depict in Figure 1.

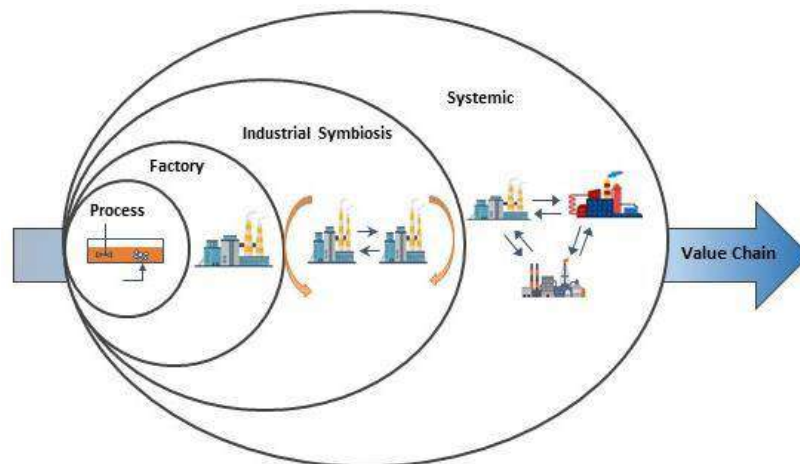


Figure 1. Levels of modelling in the equivalent sector to be deployed.

To demonstrate the methodology for the discrete case studies, the six-step analysis shall be followed. The first step includes the definition of the system boundaries by describing all the flow streams (input, output) and the goals for sustainable water management (freshwater intake reduction, increase the reuse of reclaimed water, increase the efficiency of the existing water treatment technologies, reduction of the water footprint, or increase cost savings). Secondly, the process flow diagram should be created including the technologies, the direction of the processed streams, and all the target parameters. Mapping the water sources involves the compilation of rivers, lakes, sea and raw water suppliers. Reuse and recycle options require the clarification of the reuse purposes and the processes where recycling could contribute to a more sustainable industry. Therefore, the quality of the reclaimed water (e.g., total organic content, biochemical oxygen demand, nitrates, phenolic compounds, etc.) should be defined in order to be reused reasonably. The fifth step encompasses the identification of the involved actors (industries, public or private companies) that may operate in the same or different sectors. Based on the aforementioned steps, the most appropriate model is selected. The distinct models are explained in the following sections.

3.1. In-process modelling

Monitoring a treatment process is necessary for the industry. The prediction of the effluent quality and the understanding of the occurring reactions within a treatment unit are fundamental objectives of the in-process modelling, which permits efficient water management. In this regard, it appears the most reasonable tool for managing water use and reuse. In-process modelling includes the development of mathematical models to predict the performance of advanced water treatment technologies, including biological granular activated carbon, ultrafiltration, advanced oxidation, and reverse osmosis. Therefore, the removal efficiency of the target compounds (e.g., organic content, nitrates, phenolic compounds, etc.) can be predicted. It is applied to the process industry of Dow, Solvay, BASF, Agricola, and Tüpraş.

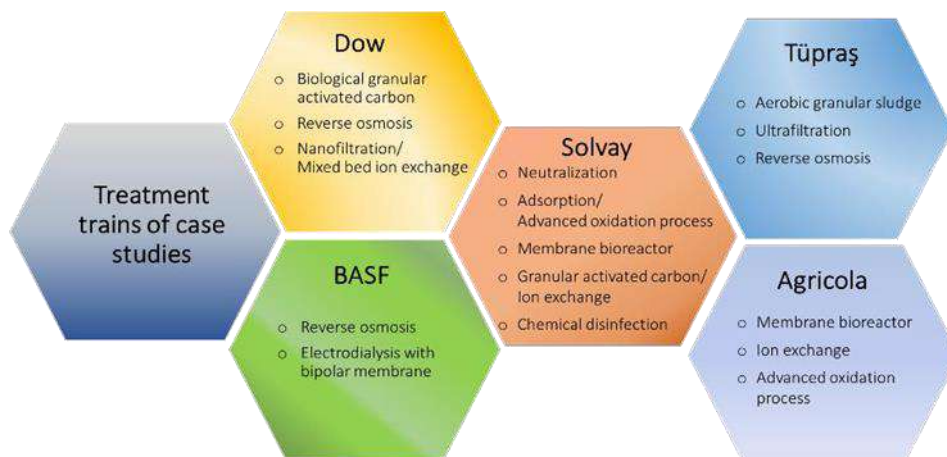


Figure 2. Water treatment technologies in each case study.



3.2. In-factory modelling

A process industry consists of several treatment processes, which are mutually linked. Each unit is fed with wastewater and in the outlet exerts the effluent stream. Water losses may be noted due to evaporation, leakages, or sludge production. To manage the quantity of the treated wastewater efficiently and determine the potential water losses, in-factory modelling is compulsory. It is demonstrated in Dow chemical plant by describing the water mass balance within the defined system boundaries. The general equation applied for the in-factory modelling for a compound (Eq. 1) declares that the accumulation rate equals the input, output, water loss, and the generation rate within the system. Specifically, the change in concentration over time, $\frac{dC}{dt}$ (mol/m³/s), within a reactor volume, V (m³) is calculated based on Eq. 2. The stream of flow rate Q_{in} (m³/s) and concentration of a specific compound C_{in} (mol/m³) inserts the system, while the exerted stream flows with rate Q_{out} (m³/s) and with the concentration of a specific compound C_{out} (mol/m³). Any water loss is quantified by the flow rate Q_{loss} (m³/s) and concentration C_{loss} (mol/m³). In case a reaction takes place, the reaction rate is described as r_i (mol/m³/s).

$$\text{Accumulation} = \text{Inflow} - \text{Outflow} - \text{Water loss} + \text{Generation} \quad (1)$$

$$\frac{dC}{dt} \cdot V = Q_{in} \cdot C_{in} - Q_{out} \cdot C_{out} - Q_{loss} \cdot C_{loss} + r_i \cdot V \quad (2)$$

This level of modelling entails the incorporation of the enmeshed processes into an integrated system in order to model and simulate the whole system, and evaluate the impact on water resource management.

3.3. Industrial symbiosis

The industrial symbiosis aims at the optimal use and reuse of materials offering economic and environmental benefits. The industries that exchange water and other materials are favored. Water and wastewater management within the boundaries of many industrial players can be optimized through synergies. The available resources are exchanged within a network of industries that operate in the same field instead of discharging them into the environment. This way, the pressure on the water sources decreases and the cost savings increase.

The process industries of Dow, BASF, Agricola, and Tüpraş may supply the generated industrial wastewater (IW) to Jems in order to transform them into valuable products. In addition, the municipality provides Solvay with municipal wastewater (MW), which is sent to the Jems plant along with industrial wastewater to be utilized. The recreation of new products by using by-products extends the life of materials and promotes circularity. Thus, the modelling and simulation of the industrial symbiosis will highlight the quantity of exchanged materials and the economic benefits for each partner. Hence, the decision-making process will indicate the scenario for the optimal management of resources. Each process industry represents a system, which shall be integrated into a broader one in order to simulate not only the individuals but also the whole system. Thus, water management, cost and environmental benefits are optimized for all actors. The synergies between the industries are depicted in Figure 3.

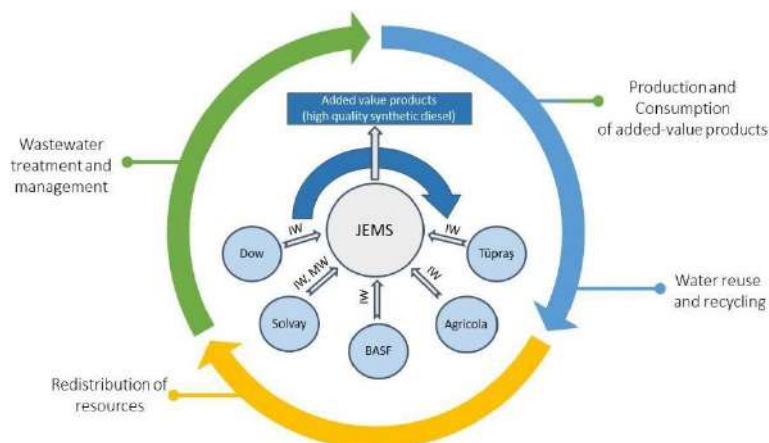


Figure 3. Synergies between the process industries that exchange industrial and municipal wastewater to transform them into valuable products.



3.4. Systemic modelling

The systemic modeling applies to Solvay chemical plant, which interacts with the wastewater reclamation plant Aretusa and the municipality by exchanging partially treated industrial wastewater. The peroxide and peracetic acid production processes at the Solvay plant result in wastewater generation, which requires further treatment in order to be reused intra-factory or discharged into the environment. In this regard, advanced wastewater treatment takes place within the factory by implementing a pilot-scale system in cooperation with Wastewater Reclamation plant Aretusa (WWRP) and the Municipal Wastewater Treatment plant (MWTP). Based on the effluent quality, there are three alternative closed-loop scenarios for achieving water efficiency and circularity:

- **Option 1:** The generated industrial wastewater is treated in the pilot-scale system using advanced treatment technologies. Then, the effluent is sent to the MWTP to be further treated. Finally, the secondary effluent is sent to WWRP Aretusa to be processed and utilized for cooling purposes at the Solvay plant as reclaimed water.
- **Option 2:** The wastewater from the peroxide and peracetic acid production is treated within the pilot-scale system. Therefore, it is sent to WWRP Aretusa and finally back to the Solvay plant to fulfill the water reuse requirements.
- **Option 3:** The pilot-scale system is fed with industrial wastewater. The effluent of this system is mixed with water provided by the WWRP Aretusa in a ratio based on water quality characteristics. The mixed stream substitutes partially for freshwater intake at the Solvay plant.

Hence, actors that operate in different sectors exchange water and wastewater. The process industry of Solvay, the ARETUSA reclamation plant, and the Municipal Wastewater Treatment plant profit from the synergies between them. The synergies between the actors are presented in Figure 4. Economic and environmental benefits act as consolidated incentives and dominate the systemic modelling.

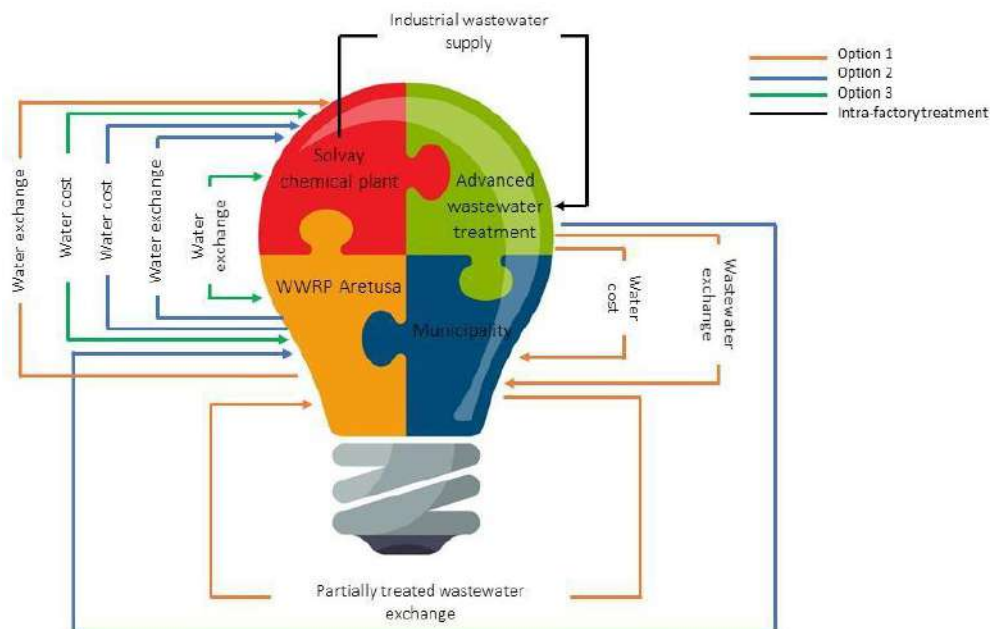


Figure 4. Interdependencies between Solvay chemical plant, Wastewater Reclamation plant Aretusa, and municipality and the exchange of water, wastewater, and partially treated wastewater.

4. CONCLUSIONS

Water is of key importance for the process industry, whose management is challenging. The transition to the circular economy requires the deployment of different levels of modelling (in-process, in-factory, industrial symbiosis, systemic) based on the case-specific requirements. It is urgent to prolong the life of water and



other materials and reduce the environmental footprint of the process industries by diminishing freshwater consumption, implementing reuse and recycling practices, and developing symbiotic relationships between several actors. Hence, fit-for-purpose closed-loop approaches are adopted to optimize the system, circulate the water, and reinforce the sustainability of the industrial sector.

5. ACKNOWLEDGEMENTS

The research methodology and results presented are part of the H2020-AquaSPICE project (EC, CE-SPIRE-07-2020, Horizon 2020). This project has received funding from the European Union's Horizon-2020 research and innovation program under grant agreement No. 958396. The responsibility for the content of this publication lies with the authors. It does not necessarily reflect the opinion of the European Union. The European Commission is not responsible for any use that may be made of the information contained therein. The authors would like to express their gratitude to all partners of the AquaSPICE project, who gave the team of the Technical University of Crete (TUC) the opportunity to develop the above methodological analysis.

REFERENCES

- Arora, M., Yeow, L. W., Cheah, L. and Derrible, S., 2022. Assessing water circularity in cities: Methodological framework with a case study. *Resources, Conservation and Recycling*, 178, 106042.
- Ashton, W. S., Chertow, M. R. and Althaf, S., 2022. Industrial Symbiosis: Novel Supply Networks for the Circular Economy. In *Circular Economy Supply Chains: From Chains to Systems*, 1st ed.; Emerald Publishing: UK.
- Chen, Y., Miller, C. J. and Waite, T. D., 2021. Heterogeneous Fenton chemistry revisited: Mechanistic insights from ferrihydrite-mediated oxidation of formate and oxalate. *Environmental Science and Technology*, 55, 14414–14425.
- Diaz, L., 2021. Water footprint: A sustainability tool for industries. In *Sustainable Industrial Water Use: Perspectives, Incentives, and Tools*, 1st ed.; IWA Publishing: London, UK.
- Dutta, D., Arya, S. and Kumar, S., 2021. Industrial wastewater treatment: Current trends, bottlenecks, and best practices. *Chemosphere*, 285, 131245.
- Ezemagu, I. G., Ejimofor, M. I., Menkiti, M. C. and Nwobi-Okoye, C. C., 2021. Modeling and optimization of turbidity removal from produced water using response surface methodology and artificial neural network. *South African Journal of Chemical Engineering*, 35, 78–88.
- Kinnunen, P., Obenaus-Emler, R., Raatikainen, J., Guignot, S., Guimerà, J., Ciroth, A. and Heiskanen, K., 2021. Review of closed water loops with ore sorting and tailings valorisation for a more sustainable mining industry. *Journal of Cleaner Production*, 278, 123237.
- Lindamulla, L. M. L. K. B., Jegatheesan, V., Jinadasa, K. B. S. N., Nanayakkara, K. G. N. and Othman, M. Z., 2021. Integrated mathematical model to simulate the performance of a membrane bioreactor. *Chemosphere*, 284, 131319.
- Lizot, M., Goffi, A. S., Thesari, S. S., Trojan, F., Afonso, P. S. L. P. and Ferreira, P. F. V., 2021. Multi-criteria methodology for selection of wastewater treatment systems with economic, social, technical and environmental aspects. *Environment, Development and Sustainability*, 23 (7), 9827–9851.
- Mbavarira, T. M. and Grimm, C., 2021. A systemic view on circular economy in the water industry: Learnings from a belgian and dutch case. *Sustainability*, 13, 3313.
- Mohan, S. V. and Katakojwala, R., 2021. The circular chemistry conceptual framework: A way forward to sustainability in industry 4.0. *Current Opinion in Green and Sustainable Chemistry*, 28, 100434.
- Panagopoulos, A., 2022. Brine management (saline water & wastewater effluents): Sustainable utilization and resource recovery strategy through Minimal and Zero Liquid Discharge (MLD & ZLD) desalination systems. *Chemical Engineering and Processing - Process Intensification*, 176, 108944.



Development of a greenhouse and screw conveyor solar driers for the treatment of faecal sludge from on-site sanitation facilities

S. Septien¹, P. Naidoo¹, A. Ramlucken¹, A. Ganapathie², Y. Pather², A. Singh², J. Pocock², F. Inambao³ and C. McGregor⁴

¹WASH R&D Centre, University of KwaZulu-Natal, Durban, South Africa

²Chemical Engineering Discipline, University of KwaZulu-Natal, Durban, South Africa

³Mechanical Engineering Discipline, University of KwaZulu-Natal, Durban, South Africa

⁴STERG, University of Stellenbosch, Stellenbosch, South Africa

Corresponding author email: septiens@ukzn.ac.za

ABSTRACT

Thermal drying is an important unit operation in faecal sludge treatment. However, this process requires a high energy input leading to high running costs due to high electricity or fuel consumption. Solar thermal energy can be used to decrease the costs of the drying process. The aim of this work is to develop solar thermal drying technologies that harness the solar thermal energy in an efficient way and are adapted to the sludge characteristics. Two different types of technologies were selected for their development, i.e. greenhouse-type solar drier and screw conveyor solar drier. After construction, the technologies were tested to measure their performance, find the optimum operating conditions, and identify improvement points. During the tests in the solar driers, it was observed that temperatures inside the enclosure were higher with respect to the ambient conditions (+10-15°C for the greenhouse and +15-25°C for the screw conveyor drier), leading to relative humidities lower than 30%. An evaporation rate in the greenhouse was measured in the order of 0.8 kg/h/m² when conducting the tests with water. The drying tests with wetted soil in the screw conveyor solar drier resulted in a good performance with most of moisture being removed from the soil after less than 30 minutes of operation. Testing with synthetic sludge showed also positive results, with moisture removal in the region of 20% to 50% in 2 hours. The most optimal conditions were obtained when the ventilation was operated at low air flowrate, as the maximum temperatures achieved in the system were higher (after the solar air heater), leading to a higher moisture removal from the synthetic sludge. The results from the tests were promising. After the testing phase for both prototypes, improvements have been identified for the next round of iteration. In particular, the sludge stickiness is a critical problem that must be resolved to achieve sustainable long operation times.

Keywords: Faecal sludge; On-site sanitation; Solar thermal drying; Temperature; Drying rate.

1. INTRODUCTION

The World Health Organization estimates that 50% of the worldwide population does not have access to safely managed sanitation service, among which over 1.7 billion people do not have basic sanitation service, causing 494 million still practicing open defecation (WHO 2021). Onsite sanitation is the most viable option to provide sanitation to the poor communities where this basic service is lacking, as the high costs for the development and maintenance of sewage system are usually unaffordable for developing countries. Moreover, many regions in the world already rely on onsite sanitation with 2.7 billion people served by this type of sanitation technology (Strande et al., 2014). Onsite sanitation can also serve in developed areas and cities to change the paradigm of sewage sanitation into a more water-sensitive, climate change-resilient and sustainable model.

One of the main challenges of onsite sanitation is the accumulation of the faecal waste in the site of generation (i.e. faecal sludge). Methods have to be therefore developed for its in-situ treatment, or its collection and transportation to a faecal sludge treatment plant for its disposal and eventual resource recovery. The implementation of safely managed onsite sanitation with the recovery of valuable resources (e.g., reuse water, nutrients and biofuel) can be a key factor to accomplish the Sustainable Development Goals, in particularly Goal 6 ensuring safe water and sanitation for all (Andersson et al., 2018).



The removal of moisture in the sludge through drying is an important step in its treatment, as it reduces the mass and volume of the faecal waste and destroys pathogens that cannot survive without water and are deactivated at high temperatures. Conventional thermal driers present high operating costs due to the high energy demand for moisture evaporation in the form of electricity or fuel. The use of solar thermal energy for drying purposes is an interesting option because of several reasons: (i) high availability in the developing countries (including South Africa); (ii) sustainability, environmentally friendly and low greenhouse emissions; (iii) renewable and “free” energy.

The use of solar thermal energy for drying proposes could reduce drastically the energy consumption, leading to a significant cost reduction. This should involve the setup of a thermal system to harness in an efficient way the solar energy for its conversion into heat. Most of the solar drying applications are found in the agriculture and food industry sectors, for the preservation of grains and dehydration of food products. Solar thermal energy has also been widely applied for sewage sludge drying in European countries, the United States and Australia (Seginer and Bux, 2006), and has gained interest in developing countries as Greece, Turkey, Algeria, Morocco and China. The largest sewage sludge solar drying applications consist in greenhouses with units that are able to process around 30,000 ton per year (Meyer-Scharenberg and Pöppke, 2010; Socias, 2011). Different types of solar thermal technologies are under development, such as solar roof dryers (Wang et al., 2019) and cabinet solar dryer (Ameri et al., 2018). Nonetheless, almost no information has been found in literature for faecal sludge solar drying apart some isolated cases where the sludge was dried in greenhouses with a simplistic design (Muspratt et al., 2014; Seck et al., 2015).

The aim of this work is to develop solar thermal drying technologies that have been designed to harness the solar thermal energy in an efficient way and that are adapted to the sludge characteristics. Two different types of technologies were selected for their development, i.e. greenhouse-type solar drier and screw conveyor solar drier. The prototypes were built at pilot-scale to be able to process several kg of faecal sludge per day. After construction, the technologies were tested to measure their performance, find the optimum operating conditions, and identify improvement points. Based on these results, a technical-economic analysis will be performed for the upscaling and implementation of the technologies in faecal sludge treatment facilities.

2. MATERIAL AND METHODS

2.1. Description of the solar thermal drying prototype

The greenhouse prototype consists in a solar dryer where faecal sludge will be placed in a bed and dried using solar thermal energy. The prototype offers an enclosed space where the solar thermal energy can be collected through greenhouse effect and the presence of an absorber wall. It includes a ventilation system and sludge rake system to boost the drying process. The sludge bed will stand on a suspended grid, which will let the sludge to dry also from the bottom. The prototype scheme can be found in Figure 1.

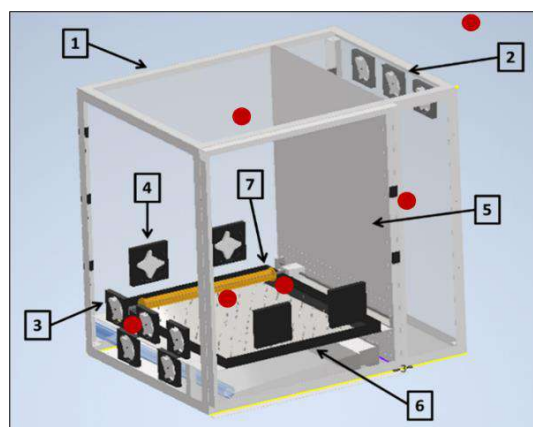


Figure 1. Drawing of the greenhouse solar dryer (1: enclosure; 2: air inlet; 3: air outlet; 4: circulation fans; 5: absorber wall; 6: sludge bed support; 7: rake system; red points: sensors).



In the screw conveyor solar drier prototype, the sludge will be dried during its passage through a transparent tube exposed to solar radiation (drying chamber). During this process, the sludge will absorb the solar thermal energy and use it as latent heat for moisture evaporation. An air stream will circulate inside the drying chamber to enhance the drying process. The air stream will be dehumidified and heated before introduction in the drying chamber. Reflectors will be placed next to the drying chamber to increase the amount of solar radiation received by the sludge. Figure 2 schematizes the screw conveyor solar drier setup.

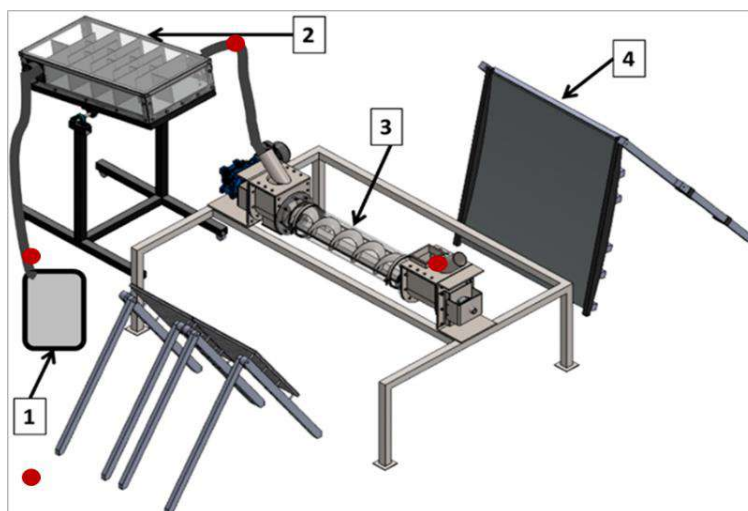


Figure 2. Schematic representation of the screw conveyor solar drier prototype (1: air dehumidifier; 2: solar air heater; 3: drying chamber; 4: reflector; red points: sensors).

2.2. Testing of the solar thermal drying prototypes

The greenhouse was tested initially without feedstock to assess the functionality of the system and find the optimal ventilation operating conditions based on the temperature measurements. Water evaporation tests were then carried out, where several 55 mm diameter containers with water (100 g/container) were placed inside the greenhouse. After a few hours of operation, the mass of evaporated water was measured by comparing the initial and final mass of the containers.

Concerning the screw conveyor solar drier, the first tests were carried out to test the individual components of the prototype and the integrated system without feedstock. Thereafter, the solar drier was tested using wetted soil (400 g water added per 1 kg of dry soil) and synthetic faecal sludge (with 80% initial moisture content) as feedstock, for 1 – 2 hours of operation. The synthetic faecal sludge recipe was made of water, psyllium husk, peanut oil, miso paste, ground dried vegetables, cellulose, polyethylene glycol and calcium phosphate (Penn et al., 2021). The effect of the ventilation rate was studied by the measurement of the temperatures obtained inside the system and the moisture content of the synthetic sludge at the outlet of the dryer.

The prototypes were placed at the roof of the Chemical Engineering building (latitude: 29°52'08.1" S; longitude: 30°58'46.6"E), at Howard College campus, University of KwaZulu-Natal, Durban, South Africa. The prototypes were tested during the month of May and June, corresponding to austral autumn, where the average irradiances are typically comprised between 90 to 105 W/m². The tests were carried out between 9:30 AM and 2:30 PM, range where the solar irradiance has attained its peak value and does not vary significantly.

3. RESULTS AND DISCUSSIONS

3.1. Results of the greenhouse testing

Table 1 shows the temperature difference between the air inside the dryer as compared to the temperature of ambient air at different ventilation conditions.



Table 1. Temperature measurement during tests of the greenhouse without feedstock.

Time	Outside Temp (°C)	GH Temp (°C) no ventilation	GH Temp (°C) ventilation full	GH temp (°C) ventilation half
09:30	34.4	42.9	41.2	40.2
10:00	34.3	43.7	38.3	37.5
10:30	34.4	43.1	38.1	37.6
11:00	32.2	42.9	38	38.7
11:30	31.3	42.4	38.5	39.6
12:00	30.0	41.4	37.6	36.8

It can be observed that temperatures higher than 10°C with respect to the ambient conditions can be obtained in the greenhouse without ventilation. If the fans are turned on, the temperature in the greenhouse decreases by a few degrees. There is no significant difference between the ventilation at full and half capacity. This result suggests that the increase of ventilation leads to lower temperatures inside the greenhouse.

During the evaporation tests, approximately 20 g of water was evaporated from each container after 4 hours of operation, demonstrating that evaporation occurred similarly at the different positions inside the greenhouse. The evaporation rate was then calculated at 2.1 kg/h/m² from the loss of mass of water, time of the test and surface area of the containers. From this result, it was estimated that the greenhouse would be able to dry faecal sludge in a bed of 1 m² surface area and 0.1 m of thickness (leading to a sludge volume of 0.1 m³ and weight of 120 kg considering a density of 1000 kg/m³) from an initial moisture content of 80% (typical value for the sludge from local pit latrines) to 20% in theoretically 35 h (equivalent to 7 days considering 6 hours of full sunlight per day). Nonetheless, sludge drying takes more time than water evaporation, so the drying time will take probably longer than the calculated value above in a real scenario.

3.2. Results of the screw conveyor solar dryer testing

Table 2 displays the results from the tests without feedstock, with wet soil and synthetic sludge in the screw conveyor solar drier, including temperature measurements and final moisture content. The tests were conducted at different ventilation rates.

The dehumidifier incremented the temperature of the air flowrate of a few degrees and led to the drop of the relative humidity to values around 35%, which is favorable for the drying process. After the solar air heater, the airflow gained a significant higher temperature and its humidity further decreased. Therefore, the combination of an air dehumidifier with solar heater allowed to obtain airflow temperatures up to 45 °C and relative humidities almost as low as 25%. In the drying chamber, the temperature tended to drop and the humidity to rise, which could be due to heat losses and the drying process that absorbs heat and releases humidity.

During the wet soil tests, most of the added moisture in the solid was removed in less than 30 minutes, showing that the system was able to completely dry the sample in a relative short amount of time. With synthetic faecal sludge as feedstock, it could be observed that a lower ventilation rate led to a slightly higher temperature at the inlet of the drying chamber and a better moisture removal. Indeed, the airflow temperature at the inlet of the drying chamber was around 45°C at airflow below 130 m³/h, whereas it was measured at 40°C at an airflow of 203 m³/h. In addition, the simulant was dried to 30% moisture content after 2 hours of residence time at 75 m³/h air flowrate, whereas a final moisture of 55% and 60% was achieved at 130 and 203 m³/h air flowrate, respectively. Therefore, operating the solar drier at low ventilation rate seems more optimal as the airflow was heated at higher temperature inside the system, providing more thermal energy for moisture evaporation.



Table 2. Results of the tests in the screw conveyor solar drier (SAH: solar air heater; DC: drying chamber).

Feedstock	Residence time	Ventilation rate	Temperature / humidity				Final moisture content
			Ambient	Outlet dehumidifier	Outlet SAH	Outlet DC	
None	N.A.	203 m ³ /h	24°C / 67%RH	32°C / 35%RH	38°C / 31%RH	34°C / 33%RH	N.A.
Wet soil	30 min	203 m ³ /h	30°C / 80%RH	34°C / 53%RH	43°C / 30%RH	35°C / 70%RH	0%
	1 h	203 m ³ /h	31°C / 67%RH	40°C / 45%RH	45°C / 30%RH	90°C / 67%RH	0%
Synthetic sludge	2 h	203 m ³ /h	27°C / 98%RH	35°C / 58%RH	42°C / 39%RH	40°C / 62%RH	60%
		130 m ³ /h	33°C / 85%RH	35°C / 52%RH	45°C / 30%RH	40°C / 55%RH	55%
		75 m ³ /h	32°C / 80%RH	36°C / 52%RH	45°C / 67%RH	41°C / 650%RH	30%

During these tests, one of the major observations was how challenging it was to work with synthetic sludge. The sludge tended to stick to all surfaces within the dryer and coat the blades of the auger in a thin layer (Figure 3). As the sludge dried, it acquired a rubber like consistency and stuck to the blades. This meant that a considerable amount of sludge tended to get stuck within the dryer and not exit the system (making difficult its quantification). However, the sludge stuck to the blades tended to get dried well with time, due to how hot the auger gets while the reflectors were in place.



Figure 3. Photograph displaying how synthetic sludge tended to stick to the auger surface.

4. CONCLUSIONS

The testing results were promising with the functionality tests showing that the systems functioned well together. The solar thermal systems increased the temperature by 10-25°C with respect to the ambient conditions, leading to relative humidities lower than 30%, which is favorable for the drying process. The temperature increase tended to be higher in the screw conveyor solar drier than the greenhouse solar drier. The greenhouse could evaporate water at a rate of 0.8 kg/h/m², whereas the screw conveyor dried completely the wet soil (40% moisture content) in less than 30 minutes and reduced the synthetic sludge moisture content from 80% to 60 – 30%. The most optimal conditions were obtained when the ventilation was operated at low air flowrate for both systems as the temperatures achieved in the drying chamber were higher. This led to a higher moisture removal from the synthetic sludge in the case of the screw conveyor solar drier. It was suspected that high ventilation rate led to a cooling effect of the system.



After the testing phase for both prototypes, improvements have been identified for the next round of iteration. In particular, the sludge stickiness is a critical problem that must be resolved to achieve sustainable long operation times.

5. ACKNOWLEDGEMENTS

The authors would like to acknowledge the funders from this project (Water Research Commission through the K5/2852 project and the Royal Academy of Engineering through TSP2021_100224 Grant), as well as the eThekweni municipality and the administrative and technical staff from the WASH R&D Centre (in particular, Poovalingum Govender, Thabiso Zikalala, Kerry Lee Philp, Nombuso Mtshali and Lungile Ndlela).

REFERENCES

- Ameri, B., Hanini, S., Benhamou, A. and Chibane, D., 2018. Comparative approach to the performance of direct and indirect solar drying of sludge from sewage plants, experimental and theoretical evaluation. *Solar Energy*, 159, 722-732.
- Andersson, K., Otoo, M. and Nolasco, M., 2018. Innovative sanitation approaches could address multiple development challenges. *Water Science and Technology*, 77(4): 855-858.
- Meyer-Scharenberg, U. and Pöppke, M., 2010. Large-scale Solar Sludge Drying in Managua/Nicaragua. *Wasser und Abfall*, 12(3):26.
- Murray Muspratt, A., Nakato, T., Niwagaba, C., Dione, H., Kang, J., Stupin, L., Regulinski, J., Mbéguéré, M., and Strande, L., 2014. Fuel potential of faecal sludge: calorific value results from Uganda, Ghana and Senegal. *Journal of Water, Sanitation and Hygiene for Development*, 4 (2): 223–230.
- Penn, R., Ward, B. J., Strande, L. and Maurer, M., 2021. Faecal sludge simulants: review of synthetic human faeces and faecal sludge for sanitation and wastewater research. *Methods for Faecal Sludge Analysis*. IWA Publishing.
- Seck, A., Gold, M., Niang, S., Mbéguéré, M., Diop, C. and Strande, L., 2015. Faecal sludge drying beds: increasing drying rates for fuel resource recovery in Sub-Saharan Africa. *Journal of Water, Sanitation and Hygiene for Development*, 5(1): 72-80.
- Seginer, I. and Bux, M., 2006. Modeling solar drying rate of wastewater sludge. *Drying Technology*, 24(11): 1353–1363.
- Shanahan, E. F., Roiko, A., Tindale, N. W., Thomas, M. P., Walpole, R., & Kurtböke, D. İ., 2010. Evaluation of pathogen removal in a solar sludge drying facility using microbial indicators. *International Journal of Environmental Research and Public Health*, 7(2), 565-582.
- Socias, I., 2011. The solar drying plant in Mallorca: the drying process in waste management. *European Drying Conference*. Palma de Mallorca, Spain.
- Strande, L., Ronteltap, M. and Brdjanovic, D., 2014. The global situation. Faecal Sludge Management: Systems Approach for Implementation and Operation. *IWA Publishing*, London.
- Wang, P., Mohammed, D., Zhou, P., Lou, Z., Qian, P. and Zhou, Q., 2019. Roof solar drying processes for sewage sludge within sandwich-like chamber bed. *Renewable Energy*, 136, 1071-1081.
- World Health Organization, 2021. Progress on household drinking water, sanitation and hygiene 2000-2020: five years into the SDGs.



Solar cell elements based on graphene-porphyrin nanocomposites

G. Gyulkhandanyan¹, P. Gikas² and G. Shmavonyan³

¹Laboratory of Bioengineering, Institute of Biochemistry of the NAS of Armenia, Yerevan, Armenia

² Design of Environmental Processes Lab/School of Chemical and Environmental Engineering, Technical University of Crete, Rethymno, Crete, Greece

³Laboratory of 2D materials Engineering and Nanotechnology Innovation, National Polytechnic University of Armenia, Yerevan, Armenia

Corresponding author email: gshmavon@yahoo.com

ABSTRACT

Designing and fabricating new generation solar cells based on unique nanocomposites consisting of porphyrins (an effective element for absorbing solar energy) and graphene (a binding element and effectively transferring energy without loss to the next nodal element, the semiconductor part of the battery) is important. Porphyrins become photobleached when modified or destroyed by light. In the present research, in order to obtain stable and durable solar cell components the effect of photobleaching (photostability) of photosensitizers (PSs), such as a) cationic and anionic porphyrins in solutions (aqueous and organic) and b) layered films of the same PSs obtained on glass microscope slides by substrates rubbing method is investigated. The photobleaching of PSs was evaluated using absorbance and fluorescence measurements. Experiments showed that when porphyrins are photosensitized by sunlight, water can have a significant effect on the absorption of PSs in solution. The mechanism of such a change in absorption can occur both by the formation of singlet oxygen $^1\text{O}_2$ and other reactive oxygen species, in particular, the $\bullet\text{OH}$ radical dissolved in water. The study of the photobleaching of PSs (both cationic and anionic) in bright sunlight, immobilized and dried on a glass substrate, gave promising results: photobleaching of cationic porphyrin (TOEt4PyP) also depended on the concentration of the applied material, but photobleaching occurred to a much less extent than in solutions; for the anionic porphyrin (Al-phthalocyanine), photobleaching was even less significant. Under determined experimental conditions third generation efficient solar cell elements based on unique layered structure of graphene quantum dots (GQDs) - porphyrin nanocomposites on glass substrates were obtained.

Keywords: solar cell; cationic and anionic porphyrins; graphene; quantum dot; photobleaching; glass plates.

1. INTRODUCTION

Photovoltaic cells convert sunlight directly into electricity through the photovoltaic effect. The following three processes determine the conversion of solar energy: (I) light harvesting and exciton diffusion, (II) charge separation, and (III) carrier transport (Hasobe, 2010). The absorption of light and the subsequent transfer of an electron through an excited state are important processes for the final energy conversion (Hasobe, 2013). The design of the solar cell requires a light-absorbing material to absorb photons and generate free electrons by the photovoltaic effect (Mao, et al., 2021). The third generation is a step beyond the single-junction cells that include not only multijunction cells but also polymer and organic and dye-sensitized solar cells (DSSCs) (Dragonetti and Colombo, 2021). As such elements, photosensitizing dyes (mainly of a porphyrin structure), which have absorption in both ultraviolet (UV) and visible regions of the spectrum, have now begun to be widely used.

As PSs, porphyrins are widely used in biophotonics, in particular, for photodynamic therapy (PDT) of tumors, as well as in phototherapy of microorganisms and viruses. Another rapidly developing area is their use as elements of third-generation solar cells. In solar batteries, one of the most important processes is the most efficient capture/absorption of solar energy in a wide range of light spectrum and the efficient transfer process (the first nodal element of the solar battery) for further conversion into electricity. The important nodal element of a solar battery is a nanocomposite consisting of porphyrins/metalloporphyrins (an effective element for absorbing solar energy) and graphene (a binding element effectively transferring energy without loss to the next nodal element, the semiconductor part of the battery) (Mao, et al., 2021).



The aim of the study is to obtain unique layered nanocomposite structure consisting of porphyrins and GQDs for high efficient third generation solar cells.

Porphyrins as PSs can convert solar energy according to the first of the three processes, namely - (I) light harvesting and exciton diffusion. A simple synthesis pathway, a high molar extinction coefficient, and a lower fabrication cost compared to other PSs give to porphyrin sensitizers a big advantage (Armel, et al., 2011). Graphene, which has a high conductivity and unique electronic properties, can convert solar energy by the second of the three processes - (II) charge separation. These two substances, porphyrin and graphene, forming a nanocomposite, turned out to be extremely promising and effective in terms of converting solar energy into electrical energy without loss of light energy (Mao, et al., 2021; Ge, et al., 2015). GQDs are known to have high photostability and an important quality of binding and self-assembly with porphyrins (protoporphyrin IX) (Gao, Song, et al., 2020). The interaction of graphene with porphyrin can be studied by Fourier transform Raman spectroscopy, atomic force microscopy, and the fluorescent resonance energy transfer method (Gao, Ma, et al., 2020; Clapp, et al., 2004).

For the normal functioning of the solar battery, it is necessary that its component parts (nodes) work in conditions of solar radiation stability for a long time. High-energy light (especially its UV component) can change and destroy elements of the nanocomposite (in particular, porphyrin), significantly reducing its effectiveness. The photobleaching factor has not been sufficiently studied, although it is one of the decisive factors for the long-term operation of solar cells. In this case, for each specific PS, photobleaching should be studied separately due to the difference in their structure and interaction with graphene. Porphyrins become photobleached when modified or destroyed by light (Spikes, 1992; Moan, 1986; Ma, et al., 1994) and this process must be strictly considered. The phenomenon of photobleaching (photodegradation) of porphyrins has been well studied in solutions. Illumination of a porphyrin solution usually leads to changes (degradation) of its macrocycle, resulting in a decrease in the absorption intensity of spectral bands in the visible part of its spectrum, especially the Soret band (400 nm - 450 nm) (Spikes, 1992). Changes in the fluorescence spectra of porphyrins reflect not only photodestruction of the porphyrin macrocycle, but also changes in the porphyrin environment, state of aggregation, and reaction conditions (Schneckenburger et al., 1988; Margalit et al., 1983).

In this work photobleaching of both solutions of PSs (aqueous and organic) and films of the same PSs in the solid state on glass microscope slides were investigated. Spectral measurements made it possible to study not only changes in the nanocomposite components, but also their interaction. Based on these results efficient solar cell elements based on unique layered structure of graphene quantum dots (GQDs) - porphyrin nanocomposites on glass substrates were obtained.

2. MATERIALS AND METHODS

2.1. Porphyrins in solution

As a component of nanocomposites meso-substituted cationic 3- and 4-pyridylporphyrins and metalloporphyrins with various peripheral functional groups (butyl-, hydroxyethyl-, allyl-, and metallyl-) were synthesized in Armenia and in the UK (Tovmasyan, et al., 2008). The absorption spectra of PSs were recorded on a Shimadzu UV-VISIBLE Recording UV-2100 spectrophotometer (Japan), as well as on a Cary 60 UV-Vis spectrophotometer (Agilent Technologies Co., USA) in a quartz cuvette (0.1 cm or 1 cm), in the range of 200 nm - 850 nm. The initial preparations (powders) of porphyrins and metalloporphyrins and other PSs (Al-phthalocyanine) were dissolved in an appropriate organic solvent (dimethyl formamide, dimethyl sulfoxide or acetonitrile) and, as a control, in distilled water at a concentration of 10^{-3} M one hour before the experiment. All the solutions were stored at room temperature or at 6 - 8°C in the dark.

2.2. GQDs films and layered structures of GQDs – porphyrin nanocomposites

Films of graphene and PSs (anionic and cationic porphyrins) and layered structure of graphene (GQDs) – porphyrin nanocomposites were obtained on glass microscope slides 25.4 mm x 76.2 mm and 1.0 nm - 1.2 mm thick (Medisar Co., Yerevan, Cat. No. 7105-F) by substrates rubbing method (Shmavonyan, et al., 2017, López-Quintela, et al., 2016, López-Quintela, et al., 2021) by rubbing graphite and/or porphyrin powders on a glass substrate at atmospheric pressure conditions.



2.3. Photobleaching

Studies of the photostability (photobleaching) of porphyrins (cationic and anionic Al-phthalocyanine) as solutions, as well as PSs applied on microscope slides as films, were carried out by exposure against solar radiation ($\sim 100 \text{ mW/cm}^2$, irradiation for 1, 3, 6 and 12 hours).

3. RESULTS AND DISCUSSION

In order to obtain layered structure of graphene - porphyrin nanocomposites obtained by substrates rubbing technology, first we studied the photobleaching phenomena for a number of cationic and anionic porphyrins in solutions, since this phenomenon can lead to a decrease in the efficiency of collecting sunlight by the porphyrin molecule, as well as damage to the solar battery. To study the effect of photobleaching in PSs in case of bright sunlight ($\sim 100 \text{ mW/cm}^2$) and to compare both PSs and to study the concentration dependence (10^{-4} M and 10^{-5} M), aqueous solutions of two types of PSs: cationic (meso-tetra[4-N-(2'-oxyethyl)pyridyl] porphyrin: TOEt4PyP) and anionic (Al-phthalocyanine) were studied. Subsequently, the results obtained were compared with the data obtained for films of PSs on microscopic glass slides by substrates rubbing method.

Photobleaching studies of preparations were studied spectrophotometrically. A typical spectrum of an anionic PS Al-phthalocyanine ($[C] = 10^{-5} \text{ M}$) presented (the spectrum was studied in a cuvette with an optical path length of 1 mm) (Figure 1). The study of photobleaching for this PS was performed on the most intense absorption band at wavelength of $\lambda = 679 \text{ nm}$ (the spectrum also shows less intense absorption bands at wavelength of $\lambda = 352 \text{ nm}$ and 215 nm).

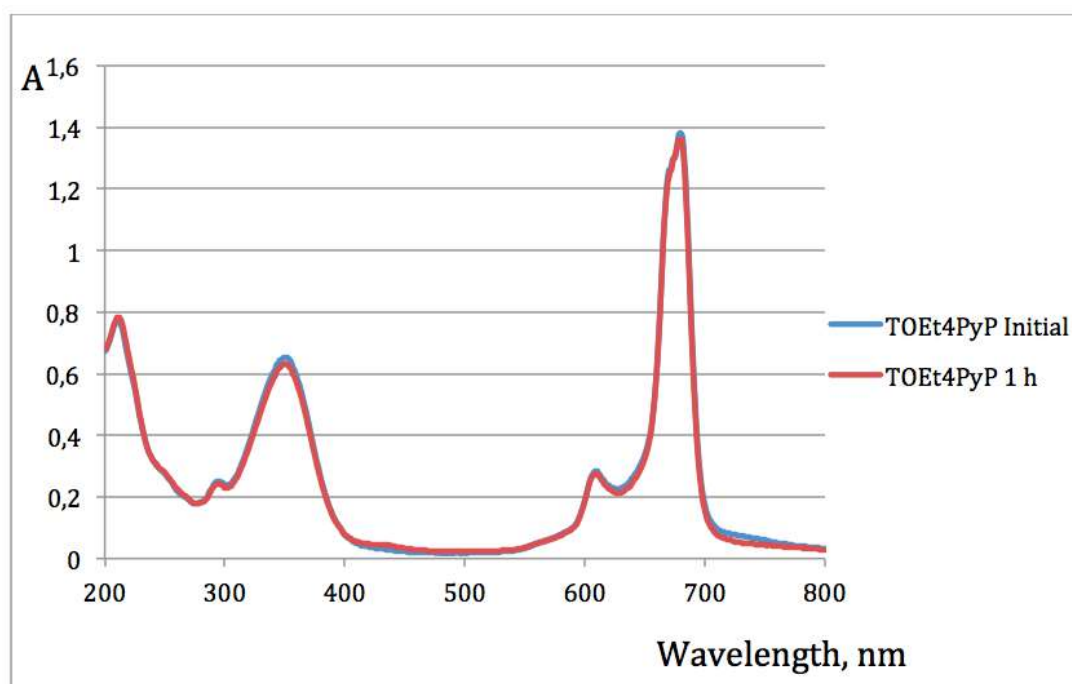


Figure 1. Absorption spectra of the anionic PS Al-phthalocyanine ($[C] = 10^{-5} \text{ M}$) (the spectrum was studied in a cuvette with an optical path length of 1 mm). The blue and red colors show the spectra of the initial PS solution and after its illumination after 1 hour, respectively.

The results of the photobleaching study of the anionic PS Al-phthalocyanine under sunlight ($\sim 100 \text{ mW/cm}^2$) are shown in Table 1.



Table 1. The data obtained from a typical spectrum of the anionic PS Al-phthalocyanine after photobleaching (Figure 1).

Concentration of porphyrin, [C]	Initial		Duration of photobleaching, 1 hour		Duration of photobleaching, 3 hours		Duration of photobleaching, 12 hours		Decrease of concentration ... times
	λ (nm)	A	λ (nm)	A	λ (nm)	A	λ (nm)	A	
10^{-5} M	678.5	0.136	679.0	0.137	678.5	0.120	679.0	0.077	1.77
	348.0	0.063	347.5	0.066	348.0	0.056	352.0	0.038	
10^{-4} M	679.0	1.248	679.0	1.245	679.0	1,156	679.0	0.866	1.44
	352.0	0.596	351.0	0.584	351.0	0.531	352.0	0.386	

From the results of Table 1 it follows that the anionic photosensitizer Al-phthalocyanine is subject to photobleaching, while sunlight does not damage the PS for 1 hour (the spectra practically coincide), while further exposure to light reduces the intensity of light absorption at $\lambda = 679.0$ nm, which is more significant for low concentration (10^{-5} M) than for high concentration (10^{-4} M), by factors of 1.77 and 1.44, respectively.

The data obtained from a typical spectrum of the cationic porphyrin TOEt4PyP ($[C] = 10^{-5}$ M) (the spectrum was studied in a cuvette with an optical path length of 1 mm) are shown on Figure 2. The study of photobleaching for this PS was carried out using the most intense Soret absorption band at a wavelength of $\lambda = 424$ nm (the spectrum also shows much weaker absorption peaks in the Q region from 650 nm to 520 nm, as well as in the UV part of the spectrum).

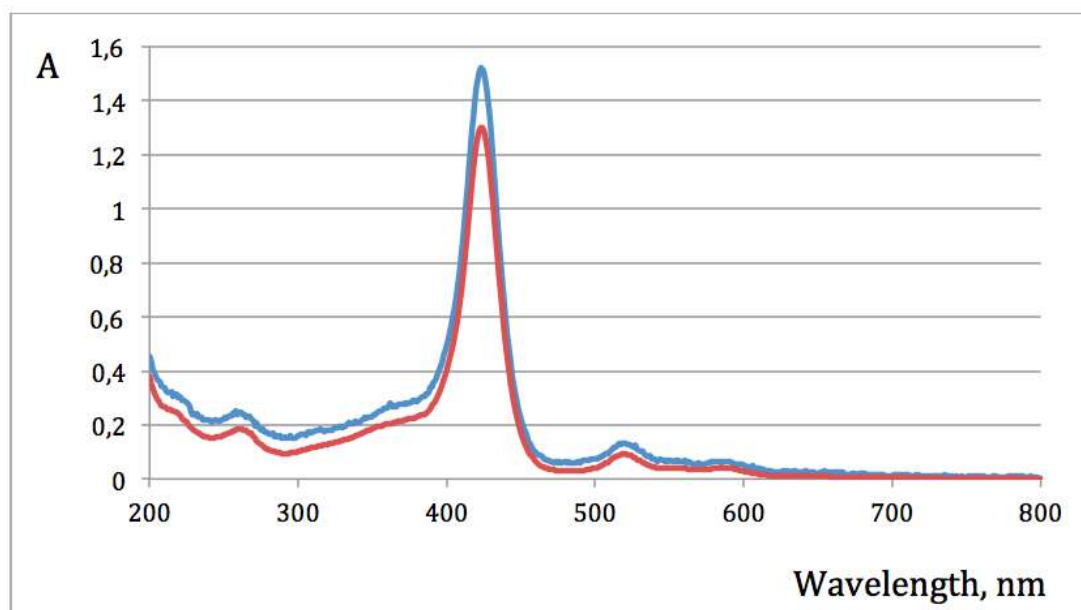


Figure 2. Absorption spectra of the cationic porphyrin TOEt4PyP ($[C] = 10^{-5}$ M) (the spectrum was studied in a cuvette with an optical path length of 1 mm). The blue and red colors show the spectra of the initial PS solution and after its illumination after 1 hour, respectively.

The results of the photobleaching study of the cationic porphyrin TOEt4PyP under its illumination by the sun (~ 100 mW/cm²) are shown in Table 2. From the results of Table 2 it follows that the cationic porphyrin TOEt4PyP is subject to significantly stronger photobleaching than the anionic Al-phthalocyanine. Already after 1 hour of exposure of the TOEt4PyP porphyrin solution against the sun, it changes the absorption at the peak of the Soret band ($\lambda = 424$ nm), and further, after 12 hours of exposure against the sun, a very significant decrease in absorption occurs at $\lambda = 424$ nm (more than 9 and 1.7 times for porphyrin concentrations of 10^{-5} M and 10^{-4} M, respectively).



Table 2. The data obtained from a typical spectrum of the cationic porphyrin TOEt4PyP after photobleaching.

Concentration of porphyrin, [C]	Initial		Duration of photobleaching, 1 hour		Duration of photobleaching, 3 hours		Duration of photobleaching, 12 hours		Decrease of concentration ... times
	λ (nm)	A	λ (nm)	A	λ (nm)	A	λ (nm)	A	
10^{-5} M	423.5	0.257	424.0	0.207	424.0	0.144	425.0	0.028	9.18
	260.5	0.051	256.0	0,043	256.5	0.033	-	-	
10^{-4} M	424.0	2.459	423.5	2.366	424.0	2.217	424.0	1.438	1.71
	260.5	0.314	261.0	0.305	260.5	0.305	260.5	0.305	

Thus, experimental results show that water can have a significant effect on the absorption of light by PSs. The mechanism of such a change in absorption can occur both by the formation of singlet oxygen 1O_2 and other reactive oxygen species, in particular, the $\bullet OH$ radical dissolved in water (the effects of these reactive oxygen species and possible partial protection from them by L-histidine and D-mannitol are considered in detail (Khaled et al., 2011)).

Since we propose the use of water-soluble PSs, cationic porphyrins, in solar cells (the advantage of such porphyrins is high fluorescence and a very high quantum yield of singlet oxygen $\Phi_{\Delta} = 0.85 - 0.95$ (Stasheuski, et al., 2014), the purpose of this work is also to show the possibility of using cationic porphyrins in an anhydrous medium (in the form of thin films on a microscope slide). In this regard, our further experiments were directed to the study of photobleaching of the cationic porphyrin TOEt4PyP and the anionic photosensitizer Al-phthalocyanine immobilized on glass microscope slides.

The study of photobleaching of PSs (both cationic and anionic) in bright sunlight, immobilized and dried on a glass substrate, gave much more optimistic results: photobleaching of cationic porphyrin (TOEt4PyP) also depended on the concentration of the applied preparation, but photobleaching occurred to a much less extent (up to 15 % within 12 hours) than in solutions; for the anionic porphyrin Al-phthalocyanine, photobleaching was even less significant, up to 5 %. This result can be explained by the fact that reactive oxygen species (and, in particular, singlet oxygen) are formed in solutions, leading to the photodegradation of PSs (porphyrins), while in the dry immobilized state this phenomenon is apparently insignificant (formation of the reactive oxygen species in the air is insignificant due to the low content of water vapor in the air in dry weather).

To achieve a homogeneous (uniform) incorporation (interaction) of porphyrin molecules with graphene, the solubility of the studied PSs in various organic solvents was studied, for which the solubility of graphene was previously studied: acetonitrile, dimethylformamide, and dimethyl sulfoxide. All the studied compounds of PSs showed good solubility in these solvents in a wide range of concentrations. The study of photobleaching in acetonitrile showed that photobleaching occurred in this solvent also at a low level (up to 13 % within 12 hours).

Thus, based on the above-mentioned results we obtained nanocomposites of layered structure of GQDs and porphyrin on a glass substrate (Shmavonyan, et al., 2017, López-Quintela, et al., 2016, López-Quintela, et al., 2021). During the formation of a nanocomposite with porphyrin, apparently, along with π - π interaction, electrostatic interaction with a positively charged porphyrin cycle takes place (Xu, et al., 2009; Chunder, et al., 2010).

4. CONCLUSIONS

Absorbance and fluorescence measurements of cationic and anionic porphyrins in solutions and layered films obtained by rubbing the same PSs in the solid state under determined experimental conditions (the effects of photobleaching (photostability) of PSs and homogeneous (uniform) incorporation (interaction) of porphyrin molecules with graphene by rubbing) allow obtaining stable and durable solar cell components based on GQDs - porphyrin nanocomposites on glass by substrates rubbing method.



REFERENCES

- Armel, V., Pringle, J. M., Wagner, P., Forsyth, M., Officer, D. and MacFarlane, D. R., 2011. Porphyrin Dye-Sensitized Solar Cells Utilising a Solid-State Electrolyte. *Chem. Commun.*, 47, 9327.
- Chunder, A., Pal, T., Khondaker, S.I. and Zhai, L. 2010. Reduced Graphene Oxide/Copper Phthalocyanine Composite and Its Optoelectrical Properties. *J. Phys. Chem. C*, 114, 35, 15129 – 15135.
- Clapp A. R., Medintz I. L., Mauro J. M., Fisher, B.R., Bawendi, M. G. and Mattoussi, H., 2004. Fluorescence resonance energy transfer between quantum dot donors and dye-labeled protein acceptors. *J Am Chem Soc.*, 126, 301–310.
- Dragonetti, C. and Colombo A., 2021. Recent Advances in Dye-Sensitized Solar Cells. *Molecules*, 26(9), 1-3, 2461.
- Gao, X., Ma, Z., Liu, X., Tang, L. and Li, J., 2020. A Fluorescence Resonance Energy Transfer Biosensor Based on Graphene Quantum Dots and Protoporphyrin IX for the Detection of Melamine. *Journal of Fluorescence*, 30(6):1463-1468.
- Gao, X., Song, Y., Zhang, Q., Liu, X., Tang, L. and Li, J., 2020. Application of maleimide modified graphene quantum dots and porphyrin fluorescence resonance energy transfer in the design of "turn-on" fluorescence sensors for biothiols. *Anal Chim Acta.*, 1108, 46-53.
- Ge, R., Wang, X., Zhang, C., Kang, S.-Z., Qin, L., Li, G. and Li, X., 2015. The influence of combination mode on the structure and properties of porphyrin–graphene oxide composites. *Colloids Surf. A*, 483, 45-52.
- Hasobe, T., 2010. Supramolecular Nanoarchitectures for Light Energy Conversion. *Phys. Chem. Chem. Phys.*, 12, 44–57.
- Hasobe, T., 2013. Porphyrin-Based Supramolecular Nanoarchitectures for Solar Energy Conversion. *The Journal of Physical Chemistry Letters*, 4(11), 1771–1780.
- Khaled, A., Khalid, O. and Mohamad, J., 2011. Photobleaching of Sn(IV) chlorine e6 dichloride trisodium salt in different environments, *African Journal of Biotechnology*, 10 (45), 9137-9144.
- López-Quintela, M. A., Shmavonyan, G. Sh. and Vázquez Vázquez C., 2016. Method for producing sheets for graphene Spanish patent ES2575711 B2.
- López-Quintela, M. A., Shmavonyan, G. Sh. and Vázquez Vázquez C., 2021. Method for producing sheets of graphene. USPTO patent US 10,968,104 B2.
- Mao, B., Hodges, B., Franklin, C., Calatayud, D. G. and Pascu, S. I., 2021. Self-Assembled Materials Incorporating Functional Porphyrins and Carbon Nanoplatfoms as Building Blocks for Photovoltaic Energy Applications. *Front Chem*, 9, 1-36, 727574.
- Margalit, R., Shaklai, N. and Cohen, S., 1983. Fluorimetric studies on the dimerization equilibrium of protoporphyrin IX and its haemato derivative. *Biochem. J.*, 29, 547-552.
- Moan, J., 1986. Effect of bleaching of porphyrin sensitizers during photodynamic therapy. *Cancer Left.*, 44, 45-53.
- Schneckenburger, H., Ruck, A., Bartos, B. and Steiner, R., 1988. Intracellular distribution of photosensitizing porphyrins measured by video-enhanced fluorescence microscopy. *J. Photochem. Photobiol. B*, 2, 355-366.
- Shmavonyan, G. Sh., Vázquez-Vázquez, C. and López-Quintela, M. A., 2017. Single-step rubbing method for mass production of large-size and defect-free 2D materials. *Trans. Mater. Res.*, 4(2), 025001.
- Spikes, J. D., 1992. Quantum yields and kinetics of the photobleaching of hematoporphyrin, photofrin 11, tetra (4-sulfonatopheny1)-porphyrine and uroporphyrin. *Phorochem. Photobiol.*, 55, 797-808.
- Stasheuski, A. S., Galievsky, V. A., Knyukshto, V. N., Ghazaryan, R. K., Gyulkhandanyan, A. G., Gyulkhandanyan, G. V. and Dzhagarov, B. M., 2014. Water-Soluble Pyridyl Porphyrins with Amphiphilic N-Substituents: Fluorescent Properties and Photosensitized Formation of Singlet Oxygen. *Journal of Applied Spectroscopy*, 80(6), 813–823.
- Tovmasyan, A. G., Babayan, N. S., Sahakyan, L. A., Shahkhatuni, A. G., Gasparyan, G. H., Aroutiounian, R M. and Ghazaryan, R. K., 2008. Synthesis and in vitro anticancer activity of water-soluble cationic pyridylporphyrins and their metallocomplexes. *J. Porphyrins Phthalocyanines*, 12, 1100-1110.
- Xu, Y., Zhao, L., Bai, H., Hong, W., Li, Ch. and Shi, G., 2009. Chemically Converted Graphene Induced Molecular Flattening of 5, 10, 15, 20 - Tetrakis (1-methyl-4-pyridinio)porphyrin and Its Application for Optical Detection of Cadmium(II) Ions. *J. Am. Chem. Soc.*, 131, 37, 13490 – 13497.



Synthesis and Study of starch/CeO₂ Nanoparticle Composite Material for Removal of Hexavalent Chromium from Synthetic Wastewater Solutions

O. Jaiyeola¹ and C. Mangwandi¹

¹School of Chemistry and Chemical Engineering, Queen's University Belfast, Belfast BT9 5AG, Northern Ireland, UK

Corresponding author email: c.mangwandi@qub.ac.uk

ABSTRACT

In this study starch/CeO₂ nano-composite was synthesised using the sol-gel method. The aim was to use the nano-composites for the removal of Cr(VI) from aqueous solution. The adsorbent was characterised using FTIR, TGA, BET analyses. The effects of dosage, initial concentration, pH, contact time and temperature were thoroughly investigated. The results showed that the optimum pH for Cr(VI) removal was pH 2 and the removal of Cr(VI) was increased with increasing dosage, smaller initial concentrations, longer contact times and higher temperatures. The data indicated that the adsorption process was a chemisorption process and the reaction was endothermic.

Keywords: Chromium; Starch, biosorption; Starch cerium oxide; Isotherm.

1. INTRODUCTION

Heavy metals, widely found in industrial wastewater, are extremely toxic to human kidneys, liver, lungs and intestines. Chromium (Cr) is among the toxic heavy metals present in wastewater, where it basically exists in two stable oxidation states, i.e., trivalent chromium (Cr(III)) and hexavalent chromium (Cr(VI)). Chromium is widely used in industries like electroplating, leather tanning, ceramics, pigment manufacturing, ceramics, wood preservation and manufacturing of paper. Chromium is used in leather tanning process in large quantity to stop water diffusion inside leather pores. Cr(VI) is primarily present in the form of chromate (CrO₄²⁻) and dichromate (CrO₇²⁻) ions. On the other hand the Cr(VI) is also 500 times more toxic than the trivalent form (Garg et al., 2007; Fahim et al., 2006). Hexavalent chromium Cr(VI) is a very soluble and toxic chromate anion and is carcinogenic and a mutagen. It is also known to be very toxic to humans and animals due to its ability to diffuse freely across cell membranes and its high oxidation potential (Mona et al., 2011). The common methods used for the chromium removal from wastewater include precipitation, ion exchange, membrane filtration, reverse osmosis and adsorption. Precipitation process is usually favoured, but the major drawback is sludge formation. Biosorption however, is an innovative method that uses biomaterials which are either inexpensive or highly available, for instance; olive oil industry waste (Malkoc et al., 2006).

This study uses the biomaterial starch-based as an adsorbent material for the removal of Cr(VI) ions. In this project the new adsorbent material starch/cerium oxide nanocomposite was produced as low-cost absorbents for complete removal of chromium (hexavalent/trivalent) from synthetic aqueous solutions. The effect of pH, temperature and dosage were evaluated.

2. MATERIALS AND METHODS

A dispersed solution of starch was prepared by mixing 3.0 g of starch in 100 ml of deionised water. 3.0 grams of citric acid (the crosslinking agent) and 1.5 g of the sodium hypophosphite monohydrate catalyst (NaH₂PO₂·H₂O) was dissolved in the starch solution for cross-linking (Naushad et al., 2016). The resulting starch suspension was continuously stirred at 60 °C for 2 hours, then left to cool to room temperature.

To prepare the hydrous cerium oxide, 0.02 moles of sodium hydroxide powder was dissolved in 100 mL of ethanol (absolute) to prepare 0.2 M sodium hydroxide/ethanol solution. 0.005 moles of Ce(NO₃)₃·6H₂O powder was dissolved in 100 mL of ethanol (absolute) to prepare 0.05 M Ce(NO₃)₃/ethanol solution. The sodium hydroxide/ethanol solution was then added into the Ce(NO₃)₃/ethanol solution at ambient temperature under vigorous stirring.

After the two solutions were mixed, the colour of the precipitates was white in just 20 minutes after continuous stirring. Precipitate was collected by centrifugation, rinsed with deionised water and ethanol



(absolute) three to four times and then dried in an oven at 60 °C for 12 hours to obtain Starch/CeO₂ adsorbent. Finally, the dried product was crushed using a mortar and pestle into fine particles of uniform size and shape (Li et al., 2012). The Cr(VI) concentration in solid phases was calculated from the equation:

$$Q_e = \frac{(C_i - C_e)V}{m} \quad \text{Eq. (1)}$$

where C_i and C_e are the liquid-phase concentrations of chromium initially and at equilibrium respectively and both measured in mg/L. Volume of solution (L) and m is the mass of dry adsorbent used for the experiment in grams. A colour reagent was synthesized using methods reported by (Albadarin et al., 2013) by adding 0.25 g of 1,5-diphenylcarbohydrazide to 50 mL methanol, 14 mL sulfuric acid and 500 mL deionised water. To determine Cr(VI) concentration after treatment using the nanocomposites 6 mL of the solution was added to 2 mL of the colour reagent for each sample.

3. RESULTS AND DISCUSSION

3.1 CHARACTERISATION

3.1.1. FTIR ANALYSIS

The FT-IR analysis was generally used to confirm the successful assembly of the target *starch/CeO₂* nanocomposite. This technique is used to obtain the infrared spectrum of absorbents. Peaks produced in graphs gives specific details on the chemistry within the absorbent. Intermolecular bonding and the presence of specific functional groups can be confirmed here. Figure 1 shows the FTIR spectra of starch, CeO₂ and the starch/CeO₂ nanocomposites. The peak at 3450 cm⁻¹ is from O-H stretching vibrations. The broadening of these peaks may be due to intermolecular hydrogen bonding (Naushad et al., 2016). The absorption bands at 2885 cm⁻¹ in the starch and nanocomposites spectra correspond to C-H stretching vibrations. The peak at 1702 cm⁻¹ is due to C=O stretch of the starch and the peak at 1590 cm⁻¹ is from Ce=O (De Marzi et al., 2013). The signals at 1400 cm⁻¹ are due to CH₂ bending modes. The peak at 1149 cm⁻¹ is from the C-O bending of the starch. The peak at 1060 is due to the stretching vibrations of Ce-O-C. (Calvache-Muñoz et al., 2017). The peaks at 1015 cm⁻¹ and 922 cm⁻¹ correspond to C-C and C-O bending respectively. The peak at 838 is due to Ce-O stretching (Babitha et al., 2015). The signals between 800-400 cm⁻¹ are from C-H bending from the starch. (Tarun et al., 2011) reports the presence of similar functional groups in the removal of Cr(VI) ions.

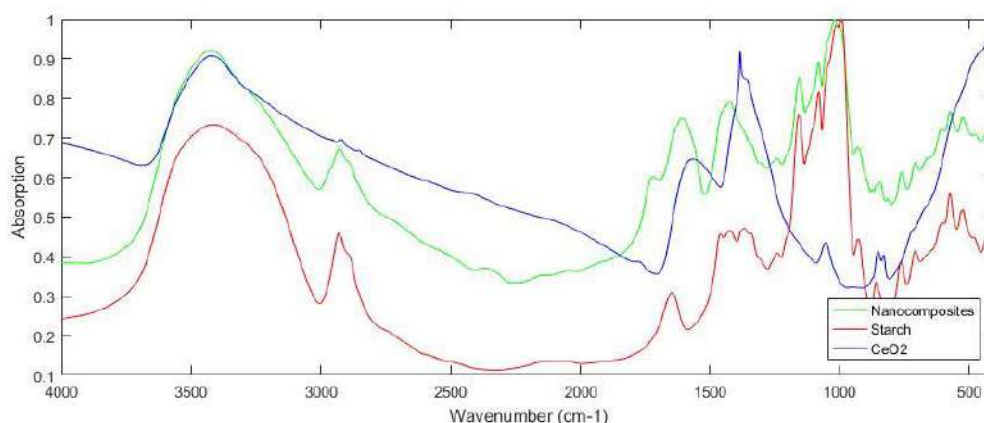


Figure 1 FTIR spectra of starch/CeO₂ nanocomposites, starch and CeO₂ nanoparticles.

3.1.2. BET ANALYSIS

BET surface area analysis, nitrogen is usually used because of its availability in high purity and its strong interaction with most solids. The the interaction between gaseous and solid phases is usually weak, the surface is cooled using liquid N₂ to obtain detectable amounts of adsorption. The nanocomposites displayed a BET surface area of 0.3204 m²/g. The nanocomposites had a single point surface area at P/P₀ of 0.3202 m²/g. A t-Plot micropore volume of 0.000946 cm³/g (Tarun et al., 2011) recorded similar surface area using rice as an adsorbent material for the removal of Cr(VI) ions.



3.1.3. TGA ANALYSIS

TGA was performed on starch/CeO₂ nanocomposite to evaluate its thermal stability in the temperature range of 25 °C to 800 °C, as illustrated in figure 2 below. The thermogravimetric curve of the starch/CeO₂ nanocomposites showed a weight loss with increasing temperature that could be due to the desorption of surface water and interlayer-adsorbed water. The nanocomposites showed a gradual mass loss of 10.03% in the 25-105°C range due to the possible evaporation of adsorbed water from the surface of this nanocomposite. This shows the adsorbent material will remain stable with an increase in temperature. This is important due to the fact that the adsorption process is an endothermic reaction.

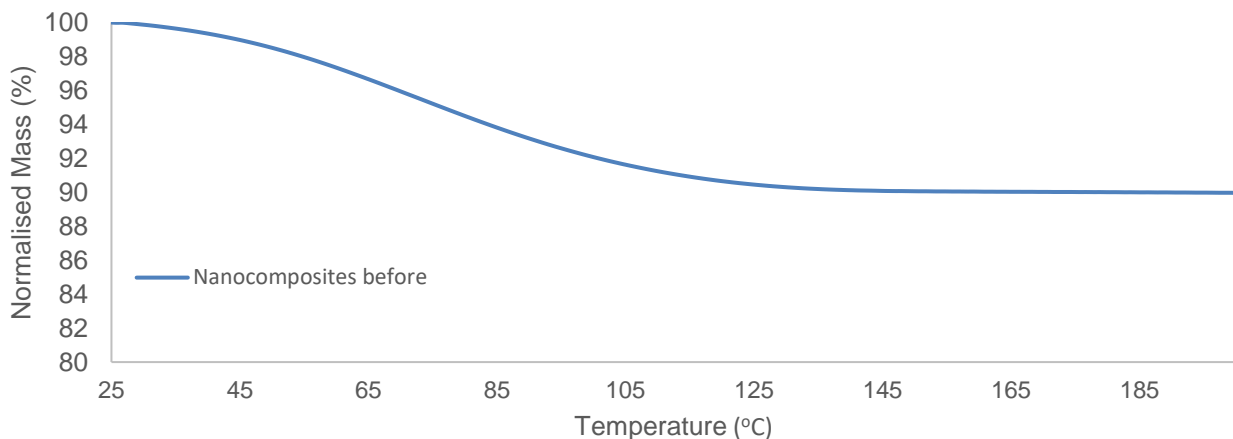


Figure 2: TGA curve of nanocomposite material.

3.2. EFFECT OF PH

pH is a key factor to consider during the adsorption process, because it affects the transfer of charges between solids and liquids. For this adsorption process, the effect of pH for the adsorption of Cr(VI) on to the starch nanocomposite material was investigated at different pH's, it was identified that for this research, the removal efficiency increases with a decrease in pH. Figure 3 below, shows that at pH 2 the percentage removal was 99.54% at neutral pH 7 there was a decrease in removal percentage which was 56.32%. At a pH of 9, removal efficiency had further reduced to 41%. The general interpretation of the influence of pH on Cr(VI) metal adsorption is according to literature and in this experiment, based on the functional group as well as the ionic composition that is present in the nanocomposite adsorbent. The high percentage removal at low pH is related to the composition of the Cr and the starch nanocomposite surface. In acidic conditions the dominant species of Cr present is Cr²⁺O₇²⁻ (Alfa-Sika et al., 2010).

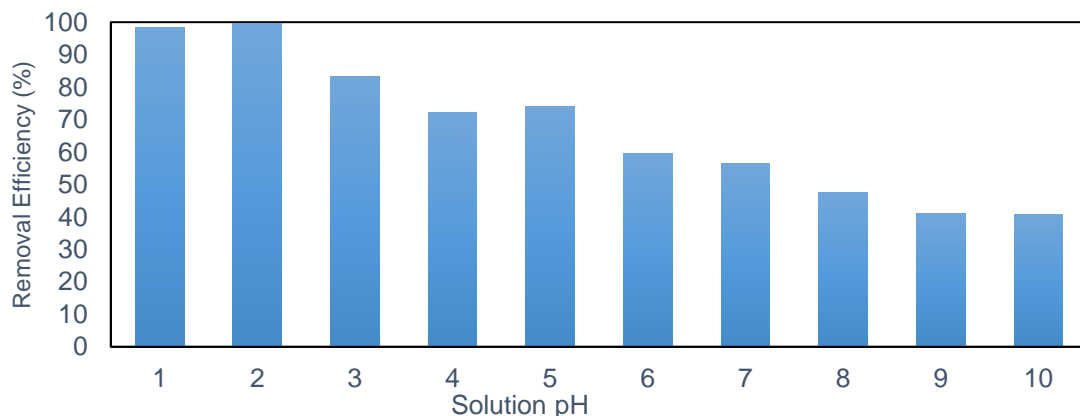


Figure 3. pH Test: The effect of solution pH on Removal % with initial concentration of 100ppm and adsorbent dosage of 2.5 g/L.



3.3. DOSAGE EFFECT OF REMOVAL OF CHROMIUM

The impact of dosage of the starch nanocomposite material was studied, Figure 4 below shows the general trend obtained from the experiment. An increase in the dosage of the adsorbent led to an increase in adsorption. Based on literature and the experiment carried out, the reason for this trend is as a result of the increase in the surface area and the presence of more active sites as the dosage is increased. The experiment was carried out with a constant volume of the adsorbate (20 ml), a constant pH of 2, a known concentration of 50 ppm and a varying mass of adsorbent material. An example of the trend observed, at mass of adsorbent 0.02 g the percentage removal of chromium (VI) in the experiment was 53.20%, however when the mass of the adsorbent was increased to 0.05 g, the percentage removal also increased to 99.54%. This is attributed to increased adsorbent surface area and availability for more adsorption sites (Rao et al., 2002; Umoren et al., 2013).

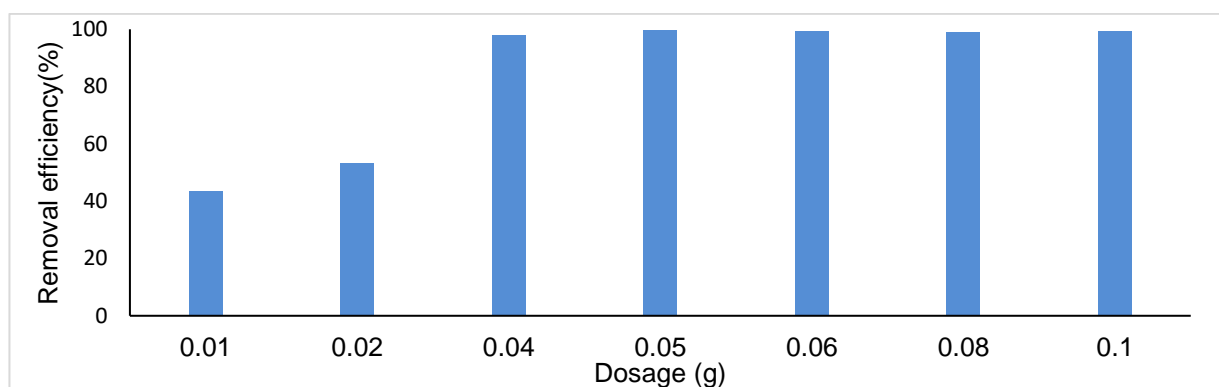


Figure 4. Dosage Test: The effect of adsorbent concentration on the Removal %.

3.4. ISOTHERM

To evaluate the adsorption capacity of the nanocomposite material, isotherm study was done. The most commonly used isotherms Langmuir and Freundlich adsorption were tested on the isotherm data.

The Langmuir isotherm model can be written as:

$$q_e = \frac{q_m b C_e}{1 + b C_e} \quad \text{Eq. 2}$$

where q_m and b are the Langmuir constants related to maximum monolayer adsorption capacity and energy of adsorption, respectively.

The Freundlich isotherm is the other empirical model which is commonly used to describe adsorption data. The Freundlich isotherm is expressed by the following equation:

$$q_e = k_f C_e^{\frac{1}{n}} \quad \text{Eq. 3}$$

where, k_f and n are the Freundlich adsorption constants.

Equations (2) and (3) were fitted to the experimental data using non-linear regression with a custom –built MATLAB app and the results are presented in Table 1. The separation factor was determined from the Langmuir parameters using the equation (4):

$$R_L = \frac{1}{1 + C_0 b} \quad \text{Eq. 4}$$

The calculated value of the separation of 0.92 indicate the adsorption was favourable under normal condition (Mckay et al., 1982). Judging from the R2 values for the different isotherms, the Langmuir isotherm fit the data better the Freundlich isotherm. It can therefore inferred that Cr(VI) ions from monolayer on the surface of the adsorbent during adsorption and that the adsorbate ions do not interact with each other during this process.

Comparison of the Langmuir capacity value for the nano-composite material with the other material in literature is reported in Table 2. The adsorption capacity reported in the current work is higher than reported values for Hazelnut shells, activated carbon from fertiliser slurry clarified sludge. It is similar to value reported for chemical activated date pits (Mangwandi et al., 2020) and hydrous Cerium Oxide nanoparticles (Albadarin



et al., 2014). This show that the material developed in this work has a good potential for use as an adsorbent material.

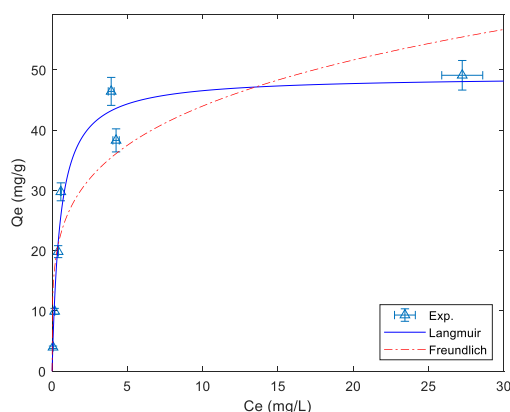


Figure 5. Isotherm models comparison for Cr(VI) removal from solution by CeO₂ starch nanocomposite adsorbent with constant pH 2 and adsorbent dosage of 2.5 g/L.

Table 1. Evaluation of correlation coefficient as well as model constants from isotherm models.

Model	Langmuir			Freundlich		
Parameter	Q _m (mg/g)	R _L	R ²	1/n	K _f	R ²
Value	48.54	0.92	0.99	0.25	18.98	0.56

Table 2. A comparative look at other adsorbents with similar results to this study.

Material	Q _m (mg/g)	pH	Reference
Carbon slurry from fertilizers	15.24	2	Gupta et al., 2010
Hazelnut shell	17.7	2	Cimino et al., 2000
CM-date pit	53.31	2	Mangwandi et al., 2020
Clarified sludge	26.31	3	Bhattacharya et al., 2008
Hydrous Cerium oxide Nanoparticles	43.1		Albadarin et al., 2014
Tea factory waste	54.65	2	Malkoc et al., 2007
Starch-CeO ₂	48.54	2	Current Study

4. CONCLUSIONS

In conclusion, there was a successful synthesis of starch/CeO₂ nanocomposites via the sol-gel method and was applied for the removal of Cr(VI) from aqueous solution. The optimum pH for this study was found to be 2 which was in agreement with earlier studies reported in literature. The detailed adsorption study shows that increasing the dosage, decreasing the initial Cr(VI) concentrations, increasing the contact time and temperature resulted in better removal percentages. The detailed adsorption study also showed that starch cerium oxide nanocomposite material had Cr(VI) removal capacity of 48.54 mg/g which is competitively high when compared to other adsorbent materials reported in literature. The new adsorbent developed in this work show great potential for removal of hexavalent chromium. Future studies will focus on evaluating its performance in a continuous system.



REFERENCES

- Aksu Z., 2002. Determination of the equilibrium, kinetic and thermodynamic parameters of the batch biosorption of nickel(II) ions onto *Chlorella vulgaris*. *Process Biochem*, 38 pp. 89–99.
- Albadarin, A. B., Mangwandi, C., Walker, G. M., Allen, S. J., Ahmad, M. N. M. and Khraisheh, M., 2013. Influence of solution chemistry on Cr (VI) reduction and complexation onto date-pits/tea-waste biomaterials. *Journal of Environmental Management*, 114, 190-201.
- Albadarin, A.B., Yang, Z., Mangwandi, C., Glocheux, Y., Walker, G. and Ahmad, M. N. M., 2014. Experimental design and batch experiments for optimization of Cr(VI) removal from aqueous solutions by hydrous cerium oxide nanoparticles. *Chemical Engineering Research and Design*, 92 (7), 1354 – 1362.
- Alfa-Sika M. S., Liu, F. and Chen, H., 2010. Optimization of key parameters for chromium(VI) removal from aqueous solutions using activated charcoal. *J Soil Sci Environ Manage*, 1, 55–62.
- Babitha, K. K., Sreedevi, A., Priyanka, K. P., Sabu, B. and Varghese, T., 2015. Structural characterization and optical studies of CeO₂ nanoparticles synthesized by chemical precipitation. *Indian Journal of Pure and Applied Physics*, 53, 596-603.
- Bhattacharya, A. K., Naiya, T. K., Mandal, S. N. and Das, S.K., 2008. Adsorption, kinetics and equilibrium studies on removal of Cr(VI) from aqueous solutions using different low-cost adsorbents. *Chemical Engineering Journal*, 137, 3.
- Calvache-Muñoz, J., Prado, F. A., and Rodríguez-Páez, J. E., 2017. Cerium oxide nanoparticles: Synthesis, characterization and tentative mechanism of particle formation. *Colloids and Surfaces A: Physicochemical and Engineering Aspects*, 529, 146-159.
- Cimino G., Passerini, A. and Toscano, G., 2000. Removal of toxic cations and Cr(VI) from aqueous solution by hazelnut shell. *Water Res.*, 34, 2955-2962.
- De Marzi L., Monaco, A., De Lapuente, J., Ramos, D., Borrás, M., Di Gioacchino, M., Santucci, S., and Poma, A., 2013. Cytotoxicity and Genotoxicity of Ceria Nanoparticles on Different Cell Lines *in Vitro*. *International Journal of Molecular Sciences*, 14, 3065-3077.
- Freundlich H. M. F., 1906. Over the adsorption in solution. *J Phys Chem*, 57, 385–471.
- Garg, U. K., Kaur, M. P., Garg, V. K. and Sud, D., 2007. Removal of hexavalent chromium from aqueous solution by agricultural waste biomass. *J Hazard Mater*, 140:60–68.
- Gupta, V., K., Rastogi, A., Nayak, A., 2010. Adsorption studies on the removal of hexavalent chromium from aqueous solution using a low cost fertilizer industry waste material. *J Colloid Interface Sci.*, 342(1), 135-41.
- Kumar, T., Singha, B. and Das, S. K., (2011). FTIR Study for the Cr(VI) Removal from Aqueous Solution Using Rice Waste. *International Conference on Chemistry and Chemical Process*, IPCBEE vol.10, IACSIT Press, Singapore.
- Langmuir, I., 1918. The adsorption of gases on plane surfaces of glass, mica and platinum. *J. Am. Chem. Soc.*, 1918, 40, 9, 1361–1403.
- Li, R., Li, Q., Gao, S., Shang, J. K., 2012. Exceptional arsenic adsorption performance of hydrous cerium oxide nanoparticles: Part A. Adsorption capacity and mechanism, *Chemical Engineering Journal*, 246(1), 127-135.
- Malkoc E., Nuhoglu, Y. and Dundar, M., 2006. Adsorption of chromium(VI) on pomace-an olive oil industry waste: batch and column studies. *Journal of Hazardous Materials*, 138, 142-151.
- Mangwandi C., Kurniawan T. A. and Albadarin A. B., 2020. Comparative biosorption of chromium(VI) using chemically modified date pits (CM-DP) and olive stone (CM-OS): Kinetics, isotherms and influence of co-existing ion. *Chemical Engineering Research and Design*, 156, 251-262.
- McKay, G., Blair, H. S., Gardener, J. R., 1982. Adsorption of dyes on chitin. I. Equilibrium studies. *J. Appl. Polym. Sci.*, 27, 3043-3057.
- Naushad, M., Ahamad, T., Sharma, G., Al-Muhtaseb, A. a. H., Albadarin, A. B., Alam, M. M., Alothman, Z. A., Alshehri, S. M. and Ghfar, A. A., 2016. Synthesis and characterization of a new starch/SnO₂ nanocomposite for efficient adsorption of toxic Hg²⁺ metal ion. *Chemical Engineering Journal*, 300, 306-316.
- Rao, M., Parwate, A. V., Bhole, A. G., 2002. Removal of Cr⁶⁺ and Ni²⁺ from aqueous solution using bagasse and fly ash. *Waste Manage*, 22, 821–830.
- Tella, A. C., Owulude, S. O., Ojekanmi, C. A., Oluwafemi, O. S., 2014. Synthesis of copper–isonicotinate metal–organic frameworks simply by mixing solid reactants and investigation of their adsorptive properties for the removal of the fluorescein dye. *New J Chem*, 38, 4494–4500.4.
- Umoren S. A., Etim, U. J., Israel, A. U., 2013. Adsorption of methylene blue from industrial effluent using.



Nutmeg seed shell-based silver nanoparticle/PVA composite for the synthesis of antimicrobial food packaging films

T. Thomas¹ and A. K. Thalla¹

¹Center for sustainable development, National Institute of Technology Karnataka, India

Corresponding author email: teemathomas111@gmail.com

ABSTRACT

Nutmeg seed shell extract which included reducing and capping agents is used to synthesise silver nanoparticles. These silver nanoparticles are embedded into polyvinyl alcohol films for antimicrobial food packaging applications. In situ preparation of these polymer composites is confirmed with the help of the XRD analysis. The films produced showed better UV blocking properties which are confirmed by transparency at 280 nm using UV visible double beam spectrophotometer. The antioxidant properties of the films are determined by the DPPH scavenging assay. With the increase in silver concentration antioxidant properties also showed better results. Moisture absorption tests were all performed on films, which resulted in the increase of moisture content with the increase in silver nanoparticle concentration. The antibacterial activity against gram-positive and gram-negative bacteria (*E. coli*, *Bacillus subtilis*) shows the film inhibits the action of bacteria with the presence of silver nanoparticles than plain PVA films. Thus, in situ production of Ag NP embedded PVA film formation by the addition of nutmeg seed shell extract as a reducing and capping agent proposes for use in food packaging.

Keywords: Nutmeg seed shell; Aqueous extract; PVA; Antimicrobial property.

1. INTRODUCTION

Pollution is happening due to over conception of polymer items in day-to-day life. Thus, the research is moving to biodegradable polymer materials. Especially food packaging materials are mainly concentrated on biopolymer composite which will preserve the food items due to its antioxidant and antimicrobial activity (Zhang et al. 2020). Polyvinyl alcohol (PVA) is a biodegradable, water-soluble, non-toxic polymer which has a growing demand in food packaging and other applications. PVA hydrophilic, polymer with, emulsifying, and adhesive capabilities as well as having superior film-forming property, flexibility and tensile strength (Jayakumar et al. 2019). It is vital to enhance its mechanical antioxidant and antibacterial properties (Balavairavan et al. 2020).

Silver nanoparticles have enhanced properties of antimicrobial antioxidant properties which is more favourable for food preservation considering their biocompatibility and non-toxicity (Yugandhar and Savithamma 2016). PVA added with silver nanoparticles (AgNP) enhances the antimicrobial property (Badawy 2014; Tanwar et al. 2021). Silver nanoparticles can be synthesized by the biological method by using biological reducing and capping agents considering environmental pollution created by another chemical and physical nanoparticle synthesis. The green synthesis of silver nanoparticles from their metal precursor can be done by adopting an apt reducing and capping agent. Nutmeg seed shell is an agricultural waste which has a high content of these reducing agents and capping agents in terms of flavonoids, myristicin, polyphenols and tannins (Latha et al. 2005; Thomas and Thalla 2022).

Here, the approach is to enhance the desired material characteristics of biodegradable polymers by adding nontoxic nanoparticles and other bioactive natural ingredients. Thus, improving the UV barrier property, antioxidant property and antimicrobial properties of food packaging polymer films. As an outcome, the food products will be well-protected, preserved, long shelf life, and have better marketing than conventional food packaging systems.

2. MATERIALS AND METHODS

Preparation of nutmeg seed shell aqueous extract

The aqueous extract from the nutmeg seed shell is prepared by adding 10 g, 105 µm size nutmeg seed shell powder into 100 mL deionized water and boiled for 1 hour and then centrifuged to separate the supernatant at 5000 rpm for 5 min.



Preparation of polymer films

In-situ preparation of polymer film is carried out by adding 5 mL of nutmeg seed shell aqueous extract to 95 mL of 1mM silver nitrate solution then, 10 g of PVA is added and continuously stirred at 1000 rpm at 90°C for One hour. The solution is poured into a Petri dish and dried for 6 hours in a hot air oven to prepare films. The polymer films were cast with 1 mM, 2 mM, 3 mM, 4 mM, and 5 mM concentrations of silver nitrate solution and control as only PVA for further analysis.

DPPH radical scavenging

To assess the radical scavenging capacity of antioxidants, the DPPH radical scavenging technique is frequently utilised. Films were divided into pieces and 0.5g is added in 10 mL methanol and stirred for 24 hours at room temperature. Supernatant and methanolic solution of DPPH (5 mg/100 mL) were combined well for an hour in dark condition. The solution's absorbance is then tested using a visible UV-visible double beam spectrophotometer (Analytical technologies 3080-TS) at 517 nm. The negative control was set to DPPH and methanol, with methanol serving as the blank. The following formula was used to determine the capacity to scavenge DPPH radicals:

$$\text{Radical scavenging activity (\%)} = (1 - A_s / A_c) * 100$$

where, A_s is the absorbance of the specified sample and A_c is the absorbance of the control.

Moisture content

Specimens measuring 20 mm×20 mm were cut from nanocomposite films, oven-dried at 60 °C for 48 hours and then weighed. The films were subsequently conditioned at 25 °C, weighing the sample every 30 min. to a constant value. For estimating the moisture content, an increase in the mass of the films is noted. The net variation between the film's initial and final moisture content provides statistics about the moisture content, according to the formula (Ramaraj 2006):

$$\text{Moisture Content (\%)} = (W - W_{\text{dry}}) * 100 / W$$

where, W = Initial weight and

W_{dry} = Dry weight

UV barrier property

Food photodegradation during storage and transportation should be prevented by the food packaging material. Food deterioration can be brought on by oxidation, which is a result of UV radiation. Thus, it is crucial to guarantee that food packaging sheets have UV light barrier qualities (Jayakumar et al. 2019). The barrier properties of produced nanocomposite films against ultraviolet (UV) was evaluated by recording transmittance (T) on a UV-visible double beam spectrophotometer within a wavelength of 280 nm. The transmittance spectra were acquired using air as background (He et al. 2019).

Antimicrobial property

The antibacterial property of films is determined by inhibition zone analysis. Escherichia coli and Bacillus subtilis were used as model bacteria to evaluate the antibacterial properties of the PVA-AgNP films prepared in this study, and the standardized agar disk diffusion plate test method was used. The nutrient broth is poured into each sterilized petri dish and microbes are uniformly spread onto it. Plates were incubated for 24 h at 37°C immediately after placing the test specimens with 5 mm circular diameter PVA-AgNP films on the agar. The bacterial growth was then checked (Maruti Kesava Kumar et al. 2015).

XRD analysis

Silver nanoparticle formation on PVA films are analysed by X-ray diffraction (XRD) analysis. X-ray diffraction was recorded by diffractometer (model: Empyrean 3rd Gen, Malvern PANalytical operated at 45 kV and a current of 40 mA using a copper (Cu) tube with Cu K α radiation ($\lambda = 1.540598 \text{ \AA}$). The diffraction intensities were recorded from 4° to 80°.

3. RESULTS AND DISCUSSION

UV barrier property



Films prepared by the addition of silver nanoparticles with the help of nutmeg seed shell aqueous extract is shown in figure 1. Here, the PVA neat film was found to be highly transparent at 280 nm with a value of 90.36 % and with the increase in the silver nanoparticle with the help of nutmeg seed shell extract the transparency decreased up to 4.04 % (Figure 2). The addition of nutmeg seed shell extract helped the formation of silver nanoparticles due to the presence of antioxidants, reducers and capping agents such as flavonoids and polyphenols. As the developed film is likely to prevent oxidation-induced food spoiling due to its outstanding UV barrier qualities and is also consistent with other research, it might be employed for active and intelligent food packaging (Jayakumar et al. 2019).

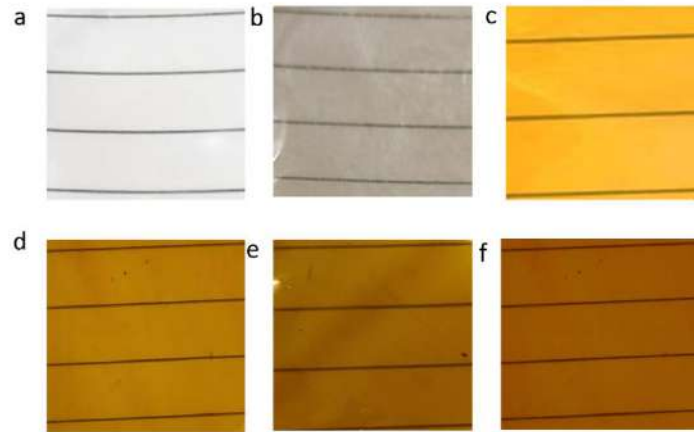


Figure 1: Photographs of PVA-Silver nanoparticles bio composite films a) PVA b) PVA1 c) PVA2 d) PVA3 e) PVA4 f) PVA5.

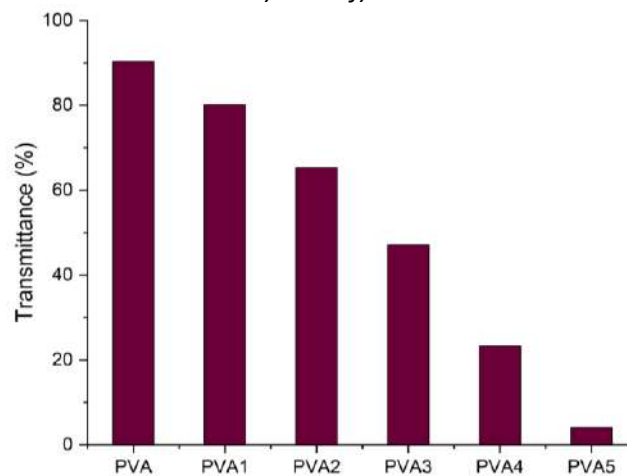


Figure 2: UV Transmittance at 280 nm.

Moisture absorption test

To ascertain a material's moisture absorptivity, a moisture absorption test is utilised. According to figure 3, the composite's ability to absorb moisture improved as the number of silver nanoparticles in the biopolymer increased. The outcome demonstrates that the composite becomes thicker when nanoparticles are introduced to the biopolymer mix, indicating that the amount of moisture absorption relies on the blend's nanoparticle concentration (Ernest Ravindran et al. 2020).

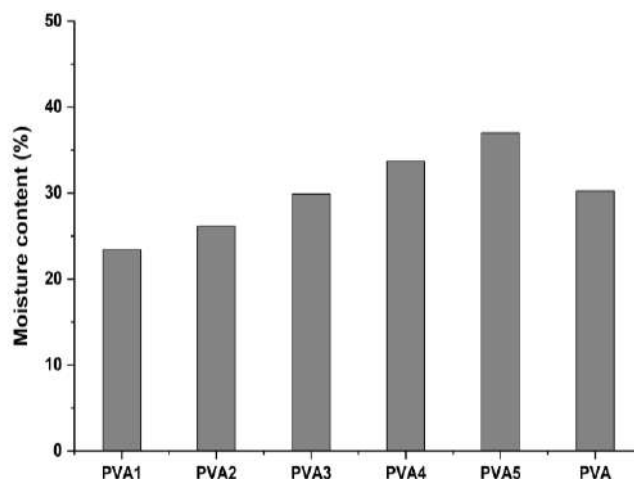


Figure 3: Moisture content.

Antimicrobial property

Antimicrobial property analysis with gram-positive and gram-negative bacteria shows that with respect to PVA films PVA-AgNP polymer composite shows better antimicrobial character and it is evident from the inhibition zone analysis (Table: 1). The inhibition of cell growth of microorganisms is due to the distortion of cytoplasm by silver nanoparticle. The distortion of microbe can be attained by two mechanisms: it will attach to the proteins that contain sulphur and result in the cell malfunctioning. The other mechanism is attachment or penetration through the cell wall, resulting in cell degradation (Haider and Kang 2015).

Table 1: Inhibition zone diameter for silver nanoparticles embedded film against bacterial strains.

Microbes	Inhibition zone (mm)			
	1 mM silver nitrate	Nutmeg seed shell extract	PVA	PVA5
<i>Ecoli rosetta</i>	6	6	0	10
<i>Bacillus subtilis</i>	0	6	0	11

DPPH scavenging assay

Food decaying enhance due to the lipid oxidation process. Antioxidant agents will inhibit this process and thus increase the shelf life of food items. Food packaging materials with antioxidant nature will thus helps to preserve the food (Tanwar et al. 2021). 2,2-diphenyl-1-picrylhydrazyl (DPPH) radicals scavenging activity of prepared films are analysed to determine the antioxidant property. The ability to change the colour of DPPH IN methanol solution to yellowish diphenyl picryl hydrazine shows the ability to reduce the radical effect by donating hydrogen (Tanwar et al. 2021). Increasing the concentration of silver nanoparticle causes a drastic colour change from purple to yellow. The samples are tested in UV-visible double beam spectrophotometer at 517 nm to determine the DPPH radical scavenging effect of prepared silver nanoparticle embedded polymer sheet. It was qualitatively obvious that films have better antioxidant property about 91 % at a 5 mM concentration of silver nitrate which is much more than plain PVA film (Figure 4). Nutmeg seed shell is also have high content of phenolic compounds responsible for the formation of silver nanoparticles from silver nitrate and the antioxidant activity of whole polymer films (Sulaiman and Ooi 2012).

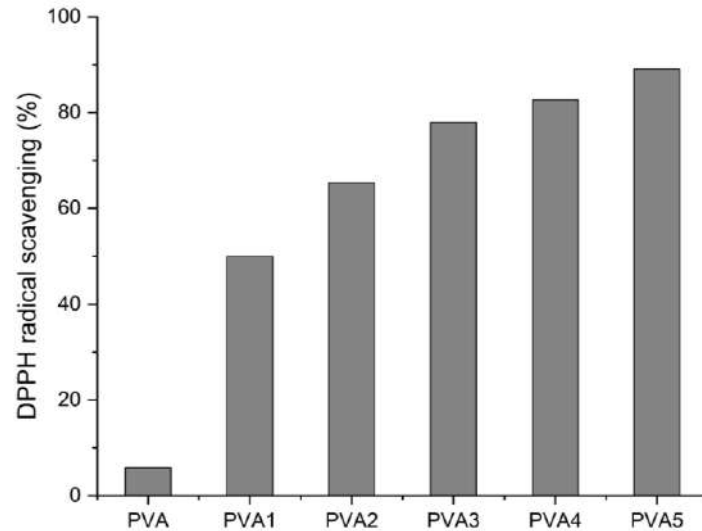


Figure 4: DPPH radical scavenging

Moisture absorption test

To ascertain a material's moisture absorptivity, a moisture absorption test is utilised. According to figure 3, the composite's ability to absorb moisture improved as the number of nanoparticles in the biopolymer increased. The outcome demonstrates that the composite becomes thicker when nanoparticles are introduced to the biopolymer mix, indicating that the amount of moisture absorption relies on the blend's nanoparticle concentration (Ernest Ravindran et al. 2020).

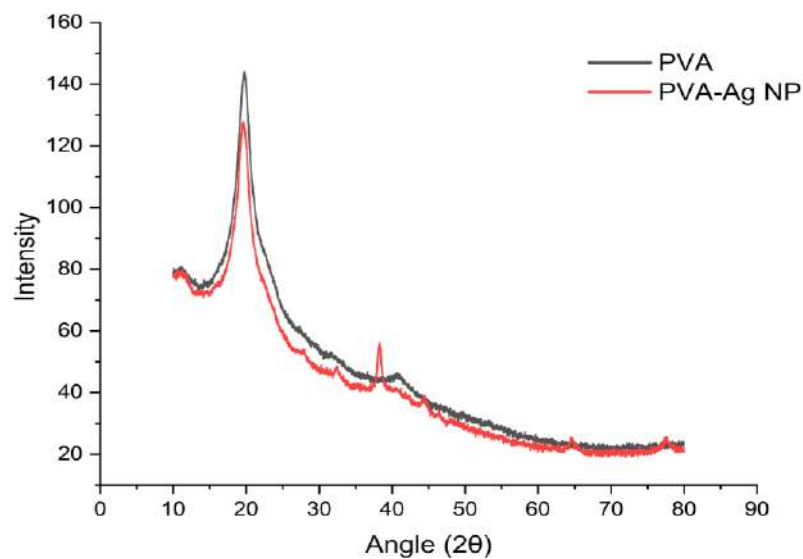


Figure 5. XRD analysis for polymer sheet with and without Ag NP

XRD analysis

The AgNPs were well crystallized and showed sharp peaks at 2θ angles of 37.5° , 45° , 63.8° and 76° (figure 5). These were assigned to the (111), (022), (220) and (131) planes of the Ag and confirm that the AgNP crystals were successfully prepared (Aravind et al. 2021). The tensile strength of the CNC-PVA-AgNP nanocomposite films increased from 42.4 MPa to 81 MPa for 10% PVA and 10% PVA with 5 mM silver nitrate solution and 5 mL extract.

4. CONCLUSIONS

PVA films are mostly used as food packaging material which is having less antimicrobial potential. In this study agricultural waste: nutmeg seed shell-based nanoparticle infusion into PVA films in a one-step process



is implemented successfully with better antimicrobial properties, antioxidant properties and UV barrier property. PVA a film with silver nitrate and extract reduced silver nitrate to form silver nanoparticles which is evidently resulted as peaks in XRD analysis. The extract and its phenolic and flavonoid content along with silver nanoparticle resulted in the enhanced properties PVA films. The PVA films shows better antimicrobial property against both gram-positive and gram-negative bacteria. And antioxidant property of PVA films with silver nanoparticles is proven by the scavenging activity against DPPH radicals. The work done shows that agricultural waste as nutmeg seed shell and its extract can act as reducing and capping agent to support the formation of silver nanoparticles and helps to improve the properties of packaging material with higher antioxidant property, UV barrier property and antimicrobial property.

5. ACKNOWLEDGEMENTS

The authors express their heartfelt gratitude to Center for sustainable development NITK Surathakal (UV-visible spectrophotometer and centrifuge), Department of chemistry, NITK Surathkal (FTIR) and Department of Metallurgy NITK Surathakal (XRD) for providing the instrumental analysis for this research work.

Funding

Authors didn't receive any funding from any organization.

REFERENCES

- Aravind, M., Ahmad, A., Ahmad, I., Amalanathan, M., Naseem, K., Mary, S. M. M., Parvathiraja, C., Hussain, S., Algarni, T. S., Pervaiz, M. and Zuber, M., 2021. Critical green routing synthesis of silver NPs using jasmine flower extract for biological activities and photocatalytic degradation of methylene blue. *J. Environ. Chem. Eng.*, 9(1), 104877.
- Badawy, S. M., 2014. Green synthesis and characterisations of antibacterial silver-polyvinyl alcohol nanocomposite films for wound dressing. *Green Processing and Synthesis*, 3(3), 229–234.
- Balavairavan, B., Saravanakumar, S. S. and Manikandan, K. M., 2020. Physicochemical and Structural Properties of Green Biofilms from Poly (Vinyl alcohol)/Nano Coconut Shell Filler. *J. Nat. Fibers.*, 18(12), 2112-2126 .
- Ernest Ravindran, R. S., Subha, V. and Ilangovan, R., 2020. Silver nanoparticles blended PEG/PVA nanocomposites synthesis and characterization for food packaging. *Arab. J. Chem.*, 13(7), 6056–6060.
- Haider, A. and Kang, I. K., 2015. Preparation of silver nanoparticles and their industrial and biomedical applications: A comprehensive review. *Adv. Mater. Sci. Eng.*, 2015.
- He, X., Luzi, F., Hao, X., Yang, W., Torre, L., Xiao, Z., Xie, Y. and Puglia, D., 2019. Thermal, antioxidant and swelling behaviour of transparent polyvinyl (alcohol) films in presence of hydrophobic citric acid-modified lignin nanoparticles. *Int. J. Biol. Macromol.*, 127, 665–676.
- Jayakumar, A., K.V., H., T.S., S., Joseph, M., Mathew, S., G., P., Nair, I. C. and E.K., R., 2019. Starch-PVA composite films with zinc-oxide nanoparticles and phytochemicals as intelligent pH sensing wraps for food packaging application. *Int. J. Biol. Macromol.*, 136, 395–403.
- Latha, P. G., Sindhu, P. G., Suja, S. R., Geetha, B. S., Pushpangadan, P. and Rajasekharan, S., 2005. Pharmacology and chemistry of *Myristica fragrans* Houtt. – a review. *J. Spices Aromat. Crop.*, 4(2), 94–101.
- Ramaraj, B., 2006. Modified poly(vinyl alcohol) and coconut shell powder composite films: Physico-mechanical, thermal properties, and swelling studies. *Polym. - Plast. Technol. Eng.*, 45(11), 1227–1231.
- Sulaiman, S. F. and Ooi, K. L., 2012. Antioxidant and anti food-borne bacterial activities of extracts from leaf and different fruit parts of *Myristica fragrans* Houtt." *Food Control*, 25(2), 533–536.
- Tanwar, R., Gupta, V., Kumar, P., Kumar, A., Singh, S. and Gaikwad, K. K., 2021. Development and characterization of PVA-starch incorporated with coconut shell extract and sepiolite clay as an antioxidant film for active food packaging applications." *Int. J. Biol. Macromol.*, 185, 451–461.
- Thomas, T. and Thalla, A. K., 2022. Nutmeg seed shell biochar as an effective adsorbent for removal of remazol brilliant blue reactive dye: kinetic, isotherm, and thermodynamic study." *Energy Sources, Part A Recover. Util. Environ. Eff.*, 44(1), 893–911.
- Yugandhar, P. and Savithramma, N., 2016. Biosynthesis, characterization and antimicrobial studies of green synthesized silver nanoparticles from fruit extract of *Syzygium alternifolium* (Wt.) Walp. an endemic, endangered medicinal tree taxon. *Appl. Nanosci.*, 6(2), 223–233.
- Zhang, X., Liu, W., Liu, W., and Qiu, X., 2020. High performance PVA/lignin nanocomposite films with excellent water vapor barrier and UV-shielding properties." *Int. J. Biol. Macromol.*, 142, 551–558.



Production of Phase Change Material from Waste Low Density Polyethylene for Thermal Energy Storage Applications

H. Akgün¹, A. Özkan¹, Z. Günkaya¹ and M. Banar¹

¹Environmental Engineering Department of Eskisehir Technical University, Eskisehir, Turkey
Corresponding author email: hasretakgun@eskisehir.edu.tr

ABSTRACT

In this study, it was aimed to investigate the potential of using pyrolysis liquid product as a phase change material (PCM). For this purpose, waste low-density polyethylene (LDPE) was pyrolyzed at 450 °C and 10 °C/min heating rate. Then, the liquid product and waste LDPEs were blending with at different mixing ratios (10/90- 30/ 70- 50/50) by extrusion method. In addition to these, same procedure was applied for commercial wax instead of pyrolysis liquid product and the results were compared. Initial characterization for the liquid product and commercial wax was carried out. For the mixtures, elemental analysis, FT-IR, TGA and DSC were used to determine the structure and properties. When the analysis results are examined, elemental content of pyrolysis product was found to be very close to commercial wax. For the mixtures, it is seen that the results of the commercial wax and the pyrolysis product are similar. DSC analyzes showed that the increase in wax content in the mixture lowered the melting and crystallization temperatures, although not significantly.

Keywords: low density polyethylene; phase change material; thermal energy storage; waste plastic.

1. INTRODUCTION

After the petroleum crises experienced in recent years, the thermal energy storage (TES) by using heat transfer media such as phase change materials (PCM) has become an increasingly important research area. The necessity to reduce the use of fossil fuels and the increasing demand in the energy sector widened the gap between energy supply and consumption (Peng et al., 2021). TES technologies basically include sensible heat thermal energy storage (SHTES), latent heat thermal energy storage (LHTES), and adsorption and chemical reaction thermochemical energy storage. Phase change materials (PCMs) used in LHTES have a compound annual growth rate (CAGR) which is 16 % (http 1, 2021). PCMs are special materials that can store a high amount of heat as energy during phase change at constant temperature and are classified as organics (paraffins and fatty acids), inorganics (salt hydrates and metals), and eutectic combinations of organic and/or inorganic materials (Abdelrazeq, 2016). Fatty acids and paraffins, as PCMs among organic materials, are the substances that have shown the most interest by researchers. They do not have corrosive and toxic effects and have a thermally stable structure, which makes organic substances superior to inorganic ones (Acar, 2014; George et al., 2020). Paraffins provide high energy storage density relative to their low mass and exhibit favorable melting and solidification with negligible supercooling, are very chemically stable and do not react with most chemicals. In order to a material to be used as PCM, its latent heat of fusion and thermal conductivity must be high, and it must have a low density for low volume change during phase change. However, since the phase changes of paraffin waxes are between solid and liquid phases, they cannot be used directly in applications. Paraffin waxes can be fixed in stable forms by blending with certain polymers or by encapsulation in a polymeric shell to prevent the leakage tendency of the PCM after melting and the loss of the liquid phase, and to isolate the PCM material from its surroundings.

Polymer composites are increasingly used in a wide variety of industrial applications (Stan et al., 2019). At this point, PE is seen as the most widely used polymer for mixing with paraffin waxes as PCM, due to its high structural and chemical similarity and features such as preventing wax leakage and allowing the inclusion of large amounts of wax in the polyethylene matrix (Sobolčiak et al., 2015; Abdelrazeq et al., 2016). Low-density polyethylene (LDPE), as a PE derivative, accounts for 17.4% of global plastics demand (Europe Plastic, 2020) and is expected to grow over 3% from 2021-2026 (http 2, 2021). The increase in the use of LDPE also brings about waste generation. It is important to use waste LDPEs in composite materials both for increasing environmental concerns and for improving the properties of materials and reducing overall production costs (Sobolčiak et al., 2015). For instance, the use of waste LDPEs as a matrix in PCM production may be an



alternative to the solution of the growing waste problem. At that point, pyrolysis comes to front since it can provide an opportunity to convert low-energy density materials into liquid energy carriers with high energy density, while also recovering certain high-value chemicals. Similarly, based on the studies examined, the potential of the wax product obtained by pyrolysis of LDPE to be used as a paraffin wax or its machinability to obtain some components for industrial use attracts attention (Onwudili et al., 2009). Compared to commercial wax obtained from petroleum, it has properties such as high softening point, excellent dispersion, flow, greater resistance to water and chemicals, as well as good chemical stability. The world market of PE wax is insufficient and relatively costly, so PE waste, PE wax conversion technology has a large potential market (Jixing, 2003). In this study, it was aimed to obtain paraffin wax by pyrolysis of LDPE packaging wastes and to use it as a PCM.

2. MATERIALS AND METHODS

This study was realized at two experimental stages; pyrolysis and extrusion. In the first stage, LDPE packaging waste collected from local markets was reduced to 5 mm x 5 mm. The pyrolysis conditions were determined through realizing Thermogravimetric analysis (TGA) and literature search and applied as 450 °C and 10 °C/min. Elemental analysis, Fourier Transform Infrared Spectroscopy (FT-IR) analysis, TGA, and differential scanning calorimetry analysis (DSC) were performed for the liquid product of pyrolysis (labeled as LDPE-Wax). Additionally, for the comparison, these analyzes were also performed for waste LDPE and commercial wax. In the second stage, LDPE-Wax was mixed with waste LDPE (1 mm x 1 mm) in different ratios (10/90, 30/70, 50/50) as supporting polymer material by extrusion method. The mixtures were blended in an 8-zone twin screw extruder with a diameter of 16 mm with an initial temperature of 130 °C, 140 °C in the other 7 zones and a screw speed of 35 rpm. Thus, PCM composites were prepared. For the comparison, the same process was repeated for commercial wax.

Elemental contents of waste LDPE and wax were determined by LECO brand elemental analyzer by taking 1-2 mg from analytical samples for analysis. The functional groups of waxes and their composites formed with waste LDPE were determined with Shimadzu IR Tracer 100 brand Fourier Transform Infrared Spectroscopy (FT-IR) analyzer. The purpose of TGA analysis is to examine the thermal stability, immiscibility, and homogeneity of PCMs over the operating temperature range. In TGA analysis, all samples (approximately 10-15 mg) were heated from 30 °C to 800 °C at a heating rate of 10 °C/min in nitrogen atmosphere and measured using the TGA Q500 - TA instrument. One of the critical parameters in PCM applications is the storage and release of thermal energy. All samples (5-7 mg) were cycled from 20 °C to 160 °C (heating/cooling) in nitrogen atmosphere with a heating/cooling rate of 10 °C/min. For the comparison, analyses were also performed for the commercial wax composites.

3. RESULTS AND DISCUSSION

Elemental analysis results are given Table 1. According to these results, the carbon content of the product obtained by the pyrolysis of waste LDPE decreases compared to waste LDPE because since some of the carbon remains in the solid and gaseous product. On the other hand, elemental content of pyrolysis wax was found to be very close to commercial wax.

Table 1. Elemental analysis results

%	C	H	O	N
Waste LDPE	87.9	10.5	1.1	0.5
LDPE-Wax	55.6	9.2	34.4	0.8
Commercial wax	57.6	9.4	32.3	0.7

The functional groups forming the obtained composites were carried out by Fourier Transform Infrared Spectroscopy (FT-IR) analysis. Since the composites are solid at room temperature, the spectra were taken by ATR attachment and the chemical compatibility between waste LDPE, PE-Wax produced from waste LDPE, commercial wax and PCMs prepared by mixing them in different ratios was tried to be determined in this way (Figure 1). When the spectra given in the figure are examined, the peaks at 2848, 2872, 2915 and 2956



represent the symmetrical stretching vibration of paraffin and LDPE in the (-CH₃) and (-CH₂) groups. The peaks at 719, 890, 1377 and 1456 are the deformation vibration of (-CH₂) and (-CH₃) groups and the swing vibration of (-CH₂). For PCM prepared with Wax / Waste LDPE, the characteristic peaks of the components can be clearly identified.

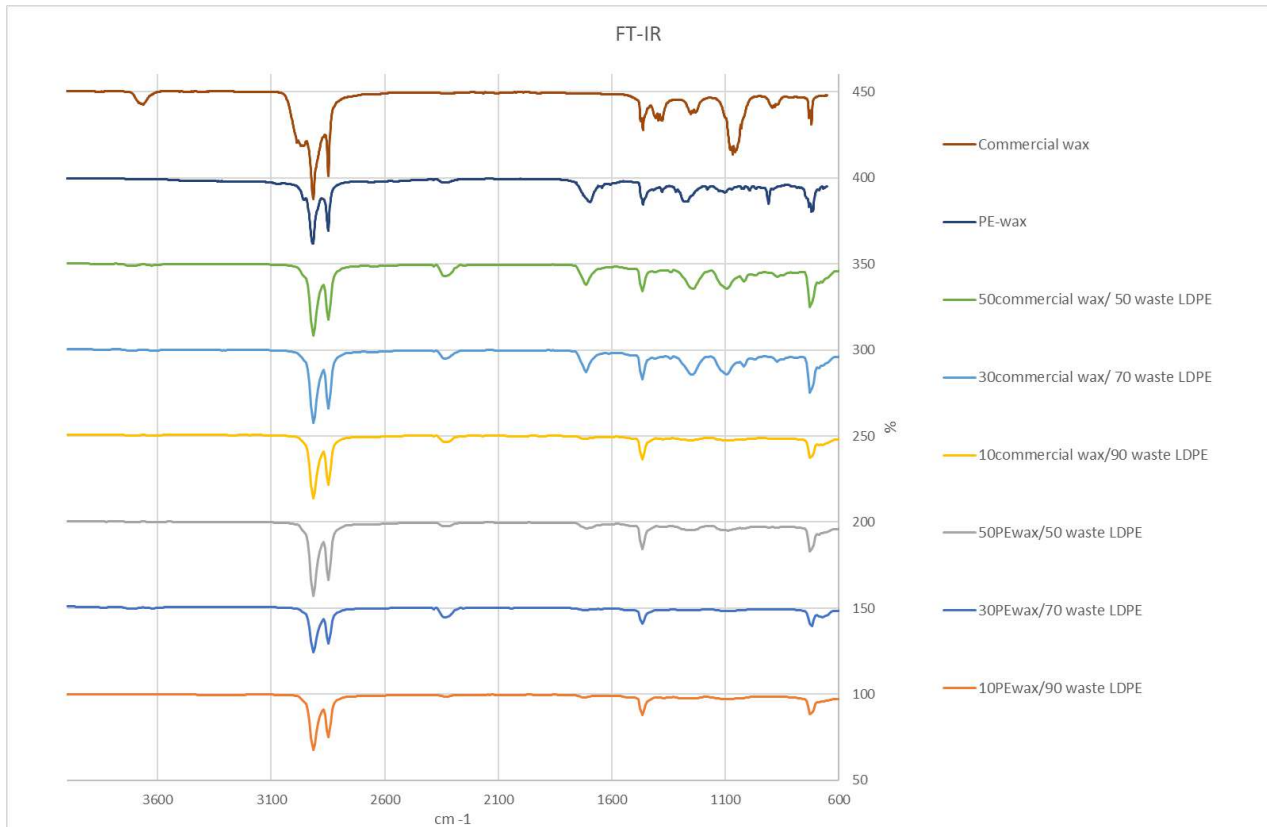


Figure 1. FT-IR Spectra.

Figures 2-9 show the TG curves of the prepared samples. Waste LDPE exhibited a single-phase degradation to 0% by weight. While waste LDPE has a decomposition temperature of 444 °C, decomposition of paraffin-LDPE mixtures increases proportionally with the increase of wax mass fraction in the mixture. Wax-waste LDPE degradation took place in two separate phases. The results of TGA reveal that the extrusion process provides a shape stable PCM. The decomposition temperatures and masses of the mixtures prepared by mixing the wax obtained from LDPE and commercial wax with waste LDPE are quite similar.

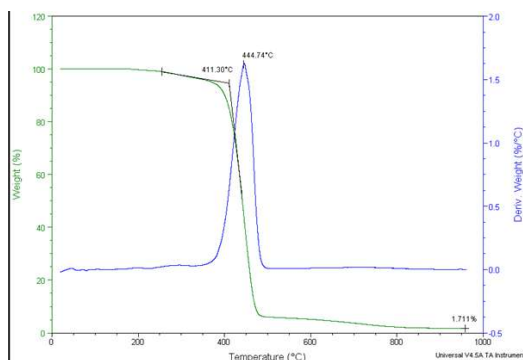


Figure 2. TGA curve of the waste LDPE.

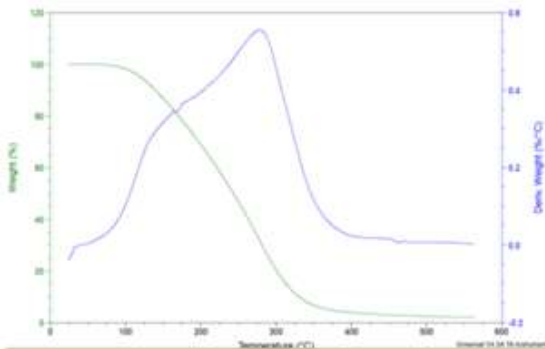


Figure 3. TGA curve of the PE-Wax.

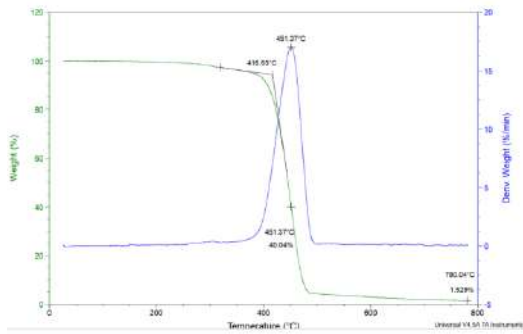


Figure 4. PE-wax/ Waste LDPE mixture (10/90).

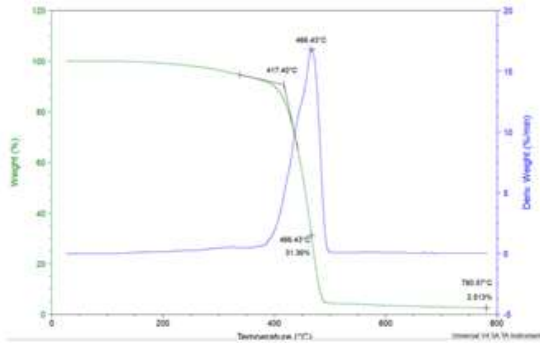


Figure 5. Commercial wax/ Waste LDPE mixture (10/90)

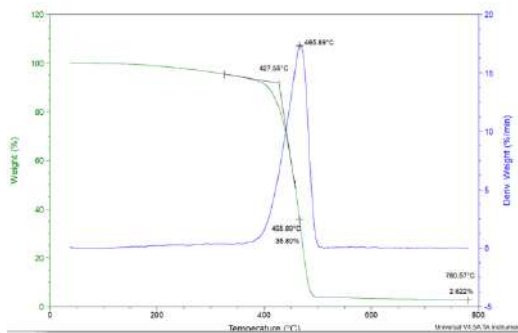


Figure 6. PE-wax/ Waste LDPE mixture (30/70).

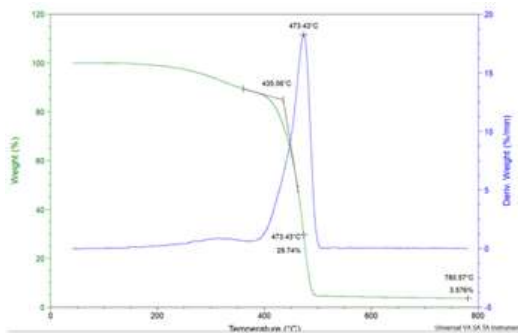


Figure 7. Commercial wax/ Waste LDPE mixture (30/70)

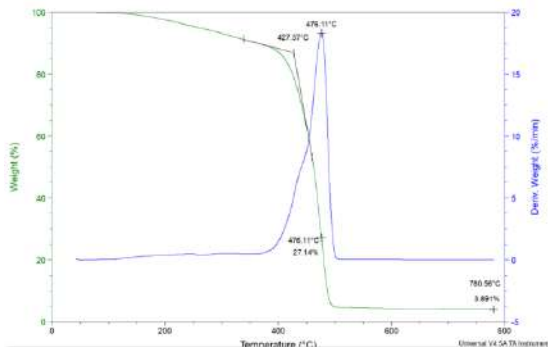


Figure 8. PE-wax/ Waste LDPE mixture (50/50).

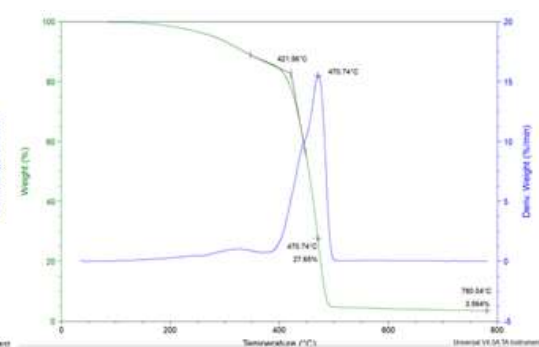


Figure 9. Commercial wax/ Waste LDPE mixture (50/50)

Melting and solidification temperatures and melting enthalpy values of wax / Waste LDPE PCMs obtained from DSC graphs are summarized in Table 2. Two peaks representing solid-solid phase transition and solid-liquid phase transition were observed in DSC plots. In cooling, reverse transitions were observed with ~10-20 °C subcooling.

In most studies in the literature, crystallization and/or melting temperature peaks for the wax component have not been reported for polyethylene/wax mixtures. This may be because the wax chains are trapped in the amorphous part of the polyethylene chains. Another possibility is the miscibility effect between polyethylene and wax in the crystal region. Conversely, some studies reported the crystallization and/or melting temperatures of both wax and polyethylene in PE/wax mixtures. This shows that a significant part of the wax and polyethylene chains crystallize and melt separately. In other cases, the wax peak crystallized and melted to form several multiple peaks. This is indicative of some degree of heterogeneity in sequence lengths, as well as discrete crystal populations consisting of chains of different crystallizable lengths. However, many reports have revealed that when the wax content is increased in PE/wax blends, there is a decrease in the crystallization and melting temperatures of the blends. This is an indication that polyethylene is plasticized by the molten wax, increasing chain mobility and reducing the temperature at which it starts to crystallize (Gumede, 2021). The melting temperature of the waste LDPE was determined as 108 °C and the melting temperature of the wax obtained by pyrolysis was determined as 88 °C. It is seen that the PCMs prepared by



extrusion rise according to the melting and crystallization temperatures of the raw materials. The increase in wax content in the mixture decreased the melting and crystallization temperatures, although it was not obvious. Wax / Waste enthalpies for LDPE decreased, although the increase in wax content had no significant effect.

Table 2. Melting and solidification temperatures and latent heat values of Wax / Waste LDPE PCMs.

Mass fraction %	Solid-liquid			
	Crystallization temperature °C	Enthalpy of crystallization (J/g)	Melting temperature °C	Enthalpy of melting (J/g)
10-90 PE-wax/waste LDPE	113.82	7.87	123.44	7.50
30-70 PE-wax/ waste LDPE	109.47	4.44	121.58	5.71
50-50 PE-wax/ waste LDPE	109.73	3.66	122.15	6.33
10-90 commercial wax /waste LDPE	108.69	5.19	122.63	6.44
30-70 commercial wax / waste LDPE	108.05	4.37	124.48	4.72
50-50 commercial wax / waste LDPE	107.63	4.57	120.78	7.58

4. CONCLUSIONS

In this study, as an alternative to paraffin wax (produced from crude oil), which is a low-cost thermal energy storage material, wax was produced from waste LDPE with good thermal stability and suitable latent heat in a certain temperature range and used as PCM. According to the analysis results obtained, the decomposition temperatures of the PCMs prepared with the wax produced from waste LDPE and commercial wax are similar. In addition, while the mixing ratios did not differ in functional groups, crystallization and melting temperatures, changes were observed in crystallization and melting enthalpies.

It is thought that it will guide future studies to make suggestions about which application areas the produced PCMs can be used according to their determined thermal properties.

5. ACKNOWLEDGEMENTS: This study was supported by Eskişehir Technical University Scientific Research Projects Commission under the grant number 22DRP156 and 22ADP097.

REFERENCES

- Abdelrazeq, H., W., 2016. Heat Absorbers Based on Recycled Polyethylene and Paraffin Wax for Energy Storage. Master's Thesis, Qatar University, College of Arts and Sciences.
- Acar, S. Ş., 2014. Phase change materials and applications.
- Chi, Y. L., Mei, T., Yi, Y. F., Ji, D. K., Ding, F. C., & Chen, L., 2012. Preparation of polyethylene wax from LDPE in the solvent. *In Advanced Materials Research* (Vol. 550, pp. 771-776). Trans Tech Publications Ltd.



- Erdoğan, S., 2020. Recycling of waste plastics into pyrolytic fuels and their use in IC engines. *In Sustainable Mobility*. IntechOpen.
- Europe, P., 2020. Plastics-the Facts 2020 An analysis of European plastics production, demand and waste data. Available on the website: <http://www.plasticseurope.org>.
- George, M., Pandey, A. K., Abd Rahim, N., Tyagi, V. V., Shahabuddin, S., and Saidur, R., 2020. A novel polyaniline (PANI)/paraffin wax nano composite phase change material: Superior transition heat storage capacity, thermal conductivity and thermal reliability. *Sol. Energy*, 204, 448-458.
- Gumede, T. P., 2021. The overall crystallization behavior of polyethylene/wax blends as phase change materials for thermal energy storage: A mini review. *J. Vinyl Add. Tech.*, 27(3), 469-484.
- http 1, 2021. Global Phase Change Materials Market - Segmented by Product Type, End-User, Encapsulation Technology and Geography - Growth, Trends and Forecasts (2018 - 2023) (accessed 18.06.2021).
- http 2, <https://www.mordorintelligence.com/industry-reports/low-density-polyethylene-market> (Accessed 27.10.2021).
- Jeswani, H., Krüger, C., Russ, M., Horlacher, M., Antony, F., Hann, S. and Azapagic, A., 2021. Life cycle environmental impacts of chemical recycling via pyrolysis of mixed plastic waste in comparison with mechanical recycling and energy recovery. *Sci. Total Environ.*, 769, 144483.
- Jixing, L. I., 2003. Study on the conversion technology of waste polyethylene plastic to polyethylene wax. *Energy sources*, 25(1), 77-82.
- Onwudili, J. A., Insura, N. and Williams, P. T., 2009. Composition of products from the pyrolysis of polyethylene and polystyrene in a closed batch reactor: Effects of temperature and residence time. *J. Anal. Appl. Pyrolysis*, 86(2), 293-303.
- Peng, H., Wang, J., Zhang, X., Ma, J., Shen, T., Li, S. and Dong, B., 2021. A review on synthesis, characterization, and application of nanoencapsulated phase change materials for thermal energy storage systems. *Appl. Therm. Eng.*, 185, 116326.
- Sobolčiak, P., Abdelrazeq, H., Ouederni, M., Karkri, M., Al-Maadeed, M. A. and Krupa, I., 2015. The stabilizing effect of expanded graphite on the artificial aging of shape stabilized phase change materials. *Polym. Test.*, 46, 65-71.
- Stan, F., Stanciu, N. V., Fetecau, C., & Sandu, I. L., 2019. Mechanical Recycling of Low-Density Polyethylene/Carbon Nanotube Composites and Its Effect on Material Properties. *J. Manuf. Sci. Eng.*, 141(9), 091004.



Effect on the thermal sensation of outdoor users due to the age of the granite blocks used in the coating of public areas

K. Stefanopoulos¹, N. Lianos¹, D. Polychronopoulos¹ and S. Zoras²

¹Dept. of Architectural Engineering, Democritus University of Thrace, Xanthi, Greece

²Dept. of Environmental Engineering, Democritus University of Thrace, Xanthi, Greece

Corresponding author email: kstefanopoulo@gmail.com

ABSTRACT

In this research we will see the results from the comparison of the temperature measurements that were made over different external points of public spaces in the old town of Xanthi. The area is located in northern Greece and is a protected settlement. All the points where the measurements were made are covered with dark gray granite blocks. This material has always been used to pave the public open spaces of the old town. Through the comparison of temperature measurements, it was found that the older coating materials develop higher temperatures compared to the same but newer materials. Thus, it was concluded that the age of the paving materials affects the comfort conditions of the users of the open public spaces. To find it out, the measurements were made during two months of spring and summer. During this period the temperatures are higher and they affect the users of the outdoor areas more, as well as the results in the comparison of the coating materials.

Keywords: granite; blocks; coating; outdoor; public area; urban; temperature; thermal sensation, comfort conditions.

1. INTRODUCTION

The aim of this work is the study of the differentiation of responses among newer materials compared to the same but older materials that have been used and exposed for a longer period of time.

The old town of Xanthi is located at the north-eastern edge of Greece in the homonymous prefecture and the Region of Eastern Macedonia and Thrace. After the catastrophic earthquake of 1829 with which the town of Xanthi was levelled, the new period of its reconstruction began with particular prosperity due to the tobacco trade from 1870-1910. Reconstruction and economic prosperity stopped in 1912 with the start of the Balkan Wars. To this day, the traditional character of the old town of Xanthi has been preserved and is a protected settlement. The streets of the old city have always had as a paving material the dark grey granite blocks that are placed with a special technique and due to their great durability are kept for many years in very good condition.

2. THE RESEARCH

The difference in climatic conditions between the city and its periphery is greatly influenced by the response of sunlight that falls and is trapped in the ground, in the coating materials and in the various general constructions (Chrysomallidou et al., 2002). This response also depends on other factors concerning the paving materials of public areas. On the one hand atmospheric air is heated by the sun rays that penetrate it and on the other hand by the surface of the earth. The comparison is made between different points in the urban area of the old town of Xanthi, which is paved with grey granite cobblestones. These areas are important road intersections, squares but also parking lots. These points have been reconstructed in different periods of time, which we know from an archive of the Municipality of Xanthi with projects carried out from 1992 until today. During the day the selected areas are exposed to the sun as well as they are in the shadow caused by vegetation or buildings, due to the course of the sun.

An effort has been made to demonstrate whether newer or older coating materials respond better in the comfort conditions of their users and especially the thermal sensation. For this purpose, the temperature was recorded at the height of a person, above specific areas that are covered with grey granite blocks, during the warm period of the year. The comparison was made between the means of the temperature



measurements recorded at each point. The measurements were made hours of the day when the sun most influences the response of the materials and specifically at 12:00 pm, 15:00 pm and 18:00 pm.

2.1 STUDY AREA

The old town of Xanthi is the study area. Occupies 380,000 sq.m. It is built at the foot of the mountain Achladovouno, the river Kosynthos passes next to the settlement and has a southern orientation. It retained its old road plan and its building stock due to its proclamation in a protected settlement. In the old town there are 1,200 protected listed buildings. Of these 140 are characterized as very remarkable, 130 as remarkable and 260 as interesting. Dark gray granite cobblestones are the main coating material of the external public common areas, which are the squares, streets, parking lots and other plateaus. In various places there is tall vegetation, the buildings have a low height and are covered with tiled roofs. The presence of trees and grass in the outdoor public areas can help develop social bonds. Vegetation also helps people relax and rejuvenate, reducing aggression (Kosmopoulos, 2001).

Temperature measurements were made at fifteen different points throughout the urban area of the old town. Every three of these points are relatively in close distance or in the same square (Figure 1). All fifteen points are important outdoor public spaces of the old town. The measuring points are sometimes near trees or buildings and other times exposed in an open area. Due to the knowledge of the time when the reconstructions of the paving of the cobblestones were done in these points, it was possible to make a comparison between points that had been reconstructed in near or distant times.

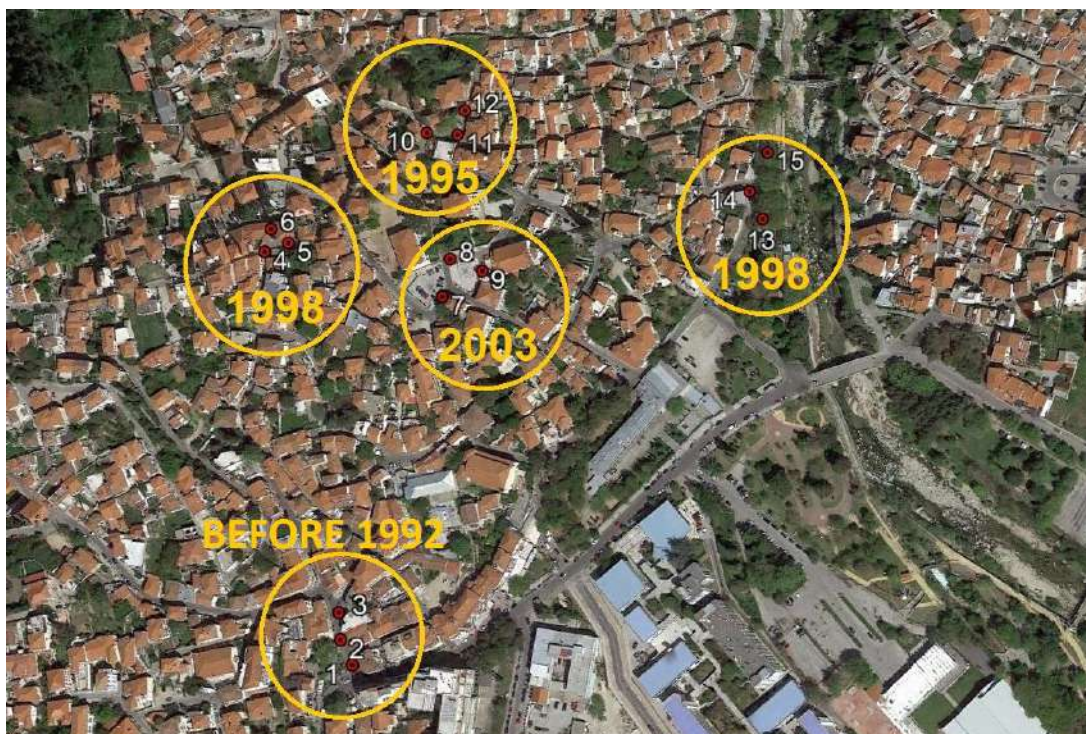


Figure 1. Measurement points and years of cobblestone reconstruction.

2.2 METHOD

The device that made the measurements for the purpose of comparing temperatures is the thermometer. Air temperature is one of the most important meteorological and climatic elements and its change is of great importance for the study of weather and climate (Flokas, 1994). The thermometer that made the measurements was connected to a digital hand measuring device of the company Kimo instruments. The model of the device is the HD 200 (Figure 2). A hygrometer with a built-in thermometer was also connected to the digital device.

To make the measurements, the measuring device went to the selected points at the selected time points. The device remained open for a period of time until the readings were stabilized and then recorded and collected to compare their values.



Figure 2. Digital measuring device HD 200 by Kimo instruments.

More specifically, the thermometer with which the ambient temperature was determined is of the black sphere type as shown in Figure 3, which can and does record values ranging from 0 °C to + 60 °C with an error of the order of 0, 5 °C and temperature resistance up to 600 °C. The measurements of this thermometer are seen in Table 1 as Tr2. This fact shows us the great accuracy of the device which is equal to +/- 0.417% of the reading.

Table 1. Indicative table of two-day measurements.

		INDICATIVE TABLE OF MEASUREMENTS																	
		ANTIKA SQUARE			PYG. CHRISTIDI & FILIPPOU			METROPOLIS SQUARE			MATSINI SQUARE			PINDAROU - WATERMILL					
DATE	HOURS	DATA	POINT 1	POINT 2	POINT 3	POINT 4	POINT 5	POINT 6	POINT 7	POINT 8	POINT 9	POINT 10	POINT 11	POINT 12	POINT 13	POINT 14	POINT 15	EMY	WEATHER
1/6/2022	12:00	RH %	22,70	24,40	23,40	28,80	26,20	28,10	30,20	28,10	26,10	26,80	26,80	30,10	28,90	27,90	29,60	36,00	☀
1/6/2022	12:00	WBGT oC	25,90	26,40	26,50	26,10	25,90	26,00	25,30	26,10	26,00	25,80	25,90	25,60	25,40	25,10	25,10	<26,6	☀
1/6/2022	12:00	Tr1	37,00	37,10	37,60	35,30	35,90	35,40	33,80	36,20	36,40	35,70	36,20	34,40	34,40	34,50	34,20	29,00	☀
1/6/2022	12:00	Tr2	38,22	38,72	39,02	37,98	37,68	37,88	37,10	38,45	38,12	37,37	37,45	36,86	37,22	36,41	35,73		☀
1/6/2022	15:00	RH %	28,70	29,80	27,70	33,20	32,30	34,50	31,10	30,40	28,60	27,20	28,00	30,10	30,80	31,30	31,50	33,00	☁
1/6/2022	15:00	WBGT oC	26,30	26,20	26,60	25,20	25,10	25,10	25,90	26,20	26,50	26,60	26,60	26,40	26,00	25,90	26,60	<26,6	☁
1/6/2022	15:00	Tr1	36,60	36,10	37,20	33,90	34,00	33,20	34,90	35,90	36,40	36,00	36,20	34,50	34,40	34,60	34,10	30,00	☁
1/6/2022	15:00	Tr2	37,51	37,88	38,83	35,62	35,68	35,13	35,63	37,32	38,03	39,48	39,64	39,27	37,53	38,03	37,87		☁
1/6/2022	18:00	RH %	29,70	30,50	28,30	35,00	34,20	35,50	33,10	31,50	28,70	28,30	29,10	30,60	31,70	32,40	32,60	31,00	☀
1/6/2022	18:00	WBGT oC	26,40	26,50	26,80	25,50	25,50	25,60	26,10	26,40	26,60	26,50	26,50	26,40	26,00	25,90	26,30	<26,6	☀
1/6/2022	18:00	Tr1	36,70	36,50	37,20	34,10	34,40	33,60	35,40	34,20	34,30	35,10	34,20	34,40	33,10	33,30	33,10	31,00	☀
1/6/2022	18:00	Tr2	37,68	37,62	38,81	35,75	35,62	35,42	37,18	35,85	35,94	37,53	36,67	36,85	36,34	36,75	36,31		☀
2/6/2022	12:00	RH %	37,30	36,10	36,30	41,70	39,00	43,20	39,40	37,50	35,30	35,30	33,80	35,30	37,80	36,30	38,30	34,00	☁
2/6/2022	12:00	WBGT oC	24,60	24,70	25,20	24,50	24,70	24,40	25,10	25,90	25,90	26,20	26,20	26,30	25,40	25,70	25,30	<26,6	☁
2/6/2022	12:00	Tr1	32,50	32,70	33,20	31,20	32,10	30,70	32,10	33,80	34,30	34,30	34,60	34,20	32,60	33,60	32,50	31,00	☁
2/6/2022	12:00	Tr2	32,43	32,85	33,84	32,72	32,57	32,61	34,51	34,40	34,68	36,36	36,48	36,88	35,53	35,07	35,10		☁
2/6/2022	15:00	RH %	32,60	33,70	30,90	36,50	35,30	37,70	33,20	32,30	31,70	30,40	30,90	31,60	34,10	34,30	34,60	27,00	☀
2/6/2022	15:00	WBGT oC	26,20	26,00	26,30	24,90	25,00	24,80	25,70	25,90	26,20	26,30	26,30	26,20	25,10	25,10	25,00	<26,6	☀
2/6/2022	15:00	Tr1	35,70	35,30	36,10	32,70	32,00	31,80	32,60	33,40	33,20	33,90	33,50	33,80	33,20	31,70	32,80	33,00	☀
2/6/2022	15:00	Tr2	37,26	37,21	38,46	35,31	34,79	33,58	34,82	35,36	35,21	36,23	35,86	36,20	35,14	33,75	34,85		☀
2/6/2022	18:00	RH %	33,30	33,90	30,80	36,80	35,40	36,10	33,20	32,50	31,90	30,50	30,90	31,30	34,50	34,70	34,80	29,00	☀
2/6/2022	18:00	WBGT oC	26,10	26,00	26,20	24,80	24,90	24,70	25,50	25,70	26,10	26,20	26,10	25,00	25,00	24,90	<26,6	☀	
2/6/2022	18:00	Tr1	35,50	35,30	36,00	32,40	32,60	31,50	32,80	32,40	32,20	34,20	33,50	33,30	32,70	32,90	32,60	32,00	☀
2/6/2022	18:00	Tr2	37,13	37,24	38,38	35,14	34,79	33,58	35,14	34,79	34,62	36,41	35,46	35,35	35,47	35,57	35,64		☀

It was able to record both liquid and spherical thermometer temperature (WBGT). This indicator expresses the thermal stress to which a person is exposed when exposed to a very hot outdoor environment. This thermal stress is a function of the heat produced within the body due to the physical activity that the individual develops and those parameters of the workplace that affect the heat exchange between the human body and the environment. The hygrometer measures a percentage of % while it has a built-in thermometer that performs measurements from -50 °C to + 250 °C. The measurements of this thermometer are seen in Table 1 as Tr1. Therefore, during the measurements, double temperature measurements were made, both of which were used for comparison, for more detailed and reliable results.

The temperature was recorded at the fifteen points of Figure 1, due to the importance of these points for the urban area of the old town. It was done for three times of each day, at 12:00, 15:00 and 18:00 in the afternoon, so that there is a set of measurements from noon until late in the afternoon. The measurements were carried out for two months, from April 14 to June 14, 2022, a period during which the sun is intense and significantly affects the comfort conditions of the users of the outdoor public spaces that we examine.

The daily measurements for its three time points and for the fifteen measurement points were placed in tables (Table 1). The comparison was made between the temperatures obtained from the average of the temperatures of all days of each point at one of the selected time points. The comparison between the points was performed twice. The first time temperatures recorded by the black sphere thermometer (Tr2) and the



second with the built-in dry type thermometer of the hygrometer (Tr1). Measurements were compared both between points that were reconstructed in the near and distant periods. This was done to see if the granite paving blocks perform differently depending on their age and which of the newer or older materials perform better.

2.3 RESULTS

A comparison was made between points that were reconstructed in the same year and specifically in 1998, such as points 4 and 14. In addition, the comparison was made between points that were reconstructed in close years, such as points 4 and 10 with respective reconstructions years of 1998 and 1995 (Figure 1). It was made at the same time of the day as well as the measurements were made when the two points that compared were both exposed to the sun or in the shadow. This choice was necessary so the worst case of sun exposure not to affect the outcome. The comparison for points 4 and 14 was made for 12:00 pm and while they were exposed to the sun, while for points 4 and 10 the comparison was made for 15:00 pm and while they were exposed to the sun too (Table 2).

Table 2. Sun exposure & shadowing table of measurement points.

		SUN EXPOSURE TABLE & SHADOWING OF MEASUREMENT POINTS - PERIOD FROM 14/4 TO 30/9 2022															
		ANTIKA SQUARE			PYG. CHRISTIDI & FILIPPOU			METROPOLEOS SQUARE			MATSINI SQUARE			PINDAROU - WATERMILL			
DATE	HOURS	DATA	POINT 1	POINT 2	POINT 3	POINT 4	POINT 5	POINT 6	POINT 7	POINT 8	POINT 9	POINT 10	POINT 11	POINT 12	POINT 13	POINT 14	POINT 15
YEAR OF GRANITE CUBE COATING CONSTRUCTION			BEFORE 1992			1998			2003			1995			1998		
PERIOD FROM 14/04 TO 14/06	12:00	SYMBOLISM OF SUN EXPOSURE & SHADOWING OF THE POINTS	●	●	●	●	●	■	■	●	■	●	●	●	■	●	■
MEMORANDUM																	
SUN	15:00	SYMBOLISM OF SUN EXPOSURE & SHADOWING OF THE POINTS	●	■	●	●	●	■	●	●	●	●	●	●	●	■	●
SHADOW	18:00	SYMBOLISM OF SUN EXPOSURE & SHADOWING OF THE POINTS	■	■	■	■	■	■	●	■	■	●	■	■	■	■	■

During this comparison it was found that the two points compared to each other were very close to the temperatures measured. The difference is less than 1.00 °C between points 4 and 14 as well as between points 4 and 10 (Figure 3).



Figure 3. Measurement points in the old town of Xanthi.

Specifically, the average temperatures recorded by the black sphere thermometer for the 12:00 pm at point 4 was 28.92 °C and at point 14 was 28.10 °C with their difference in 0.82 °C. Respectively, the average of the temperatures recorded by the built-in thermometer of the hygrometer for the 12:00 pm at point 4 was 26.99 °C and at point 14 was 26.40 °C, with their difference in 0.59 °C. This can be justified due to the riparian location of the point 14 in comparison with the point 4 located in the heart of the settlement with the narrow streets and a larger number of buildings. The average temperatures recorded by the black sphere thermometer for the 15:00 pm at point 4 was 29.00 °C and at point 10 was 29.32 °C with their difference in 0.32 °C. Respectively, the average of the temperatures recorded by the built-in thermometer of the



hygrometer for the 15:00 pm at point 4 was 27.67 °C and at point 10 was 27.39 °C, with their difference in 0.28 °C (Fig. 4).

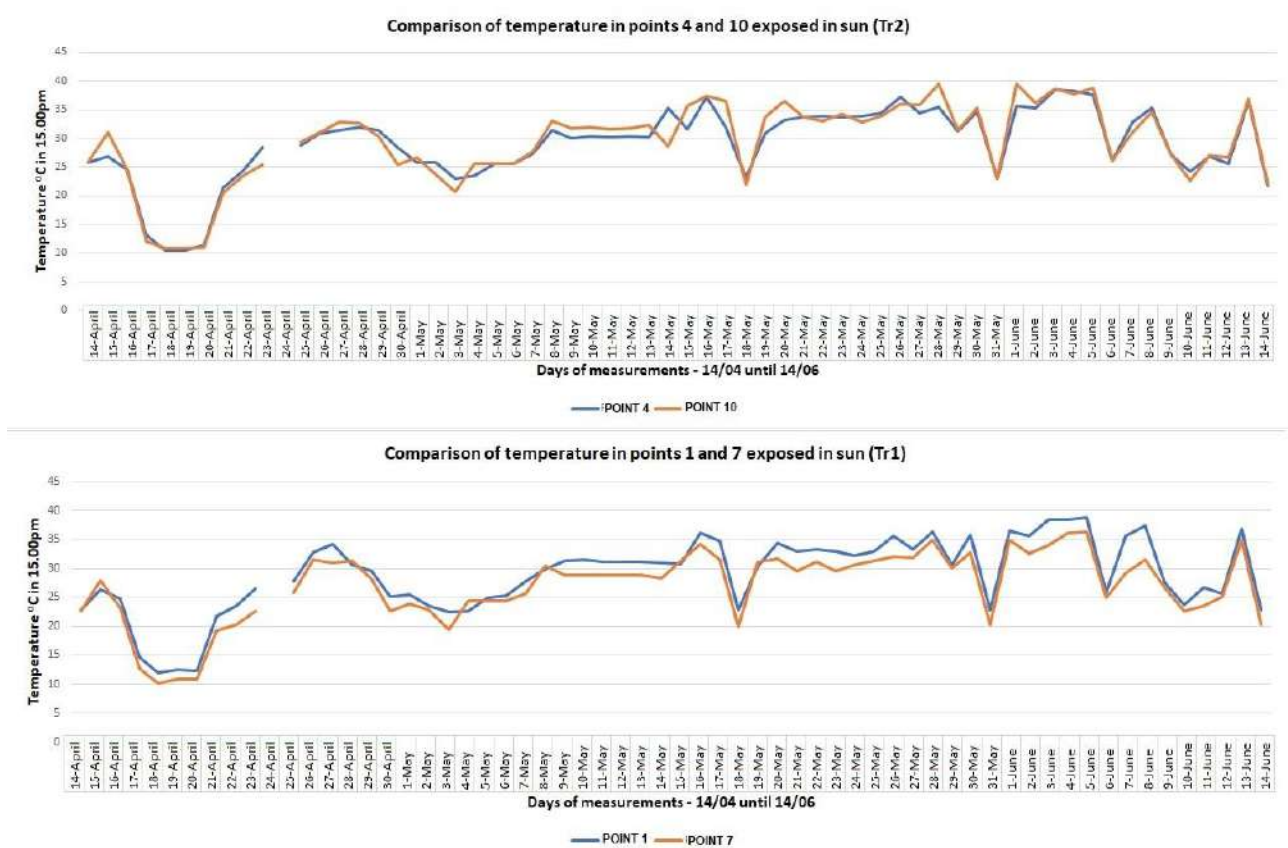


Figure 4. Linear graphs of temperature comparison between two points.

In the comparison between points that were reconstructed at long intervals between each other and specifically before 1992 and 2003, the points selected were 3 to 8 as well as 1 to 7 (Figure 3). Points 7 and 8 were reconstructed in 2003 and points 1 and 3 before 1992. The measurements were made for the same time of day and specifically at 15:00 pm and while the spots were exposed to the sun (Table 2). During this comparison it was found that the two points compared of each other had a more significant deviation in the temperatures measured (Figure 4).

There was a difference in the averages of the temperatures of all days that the measurements were made, greater than 1.0 °C between points 3 and 8 as well as between points 1 and 7. Specifically, the average temperatures recorded by the black sphere thermometer for the 15:00 pm at point 3 was 30.30 °C and at point 8 was 28.76 °C with their difference in 1.54 °C. Respectively, the average of the temperatures recorded by the built-in thermometer of the hygrometer for the 15:00 pm at point 3 was 29.00 °C and at point 8 was 27.16 °C, with their difference in 1.84 °C. Also, the average temperatures recorded by the black sphere thermometer for the 15:00 pm at point 1 was 29.81 °C and at point 7 was 28.52 °C with their difference in 1.29 °C. Respectively, the average of the temperatures recorded by the built-in thermometer of the hygrometer for the 15:00 pm at point 1 was 28.94 °C and at point 7 was 27.00 °C, with their difference in 1.94 °C (Fig. 4). All four points are located in the old town of Xanthi in similar morphologically areas. The highest temperatures were measured in the older granite cobblestone coatings.

3. CONCLUSIONS

The comparison was made between points that were reconstructed in the same year or in nearest years as well as the comparison between points that were reconstructed in distant years. Also was made for the same time of the day which was, 12:00 pm, 15:00 pm and 18:00 pm. The measurements were made when the two points that compared were both exposed to the sun or in the shadow.



The results of the comparison were found that the two points which compared with the nearest years of reconstruction, were very close to the temperatures measured, with a difference less than 1.00 °C and exactly 0.82 °C and 0.59 °C between points 4 and 14 and exactly 0.32 °C and 0.28 °C between points 4 and 10. The comparison between points that were reconstructed in distant years had a more significant deviation in the temperatures measured, with a difference of more than 1.00 °C and exactly 1.54 °C and 1.84 °C between points 3 and 8 and exactly 1.29 °C and 1.94 °C between points 1 and 7. Corresponding conclusions were found in the comparison of other points with similar conditions. The comparison was made for the temperatures recorded by both the black sphere thermometer and the temperatures recorded by the built-in thermometer of the hygrometer.

As we have seen, the highest temperatures were measured in the older granite cobblestone coatings. This leads us to the conclusion, that the newer grey granite blocks respond better in terms of comfort conditions to users of the outdoor public areas where they have been coated. The temperature difference between the newer and the older granite blocks used for outdoor coating, is more than 1,0 °C and approaches 2,0 °C.

REFERENCES

- Chrysomallidou, N., Theodosiou, Th. and Tsikaloudaki K., 2002. Sustainable development of free spaces in an urban environment, paragraph 5.1., Conference: *Bioclimatic design in urban outdoor space*.
- Kosmopoulos, P. 2001. Essay on introduction to environmental design. Thessaloniki.
- Flokas, A. A., 1994. *Courses in Meteorology and Climatology*. Ziti Publications, Thessaloniki.



Improving Groundwater Quality Using Hybrid Constructed Wetland in a Coastal Environment in Sub-Saharan Africa

R. N. Okparanma¹ and V. O. Ahiakwo¹

¹Department of Agricultural and Environmental Engineering, Rivers State University, Nkpolu-Oroworukwo, PMB 5080 Port Harcourt, Nigeria
Corresponding author email: okparanma.reuben@ust.edu.ng

ABSTRACT

Developing a simple, low-cost, and easy-to-maintain groundwater remediation system would benefit coastal communities in low-income economies like Nigeria in sub-Saharan Africa struggling with high levels of heavy metals in local groundwater sources. In this study, we constructed a simple, low-cost, and easy-to-maintain hybrid wetland with locally available materials and used it for the removal of Fe³⁺, Mn²⁺, and colour from groundwater collected from Yenagoa, a coastal community in Bayelsa State in the Niger Delta region of Nigeria (5.317°N, 6.467°E). The experimental setup consisted of three plastic containers (Cells) connected in series at decreasing elevations. The cells were packed with loamy soil (as microbe carrier), fine and coarse aggregates, and planted with water hyacinth to enhance Fe³⁺ and Mn²⁺ removal. The system flow rate was 43,200 cm³/day, retention time was 1.02 days, and hydraulic loading rate was 2.21 cm/day. The concentrations of Fe³⁺ and Mn²⁺ in the groundwater, as well as pH and colour, were determined periodically using standard analytical protocols. Before treatment, results showed that the groundwater was objectionable for domestic use with reddish-brown colour and concentrations of Fe³⁺ (1.094 mg/L) and Mn²⁺ (1.043 mg/L) about 4- and 5-folds higher than their respective WHO permissible limits. However, after 12 days of treatment, the water colour changed to almost colourless, while Fe³⁺ and Mn²⁺ were reduced to less than their respective permissible limits. Similarly, the pH dropped from an initial 8.94 to 6.8 (Cell-1), 7.15 (Cell-2), and 7.25 (Cell-3); all within the WHO's permissible range of 6.5–8.5. These suggest that the simple, low-cost, and easy-to-maintain hybrid constructed wetland improved the quality of the groundwater for domestic use, especially for washing purposes. Therefore, homegrown hybrid constructed wetlands could be used to tackle the pressing challenges of declining access to pipe-borne water in coastal communities in low-income economies in sub-Saharan Africa.

Keywords: Artificial Wetland; Groundwater Quality; Groundwater Remediation; Heavy Metals; Developing Economies.

1. INTRODUCTION

The provision of potable water is arguably one of the most important municipal services any government can provide for its residents. It is also widely known that achieving a well-functioning and sustainable water treatment facility is capital intensive. This explains why providing this all-important municipal service to its teeming residents has continued to elude many low-income economies in sub-Saharan Africa including Nigeria. In Nigeria, the proportion of urban households with access to pipe-borne water to their premises declined significantly from 33% in 1990 to 3% in 2015 (USAID, 2020). This trend left residents with little or no option other than self-help, resulting in the unregulated construction of water boreholes in almost every neighborhood in the country with a huge financial burden on residents and concomitant health risks. The situation is expected to worsen with a rapidly growing population if nothing is done to reverse the trend.

From available records, Nigeria is one of the major producers of crude oil and natural gas in the world. The Niger Delta region (5.317°N, 6.467°E), which is the hub of crude oil and natural gas activities in Nigeria is predominantly a coastal environment (NDES, 2005). It has been widely reported that coastal environments in crude oil-producing areas are highly vulnerable to crude oil pollution due to land-based oil and gas activities. For instance, groundwater, a major constituent of coastal environments is frequently polluted by a wide range of contaminants including hydrocarbons and heavy metals (e.g., UNEP, 2011; Amnesty International, 2018). Thus, groundwater quality needs to be monitored regularly across aquifers to determine the type of contaminants, extent of contamination, and required intervention approach (if



need be). Several methods exist for determining the compounds contributing to the contamination of groundwater; however, the analytical methods have been mostly adopted (Vymazal, 2007). In the same vein, several treatment methods that have proven to be economical and effective in removing contaminants from groundwater are available (Ani, 2016). Treatment of domestic and industrial wastewater can be integrated with constructed wetland system.

Constructed wetland is an emerging eco-sound technology for water treatment by mimicking the natural wetland's original functions and improving the natural wetland's limiting factors (Lim et al., 2001). In this technology, plants are usually planted in well-arranged beds of fine and coarse aggregates, which act as a filtering medium and slow down water velocity thereby allowing suspended solids to settle out. This enables the intake of elements like carbon, nitrogen, and iron in nutrient forms and converts them to plant tissues (Rouso et al., 2019). Equally important in wetland systems is the concept of photosynthesis by algae, which increases the dissolved oxygen content of the water and affects nutrients and metals distribution (Lim et al., 2001).

Wetland plants also provide the necessary conditions for microorganisms to live, transform, and remove pollutants from the water (Abbassi et al., 2018). Generally, constructed wetland can remove organic matter, suspended solids, and heavy metals from wastewater (Abbassi et al., 2018). Constructed wetlands are cost-effective, cheap to maintain, and suitable for wastewater treatment in low-population communities where lands are available (Rozema et al., 2016). Brad (2016) reported the high removal of iron from mining industry wastewater and outlined the effectiveness of aerobic wetland for metal polishing in mine water treatment. Also, planting young growing macrophytes on wetland remarkably removed total dissolved solids and phosphorus (Bodin, 2013).

Despite reports that constructed wetlands are cost-effective, cheap to maintain, and suitable for wastewater treatment, no studies could be found in the open literature on their application in Nigeria where local groundwater sources in some crude oil-bearing coastal communities are characterized by high contents of heavy metals due to oil pollution. Therefore, this study would benefit residents in coastal communities in low-income countries like Nigeria struggling with high contents of heavy metals in local groundwater sources. The objective of this study was to develop a hybrid constructed wetland for the removal of Fe^{3+} and Mn^{2+} in groundwater within a coastal environment to improve its quality for domestic use, especially for drinking and washing.

2. MATERIALS AND METHODS

2.1. Brief description of the study area

Bayelsa is one of southern Nigeria's nine states in the Niger Delta region (Figure 1). Yenagoa is the state capital and is located at Latitude $4^{\circ}55'29''\text{N}$ and Longitude $6^{\circ}15'51''\text{E}$ with a land area of 706 km^2 . Yenagoa had a population of 352,285 as of the 2006 census and is projected to have a population of 470,800 by 2016 (Idhoko et al., 2016).

Geologically, the State is located within the lower delta plain with a major geological characteristic of sedimentary alluvium. It has many tributaries of River Niger and is characterized by different soil types including sandy loam, loamy sand, and silty loam (soils of high-lying leaves). Others are soils of the low-lying leaves with moderately fine texture, such as red silty and clay loamy soils. The texture of a majority of the soil ranges from medium to fine grains (Dickson, 2018).

The hydrogeology of the study area based on strata logs showed multi-aquifer systems. The first aquifer is mostly unconfined and occurs between 0–45 m depth under phreatic conditions. The aquifer supplies water to small boreholes and is extensively exploited, leading to water table decline, pollution, and saline water intrusion while the remaining aquifer is confined (Maciel et al., 2018). The average depth of boreholes in Yenagoa is between 20 and 50 m (Samso, 2014). In terms of water quality, Samso (2014) reported that groundwater around 0-150 m depth in most parts of Yenagoa is high in iron content. In Bayelsa State as a whole, the static water level ranges from 0-1 m during the rainy season and 1-3 m during the dry season (Yassir et al., 2018). However, rainfall is the major source of recharge for aquifers in the area (Yassir et al., 2018).

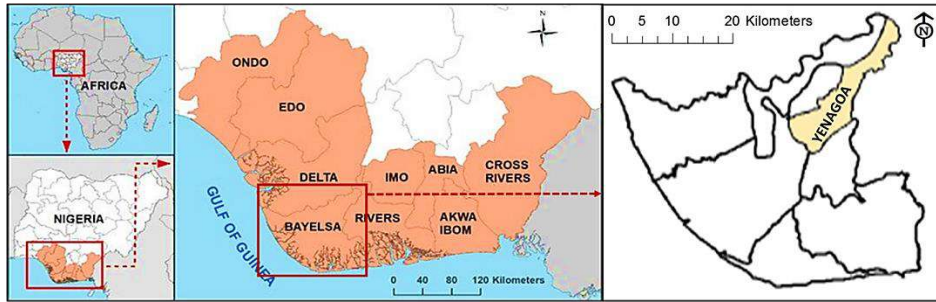


Figure 1: Map of the study area in the Niger Delta province, Nigeria [Adapted from Ebuoma et al. (2020)].

2.2. Sample collection

Using plastic containers, two 50 litres of groundwater samples were collected from two different boreholes located at Crystal Car Wash (not mapped) and Fiko Street (4.96°N, 6.35°E) along Tombia-Amassoma road all in Yenagoa. Then aliquots were immediately taken to the laboratory for baseline assessment. Water hyacinth macrophytes (free-floating plants) used as treatment were collected from surface water behind Swali Market also in Yenagoa.

2.3. Experimental procedures

The schematic of the hybrid constructed wetland without the plants, sectional diagram of the model domain, and pilot-scale setup created outdoors are shown in Figure 2. The setup was made up of three treatment PVC basins (cells 1, 2, and 3) placed in series on wooden frameworks at different elevations. This was to allow the free flow of water from the cell at a higher elevation to the cell below it under gravity. The cells were then linked with a 2-inch (5.08 cm) PVC pipe fitted at the base of each cell. A PVC valve was also fitted to the pipe to control the flow of water. A bed of filter medium consisting of fine sand ($\varnothing 0.5-1.00$ mm), gravel ($\varnothing 10-20$ mm), and a little quantity of loamy soil from a wetland (as a microbe carrier) were prepared in each of the cells. The overall thickness of the bed was 15.24 cm (i.e., sand and gravel = 14 cm and loamy soil = 1.24 cm). Thirty stands of water hyacinth (12-14 cm in height) were randomly selected, and ten stands were carefully planted in each cell at about equal spacing. These were done to produce a system with almost the same characteristics as a natural wetland. The outlet at the base of the cell was fitted with a geotextile filter gauze to prevent the passage of soil, sand, or gravel particles.

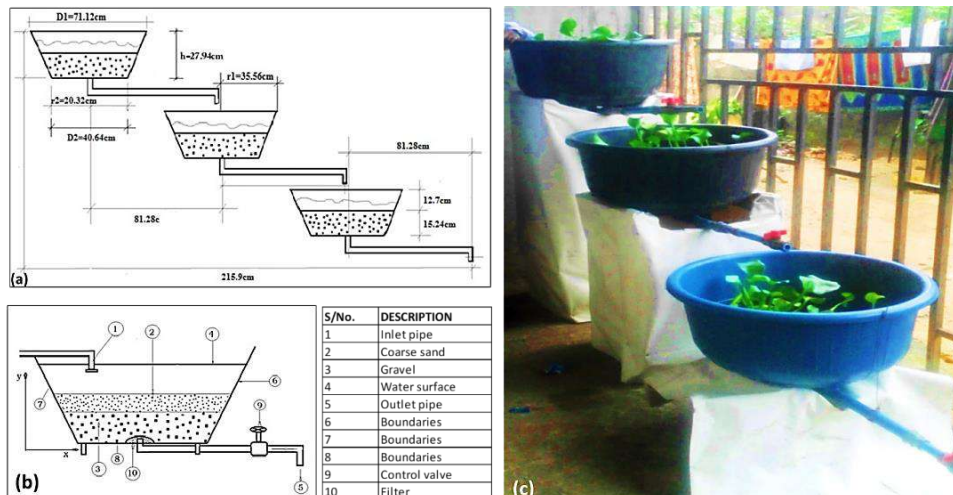


Figure 2: The hybrid constructed wetland: (a) schematic without the plants, (b) sectional diagram of the model domain, and (c) outdoor pilot setup.



2.4. Determination of selected hydraulic characteristics of the hybrid constructed wetland

2.4.1. Cell volume (V), lateral area (A_L), and surface area (A_S)

As stated, PVC basins were used as the cells of the hybrid constructed wetland. The volume of the basin was determined by assuming the basin to be a truncated cone as shown in Figure 3. We used the well-known equations 1, 2, and 3 to determine the volume (V), lateral area (A_L), and surface area (A_S), respectively of the cell.

$$V = \frac{1}{3}\pi(r_1^2 + r_1r_2 + r_2^2)h \quad (1)$$

$$A_L = \pi(r_1 + r_2)\sqrt{(r_1 - r_2)^2 + h^2} \quad (2)$$

$$A_S = A_L + \pi(r_1^2 + r_2^2) \quad (3)$$

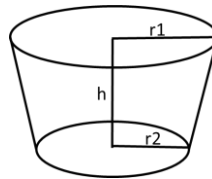


Figure 3: The assumed truncated cone of a cell of the hybrid constructed wetland.

2.4.2. Nominal residence (retention) time, t (days)

The volume of water in the wetland (V_w) in cm³ was determined using equation 4.

$$V_w = \varepsilon V \quad (4)$$

Where, ε = the fraction of cell volume that is water. From several literatures, this is usually high and taken as 0.9 approximately. Thus, the retention time was determined from equation 5.

$$t = \frac{V_w}{Q} \quad (5)$$

Where, Q = influent flow rate into the wetland (cm³/day).

2.4.3. Hydraulic loading, q (cm/day)

This is the amount of influent the wetland can handle, or the amount of influent applied to the wetland. It is also related to the size of the wetland. For constructed wetland, the size is its surface area (A_S). The amount of influent to be treated can be determined by first considering the hydraulic loading, which requires prior knowledge of the influent flow rate into the wetland (Q). The hydraulic loading of the hybrid constructed wetland was determined using equation 6.

$$q = \frac{Q}{A_S} \quad (6)$$

2.5. Characterization of water sample

To evaluate the performance of the wetland, aliquots were collected from the outlets of each cell at 3 days intervals for 12 days using amber colour vials for analysis. In this paper, only the analyses for pH level, as well as the Fe³⁺ and Mn²⁺ contents are presented. Colour change was assessed qualitatively by visual observation. The pH of the water sample was analyzed using the HI9828 Multiparameter Water Quality Meter (Hanna Instruments, USA) according to ASTM (2007) method D7315. The concentrations of Fe³⁺ and Mn²⁺ in the water were determined by flame atomic absorption spectrophotometry using a SHIMADZU® AA6800 Atomic Absorption Spectrophotometer according to APHA (1998).

3. RESULTS AND DISCUSSION

3.1. Selected hydraulic characteristics of the hybrid constructed wetland

The major dimensions of the cell for the determination of selected hydraulic characteristics of the hybrid constructed wetland are shown in Table 1. Using the values deduced in Table 1 and a system flow rate of



43,200 cm³/day (43.2 L/day), the retention time (t) and hydraulic loading rate (q) of the hybrid constructed wetland were deduced as 1.02 days and 2.21 cm/day, respectively.

Table 1. Major dimensions of the model domain (cell)

Dimension	Value
Top radius, r1 (cm)	35.56
Bottom radius, r2 (cm)	20.32
Height, h (cm)	27.94
Volume of cell, V (cm ³)	49,069
Volume of water in the cell, V _w (cm ³)	44,162
Lateral area, A _L (cm ²)	3,456
Surface area, A _S (cm ²)	19,587

3.2. Variations in colour, pH, and concentrations of Fe³⁺ and Mn²⁺ in the groundwater before and after passing through the constructed wetland

One of the indicators used to assess the performance of the treatment was a colour change in the untreated and treated water samples over the 12 days period. Figure 4 shows the colour change of the water samples on day 1 and day 12 of treatment in the hybrid constructed wetland. The reddish-brown colour in the initial water sample was due to the presence of Fe³⁺ (Khadse et al., 2015; Sharma and Bhattacharya, 2017). As can be observed in Figure 4, the intensity of the reddish-brown colour reduced from cell 1 to 3 on day 1 of treatment. However, after 12 days of treatment, the colour of the groundwater changed from the initial reddish-brown to almost colourless in cells 2 and 3. The increase in clarity of colour with the number of treatment cells over time indicates that the number of treatment cells enhanced the removal of colour caused by the concentration of Fe³⁺ in the groundwater.

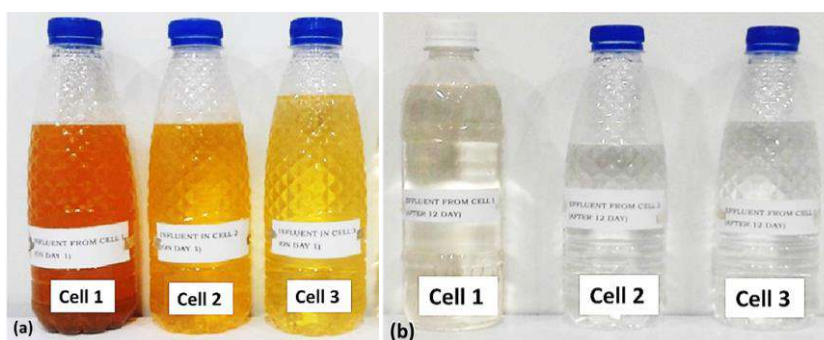


Figure 4: Colour change in the water samples on (a) day 1 and (b) day 12 of treatment in the hybrid constructed wetland.

The concentrations of Fe³⁺ and Mn²⁺, as well as pH levels in the groundwater before and after treatment in the constructed wetland in comparison with WHO permissible limits are shown in Table 2. As observed in Table 2, after treatment on day 12, both Fe³⁺ and Mn²⁺ were reduced to less than their respective WHO (2017) permissible limits with cell 3 outperforming cells 1 and 2 over time (Table 2). This indicates that an increase in stages of treatment cells enhanced the removal of Fe³⁺ and Mn²⁺ in the groundwater. The levels of Fe³⁺ and Mn²⁺ removed were higher than the level reported by Khadse et al. (2015) using Jar test experiments dosed with 5, 10, and 15 mg/L chlorine and 20 and 30 mg/L alum for treatment of surface water. However, the trends in Fe³⁺ and Mn²⁺ removal agreed with the findings of Khadse et al. (2015) and Sharma and Bhattacharya (2017) in the treatment of water contaminants. Like Fe³⁺ and Mn²⁺, the pH across the cells dropped to within WHO's permissible range after 12 days of treatment.



On the day-to-day variations in pH across the cells (Figure not shown), it was observed that pH continued to decrease up to day 6 before it increased from day 9 up to day 12, yet within the permissible range recommended by WHO (2017). The irregular variation in the pH could be attributed to the utilization of excessive dissolved oxygen through the photosynthetic and aerobic processes during the treatment process (Younger et al., 2002). Thus, during the transmitting process of treated water from one cell to another, aeration of the water takes place, especially in the case where the water was exposed to the atmosphere, as was the case in this study and in vertically constructed wetland (USEPA, 2011).

Table 2. The levels of Fe^{3+} , Mn^{2+} , and pH in the groundwater before and after treatment in the hybrid constructed wetland in comparison with WHO permissible limits.

Property	Before treatment	12 days after treatment			WHO (2017) Permissible Limit
		Cell-1	Cell-2	Cell-3	
Fe^{3+} (mg/L)	1.094	0.012	0.008	0.003	0.3
Mn^{2+} (mg/L)	1.043	0.004	0.003	0.001	0.2
pH	8.94	6.8	7.15	7.25	6.5-8.5

4. CONCLUSIONS

In this study, a simple, low-cost, and easy-to-maintain hybrid constructed wetland developed with locally available materials was used to remove Fe^{3+} , Mn^{2+} , and colour from groundwater in a coastal environment in Nigeria, sub-Saharan Africa. The system flow rate was 43,200cm³/day, retention time was 1.02 days, and hydraulic loading rate was 2.21cm/day. After 12 days of treatment, the initial reddish-brown colour of the groundwater changed to almost colourless, while Fe^{3+} and Mn^{2+} were reduced to less than their respective WHO's permissible limits; and the pH also dropped to within the permissible range. With the level of improvement in the groundwater quality achieved in this study, we believe that the development, deployment, and scaling of homegrown hybrid constructed wetlands could tackle the pressing challenges of declining access to pipe-borne water in coastal communities in low-income economies in sub-Saharan Africa.

REFERENCES

- Abbassi, B., Kinsley, C. and Hayden, J., 2018. *Constructed Wetlands Design Manual for Beef and Dairy Farm Wastewater Applications in Ontario*. Ontario Rural Wastewater Centre, Canada. Available online: <https://ontarioruralwastewatercentre.ca/wp-content/uploads/2019/03/constructed-wetlands-design.pdf> (accessed 29 June 2022).
- Amnesty International, 2018. Urgent Action: Community in Nigeria drinking polluted water. Available online: <https://www.amnesty.org/download/Documents/AFR4491722018ENGLISH.pdf> (accessed on 20 June 2022).
- Ani, C., Okogwu, O.I., Nwonumara, G.N., Nwani, C.D. and Nwinyimagu, A.J., 2016. Evaluation of physicochemical parameters of selected rivers in Ebonyi State, Southeast, Nigeria. *Greener J. Biol. Sci.*, 6(2), 34-41.
- APHA (America Public Health Association), 2013. Method 2340C: Standard methods for the examination of water and wastewater. America Public Health Association, Washington (DC).
- ASTM (American Society for Testing and Materials), 2007. Method D7315: Standard method for determination of turbidity in Turbidity Unit (TU). American Society for Testing and Materials, West Conshohocken (PA).
- Bodin, H., 2013. Wastewater treatment in constructed wetlands: Effects of vegetation, hydraulics and data analysis methods. PhD Thesis, Department of Physics, Chemistry and Biology, Linköping University Institute of Technology, Sweden.
- Dickson, A.A., 2018. Characterisation, classification, and suitability evaluation of agricultural soils of selected communities located along various river systems in Bayelsa State, Southern Nigeria. PhD Thesis, North-West University, South Africa.



- Ebhuoma, E.E., Simatele, M.D., Leonard, L., Ebhuoma, O.O., Donkor, F.K. and Tantoh, H.B., 2020. Theorizing indigenous farmers' utilization of climate services: Lessons from the oil-rich Niger Delta, *Sustainability*, 12, 7349.
- Idhoko, K.E., Ndiwari, E L., Ogeh, V.C. and Ikegbulam, S.C., 2016. Urban road network analysis of Yenagoa, Bayelsa State Using GIS. *Int. J. Eng. Comput. Sci.*, 5(1), 15605-15615.
- Khadse, G.K., Patni, P.M. and Labhassetwar, P.K., 2015. Removal of iron and manganese from drinking water supply. *Sust. Water Res. Manage.*, 1, 157-165.
- Lim, P.E., Wong, T.F. and Lim, D.V., 2001. Oxygen demand, nitrogen, and copper removal by free-water-surface and subsurface-flow constructed wetlands under tropical conditions. *Environ. Int.*, 26(5–6), 425-431.
- Maciel, P.M.F. and Sabogal-Paz, L.P., 2018. Household slow sand filters with and without water level control: Continuous and intermittent flow efficiencies. *Environ., Technol.*, 41(8), 944-958
- NDES (Niger Delta Environmental Survey), 1995. *Background and Mission: Briefing Note 1*. Publication of the Steering Committee, NDES, Falomo, Lagos, Nigeria.
- Rouso, B.Z., Pelissari, C., dos Santos, M.O. and Sezerino, P.H., 2019. Hybrid constructed wetlands system with intermittent feeding applied for urban wastewater treatment in South Brazil. *J. Water Sanitation Hygiene Dev.*, 9(3), 559–570.
- Rozema, E.R., VanderZaag, A.C., Wood, J.D., Drizo, A., Zheng, Y., Madani, A. and Gordon, R.J., 2016. Constructed wetlands for agricultural wastewater treatment in North-eastern North America: A review. *Water*, 8(5), 173.
- Samsó, C.R., 2014. Numerical modelling of constructed wetlands for wastewater treatment. PhD Thesis University Institute for Research in Sustainability Science and Technologies (IS.UPC), Barcelona, Spain. Available online: <http://hdl.handle.net/2117/95297> (accessed 15 May 2022).
- Schultz, B., 2016. Surface mining reclamation and enforcements Appalachian region technical support division. *Int. J. Environ. Res. Public Health*, 12(7), 7300-7320.
- Sharma, S. and Bhattacharya, A., 2017. Drinking water contamination and treatment techniques. *Appl. Water Sci.*, 7(3), 1043-1067.
- UNEP (United Nations Environment Programme), 2011. *Environmental Assessment of Ogoniland*. United Nations Environment Programme, Nairobi, Kenya. Available online: <http://www.unep.org> (accessed on 29 October 2012).
- USAID (United States Agency for International Development), 2020. NIGERIA: Overview. Available online: <https://www.globalwaters.org/> (accessed on 27 June 2022).
- Vymazal, J., 2007. Removal of nutrients in various types of constructed wetlands. *Sci. Total Environ.*, 380(1-3), 48-65.
- WHO (World Health Organization), 2017. *Guidelines for Drinking-water Quality: Incorporating the First Addendum*, 4th Ed.; Available online: <https://www.who.int/publications/i/item/9789241549950> (accessed on 13 May 2017).
- Yassir, B., Chaimae, Z., Abdelaziz, A.M., Eddine, K.M. and Pineau, A., 2018. New approach to understand the removal efficiency of some anions in well water by slow sand filtration. *Annual Res. Rev. Biol.*, 23(1), 1-8.
- Younger, P.L., Banwart, S.A. and Hedin, R.S., 2002. Mine Water Hydrology. In: *Mine Water*, vol. 5, p.127–270. Springer Science; Dordrecht.



Agro-food waste re-valorization through solid-state fermentation for hydrolytic enzymes production

J. Sosa-Martínez¹, J. Montañez¹, J.C. Contreras¹, S. Gadi² and L. Morales¹

¹Facultad de Ciencias Químicas. Universidad Autonoma de Coahuila. Unidad Saltillo. Saltillo, Coahuila, 25280, México

²Facultad de Ingeniería Mecánica y Eléctrica. Universidad Autonoma de Coahuila. Unidad Torreón. Torreón, Coahuila, 27276, México

Corresponding author email: lourdesmorales@uadec.edu.mx

ABSTRACT

Using agro-industrial wastes to produce fungal enzymes is a promising strategy to revalue and reuse lignocellulosic materials generated by agro-industry. This work proposes a cost-effective and environmentally friendly bioprocess for the microbial production of xylanase, cellulase and pectinase. The physico-chemical characteristics of twelve agro-food wastes were evaluated to determine their capacity to be used as support-substrate in solid-state fermentation. The relationship between the physico-chemical characteristics of the residues and the ability of fungal strains to grow on them was established. In addition, five fungal strains were screened to select the one with the capacity to synthesize the enzymes of interest. Strain G5 was chosen for process optimization to maximize hydrolytic enzymes production using a mixture of brewery spent grain and apple pomace as substrate. The parameters substrate ratio (75/25, 80/20, 85/15), pH (4.0, 4.5, 5.0) and humidity (40, 50, 60 %) were optimized via Central Composite Design. Factors' effects and optimum settings were identified to achieve the desired enzymatic cocktail composition of xylanase, cellulase and pectinase.

Keywords: agro-industrial waste, hydrolytic enzymes, solid-state fermentation.

1. INTRODUCTION

Agribusiness generates 17 million tons of waste and sub-products annually (Barcelos et al., 2020). Generated materials can be used as substrate support in solid cultures. Solid-state fermentation (SSF) is an efficient and eco-friendly alternative to revalue such materials and benefit from them (Kantifedaki et al., 2018). A bioprocess approach has been useful in obtaining value-added compounds from agro-wastes. One of the main advantages of these materials is that they can be used without pre-treatment.

Microorganisms enable obtaining valuable products in two main ways. First, their metabolism allows the release of compounds of interest present in the substrates, such as polyphenols, fatty acids, sugars, pigments, bioactive peptides, etc. (Ajmal et al., 2021). Second, the wastes are used as carbon and nitrogen sources for the biosynthesis of a metabolite of interest, such as enzymes, pigments, polymers, proteins, fatty acids, bioethanol, biogas, flavors, fragrances, among others many other biomolecules (Shen et al., 2021).

Hydrolytic enzymes are of great interest due to their vast applications. Specifically, xylanase, cellulase and pectinase play an essential role in the circular economy of bioprocesses. Enzyme production in SSF has been widely reported (Mansour et al., 2016). However, searching for new microorganisms that produce enzymes with different catalytic capacities is essential.

It is also essential to gain process knowledge about the simultaneous production of hydrolytic enzymes and to adjust the process conditions to maximize a single enzyme or a mixture of enzymes depending on the application. Therefore, this work aims to revalue the residues obtained from the agroindustry, such as pomaces and bagasse, for obtaining hydrolytic enzymes through SSF.

2. MATERIALS AND METHODS

2.1. Agro-waste potential evaluation as SSF support and substrate

Agro-food wastes used in this work were obtained from different agricultural activities, food processing and commercial activities. The substrates used were Apple pomace (AP), brewery spent grain (BSG), corn cob (CC), cotton seed (CS), carrot waste (CW), grapefruits peels (GfP), grape pomace (GP), orange peel (OP),



peanut shell (PS), pasta residue (PR), soybean waste (SW), wheat bran (WB). Materials were dried at 60 °C for 48 hours and ground in a disk mill until obtaining a homogeneous material.

The composition of the materials was determined for total nitrogen content (Kjeldahl, 1883), lipids (Annamalai et al., 2018), total sugars (Dubois et al., 1956) and reductors sugars (Miller, 1959). Dry matter was determined by weighing 1 gram of residue and bringing it to constant weight in an oven at 100 °C. Ash was determined by incinerating 1 gram sample in a tarred crucible in a muffle at 550 °C degrees for six hours. Physicochemical parameters evaluation included parameters such as water absorption index (WAI), water holding capacity (WHC) (Du et al., 2018), critical humidity point (CHP) (Orzua et al., 2009), pH, and humidity.

2.2. Screening of hydrolytic enzyme-producing fungi

2.2.1 Microorganisms and inoculum preparation

Five fungal strains isolated from a maize silage process were used to examine their qualitative enzymatic activities; named A5, A13, B1, D1 and G5. Fungal strains were grown on Sabouraud dextrose agar (DSA) at 30 °C until sporulation occurred. Spores' suspension was used as inoculum adjusted to 1×10^6 spores mL⁻¹.

2.2.2 Qualitative evaluation of hydrolytic enzyme production

The plate screening method was used to determine the ability of the fungal strains to degrade xylan, cellobiose and pectin. Solid media containing nutritive agar and 1% of xylan, cellobiose and pectin were prepared. An inoculum aliquot (50 µL) was placed on the plate's center and incubated for 5 days. The plates were stained with 10 mL Congo red (1%) for 10 minutes and subsequently washed with NaCl (1 M). The appearance of a halo without red coloration was considered a positive result for enzyme secretion.

2.2.3 Fungal growth in lignocellulosic materials

The three best strains, according to their ability to degrade polysaccharides (xylan, cellobiose and pectin), were used for SSF using the twelve agro-residues as support-substrate. An initial humidity of 70% was set, using the Czapeck-Dox mineral medium containing (g L⁻¹) NaNO₃ (3.0), KH₂PO₄ (1.0), MgSO₄ (0.5), KCl (1.0), FeSO₄ (0.1). Fermentation was monitored every 24 hours to determine radial growth; the images were analyzed with the Image J program and growth was reported in %.

2.2.4 Enzyme production and quantification

The selected strain and residues were further evaluated for enzyme production. SSF was carried out, measuring activity on days 4, 6 and 8. Crude enzyme extract was obtained by adding distilled water to the fermented medium (5:1 ratio). The mixture was centrifuged (8000 rpm, 15 min) and then filtered (Whatman 1). The enzymatic activities (U/mL) of the carbohydrases were determined using the release of reducing sugars from substrates. Pectin, xylan, and cellulose were used. Analysis was carried out with the DNS assay.

2.2.5 HPLC analysis

Monosaccharides (arabinose, galactose, glucose and xylose) were analyzed before and after fermentation. A high-performance anion-exchange chromatography with pulsed amperometric detection (HPAEC-PAD, ICS 5000, Thermo-Scientific-DIONEX, USA) was used. Before HPLC analysis, all samples and standards were filtered (0.45 µm). The CarboPacTM PA 1 column (Thermo-Scientific-DIONEX, USA) (2 x 250 mm) equipped with guard column (2 x 50 mm) was used and a volume of 10 µL of the sample was injected using 1mM NaOH solution as eluent with a flow rate of 1 mL min⁻¹ at 30 °C for 20 minutes. A calibration curve was made for standards of D-(+)glucose, D-(+)xylose, D-(+) galactose, L-(+) arabinose, D-(+) mannose.

2.3. Statistical optimization of hydrolytic enzymes production by SSF

In a previous study (data not shown), parameters influencing xylanase, pectinase and cellulase production were screened. The effect of critical parameters on the enzyme production process was studied using selected wastes and microorganism. Central Composite Design (CCD) with three factors at three levels was applied to evaluate the effect of substrate ratio BSG/AP (75/25, 80/20, 85/15), humidity (40, 50, 60 %), and pH (4.0, 4.5, 5.0) on enzyme production. Two other levels, known as star points ($\pm\alpha$), were considered.

3. RESULTS AND DISCUSSION

3.1. Agro-waste potential evaluation as SSF support and substrate

Table 1 shows the results obtained from the proximate chemical analysis of the agro-industrial wastes. This analysis shows the potential to be used as a source of nutrients and as an inducer of enzymatic activity. It is



well reported that the composition is a determinant of stimulating enzyme secretion by microorganisms (Barcelos et al., 2020). Although this article focuses on the production of enzymes using waste materials as the substrate, it is essential to highlight that some residues can be used to obtain compounds of interest, such as the case of soybean residue, which has a high percentage of protein; likewise, cottonseed can be a source of fatty acids, since it has the highest percentage of lipids among the analyzed residues.

High percentages of lignin could be detrimental to achieving the proposed objective. This component prevents access to the cell wall polysaccharides. So, the peanut shell and cotton seed composition could inhibit the microorganism's development. In the case of lignocellulosic fungi, this could be an excellent substrate. Secretion of cellulase and xylanase enzymes can be stimulated by materials such as corn cob, cottonseed, brewery spent grain, because they have cellulose and hemicellulose in greater quantities.

Table 1. Proximal chemical composition of lignocellulosic materials.

	AP	BSG	CW	CC	CS	GfP	GP	OP	PR	PS	SW	WB
Protein	10.46 ^e	16.41 ^d	10.59 ^e	3.86 ^h	21.47 ^b	7.22 ^g	19.18 ^{bc}	7.57 ^{fg}	9.83 ^{ef}	7.67 ^{fg}	45.69 ^a	17.84 ^{cd}
Lipids	3.16 ^g	3.96 ^{ef}	2.72 ^g	3.71 ^f	13.50 ^a	4.98 ^d	5.41 ^d	9.02 ^b	6.40 ^c	1.96 ^h	5.31 ^d	4.28 ^e
Carbohydrates	65.05 ^a	29.41 ^c	30.11 ^c	14.25 ^e	0.55 ^h	52.60 ^b	5.77 ^g	23.38 ^d	8.93 ^f	12.39 ^e	9.61 ^f	6.60 ^g
Hemicellulose	9.88 ^{de}	19.16 ^b	3.17 ^{fg}	44.16 ^a	11.95 ^c	5.44 ^e	7.03 ^e	6.32 ^{ef}	8.65 ^e	13.11 ^{cd}	ND	14.22 ^c
Lignin	ND	3.55 ^{de}	ND	9.73 ^{cd}	21.61 ^b	16.84 ^{cd}	13.83 ^c	13.33 ^c	3.48 ^e	52.74 ^a	ND	ND
Cellulose	12.86 ^{ef}	4.78 ^g	11.78 ^{ef}	40.57 ^c	48.09 ^b	15.70 ^{de}	10.23 ^f	23.98 ^d	0.01 ^h	63.85 ^a	4.69 ^g	8.00 ^f

Results of the physico-chemical parameters are plotted in Fig. 1. WHC of the materials is directly related to the interaction of the water molecules with the non-cellulosic cell wall polysaccharides, mainly pectins and xylan (Du et al., 2018). Materials with the highest WHC were CW, OP and CC, of which a pectin composition of 10 and 30 % are reported for CW and OP, respectively (Patience et al., 2021). Meanwhile, 32 % xylan for CC (Yan et al., 2017). Thus, WHC results were attributed to the composition of these materials, as well as the WAI, which is also closely related to the composition and interaction of water with cell wall components. While WAI determines the ability to absorb water, WHC indicates how much water is retained by the material. A high percentage of WAI is desirable for the support-substrate used in SSF (Orzua et al., 2009); however, high WHC could be detrimental to the system because water would occupy pore space for a more extended period, thus avoiding a deficient oxygen transfer.

SSF is a three-phase system; however, the potential of the solid material, as well as its interaction with the liquid and gas phase, is decisive for the success of the bioprocess (Pap et al., 2020). CHP is an important parameter because it indicates the critical moisture percentage for the system; from this value, the moisture loss will initiate to accelerate since there is no more free water. Since SSF is carried out with humidity ranging from 40 to 80 %, the CHP shouldn't be higher than 30 (Orzua et al., 2009). All materials tested meet this characteristic. Material humidity determination aids in adjusting the desired moisture in the fermentation process; the material should present a low percentage since this water is not available for the microorganism. The pH value of the substrates allowed us to understand the requirements of the microorganisms since, in SSF screening assay, this value was not adjusted. Most filamentous fungi grow at slightly acidic pH (Groff et al., 2022). The strains used in this assay also preferred substrates with pH values below 5.

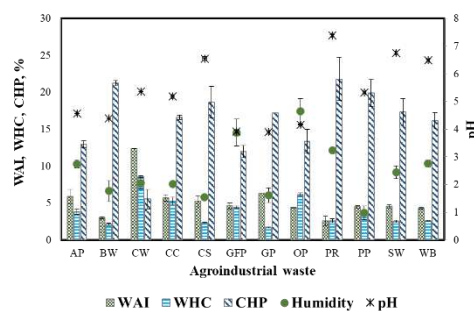


Figure 1. Physico-chemical parameters of agro-industrial wastes.



3.2. Screening of hydrolytic enzyme-producing fungi

The isolated fungal strains can produce enzymes of interest. Strains B1, D1 and G5, were able to degrade the highest number of substrates. B1 failed to degrade CMC and D1 xylan and cellobiose, while G5 degraded all substrates. The three strains were then used for the SSF using agro-industrial wastes.

Results showed maximum overall growth in AP, BSG, GP, and CW. The residues AP, BSG, OP and CW have a high percentage of sugars (65.05, 29.41, 23.38, and 30.11 %, respectively), as shown in Table 1. The growth of G5 in GP is interesting since this material has a sugar percentage of 5.77 %, much lower than the other residues. This last issue allows us to conclude that the sugar content does not necessarily influence growth but that other factors intervene. For example, GfP has 52.60 % sugar and the microorganisms achieved only 39.13, 25.01 and 11.62 % for B1, D1 and G5, respectively. This may be because it has a high WHC and insufficient space for growth and exchange of matter and gases between the solid matrices.

B1 (100 ± 0.5 %) and D1 (78.54 ± 1.22 %) reached maximum growth in AP, and G5 had good growth (98.13 ± 2.23 %). This could be due to its high sugar content. It also has a natural pH suitable for fungal growth and can absorb and retain water in adequate percentages.

On the other hand, GP was the substrate where G5 reached maximum growth (100 %), and B1 and D1 also performed well (88.46 ± 7.31 % and 54.18 ± 6.62 %, respectively). Unlike AP, GP has a much lower percentage of sugars]. Viability is interesting; the growth of the microorganism may be promoted by compounds present in the grape pomace, such as polyphenols, tannins, etc. The WAI is adequate, which may be why the microorganism develops a good percentage of growth during the first two days of fermentation. The potential of this residue is for short-time SSF since it has low WHC, and the necessary humidity to maintain the metabolism of the fungus would not be sufficient for prolonged periods, fermentations of more than 7 days. The use of this residue has been reported for transformation by biological means into bioethanol and enzymes. But the main valorization of this by-product is in the extraction of polyphenols, the most abundant being epicatechin (Cisneros-Yupanqui et al., 2022).

BSG stands out as one of the three best substrates for the growth of the three studied strains (97 ± 1.34 %, 63.85 ± 3.78 , 49.3 ± 2.23 for B1, G5 and D1, respectively). BSG has the greatest versatility of applications among evaluated wastes such as biopolymers, animal feed, raw material for bioprocesses, source of fiber, food ingredients, plant fertilizer, biosorbent for bioremediation. However, it is also the most heterogeneous due to the variability of the waste generated by each brewery (Naibaho and Korzeniowska, 2021). It is important to note that all the materials used as substrates also function as supports, were not pre-treated and were not supplemented with another carbon source or enzyme activity inducer, making this bioprocess more sustainable (low cost and environmental impact).

Since strain G5 showed the greatest potential to produce hydrolytic enzymes of interest, the potential for enzyme production in AP, BSG, GP and OP by strain G5 was analyzed. The highest enzymatic activity for xylanase was observed at day 4 in BSG (481.45 ± 4.39 U), pectinase in AP at day 4 (47.88 ± 7.09 U), cellulase in AP at day 8 (41.25 ± 3.85 U).

Regarding the percentages of sugars detected by HPLC for AP, BSG, GP and OP residues before and after SSF in BSG, there is an increase in the rate of arabinose, galactose and xylose, which is a confirmation of the hydrolytic activity performed by the enzymes. In AP there is an increase in glucose; interestingly, galactose was not detected in the unfermented sample, but the fermented sample, indicating hydrolysis of non-cellulosic polysaccharides (pectin, xyloglucans, arabinans, galactans). Fermentation-assisted extraction of galactose could be an alternative for obtaining this sugar. Interestingly, the OP residue, where the lowest enzyme activity for xylanase, pectinase and cellulase was detected, is where the highest percentage of glucose was quantified in the unfermented material, so fungal metabolism was performed using the available glucose, and there were no conditions to secrete hydrolytic enzymes.

GP is a material with potential to promote the synthesis of hydrolytic enzymes, its percentage of glucose is lower than OP. The growth of the tested fungal strains had high percentages. The increase in the percentage of galactose indicates hydrolysis of hemicellulose and other polysaccharides, other enzymes such as β -D-galactosidase y β -D-glucosidase, etc. could be acting.

Enzyme production from low-cost substrates is on the rise. Especially in SSF processes where filamentous fungi find the ideal niche to grow and produce (Mansour et al., 2016). However, one of the challenges is to



find the ideal substrate for the development of the fungal strain, as well as the characteristics of the substrate itself. The properties of the components of solid materials determine the interaction with the environment.

Apple pomace has a high composition of fermentable sugars and pectins. Nevertheless, the particle size is low, making this material more suitable for submerged fermentation. Therefore, mixing it with a substrate would improve the SSF process. BSG would function as support (although not exclusively) and AP as a substrate. Thus, for SSF optimization, the G5 strain was selected with a BSG-AP mixture.

The production of enzymes using BSG has previously been applied but to our knowledge, no enzyme production using a mixture of AP with BSG has been reported.

3.3. Statistical optimization of hydrolytic enzymes production by SSF

Table 2 summarizes the optimum levels, predicted response and the validation results. Overall, the polynomial model presented good correlations between predicted and experimental data ($R^2 = 0.81, 0.82$ and 0.88 for xylanase, cellulase and pectinase, respectively). The effects of the evaluated factors were different for each enzyme. The linear effect of ratio substrate, the quadratic effect of humidity and interactions between substrate/pH and pH/humidity were significant in producing the three enzymes. Interestingly, pH was not significant in its quadratic terms for cellulase and pectinase and linear term for xylanase; however, the interaction of pH with the other two factors was significant for the three enzymes. For xylanase production, all effects were significant (linear, quadratic and interactions) except the linear effect of pH. The interactions of the three factors were most significant for cellulase synthesis. In the case of pectinase, the linear effect of substrate ratio was most significant, followed by substrate/pH and pH/humidity interactions.

Under optimal production conditions, enzyme activity increased by 20, 25 and 65 % for xylanase, pectinase and cellulase, respectively. Based on this knowledge, it is possible to produce enzymatic cocktails containing all three enzymes but maximizing one or several depending on the desired application. These multi-enzyme extracts were used to obtain value-added compounds with good yields (data not shown).

Table 2. Optimum levels predicted and observed enzymatic activity at such levels for xylanase, pectinase and cellulase conditions.

RSM Results		Xylanase	Cellulase	Pectinase
Optimum levels and expected response	BSG/AP	81/19	88/12	72/28
	pH	4.58	5.30	4.38
	Humidity	50.40	66.00	66.00
	Expected	582.38 ± 6.93	69.90 ± 3.53	61.73 ± 1.58
Experimental		578.70 ± 2.31	68.31 ± 5.57	59.97 ± 2.84

4. CONCLUSION

Studying the properties and composition of agro-industrial wastes allowed the understanding of the growth and production of enzymes by microorganisms. The G5 strain demonstrated the ability to biosynthesize xylanase, cellulase and pectinase. It was possible to gain process knowledge about the simultaneous production of xylanase, cellulase and pectinase, which will allow adjusting process conditions to maximize a single enzyme or mixture of enzymes depending on the application.

5. ACKNOWLEDGEMENTS

CONACyT-México for the financial support provided for conducting J. Sosa-Martinez PhD studies.

REFERENCES

- Ajmal, M., Shi, A., Awais, M., Mengqi, Z., Zihao, X., Shabbir, A., Faheem, M., Wei, W. and Ye, L., 2021. Ultra-high temperature aerobic fermentation pretreatment composting: Parameters optimization, mechanisms and compost quality assessment. *J. Environ. Chem. Eng.*, 9, 105453.
- Annamalai, N., Sivakumar, N. and Oleskowicz-Popiel, P., 2018. Enhanced production of microbial lipids from waste office paper by the oleaginous yeast *Cryptococcus curvatus*. *Fuel*, 217, 420–426.
- Barcelos, M.C.S., Ramos, C.L., Kuddus, M., Rodriguez-Couto, S., Srivastava, N., Ramteke, P.W., Mishra, P.K.



- and Molina, G., 2020. Enzymatic potential for the valorization of agro-industrial by-products. *Biotechnol. Lett.* 42, 1799–1827.
- Cisneros-Yupanqui, M., Zagotto, A., Alberton, A., Lante, A., Zagotto, G., Ribaudó, G. and Rizzi, C., 2022. Study of the phenolic profile of a grape pomace powder and its impact on delaying corn oil oxidation. *Nat. Prod. Res.* 36, 455–459.
- Du, J., Cheng, L., Hong, Y., Deng, Y., Li, Z., Li, C. and Gu, Z., 2018. Enzyme assisted fermentation of potato pulp: An effective way to reduce water holding capacity and improve drying efficiency. *Food Chem.* 258, 118–123.
- Dubois, M., Gilles, K.A., Hamilton, J.K., Rebers, P.A. and Smith, F., 1956. Colorimetric Method for Determination of Sugars and Related Substances. *Anal. Chem.* 28, 350–356.
- Groff, M.C., Scaglia, G., Gaido, M., Kassuha, D., Ortiz, O.A. and Noriega, S.E., 2022. Kinetic modeling of fungal biomass growth and lactic acid production in *Rhizopus oryzae* fermentation by using grape stalk as a solid substrate. *Biocatal. Agric. Biotechnol.* 39, 102255.
- Kantifedaki, A., Kachrimanidou, V., Mallouchos, A., Papanikolaou, S. and Koutinas, A.A., 2018. Orange processing waste valorisation for the production of bio-based pigments using the fungal strains *Monascus purpureus* and *Penicillium purpurogenum*. *J. Clean. Prod.* 185, 882–890.
- Kjeldahl, J., 1883. Neue methode zur bestimmung des stickstoffs in organischen körpern. *Zeitschrift für Anal. Chemie*, 22, 366–382.
- Mansour, A.A., Arnaud, T., Lu-Chau, T.A., Fdz-Polanco, M., Moreira, M.T. and Rivero, J.A.C., 2016. Review of solid state fermentation for lignocellulolytic enzyme production: challenges for environmental applications. *Rev. Environ. Sci. Biotechnol.* 15, 31–46.
- Miller, G.L., 1959. Use of dinitrosalysilic acid reagent for determination of reducing sugar. *Anal. Chem.* 31.
- Naibaho, J. and Korzeniowska, M., 2021. The variability of physico-chemical properties of brewery spent grain from 8 different breweries. *Heliyon* 7, e06583.
- Orzua, M.C., Mussatto, S.I., Contreras-esquivel, J.C., Rodriguez, R., De, H., Teixeira, J.A. and Aguilar, C.N., 2009. Exploitation of agro industrial wastes as immobilization carrier for solid-state fermentation. *Ind. Crop. Prod.* 30, 24–27.
- Pap, N., Hamberg, L., Pihlava, J.M., Hellström, J., Mattila, P., Eurola, M. and Pihlanto, A., 2020. Impact of enzymatic hydrolysis on the nutrients, phytochemicals and sensory properties of oil hemp seed cake (*Cannabis sativa* L. FINOLA variety). *Food Chem.* 320, 126530.
- Patience, N.A., Schieppati, D. and Boffito, D.C., 2021. Continuous and pulsed ultrasound pectin extraction from navel orange peels. *Ultrason. Sonochem.* 73, 105480.
- Shen, D., Kou, X., Wu, C., Fan, G., Li, T., Dou, J., Wang, H. and Zhu, J., 2021. Cocktail enzyme-assisted alkaline extraction and identification of jujube peel pigments. *Food Chem.* 357, 129747.
- Yan, Y.H., Li, H.L., Ren, J.L., Lin, Q.X., Peng, F., Sun, R.C. and Chen, K.F., 2017. Xylo-sugars production by microwave-induced hydrothermal treatment of corncob: Trace sodium hydroxide addition for suppression of side effects. *Ind. Crops Prod.* 101, 36–45.



Photoprotection of Cationic Porphyrins and Their Non-Covalent Complexes for Effective Photodynamic Therapy of Tumors

L. Mkrtchyan¹, A. Zakoyan¹, T. Seferyan², P. Gikas³, G. Shmavonyan⁴ and G. Gyulkhandanyan^{1,4}

¹Laboratory of Bioengineering, Institute of Biochemistry of the NAS of Armenia, Yerevan, Armenia

²Laboratory of Biomedical research, Institute of Biochemistry of the NAS of Armenia, Yerevan, Armenia

³Laboratory of Design of Environmental Processes, Technical University of Crete, Chania, Crete, Greece

⁴Laboratory of 2D materials Engineering and Nanotechnology Innovation, National Polytechnic University of Armenia, Yerevan, Armenia

Corresponding author email: mkrtchyanlusine709@gmail.com

ABSTRACT

Photodynamic therapy (PDT) is a treatment technique based on the combination of photosensitizer (PS), PS-specific excitation wavelength light, and intracellular oxygen. The combination of these three factors will generate cytotoxic reactive oxygen species (especially singlet oxygen - $^1\text{O}_2$) capable of inducing cancer cell death (Baydoun, et al., 2020). Because of the fast growth and cell division, numerous cancer cell lines over-express folic acid (FA) receptors (Stallivieri, et al., 2017). Accordingly, we perform non-covalent complexation of folic acid and cationic porphyrins. One of the characteristics of PS's is the photobleaching, which is the loss of absorption or emission intensity that is caused by light (Khaled, et al., 2011). The aim of this work was to gain stable complexes and enhance the effectiveness of PDT by reducing the photobleaching of FA, cationic porphyrins, and their non-covalent complexes. The study of PS's and complexes photobleaching in presence of known quenchers (L-histidine as a singlet oxygen quencher and D-mannitol as a free radicals' quencher) was also performed. The study revealed that singlet oxygen quencher L-histidine and free radicals' quencher D-mannitol, with optimal concentrations can lead to the reduction of photobleaching rate and thus the enhancement of PDT efficiency. Therefore, both singlet oxygen and $\bullet\text{OH}$ radical involved in the photobleaching of cationic porphyrins.

Keywords: porphyrins; photobleaching; folic acid; L-histidine; D-mannitol.

1. INTRODUCTION

Photodynamic therapy (PDT) is a treatment technique based on the combination of photosensitizer (PS), PS-specific excitation wavelength light and intracellular oxygen. The combination of these three factors will generate cytotoxic reactive oxygen species (especially singlet oxygen - $^1\text{O}_2$) capable of inducing cancer cell death (Baydoun, et al., 2020). A strategy for improving the efficiency of PDT is to increase the selectivity towards tumor cells in order to reduce the adverse side-effects caused by normal cell injury. It is known that numerous cancer cell lines (on prostate, brain, lung, nose, ovary, colon, cancer cells) over-express folic acid (FA) receptors because of their fast growth and cell division (Stallivieri, et al., 2017). Considering this, one of the strategies for improving the targeting nature of PDT, is the complexation of PS's with folic acid and their binding to folic acid receptors.

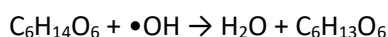
One of the characteristics of PS's is photobleaching, which is the loss of absorption or emission intensity that is caused by light. Rapid photobleaching in photosensitizer decreases the efficiency of photodynamic therapy because the tumor destruction will not be complete (Khaled, et al., 2011). Photobleaching, shown by many PS's, may reduce the concentration of PS in the tissue during irradiation. One of the main reasons photobleaching is that it leads to the decrease in the concentration and/or to the modification of the nature of the PS, thus playing a leading role in the dosimetry of the photodynamic treatment (Lassalle, 2005).

The reactive oxygen intermediates can interact with the PS, leading to its transformation and/or destruction. To determine whether singlet oxygen ($^1\text{O}_2$) is involved in the photobleaching mechanism of photosensitizer, the best way is to quench physically or chemically the $^1\text{O}_2$ immediately after his production (Lassalle, 2005).



The first excited state of oxygen - singlet oxygen ($^1\text{O}_2$), has both electrons in the same orbital with opposite spins, and exhibits longer lifetime (45 min in vacuum and 4 μsec in water) and a substantial reactivity towards electron-rich organic molecules such as dienes, olefins, phenols and polycyclic aromatic compounds. Singlet oxygen behaves as an electrophile, which can react easily with electron-rich double bonds (Kaneez, et al., 2016). The quenching of $^1\text{O}_2$ involves the deactivation of the excited singlet states of an oxygen molecule. It may be either physical or chemical quenching. Chemical quenching occurs when $^1\text{O}_2$ reacts with quencher (Q) to give product (QO_2). Physical quenching leads only to the deactivation of $^1\text{O}_2$ to its ground state without oxygen consumption or product formation. During PDT, the generation of hydroxyl radicals can also occur. In order to assess the role of this reactive oxygen species, the inhibitory action of hydrogen donors such as mannitol, ethanol, tert-butanol, acetate, formate and benzoic acid can be examined (Lassalle, 2005).

Mannitol is an effective $\bullet\text{OH}$ radical scavenger that consumes only one $\bullet\text{OH}$ radical. Mannitol combines with $\bullet\text{OH}$ radical producing water molecule (Ghimire, et al., 2018).



The aim of this work was to gain stabile complexes and enhance the effectiveness of PDT by reducing the light-induced changes of FA, cationic porphyrins, and non-covalent complexes. The stabile complexes were obtained: we chose 20 % glycerin as stabilizing agent for complexation and enhancement of photostability. The study of PS's and complexes photobleaching in the presence of known quenchers (L-histidine (L-His) as a singlet oxygen quencher and D-mannitol (Man) as a free radicals' quencher) was also performed to define the involvement of singlet oxygen and $\bullet\text{OH}$ radical in the photobleaching of cationic porphyrins.

2. MATERIALS AND METHODS

2.1. Chemicals

The cationic porphyrins and metalloporphyrins synthesized in Armenia and UK are as follows: zinc meso-tetra [4-N- (2'-oxyethyl) pyridyl] porphyrin (Zn-TOEt4PyP); zinc-meso-tetra [3-N-butyl pyridyl] porphyrin (Zn-TBut3PyP); meso-tetra [4-N- (2'-oxyethyl) pyridyl] porphyrin (TOEt4PyP). Their chemical structure is shown in figure 1.

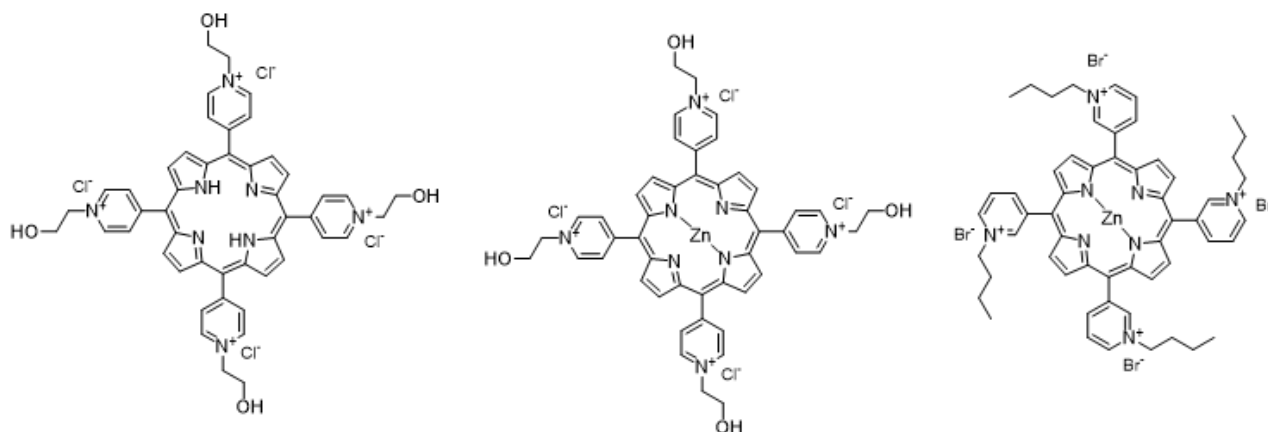


Figure 1. Chemical structure of cationic porphyrins (from left to right TOEt4PyP, Zn-TOEt4PyP and Zn-TBut3PyP).

Folic acid was obtained from the ACROS Organics Co. (Folic Acid, 97 % pure; Product code 216630100, CAS Number: 59-30-3). L-histidine and D-mannitol were purchased from Sigma-Aldrich Co.

2.2. Non-covalent complexation of FA and PS's



FA and PS were mixed in a ratio of 5/1 and incubated for 24 hours, in the dark, at 25°C. Glycerin was added to the mixture of FA and PS to make it 20 % in the final volume with additional 24-hour incubation. Unbounded components were purified using Al₂O₃ (aluminum oxide) column chromatography with 0.1 M phosphate-buffered saline (PBS) containing 20 % glycerin as eluent. The absorption spectra of porphyrins and their complexes with FA were recorded on Cary 60 UV-Vis Spectrophotometer (Agilent Co., USA), in the range 200-700 nm. Fluorescence spectra of complexes were recorded on Cary Eclipse fluorescence spectrometer (Agilent Co., USA).

2.3. Illumination of samples

Samples were illuminated under similar conditions and the changes of absorbance over time were recorded. Illumination was carried out by tungsten lamp with a range of a wavelength 380 - 1000 nm using an irradiance of 30 mW/cm², to a total of 30-minute duration. The absorptions for samples were recorded during the irradiation and after irradiation for 0 min, 5 min, 15 min, and 30 min. For photostability studies samples were FA, cationic porphyrins and their non-covalent complexes. The effect of two quenchers - histidine's and mannitol's four concentrations (0.01 mM, 0.02 mM, 0.04 mM and 0.08 mM for L-histidine and 0.1 mM, 0.2 mM, 0.4 mM and 0.8 mM for D-mannitol) on photobleaching were performed too by adding quenchers to the solution of samples providing appropriate final concentrations.

3. RESULTS AND DISCUSSION

3.1. Non-covalent complexes

We obtain non-covalent complexes of FA and PS's. In figure 2 the fluorescent spectrum one of complexes (Zn-TBut3PyP + FA) is presented. Due to complexation in the spectrum of complex there are two peaks of emission (at 422 nm and 458 nm), while the FA control has only one peak at 450 nm. Zn-TBut3PyP has two emission peaks at 610 nm and 658 nm for control and two peaks at 605 nm and 660 nm for the complex with FA. These changes suggest the formation of non-covalent bonds between the components. Similar spectra were obtained for other two porphyrins and their complexes with FA.

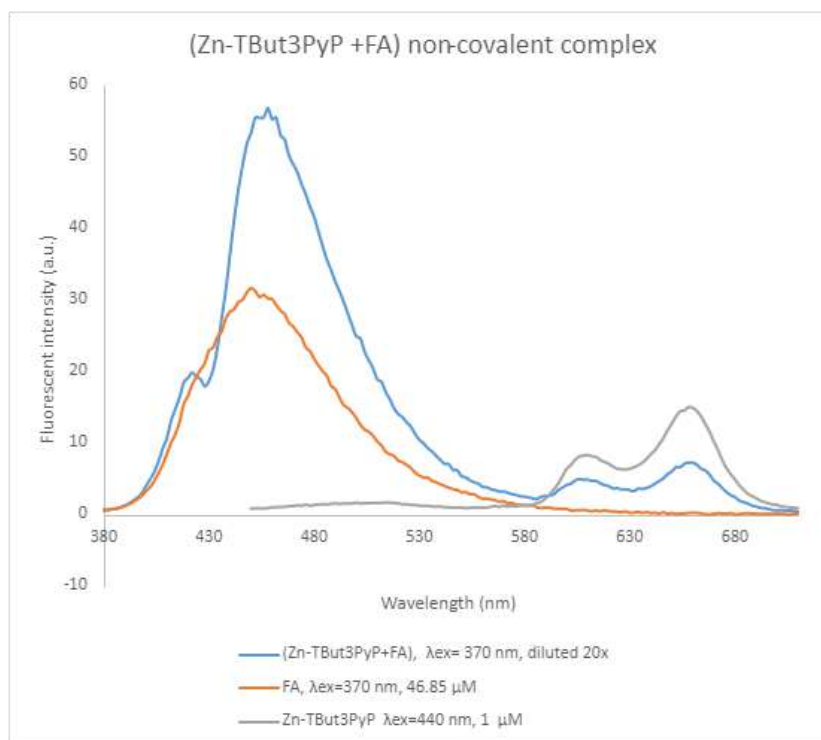


Figure 2. Fluorescent emission spectra of (Zn-TBut3PyP+FA) non covalent complex and its components.

3.2. The effect of L-histidine on photobleaching



We perform the (FA+PS) complexes and free components (FA and PS's) photobleaching study before illumination, as well as after 5 min, 15 min and 30 min of continuous exposure. It should be noted that all studies of photobleaching were performed in the presence of 20 % glycerin as it has a photostabilizing effect on the complexes and their free components (~ 2 times). Increasing the illumination duration leads to gradual reduction in the absorption of photosensitizers (free and in complexes with FA) (Mkrtchyan, 2022).

To clarify the role of singlet oxygen in the photobleaching process, L-histidine - a well-known chemical quencher of singlet oxygen, was added to the samples of the complexes and their individual components with different concentrations. It was revealed that histidine has a concentration-dependent effect on the photobleaching. Addition of 1 mM histidine resulted in up to 64 % photobleaching (decrease of absorption for Soret band at 424-440 nm): this led to 1.67- to 2.9-fold more decrease of absorption than in the case of samples with no L-histidine, following 30 min of illumination. The obtained data contradicted the result obtained by Khaled et al. 2011, according to which the addition of 1 mM of L-histidine resulted in a reduction of Sn(IV) chlorine e6's photobleaching rate. Also, it was suggested that the increased rates of porphyrin photobleaching in the presence of the photooxidizable substrate (e.g., histidine) could result from an attack on the porphyrin macrocycle by reactive 1O_2 photooxidation products of the substrates (Chekulayeva, et al., 2002).

Accordingly, to clarify the role of L-histidine as a singlet oxygen chemical quencher, we reduced the concentration and tested the effect of four lower concentrations on photobleaching (0.01 mM, 0.02 mM, 0.04 mM and 0.08 mM).

Data from the study of the effect of L-histidine on photobleaching after 30 min of illumination are shown in figure 3.

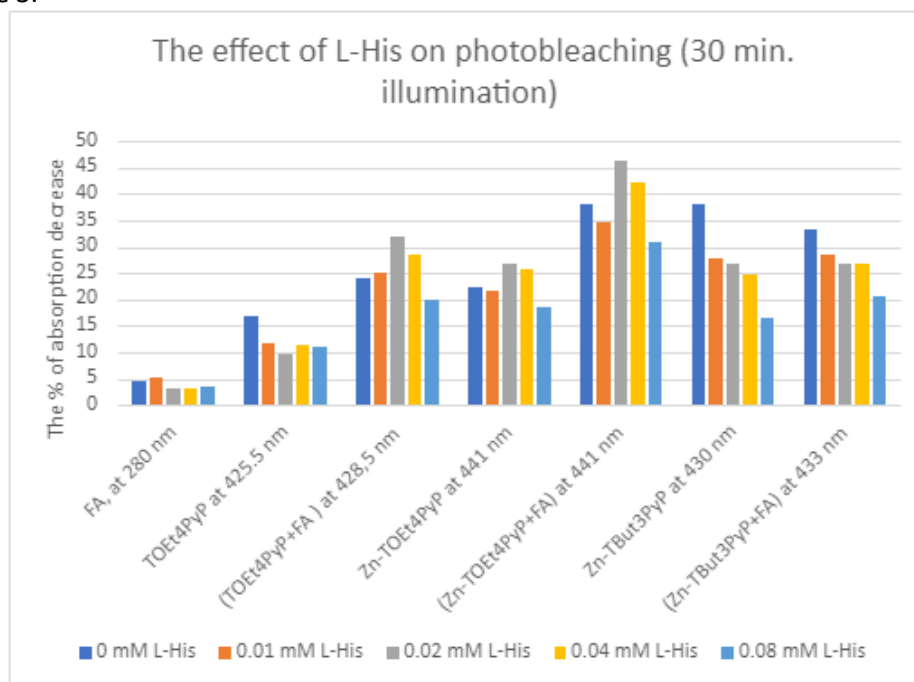


Figure 3. Photobleaching of FA, PS's and their complexes in the presence of L-His for the corresponding wavelengths of their UV-Vis spectra. The calculations were performed with respect to unlit samples (before illumination).

As it can be seen in Figure 3, for folic acid, both in the presence and absence of L-histidine, the decrease in absorbance at 280 nm is negligible and the addition of L-histidine did not result in a significant change. Therefore, we can conclude that singlet oxygen has no major role for the photobleaching process.



For porphyrins (for free PS's and in the complexes with FA), the most effective L-histidine concentration was 0.08 mM in almost all cases. L-histidine was a more effective quencher for Zn-TBut3PyP and for its complex with FA. Compared to samples without L-histidine, 30 min of illumination resulted in 2.3 times less photobleaching percentage for free Zn-Tbut3PyP and 1.6 times for the same porphyrin in the complex with porphyrin.

For metalloporphyrin Zn-TOEt4PyP, the addition of 0.08 mM L-histidine led to 1.2 times less photobleaching both for free porphyrin and in the complex with FA, after 30 min of photobleaching.

For free porphyrin TOEt4PyP the more effective L-histidine concentration was 0.02 mM that led to 1.8 times less photobleaching. For (TOEt4PyP + FA) complex, this porphyrin's absorption decrease reduced more by 0.08 mM L-histidine (by 1.2 times).

3.3. The effect of D-mannitol on photobleaching

The addition of 10 mM of D-mannitol led to ~2 times more photobleaching after 30 min of illumination. Therefore, to reveal the role of D-mannitol as a •OH radical scavenger, the concentration was decreased and four concentrations were tested to examine the role of •OH radical for the photobleaching of cationic porphyrins.

As was shown by Lassalle (2005) that in order to trap hydroxyl radical effectively, the D-mannitol and other quenchers should be present in very high concentration. Consequently, we tested 10 times higher concentrations for D-mannitol than for L-histidine. The most effective scavenging effect was obtained in the case of 0.8 mM D-mannitol for all porphyrins and for porphyrins in their complexes with FA. Data from the D-mannitol's effect on photobleaching after 30 min of illumination are shown in figure 4.

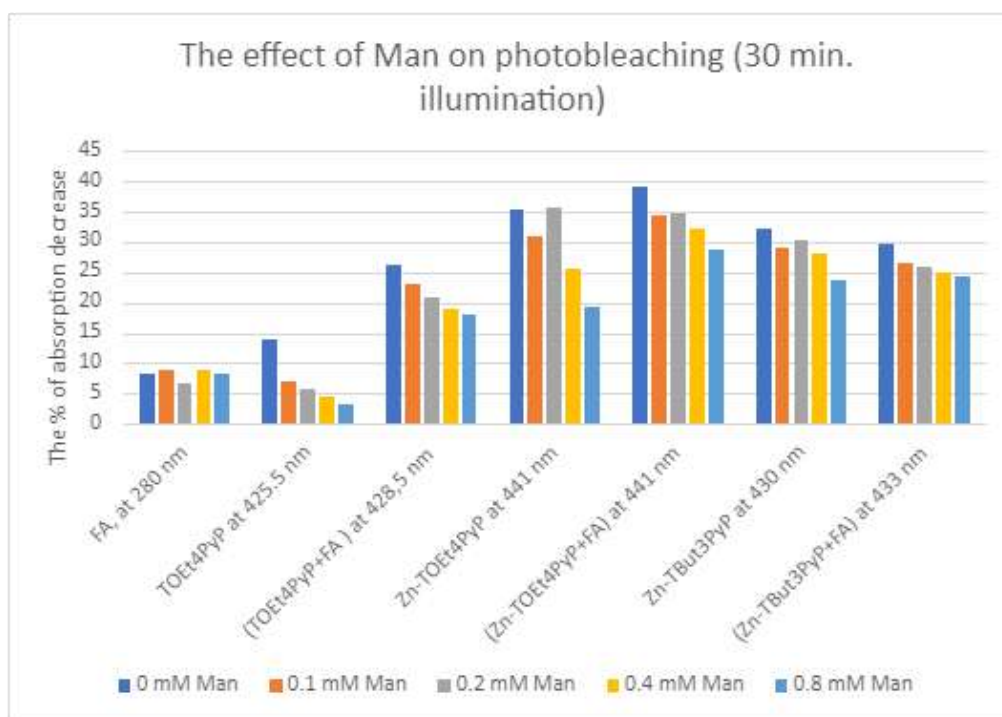


Figure 4. Photobleaching of FA, PS's and their complexes in the presence of D-mannitol (Man) for the corresponding wavelengths of their UV-Vis spectra. The calculations were performed with respect to unlit samples (before illumination).

A concentration of 0.8 mM D-mannitol most effectively reduced photobleaching of porphyrin TOEt4PyP following 30 min of illumination (only 3 % of photobleaching after the addition of D-mannitol). In the complex with FA, the photobleaching of porphyrin TOEt4PyP was reduced by 1.46 times.



D-mannitol was more effective for protection from photobleaching in case of metalloporphyrin Zn-TOEt4PyP too than the L-histidine, as the photobleaching was reduced by 2 and 2.4 times for free porphyrin and in the complex with FA, respectively.

In contrast to the aforementioned, for metalloporphyrin Zn-TBut3PyP D-mannitol was less effective than L-histidine: the reduction of photobleaching after the addition of D-mannitol was 1.3 and 1.2 times less compared with the samples with no D-mannitol, respectively, in the case of free porphyrin and for this porphyrin in non-covalent complex with FA.

We can conclude that D-Mannitol is more effective for •OH radical scavenging of TOEt4PyP and Zn-TOEt4PyP than L-histidine for quenching the singlet oxygen. The more effective photoprotection by L-histidine for Zn-TBut3PyP is correlated with higher singlet oxygen quantum yield (γ_{Δ}) of this PS ($\gamma_{\Delta}=0,98$) compared with other two PS's ($\gamma_{\Delta}=0,7$ for TOEt4PyP and $\gamma_{\Delta}=0,84$ for Zn-TBut3PyP). It should be noted that both quenchers have a protective effect, thus indicating that both singlet oxygen and •OH radical play a crucial role in the photobleaching mechanism of these cationic porphyrins.

4. CONCLUSIONS

FA forms non-covalent stable complexes with cationic porphyrins in the presence of 20 % glycerin. The advantage of gaining this type of complexes is the simplicity of method. By using singlet oxygen quencher L-histidine and free radicals' quencher D-mannitol, it was concluded that the use of quenchers with optimal concentration can lead to the reduction of photobleaching rate and thus the enhancement of PDT efficiency.

5. ACKNOWLEDGEMENTS

This study supported by the Science Committee of the Ministry of Education, Science, Culture and Sports of the Republic of Armenia (Grant No 21SC-BRFFR-1F007). The authors thank Dr. Robert Ghazaryan from Yerevan State Medical University for providing cationic porphyrins and metalloporphyrins.

REFERENCES

- Baydoun, M., Moralès, O., Frochot, C., Ludovic, C., Leroux, B., Thecua, E., Ziane, L., Grabarz, A., Kumar, A., de Schutter, C., Collinet, P., Azais, H., Mordon, S. and Delhem, N., 2020. Photodynamic therapy using a new folate receptor-targeted photosensitizer on peritoneal ovarian cancer cells induces the release of extracellular vesicles with immunoactivating properties. *J. Clin. Med.*, 9, 1185.
- Chekulayeva, L., Shevchuk, I., Chekulayev, V. and Jäälaid, R., 2002. Kinetic studies on the mechanism of haematoporphyrin derivative photobleaching. *Proc. Estonian Acad. Sci. Chem.*, 51, 1, 49–70.
- Ghimire, B., Lee, G. J., Mumtaz, S. and Choi, E. H., 2018. Scavenging effects of ascorbic acid and mannitol on hydroxyl radicals generated inside water by an atmospheric pressure plasma jet. *AIP Advances*, 8, 075021.
- Kaneez, F., Nusrat, M. and Suaib, L., 2016. Quenching of singlet oxygen by natural and synthetic antioxidants and assessment of electronic UV/Visible absorption spectra for alleviating or enhancing the efficacy of photodynamic therapy. *Biomedical Research and Therapy*, 3(2), 514-527.
- Khaled, A., Khalid, O. and Mohamad, J., 2011. Photobleaching of Sn(IV) chlorine e6 dichloride trisodium salt in different environments. *African Journal of Biotechnology*, 10 (45), 9137.
- Lassalle, H. P., 2005. Study of the photobleaching mechanisms of the 5,10,15,20-tetrakis(mhydroxyphenyl) bacteriochlorin (m-THPBC), in solution, *in vitro* and *in vivo*. *PhD thesis, Bioengineering. Université Henri Poincaré - Nancy I*.
- Mkrtychyan, L., 2022. Photobleaching of non-covalent complexes of folic acid and photosensitizers, *Biological Journal of Armenia*, 74 (1), 31-38.
- Stallivieri, A., Colombeau, L., Jetpisbayeva, G., Moussaron, A., Myrzakhmetov, B., Arnoux, P. and Frochot, C., 2017. Folic acid conjugates with photosensitizers for cancer targeting in photodynamic therapy: Synthesis and photophysical properties. *Bioorganic & Medicinal Chemistry*, 25(1), 1–10.



Influence of anthropogenic factors on pollution of arable soils and changes in the activity of enzymes in them

A. Sukiasyan¹, A. Kirakosyan¹, S. Kroyan² and P. Gikas³

¹Chair General chemistry and chemical technology,
National Polytechnic University of Armenia, Yerevan, Armenia

²National University of Architecture and Construction of Armenia, Yerevan, Armenia

³Technical University of Crete, School of Chemical and Environmental Engineering, Chania,
Greece

Corresponding author email: sukiasyan.astghik@gmail.com

ABSTRACT

The aim of this work was to combine biochemical and geo-ecological approaches to determine the degree of anthropogenic load on soils, taking into account the activity of some oxidoreductase (catalase) and hydrolytic (amylase, urease, and invertase) enzymes for comparative assessment of pollution of arable soils near the industrial zone of Hrazdan city. There are located Hrazdan Thermal Power Plant and Hrazdan Cement Plant. A soil sample from the point-area *Hrazdan1* was located next to them. Taking into consideration that the wind was rising in the southwest direction, the third point-area *Hrazdan3* was located in the same direction, at a distance of up to one kilometer from the industrial zone. The soil samples were determined for humus content, the activity of some enzymes, and d-elements of the fourth period, forming a group known as transitional heavy metals. With distance from the general industrial zone, taking into account all intermediate points of material sampling, a significant decrease in the concentration of transitional heavy metals was observed for the middle point-area (*Hrazdan2*). The values Z_c showed that all the investigated point-areas were dangerously contaminated, but the middle point-area (*Hrazdan2*) had 15% lower values Z_c compared to the extreme soil sampling points. As we moved away from the industrial zone from point-area *Hrazdan3* toward point-area *Hrazdan1*, a significant increase in humus up to 25% was found in the soil samples against the background of a gradual increase in pH in the soil samples up to 7%. According to the activity of invertase and amylase enzymes, it is well seen that their activity in the point-area *Hrazdan2* differs from the activity in other point-areas. Invertase activity in *Hrazdan2* was on average 30% lower than in soil samples from *Hrazdan1* and *Hrazdan3*.

Keywords: transition heavy metals; soil; total pollution index; humus; activity of soil enzymes.

1. INTRODUCTION

Irrational human activities as well as greedy exploitation of natural resources have destabilized the biosphere. These phenomena have become cause-and-effect pushes that require increased attention to mitigate the effects of man-made environmental problems. The problem of deterioration of soil biological properties is relevant against the background of uncontrolled environmental pollution by a wide range of pollutants (Huang et al., 2020; Sukiasyan and Kirakosyan, 2020). In this context, multi component studies may be the information needed to link the effects of adverse factors on biota and human economic activities. Soil resources, as one of the most important components of the biosphere, are the first to experience anthropogenic negative impacts (Margesin et al., 2000). At present, it has acquired a global scale with a consequent decrease in the natural fertility of soils. Among the dominant causes of soil degradation and reduction of its biological productivity is pollution by heavy metals (HMs). It is known that up to 90% of the biosphere pollutants accumulate in the soil. However, in many cases, environmental problems are not given proper attention. Areas with active industrial activities are polluted by emissions and movement of HMs, which have a highly toxic effect on the biota. HMs inhibit mineralization and synthesis of various substances in soils (Trifonova et al., 2014), oppress respiration of soil microorganisms, and cause microbostatic effects (Nannipieri et al., 2017). Most HMs in elevated concentrations irrevocably change the activity of soil enzymes: catalase, invertase, amylase, etc. (Ivshina et al., 2014; Olaniran et al.,



2013). At the same time, the sensitivity of enzymes with respect to different doses of HMs is different (Kuziemska et al., 2020; Engwa et al., 2019). Anthropogenic impact on biota leads to a change in the physical, chemical and biological state of soils, affects the activity of carbohydrate metabolism enzymes. Enzymatic activity of soils is the most important diagnostic indicator of the impact of anthropogenic load on soil systems. Despite the environmental sensitivity to enzymatic diagnostics, the impact of pollutants on the natural biochemical processes that form fertility is poorly studied.

In view of the above, the aim of this work is to combine biochemical and geoecological approaches to determine the degree of anthropogenic load on soils, taking into account the activity of some oxidoreductase and hydrolytic enzymes for a comparative assessment of bioremediation of arable soils near the industrial zone of Hrazdan town. Hrazdan is one of the most important industrial and energy centers in the Republic of Armenia. There are the Hrazdan Thermal Power Station (HTPS) and Hrazdan Cement Plant (HCP) as well as other important enterprises which formed a large industrial area.

2. MATERIALS AND METHODS

2.1. Collection and processing of soil samples

The study area covered a large part of the Hrazdan industrial area in a southwestern direction (HTPS and HCP), taking into account anthropogenic pressures and regional wind patterns (Elliott et al., 2003). A soil sample from the point-area *Hrazdan1* was located near the HTPS and HCP. The second experimental point-area *Hrazdan2* was located 380-400 m away from the first site. The third experimental point-area *Hrazdan3* was located in the same direction at a distance of 800-850 m from the industrial area (Fig. 1).



Figure 1. Scheme of the location of the soil samples (*Hrazdan1*, *Hrazdan2*, and *Hrazdan3*) near Hrazdan Thermal Power Station (HTPS) and Hrazdan Cement Plant (HCP).

Soil samples under dry-weather conditions were taken from a depth of up to 20 cm at the control points using the envelope method. Point sampling was performed by using non-metallic tools. A combined soil sample was prepared by mixing at least five incremental samples taken from the same experimental site.

2.2. Determination of the concentration of chemical elements of the fourth periodicity

The chemical elements of the fourth periodicity (scandium (Sc), titanium (Ti), vanadium (V), chromium (Cr), manganese (Mn), iron (Fe), cobalt (Co), nickel (Ni), copper (Cu) and zinc (Zn)) with different hazard classes were measured in soil samples (Sukiasyan, 2018). Soil samples were examined under direct exposure to X-rays using a Thermo Scientific™ Niton™ portable XRF analyzer (Thermo Scientific Niton XL3t Series handheld XRF analyzer instruments). Each sample was examined at least 3 times and the results were averaged



according to the arithmetic mean law. Instrument data (mg/kg) were considered as the final result for soils. Studies were performed on 10 soil samples, with the results presented in units/mg/kg, respectively (Thermo Scientific Niton XL3t Series Handheld XRF Mining Analyzers instruments).

To characterize the processes of accumulation of chemical elements in soil samples, the total pollution index (Z_c) was calculated according to the formula

$$Z_c = \sum_{i=1}^n C_{ci} - (n - 1)$$

where $C_i = C_s/B_f$ – concentration factor; C_s – concentration of chemical elements in the soil sample, mg/kg; B_f – background content of chemical elements in the soil, mg/kg (Müller, 1981); n – number of chemical elements.

2.3. Biochemical analysis of soil samples

Determination of humus in soil samples was carried out by Tyurin's method, which is based on the oxidation of humus with a sulfur-chromium mixture prepared in a ratio of sulfuric acid with a specific weight of 1.84 and water 1:1 (Tyurin, 1951, modified by GOST 26213 - 91). In soil samples, determination of catalase (1.11.1.6) activity in soil samples was carried out at 18-20 °C; $C_m O_2$ per 1 g of soil for 1 min. The total activity of α and β amylase (3.2.1.1), which act on glycosyl compounds, was determined. Invertase (3.2.1.26) is involved in the breakdown of hydrocarbons, and the activity of this enzyme can be used to judge the rate of decomposition of carbon-containing organic compounds. Urease (3.5.1.5) decomposes urea to CO_2 and NH_3 , and the resulting ammonia and ammonium salts serve as a source of nitrogen nutrition for plants and microorganisms. The activities of all of these enzymes (catalase, amylase, urease, and invertase) in soil samples were carried out according to the method by Khaziev's methods (Khaziev, 1990).

2.4 Biochemical analysis of soil samples

All experimental data had up to 5 technical repetitions and were subjected to statistical processing taking into account Student's t-test at a significance level of $p < 0.05$ (Kirakosyan and Sukiasyan, 2005).

3. RESULTS AND DISCUSSION

Accumulation of HMs causes a decrease in the biological productivity of soils, slowing down the processes of soil formation. To solve this problem it is very important to quickly and accurately assess the level of soil contamination by the most effective environmentally safe methods. Exact boundaries separating transition metals (TMs) from other groups of chemical elements have not yet been drawn. Therefore, the d-elements forming the group (d-block) known as transition heavy metals (THMs) were considered in the presented work. These chemical elements are grouped by the valence electrons with the highest energy that occupy the d-orbital in the electron shell (Jensen, 2003). THMs occur mainly as trace elements, and their general functions are related to the process of complexation between amino acids, proteins, nucleic acids, and ions of the corresponding metals. A series of experiments to study the impact of anthropogenic load of industrial enterprises in Armenia was initiated, on nearby areas of arable soils. Soil sampling was conducted from sites at distances of 0.5; 1.5; 2.5; 5; 10; 15 and 25 km from the pollution source (Sukiasyan et al., 2021). In continuation of studies in this direction in order to identify changes in HMs concentration, but in this case at close distances, up to one kilometer. According to the information on the wind rose map in Hrazdan, the prevailing wind direction is southwest (31%). Accordingly, the dispersion zone of pollutants entering the atmosphere of the industrial zone will prevail in this direction, where the arable soils of the region are located. Changes in the concentration of some THMs in soil samples located at different distances of about 350-400 m from each other were determined. The results obtained were not unambiguous. According to the results presented in Table 1, the elements Sc and Co were detected in trace amounts among the HTMs, regardless of the location of the point zones. Fe and Ti differed in the highest concentration values by an order of magnitude compared to other elements of HTMs. A peculiar anomaly was found in the general pattern of element distribution. With distance from the general industrial zone, taking into account all intermediate material sampling points, a significant decrease in HTMs concentration was observed for the point-area Hrazdan2. After that, a gradual increase in concentrations of the elements in question is observed,



and already closer to the road in the point-area of Hrazdan1 (the distance was 200 m from the road) a strong contamination is observed. Based on the results obtained (table 1), it can assume which elements are subject to air migration caused by the wind rose in the region. To interpret the results, the reduced total pollution index (Zc) was compared, taking into account the concentration of chemical elements by Clark (Sukiasyan, 2018). The calculations of Zc based on the values of THMs concentrations in soil samples showed that soil contamination in all investigated points-areas is within dangerous. In the middle point-area (Hrazdan2) the value of reduced total pollution index was on 15% lower compared to the extreme points of soil sampling.

Table 1. Concentrations of some transition metals (mg/kg) and value of in arable soil samples near industrial zone of Hrazdan.

The elements of the d-block (valence electron configuration)	The soil sampling from point-area		
	Hrazdan 1	Hrazdan 2	Hrazdan 3
Sc (4s23d1)	trace	trace	trace
Ti (4s23d2)	3702.4±5.9	3408.1±81.8	4675.6±112.2
V (4s23d3)	130.1±2.7	104.4±2.7	143.3±4.0
Cr (4s13d5)	120.5±2.9	88.4±1.9	98.1±2.4
Mn (4s23d5)	717.3±32.6	974.7±26.3	883.8±23.9
Fe (4s23d6)	27850.0±668.4	29417.0±991.0	31030.2±899.9
Co (4s23d7)	trace	trace	trace
Ni (4s23d8)	63.2±0.8	71.9±1.5	62.2±1.3
Cu (4s13d10)	66.3±1.1	57.7±0.5	51.4±1.3
Zn (4s23d10)	129.0±2.7	99.1±1.5	101.8±2.4
Total pollution index (Zc)*	63	56	66

Note: *the summary pollution level was classified as low with $Z_c < 16$ contamination is considered as non- dangerous; with $16 < Z_c < 32$ contamination is moderately dangerous; with $32 < Z_c < 128$ contamination is dangerous; with $Z_c > 128$ contamination is extremely dangerous (Müller, 1981); with a significance level of $p < 0.05$.

Soil enzymes are involved in the decomposition of plant, animal, and microbial residues, as well as in the synthesis of humus. An increase in the anthropogenic load on the soil leads to changes in the quantitative and qualitative composition of humus and the enzymatic activity of soils. This "non-standard" distribution of THMs in soil samples was duplicated in biochemical indicators as well (Table 2). Determination of the activity of soil enzymes is important to determine the degree of influence of agrotechnical measures and agrochemical means on the activity of biological processes in order to judge the rate of mobilization of major organogenic elements. Amylase enzymes carry out hydrolysis of starch, which is part of the organic residues entering the soil, with the formation of dextrans and maltose. The main producer of amylase is the root excretions of plants. The high activity of urease in the soil is an essential factor in its nitrogen metabolism.

Table 2. Major agrochemical, physico-chemical properties and enzyme activity of arable soils depending on the distance from the industrial zone of Hrazdan town.

The soil sampling from point-area	Humus (%)	pH	Enzyme activity			
			Catalase (1.11.1.6) (O ₂ cm ³ in one g of soil per one min)	Invertase (3.2.1.26) (mg of glucose in one g of soil per one day)	Amylase (3.2.1.1) (mg of maltase in one g of soil per one day)	Ureaza (3.5.1.5) (mg NH ₃ in one g of soil per one day)
Hrazdan 1	3.13±0.01	7.66	4.37±0.06	10.62±0.29	3.38±0.27	2.63±0.09
Hrazdan 2	2.23±0.03	7.47	9.93±0.21	7.67±0.16	6.06±0.61	2.39±0.21
Hrazdan 3	2.34±0.02	7.19	10.87±0.15	11.13±0.43	3.71±0.17	2.39±0.05

Thus, according to the activity of invertase and amylase enzymes, it is well seen that their activity in the point-area of Hrazdan2 differs from the activity in other point-areas. Invertase activity in Hrazdan2 was on average 30% lower than in soil samples from Hrazdan1 and Hrazdan3. Such kind of changes in activity of



enzymes was an indicator of early diagnosis of negative changes in soil properties (Sardar, 2007). Urease plays an important role in soil nitrogen conversion. The presence of urease in bacteria allows them to use urea as a source of ammonium because urease catalyzes its hydrolysis. In our case, the urease activity of soil confirms the close correlation between its indicator and anthropogenic factor (Khaziev, 1990). As the distance from the industrial zone from point-area Hrazdan3 towards point-area Hrazdan1 against the background of a gradual increase in pH in soil samples up to 7%, a significant increase in humus up to 25% was found. An important role in the processes of neutralization of hydrogen peroxide, which is toxic to soil living organisms, is played by catalase, which enters the soil as a result of their high physiological activity during the period of favorable living conditions.

The presence of THMs in the soil can affect the rate of decomposition of hydrogen peroxide by catalase (Novoselova and Volkova, 2017). The parameters of the activity of the catalase enzyme are used in the study of various types of soils in order to characterize their biological properties (Khaziev, 1990), and to assess the influence of various anthropogenic factors on the state of soil systems (Falsone, 2012). However, the decomposition of hydrogen peroxide can be carried out not only by the catalase enzyme, but also by abiotic catalysts present in soils (Marshall, 2000). They can be organic compounds, clay minerals, various chemical elements with variable valence, etc.

According to the results obtained on the activity of catalase near the industrial zone, high activity was noted, which decreases by 60% as the distance from the source of pollution decreases. The trend towards a decrease in catalase activity can be explained by the fact that catalase in the soil is synthesized mainly by aerobic microorganisms, the number of which probably decreases with distance from the main source of anthropogenic load from the industrial zone due to a decrease in the content of elements of variable valence. In addition, catalase activity is higher in soil samples with the least amount of humus, and vice versa. Statistical processing revealed an inverse functional relationship between these indicators.

4. CONCLUSIONS

Transition heavy metals (THMs) have been investigated as the most dangerous pollutants entering the environment. They are not susceptible to degradation processes and can only redistribute between individual soils components and are also capable of accumulating in individual links of the trophic chain. In continuation of studies in this direction in order to identify changes in HMs concentration, but in this case at close distances, up to one kilometer. A peculiar anomaly was found in the general pattern of element distribution. With distance from the general industrial zone, taking into account all intermediate material sampling points, a significant decrease in HTMs concentration was observed for the middle point-area (Hrazdan2). The calculations of Zc based on the values of THMs concentrations in soil samples showed that soil contamination in all investigated point-areas is within dangerous. Again, in the middle point-area (Hrazdan2) the value of reduced total pollution index was on 15% lower compared to the extreme points of soil sampling. The behavior of the most common soil enzymes during soil contamination with HMs can serve as an indicator of the degree of soil contamination. The pool of soil hydrolytic and oxidoreductase enzymes participates in all stages of transformation of organic compounds entering anthropogenically contaminated soil, is the most important regulator of soil biochemical homeostasis, and can serve as a measure of danger of anthropogenic pressure on biota.

5. ACKNOWLEDGEMENTS

This study is supported by the by the Science Committee of RA, in the frames of the research project № 21T-2H216.

REFERENCES

- Huang, H., Luo, L., Huang, L., Zhang, J., Gikas, P., and Zhou, Y., 2020. Effect of manure compost on distribution of Cu and Zn in rhizosphere soil and heavy metal accumulation by *Brassica juncea*. *Water, Air, & Soil Pollution*, 231(5), 1–10.
- Sukiasyan, A., and Kirakosyan, A., 2020. Ecological evaluation of heavy metal pollution of different soil-climatic regions of Armenia by biogeochemical coefficients. *DRC Sustainable Future: Journal of Environment, Agriculture, and Energy*, 1(2), 94–102, doi: 10.37281/DRCSF/1.2.2.



- Margesin, R., Zimmerbauer, A., and Schinner, F., 2000. Monitoring of bioremediation by soil biological activities. *Chemosphere*, 40(4), 339–346.
- Trifonova, T., Sakhno, O., Zabelina, O., and Feoktistova, I., 2014. Comparative assessment of the state of urban soils based on their biological activity. *Moscow University Soil Science Bulletin*, 69(3), 112–115.
- Nannipieri, P., Greco, S., and Ceccanti, B., 2017. Ecological significance of the biological activity in soil. *Soil biochemistry*, 293–356.
- Ivshina, I., Kostina, L., Kamenskikh, T., Zhuikova, V., Zhuikova, T., and Bezel, V., 2014. Soil microbiocenosis as an indicator of stability of meadow communities in the environment polluted with heavy metals. *Russian journal of ecology*, 45(2), 83–89.
- Olaniran, A., Balgobind, A., and Pillay, B., 2013. Bioavailability of heavy metals in soil: impact on microbial biodegradation of organic compounds and possible improvement strategies. *International journal of molecular sciences*, 14(5), 10197–10228. <https://doi.org/10.3390/ijms140510197>.
- Kuziemska B., Wysokiński A., and Trębicka J., 2020. The effect of different copper doses and organic fertilisation on soil's enzymatic activity. *Plant, Soil and Environment*, 66(2), 93–98 <https://doi.org/10.17221/671/2019-PSE>.
- Engwa, G., Ferdinand, P., Nwalo, F., and Unachukwu, M., 2019. Mechanism and health effects of heavy metal toxicity in humans. In O. Karcioglu, and B. Arslan (Eds.), *Poisoning in the Modern World - New Tricks for an Old Dog?* <https://doi.org/10.5772/intechopen.82511>.
- Elliott D., Schwartz M., Scott G., Haymes S., Heimiller D., and George R., 2003. Wind energy resource: Atlas of Armenia. *Technical report National Renewable Energy Laboratory, U.S. Department of Energy Office of Scientific and Technical Information*, July.
- Sukiasyan, A., 2018. A new approach to determining the environmental risk factor by biogeochemical coefficients of heavy metals. *South of Russia: ecology, development*. 13(4), 108–118. doi: 10.18470/1992-1098-2018-4-108-118
- Thermoscientific sample collection and preparation tools for exploration and mining <https://tools.thermofisher.com/content/sfs/brochures/sample-prep-tools-mining-final-2012feb14specsheets.pdf>, 2–3.
- Tyurin, I., 1951. On the method of analysis for comparative study of the composition of soil humus or humus. *Proceedings of Soils, Institute after Dokuchaev*, 38, p. 5–21
- GOST 26213-91 Soils. Methods for determination of organic matter. Standards Publishing, 1992. Khaziev, F., 1990. *Methods of soil enzymology*. Mi: Science, 189 p.
- Kasimov, N., and Vlasov, D., 2015. Clarkes of chemical elements as reference standards in ecogeochemistry. *Bulletin of the Moscow University*. Ser. 5. Geography, 2, 7–17.
- Kirakosyan, A. and Sukiasyan, A., 2005. *Using MATLAB as an express method for evaluating experimental results*. International Youth Conference: Information Technologies. Yerevan, Armenia, 34–37.
- William, B., 2003. The place of zinc, cadmium, and mercury. *Periodic Journal of Chemical Education Table*, 952–961.
- Sukiasyan, A., Kroyan, S., Skugoreva, S., Kirakosyan, A., and Ghazaryan, H. 2021. Consequences of the impact of some industrial plants on the content of heavy metals in soils. *Theoretical and Applied Ecology*, 4, 90–97. DOI: 10.25750/1995-4301-2021-4-090-097.
- Sardar, K., 2007. Soil enzymatic activities and microbial community structure with different application rates of Cd and Pb. *Journal of Environmental Sciences*, 19(7), 834–840.
- Khaziev, F., 1990. System-ecological analysis of the enzymatic activity of soils. Moscow, 204p.
- Müller, G., 1981. Die Schwermetallbelastung der sedimente des Neckars und seiner Nebenflüsse Eine Bestandsaufnahme. *Chemical Zeitung*, 105, 157–164.
- Novoselova, E., and Volkova, O., 2017. Influence of heavy metals on the activity of catalase of different soil types. *Bulletin of the Orenburg State Agrarian University*, 2 (64), 190–193.
- Falsone, G, Celi, L., Caimi, A., Simonov, G., and Bonifacio, E., 2012. The effect of clear cutting on podzolization and soil carbon dynamics in boreal forests (Middle Taiga zone, Russia). *Geoderma*, 177–178, 27–38.
- Marshall, V., 2000. Impacts of forest harvesting on biological processes in northern forest soils. *Forest Ecology and Management*, 133(1–2), 43–60.



Beneficiation of Coal Ash for Rare Earth Elements Enrichment

A. Tsachouridis¹ and N. Kiratzis¹

¹Department of Mineral Resources Engineering/School of Engineering, University of Western Macedonia, Kozani, Greece

Corresponding author email: nkiratzis@uowm.gr

ABSTRACT

Rare Earth Elements and Yttrium (REY), as basic raw materials for numerous high-tech applications, comprise an indispensable and invaluable component of our civilization. They have been classified as critical materials due to the combination of their supply risk for key technologies and their economic importance in the production and capabilities of products, within the electronic and energy industries. Coal fly (CFA) and bottom ash (CBA), from existing and decommissioned electric power plants, may constitute a good source for these metals. Here, the feasibility of recovering these metals from the thermal power plant of PPC Meliti, Florina is examined. Results are presented on the chemical and mineralogical analysis of the starting materials as well as on the effect of size and magnetic separation on REY enrichment and recovery.

Keywords: Coal ash; Rare Earth Elements; Beneficiation; Size Separation; Magnetic Separation.

1. INTRODUCTION

Rare Earth Elements consist an important family of metallic elements that are vital components for hundreds of industrial applications. This family of metals includes the lanthanides plus scandium and yttrium and they are generally denoted as REY. They can be classified as Heavy(H) and Light(L), based on their atomic number, with the L.REY being the elements from *La* to *Sm* (Atomic number 57 → 62) and the H.REY from *Eu* to *Lu* (Atomic Number 63 → 71) (Simoni et al., 2015). Furthermore, REY be categorized as Critical (*Nd, Eu, Tb, Dy, Y, Er*), Uncritical (*La, Pr, Sm, Gd*) and Excessive (*Ce, Ho, Tm, Yb, Lu*) (Seredin and Dai, 2012) with respect to their economic value. For further characterization of any given material, the Outlook Coefficient and the Critical Percentage indexes have been introduced and described by the equations below (w/w):

$$C_{outlook} = \frac{(Nd + Eu + Tb + Dy + Er + Y)/\sum REY}{(Ce + Ho + Tm + Yb + Lu)/\sum REY} \quad (1)$$

$$Critical \% = \frac{(Nd + Eu + Tb + Dy + Er + Y)}{\sum REY} \times 100 \quad (2)$$

Higher Outlook Coefficient values indicate a more promising REY source, with respect to its potential industrial value. According to Dai et al. (2017), sources that produce an Outlook Coefficient between 0.7 and 1.9 are considered as promising.

In the current study, samples of CFA and CBA from the active thermal power plant of PPC Meliti, Florina are evaluated as potential and valuable REY sources. The effect of size and magnetic separation on REY content is examined and, in light of these findings, appropriate subsequent enrichment processes are proposed and discussed.

2. MATERIALS AND METHODS

A large quantity of coal fly (CFA) and bottom (CBA) ash was collected every day, for five days, from the active thermal power plant of PPC Meliti, Florina. The material was thoroughly mixed and subjected to coning and quartering so as to produce two final samples of fly and bottom ash, representative of the material that the power plant produces on weekly basis.

The two ash samples were subjected to thermogravimetric analysis (TGA) for their Loss on Ignition (LOI) content. LOI content indirectly indicates the quantity of the unburned carbon in any given sample. The major and minor elements composition of the samples was examined by X-Ray fluorescence (XRF) analysis, while their REY content was determined by Inductively Coupled Plasma – Mass Spectroscopy (ICP-MS). The CFA



had the higher REY content and was further selected as the basis for beneficiation. The CFA mineralogical composition was analyzed by means of X-Ray powder diffraction (XRD, Bruker 38 Advance Series II X-ray Diffractometer).

Particle size separation was the first beneficiation method that was implemented, by means of dry sieving. For this process, an ANALYSETTE 3 PRO FRITSCH Vibratory Sieve Shaker was used. The particle size ranges that were evaluated were the following: +50 Mesh (>297 μm), 50-120 Mesh (297-125 μm), 120-200 Mesh (125-75 μm), 200-325 Mesh (75-44 μm), 325-400 Mesh (44-37 μm) and -400 Mesh (<37 μm). For each sieving test, 80 gr of fly ash were loaded on the sieving apparatus, while each test lasted 85 min approximately.

Wet magnetic separation was implemented after the size separation. The feed material of the process was obtained from the finer particle size fraction of the size separation (-400 Mesh), as it was considered the optimal material, based on the REY recovery that it yielded. For this process, a high-gradient magnetic separator (CARPCO) was used. For the slurry, 120 gr of the material were mixed with 480 ml of water (solid-to-liquid ratio 1:4) and the mixture was subjected to magnetic separation, in two different magnetic fluxes (4200 Gauss & 8420 Gauss). During the process, the magnetic minerals attach to the induced magnetic balls through which the slurry passes, while the non-magnetic minerals exit unaffected from the bottom of the separator. After the prescribed time, the magnetic field is disabled and the magnetic fraction is released from the magnetic balls. Both fractions are collected, dried overnight, weighted and given for chemical analysis.

3. RESULTS AND DISCUSSION

The REY recovery (%) and the enrichment factor (EF) (Lin et al., 2017) were defined following Lin et al., where REY_i is the concentration in the i th fraction (ppm) and W_i is the mass percentage of that fraction. Fig. 1 shows the major chemical composition and the LOI content of the various size fractions.

$$REY \text{ recovery } (\%) = \frac{REY_i W_i}{\sum_i^n REY_i W_i} \times 100 \quad (3)$$

$$EF_i = \frac{REY_i}{REY_f} \quad (4)$$

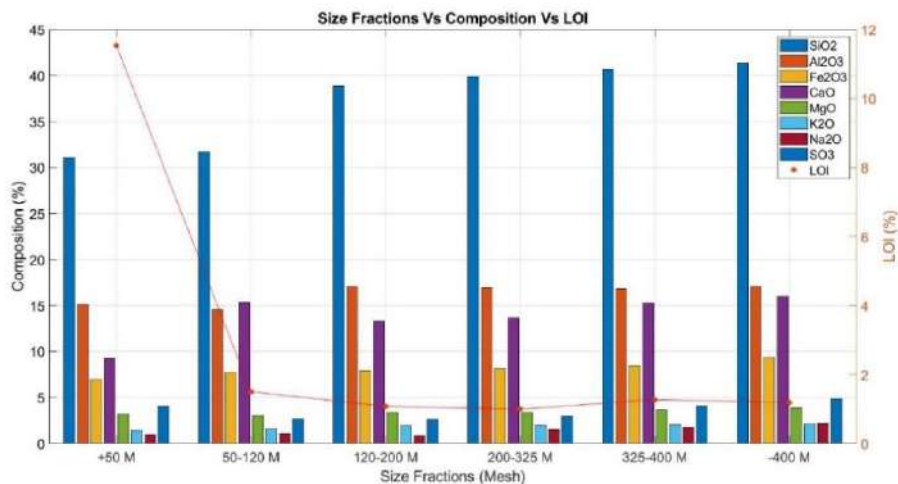


Figure 1. Chemical composition and LOI content of the various size fraction.

The REY content of the CFA was equal to 254.7 ppm and that of the CBA equal to 227.9 ppm, therefore the CFA sample was selected as the basis for the upcoming beneficiation and extraction processes. Based on the ASTM C618-12a classification, the CFA was classified as Class C, typical for lignite coals (ASTM C618, 2021).

All size fractions of CFA consisted of amorphous glass, quartz, plagioclases (albite, labradorite, bytownite), lime, gehlenite, hematite and anhydrite. The quartz content was significantly lower in the two coarser fractions (+50 Mesh, 50-120 Mesh) compared to the other fractions. Semi-quantitative XRD showed higher



concentrations of albite in the coarser fractions (+50 Mesh, 50-120 Mesh). The amorphous glass phases gehlenite, hematite and anhydrite concentrate towards the finer particle sizes.

The initial CFA sample presented a $C_{outlook}$ value equal to 0.99 and a critical REY (%) value equal to 36.66%, indicating a promising source with potential industrial value. Similar studies on Polish and United Kingdom industrial coal fly ashes report critical REY values ranging from 33%-35.8% and $C_{outlook}$ between 0.84-0.96 (Blissett et al., 2014). Generally, it has been observed that ashes of different geological origin may respond differently to the various beneficiation methods (Rosita et al., 2020). However, the overall REY concentration in CFA of the PPC Meliti (254.7 ppm) was lower than the global average (404 ppm) (Seredin and Dai, 2012), indicating the need for beneficiation methods prior to main extraction processes.

Fig. 1 reveals that the coarser fraction (+50 Mesh) contained the highest LOI content, indicating that the majority of the unburned carbon which could represent the amount of the remaining organic material after the combustion can be collected and removed with that particular size fraction, in the absence of more sophisticated and costly methods (i.e. froth flotation) (Blissett et al., 2014).

Figure 1 also shows that the concentrations of Al_2O_3 and MgO do not significantly change with size fraction. On the other hand, those of SiO_2 , Fe_2O_3 and CaO increase with decreasing particle size. In light of the mineralogical results it can be inferred that SiO_2 probably resolves mainly as quartz and to a lesser extent through the amorphous glass phase, albite and gehlenite. On the other hand, Al_2O_3 , Fe_2O_3 should constitute the major portions of amorphous glass and hematite respectively. Finally, CaO content is correlated mostly with bytownite and to a lesser degree with labradorite, gehlenite and lime. An XRD diffractogram for the -400 Mesh fraction, which yielded the highest REY recovery, is shown in fig. 2. Table 1 summarizes the results of the two beneficiation processes implemented.

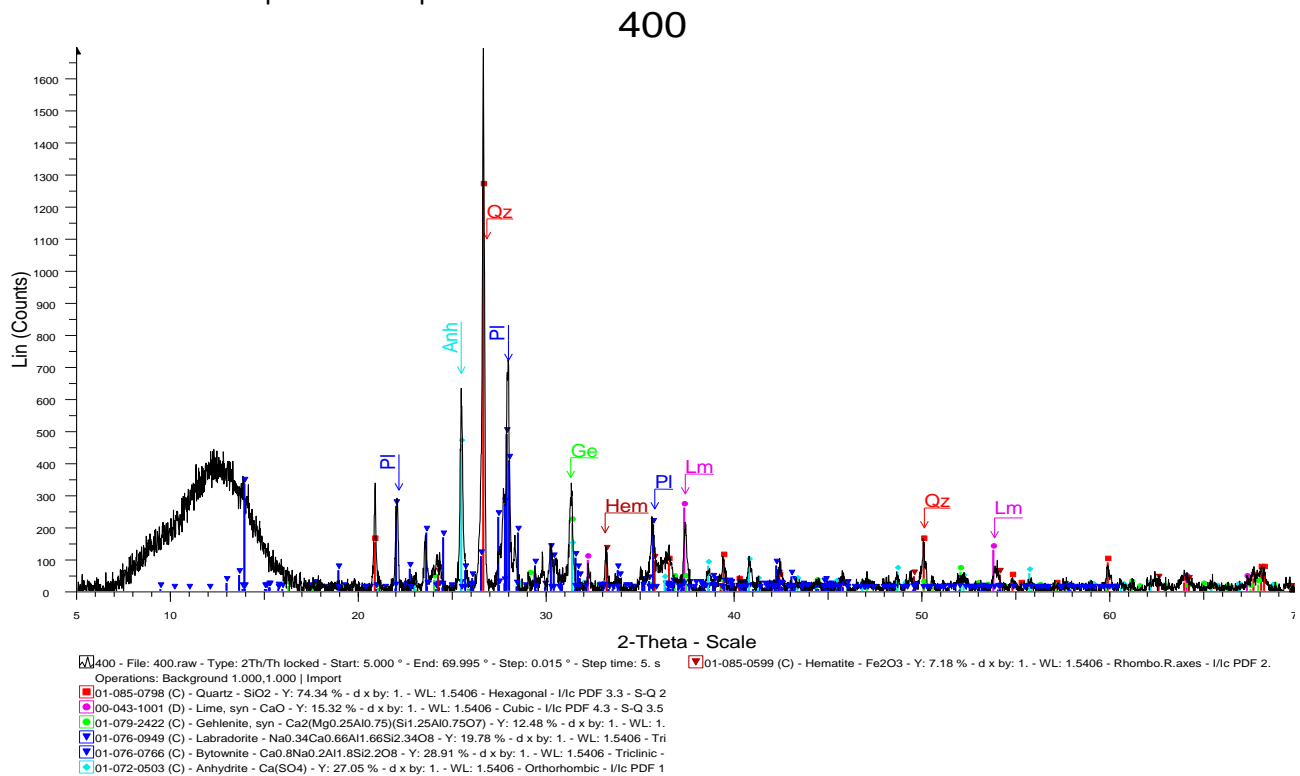


Figure 2. XRD Analysis for the -400 Mesh size fraction.

Table 1. Size and magnetic separation results.

Size Fraction	REY Conc. (ppm)	E.F.	Recovery (%)	Critical (%)
+50 Mesh	254.95	1.001	4.07	34.22
50-120 Mesh	257.90	1.013	14.59	34.63
120-200 Mesh	256.27	1.006	14.17	35.71
200-325 Mesh	255.82	1.005	18.24	36.57
325-400 Mesh	242.04	0.951	11.31	36.61
-400 Mesh (↓)	247.21	0.971	37.62	36.89



Fraction/M. Flow	REY Conc. (ppm)	E.F.	Recovery (%)	Critical (%)
Magn. 8420 G.	273.86	1.108	52.36	37.40
Non-Magn. 8420 G.	227.70	0.921	47.64	38.04
Magn. 4200 G.	283.99	1.149	45.77	36.98
Non-Magn. 4200 G.	225.22	0.911	54.23	38.49

The weight percentage along with the REY content of every fraction is presented in fig. 3. The finer particle size fraction (-400 Mesh) is predominant in the PPC Meliti CFA (38.2 %), while almost 60% of the overall particles are smaller than 200 Mesh. It can be seen that REY content does not significantly change throughout all size fractions. The effect of size separation on the REY recovery and the enrichment factor is depicted in fig. 4. REY recovery follows the trend of the REY content of fig. 3, as expected, with approximately 38% of the material resulting in the -400 Mesh fraction. Enrichment, similarly to REY content, is almost identical in all fractions. It can be inferred that size separation does not significantly affect REY content. The REY content and consequently the enrichment factor is almost equal in all the fractions, with its values ranging from 0.951 (in the 325-400 M fraction) to 1.013 (in the 50-120 M fraction). REY recovery in the -400 Mesh fraction is significantly increased to 37.62% as a result of the fact that almost 40% of the material resides in that fraction since $REY\ recovery\ (\%) = EF \times Weight\ (\%)$ and the EF is approximately 1, in all cases. Note also that the Critical (%) increases monotonically as the particle size is decreased (Table 1).

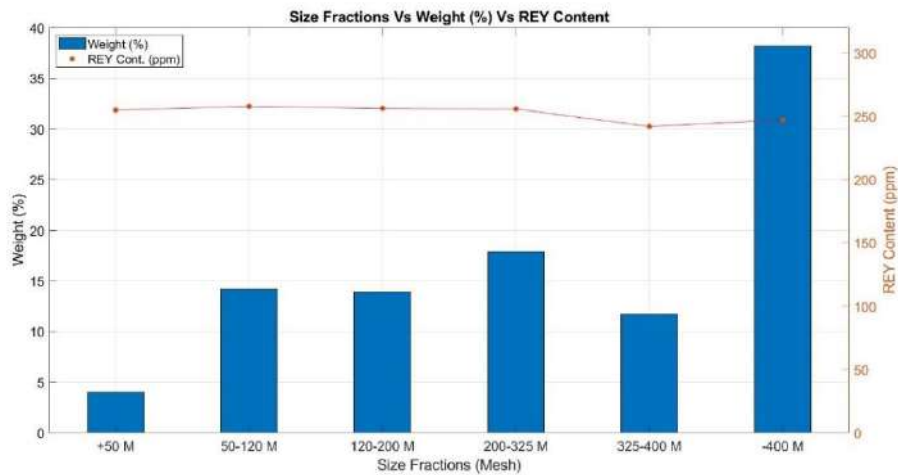


Figure 3. REY content and weight (%) distribution of the various sizes fractions.

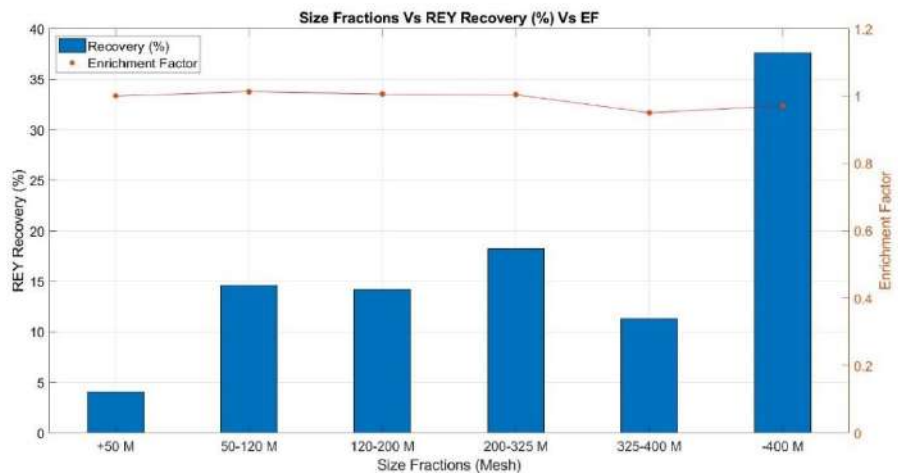


Figure 4. Enrichment factor and REY recovery (%) of the various sizes fractions.

The weight (%) along with the REY content of the magnetic and non-magnetic fractions for the -400 Mesh fraction is presented in fig. 5 while the effect of magnetic separation on enrichment factor and REY recovery (%) is shown in fig.6.

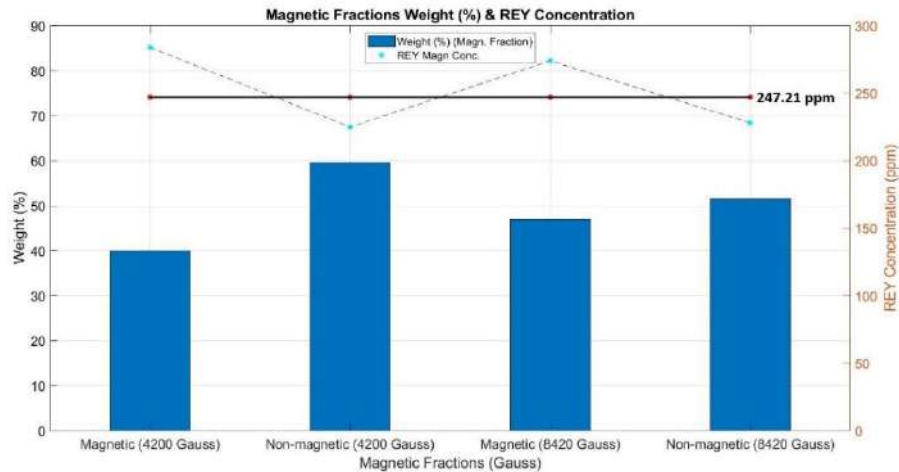


Figure 5. REY content and weight (%) distribution of the magnetic separation products.

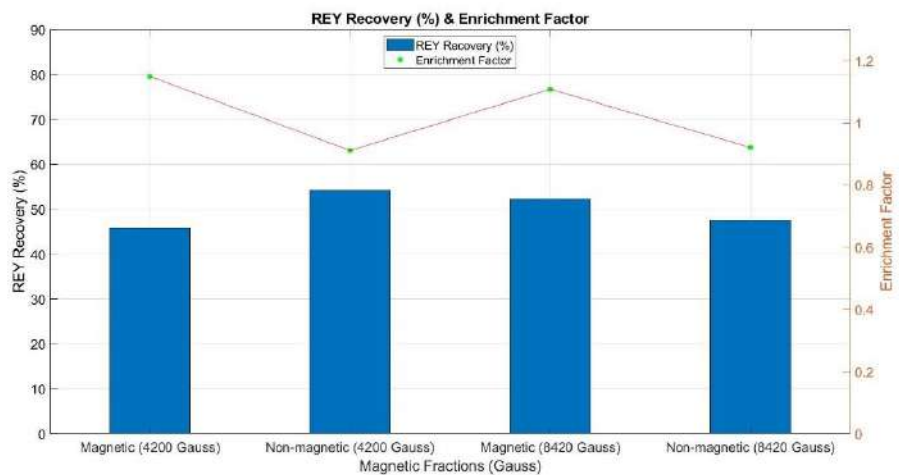


Figure 6. Enrichment factor and REY recovery (%) of the magnetic separation products.

It can be seen that, that magnetic separation results in an increase of REY concentration in the magnetic fractions of the process. In addition, the Critical (%) in all fractions (magnetic and non-magnetic) is increased, compared to the -400 Mesh feed material. This result contradicts some previous studies (Lin et al., 2017; Rosita et al., 2020), where the non-magnetic products were more enriched in REY content, but is in agreement with the findings by Honaker et al. (2015), who observed higher REY contents in the magnetic fractions in all their coal and coal by-products used in their study. These contradicted results are probably due to effect of the differences in the origin and geological background of the source materials that modify the preferential affinity of REY during a magnetic separation process. However, most of these metals are paramagnetic in room temperature (Liu, 1960), and thus, REY content should be higher in the magnetic than the non-magnetic fractions as it is observed here (Suganal, 2018).

4. CONCLUSIONS

Fly and bottom ash samples from the active thermal power plant of PPC Meliti, Florina were evaluated as potential REY sources. Coal fly ash contained higher concentrations of REY than bottom fly ash and thus, it was selected for further beneficiation. It was found that size separation did not significantly affect REY content in a specific size fraction. Almost 40% of the material resulted in the finest fraction (-400 Mesh) which resulted in a 37.62% recovery in that fraction. The Critical REY (%) was also found highest in that size fraction. Magnetic separation was subsequently implemented, with the -400 Mesh fraction as the feed material, at two different magnetic fluxes (4200 Gauss & 8420 Gauss). It was found that REY concentration was increased in the magnetic fractions for both flows. The 4200 G magnetic fraction showed the highest REY content (283.99 ppm), but REY recovery (%) was relatively low (45.77 %) since the majority of the feed material ended up in the non-magnetic fraction. A promising combination of both high REY content and recovery was found



in the 8420 G. flow, with the REY content at 273.86 ppm and recovery at 52.36 %. The Critical (%) for all the fractions of the process was increased compared to that of the -400 Mesh feed material. Future work will examine the effect of density separation by means of Sodium Polytungstate on REY enrichment. This will be complemented with selective oil agglomeration (SOA) of the coarser fraction that contains the highest amount of organic carbon.

5. ACKNOWLEDGEMENTS

The authors are indebted to Prof. K. Komnitsas and his team at the School of Mineral Resources Engineering, Technical University of Crete, for their contribution in the magnetic separation experiments.

REFERENCES

- “ASTM C618 - 12a Standard Specification for Coal Fly Ash and Raw or Calcined Natural Pozzolan for Use in Concrete.” <https://www.astm.org/DATABASE.CART/HISTORICAL/C618-12A.htm> (accessed Jun. 05, 2021).
- Bartoňová, L., 2015. Unburned carbon from coal combustion ash: An overview. *Fuel Processing Technology*, 134, 136–158.
- Blissett, R. S., Smalley, N. and Rowson, N. A., 2014. An investigation into six coal fly ashes from the United Kingdom and Poland to evaluate rare earth element content. *Fuel*, 119, 236–239.
- Dai, S., Xie, P., Jia, S., Ward, C. R., Hower, J. C., Yan, X. and French, D., 2017. Enrichment of U-Re-V-Cr-Se and rare earth elements in the Late Permian coals of the Moxinpo Coalfield, Chongqing, China: Genetic implications from geochemical and mineralogical data. *Ore Geology Reviews*, 80, 1–17.
- Lin, R., Howard, B. H., Roth, E. A., Bank, T. L., Granite, E. J. and Soong, Y., 2017. Enrichment of rare earth elements from coal and coal by-products by physical separations. *Fuel*, 200, 506–520.
- Liu, S. H.-p., 1960. MAGNETIC PROPERTIES OF RARE EARTH METALS. *PhD Dissertation*, Iowa State University Of Science and Technology Ames, Iowa.
- Honaker, R., Hower, J., Eble, C., Weisenfluh, J., Groppo, J., Rezaee, M. and Bhagavatula, A., 2015. Laboratory and Bench-Scale Testing for Rare Earth Elements. *Leonardo Technologies, Inc.*, Contractor to the U.S. Department of Energy National Energy Technology Laboratory, 626 Cochran Mill Road Pittsburgh, PA 15236.
- Rosita, W., Bendiyasa, I. M., Perdana, I. and Anggara, F., 2020. Sequential particle-size and magnetic separation for enrichment of rare-earth elements and yttrium in Indonesia coal fly ash. *Journal of Environmental Chemical Engineering*, 8(1), 103575.
- Seredin, V. v. and Dai, S., 2012. Coal deposits as potential alternative sources for lanthanides and yttrium. *International Journal of Coal Geology*, 94, 67–93.
- Simoni, M., Kuhn, E. P., Morf, L. S., Kuendig, R. and Adam, F., 2015. Urban mining as a contribution to the resource strategy of the Canton of Zurich. *Waste Management*, 45, 10–21.
- Suganal, S., 2018. Rare earth elements enrichment of fixed-bed coal ash from a pilot plant gasification by physical methods. *Indonesian Mining Journal*, 21(2), 113–125.
- Wang, S., Ma, Q. and Zhu, Z. H., 2009. Characteristics of unburned carbons and their application for humic acid removal from water. *Fuel Processing Technology*, 90(3), 375–380.



Crocin as an eco-friendly corrosion inhibitor for aluminum alloys in NaCl solution

P. Pantazopoulou¹, S. Theohari² and S. Kalogeropoulou¹

¹ Department of Electrical and Electronic Engineering, University of West Attica, Athens, Greece

² Graphic Design and Visual Communication Department, University of West Attica, Athens, Greece

Corresponding author email: parpant@uniwa.gr

ABSTRACT

Corrosion of metals has proved to be a very serious problem, leading to consumption of natural resources, energy and materials, and impeding sustainable development, especially in the fields of environment and economy. Although aluminum and aluminum alloys are protected via the natural inert oxide film formed on their surface, they are susceptible to corrosion in acidic, alkaline, and chloride-containing solutions. The necessity of the protection of aluminum and its alloys against corrosion in aggressive environments has led to a quest of new and proper inhibitors, which are effective and simultaneously eco-friendly, non-toxic and do not endanger life and the environment. This experimental research investigates the possibility of the use of a natural organic substance from the Greek plant *Crocus sativus*, Crocin, against the corrosion of four aluminum alloys in an aggressive chloride ions environment of 0.01 M NaCl. Corrosion resistance of aluminum alloy specimens in Crocin-containing solution was evaluated by the investigation of their electrochemical performance using potentiodynamic corrosion techniques, and mass loss measurements. Observation and analysis of the morphology of the surface of the specimens, before and after the corrosion measurements, was performed using Scanning Electron Microscopy, Stereomicroscopy and Glossiness measurements. Findings acquired from all experimental methods indicate that Crocin largely functions protectively against corrosion of all specimens in the corrosive environment.

Keywords: aluminum corrosion; sodium chloride environment; eco-friendly inhibitors; Crocin; electrochemical and gravimetric methods.

1. INTRODUCTION

Aluminum is a multipurpose, cost-effective, and durable metallic material with numerous applications. It is alloyed in order to ameliorate its properties, such as hardness, strength, and resistance to wear. Aluminum alloys are broadly used in the automotive and aerospace industry, as construction materials, in production of machines and appliances, etc. The 5xxx and 6xxx aluminum alloys are usually utilized in marine applications, because they present low density and good mechanical properties and corrosion behavior (Davis, 2001).

Aluminum possesses outstanding corrosion resistance owing to a colorless and transparent protective oxide film - created in air at ambient temperature - that is attached firmly to its surface. If the natural surface film of only about 5 nm is impaired, then it reforms instantaneously in non-aggressive environments and carries on protecting aluminum against corrosion. As soon as this film is detached or destroyed in acidic, alkaline, and chloride-containing solutions, where self-repair cannot follow, corrosion occurs (Davis, 2001; Ma, 2012; Natishan and O'Grady, 2014; Xhanari et al., 2017).

Commercial pure aluminum alloy (1xxx) is more corrosion resistant than any of the aluminum alloys. The Al-Mg alloys (5xxx) exhibit moderate resistance against uniform and localized corrosion in chloride-containing solutions. The Al-Si-Mg alloys (6xxx) present less resistance to pitting corrosion (Davis, 2001; Ezuber et al., 2008).

Corrosion inhibition of aluminum and its alloys is crucial for economic and environmental reasons and conservation of natural resources, energy and materials. Various organic substances have been used as inhibitors, but many of them are toxic with hazardous effects on life and the environment. Therefore, there is a global effort for the discovery of new green corrosion inhibitors, which are environmentally friendly, cost-effective, with minimum health and safety impacts, and can be produced from renewable resources. Many studies have focused on plant extracts, whose main constituents belong to a broad range of organic compounds, including polyphenols, terpenes, carboxylic acids and alkaloids (Badawi and Fahim, 2021; Verma



et al., 2021). Many of these substances contain phosphorus, nitrogen, sulphur, oxygen atoms and multiple bonds in their molecules, which function as bonding centers for their adsorption on the surface of aluminum materials (Amitha Rani and Basu, 2012; Byrne et al., 2022; Khanari et al., 2017).

Within the research for eco-friendly inhibitors, Crocin, a natural organic substance from the Greek plant *Crocus sativus* (saffron), is examined against corrosion of AA 1050, 5083, 5754 and 6082 aluminum alloys in a highly corrosive environment such as sodium chloride solution (Pantazopoulou et al., 2021). Crocin is water-soluble carotenoid forming an orange-colored solution with protective antioxidant function (Bathai et al., 2014; Cerdá-Bernad et al., 2020; Rahaiee et al., 2015; Soror, 2013). Its anti-corrosive behavior is attributed to the extended pi-electron conjugated system in the main chain of its molecule whereas the sugar moiety of its molecule is assumed to play a key beneficial role too, although it does not contribute to the conjugation system (Akhtari et al., 2013).

Linear and Tafel polarization, mass loss measurements, Scanning Electron Microscopy, Stereomicroscopy and Glossiness measurements were used for the study of the effectiveness of Crocin against corrosion of aluminum alloys in NaCl solution.

2. MATERIALS AND METHODS

Specimens of aluminum alloys with %wt composition as displayed in Table 1 were tested. The corrosive environment was either a solution of 0.01M NaCl p.a. (reference solution) or a solution of 0.01M NaCl with 1.25mM Crocin (inhibiting solution). Crocin or 8,8-diapo-8,8-carotenoid acid ($C_{44}H_{64}O_{24}$) was supplied from Sigma-Aldrich. 1.25mM concentration of Crocin was used, as it was proved in a previous experimental work that it offered significant protection against corrosion of 1050 aluminum alloy in sodium chloride environment (Pantazopoulou et al., 2021).

Table 1. Composition (%wt) of aluminum and aluminum alloys.

Type	Si	Fe	Mn	Mg	Cu	Ti	Cr	Zn	Al
1050	0.168	0.245	0.003	0.001	0.001	0.006	0.002	0.013	balanced
5083	0.133	0.318	0.523	4.698	0.061	0.015	0.061	0.117	balanced
5754	0.125	0.273	0.142	2.939	0.017	0.014	0.052	0.008	balanced
6082	0.900	0.430	0.460	0.800	0.080	0.030	0.020	0.050	balanced

Linear and Tafel Polarization measurements were performed by a Gamry Interface 1000 and DC105 Corrosion Software. The reference electrode (RE) was Ag/AgCl, the counter electrode (CE) was Pt and the working electrode (WE) was the aluminum alloys specimens with a 1 cm² surface area in contact with the electrolyte. Open Circuit Potential (OCP) was recorded for 60 min until an almost steady value was reached. Linear Polarization scan was carried out at a potential range of ± 0.02 V vs. OCP and a scan rate of 0.125 mV/s whereas Tafel Scan was performed at a potential range of -0.250 V to +0.400 V vs. OCP and a scan rate of 0.166 mV/s.

The inhibition efficiency of Crocin was calculated from corrosion currents derived from Tafel curves by the equation:

$$IE (\%) = [(I_{\text{corr,R}} - I_{\text{corr,I}}) / I_{\text{corr,R}}] \times 100 \quad (1)$$

where $I_{\text{corr,R}}$ and $I_{\text{corr,I}}$ are the corrosion currents in the reference and inhibiting solutions, respectively.

Mass loss of aluminum alloys samples was measured weekly for a total immersion period of 13 weeks in the test solutions at room temperature. Prior to weighing specimens were descaled in HNO_3 according to ISO 8407 standard.

Inhibition efficiency of Crocin was also calculated from mass loss measurements using the equation:

$$IE (\%) = [(\Delta m_{\text{corr,R}} - \Delta m_{\text{corr,I}}) / \Delta m_{\text{corr,R}}] \times 100 \quad (2)$$

where $\Delta m_{\text{corr,R}}$ and $\Delta m_{\text{corr,I}}$ are the mass loss values in the reference and inhibiting solutions, respectively.

Observation and analysis of the specimens' surface were carried out by Stereomicroscopy via an Olympus SZ61 Stereo Microscope equipped with a camera (Image Pro Plus - Infinity Capture) and by Scanning Electron Microscopy (SEM) equipped with Energy Dispersive Spectroscopy (EDS) (JEOL JSM-6510 LV - EDAX / Oxford Instruments).



Moreover, the surface gloss of the specimens was measured using a TG 60/268 Lovibond gloss meter and GQC6 Quality Control Software, according to ISO 7668 standard. The gloss meter determines the intensity of light reflected from the aluminum alloy surface at three measurement angles of 20°, 60° and 85°, giving information on the status of the surface.

3. RESULTS AND DISCUSSION

Tafel potentiodynamic polarization curves for all aluminum alloys specimens in contact with reference and inhibiting solutions are presented in Figure 1, where overpotential (η) - calculated as the difference between the potential (E) and the corrosion potential (E_{corr}) - is given as a function of current (I). It is observed that in the absence of Crocin the corrosion potentials coincide with the pitting potentials with the exception of the 1050 alloy, indicating an extended corrosion of the surfaces of these alloys in the sodium chloride solution. Instead, in the inhibiting solution a separation of these values is visible in all cases. Moreover, the current has lower values both in cathodic and anodic areas than in the reference solution for all the aluminum alloys, which means that Crocin acts as a mixed type inhibitor. This is indicative of a protective film formation on the specimens via adsorption of Crocin on the surfaces through the hydroxyl groups of the extreme glucose rings of its molecules. Thus, Crocin blocks the access of chloride ions by covering a large part of the Al and Al_2O_3 surfaces available for corrosion reactions.

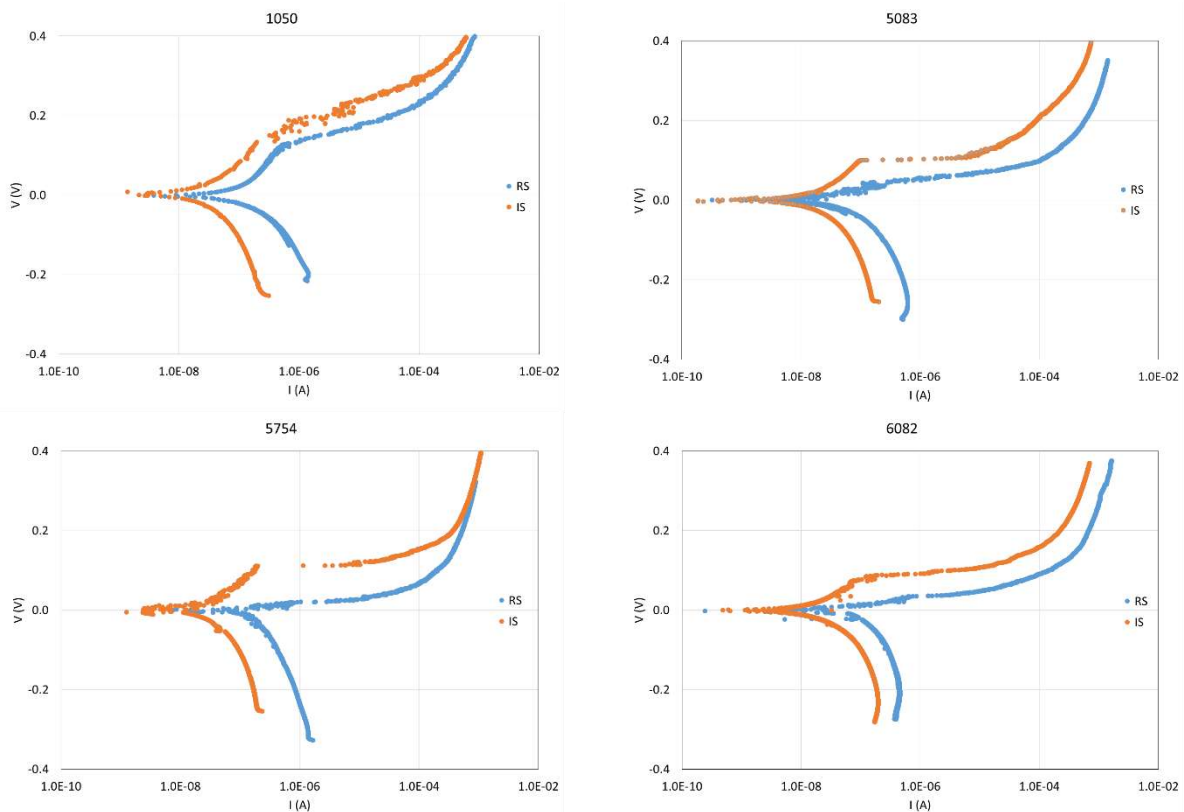


Figure 1. Tafel Polarization curves for aluminum alloy test specimens immersed in the reference (RS) and the inhibiting solutions (IS).

The inhibition efficiency (IE) of Crocin calculated from corrosion currents is presented in Figure 2. All values are high, varying from 80% to 93%, which confirm the protecting action of Crocin against corrosion for all the aluminum alloys.

Mass loss tests also proved the positive influence of Crocin, as it can be observed by the weight loss of specimens vs. immersion time in the reference and inhibiting solutions given in Figure 3, from which IE values between 80 and 95% are derived. It is noticeable that for the 5083 specimens the protective performance of Crocin was more pronounced than for the others. This is attributed to the higher tendency of this alloy for corrosion, due to its elevated content of Mg, in the reference solution which is significantly reduced by the presence of Crocin.

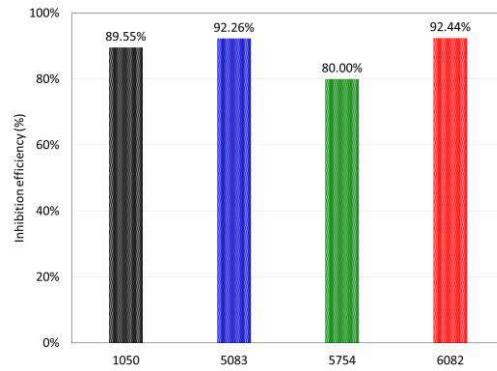


Figure 2. Inhibition efficiency of Crocin for aluminum alloy specimens obtained from corrosion currents.

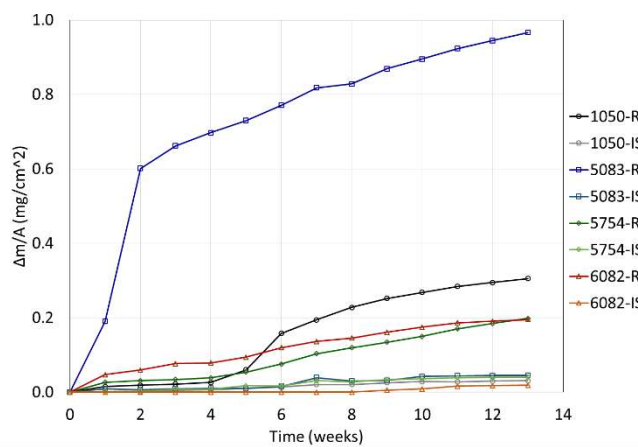


Figure 3. Mass loss of the specimens vs. immersion time.

Observation of the surfaces of specimens immersed in the reference and the inhibiting solutions for 13 weeks performed by SEM, revealed less corroded surfaces, without any signs of localized pitting corrosion in the presence of Crocin, as shown in micrographs of Figure 4.

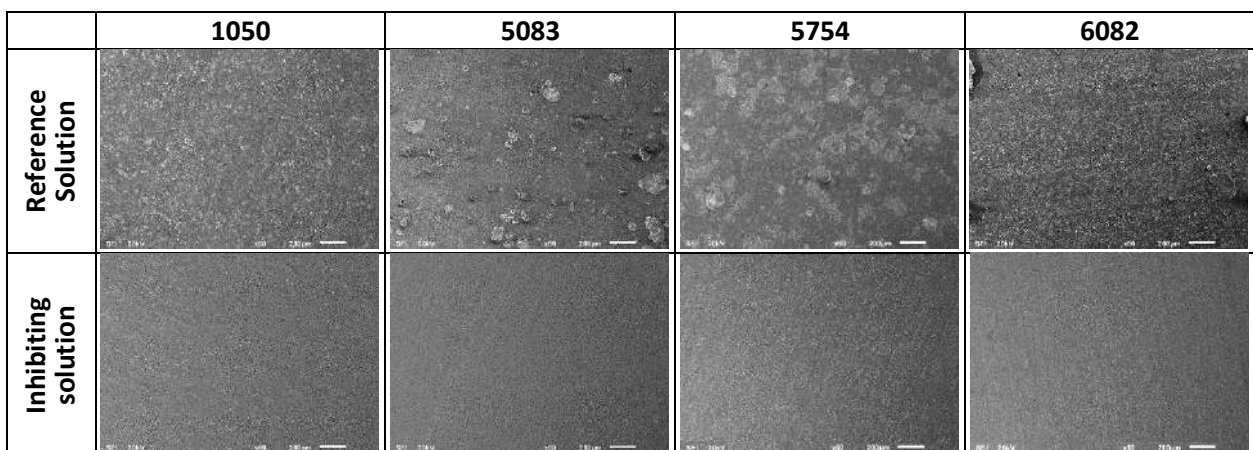


Figure 4. SEM micrographs (X60) of specimens' surfaces after immersion in test solutions for 13 weeks.

Elemental analysis by EDS showed that the surfaces of all samples immersed in the reference solution had Al/O weight ratios lower than those before their exposure to the testing solution, indicating the existence of corrosion products rich in O on them. Moreover, a depletion of the alloying elements (Fe, Mg, and Mn) in the case of the 5083, 5754 and 6082 alloys was found. On the contrary, the surfaces of the samples immersed in



the Crocin containing solution had similar chemical composition with the initial uncorroded surfaces of the alloys. These results validate the favorable influence of Crocin as corrosion inhibitor and confirm the findings of the electrochemical corrosion tests and mass loss measurements. Additionally, even in the case where pitting corrosion has initiated, the intense presence of Crocin detected on defects of the specimens' surface by Stereomicroscopy (Figure 5) indicates that Crocin impedes the further progress of corrosion.



Figure 5. Crocin adsorbed on surface defects of 1050 specimen after immersion in the inhibiting solution for 13 weeks, as observed by Stereomicroscopy.

Finally, additional evaluation of the aluminum alloys surface after immersion in the reference and the inhibiting solutions for 13 weeks was performed by glossiness measurements (Figure 6). A pronounced difference in Glossiness Units (GU) values between the specimens immersed in Crocin solution and the ones in the reference solution is observed. In the presence of Crocin the specimens' surface reflects the major part of the incident light presenting shiny appearance. In the reference solution, lower GU values are due to an increased scattering of light on the surfaces, producing a matt appearance, which indicates the presence of corrosion products (oxides and hydroxides) and defects on the surfaces.

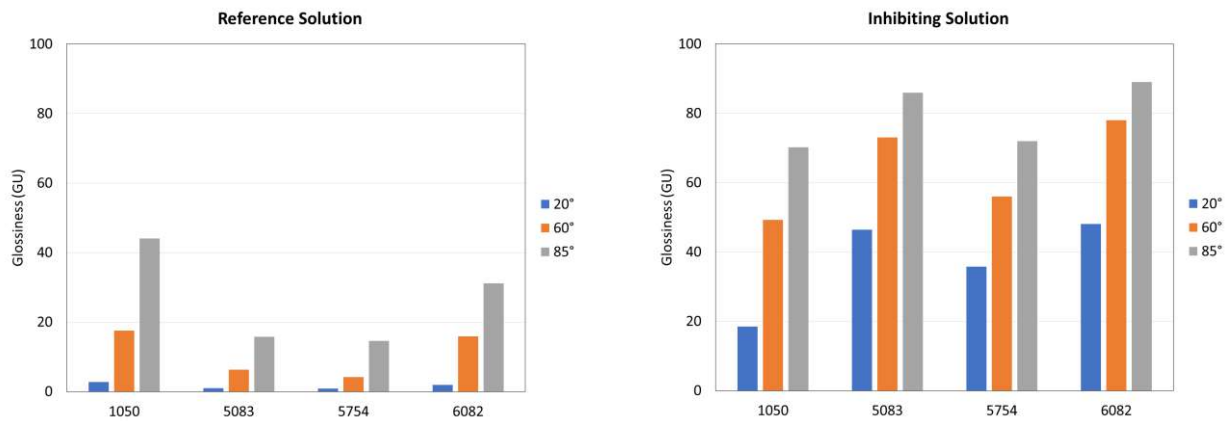


Figure 6. Glossiness of aluminum alloys after immersion in the test solutions for 13 weeks.

4. CONCLUSIONS

This study evidences the effectiveness of Crocin as an eco-friendly corrosion inhibitor for aluminum alloys in the NaCl corroding environment. Crocin was found to retard the dissolution of the natural protective aluminum oxide layer, obstruct pitting corrosion and reduce the formation of corrosion products. Particularly:

- Electrochemical measurements showed that Crocin acts as a mixed type inhibitor for the corrosion of the 1050, 5083, 5754 and 6082 aluminum alloys in the 0.01 M NaCl solution, as both the anodic and cathodic currents are decreased in the inhibiting solution.
- The inhibition efficiency of Crocin calculated from corrosion currents and mass loss measurements is high, varying from 80% to 95%.
- Observation and analysis of the alloys surface performed by SEM and EDS revealed less corroded surfaces, without any signs of localized pitting corrosion, in the presence of Crocin.



- Glossiness measurements confirmed the positive influence of Crocin, as the alloys surfaces had more shiny appearance after exposure in the inhibiting solution than in the reference solution.
- Inhibiting action of Crocin is attributed to a protective film formation on the specimens via adsorption of its molecules through the hydroxyl groups of their extreme glycoside rings. Crocin blocks the access of chloride ions by covering a large part of the Al and Al₂O₃ surfaces available for corrosion reactions.
- Even in the case where pitting corrosion initiates, Crocin is adsorbed preferentially on the defects of the specimens' surface indicating that it impedes the further progress of corrosion.

5. ACKNOWLEDGEMENTS

This research is co-financed by Greece and the European Union (European Social Fund- ESF) through the Operational Programme «Human Resources Development, Education and Lifelong Learning» in the context of the project “Reinforcement of Postdoctoral Researchers - 2nd Cycle” (MIS-5033021), implemented by the State Scholarships Foundation (IKY).



REFERENCES

- Akhari, K., Hassanzadeh, K., Fakhraei, B., Fakhraei, N., Hassanzadeh, H., Zarei, S.A. 2013. A density functional theory study of the reactivity descriptors and antioxidant behavior of Crocin. *Comput. Theor. Chem.*, 1013, 123-129.
- Amitha Rani, B.E., Basu, B.B.J., 2012. Green Inhibitors for Corrosion Protection of Metals and Alloys: An Overview. *Int. J. Corros.*, 380217.
- Badawi, A.K. and Fahim, I.S., 2021. A critical review on green corrosion inhibitors based on plant extracts: Advances and potential presence in the market. *Int. J. Corros. Scale Inhib.*, 10, 1385–1406.
- Bathaie, S.Z., Farajzade, A., Hoshyar, R. 2014. A review of the chemistry and uses of crocins and crocetin, the carotenoid natural dyes in saffron, with particular emphasis on applications as colorants including their use as biological stains. *Biotech Histochem.*, 89(6), 401-411.
- Byrne, C.E., D’Alessandro, O., Deyá, C., 2022. Tara Tannins as a Green Sustainable Corrosion Inhibitor for Aluminum, *J. Mater. Eng. Perform.*, 31, 2918-2933.
- Cerdá-Bernad, D., Valero-Cases, E., Pastor, J.J., Frutos, M.J., 2020. Saffron bioactives crocin, crocetin and safranal: effect on oxidative stress and mechanisms of action. *Crit. Rev. Food Sci. Nutr.*, 62(12), 3232-3249.
- Davis, J.R., 2001. Alloying: Understanding the Basics, *ASM International*, 351-416.
- Ezuber, H., El-Houd, A., El-Shawesh, F., 2008. A study on the corrosion behavior of aluminum alloys in seawater. *Materials and Design*, 29, 801–805.
- Ma, F.Y., 2012. Corrosive Effects of Chlorides on Metals. *Pitting Corrosion*. Intech., 139.
- Natishan, P.M. and O’Grady, W.E., 2014. Chloride Ion Interactions with Oxide-Covered Aluminum Leading to Pitting Corrosion: A Review. *J. Electrochem. Soc.*, 161, C421-C432.
- Pantazopoulou, P., Theohari, S., Kalogeropoulou, S., 2021. Organic dyes as corrosion inhibitors of commercial AA1050 aluminum alloy in sodium chloride environment. *MATEC Web of Conference* 349, 02017, ICEAF-VI 2021.
- Rahaiee, S., Moini, S., Hashemi, M., Shojaosadati, S.A., 2015. Evaluation of antioxidant activities of bioactive compounds and various extracts obtained from saffron (*Crocus sativus* L.): a review. *J. Food Sci. Technol.*, 52(4), 1881–1888.
- Soror, T.Y., 2013. Saffron extracts as environmentally safe corrosion inhibitors for aluminium dissolution in 2M HCl solution. *Eur. Chem. Bull.*, 2(4), 191-196.
- Verma, C., Ebenso, E., Quraishi, M.A., Hussain, C.M., 2021. Recent developments in sustainable corrosion inhibitors: design, performance and industrial scale applications. *Mater. Adv.*, 2, 3806-3850.
- Xhanari, K., Finšgar, M., Hrnčič, M.K., Maver, U., Knez, Z., Seiti, B., 2017. Green corrosion inhibitors for aluminium and its alloys: a review. *RSC Adv.*, 7, 27299-27330.



Investigation of the processes occurring in water of acid mine drainage during their exposure

S. Hayrapetyan¹, M.Chobanyan¹, V. Hovhannisyan¹, A. Kirakosyan², A. Sukiasyan² and P. Gikas³

¹ Faculty of Chemistry of Yerevan State University, Yerevan, Armenia

²Chair General chemistry and chemical technology, National Polytechnic University of Armenia, Yerevan, Armenia

³Technical University of Crete, School of Chemical and Environmental Engineering, Chania, Greece

Corresponding author email: sukiasyan.astghik@gmail.com

ABSTRACT

The most actual environmental problem currently faced by the coal and metal mining industry is acid mine drainage. The aim of the article is to study a number of physicochemical properties of the acid mine drainage waters, which will serve as a basis for the development of new competitive approaches to their purification. Using inductively coupled plasma-optical emission spectrometry and pH-measurement processes occurring in the acid mine drainage waters under their long-term exposure under normal conditions were investigated. The drainage water of 10-days' exposure in the laboratory was studied. As a result of the oxidation of divalent iron into trivalent iron in the acid mine drainage waters the precipitation of iron as $\text{Fe}(\text{OH})_3$. Direct contact of water with atmospheric oxygen after the outlet initiated the oxidation process. In order to restore the true picture of the content of metal cations and sulfate ions, we analyzed both the water and the sediment, which was formed during water sedimentation. It has been reliably established that as the pH decreases, the turbidity of the source water increases, which has a linear character. The main, but not the only, component of the precipitate is $\text{Fe}(\text{OH})_3$, while its share in terms of Fe^{3+} is 64.01 wt %. But if calcium precipitates in the form of insoluble sulfates, then in the case of other metals, precipitation occurs with iron hydroxide in adsorbed form. In the case of the transition of sodium and magnesium to the precipitate, they are precipitated with iron hydroxide in adsorbed form. There is also a transition to the precipitate of sulfate ions. The gypsum nature of sulfate ions in the sediment is about 1/3 of the total sulfur content in the sediment. The rest of the sulfate ions are precipitated with iron hydroxide in adsorbed form.

Keywords: acid mine drainage; metals; total suspended solid; pH.

1. INTRODUCTION

Acid rock drainage (ARD) is a natural process that occurs when sulfur-containing compounds in rocks are exposed to air and water. In the context of mining operations, sulfur-bearing rocks are exposed during open-pit or underground mining was caused by acid mine drainage (AMD). The management, storage, and processing of the mine-impacted waters is a serious environmental problem in all mining areas (Blowes et al., 2003). The process produces acidic waters by oxidizing the minerals pyrite (FeS_2) and pyrotite (FeS) and other sulfur-containing compounds to form sulfuric acid. Typically, the pH of acidic water is between 2.1 and 3.5, which encourages leaching metals from the rock and soil in contact with them. The AMD waters (AMDW) are high iron content, and sulfate promotes the oxidation of sulfur minerals associated with metals such as As, Cd, Co, Cu, Pb, and Zn. The bacterially catalyzed oxidation of pyrite is particularly common in coal mining operations and usually results in low-pH water polluted with toxic metals and sulfate. Although high sulfate concentrations can be reduced by gypsum precipitation, removing lower concentrations (below 1200 mg/L) remains a challenge (Gupta and Ali, 2012; Guimaraes and Leao, 2014; Vecino et al., 2021). On the other hand, AMD is one of the most serious environmental problems currently faced by the coal and metal mining industry. For example, the formation of drainage with low pH increases the dissolution of heavy metals (HMs) in water (Sountharajah et al., 2015). HMs pollution has become one of the most serious environmental problems today. The treatment of HMs is of special concern due to their recalcitrance and persistence in the environment. In recent years, various methods for HMs removal



from wastewater have been extensively studied. These technologies include chemical precipitation, ion exchange, adsorption, membrane filtration, coagulation-flocculation, flotation, and electrochemical methods (Vecino et al., 2021; Fu and Wang, 2011). In addition, the concentration of HMs in groundwater can be controlled mainly by pH (Glover-Kerkvilet, 1995).

Today, many countries have laws and regulations governing the treatment of wastewater before it enters water bodies. Of particular note in this context is the widespread integration of treatment methods to remove pollutants from wastewater (Chen, 2012). Among these, adsorbent filtration has been widely used as an effective treatment strategy for removing organic and inorganic pollutants from stormwater (Glover-Kerkvilet, 1995; Roesner and Charles, 1996). Of course, stormwater runoff can also acidify and contaminate soils near mining areas and in floodplains (Lottermoser, 2011). The mining industry is a major producer of AMD systems, with both active and abandoned mines affected. Of all the pollutants in runoff, AMD is perhaps one of the most serious because of its nature, scale, and recovery complexity (Fu and Wang, 2011; Strosnider et al., 2015). Therefore, AMDW treatment is necessary in the first place to prevent large-scale surface water pollution. Obviously, a fundamental study of AMDW properties is a necessary need to select the most appropriate technological approach for their processing and treatment. There is a great variety of AMD, and each type of AMD requires an individual approach. Among the currently available approaches, the most popular is alkaline neutralization, which uses lime to remove sulfates from the aqueous medium (Johnson, 2005; Akcil and Koldas, 2006). The use of alkaline materials is associated with expensive technologies. Of particular technological interest is the development of new processes based on the use of precipitated calcium carbonate and lime pretreatment to neutralize AMDW and partial desalination (Kurniawan, 2006). Wastewater treatment methods based on sorption processes are also being developed (Scherrenberg et al., 2008; Goldberg, 2002). Based on flocculation and coagulation, they mainly focus on the physicochemical properties of colloidal suspensions, and the effectiveness of the treatment depends mainly on the reaction dynamics between colloidal suspensions and coagulants (Sincero and Sincero, 2003; McCurdy et al., 2004).

In view of the above, and considering that the recovery processes of many dangerous ecological deviations promoted all over the world seek to build a sustainable ecological reality, the aim of our work is to study a number of physical and chemical properties of AMDW, which will serve as a basis for developing new competitive approaches to their purification.

2. MATERIALS AND METHODS

2.1. Process of preparation and separation of drainage water

The drainage water of ten days in the laboratory was investigated. During this period a certain amount of ions precipitated in water. To determine the content of the precipitate formed, after careful shaking, a suspension of the said precipitate was taken into a uterine solution of 500 ml. Then, after complete sedimentation, the sediment is first decanted and then filtered. The sediment from the surface of the filter paper is washed with distilled water, 15 ml of hydrochloric acid is added to the resulting suspension, as a result of which the suspended particles are completely dissolved, and then the volume of the resulting solution is brought to the mark (50 ml) with distilled water. Before analysis by optical emission spectroscopy (ICP-OES, Perkin Elmer Optima DV 7000, USA) the samples were filtered (0.2 μm) and acidified with 2% HNO_3 .

2.2. Reagents

Hydrochloric acid (30% (v/v)) was used to dissolve the sediment that formed after 10 days in the drain water. Nitric acid (62 % (v/v)) was used to oxidize the samples prior to analysis. All chemicals were analytical grade reagents and were supplied by Panreac. Distilled water was used to adjust sample volumes.

2.3. Chemical compounds of acid mine drainage water

The water samples sampled came from an open pit mine and were obtained from polymetallic sulfide processing. The results on determining the chemical composition were summarized in Table 1. So, the major elements in the mine water were calcium, followed by magnesium, aluminum, manganese, iron, and zinc. In addition, other metals (such as copper, tungsten, cobalt, and nickel) were also present in minor concentrations. The pH of the sample was 3.4 ± 0.1 , measured with a pH / Ion 340i meter (Weilheim 2004, WTW GmbH) was used to measure pH, given that the main acid present in the sample was sulfuric acid.

2.4. Assessment of water quantity and sludge composition



Experiments were conducted to evaluate the amount and composition of sludge as a function of water exposure as a function of pH. Batch experiments were performed by sampling and measuring pH. The following pH range (with 1 M H₂SO₄, adjusted if necessary) was used for the study: 1.0, 1.5, 2.0, 2.5, 3.0, 4.0 and 5.0. Each solution was equilibrated by stirring for 2 h at room temperature (23 ± 1°C) to reach equilibrium. The pH value was monitored and corrected every 30 min by taking up to 1 mL fraction of each solution. It was measured with a pH/Ion 340i Meter used for pH measurement (Weilheim 2004, WTW GmbH) and corrected to the initial value by stirring for 2 h. The final solutions were then analyzed by ICP-OES (Perkin Elmer Optima DV 7000, USA). To increase the accuracy of the results, up to five repeated experiments were performed. Experimental data are presented as the mean ± standard deviation of the number of determinations.

2.5. Turbidity measurement

Using turbidity measurements, total suspended solids (TSS) were estimated in situ, and then the qualitative indicator is converted to a quantitative one using the formula (Ntwampe et al., 2015)

$$\ln(TSS) = 0.574 + 0.979 \cdot \ln(\text{turbidity}) .$$

A portable turbidity meter HI 98713 ISO (HANNA Instruments, USA) was used to evaluate the deposition processes of metal ions in AMDW. Formazine nephelometric units (FNU) were used as the unit of measurement to determine turbidity or suspended particles in the supernatant, which were calibrated with standard solutions of 0.10, 10, 100, 1000, and 10000 FNU. The FNU is most commonly used when referring to the ISO 7027 (European) turbidity method.

3. RESULTS AND DISCUSSION

3.1. Chemical composition of acid mine drainage water

The contents of some chemical elements in the samples of AMDW after their 10-day exposure are presented in table 1 at room temperature in an open container (2nd column). After appropriate treatment in a hydrochloric acid solution, a precipitate formed at the bottom of the container, in which the concentration of these chemical elements was also determined (table 1, 3rd column). On the basis of these data, in order to determine the real of concentration of chemical elements in the source water (at zero exposure), the calculated values of the metal content in the sediment are presented, giving an idea of the real concentration chemical elements. When preparing the sample for analysis, the concentration factor must be taken into account. According to the method of solution preparation (see 2.1) the analyzed solution was concentrated 10 times with respect to the initial water. Based on this, the concentration of metals must be reduced by a factor of 10 (table 1, 4th column). Zero-impact analysis becomes unrealistic due to the fact that immediately after taking water from the mine, iron is oxidized, and while the sample is taken to the laboratory and analyzed (which can last from several hours), a precipitate is formed. This is why the metal content needs to be corrected. In this case, the data presented in columns 2nd and 4th of table 1 are added. Finally, in column 6th presents the resulting corrected AMDW composition.

Table 1. Chemical composition in samples of acid mine drainage water (AMDW).

Chemical element	AMDW after 10 days of exposure (mg/l)	Original acidic sediment solution (mg/l)	Corrected composition of acid solution sediment (mg/l)	Composition of sediment (%)	Corrected composition of solution AMDW (mg/l)	% of precipitated metals from their total content
Al	223.2±5.0	17.1±0.4	1.71	1.78	225.6 ±5.0	0.76
Ca	312.1±7.0	76.3±1.7	7.59	7.90	319.2±7.0	2.44
Cd	0.23±0.01	0.03±0.007	0.003	0.003	0.26±0.01	1.30
Cu	4.02±0.08	0.49±0.009	0.049	0.051	4.5 ±0.1	1.22
Fe	125.3±3.0	61.6±1.5	61.53	64.01	184.7±4.0	49.07
Mg	298.8±6.0	40.4±0.9	3.96	4.12	302.4±6.0	1.33
Mn	174.1±3.5	15.3±0.4	1.50	1.56	175.7±3.5	0.86
Na	27.5±0.6	25.8±0.6	2.49	2.59	30.9±0.6	9.05



Pb	0.024±0.0014	0.04±0.003	0.004	0.004	0.024±0.006	20.00
S	1347.9±27.0	167.4±3.8	16.67	17.35	1363.8±27.5	1.24
Zn	70.5±1.5	5.5±0.1	0.55	0.57	71.4±1.5	0.78

As follows from the results of table 1, the main component of the precipitated sediment is iron - 64.01 wt %, (61.53 mg, which is 49.07 wt % of the total iron content in AMDW samples. The mechanism of iron precipitation is not fully understood, as well as there is no strict information on the precipitation of other metals and anions (in particular, sulfate ions) [24]. On this basis, in our experiments, an important indicator is the percentage of precipitated content of this metal from the total mass in AMDW samples as a result of pH reduction. Further, the calcium content in the precipitate is 8.05 wt % (7.59 g, which is 2.44 wt % of the total calcium content in the AMDW samples), the precipitation mechanism of which is probably related to the formation of its insoluble sulfates. The aluminum content of the precipitate is negligible at 1.81 wt% (1.71 g, which is 0.76 wt% of the total aluminum content of the AMDW samples), which is due to partial precipitation of aluminum as hydroxide. It is assumed that the deposition of other metals and sulfate ions occurs as a result of adsorption of iron hydroxide due to the significant active surface. It has been shown that iron-containing materials can absorb metal cations depending on the pH of the medium (Ghaly et al., 2006; Alyaseri et al., 2007). On the one hand, copper, lead and cadmium have specific adsorption on goethite, since the capacity of these chemical elements on the goethite surface increases with increasing electro negativity of the metal: $Cu > Pb > Cd$. On the other hand, the equilibrium constant for lead was greater than for copper, which agrees with their hydration radius ($Pb < Cu < Cd$) (McKenzie, 1980). The transition of sodium ions to precipitate was of particular interest because they do not form insoluble compounds. The sodium content is 2.49 wt % (2.59 g, which is 9.05 wt % of the total sodium content in AMDW samples). The only possible explanation for this process may be adsorption. Based on these results, sodium ranks 4th after iron, calcium, and magnesium (i.e., 9.05 wt% sodium of the total sediment mass (table 1)). For magnesium, it is 4.12 wt% (3.956 g, which is 1.33 wt% of the total magnesium content in AMDW). The amount of phosphorus and ammonia is negligible or nonexistent to form struvite ($MgNH_4PO_4$), the only insoluble magnesium compound, i.e., magnesium precipitation with struvite is excluded. Precipitation of 3.956 mg of magnesium would require 5.11 mg of phosphorus. The phosphorus content in the test water is only 0.014 mg/L. For sulfur, it is 17.35 wt % (16.67 g, which is 1.24 wt % of the total sulfur content of the AMDW samples). In this case, our calculations show that the amount of precipitated sulfur as gypsum is only 34.99 wt % of the total mass of sulfur contained in the sediment. The precipitated sulfur is negligible compared to the total mass of sulfur in AMDW samples - 1.24 wt %, but determination of its precipitation mechanism can provide insight into the way sulfate ions are removed from AMDW samples. Removal of sulfur in the form of sulfate ions is associated not only with the formation of gypsum because only 19.32 mg/l is deposited as gypsum but also when 17.69 mg of sulfur (corresponding to 53.07 mg of sulfate ion), i.e. $53.07 - 19.32 = 33.75$ mg of sulfate ions are not gypsum. The gypsum nature of sulfate ions accounts for only 1/3 of the precipitated sulfate ions (34.99 wt %). The remaining part of sulfate ions (65.01 wt %) appears to be deposited by adsorption on the surface of iron hydroxide. Sulfate ions are sorbed on the surface of iron compounds. It was found that the consumption of SO_4^{2-} on hematite occurs mainly in the form of intraspherical complexes. However, the use of extended spectroscopic analysis and complexation models showed that SO_4^{2-} appears on hematite as both internal and external complexes (Strawn, 2021).

3.2. Physicochemical parameters of acid mine drainage water

Among the different physico-chemical parameters of AMDW was chosen to determine its turbidity and pH (table 2). Water taken directly from the source had turbidity 5 ± 0.4 FTU and pH 3.48. Being in an open vessel, the water underwent certain qualitative changes. After 8 hours of exposure, the visually transparent material became light green in color. Then, after 24 hours of exposure, the color of AMDW samples became yellowish orange, and the pH decreased to a value of 3.2. At the same time, the downward trend in pH persisted and was 2.61 by the 10th day of exposure. By 30 hours of standing water, the formation of a precipitate dominated by $Fe(OH)_3$ as a result of iron oxidation to iron was visually observed (table 1). As follows from the presented results, the values of both turbidity and TSS of AMDW increase during exposure. On the fourth day of exposure this dependence has a plateau, and in the next six days the increase in turbidity and TSS values of AMDW becomes insignificant. That is why the water sampling as a



sample for the study was conducted after 10 days of exposure after sampling from the source in an open container (table 2).

Table 2. Value of physicochemical parameters in samples of acid mine drainage water at the time of its exposure to air.

Exposition times (day)	Turbidity	TSS	pH
0	5.2±0.4	9.09±1.0	3.45±0.03
1	55.4±4.5	90.2±7.5	3.21±0.03
2	98.2±8.6	158.4±13.7	3.06±0.03
3	127.7±11.3	204.6±18.4	2.95±0.03
5	135.3±12.6	216.7±19.3	2.79±0.02
7	140.2±12.5	224.5±19.1	2.70±0.02
10	145.5±13.2	232.8±21.2	2.61±0.02

Then, considering the TSS values (table 2) and the equation $\text{Fe}^{3+} + 3\text{H}_2\text{O} \rightarrow \text{Fe}(\text{OH})_3 + 3\text{H}^+$ (Wang et al., 2018), was estimated the amount of sulfuric acid formed when the pH of the sediment decreased. As the water exposure time increases up to 10 days, simultaneously with the decrease in pH, the values of turbidity and TSS increase, which we tend to attribute to the formation of $\text{Fe}(\text{OH})_3$ (table 1). It should also be noted that in addition to iron hydroxide, 18.22 mg of gypsum (CaSO_4) is also formed in the sediment, which is comparable to the calcium content. In fact, the turbidity of water is due to iron hydroxide with adsorbed metals and gypsum. So, the system contains 18.22 mg of gypsum, 117.57 mg of iron hydroxide, 39.70 mg of adsorbed sulfate ions, 1.56 mg of manganese, 2.59 mg of sodium and 1.78 mg of aluminum. A total of 181.11 mg and from table 2 shows that the TSS is 230 mg. The difference is $230 - 181 = 49$, which is 21.30%. Light scattering cannot characterize the amount of sediment because the dispersed particles can be very different, from colloids to particles as small as a few microns. But having an approximate TSS distribution of turbidity values, one can quickly estimate the amount of dispersed particles, which is a good way to characterize sedimentation processes in AMDW samples. The dependence of turbidity on the pH value of AMDW samples was established (figure). It was found that the turbidity increased almost linearly with decreasing pH. This indicates that the formation of $\text{Fe}(\text{OH})_3$ at decreasing pH (according to the equation $\text{Fe}^{3+} + 3\text{H}_2\text{O} \rightarrow \text{Fe}(\text{OH})_3 + 3\text{H}^+$) is directly proportional to the amount of hydrogen ions formed. With the cessation of the lowering pH process, the formation of $\text{Fe}(\text{OH})_3$ also stops, and at a certain pH value an equilibrium state is established.

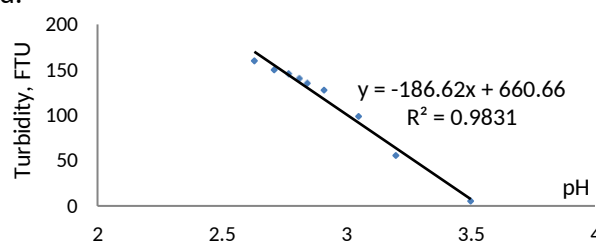


Figure. Functional dependence of turbidity of acid mine drainage water samples on pH value.

In this case, it is possible to artificially stop the formation of $\text{Fe}(\text{OH})_3$ and lower the pH by adding mineral acid, which will lead to the stabilization of AMDW samples. Apparently, there is an influence of various anions on these processes. On the basis of this sulfuric acid was chosen to lower the pH. Indeed, after lowering the pH to 2.5 with sulfuric acid, exposure of AMDW samples did not cause any changes over the next three months.

4. CONCLUSIONS

The processes that occur in AMDW samples during their long exposure under normal conditions lead to changes in such characteristics as pH, TSS, turbidity, and metal content. It has been reliably established that as the pH decreases, the turbidity of the source water increases, which has a linear character. The main, but not the only, component of the precipitate is $\text{Fe}(\text{OH})_3$, while its share in terms of Fe^{3+} is 64.01 wt %.



Calcium precipitates in the form of insoluble sulfates, and in the case of other metals, precipitation occurs with iron hydroxide in adsorbed form. In the case of transition of sodium and magnesium to the precipitate, they are precipitated with iron hydroxide in adsorbed form. The gypsum nature of sulfate ions in the sediment is about 1/3 of the total sulfur content in the sediment. The rest of the sulfate ions are precipitated with iron hydroxide in adsorbed form.

5. ACKNOWLEDGEMENTS

This study is supported by the by the Science Committee of RA, in the frames of the research project № 21T-2H216.

REFERENCES

- Blowes, D., Ptacek, C., Jambor, J., Weisener, C., 2003. The geochemistry of acid mine drainage. *Treatise Geochem*, 9, 612.
- Gupta, V., Ali, I., 2012. *Environmental Water: Advances in Treatment, Remediation and Recycling*; Elsevier: Amsterdam, The Netherlands.
- Guimaraes, D., Leao, V., 2014. Fundamental aspects related to batch and fixed-bed sulfate sorption by the macroporous type 1 strong base ion exchange resin Purolite A500. *J. Environ. Manag.* 145, 106–112.
- Vecino, X., Reig, M., López, J., Valderrama, C., Cortina, J., 2021. Valorisation options for Zn and Cu recovery from metal influenced acid mine waters through selective precipitation and ion-exchange processes: promotion of on-site/off-site management options. *J Environ Manage.* Apr 1(283:112004. doi: 10.1016/j.jenvman.2021.112004.
- Sountharajah, D. P., Loganathan, P., Kandasamy, J., Vigneswaran, S., 2015. Effects of Humic Acid and Suspended Solids on the Removal of Heavy Metals from Water by Adsorption onto Granular Activated Carbon. *Int. J. Environ. Res. Public Health*, 12, 10475-10489. doi:10.3390/ijerph120910475.
- Fu, F., Wang, Q., 2011. Removal of heavy metal ions from wastewaters: a review. *J. Environ. Manag.* 92, 407–418.
- Glover-Kerkvilet, J., 1995. Environmental assault on immunity. *Environ. Health Persp.*, 103,236–237.
- Chen, J., 2012. *Decontamination of Heavy Metals: Processes, Mechanisms, and Applications*; CRC Press: Boca Raton, FL, USA.
- Roesner, L., Charles, R., 1996. National storm water quality regulations and standards. *J. Hydraul.Res.*, 34, 841–856.
- Lottermoser, B., 2011. *Mine Wastes: Characterization, Treatment and Environmental Impacts*. 2nd edit., Springer, Berlin Nordstrom DK Mine waters: acidic to circum neutral. *Elements* 7:393–398.
- Strosnider, W., Llanos, F., Marcillo, C., Callapa, R., Nairn, R., 2014. Impact on tributaries of the Pilcomayo River by additional pollutants from mine acid drainage from Cerro Rico de Potosí-Bolivia. *Adv. Sci. Eng.*, 5, 1–17.
- Johnson, D., Hallberg, K., 2005. Acid mine drainage remediation options: a review. *Science of the Total Environment*, 338, 3– 14.
- Akcil, A., Koldas, S., 2006. Acid mine drainage (AMD): Causes, treatment and case studies. *J. Cleaner Prod.* 14(12-13):1139-1145.
- Kurniawan, T., Chan, W., Lo, W-S., Babel, S., 2006. Physico-chemical treatment techniques for wastewater laden with heavy metals. *Chem. Eng.*, 118:83-87.
- Scherrenberg, S., Menkveld, H., Schuurman, D., den Elzen, J., van der Graaf, J., 2008. Advanced treatment of WWTP effluent; no use or reuse? *Wat. Pract. Technol*, 3(2).
- Goldberg, S., 2002. Competitive Adsorption of Arsenate and Arsenite on Oxides and Clay Minerals. *Soil Sci. Soc. Am.*, 66: 413-421.
- Sincero, A., Sincero, G., 2003. *Physical-chemical treatment of water and wastewater* IWA Publishing, London, USA.
- McCurdy, K., Carlson, K., Gregory, D., 2004. Floc morphology and cyclic shearing recovery: comparison of alum and polyaluminum chloride coagulants. *Wat. Res.* 38(2):486-494.
- Ntwampe, I., Waanders, F., Bunt, T., 2015. Comparison between mixing and shaking techniques during the destabilization-hydrolysis of the acid mine drainage (AMD) using Ca(OH)₂ and Mg(OH)₂. *J.Chemical Engineering and Materials Science.* 6(3), pp. 15-33, doi:10.5897/JCEMS2015.0212.
- Ghaly, A., Snow, A., Faber, B., 2006. Treatment of grease filter wash water by chemical coagulation. *Can. Biosyst. Eng.* 48:6.13-6.22.
- Alyaseri, I., Morgan, S., Retzlaff, B., 2007. Using Turbidity to Determine Total Suspended Solids in Storm-Water Runoff from Green Roofs. *J. Environmental Engineering*, 139(6): 822-828. DOI:10.1061/(ASCE)EE.1943-7870.0000685.
- McKenzie, R., 1980. The adsorption of lead and other heavy metals on oxides of manganese and iron. *Soil Res.*, 18, 61–73.
- Strawn, D., 2021. Sorption Mechanisms of Chemicals in Soils. *Soil Syst.*, 5(1), 13. <https://doi.org/10.3390/soilsystems5010013>.
- Wang, X., Wang, Z., Peak, D., Tang, Y., Feng, X., Zhu, M., 2018. Quantification of coexisting inner- and outer-sphere complexation of sulfate on hematite surfaces. *ACS Earth Space Chem.*, 2, 387–398.



Biodiesel production, properties and sustainability from the biomass of *Chlorella sorokiniana* grown heterotrophically with glycerol and anaerobic digestate

D. Kasiteropoulou¹, G. Papapolymerou¹, A. Kokkalis², M. N. Metsoviti¹, X. Spiliotis¹ and A. Mpesios¹

¹ Dept. of Environmental Studies, University of Thessaly, Gaiopolis, Larissa, Greece

² GRINCO S.A., Industrial Area of Larisa, Makrychori Larisas, Greece

Corresponding author email: dkasiter@uth.gr

ABSTRACT

The bio-oil and biodiesel production process from the bio-oil of *Chlorella sorokiniana* biomass is reported. The bio-oil extraction parameters from the biomass of *Chlorella sorokiniana* were examined and two successive base-catalyzed transesterifications were carried out. Bio-oil, biodiesel and glycerin yields were determined and basic bio-oil and biodiesel properties were measured. Also, maximum biomass yields were estimated in order that biodiesel production using glycerol as a carbon source be competitive, from an energy point of view, to the anaerobic production of biogas from glycerin. Optimum extraction parameter values are a solvent to biomass ratio 20:1 (v/w), an extraction time of 48 hours and an extraction temperature 40 °C but, in any potential industrial application the combination of these parameters may be different. Biodiesel conversion efficiency (w/w) is 96% and all basic bio-oil and biodiesel properties measured were within acceptable ranges. Biomass yields of about 11 gr/l with a minimum lipid content of 35% and a carbon yield coefficient of 0.40 are needed in order for the biodiesel produced per ton of glycerin be comparable to the electrical energy produced from biogas from the anaerobic digestion also of 1 ton of glycerin.

Keywords: bio-oil; biodiesel; *Chlorella sorokiniana*; heterotrophic; glycerol; anaerobic digestate.

1. INTRODUCTION

Microalgae are unicellular photosynthetic organisms that use light and carbon dioxide, with higher photosynthetic efficiency than plants, for the production of biomass. Some microalgae species can also grow and multiply heterotrophically in the absence of light if an organic carbon source becomes available (Mata *et al.*, 2010). The main advantage of heterotrophic growth is higher biomass growth rates and biomass production because, unlike autotrophic growth, heterotrophic growth is not limited by light transmission through the growth medium. Another advantage of heterotrophic growth is the potential of achieving higher lipid content and, as a result, higher lipid productivities can be obtained. A number of review papers focus on the heterotrophic growth of several microalgal species and the trend is that heterotrophic growth enhances both the biomass and lipid productivity (Bumbak *et al.*, 2011; Perez-Garcia & Bashan, 2015). In the heterotrophic growth, industrial by-products or waste streams containing dissolved organic carbon, macronutrients and micronutrients can be used in terms of nutrient recovery, waste minimization and cyclic economy. Anaerobic digestate (AD) is a rich source of macro and micronutrients while, crude glycerol has a very high content in organic carbon.

The main challenges concerning cost-competitive production of biodiesel from microalgal bio-oil are high lipid productivities and cost-efficient bio-oil extraction technologies. Efficient biomass harvesting techniques are also needed while, conversion of bio-oil to biodiesel is less of a problem. However, a number of alternative to classical transesterification technologies have been researched which, are promising in decreasing production related costs. Such technologies are enzyme catalyzed transesterification and solid catalyst transesterification. With respect to extraction technologies many different ones, such as ultrasound and microwave assisted extraction, supercritical fluid extraction, have been proposed. Solvent extraction is a technology used more often. Roy A. (2017), Kumar R.R. *et al.* (2015) and Roux J-M *et al.* (2017) review the various extraction technologies that have been researched. In any case, the major problem in the lipid extraction process is the breaking up of the microalgal cell membrane. A wide variety of organic carbon sources have been used for the heterotrophic growth of various microalgal species such as glucose, sucrose, fructose, mannose, glycerol, lactose or galactose (Perez-Garcia *et al.*, 2011). Additionally, various industrial effluents and by-products, such as anaerobic digestate can be used as a carbon and nitrogen source. Studies on the heterotrophic cultivation of different microalgal species using glucose as carbon source have been published (Li *et al.*, 2007; Xiong *et al.*, 2008), while work on the cultivation of microalgae using glycerol is



limited. It should be mentioned that studies on cultivation using industrial effluents and by-products, such as anaerobic digestate are lacking. The aim of this work is two-fold: a) to examine the effect of the extraction parameters on the efficiency of bio-oil extraction from the biomass of *Chlorella sorokiniana* cultivated heterotrophically and its subsequent conversion to biodiesel and b) to estimate the biomass and lipid productivities needed in order for the biodiesel produced per ton of glycerin consumed to be competitive, from an energy point of view, to the energy obtained from the biogas produced via anaerobic digestion from the same amount of glycerin. For this estimation of biomass and lipid productivities needed, an average carbon fraction of the biomass and the maximum theoretical carbon yield coefficients are used. Also, basic bio-oil and biodiesel properties are reported from two cultivation experiments using glycerin as the main carbon source and anaerobic digestate as the macro and micronutrient source. The biomass used to evaluate the bio-oil extraction and biodiesel production efficiencies was obtained from two experiments using glycerin and 30% and 50% anaerobic digestate (Papapolymerou et. al., 2021).

2. MATERIALS AND METHODS

The cultivation of *C. sorokiniana* carried out in 42 L cylindrical glass bioreactors of 42L filled to 75% of their volume. Air was continuously provided to each bioreactor through perforated steel tubing placed at the bottom of the bioreactors at a rate of about 40 L/(L-h). The bioreactors, the glass tubing and the culture medium were sterilized before use.

At the end of each experiment, and specifically at the stationary growth phase, the biomass was collected by centrifugation, it was rinsed with distilled water and was re-centrifuged. Finally, it was dried in an air circulation oven at 45 °C until constant weight. Prior to lipid extraction, the biomass was pulverized using a planetary ball mill at 200 rpm for 10 minutes (FRITSCH, Idar-Oberstein, Germany). The total lipid content was determined with extraction using co-solvents of n-hexane/isopropanol in a 3:2 ratio according to the Bian method (Bian et. al., 2018). Extraction of the bio-oil was carried out in a horizontal extraction apparatus (tehnica ZELEZNIKI EV-402) at 300 rpm. Following extraction, the biomass was filtered out and the solvent was evaporated. The bio-oil was subjected to transesterification via a double classical transesterification procedure. The microalgal species *Chlorella sorokiniana* (SAG strain 211-31) was obtained from Culture Collection of Algae from the University of Göttingen in Germany (EPSAG). Glycerin and anaerobic digestate (AD) were obtained from local biodiesel and biogas plants. AD was filtered, centrifuged and sterilized before use.

3. RESULTS AND DISCUSSION

3.1 Bio-oil extraction process, extraction efficiency and bio-oil basic properties

In this work for the extraction of bio-oil from microalgae, the following procedure was used: a) concentration of the biomass, b) centrifugation, c) drying, d) milling, e) extraction of the solid phase with a mixture of solvents, f) filtration and g) evaporation of the solvents. The percentage of oil extraction that can be achieved using this technique is almost 95-96% while up to about 4-6% bio-oil are expected to remain within the biomass. The bio-oil extraction yield depends on the following factors: a) the grinding method (manually or using a planetary ball mill), b) the time speed of grinding, c) the extraction time, d) the ratio of biomass to solvent mixture and e) the extraction temperature. This technique may be suitable for use in processing large amounts of microalgal biomass if suitably modified for a large-scale application. The main points that this technology should focus to be cost-efficient for use on a large scale are: 1) the effective concentration of the culture solution of the microalgae to a percentage of solids above 50%-60%, 2) A second concentration step to a percentage more than 80% solids content with as little energy consumption as possible and the subsequent drying of the biomass, 3) the grinding of microalgae biomass with a small percentage of moisture (up to about 3-5%), 4) extraction with a solvent mixture and 5) efficient recovery of the solvent so as to minimize the operating cost of this material.

After the biomass was concentrated and dried, as microalgae have rigid cell walls and lipids are located within these cell walls, a planetary ball mill type setup with zirconium oxide beads was used for grinding in order to rupture the cell wall of the microalgae and make the lipids accessible to the solvent mixture. Grinding was done with constant and equal amounts of dry biomass in each of the four containers of the planetary ball mill for a period of 10 min and with a rotation speed of 200 rpm. Afterwards, the oil was extracted from



the dry biomass of the microalgae with a conventional extraction device (tehtnica ZELEZNIKI EV-402) at 300 rpm, using a solvent mixture of hexane and isopropanol in a ratio of 3:2. The following three parameters were investigated in order to determine the optimal conditions for oil extraction performance: a) solvent to biomass ratio (v/w), b) extraction time and c) extraction temperature. The methodology-procedure was to subject quantities of microalgal biomass from the same cultivation treatment to homogenization and grinding, then to obtain batches of biomass and divide them in equal amounts and study them comparatively in order to determine the effect of the aforementioned three extraction parameters on the amount of bio-oil extracted. Each time, one of the three extraction parameters was varied while the other two were held constant.

a) Effect of solvent to biomass ratio (v/w)

Three solvent-to-biomass ratios i.e., 5/1, 10/1 and 20/1 were studied. The 3 batches of biomass were 10 g each. The three 500 mL conical flasks contained 50 mL, 100 mL, and 200 mL of solvent respectively in a 3:2 ratio (n-hexane/isopropanol). The shaking time was 48 hours at a temperature of 25 °C. By recovering the bio-oil after filtration and evaporation of the solvent, the following amounts of bio-oil were recovered: a1) Solvent/biomass ratio (v/w) 5:1 = 2.2 g, a2) Solvent/biomass ratio (v/w) 10:1 = 2.8 g and a3) Solvent/biomass ratio (v/w) 20:1 = 2.9 g. There is no significant difference between the last two treatments and since a solvent to biomass ratio of 20:1 is demanding in terms of the amount of solvent used and the volume of the conical flask it occupies, a solvent/biomass ratio of 10:1 appears to be optimum.

b) Effect of the extraction time

Three extraction times were studied, i.e., 24, 48 and 72 hours. The amount of bio-oil extracted from each batch was compared. The 3 batches of biomass used were 20 g each. The three 500 mL conical flasks contained 200 mL of solvent each, i.e., a constant solvent to biomass ratio of 10:1 was used. The extraction took place at a temperature of 25 °C. By recovering the bio-oil after filtration and evaporation of the solvent, the following amounts of bio-oil were recovered: b1) extraction time 24 hours = 5.2 g, b2) extraction time 48 hours = 5.7 g, b3) extraction time 72 hours = 5.7 g. There is no difference between the last 2 conditions and since an extraction time of 72 hours is costly, an extraction time of 48 hours appears to be optimum. The difference between the first two (shake for 24 hours vs. shake for 48 hours) is 9.6%.

c) Effect of the extraction temperature

Two extraction temperatures were studied namely 25 °C and 40 °C. The 2 batches of biomass used were 20 g each. The two 500 mL conical flasks contained 200 mL of solvent each with a constant ratio of solvent to biomass equal to 10:1. Extraction time was 48 hours. By recovering the bio-oil after filtration and evaporation of the solvent, the following amounts of bio-oil were recovered: c1) extraction temperature 25 °C = 5.5 g and c2) extraction temperature 40 °C = 5.8 g. 5.4% greater amount is recovered at the higher temperature. Given that an estimated 3-6% of the bio-oil cannot be extracted from the biomass and that by increasing the biomass treatment (amount of solvent to bio-oil, extraction time and extraction bath temperature) no further increase seems to be achieved in the amount of bio-oil recovered. Therefore, the bio-oil extraction efficiency is estimated to be between 93% and 96%. From these results the optimal extraction conditions are: a) solvent to biomass ratio 10:1 (v/w), b) extraction time 48 hours and c) extraction temperature 40 °C. In any potential industrial application, the combination of these parameters may be different because the cost of extraction increases disproportionately compared to the increase in extraction efficiency and also other parameters not studied here such as milling time and speed as well as cell wall strength, which is different among microalgal species, may be affecting the optimum extraction parameters.

The characterization-property measurement of the bio-oil extracted from the above biomass of the microalgae *Chlorella sorokiniana* includes the determination of acidity, density, viscosity, moisture and sulfur content. Measurements were made according to the following protocols: a) acidity: EN 14104, b) density: EN ISO 3675, c) viscosity: EN ISO 3104 (40 °C), d) moisture: EN ISO 12937, and e) sulfur content: EN ISO 20846. Table 1 shows the bio-oil properties from the cultivation of *Chlorella sorokiniana* with 30% and 50% AD.



Table 1. Basic properties of the bio-oil produced from the cultivation of *Chlorella sorokiniana* with 30% and 50% AD.

Property → Cultivation ↓	Acidity (mg KOH/g)	Density (kg/m ³)	Viscosity (mm ² /sec)	Moisture (ppm)	sulfur content (ppm)
Accepted values →	<2	910-930	<36	≤750	<10
30% AD	0.45	921	30.7	750	<10
50% AD	0.45	917	30.2	700	<10

From table 1 it is noted that the bio-oil of *Chlorella sorokiniana*, for both treatments, is of proper properties for subsequent conversion to biodiesel.

3.2 Conversion to biodiesel process, transesterification yield and basic biodiesel properties

Transesterification took place in two successive stages and each time two washes were performed. The bio-oil transesterification method was carried out in a batch reactor. The bio-oil from microalgae was placed in the reactor and then heated to a temperature of 50-53°C and the stirrer, at 300 rpm, was put into operation in order to achieve complete mixing of the bio-oil with the reagents and to increase the contact surface area between the two phases. Excess alcohol was used to increase the yield and to allow separation from the glycerin formed. The amounts of methanol (CH₃OH) and catalyst (CH₃ONa) were added at 11% of the oil and 1.1% respectively (w/w). The transesterification reaction is exothermic, so the temperature was raised and held constant at 55°C for 20 minutes. Then, the stirrer was turned off and the solution was left to stand. The biphasic solution was transferred to a conical separating flask and after 1.5h the formed glycerin was separated and removed. The 2nd transesterification followed. Amounts of methanol (CH₃OH) and catalyst (CH₃ONa) were added for the 2nd transesterification. Their percentages in relation to the initial amount of bio-oil (before the 1st transesterification) were 3% and 0.5% respectively. The formed glycerin was separated and removed. In the biodiesel produced after the 2nd transesterification, amounts of soaps and glycerin remain which were not removed by separating the glycerin. Two washes were performed to remove residual soaps and glycerin. In each one, the stirrer was started and the temperature was set to 60 °C. Water was added at a percentage of 5% of the original oil in each wash and agitation lasted for 15 minutes. The stirrer was turned off and the solution was allowed to stand. After an hour and a half of rest, the soapy water was separated and removed. The last stage of transesterification is distillation to remove the residual moisture of biodiesel from bio-oils. The stirrer was started, the temperature was set to 90 °C and the vacuum to 0.1 bar. The distillation took about an hour.

From two batches of bio-oil, 95 gr and 75 gr, 91 gr and 72 gr of biodiesel were produced respectively with a yield (biodiesel/bio-oil, w/w) equal to 0.96. The glycerin yield was 13 gr from the 95 gr of bio-oil and 10 gr from the 75 gr bio-oil batch. Therefore, the glycerin yield with respect to the amount of bio-oil was 14% and 13.5% respectively.

The following biodiesel properties were studied: a) density, b) viscosity and c) the flash point. The density (15 °C) and viscosity (40 °C) were measured with the EN ISO 3675 and EN ISO 3104 standards respectively, while the flash point was measured with the EN ISO 2719 standard. Table 2 shows the biodiesel properties for the biodiesel produced from the cultivation of *Chlorella sorokiniana* with 30% and 50% AD. As it is noted from Table 1 all values for both cultivation treatments are within acceptable ranges.

Table 2. Basic properties of the biodiesel produced from the cultivation of *Chlorella sorokiniana* with 30% and 50% AD.

Property → Cultivation ↓	Density (kg/m ³)	Viscosity mm ² /sec	Flash point (°C)
Accepted values →	860-900	3.5-5.0	>101
30% AD	881	4.0	154
50% AD	879	3.8	151



3.3 Biomass and Lipid Productivities for biodiesel production sustainability

In order to determine sustainability for the use of glycerin as a carbon source for cultivating microalgae, we can estimate the maximum biomass and lipid yield needed from the cultivation of *Chlorella sorokiniana* from 1 ton of glycerin in order to obtain the same amount of energy from the use of glycerin for the production of biogas via anaerobic digestion. This is done only from an energy point of view and not from a process cost, which for the case of biodiesel is expected to be high. Proper assumptions for the carbon yield coefficient and lipid content of the biomass were made (Papapolymerou et. al., 2021).

a) Production of methane per ton of glycerin

Glycerin, among other uses, is also used in biogas production plants. The amount of methane produced per kg of glycerin containing 86% glycerol is about 320 m³, assuming a 95% conversion efficiency (Viana et. al., 2012). The heating value of methane is about 36.4 MJ/m³. Therefore, from 1 ton of glycerin it is expected that 320 m³ of methane will be produced with a heating value of 320x36.4 = 11.6x10³ MJ. In the case where this methane produced in biogas plants is used only for the production of electricity, a conversion factor of 0.42 would yield 4.9x10³ MJ of electrical energy.

b) Biomass and bio-oil yield needed per ton of glycerin used in the cultivation of *Chlorella sorokiniana*:

For every 1000 kg of glycerin used (about 800 m³), approximately 3.2x10⁴ liters of cultivation growth medium can be prepared having an initial carbon concentration equal to about 14 gr/l. Therefore, the total amount of carbon in the cultivation medium is 14x3.2x10⁴ = 448 kg of carbon. The carbon yield coefficient is defined as the ratio of the carbon (in gr) in the biomass of the microalgae to the carbon consumed during the cultivation (in gr) and the carbon fraction of the biomass is the ratio of the amount of carbon found in the biomass to the weight of the biomass. Assuming a maximum carbon yield coefficient of 0.40 and a typical carbon fraction in the biomass of *Chlorella sorokiniana* of 0.52, which corresponds to about 35% lipids (Papapolymerou et. al., 2021), the maximum weight of carbon which can be incorporated in the biomass is equal to: 448 kg x 0.40 = 179.2 kg of carbon. From the carbon fraction of the biomass of 0.52, the maximum weight of biomass which can be produced is equal to: 179.2/0.52 = 344.6 kg of biomass. This biomass is obtained, as aforementioned, from 3.2x10⁴ liters of cultivation growth medium. Therefore, the maximum biomass yield is: 344.6x10³ gr/3.2x10⁴ liters = 10.8 gr/l. For a 35% content in lipids of the biomass and a 97% conversion efficiency of the lipids to biodiesel, the maximum amount of biodiesel which can be produced is equal to: 344.6x0.35x0.96 = 115.8 kg of biodiesel. For a mean value of 41 MJ/kg for the biodiesel (Sivaramakrishnan, 2011), a maximum heating value of the maximum amount of biodiesel produced per ton of glycerin used is equal to: 115.8x41 = 4.7x10³ MJ. This value is quite smaller than the heating value of 11.6x10³ MJ which is obtained from the methane produced from the anaerobic digestion of 1 ton of glycerin. So, a biomass yield of 21.6 gr/l is needed instead. But, if it is compared only to the electrical energy produced from the anaerobic digestion of 1ton glycerin, equal to 4.9x10³ MJ, the two values are comparable. However, still, a biomass yield of 10.8 gr/l with a lipid content of 35% is needed. This is not difficult to achieve but a carbon yield coefficient equal to 0.40, in order to be achieved, a high initial nitrogen concentration is needed, which in turn leads to a biomass with lower lipid and higher protein content (Papapolymerou, et. al., 2021). Other modes of cultivation such as semi-batch cultivation, mixotrophic cultivation or a combination of the two may achieve both a high biomass yield with high lipid content and a high carbon yield coefficient.

4. CONCLUSIONS

Bio-oil extraction from the biomass of *Chlorella sorokiniana* via a combination of mechanical pre-treatment in a planetary ball mill and solvent extraction has an extraction efficiency over 93%. Increasing the solvent/biomass ratio from 5:1 to 10:1, the extraction time from 24 hours to 48 hours and the extraction temperature from 25°C to 40°C and the increases the extraction efficiency by 27%, 9.6% and 5.5% respectively. The efficiency of bio-oil to biodiesel conversion via two successive base-catalyzed transesterifications is 96%. 14% (w/w) of the bio-oil-methanol reactive mixture was converted to glycerin. The bio-oil of *Chlorella sorokiniana* cultivated heterotrophically with glycerol and anaerobic digestate is appropriate for use for biodiesel production as all basic bio-oil and biodiesel properties measured are within acceptable ranges. In order for the biodiesel produced from the cultivation of *Chlorella sorokiniana* to be



competitive, from an energy point of view, to the biogas produced from the anaerobic digestion of an equal amount of glycerin a biomass yield of 21.6 gr/l with a 35% lipid content is needed. Semi-batch mode or mixotrophic mode cultivation, a combination of the two, use of genetically modified microalgae may achieve this.

5. ACKNOWLEDGEMENTS

The study was co-financed by the European Regional Development Fund of the European Union and Greek national funds through the Operational Program Competitiveness, Entrepreneurship and Innovation, under the call RESEARCH – CREATE - INNOVATE (project code: T1EDK-01580).

REFERENCES

- Bian, X., Jin, W., Gu, Q., Zhou, X., Xi, Y., Tu, R., Han, S., Xie, G., Gao, S. and Wang, Q., 2018. Subcritical n-hexane/isopropanol extraction of lipid from wet microalgal pastes of *Scenedesmus obliquus*. *World Journal of Microbiology and Biotechnology*, 34 (3), 39.
- Bumbak, F., Cook, S., Zachleder, V., Hauser, S. and Kovar, K., 2011. Best practices in heterotrophic high-cell-density microalgal processes: achievements, potential and possible limitations. *Applied microbiology and biotechnology*, 91(1), 31-46.
- Kumar, R. R., Rao, P. H. and Arumugam, M, 2015. Lipid extraction methods from microalgae: a comprehensive review. *Frontiers in Energy Research*, Vol. 2, Article 61.
- Li, X., Xu, H. and Wu, Q., 2007. Large-scale biodiesel production from microalga *Chlorella protothecoides* through heterotrophic cultivation in bioreactors. *Biotechnology and bioengineering*, 98(4), 764-771.
- Mata, T. M., Martins, A. A. and Caetano, N. S., 2010. Microalgae for biodiesel production and other applications: a review. *Renewable and sustainable energy reviews*, 14(1), 217-232.
- Papapolymerou, G., Kokkalis, A., Kasiteropoulou, D., Gougoulas, N., Mpesios, A., Papadopoulou, A., and Metsoviti, M. N., 2021. Fatty Acid Distribution of *Chlorella sorokiniana* grown with crude glycerol and Anaerobic Digestate as an alternative source of bio-oil for biodiesel production, *16th Conference on Sustainable Development of Energy, Water and Environment Systems (SDEWES)*, page 606, October 10-15, 2021, Dubrovnik, Croatia, ISSN – 1847-7178.
- Perez-Garcia, O., Escalante, F. M., De-Bashan, L. E and, Bashan, Y., 2011. Heterotrophic cultures of microalgae: metabolism and potential products. *Water research*, 45(1), 11-36.
- Perez-Garcia, O. and Bashan, Y. (2015). Microalgal heterotrophic and mixotrophic culturing for bio-refining: from metabolic routes to techno-economics. *Algal biorefineries*, 61-131.
- Roux J-M., Lamotte, H. and Achard J-L., 2017. An Overview of Microalgae Lipid Extraction in a Biorefinery Framework, *Energy Procedia*, 112, 680 – 688.
- Aprita, R., 2017. A Review on Harvesting and Lipid Extraction Methods for Biodiesel Production from Microalgae. *Biochemistry & Molecular Biology Letters*, Vol. 12, Issue 3.
- Sivaramakrishnan K., 2011. Determination of higher heating value of biodiesels”, *Intern. J. of Eng. Science and Technol.*, Vol. 3 No.11.
- Xiong, W., Li, X., Xiang, J. and Wu, Q., 2008. High-density fermentation of microalga *Chlorella protothecoides* in bioreactor for microbio-diesel production. *Applied microbiology and biotechnology*, 78(1), 29-36.
- Viana M.B., Freitas, A. V., Leitao, R. C., Pinto, G. A. S. and Santaella, S. T., 2012. Anaerobic digestion of glycerol: a review”, *Envir. Tech. Reviews*, Vol. 1 (1).



Heterotrophic growth of *Chlorella sorokiniana* with glycerol and anaerobic digestate: carbon uptake rate and phenolic content

D. Kasiteropoulou¹ G. Papapolymerou¹, D. Ladas¹, A. Mpesios¹ and M. N. Metsoviti¹

¹Dept. of Environmental Studies, University of Thessaly, Gaiopolis, Larissa, Greece
Corresponding author email: dkasiter@uth.gr

ABSTRACT

The heterotrophic cultivation of the microalgal species *Chlorella sorokiniana* using glycerol and low percentages of anaerobic digestate is examined. The effect of anaerobic digestate on the carbon uptake rate is examined. Also, the effect of the nitrogen concentration on the total phenolic content of the biomass of *Chlorella sorokiniana* is examined. Cultivations were carried out in 5L cylindrical and 42 L orthogonal glass bioreactors and air was provided at a rate of about 40 L/(L-hr). The temperature and pH were kept constant. The biomass productivity is equal to 0.12, 0.12, 0.13 and 0.13 for 0%, 4%, 8% and 16% anaerobic digestate respectively. The anaerobic digestate, at 16% in the growth medium, increases the carbon uptake rate by 13%. The biomass of *Chlorella sorokiniana* grown heterotrophically is rich in polyphenols. For a wide variation in the initial nitrogen concentration in the growth medium the phenolic concentration ranges from 2.3 mg/l to 3.6 mg/l.

Keywords: *Chlorella sorokiniana*; heterotrophic; glycerol; anaerobic digestate; phenolic content.

1. INTRODUCTION

Microalgae are unicellular photosynthetic organisms and some microalgae species can also grow and multiply heterotrophically in the absence of light if an organic carbon source becomes available and several advantages of heterotrophic growth are discussed and reviewed by Bumbak *et al.*, (2011) and Perez-Garcia & Bashan, (2015). In the heterotrophic growth, industrial by-products or waste streams containing dissolved organic carbon, macronutrients and micronutrients can be used in terms of nutrient recovery, waste minimization and cyclic economy. The main advantages of heterotrophic growth are higher biomass growth rates and biomass production because, unlike autotrophic growth, heterotrophic growth is not limited by light transmission through the growth medium and the potential of achieving higher lipid content. This combined effect leads to lipid productivities, which is needed if the bio-oil is to be used for biodiesel production. Disadvantages of heterotrophic growth are the susceptibility to contamination which requires that all parts of the bioreactors as well as all growth media must be carefully sterilized in order to minimize the risk of contamination and the cost of organic carbon which must be provided to the growth medium.

Depending on the cultivated species and the cultivation mode and parameters the microalgal biomass can be directed towards specific uses, since various components such as proteins, lipids, antioxidants and other compounds can be maximized (Dean *et al.*, 2010). The microalgae growth rate as well as the protein and lipid content are influenced by many parameters, such as the cultivated species, the temperature, the concentration of carbon, the ratio of carbon to nitrogen, the medium pH, the concentration of potassium, phosphorus and micronutrients, dissolved oxygen availability and the mixing rate (Gouveia & Oliveira, 2009). Except for the production of biodiesel, the biomass can be used in a variety of applications. The biomass of microalgae is rich in antioxidants, and some organic substances of pharmaceutical value so, some applications are in the cosmetic and pharmaceutical industry (Spolaore *et al.*, 2006). The high protein and lipid content can be of value in aquaculture for the replacement of fishmeal in fish feeds and in the poultry industry (Patil *et al.*, 2005). The biomass of microalgae is also reported to contain antioxidant compounds (Coulombier, N. 2021).

Anaerobic digestate (AD) produced by biogas plants is mainly used for field fertilization in various crops such as corn. When there are no adequate fields available or the land is not sufficiently flat, nitrification of underground and surface water and high soil salinity may result because excess anaerobic digestate is applied. Therefore, developing new applications for the efficient use of anaerobic digestate is needed in order to utilize the macro and micro nutrient content of the AD in the framework of circular economy. A good solution is the use of anaerobic digestate for microalgae cultivation since it is a good source of nitrogen,



phosphorus and potassium, as well as a source of over 30 different micronutrients. Potassium and phosphorus availability is projected to decrease in the future.

A wide variety of organic carbon have been used for the heterotrophic growth of various microalgal species such as glucose, sucrose, fructose, mannose, glycerol, lactose or galactose (Perez-Garcia et al., 2011). Additionally, various industrial effluents and by-products, such as anaerobic digestate can be used as a carbon and nitrogen source. Studies on the heterotrophic cultivation of different microalgal species using glucose as carbon source have been published (Li et al., 2007; Xiong et al., 2008), while work on the cultivation of microalgae using glycerol is limited. It should be mentioned that studies on cultivation using industrial effluents and by-products, such as anaerobic digestate are lacking.

The aim of this work is to examine the effect of low percentages of anaerobic digestate in the growth medium on the carbon uptake rate using glycerol as the main source of organic carbon and also examine the biomass of *Chlorella sorokiniana* grown with low percentages of anaerobic digestate and glycerol for its content in antioxidants, namely phenolic compounds.

2. MATERIALS, METHODS AND EXPERIMENTAL SET UP

2.1 Bioreactors, Materials and Methods

The cultivation of *C. sorokiniana* carried out in 5 L cylindrical glass bioreactors as well as in orthogonal glass bioreactors of 42 L. Air was continuously provided to each bioreactor at a rate of about 40 L/(L-h). The bioreactors, the glass tubing and the culture medium were sterilized before use.

The microalgae species *C. sorokiniana* (SAG strain 211-31) was obtained from Culture Collection of Algae from the University of Göttingen in Germany (EPSAG). The cultivation medium used for the inoculum growth was the Basal Medium (= ES "Erddekokt + Salze") and each liter of it contained: 0.2g KNO₃/L, 0.02 g K₂HPO₄/L, 0.02 g MgSO₄·7H₂O/L, 30 mL of soil extract/L and 5 ml/L, of a solution containing the following micronutrients: (1 mg ZnSO₄·7H₂O, 2 mg MnSO₄·4H₂O, 10 mg H₃BO₃, 1 mg Co(NO₃)₂·6H₂O, 1 mg MoO₄·2H₂O, 0.005 mg CuSO₄·5H₂O, 700 mg FeSO₄·7H₂O and 800 mg EDTA)/L (SAG, 2007).

Glycerol and AD were obtained from local biodiesel and biogas plants respectively. Crude glycerol was used as the carbon source. Its methanol was removed and its composition was 86 % glycerin, 0.5% methanol, 7.5% water, 3.5 % MONG (Non-Glycerin Organic Matter) and 2.5 % ash. The anaerobic digestate was first filtered through three successive sieves and then centrifuged at 4000 rpm for 10 minutes. It was then sterilized by boiling for about 10 minutes. Following its cooling the macronutrient content of the AD was determined. Nitrogen is present only in the form of ammonium ions while carbon comes from partly digested organic material. The carbon content was calculated according to the Walkley-Black method. In this method, the sample is first centrifuged and then filtered. Organic carbon is then oxidized by a mixture of K₂Cr₂O₇ and H₂SO₄ in a ratio of 1:2. The remaining K₂Cr₂O₇ was titrated with 0.5 N FeSO₄ 7H₂O.

The biomass was collected 2-3 days after the stationary phase had been achieved. The cultivation medium was centrifuged at 4000 rpm for 10 min and the biomass was dried in an air circulating oven at 45 °C until constant weight.

For the determination of phenolic content, the collected biomass was first milled in a planetary mill for 10 min at 200 rpm and then a pre-weighted sample was extracted in a polar solvent. An innovative extraction method with the use of vacuum microwave extraction technology (MAW) was used under the following conditions: 60 °C temperature, 1:10 ratio of solid material to solvent and 30 min extraction time. These conditions proved to be optimum for the extraction of polyphenolic compounds. The polyphenolic content was determined using the Folin-Ciocalteu method (Singleton, et. al. 1999).

2.2 Initial parameters of the experiments

The experimental set up of the two sets of experiments is shown in tables 1 and 2. In the first set of experiments, nitrogen (atomic nitrogen) was both in the form of nitrate, from potassium nitrate (KNO₃) and in the form of ammonium from either the anaerobic digestate or from ammonium chloride (NH₄Cl), such that in all experiments: a) the total atomic nitrogen was constant and equal to 129.9 mg/l, b) the nitrate nitrogen was equal to 74.8 mg/l and c) the total ammonium nitrogen was equal to 55.1 mg/l. Ammonium chloride was added in such a way as to keep total ammonium nitrogen constant in all four experiments since the anaerobic digestate contained 211 mg/l ammonium nitrogen.



Table 1. Experimental set up of the two sets of experiments for the study of the percentage of anaerobic digestate on the rate of carbon uptake and of the experiments for the study of the effect of initial nitrogen concentration on the total phenolic content of the biomass of *Chlorella sorokiniana*.

BR*	No (mg/l)	Co (gr/L)	% AD	Co/No	T (±1 °C)	pH (±0,3)
Effect of the % of the AD on the carbon uptake rate						
1	129.9	6.62	0	51.0	30	7.3
2	129.9	6.51	4	50.1	30	7.3
3	129.9	6.41	8	49.3	30	7.3
4	129.9	7.76	16	59.7	30	7.3
Effect of the No on the total phenolic content						
1	108.2	14.09	12	130.2	28	7.0
2	300	13.89	12	46.3	28	7.0
3	800	13.99	12	17.7	28	7.0
4	2000	13.95	12	7.0	28	7.0

* BR=Bioreactor

3. RESULTS AND DISCUSSION

a) Effect of low percentages of AD on the carbon uptake rate

Figure 1 shows the reduction in organic carbon as a function of culture time of *Chlorella sorokiniana* for the initial carbon concentrations as shown and for AD percentages in the four growth media equal to 0% (blank), 4%, 8% and 16%. Cultivation time is about 15 days. Nearly all carbon has been utilized at the end of the cultivation period (about 96%). The carbon uptake rate is obtained from the average slope in the exponential phase and it is shown versus the Co/No ratio in figure 2. The anaerobic digestate (AD) affects the organic carbon uptake rate above 8% AD. The increase is 6% and 13% at AD percentages of 8% and 16% respectively.

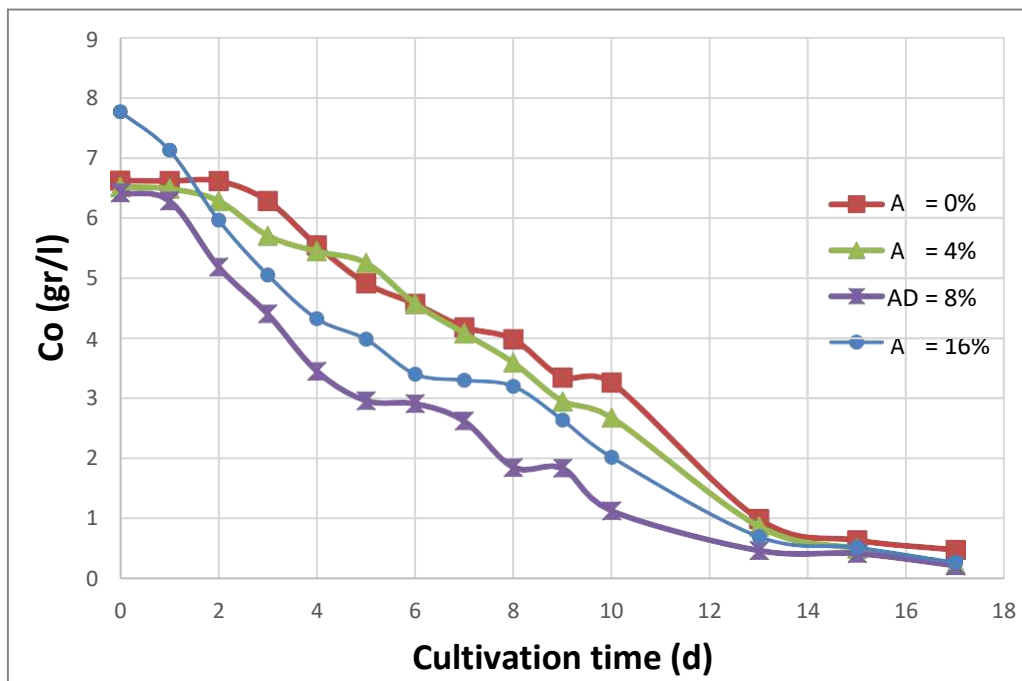


Figure 1. The reduction in organic carbon as a function of culture time of *Chlorella sorokiniana*.

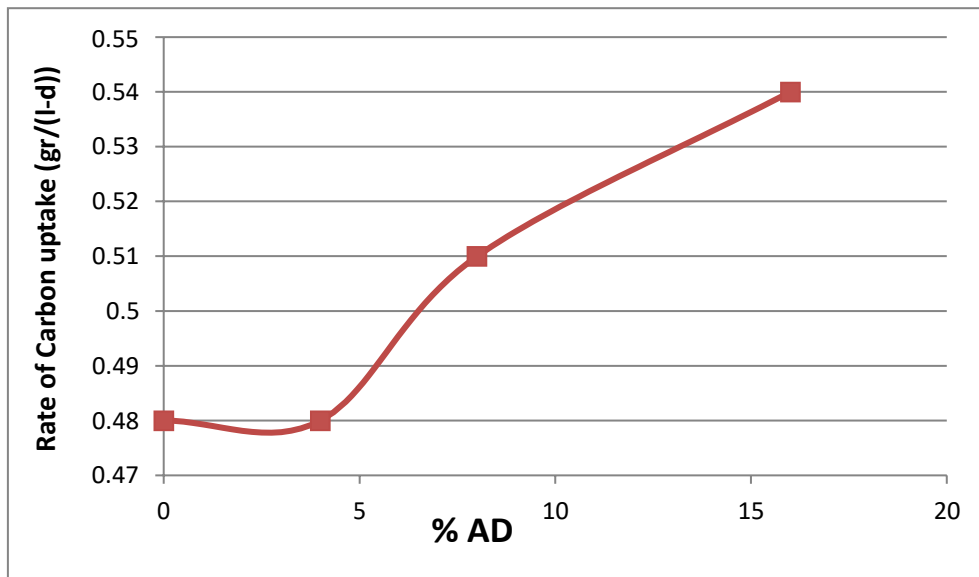


Figure 2. The rate of carbon uptake of organic carbon versus the percentage of the anaerobic digestate in the growth medium *Chlorella sorokiniana*. A line was drawn through the data points for clarity.

From figure 2 it is seen that the anaerobic digestate, at a percentage higher than 8%, affects the rate of carbon uptake of organic carbon. Specifically, the carbon uptake rate increases by 6% and 13% at biofertilizer rates of 8% and 16% respectively. The anaerobic digestate is a very complex medium. It contains a great number of elements, basically all elements, as well as various organic compounds. To add to this complexity, other unknown compounds are present such as tannins and phenolic compounds and also compounds formed from partial anaerobic digestion. Micronutrients present in the AD, especially cobalt, molybdenum and iron, may be affecting carbon uptake kinetics and this is presently being investigated. Cobalt and especially molybdenum may also be affecting nitrogen uptake by the microalgal cells which utilize these micronutrients for cell growth and therefore directly may be involved in carbon utilization process.

b) Biomass productivities

The biomass productivity is defined as the dry biomass collected in gr per liter of cultivation medium divided by the cultivation time, the lag phase excluded and is expressed in gr/(l-d). Therefore, it depends on both the biomass yield of the cultivation and on the biomass rate of growth. For the first set of experiments the biomass productivity is equal to 0.12, 0.12, 0.13 and 0.13 for 0%, 4%, 8% and 16% anaerobic digestate respectively. For the second set of experiments the biomass productivity is equal to 0.11, 0.14, 0.15 and 0.17 gr/(l-d) for initial atomic nitrogen concentrations (table 1) equal to 108.2, 300, 800 and 2000 mg/l respectively (Papapolymerou et. al., 2022).

The biomass yield depends strongly on both on initial nitrogen and initial carbon concentrations but, more on the initial nitrogen concentration. Although carbon is found in all three biomass macronutrients, namely protein, lipids and carbohydrates, atomic nitrogen, assuming carbon is present in adequate amount, affects and increases the biomass to a greater extent because, it is a necessary element for protein synthesis without which no biomass growth can occur.

c) Phenolic content of the biomass of *Chlorella sorokiniana* using glycerol and AD

The phenolic content of four samples of biomass of *Chlorella sorokiniana* grown heterotrophically with glycerol and anaerobic digestate was analyzed. For the extraction, as aforementioned, the use of innovative microwave assisted extraction (MAE) technology was used under the following conditions: a) 60 °C temperature, b) 1:10 ratio of solid to solvent and c) 30 min extraction time. The samples were obtained from four cultivation experiments in which took place in 42-liter bioreactors. The initial concentration of ammonium nitrogen was varied in the four cultivations and it was equal to 108.2 mg/l, 300 mg/l, 800 mg/l and 2000 mg/l while the initial concentration of carbon which, was provided by glycerin, was held nearly constant and equal to 14±0.1 g/l. 12% anaerobic digestate was used. Table 2 summarizes the values of total phenolic compounds measured.



Table 2. Concentration of polyphenols (expressed in mg of gallic acid/g dry weight) of *Chlorella sorokiniana* extracts (100 mg of dry matter/ml H₂O, extraction at 60 °C temperature, 1:10 ratio of solid material to solvent, 30 min extraction time and microwave intensity 100W).

N →	108 mg N/L	300 mg N/L	800 mg N/L	2000 mg N/L
Polyphenols (mg/L) →	3.6	2.8	3.4	2.3

We note that in these measurements a significant amount of polyphenols is measured in the biomass of *Chlorella sorokiniana* grown heterotrophically. In these preliminary experiments, no trend of polyphenol concentration with initial nitrogen concentration is evident.

4. CONCLUSIONS

Glycerol is easily absorbed and utilized by *Chlorella sorokiniana*. The anaerobic digestate is a good source for the formulation of growth media for cultivating microalgae heterotrophically and possibly autotrophically. It provides macro and micronutrients and some carbon from undigested organic material thus, reducing the cost of the growth media for microalgal cultivation and also contributes to the recycling of important nutrients such as phosphorus and potassium. At 16%, it increases the carbon uptake rate by 13%. The biomass of *Chlorella sorokiniana* grown heterotrophically is rich in polyphenols. Their concentration mg ranges from 2.3 mg/l to 3.6 mg/l.

5. ACKNOWLEDGEMENTS: The study was co-financed by the European Regional Development Fund of the European Union and Greek national funds through the Operational Program Competitiveness, Entrepreneurship and Innovation, under the call RESEARCH – CREATE - INNOVATE (project code: T1EDK-01580).

REFERENCES

- Bian, X., Jin, W., Gu, Q., Zhou, X., Xi, Y., Tu, R., Han, S., Xie, G., Gao, S. and Wang, Q., 2018. Subcritical n-hexane/ isopropanol extraction of lipid from wet microalgal pastes of *Scenedesmus obliquus*. *World J. Microbiol. Biotechnol*, 34, 39.
- Bumbak, F., Cook, S., Zachleder, V., Hauser, S. and Kovar, K., 2011. Best practices in heterotrophic high-cell-density microalgal processes: achievements, potential and possible limitations. *Applied microbiology and biotechnology*, 91(1), 31-46.
- Coulombier, N., Jauffrais, T. and Lebouvier, N., 2021. Antioxidant Compounds from Microalgae: A Review. *Mar. Drugs*, 19, 549.
- Dean, A., Sigee, D., Estrada, B. and Pittman, J., 2010. Using FTIR spectroscopy for rapid determination of lipid accumulation in response to nitrogen limitation in freshwater Microalgae. *Bioresource Technology*, 101, 4499–4507.
- Gouveia, L. and Oliveira, A. C., 2009. Microalgae as a raw material for biofuels production. *Journal of industrial microbiology and biotechnology*, 36(2), 269-274.
- Li, X., Xu, H. and Wu, Q., 2007. Large-scale biodiesel production from microalga *Chlorella protothecoides* through heterotrophic cultivation in bioreactors. *Biotechnology and bioengineering*, 98(4), 764-771.
- Papapolymerou, G., Metsoviti, M. N., Katsoulas, N., Karapanagiotidis, I. T., Kasiteropoulou, D., Mpesios, A. and Papadopoulou, A., 2022. *FAME properties and productivity of the bio-oil of Chlorella sorokiniana grown with low and high initial nitrogen concentrations*. Proceedings of the 9th Intern. Conference CEMEPE & SECOTOX, Mykons, June 3-9 2022, Greece.
- Patil, V., Reitan, K. I., Knutsen, G., Mortensen, L.M., Källqvist, T., Olsen, E., Vogt, G. and Gislerød, H.R., 2005. Microalgae as source of polyunsaturated fatty acids for aquaculture. *Plant Biology*, 6(6), 57-65.
- Perez-Garcia, O., Escalante, F. M., De-Bashan, L. E. and Bashan, Y., 2011. Heterotrophic cultures of microalgae: metabolism and potential products. *Water research*, 45(1), 11-36.
- Perez-Garcia, O. and Bashan, Y., 2015. Microalgal heterotrophic and mixotrophic culturing for bio-refining: from metabolic routes to techno-economics. *Algal biorefineries*, 61-131.
- Singleton L., V., Orthofer, R., Lamuela-Raventós M., R., Singleton, V.L., Orthofer, R. and Lamuela-Raventós, R.M., 1999. Analysis of total phenols and other oxidation substrates and antioxidants by means of folin-ciocalteu reagent. *Oxid. Antioxidants*, Part A Volume 299, 152–178.



- Spolaore, P., Joannis-Cassan, C., Duran, E. and Isambert, A., 2006. Commercial applications of microalgae. *Journal of bioscience and bioengineering*, 101(2), 87-96.
- Xiong, W., Li, X., Xiang, J. and Wu, Q., 2008. High-density fermentation of microalga *Chlorella protothecoides* in bioreactor for microbio-diesel production. *Applied microbiology and biotechnology*, 78(1), 29-36.



Mixotrophic cultivation of *Microchloropsis gaditana*

G. Papapolymerou¹, N. Katsoulas², I. T. Karapanagiotidis³ and M. N. Metsoviti¹

¹Dept. of Environmental Studies, Univ. of Thessaly, Gaiopolis, Larissa, Greece

²Dept. of Agriculture, Crop production and Rural Development, University of Thessaly, Volos, Greece

³Dept. of Ichthyology and Aquatic Environment, University of Thessaly, Volos, Greece

Corresponding author email: papapoly@uth.gr

ABSTRACT

The mixotrophic cultivation of *Microchloropsis gaditana* is studied. The microalgal species was cultivated in 10-liter cylindrical bioreactors filled up to 6 liters. All six cultivations were carried out in identical conditions in a glass greenhouse in the month of October. So, the temperature and the light intensity were allowed to vary naturally. Four cultivations were mixotrophic while, for comparison, one cultivation was autotrophic and one cultivation was totally heterotrophic as all light was excluded. In the four mixotrophic cultivations and in the heterotrophic cultivation the carbon (Co) was supplied from glycerol. In the autotrophic cultivation, the macro and micronutrients were supplied by inorganic salts. Air was supplied with a rate of 150 l/hr corresponding to 25 l/(l-hr). In the mixotrophic cultivations Co was equal to 2.87 g/l, 2.92 g/l, 3.96 g/l and 4.96 g/l and in the heterotrophic cultivation Co was equal to 2.24 g/l. The initial nitrogen concentration (No) was the same in all six cultivation and equal to 77.1 mg N/l as nitrate nitrogen. The Co/No ratio influenced both the time necessary for the organic carbon to be fully utilized and the rate of carbon uptake. For the heterotrophic cultivation, within 15 days, 92% of the carbon has been utilized, while for the mixotrophic cultivations after 32 days of cultivation 79%, 68% and 37% of the carbon has been utilized for Co equal to 2.92, 3.96 and 4.96 gr/l respectively. The organic carbon uptake rate, compared to the mixotrophic cultivations, is higher in the heterotrophic growth because during the day the microalgal cells via photosynthesis utilize CO₂ instead. The biomass yield, expressed per gr of organic carbon added to the growth medium, decreases for the high Co=4.96 gr/l and it is highest for the heterotrophic growth.

Keywords: *Microchloropsis gaditana*; mixotrophic; heterotrophic, autotrophic; biomass yield.

1. INTRODUCTION

Microalgae are unicellular photosynthetic organisms that use light and carbon dioxide, with higher photosynthetic efficiency than plants, for the production of biomass. Some microalgae species can also grow and multiply heterotrophically in the absence of light if an organic carbon source becomes available (Mata et. al., 2010). The main advantage of heterotrophic growth is higher biomass growth rates and biomass production because, unlike autotrophic growth, heterotrophic growth is not limited by light transmission through the growth medium (Liang Y., 2013). Another advantage of heterotrophic growth is the potential of achieving higher lipid content and, as a result, higher lipid productivities (Huang et. al., 2010). This is needed if microalgal cultivation is to be useful for biodiesel production. Disadvantages of heterotrophic growth are the susceptibility to contamination which requires that all parts of the bioreactors as well as all growth media must be carefully sterilized and the cost of organic carbon which must be provided to the growth medium (Embury et. al., 2012). Mixotrophic cultivation is a combination of cultivation in autotrophic and heterotrophic modes. The major advantages of mixotrophic cultivation are the higher growth rate and biomass productivity, as well as the higher lipid and protein content of the biomass (Burkholder et. al., 2008). Additionally, it should be mentioned that the process can easily scaled-up and it can result in increased growth and resource utilization by the microalgae (Wan et. al., 2011). On the other hand, the major disadvantages of mixotrophic cultivation are the simultaneous need for light, CO₂, organic carbon, and O₂ and the reduced energy conversion efficiency in comparison to heterotrophic cultivation (Yang et. al., 2000). The biodiversity of microalgae is large; there are species that prosper in fresh water and others in saltwater.

It should be mentioned that they are used in pharmaceutical industry, in biodiesel production, in wastewater management, as nutritional supplements for human nutrition and as feed for animals and fish (Pulz & Gross 2004). What is more, they contain a high percentage of proteins, (with a good amino acid profile) and lipids (with significant amounts of DHA and EPA that are essential for fish feeds), varying by algal species (Brown et. al., 1997). In addition, they have a high content of vitamins such as, A, B1, B2, B6, B12, C,



E and biotin, folic acid and inorganic salts (phosphate, zinc, iron, calcium, selenium, magnesium), antioxidants and pigments such as chlorophylls, carotenoids and phenolic compounds (Lubian et. al., 2000). Cultivation of microalgae can be carried out either in open or closed systems. Open-field cultivation is usually conducted in open raceway bioreactors that are exposed to the environment. Cultivation in closed systems can be carried out in photobioreactors of various configurations. However, their culture systems are quite complex and microalgal growth is influenced by different factors, such as light intensity, temperature, pH, carbon dioxide, mixing rate, salinity and nutrient composition of the culture medium (Dean et. al., 2010).

The aim of this study is to cultivate *Microchloropsis gaditana* in three different modes, i.e. autotrophically, mixotrophically and heterotrophically and compare the biomass yields and productivities. Also, for the heterotrophic and mixotrophic cultivations, the aim is to determine the effect of the initial carbon concentration on the carbon uptake rate and the biomass yield expressed in gr of biomass/(l-gr of organic carbon added).

2. MATERIALS AND METHODS

2.1 Bioreactors

The cultivations were carried out in cylindrical bioreactors each of 10 L capacity that were filled up to 6L. Air was continuously passed through the solution in each bioreactor at 150 L/hr through 2 mm glass tubing positioned at the tip of a magnetic bar and the air bubbles were dispersed with the magnetic bar at the bottom of the glass flasks at a rotational speed of 500 rpm. The carbon dioxide feed rate corresponds to 0.062 L CO₂ h⁻¹ or 0.026 mole CO₂ h⁻¹. The experiments were performed in the greenhouse of the University of Thessaly under the same conditions of temperature, light intensity, orientation and aeration each time. The pH in all six bioreactors was fixed at 8.5 ±0.3 with the addition of a weak base or weak acid. This cultivation set up in a greenhouse environment where temperature and sun illumination vary naturally is useful since it can examine differences in biomass productivities for these different modes of cultivations under identical external conditions in a natural environment and could be useful in a potential application in open bioreactors.

2.2 Materials and Methods of Analyses

The microalgae *Microchloropsis gaditana*, a species growing in brackish waters, SAG strain number 2.99, was obtained from the University of Göttingen and the inoculum was cultivated in a Brackish Water Medium (Sammlung von Algenkulturen der Universität Göttingen (SAG), Göttingen, Germany) (= 1/2 SWES) (SAG, 2007). Each liter of the culture medium contained: 0.2 g KNO₃/L, 0.02 g K₂HPO₄/L, 0.02 g MgSO₄·7H₂O/L, 30 mL of soil extract/L and 5 ml/L, of a solution containing the following micronutrients: (1 mg ZnSO₄·7H₂O, 2 mg MnSO₄·4H₂O, 10 mg H₃BO₃, 1 mg Co(NO₃)₂·6H₂O, 1 mg MoO₄·2H₂O, 0.005 mg CuSO₄·5H₂O, 700 mg FeSO₄·7H₂O and 800 mg EDTA)/L. Also, synthetic salt was used to make the culture water brackish (455 mL filtered brackish water in 1 L water). Each bioreactor was inoculated with a standard quantity of 60 mL of *M. gaditana* inoculum of approximately 0.5 optical density.

Crude glycerol was obtained from a local biodiesel manufacturing plant. Its composition was approximately 86% glycerol, 0.5% methanol, 4% free fatty acids and 7.5% H₂O. The carbon content was calculated so that the approximate C/N ratios could be pre-estimated. Initial atomic nitrogen concentration was fixed in all six bioreactors at 77.1 mg/l and it was in the nitrate form (NaNO₃). Potassium was supplied from potassium chloride (KCl). The average daily temperature was 25.3 °C and the average sun illumination was 10.9 (MJ/m²-d). Table 1 shows the initial parameters of each of the six experiments.

For the determination of organic carbon, the method of Ciavatta *et al.* was used (1991). The samples were first centrifuged and then filtered. According to this method, organic carbon was oxidized by a mixture 5 ml of 2N K₂Cr₂O₇ and 20 ml of concentrated H₂SO₄ at 160 ± 2 °C. The excess dichromate was titrated with iron (II) sulphate. The ammonium nitrogen content was measured by distillation in the presence of MgO and collection of the product in a solution 2% H₃BO₃ in presence of indicator methyl red, and subsequently titration of the product with 0.1 N HCl. The biomass, at the end of the cultivation period, was collected via centrifugation at 4000 rpm for 5 minutes and was dried in an air circulation oven at 45 °C.



Table 1 The basic experimental set up for the six cultivations of *M. gaditana* in a glass greenhouse.

BR	No (mg/l)	K (mg/l)	Trace Elements & P	Co (gr/l)	Co/No	Mode of Cultivation	pH (± 0.3)
1	77.1	138.7	SAG, 1/2 SWES	0	----	Autotrophic	8.5
2	77.1	138.7	SAG, 1/2 SWES	2.24	29.0	Heterotrophic	8.5
3	77.1	138.7	SAG, 1/2 SWES	2.87	37.2	Mixotrophic	8.5
4	77.1	138.7	SAG, 1/2 SWES	2.92	37.8	Mixotrophic	8.5
5	77.1	138.7	SAG, 1/2 SWES	3.69	47.9	Mixotrophic	8.5
6	77.1	138.7	SAG, 1/2 SWES	4.96	64.3	Mixotrophic	8.5

3. RESULTS AND DISCUSSION

Figure 1 shows the carbon reduction versus the cultivation time for the heterotrophic and the four mixotrophic cultivations. The two curves having Co= 2.87 and 2.92 g/L with Co/No equal to 37.2 and 37.8 respectively and are independent cultivations are basically identical.

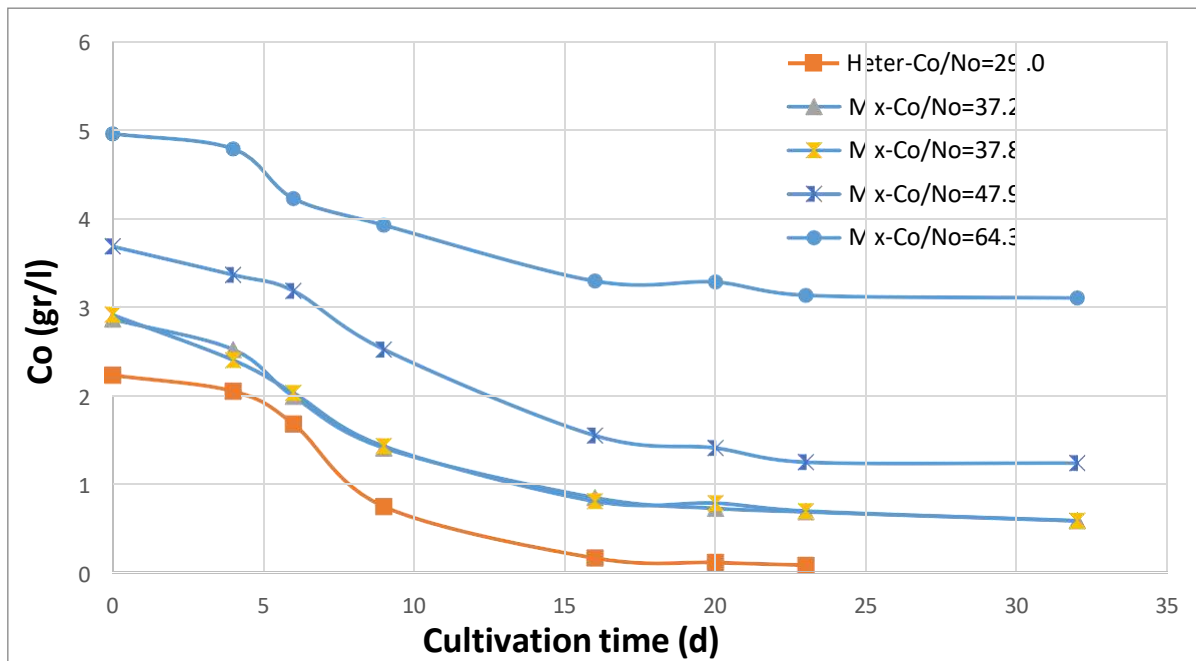


Figure 1. The carbon reduction versus the cultivation time for the heterotrophic and the four mixotrophic cultivations for the initial carbon concentrations equal to 2.24, 2.87, 2.92, 3.69 and 4.96 gr/l and for Co/No ratios shown in the figure. Initial atomic nitrogen concentration is equal to 77.1 mg/l. Curves were drawn between data points for clarity.

It is evident from figure 1 that the cultivation time is strongly dependent on the initial carbon concentration and as Co increases so does the cultivation time. For the heterotrophic cultivation, within 15 days, 92% of the carbon has been utilized. For the mixotrophic cultivations after 32 days of cultivation 79%, 68% and 37% of the carbon has been utilized for Co equal to 2.92, 3.96 and 4.96 gr/l (Co/No=37.8, 47.9 and 64.3) respectively. This substantially increased cultivation time required for the reduction of organic dissolved carbon (compared to the corresponding one for the heterotrophic cultivation) is probably due to the decreased carbon uptake rate because during the daylight hours in the mixotrophic cultivations the microalgal cells work via photosynthesis and therefore do not absorb dissolved organic carbon as efficiently.

Figure 2 shows the carbon uptake rate versus the Co/No ratio for the four mixotrophic cultivations of table 1.

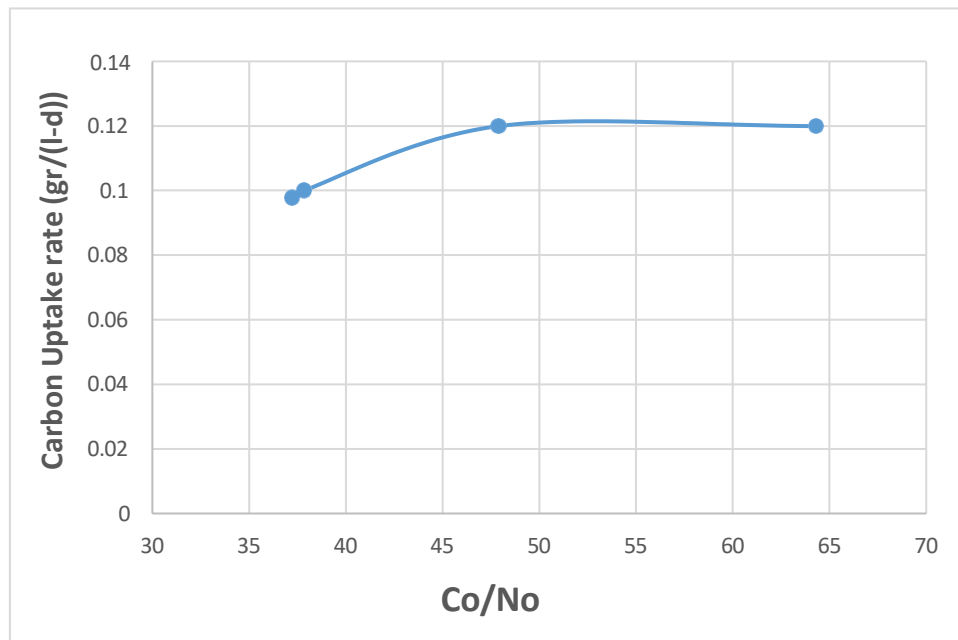


Figure 2. The carbon uptake rate versus the Co/No ratio for the four mixotrophic cultivations of table 1. Curves were drawn through the data points for clarity. For comparison the carbon uptake rate for the purely heterotrophic cultivation with Co/No=29.0 is 0.14 gr/(l-d).

From figure 2 it is seen that carbon uptake initially increases and then above Co=3.96 gr/l (Co/No=47.9) it remains constant. For comparison the carbon uptake rate of the heterotrophic cultivation, although it had a lower Co and Co/No equal to 2.24 gr/l and 29.0 respectively, is equal to 0.14 gr/(l-d) higher by 40% than the 0.1 gr/(l-d) for the mixotrophic cultivations with Co=2.87 and 2.92 gr/l and Co/No= 37.2 and 37.8. As discussed previously, this is most likely due to the decreased carbon uptake rate for the mixotrophic cultivations because during the day they photosynthesize and therefore do not utilize dissolved organic carbon as efficiently. Therefore, both the mode of cultivation and the initial carbon to nitrogen ratio influenced both the time necessary for the organic carbon to be utilized and the rate of carbon uptake.

Table 2 shows the biomass yield and the biomass productivities of the six cultivations namely, the autotrophic, the heterotrophic and the four mixotrophic cultivations of *Microchloropsis gaditana*. As noted in table 2 the biomass yield differed in these cultivations. In the mixotrophic cultivations as the Co/No ratio increased the biomass yield as well as the biomass productivity increase as the carbon added to the growth medium increases. However, when the biomass yield is expressed per gr of organic carbon added to the growth medium, it is equal to 1.1, 1.1 and 0.96 gr/(l-gr of C) for Co/No=37.2, 37.8 and 47.9 respectively, declining to 0.85 for Co/No=64.3. For the heterotrophic growth for Co/No=29 the biomass yield as well as the biomass productivity are higher and equal to 1.3 gr/(l-gr of C) and 145 mg/(l-d) respectively. The autotrophic cultivation gave a biomass yield of 2.8 g/l. The productivity is higher for the heterotrophic growth because of the shorter cultivation period required. For the autotrophic growth the biomass productivity was 0.086 g/(l-d).

Table 2. The biomass yield (M_b), the biomass productivity (P_b) and the biomass yield per gr of organic carbon added in the growth medium (M'_b) for the autotrophic, the heterotrophic and the four mixotrophic cultivations of *Microchloropsis gaditana*.

	Mode of Cultivation					
	Autotrophic	Heterotrophic	Mixotrophic	Mixotrophic	Mixotrophic	Mixotrophic
Co → Quantity ↓	-----	2.24 gr/l	2.87 gr/l	2.92 gr/l	3.96 gr/l	4.96 gr/l
M_b (gr/l)	2.8	2.9	3.2	3.2	3.8	4.2



P _b (mg/(l-d))	86	145	107	107	125	140
M' _b (gr/(grC-l))	-----	1.3	1.1	1.1	0.96	0.85

4. CONCLUSIONS

The species *Microchloropsis gaditana* can grow in a variety of modes since it absorbs and utilizes glycerol efficiently. The mode of cultivation of the microalgal species *Microchloropsis gaditana* affects the kinetics of carbon reduction as well as the carbon uptake rate. The biomass productivity for the autotrophic growth is 0.086 g/(l-d). Heterotrophic growth appears to be superior if the biomass productivity is expressed in gr/(l-d-gr of carbon supplied). Excess carbon, 4.96 gr/l, in the mixotrophic growth leads to a decrease in biomass productivity per gr of carbon and does not appear to increase the kinetics of carbon reduction because, after 30 days of cultivation only about 37% of the carbon supplied is utilized. This is to compare with a 79% and a 68% reduction for 2.92 gr/l and 3.69 gr/l carbon added respectively. For the heterotrophic growth at the end of the cultivation with 2.24 gr/l carbon added 96% of the carbon had been utilized. Therefore, other modes of heterotrophic or mixotrophic cultivation such as heterotrophic semi-batch or mixotrophic semi-batch, in which carbon is added in small amounts, may lead to higher productivities.

5. ACKNOWLEDGEMENTS

This study was part of the project coded MIS 5045804 that has been co-financed by Greece and EU under the "Operational Programme Competitiveness, Entrepreneurship and Innovation - EPAnEK 2014-2020".

REFERENCES

- Brown, M. R., Jeffrey, S. W., Volkman, J. K. and Dunstan, G. A., 1997. Nutritional properties of microalgae for mariculture. *Aquaculture*, 197, 151, 315-331.
- Burkholder, J. M., Glibert, P. M. and Skelton, H. M., 2008. Mixotrophy, a major mode of nutrition for harmful algal species in eutrophic waters. *Harmful Algae*, 8:77-93
- Ciavatta, C., Govi M., Antisari L. V. and Sequi P., 1991. Determination of organic carbon in aqueous extracts of soils and fertilizers. *Commun. Soil Sci. Plant Anal.*, 22(9-10), 795-807.
- Dean, A., Sigee, D., Estrada, B. and Pittman, J., 2010. Using FTIR spectroscopy for rapid determination of lipid accumulation in response to nitrogen limitation in freshwater microalgae. *Bioresour. Technol.* 101: 4499-4507.
- Embury, O., Merchant, C. J. and Filipiak, M. J., 2012. A reprocessing for climate of sea surface temperature from the along-track scanning radiometers: Basis in radiative transfer. *Remote Sens. Environ.*, 116, 32-46.
- Huang, G., Chen, F., Wei, D., Zhang, X. and Chen, G., 2010. Biodiesel production by microalgal biotechnology. *Appl. Energy*, 87, 38-46.
- Liang, Y., 2013. Producing liquid transportation fuels from heterotrophic microalgae. *Appl. Energy*, 104, 860-868.
- Lubián, L. M., Montero, O., Moreno-Garrido, I., Huertas, I. E., Sobrino, C., González-Del Valle, M. and Parés, G., 2000. *Nannochloropsis* (Eustigmatophyceae) as source of commercially valuable pigments. *J. Appl. Phycol.*, 12, 249-255.
- Mata, T. M., Martins, A. A. and Caetano, N. S., 2010. Microalgae for biodiesel production and other applications: a review. *Renew. Sust. Energ. Rev.*, 14, 217-232.
- Wan, M., Liu, P., Xia J., Rosenberg, J. N., Oyler, G. A., Betenbaugh, M. J., Nie, Z. and Qiu, G., 2011. The effect of mixotrophy on microalgal growth, lipid content, and expression levels of three pathway genes in *Chlorella sorokiniana*. *Appl Microbiol Biotechnol*, 91:835-844.
- Yang, C., Hua, Q. and Shimizu K., 2000. Energetics and carbon metabolism during growth of microalgal cells under photoautotrophic, mixotrophic and cyclic light-autotrophic/dark-heterotrophic conditions. *Biochem Eng J*, 6:87-102.
- Pulz, O. and Gross, W., 2004. Valuable products from biotechnology of microalgae. *Applied Microbiology and Biotechnology*, 65 (6), 635-648
- SAG. (2007). Sammlung von Algenkulturen der Universität Göttingen. Culture Collection of Algae, [https://www.uni-goettingen.de/Abteilung Experimentelle Phykologie und Sammlung von Algenkulturen \(EPSAG\), Universität Göttingen, Deutschland. Available at: http://epsag.uni-goettingen.de.](https://www.uni-goettingen.de/Abteilung%20Experimentelle%20Phykologie%20und%20Sammlung%20von%20Algenkulturen%20(EPSAG),%20Universit%C3%A4t%20G%C3%B6ttingen,%20Deutschland.%20Available%20at%20%3A%3A%3Ahttp://epsag.uni-goettingen.de.)



Energetic potential evaluation of medical wastes for using as solid recovered fuels

D. Torres¹, M. Fonseca Almeida¹ and S. C. Pinho¹

¹LEPABE, Laboratory for Process Engineering, Environment, Biotechnology and Energy,
Faculty of Engineering, University of Porto
Corresponding author email: scpinho@fe.up.pt

ABSTRACT

Using wastes as alternative fuels is an efficient way of energy recovery, a process currently applied by the cement industry worldwide. Nevertheless, current laws only recognize nonhazardous wastes as potential solid recovered fuels, excluding hazardous medical wastes. Microwave technology shows a high efficiency on microbial inactivation thus, after treatment, medical wastes are equated to nonhazardous wastes and can be landfilled. Therefore, using the treated wastes having enough energetic potential not only recovers energy but also avoids landfilling and it could be an option to consider. The aim of this study was to evaluate the energetic potential of medical wastes from a microwave treatment plant. Their calorific values demonstrated the potential of the medical wastes as an alternative fuel. Also, its classification according to ISO 21640:2021 is in class 1 regarding the net calorific value and mercury content and relatively chlorine content is in class 3, fulfilling the requirements from the standard.

Keywords: medical wastes; solid recovered fuels; alternative fuel.

1. INTRODUCTION

The growth of medical waste production and the need for a specific treatment made those responsible for managing such wastes look for new and more efficient ways to treat them. Over the last decades, incineration and autoclaving have been the most commonly used technologies for treating medical wastes (Sukandar et al., 2006). Microwave treatment is an innovative, clean and effective technology in eliminating pathogens, resulting in a treated, unrecognizable, homogeneous waste, composed of very fine particles, constituting a potentially recoverable or recyclable product. Due to the fragmentation process to which it is subjected, the residue reduces about 80 % of the initial volume, although its mass remains practically unchanged. This treatment shows solid indications of becoming more common for medical waste, giving a residue that continues to be landfilled. Disposal is the last option in the waste management hierarchy that must be adopted when there are no other possibilities. Therefore, proceeding with the disposal of treated medical wastes should only occur if there is no way to give useful use to the wastes resulting from this treatment (Chartier et al., 2014).

In the last years, the use of alternative fuel (such as refuse derived fuel (SFR), tire derived fuel, sewage sludge, and municipal solid wastes) has shown to be ecologically and economically profitable (Chatziaras and Psomopoulos, 2016). Although SFR has advantages in terms of the management of natural resources and the diversion of waste to landfills, it must have a homogeneous chemical and physical composition and not present variations in energy so as not to interfere with the conditions of the process where it will be used.

The utilization of wastes that have the potential of being used to recover energy could be an option to consider. The current laws only recognize nonhazardous wastes as potential solid recovered fuels which does not include hazardous medical wastes. Since microwave technology shows a high efficiency on microbial inactivation (Zimmermann, 2017), and, after treatment, medical wastes are equated to nonhazardous wastes, it could be possible to produce SRF from these wastes. The objective of this study was to evaluate the energetic potential of using treated medical wastes as SRF, analyzing the parameters set as mandatory by the European standards.

2. MATERIALS AND METHODS

2.1. Materials

The three samples of medical waste samples used in this study were collected in a microwave treatment unit at three different months to cover possible changes in the constitution of medical wastes. Medical wastes



are mainly constituted by plastics (33 %), paper (24 %), absorbents (34 %), glass (3 %), metals (2 %) and others (2 %) (Alvim-Ferraz and Afonso, 2005). Figure 1 shows the sample of medical wastes, looking *fluff*, after microwave treatment. To ensure the homogeneity of the samples they were quartered and comminuted using a RETSCH SM 200 equipment with a 2 mm sieve. In the size sample distribution analysis, 7 sieves with a mesh between 1.00 mm and 12.50 mm were used and determinations were made on the three samples.



Figure 1. Sample of medical wastes after microwave treatment.

2.2. Methods

The gross calorific value was obtained at 25 °C in a bomb calorimeter model Parr 1672 according to EN 15400:2011. The chlorine was determined according to EN 15408:2011 and total carbon following EN 13137:2001 standard procedure. The ash content and the moisture content followed the EN 15403:2011 and EN 15414-1: 2011 standards, respectively. For metals quantification, the samples were subjected to chemical attack with aqua regia, according to the ISO 11466:1995 standard and the solutions were analyzed by Atomic Absorption Spectrometry (AAS). All parameters were carried out in triplicate, the depicted values being the average with a standard deviation of less than 5–6 %.

3. RESULTS AND DISCUSSION

The ISO 21640:2021 standard uses a classification system for SRF based on three parameters: an economic parameter (net calorific value), a technical parameter (chlorine content), and an environmental parameter (mercury content). Each parameter is divided into five classes (described in table 2 of the standard), and the class code consists on the combination of these three classifications. The standard also defines mandatory specifications such as origin, shape and size of particles, ash content, moisture content, and chemical parameters, namely some metals.

All of the following values reported correspond to the average of the three samples collected in a microwave treatment unit in three different months.

The particle size distribution in Figure 2, proves the heterogeneity of the samples in terms of their size. However, there is a large percentage of particles smaller than 6.30 mm, and the oversize from 8.00 mm has the highest percentage, around 55 %.

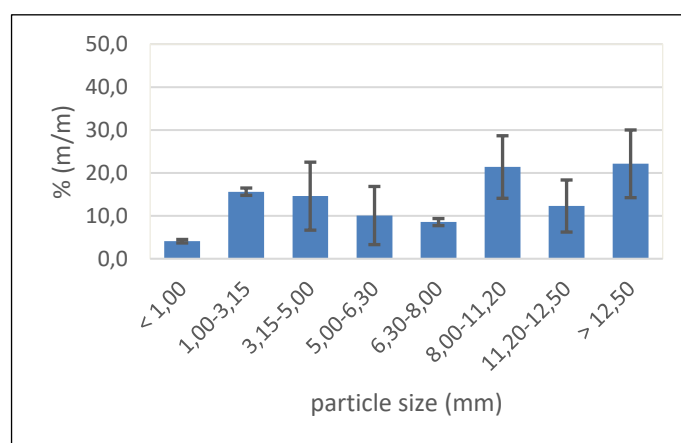


Figure 2. Particle size distribution of medical waste samples after microwave treatment.



The values reported correspond to the average of the three samples collected in a microwave treatment unit in three different months. Table 1 reports the values of the mandatory specification physical parameters obtained on the medical wastes. Medical wastes show a high net calorific value of dry (d), and as received (ar) samples nearly the heating value of coal, which is about 30 MJ/kg (Dincer at al., 2018). Concerning ash and moisture content, these wastes have low values. The medical waste samples show, also a high total carbon content, 68.7 %, and high gross calorific value, 33.40 MJ/kg, as expected due to its composition, mainly plastics and paper.

Table 2 shows the values of the mandatory specification chemical parameters in samples the mercury content was low but chlorine content was slightly significant. The chlorine in the samples is from plastic components made of polyvinyl chloride, such as transfusion tubes and/or collection bags.

Table 1. Mandatory specification physical parameters.

Parameter	Value
Ash content, %	6.0 ± 0.8
Moisture content, %	8.4 ± 1.7
Net calorific value, MJ/kg (ar)	31.0 ± 3.9
Net calorific value, MJ/kg (d)	33.9 ± 1.7

Table 2. Mandatory specification chemical parameters.

Parameter	Value
Antimony, mg/kg (d)	< 20.67±0.79
Arsenic, mg/kg (d)	0.63±0.02
Cadmium, mg/kg (d)	< 1.79±0.07
Chlorine, mg/kg (d)	0.84±0.14
Chromium, mg/kg (d)	72.97±36.6
Cobalt, mg/kg (d)	8.96±6.18
Copper, mg/kg (d)	97.31±34.68
Lead, mg/kg (d)	<5.59±0.21
Manganese, mg/kg (d)	43.31±3.56
Mercury, mg/kg (d)	0.19±0.01
Nickel, mg/kg (d)	46.60±14.90
Thallium, mg/kg (d)	29.55±1.04
Vanadium, mg/kg (d)	< 19.25±0.76
∑ Heavy metals (mg/kg)	315.32±10.9

The net calorific value of the medical waste obtained was greater than 25 MJ/kg; therefore, it is in class 1; the chlorine content was lower than 1.0 %, corresponding to class 3. The median mercury content and the 80th percentile were $\leq 0,02 \leq 0,04$ mg/MJ, respectively, thus corresponding to class 1, as reported in Table 3. Therefore, the medical waste with these determined characteristics is coded as PCI 1; Cl 3; Hg 1, according to ISO 21640:2021.

Table 3. Classification of medical waste according ISO 21640:2021 standard.

Parameter	Value	Classes
Net calorific value, MJ/kg (ar)	33.9	1
Chlorine, % (d)	0.84	3
Mercury [mg/MJ], (ar)	0.0082	1
Median 80 th percentile	0.0092	



4. CONCLUSIONS

The heat of combustion determined for the samples show the potential of using this waste as one more alternative for solid recovered fuels. Besides, the ash content is low, and the values in the samples were consistent, which is favorable to the use of medical wastes in specific incineration or co-incineration processes. This ability is also supported by its classification according to the ISO 21640:2021 standard, which, in terms of net calorific value, chlorine content and mercury content ranks this waste good. In terms of economic and environmental parameters it is class 1, the best value provided by the standard. Indeed, based on the analyzed hospital waste's characteristics, energy production can be an asset in its management both from an environmental and economic point of view.

5. ACKNOWLEDGEMENTS

This work was financially supported by LA/P/0045/2020 (ALiCE), UIDB/00511/2020 and UIDP/00511/2020 (LEPABE), funded by national funds through FCT/MCTES (PIDDAC).

REFERENCES

- Alvim-Ferraz, M. C. M., Afonso, S. A. V., 2005. Incineration of healthcare wastes: management of atmospheric emissions through waste segregation. *Waste Management*, 25(6), 638–648.
- Chartier, Y., Emmanuel, J., Pieper, U., Pruss, A., Rushbrook, P., Stringer, R., Townend, W., Wilbum, S., Zghondi, R. 2014. Safe Management of Wastes from Health Activities. 2nd edition, World Health Organization, Geneva
- Chatziaras, N, Psomopoulos, C. S., 2016. Use of waste derived fuels in cement industry: a review. *Management of Environmental Quality: An International Journal*, 27, 178–193
- Dincer, I., Rosen, M.A., Khalid F., 2018. 3.16 Thermal Energy Production. *Comprehensive Energy Systems*, 3, 673–706
- EN 15400:2011. Solid recovered fuels - Determination of calorific value.
- EN 15408:2011. Solid recovered fuels - Methods for the determination of sulphur (S), chlorine (Cl), fluorine (F) and bromine (Br) content.
- EN 13137:2001. Characterisation of waste – Determination of total organic carbon (TOC) in wastes, sludges and sediments.
- EN 15403:2011. Solid recovered fuels - Determination of ash content.
- EN 15414-1: 2011. Solid recovered fuels - Determination of moisture content using the oven dry method - Part 3: Moisture in general analysis sample.
- ISO 11466:1995. Soil quality—Extraction of trace elements soluble in aqua regia.
- ISO 21640:2021. Solid recovered fuels — Specifications and classes.
- Sukandar, S., Yasuda, K., Tanaka, M., Aoyama I., 2006. Metals leachability from medical waste incinerator fly ash: A case study on particle size comparison. *Environmental Pollution*, 144, 726–735.
- Zimmermann, K. (2017). Microwave as an emerging technology for the treatment of biohazardous waste: A mini-review. *Waste Management & Research*, 35(5), 471 – 479.



Contact

Professor Petros Gikas

Design of Environmental Processes Laboratory

School of Chemical and Environmental Engineering Technical University of Crete, Greece

T: +30 28210 37836

E: pgikas@tuc.gr, secretariat@susteng.eu

W: www.deplab.tuc.gr, www.susteng.eu



organizers



Technical University of Crete
School of Chemical and
Environmental Engineering



LIFE B2E4 sustainable - WWTP
LIFE16 ENV/GR/000298

funders



sponsors



Co - organizer



Gold sponsor



Gold sponsor



Gold sponsor



SEKA bunkering station S.A.
BUNKERING IN PIRAEUS & KALI LIMENES

Gold sponsor



Silver sponsor



Silver sponsor



Sponsor



Sponsor



Silver sponsor



Media sponsor



Supporter



Supporter



Supporter



Supporter